

Analysis of Aircraft Structures

An Introduction

SECOND EDITION

Bruce K. Donaldson



CAMBRIDGE AEROSPACE SERIES

Analysis of Aircraft Structures

Second Edition

As with the first edition, this textbook provides a clear introduction to the fundamental theory of structural analysis as applied to aircraft, spacecraft, automobiles, and ships. The emphasis is on the application of fundamental concepts of structural analysis that are employed in everyday engineering practice. All approximations are accompanied by a full explanation of their validity. Repetition is an important learning tool; therefore some redundancy is used to dispel misunderstanding. In this new edition, more topics, figures, examples, and exercises have been added. There is also a greater emphasis on the finite element method of analysis. Clarity remains the hallmark of this text.

Bruce K. Donaldson was first exposed to aircraft inertia loads when he was a carrier-based U.S. Navy antisubmarine pilot. He subsequently worked in the structural dynamics area at the Boeing Company and at the Beech Aircraft Corporation in Wichita, Kansas, before returning to school and embarking on an academic career in the area of structural analysis. He became a professor of aerospace engineering and then a professor of civil and environmental engineering at the University of Maryland. Professor Donaldson is the recipient of numerous teaching awards and has maintained industry contacts, working various summers at government agencies and for commercial enterprises, the last being Lockheed Martin in Fort Worth, Texas. He is the author of *Introduction to Structural Dynamics*, also published by Cambridge University Press.

Cambridge Aerospace Series

Editors

Wei Shyy

and

Michael J. Rycroft

1. J. M. Rolfe and K. J. Staples (eds.): *Flight Simulation*
2. P. Berlin: *The Geostationary Applications Satellite*
3. M. J. T. Smith: *Aircraft Noise*
4. N. X. Vinh: *Flight Mechanics of High-Performance Aircraft*
5. W. A. Mair and D. L. Birdsall: *Aircraft Performance*
6. M. J. Abzug and E. E. Larrabee: *Airplane Stability and Control*
7. M. J. Sidi: *Spacecraft Dynamics and Control*
8. J. D. Anderson: *A History of Aerodynamics*
9. A. M. Cruise, J. A. Bowles, C. V. Goodall, and T. J. Patrick: *Principles of Space Instrument Design*
10. G. A. Khoury and J. D. Gillett (eds.): *Airship Technology*
11. J. Fielding: *Introduction to Aircraft Design*
12. J. G. Leishman: *Principles of Helicopter Aerodynamics*, 2nd Edition
13. J. Katz and A. Plotkin: *Low Speed Aerodynamics*, 2nd Edition
14. M. J. Abzug and E. E. Larrabee: *Airplane Stability and Control: A History of the Technologies That Made Aviation Possible*, 2nd Edition
15. D. H. Hodges and G. A. Pierce: *Introduction to Structural Dynamics and Aeroelasticity*
16. W. Fehse: *Automatic Rendezvous and Docking of Spacecraft*
17. R. D. Flack: *Fundamentals of Jet Propulsion with Applications*
18. E. A. Baskharone: *Principles of Turbomachinery in Air-Breathing Engines*
19. D. D. Knight: *Numerical Methods for High-Speed Flows*
20. C. Wagner, T. Hüttl, and P. Sagaut: *Large-Eddy Simulation for Acoustics*
21. D. Joseph, T. Funada, and J. Wang: *Potential Flows of Viscous and Viscoelastic Fluids*
22. W. Shyy, Y. Lian, H. Liu, J. Tang, and D. Vieru: *Aerodynamics of Low Reynolds Number Flyers*
23. J. H. Saleh: *Analyses for Durability and System Design Lifetime*
24. B. K. Donaldson: *Analysis of Aircraft Structures*, 2nd Edition

Analysis of Aircraft Structures

An Introduction

Second Edition

BRUCE K. DONALDSON, Ph.D.

*Department of Civil and Environmental Engineering
University of Maryland*



CAMBRIDGE
UNIVERSITY PRESS

CAMBRIDGE UNIVERSITY PRESS

Cambridge, New York, Melbourne, Madrid, Cape Town, Singapore,
São Paulo, New Delhi, Mexico City

Cambridge University Press
c/o Cambridge University Press India Pvt. Ltd.
Cambridge House
4381/4, Ansari Road, Daryaganj
New Delhi 110002
India

www.cambridge.org
Information on this title: www.cambridge.org/9780521865838

© Bruce K. Donaldson 2008

This publication is in copyright. Subject to statutory exception and to the provisions of relevant collective licensing agreements, no reproduction of any part may take place without the written permission of Cambridge University Press.

First published 2008
First South Asian edition 2012

This South Asian edition is based on Bruce K. Donaldson / *Analysis of Aircraft Structures: An Introduction* – 2 ed. / 9780521865838 / 2008

Printed in India at Raj Press, R-3 Inderpuri, New Delhi 110012

A catalogue record for this publication is available from the British Library

Library of Congress Cataloging in Publication data

Donaldson, Bruce K.,

Analysis of aircraft structures : an introduction / Bruce K. Donaldson. – 2nd ed.

p. cm. – (Cambridge aerospace series)

Includes bibliographical references and index.

ISBN 978-0-521-86583-8 (hardcover)

1. Airframes. 2. Structural analysis (Engineering) 3. Vehicles – Design and construction. I. Title.

TL671.6.D56 2008

629.134'31 – dc22

2008002226

ISBN-13 978-1-107-63816-7 (Paperback)

Cambridge University Press has no responsibility for the persistence or accuracy of URLs for external or third-party internet websites referred to in this publication, and does not guarantee that any content on such websites is, or will remain, accurate or appropriate.

TO MY WIFE, LOIS,
AND CHILDREN,
LEXA, SARA, AND KENNETH

Greek Alphabet

Forms	Name
$A \alpha$	alpha
$B \beta$	beta
$\Gamma \gamma$	gamma
$\Delta \delta$	delta
$E \epsilon$	epsilon
$Z \zeta$	zěta
$H \eta$	ěta
$\Theta \theta$	thěta
$I \iota$	iota
$K \kappa$	kappa
$\Lambda \lambda$	lambda
$M \mu$	mu
$N \nu$	nu
$\Xi \xi$	xi
$O \omicron$	omicron
$\Pi \pi$	pi
$P \rho$	rhó
$\Sigma \sigma$	sigma
$T \tau$	tau
$\Upsilon \upsilon$	upsilon
$\Phi \phi$	phi
$X \chi$	chi
$\Psi \psi$	psi
$\Omega \omega$	ömega

Contents

<i>Introduction to the Second Edition</i>	page xix
<i>Introduction to the First Edition</i>	xxi
<i>List of Repeated Engineering Symbols</i>	xxv
<i>Acknowledgments</i>	xxxiii

Part I The Fundamentals of Structural Analysis

1.1	An Overview of Part I	1
1.2	Summary of Taylor's Series	2
1.3	Summary of Newton's Method for Finding Roots	2
1.4	The Binomial Series	3
1.5	The Chain Rule for Partial Differentiation	4
1	Stress in Structures	5
1.1	The Concept of Stress	5
1.2	The General Interior Equilibrium Equations	12
1.3	Equilibrium at the Outer or Inner Boundary	19
1.4	Plane Stress	23
1.5	Summary	27
	Chapter 1 Exercises	29
2	Stresses and Coordinate Axis Rotations	38
2.1	Introduction	38
2.2	Stress Values in Other Cartesian Coordinate Systems	38
2.3	The Determination of Maximum Stress Values	43
2.4	Mohr's Circle	47
2.5	A Three-Dimensional View of Plane Stress	52
2.6	**Principal Stresses in the General Three-Dimensional Case**	53
2.7	Summary	59
2.8	Octahedral (von Mises) Shearing Stresses	59
2.9	**The Mathematical Description of Stresses**	62
	Chapter 2 Exercises	63
	Endnote (1) Solution for the Planes of Principal Stress	67
3	Displacements and Strains	68
3.1	Introduction	68
3.2	Displacements	68
3.3	Longitudinal Strains	69
3.4	Shearing Strains	77
3.5	Other Strain Definitions	79
3.6	The Strain-Displacement Equations	80

3.7	The Compatibility Equations	81
3.8	Plane Strain	85
3.9	Summary	86
	Chapter 3 Exercises	87
	Endnote (1) The Derivation of the Strain–Displacement Equations for Cylindrical Coordinates	89
	Endnote (2) A Third Derivation of the Compatibility Equations	90
4	Strains in Rotated Coordinate Systems	95
4.1	Introduction	95
4.2	Strains in Other Cartesian Coordinate Systems	95
4.3	Strain Gauges	98
4.4	The Mathematical Properties of Strains	102
4.5	Summary	102
	Chapter 4 Exercises	105
5	The Mechanical Behavior of Engineering Materials	109
5.1	Introduction	109
5.2	The Tensile Test	116
5.3	Compression and Shear Tests	124
5.4	Safety Factors	125
5.5	Factors Other than Stress That Affect Material Behavior	127
5.6	**Biaxial and Triaxial Loadings**	136
5.7	Simplifications of Material Behavior	138
	Chapter 5 Exercises	140
	Endnote (1) Residual Stress Example Problem	143
	Endnote (2) Crack Growth Example	144
6	Linearly Elastic Materials	146
6.1	Introduction	146
6.2	Orthotropic Materials	148
6.3	Isotropic and Other Linearly Elastic Materials	153
6.4	The Plane Stress Constitutive Equations	157
6.5	**Applications to Fiber Composites**	157
6.6	Summary	159
	Chapter 6 Exercises	160
	Endnote (1) Negative Poisson Ratios	163
Part II **Introduction to the Theory of Elasticity**		
II.1	Introduction	165
7	The Theory of Elasticity	167
7.1	Introduction	167
7.2	A Theory of Elasticity Solution Using Stresses	168
7.3	A Theory of Elasticity Solution Using Displacements	173
7.4	Reprise	177
7.5	Summary	181
	Chapter 7 Exercises	181
	Endnote (1) General Problem Formulations	187

Endnote (2) Another Solution to the Disk Displacement Equation	190
Endnote (3) Example 7.1 Compatibility Equation	190
8 Plane Stress Theory of Elasticity Solutions	192
8.1 Introduction	192
8.2 Solution Examples	192
8.3 St. Venant's Principle	198
8.4 **Review Problem**	199
8.5 Summary	202
8.6 **The Airy Stress Function**	202
Chapter 8 Exercises	204
Endnote (1) An Example of Calculating Displacements from a Stress Solution	209
Parts I and II Review Questions	211
Part III Engineering Theory for Straight, Long Beams	
III.1 Aircraft and Other Vehicular Structures	219
III.2 The Method of Undetermined Coefficients	221
III.3 Linear Independence	223
III.4 The Mean Value Theorem	224
9 Bending and Extensional Stresses in Beams	225
9.1 Introduction	225
9.2 An Elaboration on the Scope of Strength of Materials	226
9.3 Stress Resultants	227
9.4 The Approximate Pattern for Beam Displacements	230
9.5 The Accuracy of the Beam Stress Equation	238
9.6 Calculation of the Area Properties of the Nonhomogeneous Cross-Section	241
9.7 Calculation of Equivalent Thermal Loads	249
9.8 Principal Axes for the Beam Cross-Section	252
9.9 Summary	254
Chapter 9 Exercises	259
Endnote (1) The Predominance of the Normal Axial Stress	268
Endnote (2) Schwartz's Inequality	270
10 Beam Bending and Extensional Deflections	271
10.1 Introduction	271
10.2 The Small Deflection Beam Equilibrium Equations	272
10.3 Nonlinear Beam Equilibrium Equations	274
10.4 Boundary Conditions and the Boundary Value Problem	282
10.5 Uncoupled Forms of the GDEs and the BCs	285
10.6 Solutions for Beam Deflection Problems	286
10.7 Summary	296
Chapter 10 Exercises	300
Endnote (1) Different BCs in Different Planes at the Same Beam End	305
Endnote (2) The Nonlinear Form of the Axial Deflection Equation	306

Endnote (3) The Presence of the Moment per Unit Length Terms in the Shear Force Boundary Condition Expressions	307
Endnote (4) Exact Integrations for a Nonuniform Beam	307
11 Additional Beam Bending Topics	310
11.1 Introduction	310
11.2 The Concept of Elastic Boundary Conditions	310
11.3 Elastic Support Boundary Conditions	312
11.4 Concentrated and Partial Span Loads	316
11.5 Partial Span and Concentrated Load Example Problems	320
11.6 Introduction to Beam Buckling	329
11.7 **Additional Comments on Beam Buckling**	334
11.8 Summary	336
Chapter 11 Exercises	346
Endnote (1) The Bending Slope Sign Convention	359
Endnote (2) Combined Beam Axial and Lateral Loadings	359
Endnote (3) Heaviside Step Function Additional Comments	363
Endnote (4) Combined Bending and Torsional Loadings	364
Endnote (5) Beams Continuous over Several Supports	366
12 Uniform Torsion of Beams	368
12.1 Introduction	368
12.2 The Stress Formulation for Uniform Torsion	369
12.3 Further Properties of the Prandtl Stress Function	376
12.4 The Membrane Analogy	378
12.5 Closed Form Beam Torsion Analytical Solutions	382
12.6 Open Form Uniform Beam Torsion Solutions	387
12.7 Summary	391
Chapter 12 Exercises	396
Endnote (1) A Comment on the Solution for a Circular Shaft with a Keyway	400
Endnote (2) Orthogonality	400
Endnote (3) A Separation of Variables Approach to Example 12.1	401
13 Beam Torsion Approximate Solutions	403
13.1 Introduction	403
13.2 Open Cross-Section Beam Torsion	404
13.3 Closed Section Beam Torsion	410
13.4 Accuracy of the Uniform Torsion Theory	420
13.5 Beams Subjected to a Variable Torque	421
13.6 Summary	424
Chapter 13 Exercises	426
Endnote (1) Torsion Constants for Rolled and Extruded Beams	430
Endnote (2) Warping Constraint Due to Varying Torque	433
Beam Bending and Torsion Review Questions	434
14 Beam Shearing Stresses Due to Shearing Forces	444
14.1 Introduction	444
14.2 Thin-Walled Open Cross-Sections	444
14.3 Thin-Walled Open Cross-Section Example Problems	448

14.4	The Open Section Shear Center	457
14.5	Shear Flows in Thin-Walled Closed Cross-Sections	459
14.6	Summary	464
	Chapter 14 Exercises	469
	Endnote (1) The Shear Center as the Center of Twist	473
Part IV Work and Energy Principles		
IV.1	Preface	475
IV.2	The Green–Gauss Theorem	475
15	Work and Potential Energy Principles	479
15.1	Introduction	479
15.2	Work and Potential Energy	481
15.3	Virtual Work and Virtual Potential Energy	483
15.4	The Variational Operator	486
15.5	The Principle of Virtual Work	490
15.6	Internal Virtual Work	495
15.7	Complementary Virtual Work	497
15.8	**Energy and Other Principles**	502
15.9	**Modifications for Temperature Changes**	504
15.10	Summary	506
	Chapter 15 Exercises	507
	Endnote (1) Further Explanation of the Variational Operator	510
	Endnote (2) Proof That the Principle of Virtual Work Is a Sufficient Condition for Equilibrium	514
	Endnote (3) Proof of the Pairing of BCs for the Beam Fourth Order Bending Equations and the Second Order Extension Equations	516
	Endnote (4) Derivation of the Uniform Torsion Beam Equations Using the Principle of Complementary Virtual Work	518
Part V Energy-Based Numerical Solutions		
V.1	Preface	521
16	**Precursor Numerical Analyses**	523
16.1	Introduction	523
16.2	Numerical Methods of Note	523
16.3	Summary	540
	Chapter 16 Exercises	542
17	Introduction to the Finite Element Method	545
17.1	Introduction	545
17.2	Generalized Coordinates	546
17.3	The Beam Bending Finite Element	551
17.4	The Bar and Spring Element Stiffness Matrix Equations	556
17.5	Assembling the System Matrix Equation	558
17.6	Solving the System Matrix Equation	565
17.7	Example Beam Frame and Grid Problems	567
17.8	More Extensive Example Problems	574
17.9	Summary	581

Chapter 17 Exercises	592
Endnote (1) Distributed Coordinates	598
Endnote (2) Accuracy of the Concentrated Load Approximation	599
Endnote (3) The Reason for the Name “Generalized Coordinates”	600
18 Finite Element Truss Problems	602
18.1 Introduction	602
18.2 The Rotated Bar Element	602
18.3 Equivalent Thermal Loads	607
18.4 Other Initial Strains	610
18.5 Enforced Deflections	611
18.6 Summary	612
Chapter 18 Exercises	617
Endnote (1) Substructuring in Static Analyses	620
19 Basic Aspects of Multidimensional Finite Elements	623
19.1 Introduction	623
19.2 A Rectangular Plane Stress Finite Element	623
19.3 A Triangular Plane Stress Element in Brief	635
19.4 Three-Dimensional Finite Elements	636
19.5 Refined Finite Elements of Simple Shapes	637
19.6 **The Finite Element Method with Time-Varying Loads**	642
19.7 Summary	649
Chapter 19 Exercises	650
Endnote (1) An Explanation for Rigid Body Motion-Induced False Strains	653
Endnote (2) Reducing the Number of DOF in a Dynamic Analysis	653
20 The Unit Load Method for Determinate Structures	655
20.1 Introduction	655
20.2 External Complementary Virtual Work in the Unit Load Method	656
20.3 Internal CVW for Beam Bending and Extension	658
20.4 Internal Complementary Virtual Work for Beam Torsion	667
20.5 **Internal CVW for Beam Shearing**	669
20.6 Additional Illustrative Examples	670
20.7 **Examples of Using the ULM for Design Purposes**	677
20.8 **General Deflection Solutions**	682
20.9 **Large Radius Curved Beams**	683
20.10 Summary	688
20.11 Maxwell’s Reciprocity Theorem	689
Chapter 20 Exercises	693
Endnote (1) ULM Limitations	698
Endnote (2) Internal Complementary Virtual Work	699
21 The Unit Load Method for Indeterminate Structures	700
21.1 Introduction	700
21.2 Identifying Redundant Forces and Moments	700
21.3 The Coiled Spring Structural Elements	704
21.4 The Strategy of Releases and Reattachments	707
21.5 Example Problems	711

21.6	**Further Example Problems**	724
21.7	Summary	729
	Chapter 21 Exercises	737
	Parts IV and V Review Questions	747
Part VI Thin Plate Theory and Structural Stability		
	VI.1 Introduction	757
22	Thin Plate Theory	759
22.1	Introduction	759
22.2	The Plate Midplane	760
22.3	The Plate Stress Resultants	761
22.4	The Approximate Pattern for Plate Displacements	763
22.5	The Small Deflection Thin Plate Bending Equation	766
22.6	Thin Plate Boundary Conditions	770
22.7	**Classical Small Deflection Plate Bending Solutions**	773
22.8	**Plate Buckling and Its Uses**	777
22.9	A Simple Plate Bending Finite Element	781
22.10	Summary	788
	Chapter 22 Exercises	788
	Endnote (1) The Second Finite Deflection Plate Equation	791
23	Elastic and Aeroelastic Instabilities	792
23.1	Introduction	792
23.2	An Energy Formulation of the Beam Buckling Problem	792
23.3	A Beam Buckling Finite Element	795
23.4	Further Aspects of the Energy Formulation	800
23.5	Types of Fluid–Structure Interaction Instabilities	806
23.6	Airfoil Divergence	808
23.7	Airfoil Flutter	814
23.8	Matrix Iteration for Symmetric Matrices	820
	Chapter 23 Exercises	829
	Endnote (1) Resonance	831
	Endnote (2) Diagonalization and Functions of Matrices	833
	<i>Appendix A: Additional Topics</i>	839
A.1	Integration of the Strains to Obtain Displacements	839
A.2	Proof of the Symmetry of the Compliance Matrix	841
A.3	Uniform Torsion Stress Resultants for Multiply Connected Cross-Sections	846
A.4	The Uniform Torsion GDE for Multiply Connected Cross-Sections	848
A.5	Calculation of the Twist per Unit Length of a Single Cell of an N -Cell Cross-Section	850
	<i>Appendix B: Selected Answers to Exercises</i>	851
	<i>References</i>	925
	<i>Index</i>	929

Introduction to the Second Edition

In an attempt to improve the first edition, more topics, figures, examples, and exercises have been added. The author hopes all the old errors have been removed and few new errors have been introduced. The primary change has been a greater emphasis on preparing the student for a broad understanding of the finite element method of analysis. In the author's experience, various finite element method software packages are almost, if not totally, the only means of structural analysis used today in the aerospace industry and in the associated federal and state government agencies. The three chapters dealing with the finite element method of analysis, Chapters 16, 17, and 18, are hopefully just the right amount of exposure suitable for undergraduates.

The style of presentation has remained the same. Clarity rather than brevity has been the consistent goal. Hence, there is a purposeful use of extra words and sentences in order to try to assist the reader who is new to the material. This strategy of being wordy admittedly makes this textbook less useful as a reference for the instructor who already is quite familiar with the chosen material. Perhaps this wordiness will allow that instructor the luxury of being brief in his or her lectures, knowing that this textbook is available as a backup to those lectures.

The author would appreciate any suggestions or corrections. He can be reached at bkdonaldson@verizon.net.

B. D.

Introduction to the First Edition

This text has a single purpose. That purpose is to provide clear instruction in the fundamental concepts of the theory of structural analysis as applied to vehicular structures such as aircraft, automobiles, ships, and spacecraft. To this end, the text offers explanations and applications of the fundamental concepts of structural analysis and indications of how those concepts are employed in everyday engineering practice. The text endeavors to foster in the reader the habit of asking questions until the reader is thoroughly clear on all important details within the scope of this text.

Three strategies are followed to achieve clarity with regard to the basic concepts of structural analysis. The first strategy is to be thoroughly logical within the scope of the presented material. No “assumptions” with regard to method of analysis are made anywhere in this textbook. All approximations are accompanied by a full explanation of their validity. The second strategy is to be repetitious and redundant. Repetition is an important learning tool, and redundancy dispels misunderstandings. The third strategy to obtain the goal of clarity is to limit the number of topics covered in detail in this text to only those that are essential to an introduction to modern structural analysis.

This text is meant to serve as a basis for, or a supplement to, a series of introductory courses for undergraduates. It may be necessary to justify beginning a course of undergraduate study with the mathematics-encumbered elements of the theory of elasticity. If so, note that for an engineer to properly use any method of structural engineering analysis, that engineer must understand both the breadth and the limitations of that method of analysis. Such knowledge is invariably based, at least in large part, upon a derivation of the method in question. A background in the elements of the theory of elasticity is essential to interpreting the choices made in a structural analysis derivation with respect to the applicability of the result. The challenge posed to undergraduates by the theory of elasticity is further justified by the fact that the need to achieve vehicular structural components that are as lightweight and as easy to manufacture as possible requires an accuracy of analysis that is only possible with sophisticated, modern methods of analysis. The theory of elasticity is the one basis of that sophistication.

The educational price to be paid for the more encompassing view of structural mechanics made possible by means of an introduction to the theory of elasticity and a more rigorous introduction to work and energy methods is the loss of time for repetition of structural analysis solution techniques. This loss of repetition quite often means that students quickly forget what structural mechanics theory and solution techniques they quickly learned in their undergraduate courses. This fact, and the additional, more advanced material scattered throughout the text, make this text also suitable as a basis for, or supplement to, first-year graduate courses.

The organization of the text is largely conventional. Part I provides an introduction to structural mechanics and a single, logical basis for proceeding through the remaining parts of the text. Part II combines the separate topics of Part I to offer a brief introduction to the theory of elasticity at as close to an elementary level as possible. Part III develops the strength of materials approach to elementary straight-beam theory. Part IV introduces

work and energy principles, and Part V offers the unit load and finite element methods of analysis as two distinct types of work or energy methods. The development of the finite element method is limited to only that material which is suitable as an introduction to the topic. Part III and Parts IV plus V can be studied sequentially or concurrently, or their order can be interchanged if the reader/student has some knowledge of beam theory such as that normally obtained from a prior course in strength of materials. A full undergraduate use of Parts I and II together, and Part III, requires something more than one semester each, while Parts IV plus V, through Chapter 21, requires about one semester. Time pressure to meet this undergraduate semester schedule requires omitting some parts of this textbook and very quick treatment of the more advanced chapters that are heavy with theory, such as Chapter 15. Undergraduates, like the rest of us, often only develop an interest in the details of a theory after enjoying its applications. If this textbook is used to instruct junior-year students, then the teaching schedule may omit more topics (even most of some chapters such as Chapters 7 and 8) than would be proper for more advanced students. The purpose of Part VI is to make the textbook more useful for those curriculums that include (i) some plate theory or aeroelasticity and (ii) a more in-depth look at elastic stability than is incorporated in the last of the three beam bending chapters. Most advanced topics of interest to graduate students are located in sections that are identified by a double asterisk, or relegated to endnotes and the more difficult exercises, and Appendix A.

In order to use this text effectively, the reader is expected to have the knowledge base that is usually obtained by completing (i) three semesters of college-level analytical geometry and the calculus, one semester of linear algebra, and an additional course in ordinary differential equations; and (ii) courses of study concerning engineering statics and dynamics. The required mathematics cited above is often a stumbling block for students. It is good for all students to realize that this body of mathematics is the tool that makes modern structural engineering methods both possible and comprehensible. In other words, understanding mathematics makes engineering easy. This text uses only the above-cited body of mathematics to formulate the engineering concepts presented herein. Occasionally a more elegant mathematical tool will be mentioned but not used. The mention of a more elegant mathematical tool is made only in order to prepare the reader for future professional growth. When a mathematical tool at the edge of the reader's assumed knowledge base is used, a brief review of that technique is provided in the preface to the part of the textbook in which its use is first encountered. While highly desirable as further practice in summing forces and moments for structural bodies, a prior course in strength of materials is not strictly necessary. However, the absence of sufficient prior drill in summing forces and moments means that that drill would have to be inserted into this study program.

Reference numbers are enclosed within brackets, and endnotes are enclosed within parentheses. The matrix and determinant symbols used are

- [] is a square or rectangular matrix
- { } is a column matrix, often called a vector
- [] is a row matrix, also sometimes called a vector
- | | is a determinant
- []^t is the transpose of the original matrix
- []⁻¹ is the inverse of the original matrix

A ■ is used to indicate the end of an example problem.

Finally, since this text is almost exclusively devoted to explaining the methods needed for the analysis of the structural portion of whatever system is under study, it is appropriate

to mention briefly the other activities that are also essential parts of the process of creating a land, marine, or flight vehicle. Analysis is but one part of the continuous product production chain – marketing to design to analysis to manufacturing to testing, and back to marketing. The above activities are somewhat ordered in time as stated. However, for any complex product, each activity is linked with every other activity with considerable overlap. In particular, the people responsible for the design and analysis activities work interactively in order to achieve better products. Expert analysis is an essential part of any vehicular design today.

List of Repeated Engineering Symbols

a	The vector of acceleration
<i>a, b, c</i>	Lengths; with subscripts, series coefficients
<i>a</i>	Distance aft from midchord to the elastic axis as a fraction of the semi-chord length, <i>b</i>
<i>a</i>	An arbitrary parameter
<i>b</i>	Width (Parts II–VI) or depth (Part I) of a rectangular beam cross-section; <i>y</i> axis intercept of a straight line; semichord length, $\frac{1}{2}c$
<i>c</i>	Airfoil chord length, $2b$
<i>c_{mn}</i>	Double Fourier series coefficients used in the solution for the twisting of a uniform beam with a rectangular cross-section
<i>c_{nx}, c_{ny}, c_{nz}</i>	The three direction cosines for the normal to a plane; that is, the respective cosines of the angles between the normal direction and the Cartesian coordinate axes; entirely equivalent to lower-case <i>v</i> with single coordinate subscripts
<i>c_{xz}</i>	Typical coordinate rotation direction cosine, which, in this case, is the cosine of the angle between the (rotated) <i>x*</i> Cartesian coordinate axis and the (original) <i>z</i> Cartesian coordinate axis. The first subscript always indicates the rotated coordinate system axis, while the second subscript always indicates the original coordinate system axis. See the next entry.
[<i>c</i>]	Three by three matrix of direction cosines of a rotated coordinate system arranged so that the first element subscript indicates the row number and the second element subscript indicates the column number
<i>d₀, D₀</i>	A rectilinear deflection of a structural support causing the structure to deform
<i>e</i>	A distance from some reference point; that is, an eccentricity; chord length distances, dimensional or nondimensional
<i>e_y, e_z</i>	Rectilinear distances to the beam cross-section shear center from an arbitrarily chosen moment center; these distances respectively parallel the <i>y</i> and <i>z</i> coordinate axes, and they are without a sign convention
<i>f</i>	Vibratory frequencies in units of cycles per second = Hz
<i>f, f</i>	Arbitrary function
<i>f₀</i>	A magnitude associated with an applied force per unit length of beam axis, or an applied force per unit area in the case of a plate analysis
<i>f_x, f_y, f_z</i>	Externally applied force components per unit length applied along the beam centroidal axis in the respective coordinate directions of the subscripts, or similar forces per unit area applied at a plate midplane
<i>f_{ij}</i>	The <i>i, j</i> flexibility coefficient; sometimes called the <i>i, j</i> flexibility influence coefficient
[<i>f</i>]	Flexibility influence coefficient matrix; that is, the array of <i>f_{ij}</i>
<i>g</i>	Acceleration of gravity; damping factor; arbitrary function

h	Depth of rectangular beam cross-section; plate thickness
$h(t)$	Downward deflection of an airfoil
$[h]$	Elastic stability matrix defined in Chapter 23, which has as a factor the unknown value of the compressive load that causes buckling
i	Square root of -1
i, j, k	Integer indices
k	Spring constant/factor [units of force over length]; plate buckling coefficient defined in Example 22.4
k_{ij}	The i, j element of a stiffness coefficient matrix. It represents the value of the i th generalized external force required by a unit value of the j th generalized deflection (i.e., generalized coordinate) when all other generalized deflections are zero
$[k]$	Element stiffness coefficient matrix whose square size depends upon the number of generalized coordinates required, perhaps approximately, to uniquely specify the structural element deflections
$[\tilde{k}]$	Element stiffness matrix reduced in size by the application of the global or system boundary conditions to the element degrees of freedom
l	Length of beam finite element, usually a fraction of the total beam length; beam length
m	A discrete mass; slope of a straight line
m_y, m_z	Applied beam moments per unit length
m, n	Integers or integer indices, sometimes maximum values for the indices i, j, k
n, s	Respective normal and tangential orthogonal coordinates at any point along a line on a flat surface. When the curve is a closed curve, s is positive counterclockwise, and n is positive in the outer normal direction
p	Pressure on the surface of a structural body
q	Shear flow; that is, the product of (i) the shearing stress on the surface of the beam cross-section in the direction of the centerline of the thin skin and (ii) the thickness of the thin skin
q	Fluid dynamic pressure equal to one-half the fluid mass density multiplied by the fluid velocity squared
q_i	The i th generalized coordinate
$\{q\}$	Column matrix of generalized coordinates; specifically, without modification, the element degrees of freedom of a finite element; with a $\hat{\quad}$, the structural system degrees of freedom; with a $\tilde{\quad}$, the DOF vector reduced by use of the system boundary conditions (later the tildes are dropped from use)
r	Radial coordinate of a cylindrical or spherical coordinate system, or a moment arm for shear flows and shearing stresses about an arbitrary moment center
\mathbf{r}	Position vector from the coordinate origin to the geometric point under consideration
$[r(\theta)]$	A coordinate rotation matrix for strains; see Eq. (6.15)
s	Arc length coordinate, usually with an arbitrary origin; also see statement regarding n, s
$\text{stp}(x - x_0)$	Heaviside (unit) step function; see Section 11.4
t	Thickness; the addition of an asterisk indicates a modulus weighted thickness, $(G/G_0)t$, in the case of beam torsion

t, t_0	Time, as a variable and as a parameter
u, v, w	Orthogonal displacement components of a material point within or on the surface of a structural body, hence a function of all three spatial coordinates, and perhaps time also
u, v, w	Deflections of points along the beam axis, hence a function only of x and perhaps time also; similarly for a plate midplane, as functions of x, y and perhaps t
$\bar{u}, \bar{v}, \bar{w}$	Known orthogonal components of displacements on the surface of a structural body; that is, displacement boundary conditions
u_i, v_i, w_i	Finite element DOF; modified with $\hat{\quad}$, structural system DOF; modified with $\tilde{\quad}$, structural system degrees of freedom retained after application of system boundary conditions
x, y, z	Cartesian coordinates that locate material points before or after deformation
y, z	Coordinates of a beam cross-section originating at the centroid
y_0, z_0	Coordinates for a beam cross-section with an arbitrarily selected origin
A	Cross-sectional area of a beam
\hat{A}	Area enclosed within the centerline of a thin, closed beam cross-section
A_x, A_y, A_z	Areas perpendicular to the x, y, z axes, respectively
$\{A\}$	$[E]\{\alpha\}$, a vector associated with thermal strains and the resulting stresses
$\{A\}$	One of several aerodynamic matrices in Chapter 23
$[A], [B]$	Arbitrary square matrices
A_i, B_i, C_i, D_i	Constants of integration
A, B	Arbitrary vectors
ALS	Abbreviation for "actual load system"; the system of externally applied loads and the corresponding internal stress resultants induced by the applied loads as used by the unit load method for calculating unknown or known deflections
B	With coordinate subscripts, the body force per unit mass in the indicated coordinate direction
$[B]$	Coefficient matrix for finite element degrees of freedom in the expression for the intraelement strains
BC	Abbreviation for "boundary condition"
$[C]$	Damping coefficient matrix used to represent velocity-dependent forces
C_l	Lift coefficient; an empirical factor, which, when multiplied by the fluid dynamic pressure and a relevant area, yields the lift component of the total aerodynamic force [nondimensional]
$C_{l\alpha}$	Lift curve slope; that is, the slope of the straight-line portion of the curve on the plot of lift coefficient (C_l) versus angle of attack (α)
C_m	Aerodynamic moment coefficient; that is, an empirical factor, which, when multiplied by the fluid dynamic pressure, an appropriate area, and an appropriate moment arm, yields the moment acting upon an airfoil at the aerodynamic center
C	Centerline of symmetry
D	Diameter
D	Plate bending stiffness coefficient equal to $Eh^3/[12(1 - \nu^2)]$
D	The total displacement vector whose components are u, v , and w
DOF	Abbreviation for "degree(s) of freedom"

$\%D$	Percent fatigue damage as represented by the Palmgren–Miner rule of Eq. (5.2), with 100-percent damage indicating a 50-percent probability of fracture failure as a result of a disordered sequence of loading cycles
$[D]$	The dynamic matrix; see Eq. (23.18)
E	Young’s modulus, the modulus of elasticity; coordinate subscripts indicate the direction in which this material property is measured; the lack of a subscript indicates an isotropic material
E_0	Reference value for Young’s modulus, chosen arbitrarily in order to produce more natural units for quantities useful in beam bending analyses
$[E]$	The material stiffness matrix that, when postmultiplied by the strain vector, often provides the stress vector
F	Applied force, often with numerical subscripts
\mathbf{F}	A force vector
F, G, H	Arbitrary functions
FEM	Abbreviation for “finite element method”; see Chapter 17 and subsequent chapters
G	Shear modulus, the modulus of rigidity; double coordinate subscripts indicate that the shear modulus is referred to the material axes of an orthotropic material
G_0	Reference value for the shear modulus, akin to E_0
GDE	Abbreviation for “governing differential equation”
$[H]$	The assembled elastic stability matrix, see Example 23.1
I	An integral
\bar{I}	Moments or product of inertia about the sub-area centroid
I_x, I_y, I_z	Mass moments of inertia about the axis indicated by the subscript
I_{yy}, I_{zz}	Area moments of inertia for a beam cross-section about the y and z axes, respectively, see Eqs. (9.6)
I_{yz}	Area product of inertia for a beam cross-section, see Eqs. (9.6)
J	The St. Venant constant for uniform beam torsion, which is calculated on the basis of the classification of the type of beam cross-section; an asterisk indicates that J is modulus weighted
K	Torsional spring constant or factor; units of force length, with various subscripts; in-plane plate stiffness coefficient
K_t	Stress concentration factor; the t subscript indicates that the factor is theoretical
$[K], [\tilde{K}]$	Structural stiffness matrix assembled from element stiffness matrices, after the application of the global or system boundary conditions; the tilde is omitted in later equations when it is clear that the stiffness matrix is associated with only the unknown degrees of freedom
$[\hat{K}]$	Singular structural stiffness matrix assembled from the element stiffness matrices, before the application of the global boundary conditions
L	Beam length; or length, in general
\mathcal{L}	Lift force; that is, the component of the net aerodynamic force acting upon an airfoil or other solid body perpendicular to the direction of the motion of the body or the fluid stream. (The drag is the force component in the direction of the fluid stream.) For an airfoil, the lift force acts at the airfoil aerodynamic center.
M	Often with subscripts 0, 1, 2, . . . , bending or twisting moment applied to beam or other structures
\mathcal{M}	Aerodynamic moment at the airfoil aerodynamic center

$M_t(x)$	Internal beam twisting moment at the beam cross-section identified by the coordinate x
M_x, M_y	When functions of x, y : plate bending moments about the y, x axes, per unit length along the y, x axes, respectively; units of [force]
M_y, M_z	When functions of x only: internal beam bending moments about the y and z axes, respectively, at the beam cross-section identified by the coordinate x
$M_{xy}(x, y)$	Plate twisting moment about the x axis per unit length in the y coordinate direction; units of [force]
$M_{yx}(x, y)$	Plate twisting moment about the y axis per unit length in the x coordinate direction; units of [force]
$[M]$	Mass matrix in the system matrix equations of motion, which, when postmultiplied by the negative of the acceleration vector, produces the system inertia forces
N, N_0	Applied beam axial force, or, more generally, a force normal to a specified plane in space
$N(x)$	Internal beam axial force acting at the beam cross-sectional centroid, positive in tension
N_i	The number of fatigue cycles to failure for a single specified mean and alternating stress; or, when a function of one or more spatial coordinates, the deflection shape function associated with the i th structural element generalized coordinate
N_x, N_y	Internal or externally applied tensile or compressive forces that act in the indicated coordinate direction per unit length in the other coordinate direction and that lie within the midplane of a membrane or plate; units of [force/length]; or, more generally, a force acting on a plane in the coordinate subscript direction
N_{xy}, N_{yx}	Internal or externally applied shearing forces per unit length that lie within the midplane of a membrane or plate, and that follow the same sign convention as do shearing stresses; units of [force/length]
O, P, Q, R, S	Points in the volume of the structural body
P	Replacement symbol for $N(x)$ when the axial force in the beam is negative, that is, a compressive beam loading
Q_i	The i th generalized force, which is determined by use of the virtual work expression in conjunction with a variation of the i th generalized coordinate
$Q_y(s), Q_z(s)$	First moments of those portions of the beam cross-sectional area that lie behind the point s on the thin-beam centerline
Q_x, Q_y	Plate internal shear forces acting in the thickness direction, per unit length in the y, x directions, respectively; units of [force/length]
$\{Q\}$	Column matrix of generalized forces
R	A fixed radius; a force or moment reaction at a support
R	With two coordinate subscripts, ratios of inertia defined by Eqs. (10.6)
$[R(\theta)]$	A coordinate rotation matrix for stresses; see Eq. (6.14)
S	Beam-column slenderness ratio; an airfoil planform area
S_1, S_2	Surface areas for a structural body; subscript 1 indicates an area where forces/tractions, rather than deflections, are prescribed, and subscript 2 indicates the opposite
$[S]$	The material compliance matrix, which, when postmultiplied by the stress vector, produces the strain vector; see Eq. (6.1)

T	Either (i) kinetic energy; or (ii) a torque; or (iii), when modified by subscripts, and so on, a specified temperature change
T_x, T_y, T_z	Surface tractions (forces per unit area) acting upon the surface of the structural body in the x , y , and z directions, respectively
$\{T\}$	The vector of surface tractions
$[T]$	A rectangular transformation matrix between two sets of generalized coordinates
\mathcal{T}	A twisting moment of aerodynamic origin
U	Total strain energy of a structural body
U_0	Strain energy density; that is, the strain energy per unit volume
ULM	Abbreviation for the "unit load method"; see Chapters 20 and 21
ULS	Abbreviation for a "unit load system"; a system of self-equilibrated virtual forces and virtual moments used by the ULM to calculate known or unknown actual deflections
Vol.	Volume
V	Potential function for body forces per unit volume; see Eq. (8.10); with an upper bar, a similar potential function in plate theory
V	Potential energy of the externally applied loads that are the surface tractions and the body forces
V_y, V_z	Internal shear forces acting upon a beam cross-section in the indicated coordinate directions
V_x, V_y	Kirchhoff plate shearing forces that are important to plate boundary conditions. They are a combination of the ordinary plate shearing forces per unit length and derivatives of the twisting moment; see Fig. 22.3
W	Total work, that is, the work done by both the external and internal forces acting upon a structure
W_{ex}	Work done by the external forces acting upon a structure
W_{in}	Work done by the internal forces acting upon a structure
X, Y	x/a , y/b , respectively, nondimensional Cartesian coordinates used in certain finite element derivations
Y, Z	The principal centroidal coordinates of a beam cross-section (used only when a clear distinction is useful)
α	An angle, sometimes specifically the angular coordinate of the cylindrical coordinate system when θ has another meaning in the same analysis; an airfoil angle of attack; or a nondimensional factor
α	The coefficient of thermal expansion; coordinate subscripts indicate the material direction for which this material property is measured
$\{\alpha\}$	The 6×1 vector of the coefficients of thermal expansion for each of the three coordinate directions, plus three zeros; or the corresponding 3×1 plane stress vector
α, β	Factors, depending upon the aspect ratio of the rectangular beam cross-section, that arise from the calculation of the maximum shear stress and the St. Venant constant for uniform torsion, respectively
β	An angle, or a nondimensional or other parameter
γ	A nondimensional factor for the beam cross-sectional stiffness for shearing deformation γGA ; see Section 20.5
γ	An engineering shearing strain, usually with two different coordinate subscripts; that is, the change in the original right angle defined by the two subscripted coordinates as a result of structural deformation

$\{\gamma\}$	The 6×1 vector of the three longitudinal strains and the three engineering shearing strains; or, in the case of plane strain, the 3×1 vector whose elements are ϵ_{xx} , ϵ_{yy} , and γ_{xy}
$\delta(x - x_0)$	Dirac delta function; see p. 317
ϵ	A very small number
ϵ	Longitudinal strain = normal strain = direct strain; two identical subscripts indicate the coordinate direction of this normalized change in length; two dissimilar coordinate subscripts indicate a Green shearing strain; a single subscript a , b , c indicates the strain measured by a strain gauge; numerical subscripts indicate principal strains
$[\epsilon]$	Three by three symmetric matrix of the 6 Green strains
ζ, η	Varieties of Cartesian coordinates
θ	Beam twist per unit length
θ	The angular coordinate of a cylindrical or spherical coordinate system
θ	The angle of rotation of the rotated orthogonal coordinate system when the entire rotation is confined to a single plane (the z plane)
θ	With various letter subscripts, a rotation about the axis indicated by the subscript; with various numerical subscripts, a finite element rotational DOF
λ	An eigenvalue; in the principal stress equations, λ is any one of the three principal stresses; in the beam buckling case, λ is the square root of the product of the unknown compressive axial force and the inverse of EI
λ, μ	Lamé material constants; see Eqs. (6.5, 6.6)
μ	Nondimensional parameter
ν	Poisson's ratio, the negative of the ratio between the lateral strain and the longitudinal strain; two coordinate subscripts indicate that the Poisson's ratios are for the material axes of an orthotropic material (see Section 6.2)
$\{v\}$	The 3×1 vector of direction cosines of the normal vector to a plane; the components of the vector are indicated by either ν with a single coordinate subscript or by c with an n subscript followed by a coordinate subscript
ξ	A linear coordinate
ρ	Mass density, units of force-time squared/(length to the fourth power)
σ	Stress, usually with two orthogonal coordinate subscripts according to the convention set forth in Chapter 1; repeated coordinate subscripts indicate a normal stress, while different subscripts indicate a shearing stress; numerical subscripts indicate principal stresses
$[\sigma]$	Three by three symmetric matrix of the 6 stresses
$\{\sigma\}$	Six by one vector of the stresses in alphabetical order
ϕ	The angle of twist of a beam; spherical coordinate; or an angle in general
ϕ	With numerical subscripts, finite element rotational DOF
ψ	An arbitrary angle; with subscripts, a FEM rotational generalized coordinate
ω	With two nonidentical coordinate subscripts, the rigid body (i.e., the average) rotation about the coordinate axis not present among the two subscripts; see Eqs. (3.13)
Γ	Function defining the geometry of the boundary of the area or volume under consideration

Γ	Warping constant; see Endnote (2) of Chapter 13
ΔT	A temperature change, usually from room temperature
Π	Total potential energy; that is, the sum of $U + V$
Σ	Stress in an adjacent structural body
Υ	An unknown redundant force or moment in a unit load method analysis
$\Phi(x, y)$	Airy stress function; see Section 8.6
$[\Phi]$	The modal matrix; see Eq. (23.23)
$\Psi(y, z)$	Prandtl stress function for torsional shearing stresses; see Chapter 12
Ω	Angular velocity

Subscripts and Superscripts

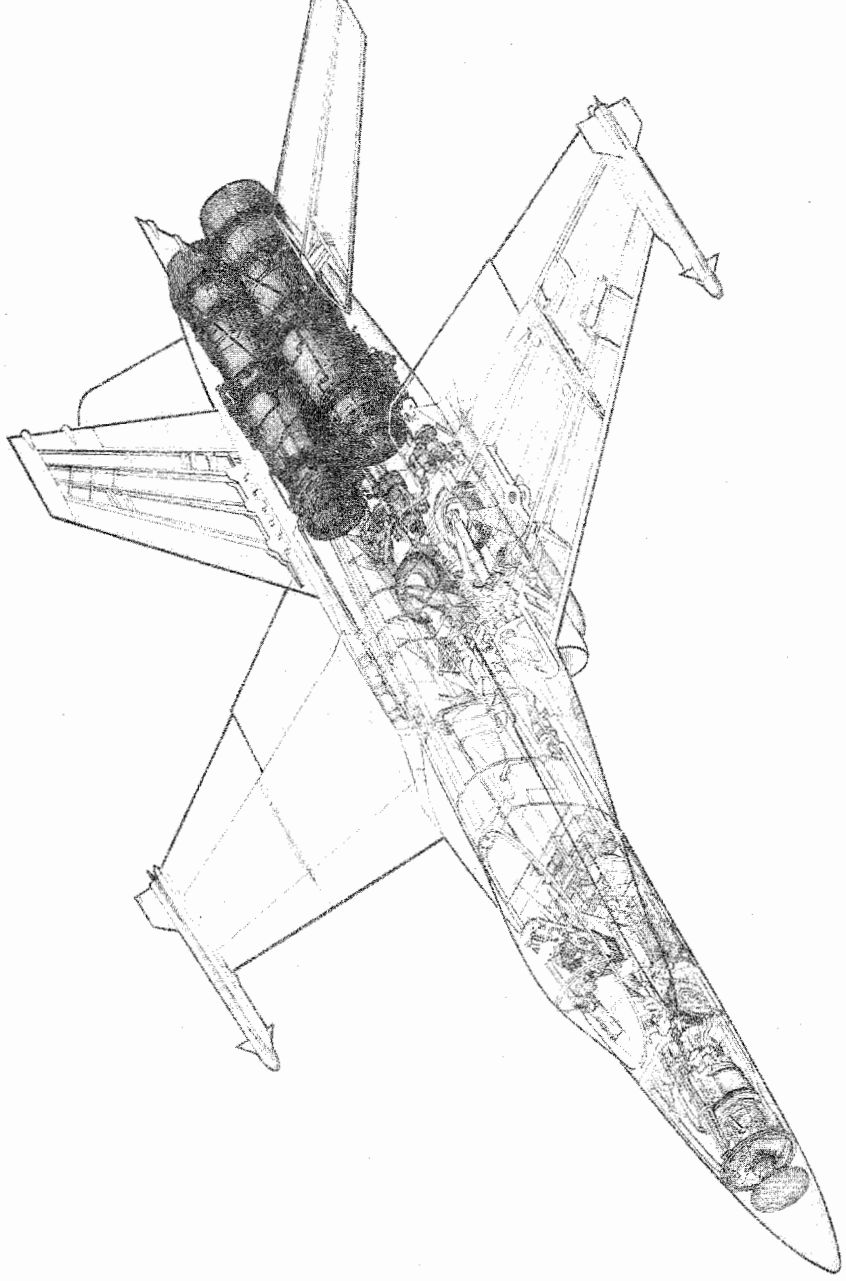
0	Generally indicates a fixed or constant value
c	As a subscript, indicates a complementary solution, that is, a solution for the homogeneous portion of a differential equation
c	As a superscript, indicates an applied force per unit length, a force, or moment that is a combination of a mechanical component and an equivalent thermal component
cr	Critical value for stability
f	Indicates that the quantity is associated with the flutter neutral point in the flight regime
p	Indicates a particular solution for a differential equation
D	Indicates that the quantity is associated with the divergence point in the flight regime
T	Indicates that the subscripted quantity is the result of a temperature change
,	As a subscript followed by a variable, indicates partial differentiation with respect to that variable
*	Distinguishes coordinates, unit vectors, deflections, stresses, or strains referred to a rotated coordinate system as opposed to those coordinates, unit vectors, deflections, stresses, or strains without such a superscript that refer to the unrotated (i.e., the original) coordinate system; and the same for matrices of material properties
*	When applied to beam area cross-sectional properties (including thickness when dealing with beam torsion), this superscript indicates that the effect of beam material nonhomogeneity has been accounted for, and an arbitrary material constant (either E_0 or G_0) has been selected
*	When applied to work or potential energy expressions, the complementary form of those quantities
1, 2, 3	Subscripts used to indicate principal directions for stresses and strains
—	An upper bar indicates that the modified internal stress resultant is associated with the virtual load system
—	An upper bar indicates an average value and, in particular, when applied to coordinate distances, the upper bar indicates a distance from a coordinate axis to an area or sub-area centroid

Acknowledgments

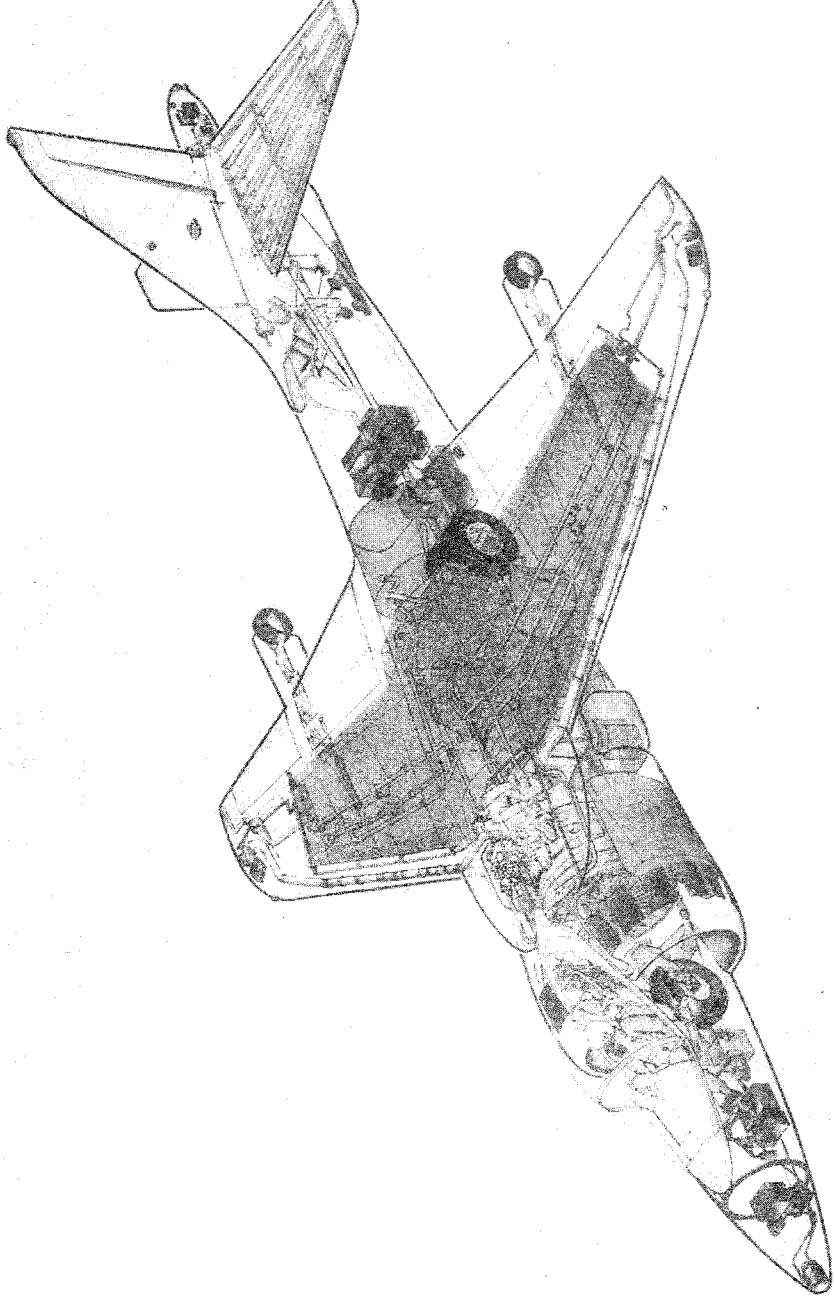
For this edition (as well as the first edition), the author sincerely thanks all of the teachers and students who have helped formulate the presentation of the material herein. It is necessary to note that two textbooks have particularly influenced the choice of material and its organization. The first of these textbooks was written by the author's colleague Robert M. Riveilo (Ref. [16]), and the second was written by Clive L. Dym and Irving H. Shames (Ref. [3]). This author is greatly indebted to them for their work. For this second edition, the author would like to thank those who labored to put this book into print, particularly Peter C. Gordon, Senior Editor, and Katie Greczylo, Project Manager.

The author would also like to thank the following reviewers for their comments and suggestions: John Dugundgi, Massachusetts Institute of Technology; David W. Jensen, Pennsylvania State University; Rakesh K. Kapania, Virginia Polytechnic Institute and State University; James A. Milke, University of Maryland; Walter D. Pilkey, University of Virginia; Brent Sherwood, Applied Physics Laboratory; Howard W. Smith, University of Kansas; Alfred G. Striz, University of Oklahoma; and Anthony M. Waas, University of Michigan. The author would be happy to receive further comments and corrections, large or small, on any aspect of this textbook.

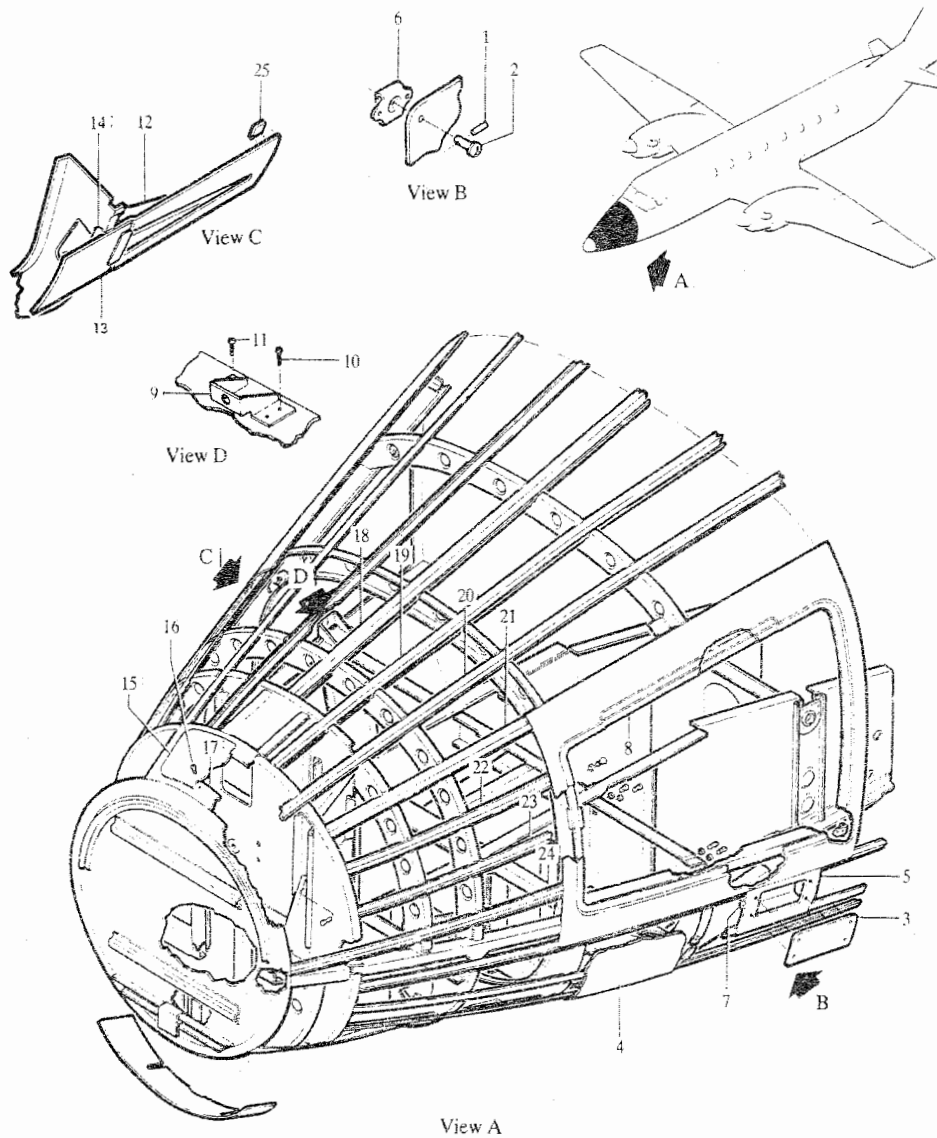
B. D.



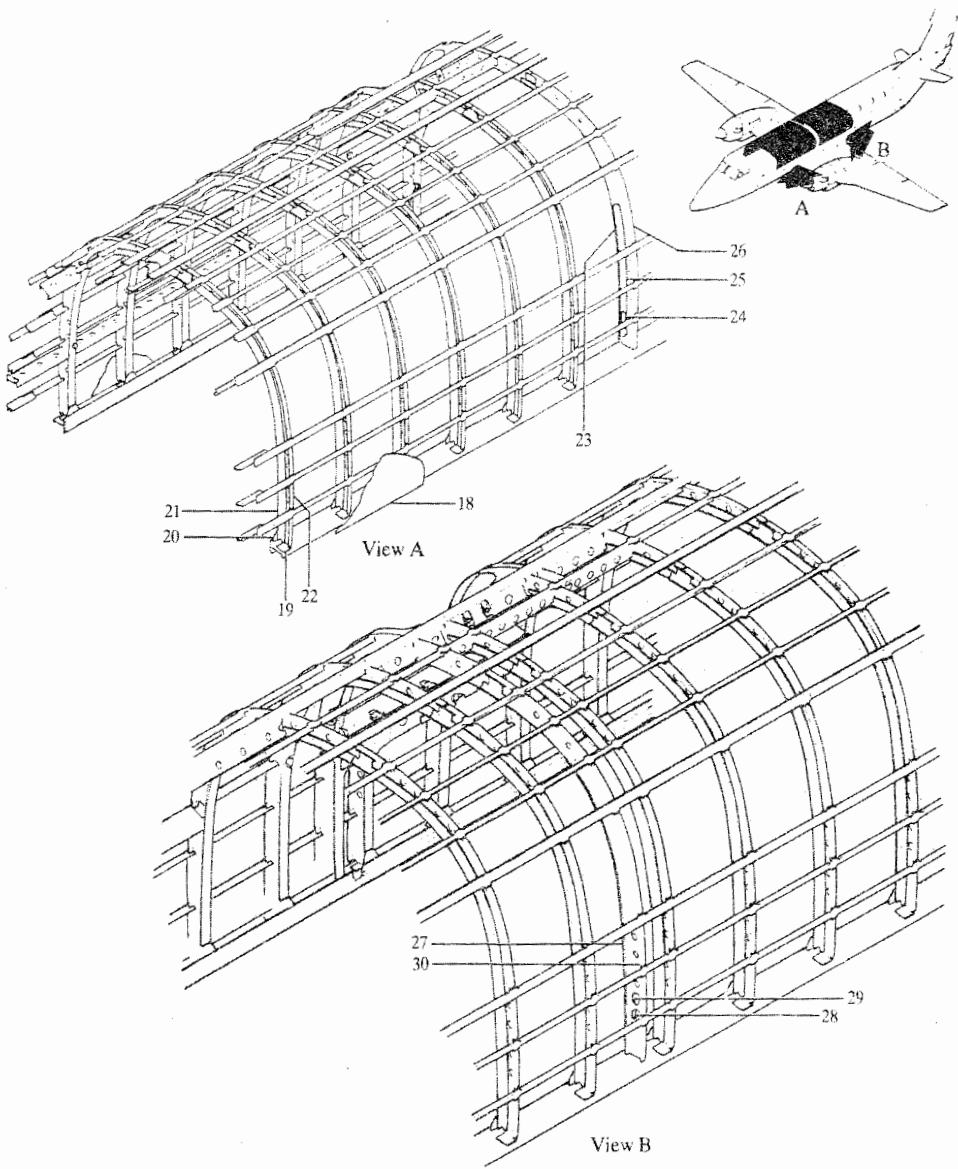
Partial structural details of an F/A-18 wing and vertical stabilizer. Courtesy of the McDonnell-Douglas Corp., St. Louis, Missouri.



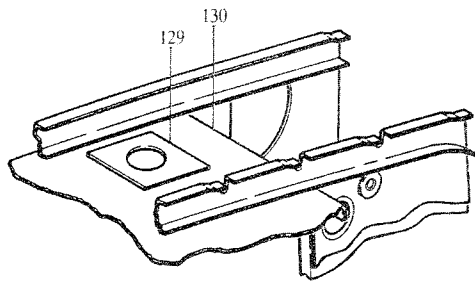
Partial structural details of the horizontal stabilizer of the AV-8B. Courtesy of the McDonnell-Douglas Corp., St. Louis, Missouri.



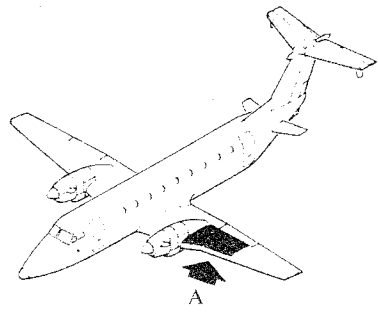
A structural component assembly drawing, with most of the outer skin removed. Courtesy of the Beech Aircraft Corporation, Wichita, Kansas.



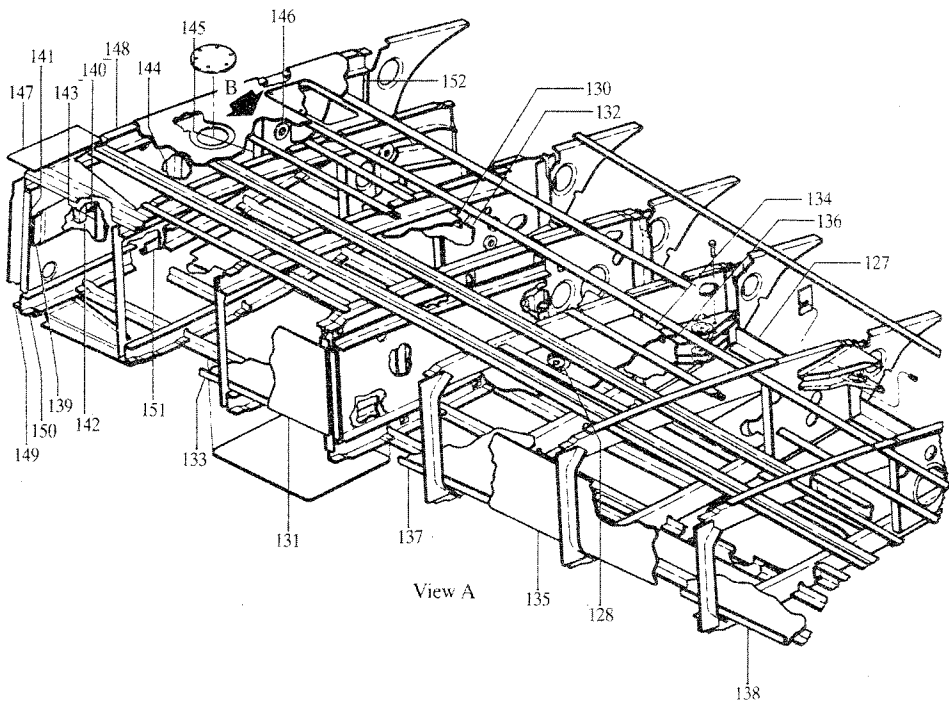
A structural component assembly drawing, with most of the outer skin removed. Courtesy of the Beech Aircraft Corporation, Wichita, Kansas.



View B

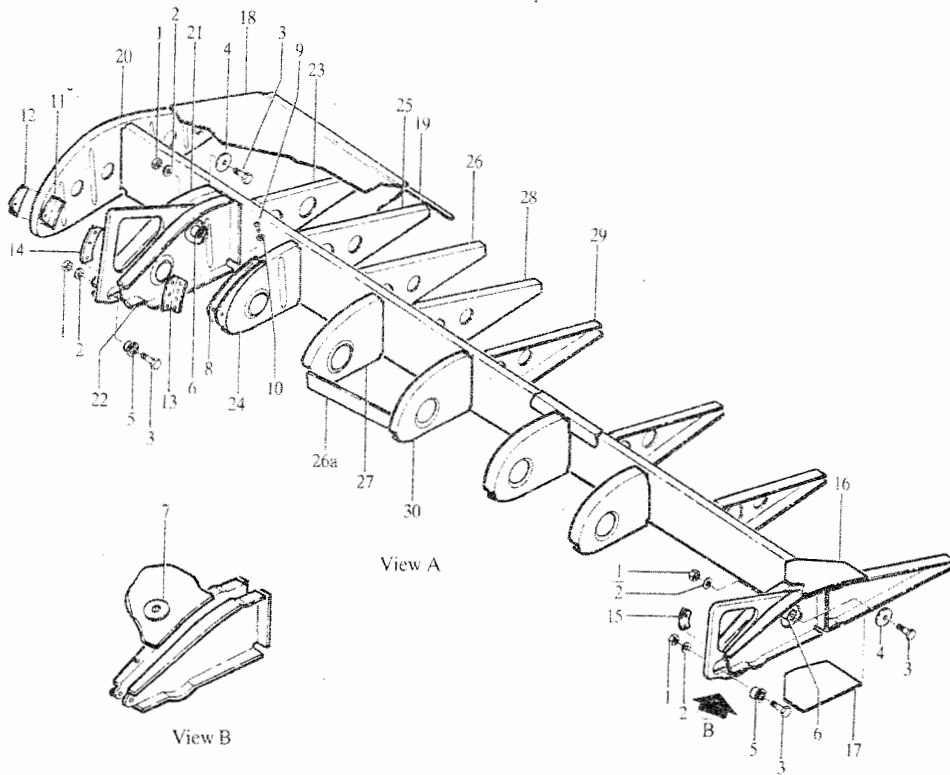


A

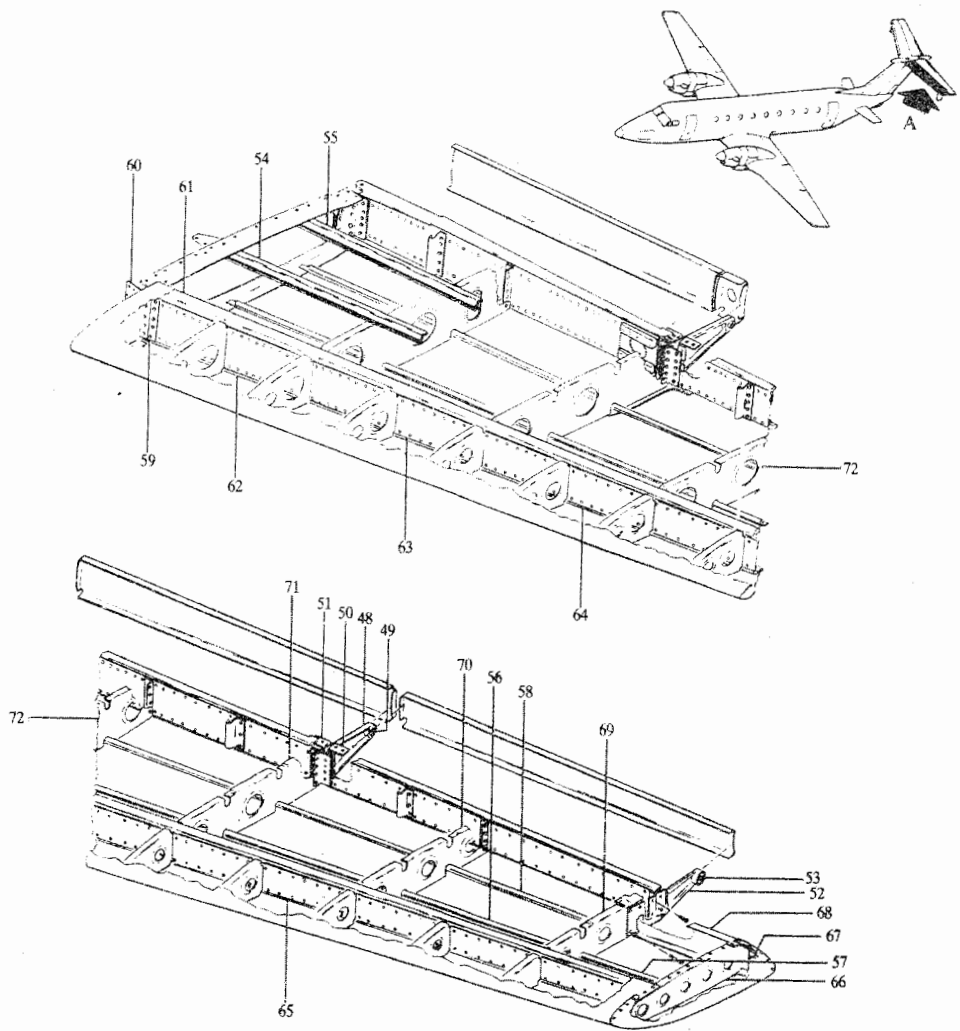


View A

A structural component assembly drawing, with most of the outer skin removed. Courtesy of the Beech Aircraft Corporation, Wichita, Kansas.

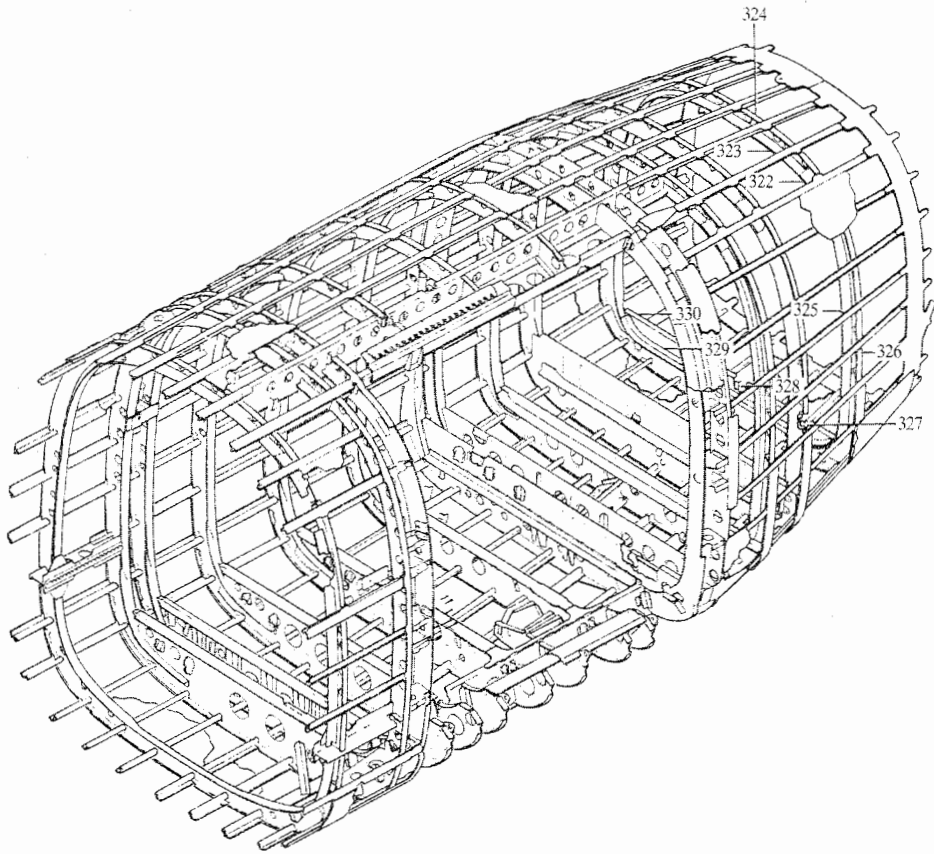


A structural component assembly drawing, with most of the outer skin removed. Courtesy of the Beech Aircraft Corporation, Wichita, Kansas.



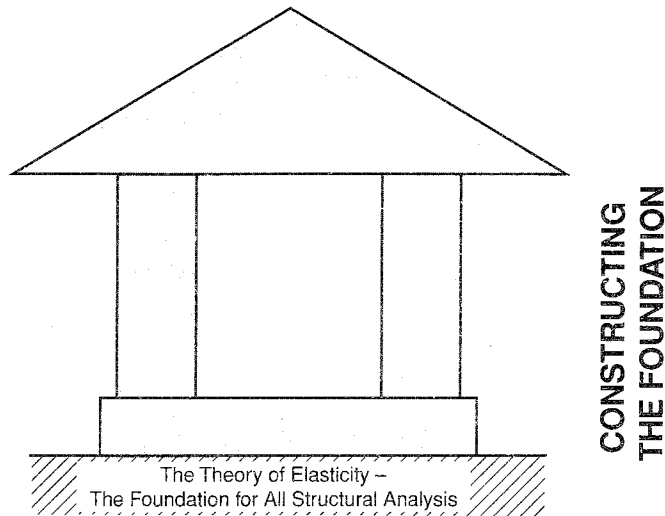
View A

A structural component assembly drawing, with most of the outer skin removed. Courtesy of the Beech Aircraft Corporation, Wichita, Kansas.



A structural component assembly drawing, with most of the outer skin removed. Courtesy of the Beech Aircraft Corporation, Wichita, Kansas.

THE FUNDAMENTALS OF STRUCTURAL ANALYSIS



I.1 An Overview of Part I

Vehicular weight, particularly that of aircraft and spacecraft, has a strong effect on the performance or economics of all such vehicles. Thus it is well worth spending many engineering man-hours on their design and analysis so as to make those vehicles as light-weight as possible. To make those many engineering hours of analysis as effective as possible, it is important that all the different types of loads that the vehicle will bear be well estimated, and then the structural response to those loads be carefully calculated. To carefully calculate the response of structures to estimated or measured loadings, it is important to use structural analysis techniques to which considerable confidence can be assigned. High degrees of confidence are achieved through experience and through thorough understanding of any approximations that are incorporated within the derivations of the selected structural analysis techniques. Thus it would seem that, in general, the fewer and the smaller the approximations, the more useful the structural analysis technique. This surmise is only partially true. As will be seen as the material of this textbook unfolds, the use of structural analysis techniques that contain essentially no approximations for many circumstances can be much too expensive and time consuming. Hence a compromise between cost and accuracy is necessary for good engineering practice. To understand how that compromise is found, this introduction to aerospace structures begins with the fundamentals of structural mechanics where the approximations are few in number and small in impact.

Part I of this textbook presents structural mechanics on a differential scale. That is, the focus of the analysis is typically on a volume of engineering material whose rectangular volume is $dx dy dz$. The enormous advantage of this approach is that the equations that are so established by this process apply to any type of component (beam, shell, solid) of any engineering structure simply because such a differential volume can be visualized as being part of the finite volume of that type of structural component. The frequent use of differential distances like dx should suggest that the calculus, a powerful analytic tool, figures prominently in Part I. The calculus is also vital to the remainder of the textbook because so much of that remainder is based upon the material of Part I. Not only is a knowledge of differential and integral calculus important, but certain other calculus-related aspects of mathematics should be well understood. The remaining four sections of this preface to Part I provide a review of those additional mathematical topics that are essential for a thorough understanding of the Part I material. Knowing the required mathematics makes the engineering much easier.

I.2 Summary of Taylor's Series

Let $f(x)$ be a function of single variable. The Taylor's series for $f(x)$ about $x = a$ may be written as

$$f(x) = f(a) + (x - a)f'(a) + \frac{1}{2!}(x - a)^2 f''(a) + \cdots + \frac{1}{n!}(x - a)^n f^{(n)}(a) + \cdots$$

when all the derivatives exist and are continuous in a closed interval containing $x = a$. This same series is written in a slightly different style at the end of this section. The question of exactly when a Taylor's series is valid is not a simple one. The use of Taylor's series to represent the exceptionally smooth functions that generally describe stresses, strains, displacements, and the derivatives of these quantities in continuous structures has never led to contradictions. Hence this series is used freely whenever discontinuities are not suspected. A function that has a Taylor's series expansion is called "analytic."

In two dimensions, at $x = a$ and $y = b$, Taylor's series, written in a slightly different style, is

$$F(a + h, b + k) = F(a, b) + \sum \frac{1}{n!} \left[h \frac{\partial}{\partial x} + k \frac{\partial}{\partial y} \right]^n F(x, y) \Big|_{x=a, y=b}$$

where the summation is from $n = 1$ to infinity. If the reader finds the style of presentation for the Taylor's series in two dimensions unfamiliar, it may help to note that, for example, the first series can be written in the style of the second series simply by substituting $(a + h)$ for the variable x . That is, where h is now the variable

$$f(a + h) = f(a) + hf'(a) + \frac{h^2}{2!} f''(a) + \cdots + \frac{h^n}{n!} f^{(n)}(a) + \cdots$$

I.3 Summary of Newton's Method for Finding Roots

There are numerous approximate methods for finding the roots of polynomial equations, many of which are not limited to real roots. Newton's method is a simple matter when limited to real roots, and this method is not limited to polynomial equations. Newton's method is an iterative procedure, which means the same procedure is applied repeatedly until the results exhibit convergence to the degree of accuracy desired. Newton's method

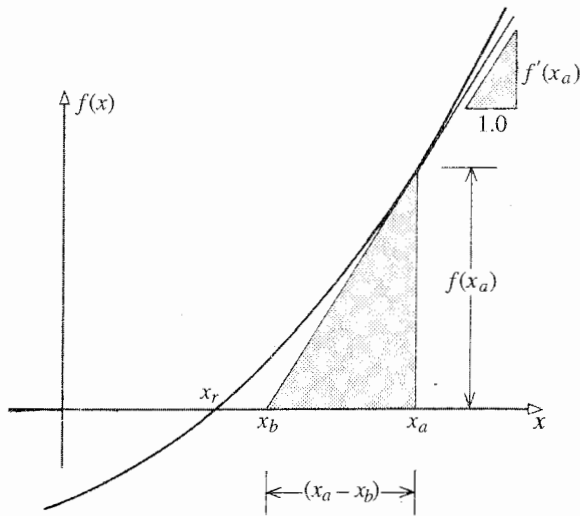


Figure I.1. A tangent (as opposed to secant) approach to determining the real roots of a single variable function.

begins with a first estimate for the location of the desired polynomial root, x_a . It does not matter how this initial estimate x_a is obtained. For example, the initial estimate of the root could be obtained from a rough graph of the polynomial equation. The first estimate is used in this iterative procedure to calculate a second estimate that is closer to the actual root, and the second estimate is used to calculate a still closer third estimate, and so forth. From Fig. I.1, it can be seen that from the interpretation of the derivative as a slope, $f'(x_a) = f(x_a)/(x_a - x_b)$. Solving this equation for the second estimate x_b yields

$$x_b = x_a - \frac{f(x_a)}{f'(x_a)}$$

Used repeatedly, this equation is the means of obtaining a series of improved estimates. The only caution is that the initial estimate has to be “close” enough to the desired root so that the process converges to that root. For example, if it were desired to discover the root $x = \pi$ of the equation $\sin x = 0$, then an initial guess of $x_a = 1$ would lead to the root $x = 0$ rather than the desired root.

See Refs. [44, 60] for a discussion of the intricacies of using Newton’s method to find complex roots.

I.4 The Binomial Series

From Ref. [1], it may be proved via use of Taylor’s series, that for any real number m , and for any x such that $|x| < 1$,

$$(1 + x)^m = 1 + mx + m(m - 1)\frac{x^2}{2!} + m(m - 1)(m - 2)\frac{x^3}{3!} + \dots$$

$$+ [m(m - 1)\dots(m - n + 1)]\frac{x^n}{n!} + \dots$$

This series is only of finite length when m is equal to a positive integer.

I.5 The Chain Rule for Partial Differentiation

Consider a variable $q = Q(r, s, t)$. In this case, Q is an arbitrary function of the variables $r, s,$ and t , which are called the first class variables. Let the first class variables be in turn functions of the second class variables $x, y,$ and z ; that is, $r = R(x, y, z)$, $s = S(x, y, z)$, and $t = T(x, y, z)$. Since the first class variables are dependent on the values of the second class variables, q can also be considered to be a function of the second class variables. Therefore derivatives of q can be taken with respect to the second class variables $x, y,$ and z . The chain rule for partial differentiation of q with respect to x is as follows (Ref. [1]):

$$\frac{\partial q}{\partial x} = \frac{\partial Q}{\partial r} \frac{\partial R}{\partial x} + \frac{\partial Q}{\partial s} \frac{\partial S}{\partial x} + \frac{\partial Q}{\partial t} \frac{\partial T}{\partial x}$$

Notice the pattern of the variables. Each of the first class variables $r, s,$ and t gets its chance to be part of a derivative of Q . Then each first class variable in turn is differentiated with respect to x , which is the second class variable with which the top variable q is differentiated in this illustration. The pattern for $\partial q/\partial x$ is that the leading function of each pair of products is always Q , the trailing variable is always x , and the connecting terms are always related to the first class variables.

The partial derivative of q with respect to y or z is the same as above but for x replaced by y or z . If the first class variables $r, s,$ and t were only functions of x instead of $x, y,$ and z , then $\partial q/\partial x$ would become dq/dx , and $\partial R/\partial x$ would become dR/dx , and so on. It is common practice to write $\partial r/\partial x$ in place of $\partial R/\partial x$, or dr/dx in place of dR/dx , and so on.

Stress in Structures

1.1 The Concept of Stress

Structural engineers are concerned with the effects that forces produce on structures. That forces produce results such as deformations or structural collapse is the usual structural engineering cause-to-effect point of view. Even though this viewpoint is not the only possible or even useful viewpoint, it is the one adopted implicitly in Parts I, II, and III of this text as a temporary convenience until it becomes necessary to adopt a more general viewpoint. In other words, the usual engineering viewpoint is that the forces are an input, the structure is the system, and the effects of the forces acting on the structure (deformations, cracking, etc.) are the output. If a structural effect in turn influences the forces acting on the structure, then a feedback loop involving the forces and the structural effect exists. An example of structural feedback is first encountered in Part III of this text in the form of a beam buckling problem.

The theory that is developed in the next four chapters is valid for *any* type of force or combination of forces (within certain limits), and *any* type of structure. The task of classifying types of forces and structures can wait until it becomes necessary. What is necessary now is to begin to discuss the types of effects that forces produce on structures. One effect that forces can produce is *structural failure*. Structural failure is defined simply as occurring whenever a structure no longer can serve its intended use. A structural failure can be the dramatic collapse or rapid chain reaction disintegration of a large, enormously expensive structure (e.g., the Challenger space shuttle), or it can be as trivial as a wire clothes hanger being sufficiently bent out of shape that its usefulness as a clothes hanger is outweighed by the bother of straightening it. Clearly, certain structural failures are acceptable after an appropriate service life, and the service lives and performance of some structures have to be monitored or ended so as to avoid failures. The resulting question that structural engineers must address is the one that asks how structural failures can be anticipated with reasonable precision; that is, how can failures be predicted mathematically? In order to focus on the preliminary steps essential to predicting structural failures, this text omits discussion of the important topics of confirming mathematical predictions through testing or service experience monitoring.

The question of how to predict structural failures is a difficult question because there are many types of structural failure, and each type of failure has its own complexity. Returning to the example of wire clothes hangers, the large-deformation “bent-out-of-shape” type failure of the wire hanger to support three or more heavy winter coats is quite different from the fracture type of failure that results when a small portion of the hanger is repeatedly bent back and forth upon itself until the wire fractures. The process of predicting structural failures can be conveniently divided into two steps. The first step is the calculation of either or both of the analytical quantities called “stresses” and “displacements.” (Definitions of stress and displacement are decided upon later.) The second step is to use, for example, the calculated stresses, the known material characteristics of the structure, and the loading characteristics to estimate the safety of the structure. This introductory text concentrates on

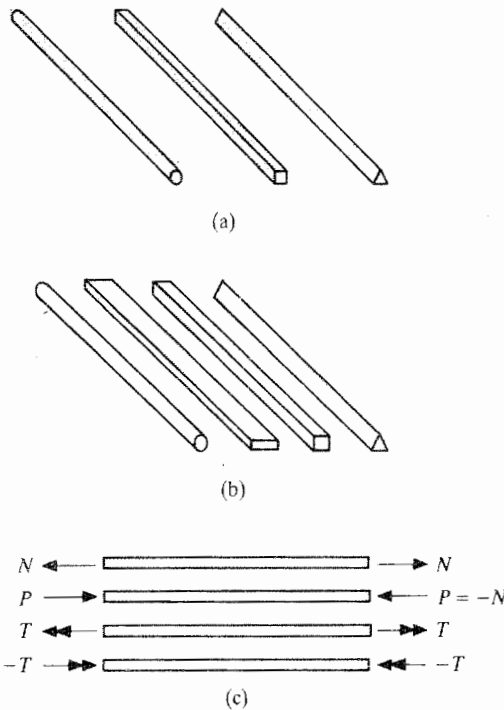


Figure 1.1. (a) Same length, uniform bars with the same cross-sectional area, but different cross-sectional shapes. (b) Same length, uniform bars with twice the cross-sectional area of the previous set. (c) By definition, “bars” only transmit axial forces (tensile or compressive) and twisting moments.

explaining the preliminary step of calculating stresses and displacements. Explanations of the process of using the calculated stresses or displacements to estimate the likelihood of failure is mostly left to more advanced texts, each of which generally concentrates on only one type of failure.

In this chapter the topic of stresses is introduced. The introduction is done in a complete manner that will not require extension or further elaboration short of the most advanced studies in solid mechanics. Thus this approach will save the reader time and effort in the process of learning the elements of structural mechanics. The first thing to be done is to provide an illustration of why engineers have developed the concept of stress, and the usefulness of that concept for determining when a structure will fail in a simple way. The same illustration will provide a basis for choosing a definition for stress. Consider the two sets of bars shown in Figs. 1.1(a) and 1.1(b). A bar is a long thin object of any constant cross-sectional shape that is subjected to only two types of loads. The first type of load is an axial force, that is, a force whose vector representation parallels an axis along the length of the bar. The second type of load is a twisting moment, also called a torque. Its double arrowhead vector representation (right-hand rule) is also one where the vector is parallel to an axis along the length of the bar. The conventional representations of bars loaded in the above manner are shown in Fig. 1.1(c). Let the bars in Fig. 1.1(a) all be well made from the same material and have the same cross-sectional area as that of a typical pencil. Let the bars in Fig. 1.1(b) have twice that cross-sectional area, and be well made of the same material as the bars in Fig. 1.1(a). If increasing tensile forces, that is, forces that tend to stretch the bars, are

applied to each of the bars in Fig. 1.1(a), then it would be determined experimentally that all of the bars in Fig. 1.1(a) pulled apart (failed) at approximately the same final value of the applied-tensile force. The small differences between the magnitudes of the tensile forces at failure for each of the bars in Fig. 1.1(a) would be due to experimental measurement errors and small, unobserved differences between the bars. For cross-sectional areas like those of a typical pencil, or greater, it could also be discovered that the length of the bar has no appreciable effect on the magnitude of the failure load. Thus, from this first set of experimental results it can be concluded that, for this type of loading, the shape of the bar cross-section and its length are immaterial. Let the larger cross-section bars of Fig. 1.1(b) be subjected to the same experimental routine. Again it would be observed that each bar of this set failed at approximately the same final load value. Moreover, it would be observed that the failure loads for the bars of Fig. 1.1(b) are twice those of Fig. 1.1(a). In other words, doubling the cross-sectional area doubles the magnitude of the tensile failure load. Furthermore, this proportionality would continue for all larger and many smaller multiples of the cross-sectional area. (If the bar cross-sections are very small, for example, like those of thin wires, then small manufacturing imperfections may have large effects on the magnitude of the tensile load at failure.) Since a consistent goal of all engineers is to simplify their understanding of physical phenomena wherever possible, it is desirable to seek the best possible way to organize this simple data set. This can be done by noticing that the *one* thing that *all* the bars of Figs. 1.1(a) and 1.1(b) have in common is the ratio of the failure load value to the value of the cross-sectional area. The simple experiment described above suggests that the ratio of force to area is a primary means of predicting the behavior of structures and the materials from which they are made. Experiments with different materials, loadings and structural shapes would show that this conclusion is generally true. Hence a special name is bestowed on the ratio of force to area. The name is, of course, *stress*.

Very few useful structures are as simple as the bars in Fig. 1.1. No loadings are simpler than the tensile forces sketched in Fig. 1.1. The latter statement is based on the implication inherent in the sketch as it is drawn that the stress produced by the normal force, N , is evenly (i.e., "uniformly") distributed over the bar cross-sectional area, A . In other words, for this type of loading, the stress everywhere on the bar cross-section is equal to the average stress. In symbolic form, if σ_{av} is the average stress, then by the ratio concept of the preceding paragraph, $\sigma_{av} = N/A$. The question arises as to whether all stress distributions are necessarily uniform. To answer this question, consider two bars of equal length with equal-area square cross-sections. Let the first bar be made of rubber and let the second bar be made of steel. Let axial tensile forces be applied separately to each bar so as to stretch each bar exactly the same distance. The reader recognizes that a much greater force is required to stretch the steel bar the specified distance than is required to stretch the rubber bar that same distance. Thus, in these circumstances of equal areas, the average stress in the steel bar is much greater than the average stress in the rubber bar. Now consider the situation where the two bars in their equally stretched condition are bonded together to form one stretched bar. Clearly, from the viewpoint of the now single bar, the stress distribution is not uniform since the stress is much higher over the steel portion of the bar than over the rubber portion.

It is also true that a nonuniform stress distribution can exist over a cross-section of a bar made of only one material. Consider two square cross-section bars of cross-sectional area A which are made of the same material. Let the first of these two bars be loaded by a tensile force of magnitude 9000 lb, and the second by a tensile force of 1000 lb, where both forces are uniformly distributed over their respective cross-sections. Let the unloaded length of the first bar be just slightly and sufficiently shorter than that of the second bar so

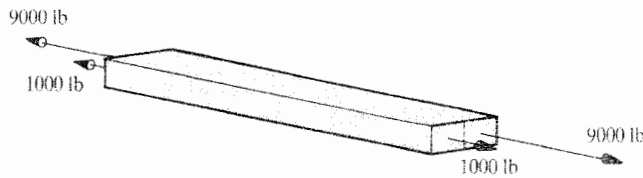


Figure 1.2. Illustration of the possibility of a nonuniform distribution of axial stresses across the cross-section of a bar.

that the stable loaded lengths of both bars are exactly the same. If the two bars are now fused together along their lengths to form one bar of cross-sectional area $2A$, while the respective loads are maintained on both halves of the now single bar, the result is a bar as shown in Fig. 1.2. In this case the bar is made of a single material with a stress acting over one half of the new cross-section that is nine times as great as that acting over the other half of the cross-section. When the stress does vary significantly, it is not useful to work with a value of the average stress over the entire cross-section. Clearly the more heavily loaded half of the fused bar is closer to rupture than the less loaded half. For that type of reason, engineers are usually much more interested in knowing the values of the peak stresses and knowing how extensive are the areas over which high stresses act. This latter information is much more useful when estimating the likelihood of local material failures or more general structural failures.

It is also important to note that simply stating that the two loads acting upon the combined bar's end cross-sectional area have a combined magnitude of 10000 lbs would not be sufficiently informative with regard to the load distribution on the end surfaces of that bar. It will be necessary to be more precise when specifying the loads acting on the outer surfaces of the bodies under study.

The fact that stresses are not always constant over a given internal planar area requires careful consideration about how stress is to be defined. The definition must not compromise the basic concept of stress being the ratio of force over area. Since both force and area are measurable quantities, so then their ratio must also be a measurable quantity. Therefore it is necessary that the definition produce a unique measure; that is, that there be no ambiguity as to the magnitude of the stress. Consider Fig. 1.3(a). That sketch shows an edge view of a varying stress distribution acting over a beam cross-section that is positioned somewhere along the length of a loaded beam. (Beams have the same general geometry as bars, but the name "beam" indicates a more general type of loading.) Since an average stress value based on a total area is not a satisfactory measure, explore the possibility of a stress value that can be associated with smaller portions of the total area. A definition of stress based on sub-areas would permit having separate stress values where the stresses are high, or anywhere else. Therefore consider an arbitrarily located sub-area. Better yet, consider the arbitrarily located sequence of three sub-areas, from larger to smaller, as drawn in Fig. 1.3(b). Each sub-area in the sequence has been chosen as an included square, and each square has the point P as one vertex. Figure 1.3(c) shows edge views of the stress distributions acting on that sequence of sub-areas. For the lack of a better idea, let it be said that the stress to be associated with each sub-area of the sequence is the average stress for that sub-area. Geometrically, the average stress is represented by the dashed line ordinate in Fig. 1.3(c). It is easily seen that in this case the value of the stress to be associated with each sub-area decreases as the area decreases. Similarly, if the sequence of squares approached point Q , instead of point P , the stress values would increase as the total force and the magnitude of the sub-area decreased. It also should be clear from the geometry that if the sequence of sub-area was greatly extended in an orderly fashion beyond three in number, the value of the average

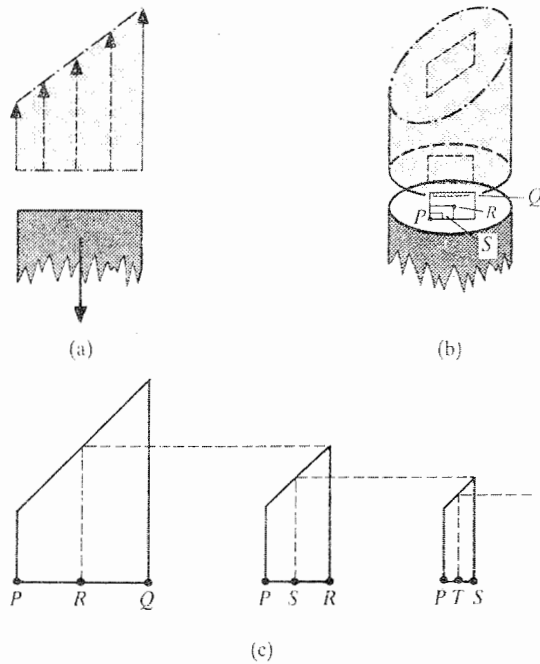


Figure 1.3. (a) Side view of a tensile force whose effect is distributed linearly over the bar cross-section. (b) The process of considering smaller and smaller portions of the bar cross-section at the fixed-point P . (c) A geometric illustration of how the average intensity of the distributed force near point P approaches a unique value as the small portion of the total cross-sectional area anchored at point P is systematically reduced by a factor of 4.

stress would stabilize (i.e., converge) as the sequence of dashed lines representing the stress magnitude approached either point P or Q . For example, for an approach to point P , the dashed line that depicts the average value of the stress over the sub-area in the sequence of sub-areas would irresistibly approach, and be confined by, the stress magnitude line at point P . This fixed stress magnitude at point P is precisely the unique force over area measure that is sought. This measure needs only to be expressed mathematically as the following limit,¹ where N , the total force acting over the sub-area A , is a function of A :

$$\text{Stress} \equiv \lim_{A \rightarrow 0} \frac{N}{A} \quad (1.1)$$

In this limit both the numerator and denominator decrease jointly to very small, even infinitesimal quantities.² Recall that the definition of a derivative is exactly the same type of limit. For example, the derivative of the function $f(x)$ at the point x_p is the limit as

¹ The three-bar symbol signifies that the relationship between the left-hand side and the right-hand side is that of an identity. An identity is an equality that is true in *all* circumstances. A simple way of appreciating the difference between an identity and a mere equality is to recall that for $0 \leq \theta \leq 2\pi$, the formula $\cos^2 \theta + \sin^2 \theta \equiv 1.0$ is true for all θ , while $\cos \theta + \sin \theta \equiv 1.0$ is only true for two values of θ . All definitions are identities.

² The atomic nature of materials is ignored in preference to the convenient fiction that all pure materials exhibit the same physical properties for small samples, no matter how small, as are exhibited on average for large samples of the material. This convenient approximation leads to the material being called a *continuum* and thus the material of Chapters 1–4 is called *solid mechanics*, a branch of continuum mechanics.

x approaches x_p of the ratio of $[f(x_p) - f(x)]/[x_p - x]$. Note how closely the above definition of the derivative fits the illustration in Fig. 1.3(c) where x_p is analogous to the point P , and x is analogous to the right-hand point in the sequence Q, R, S, \dots . This argument allows rewriting of the above definition, Eq. (1.1), as the ratio of two differentials; that is, as

$$\text{Stress} = \frac{dN}{dA} \quad (1.2)$$

This definition of stress is well and good as far as it goes, but it does not take into account the one further fact that the stress acting upon the cross-sectional area need not, as always assumed in the above discussion, act perpendicularly to the surface of the area under discussion. A simple demonstration that stress can act in the plane of the area as well as perpendicularly to the area occurs when one places one's hand firmly on a flat surface, and then rubs the surface with that hand, creating, by means of the friction between the hand and the surface, an in-plane stress on the flat surface. Note that the total force N acting upon the flat surface beneath the hand is the vector sum of the normal component (from pressing down with the hand) and the in-plane component. Since neither component is zero in this case, the total force vector N is neither normal to nor within the plane of the surface. Another confirmation of the possibility that the stress does not always act in a direction that is normal to the area under consideration can be obtained by merely passing an oblique plane through the first or second bar in Fig. 1.1(c). Since the total force, and hence the total stress, in the bar parallels the bar axis, and the normal to the oblique plane is not parallel to the bar axis, the stress is not normal to the oblique plane. Therefore, it is now necessary to adjust the above definition of stress to account for the directional properties of forces and stresses. When considering an area with a fixed orientation in space, stress is a vector quantity because it is a force vector (dN) divided by a scalar (dA). (The qualification "when considering an area with a fixed orientation" is important, and is developed later.)

On the basis of the above discussion, it is now a simple matter to define a *normal* stress as the limit of the ratio of the normal force acting upon an area of fixed orientation, as the magnitude of that area approaches zero. The same can be done for the in-plane stress, called the total *shearing stress*. This decomposition of the total stress into a normal stress and a total shear stress is significant because the effects of these two different types of stresses on materials can be quite different. Two more steps are necessary to make the above definitions still more useful. The first step is to introduce a coordinate system. To begin simply, consider a right-handed Cartesian³ coordinate system where the x axis is normal to the area being studied, while the y and z axes lie in the tangent plane of the area under study. In this case the area is called an " x area," or " x surface," or " x plane," since the orientation of the plane is precisely located by its normal, the x axis. In other words, when the x axis is fixed in space, then any plane perpendicular to that axis is an x plane.

Lower-case sigma (σ) is chosen to symbolize stress. A double-subscript notation is used to identify which of the possible stress components is meant; see Fig. 1.4. The first subscript designates the plane of the area upon which the stress acts, while the second subscript designates the direction in which the stress acts. Looking at Fig. 1.4, for example,

$$\sigma_{xy} = \frac{dN_y}{dA_x} \quad (1.3)$$

³ From Ref. [2], the adjective "Cartesian" is derived from the family name of René Descartes (1596–1650), who first introduced the coordinate method and established analytical geometry.

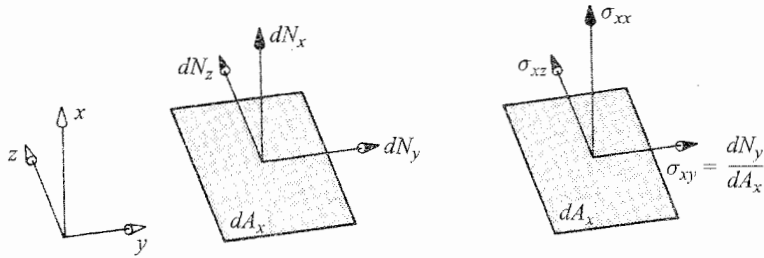


Figure 1.4. The total force acting upon a differential area, dA_x , can have no more than a differential magnitude, dN . Like any force vector, dN can be resolved into three Cartesian components. When these vector components are divided by the scalar value dA_x , the corresponding components of the total stress vector are obtained.

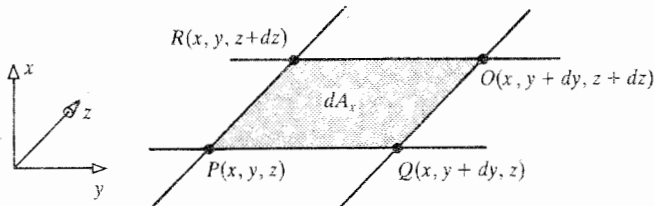


Figure 1.5. The bounds of the differential area dA_x that are always to be associated with the point P .

where dN_y is the y component of the total differential force acting over the differential area, dA_x . The double-subscript notation is illustrated more extensively below.

The second and final step to enhance the usefulness of the above definition of stress with its associated subscript protocols is to establish that stress, a quantity tied to an area, can be treated as an ordinary mathematical function of the coordinates of the chosen spatial coordinate system. A function that is solely a function of the spatial coordinates is called a "point function." Temperature is an example of a physical phenomena representable as a point function since a temperature value can be assigned to each point in the volume of the structure. In order to consider stress as a point function, let it be agreed that any point P in the structure can be identified by a set of Cartesian or other coordinates. In keeping with the double-subscript notation, let it also be agreed that the differential area that is associated with the stress definition at point P always lies in the plane defined by the coordinate axis of the first stress subscript. Let it be further agreed that the differential area always extends from point P in the direction of the two positive coordinate axes that parallel that plane, and the shape of the differential area is defined by constant values of the in-plane coordinates. Thus, for example, for Cartesian coordinates, an x plane differential area would have the shape of a rectangle of differential dimensions dy by dz as shown in Fig. 1.5. In this way, for all coordinate systems, a unique differential area consistent with the stress definition is automatically associated with any given point in the space of the structure. Therefore, by reversing the above viewpoint, the value of the stress acting on that differential area can be associated with a given point in the space of the structure. That is, it is now possible with clear meaning to speak, in terms of a coordinate system, about the stress or stresses "acting at a point." Therefore it is also possible to say that the stress components vary as the coordinates vary; or equivalently, that the stress is a function of the spatial coordinates. One result of the above convention is that it is now possible to understand clearly the meaning

of a partial derivative of a stress component such as $\sigma_{xz}(x, y, z)$ with respect to a spatial coordinate such as y ; that is, $\partial\sigma_{xz}/\partial y$.

Another way to suggest that such partial differentiation is valid is simply to note that (1) if, say, all the normal stresses acting on all the differential areas of a cross-section were added up (i.e., integrated), then the result would be the normal component of the total force acting across that cross-section; and (2) partial differentiation is the inverse operation of integration. Hence, if integration is valid, as it is since it is just the process of putting the stresses over the sub-areas together to form the total force N acting over the area, then the inverse operation of partial differentiation should also be possible for this physical phenomenon.

The next question to be addressed is: What is to be done with the various stress components? The present point of view is that the stresses arise as a result of external forces being applied to the structure under consideration. The stresses can be considered as the result of the forces being transmitted through, or equivalently, diffused throughout the structure. To illustrate this remark, think again of the first or second bar in Fig. 1.1(c). From simple static equilibrium considerations, if the bar is cut through anywhere in its interior, the same force that appears at an end will be found at the cut. In other words, the bar transmits the force from one of its ends to the other. The same *continuity of forces* exists in all loaded structures, and the force transmission requirement point of view is one starting point for the design of structural components. This concept of the continuity of forces, via internal stresses in this case, is but one aspect of Newton's laws of motion.⁴ Newton's second law will now be used to quantify the above ideas.

1.2 The General Interior Equilibrium Equations

Newton's second law is applicable only to bodies of fixed mass. It is thus necessary to consider a structure of fixed mass that is completely enclosed by a fully specified outer boundary whose shape and size may change with time. To draw general conclusions using Newton's second law it is necessary to consider a structure of general shape. In this text, as in all others, bodies of general shape are always represented as having the shape of potatoes, potatoes with forces and moments acting upon them, with perhaps a hole or two. If there is a significant temperature change, (an important form of loading for vehicles of all kinds), then the body of general shape is a hot potato. Consider such a hot potato at a particular instant in time. Since the potato has no specific geometry, the only way available for discussing the stresses that exist in a potato in an unambiguous way is to examine the stresses acting upon infinitesimal areas. Hence consider an infinitesimal body in the interior of the general body. The infinitesimal body is chosen so that it is bounded by the distinct infinitesimal areas defined by the intersecting planes of the chosen coordinate system. To begin simply, a Cartesian coordinate system is first discussed. Hence, in this case, the infinitesimal areas are rectangles and the volume is a rectangular parallelepiped; see Fig. 1.6(a). The entire interior of the body up to, but not including, the boundary surface or surfaces (the skin of the potato) can be fashioned from such differential volumes.

The Cartesian components of the stresses that act upon this differential volume are shown from two different viewpoints in Figs. 1.6(b) and 1.6(c). The stress vector magnitudes are, as adopted previously, average values for the stress over their respective differential areas. Since the differential areas are so very small, the variation in the stress magnitude is very

⁴ According to Ref. [2], Sir Isaac Newton (1642–1727) published the laws of motion in his famous *Philosophiae Naturalis Principia Mathematica* in 1687.

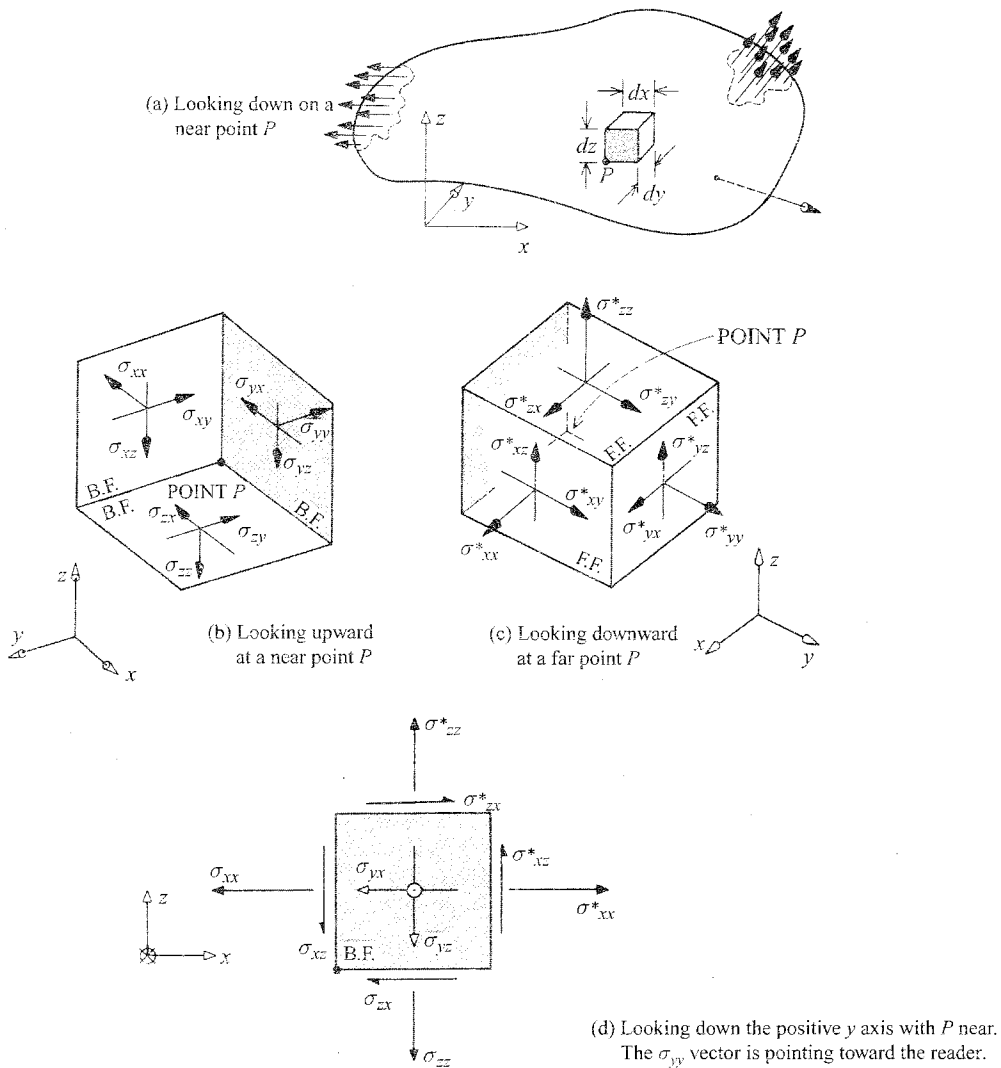


Figure 1.6. (a) A structural body of general shape subjected to any loadings acting upon its surface and any body forces acting throughout its volume. In accord with the selected coordinate system, there is a unique differential volume extending in the positive coordinate axis directions from the arbitrarily selected point P . When the coordinate system is Cartesian, the differential volume has the shape of a rectangular parallelepiped. (b) A view of the rectangular parallelepiped faces, called “back faces,” temporarily abbreviated as B.F., that intersect at point P . To help interpret the orientation of these rectangular parallelepipeds, in all four different views of this same parallelepiped, the back y face is shaded. (c) A view of the three “front faces” (F.F.) associated with the point P . In order to distinguish between the corresponding stresses on the front and back faces, an asterisk is *temporarily* added to the front face stress symbols. (d) A side view of the same parallelepiped showing the back y face. Note the convention that the arrowheads of vectors coming directly out of the paper appear as small circles with a dot at the center, while vectors into the paper are symbolized by small crosses (the feathers) centered on small circles.

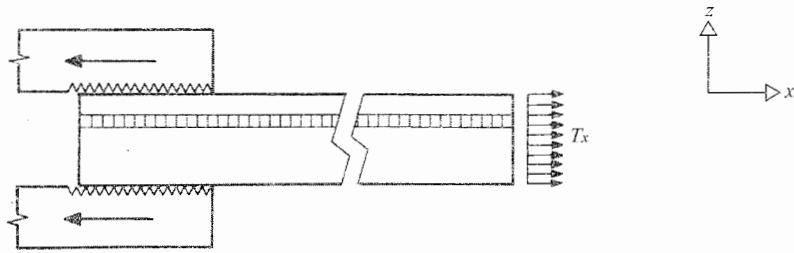


Figure 1.7. A test specimen gripped on one end and loaded upon the other end by a uniform traction.

close to being planar (a plane at a tilt). Therefore the average value of the stress magnitude occurs very close to the centroid of the differential area: in this case, at the center of each rectangular face. Figure 1.6(d), a side view of the same infinitesimal element, ties together the three faces shown in Fig. 1.6(b) with the other three faces shown in Fig. 1.6(c). Note that the point P in Fig. 1.6(b) is the corner of the rectangular parallelepiped that has the lowest coordinate values. Accordingly, by the convention adopted above for associating the areas over which the stresses act with a nearby point, the stresses acting upon the faces shown in Fig. 1.6(b) are the stresses “acting at point P .” The three faces of the rectangular parallelepiped that intersect at point P are called “back faces.” On the back faces the standard convention for positive stress vectors is that they are always oppositely directed from the positive coordinate axes that they parallel. The front faces shown in Fig. 1.6(c) have higher coordinate values than the corresponding back faces, and the front face stress vectors are always positive in the positive coordinate axis direction. Note again the pattern of the double subscripts where, for both front and back faces, the first subscript identifies the (x , y , or z) face upon which the stress acts while the second subscript identifies the axis paralleled by the stress vector. The reader must memorize the stress sign convention and be able to apply the double subscript notation to differential elements whose geometry is defined by all common orthogonal coordinate systems, and do so from any viewing angle.

The stresses on the front faces are distinguished from those acting on the back faces by the temporary addition of an asterisk to signify that the front face stresses may be different from the stresses with the same subscripts that act on the back faces. To show that the two sets of stresses can be different, examine Fig. 1.7. At this point the term “tractions” will be introduced to refer to stresses acting on the outside of any outer boundary surface. In other words, stresses and tractions are exactly the same thing, but stresses occur inside the structural body, or on the inside of outer surface boundaries, while tractions occur on the outside of the outer surface boundaries.⁵ (A sign convention for tractions is introduced later.) The bar in Fig. 1.7 is being stretched by a uniformly distributed traction, T_x , acting on the right-hand end face of the bar. The left end of the bar is being gripped by the jaws of a clamp. The clamp equilibrates the resulting force applied to the right-hand end by producing oppositely directed shearing tractions on the cylindrical outer surface of the bar. Now consider the long row of infinitesimal rectangular parallelepipeds that runs parallel to the bar axis from the bar’s left-hand end face to the bar’s right-hand end face as is shown in Fig. 1.7. Ignoring the insignificant effect of air pressure in this situation, there is no traction acting on the left-hand face of the furthestmost left-hand infinitesimal element in the row of such elements. Isolating and internalizing this infinitesimal element, (so that the tractions can be referred to as stresses), it then can be said that there is zero stress on that left-hand

⁵ The term “surface boundaries” is meant to include the boundaries of any cavities within the general body.

face of the left-hand element. Applying the same sort of reasoning to the isolated right-hand element, it can be said that the stress acting on the right-hand face of the right-hand element has the magnitude of the applied traction, T_x . Thus over the finite length of the bar, there is a finite change in the stress σ_{xx} from a value of zero at one end to a value of T_x at the other end. Thus it is necessary to conclude that, for at least some of these infinitesimal rectangular parallelepipeds, there is a change of some sort in the values of the σ_{xx} stress from that at their left-hand face to that at their right-hand face. Thus, by extending the same sort of argument to each of the other stresses, it may be concluded that the temporary asterisks applied to the stresses on the front faces of the generally stressed rectangular parallelepiped are appropriate for making a distinction between the corresponding back face and front face stresses.

Figures 1.6(b) and 1.6(c) show a count of 18 different stresses (nine with asterisks and nine without) before application of Newton's second law. It is quite possible to proceed using those 18 quantities when summing forces in, and taking moments about, the three orthogonal directions. Summing forces and moments in that manner produces six equations relating the 18 quantities. There is a much better way of representing the stresses with asterisks so as to produce more manageable, albeit differential, equations of equilibrium. One important advantage of this second approach is that the difference between the number of unknown stresses and the number of equations that relate these stresses is only 3 as opposed to 12 when using asterisks. To begin this second approach, consider the stress σ_{xx} on the back face, and the stress σ_{xx}^* on the front face, of the rectangular parallelepiped: again see Fig. 1.6(d). Consider also the stress in the x direction on the back face of a neighboring rectangular parallelepiped of the same size lying to the right of the first parallelepiped. The back face of the neighboring parallelepiped abuts the front face of the first parallelepiped. Newton's third law concerning equal and opposite reactions establishes that the stress in the x direction on the neighboring back face is σ_{xx}^* . Then a comparison of these back face stresses in the x direction of these two adjacent elements shows that the stress values σ_{xx} and σ_{xx}^* are values of the same stress function at different points in space separated by a differential distance. Therefore these two values of the same stress function can be related by means of a Taylor's series expansion⁶ when it is assumed that the stress function varies in such a smooth fashion that it has an infinite number of derivatives. Again, a short summary of Taylor's series is presented in Section 1.2. Let $\sigma_{xx}(x, y, z)$ symbolize the stress function. When expanding this function about the x value associated with the back face at P (which is simply called x) to obtain the value of σ_{xx} at the front face, a distance dx from the back face, only the variable x undergoes a change from the value x to the value $x + dx$. Thus the Taylor's series has the form

$$\begin{aligned} \sigma_{xx}(x + dx, y, z) = & \sigma_{xx}(x, y, z) + dx \left(\frac{\partial \sigma_{xx}}{\partial x} \right) + \left(\frac{1}{2!} \right) (dx)^2 \left(\frac{\partial^2 \sigma_{xx}}{\partial x^2} \right) \\ & + \left(\frac{1}{3!} \right) (dx)^3 \left(\frac{\partial^3 \sigma_{xx}}{\partial x^3} \right) + \dots \end{aligned} \quad (1.4)$$

⁶ According to Ref. [1], Taylor's series was first published in 1715 by Brook Taylor. Taylor's formula with remainder was derived by Lagrange in 1797, and later by Ampère in 1806. The assumption of the validity of the Taylor series is not really necessary in this case. The same final result can be obtained from the simple geometric interpretation of the first derivative as a tangent that well approximates the function over infinitesimal distances. The Taylor's series argument was chosen for presentation in place of the simpler geometric argument because only the former argument makes clear the error associated with retaining only the first and second terms in the expansion. The expansion shows that the error is infinitesimal.

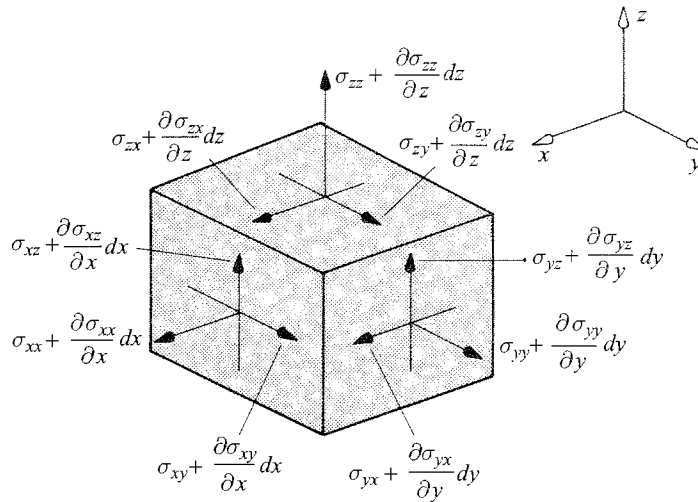


Figure 1.8. The three front faces of a rectangular parallelepiped and the stress vector components that always act upon those faces. The presence of the infinitesimal changes in the stress values, that is, changes from those values on the back faces, renders obsolete the previous use of asterisks to denote front face stresses.

where, by the previous notation

$$\sigma_{xx}^* = \sigma_{xx}(x + dx, y, z)$$

Once again, note from Fig 1.6(d) that the values of the coordinate y and z are unchanged when moving from the center of the back face to the center of the front face. Hence partial derivatives with respect to y and z , which represent changes in these directions, are zero, and do not appear in the above expansion. Examination of Eq. (1.4) shows that the difference between σ_{xx}^* , on the front face and σ_{xx} on the back face is a series of terms each of which includes an infinitesimal differential factor dx , with each succeeding term including an additional infinitesimal factor dx . Thus each succeeding term is infinitesimal compared to the preceding term. Thus all the terms after the second term are certainly negligible compared to the second term, and these terms are dropped from further consideration. Even though it is also true that the second term is infinitesimal compared to the first, it is not dropped because if it were dropped, then the entire difference over the infinitesimal distance dx between σ_{xx}^* and σ_{xx} would be lost, and that cannot be permitted without losing the possibility of coping with finite differences over finite distances. In other words, the second term is by far the largest part of the difference between the stresses at the two faces.

The final result, following the same development for the other stresses with asterisks as was done for σ_{xx}^* above, is that all the stresses with the temporary asterisks are now replaced by the two-term sums shown in Fig. 1.8. Now it is possible to apply Newton's second law and obtain manageable equations. The style of applying Newton's second law used here may require a brief explanation. Note that the usual form, where boldface terms are vector quantities, is

$$\sum \mathbf{F}_i = m\mathbf{a} \quad (i = 1, n)$$

where of course, the \mathbf{F}_i are the various forces acting upon the body of mass m , and \mathbf{a} is the total acceleration of the body. This identity may be rewritten as

$$\sum \mathbf{F}_i - m\mathbf{a} = 0 \quad (i = 1, n)$$

By choosing to define the term $-m\mathbf{a}$ as a force called the “inertia force,” which is possible since it too is a vector with units of force, the inertia force can be included in the summation with all the other forces. Then, in these circumstances, Newton’s second law has the appearance

$$\sum \mathbf{F}_i = 0 \quad (i = 1, n + 1) \quad (1.5)$$

This latter equation is the equation of “dynamic equilibrium” when inertia forces are actually included in the sum, that is, when either the magnitudes or directions of the accelerations are functions of time. It is the familiar equation of “static equilibrium” when all included accelerations are constants. This latter, yet all-inclusive, form of Newton’s second law is used whenever it is desired to sum forces and moments and not make a distinction between static and dynamic equilibrium. In other words, adopting the inertia force point of view is simply a means of retaining the generality necessary to meet the problems of structural dynamics, yet at the same time not divert attention from the focus of this text, which is on structural mechanics.

Inertia forces (the negative of mass multiplied by acceleration) are tied to the mass of the body. The reader has probably experienced on his or her body the thrilling effects of the inertia forces that result from the accelerations imposed by the convoluted paths followed by carnival rides. A simpler example for inertia forces is provided by a high-speed elevator in a tall building. When the elevator accelerates upward, a passenger feels his or her entire body being pulled downward. When the elevator decelerates (i.e., has a negative acceleration), the passenger feels almost able to float. Such forces that act over the mass of a body are simply called “body forces.” It is irrelevant whether or not the accelerations vary with time as in the above-cited examples, or are constant as in the case of weight forces. The vector sum of all the body forces is the total body force, and the magnitudes of its three Cartesian components per *unit mass* (which are just the total acceleration components) are identified herein as B_x , B_y , and B_z . Similar designations are used with other coordinate systems. All such components are positive in the direction of the positive coordinate axes.

Now, at long last, everything is in place to write the equations of equilibrium for the infinitesimal element of Fig. 1.8 whose geometry is defined by the choice of a Cartesian coordinate system. Note that the sketch of the infinitesimal element constitutes a free body diagram, and this is the only free body diagram that can be drawn for a body of general shape. The reader is cautioned that it is absolutely necessary to draw free body diagrams before summing forces and moments. Begin by summing forces in the x direction. Since Newton’s second law involves forces, not stresses, each stress has to be multiplied by the area over which it acts to obtain the corresponding force. Similarly, the body force components per unit mass need to be multiplied by the body mass, that is, mass density symbolized by lower-case rho, ρ , multiplied by body volume. Then

$$\begin{aligned} & -\sigma_{xx} dy dz + \left[\sigma_{xx} + \left(\frac{\partial \sigma_{xx}}{\partial x} \right) dx \right] dy dz \\ & -\sigma_{yx} dx dz + \left[\sigma_{yx} + \left(\frac{\partial \sigma_{yx}}{\partial y} \right) dy \right] dx dz \\ & -\sigma_{zx} dx dy + \left[\sigma_{zx} + \left(\frac{\partial \sigma_{zx}}{\partial z} \right) dz \right] dx dy + \rho B_x dx dy dz = 0 \end{aligned}$$

The above identity can be simplified by canceling terms of opposite sign, and dividing through by the quantity $dx dy dz$. Such a division is permissible because, although each of

these differentials is made to approach zero, they are not permitted to be zero. The result is

$$\boxed{\frac{\partial \sigma_{xx}}{\partial x} + \frac{\partial \sigma_{yx}}{\partial y} + \frac{\partial \sigma_{zx}}{\partial z} + \rho B_x = 0} \quad (1.6a)$$

The reader can readily verify that the summation of forces in the y and z directions leads to the following two additional identities

$$\boxed{\begin{aligned} \frac{\partial \sigma_{xy}}{\partial x} + \frac{\partial \sigma_{yy}}{\partial y} + \frac{\partial \sigma_{zy}}{\partial z} + \rho B_y &= 0 \\ \frac{\partial \sigma_{xz}}{\partial x} + \frac{\partial \sigma_{yz}}{\partial y} + \frac{\partial \sigma_{zz}}{\partial z} + \rho B_z &= 0 \end{aligned}} \quad (1.6b)$$

Now sum moments about an axis parallel to the z axis that passes through the center of the parallelepiped. The advantage of placing the axis at the center of the differential element is that all of the body forces and all the forces associated with the normal stresses have zero moment arms. In addition, the shear stresses on the z faces also have zero moment arms. The shear stresses on the x and y faces that have z subscripts parallel the z axis and thus also do not result in a moment about the z axis. Furthermore, assume there are no body moments such as might result from a magnetic field acting upon a magnetic material.⁷ The sum of the moments therefore reduces to

$$\begin{aligned} +\sigma_{xy} dy dz \left(\frac{1}{2} dx\right) + \left[\sigma_{xy} + \left(\frac{\partial \sigma_{xy}}{\partial x}\right) dx\right] dy dz \left(\frac{1}{2} dx\right) \\ -\sigma_{yx} dx dz \left(\frac{1}{2} dy\right) - \left[\sigma_{yx} + \left(\frac{\partial \sigma_{yx}}{\partial y}\right) dy\right] dx dz \left(\frac{1}{2} dy\right) = 0 \end{aligned}$$

Dividing through by the quantity $dx dy dz$ yields

$$+\sigma_{xy} - \sigma_{yx} + \frac{1}{2} \left(\frac{\partial \sigma_{xy}}{\partial x}\right) dx - \frac{1}{2} \left(\frac{\partial \sigma_{yx}}{\partial y}\right) dy = 0$$

The latter two terms each contain an infinitesimal differential factor. Thus they are infinitesimal compared to the first two terms and are accordingly dropped.⁸ If inertial torques, that is, torques due to angular accelerations, were included in this sum of moments acting upon the differential rectangular parallelepiped, the inertial torques would initially involve five

⁷ The astute reader recalls that the stress profile over any infinitesimal area is, in general, planar. Since it is not a constant, there is a moment on each surface area due to the variation in the stress distribution. However, this type of moment involves four differential factors. Thus it, like the other partial derivative terms in the moment summation, makes only a negligible contribution to the total summation. See the exercises at the end of this chapter for an illustration of this point.

⁸ Note that for the sole purpose of deriving these moment equations, the differential element in Fig. 1.8 could have been drawn without the stress magnitudes on the front faces including the additional differential terms that distinguish the front face stresses from the back face stresses. The reader is advised not to be confused by the fact that it is not unusual for basic engineering textbooks dealing with the mechanics of fluid flow, heat transfer, and structural mechanics to omit such differential increments whenever these differential increments, as in this case of the moment equations, have no effect on the equation being derived. It should be remembered that in general, whether or not they contribute to the final equation, differential increments are always actually present on differential elements.

differential factors. Hence they too would be negligible: The final result for this summation, and similarly for the other two summations, is

$$\boxed{\sigma_{xy} = \sigma_{yx} \quad \sigma_{xz} = \sigma_{zx} \quad \sigma_{yz} = \sigma_{zy}} \quad (1.7)$$

The happy conclusions from the moment equilibrium equations are that there are only six (σ_{xx} , σ_{yy} , σ_{zz} , σ_{xy} , σ_{xz} , and σ_{yz}) rather than nine distinct stresses with which it is necessary to contend, and the order of the stress subscripts is immaterial. These two conclusions are incorporated in all the work that follows. Therefore there is no need to refer to Eqs. (1.7) again, and Eqs. (1.6) alone are henceforth referred to as the *equilibrium equations*. Since Newton's second law applies to any engineering structure, Eqs. (1.6) always apply everywhere in the interior of a structure of any shape made of any material subjected to any mechanical and thermal loading.

1.3 Equilibrium at the Outer or Inner Boundary

It is now necessary to examine the boundary of the structural body of general shape on the same infinitesimal scale as was used for the interior of this structural body. The purpose is to discover what conditions on the stresses result from requiring that a differential mass at the outer boundary of the general body be in a state of equilibrium. In parallel to the development for the interior of the general body, the first thing to be done here is to deal with the geometry of a general body boundary. It is easy to see that any closed curve that lies in a plane can be approximated with any degree of desired accuracy by joining smaller and smaller secants in the same fashion that a given circle can be approximated by an inscribed regular polygon as the number of polygonal sides increases without bound. In three dimensions, in a similar fashion, a surface in three-dimensional space can be approximated to any degree of desired accuracy by connecting planar triangles as the triangles are made smaller and smaller. Hence, to examine a portion of a general surface is to examine an infinitesimal plane triangle that is as close an approximation to that surface as desired. Again, since Newton's second law is for bodies rather than surfaces, it is necessary to form a body which has the infinitesimal triangle of the boundary surface as one of its distinct surfaces. When Cartesian coordinates are used, the body to be formed requires x , y , and z faces as well as the triangular area of the boundary surface. The body that meets these requirements is simply an irregular tetrahedron as shown in Fig. 1.9(a).

It is now necessary to introduce a sign convention for the tractions acting on the boundary. Let the tractions be positive in the positive coordinate directions regardless of the boundary surface on which they act. Recall that just as the total stress vector acting on a given internal surface can be at any angle to that surface, the total traction vector can have any angular orientation with respect to the boundary surface. Thus the components of the total traction vector are wholly independent of each other. Figure 1.9(b) illustrates the sign convention for the tractions in Cartesian coordinates. The tetrahedron's interior surfaces bear the stresses shown because they are back faces; that is, they pass through the point with the lowest coordinate values, point P .

As an aside, note that on the infinitesimal scale being discussed here, even a "concentrated force" acting upon an outer surface is just an intense traction. Indeed, a concentrated force is just a convenient mathematical fiction for an intense traction acting over a very small area compared to the total area of the body under discussion. That is, no force, finite or infinitesimal, can act upon a single point because a point has a zero area. The pressure (i.e., traction) would be infinite, and thus beyond engineering experience.

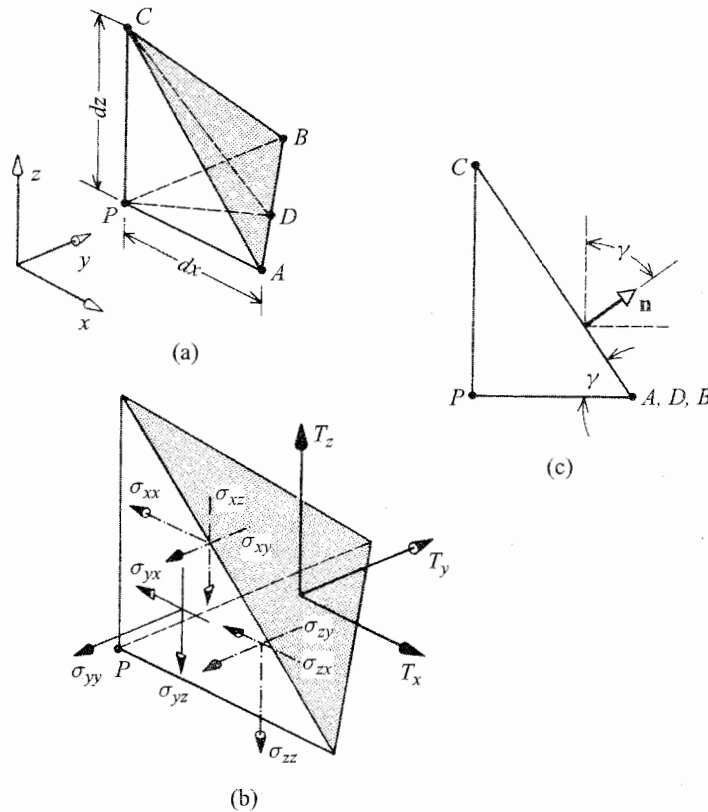


Figure 1.9. (a) Geometry of the irregular tetrahedron extending from the point P very near the boundary surface of the general structural body. The oblique triangle ABC is a very close approximation to the boundary surface in the neighborhood of point P . (b) Stresses and tractions acting upon the tetrahedron at the boundary surface. The total traction vector on the boundary surface is resolved into Cartesian coordinate components. (c) Side view of the internal triangle PDC showing the unit vector normal to the plane boundary surface ABC .

Consider summing forces in any direction. The force in any direction is again, from the definition of stress, the stress in that direction multiplied by the total area over which the stress acts. It is necessary to describe the area of the oblique triangle, and for that matter, to describe its orientation with respect to the Cartesian coordinate axes. Exactly as was done previously with x , y , and z planes, the orientation of this or any plane is known by specifying the orientation of the normal to the plane. The convenient way of denoting the orientation of the normal to the oblique plane is to specify the direction cosines of the normal. These direction cosines are the cosines of the angles between the normal and the three Cartesian coordinate axes. Thus the direction cosines are also the components along the coordinate axes of the unit normal vector. Let the cosine of the angle between the normal to the plane and, for example, the x axis, be denoted as $\cos(n, x)$. The area of the oblique triangle, dA , can be deduced as follows. Referring to Fig. 1.9(a), pass a plane through the line CP and rotate the plane like a revolving door until it is perpendicular to the line AB . Let the point of intersection of the plane with line AB be designated as point D . Since the line AB is normal to the plane PCD , it is perpendicular to every line in that plane. In particular, line

AB is perpendicular to lines CD and DP . Thus the ratio of the area of the z face triangle ABP to the area of the oblique triangle ABC , dA_z/dA , is the ratio of the lengths of the two line segments, DP/CD . This is so because these two line segments are the heights of their respective triangles, and because both triangles have the same base length, AB . From Fig. 1.9(c), which is a side view of triangle CDP , it is clear that $\cos(\gamma) = \cos(n, z)$ is also the same ratio of line segments. Thus the ratio of the z face differential area to the oblique face differential area, dA_z/dA , is $\cos(n, z)$. Similarly, the ratios of the x and y face triangular areas to the area of the oblique triangle are $\cos(n, x)$ and $\cos(n, y)$, respectively. These same results could have been obtained more elegantly using vector notation. See the exercises at the end of this chapter.

Now all is ready for summing forces. For example, summing forces in the x direction:

$$T_x dA = \sigma_{xx} dA_x + \sigma_{yx} dA_y + \sigma_{zx} dA_z - \frac{1}{3} \rho B_x dz dA_z$$

Note that the x direction force on the oblique face is the x direction traction multiplied by the actual area of the oblique triangle rather than a projected area. The last term on the right-hand side is, of course, the product of the x direction body force per unit mass, the mass density, and the volume of the tetrahedron, which is one-third the base, dA_z , multiplied by the height, dz . Note that this last term includes one more differential factor than the other terms in the relation. Thus it is infinitesimally small in comparison to the other terms in the identity, and at this point is dropped from further consideration. Dividing through by the nonzero quantity dA yields

$$T_x = \sigma_{xx} \cos(n, x) + \sigma_{yx} \cos(n, y) + \sigma_{zx} \cos(n, z) \quad (1.8a)$$

Similarly, for the other two orthogonal directions

$$\begin{aligned} T_y &= \sigma_{xy} \cos(n, x) + \sigma_{yy} \cos(n, y) + \sigma_{zy} \cos(n, z) \\ T_z &= \sigma_{xz} \cos(n, x) + \sigma_{yz} \cos(n, y) + \sigma_{zz} \cos(n, z) \end{aligned} \quad (1.8b)$$

Note that Eqs. (1.8a) may be written more compactly in matrix form:

$$\begin{Bmatrix} T_x \\ T_y \\ T_z \end{Bmatrix} = \begin{bmatrix} \sigma_{xx} & \sigma_{xy} & \sigma_{xz} \\ \sigma_{xy} & \sigma_{yy} & \sigma_{yz} \\ \sigma_{xz} & \sigma_{yz} & \sigma_{zz} \end{bmatrix} \begin{Bmatrix} \cos(n, x) \\ \cos(n, y) \\ \cos(n, z) \end{Bmatrix} \quad (1.9)$$

or simply as

$$\boxed{\{T\} = [\sigma]\{v\}}$$

where (lower-case nu) $\{v\}$ represents the 3×1 matrix of direction cosines. These equations are cast in matrix form because matrix algebra becomes increasingly useful as the complexity of the structure to be analyzed increases. Note that $[\sigma]$ is a symmetric matrix. Equations (1.8) or Eqs. (1.9) are algebraic equations that tie together (i) the tractions on the outer surface and (ii) the stresses which are the internal response to the input of the tractions and the body forces per unit mass. These are the equilibrium equations on the boundary. They are often referred to as the *Cauchy equation*⁹ (Ref. [3]).

The development of boundary equilibrium equations in coordinate systems other than Cartesian coordinates is usually not necessary because the other coordinate systems are usually employed only when a body's surface or surfaces are congruent with one of the

⁹ Augustin Louis Cauchy (1789–1857), French mathematician (Ref. [71]).

surfaces defined by that other coordinate system.¹⁰ For example, a circular cylindrical outer surface of a body can be made congruent with a surface defined by the radius coordinate of a cylindrical coordinate system when the origin of that radius coordinate is placed at the central axis of the cylinder. In other words, that surface can be specified mathematically by setting the cylindrical radius coordinate, r , equal to the given radius, say r_0 . On that given outer surface, the normal component of the total traction, T_r , for example, would simply coincide with the normal outward pressure on that same surface. Thus, in the cylindrical coordinate system, which is of course the most convenient for a cylindrical surface, this one equilibrium boundary equation would be simply

$$\sigma_{rr}(r_0, \theta, z) = T_r \quad (\text{where } T_r \text{ is a given quantity})$$

If the surface is more complicated than a simple cylindrical, spherical, or other such surface, the usual choice is between using surface-based coordinates, which are of no present interest, or Cartesian coordinates and direction cosines.

In summary, Eqs. (1.6) and Eqs. (1.9) are respectively the internal and external equilibrium equations. The latter equations, the Cauchy equations, relate the internal stresses to the applied tractions. The six distinct stress functions must satisfy both of these sets of equations over their separate domains, that is, over their separate regions of applicability. In addition to the specific names given to these equilibrium and Cauchy equations, there are also general names that apply. These general names emphasize the domain of the equations. Equations that are valid at the boundaries, such as Eqs. (1.9), are called *boundary equations*, or more often *boundary conditions*. Equations that are valid over the interior, such as Eqs. (1.6a), are called *field equations*, or more often *governing differential equations*. The two sets of equations are always distinct and are not interchangeable. The boundary conditions do not add to the number of equations available to determine the unknown functions, which in this case are the six unknown stresses as functions of three spatial coordinates. This is because the boundary conditions are only valid for values of the unknown functions at those fixed values of the spatial coordinates that specify the boundary. Thus the boundary condition equations do not refer to the unknown functions in their general form, and thus do not directly assist in determining the general form of the unknown functions. Hence the boundary equations are not to be counted for determining the adequacy of the number of equations relative to the number of unknowns. In later chapters it will be seen that the solutions to field equations (whether or not they are easily obtained) are applicable to many different forms of the same type of problem, and as such contain unspecified parts (such as constants of integration) that are specialized to the problem at hand by the boundary condition equations. Therefore, after developing the equilibrium boundary conditions, the situation is still one where there are six unknown stresses, but only the three equilibrium equations with which to determine those six unknowns in their general form. Any situation where the number of unknowns exceeds the available number of equations is described as "indeterminate." Clearly, additional equations need to be found. Such equations are found in subsequent chapters by investigating quantities other than stresses. The development of those equations is postponed until several other matters related to stresses alone have been discussed.

¹⁰ A coordinate system is an *orthogonal* coordinate system when the curved surfaces or planes defined by constant values of its coordinates are perpendicular to each other everywhere they meet. *Cartesian*, *cylindrical*, and *spherical* coordinate systems are examples of orthogonal coordinate systems.

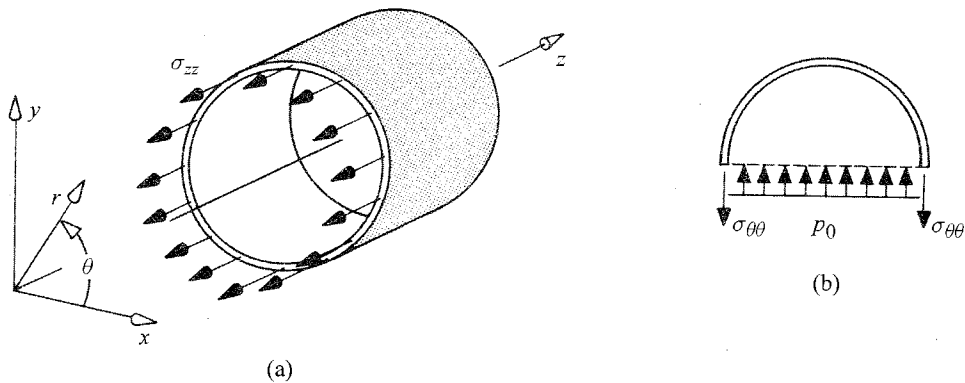


Figure 1.10. (a) Free body diagram of approximately half of a cylindrical pressure vessel showing the cylindrical coordinate system used for the approximate analysis and the only internal stresses that act at the z plane partition. (b) Free body diagram of half of this pressure vessel, and half of the internal gas, showing only the stresses and the pressure acting upon this θ plane partition.

1.4 Plane Stress

The above equations were developed in three spatial dimensions for a general (three-dimensional) state of stress. Occasionally, the shape of the body and the nature of the loading are such as to produce a simpler, essentially two-dimensional, stress state. Examples of such a simpler state of stress are often found in thin (flat or curved) sheets of material. Thin sheet and thin plate construction is commonplace in vehicular structures such as aircraft and ships, where thin skins cover reinforcing grids of beams. An algebraic demonstration of this situation where a common body geometry and a common loading very nearly produce only stresses within the plane of a thin sheet is offered in the next paragraph.

Consider the case of a circular cylinder with closed ends that is loaded with either an internal pressure that exceeds the small external pressure by the amount p_0 , or is loaded by an external pressure that exceeds the small internal pressure by the same value. In the first case, this cylindrical pressure vessel could be a very simplified version of a pressurized aircraft fuselage, and in the second case, a very simplified version of a submarine hull. Let the cylindrical wall thickness, t , be very small compared to the radius of the cylinder, R . With $t \ll R$, the following approximate approach for estimating the stresses within the cylindrical shell is valid away from the juncture of the circular cylinder and the circular end plates. To calculate σ_{zz} , which does not vary with the coordinate θ because of the symmetry of the pressure vessel, consider the free body diagram (FBD) shown in Fig. 1.10(a). Choosing the internal pressure case, the internal force on the endplate is $\pi R^2 p_0$. This force is equilibrated by the total axial force, $2\pi R t \sigma_{zz}$, supplied by the normal stresses, σ_{zz} , which are virtually constant over the shell thickness. Equating the magnitudes of these equal and opposite forces leads to

$$\sigma_{zz} = \frac{p_0 R}{2t}$$

Figure 1.10(b) shows a z plane view of a FBD consisting of the thin sheet of a semicircular part of the original cylinder which has a depth \bar{d} into the paper, and the fluid within that semicircular cylinder. Recalling that pressure is transmitted uniformly throughout a fluid

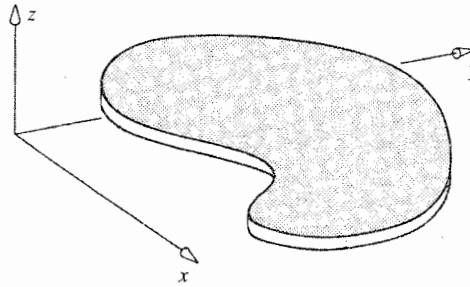


Figure 1.11. A thin, structural body of general planform geometry. If applied loads bend this body, the body is then called a “plate.” If this body is only stretched and/or compressed by loadings in its own plane, then this body is called a “sheet” or a piece of “skin” if thin, or it is called a “slab” if thick.

at rest, the upward fluid pressure, $2R\bar{d}p_0$, is exactly balanced by the total downward force produced by the hoop stress, $2t\bar{d}\sigma_{\theta\theta}$. Thus,

$$\sigma_{\theta\theta} = \frac{p_0 R}{t}$$

It is not possible to calculate the stress in the radial direction by this simple approach. However, an exact analysis to be considered in Chapter 7 shows that its maximum value is the small value

$$\sigma_{rr}|_{max} = -p_0$$

The symmetry of the structure and loading indicates that the shearing stresses in the central portion of the cylinder are all zero. Now compare the magnitudes of the three normal stresses. Since $R \gg t$, the axial stress and the hoop stress, both in-plane stresses, are clearly much greater than the radial stress, an out-of-plane stress. In fact, the radial stress can be ignored in preference to the other two stresses without any significant loss of accuracy. Hence this is a case where the significant stresses are only within the (tangent) plane.

It is worth using the above pressure vessel example to note also that engineers use mathematics as an aid for making engineering decisions, and can sometimes, but not always, leave mathematical purity to those who relish such purity. In other words, for many important structures or structural components subjected to actual loadings, simplifications are possible with regard to describing the state of stress without serious loss of accuracy.

In more general terms, consider the structural body in Fig. 1.11 which has the special shape of a thin, flat sheet. If that body were loaded only with the tractions $T_x(x, y)$ and $T_y(x, y)$ on the cylindrical surface that defines the sheet edges, and the body forces per unit mass were limited to $B_x(x, y)$ and $B_y(x, y)$ then neither the geometry nor the loading would vary in the z direction.¹¹ In this special case all the stresses with a z subscript would be exactly zero, and the remaining stresses would be functions of the x and y variables only. To formally describe this and similar situations, the following definition is introduced. A state of *plane stress* exists when there exists a z axis (or some other such orthogonal axis) such that $\sigma_{xz} = \sigma_{yz} = \sigma_{zz} = 0$, and the loading and remaining stresses are only functions of the x and y coordinates. Thus the above-discussed cylindrical vessel case, where all the

¹¹ Recall that the weight forces are just a special case of the body forces, and in this discussion either the sheet is oriented within the gravitational field so that the weight forces do not have a component in the z direction, or that component is negligibly small compared to the other loads.

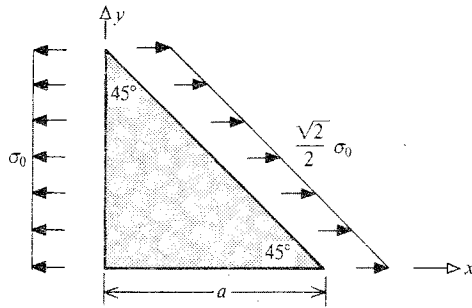


Figure 1.12. Example 1.1. A plane stress problem.

stresses with an r subscript are effectively zero, closely fits the plane stress definition above. The θ, z coordinates are, of course, the plane stress coordinates. In the case of plane stress as described by Cartesian coordinates, the equilibrium and boundary equilibrium (Cauchy) equations respectively reduce to

$$\begin{aligned} \frac{\partial \sigma_{xx}}{\partial x} + \frac{\partial \sigma_{xy}}{\partial y} + \rho B_x &= 0 \\ \frac{\partial \sigma_{xy}}{\partial x} + \frac{\partial \sigma_{yy}}{\partial y} + \rho B_y &= 0 \end{aligned} \quad (1.10)$$

and

$$\begin{aligned} T_x &= \sigma_{xx} \cos(n, x) + \sigma_{xy} \cos(n, y) \\ T_y &= \sigma_{xy} \cos(n, x) + \sigma_{yy} \cos(n, y) \end{aligned} \quad (1.11)$$

In the case of plane stress, there are in general three unknown stresses and just two available equilibrium equations, Eqs. (1.10). Thus this special case is also indeterminate.

The following two example problems are intended to help acclimate the reader to (i) the association between stresses and tractions and (ii) dealing with stresses and tractions as functions of spatial variables.

Example 1.1. Consider a uniformly thin, isosceles, right triangularly shaped piece of sheet material which, in plan view, is located in the upper right quadrant of the xy plane. The vertex opposite to the hypotenuse is at the coordinate origin. The triangle's equal-length edges of length a lie along the x and y axes. The thickness in the z direction is t . The state of stress within the slab is $\sigma_{xx} = \sigma_0$, where σ_0 is a constant with units of stress, and all other stresses are zero. (a) Is this slab in a state of internal equilibrium? (b) Sketch and label the tractions necessary for equilibrium at the boundaries. (c) Are the external loads that result from the applied tractions in equilibrium?

Solution. (a) This is a plane stress problem because all stresses with z subscripts are zero. To test internal equilibrium, it is only necessary to substitute the given stress field into Eqs. (1.10). Since those two equations are satisfied identically, the slab is in a state of internal equilibrium.

(b) The tractions on the three sides of the triangular slab can be calculated using Eqs. (1.11), which in this case reduce to $T_x = \sigma_0 \cos(n, x)$. On the face $y = 0$, $\cos(n, x) = 0$; on the face $x + y = a$, $\cos(n, x) = \sqrt{2}/2$; and on the face $x = 0$, $\cos(n, x) = -1.0$. Hence the tractions are as shown in Fig. 1.12.

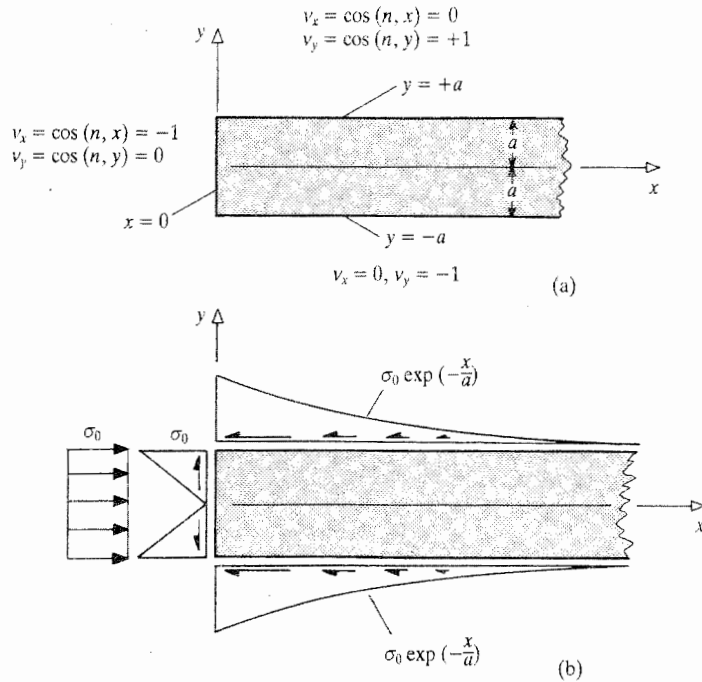


Figure 1.13. Example 1.2. A plane stress problem.

(c) To check that the external loads due to the edge tractions are in equilibrium among themselves, it is sufficient to sum forces and moments with respect to those tractions. Summing forces in the x direction

$$-at\sigma_0 + \frac{2a}{\sqrt{2}}t \frac{\sigma_0\sqrt{2}}{2} = 0$$

Summing forces in the y direction and summing moments in the xy plane about the point $(0, a/2)$ leads to the equalities $0 = 0$. Therefore the external loads are also in equilibrium. ■

Example 1.2. For a case of plane stress (a) show that the following stresses satisfy the equations of equilibrium; and (b) determine and sketch the tractions that must act on the three edges of the semiinfinite, rectangular structure shown in Fig. 1.13(a) in order for these stresses to be in equilibrium with the tractions at the boundary of the structure.

$$\sigma_{xx} = -\sigma_0 \exp\left(\frac{-x}{a}\right) \quad \sigma_{xy} = -\sigma_0 \frac{y}{a} \exp\left(\frac{-x}{a}\right)$$

$$\sigma_{yy} = \frac{1}{2}\sigma_0 \left[1 - \left(\frac{y}{a}\right)^2\right] \exp\left(\frac{-x}{a}\right)$$

where σ_0 is a constant with units of stress, and “exp,” with an argument, is an alternative symbol for e , with a superscript, that is, for the exponential function.

Solution. (a) The plane stress equilibrium equations are Eqs. (1.10). Since there is no mention of body forces, it is implied that they are zero. Direct substitution into Eqs. (1.10) and differentiation yields

$$\frac{\sigma_0}{a} \exp\left(\frac{-x}{a}\right) - \frac{\sigma_0}{a} \exp\left(\frac{-x}{a}\right) \equiv 0$$

$$\frac{\sigma_0}{a} \frac{y}{a} \exp\left(\frac{-x}{a}\right) - \frac{y}{a^2} \sigma_0 \exp\left(\frac{-x}{a}\right) \equiv 0$$

Hence the equilibrium equations are identically satisfied, and therefore these stresses are in a state of internal equilibrium.

(b) This part of the example problem is a bit different in that no tractions are given; that is, it is necessary to use the Cauchy equations, Eqs. (1.11) in order to determine the tractions on the given boundary that complete the equilibrium state of the structure. Figure 1.13(a) provides the values of the direction cosines, and carries forward the notation of subscripted lower-case v 's for the direction cosines of the normal unit vectors that is partly suggested by Eqs. (1.9). Equations (1.11) for the three edges are

At the top edge, $y = +a$

$$T_x(x, a) = \sigma_{xy}(x, a) = -\sigma_0 \exp\left(\frac{-x}{a}\right) \quad \text{and} \quad T_y = 0$$

At the bottom edge, $y = -a$

$$T_x(x, -a) = \sigma_{xy}(x, -a) = -\sigma_0 \exp\left(\frac{-x}{a}\right) \quad \text{and} \quad T_y = 0$$

At the left edge, $x = 0$

$$T_x(0, y) = -\sigma_{xx}(0, y) = +\sigma_0 \quad \text{and} \quad T_y = -\sigma_{xy}(0, y) = \sigma_0 \left(\frac{y}{a}\right)$$

A sketch of these tractions on the rectangular body is provided in Fig. 1.13(b). That sketch concludes the solution. ■

It is necessary to comment upon the above "solution." Integration of the tractions over the semiinfinite top and bottom surfaces confirms the equilibrium of the external loads. However, while these stresses and tractions do satisfy equilibrium everywhere within and upon this body, they are NOT a solution to ANY problem because there are other required conditions that these stresses do not meet. These other requirements are discussed fully in later chapters, and are brought together with the equilibrium requirements to form a complete analysis in Chapters 7 and 8. In other words, the satisfaction of internal and external equilibrium equations is only a beginning, and not always sufficient in itself for a stress solution.

1.5 Summary

Rather than attempt to study each different type of structural system or structural element as a separate entity, the approach taken here is to discover what equations apply

to all structures. Once comprehensive equations are developed, then convenient specializations to particular structural elements can proceed on a more informed basis. To achieve such a sweeping generality, it is necessary to begin the investigation on the differential scale. Differential-sized bodies are the only shapes that can be visualized inside or at the boundary of any structural element, be it a beam, or a plate, or whatever. Concurrent with this geometric choice is the decision to describe all external and internal mechanical loadings in terms of tractions and stresses, respectively. The decision to focus on stresses was prompted by the convenience that the stress concept affords when organizing descriptions of material behavior. Chapters 5 and 6 elaborate upon material behavior in response to stresses. The focus of this chapter, the (internal) equilibrium equations and the Cauchy (boundary condition) equations are simply Newton's laws in terms of stresses and tractions. The equilibrium equations, which are partial differential equations, indicate the price to be paid for complete generality. That price is mathematical complexity. Thus the course of this textbook is to first establish the extent of that complexity, and then to find ways to circumvent that complexity.

When stress components are referenced to an orthogonal coordinate system, they are point functions that describe the magnitude and direction of the force components acting normal to, and in the plane of, areas extending from the point under consideration. All stress components have the units of force over area. The areas associated with the stress components are understood to extend in the positive coordinate axis directions from the point under consideration. It is desirable to distinguish between stresses that act over areas within the body volume and those that act on areas of the outer boundary surfaces. The term "stress" is hereafter reserved for stresses within the volume of the structural body, while the term "traction" is reserved for stresses on the outer boundary surface. The sign conventions for stresses and tractions must be thoroughly memorized.

Every structural body is either in a state of static equilibrium or in a state that can be described as dynamic equilibrium. If the inertia forces are treated like any other body forces, it is not necessary to distinguish between the two types of equilibrium. Every portion of a structural body in equilibrium, including differential-sized elements, must also be in equilibrium. Again, in order to treat a body of general shape in a general way, it is necessary to examine differential-sized sub-volumes of the general body. The application of Newton's second law to differential-sized elements within the body volume and at the boundary surface produces the "equilibrium equations" and "Cauchy's equations," respectively. The equilibrium equations relate the stress components within the body, while Cauchy's equations relate the tractions to the stresses at the boundary. Having available only these equations of equilibrium for the interior and at the boundary of a body is usually not sufficient to determine the stress distribution within that body given the tractions and body forces acting on and throughout the body.

Example 1.3. Write the fully elaborated Cauchy equations for the single boundary edge shown in Fig. 1.14. In this case, "fully elaborated" means write the appropriate argument for each function in your answer. (This way of restricting the variables of the functions that appear in the boundary condition statements is always necessary.) The body possessing the edge in question is in a state of plane stress.

Solution. The equation for the boundary edge is $y = x + a$. The direction cosines for this edge are $v_x = \cos(n, x) = \cos(135^\circ) = -\sqrt{2}/2$, and $v_y = \cos(n, y) = \cos(45^\circ) = +\sqrt{2}/2$. Along that edge $T_x = 0$, and $T_y = -p_0$. Thus, after multiplying through

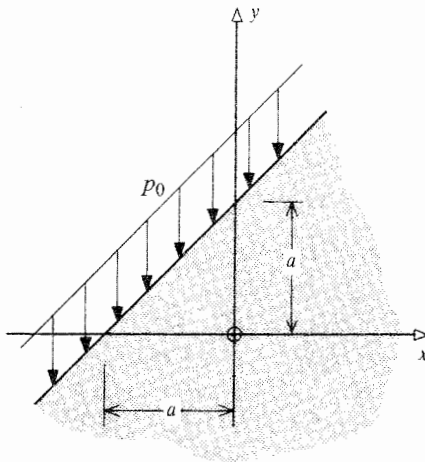


Figure 1.14. Example 1.3. The stipulated boundary and traction.

by 2, the Cauchy equations for this edge are

$$0 = -\sqrt{2}\sigma_{xx}(x, x+a) + \sqrt{2}\sigma_{xy}(x, x+a)$$

$$-2p_0 = -\sqrt{2}\sigma_{xy}(x, x+a) + \sqrt{2}\sigma_{yy}(x, x+a)$$

Of course, the first of the above two equations can be further simplified by division by $\sqrt{2}$. ■

What can be done at this point in the way of exercises is such things as: (i) determine whether proposed states of equilibrium are valid in the interior and at the boundary; (ii) determine tractions given internal stresses; and (iii) pursue the interior and boundary equilibrium concepts in other useful coordinate systems. The following exercises address these possibilities. The first exercise is thrown in to have something to do before the equilibrium equations are established, and just for the fun of it.

Chapter 1 Exercises

- 1.1. Lexa is 12 years old. Lexa is twice as old as Sara was when Lexa was as old as Sara is now. How old is Sara?
- 1.2. (a) Using the standard convention, show the positive stresses with respect to the Cartesian coordinate system that act on the nonhidden faces of the differential-sized rectangular parallelepiped shown in Fig. 1.15(a).
 (b) Do the same for the infinitesimal element defined by cylindrical coordinates as shown in Fig. 1.15(b).
 (c) Do the same for the differential element bounded by surfaces defined by constant values of the spherical coordinates (ρ, θ, ϕ) and which extends from the point P as shown in Fig. 1.15(c). When doing so, be sure to note the direction in which the coordinate ϕ is positive.
 (d) Locate and label the appropriate body force components for each of the three cases above.
- 1.3. (a) Figure 1.16 shows a rectangular piece of sheet metal in a state of plane stress. The rectangular piece is loaded on its thin edges by constant tractions that

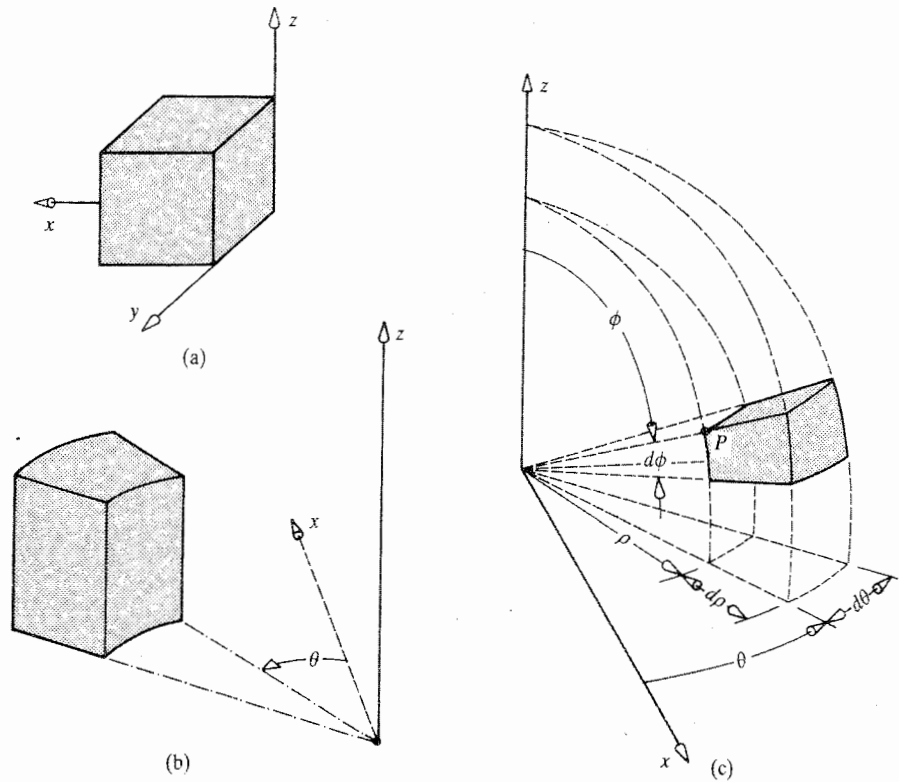


Figure 1.15. (a) Exercise 1.2(a). A differential element defined by Cartesian coordinates. (b) Exercise 1.2(b). A differential element defined by cylindrical coordinates. (c) Exercise 1.2(c). A differential element defined by spherical coordinates. Be sure to note the positive direction of the colatitude coordinate ϕ .

lie in its own plane. Write the mathematical description of the two traction components T_x and T_y for each of the four edges with due regard for the traction sign convention.

- (b) Is $\sigma_{xx}(x, y) = +2p_0$, $\sigma_{yy}(x, y) = -p_0$, and $\sigma_{xy}(x, y) = 0$ a solution of the plane stress equilibrium equations and the plane stress Cauchy equations?
- (c) The quantity σ_0 is a constant with units of stress. Determine the traction boundary conditions on the straight boundary shown in Fig 1.16(b) when the solution for the overall geometry and loading are

$$\sigma_{xx}(x, y) = \sigma_0 \left[\left(\frac{x}{a} \right)^3 \sin \frac{\pi y}{b} + \frac{3}{2} \right],$$

$$\sigma_{xy}(x, y) = \sigma_0 \left[1 - \left(\frac{y}{b} \right)^2 \right] \left[\cos \frac{x}{a} + \frac{2}{3} \left(\frac{x}{a} \right)^2 \right],$$

$$\sigma_{yy}(x, y) = \sigma_0 \left[\frac{1}{2} + \left(\frac{y}{b} \right) \sin \frac{\pi y}{b} \right],$$

and

$$\sigma_{xz} = \sigma_{yz} = \sigma_{zz} = 0$$

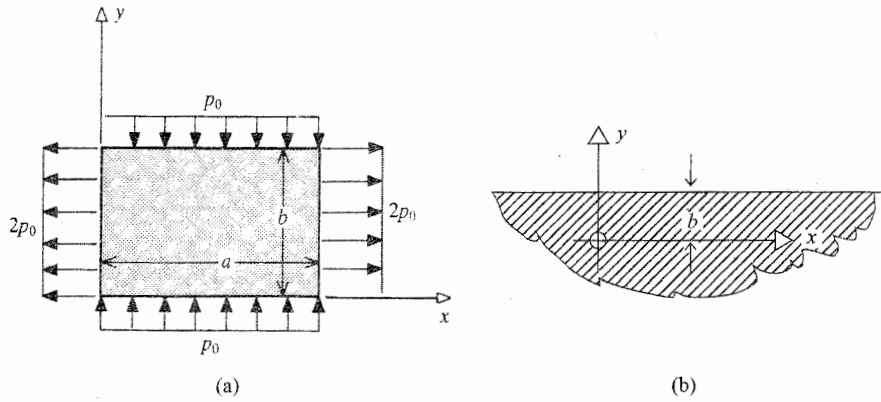


Figure 1.16. Exercise 1.3. Plane stress problems.

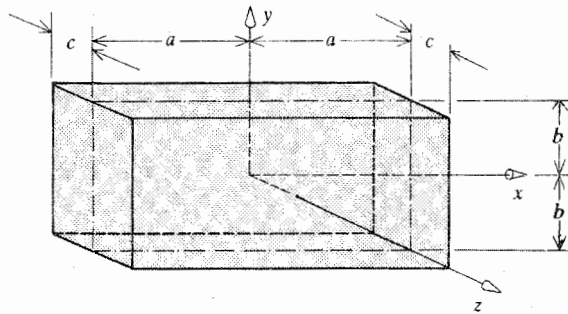


Figure 1.17. Exercises 1.4 and 1.5. The structural body dimensions and coordinate system.

- 1.4. Consider the rectangular piece of sheet metal shown in Fig. 1.17, which has the dimensions $2a \times 2b \times 2c$, where the relative size of $2c$ has been exaggerated for the sake of visual clarity. For the Cartesian coordinate system shown, determine the direction cosines of the normals to the three visible surfaces (i.e., the surfaces $(x = -a, y = +b, z = +c)$) with respect to each Cartesian coordinate.
- 1.5. If the piece of sheet metal of the previous problem (Fig. 1.17) is in a state of plane stress, the body forces are zero, σ_0 is an arbitrary stress value, and if

$$\sigma_{xx} = 0 \quad \sigma_{xy} = -3 \left(\frac{x}{a} \right)^2 \sigma_0 \quad \sigma_{yy} = C \left(\frac{xy}{a^2} \right) \sigma_0$$

- (a) What then must be the value of the constant C in the expression for σ_{yy}
 - (b) What must be the tractions on the faces $x = \pm a$?
 - (c) What must be the tractions on the faces $y = \pm b$?
 - (d) What must be the tractions on the faces $z = \pm c$?
- 1.6. If the carbon fiber composite material sheet shown in Fig. 1.18 is in a state of plane stress where all body forces are zero, and the analytical expressions for the stresses are known to have the forms listed in the diagram, then:
- (a) What relations must exist between the constants $A, B, C,$ and D for the interior of this body to be in a state of equilibrium?

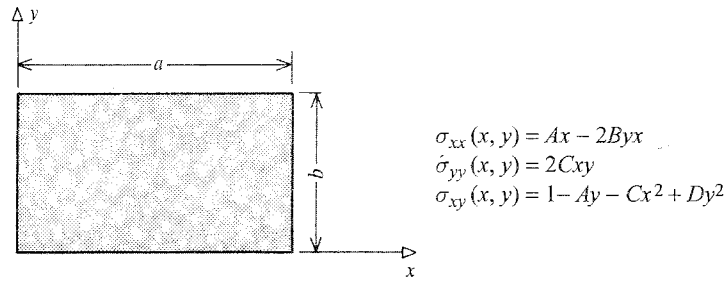


Figure 1.18. Exercise 1.6. A thin sheet and partially determined stresses.

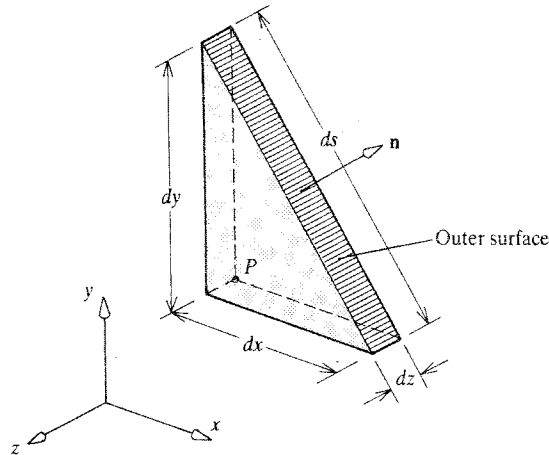


Figure 1.19. Exercise 1.8. A plane stress infinitesimal boundary element and the boundary outer normal.

- (b) Determine all the tractions that must exist on the edge $x = 0$ for that portion of the boundary to be in a state of equilibrium.
- 1.7.** In a variation upon Example 1.1, consider a thin sheet of material (any material) which has the planform shape of a 30° , 60° , 90° ; triangle. The length of the hypotenuse is a . If the Cartesian coordinate system used to describe points on the triangular sheet originates at the right angle, with the positive x axis coinciding with the short side of length $\frac{1}{2}a$, and the positive y axis coinciding with the side of length $(\sqrt{3}/2)a$, and if each side is loaded by an edge traction of magnitude σ_0 that is everywhere perpendicular to, and directed inward towards each thin edge, then determine:
- Whether the triangular shaped body is in a state of external equilibrium, that is, whether the externally applied force vectors, produced by the tractions acting upon the three triangular edges, sum to zero.
 - Whether the plane stress solution $\sigma_{xx}(x, y) = \sigma_{yy}(x, y) = -\sigma_0$, and $\sigma_{xy}(x, y) = 0$ satisfies both the interior and boundary equilibrium equations.

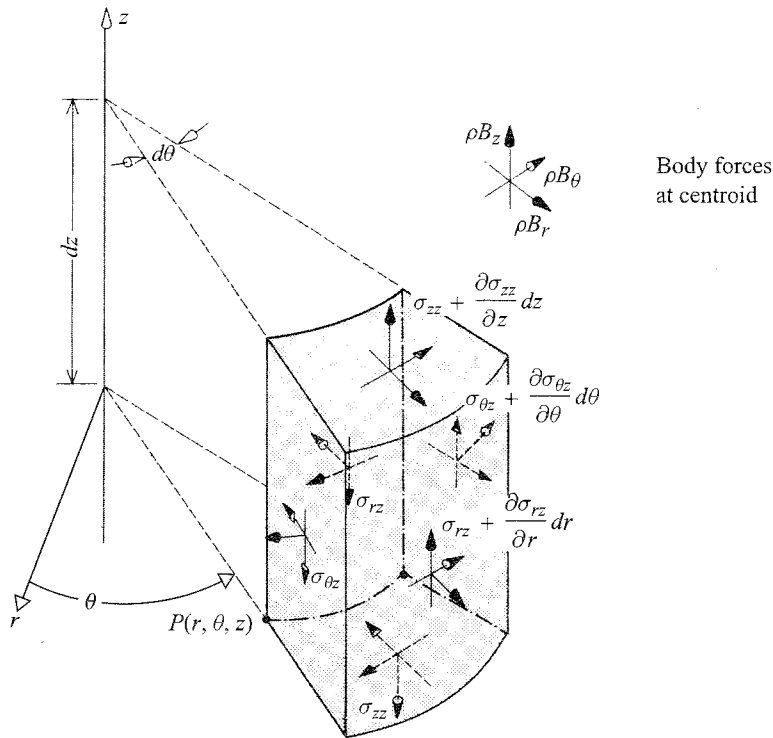


Figure 1.20. Exercise 1.9. A partially labelled free body diagram.

- 1.8. In the case of plane stress, directions can be specified by use of a single angle. Use Fig. 1.19 to derive the plane stress Cartesian boundary condition (i.e., Cauchy) equations in terms of the angle θ , where θ is the angle between the normal to the outer boundary surface and the x axis. It is left to the reader to augment the drawing with the positive representations of the appropriate stress and traction vectors. *Hint:* From the geometry of the triangle, $dy/ds = \cos \theta$, and $dx/ds = \sin \theta$.
- 1.9. Figure 1.20 depicts a differential element defined by cylindrical coordinates. For the sake of clarity, only those stresses that act in the z direction are labelled.
- (a) Use Fig. 1.20 to show that the interior equilibrium equation in terms of cylindrical coordinates for the z direction at the arbitrary point P is as stated below. *Hint:* Be sure to correctly calculate the areas associated with each stress; for example, the front r face has an area equal to $(r + dr) d\theta dz$. The volume is $(r + dr/2) dr d\theta dz$.

$$r \left(\frac{\partial \sigma_{rz}}{\partial r} \right) + \sigma_{rz} + \frac{\partial \sigma_{\theta z}}{\partial \theta} + r \left(\frac{\partial \sigma_{zz}}{\partial z} \right) + r \rho B_z = 0$$

- (b) Determine whether or not the order of the subscripts is significant for stresses defined in terms of cylindrical coordinates by investigating whether or not $\sigma_{rz} = \sigma_{zr}$.
- (c) Determine whether $\sigma_{r\theta} = \sigma_{\theta r}$.
- (d) Determine whether $\sigma_{z\theta} = \sigma_{\theta z}$.

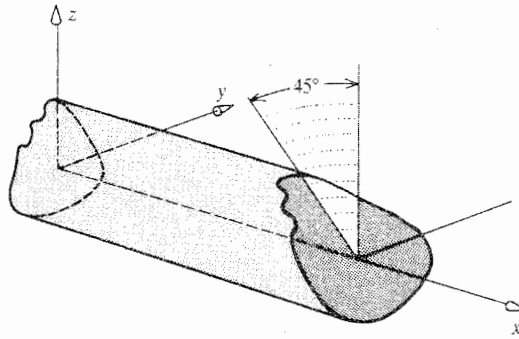


Figure 1.21. Exercise 1.12(b). The structural body geometry.

- 1.10. (a) Plane stress in terms of cylindrical coordinates is exactly the same as for Cartesian coordinates; that is, all z -subscripted stresses are zero, and so forth. Show that the plane stress interior equilibrium equations for the r and θ directions are

$$r \left(\frac{\partial \sigma_{rr}}{\partial r} \right) + \frac{\partial \sigma_{r\theta}}{\partial \theta} + \sigma_{rr} - \sigma_{\theta\theta} + r\rho B_r = 0$$

$$r \left(\frac{\partial \sigma_{\theta r}}{\partial r} \right) + \frac{\partial \sigma_{\theta\theta}}{\partial \theta} + 2\sigma_{r\theta} + r\rho B_\theta = 0$$

Hint: Note that the stresses acting on the theta faces are at an angle of $\pm d\theta/2$ or $\pm(\pi/2 + d\theta/2)$ to the axis of symmetry for the element geometry. Note further that $\sin(d\theta/2) \approx d\theta/2$ and $\cos(d\theta/2) \approx 1.0$ are very good approximations for infinitesimal angles.

- (b) By both direct summation for a differential element, and also by substitution into the equilibrium equations derived in part (a), show that the following constant stresses are a possible equilibrium plane stress state when the body forces are zero: $\sigma_{rr} = \sigma_{\theta\theta} = \sigma_0$, and $\sigma_{r\theta} = 0$.
- (c) Extend the above plane stress equations to the three-dimensional case of Fig. 1.20.
- 1.11. Are the units of each term in each interior equilibrium equation of Exercises 1.9 and 1.10 consistent with every other term?
- 1.12. Consider a straight, uniform bar of long or short length L , and an arbitrary cross-sectional area A . Let the two ends of the bar be planes that are perpendicular to the cylindrical surface. Let all body forces and temperature changes be negligible, and let N be the magnitude of the total tensile force acting at each end of the bar.
- (a) If the x axis runs the length of the bar, and if the bar's cylindrical surface is traction-free while the result of the tensile load N is that the end cross-sections are loaded uniformly with a traction $T_x = N/A$ on the $x = L$ face and a traction $T_x = -N/A$ at the $x = 0$ face, then show that the solution $\sigma_{xx} = +N/A$ with all other stresses equal to zero satisfies the interior equilibrium equations and the Cauchy equations on the boundary.
- (b) As shown in Fig. 1.21, if the end plane at $x = L$, which was previously perpendicular to the x axis, is now rotated 45° about the y axis so that $\cos(n, x) = \cos(n, z) = \sqrt{2}/2$, and $\cos(n, y) = 0$, then with the same

uniform tensile loading in the x direction of total magnitude N , what now is the mathematical description of the tractions at this right-hand end? Is the stress solution of part (a) still valid in this case? If so, how can this problem be extended so as to draw a conclusion for a body of a general shape subjected to this special type of traction which acts only in either a positive or negative coordinate direction? *Hint:* Exercise 1.14 shows that an oblique area is equal to its projected area divided by the cosine of the angle between the normals to the two areas.

FOR THE EAGER

- 1.13. A force acting in the (a) z direction; (b) y direction; (c) x direction, of magnitude N is uniformly distributed over a triangular plane whose vertices are the three points $(a, 0, 0)$, $(0, 2a, 0)$, and $(0, 0, 3a)$. What then are the magnitudes of the normal and total shear stress vectors acting upon the triangular area? What are the stress components on this oblique triangular area in the directions of the positive coordinate axes? *Hints:* For part (a), write $\mathbf{N} = N\mathbf{k}$; determine the expression for the unit vector normal to the triangular area by recalling the result for the cross product of two vectors; and a unit vector is obtained by dividing a vector by its magnitude.
- 1.14. Consider again the tetrahedron used to determine the boundary equilibrium equations, Fig. 1.9(a). Define three vectors each originating at point P , and extending to the respective points A , B , and C . Use these vectors and their differences to determine the relations between the oblique differential area and the other three differential areas. *Hint:* Recall again that one-half of the cross product of two vectors with a common origin is a vector whose magnitude is the area of the triangle defined by the two vectors, and whose direction is normal to both of the product vectors.
- 1.15. In cylindrical coordinates, what is meant by the positive " θ direction" is the direction of increasing θ along a circular arc of fixed values of the coordinates r and z . Since all previous changes in stress quantities have been described using partial derivatives with respect to a coordinate that directly measures distance, justify using a partial derivative with respect to θ , an angle, to describe changes in the positive θ direction as is done, for example, in Exercise 1.10.

FOR THE ESPECIALLY EAGER

- 1.16. In order to illustrate that the resulting moment on a differential face resulting from a planar (tilted) stress distribution acting over that differential face does involve four differential factors, consider the special case where the tilt is in only one direction, say the x direction on a z face as shown in Fig. 1.22. For ease of orientation, choose the front z face, which is at the top of the differential element, and focus only on the normal stress there which, for brevity, is identified by the temporary symbol σ_{zz}^* . Recall that the value of the normal stress on this or any other such differential surface is the average stress. Since the distances are infinitesimal, the average stress is the stress at the center of the differential face. The slope of the stress distribution in this situation is simply $\partial\sigma_{zz}^*/\partial x$. Since slope multiplied by "run" equals "rise," the maximum changes in the stress distribution are as shown. Using the given sketch, proceed to calculate the moment produced by the change in the stress distribution over the area of the differential face.

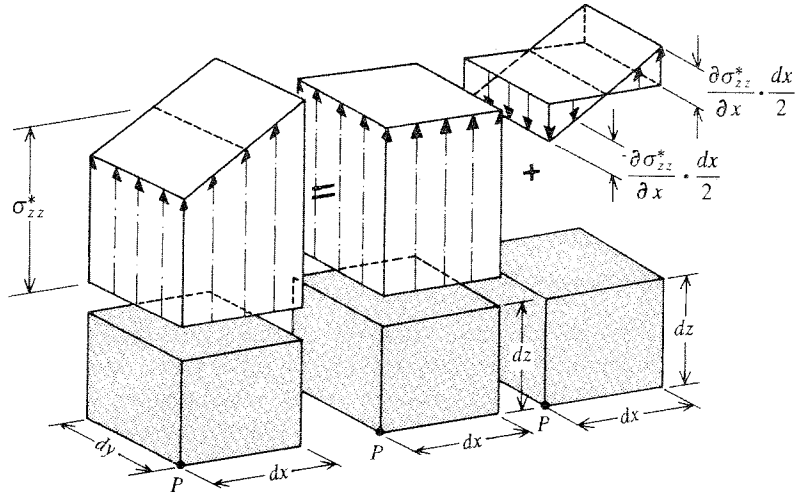


Figure 1.22. Exercise 1.16. The stress distribution diagram for the purpose of showing that the surface moments are insignificant.

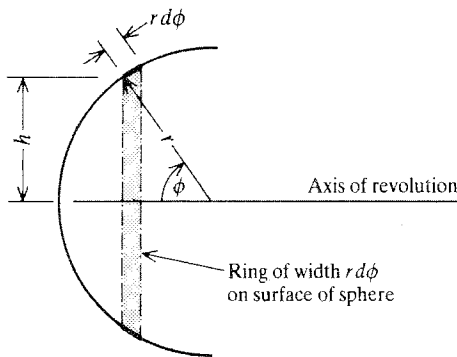


Figure 1.23. Exercise 1.17. The geometric details of a spherical surface of revolution.

1.17. Use Fig. 1.15(c) to write the general stress equilibrium equation in terms of spherical coordinates for

- The radial direction (use r instead of ρ , saving ρ as the symbol for the mass density).
- The ϕ direction.
- The θ direction.

Hint: The surface areas of the differential-sized element are as follows.

$$\text{For either } \theta \text{ face} \quad (r + \frac{1}{2}dr)d\phi dr \approx r d\phi dr$$

$$\text{For an upper } \phi \text{ face} \quad (r + \frac{1}{2}dr) \sin \phi d\theta dr \approx r \sin \phi d\theta dr$$

$$\text{For a lower } \phi \text{ face} \quad (r + \frac{1}{2}dr) \sin(\phi + d\phi) d\theta dr \approx r(\sin \phi + d\phi \cos \phi) d\theta dr$$

$$\text{For an inner } r \text{ face} \quad r^2 \sin \phi d\phi d\theta$$

$$\text{For an outer } r \text{ face} \quad (r + dr)^2 \sin \phi d\phi d\theta \approx (r + 2r dr) \sin \phi d\phi d\theta$$

Comment. The primary difficulty of this task is determining the areas of the six faces of, and the volume of, the differential-sized free body defined by

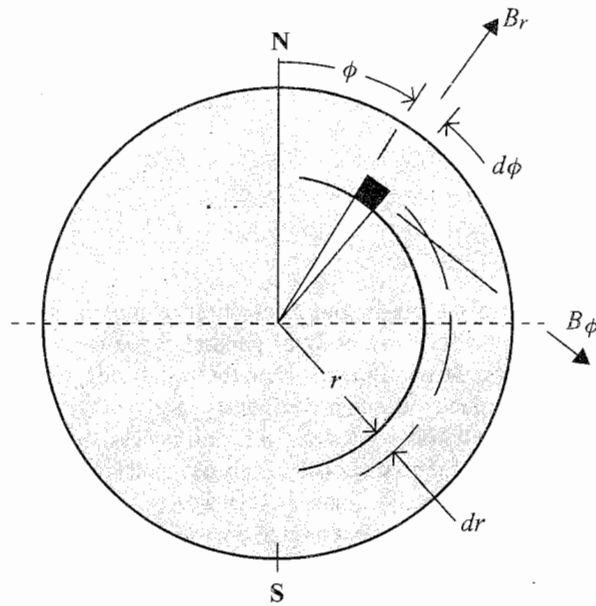


Figure 1.24. Exercise 1.18.

constant values of the three spherical coordinates. The areas of the θ and ϕ faces are determined simply from the planar geometry of circular sectors. However, it is necessary to recognize that the arc length for a ϕ surface is $r \sin \phi d\theta$, which fact is easily established by use of the result of Exercise 10.19. The third area, the area of the spherical differential surface at the radius value r and colatitude angle ϕ can be determined by treating the spherical segment as part of a surface of revolution about an x axis. See Fig. 1.23 for the meaning of the temporary symbol h . By this approach, first convert the expression for the area of the differential ring of revolution ($2\pi h ds$) into spherical coordinates ($ds = r d\phi$, $h = r \sin \phi$); and then proportionalize that area on the basis of the equatorial arc that defines the differential area in question (i.e., multiply by the factor $d\theta/2\pi$), and thus obtain the area solution as $r^2 \sin \phi d\phi d\theta$.

One way to obtain the expression for the differential volume is to calculate the value of the Jacobian. On the other hand, a purely geometric approach would be to take a cue from the answer for the differential volume in cylindrical coordinates. In the cylindrical coordinate case, the differential volume is $r dr d\theta dz$, which is simply the product of the edge lengths at point P . Mimicking that answer, the differential volume for spherical coordinates is $d(\text{Vol.}) = r^2 \sin \phi d\theta d\phi dr$.

- 1.18. The dense, uniform spherical object shown in Fig. 1.24 is known to rotate about its own axis of rotation with a constant angular velocity Ω . If the radius of the sphere is R , and the law of gravitational attractions *within* the sphere is $g(r) = rg_0/R$,
- what are the body forces per unit mass B_r , B_θ , and B_ϕ ?
 - by symmetry, what stresses must be zero throughout the sphere?
 - which derivatives with respect to the spherical coordinates r , θ , and ϕ must be zero?

Stresses and Coordinate Axis Rotations

2.1 Introduction

In Chapter 1 the choice of the origin and orientation of the analysis Cartesian coordinate system was made arbitrarily. For a body of general shape there simply is no geometric feature with which to align the coordinate system for the advantage of the analyst. Even if the structure has a special geometry that clearly suggests an advantage for a particular origin or orientation of a Cartesian coordinate system, it is still necessary to consider the following question. What effect would there be upon the analysis results (e.g., the calculated values of the stresses) if another Cartesian coordinate system were selected that is different from the first in its origin and orientation? In general, the answer is that the set of stresses associated with the second Cartesian coordinate system are different from those that are associated with the first Cartesian coordinate system. For example, consider the first bar of Fig. 1.1(a). If the first Cartesian coordinate system is such that the x axis runs along the length of the bar, then with the end forces applied as uniform tractions, the first set of stresses would be $\sigma_{xx} = N/A$ with the other five stresses equal to zero. Similarly, if the second Cartesian coordinate system were such that the y axis ran the length of the bar, the second set of stresses would be $\sigma_{yy} = N/A$ with the other five stresses equal to zero. These two sets of stresses are different, but the physical reality of the loaded bar is not changed in the slightest by the analyst's choice of coordinate system. The only thing that does change is the mathematical description of that unchanged physical reality. Note that nothing was said about the origins of the above two Cartesian coordinate systems. In this case only their orientation mattered.

The above observation suggests that there may be a relationship between the above two sets of stresses, or any two sets of stresses, at a given interior point based on the extent of the relative rotation of the Cartesian coordinate systems. Thus the question: Is knowing the values of the set of six stresses in one Cartesian coordinate system at an arbitrary interior point sufficient, at the same arbitrary point in the structure, to know all six stresses in any other Cartesian coordinate system? Another related question is, How is it possible to determine the coordinate system that is associated with the greatest values of each of the six stresses? If the information contained in one set of stresses for one coordinate system is not sufficient to develop the values of another such set of stresses for another coordinate system, then a very large number of repetitive analyses may be necessary to develop a complete picture of how the stresses at a particular point vary as the various planes passing through the point of interest are rotated relative to each other. The purpose of this chapter is to answer these questions for Cartesian coordinate systems, and, after that, to deal with other orthogonal coordinate systems as well.

2.2 Stress Values in Other Cartesian Coordinate Systems

Recall that stresses are associated with a particular coordinate system because the coordinate system defines the surfaces on which the stresses act. Consider two Cartesian coordinate systems each of which is arbitrarily located in space. In general, either coordinate

system can be made coincident with the other by a series of three translations and three rotations. Hence, when discussing stresses in different coordinate systems, it is perhaps necessary to consider both translations and rotations of coordinate axes. The next paragraph disposes of the need to consider translations of coordinate axes.

As a starting point, let it be assumed that the stresses associated with one particular Cartesian coordinate system are known. Consider a second Cartesian coordinate system that is arbitrarily translated in space relative to the first coordinate system. The orientations of the planes defined by the two coordinate systems at any point of interest are exactly the same. That is, the x planes, y planes, and z planes are identical because, for example, it is the orientation of the x direction, not the x value that defines the x plane. In other words, the geometries of the differential-sized planes at any point P are exactly the same in either coordinate system. Also note again that the applied loads, material, and the geometry of the structure are not in any way affected by the analyst's choice of a coordinate system. Therefore the internal response to those applied loads, that is, the internal load distribution, is also unaffected by the choice of the coordinate system. Neither the interior stress distribution nor the planes through which that interior stress system acts, are altered by use of a translated coordinate system. Hence the stresses associated with two such Cartesian coordinate systems are the same, and Cartesian coordinate system translations need not be given any further attention with respect to stresses.

Now let the second Cartesian coordinate system be rotated in an arbitrary manner in space relative to the first Cartesian coordinate system. The first coordinate system is referred to as the original coordinate system; see Fig. 2.1(a). Let the coordinates of, and the stresses associated with, the second, rotated coordinate system be distinguished from those of the first system by the use of asterisks.¹ Consider the plane defined by the x^* coordinate. Let the previously adopted stress naming convention be slightly simplified so that the normal and shear stresses on the x^* plane are symbolized as σ_{xx}^* , σ_{xy}^* , and σ_{xz}^* . In order to pursue a possible relationship between the first and second sets of stresses, put a differential-sized x^* plane together with the three differential-sized planes of the original coordinate system. The result is the differential-sized tetrahedron extending from the arbitrary point P as shown in Fig. 2.1(b). Unlike the tetrahedron used to derive the Cauchy equations, this one is at an arbitrary *interior* point, and thus stresses rather than tractions act on the oblique face. Since it previously proved useful to sum forces on such stress-decorated differential bodies, that summation process is repeated below. The question immediately arises as to the direction in which forces should be summed. If forces are summed, for example, in the x direction, then components of all three of the x^* face stresses will appear in the result. On the other hand, if forces are summed in one of the directions of the rotated coordinate system, then only one x^* face stress will appear in the result along with the many components of the stresses associated with the original (without asterisk) coordinate system. The purpose of the summation is to determine whether the values of the rotated set of stresses are uniquely determined by those of the original set. Thus it is preferable that the individual values of the rotated set of stresses be sought in terms of the stresses associated with the original coordinate system. In other words, summing in the direction of the rotated coordinates is preferable.

Consider summing forces in the x^* direction. At first glance, this appears to be a daunting task. It is necessary to obtain the components of all the back face stresses and body forces

¹ Note that the asterisks of this and succeeding chapters have no relation whatsoever to the temporary asterisks used in the previous chapter.

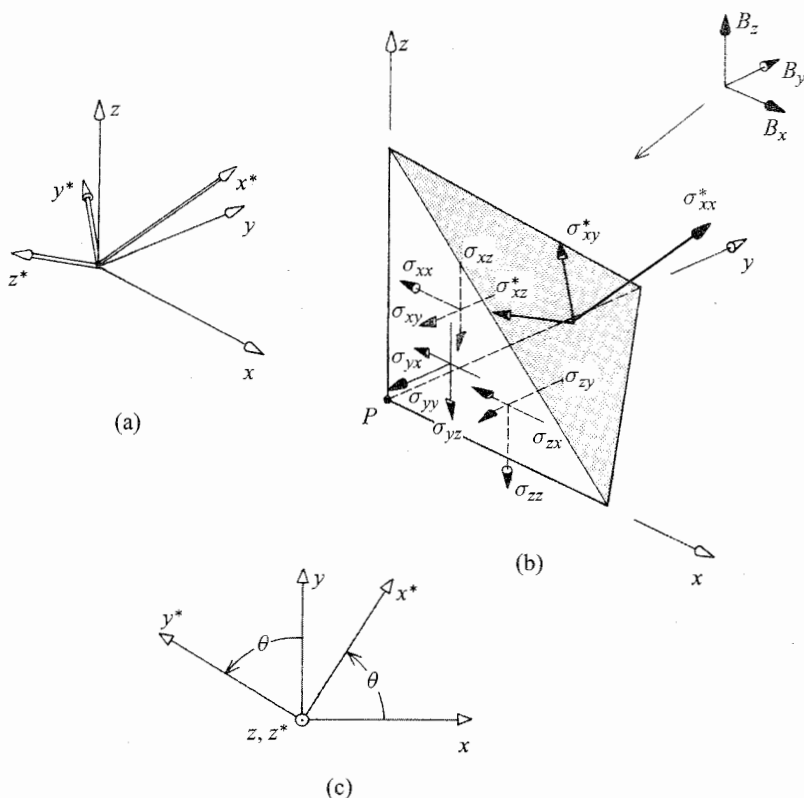


Figure 2.1. (a) Both the original and arbitrarily rotated Cartesian coordinate systems, where the latter coordinates are designated by asterisks. (b) A free body diagram in the shape of an irregular tetrahedron whose oblique face is perpendicular to the x^* axis. (c) Coordinate axis rotations confined to the z plane.

per unit mass in the x^* direction. The size of the task at hand requires careful organization and some discussion. As a preliminary step, consider the vectors \mathbf{A} and \mathbf{B} shown in Fig. 2.2(a). If θ is the angle between the two vectors, then the magnitude of the component of the vector \mathbf{A} in the direction of the vector \mathbf{B} is $A \cos \theta$. Similarly, if the angle between the vectors \mathbf{B} and \mathbf{C} is ϕ , then the magnitude of the component of the vector \mathbf{C} in the direction of the vector \mathbf{B} is $C \cos \phi$ where $\cos \phi$ is a negative quantity. It is important to note that the direction of the component is accounted for by the sign of the cosine. This means that all that is necessary to obtain the magnitude of the component of one vector in the direction of another vector is simply to multiply the magnitude of the first vector by the cosine of the angle between the two vectors.

In order to describe the angles between the stress vectors acting upon the differential tetrahedron, first note that the orientation of the rotated Cartesian coordinate system relative to the original coordinate system can be fully specified by means of the angles between their respective coordinate axes. Between any one coordinate axis of the original coordinate system and any one coordinate axis of the rotated coordinate system, either one of two angles can be used to describe the relative rotation of those two coordinate axes. One of these two angles is always less than 180° , and the other is always greater than 180° . Let the nine angles

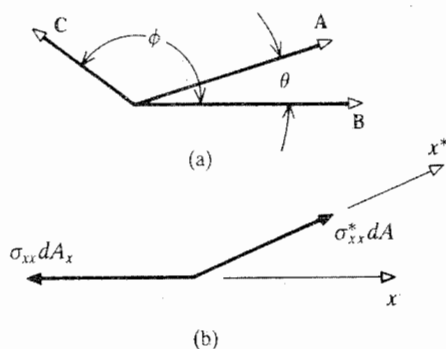


Figure 2.2. A diagram for explaining how to routinely obtain vector components in a given direction.

that describe the relative rotations between such pairs of coordinate axes always be chosen so that they lie within the closed interval $[0, \pi]$. For this range of values for the nine angles, the cosines of these angles are unambiguously related to the angles themselves.² In all that follows, these orientation-determining cosines are referred to as the *direction cosines*.

Since there are nine different direction cosines, and they are used extensively, it is desirable to introduce a brief notation. First let, for example, the direction cosine between the x^* axis and the y axis be denoted as $\cos(x^*, y)$. Then, for brevity, let $\cos(x^*, y)$ be denoted as c_{xy} , where the first subscript *always* refers to the rotated coordinate system, that is, the coordinate system denoted by asterisks, while the second subscript *always* refers to the original coordinate system. Note that $c_{xy} \neq c_{yx}$ because the angle between the x^* and y axes is in general not the same as the angle between the y^* and x axes. They are two different pairs of axes.

In the summation of forces acting upon the tetrahedron that follows, be sure to understand that the angles of the direction cosines are those between the positive directions of the coordinate axes, not those between the positive directions of the stresses. All the back face stress vectors acting on the differential tetrahedron faces are positive in the negative directions of the original coordinate axes. Therefore all the cosines of the angles between the various stress vectors of the original coordinate system and the stress vectors of the rotated coordinate system are negative values of the direction cosines. That is, $\cos(\theta + \pi) = -\cos \theta$. On the other hand, the body force vectors are in the positive original coordinate axis directions, and thus the cosines of the angles between them and the stresses of the rotated coordinate system are the positive values of the direction cosines.

To test the contemplated summation procedure simply, examine Fig. 2.2(b), which is just a variation on a small portion of Fig. 2.1(b). The variation is, of course, that force vectors rather than stress vectors are shown in Fig. 2.2(b). Summing forces in the x^* direction for just those two forces yields $\sigma_{x^*x^*} dA - \sigma_{xx} dA_x c_{xx}$. Again, the minus sign is used because the σ_{xx} vector is in the negative x direction. Since the angle between the x^* and x axes is acute as drawn, c_{xx} is a positive number, and thus the summation procedure is correct in that the two force vectors shown are somewhat opposing each other. With this small confidence-building

² In mathematics, this unambiguous situation is called a "one-to-one mapping."

exercise completed, all is ready for summing forces on the tetrahedron of Fig. 2.1(b). Doing so in the x^* direction yields

$$\begin{aligned} \sigma_{xx}^* dA - \sigma_{xx} dA_x c_{xx} - \sigma_{xy} dA_x c_{xy} - \sigma_{xz} dA_x c_{xz} \\ - \sigma_{yx} dA_y c_{yx} - \sigma_{yy} dA_y c_{yy} - \sigma_{yz} dA_y c_{yz} \\ - \sigma_{zx} dA_z c_{zx} - \sigma_{zy} dA_z c_{zy} - \sigma_{zz} dA_z c_{zz} \\ + \frac{1}{3} \rho [B_x c_{xx} + B_y c_{yy} + B_z c_{zz}] dz dA_z = 0 \end{aligned}$$

Divide through by the nonzero quantity dA . Since the x^* direction is the normal direction for the oblique face, the result from the previous chapter that $dA_x/dA = \cos(n, x)$ means here that the same ratio equals $\cos(x^*, x) = c_{xx}$. Furthermore, $dA_y/dA = c_{xy}$, and $dA_z/dA = c_{xz}$. Since the body force terms include an extra differential factor, they may be discarded as before. Regrouping terms leads to the result

$$\sigma_{xx}^* = \sigma_{xx} c_{xx}^2 + \sigma_{yy} c_{xy}^2 + \sigma_{zz} c_{xz}^2 + 2(\sigma_{xy} c_{xx} c_{xy} + \sigma_{xz} c_{xx} c_{xz} + \sigma_{yz} c_{xy} c_{xz}) \quad (2.1)$$

The same mechanical process works when summing forces in the y^* direction. It is worth repeating the process to develop mastery. Summing forces in the y^* direction yields

$$\begin{aligned} \sigma_{xy}^* dA - \sigma_{xx} dA_x c_{yx} - \sigma_{xy} dA_x c_{yy} - \sigma_{xz} dA_x c_{yz} \\ - \sigma_{yx} dA_y c_{yx} - \sigma_{yy} dA_y c_{yy} - \sigma_{yz} dA_y c_{yz} \\ - \sigma_{zx} dA_z c_{yx} - \sigma_{zy} dA_z c_{yy} - \sigma_{zz} dA_z c_{yz} \\ + \frac{1}{3} \rho [B_x c_{yx} + B_y c_{yy} + B_z c_{yz}] dz dA_z = 0 \end{aligned}$$

Again, dividing by dA , dropping the body force terms as negligible, and regrouping for clarity, yields

$$\begin{aligned} \sigma_{xy}^* = \sigma_{xx} c_{xx} c_{yx} + \sigma_{yy} c_{xy} c_{yy} + \sigma_{zz} c_{xz} c_{yz} + \sigma_{xy} (c_{xx} c_{yy} + c_{xy} c_{yx}) \\ + \sigma_{xz} (c_{xx} c_{yz} + c_{xz} c_{yx}) + \sigma_{yz} (c_{xy} c_{yz} + c_{xz} c_{yy}) \end{aligned} \quad (2.2)$$

Note the regular pattern that the subscripts follow in Eqs. (2.1) and (2.2). The first subscripts in each pair of direction cosines refer to the stress on the left-hand side. The second subscripts refer to the right-hand side stress for which the direction cosines are factors. Regular patterns should always be sought and then used to check whether there are mistakes.

The above process is quite manageable for the x^* face. A particularly interesting aspect of this process compared to the corresponding and usual (two-dimensional) plane stress derivation is that this process works just as well and exactly the same way for the y^* and z^* faces. If a diagram is desired, it is only necessary to relabel the oblique face in Fig. 2.1(b) as the y^* or z^* face, as desired. The corresponding change in the equations is, for example for a z^* face, the replacement of σ_{xx}^* by σ_{zz}^* and σ_{xy}^* by σ_{zy}^* , and the replacement of x as the first subscript for all the direction cosines by z . The result for all six of the stresses in the rotated coordinate system can be written compactly in matrix form as

$$[\sigma^*] = [c][\sigma][c]^t \quad (2.3)$$

where the nonsymmetrical matrix of direction cosines, $[c]$, and the symmetrical stress matrix $[\sigma]$ are defined as

$$[c] = \begin{bmatrix} c_{xx} & c_{xy} & c_{xz} \\ c_{yx} & c_{yy} & c_{yz} \\ c_{zx} & c_{zy} & c_{zz} \end{bmatrix} \quad [\sigma] = \begin{bmatrix} \sigma_{xx} & \sigma_{xy} & \sigma_{xz} \\ \sigma_{xy} & \sigma_{yy} & \sigma_{yz} \\ \sigma_{xz} & \sigma_{yz} & \sigma_{zz} \end{bmatrix} \quad (2.4)$$

The matrix $[\sigma^*]$ has the same form as the $[\sigma]$ matrix. Equation (2.3) clearly demonstrates that all the stresses in one Cartesian coordinate system are uniquely determined by those in any other Cartesian coordinate system. Equation (2.3) is also valid for non-Cartesian orthogonal coordinate systems.

Before proceeding to the determination of the maximum values of the stresses and the coordinate system associated with those maximum values, the above equations will be specialized for the important case of plane stress. As the reader recalls, the plane stress state is one where there exists a z axis such that there are no stresses on any z plane, and none of the applied loadings or other stresses vary in the z direction. The best way of dealing with the rotation of axes in the case of plane stress is to require that the z^* axis parallel the z axis. The two sets of coordinate axes for plane stress are shown in Fig. 2.1(c). When the requirement that the z^* axis parallel the z axis is met, it is possible to conclude immediately that all three of the z -subscripted stresses in the rotated coordinate system are zero. It is also evident that $c_{zx} = c_{zy} = c_{xz} = c_{yz} = 0$, and $c_{zz} = 1.0$. Substituting the above special values for the direction cosines into Eq. (2.3) provides confirmation that the z -subscripted stresses in the rotated coordinate axes are zero, and the other stresses are not zero in general. Extracting the nonzero matrix elements for close inspection, yields the result

$$\begin{aligned}\sigma_{xx}^* &= \sigma_{xx}c_{xx}^2 + \sigma_{yy}c_{xy}^2 + 2\sigma_{xy}c_{xx}c_{xy} \\ \sigma_{yy}^* &= \sigma_{xx}c_{yx}^2 + \sigma_{yy}c_{yy}^2 + 2\sigma_{xy}c_{yx}c_{yy} \\ \sigma_{xy}^* &= \sigma_{xx}c_{xx}c_{yx} + \sigma_{yy}c_{xy}c_{yy} + \sigma_{xy}(c_{xx}c_{yy} + c_{xy}c_{yx})\end{aligned}\quad (2.5)$$

or

$$\begin{bmatrix} \sigma_{xx}^* & \sigma_{xy}^* \\ \sigma_{xy}^* & \sigma_{yy}^* \end{bmatrix} = \begin{bmatrix} c_{xx} & c_{xy} \\ c_{yx} & c_{yy} \end{bmatrix} \begin{bmatrix} \sigma_{xx} & \sigma_{xy} \\ \sigma_{xy} & \sigma_{yy} \end{bmatrix} \begin{bmatrix} c_{xx} & c_{xy} \\ c_{yx} & c_{yy} \end{bmatrix}^t$$

Referring again to Fig. 2.1(c), for this simpler situation the four nonzero direction cosines of interest can be rewritten in terms of the single angle θ which as shown is positive when the x^* axis is rotated counterclockwise from the x axis. Specifically, $c_{xx} = \cos \theta$, $c_{xy} = \cos((\pi/2) - \theta) = \sin \theta$, $c_{yx} = \cos((\pi/2) + \theta) = -\sin \theta$, and $c_{yy} = \cos \theta$. Substituting for the direction cosines yields

$$\begin{aligned}\sigma_{xx}^* &= \sigma_{xx} \cos^2 \theta + \sigma_{yy} \sin^2 \theta + 2\sigma_{xy} \sin \theta \cos \theta \\ \sigma_{yy}^* &= \sigma_{xx} \sin^2 \theta + \sigma_{yy} \cos^2 \theta - 2\sigma_{xy} \sin \theta \cos \theta \\ \sigma_{xy}^* &= (\sigma_{yy} - \sigma_{xx}) \sin \theta \cos \theta + \sigma_{xy}(\cos^2 \theta - \sin^2 \theta)\end{aligned}\quad (2.6)$$

Equations (2.6), the plane stress equivalent to the more general case represented by Eq. (2.3), are the subject of exercises designed to involve the reader in the process of rotating Cartesian coordinate axes. The rotation process is important because it is the means by which the maximum tensile, compressive, and shear stresses can be identified.

2.3 The Determination of Maximum Stress Values

Before beginning the somewhat lengthy development of the solution for the maximum values for the normal and shear stresses, it may be worthwhile to recall the differential calculus procedure for determining the relative extreme values, that is, the relative maximums and relative minimums, of any function, $f(\theta)$. The first thing to note is that when θ is a continuous angle of rotation over the interval $[0, 2\pi)$, there are actually no end points to the interval since the angle just repeats itself. Thus in this case all relative extreme values are

absolute extreme values. As the reader undoubtedly recalls, all that is necessary to discover the extreme values of $f(\theta)$ is to: (i) set the derivative of $f(\theta)$ equal to zero; (ii) solve for the values of θ that satisfy that equation, $f'(\theta) = 0$; and then (iii) substitute those solutions for θ into the expression for $f(\theta)$. The values of $f(\theta)$ for those values of θ are the extreme values of $f(\theta)$. This three-step procedure is the road map for what follows.

The equations available for determining the maximum stresses are Eqs. (2.3) and (2.6). Since it appears that Eqs. (2.6) are easier to deal with in a direct manner, the discussion begins with the plane stress equations. An interesting aspect of Eqs. (2.6) is the appearance of the factors $(2 \sin \theta \cos \theta)$ and $(\cos^2 \theta - \sin^2 \theta)$. These two factors are identified as $\sin 2\theta$ and $\cos 2\theta$, respectively. This suggests, and it turns out to be true, that there is an advantage to rewriting Eqs. (2.6) in terms of the quantity 2θ rather than just θ . The equations can be so rewritten by employing the further identities³

$$\sin^2 \theta \equiv \frac{1}{2}(1 - \cos 2\theta) \quad \text{and} \quad \cos^2 \theta \equiv \frac{1}{2}(1 + \cos 2\theta)$$

Substituting the above four trigonometric identities into Eqs. (2.6) yields

$$\begin{aligned} \sigma_{xx}^* &= \frac{1}{2}(\sigma_{xx} + \sigma_{yy}) + \frac{1}{2}(\sigma_{xx} - \sigma_{yy}) \cos 2\theta + \sigma_{xy} \sin 2\theta \\ \sigma_{yy}^* &= \frac{1}{2}(\sigma_{xx} + \sigma_{yy}) - \frac{1}{2}(\sigma_{xx} - \sigma_{yy}) \cos 2\theta - \sigma_{xy} \sin 2\theta \\ \sigma_{xy}^* &= -\frac{1}{2}(\sigma_{xx} - \sigma_{yy}) \sin 2\theta + \sigma_{xy} \cos 2\theta \end{aligned} \quad (2.6a)$$

If it was not evident in Eqs. (2.6), it should now be obvious that

$$\sigma_{xx}^* + \sigma_{yy}^* = \sigma_{xx} + \sigma_{yy} \quad (2.7)$$

That is, the sum of the normal stresses is the same regardless of the orientation of the coordinate system. (The analogous result is also true in the three-dimensional case.) This result is convenient for checking maximum normal stress calculations and should be remembered for that purpose. Equation (2.7) also is used in demonstrating that other important quantities, such as certain energy expressions, are independent of the coordinate system in which they are described. Thus a special name is given to the sum of the normal stresses. This sum is called the *first stress invariant*. There are two other such basic stress invariants, which, as the reader might guess, are called the second and third stress invariants. They are not important to our present purposes.

The task of finding the extreme values of the three stresses of Eq. (2.6a) can be dealt with in the familiar terms of differential calculus as outlined above. Note that since this discussion deals with a single material point, the stresses in the original coordinate system, σ_{xx} and so forth, are here considered to be known constants, while the stresses of the rotated coordinate system, σ_{xx}^* and so forth, vary with the single variable, θ . Thus it is only necessary to differentiate each rotated coordinate system stress with respect to θ , or better yet 2θ , and set the result equal to zero in order to determine the value or values of 2θ for which the stresses in the rotated coordinate system are a maximum or minimum. Doing so yields

$$\frac{d\sigma_{xx}^*}{d(2\theta)} = -\frac{1}{2}(\sigma_{xx} - \sigma_{yy}) \sin 2\theta + \sigma_{xy} \cos 2\theta = 0$$

³ The only trigonometric identities that the reader ever need memorize are stated below. All others can be derived, usually with only a few steps, from $\sin(\alpha \pm \beta) = \sin \alpha \cos \beta \pm \cos \alpha \sin \beta$ and $\cos(\alpha \pm \beta) = \cos \alpha \cos \beta \mp \sin \alpha \sin \beta$.

so

$$\tan 2\theta_x = \frac{\sigma_{xy}}{\frac{1}{2}(\sigma_{xx} - \sigma_{yy})}$$

$$\frac{d\sigma_{yy}^*}{d(2\theta)} = \frac{1}{2}(\sigma_{xx} - \sigma_{yy}) \sin 2\theta - \sigma_{xy} \cos 2\theta = 0$$

so

$$\tan 2\theta_y = \frac{\sigma_{xy}}{\frac{1}{2}(\sigma_{xx} - \sigma_{yy})}$$

$$\frac{d\sigma_{xy}^*}{d(2\theta)} = -\frac{1}{2}(\sigma_{xx} - \sigma_{yy}) \cos 2\theta - \sigma_{xy} \sin 2\theta = 0$$

so

$$\tan 2\theta_s = \frac{-\frac{1}{2}(\sigma_{xx} - \sigma_{yy})}{\sigma_{xy}}$$

The solutions for $2\theta_x$ and $2\theta_y$, which locate the extreme values of the two normal stresses, are exactly the same. From a sketch of the tangent function over the range of all physically meaningful values of 2θ , the interval $[0, 2\pi)$, it can be seen that there are two possible solutions for $2\theta_x$ and $2\theta_y$, and those two solutions for these double angles are 180° apart. Therefore the two solutions for either angle of rotation, θ_x or θ_y , are 90° apart. By considering Eq. (2.7), which states that any sum of σ_{xx}^* and σ_{yy}^* is a constant, it is clear that at either of the two equal single-angle solutions it is not possible for both normal stress values to be a maximum. Nor is it possible for both to be a minimum. Therefore at each of the two equal, single-angle solutions, one of these two normal stresses must be a maximum and the other a minimum. Then the 90° difference between the planes on which the maximum and minimum stresses act can be understood as two different mathematical descriptions of the same physical state simply because σ_{xx}^* and σ_{yy}^* are always 90° apart. In other words, all four of the $\tan 2\theta_x$ and $\tan 2\theta_y$ solutions are the same solution. That is, each contains exactly the same information about the orientation of the two perpendicular planes of the rotated element on which one of the normal stresses is a maximum and the other is a minimum.

Having this interpretation of the solution for the rotational angle $\theta_x = \theta_y = \theta$ that produces the extreme values of the normal stresses, consider the solution for the angle θ_s that produces an extreme value of the shear stress. The $\tan 2\theta_s$ solution for the extreme value of the shear stress is seen to be the negative reciprocal of the normal stress $\tan 2\theta$ solution. Since tangents are slopes, and since slopes that are negative reciprocals of each other are normal to each other, then the shear stress $2\theta_s$ solution is 90° from the normal stress 2θ solution; that is, the two different single angle solutions are separated by 45° . (Fortunately, as is demonstrated later, there is a simple mnemonic device to help the reader remember all of the above plus the results of the remaining task of calculating the extreme values of the normal and shear stresses.)

In the above paragraph, the angular locations of the extreme values for the normal and shear stresses were developed. Now it is necessary to substitute those angular locations into the expressions for the normal and shear stresses, Eqs. (2.6a), in order to determine the magnitudes of the extreme values of the stresses. In order to obtain the necessary values of the sines and cosines from a knowledge of the tangents, the convenient diagrams of Fig. 2.3 can be consulted. Note, however, that these convenient diagrams as they stand do not account for the sign changes that occur between tangent functions on the one hand, and

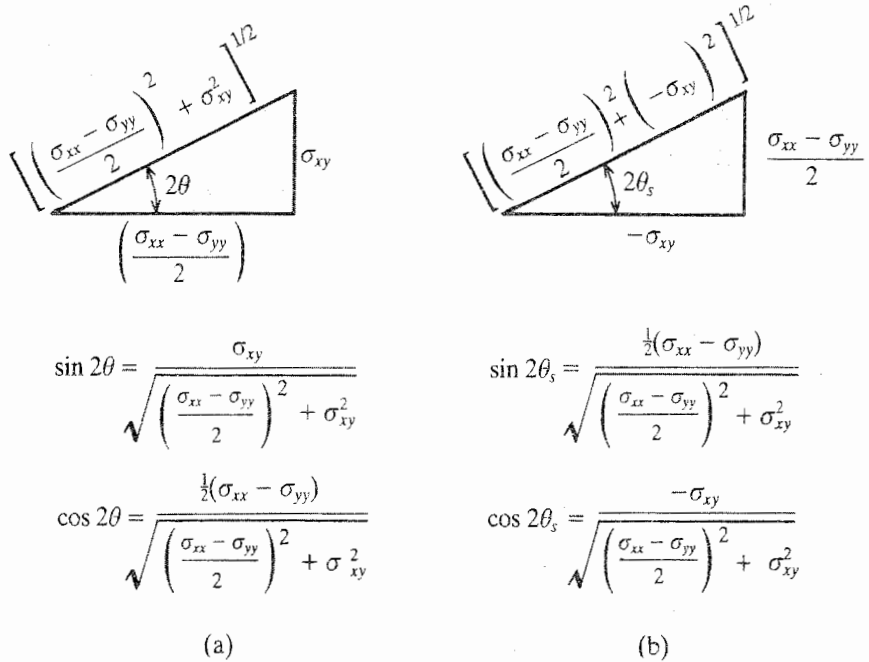


Figure 2.3. (a) A diagram for converting tangent values into sine and cosine values in the case of the normal stresses. (b) A similar diagram for the shearing stress case.

the sine and cosine functions on the other, when the solution for 2θ lies outside the first quadrant. Substituting for the sines and cosines of the normal and shear solutions for 2θ yields

$$\sigma_{xx}^* = \frac{1}{2}(\sigma_{xx} + \sigma_{yy}) + \left[\frac{1}{4}(\sigma_{xx} - \sigma_{yy})^2 + \sigma_{xy}^2\right]^{1/2}$$

$$\sigma_{yy}^* = \frac{1}{2}(\sigma_{xx} + \sigma_{yy}) - \left[\frac{1}{4}(\sigma_{xx} - \sigma_{yy})^2 + \sigma_{xy}^2\right]^{1/2}$$

and

$$\sigma_{xy}^* = -\left[\frac{1}{4}(\sigma_{xx} - \sigma_{yy})^2 + \sigma_{xy}^2\right]^{1/2}$$

Since the square roots must be positive real quantities, clearly the first listed normal stress is the maximum normal stress while the second listed is the minimum normal stress. However, if the third-quadrant solution for $\tan 2\theta$ were used instead of the first quadrant solution, the sign before all three radicals would change so that the first listed normal stress would be the minimum stress, the second listed would be the maximum stress, and the shear stress would have a positive value. Hence there is no significance to be attached to the sign of the maximum shear stress and, as discussed previously, the first- and third- (or second- and fourth-) quadrant solutions describe the exact same physical state. The final result is organized as follows. Let σ_{11} be the symbol for the largest of these two normal stresses in

the algebraic sense that $(+2) > (-3)$, let σ_{22} be the other normal stress, and let σ_s be the magnitude of the maximum shear stress in the z plane, then

$$\begin{aligned}\sigma_{11} &= \frac{1}{2}(\sigma_{xx} + \sigma_{yy}) + \left[\frac{1}{4}(\sigma_{xx} - \sigma_{yy})^2 + \sigma_{xy}^2 \right]^{1/2} \\ \sigma_{22} &= \frac{1}{2}(\sigma_{xx} + \sigma_{yy}) - \left[\frac{1}{4}(\sigma_{xx} - \sigma_{yy})^2 + \sigma_{xy}^2 \right]^{1/2}\end{aligned}\quad (2.8)$$

and

$$\sigma_s = \left[\frac{1}{4}(\sigma_{xx} - \sigma_{yy})^2 + \sigma_{xy}^2 \right]^{1/2}$$

The two normal plane stresses listed above are called the *principal stresses*. Be sure to note the “-al” ending. As in life, *principles* come later.

There is an important feature associated with the principal stresses which can now be recognized. Recall that the principal stresses were derived from Eqs. (2.6a) by inserting the values of 2θ that extremize the normal stresses into the expressions for the normal stresses. Now note that when the values of 2θ that so specialize the normal stresses as principal stresses are inserted into the *shear* stress equation, the shear stress has a zero magnitude. In other words, when the plane stress differential rectangular parallelepiped is rotated through the angle θ that results in the principal stresses acting on those particular x^* and y^* faces, the shear stresses acting on those particular x^* and y^* faces are nil. (In three dimensions it is also true that on the planes of the principal stresses, the shear stresses have zero values.) The absence of shear stresses can even be used to define the planes on which the principal stresses act. (Such a change in definition is made below.) In the opposite of the above procedure, when the values of 2θ that extremize the shear stress are substituted into the normal stress equations, both normal stresses take on the value of the average normal stress, $\frac{1}{2}(\sigma_{xx} + \sigma_{yy})$. Thus on the x^* and y^* planes on which the maximum in-plane shear stresses act, the normal stresses have their average values.

Often it is important to know the direction in which the principal stresses act, or, what amounts to the same thing, the orientation of the maximum in-plane shear stress vectors. The equations developed prior to Eqs. (2.8) are adequate to the task. However, there is a single mnemonic device that combines the calculations of the maximum magnitudes and their directions. The same device clearly exhibits all the special relations mentioned above. Its use is explained below.

2.4 Mohr's Circle

The derivation of Mohr's circle is of little importance. It is relegated to being an additional exercise. Mohr's circle is constructed with reference to the differential-sized rectangular parallelepiped in the state of plane stress shown in Fig. 2.4. All the stresses and coordinates shown in that figure are in conformity with the previously adopted positive conventions. The differential-sized differences between stresses on opposite faces of the differential element as sketched in Fig. 2.4 are not relevant to, and are thus omitted from, the present endeavor because the focus is on the rotation of the stresses at the arbitrary point P , which are, of course, the back face stresses. That is, the front face stresses appear on the rectangle only to provide the comforting appearance of equilibrium. The body forces, which are of the same order of magnitude as the stress increments, are also omitted. In addition, it is not possible to quantify numerically a differential quantity.

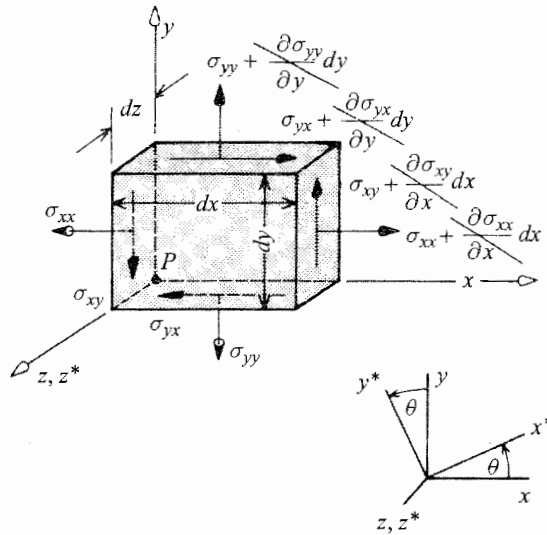


Figure 2.4. A plane stress free body diagram for use with Mohr's circle and the associated coordinate rotation.

This is how to construct Mohr's circle. Let a horizontal axis represent the normal stresses. Let a vertical axis represent shear stresses. Normal stresses to the right of the origin are positive or tensile stresses, while the negative stresses are of course interpreted as compressive stresses. This is the part that is peculiar to Mohr's circle: positive shear stresses on the x face are positive down, and positive shear stresses on the y face are positive up. On this grid, plot the point in normal and shear stress coordinates that represents the x face stresses and similarly the point that represents the y face stresses; see Fig. 2.5(a). Draw a straight line connecting these two stress points. This line defines the diameter of the Mohr's circle. The Pythagorean theorem⁴ shows that the radius of the circle is $[\frac{1}{4}(\sigma_{xx} - \sigma_{yy})^2 + (\sigma_{xy})^2]^{1/2}$. The center of the circle is at the average stress value of $\frac{1}{2}(\sigma_{xx} + \sigma_{yy})$. At this point refer to Eqs. (2.8) to note the relevance of those quantities. It is hopefully clear on the basis of Eqs. (2.8) and the algebraic maximum and minimum stress values indicated by Mohr's circle that: (i) the points where the circle crosses the horizontal axis represent both the values and the planes of the principal stresses; and (ii) the very top and very bottom of the circle represent the magnitudes and the planes on which the maximum shear stresses act.

By referring to Fig. 2.5(b) and back to the $\tan 2\theta$ solutions that locate the planes of the principal stresses and the planes of maximum in-plane shear stress, it can be confirmed that the double angle (2θ) rotations from the x and y planes derived there have the same double angle magnitude and direction of rotation as those indicated by Mohr's circle. That is, Mohr's circle is merely a graphical representation of Eqs. (2.6, 2.7, 2.8) plus the $\tan 2\theta$ equations. As a result, of course, angular rotations around the perimeter of Mohr's circle are twice those of the physical state. That is why, for example, the x and y faces are plotted diametrically opposite each other, and the planes of the principal stresses are also 180° apart on Mohr's circle.

⁴ Pythagoras (c. 582–c. 500 BC), Greek philosopher, religious teacher, and mathematician.

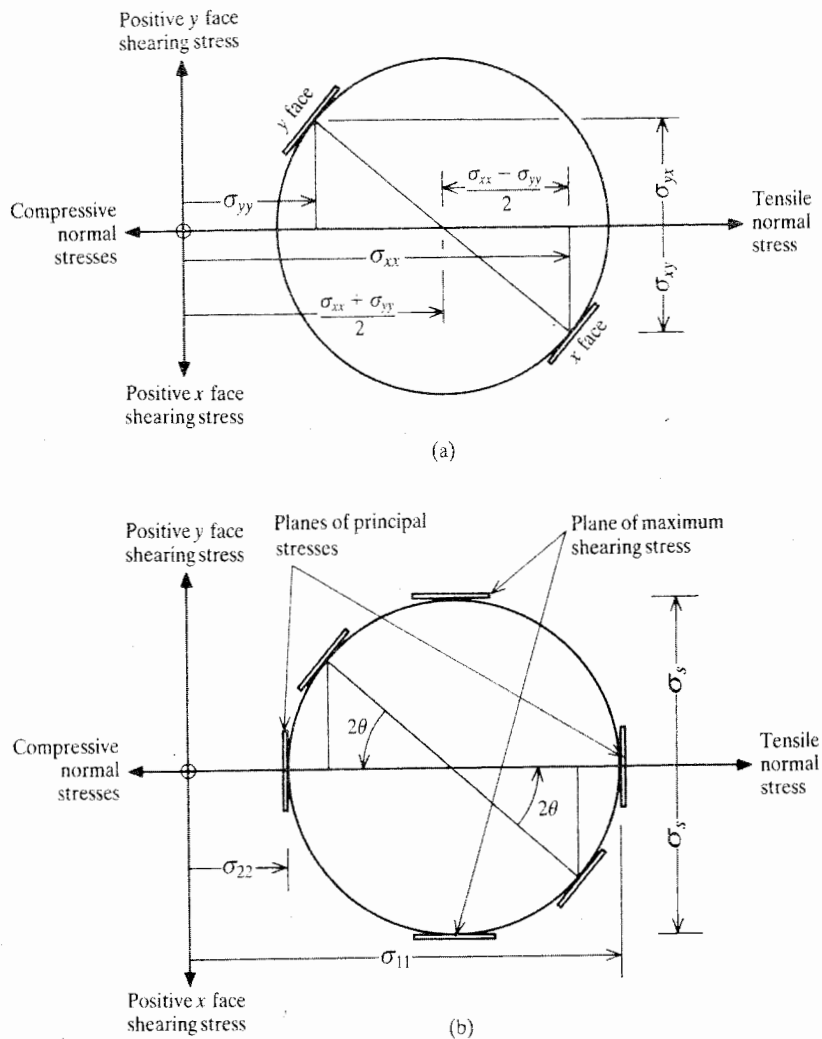


Figure 2.5. (a) Coordinate axes to be used to set up Mohr's circle and an illustration of how to plot σ_{xx} , σ_{yy} , and σ_{xy} so as to obtain a Mohr's circle for the case of plane stress. (b) For the same Mohr's circle, the location of the planes of the principal stresses and the planes of the maximum shearing stress. The rotation to the planes of the principal stresses is shown explicitly.

Mohr's circle is learned through practice. The exercises at the end of the chapter provide opportunity for practice, and two examples are given below. Mohr's circle is best used as a bridge between (i) input information that consists of the plane stresses associated with the originally chosen analysis coordinate system and (ii) clearly presented information on the principal stresses and the maximum shear stresses at the point under study. In other words, good engineering practice does not make Mohr's circle the end product. Instead, the end product should be a pair of diagrams of appropriately rotated differential-sized elements, at the point under study, that display the principal stresses and the maximum in-plane shear stresses.

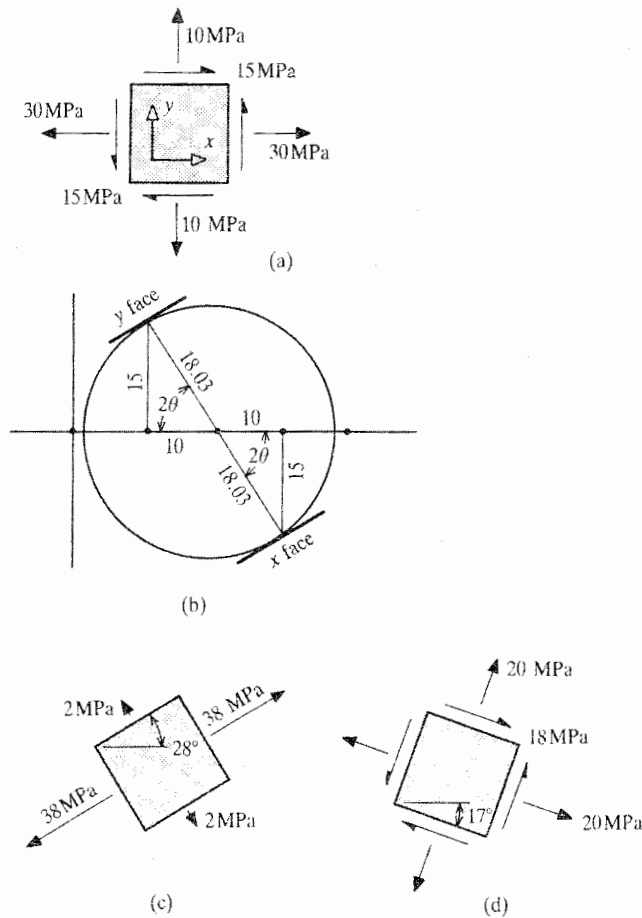


Figure 2.6. (a) Example 2.1. The free body diagram of the stresses at point P from which Mohr's circle is to be constructed. (b) Example 2.1 Mohr's circle of radius $[(10)^2 + (15)^2] = 18.03$ MPa. For the rotation angle to the principal stresses, $\tan 2\theta = 15/10$, so $\theta = 28.15^\circ$ counterclockwise. The rotation angle for the maximum shear stresses is $45^\circ - 28.15^\circ$ in the opposite direction. Both principal stresses are tensile, with $\sigma_{11} = 20 + 18.03 = 38$ MPa, and $\sigma_{22} = 20 - 18.03 = 2$ MPa. (c) Correctly oriented free body diagram showing the principal stresses for this plane stress problem. (d) Correctly oriented free body diagram showing the maximum shearing stresses and their associated normal stresses.

Example 2.1. Consider that, in terms of the original (analysis) Cartesian coordinate system, the plane stresses at point P are as illustrated in Fig. 2.6(a). Draw similar, fully detailed differential-sized elements that illustrate the principal and maximum shear stresses in the z plane, and the physical rotations necessary to achieve those maximum stresses.

Solution. All the stress vectors on the given differential element conform to the positive sign convention. In order to determine the signs to be assigned to each stress, the reader can focus on either the front or back faces. However, the front faces are recommended since the convention there is in harmony with the coordinate axes. The units associated with

the stress magnitudes are megapascals (MPa), which are millions of newtons per square meter.⁵

Draw the stress axes for Mohr's circle. Plot the location of the x face as 30 MPa to the right of the origin, and 15 MPa down from the horizontal axis. Plot the location of the y face as 10 MPa to the right of the origin, and 15 MPa up from the horizontal axis. Draw the diameter of the Mohr's circle by connecting these two stress state points, and complete the circle; see Fig. 2.6(b). The calculation for the magnitude of the radius of Mohr's circle can simply be done by employing the Pythagorean theorem with either of the right triangles whose base lies on the horizontal axis. This and the few other necessary calculations are shown on the figure. The differential element that displays the principal stresses is rotated 28° counterclockwise from either the x or y face orientation. The element that displays the maximum shear stresses in the z plane is rotated 17° clockwise. Do not forget to include the average normal stresses on the maximum in-plane shear sketch. Also check to make sure that all the shear stress vectors are drawn head-to-head and toe-to-toe. Finally, note that the input data contained at most two significant digits. Therefore the output must be limited to two significant digits.

There is a quick mental check that can be made to determine whether the two sketches Figs. 2.6(c) and (d) are reasonable. Consider the original element stress diagram. Imagine that the two front face shear vectors add to a vector going towards the upper right, with an approximate magnitude of 20+ MPa, half-way between the directions of the 10 and 30 MPa vectors. The largest vector, that is, the larger of the principal stress vectors, can then be imagined as a combination of the 20+ and 30 MPa vectors going in approximately the two o'clock direction. That is exactly what is seen in the principal stress diagram. Doing the same thing with the maximum in-plane shear diagram, again relative to the principal stress diagram, confirms the reasonableness of both. ■

Example 2.2. Given the stress state at point P shown in Fig. 2.7(a), sketch and fully detail the differential elements that show the associated principal stresses and maximum in-plane shear stresses.

Solution. The x face normal stress is compressive, and therefore is assigned a negative value. Thus the x face is plotted with the normal stress coordinate of -50 ksi (1 ksi \equiv 1000 psi, where psi stands for pounds per square inch) and the shear stress coordinate of $+30$ ksi. That is, the x face is located 50 units to the left of the origin, and 30 units down. The stresses on the y face are positive. Hence the y face position is 30 units to the right and above the origin. These two stress state points define the diameter of the Mohr's circle, and hence the circle itself; see Fig. 2.7(b). Note that the center on a Mohr's circle always lies on the normal stress axis.

The Mohr's circle shows that a rotation of 18° clockwise from either the y or x face produces the principal planes and stresses which are shown in Fig. 2.7(c). Similarly for the maximum shear stress diagram. Note that it is absolutely necessary to include the units as well as the magnitude of the stress vector. Also note that the arrowhead indicates the direction of the stress, so do not label a vector with a negative magnitude. Since opposite vectors have the same magnitudes, it is permissible to label only two adjacent sides. Note that in both example solutions the sum of the normal stresses is the same for all three differential elements. ■

⁵ Blaise Pascal (1623–1662), French mathematician and philosopher.

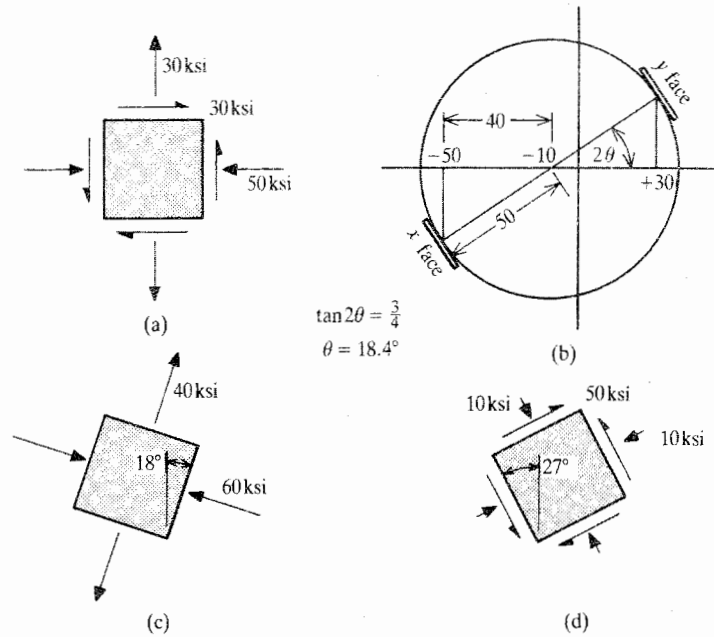


Figure 2.7. (a) Example 2.2. The point P free body diagram for the x and y coordinate axes. (b) Corresponding plane stress Mohr's circle. (c) Properly oriented free body diagram for the principal stresses. (d) Properly oriented free body diagram for the maximum shearing stresses.

Mohr's circle is a small joy because once learned it is easily remembered. Thus it can be used more easily and with better effect than all the plane stress equations of this chapter. There is also the slight advantage that, while Mohr's circle is generally only used by structural engineers for stresses, it can be used with other two-dimensional engineering quantities that rotate the same way that stresses rotate. Strains, and area moments of inertia are topics to be discussed later that provide examples of quantities that rotate as stresses rotate.

2.5 A Three-Dimensional View of Plane Stress

The first thing to be said is that the above exposition of Mohr's circle must be extended to account for the fact that while the more noticeable aspects of plane stress are confined to the plane formed by the x and y axes (the z plane), the other two orthogonal planes are also always present in any real structure. This means that in the case of plane stress, the third principal stress is the zero value of σ_{zz} because, by the definition of plane stress, the shear stresses on the z plane are zero.⁶ With this realization and a sense of fair play

⁶ The definition of a principal stress has now been changed from that of being a maximum or minimum stress (which description is not wholly suitable to three dimensions because there are three principal stresses), to that of being a normal stress that occurs on a plane on which there are no shear stress components. The previous development of the plane stress equations can simply be reordered to fit the new definition by first using the third of Eqs. (2.6a) to determine the value of the rotational angle θ at which the shear stress σ_{xy}^* is zero. Since, as was noted previously, this is the same angle that extremizes the normal stresses, all the previous results follow.

for the other two planes, Mohr's single circle can immediately be extended to a grouping of three such circles as shown in Fig. 2.8(a) where each plane is conveniently identified by its horizontal axis intercepts, the principal stresses. The additional two circles are dashed, not because they are less real, but just for clearer identification. In the case of plane stress, one of the three circles always represents the z plane. In Fig. 2.8(a), the z plane happens to be the 3-plane, that is, the plane formed by the 1- and 2-axes. In Fig. 2.8(b), the z plane happens to be the 2-plane. Examination of Fig. 2.8(a) shows something of potential significance. Unlike the situation in Fig. 2.8(b), in 2.8(a) the overall maximum shear stress does not lie in the z plane. The maximum shear stress lies in the 2-plane, and its magnitude can be considerably larger than the shear stress in the z plane. The same thing can happen when the z plane Mohr's circle lies entirely on the compression side of the horizontal stress axis. This can be a significant matter for a material that has poor resistance to shear stresses. Figures 2.8(c, d) illustrate a three-dimensional view of the planes upon which these maximum shear stresses act.

There is a small variation upon the above discussion that is worth mentioning. If the stress σ_{zz} is not equal to zero, but the z face shear stresses are zero, then the $\sigma_{zz} = \sigma_{zz}^*$ stress is again a principal stress, and the rotation to the differential element orientation for all three principal stresses is again exclusively about the z axis. This situation is sometimes referred to as that of *generalized plane stress* (Ref. [6]). Mohr's circle easily accommodates this situation when σ_{zz} is plotted at its nonzero value on the horizontal axis. This nonzero value is now the anchor for the other two Mohr's circles in exactly the same way as when σ_{zz} was zero. To illustrate this point, consider Figs. 2.8(e, f, g). In each of these three example sketches, σ_{zz} is a small compressive normal stress. In Fig. 2.8(e), $\sigma_{11}, \sigma_{22} > 0$, so $\sigma_{zz} = \sigma_{33}$. In Fig. 2.8(f) $\sigma_{zz} = \sigma_{22}$, and in Fig. 2.8(g) $\sigma_{zz} = \sigma_{11}$. Note that in all cases, the overall maximum shear stress has the value

$$\sigma_s |_{max} = \frac{1}{2}(\sigma_{11} - \sigma_{33})$$

2.6 ** Principal Stresses in the General Three-Dimensional Case **

The plane stress situation is but a special case of the more general three-dimensional stress state. Mohr's circle can be adapted to the general three-dimensional case (Ref. [4]), but then it loses some important advantages, particularly its simplicity. There is another approach that is quite simple, particularly if all that is desired is the values of the principal stresses. This limited knowledge is often satisfactory because all maximum shear stress magnitudes can be easily calculated from a knowledge of the principal stresses. The planes on which the principal stresses act are not difficult to obtain by this same procedure, but the details of that aspect of the total procedure are relegated to Endnote (1). This alternate solution technique (Ref. [3]) begins with the later adopted definition that the principal stresses occur as normal stresses on those planes passing through the point of interest which are without shear stresses. Thus the normal stress vector is the total stress vector on any principal plane. Then the total/normal stress vector, $\{t\}$, is collinear with, and thus proportional to, the unit (geometric) normal vector to that principal plane, $\{v\}$. This statement that the total stress vector must be proportional to the unit normal is stated mathematically by writing

$$\begin{Bmatrix} t_x \\ t_y \\ t_z \end{Bmatrix} = \lambda \begin{Bmatrix} \cos(n, x) \\ \cos(n, y) \\ \cos(n, z) \end{Bmatrix} \equiv \lambda \begin{Bmatrix} v_x \\ v_y \\ v_z \end{Bmatrix}$$

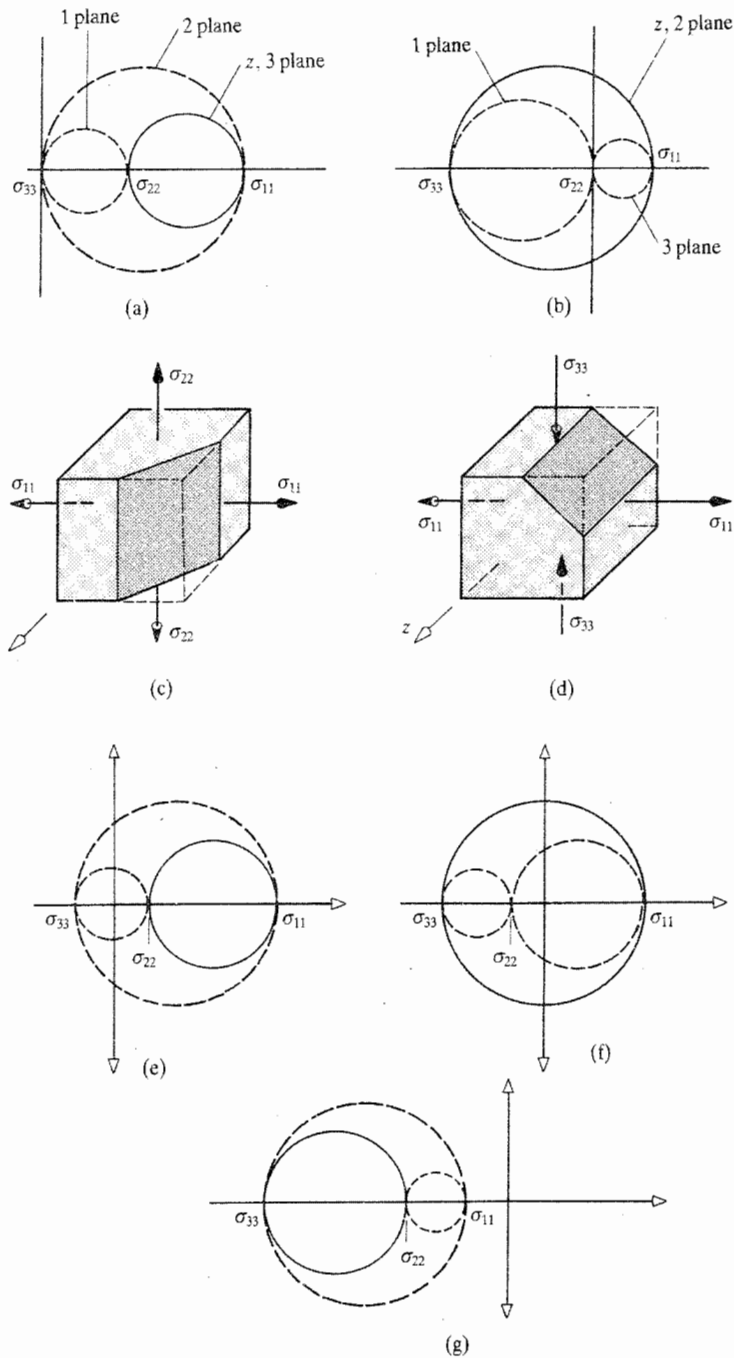


Figure 2.8. (a) Illustration of the two additional Mohr's circles for the plane stress case where the first two principal stresses are both tensile. (b) Illustration of the two additional Mohr's circles for the plane stress case where one principal stress from the rotation in the x, y plane is tensile while the other is compressive. (c) Location of a plane of maximum shearing stress for case 2.8(a). (d) Location of a plane of maximum shearing stress for case 2.8(b). (e) The three Mohr's circles for the generalized plane stress case where $\sigma_{33} = \sigma_{zz}$. (f) The three Mohr's circles for the generalized plane stress case where $\sigma_{22} = \sigma_{zz}$. (g) The three Mohr's circles for the generalized plane stress case where $\sigma_{11} = \sigma_{22}$.

In this equation, the components of the total stress vector are parallel to the directions of the original Cartesian coordinate system as per Fig. 1.9. The factor λ is the unknown constant of proportionality. The 3×1 matrix $\{v\}$, as before, is the unknown vector of the direction cosines which locates the orientation of the unit normal with respect to the original, nonrotated Cartesian coordinate system. Now reconsider Eq. (1.9), which is $\{T\} = [\sigma]\{v\}$. This Cauchy matrix equation was originally constructed to relate the Cartesian components of the tractions on a boundary surface, $\{T\}$, to the internal stresses $[\sigma]$. All that is necessary to do for the present purpose is to proclaim that what was once a planar approximation to a portion of the boundary surface is now to be viewed as an internal principal plane. Planes are planes, and as long as all other circumstances are the same, different names (interpretations) can be assigned as is convenient. When these two different equations for the total stress vector on the principal plane are combined so as to eliminate $\{t\} \equiv \{T\}$, the result is

$$[\sigma]\{v\} = \lambda\{v\} \quad (2.9a)$$

It is important to point out the special characteristics of the above matrix equation. As preliminary to that purpose, first consider the matrix formulation of a general set of simultaneous equations where the number of equations equals the number of unknown quantities in the vector of unknown quantities, $\{x\}$. If $[A]$ is the coefficient matrix, and $\{b\}$ is a matrix of known constants, then the set of simultaneous equations can be written as

$$[A]\{x\} = \{b\} \quad (2.10)$$

For example, if

$$\begin{aligned} 2x + 3y - 4z &= 10 \\ 3x - 4y + 5z &= -3 \\ 4x + 5y - 6z &= 56 \end{aligned} \quad \text{then} \quad \begin{bmatrix} 2 & 3 & -4 \\ 3 & -4 & 5 \\ 4 & 5 & -6 \end{bmatrix} \begin{Bmatrix} x \\ y \\ z \end{Bmatrix} = \begin{Bmatrix} 10 \\ -3 \\ 56 \end{Bmatrix}$$

where the square matrix is $[A]$, $\{x\} \equiv \{x\}^t = [x \ y \ z]$, and $\{b\} = [10 \ -3 \ 56]$. This example equation has a single solution for the vector of unknown quantities $\{x\}$, which is $\{x\} = [5 \ 72 \ 54]$. Similarly, in the general case, the matrix equation $[A]\{x\} = \{b\}$ has the unique solution, which can be written as

$$\{x\} = [A]^{-1}\{b\}$$

whenever $[A]^{-1}$ exists, that is, whenever $|A|$ is not zero. That solution is a null vector (all zeros) if and only if $\{b\}$ is a null vector.

Contrast the above situation to the matrix equation of present interest, which is Eq. (2.9). As is typical for this type of equation, even with $[\sigma]$ being a square matrix, there is one more unknown (four) than the number of equations (three). The four unknowns are: λ , v_x , v_y and v_z . That is, neither the constant of proportionality, λ , nor the direction cosines of any of the principal planes are known relative to the fixed Cartesian axes. Like many examples of this type of equation, such as are met in Parts III, V, and VI of this text, the solution technique proceeds without any immediate attention to this imbalance. *Unlike* many examples of this type of equation, in this case there is an auxiliary equation (the sum of the squares of the direction cosine equals 1; see exercises) that provides that extra equation which fully specifies the last three unknowns, the direction cosines. In order to discuss all equations of the general form of Eq. (2.9), set the unusual auxiliary equation aside for the moment. In the general case, without an auxiliary equation, there is always a solution where the column vector of unknowns is the zero vector. This is called the *trivial solution* and it is valid regardless of the value of the unknown proportionality factor of the right-hand side vector, λ . The trivial solution generally has a physical interpretation, but as the name suggests,

it is not the solution of interest. The proof of this statement is accomplished simply by substituting a zero vector for the unknown vector $\{v\}$ and carrying out the multiplications. Another special feature of the general matrix equation form, which is also true for Eq. (2.9) with the auxiliary equation, is that the solutions for the unknown proportionality factor λ are always a finite number of discrete values. This latter aspect is made clear when the solution is developed for λ from Eq. (2.9). These special features call for a special name for this general type of matrix equation. Such an equation is called a *matrix eigenvalue problem*. The word "eigen" is German for, among other things, "characteristic," and therefore there is the alternate name of *matrix characteristic value problem*. The factor λ is called the eigenvalue or characteristic value. Other physical phenomena, such as some vibration and buckling problems, can be formulated as either matrix eigenvalue problems or equivalent differential equation eigenvalue problems.

The solution of the matrix eigenvalue problem of immediate interest begins as follows: Rewrite the equation as

$$[\sigma]\{v\} = \lambda[I]\{v\} \quad \text{or} \quad ([\sigma] - \lambda[I])\{v\} = \{0\} \quad (2.9b)$$

where $[I]$ is the identity matrix. The latter form appears to be a special case of Eq. (2.10), but the difference is that this coefficient matrix, $[A]$, is not a matrix of fixed constants since this coefficient matrix contains the unknown eigenvalue λ . It is however instructive to proceed as if this were merely a variation on Eq. (2.10), and to use the simultaneous equation solution technique called Cramer's rule (Ref. [5]) in order to obtain a solution for the n th direction cosine ($n = 1, 2, 3$). Remember that the matrix equations are nothing but simultaneous equations. Cramer's rule states that the solution for the n th unknown direction cosine is equal to a ratio of two determinants. The determinant in the denominator is the determinant of the coefficient matrix $([\sigma] - \lambda[I])$. The determinant in the numerator is the same as that in the denominator with the one exception that the n th column is replaced by the right-hand side vector $\{b\}$, which in this case is $\{0\}$. A complete column of zeros makes any determinant have the unequivocal value of zero. Thus at this point it would appear at first glance that zero is the solution for all the direction cosines. However, since there is the auxiliary equation that the sum of the squares of the direction cosines is 1, it is clear that this trivial solution is nonsense. Therefore a loophole must be sought in Cramer's rule.⁷ The loophole can be found in the determinant that is the denominator. If the eigenvalue is required to be such that the determinant of the coefficient matrix also has a zero value, then Cramer's rule would produce the undefined ratio of $0/0$. In this situation, the ratio $0/0$ has the merit of not necessarily being zero. This is exactly what is needed to avoid the trap of all-zero direction cosines. This requirement on the eigenvalue is enforced by simply writing for the determinant of the denominator

$$|[\sigma] - \lambda[I]| = 0 \quad (2.11)$$

Since the size of the square matrices is 3×3 , the expanded determinant is a cubic equation in the unknown eigenvalue, λ . A corollary of the fundamental theorem of algebra states that there are three solutions to the cubic equation. From either Eq. (2.9) or (2.11), it is clear that the eigenvalue has the units of stress. Going back further in the development, the eigenvalue was introduced in the relation $\{t\} = \lambda\{v\}$ as the proportionality factor between the total stress vector, $\{t\}$, and the unit (nondimensional) geometric normal vector on the principal plane, $\{v\}$. Since the magnitude of the unit normal is 1, then any solution for an

⁷ Gabriel Cramer (1704–1752), Swiss mathematician (Ref. [71]).

eigenvalue is the full magnitude of a normal stress vector on a principal plane. Thus the magnitude of each eigenvalue is the magnitude of a principal stress, and the three solutions for the eigenvalue are the magnitudes of the three principal stresses.

After this long development for the general case of three-dimensional principal stresses, the solution process all comes down to simply solving the cubic equation, that is, Eq. (2.11), for the values of the three principal stresses. This procedure is illustrated in the following example, and reinforced in the exercises. One of many approximate methods for solving for a real root of a cubic equation is outlined in Section I.3. The following theorems regarding the solutions for the roots of the cubic equation produced by Eq. (2.11) can be proved (Ref. [3]): (i) all three of these principal stresses will always have solutions that are real numbers; and (ii) these solutions are indeed the extreme normal stress values, and they occur on mutually perpendicular planes.

Example 2.3. Given the following three-dimensional stress state in matrix form, determine the magnitudes of the principal stresses.

$$[\sigma] = \begin{bmatrix} 20 & 0 & 15 \\ 0 & 85 & 12 \\ 15 & 12 & -12 \end{bmatrix} \text{ MPa}$$

Solution. The equation to be solved for the eigenvalues is Eq. (2.11). In its determinant and expanded forms, it is, respectively,

$$\begin{vmatrix} (20 - \lambda) & 0 & 15 \\ 0 & (85 - \lambda) & 12 \\ 15 & 12 & (-12 - \lambda) \end{vmatrix} = 0$$

and

$$(20 - \lambda)(85 - \lambda)(12 + \lambda) + 225(85 - \lambda) + 144(20 - \lambda) = 0$$

Since there are no common factors for all the terms of the above sum, it is best to rewrite this equation in the standard cubic polynomial form

$$f(\lambda) = 0 = \lambda^3 - 93\lambda^2 + 71\lambda + 42\,405$$

With a modern, hand-held, programmable calculator, the principal stress roots of this cubic equation are easily obtained. In the absence of such a calculator, the following procedure, one of many possible procedures, is recommended. First make a rough sketch of the cubic function. The sketch is aided by a rough estimate of the λ values where the tangents to the cubic are zero. The zero tangent points are obtained from

$$f'(\lambda) = 0 = 3\lambda^2 - 186\lambda + 71$$

or roughly

$$0 = \lambda^2 - 62\lambda + 24$$

The quadratic equation solution shows that the zero tangent points are approximately 0.4 and 61.6 MPa. Noting further that (i) $f(0) = +42\,405$ (ii) when λ is large and positive, the value of the cubic is very large and positive, and (iii) when λ is large and negative, the value of the cubic is very large and negative; then the cubic polynomial has the rough form shown in Fig. 2.9. Since all three roots are real, application of Descartes' rule confirms that there are two positive roots and one negative root. A convenient first root to search

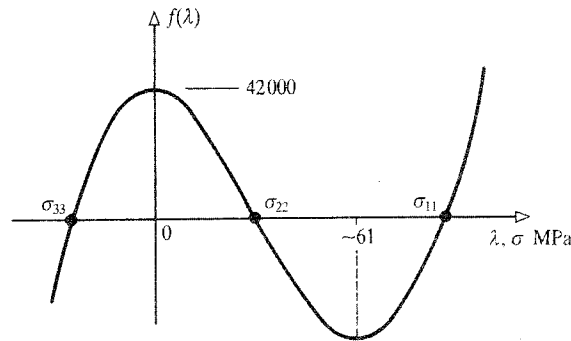


Figure 2.9. Example 2.3. The approximate plot of the cubic polynomial $f(\lambda) = \lambda^3 - 93\lambda^2 + 71\lambda + 42405$.

for is σ_{22} , which clearly has a value in the neighborhood of 30 MPa. Using Newton's method (see Section I.3) with a first estimate of 30 MPa, continued estimates converge to $\sigma_{22} = 25.62$ MPa.

The other two principal stresses could be obtained in exactly the same way as the above principal stress, again starting with initial estimates of their values from Fig. 2.9. An easier way is to factor out the above solution from the original cubic equation, thereby reducing it to a quadratic equation that is quickly solved. This reduction to a quadratic equation can be achieved by long division of $(\lambda - 25.62)$ into the cubic polynomial. A more efficient variation on the long division process is synthetic division. For those familiar with that process, the result is

$$\begin{array}{r|rrrr}
 25.62 & 1 & -93 & +71 & +42405 \\
 & & 25.62 & -1726.28 & -42408 \\
 \hline
 & 1 & -67.38 & -1655.28 & -3
 \end{array}$$

which is an error of less than one-hundredth of one percent. The coefficients of the quadratic are the three boxed numbers on the lower line, the quadratic equation solution yields the additional roots

$$\sigma_{11} = 86.51 \text{ MPa} \quad \text{and} \quad \sigma_{33} = -19.13 \text{ MPa}$$

As a check on the numerical accuracy, note that: (i) the sum of the three roots is 93.00, which is close enough to the exact value of 93, which is the negative of the first coefficient of the cubic after the leading value of 1; and (ii) the product of the three roots is $-42\,399$, which is close enough to the negative of the last coefficient value. Those readers who are familiar with matrix iteration techniques can perhaps find a first root, of the cubic more efficiently than by use of Newton's method regardless of how the eigenvector is normalized. Matrix iteration is discussed in the last chapter. ■

All of the above work concerned rotated Cartesian coordinate systems. Other orthogonal coordinate systems fit the exact same mold. The cylindrical and spherical coordinate systems are examples of other orthogonal coordinate systems because, at any given point P , the (r, θ, z) and the (θ, ρ, ϕ) coordinate directions (i.e., the directions of the tangents in the case of the curvilinear coordinates) are mutually perpendicular. The average stress vectors

on the differential planes that intersect at the point P differ from perpendicularity only by infinitesimal values that cannot be quantified. Therefore, all the above conclusions reached regarding rotating stresses aligned with Cartesian coordinates apply equally well to all other orthogonal coordinate systems.

2.7 Summary

At this point the means for determining the six stresses in a general structural body subjected to a general mechanical and thermal loading are still limited to the three equilibrium equations of Chapter 1. Again, the three stress/traction boundary equations are not contributors to the general form of the stress solutions. However, as a result of the material developed in this chapter, once the stresses are determined in the orthogonal coordinate system of the analysis, they can be determined for any translated or rotated orthogonal coordinate system. Furthermore, by means of Mohr's circle or the described eigenvalue problem, the values of the principal stresses can be determined along with the value of the maximum shear stress or any other shear stress related to a failure theory.

Example 2.4. The infinitesimal element sketched in Fig. 2.10(a) is in a state of generalized plane stress. From this information, sketch (a) the properly oriented differential element upon which the principal stresses act, and (b) the properly oriented differential element which bears the maximum shearing stresses in the xy plane. (c) Identify the overall maximum shearing stress, and list the three principal stresses in their proper order.

Solution. Figure 2.10(b) shows the Mohr's circles. Figure 2.10(c) shows the sketch for the principal stresses. Figure 2.10(d) shows the sketch for the maximum shearing stresses in the xy plane. The overall maximum shearing stress is 19.1 ksi, and from Fig. 2.10(b), the principal stresses are: $\sigma_{11} = 4.0$ ksi, $\sigma_{22} = -5.9$ ksi, and $\sigma_{33} = -34.2$ ksi. ■

2.8 Octahedral (von Mises) Shearing Stresses

A full discussion of the importance of octahedral, or von Mises, shearing stresses must be postponed to Section 5.6 where the general topic of engineering material behavior under general states of stress is considered. However, the interpretation of the von Mises stresses, and the determination of their magnitudes are appropriately addressed here because this topic requires the rotation of coordinate axes and the use of direction cosines.

First recall that a regular octahedron is a solid shape that can be likened to two Egyptian pyramids stuck together, square base to square base. The surface of the regular octahedron is composed of eight identical, equilateral triangles. Consider such an infinitesimal-sized regular octahedron centered at a point of interest, point O , within a loaded structure. Let the local Cartesian coordinate axes coincide with the directions of the principal stresses at point O , and arrange the octahedral surfaces so that they all are equally inclined to the three coordinate axes as illustrated in Fig. 2.11(a). For convenience, focus upon the shaded equilateral triangle lying in the octant defined by the positive coordinate axes. Since the normal to this triangular surface makes the same angle with each of the three coordinate axes, $c_{nx} = c_{ny} = c_{nz}$. Recall that any unit normal vector can be written as $\mathbf{i}^* = c_{nx}\mathbf{i} + c_{ny}\mathbf{j} + c_{nz}\mathbf{k}$. Then taking the dot product $\mathbf{i} \cdot \mathbf{i}^*$ yields $c_{nx}^2 = c_{ny}^2 + c_{nz}^2 = 1$. Therefore in the case of the octahedral surface where the three direction cosines have the same value, it can be concluded that $c_{nx} = c_{ny} = c_{nz} = 1/\sqrt{3}$. Now, from the general stress rotation equation, Eq. (2.1), and remembering that these coordinate axes are parallel the

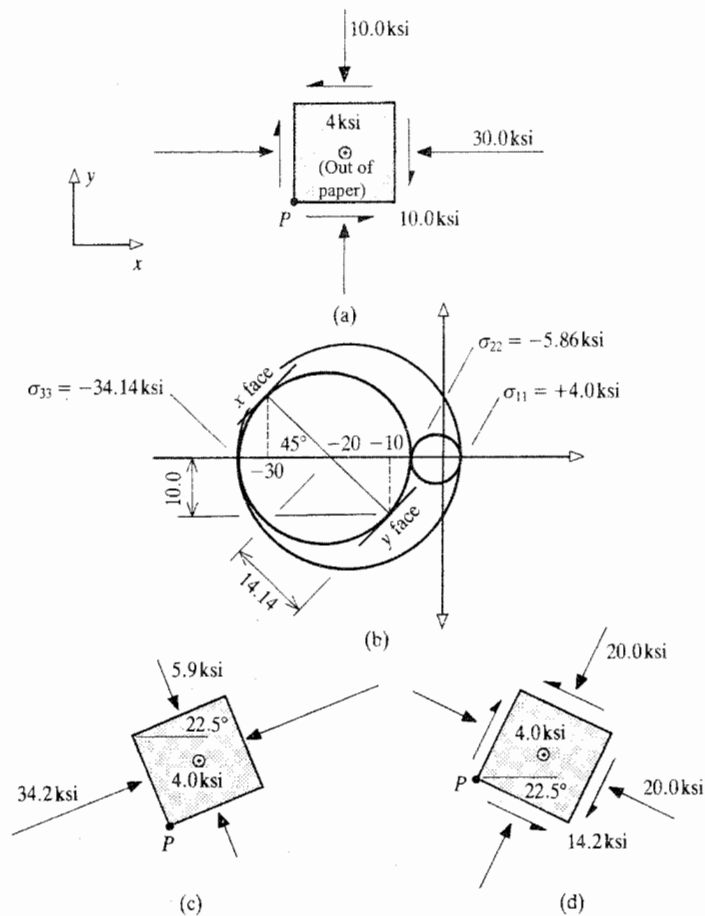


Figure 2.10. (a) Example 2.4. A generalized plane stress free body diagram at the point P . (b) The three corresponding Mohr's circles. (c) The properly oriented free body diagram of the three principal stresses. (d) The properly oriented free body diagram of the maximum shearing stresses obtained from a rotation about the z axis, which shearing stresses are slightly less than the overall maximum shearing stresses.

principal axes and thus there are no shearing stresses associated with these coordinate axes, the normal stress acting upon the octahedral surface is

$$\sigma_n = (1/3)(\sigma_{11} + \sigma_{22} + \sigma_{33})$$

This result that the normal stress on each octahedral surface is the same, and that common value is the average of the principal stresses (sometimes called the "spherical" or "hydrostatic" stress), suggests the octahedral surfaces are significant because of the analogy to the plane stress situation, pictured for example in Figs. 2.6(d) and 2.7(d) where the normal stresses are the same on all loaded surfaces, and the shear stresses are a maximum.

The three components of the *total* stress vector acting on an octahedral surface are easily obtained from the Cauchy equation. Again, since there are no shearing stresses associated

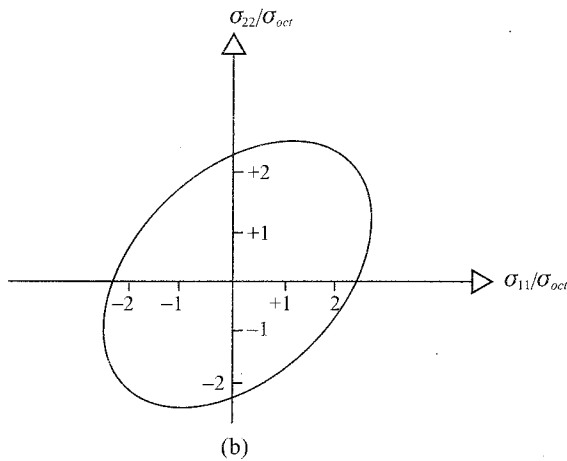
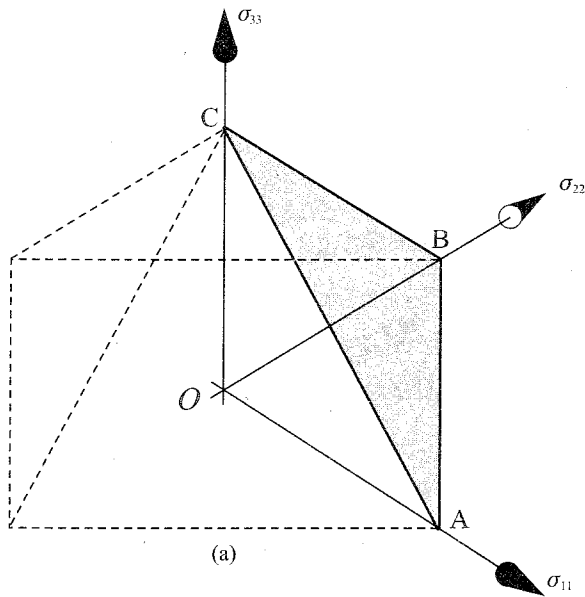


Figure 2.11. (a) Top half of a regular octahedron where the octahedral surfaces are situated between axes paralleling the principal stresses at point O . (b) Plane stress limits of linear material behavior.

with these coordinate axes, and the direction cosines $c_{nx} = c_{ny} = c_{nz} = (1/\sqrt{3})$, the product $[T] = [\sigma] \{v\}$ becomes

$$[\sigma_{tot}] = (1/\sqrt{3})[\sigma_{11} \quad \sigma_{22} \quad \sigma_{33}]$$

To obtain the magnitude of the octahedral shear stress vector, the purpose of this investigation, it is necessary to use only the Pythagorean theorem with the total stress vector and

the normal stress vector because this shearing stress vector is perpendicular to the normal stress vector. That is

$$\begin{aligned}\sigma_{oct}^2 &= (1/3)(\sigma_{11}^2 + \sigma_{22}^2 + \sigma_{33}^2) \\ &\quad - (1/9)(\sigma_{11}^2 + \sigma_{22}^2 + \sigma_{33}^2 - 2\sigma_{11}\sigma_{22} - 2\sigma_{22}\sigma_{33} - 2\sigma_{33}\sigma_{11})\end{aligned}$$

or

$$\sigma_{oct}^2 = (1/9)(2\sigma_{11}^2 + 2\sigma_{22}^2 + 2\sigma_{33}^2 - 2\sigma_{11}\sigma_{22} - 2\sigma_{22}\sigma_{33} - 2\sigma_{33}\sigma_{11})$$

or

$$\begin{aligned}\sigma_{oct}^2 &= (1/9)[(\sigma_{11}^2 - 2\sigma_{11}\sigma_{22} + \sigma_{22}^2) + (\sigma_{22}^2 - 2\sigma_{22}\sigma_{33} + \sigma_{33}^2) \\ &\quad + (\sigma_{11}^2 - 2\sigma_{11}\sigma_{33} + \sigma_{33}^2)]\end{aligned}$$

or

$$\sigma_{oct} = (1/3)[(\sigma_{11} - \sigma_{22})^2 + (\sigma_{22} - \sigma_{33})^2 + (\sigma_{33} - \sigma_{11})^2]^{1/2}$$

There is one more point to be made for future reference. Consider the plane stress case where $\sigma_3 = 0$. This case is important because thin skins are common in aerospace structures. In this case, the above equation may be rewritten as

$$9/2 = (\sigma_{11}^2 - \sigma_{11}\sigma_{22} + \sigma_{22}^2)/\sigma_{oct}^2$$

where the principal stresses are referenced to (i.e., nondimensionalized by) the magnitude of the octahedral stress. A plot of this equation is shown in Fig. 2.11(b). In Section 5.6, this plane stress curve will be interpreted to say, according to either the proposed octahedral shearing stress theory or the proposed maximum energy of distortion theory, that the material will obey Hooke's law (to be explained) as long as the pair of principal stresses, nondimensionalized by the material's maximum allowable octahedral shearing stress, plot within this ellipse.

Every structural analysis digital computer program can be expected to offer the analyst the option of listing the principal stresses and the octahedral (von Mises) shearing stresses at representative points within the structural elements (see Chapters 17 and 19) that are used to model the structure. As discussed in detail in Chapter 5, the maximum tensile stress among the principal stresses is useful in judging the possibility of fracture, particularly in brittle materials, and the possibility of crack propagation. The maximum compressive stress among the principal stresses is useful in judging the possibility of buckling of the structure. The von Mises shearing stress is useful in judging the possibility of the advent of plasticity in response to further stress.

2.9 **The Mathematical Description of Stresses**

There is one additional feature of both the plane stress equations and the three-dimensional stress equations that requires attention. This feature is evident in Eqs. (2.6) where the sine and cosine functions do not appear individually, but in pairs as coefficients for the stresses. If the rotated stresses for arbitrarily oriented areas were vector quantities, dealing with the rotated coordinate system would just be a matter of taking components of the stress vectors in different directions. In that case, the sines and cosines would appear individually, or in other words, to the first power. Thus it appears that rotated stresses, that is, stresses in general, are not vector quantities. From another viewpoint, vectors contain two items of information, a magnitude and a direction. The rotated stresses require the

specification of three items of information: a magnitude, a direction (normal or one of the shear directions or anything in between), and the direction of the normal to the plane on which the stress acts, which could be defined by a single coordinate. Clearly, while vectors are sufficient to describe stresses on fixed planes, they are insufficient to describe stresses in general. Thus the question arises as to what mathematical quantities are sufficient to describe stresses in general. An approach to the answer to that question can be inferred from the other quantity that goes by the name “vector,” which is a column or row matrix. The next step in the extension of a 3×1 column matrix or 1×3 row vector is a 3×3 square matrix. Indeed such square matrices are exactly what are used in Eq. (2.3) for the general equation describing rotated stresses. Thus it is inferred that the six stress values can be treated in generality when they are grouped as the 3×3 symmetric matrix of Eq. (2.4).

In this text matrices are used extensively because the reader is presumed to be well acquainted with them, and most actual structural computations today are matrix-based. However, matrices are not the only possible choice, or even always the best choice for the development of the theory of structural mechanics. There are other mathematical quantities called “tensors” that are suitable for the representation of the six stress components and even more extensive informational requirements. Second order tensors correspond roughly to square matrices. The differences between second order tensors and square matrices can be likened to the differences between a complex number and an ordinary vector confined to a plane. They both contain two bits of information, two components, but they obey different algebras, that is, they have different rules for multiplication. Tensors are not used at all in this introductory text because (i) an explanation of tensors would interrupt the development of the discussion of structural mechanics; and perhaps more importantly, (ii) their very elegance and conciseness in the management of the equations of structural mechanics, which is a boon to clarity in advanced texts, here might act to obscure the details of those equations as well as the engineering quantities the tensors represent. Nevertheless, as is pointed out occasionally in succeeding chapters, the results of tensor formulations guide the choices that are made between competing developments.

The choice between using matrix algebra or tensor algebra can be made on the basis that matrices are superior for organizing large or small numbers of ordinary differential equations, while tensors are generally superior for dealing with partial derivatives and partial differential equations.

Chapter 2 Exercises

- 2.1. (a) Confirm that the matrix product of Eq. (2.3) actually does provide the results displayed in Eq. (2.1).
(b) As in part (a), but this time for Eq. (2.2).
- 2.2. Starting with the case of plane stress and Fig. 2.12, rederive the two of the three stress rotation equilibrium equations for rotation of Cartesian coordinate axes that are associated with the stresses that appear in the figure. Do so in terms of the rotation angle θ , that is, without the use of direction cosines. Note that the differential element extending from the point P shown in Fig. 2.12 is constructed of an x^* plane as well as x , y , and z planes. Of course the z^* and z planes coincide. Only the stresses on the x^* face are provided for the reader.
- 2.3. (a) Justify the free body diagram (FBD) in Fig. 2.13 as a basis for deriving the third of the three plane stress rotation equations, the equation for σ_{yy}^* , and as

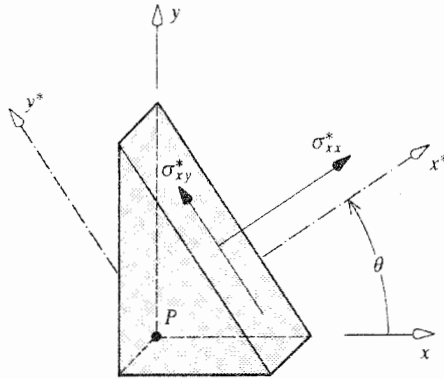


Figure 2.12. Exercise 2.2. A partially labelled free body diagram, which can be used to obtain formulas for two of the rotated plane stresses.

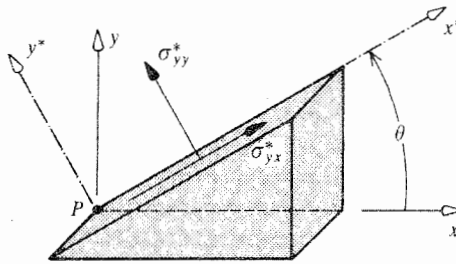


Figure 2.13. Exercise 2.3(a, b). A partially labelled free body diagram, which can be used to obtain formulas for two other rotated plane stresses.

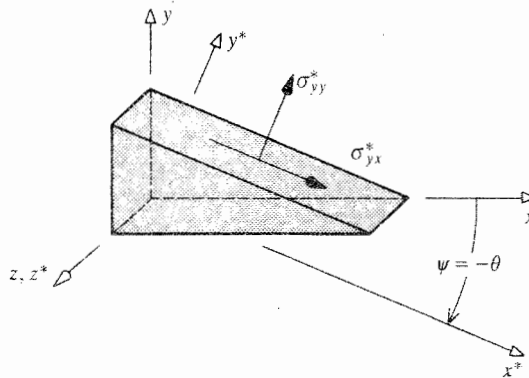


Figure 2.14. Exercise 2.3(c). A partially labelled free body diagram.

a basis for checking the equation for σ_{xy}^* . In particular, justify the direction of the σ_{xy}^* vector.

- (b) Use that same FBD to actually derive the equations for those two stresses in terms of the rotation angle θ , and compare these two results to the previous two results.

(c) As an example of still another approach, complete the FBD of Fig. 2.14 and determine the equations for the stresses σ_{xy}^* and σ_{yy}^* in terms of the angle ψ . Then set ψ equal to the negative of the angle θ , and compare these results to the previous solutions.

2.4. (a) Prove that the sum of the squares of the direction cosines of the normal to a rotated plane, relative to a fixed Cartesian coordinate system, equals 1. That is, prove $c_{nx}^2 + c_{ny}^2 + c_{nz}^2 = 1$. *Hint:* Represent the normal by a unit normal vector, and take the dot product of that vector with itself.

(b, c, d) Sketch the orientation of the rotated coordinate system relative to the original coordinate system when the matrix of direction cosines for the rotated coordinate system is

$$(b) \begin{bmatrix} 0 & 0 & -1 \\ 0 & 1 & 0 \\ 1 & 0 & 0 \end{bmatrix} \quad (c) \begin{bmatrix} 1 & 0 & 0 \\ 0 & -1 & 0 \\ 0 & 0 & -1 \end{bmatrix} \quad (d) \begin{bmatrix} 1 & 0 & 0 \\ 0 & 0.707 & 0.707 \\ 0 & -0.707 & 0.707 \end{bmatrix}$$

2.5. With respect to the analysis Cartesian coordinate system, the stress state at a certain point P in a certain loaded structure was determined to be as follows:

Case	σ_{xx}	σ_{yy}	σ_{zz}	σ_{xy}	σ_{xz}	σ_{yz}
(1)	-120 MPa	80 MPa	0	-100 MPa	0	0
(2)	-18 ksi	6 ksi	0	9 ksi	0	0
(3)	0	24 ksi	10 ksi	5 ksi	0	0
(4)	10 ksi	0	-8 ksi	$-5\sqrt{3}$ ksi	0	0
(5)	200 MPa	0	-90 MPa	$100\sqrt{3}$ MPa	0	0
(6)	70 MPa	70 MPa	70 MPa	0	0	0
(7)	100 MPa	20 MPa	-50 MPa	90 MPa	0	0
(8)	40 ksi	40 ksi	0	-45 ksi	0	0
(9)	-32 MPa	16 MPa	-12 MPa	10 MPa	0	0

(a) For these cases of plane stress, or plane stress augmented by a nonzero value of σ_{zz} (generalized plane stress), draw the Mohr's circle that represents the z plane. On the same sketch, draw the other two Mohr's circles that link the two principal planes determined by the first Mohr's circle to the third principal plane.

(b) Sketch and fully label the two differential elements at point P that when rotated in the z plane illustrate the z plane principal stresses and the maximum z plane shear stresses. Complete these two diagrams by including the σ_{zz} stresses as in Fig. 2.10.

(c) From the above, determine the absolute value of the overall maximum shear stress in the three-dimensional body.

2.6. If the matrix of stresses in the original coordinate system, and the matrix of direction cosines are, respectively,

$$[\sigma] = \begin{bmatrix} 15 & -10 & 0 \\ -10 & 5 & 0 \\ 0 & 0 & 20 \end{bmatrix} \text{ ksi} \quad [c] = \begin{bmatrix} 3/5 & 0 & -4/5 \\ 0 & 1 & 0 \\ 4/5 & 0 & 3/5 \end{bmatrix}$$

- (a) Calculate the stresses associated with the rotated coordinate system
 (b) Sketch the rotated axes relative to the original axis system.
- 2.7. (a) For the stress matrix of Exercise 2.6, determine the Cartesian components of the total stress vector (or, if the surface is regarded as a boundary surface, the Cartesian components of the total traction vector) acting on the plane that intersects the coordinate axes at the points (2, 0, 0), (0, 3, 0), and (0, 0, 4).
 (b) Determine the magnitude of the total stress vector (or total traction vector), and the magnitude of the normal component of the total stress vector for the given plane of part (a).
 (c) Determine the magnitude of the total shear vector acting on the given surface of part (a).

FOR THE EAGER

- 2.8. (a) Given that the cubic polynomial equation for the principal stresses in a certain case is

$$\sigma^3 + 3\sigma^2 - 58\sigma + 122 = 0$$

determine the middle root of this equation by any iterative method (not a programmable hand calculator). Converge to at least two significant digits. The stress units are MPa.

- (b) Determine the middle root of the principal stress polynomial equation $\sigma^3 + 8\sigma^2 - 612\sigma + 3568 = 0$, where σ has the units of ksi.
 (c) Determine the one negative root of the principal stress polynomial equation $\sigma^3 - 22\sigma^2 - 5\sigma + 1498 = 0$, where σ has the units of ksi.
 (d) Given that the cubic equation $\sigma^3 - 2\sigma^2 - 83\sigma + 300 = 0$ has a root $\sigma = 7.7178$ MPa, determine the quadratic equation that contains the other two roots.
- 2.9. For each of the following orthogonal stress matrices associated with an analysis Cartesian coordinate system, determine the values of the principal stresses. Do not determine their orientation. *Hint:* In part (a) there is a negative integer root. For all parts, recall that in a cubic equation, the sum of the three roots is equal to the negative of the coefficient of the quadratic term, and the product of the three roots is equal to the negative of the constant term. Use the first of these two facts in conjunction with the invariance of the sum of the normal stresses to check on the second coefficient of the polynomial equation result of your determinant expansion, and both facts to check on the values of your roots.

$$(a) [\sigma] = \begin{bmatrix} -10.0 & 4.0 & -5.0 \\ 4.0 & 0 & 4.0 \\ -5.0 & 4.0 & -10.0 \end{bmatrix} \text{ ksi} \quad (b) [\sigma] = \begin{bmatrix} 70 & 40 & 10 \\ 40 & 80 & 20 \\ 10 & 20 & 30 \end{bmatrix} \text{ MPa}$$

$$(c) [\sigma] = \begin{bmatrix} 60 & 20 & 0 \\ 20 & 20 & -30 \\ 0 & -30 & 0 \end{bmatrix} \text{ MPa} \quad (d) [\sigma] = \begin{bmatrix} 14.0 & 0 & -5.0 \\ 0 & 8.0 & -9.0 \\ -5.0 & -9.0 & -10.0 \end{bmatrix} \text{ ksi}$$

$$(e) [\sigma] = \begin{bmatrix} 12.0 & 5.0 & -6.0 \\ 5.0 & 0 & 8.0 \\ -6.0 & 8.0 & 10.0 \end{bmatrix} \text{ ksi} \quad (f) [\sigma] = \begin{bmatrix} 20 & 5 & 0 \\ 5 & -10 & 10 \\ 0 & 10 & -5 \end{bmatrix} \text{ MPa}$$

$$(g) [\sigma] = \begin{bmatrix} 20.0 & -12.0 & 0 \\ -12.0 & -16.0 & 10.0 \\ 0 & 10.0 & -12.0 \end{bmatrix} \text{ ksi}$$

- 2.10.** Justify Mohr's circle by demonstrating that the first and third of the plane stress equations, Eqs. (2.6a), are the parametric forms for a circle centered at the mean normal stress point $(\sigma_{xx} + \sigma_{yy})/2, 0$ on the stress plane used to construct Mohr's circle. *Hint:* Recall that the general equation of a circle centered at (h, k) on the x, y plane is $(x - h)^2 + (y - k)^2 = r^2$; and recall that the radius of Mohr's circle is the square root of the sum of the squares of one half the difference between the normal stresses and shearing stress.
- 2.11.** Equation (2.3) describes the stresses in a rotated Cartesian coordinate system with respect to the stresses of an original Cartesian coordinate system. Explain why this same equation is valid for cylindrical, spherical, and mixed orthogonal coordinate systems.

Endnote (1) Solution for the Planes of Principal Stress

After the solution for the principal stresses in the form of the solution for the three eigenvalues of Eq. (2.9b), the three orthogonal planes upon which those principal stresses act can be specified by determining the direction cosines for the normal to each of those planes. For example, to determine the three direction cosines for the normal to the front face plane upon which the first principal stress acts, start by substituting the solution for the first eigenvalue into the second part of Eq. (2.9b). Recall that the coefficient matrix of these three homogeneous, simultaneous equations is singular, and thus these three equations cannot be solved simultaneously for the three direction cosines. To rid the solution process of that singularity, simply discard any one of the three simultaneous equations. Replace that discarded equation by the identity (see Exercise 2.4)

$$v_x^2 + v_y^2 + v_z^2 = 1.0 \quad (2.12)$$

The two equations retained from Eq. (2.9b) and the above equation combine to provide three equations that can be solved for the three direction cosines. Since the last of these three equations is nonlinear, it is best to simultaneously solve the two linear equations so as to obtain any two of the direction cosines in terms of the third, and then substitute for those direction cosines into Eq. (2.12). The result is one quadratic equation Eq. (2.12), in terms of one direction cosine. Of course, the square of that direction cosine will always equal a positive quantity less than 1, and the positive and negative values that are the solution for the direction cosine itself represent the outer normals of the planes on opposite sides of the rectangular parallelepiped. Front face planes have two or three positive direction cosines. The interdependence of all of the direction cosines is further explored in Exercise 4.2.

Displacements and Strains

3.1 Introduction

At this point, all that is available for the purpose of accomplishing a general structural analysis are the three equilibrium equations, Eqs. (1.6). These equations pertain to the stress state in a general structural body subjected to a general mechanical loading (including dynamic loads) and a temperature change. These three equations are insufficient to deduce the six stresses that define the stress state. Since the reader's ambition and good sense require nothing less than a complete set of equations that are applicable to a structure of any shape or material, as well as any loading, it is necessary to look beyond equilibrium considerations in order to describe fully the response of a general structural body. The two other physical phenomena that need to be investigated in order to obtain additional equations are the geometry of the deformations of the general structure, and the response of materials to mechanical and thermal loadings. Descriptions of the deformations of loaded structures are the focus of this chapter and Chapter 4. Chapters 5 and 6 discuss the response of structural materials to loadings and temperature changes.

3.2 Displacements

The general concept of a *displacement* is simply that of a movement; a change in position that has been completed or is in progress. The change in position involves both a direction and a distance. Thus a displacement is defined as a vector quantity. For engineering purposes, the displacement concept must be susceptible to precise description and measurement. For this purpose, a displacement is associated with every geometric point within and on the boundaries of a structural body, and the components of each displacement vector can be referenced to a specific coordinate system. As with stresses, the association of displacements with geometric points allows the mathematical treatment of displacement components as point functions. This, in turn, allows the full use of the calculus in dealing with displacements and their components. Depending on the choice of the coordinate system, the components of the total displacement can be described as straight-line distances, curvilinear distances, angles, and so forth. As was done previously, for the sake of simplicity, the discussion begins with a Cartesian coordinate system. When a Cartesian coordinate system is used, the displacement components in the x , y , and z directions, at the general point $P(x, y, z)$, are symbolized as $u(x, y, z; t)$, $v(x, y, z; t)$, $w(x, y, z; t)$, respectively, where t is the symbol for time. For the reason of lack of emphasis in this textbook, all explicit references to a functional dependence on time are omitted hereafter. Short-hand variations on the displacement symbols are $u(P)$, $v(P)$, and $w(P)$, or just u , v , and w . Thus the total displacement vector at a point P can be written as

$$\mathbf{D} = u\mathbf{i} + v\mathbf{j} + w\mathbf{k} \quad (3.1)$$

where \mathbf{i} , \mathbf{j} , and \mathbf{k} are the Cartesian unit vectors.

Let a cooked potato represent a structural body of general shape. Picture gently supporting the potato in one's hand and very slowly moving it about along an arbitrary path. The intermediate and final translations and rotations experienced by the potato can all be described by the three functions u , v , and w for each point within the potato and for each point on its outer boundary. Since the potato is being moved very slowly, there is no appreciable development of kinetic energy, or what amounts to the same thing, no appreciable development of inertia forces. Thus, while there are all sorts of displacements as the potato is moved about, there are no noticeable changes in the shape or size of the potato beyond those which were previously incurred due to the initial support provided by the hand. If now the supporting hand mashes the potato, the result is a considerable change in the shape of the potato, and perhaps some change in the size of the potato as well. Changes in size or shape are collectively called *deformations*. While the above-described physical situation may have small complications, it is possible to concentrate wholly on the motion (kinematics) of points within the volume of the potato and see that there are two mutually exclusive and exhaustive categories into which the displacements may be separated. The first category is the one where the body moves without undergoing any deformations of either kind. The displacements of this category are called, for self-evident reasons, *rigid body displacements*. A useful way of characterizing rigid body displacements is to note that there are no relative displacements between points within the volume of the body.

It is only the second category of displacements that is of present concern. That is the category of displacements that result in deformations, and these displacements are the relative displacements between different points within the structural body. These relative displacements precisely quantify the deformation of the structure, and vice versa. That is, anticipating developments in later chapters, it can be expected that the relative displacements (deformations) fully describe the structural response of any body to the loads and temperature changes acting throughout the body. The relative displacements are separated from the rigid body displacements merely by referencing all the displacements that produce relative changes in position to the undeformed geometry of the structural body. Hereafter, the relative displacements are referred to as the *structural displacements*, or simply as the displacements. Figure 3.1 provides a pictorial explanation of rigid body and relative displacements.

Before proceeding to discuss structural displacements, there is one other widely used term that is mentioned now so as to avoid confusion. As is explained in Part III, *deflections* are the lateral and longitudinal displacements of specially designated axes within bars and beams, and the normal and in-plane displacements of specially designated surfaces within membranes, plates, and shells. By extension, the term deflections is also used to describe the changes in position of whole structures that are viewed as being composed of those types of structural elements.

3.3 Longitudinal Strains

To begin the formal discussion of the engineering organization of structural displacements, consider the now familiar, differential, rectangular parallelepiped extending from the arbitrary point $P(x, y, z)$ inside a general body as is shown in Fig. 3.2(a). Again, for the sake of clarity, the size of the infinitesimal parallelepiped has been greatly exaggerated. Since the ultimate purpose is to relate the deformations within the structural body at point P to the stresses at the same point P , and since the stresses at point P are the back

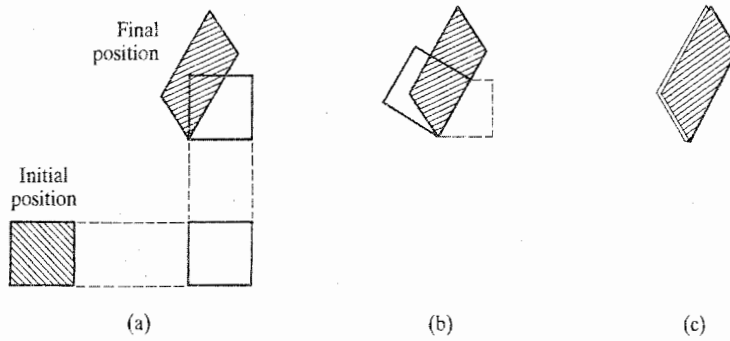


Figure 3.1. (a) Two “rigid body” translations in the plane of the paper as the first two parts of the total displacement from the initial to final positions of a representative structural element. (b) A “rigid body” rotation as the third step in formulating a combination of rigid body displacements and relative displacements that link the initial position to the final position of the representative element. (c) Relative displacements in the form of changes in size and changes in shape to complete the movement of the structural element to its final position.

face stresses, the edges of the intersecting back faces are emphasized as solid lines while the other edges are represented as dashed lines.

After the application of the loads and temperature changes, the structural body deforms, and the material point P , formerly at the geometric point $P(x, y, z)$, moves through the structural displacements u, v, w to the new geometric point $P'(x + u, y + v, z + w)$. Similarly, the other parallelepiped corner points Q, R , and S move to Q', R' , and S' ; see Fig. 3.2(b). Note that the Cartesian coordinate system chosen to locate position and identify material points in the undeformed body is not altered by the application of loads to the body of interest. In other words, the coordinate system associated with the undeformed structure is also here used to identify “material points” for the deformed state. Such a coordinate system is called a *Lagrangian* coordinate system.¹ (When a coordinate system chosen for the deformed state is used to identify material points for the analysis, that coordinate system is called an *Eulerian* coordinate system.²) The deformed line segments $P'Q', P'R', P'S'$ are still drawn as straight lines because of their differential lengths. However, after deformation these differential-sized lengths no longer have the values dx, dy , and dz , and the line segments are no longer perpendicular to each other. Figure 3.3 shows, in one sketch, the parallelepiped back face edges before and after deformation in order to focus upon the displacements that tie together those two back face edge configurations. In Fig. 3.3, the size of these before and after differential line segments has been greatly exaggerated relative to the displacements in order to make the sketch more easily understood. Be sure to understand that the displacements u, v , and w are not differential quantities. While the displacements

¹ Giuseppe Luigi Lagrange was born in Turin in 1736, died in Paris in 1813, and is buried in the Pantheon in Paris. According to Ref. [2], “Lagrange has been said to be second only to Newton among the modern mathematicians. He is the discoverer of the calculus of variations, and he is considered the father of analytic mechanics.”

² Leonhard Euler, a Swiss mathematician and scientist, was born in Basel in 1707 and died in St. Petersburg in 1783. According to Ref. [2], he is considered the greatest mathematician of the eighteenth century.

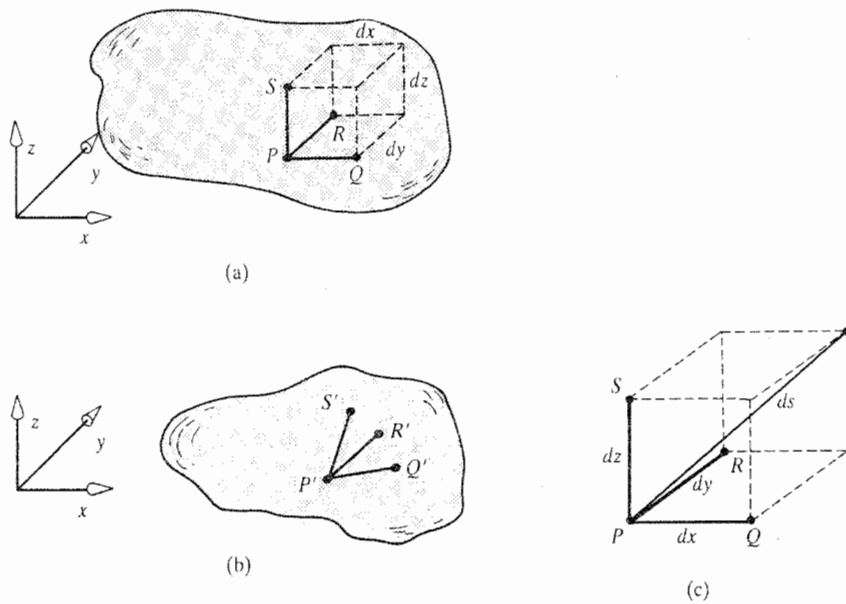


Figure 3.2. (a) A structure of general shape before the application of loads with the usual differential rectangular parallelepiped extending from point P . (b) The same structure of general shape after the application of loads, showing the distortions of the three edges of the original rectangular parallelepiped when the material points P , Q , R , S move to locations P' , Q' , R' , S' of the fixed coordinate system. (c) Examination of the changes in the lengths and orientations of dx , dy , and dz is equivalent to examining changes in length and orientation of the length ds .

are generally very much smaller than the dimensions of the structure, they are nevertheless finite quantities, and hence are very much larger than the infinitesimal parallelepiped edges.

Before discussing the features of Fig. 3.3, let the requirement of being differentiable be imposed upon the mathematical descriptions of the three displacement component functions $u(P)$, $v(P)$, and $w(P)$. The need for such a requirement can be explained as follows. In order to reflect the everyday experience with loaded structures that, short of failure, the material points do not separate or overlap, it must be required that the displacement functions be single-valued, continuous functions of the geometric coordinates. To reflect the further experience that, within solid bodies, all the displacement functions have only smooth changes from one point to another, it is required that the displacement functions be differentiable. Not caring to be economical on this matter, and with a view to the further use of Taylor's series, it is temporarily assumed that the displacement functions possess an infinite number of successive partial derivatives, just as was initially done with stress functions.

Again, the Cartesian components of the displacement of the material point P from the geometric point $P(x, y, z)$ to the geometric point $P'(x + u, y + v, z + w)$ are defined as u , v , and w . Since the point Q is different from the point P , all the displacement components at point Q have to be assumed to be different from those of point P . The point Q is not an arbitrary point in relation to point P . Point Q is a distance dx in the x direction from

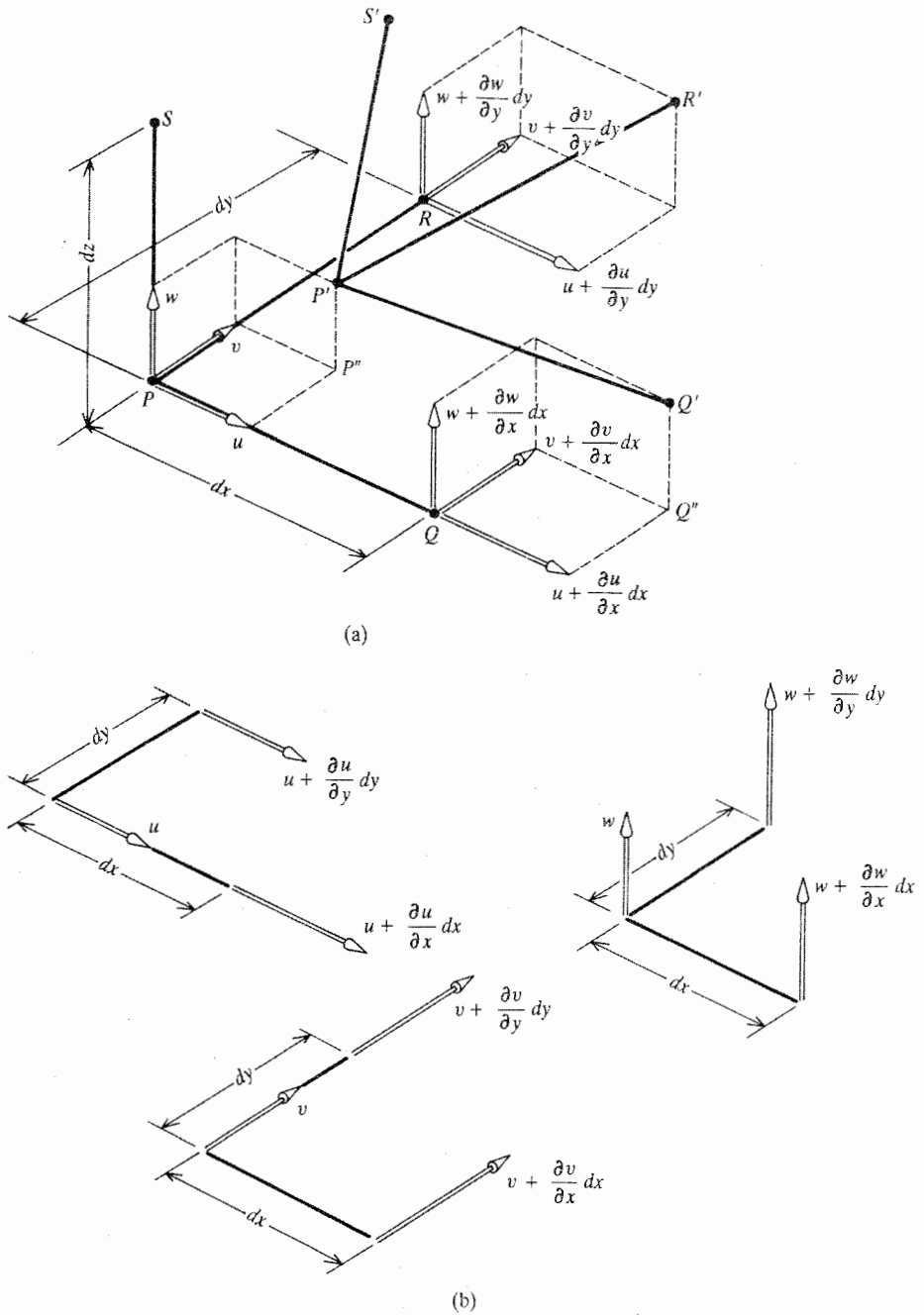


Figure 3.3. (a) A smaller scale, before and after deformation, view of the three differential rectangular parallelepiped edges that extend from point P , plus the Cartesian components of the deformation vectors that link the points P, Q, R, S to the points P', Q', R', S' . (b) A pictorial explanation of the differential-sized changes in each of the three Cartesian components of the total deflection vector at point P . Note that changes with respect to z have been omitted for clarity.

point P . Such a knowledge of the spatial separation of these two points allows the use of a one-dimensional Taylor's series to describe the relation between any two point functions evaluated at P and Q . For example, the x direction component of the displacement of the material point Q , symbolized as $u(x + dx, y, z)$, can be related to the same quantity at point P , which is $u(x, y, z)$. Again, since the spatial separation between this pair of points is entirely in the x direction, the Taylor's series does not involve any changes (derivatives) in either the y or z directions. Thus this Taylor's series, for zero y and z direction changes, is

$$\begin{aligned} u(x + dx, y, z) = & u(x, y, z) + dx \left(\frac{\partial u}{\partial x} \right) + \frac{1}{2!} (dx)^2 \left(\frac{\partial^2 u}{\partial x^2} \right) \\ & + \frac{1}{3!} (dx)^3 \left(\frac{\partial^3 u}{\partial x^3} \right) + \dots \end{aligned} \quad (3.2)$$

where all the derivatives are evaluated at $P(x, y, z)$. Once again, all terms after the second right-hand side term can be discarded as infinitesimal compared to the second right-hand side term. The second right-hand side term is retained to represent the infinitesimal difference in the displacements over the infinitesimal distances dx . Now consider the y and z components of the total displacement at point Q . The functions $v(Q)$ and $w(Q)$ are functions exactly like the function $u(Q)$. The values of these two functions at the point Q can be related to their respective values at the neighboring point P in exactly the same fashion as used above for the x component of the total displacement. It does not matter that these functions have the meanings of displacements in directions other than the x direction. The fact that does matter is that in both cases the three displacement component functions are being related across a separation in the x direction only. Thus, with the same Taylor's series and the same truncation as above

$$v(x + dx, y, z) = v(x, y, z) + \left(\frac{\partial v}{\partial x} \right) dx \quad (3.3a)$$

$$w(x + dx, y, z) = w(x, y, z) + \left(\frac{\partial w}{\partial x} \right) dx$$

Once again, as with the stresses, a simple geometric argument based on the interpretation of the derivative as a tangent to the function at point P could have been used to obtain Eqs. (3.3a) as an approximation. However, the insignificance of the error of the approximation would not have been as evident.

The same techniques can be used to describe the displacements at the point R . In this case the separation from the reference point P is entirely in the y direction, so all changes in the three displacement functions evaluated at the point R are y direction changes. Their mathematical representations are as follows:

$$\begin{aligned} u(x, y + dy, z) &= u(x, y, z) + \frac{\partial u}{\partial y} dy \\ v(x, y + dy, z) &= v(x, y, z) + \frac{\partial v}{\partial y} dy \\ w(x, y + dy, z) &= w(x, y, z) + \frac{\partial w}{\partial y} dy \end{aligned} \quad (3.3b)$$

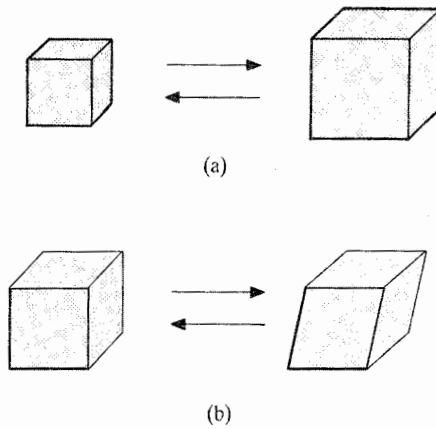


Figure 3.4. Division of deformations into two mutually exclusive categories that in combination describe any total deformation: (a) changes in size without changes in shape; (b) changes in shape without changes in size. Note again that the changes in the parallelepiped edges that emanate from point P fully describe the changes in the total parallelepiped.

Finally, for the point S :

$$\begin{aligned}
 u(x, y, z + dz) &= u(x, y, z) + \frac{\partial u}{\partial z} dz \\
 v(x, y, z + dz) &= v(x, y, z) + \frac{\partial v}{\partial z} dz \\
 w(x, y, z + dz) &= w(x, y, z) + \frac{\partial w}{\partial z} dz
 \end{aligned}
 \tag{3.3c}$$

The last set of displacements are not shown in Fig. 3.3 in order to simplify the sketch.

There are two types of deformations in Fig. 3.3. There are overall and local changes in body size and there are overall and local changes in body shape. From Fig. 3.4 it should be clear that local changes in body size at point P can be described by the changes in the lengths of the original rectangular parallelepiped edges. Also, at point P , there are local changes in body shape represented on this differential scale by the changes in the three right angles of the original rectangular parallelepiped. Since these two types of deformations can occur independently of each other, they can be investigated separately. Since they can occur simultaneously, the total deformation is considered to be the sum of these two types of deformations. In other words, the total deformation consists of a change in size plus a change in shape. The change in size is measured by measuring changes in length, while the change in shape is measured by changes in right angles.

The change in length of the parallelepiped edge PQ is the difference between the lengths $P'Q'$ and PQ . It is reasonable to compare these two lengths because the line segment $P'Q'$ is very nearly parallel to the line segment PQ in all the "small-displacement" cases considered in this introductory text. This is so in such cases because, as is discussed in the later chapters dealing with engineering materials, all nondimensional (angular) quantities, such as $\partial v/\partial x$ and $\partial w/\partial x$, generally have magnitudes on the order of 0.001 (one-twentieth of one degree) or less.

The length PQ is simply dx . The length $P'Q'$, call it $d\hat{x}$, can be calculated using the Pythagorean theorem with a knowledge of the displacements. Referring to Fig. 3.3, the projection of the line segment $P'Q'$ on the $z = 0$ plane is the line segment $P''Q''$. The

projection of $P''Q''$ on the x axis has the length

$$\left\{ dx + \left[u + \frac{\partial u}{\partial x} dx \right] - u \right\} = dx + \frac{\partial u}{\partial x} dx$$

where, again, u and its derivatives are evaluated at $P(x, y, z)$. Now the Pythagorean theorem can be used to calculate the length of the hypotenuse $P''Q''$. The length of the other side of the triangle adjacent to the right angle is $\left\{ \left[v + \left(\frac{\partial v}{\partial x} \right) dx \right] - v \right\}$. The square of the length of $P''Q''$ is then

$$\overline{P''Q''}^2 = \left[dx + \frac{\partial u}{\partial x} dx \right]^2 + \left[\frac{\partial v}{\partial x} dx \right]^2$$

The last step in calculating the length of $P'Q'$ is repeating what was done in the horizontal plane $z = 0$, in the vertical plane of $P'Q'$ and $P''Q''$. Then³

$$d\hat{x} = \left\{ \left[dx + \frac{\partial u}{\partial x} dx \right]^2 + \left[\frac{\partial v}{\partial x} dx \right]^2 + \left[\frac{\partial w}{\partial x} dx \right]^2 \right\}^{1/2} \quad (3.4)$$

Now all is ready to compute the change in length of the original line segment PQ , which is simply the difference between the lengths $d\hat{x}$ and dx . (The question as to whether or not this is the best way to measure changes in size in the x direction irrespective of changes in shape is addressed later.) Before calculating that difference, note that engineers generally favor the use of nondimensional quantities because no system of units is inherent in physical laws. The use of nondimensional quantities provides the small convenience of not having to list units and the more important advantage of clarifying the relative magnitudes of the terms involved. Moreover, there is also a particular advantage to nondimensionalizing the difference between $d\hat{x}$ and dx by referencing (dividing) that difference to (by) the original differential length, dx . As is seen in the following, dividing the difference in differential lengths by the original differential length eliminates the indefinite quantity dx from the result.

As an elaboration on the second cited general advantage of nondimensionalizing, consider two rubber bands with the same cross-sectional area. Let the first rubber band have a unit length, and the second a length of ten units. If both rubber bands are stretched by equal forces, the second rubber band has ten times the total change in length as that of the first, because each unit length of the second rubber band duplicates the stretch of the unit length of the first rubber band. Since the ultimate goal is to relate deformations to stresses, it is clear that there is the problem here of two different changes of length associated with a single stress value. The problem is resolved by dividing the different total changes in length by the respective original lengths. Then this ratio of change in total length over original length is the same value for the two different rubber bands with the same stress. Thus there is the prospect of a unique relationship between such an elongation ratio and stress.

On the above-cited bases, it is the nondimensionalized difference between the before and after lengths that is used to describe a change in length. A special name is adopted. The nondimensionalized change in length associated with each of the three orthogonal coordinate directions is called a *longitudinal strain*, or a *normal strain*. A normal or longitudinal strain

³ Note that the final result is what may be called the Pythagorean theorem in three dimensions; that is, with respect to three right angle components, the square of the diagonal is equal to the sum of the squares of the components. Another, more simple proof can be based upon representing the diagonal as a vector that is described in terms of its three orthogonal components, and then taking the vector's dot product with itself.

is symbolized by a lower-case epsilon (ϵ) plus a double subscript that indicates the direction in which the change in length is measured. For the case at hand

$$\epsilon_{xx} \equiv \frac{d\hat{x} - dx}{dx} \quad \epsilon_{yy} \equiv \frac{d\hat{y} - dy}{dy} \quad \epsilon_{zz} \equiv \frac{d\hat{z} - dz}{dz} \quad (3.5)$$

In Eq. (3.4), the differential distance dx that appears inside the radical as a squared term, can be factored out of the radical as simply dx . Then substitution into Eq. (3.5) yields:

$$\epsilon_{xx} = \left[1 + 2 \left(\frac{\partial u}{\partial x} \right) + \left(\frac{\partial u}{\partial x} \right)^2 + \left(\frac{\partial v}{\partial x} \right)^2 + \left(\frac{\partial w}{\partial x} \right)^2 \right]^{1/2} - 1 \quad (3.6)$$

The lack of simplicity in the above right-hand side is sufficient to raise the question as to what other means can be employed to describe changes in size. However, Eq. (3.6) is easily salvaged when the partial derivative terms are small quantities. Such is the case in almost all engineering structures. For example, consider the floor of any building or deck of any vehicle. Floors and decks do have their importance, particularly in tall buildings, ships, and aircraft. A sag with a 6° slope (0.1 radian) in a floor that was expected to be flat would be a rather disturbing slope for anyone supported by that floor. In the circumstances of a ship or aircraft deck, a perceived change in the difference in slope of 6° between one location and another would also produce considerable unease. Yet a slope value of one-tenth for $\partial w/\partial x$ and similarly for $\partial u/\partial x$ and $\partial v/\partial x$, when squared, makes these three terms quite small relative to the value of 1.0 in the radical of Eq. (3.6). Another aspect contributing to the smallness of these terms is that, in the cases of beams or plates respectively, one or two of these partial derivatives would not be slopes, rather they would be measures of stretching. On this point, note that while it is not difficult to bend a plastic ruler to a slope along its length (call the lengthwise direction the x direction) of 0.1 radian, not many people are strong enough to pull on a 12-inch plastic ruler and stretch it 1.2 inches, so that the value of $\partial u/\partial x$ would be also approximately one-tenth.

Although they may not be commonplace, slopes on the order of one-tenth or more do occur in some vehicular structures. If one were to compare photographs of the wings of the world circumnavigating Voyager experimental aircraft in flight, where the wings are bent upward as they support the weight of the aircraft, with photographs of the same wings loaded with fuel scraping the runway as that aircraft started its take-off run, it would be clear that there were cumulative changes in spanwise wing bending slopes considerably greater than 0.1 radian. Even then, and for almost all engineering applications, the radical in Eq. (3.6) is dominated by the term 1.0. This fact suggests how this radical can be greatly simplified. To this end, use may be made of the binomial series, which is reviewed in Section I.4. In this case the exponent of the binomial term is $\frac{1}{2}$, and the quantity whose absolute value is less than 1 is everything in the radical but the integer 1. Carrying out the expansion yields

$$\begin{aligned} \epsilon_{xx} = & 1 + \frac{1}{2} \left[2 \frac{\partial u}{\partial x} + \left(\frac{\partial u}{\partial x} \right)^2 + \left(\frac{\partial v}{\partial x} \right)^2 + \left(\frac{\partial w}{\partial x} \right)^2 \right] \\ & - \frac{1}{8} \left[4 \left(\frac{\partial u}{\partial x} \right)^2 + 4 \left(\frac{\partial u}{\partial x} \right)^3 + 4 \frac{\partial u}{\partial x} \left(\frac{\partial u}{\partial x} \right)^2 \right] \\ & + [\text{Seven other products involving the slopes with combined exponents of three or four}] \\ & + \left[\text{other terms where } \frac{1}{2} \left(\frac{\partial u}{\partial x} \right)^3 \text{ is the largest of the lot} \right] + [\text{still smaller terms}] - 1 \end{aligned}$$

Note that the leading +1 and ending -1 cancel each other. Striking a compromise between the need to save more than just the remaining most dominant terms on the one hand and the desire to simplify by discarding the smaller terms on the other hand, leads to discarding all triple and higher products of these nondimensional slopes whose maximum magnitudes for individual structural elements can be taken to be on the order of one-tenth. The result is

$$\epsilon_{xx} = \frac{\partial u}{\partial x} + \frac{1}{2} \left[\left(\frac{\partial v}{\partial x} \right)^2 + \left(\frac{\partial w}{\partial x} \right)^2 \right] \quad (3.7)$$

The longitudinal strain terms that measure changes in size in the y and z directions follow exactly the same form as that in Eq. (3.7). See the exercises. (The statement of these other two equations, or another, similar set of equations, is postponed until after discussion of changes in shape.) This measure of the change in size in the x direction has a linear part, $\partial u/\partial x$, and a nonlinear part which is enclosed in brackets. The nonlinear part, not always, but most often greatly complicates analyses, and is thus to be avoided whenever its contribution to the final result is believed to be secondary. The nonlinear part is only significant when the deformations described by the above partial derivatives have values on the order of one-tenth or more. Skipping over some possible refinements, such a situation, where the nonlinear terms have significance, is here called a case of *finite deformations*. Otherwise the situation is called a case of *small deformations*. In the theory beyond this chapter, and in all exercises and all examples presented in this text, it is implicitly presumed, unless otherwise stated, that the deformations are small, and thus the nonlinear portion of each strain expression can be dropped as insignificant. However, there is a routine exception where finite deformations are always considered, but sometimes without special mention. The exception is the case of elastic stability analyses. In such analyses, the nonlinear part of a slope-type strain combines with a large force or moment component to become an essential part of the analysis. The importance of such analyses requires that this text present the nonlinear portions of the six strain expressions in this chapter, and of course use them (perhaps indirectly) when investigating the elastic stability of a structure.

3.4 Shearing Strains

Recall that the means adopted above for measuring changes in size were to measure changes in length in the three orthogonal directions. The means adopted for measuring changes in shape are those of measuring the changes in the three right angles between those edges of the differential rectangular parallelepiped extending from point P . Note the unusual circumstance here where a decrease in the right angles is taken to be a positive change. This is so because the positive changes in displacements cause the right angles of the parallelepiped at point P to diminish, and it is desired to associate positive changes in shape with positive displacements.

Consider again the right angle RPQ , which is transported during the deformation process into $R'P'Q'$ as shown in Fig. 3.3. The total change in the original right angle RPQ is called an *engineering shearing strain*, or an *engineering shear strain*. To be wholly clear, the engineering shearing strain in the z plane is the difference between the right angle RPQ and the angle $R'P'Q'$, which has a very slightly skewed orientation, and which is something very slightly less than a right angle. Like longitudinal strains, the units of shearing strain are never degrees, but are always radians, or equivalently m/m , in/in , mm/mm , and so on. Engineering shearing strains are denoted by lower-case gamma (γ) with coordinate subscripts that indicate the orthogonal axes that define the original right angle. In the case

of the right angle RPQ , the axes that parallel the original line segments are the x and y axes, so the associated engineering shearing strain is symbolized by γ_{xy} . If ϕ denotes the near $\pi/2$ magnitude of the angle $R'P'Q'$, then $\gamma_{xy} = (\pi/2) - \phi$. It is of no importance that there is no plane to which the angle γ_{xy} can be precisely ascribed. Again, since the tilt of the plane of the angle $R'P'Q'$ is quite small, the angle γ_{xy} is simply associated with the z plane. Note further that since the change in angle between the line segment paralleling the x axis and the one paralleling the y axis is the same as the change in angle between the line segment paralleling the y axis and the one paralleling the x axis, $\gamma_{xy} = \gamma_{yx}$.

The task ahead is to develop an expression for this engineering shearing strain in terms of the displacements. The task is accomplished as follows. The change in the original right angle is determined by calculating the cosine of the angle $R'P'Q'$, which is $\cos \phi = \cos[(\pi/2) - \gamma_{xy}] = +\sin \gamma_{xy} \approx \gamma_{xy}$. The approximation of the sine of an angle by the angle is in error by less than 0.5 percent even when the angle is as large as 0.1 radian (5.7°). Check that statement on a hand calculator, or better yet, by reference to the series expansion for the sine function. Such a large shearing angle as 0.1 radian is, to say the least, highly unusual in an engineering structure. Thus it may be concluded that replacing the sine by the angle in this case is well warranted.

The cosine of ϕ can be determined by creating the vectors $P\bar{Q}' = \mathbf{Q}$, and $P\bar{R}' = \mathbf{R}$, and dividing by their magnitudes, Q and R , respectively, to form unit vectors, and then taking their dot product. Since

$$\mathbf{Q} = dx \left[\left(1 + \frac{\partial u}{\partial x} \right) \mathbf{i} + \frac{\partial v}{\partial x} \mathbf{j} + \frac{\partial w}{\partial x} \mathbf{k} \right]$$

and

$$\mathbf{R} = dy \left[\frac{\partial u}{\partial y} \mathbf{i} + \left(1 + \frac{\partial v}{\partial y} \right) \mathbf{j} + \frac{\partial w}{\partial y} \mathbf{k} \right]$$

By taking the square root of the dot product of each of the two vectors with itself, the vector magnitudes are

$$Q = dx \left[\left(1 + \frac{\partial u}{\partial x} \right)^2 + \left(\frac{\partial v}{\partial x} \right)^2 + \left(\frac{\partial w}{\partial x} \right)^2 \right]^{1/2}$$

$$R = dy \left[\left(\frac{\partial u}{\partial y} \right)^2 + \left(1 + \frac{\partial v}{\partial y} \right)^2 + \left(\frac{\partial w}{\partial y} \right)^2 \right]^{1/2}$$

Then $\cos \phi = (\mathbf{R} \cdot \mathbf{Q})/(RQ)$. After canceling the differentials dx and dy in the numerator and denominator, the numerator, temporarily called "num," is

$$\text{num} = \frac{\partial u}{\partial y} + \frac{\partial v}{\partial x} + \frac{\partial u}{\partial x} \frac{\partial u}{\partial y} + \frac{\partial v}{\partial x} \frac{\partial v}{\partial y} + \frac{\partial u}{\partial x} \frac{\partial w}{\partial y}$$

The denominator is a bit of a mess. The best way of dealing with the denominator is to use the binomial expansion with the exponent of $-\frac{1}{2}$ for both R and Q in order to have a product rather than a divisor to interact with the numerator. Looking ahead, the only terms worth keeping from the inverse of the denominator are terms involving slopes to the first and zeroth powers. This is so because the numerator only involves slopes to the first and second powers, and on the same basis used for the longitudinal strains, it is desired that the product of the numerator and inverse of the denominator also retain slopes to the first and

second powers. So, with the above-indicated truncation and $|q| < 1$, the binomial series for a term of the form of

$$\frac{1}{(1+q)^{1/2}} \approx 1 - \frac{q}{2}$$

Thus the inverse of the denominator without the canceled differentials dx and dy is reduced to $[1 - (\partial u/\partial x)][1 - (\partial u/\partial y)]$. Therefore, the final result is

$$\cos \phi = \gamma_{xy} = \frac{\partial u}{\partial y} + \frac{\partial v}{\partial x} - \frac{\partial u}{\partial x} \frac{\partial v}{\partial x} - \frac{\partial u}{\partial y} \frac{\partial v}{\partial y} + \frac{\partial w}{\partial x} \frac{\partial w}{\partial y} \quad (3.8)$$

Similar expressions for γ_{xz} and γ_{yz} can be obtained by cycling the displacement and coordinate symbols. Alas, Eq. (3.8) and the similar nonlinear expressions for the other two pairs of coordinate axes are seldom used.

3.5 Other Strain Definitions

In the above it was hinted that the above-chosen measures of deformation with respect to size and shape might not be the best in some sense. However, the above definitions do have the advantage of simplicity, and this is an important advantage in the laboratory. In order to pursue this matter further, it is useful to look at the two more prominent competing strain definitions. The first of these competing strain definitions may be called the definition for *tensor strains*.⁴ In the coordinate system of the undeformed body, according to Ref. [3], these strains are more properly called the *Green strains*.⁵ In tensor notation a single strain definition encompasses both longitudinal and shearing strains. To present a sample of this definition here, say for the longitudinal strain in the x direction, it is necessary to adapt the tensor definition to the present style and symbols. Upon doing so, the definition may be written as

$$\epsilon_{xx} = \frac{1}{2} \frac{(d\hat{x})^2 - (dx)^2}{(dx)^2} = \left(\frac{d\hat{x} - dx}{dx} \right) \left(\frac{d\hat{x} + dx}{2dx} \right) \quad (3.9)$$

Of course, similar expressions can be written for the longitudinal strains in the other two orthogonal directions. The second of the above factors within parentheses is just the average value of the two differential lengths divided by the original differential length, and is thus very close to the value of 1. Thus this definition involving the squares of the differential lengths is very little different from the one developed above. In fact, the linear terms of the longitudinal strains are exactly the same as those developed above, and the differences appear only in the nonlinear terms. While this definition appears to be unnecessarily more complicated than that first discussed, it is a simple form in tensor notation. Its major advantage is simply that the tensor definition produces a quantity that is a tensor, and therefore possesses very helpful mathematical properties. For example, a transformation to another type of coordinate system, such as cylindrical coordinates, is a well defined and thus comparatively simple process. Rotations of coordinate axes are also accomplished simply with tensor quantities. A minor advantage is that the tensor definition only gives rise to linear and quadratic terms.

⁴ For a brief comment on tensors, see Section 2.9.

⁵ George Green (1793–1841), an English mathematician and physicist (Ref. [71]).

The second of the prominent definitions competing with the original definition of strain is called the *true strain* definition. For longitudinal strain, the definition is

$$d\epsilon \equiv \frac{dL}{L}$$

where L is any length in the direction of the strain to be measured. This definition can be integrated to obtain

$$\begin{aligned}\epsilon &= \int_0^\epsilon d\epsilon = \int_{L_0}^{L_1} \frac{dL}{L} = \ln\left(1 + \frac{\Delta L}{L_0}\right) \\ &= \frac{\Delta L}{L_0} - \frac{1}{2}\left(\frac{\Delta L}{L_0}\right)^2 + \frac{1}{3}\left(\frac{\Delta L}{L_0}\right)^3 - \dots\end{aligned}\quad (3.10)$$

where $\Delta L = L_1 - L_0$ is the finite change of length from the original length, L_0 . The first term of the series expansion of the natural logarithm, Eq. (3.10), is essentially the definition of the first-discussed strain. Thus, once again, this strain definition differs from the other definitions only with respect to the nonlinear terms. A somewhat appealing aspect of this third-discussed strain definition is its ease in combining successive strains at the same point in the same direction. That is, because this definition is in terms of a differential of strain, the reference length used for a second successive strain at the same point in the same direction as the first strain is the length L_1 . The other two strain definitions necessarily use the original length L_0 that was established before the first straining.

3.6 The Strain–Displacement Equations

Since all three of the prominent strain definitions agree on the linear portions of the six strain expressions, except for a wholly stylistic adjustment discussed below, these common linear expressions can be, and universally are, adopted with confidence for the case of small deformations. Thus the simple first-discussed definition can be used in the laboratory for measuring all small strains. Since the tensor definition for the Green strains is the most convenient when dealing with those situations where the nonlinear terms are significant, the nonlinear terms derived from that definition are those that are generally used, and are those that are adopted by this text hereafter.

There is a special characteristic of the Green shearing strains that now needs to be mentioned. The tensor strain definition produces linear shearing strain expressions that are exactly one-half of those produced by the first definition. In other words, the tensor definition averages the two rotations of the line segments that originally paralleled the coordinate axes. The only significance this has is that the engineer has to communicate clearly which of the two shearing strains is being discussed: the engineering shearing strains, or the Green shearing strains. Like the longitudinal strains, the Green shearing strains are here symbolized by the use of ϵ . A summary of what are now to be called the nonlinear and linear forms of the six *strain–displacement equations* follows.

Nonlinear forms (finite displacements)

$$\begin{aligned}\epsilon_{xx} &= \frac{\partial u}{\partial x} + \frac{1}{2} \left[\left(\frac{\partial u}{\partial x} \right)^2 + \left(\frac{\partial v}{\partial x} \right)^2 + \left(\frac{\partial w}{\partial x} \right)^2 \right] \\ \epsilon_{yy} &= \frac{\partial v}{\partial y} + \frac{1}{2} \left[\left(\frac{\partial u}{\partial y} \right)^2 + \left(\frac{\partial v}{\partial y} \right)^2 + \left(\frac{\partial w}{\partial y} \right)^2 \right]\end{aligned}$$

$$\begin{aligned}\epsilon_{zz} &= \frac{\partial w}{\partial z} + \frac{1}{2} \left[\left(\frac{\partial u}{\partial z} \right)^2 + \left(\frac{\partial v}{\partial z} \right)^2 + \left(\frac{\partial w}{\partial z} \right)^2 \right] \\ \gamma_{xy} = 2\epsilon_{xy} &= \frac{\partial u}{\partial y} + \frac{\partial v}{\partial x} + \frac{\partial u}{\partial x} \frac{\partial u}{\partial y} + \frac{\partial v}{\partial x} \frac{\partial v}{\partial y} + \frac{\partial w}{\partial x} \frac{\partial w}{\partial y} \\ \gamma_{xz} = 2\epsilon_{xz} &= \frac{\partial u}{\partial z} + \frac{\partial w}{\partial x} + \frac{\partial u}{\partial x} \frac{\partial u}{\partial z} + \frac{\partial v}{\partial x} \frac{\partial v}{\partial z} + \frac{\partial w}{\partial x} \frac{\partial w}{\partial z} \\ \gamma_{yz} = 2\epsilon_{yz} &= \frac{\partial v}{\partial z} + \frac{\partial w}{\partial y} + \frac{\partial u}{\partial y} \frac{\partial u}{\partial z} + \frac{\partial v}{\partial y} \frac{\partial v}{\partial z} + \frac{\partial w}{\partial y} \frac{\partial w}{\partial z}\end{aligned}\quad (3.11)$$

Linear forms (small displacements)

$$\begin{aligned}\epsilon_{xx} &= \frac{\partial u}{\partial x} & \gamma_{xy} = 2\epsilon_{xy} &= \frac{\partial u}{\partial y} + \frac{\partial v}{\partial x} \\ \epsilon_{yy} &= \frac{\partial v}{\partial y} & \gamma_{xz} = 2\epsilon_{xz} &= \frac{\partial u}{\partial z} + \frac{\partial w}{\partial x} \\ \epsilon_{zz} &= \frac{\partial w}{\partial z} & \gamma_{yz} = 2\epsilon_{yz} &= \frac{\partial v}{\partial z} + \frac{\partial w}{\partial y}\end{aligned}\quad (3.12)$$

While they have no great importance to the linear, that is, small-deformation theory developed here, there are three other independent quantities which are mentioned because the reader may occasionally encounter them. These quantities are the small *average rotations* about (or very nearly about) the three orthogonal axes. Again, “small” is limited by the approximation of the sine of the angle being nearly equal to the angle. The average rotations are also referred to as the *rigid body rotations*, because such a small rigid body rotation can be described by exactly the same equations. Lower-case omega (ω) is the usual symbol employed to represent the average rotations. Again, a double subscript notation is used to note the axes being rotated, and because these quantities can be arranged in a skew-symmetric matrix, which is a matrix where the (i, j) th element is equal to the negative of the (j, i) th element. From Fig. 3.3, it can be seen that the average rotations, positive in a clockwise sense, are

$$\begin{aligned}\omega_{xy} = -\omega_{yx} &= \frac{1}{2} \left(\frac{\partial u}{\partial y} - \frac{\partial v}{\partial x} \right) \\ \omega_{zy} = -\omega_{zy} &= \frac{1}{2} \left(\frac{\partial v}{\partial z} - \frac{\partial w}{\partial y} \right) \\ \omega_{zx} = -\omega_{xz} &= \frac{1}{2} \left(\frac{\partial w}{\partial x} - \frac{\partial u}{\partial z} \right)\end{aligned}\quad (3.13)$$

3.7 The Compatibility Equations

The linear strain–displacement equations, Eqs. (3.12), are six equations that provide the means by which the six small displacement strains can be obtained from the three independent displacement functions. It is simply a matter of differentiating any known displacement field (u, v, w) to obtain the six strains. Since the displacement functions are required to be differentiable functions, there is never any difficulty carrying out the

differentiation. Now consider the reverse task of determining the three displacement functions knowing the six strains. This is a much more complicated undertaking. The first reason that this reverse task is more complicated is simply that integration is often more complicated than differentiation. The second reason is even more basic. The six strains are not totally independent of each other over the volume of the structural body. That is, six *strain functions* cannot be arbitrarily chosen with the expectation that those six functions are related via Eqs. (3.12), without contradiction, to three single-valued structural displacements. In order to illustrate in simple algebraic terms the idea that any given number of independent functions can only be transformed into the same number of independent functions, let $F(x)$ and $G(x)$ be two linearly independent functions.⁶ Let $\alpha, \beta, \gamma, \delta, \theta, \mu, \rho,$ and σ be a set of arbitrary constants, and let

$$\begin{aligned} Q(x) &= \alpha F(x) + \beta G(x) & R(x) &= \gamma F(x) + \delta G(x) \\ S(x) &= \theta F(x) + \mu G(x) & T(x) &= \rho F(x) + \sigma G(x) \end{aligned}$$

The four functions $Q(x), R(x), S(x),$ and $T(x)$ are not linearly independent of each other. Only two of those four functions can be linearly independent. For example, if the two functions $Q(x)$ and $R(x)$ are chosen to be the two independent functions that are created from the two independent functions $F(x)$ and $G(x)$, then it is not difficult to show by first solving for $F(x)$ and $G(x)$ in terms of $Q(x)$ and $R(x)$ that the functions $S(x)$ and $T(x)$ are related to $Q(x)$ and $R(x)$ by the relations (provided that $\alpha\delta \neq \beta\gamma$)

$$\begin{aligned} S(x) &= \frac{(\theta\delta - \mu\gamma)Q(x) + (\mu\alpha - \theta\beta)R(x)}{\alpha\delta - \beta\gamma} \\ T(x) &= \frac{(\rho\delta - \sigma\gamma)Q(x) + (\sigma\alpha - \rho\beta)R(x)}{\alpha\delta - \beta\gamma} \end{aligned}$$

These two equations clearly illustrate the dependence of $S(x)$ and $T(x)$ on $Q(x)$ and $R(x)$. Similarly, derivatives of the three independent displacement functions can give rise only to three independent strain functions, not six independent strain functions. In other words, the task of finding three single-valued displacement functions from six arbitrarily chosen strain functions would be overprescribed. Hence it is to be expected that there is a set of three independent relations between the six strains.

Relations among the strains, which demonstrate their dependence upon each other, can be discovered in any number of ways. One way, and perhaps the most direct, is to begin to apply what are the standard procedures for directly integrating first order partial differential equations to Eqs. (3.12) in order to solve for the three displacements in terms of the six strains. Eliminating the resulting functions of integration⁷ produces the desired results. However, it is not expected that all readers are familiar with those procedures, so a sample of that approach is relegated to Appendix A and left for a rainy night.

The equations that relate the strains can also be derived, and done so most easily, by differentiating and combining the strain–displacement equations so as to eliminate the

⁶ Linear independence is a weak form of independence. Two functions $f(x)$ and $g(x)$ are linearly independent if and only if the relation, for all values of x , $af(x) + bg(x) = 0$, requires that the constants a and b are both zero. Examples of pairs of linearly independent functions are $\sin x$ and $\cos x$, and \sqrt{x} and x^2 . Note that for the first pair the two functions are not “independent” because the sum of their squares is 1. The second pair are not independent because the fourth power of the first function is equal to the second function.

⁷ Functions of integration that result from integrating partial differential equations are analogous to constants of integration that result from integrating ordinary differential equations.

displacements. For example, as is demonstrated immediately below, one such equation can be derived by simply differentiating $\epsilon_{xx} = \partial u / \partial x$ with respect to y twice, adding that to the result of differentiating $\epsilon_{yy} = \partial v / \partial y$ with respect to x twice, and then factoring the second partial derivative operator with respect to x and y . That is, assuming that all the stated higher order partial derivatives are continuous functions, so that the order of partial differentiation can be interchanged, then

$$\frac{\partial^2 \epsilon_{xx}}{\partial y^2} + \frac{\partial^2 \epsilon_{yy}}{\partial x^2} = \frac{\partial^3 u}{\partial x \partial y^2} + \frac{\partial^3 v}{\partial x^2 \partial y} = \frac{\partial^2}{\partial x \partial y} \left(\frac{\partial u}{\partial y} + \frac{\partial v}{\partial x} \right) = \frac{\partial^2 \gamma_{xy}}{\partial x \partial y}$$

which is indeed one relationship among the strains without any reference to the displacements. Following a similar procedure with ϵ_{xx} and ϵ_{zz} , and then with ϵ_{yy} and ϵ_{zz} (or simply cycling the subscripts so that $x \rightarrow y$ while $y \rightarrow z$, and then again as $y \rightarrow z$ while $z \rightarrow x$), produces two more equations of the same form between the six strains. At first glance it appears that these are the expected three equations that relate the six strains. However, the results from Appendix A are another, different set of three equations among the six strains. Thus the following questions arise: (i) how many such equations are there? (ii) how many of those equations are independent of each other? and (iii) what do they all mean? Since simply eliminating displacements by partial differentiation provides no answers to the first two of these questions, and only a partial answer to the third question, it is necessary to look elsewhere for a third approach to the derivation of these equations that relate the strains.

Endnote (2) details a third derivation procedure. That endnote provides a proof of the following answers to the first two questions. There are a total of six distinct second order partial differential equations that relate the strains, but only three of those six equations are independent equations. However, all six of those equations are used together in order to avoid selecting between them and thus upsetting the symmetry of the two groups of three equations. A full listing of the six equations is as follows:

$$\frac{\partial^2 \epsilon_{xx}}{\partial y^2} + \frac{\partial^2 \epsilon_{yy}}{\partial x^2} = \frac{\partial^2 \gamma_{xy}}{\partial y \partial x} \quad (3.14a)$$

$$\frac{\partial^2 \epsilon_{xx}}{\partial z^2} + \frac{\partial^2 \epsilon_{zz}}{\partial x^2} = \frac{\partial^2 \gamma_{xz}}{\partial x \partial z} \quad (3.14b)$$

$$\frac{\partial^2 \epsilon_{yy}}{\partial z^2} + \frac{\partial^2 \epsilon_{zz}}{\partial y^2} = \frac{\partial^2 \gamma_{yz}}{\partial y \partial z} \quad (3.14c)$$

$$\frac{\partial}{\partial z} \left(\frac{\partial \gamma_{yz}}{\partial x} + \frac{\partial \gamma_{xz}}{\partial y} - \frac{\partial \gamma_{xy}}{\partial z} \right) = 2 \frac{\partial^2 \epsilon_{zz}}{\partial x \partial y} \quad (3.14d)$$

$$\frac{\partial}{\partial y} \left(\frac{\partial \gamma_{yz}}{\partial x} - \frac{\partial \gamma_{xz}}{\partial y} + \frac{\partial \gamma_{xy}}{\partial z} \right) = 2 \frac{\partial^2 \epsilon_{yy}}{\partial x \partial z} \quad (3.14e)$$

$$\frac{\partial}{\partial x} \left(-\frac{\partial \gamma_{yz}}{\partial x} + \frac{\partial \gamma_{xz}}{\partial y} + \frac{\partial \gamma_{xy}}{\partial z} \right) = 2 \frac{\partial^2 \epsilon_{xx}}{\partial y \partial z} \quad (3.14f)$$

The answer to the third question, regarding the meaning of these six equations, is as follows. These six equations are the constraints with which the small strains must comply in order for the strains to be compatible with any differentiable displacement field in the manner stated

in Eqs. (3.12). For this reason, the six equations are called the *compatibility equations*. The compatibility equations are attributed to St. Venant.⁸

The compatibility equations are the closest thing available to an inversion of the strain–displacement equations; that is, there are no displacement–strain equations as such. The compatibility equations contain the same information as the strain–displacement equations, but they express that information entirely in terms of the strains. Hence compatibility equations are a necessary part of any structural analysis for which the equilibrium equations alone are insufficient for a solution, and the displacements themselves are not explicitly part of the analysis.

Once the approach to the compatibility equations discussed in the endnote answers the questions regarding the number and meaning of the compatibility equations, the derivation of other forms of the compatibility equations is best achieved by using the relatively simple second approach, which is just that of eliminating displacements via differentiation. Other forms of the compatibility equations are (i) compatibility equations for strains in terms of other orthogonal coordinate systems; or (ii) compatibility equations for special circumstances. In the latter situation, it is important to realize that special circumstances are opportunities to seek to reduce the order of the derivatives in the compatibility equations needed for the special case. Each reduction in the order of the derivatives is equivalent to one integration in the overall solution process. The following are two examples that illustrate that second situation. An exercise and an endnote deal with the first situation in the important general case of cylindrical coordinates.

Example 3.1. When a body is in a state of axisymmetric plane stress, then in terms of cylindrical coordinates, the displacement in the θ direction, v , can be taken to be zero, and the displacement in the radial direction, u , is only a function of the radial coordinate, r . That is $u = u(r)$. Devise a compatibility equation for this special case where, from Endnote (1), the cylindrical coordinate strains reduce to

$$\epsilon_{rr} = \frac{du}{dr} \quad \epsilon_{\theta\theta} = \frac{u}{r} \quad \gamma_{r\theta} = 0$$

Solution. Since the shearing strain is always zero, no other conditions can be placed upon it. Thus the shearing strain does not appear in the compatibility equation. The single displacement u can be eliminated as follows. From the θ direction strain expression, $u = r\epsilon_{\theta\theta}$. Substituting this expression for the radial displacement into the expression for the radial direction strain leads to the equation

$$\epsilon_{rr} = \left(\frac{d}{dr} \right) (r\epsilon_{\theta\theta})$$

This is the desired compatibility equation because it involves only the strains and not the displacements. Note that in this special case the resulting differential equation is only of the first order. The general forms of the compatibility equations written in cylindrical

⁸ Barré de Saint-Venant (1797–1886), French engineer and mathematician (Ref. [2]). Reference [9] states that St. Venant gave the relations among the strain components in an appendix of his edition of Navier's *Résumé des Leçons sur l'application de la Mécanique*, 1864.

coordinates are, like those written in Cartesian coordinates, second order partial differential equations. Just as is the case with ordinary differential equations, it is a lot easier to work with first order partial differential equations than second order partial differential equations. ■

Example 3.2. If it is known that the two Cartesian coordinate displacements u , v are related by $v(x, y) = -cu(x, y)$, where c is a known constant, then determine a compatibility equation for this situation

Solution. In this case, writing all the strains in terms of the x direction displacement by direct use of Eqs. (3.12) leads to

$$\epsilon_{xx} = \frac{\partial u}{\partial x} \quad \epsilon_{yy} = -c \frac{\partial u}{\partial y} \quad \gamma_{xy} = -c \frac{\partial u}{\partial x} + \frac{\partial u}{\partial y}$$

Substituting the first two equalities into the third produces the solution

$$c^2 \epsilon_{xx} + \epsilon_{yy} + c \gamma_{xy} = 0$$

which in this case is only an algebraic equation, and therefore much easier to use than an ordinary differential equation or a partial differential equation. ■

3.8 Plane Strain

In an exact analogy to the definition of plane stress, *plane strain* is defined as the situation where there exists a Cartesian coordinate axis z such that $\gamma_{xz} = \gamma_{yz} = \epsilon_{zz} = 0$. Adding the further requirement that neither of the displacements u and v varies in the z direction allows the immediate conclusion that the displacement w must be a constant with respect to, the spatial variables; see the exercises. Situations that exactly meet the definition of plane strain are rare occurrences. However, in everyday engineering work where acceptable approximations are routinely, and properly, made to cut costs, certain approximations equivalent to assuming a state of plane strain are commonplace. A summary of the nontrivial linear equations applicable for a state of plane strain are listed below. This list also serves as a condensed summary of all the three-dimensional linear strain equations.

The plane strain displacements (time omitted as per usual)

$$u = u(x, y) \quad v = v(x, y) \quad w = \text{constant}$$

The plane strain small-strain–displacement equations

$$\epsilon_{xx} = \frac{\partial u}{\partial x} \quad \epsilon_{yy} = \frac{\partial v}{\partial y} \quad \gamma_{xy} = 2\epsilon_{xy} = \frac{\partial u}{\partial y} + \frac{\partial v}{\partial x}$$

The plane strain linear compatibility equation

$$\boxed{\frac{\partial^2 \epsilon_{xx}}{\partial y^2} + \frac{\partial^2 \epsilon_{yy}}{\partial x^2} = \frac{\partial^2 \gamma_{xy}}{\partial x \partial y}} \quad (3.14a)$$

There is only one plane strain compatibility equation because the other five equations reduce to the trivial case of zero equals zero. Note that since plane stress is not the same as plane strain, all six compatibility equations must be considered in the case of plane stress. The use of the compatibility equations in the case of plane stress is discussed at some length later. Note also that in the plane strain case, three strain functions are defined from two independent displacement functions. Hence there is only one constraint necessary for the three strains in order for them to be compatible with the two differentiable displacements. Since this single constraint equation must be an independent equation, there are two independent strain functions and one dependent strain function. It does not matter which strain is considered to be the dependent strain function. This reduced situation is clearly more tidy than the full three-dimensional case.

3.9 Summary

Deformations are the result of relative motion between material points. Deformations can be studied as simply a matter of geometry without any reference to either the nature of the material or the loads acting on the structure. The only possible types of deformation on a differential scale are changes in size and changes in shape. Changes in size are routinely described by measuring changes in length on a differential scale in three orthogonal directions. When referenced to (i.e., divided by) the original length, these measurements are called longitudinal strains. Changes in shape are routinely described by measuring the changes on a differential scale in the three right angles that exist prior to deformation between the same three orthogonal lengths used to describe longitudinal strains. These changes in the three right angles are called shearing strains. Hence the longitudinal and shearing strains completely describe the deformation of a structural body.

It turns out that the change in length divided by original length definition for longitudinal strains and the change in right angle definition for shearing strains, are only easy to deal with in terms of Cartesian coordinates. (See the comment in Endnote (1).) Satisfactory strain definitions should accommodate any standard coordinate system. Hence slightly different definitions of strain have been considered. Green strains, which are easy to deal with in any coordinate system, are the strains to be used when dealing with finite deformations.

The three longitudinal and three shearing strains are related to the three displacement components in a complicated fashion that can be greatly simplified, as is done in this text, by restricting further consideration of deformations to small relative displacements. By definition, such a restriction allows the discarding of the nonlinear terms in the strain–displacement relations, leaving only linear differential relations between the strains and the displacements. The six linear strain–displacement equations are easily memorized through use, and they are the same six relations regardless of the choice that is made between Green strain definition and the “engineering” strain definitions, except for a factor of 2 for the shearing strains.

Determining the strains from the displacements is merely a matter of differentiation. Consideration of the reverse problem of determining the displacement functions from specified strain functions shows that the six strain functions are related to each other by means of the six compatibility equations. Only three of the six compatibility equations are independent. The compatibility equations ensure that the strains are compatible with differentiable displacements. In the case of plane strain, the situation is simpler in that there are only two relevant independent displacement components, three nonzero strains, and one compatibility equation that relates the three strains.

With regard to the overall analysis of loaded structures, the development of the strain–displacement equations has introduced six more equations, but added nine more unknowns over the volume (domain) of the structural body. The nine unknowns are, of course, the three displacement components and the six strain functions. The alternative approach is to use the six compatibility equations, which do not involve the displacements, rather than use the six strain–displacement equations. This route introduces the six unknown strains into the analysis, but only three independent equations. With either approach, there is an additional net deficit of three equations to be added to the previous deficit of three equations, for a total requirement for six more equations.

Chapter 3 Exercises

- 3.1. If the displacements in a certain body are known to be those listed below, where C is a nondimensional constant and L a known length, what then are the corresponding strains?
- (a) $u = C(x + 2y)$; $v = -C(2x + y)$; $w = -Cz$.
 (b) $u = 2LC \ln[1 + (x/L)]$; $v = LC \exp(-x/L)$; $w = 0$.
- 3.2. Discuss the geometric/mathematical difficulties that occur with the following description of displacements: $u = C|x|$; $v = Cy$; $w = Cz$. Again, C is a nondimensional constant.
- 3.3. (a) By using the change in length over length definition of longitudinal strain, and by totally disregarding the small angles between the original rectangular parallelepiped edge length, dy , and the edge length after deformation, $d\hat{y}$, show that the strain $\epsilon_{yy} = \partial v/\partial y$.
 (b) Again use the change in length over length longitudinal strain definition to show that $\epsilon_{yy} = \partial v/\partial y$. This time account for the small angles between dy and $d\hat{y}$, but discard all derivatives of higher order than the first. *Hint*: Make use of the displacements sketched in Fig. 3.3.
- 3.4. A certain body in a state of plane strain is determined to have the strains listed below where the coefficients A , B , and C are nondimensional constants, and L is a known length. Determine what relations must exist between the constants A , B , and C , if any.

$$(a) \quad \epsilon_{xx} = \frac{Ay^2}{L^2} + \frac{Cxy}{L^2}$$

$$\epsilon_{yy} = \frac{A(x^2 + y^2)}{L^2}$$

$$\gamma_{xy} = \frac{Cxy}{L^2}$$

$$(b) \quad \epsilon_{xx} = 3A \cos\left(\frac{\pi x}{L}\right) \sin\left(\frac{2\pi y}{L}\right)$$

$$\epsilon_{yy} = C \cos\left(\frac{\pi x}{L}\right) \sin\left(\frac{2\pi y}{L}\right)$$

$$\gamma_{xy} = 2A \sin\left(\frac{\pi x}{L}\right) \cos\left(\frac{2\pi y}{L}\right)$$

$$\begin{aligned}
 \text{(c) } \epsilon_{xx} &= \frac{A \cos(\pi y/L)}{[1 + (\pi x/L)]^2} \\
 \epsilon_{yy} &= B \exp\left(\frac{-\pi x}{L}\right) \cos\left(\frac{\pi y}{L}\right) \\
 \gamma_{xy} &= A \exp\left(\frac{-\pi x}{L}\right) \sin\left(\frac{\pi x}{L}\right) + \left(\frac{C}{1 + (\pi x/L)}\right) \sin\left(\frac{\pi x}{L}\right)
 \end{aligned}$$

3.5. By means of direct substitution of the strain–displacement relations, demonstrate the validity of the compatibility equation that is (a) the fourth of Eqs. (3.14); (b) the fifth of Eqs. (3.14); (c) the first of the Bianchi identities, Eqs. (3.18), which is found in the endnote.

3.6. The plane strain compatibility equation for cylindrical coordinates has the general form shown below. Use the general linear strain–displacement equations

$$\epsilon_{rr} = \frac{\partial u}{\partial r}, \quad \epsilon_{\theta\theta} = \frac{u}{r} + \frac{1}{r} \frac{\partial v}{\partial \theta}, \quad \text{and} \quad \gamma_{r\theta} = \frac{1}{r} \frac{\partial u}{\partial \theta} + \frac{\partial v}{\partial r} - \frac{v}{r}$$

to determine what integer values are represented by the factors A , B , and C ?

$$\frac{\partial^2(r\gamma_{r\theta})}{\partial r \partial \theta} = A \frac{\partial^2 \epsilon_{rr}}{\partial \theta^2} + Br \frac{\partial \epsilon_{rr}}{\partial r} + Cr \frac{\partial^2(r\epsilon_{\theta\theta})}{\partial r^2}$$

Hint: (i) Recall that any compatibility equation must hold true for the general form of the strains in terms of displacements; and (ii) recall the product rule for differentiation that, for example, $(\partial/\partial r)[rF(r, \theta)] = F(r, \theta) + r(\partial F/\partial r)$.

Comment: Note that v is the displacement in the positive theta direction along a line tangent to the line of fixed radius, and the other three linear strain–displacement equations in terms of cylindrical coordinates are

$$\epsilon_{zz} = \frac{\partial w}{\partial z}, \quad \gamma_{rz} = \frac{\partial v}{\partial z} + \frac{\partial w}{\partial r}, \quad \text{and} \quad \gamma_{\theta z} = \frac{1}{r} \frac{\partial w}{\partial \theta} + \frac{\partial v}{\partial z}$$

- 3.7. (a) If the Cartesian displacement $u = u(x, y)$, and the Cartesian displacements $v = w = 0$, devise a single, first order compatibility equation for this special circumstance.
- (b) In the special case where $u = \epsilon_{rr} = 0$, and $\epsilon_{\theta\theta}$ and $\gamma_{r\theta}$ are functions of the cylindrical coordinates r, θ only, devise a compatibility equation for the above two nonzero strains. Note that in this special case, the strain–displacement $(\epsilon - u)$ relations are $\epsilon_{\theta\theta} = (1/r)(\partial v/\partial \theta)$, and $\gamma_{r\theta} = \partial v/\partial r - v/r$.
- (c) If the Cartesian coordinate system displacements are such that $u(x, y) = f(x)v(x, y)$, where $f(x)$ is a known function, determine a first order compatibility equation that involves all three strains for the case of plane strain.
- 3.8. Using a Cartesian coordinate system, show that for the case of plane strain and no change in displacements with respect to time, the displacement in the z direction must be a constant.
- 3.9. The following equation is listed in Ref. [24] as a compatibility equation for cylindrical coordinates. Why is there obviously a typographical error in the statement of this equation?

$$\frac{\partial}{\partial z} \left[2r \frac{\partial \epsilon_{rr}}{\partial \theta} - \frac{\partial}{\partial r} (r\gamma_{r\theta}) \right] + r^2 \frac{\partial}{\partial r} \left[\frac{1}{r} \left(\frac{\partial}{\partial r} (r\gamma_{\theta z}) - \frac{\partial \gamma_{zr}}{\partial \theta} \right) \right] = 0$$

FOR THE EAGER

3.10. Which of the following are true identities?

- (a) $\epsilon_{xx,y} = \frac{1}{2}\gamma_{xy,x} + \omega_{xy,x}$
 (b) $\epsilon_{yy,x} = \frac{1}{2}\gamma_{xy,y} - \omega_{xy,y}$
 (c) $\omega_{xy,z} = \frac{1}{2}[\gamma_{xz,y} + \gamma_{yz,x}]$
 (d) $\omega_{yz,x} = \frac{1}{2}[\gamma_{xy,z} - \gamma_{xz,y}]$

Endnote (1) The Derivation of the Strain–Displacement Equations for Cylindrical Coordinates

The derivation of the strain–displacement equations presented in this chapter for Cartesian coordinates was a mostly geometric argument in conjunction with the $\Delta L/L$ definition of strain. After completing that process, other definitions of strain were mentioned. It was stated that all accepted definitions of strain produced the same results for the linear portions of the strain–displacement equations, but differed in their quadratic terms. Then the tensor definition of strain was declared to be the preferred choice when it came to the quadratic (nonlinear) terms. This endnote provides a bit of justification for the greater acceptance of the tensor definition for strain. This present justification rests upon the difficulty of a geometric approach to determining the strain–displacement equations in other important coordinate systems. If the reader were to attempt to use the original $\Delta L/L$ definition of strain with a cylindrical coordinate system, then the reader would be immediately confronted with such questions as how does one define displacements in the cylindrical coordinate system. When attempting to work through the geometry, while it can be done, it would be difficult enough to obtain the accepted linear terms, and it would be clear that there would be little hope of agreeing on the quadratic terms. The situation would be even more complicated in spherical coordinates. The great advantage of the tensor approach is that it is mostly algebraic, and that is indeed a great advantage. As stated earlier, the 32 definition of strain for cylindrical coordinates, translated from indicial notation, is

$$(ds^*)^2 - (ds)^2 \equiv 2(\epsilon_{rr} dr dr + \epsilon_{\theta\theta} r^2 d\theta d\theta + \epsilon_{zz} dz dz + \gamma_{r\theta} r dr d\theta + \gamma_{z\theta} r dz d\theta + \gamma_{rz} dr dz)$$

To implement this approach, it is necessary to work out the details of the left-hand side of the above equality. To that end, note that in cylindrical coordinates, the position vector to an arbitrary position in space is $\mathbf{r} = r\mathbf{i}_r + z\mathbf{k}$, where \mathbf{i}_r is the unit vector in the radial direction. Since $\mathbf{i}_r = \mathbf{i} \cos \theta + \mathbf{j} \sin \theta$, then $d\mathbf{i}_r = (-\mathbf{i} \sin \theta + \mathbf{j} \cos \theta) d\theta = \mathbf{i}_\theta d\theta$. Again vector differentiation produces a ninety degree counterclockwise rotation. The differential line segment extending from the arbitrarily selected point in space—the line segment that represents the undeformed geometry—is $d\mathbf{r} = dr\mathbf{i}_r + r d\theta\mathbf{i}_\theta + dz\mathbf{k}$. The magnitude of the $d\mathbf{r}$ vector is the quantity ds on the left-hand side of the above strain definition equation.

After deformation, the arbitrarily chosen material point moves through the three displacement components to a new geometric position identified by the position vector $\mathbf{r}^* = (u + r)\mathbf{i}_r + v\mathbf{i}_\theta + (w + z)\mathbf{k}$. It is important to note that the displacements u , v , and w are tied to the unit vectors, and therefore are measured in the straight line directions of the unit vectors. The undeformed differential line segment becomes, after deformation, the line segment represented by $d\mathbf{r}^* = (dr + du - v d\theta)\mathbf{i}_r + (r d\theta + u d\theta + dv)\mathbf{i}_\theta + (dw + dz)\mathbf{k}$, where $d\mathbf{i}_\theta = -\mathbf{i}_r d\theta$. Now $ds^* ds^* = d\mathbf{r}^* \cdot d\mathbf{r}^*$ and $ds ds = d\mathbf{r} \cdot d\mathbf{r}$. Taking those dot products and inserting those results into the above strain definition equation,

and then associating terms on the basis of equal differential products, leads to the result that

$$\begin{aligned}\epsilon_{rr} &= \frac{\partial u}{\partial r} + \frac{1}{2} \left[\left(\frac{\partial u}{\partial r} \right)^2 + \left(\frac{\partial v}{\partial r} \right)^2 + \left(\frac{\partial w}{\partial r} \right)^2 \right] \\ \epsilon_{\theta\theta} &= \frac{u}{r} + \frac{1}{r} \frac{\partial v}{\partial \theta} + \frac{u^2 + v^2}{2r^2} + \frac{1}{r^2} \left[u \frac{\partial v}{\partial \theta} - v \frac{\partial u}{\partial \theta} \right] \\ &\quad + \frac{1}{2r^2} \left[\left(\frac{\partial u}{\partial \theta} \right)^2 + \left(\frac{\partial v}{\partial \theta} \right)^2 + \left(\frac{\partial w}{\partial \theta} \right)^2 \right] \\ \epsilon_{zz} &= \frac{\partial w}{\partial z} + \frac{1}{2} \left[\left(\frac{\partial u}{\partial z} \right)^2 + \left(\frac{\partial v}{\partial z} \right)^2 + \left(\frac{\partial w}{\partial z} \right)^2 \right] \\ \gamma_{r\theta} &= \frac{1}{r} \frac{\partial u}{\partial \theta} + \frac{\partial v}{\partial r} - \frac{v}{r} + \left[\frac{u}{r} \frac{\partial v}{\partial r} - \frac{v}{r} \frac{\partial u}{\partial r} \right] + \frac{1}{r} \left[\frac{\partial u}{\partial r} \frac{\partial u}{\partial \theta} + \frac{\partial v}{\partial r} \frac{\partial v}{\partial \theta} + \frac{\partial w}{\partial r} \frac{\partial w}{\partial \theta} \right] \\ \gamma_{rz} &= \frac{\partial u}{\partial z} + \frac{\partial w}{\partial r} + \frac{1}{2} \left[\frac{\partial u}{\partial r} \frac{\partial u}{\partial z} + \frac{\partial v}{\partial r} \frac{\partial v}{\partial z} + \frac{\partial w}{\partial r} \frac{\partial w}{\partial z} \right] \\ \gamma_{\theta z} &= \frac{\partial v}{\partial z} + \frac{1}{r} \frac{\partial w}{\partial \theta} - \frac{v}{r} \frac{\partial u}{\partial z} + \frac{1}{r} \left[\frac{\partial u}{\partial \theta} \frac{\partial u}{\partial z} + \frac{\partial v}{\partial \theta} \frac{\partial v}{\partial z} + \frac{\partial w}{\partial \theta} \frac{\partial w}{\partial z} \right]\end{aligned}$$

Remember that tensors form just another algebra, and that Cartesian tensors, those referenced to Cartesian coordinates are particularly simple. The algebra of Cartesian tensors somewhat resembles matrix algebra. Addition and subtraction are the same, but the multiplication rule is a bit different. The algebra of Cartesian tensors is sometimes referred to as "index notation." Again, one reason that engineers and scientists use both matrix algebra and tensor algebra is that matrices are more convenient when dealing with groups of ordinary differential equations, while tensors are more convenient when dealing with partial differential equations.

Endnote (2) A Third Derivation of the Compatibility Equations

A third approach to the derivation of the compatibility equations is as follows. The strain-displacement equations imply the unique existence of all the first order partial derivatives of the displacements. These partial derivatives in turn imply that the displacement functions possess a differential, and that the displacement functions are single valued, continuous functions. Thus, for example, it is possible to write the chain rule expansion for the differential change in the deflection in the x direction as

$$du = \left(\frac{\partial u}{\partial x} \right) dx + \left(\frac{\partial u}{\partial y} \right) dy + \left(\frac{\partial u}{\partial z} \right) dz \quad (3.15a)$$

The following physical meaning can be assigned to this version of the chain rule. Consider two material points in a general structural body. Label these points P_1 and P_2 . Let these two points be separated by the infinitesimal distance whose components in the selected Cartesian coordinate system are dx , dy , and dz . Another way of saying the same thing is to let the Cartesian coordinates of point P_1 be (x, y, z) , and let the coordinates of P_2 be $(x + dx, y + dy, z + dz)$. During the loading process, the two material points undergo displacements. Let the x component of the total displacement of point P_1 , be called, as usual, $u = u(x, y, z)$. Since point P_2 is only an infinitesimal distance from point P_1 , the x component of the P_2

displacement differs only infinitesimally from that at point P_1 . Therefore the x component of the total displacement vector for point P_2 is called $u + du$. Thus the difference between the displacement x components of the two points is $du(x, y, z)$. The above chain rule equation ties du to the changes in the function $u(x, y, z)$ in each of the Cartesian directions. It does so in terms of the extent of the infinitesimal components of the distance between the two points.

Using the strain–displacement equations, Eq. (3.15a) can be rewritten as

$$du = \epsilon_{xx} dx + \left(\gamma_{xy} - \frac{\partial v}{\partial x} \right) dy + \left(\gamma_{xz} - \frac{\partial w}{\partial x} \right) dz \quad (3.15b)$$

where use is made of the linear engineering strain–displacement equations. Recall the mathematical theorem (Ref. [1]) that states that $df = P dx + Q dy + R dz$ is an exact differential if and only if $\partial P/\partial y = \partial Q/\partial x$, $\partial P/\partial z = \partial R/\partial x$, and $\partial Q/\partial z = \partial R/\partial y$. Application, for example, of the first of these three necessary equalities leads to

$$\frac{\partial \epsilon_{xx}}{\partial y} = \frac{\partial}{\partial x} \left(\gamma_{xy} - \frac{\partial v}{\partial x} \right) \quad (3.15c)$$

Differentiating this equation with respect to y , interchanging the order of differentiation, and using the strain–displacement relation for ϵ_{yy} , yields

$$\frac{\partial^2 \epsilon_{xx}}{\partial y^2} + \frac{\partial^2 \epsilon_{yy}}{\partial y^2} = \frac{\partial^2 \gamma_{xy}}{\partial x \partial y} \quad (3.14a)$$

As an illustration of a different type of result, consider the third necessary equality for the single-valuedness of the function $u(x, y, z)$, that is, $\partial Q/\partial z = \partial R/\partial y$:

$$\frac{\partial}{\partial z} \left(\gamma_{xy} - \frac{\partial v}{\partial x} \right) = \frac{\partial}{\partial y} \left(\gamma_{xz} - \frac{\partial w}{\partial x} \right)$$

or

$$\frac{\partial \gamma_{xy}}{\partial z} - \frac{\partial \gamma_{xz}}{\partial y} = \frac{\partial^2 v}{\partial x \partial z} - \frac{\partial^2 w}{\partial x \partial y}$$

It is not immediately clear what to do with the above in order to obtain another equation solely in terms of derivatives of the strains. Moving toward some sort of balance of form, consider adding to, or subtracting from, the left-hand side the quantity $\partial \gamma_{yz}/\partial x$, and, to maintain the equality, adding to or subtracting from the left-hand side

$$\frac{\partial \gamma_{yz}}{\partial x} = \frac{\partial^2 v}{\partial x \partial z} + \frac{\partial^2 w}{\partial x \partial y}$$

Choosing the addition option first leads to the result

$$\frac{\partial \gamma_{xy}}{\partial z} - \frac{\partial \gamma_{xz}}{\partial y} + \frac{\partial \gamma_{yz}}{\partial x} = 2 \frac{\partial^2 v}{\partial x \partial z}$$

In order to write the right-hand side in terms of a strain, differentiate both sides of the above equation with respect to y and obtain the following equation entirely in terms of strains

$$\frac{\partial}{\partial y} \left(\frac{\partial \gamma_{yz}}{\partial x} - \frac{\partial \gamma_{xz}}{\partial y} + \frac{\partial \gamma_{xy}}{\partial z} \right) = 2 \frac{\partial^2 \epsilon_{yy}}{\partial x \partial z} \quad (3.14e)$$

It may be tempting to stop here now that the objective of an equation entirely in terms of the strains has been achieved. Nevertheless, the subtraction option needs to be explored. The result obtained in the same fashion as that above is

$$\frac{\partial}{\partial z} \left(\frac{\partial \gamma_{yz}}{\partial x} + \frac{\partial \gamma_{xz}}{\partial y} - \frac{\partial \gamma_{xy}}{\partial z} \right) = 2 \frac{\partial^2 \epsilon_{zz}}{\partial x \partial y} \quad (3.14d)$$

Note that Eqs. (3.14e) and (3.14d) are unrelated in themselves because one contains ϵ_{yy} and not ϵ_{zz} , while the reverse is true for the other equation. The three necessary equalities of the above-stated theorem for the exact differentials dv and dw , and the middle requirement for du produce nine duplications of these types of equations, but only three more equations that are different from the above three. Therefore, this process establishes the fact that there is a total of exactly six of these equations. These six equations can be summarized in the following way, where the S_{ij} terms are used later:

$$\begin{aligned} S_{zz} &= \frac{\partial^2 \epsilon_{xx}}{\partial y^2} + \frac{\partial^2 \epsilon_{yy}}{\partial x^2} - \frac{\partial^2 \gamma_{xy}}{\partial x \partial y} = 0 \\ S_{yy} &= \frac{\partial^2 \epsilon_{xx}}{\partial z^2} + \frac{\partial^2 \epsilon_{zz}}{\partial x^2} - \frac{\partial^2 \gamma_{xz}}{\partial x \partial z} = 0 \\ S_{xx} &= \frac{\partial^2 \epsilon_{yy}}{\partial z^2} + \frac{\partial^2 \epsilon_{zz}}{\partial y^2} - \frac{\partial^2 \gamma_{yz}}{\partial y \partial z} = 0 \\ S_{xy} &= \frac{\partial}{\partial z} \left(\frac{\partial \gamma_{yz}}{\partial x} + \frac{\partial \gamma_{xz}}{\partial y} - \frac{\partial \gamma_{xy}}{\partial z} \right) - 2 \frac{\partial^2 \epsilon_{zz}}{\partial x \partial y} = 0 \\ S_{xz} &= \frac{\partial}{\partial y} \left(\frac{\partial \gamma_{yz}}{\partial x} - \frac{\partial \gamma_{xz}}{\partial y} + \frac{\partial \gamma_{xy}}{\partial z} \right) - 2 \frac{\partial^2 \epsilon_{yy}}{\partial x \partial z} = 0 \\ S_{yz} &= \frac{\partial}{\partial x} \left(-\frac{\partial \gamma_{yz}}{\partial x} + \frac{\partial \gamma_{xz}}{\partial y} + \frac{\partial \gamma_{xy}}{\partial z} \right) - 2 \frac{\partial^2 \epsilon_{xx}}{\partial y \partial z} = 0 \end{aligned} \quad (3.16)$$

Equations (3.16) are a direct result of the displacement functions being differentiable, single-valued point functions and the small-strain–displacement equations, Eqs. (3.12). Equations (3.16) are the constraints that the six small strains must meet in order to be compatible with (i.e., not cause contradictions within) a differentiable, single-valued structural displacement field (u, v, w). Again, for that reason, Eqs. (3.16) are referred to as the compatibility equations. A fourth proof of the compatibility equations, which is credited to E. Cesaro, can be found in Ref. [37].

Thus it is clear that the strain–displacement equations imply (are sufficient conditions for) the compatibility equations. The question to be addressed now is this: Can it be proved that single-valued, continuous displacements or the strain–displacement equations are implied by (are necessary conditions for) the compatibility equations? The answer to this question is yes for both single-valued, continuous displacements and the strain–displacement equations. The former is an immediate consequence of the latter. A direct proof that the compatibility equations imply the strain–displacement equations makes use of potential functions. Potential functions are discussed in some detail in Section 8.6 and Section 13.2. The proof is as follows. Define the three potential functions U, V , and W from which the six strains can be determined as shown in Eqs. (3.17) in terms of cartesian coordinates. Let all

derivatives of these three potential functions through the third order be continuous. (This last sentence is often phrased as let “ $U, V,$ and W be in C^3 ”).

$$\begin{aligned}\epsilon_{xx} &\equiv \frac{\partial U}{\partial x} & \gamma_{xy} &\equiv \frac{\partial U}{\partial y} + \frac{\partial V}{\partial x} \\ \epsilon_{yy} &\equiv \frac{\partial V}{\partial y} & \gamma_{xz} &\equiv \frac{\partial U}{\partial z} + \frac{\partial W}{\partial x} \\ \epsilon_{zz} &\equiv \frac{\partial W}{\partial z} & \gamma_{yz} &\equiv \frac{\partial V}{\partial z} + \frac{\partial W}{\partial y}\end{aligned}\quad (3.17)$$

Substitution of Eqs. (3.17) into the small-displacement compatibility equations, Eqs. (3.14), shows that each of those six equations is identically satisfied after reordering the partial derivatives of the potential functions. Thus Eqs. (3.17) are solutions to (i.e., integrate) Eqs. (3.14). When the potential functions are interpreted as the respective displacement components, the proof is complete.⁹

Instead of three equations of constraint on the six strains, as originally expected so as to have three independent strains, Eqs. (3.16) at first glance appear to offer six constraints on the six strains. The appearance is deceiving because three of the six equations are dependent equations.¹⁰ Before going to the mathematical demonstration of this fact, first consider the physics of the situation. If the six compatibility equations were six independent equations, then they could conceivably be solved in one fashion or another to determine the mathematical form of the six strains over the interior domain, and thus the form of the deformation field of the structural body without (i) any reference to the mechanical or thermal loading throughout the body, or (ii) the properties of the materials from which the structure is made. This should seem unlikely. The three mathematical relations between the six compatibility equations that demonstrate that only three of the compatibility equations are independent are listed below as a form of Bianchi’s identities (Ref. [8]).

$$\begin{aligned}\frac{\partial S_{xx}}{\partial x} - \frac{\partial S_{xy}}{\partial y} - \frac{\partial S_{xz}}{\partial z} &= 0 \\ -\frac{\partial S_{xy}}{\partial x} + \frac{\partial S_{yy}}{\partial y} - \frac{\partial S_{yz}}{\partial z} &= 0 \\ -\frac{\partial S_{xz}}{\partial x} - \frac{\partial S_{yz}}{\partial y} - \frac{\partial S_{zz}}{\partial z} &= 0\end{aligned}\quad (3.18)$$

These equations, which will have no further use in this text, can be verified by direct substitution. Another viewpoint is to ignore the compatibility equations and consider the above equations as the three independent equations that relate the six strains. The severe drawback to this approach is that Eqs. (3.18) involve higher-order partial derivatives than the compatibility equations. As a result, this latter approach is rarely used.

⁹ The validity of this simple proof, original to the author, has been challenged. An accepted proof that the compatibility equations imply the strain–displacement equations can be found in the discussion of linear elasticity in Ref. [70].

¹⁰ To understand what is meant by a dependent equation, as opposed to a dependent function, consider the simple case of the three algebraic equations: $x + 2y + 3z = 4$, $3x + 4y - 5z = 2$, and $4x + 6y - 2z = 6$. These are three dependent equations as can be seen by adding the first two equations to obtain the third. Therefore there are only two independent equations, and it matters not which two equations are retained and which one is discarded as not containing any additional information. Hence dependency among equations and functions is much the same idea.

To conclude the discussion of compatibility equations, the following is a list of the five compatibility equations for the strains in terms of cylindrical coordinates that, together with the one compatibility equation in Exercise 3.6, make the complete list of six. (From Ref. [35], with the third equation corrected.)

$$\begin{aligned} \frac{\partial^2 \epsilon_{rr}}{\partial z^2} + \frac{\partial^2 \epsilon_{zz}}{\partial r^2} - \frac{\partial^2 \gamma_{zr}}{\partial z \partial r} &= 0 \\ r \frac{\partial}{\partial z} \left(2\epsilon_{rr} - 2\frac{\partial}{\partial r}(r\epsilon_{\theta\theta}) + \frac{\partial \gamma_{r\theta}}{\partial \theta} \right) + \frac{\partial}{\partial \theta} \left(\frac{\partial}{\partial r}(r\gamma_{r\theta}) - \frac{\partial \gamma_{zr}}{\partial \theta} \right) &= 0 \\ \frac{\partial}{\partial z} \left(2r \frac{\partial \epsilon_{rr}}{\partial \theta} - \frac{\partial}{\partial r}(r^2 \gamma_{r\theta}) \right) + r^2 \frac{\partial}{\partial r} \left[\frac{1}{r} \left(\frac{\partial}{\partial r}(r\gamma_{\theta z}) - \frac{\partial \gamma_{zr}}{\partial \theta} \right) \right] &= 0 \\ r^2 \frac{\partial^2 \epsilon_{\theta\theta}}{\partial z^2} + r \frac{\partial \epsilon_{zz}}{\partial r} + \frac{\partial^2 \epsilon_{zz}}{\partial \theta^2} - r \frac{\partial}{\partial z} \left(\frac{\partial \gamma_{\theta z}}{\partial \theta} + \gamma_{rz} \right) &= 0 \\ 2 \frac{\partial}{\partial r} \left(\frac{1}{r} \frac{\partial \epsilon_{zz}}{\partial \theta} \right) + \frac{\partial}{\partial z} \left(\frac{\partial \gamma_{r\theta}}{\partial z} - r \frac{\partial}{\partial r} \left(\frac{\gamma_{\theta z}}{r} \right) - \frac{1}{r} \frac{\partial \gamma_{zr}}{\partial \theta} \right) &= 0 \end{aligned}$$

Strains in Rotated Coordinate Systems

4.1 Introduction

In Chapter 3 the concept of strains was developed for a single Cartesian coordinate system. The same two questions that were raised with regard to stresses referenced to a single Cartesian coordinate system can be raised with respect to strains: (i) do the strains in one Cartesian coordinate system uniquely determine the strains in another Cartesian coordinate system that is translated and rotated with respect to the first coordinate system; and (ii) how are the maximum strains determined? After the experience gained with stresses, it may be tempting to assume that the answer to the first question is in the affirmative. However, unlike stresses which involve force components, and therefore can be summed using Newton's second law, strains are only a matter of geometry. Therefore, at this point, since they do not share a common basis, no parallel can be drawn between stresses and strains with regard to the translation and rotation of Cartesian coordinate axes. The question has to be investigated anew.

4.2 Strains in Other Cartesian Coordinate Systems

The translation of Cartesian coordinate axes has no effect on longitudinal strains simply because longitudinal strains are measures of the differences between displacements at neighboring material points in a structural body. The description of the magnitudes of relative displacements in any particular coordinate axis direction is wholly unaffected by a translation of the origin of that coordinate axis. To say the same thing in other terms, recall that, for any coordinate axis direction, a longitudinal strain is the difference between the after deformation length to the first or second power, and the before deformation length to the first or second power, all divided by the original length to the first or second power, respectively, where all lengths parallel the coordinate axis direction. Mathematical descriptions of lengths paralleling the coordinate axes are totally unaffected by translations of the coordinate system used to measure length. Similarly, the shearing strains are also unaffected by a translation of a Cartesian coordinate system because the right angles and their changes are exactly the same right angles and changes in right angles in the translated Cartesian coordinate system as they are in the original system.

The rotation of a Cartesian coordinate system results in the consideration of different lengths and changes in length, and different right angles and changes in right angles. Thus the magnitudes of the various strain components are generally different when strain components are referred to a rotated coordinate system. Therefore, consider two Cartesian coordinate systems with arbitrarily different rotational orientations. Let one system be called the *original coordinate system* with coordinates x , y , and z , and let the other be called the *rotated coordinate system* with coordinates x^* , y^* , and z^* . Let the displacements measured in the rotated coordinate system be designated as u^* , v^* , and w^* . Consider, for example, the longitudinal strain ϵ_{xx}^* associated with the rotated coordinate system. Since the choice of which of the two coordinate systems is called the rotated coordinate system is entirely

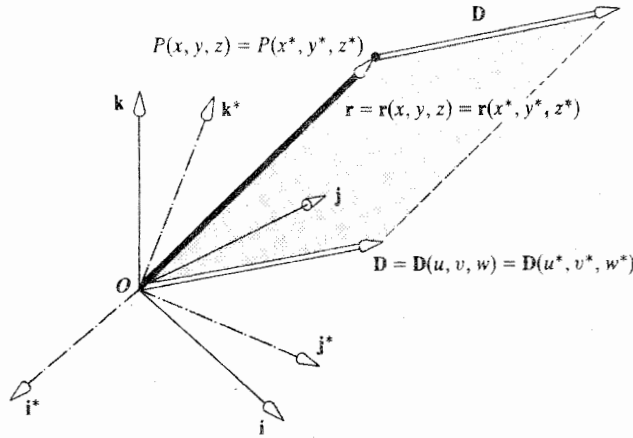


Figure 4.1. The original (without asterisks) and rotated (with asterisks) coordinate system unit vectors plus the position vector \mathbf{r} for point P , and the displacement vector $\mathbf{D}(P)$. The components of both $\mathbf{r}(P)$ and $\mathbf{D}(P)$ can be referred to either the original or the rotated coordinate system.

arbitrary, any strain has exactly the same *form* in any Cartesian coordinate system. That is,

$$\epsilon_{xx}^* = \frac{\partial u^*}{\partial x^*} \quad (4.1)$$

In order to attempt to develop an expression for the strain in the rotated coordinate system in terms of the strains in the original coordinate system, it is necessary to recognize that both coordinate systems cover the volume of the structural body. Thus the position vector \mathbf{r} to an arbitrary point P within the structural body from point O , the joint origin of the original and rotated coordinate systems, can be expressed in terms of either set of coordinates (see Fig. 4.1). Hence

$$\overline{OP} = \mathbf{r} = x\mathbf{i} + y\mathbf{j} + z\mathbf{k} = x^*\mathbf{i}^* + y^*\mathbf{j}^* + z^*\mathbf{k}^* \quad (4.2)$$

where the unit vectors with asterisks are, of course, aligned with the axes of the rotated coordinate system. Similarly, the displacement components $[u \ v \ w]$ on the one hand, and $[u^* \ v^* \ w^*]$ on the other hand, describe the same physical displacement field of the structural body. Therefore, at the same arbitrary point P , the total displacement vector \mathbf{D} can be written in terms of both sets of displacement components as

$$\mathbf{D} = u\mathbf{i} + v\mathbf{j} + w\mathbf{k} = u^*\mathbf{i}^* + v^*\mathbf{j}^* + w^*\mathbf{k}^* \quad (4.3)$$

Again, see Fig. 4.1. Now, by taking dot products between the unit vectors of one coordinate system and the unit vectors of the other coordinate system, the coordinates or displacement components of one coordinate system can easily be determined in terms of the coordinates or displacement components of the other coordinate system, respectively. (This fact immediately encourages the expectation that the strains associated with the two coordinate system can also be related to each other.) For example,

$$x = x^*(\mathbf{i}^* \cdot \mathbf{i}) + y^*(\mathbf{j}^* \cdot \mathbf{i}) + z^*(\mathbf{k}^* \cdot \mathbf{i})$$

and

$$u^* = u(\mathbf{i}^* \cdot \mathbf{i}) + v(\mathbf{i}^* \cdot \mathbf{j}) + w(\mathbf{i}^* \cdot \mathbf{k}) \quad (4.4)$$

The dot products are just the cosines of the angles between the coordinate axes. These are identical to the direction cosines that describe the rotations from the original coordinate system to the rotated coordinate system. Thus Eqs. (4.4) can be rewritten in terms of the direction cosine symbols introduced in Chapter 2 where again, for example, $c_{yz} = \mathbf{j}^* \cdot \mathbf{k}$ is the cosine of the angle between the y^* and the z axis, and the first subscript always refers to the rotated coordinate system. Extending Eqs. (4.4) to include the other two coordinates and other two displacement components yields

$$\begin{Bmatrix} x \\ y \\ z \end{Bmatrix} = \begin{bmatrix} c_{xx} & c_{yx} & c_{zx} \\ c_{xy} & c_{yy} & c_{zy} \\ c_{xz} & c_{yz} & c_{zz} \end{bmatrix} \begin{Bmatrix} x^* \\ y^* \\ z^* \end{Bmatrix} \quad \text{or} \quad \{x\} = [c]^t \{x^*\} \quad (4.5)$$

and

$$\begin{Bmatrix} u^* \\ v^* \\ w^* \end{Bmatrix} = \begin{bmatrix} c_{xx} & c_{xy} & c_{xz} \\ c_{yx} & c_{yy} & c_{yz} \\ c_{zx} & c_{zy} & c_{zz} \end{bmatrix} \begin{Bmatrix} u \\ v \\ w \end{Bmatrix} \quad \text{or} \quad \{u^*\} = [c] \{u\} \quad (4.6)$$

Now all is ready to work with the expression $\epsilon_{xx}^* = \partial u^* / \partial x^*$. The development process is the repeated use of the chain rule for partial differentiation. Those readers who need to review the chain rule can refer to Section I.5. Since the deformations in the rotated coordinate system can be considered to be functions of the deformation components of the original coordinate system, as specified in Eqs. (4.6), it is possible to write

$$\epsilon_{xx}^* = \frac{\partial u^*}{\partial x^*} = \frac{\partial u^*}{\partial u} \frac{\partial u}{\partial x^*} + \frac{\partial u^*}{\partial v} \frac{\partial v}{\partial x^*} + \frac{\partial u^*}{\partial w} \frac{\partial w}{\partial x^*} \quad (4.7)$$

$$\epsilon_{xx}^* = c_{xx} \frac{\partial u}{\partial x^*} + c_{xy} \frac{\partial v}{\partial x^*} + c_{xz} \frac{\partial w}{\partial x^*}$$

where the deformations in either coordinate system can be considered as functions of either set of coordinates. However, it is preferable always to match the displacements with the associated coordinate system. Therefore, write

$$\begin{aligned} \frac{\partial u}{\partial x^*} &= \frac{\partial u}{\partial x} \frac{\partial x}{\partial x^*} + \frac{\partial u}{\partial y} \frac{\partial y}{\partial x^*} + \frac{\partial u}{\partial z} \frac{\partial z}{\partial x^*} = \frac{\partial u}{\partial x} c_{xx} + \frac{\partial u}{\partial y} c_{xy} + \frac{\partial u}{\partial z} c_{xz} \\ \frac{\partial v}{\partial x^*} &= \frac{\partial v}{\partial x} \frac{\partial x}{\partial x^*} + \frac{\partial v}{\partial y} \frac{\partial y}{\partial x^*} + \frac{\partial v}{\partial z} \frac{\partial z}{\partial x^*} = \frac{\partial v}{\partial x} c_{xx} + \frac{\partial v}{\partial y} c_{xy} + \frac{\partial v}{\partial z} c_{xz} \\ \frac{\partial w}{\partial x^*} &= \frac{\partial w}{\partial x} \frac{\partial x}{\partial x^*} + \frac{\partial w}{\partial y} \frac{\partial y}{\partial x^*} + \frac{\partial w}{\partial z} \frac{\partial z}{\partial x^*} = \frac{\partial w}{\partial x} c_{xx} + \frac{\partial w}{\partial y} c_{xy} + \frac{\partial w}{\partial z} c_{xz} \end{aligned} \quad (4.8)$$

Substituting Eqs. (4.8) into the second of Eqs. (4.7) yields

$$\begin{aligned} \epsilon_{xx}^* &= \epsilon_{xx} (c_{xx})^2 + \epsilon_{yy} (c_{xy})^2 + \epsilon_{zz} (c_{xz})^2 \\ &\quad + \gamma_{xy} c_{xx} c_{xy} + \gamma_{xz} c_{xx} c_{xz} + \gamma_{yz} c_{xy} c_{xz} \end{aligned} \quad (4.9a)$$

or

$$\begin{aligned} \epsilon_{xx}^* &= \epsilon_{xx} (c_{xx})^2 + \epsilon_{yy} (c_{xy})^2 + \epsilon_{zz} (c_{xz})^2 \\ &\quad + 2[\epsilon_{xy} c_{xx} c_{xy} + \epsilon_{xz} c_{xx} c_{xz} + \epsilon_{yz} c_{xy} c_{xz}] \end{aligned} \quad (4.9b)$$

where, in this coordinate rotation equation for the strain ϵ_{xx}^* , the Green shearing strains are introduced in place of the engineering shearing strains in order to obtain exactly the

same form for Eq. (4.9b) as that which exists for the coordinate rotation equation for the corresponding stress, σ_{xx}^* . That latter equation is Eq. (2.1).

The same process can be carried out for each of the other strains in the rotated coordinate system. See Exercise 4.1, which shows that the Green shearing strain

$$\begin{aligned}\epsilon_{xy}^* &= \frac{1}{2}\gamma_{xy}^* = \epsilon_{xx} c_{xx} c_{yx} + \epsilon_{yy} c_{xy} c_{yy} + \epsilon_{zz} c_{xz} c_{yz} \\ &\quad + \epsilon_{xy}(c_{xx} c_{yy} + c_{xy} c_{yx}) + \epsilon_{xz}(c_{xx} c_{yz} + c_{xz} c_{yx}) \\ &\quad + \epsilon_{yz}(c_{xy} c_{yz} + c_{xz} c_{yy})\end{aligned}\quad (4.9c)$$

The above shearing strain result is entirely analogous to the corresponding shearing stress result, Eq. (2.2). All the strain rotation equations can be cast in matrix form as

$$[\epsilon^*] = [c][\epsilon][c]^t \quad \text{where} \quad [\epsilon] = \begin{bmatrix} \epsilon_{xx} & \epsilon_{xy} & \epsilon_{xz} \\ \epsilon_{xy} & \epsilon_{yy} & \epsilon_{yz} \\ \epsilon_{xz} & \epsilon_{yz} & \epsilon_{zz} \end{bmatrix}\quad (4.10)$$

and where $[\epsilon^*]$ follows the same pattern as $[\epsilon]$. Equation (4.10) clearly demonstrates that the strains in any Cartesian coordinate system define the strains in all Cartesian coordinate systems.

The exact analogy between the matrix equation that describes the rotation of the Green strains, Eq. (4.10), and that which describes the rotation of stresses, Eq. (2.3), leads to the following conclusion. All results that apply to the rotation of stresses, such as Mohr's circle and the eigenvalue solution for principal stresses, apply to the Green strains (not the engineering strains) as well. However, Mohr's circle and the eigenvalue problem are usually treated in terms of stresses, rather than strains, after a conversion from strains to stresses as is discussed in Chapter 6. Nevertheless, there is an important, direct application of the strain rotation equations, which is developed below.

4.3 Strain Gauges

As is quantified in the next chapter, if a piece of metal is elongated in one direction, it tends to shrink in all directions perpendicular to the direction of elongation. Similarly, if the piece of metal is compressed in one direction, it tends to expand in all directions perpendicular to the direction in which it is compressed. In particular, if a piece of electrical wiring is stretched, the cross-sectional area of the wire will diminish. The decrease in the cross-sectional area results in an increase in the electrical resistance over the length of the wire. Similarly, if the wire contracts without buckling, the cross-sectional area increases and the electrical resistance of the wire decreases. These changes in electrical resistance can be calibrated with respect to the changes in length of the wire. If the insulated wire is bonded to a surface of a structural body so that the wire stretches or contracts as the body stretches and contracts, then the change in electrical resistance is a measure of the surface extension or contraction (i.e., the longitudinal strain) of the body in the direction of the wire. In order to achieve greater accuracy, it is desirable to have as long a piece of wire as possible. If the wire extends over any significant distance (relative to the dimensions of the structure), then the change in electrical resistance is tied to a less useful average strain over the length of the wire, rather than a strain that can be closely ascribed to a point. This difficulty can be mitigated by repeatedly doubling back the wire upon itself so as to have one long wire bent so that its segments run predominantly in one direction; see Fig. 4.2(a). The point on the structural surface to which the measured strain would be ascribed would

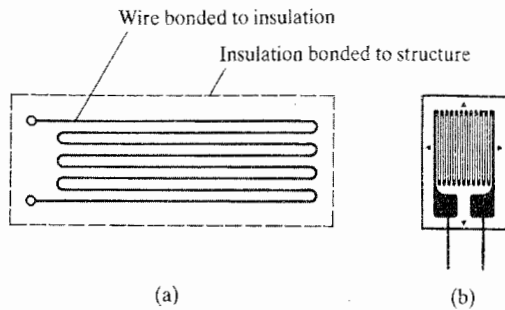


Figure 4.2. (a) The basic (and original) strain gauge was a wire folded back and forth in order to concentrate the wire nearer to the point of interest while still providing increased length for greater accuracy of measurement. (b) A readily available, modern foil type strain gauge length can be smaller than half a centimeter. Typically, the modern gauge can operate within a temperature range of -150°F to 175°F , and is manufactured to have the same thermal expansion coefficient of either steel, or copper, or aluminum. Epoxy cement is one means of bonding the strain gauge to the structure.

be the center of the wire pattern. This use of a folded wire is precisely how strain gauges used to be made. Today, this type of strain gauge, like much other modern circuitry, is a foil rather than a wire device; see Fig. 4.2(b).

Consider a structural body that is subjected to a loading. Consider a point on an outer surface of such a body and a Cartesian coordinate system oriented so that the z axis is perpendicular to the body surface. To obtain the values of two longitudinal strains and the shearing strain associated with the x, y axes, three (longitudinal) strain gauges are clustered on the surface around the point where the strain is to be measured. Regardless of the relative orientation of the three strain gauges, the cluster of three is called a *strain gauge rosette*. Figure 4.3 illustrates a typical rosette centered at the point P . With the z axis normal to the plane of the rosette, the strain rotation equation, Eq. (4.9a), reduces to

$$\epsilon_{xx} c_{xx} c_{xx} + \epsilon_{yy} c_{xy} c_{xy} + \gamma_{xy} c_{xx} c_{xy} = \epsilon_{xx}^* \quad (4.11)$$

because all the direction cosines with z subscripts are zero. Notice that the engineering shearing strain is being used in this discussion. Recall that the orientation of the x^* axis relative to the x or y axes is entirely arbitrary. This allows the analyst to choose to have the x^* axis to be successively directed along the axes of each of the three strain gauges of the rosette, and to thus, in turn, call the strain measured by each of the three strain gauges the ϵ_{xx}^* of Eq. (4.11). The result is that the three measured strain values taken from the rosette can be used to form the right-hand side of a system of three simultaneous equations in terms of the three unknown strain values, ϵ_{xx} , γ_{xy} , and ϵ_{yy} . The following example problems illustrate this process. Similar problems are available in the exercises.

Example 4.1. For the sake of ease of illustration, let the x and y axes be oriented with respect to the rosette as shown in Fig. 4.3. The task at hand is to determine the values of the strains ϵ_{xx} , γ_{xy} , and ϵ_{yy} , at the surface point P . Let the input, the measured strain values obtained from their respective gauges, be $\epsilon_a = +0.000\,044$ mm/mm, $\epsilon_b = -0.000\,055$ mm/mm, and $\epsilon_c = +0.000\,066$ mm/mm = 66×10^{-6} mm/mm. The output, $[\epsilon_{xx} \ \epsilon_{yy} \ \gamma_{xy}]$, is obtained through the repeated use of Eq. (4.11) with the x^* axis directed in turn along each strain gauge axis. That is, in order to apply Eq. (4.11) to strain gauge a , first direct the x^* axis from point P outward along the a gauge axis. Note that for this first application of

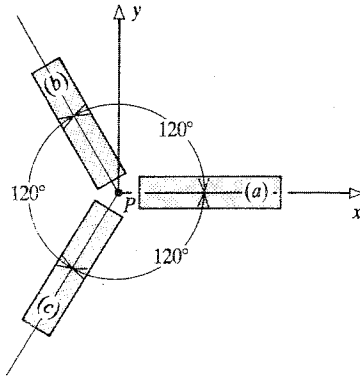


Figure 4.3. Example 4.1. A strain gauge rosette.

Eq. (4.11), the angle between the x^* and x axis is zero degrees, and the angle between the x^* axis and y axis is 90° . Thus $c_{xx} = 1.0$, and $c_{xy} = 0.0$. Hence the first of the necessary three solution equations is simply

$$\epsilon_{xx} = \epsilon_a$$

Note that this solution is exactly what should be expected for the case where the a gauge lies along the x axis. Now direct the x^* axis along the axis of the b gauge so that it is 120° counterclockwise from the x axis. Note that since the three-dimensional direction cosine notation is being used, there is no positive sign convention for the angles of rotation. That is, in itself, a clockwise or counterclockwise direction of rotation is immaterial when using direction cosines. Now $c_{xx} = \cos(120^\circ) = -\sin(30^\circ) = -0.5$, and $c_{xy} = \cos(30^\circ) = 0.866$. Thus the b gauge equation derived from Eq. (4.11) becomes

$$0.25\epsilon_{xx} + 0.75\epsilon_{yy} - 0.433\gamma_{xy} = \epsilon_b$$

Directing the x^* axis along the axis of the c gauge results in $c_{xx} = \cos(120^\circ) = -0.5$, and $c_{xy} = \cos(150^\circ) = -\sin(60^\circ) = -0.866$. Thus the c gauge equation derived from Eq. (4.11) is

$$0.25\epsilon_{xx} + 0.75\epsilon_{yy} + 0.433\gamma_{xy} = \epsilon_c$$

Solving these three forms of Eq. (4.11) simultaneously first produces:

$$0.75\epsilon_{yy} - 0.433\gamma_{xy} = \epsilon_b - 0.25\epsilon_a$$

$$0.75\epsilon_{yy} + 0.433\gamma_{xy} = \epsilon_c - 0.25\epsilon_a$$

and then

$$\epsilon_{xx} = \epsilon_a = +44 \times 10^{-6} \text{ mm/mm}$$

$$\epsilon_{yy} = \frac{1}{3}(-\epsilon_a + 2\epsilon_b + 2\epsilon_c) = -7.3 \times 10^{-6} \text{ mm/mm}$$

$$\gamma_{xy} = \frac{1}{\sqrt{3}}(-2\epsilon_b + 2\epsilon_c) = +140 \times 10^{-6} \text{ radians or mm/mm}$$

Note that this example calculation illustrates a situation where a strain in the x, y coordinate system can be significantly larger than the absolute value of any one of the three strain gauge measurements. Also note that strains have units of length divided by length, that is, radians. It does not matter whether the length is meters, millimeters, inches, or whatever.

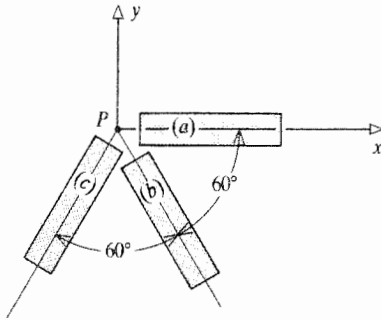


Figure 4.4. Example 4.2. Another strain gauge rosette.

Strains expressed in terms of millionths of a radian are sometimes informally referred to as having units of “microstrains.” ■

Example 4.2. Owing to interference from other parts of the structure, the strain gauge rosette placed at point P is arranged as shown in Fig. 4.4. As a result of a certain loading, the strain gauge readings ϵ_a , ϵ_b , and ϵ_c are obtained. Calculate the z plane strains at the surface point P in terms of those strain gauge measurements.

Solution. Apply Eq. (4.11) to each of the three strain gauges. Starting with the strain gauge a where the angle between the x^* and the x axis is zero, and with the y axis it is 90° , the result is again $\epsilon_{xx} = \epsilon_a$. To obtain the second equation, direct the x^* axis from point P through the b gauge so that $c_{xx} = \cos(60^\circ) = 0.5$, and $c_{xy} = \cos(150^\circ) = -0.866$. Note again that there is no required sign convention for the angles between coordinate axes. Indeed, since the cosine function is an even function (the function has the same value for positive or negative arguments), it matters not whether an angle is called positive or negative. Applying Eq. (4.11) yields

$$0.25\epsilon_a + 0.75\epsilon_{yy} - 0.433\gamma_{xy} = \epsilon_b$$

Similarly for strain gauge c ,

$$0.25\epsilon_a + 0.75\epsilon_{yy} + 0.433\gamma_{xy} = \epsilon_c$$

Simultaneous solution of the above two equations completes the problem. The list of solutions is

$$\begin{aligned}\epsilon_{xx} &= \epsilon_a & \epsilon_{yy} &= 0.667(-0.5\epsilon_a + \epsilon_b + \epsilon_c) \\ \gamma_{xy} &= 1.155(-\epsilon_b + \epsilon_c)\end{aligned}$$

which is the same algebraic solution as in Example 4.1, because the b gauge orientation here is the same as that in the previous example problem. ■

Note that in the foregoing exposition, nothing was said about the values of γ_{xz} , γ_{yz} , or ϵ_{zz} at the surface of the structure. Since the structural surface on which the strain gauges are applied is accessible to strain gauges, in general, the loads on such a surface are limited to fluid pressures and fluid friction shearing tractions. If the surface is that of a “thin” metal, or fiber composite sheet, as is often the case for many types of vehicles from submarines to spacecraft, then an approximate state of plane stress would likely exist. Then the longitudinal strain ϵ_{zz} is unimportant, and, again for metal structural materials, it will be possible to

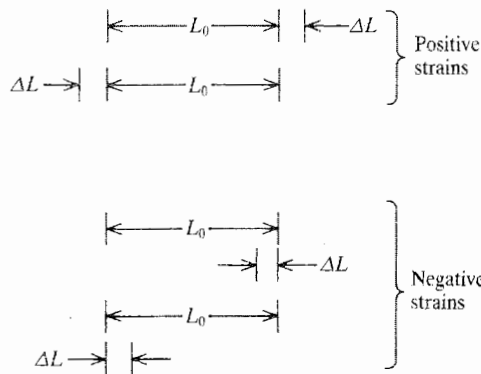


Figure 4.5. Possible combinations of changes in length with respect to original length for the purpose of demonstrating that strains are not vector quantities.

conclude that the shearing strains γ_{xz} and γ_{yz} are also negligible. In other words, it is often the case that knowing the strains in the x, y plane is all that is important with respect to vehicular strains.

4.4 The Mathematical Properties of Strains

At the beginning of Chapter 3 it was pointed out that displacements are vector quantities. Thus the collection of all displacements located at their points of origin, which is called the displacement field, is a vector field. Since the displacements are vectors, the question is: Are the strains also vector quantities? At first glance, it might seem so because strains are related to displacements, and the strains appear to have magnitudes and distinct directions. However, this is not so with regard to directions. For example, what is the direction of a positive value of ϵ_{xx} ? If the answer offered is the positive x direction, consider an x^* axis that is positive in the direction that is 180° from the positive x axis direction, and a y^* axis that is directed 180° from the direction of the positive y axis. (This means that the z^* and z axis must coincide.) If the strains were vectors, then it would seem reasonable that ϵ_{xx}^* would equal the negative of ϵ_{xx} . However, referring to Eq. (4.9), the two strains are seen to be exactly the same. This is so because the sign assigned to a strain depends only upon whether the change in length increases or decreases the original length, and does not depend on the direction of the change. Figure 4.5 illustrates this point. Furthermore, consider Eq. (4.11): That equation shows that the addition of strains is not in accord with the rules of vector addition because the direction cosines do not appear to the first power but to the second power. That is, ϵ_{xx}^* is not composed of the components in the x^* direction of ϵ_{xx} , ϵ_{yy} , and ϵ_{xy} as it would be if the strains were vectors. This is sufficient proof that the strains are not vectors. The unavailability of vector properties is not a great loss since the Green strains can be arranged in either the matrix form shown in Eq. (4.10), or as a second order tensor.

4.5 Summary

Strains in a Cartesian or other orthogonal coordinate system rotate according to Eq. (4.10). The application of that equation to strain gauges leads to the reduced form of that equation, which is Eq. (4.11). Strain gauges allow the direct measurement of strains at

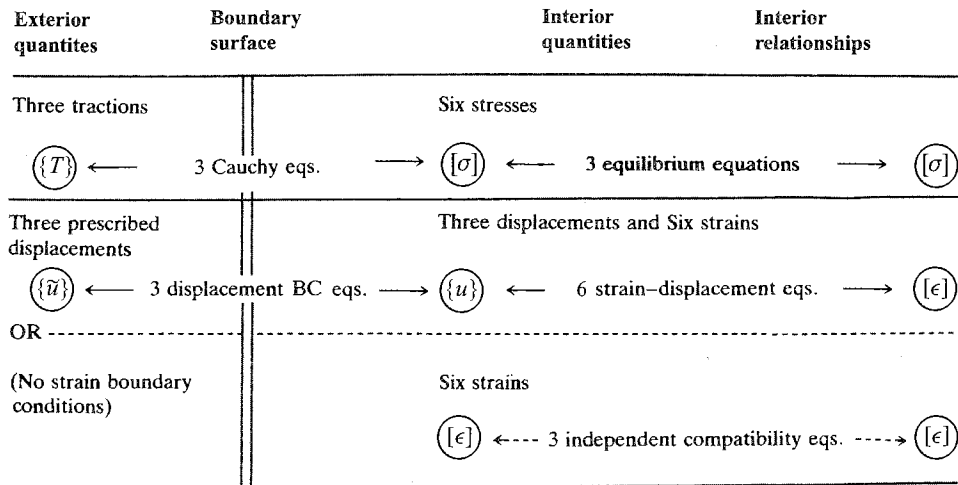


Figure 4.6. The solid mechanics analytical landscape.

something like a point on the surface of a structure. This is important since no such direct measurement of stress is usually possible.

At this point in this development of the basic equations of structural mechanics, within the domain (interior volume) of the structural body, there are the following quantities to be determined: (i) Six stresses, which can be arranged in a 3×3 matrix, or, if desirable, a 6×1 column matrix, (ii) Six strains, which can also be arranged as above, and (iii) Three displacements.

The number of quantities to be determined totals 15. The number of equations available to determine these quantities is as follows: (i) three equilibrium equations, which are first order partial differential equations that relate the stresses; (ii) six strain-displacement equations, *or* three independent compatibility equations which are second order partial differential equations that relate the strains. In the latter case, it is not necessary to count the displacements among the functions to be determined since they then do not enter into the formulation of the total structural analysis problem.

In either case, there are six more quantities to be determined than there are equations available to determine them. The diagram of Fig. 4.6 is helpful in viewing the entire analytical landscape. First note that three new quantities have been introduced. The new quantities are the prescribed displacements, which are symbolized by the addition of a tilde to the usual displacement symbols. Prescribed displacements are simply displacements at the boundary surface whose values are known after the application of the loading. To illustrate prescribed displacements, consider the end displacements of a bar subjected to axial forces. If the bar were fastened at its left end so that end surface did not move, and a tensile force of magnitude F were applied uniformly over the right-hand end cross-sectional area, then there would be a displacement boundary condition at the fixed left end, and a force or traction boundary condition at the right end where the force was applied. These boundary conditions could be written as

$$\bar{u} \text{ (left end } x \text{ coordinate value)} = 0 \quad \text{and} \quad T_x \text{ (right end)} = \frac{F}{A}$$

If, to change the circumstances of the bar, the left end were fixed as before, and the right end were pulled with an unknown force so that the end moved 1 mm, then there would

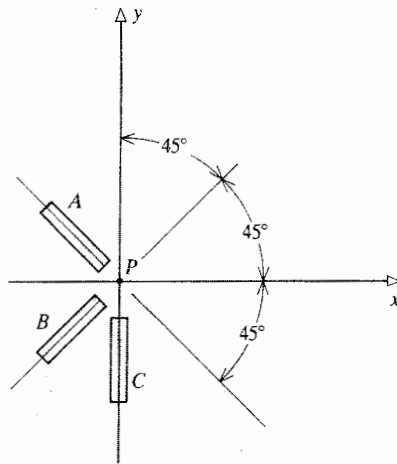


Figure 4.7. Example 4.3. Several strain gauge rosette.

be displacement boundary conditions at both ends of the spring. These latter boundary conditions could be written

$$\tilde{u} \text{ (left end)} = 0 \quad \text{and} \quad \tilde{u} \text{ (right end)} = 1.0 \text{ mm}$$

Returning now to the purpose of Fig. 4.6: on the one hand the prescribed displacements are analytically connected to the interior displacements, and the interior displacements are analytically connected to the strains. On the other hand the tractions are connected to the stresses:



What have yet to be connected are the six strains and the six stresses in this chain of quantities that define structural analysis. That connection in the form of the required six equations that bring into balance the number of equations and the number of unknowns, is the subject of the next two chapters. When the stresses and strains are related so that there are the same number of equations as there are unknown quantities, then this linear solid mechanics problem is said to be *well formulated*.

Example 4.3. Use the three strain gauge readings ϵ_a , ϵ_b , and ϵ_c from the indicated strain gauges shown in Fig. 4.7 in order to determine the three surface strains at point P .

Solution. The direction cosines are (a) $c_{xx} = -\sqrt{2}/2$, $c_{xy} = \sqrt{2}/2$ (b) $c_{xx} = -\sqrt{2}/2$, $c_{xy} = -\sqrt{2}/2$; and (c) $c_{xx} = 0$, $c_{xy} = -1$.

From Eq. (4.11)

$$\epsilon_a = \frac{1}{2}\epsilon_{xx} + \frac{1}{2}\epsilon_{yy} - \frac{1}{2}\gamma_{xy}$$

$$\epsilon_b = \frac{1}{2}\epsilon_{xx} + \frac{1}{2}\epsilon_{yy} + \frac{1}{2}\gamma_{xy}$$

$$\epsilon_c = \epsilon_{yy}$$

The three solutions for the strains at point P are

$$\epsilon_{xx} = \epsilon_a + \epsilon_b - \epsilon_c \quad \epsilon_{yy} = \epsilon_c \quad \gamma_{xy} = \epsilon_b - \epsilon_a$$

■

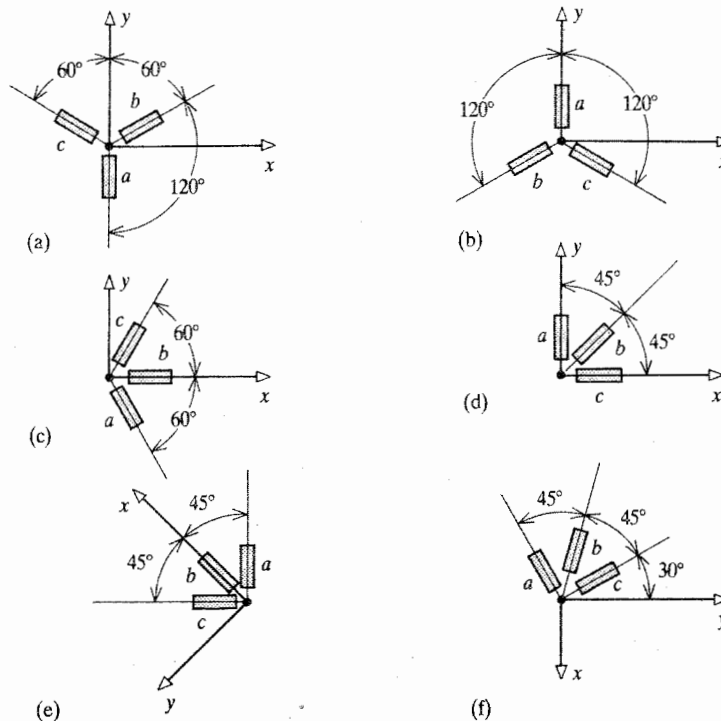


Figure 4.8. Exercise 4.4. Several strain gauge rosettes.

Chapter 4 Exercises

- 4.1. In order to practice the chain rule for partial differentiation, consider the shearing strain $\gamma_{xy}^* = 2\epsilon_{xy}^* = (\partial u^*/\partial y^*) + (\partial v^*/\partial x^*)$.
- Write the chain rule expansion for the quantity $\partial u^*/\partial y^*$, where u^* is properly taken to be a function of u , v , and w .
 - Continue the above development by considering the u , v , and w displacements each to be functions of x , y , and z in order to eliminate such expressions as $\partial u/\partial y^*$, $\partial v/\partial y^*$, and $\partial w/\partial y^*$, which are obtained in the first part of this exercise.
 - Combine the results of the first two parts in order to have an expression for $\partial u^*/\partial y^*$ only in terms of direction cosines and the terms such as $\partial u/\partial x$, $\partial u/\partial y$, ..., $\partial w/\partial z$.
 - Do the same as the above for $\partial v^*/\partial x^*$ to obtain the expression for γ_{xy}^* in terms of the strains in the original Cartesian coordinate system.
 - Confirm the similarity in form between the result for ϵ_{xy}^* (not γ_{xy}^*) and the previous result for σ_{xy}^* , thus providing further partial confirmation for Eq. (4.10).
- 4.2. (a) As a variation on Exercise 2.4, note that $\mathbf{i}^* = c_{xx}\mathbf{i} + c_{xy}\mathbf{j} + c_{xz}\mathbf{k}$, and so forth. The three dot products of each such unit vector in the rotated coordinate system with itself, and the three independent dot products of the different unit vectors in the rotated coordinate system (such as $\mathbf{i}^* \cdot \mathbf{j}^*$) yield six independent

equations in terms of the nine direction cosines. Show that these six equations are the basis for the matrix equation

$$[c][c]^t = [I]$$

Note that matrices where the transpose is the same as the inverse are called "unitary matrices" (Ref. [20]). It is also true that $[c]^t [c] = [I]$.

- (b) Use the above matrix equation to determine the solution for the matrix $[\epsilon]$ in terms of $[\epsilon^*]$, and $[\sigma]$ in terms of $[\sigma^*]$.

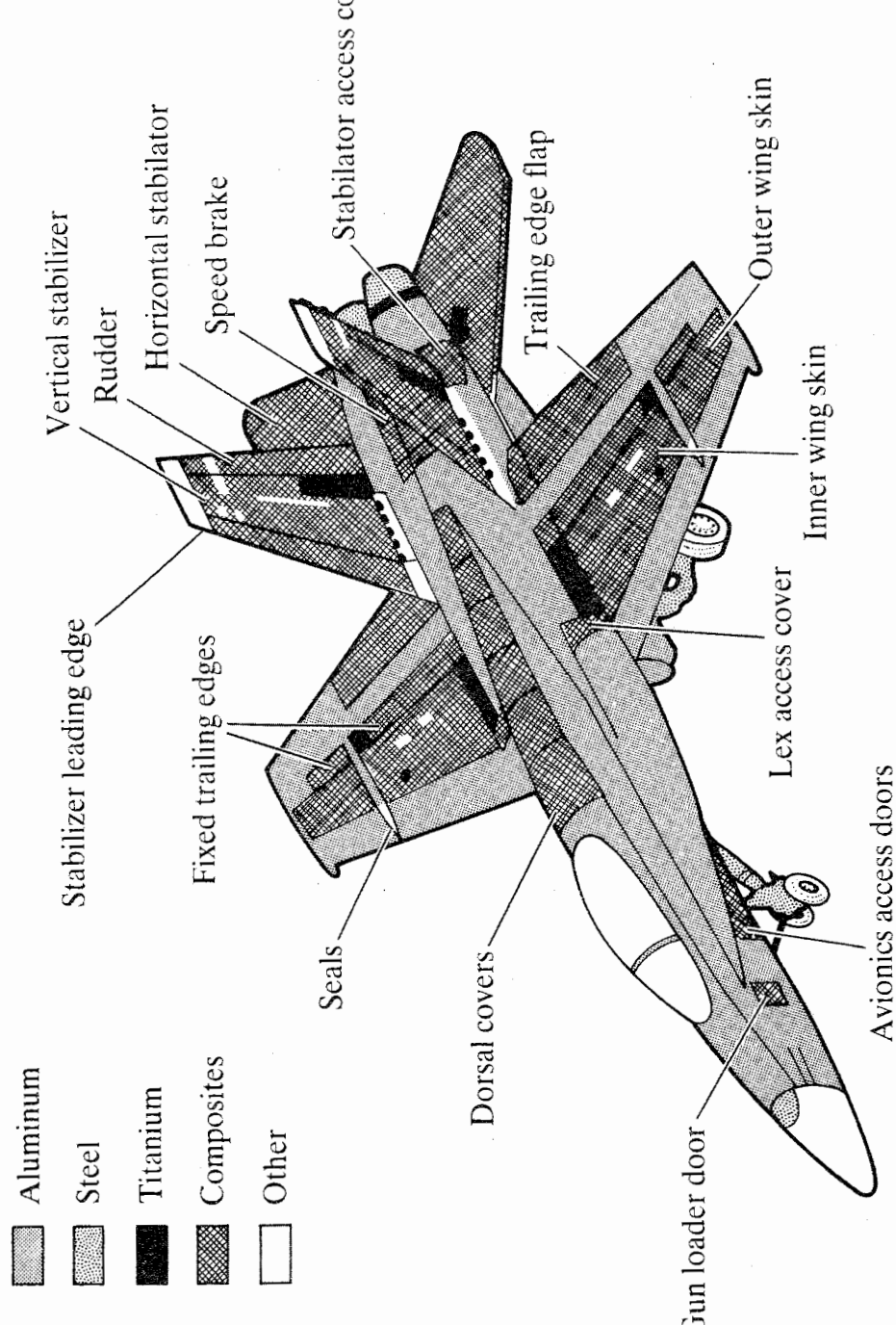
- 4.3. Is the following proposed matrix of direction cosines a valid matrix of direction cosines?

$$[c] = \begin{bmatrix} 3/7 & 6/7 & 2/7 \\ -6/7 & 2/7 & 3/7 \\ 2/7 & -3/7 & 6/7 \end{bmatrix}$$

- 4.4. For each of the strain gauge rosette configurations shown in Fig. 4.8, determine the expressions for ϵ_{xx} , γ_{xy} , and ϵ_{yy} in terms of the measured values ϵ_a , ϵ_b , and ϵ_c .

FOR THE EAGER

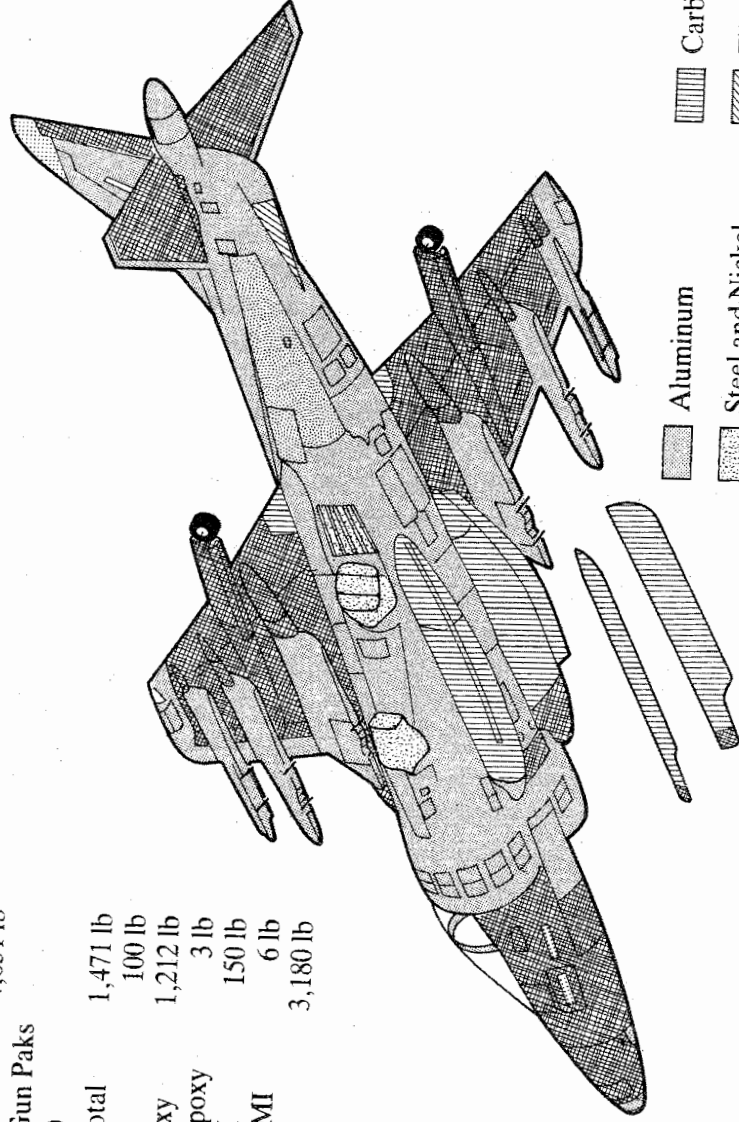
- 4.5. As an exercise in linear algebra, prove that the value of the determinant of $[c]$, the matrix of direction cosines, is 1.0. *First hint:* Recall that the scalar value of any triple vector product can be written in matrix form, and then consider the product $\mathbf{i}^* \times \mathbf{j}^* \cdot \mathbf{k}^*$, where each of these three rotated unit vectors is written in terms of its direction cosine relative to the original coordinate system. *Second hint:* A better motivated proof begins with the result of Exercise 4.2 and the theorem that if $[m] = [n][p]$, then $|m| = |n||p|$. In order to exclude the possibility that $|c| = -1$, first show that $|c| = +1$ for various, specific, right angle rotations. Then, by way of contradiction, postulate there exists a rotation for which $|c| = -1$. Then consider successive small changes in that rotation, proving that they are individually insufficient to go from -1 to $+1$.



Canadian Forces CF-18 materials usage. Like the U.S. Navy F/A-18, it has about 40 per cent of its surface covered by composite skin that is difficult to repair quickly.

Structural Wt. 4,651 lb
 (Including Gun Paks
 and Strakes)

Nonmetallics Total 1,471 lb
 Acrylic 100 lb
 Carbon/Epoxy 1,212 lb
 Fiberglass/Epoxy 3 lb
 Carbon/BMI 150 lb
 Fiberglass/BMI 6 lb
 Metallics 3,180 lb



Aluminum
 Steel and Nickel
 Titanium
 Carbon/Epoxy
 Fiberglass/Epoxy

Carbon/BMI
 Fiberglass/BMI
 Acrylic
 Other

Materials usage for the AV-8B. Courtesy of the McDonnell-Douglas Corp., St. Louis, Missouri, U.S.A.

The Mechanical Behavior of Engineering Materials

5.1 Introduction

In the course of a career, an engineer can expect to be called upon to deal with the behavior of a great many different types of materials from which an object with a structural purpose is to be, or has been, fashioned. Metals, plastics, woods, and man-made composites of all kinds are plentiful in structural engineering practice. The paragraphs below provide a brief overview of these materials, starting with the metals.

The material that is used most extensively in modern engineering practice is steel. In comparison with other metals and composites, steels are cheap, and have the advantages of being stiff, strong, and hard. Thus steels are often the material of choice for vehicular applications such as automobile frames and aircraft landing gear. The superior high-temperature properties of certain alloy steels often results in their choice as a material for the structure of fuel-burning engines such as rockets. The principal drawback of steel for vehicular use is its relatively high weight density of approximately 0.28–0.29 lb/in³. There is presently a great variety of types of steel and steel alloys (Refs. [10–14]). There is also a great variety of designations of steels. Lists of specification equivalents can be found, for example, in Ref. [13]. The American Iron and Steel Institute (AISI) and the Society of Automotive Engineers (SAE) have agreed upon an AISI–SAE four-digit numbering system for steels that is widely, but not exclusively, used. It is outlined on p. 143 of Ref. [10]. It is important to note that steels with the same numerical designation can have rather different strengths and ductilities depending upon the heat treatment applied to the steel during manufacture. The means, if any, used to strengthen a material, such as cold working or heat treating, is called the “temper” of the material.

Other metals that are used extensively in vehicular construction are aluminum alloys, magnesium alloys, and titanium alloys. In brief, aluminum alloys have the advantages of low density (approximately 0.1 lb/in³), high strength-to-weight ratios, ease of fabrication, and generally good corrosion resistance, although some alloys in sheet form have to be clad (i.e., coated) with a purer form of aluminum in order to avoid corrosion damage to the core alloy. The Aluminum Association has established a four-digit designation system for wrought and cast aluminums that is outlined in Chapter 5 of Ref. [14]. The four-digit designations are followed by a hyphen and a temper designation. See Table 5.1. New forms of aluminum are continually under development in the highly competitive materials field.

Magnesium has the advantage that it weighs only approximately 0.06 lb/in³, but it is not as stiff or strong¹ as aluminum. Reference [14] points out that corrosion protection must

¹ With regard to materials, the term “strength” refers to the load-carrying capacity of a material; that is, the *stress* which the material can sustain without failing in one sense or another. A material “stiffness” is the *stress* necessary to achieve a specified *strain*; that is, the ratio of a stress to a strain. As is seen below, examples of strength measurements for a material are the ultimate tensile stress and the compressive yield stress, while an example of a stiffness measure for a material is the modulus of elasticity. The terms strength and stiffness are also used in reference to structures, where strength refers to a total specified *load* that a structure can bear without a failure, and stiffness refers to *loading* required to achieve a unit *deflection*.

Table 5.1. Aluminum: comparative compositions, characteristics, and applications*

Alloy designation	Nominal Composition, % (Not Specified Composition)	Commercial Forms [†]	Corrosion Resistance [‡]	Comparative Characteristics					Some Applications
				Machinability [‡]	Weldability [§]	Maximum Strength [¶]	Annealed Strength		
60	99.45 Al min 99.60 Al min	STEPBW STW	A-A —	D-C —	A-A —	27 20	10 10	Electrical con Chemical equ railroad tan	
70	99.00 Al min, 0.12 Cu	STEBWFO	A-A	D-C	A-A	24	13	Sheet metal w hollow war	
75	99.45 Al min	SO	A-A	D-C	A-A	28	12	Foil; light she	
11	5.5 Cu, 0.5 Bi, 0.5 Pb	BW	C-C	A-A	D-D	60	—	Screw machin	
14	4.4 Cu, 0.8 Si, 0.8 Mn, 0.4 Mg	STEBF	C-C	B-B	B-C	70	27	Truck frames structures	
17	4.0 Cu, 0.5 Mn, 0.5 Mg	BW	C	B	B-C	62	26	Screw machin fittings	
18	4.0 Cu, 0.6 Mg, 2.0 Ni	F	C	B	B-C	61	—	Aircraft engin heads and p	
24	4.5 Cu, 0.6 Mn, 1.5 Mg	STPEBW	C-C	B-B	B-B	75	27	Truck wheels machine pr	
25	4.5 Cu, 0.8 Si, 0.8 Mn	F	C-D	B-B	B-B	58	25	aircraft str Forgings; air propellers	
27	2.5 Cu, 0.3 Mg	WB	C	C	B-C	43	—	Rivets and re	
28	4.0 Cu, 1.5 Mg, 2.0 Ni	F	C	B	B-C	48	—	Jet engine im rings	
29	6.3 Cu, 0.3 Mn, 0.10 V, 0.15 Zr	SEF	B	B	A	70	25	Structural us temperatu 600 °F); h weldment	
38	2.3 Cu, 1.6 Mg, 1.0 Ni, 1.1 Fe	F	C	B	B-C	64	—	Aircraft engin (temperatu	

3003	1.2 Mn, 0.12 Cu	All forms	A-A	D-C	A-A	30	16	Cooking utensils; equipment; vessels; sheet metal work; building tanks
3004	1.2 Mn, 1.0 Mg	S	A-A	D-C	A-A	41	26	Sheet metal work; building tanks
4032	12.2 Si, 0.9 Cu, 1.1 Mg, 0.9 Ni	F	C-D	D-C	B-C	55	—	Pistons
4043	5.0 Si	W	—	—	—	—	—	Welding wire
4343	7.5 Si	SW	—	—	—	—	—	Brazing sheet
5005	0.8 Mg	SWO	A-A	D-C	A-A	30	18	Appliances and architectural conductor
5050	1.4 Mg	STPO	A-A	D-C	A-A	32	21	Builder's hardware; refrigerator; coiled tubing
5052	2.5 Mg, 0.25 Cr	STBWPO	A-A	D-C	A-A	42	28	Sheet metal work; application tube; applicator
5056	5.2 Mg, 0.1 Mn, 0.10 Cr	BW	A-C	D-C	A-A	63	42	Cable sheathing; magnesium zippers
5083	4.5 Mg, 0.7 Mn, 0.15 Cr	SEBF	A-C	D-C	A-B	52	42	Unfired, welded vessels; magnesium auto and auto
5086	4.0 Mg, 0.5 Mn, 0.15 Cr	SETP	A-C	D-C	A-B	50	38	Auto and auto components; cryogenics; drilling rig; transportation equipment; components

Table 5.1 (continued)

Alloy Designation	Nominal Composition, % (Not Specified Composition)	Commercial Forms [†]	Corrosion Resistance [‡]	Comparative Characteristics					Some Applications
				Machinability [‡]	Weldability [§]	Maximum Strength [¶]	Annealed Strength		
154	3.5 Mg, 0.25 Cr	STPEBW	A-A	D-C	A-A	48	35	Welded structural tanks; pressure saltwater	
252	2.5 Mg, 0.25 Cr	S	A-A	D-C	A-A	39	28	Automobile	
356	5.0 Mg, 0.1 Mn, 0.10 Cr	W	—	—	—	—	—	Welding wire	
454	2.7 Mg, 0.8 Mn, 0.10 Cr	STPEB	A-A	D-C	A-A	44	36	Welded structural pressure service	
456	5.1 Mg, 0.8 Mn, 0.10 Cr	SEP	A-B	D-C	A	56	45	High-strength structures	
657	0.8 Mg	S	A-A	D-C	A-A	32	19	pressure applications	
653	0.7 Si, 1.3 Mg, 0.25 Cr	BW	A-B	C	B-C	42	16	Anodized appliances	
661	0.6 Si, 1.0 Mg, 0.25 Cu, 0.20 Cr	STPEBWF	A-A	B-C	A-A	45	18	Wire and rod	
663	0.4 Si, 0.7 Mg	TPE	A-A	D-C	A-A	42	13	Heavy-duty where corrosion resistance and marine furniture	
666	1.3 Si, 1.1 Mg, 1.0 Cu, 0.9 Mn	TPEBF	B-C	D-B	A-A	57	22	Pipe railings and architectural forgings and welded structures	
101	0.5 Si, 0.6 Mg	TPEB	A-B	B-C	A-B	32	14	High-strength conductors	
151	1.0 Si, 0.7 Mg, 0.25 Cr	F	A-B	C	A-B	48	—	Moderate strength forgings and auto parts	

6262	0.6 Si, 1.0 Mg, 0.25 Cu, 0.09 Cr, 0.6 Pb, 0.6 Bi	WB	A-A	B-B	58	—	Screw mach
6463	0.4 Si, 0.7 Mg	E	A-A	D-C A-A	35	22	Architectural extrusions
7001	7.4 Zn, 2.1 Cu, 3.0 Mg, 0.30 Cr	TEB	C	B D	98	32	High-strength
7072	1.0 Zn	S	A-A	D-C A-A	74	13	Fin stock
7075	5.6 Zn, 1.6 Cu, 2.5 Mg, 0.30 Cr	STEBWF	C	B D	83	33	Aircraft and structures
7079	4.3 Zn, 0.6 Cu, 0.2 Mn, 3.3 Mg, 0.20 Cr	EFS	C	B D		32	Structural aircraft
7178	6.8 Zn, 2.0 Cu, 2.7 Mg, 0.30 Cr	STEP	C	B D	88	33	Aircraft and structural

* Courtesy of the Aluminum Association, Inc.; Washington, D.C.

† B—bar or rod; E—extrusions; F—forgings or forging stock; O—foil; P—pipe; S—sheet or plate; T—tube; W—wire.

‡ Relative ratings in decreasing order of merit—A, B, C, D. Where applicable ratings for both annealed and hardest tempers are given (for exam-

§ Weldability: A—generally weldable; B—weldable with special techniques for specific applications; C—limited weldability; D—not weldable, for are welding. Gas welding and brazability ratings are the same or differ by only one; exceptions are most of the 2000 and 7000 series alloys

¶ Typical maximum tensile strength in kips per square inch, for fully work-hardened condition or heat-treated to highest strength level. (Multiply by 0.703 to convert to kilograms per square millimeter.)

‡ Typical annealed tensile strength in kips per square inch. (Multiply by 0.703 to convert to kilograms per square millimeter.)

be considered in all magnesium designs, and dissimilar metal joints must be properly and completely insulated. It is also well known that magnesium would generally be inappropriate for situations where it could be ignited. Titanium alloys have good strength-to-weight ratios, weight densities of approximately 0.16 lb/in^3 , low coefficients of thermal expansion, good resistance to crack propagation, and good corrosion resistance. Titanium is better suited to high-temperature applications than aluminum, and is often used in aircraft structures near the engines. However, titanium is also used for such ordinary temperature applications as the honeycomb core and outer skin of helicopter rotor blades. There are also several difficulties associated with titanium alloys, such as problems with formability, weldability, and continued deformation under constant loading, which is called *creep* (Ref. [14]).

Beryllium is occasionally used in spacecraft. It has a very high stiffness. A peculiar difficulty with beryllium is that particles of beryllium, and its compounds including beryllium oxide, are very toxic when inhaled (Ref. [14]). In addition to extensive information on the above materials, Ref. [14] also provides data on the various "heat-resistant alloys" that are used for elevated-temperature service. The penalty to be paid for the use of these generally nickel-based alloys is, of course, a weight penalty. For example, Hastelloy B has a weight density of 0.334 lb/in^3 , while that of Inconel X-750 is 0.300 lb/in^3 .

Woods are now very rare in modern sea, land, and aviation vehicles. However, plywood, perhaps because of its low cost, is still found on some experimental aircraft constructed away from major manufacturing plants.² Balsa wood is sometimes used as a core material for "sandwich" constructions. (A sandwich construction consists of two strong outer layers separated by a usually much thicker, lightweight, low-strength core. The core serves to increase the stiffness of the construction by providing a separation between the two load-bearing outer layers.) The ease of wood fabrication also makes wood a frequently preferred material for all manner of wind-tunnel test models, ship tow models, and recreational models whose wooden parts seldom require structural analysis. More precisely, these wooden structures often are not analyzed until a failure results in a substantial loss.

Plastics and synthetic materials of all kinds are presently proliferating to the point where it behoves an engineer responsible for a new design to be in contact with chemical companies in order to ascertain what such companies can offer for structural applications under consideration. For example, drone aircraft designs have sometimes emphasized wings made with Kevlar skins, for strength, wrapped around polystyrene for form and light weight. As of this writing, Kevlar 149 is the latest Kevlar. A different type of example is the use of energy-absorbing plastic materials to partially shield delicate instrumentation, and even structures, from the severe vibration environment of a rocket or space shuttle launch.

With epoxy as the binding agent to form a matrix within which the fibers transmit loads, glass fibers, carbon fibers, and sometimes boron fibers, are becoming increasingly more important in vehicular structural applications (Ref. [27]). These fiber-epoxy composites, often simply called composites, have the advantage that the orientation of the high-strength fibers can be arranged so as to provide strength or stiffness in any given direction according to the relative need for strength or stiffness in that direction. This is possible because the fiber composites are provided by their manufacturers in very thin, separate layers called plies. In each ply the fibers run in only one direction. Each ply is very strong in the direction in which the fibers run, and relatively weak in the other two orthogonal directions. The

² An Associated Press report of January 23, 1987, stated that the Massachusetts Institute of Technology "Eagle," an 88-lb experimental aircraft that set closed-course distance records for human powered flight, was made of "light-weight carbon fiber, polystyrene foam, plywood, plastic and synthetic cloth."

plies are stacked on top of each other, and bonded to each other, in whatever directions are best suited for carrying the load the structure is intended to bear. The complete stack is called the laminate. Composite structures are combinations of laminates, sometimes with the laminates forming a sandwich around a relatively weak core material fashioned into a honeycomb pattern.

Composites have many advantages. They can often be formed into very lightweight structures, especially when the geometry of the structure is not too complicated. Composites, relative to the commonly used metals, are particularly resistant to being damaged as a result of the application of stresses that repeatedly increase above, and then decrease below some average value.³ Composites are highly corrosion-resistant. Some of the difficulties with composites are as follows: (i) Although there have been major strides taken in the automation of the ply stacking (and filament winding) procedures, they are sometimes still costly and relatively slow, small-scale processes; (ii) special care has to be taken when joining composite structures to other types of structures; and (iii) the plies of the laminate tend to separate when subjected to small, rapidly applied (dynamic) loads, and such damage is difficult to detect. In regard to item (ii), simply drilling holes for fasteners alters the directions of the total stress at the hole edges. That would create the possibility of the total stress acting in the weakest direction of the laminate, causing fractures. Adhesive bonding of disparate materials is a matter of current research.

The higher costs of carbon composites generally exclude carbon composites from most automobile applications at present. However, the higher cost for materials is less important in aircraft and spacecraft applications where the money saved by saving weight more than offsets the cost of more expensive materials. For example, it has been estimated that each pound of structure safely removed from a large passenger aircraft is worth a few hundred dollars over the lifetime of the aircraft. A more extreme illustration of the monetary value of saving structural weight in order to permit a greater cargo weight or fuel savings is that the average cost per pound of space shuttle cargo is approximately \$10 000 as of the last year for which this information was available, 2002. These financial figures not only justify the use of expensive materials to save weight, but they also justify the use of engineering man-hours for the same purpose. If fuel costs increase significantly, then the lighter weight fiber composites may be advantageous to automobile manufacturers.

The advantages cited for each of the materials discussed above have caused those materials to be used in vehicular construction. However, the above very brief survey is sufficient to describe neither (i) all the attributes, good and bad, that must be taken into account when a material is considered by a structural engineer, nor (ii) the possible means of countering some of the disadvantages associated with a particular material. Each material is a study in itself, and the process of material selection for design is a process that involves many factors outside the scope of this text. On the other hand, the mechanical behavior and mathematical description of all these materials have many common features that allow a unified approach to the analysis of structural bodies composed of such structural materials. After further general descriptions, the emphasis of this text will rest upon this common, but limited, mathematical description of material behavior.

The mechanical behavior of a material is ascertained by applying various loadings (stresses) and measuring the deformations (strains). In order to begin as simply as possible, until otherwise specified, the discussion is limited to materials that are *homogeneous*, that is, that have the same mechanical and thermal properties at every point within the

³ This form of damage, called *fatigue damage*, is discussed in Section 5.5.

structural body.⁴ An example of a nonhomogeneous material is a metal that is homogeneous when at room temperature, but now has large temperature differences throughout its volume. As is seen below, the mechanical properties of metals vary with large temperature variations. Thus the mechanical properties of this metal body would vary from point to point within the volume of the body in accordance with the temperature variation.

Materials that are routinely approximated as being homogeneous can have different mechanical and thermal properties in the different directions that are parallel and perpendicular to their grains. Small directional material differences can even exist for thin metal structural elements that are rolled or extruded as part of their manufacturing process. Rolling is a strengthening process whereby the metal is forced to move between large, oppositely rotating cylinders. Extrusion is the process of forcing metal through a die, much like forcing toothpaste from a tube.

In five of the next six sections of this chapter, general background descriptions are provided on the behavior of engineering materials in response to mechanical and thermal loadings. Metals, and fiber composites where the fibers all run in just one direction, are generally the only two types of materials considered in these discussions. The final section deals with simplified mathematical models for the behavior of these engineering materials.

5.2 The Tensile Test

To begin the discussion of the mechanical response of materials to mechanical loadings, consider firstly what is perhaps the simplest type of loading, which is a uniform tensile load. Uniform tensile loads, as well as other loadings, are applied to material samples by specially designed machines called testing machines; see Fig. 5.1. The material samples used for tensile testing are generally machined in the form of either (i) a polished short rod where the central portion of its length, called the test section, has a uniform circular cross-section, or (ii) in the case of metal sheet or composite laminate samples, a short strip with a centrally located test section where again there is a uniform cross-section, see Figs. 5.2(a, b). These rods and strips are thicker at their ends to avoid failures where the testing machine grips the rods. The testing machine itself measures the load applied to the sample, usually by the direct measurement of a calibrated displacement of a machine component, or, generally in older machines, by a weight balance mechanism involving multiple levers. The mechanical (deformation) response of the test specimen, that is, the longitudinal stretching of the test section, can be measured by use of one or more strain gauges or a spring-loaded device called an extensometer that directly measures changes in length.

As previously explained, the load per unit area (i.e., stress) is the significant load measure for material behavior. Since stress is force divided by area, and since the stretching of the tensile specimen reduces the cross-sectional area of the test specimen (a phenomenon easily observed by stretching a rubber band), the question arises as to which area should be used to calculate the stress: the original (undeformed) area or the instantaneous (deformed) area? When stress was first defined in Chapter 1, the area used was the area of the loaded

⁴ It is often best not to be too fastidious about homogeneity. For example, because of the difference between winter and summer growth rings, wood is not perfectly homogeneous. However, if the structure's dimensions are much larger than the distances between the growth rings, the mathematical simplifications that are possible by regarding the wood as homogeneous more than offset the very slight inaccuracies embodied in that assumption. In the same vein, structural elements manufactured from modern fibers (glass, carbon, boron, Kevlars, etc.) embedded in a bonding material are also regarded as homogeneous when analyzing the structural element as a whole when the dimensions of the structural element are much greater than the diameters of the fibers or the distances between fibers.

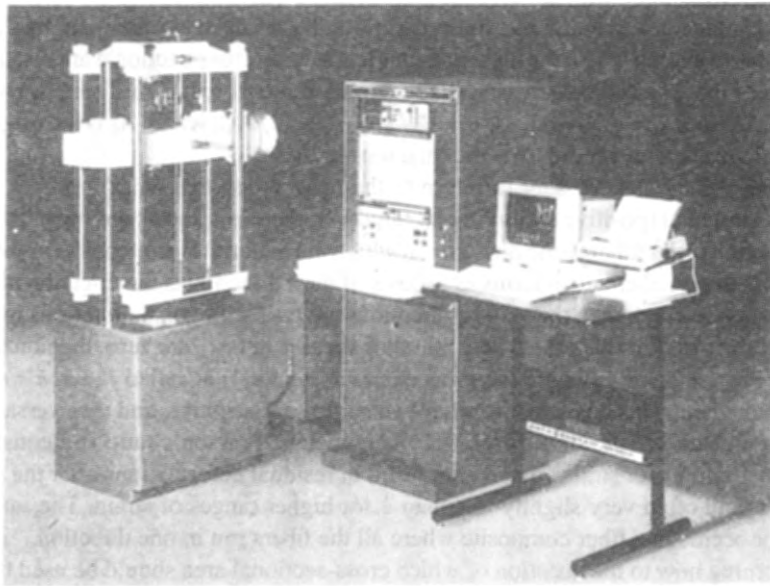
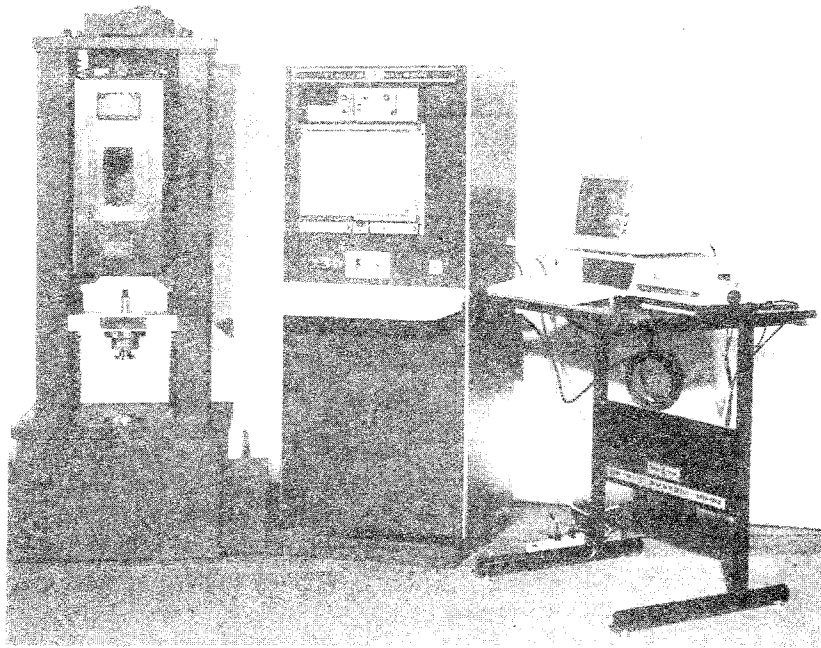


Figure 5.1. Universal testing machines. Courtesy of Tinius Olsen Testing Machine Co., Inc., Willow Grove, Pennsylvania.

rectangular parallelepiped, which is the instantaneous area of the deformed material. On the other hand, the longitudinal stretching of the test specimen is best characterized by use of strains, and strains were defined in Chapter 3 by reference to the lengths of the original, undeformed rectangular parallelepiped. Hence, stress and strain, as developed to this point, have different bases. In order to pursue further the difference in the stress definition based

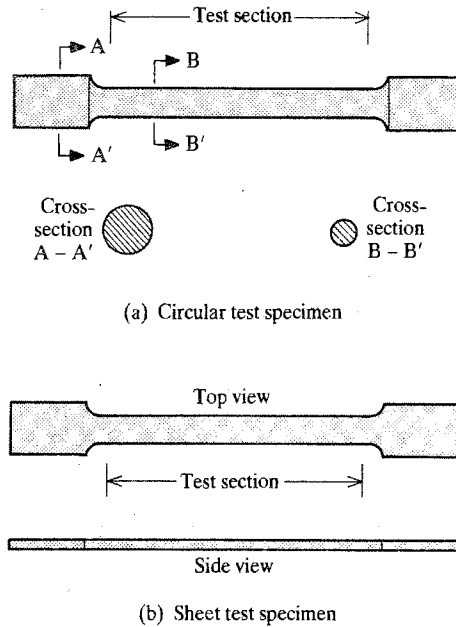


Figure 5.2. Common test specimen configurations for metals.

upon instantaneous area and the strain definition based upon original lengths, consider a tensile test specimen where the instantaneous test section cross-sectional area is, of course, a function of the longitudinal stress. Call the cross-sectional area $A(\sigma)$. Then, by the previous stress definition, $\sigma = N/A(\sigma)$, or $\sigma = (N/A_0)/[A(\sigma)/A_0]$, where A_0 is the original cross-sectional area, and as before, N is the total tensile force.

At this point it is necessary to return to the observation that when a rubber band, or a metal is stretched (positive strain) in one direction, there is a shrinkage (negative strain) in any direction orthogonal to the direction in which the material is stretched. This observation can be put into mathematical terms as follows. If the x direction is the direction in which the material is stretched, then the y and z directions are two orthogonal directions in which the material shrinks. For this case where all other stresses but σ_{xx} are zero, the nonzero strains are $\epsilon_{yy} = \epsilon_{zz} = -\nu\epsilon_{xx}$, where the proportionality factor, ν is called *Poisson's ratio*. Note again that when ϵ_{xx} is positive, the other two strains are negative, and vice versa. Poisson's ratio⁵ is a characteristic of a metal. For many metals, Poisson's ratio is a constant (often between $\frac{1}{4}$ and $\frac{1}{3}$) for strains that do not result in residual deformations after the removal of all loads, and often very slightly less than $\frac{1}{2}$ for higher ranges of strain. The same general behavior occurs in a fiber composite where all the fibers run in one direction.

Returning now to the question of which cross-sectional area should be used to calculate the stress acting on the test specimen, consider the ratio $A(\sigma)/A_0$, which is an inverse factor in the relation between the stress, σ , as defined in Chapter 1 and the stress referenced to the fixed value of the original cross-sectional area, N/A_0 . For ease of discussion only, let the test cross-section be originally circular. When the test specimen is longitudinally stretched, the cross-section will contract in equal amounts in all directions to remain circular. If the quantity r_0 is the radius of the undeformed cross-section of the test specimen, and $r(\sigma)$ is the

⁵ Simeon Denis Poisson (1781–1840), French mathematician and scientist (Ref. [2]).

radius as the specimen is stretched, then, using the change in length over the original length definition, the lateral strain in the cross-section in any direction is the negative number $\{[r(\sigma)/r_0] - 1\}$. Substituting $(-\nu\epsilon_{xx})$ for the lateral strain in the cross-section, and solving for $[r(\sigma)/r_0]$ leads to the relation $[r(\sigma)/r_0] = (1 - \nu\epsilon_{xx})$. Since the ratio of the instantaneous to original cross-sectional areas, $A(\sigma)/A_0$, is equal to the square of $[r(\sigma)/r_0]$, then

$$\frac{A(\sigma)}{A_0} = (1 - \nu\epsilon_{xx})^2 = 1 - 2\nu\epsilon_{xx} + \nu^2\epsilon_{xx}^2 \quad (5.1)$$

For structural materials, the longitudinal strain ϵ_{xx} is always a small quantity. Almost all vehicular structures are designed so that the strains will be less than approximately 0.002 because, as will be seen below, for strains beyond that approximate value, a small percentage change in the loading can result in a large percentage change in the deformation. Thus, in the circumstance where the strain is limited to a maximum value of 0.002, the difference between $A(\sigma)$ and A_0 is a little more than one-tenth of one percent. Thus, as a practical matter, it makes very little difference which area is used to calculate stresses. The simplification of using the original area to calculate stresses is now adopted. For metals and fiber composites, the error involved with this simplification is less than the usual experimental error, and is wholly consistent with the one previous simplification of discarding the nonlinear portions of the strain expressions.

The stress-strain results of typical tensile tests⁶ are shown in Figs. 5.3(a, b). Note that in both cases, the initial portion of the stress-strain curve is linear. At the end of the linear portion there is a sharp change in direction (called the knee of the curve) followed by a much more gradual increase in stress with changes in strain until a maximum stress value is reached. This maximum value is called the *ultimate stress*. After the ultimate stress is reached, the curve descends to its end point, which is where the specimen pulls apart (rupture). The stress used to plot these two curves is, again, based on the original cross-sectional area of the test specimen. If the true stress, which is based on the instantaneous area, were used, then the stress-strain curve would not descend from a maximum value, but continue to rise to the point where rupture occurs. If the material stress-strain curve has a zero tangent that occurs before the ultimate stress, as is the case in Fig. 5.3(a), the stress value where that first zero tangent occurs is called the *yield stress*. A further understanding of this first type of stress-strain curve can be had by viewing Fig. 5.4(a), which shows a specific instance of both the first and second types of stress-strain curves plus a stress-strain curve that lies between the two extreme types. Note that all three of these curves are for the same AISI 4340 steel alloy, but for different manufacturing heat treatments (tempers). The three different variations of the same material are distinguished by the values of their ultimate stress.⁷ The advantage of the temper with the lower ultimate stress is that such materials generally have greater *ductility*, that is, they can undergo greater deformation before failure. Greater ductility provides a greater warning of an overloaded structure, and is an advantage that metals generally have in comparison to other structural materials like wood and fiber composites. For example, the reader would justifiably hesitate to board an

⁶ In order to have a common basis for tensile tests, and for many other types of tests, standard test procedures have been established by the American Society for Testing and Materials. For example, the standard for tensile tests is ASTM E8.

⁷ In general, steels with high values of ultimate stress are called "hard," while those with low values are called "soft." A reason for this terminology is that there is a positive correlation between the measured hardness (i.e., the resistance to penetration by standard devices) and the ultimate stress. This correlation, along with a hardness test, can be used to estimate the ultimate stress, and hence other characteristics, of the steel.

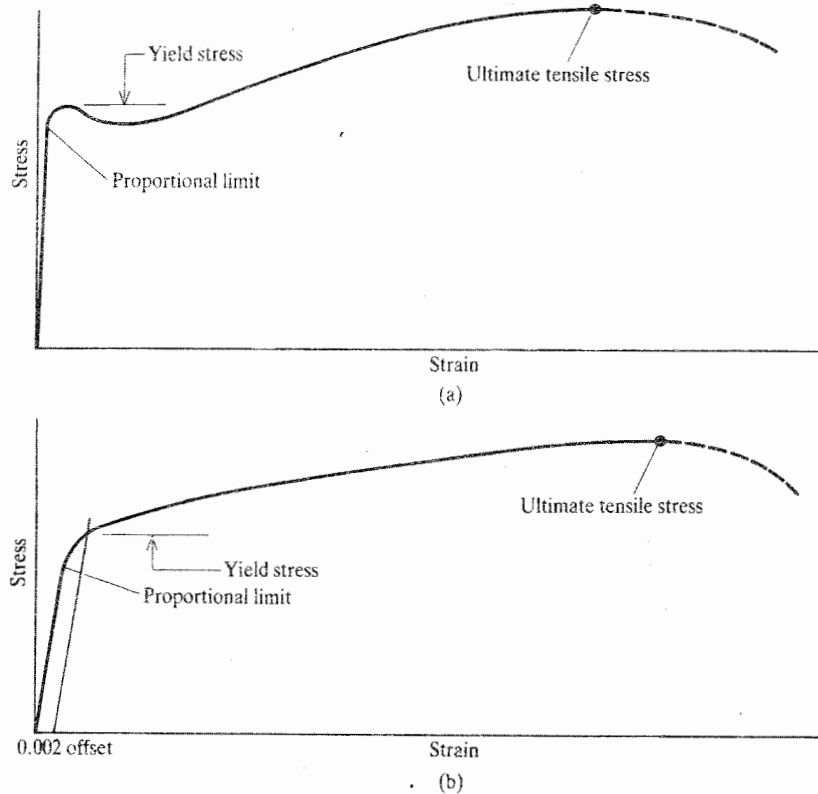


Figure 5.3. Typical stress–strain plots from MIL-HDBK-5. (a) A material having a definite yield point such as some steels. (b) A material not having a definite yield point such as aluminum alloys, some magnesium alloys, and some steels. Note that MIL-HDBK-5, which was free to the public, has been superseded by MMPDS-OZ, a quite expensive, copyrighted document. Hence this textbook utilizes the still representative material of MIL-HDBK-5.

aircraft whose ductile metal wings were bent out of shape. The tensile test strain at rupture converted to a percentage ($0.01 \text{ in/in} = 1 \text{ percent}$) is the primary measure of ductility, and it is called the *percent elongation*.

Even when there is no zero tangent line for the stress–strain curve before the ultimate stress, as is the case in Fig. 5.3(b), it is still desirable to have a measure for the point where the changes in strain become large for relatively small changes in stress. Hence the definition of the *offset yield stress* as the stress value at the point on the stress–strain curve where that curve is intersected by a straight line that is parallel to the stress–strain curve at its origin but is offset from the origin by a strain value of 0.002. Figure 5.3(b) illustrates the offset line. The point on the stress–strain curve at which the straight line portion is no longer straight (linear) is called the *proportional limit*. For many materials, particularly aluminum, it is difficult to decide where linearity stops and nonlinearity begins. In these instances, an intersecting offset line originating at a strain value of 0.0001 and, as before, parallel to the stress–strain curve at the origin, is used to define the *offset proportional limit*. The slope of the linear portion of the stress–strain curve has special importance. It is called *Young's modulus*, or the *modulus of elasticity*. Beyond the linear portion, the slope of the stress–strain curve is called the *tangent modulus of elasticity*. The slope of the line drawn

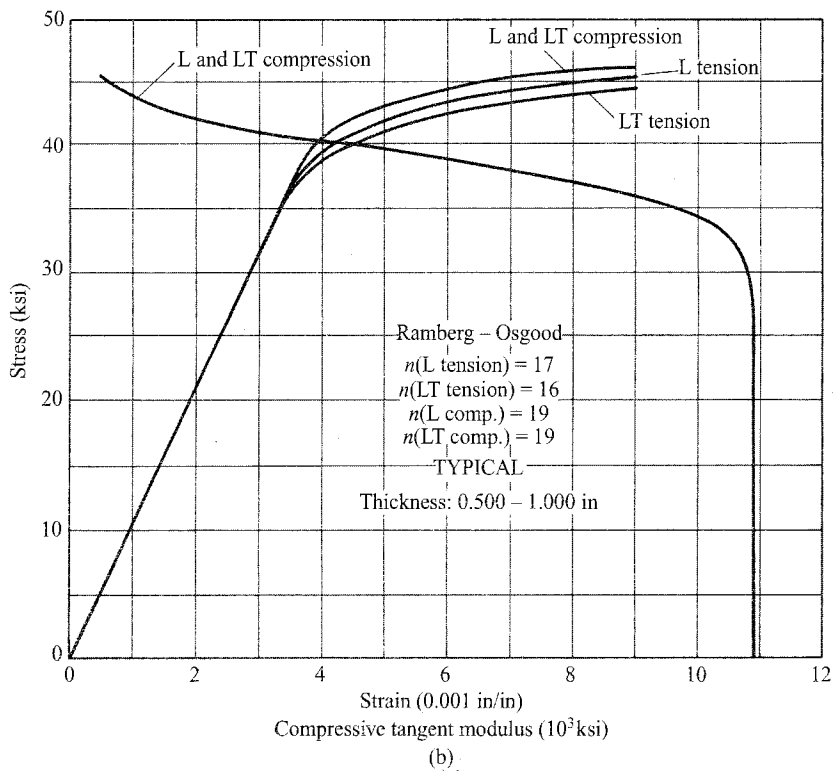
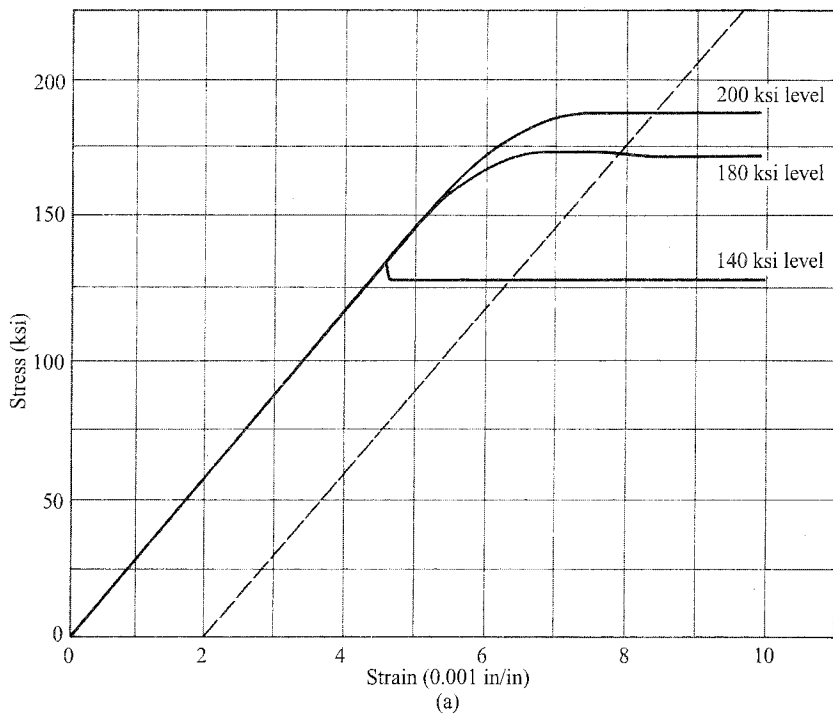


Figure 5.4. (a) Typical stress-strain curves at room temperature for heat treated AISI 4340 alloy steel, all products, from MIL-HDBK-5D. (b) Typical tensile and compressive stress-strain and compressive tangent modulus curves for 2024-T42 aluminum alloy plate at room temperature, from MIL-HDBK-5D.

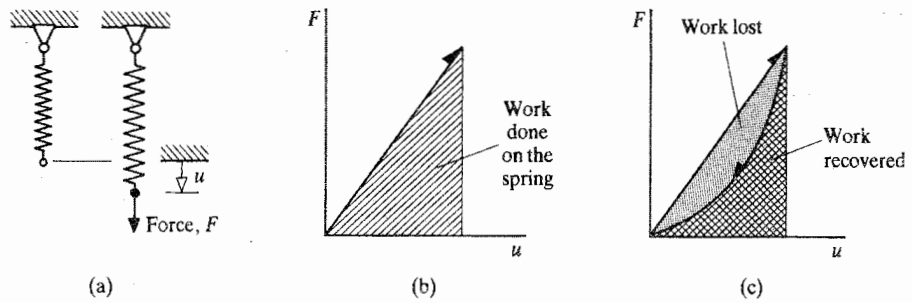


Figure 5.5. Force–displacement diagrams for a helical spring.

from the origin to any point beyond the proportional limit is called the *secant modulus of elasticity*. These three moduli are symbolized by E , E_t , and E_s , respectively. Since Young's modulus is the slope for the straight line or linear region, then for this simple one-directional loading case, $\sigma = E\epsilon$. This equation is the beginning of the present process of relating stress to strain, and is called *Hooke's law*.⁸

If the tensile test is interrupted, and the specimen is unloaded, the line on the stress–strain plot that represents the unloading has differing positions depending on the point where the loading was stopped and reversed. If the interruption occurs before a point on the stress–strain curve called the *elastic limit*, which usually very nearly coincides with the proportional limit, then the unloading curve is so nearly the same as the linear portion of the loading curve that the two curves are regarded as being the same. To elaborate on this matter, recall that work is defined as the integral of the product of force multiplied by the differential of distance in the same direction as the force. Also recall that work, when stored, is energy. For example, consider the steel coiled spring that is loaded and unloaded as shown in Fig. 5.5(a), where one end of the spring is fixed against motion. A force–displacement plot of the force that displaces the free end of the coiled spring versus the displacement at that free end is a straight line over a large range of displacements; see Fig. 5.5(b). The area under that line represents the integral of the force as a function of displacement. Thus the area under the straight line is both the work done by the force on the spring and, since the stresses in the coils of the spring do not exceed the elastic limit, the energy stored in this spring. In that circumstance, when the force at the free end of the coiled spring is reduced, the unloading path on the force–displacement diagram lies on top of the loading path, and all the work stored in the spring is recovered. If, however, the spring material characteristics are altered so that the force applied to the spring is reduced to zero along with the corresponding displacements in a way that defines the curved path shown in Fig. 5.5(c), then the work recovered would be represented by the area under the curved path. The area between the straight path and the curved path represents the work lost.

The point of this discussion is that all the above remarks regarding force–displacement plots also apply to stress–strain plots because the product of stress and strain is work per unit volume. That is, force over area multiplied by change in length over length equals, in rearranged form, force multiplied by change in length divided by the product of area

⁸ Robert Hooke (1635–1703), English experimentalist, established the linear relationship between the magnitude of the forces acting upon engineering materials and the deformations that those forces produce in 1678 (Ref. [2]). Thomas Young (1773–1829), English philosopher (Ref. [71]).

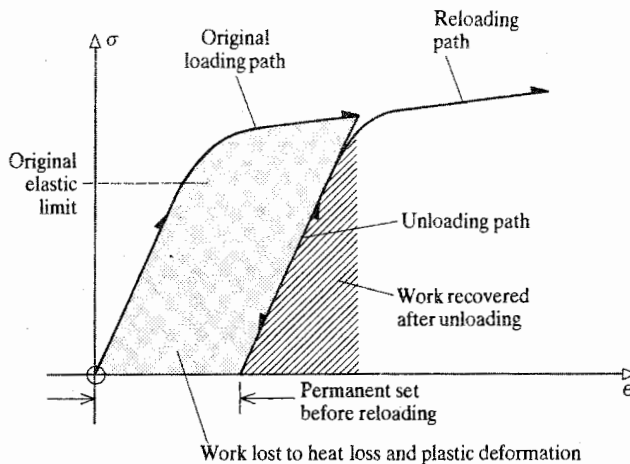


Figure 5.6. A typical unloading and reloading stress–strain plot.

and a perpendicular length (i.e., divided by volume). Hence, if, on the stress–strain diagram, the unloading path is exactly the same as the loading path, then no work per unit volume is lost. In that circumstance the material is called *elastic*. As stated above, this is very nearly the case for engineering alloys when unloading is started at or before the elastic limit. The actual very small differences between the two paths in most engineering materials are easily ignored over the course of a single loading–unloading cycle. Over many cycles, the small differences between the two paths would add up to become a quantity of work lost that would be detectable. In a vacuum, the work lost would be due to internal friction. When the work lost to internal friction is appreciable, the material is said to possess *material damping*. The energy dissipation caused by material damping, and other types of damping such as aerodynamic drag, is the reason why force-free vibrations diminish over time.

If the unloading occurs beyond the elastic limit, which again is very much the same as the proportional limit in almost all metals, the unloading path is not nearly the same as the loading path. Beyond the elastic limit, the unloading path for metals is a straight line starting at the unloading point and running parallel to the loading curve at the origin; see Fig. 5.6. It is not possible to return along the loading path while unloading past the elastic limit. Again, the area between the loading and unloading curves represents the work lost. In this case the work lost goes into producing a residual deformation and into heat generation. Since “plastic” is the opposite of elastic, and since there is some energy recovery as well as energy loss, the deformations beyond the elastic limit are called *elasto–plastic*. The energy lost through heat generation can be sufficient to burn the hand of the person who touches a ductile test specimen undergoing ample plastic deformation. The unloading curve intersects the zero-stress line at a nonzero value of strain that is called the *permanent set* since that deformation will persist in the absence of further loading. If the specimen is reloaded in tension, the reloading path has the same linear slope as it originally had, but of course it starts at the previous permanent set. However, this time the yield point is such that the reloading curve smoothly meshes with what would have been the stress–strain curve if there had been no unloading. The occurrence of a higher yield point after initial straining is called *strain hardening*.

5.3 Compression and Shear Tests

A compression test is much like a tensile test except that care must be taken to prevent the buckling of the test specimen. The prevention of buckling can be accomplished by either of two ways. The first way is, if possible, to use a rather thick test specimen. The second way is to supply adequate lateral support that does not interfere with the application of the compressive load by creating excessive friction in the loading direction. This second approach would be necessary in the case of the compressive loading of thin sheets. The required lateral support is often supplied by a series of small rollers positioned along the length of the thin sheet on both sides of the sheet.

The compressive stress–strain curves look exactly like the tensile stress–strain curves with the one exception that for ductile materials there is no compressive ultimate stress as there is in the case of tension. That is, in compression of a ductile material there is only a continuing flattening of the specimen. The ultimate compressive stress for ductile materials is arbitrarily assigned the same numerical value as the ultimate tensile stress. A *brittle* material, one that deforms very little before failure, will experience a shear-induced rupture along a plane that is approximately at 45° to the longitudinal axis of the specimen. The compressive Young's modulus, E_c , is sometimes slightly different from the tensile modulus, and the same is true for the two yield points. Figure 5.4(b) shows an overlay of typical tension and compression stress–strain curves for 2024-T42 aluminum alloy plate, as taken from Ref. [14]. In Fig. 5.4(b) the L designation stands for “longitudinal,” which means in the rolled direction, that is, in the direction in which the plate was moved through heavy cylindrical rollers. The “long transverse” direction, designated as LT, is perpendicular to both the longitudinal direction and the direction through the thickness of the plate.

Consider a test specimen that is first loaded in tension beyond the elastic limit, and then unloaded beyond the zero stress point so as to be loaded in compression. Let the compressive loading be extended beyond the point where this tensile unloading (compressive loading) line of the stress–strain diagram is no longer straight; see Fig. 5.7. Then, in general, the linear portion of this unloading–loading line does not extend on the compression side as far as it would if there had not at first been a tensile loading beyond the tensile elastic limit. The same is true if the loading is compression first and then tension. This shortening of the linear and elastic portion of the stress–strain curve in the opposite loading field is called the *Bauschinger effect* (Refs. [7, 8]). If the loading in the opposite field is continued, the loading path tends to meld with what, as shown by the dashed line in Fig. 5.7, would have been the loading path without having first had the oppositely directed loading. If the compressive loading is then unloaded and tension is reapplied so as to form a complete

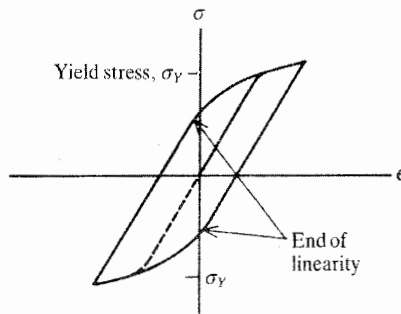


Figure 5.7. A hysteresis loop showing the Bauschinger effect.

cycle, then the closed curve is called a *hysteresis loop*. The area inside the hysteresis loop represents the work required to accomplish the loop of elasto-plastic deformations plus the work lost through heat generation.

The stress-strain curve for shear loading has the same shape as that for tensile and compressive loading. However, all the material characteristics for shear have lower values than the corresponding values for tension or compression. The only difference in names is that the slope of the linear portion of the shearing stress-strain curve is called the *shear modulus*, or the *modulus of rigidity*. There is no modern justification for the latter name.

At this point it is worth remembering that all material mechanical and thermal characteristics are determined by experiment, and all experiments have an associated error. Furthermore, no two material samples are exactly alike. As a means for reducing the error in the determination of the material's properties, tests are repeated numerous times and the test results are treated statistically to arrive at the values reported for the material's properties. In Ref. [14], referred to informally as "Mil Handbook Five," metal material properties are reported for uniform use by government contractors either as typical values or on one or more of three alphabetically named bases, A, B, or S. Quoting extensively from Mil Handbook Five, the "*typical* property value is an average value, (with) no statistical assurance being associated with it." An *A basis* value is one where "at least 99 percent of the population of values is expected to equal or exceed the A basis mechanical property allowable, with a confidence of 95 percent." A *B basis* value is one where "at least 90 percent of the population of values is expected to equal or exceed the B basis mechanical property allowable, with a confidence of 95 percent." Since fewer test results exceed the B basis value compared to the A basis value, B basis values are numerically greater than A basis values. The use of B basis values in design work for government agencies, instead of A or S values, is limited by these agencies. Reference [16] states that "in general, B values are permitted in multi-load-path structures, wherein the failure of one member will cause a transfer of load to the remaining members and no catastrophic failure will result." Quoting again from Mil Handbook Five, "the *S basis* mechanical property allowable is the minimum value specified by the appropriate Federal, Military, or SAE Aerospace Material specification for the material. The statistical assurance associated with this value is not known.

5.4 Safety Factors

One of two approaches is taken when using customer stipulated or industry standard material strength properties in an analysis of a design. The first approach is to reduce the material strength values, such as yield stresses and ultimate stresses, by dividing those material strength properties by what is called a *safety factor*, or *factor of safety*. The second approach is to multiply the estimated loads the structure must bear by the same selected safety factor. Both approaches produce exactly the same result when the analysis is linear, that is, when the differential equations that are the direct or indirect basis of the analysis are linear equations. The two approaches differ only when the analysis includes nonlinear effects.

The purpose of safety factors is to make an allowance for uncertainties. For example, since the loads that act upon a vehicle are never standard, but depend on the vehicle design, the best estimates of the magnitudes of the worst-case loads may be somewhat inadequate. It is often difficult to decide what are reasonable applied load magnitudes for a given design analysis. If the applied loads are overestimated, the vehicle must then be overdesigned, that is, made too heavy and costly to be competitive. If the design loads are underestimated, the vehicle may fail structurally when attempting to be competitive. A factor of safety,

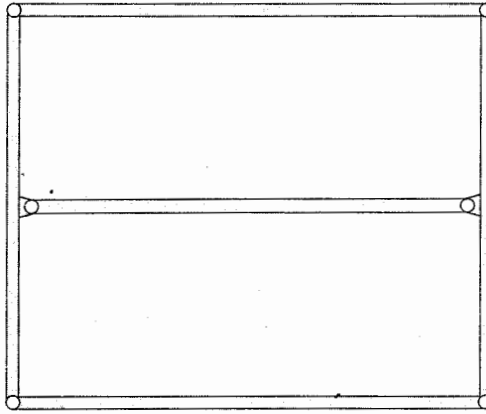


Figure 5.8. Five beams arranged to illustrate the possibility of an initial stress.

usually chosen on the basis of previous experience with similar vehicles, provides a margin for error on the less catastrophic side of avoiding a structural failure. A factor of safety is also useful for covering the possibility of unforeseen combinations of mechanical loadings, temperature changes, environmental degradations, manufacturing defects, and that very small percentage of materials that are below standard strength requirements.

To elaborate on the item of manufacturing defects, note that the geometry of the structure assumed by the analysis may differ somewhat from the actual geometry of the manufactured vehicle. Geometric irregularities, such as beam flanges and webs never being quite flat, beam axes never being quite straight, and so on, almost never have any significant effect when the flanges, webs, axes, and so on, are within manufacturing tolerances. However, to illustrate simply how imperfect geometries can induce possibly substantial, yet sometimes unaccounted for stresses in a structure, consider a structure of five identical straight beams divided into a group of three in parallel and a pair in parallel. Let the three beams be perpendicular to the pair in such a manner that the three beams connect the two ends and centers of the pair of beams so that the four outer beams form a square. See Fig. 5.8. Now, to make the point about off-nominal geometries, let the five beams be disconnected and let the middle beam be increased in length as a result of being miscut. Force the reassembly of the five beams into their original positions in this square "theta" shape. When reconnected, the longer middle beam would bend the outer pair of beams perpendicular to it, and stretch the pair parallel to it. In turn, the other four beams would compress the middle beam. Thus, before any obvious external loads were applied to this system of five beams, there would, as a result of the miscut middle beam length, be initial stresses within each of the five beams. These initial stresses could combine with those induced by the applied loading to produce an unexpected failure if no factor of safety were used to guard against this type of possibility. A quantitative approach to initial/residual stresses for a simple structure is presented in Endnote (1).

In the aerospace industry, the usual practice is to apply factors of safety so as to increase the best estimates for the worst-case loads. Two different multiplicative factors of safety are often used. The product of the *limit load factor* and the worst-case loads is used to develop "limit loads" whose corresponding stresses are required to be less than the yield stresses. The product of the *ultimate load factor*, traditionally 1.5, and the worst case loads is used to develop "ultimate loads" whose corresponding stresses are required to be less than the ultimate stresses. The *margin of safety* is a term used to describe quantitatively

the difference between the calculated stresses and the allowable stresses for each of the above sets of loads. Its precise definition, for both the stresses of the limit load case and the stresses of the ultimate load case, is

$$\text{Margin of safety} = \frac{\text{allowable stress} - \text{calculated stress}}{\text{calculated stress}}$$

A good design has small, positive margins of safety, negative margins of safety mean going back to the drawing board/computer screen.

5.5 Factors Other than Stress That Affect Material Behavior

The previous discussion is limited to the situation where the loading occurs at room temperature and at slow or moderate loading rates. Considering these factors in reverse order, the loading rate is proportional to stress rate, and stress rate is related to strain rate via the tangent modulus as determined by the stress–strain curve. Of these three rates of change with respect to time, strain rate is the one most often referenced. Test strain rates for the determination of material properties are generally between 0.001 and 0.010 rad/min. In the opinion of Ref. [14], the material test values obtained from such tests can be considered valid up to a strain rate of 0.010 rad/sec. At faster strain rates, there can be a significant effect on such properties as ultimate tensile strength, and ductility. For example, the ultimate tensile strength can nearly double at the strain rates that accompany explosions, and ductility can sharply decrease at such explosion-related strain rates.

Temperature changes, and the duration of exposure to temperature changes, can have a strong effect on material properties. Generally, increases in temperature and increases in the duration of exposure to elevated temperatures result in degraded material strength and stiffness properties in metals. Large temperature increases above room temperature can produce dramatic decreases in strength. Temperatures lower than room temperature generally produce small increases in strength properties while reducing ductility. Figure 5.9 from Mil Handbook Five illustrates the effect of temperature change and time of exposure to higher temperature on the tensile yield stress for certain 7075 aluminum alloys. It is absolutely necessary that the pertinent material properties used in any design or analysis correspond to the anticipated temperature conditions.

Temperature changes have another important effect on engineering material performance. Although they may closely approximate one or the other, all real materials are neither perfect solids nor perfect fluids. (A perfect solid is a material that has infinite viscosity, while a perfect fluid is a material that has zero viscosity.) The reader himself or herself can conduct the following simple experiment that illustrates a flow characteristic of a familiar, seemingly solid, material at room temperature. Take a rubber band and cut the band so that the result is one long piece of rubber. Fasten one end to an immovable object, and then fasten a small weight to the other end of the rubber string. Let the weight be large enough to produce an easily observable deflection at the end of the rubber string. As the reader knows, the rubber string will stretch a certain amount, and seemingly stop stretching. Either measure the length of the rubber string, or better yet, mark the deflection of the weight. Then, after a week or two, remeasure the length of the rubber string or note the new position of the weight relative to the original mark. It will be seen that the solid rubber string will have stretched further than it did initially even in this absence of an additional loading. Eventually the rubber string will rupture. From an engineering point of view, the rubber has exhibited a certain viscosity, and structural engineers call this stretching (continued deformation) under constant loading conditions by the name *creep*.

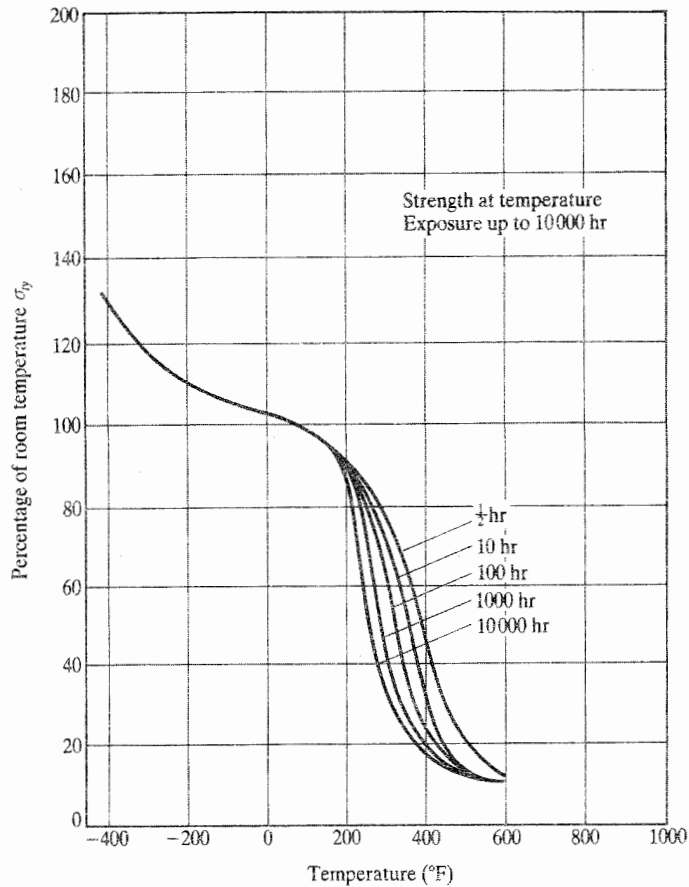


Figure 5.9. The effect of temperature on the tensile yield stress of 7075-T6, T651, T6510, and T6511 aluminum alloy, all products, from MIL-HDBK-5D.

At room temperature, and at stresses below their yield stress, most metals such as steel and aluminum have so much viscosity that their fluid characteristics can be completely ignored. (The same may not be true for some titanium alloys.) However, the viscosity of metals and other materials decreases sharply with temperature to the point where at high temperature a metal begins to plainly exhibit the characteristics of a viscous fluid as well as those of an elastic solid. Under these circumstances, metals and other materials are called *viscoelastic*, and the study of mostly solid materials for which both the elastic and viscous properties are important is called *viscoelasticity*. Certain rocket fuels (even at room temperature) are examples of linear or nearly linear viscoelastic materials. The term “linear,” as well as “nonlinear,” refers to the mathematical equations used to describe the material behavior (strain) in response to stress, and perhaps stress rate. Unfortunately for the comfort of analysts, metals at higher temperatures are nonlinearly viscoelastic, and thus their viscoelastic equations are difficult to solve. Therefore, the usual engineering approach taken to the situation where metals at higher temperatures continue to deform (i.e., creep), even at constant loadings, is to work with a creep strain rate (i.e., a time rate of change of the total strain). Under the conditions of a uniaxial load and constant temperature, strain rates for creep can be treated as constants over much of the time to rupture; see Fig. 5.10.

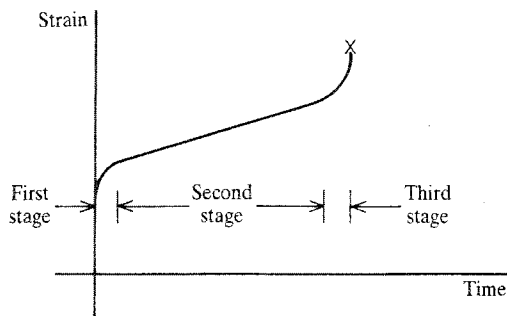


Figure 5.10. A typical creep diagram.

However, when the loading is not uniaxial and the temperature is not constant, there may be “difficulties in extrapolating from the simple to complex stress–temperature–time conditions (Ref. [14]).”

In the above discussion, time is an implicit variable in material performance because strain rates can affect material properties, and from the creep viewpoint a creep strain rate is a (temperature-dependent) material property. Time is also an explicit variable of material performance. One example of where time itself enters into the prediction of material performance is in the decrease in strength and stiffness properties with increasing time of exposure to higher temperatures. Another compelling example where a quantity directly related to a time of exposure is a direct factor in material performance occurs when the material loading is repeatedly cycled between high and low load values. For vehicular structures in particular, it is important to note that at tensile stress values significantly less than the static⁹ tensile yield stress value, a material can rupture as a result of cyclic loading. If the number of tensile, or partially tensile, load cycles is very large, say ten million, it is quite possible to have rupture when the high tensile stress value in the cycle is only one-quarter, or less, of the tensile yield stress. If the test specimen or structure has sharp notches perpendicular to the direction of loading, the nominal maximum tensile stress value that will produce a failure after, say, one million cycles can even be less than one-fifth the static tensile yield stress. (The effect of geometric irregularities, such as notches and even circular holes is briefly discussed in the paragraph after next in relation to theoretical elastic stress concentration factors.) The damage done by repeated loading cycles is called *fatigue damage*, or simply *fatigue*. The number of cycles to fatigue failure is called the *fatigue life*, which of course can be converted to the number of operating hours for a vehicular structure before an anticipated fatigue failure.¹⁰ Fatigue damage occurs only when at least some part of the loading cycle produces tensile stresses. The tensile stresses tend to increase the size of cracks that are present as a result of the manufacturing process,

⁹ Here “static” refers to the usual low-valued, test strain rates referred to previously.

¹⁰ The importance and complexity of the fatigue problem is illustrated for example by a newspaper report (*Washington Post*, October 11, 1985, p. A3) that the \$18.7 million F-18 jet fighter jointly produced by McDonnell Douglas Corp. and Northrop Corp., which was designed to have a fatigue life of 6000 flight hours, may have only a fatigue life of 2000 hours as indicated by an early test failure of the wing carry-through, structure as it was then designed. Similar reassessments of the fatigue lives of the military aircraft of many other manufacturers has also occurred. A July 24, 1991 article offers an appreciation of the costs that can be associated with wing fatigue problems. This article states that the U.S. Air Force estimates that repairs to the General Dynamics F-16 wing–fuselage junctions will cost more than \$250 million.

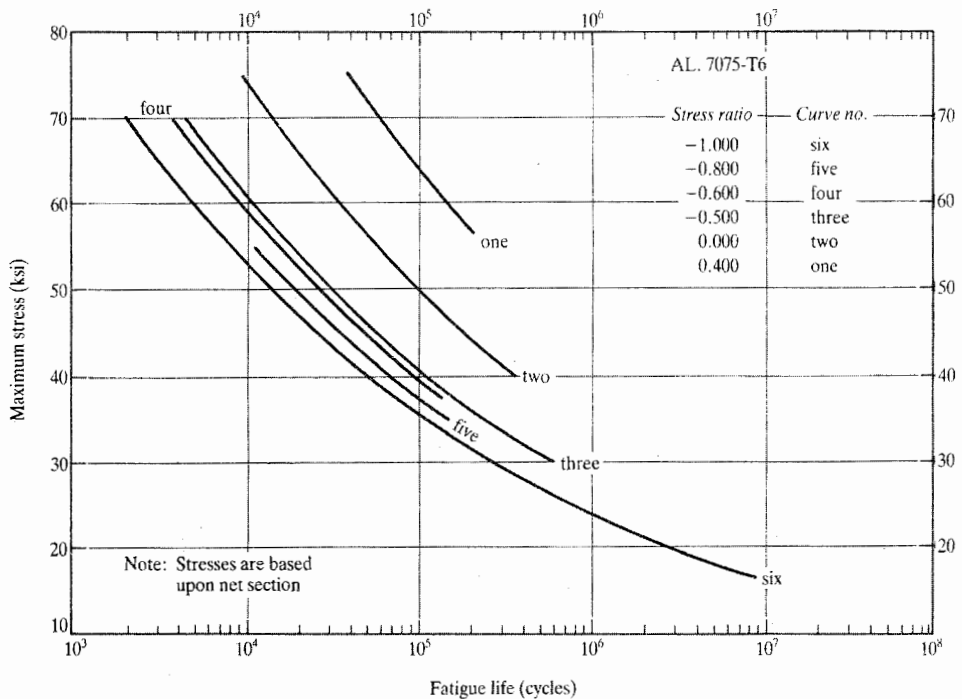


Figure 5.11. S - N curves for unnotched 7075-T6 bare, electropolished, aluminum alloy sheet (0.090 in thick), longitudinal direction, at room temperature in air. The stress ratio (R) is the ratio of the algebraic value of the minimum stress to the value of the maximum (tensile) stress. These are best fit curves, with half of the scattered data points for each curve above the curve, while the other half of the data points lie below the curve. Source: MIL-HDBK-5D.

or arise due to surface dents and scratches, or slippages aligned with the maximum shearing stresses.

Figures 5.11 and 5.12, which are from Mil Handbook Five, illustrate the usual manner in which fatigue test data are presented. Diagrams like Fig. 5.11 are called S - N diagrams, where S is for stress, and N is for number of cycles. Those like Fig. 5.12 are called constant life diagrams. Figures 5.11 and 5.12 contain the same type of information in different formats. In these illustrations, the stress ratio R is the ratio of the minimum stress to the maximum stress of the stress cycle. As usual, compressive stresses are identified as negative quantities. One half of the difference between the maximum and minimum stresses is called the alternating stress value. The average of the maximum and minimum stress values is called the mean stress value. Thus the mean and alternating pair of stress values contain exactly the same information as the maximum and minimum stress values. The quantity A in Fig. 5.12 is the ratio of the alternating stress to the mean stress. The quantity K_t is the theoretical elastic stress concentration factor. The circumstances of this latter quantity are of sufficient importance to merit digressing in order to offer an explanation.

Consider a very wide, flat metal tensile specimen with a small, circular hole in its center as shown in Fig. 5.13(a). In the absence of the hole, the specimen is in a state of uniaxial tensile stress. It can be proved (Ref. [21]) that the presence of the hole only disturbs the uniaxial stress pattern near the hole itself. Consider the stresses in the direction of loading

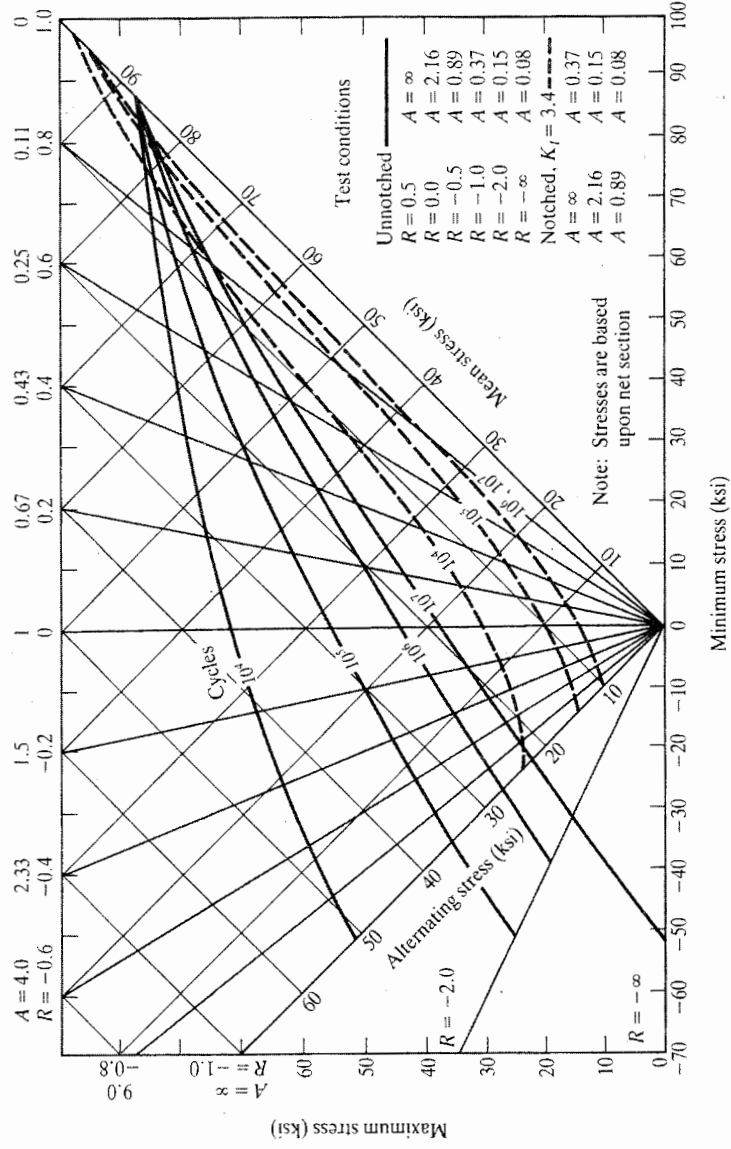


Figure 5.12. Typical constant life diagram for the fatigue behavior of various wrought products (drawn, rolled, and extruded rods and bars) of 7075-T6 aluminum alloy at room temperature in air. The symbol $A = (1 - R)/(1 + R)$ is the ratio of alternating stress value to mean stress value, and again, R is the stress ratio. A $S-N$ diagram and a constant life diagram present exactly the same type of data, where the former uses a stress value to create a family of curves while the latter uses the number of cycles to failure to identify the different curves.

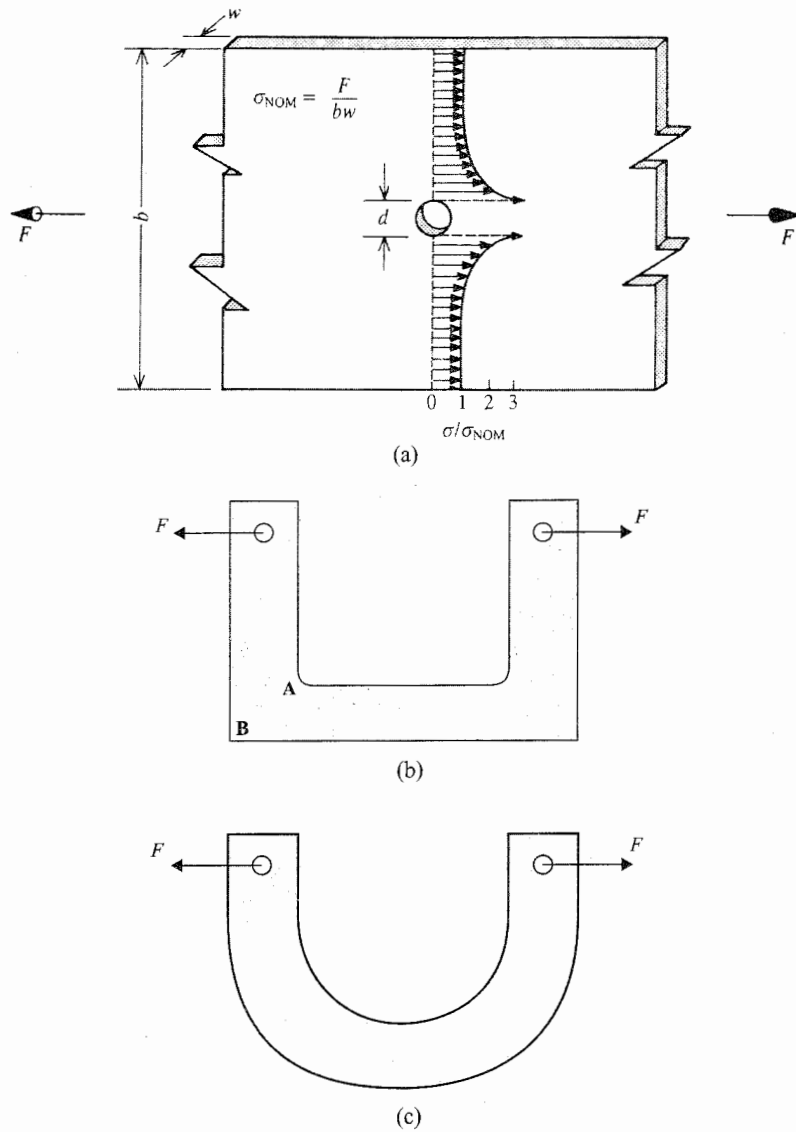


Figure 5.13. (a) The stress distribution in the loading direction across a wide metal sheet with a circular hole. (b, c) Respectively, poor and better designs for transmitting an applied force F around an abstraction from the standpoint of stress concentrations.

that act along the cross-section which is perpendicular to the loading and which also passes through the center of the hole. Since the specimen's cross-sectional area at the hole is less than that at the edges where the uniform loading is applied, it is to be expected that on average, the stresses on the cross-section through the hole are a bit larger than the tractions at the edges. Along that cross-section, at five radii away from the hole center, the stress in the direction of the loading is only 2 percent greater than the stress at the straight edge where the specimen is loaded, and it is only 1/2 percent greater than the applied traction at ten radii. It is also known both by analysis and experiment that the magnitude of the

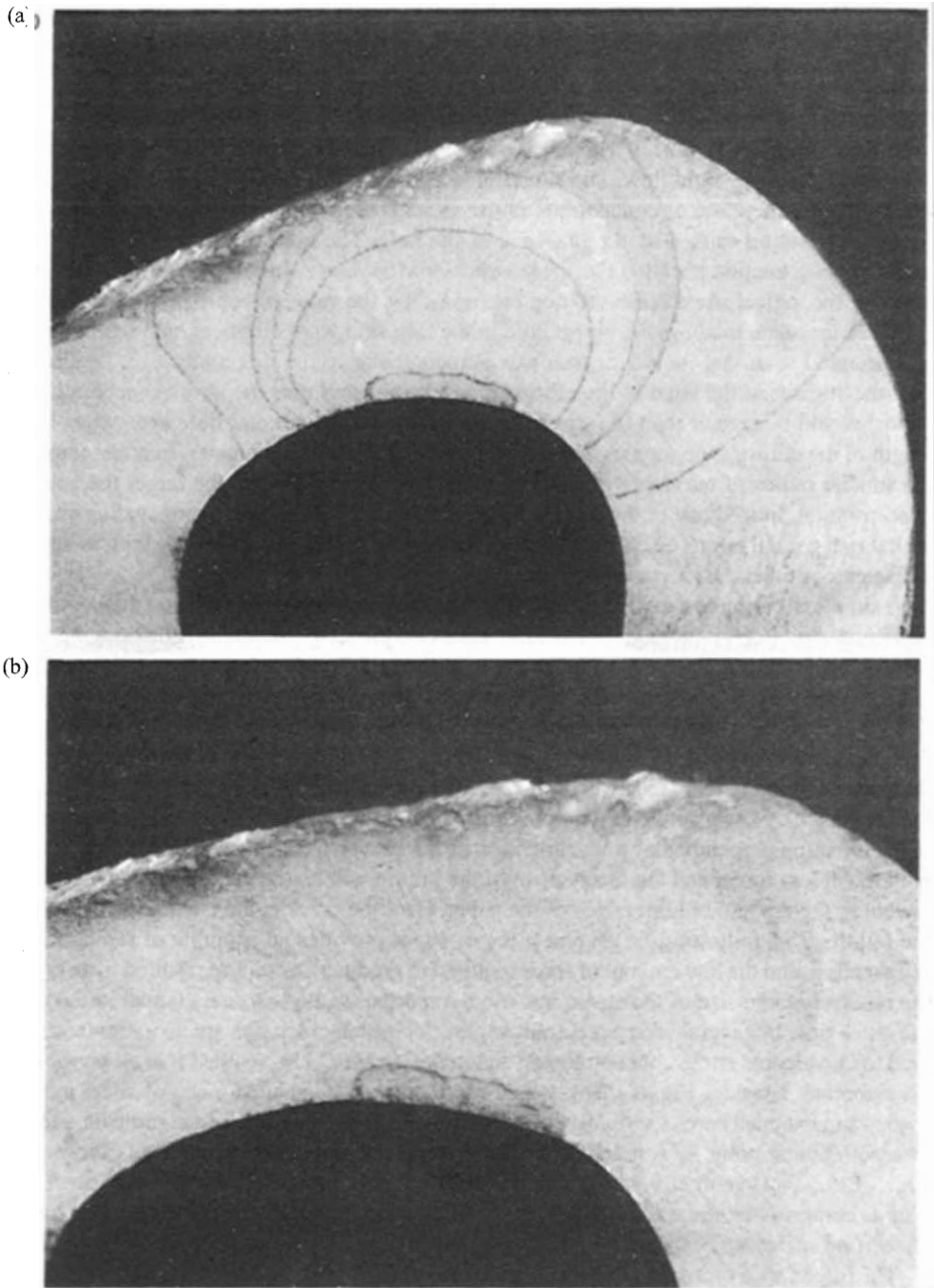
normal stress rises sharply near the edge of the hole to a maximum value at the hole edge of approximately three times the uniform traction that forms the loading at the outer edges away from the hole (Refs. [18, 21]). The stress pattern can be likened to that of fluid velocities in an incompressible fluid flow. The situation is as if the stress flow in the direction of the loading had to increase, or concentrate, in the vicinity of the hole in order to compensate for the obstruction caused by the presence of the hole. The ratio of the maximum stress to the loading traction is called the *stress concentration factor*. In this case of the circular hole, the theoretical stress concentration factor, K_t , has the value of approximately 3.0.

If, for the same loading, the above hole in the thin skin were elliptical, and that ellipse was oriented such that its longer axis was perpendicular to the direction of the loading, then the stresses at the edge of the ellipse's longer axis (and thus the stress concentration factor) would be greater than the stresses associated with the circular hole even when the length of the ellipse's longer axis equals the length of the circle's diameter. In other words, the smaller radius of curvature at the ends of hole of a given length, the larger the stress concentration. Indeed one of the routine means of dealing with a slowly propagating crack with its very small radius of curvature at the crack tip, is to drill a circular hole with as large a diameter as other considerations allow.

A simple experiment can illustrate the effect of the geometry of the void and the possible suddenness of a crack propagation failure. Take two pieces of identical photocopying, or similar, paper and, using a razor, make a cut in the middle of each paper paralleling the longer edge of the paper. Let both cuts be of equal size and approximately half the length of the piece of paper from top to bottom. With a firm grip at both the top and bottom of the first paper, pull the paper in the direction of the cut. If enough tension is applied to paper, the paper will likely tear (fail) where the person's hands grip the paper, and not at or near the cut (crack). Now grip the second piece of paper at its sides and apply tension to paper in the direction perpendicular to the direction of the cut. This time the paper will tear apart with much less force, and the mechanism of the failure will be the very rapid extension of the cut to the top and bottom edges of the paper. Here the crack is the clearly the cause of the failure. This failure of the second piece of paper provides an example of rapid crack propagation, and the low amount of force required to produce this failure resulted from both the relatively large size of the crack, and more importantly, the sharpness (small radius) at the crack tips. In general, sharp reentrant angles, for which crack tips are an extreme case, lead to unwelcome stress concentrations, and in design should be avoided if at all possible. To elaborate, consider Fig. 5.13(b), which represents a "U" shaped piece of sheet metal loaded in tension. There is virtually no stress at point B, while there is a significant stress concentration at point A. A much better design with the same basic geometry is shown in Fig. 5.13(c). This geometry will greatly reduce the stress at point A, while the price to be paid is compressive stresses at point B that could lead to out-of-plane buckling of the thin sheet if no stiffening is added.

The importance of avoiding reentrant angles in design was emphasized to the aerospace community by the catastrophic fatigue failures that afflicted the first commercial jet-powered airliner, the British-built Comet. It was determined that cracks initiated and grew outward from the sharp corners of the Comet passenger windows. That this lesson was heeded is evident in the very small size and rounded shape of the passenger windows of the British-French built Concorde.

From Ref. [17], fatigue damage in the form of cracks in a material is initiated either (i) at surface or interior imperfections in the form of small scratches or cracks resulting from the manufacturing process or subsequent handling (see following photographs) or (ii)



Photographs of the fatigue fracture surface of one blade of a B-29 propeller that was used to generate an airflow in a wind tunnel. (a) The fracture surface with the use of pencil marks to make more visible the crack edges where the advancing crack was relatively stationary. The smallest area indicates where the crack originated, apparently from a manufacturing flaw. The rough area outside the last roughly elliptical shaped crack edge is the area that failed in tension during the last load cycle. (b) The same fracture surface without the use of pencil tracings of prominent beach marks. Courtesy of Prof. Jewel Barlow and the Glenn L. Martin Wind Tunnel at the University of Maryland. Photographs by Prof. Allen Winkelmann.

in materials without such significant imperfections, at planes of shearing slippage, usually at the surface, see Endnote (2). After initiation, the growth of the cracks is in response to the cycling of tensile stresses. Crack growth phenomenon has been the subject of considerable research. There are presently two basic engineering approaches for estimating fatigue failures. The first approach is the application of linear elastic fracture mechanics (LEFM). The object of LEFM is to predict the growth per load cycle in the size of a given crack until that crack reaches the estimated critical crack size. At the critical crack size the crack grows very rapidly to complete rupture. An important aspect of this approach is the concept of what might be called a semimaterial property, strongly dependent on thickness for small thicknesses, called *fracture toughness*.

The second approach is to use a fatigue failure theory such as the linear damage accumulation theory proposed by Palmgren and revived by Miner (Ref. [26]). This is a more empirical approach that is based on the gross simplification that for a given material at given maximum and minimum stresses, given temperature, given surface finish, and given corrosive environment, each loading cycle does the same damage to the material. Hence, with each loading cycle doing a certain fixed percentage of the total damage to failure as estimated by using information like that presented in Fig. 5.10 or 5.11, the Palmgren–Miner theory is just a matter of adding damage percentages for various load cycles until 100-percent damage is accumulated. Two example calculations follow, and there are exercises on this topic as well. There are theoretical and practical difficulties with both the LEFM and the linear damage accumulation approaches, but they are generally the best of those approaches presently available, particularly when the load cycles are randomly ordered and clearly delineated.

Example 5.1. Consider an extruded angle beam of cross-sectional size $3 \times 3 \times \frac{3}{8}$ inches which is made from 7075-T6 aluminum. If the beam is without notches (i.e., the theoretical stress concentration factor, $K_t = 1.0$), and if the beam is subjected to the following axial stress history at room temperature, what then is the likelihood of this structural part experiencing a fatigue failure?

Mean stress	Alternating stress	Number of loading cycles
10 ksi	30 ksi	200 000
60 ksi	10 ksi	1 000 000
20 ksi	20 ksi	4 000 000

Solution. Figure 5.11 is for unclad sheeting, and Fig. 5.12 includes thick extruded bars. While the angle beam of this example is much thinner than the listed extruded bars, and therefore more susceptible to flaws, the data of Fig. 5.12 is clearly the more appropriate of the two data sets. Interpolating from Fig. 5.12 number of cycles to failure for these three load cycle histories are, respectively, 250 000 cycles, 10 000 000 cycles, and 4 500 000 cycles. To understand how those interpolated values are obtained, note that the lines of constant life such as 10 000 cycles and 100 000 cycles differ by factors of ten at roughly equal spacings. This strongly suggests that the interpolation must be logarithmic rather than linear. Thus half the difference between the 100 000 cycles line and the 1 000 000 cycles line is 300 000 cycles, not 500 000 cycles. This is so because for base 10, $\log 3 \approx 0.48$. Similarly, 200 000 cycles is three-tenths of the distance between those two lines on the graph because $\log 2 \approx 0.30$.

Now, by the Palmgren–Miner damage accumulation theory, the percentage of damage estimate is the sum for each combination of mean and alternating stress, of the ratio of the number of applied loading cycles at a particular mean and alternating stress, n_i , to the average number of cycles to failure at the same stress conditions, N_i . That is, the percent damage estimate, % D , is

$$\%D = (100\%) \sum \frac{n_i}{N_i} \quad (5.2)$$

In this case, the percent damage estimate is

$$\%D = \left[\frac{200\,000}{250\,000} + \frac{1\,000\,000}{10\,000\,000} + \frac{4\,000\,000}{4\,500\,000} \right] \times 100\% = 180\%$$

Since the percent damage estimate exceeds 100 percent, fatigue failure would be expected in the majority of such cases. It is not possible to be more definite because there is considerable scatter in the fatigue test data, and only average values are used for the values of the number of cycles to failure, the terms in the above denominators. ■

Example 5.2. Determine whether it is likely that a piece of unnotched 7075-T6 aluminum alloy sheet loaded axially in the longitudinal direction as follows, will experience a fatigue failure. The sheet metal is 0.125 inches thick, polished, and at room temperature.

Max. stress	Min. stress	No. of actual load cycles
30 ksi	−30 ksi	100 000
20 ksi	−20 ksi	1 000 000

Solution. The thickness cited here is a bit greater than that of sheet metal for which Fig. 5.11 was prepared. The data of Fig. 5.11 may be used in this case because the ratio of expected defect size to cross-sectional area is slightly more favorable in this case than that of the test specimen. From Fig. 5.10, the respective numbers of allowable cycles for the above two loading conditions (stress ratio $R = -1$) are approximately 300 000 and 3 000 000 cycles. Using the Palmgren–Miner damage accumulation theory,

$$\%D = \left[\frac{100\,000}{300\,000} + \frac{1\,000\,000}{3\,000\,000} \right] \times 100\% = 70\%$$

Since the damage percentage is less than 100 percent, the sheet metal is less likely to fail than not fail by fatigue cracking. ■

The American Society of Mechanical Engineers (ASME) Boiler Code specifies an extension of the Palmgren–Miner theory to include creep damage (Ref. [40]).

5.6 **Biaxial and Triaxial Loadings**

The discussion of the previous sections is generally relevant to a tensile or compressive loading applied in a single direction. Added complications arise when the applied loading occurs in two or three orthogonal directions. One possible question for biaxial loading is: If a material sample in sheet form were subjected to tensile or compressive loadings in two orthogonal directions, at what values of the two combined stresses would the sheet material yield? This particular question has received considerable attention. Two

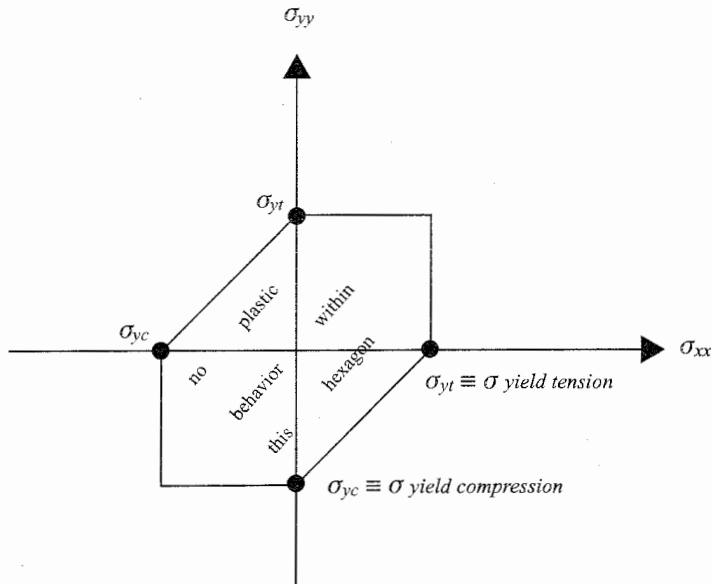


Figure 5.14. The limits of elastic behavior for the case of plane stress, as predicted by the theory of Tresca and St. Venant.

theories are currently accepted for use with ductile metals (Refs. [4, 6]). In the first, credited to Tresca and St. Venant, yielding occurs when the maximum shear stress in the material reaches the shear stress that exists at the point of yielding in a test specimen subjected to a uniaxial loading. That is, by this theory, yielding occurs when the maximum shear stress in the three-dimensional body reaches a value that is one-half that of the uniaxial tensile or compressive yield stress. It is not overly difficult to use three Mohr's circles for the two loading planes and the plane without loading to establish the following observations for biaxial loadings. (Remember that when two principal stresses have the same magnitude, the Mohr's circle for that plane has zero radius.) By this theory the two nonzero principal stresses can both have values that extend to the yield stress values without yielding occurring *if both stresses are tensile, or both stresses are compressive*. However, if the stresses are of opposite sign, then the sum of their absolute values must be less than the yield stress value to avoid yielding. Experiments show that this theory offered by Tresca and St. Venant tends to slightly underestimate the values of the combined stresses necessary to produce yielding. Thus this theory errs on the side of safety, and is termed "conservative." Figure 5.14 is a stress state plot that embodies these ideas. Exercise 5.8 deals with this theory for those who wish to explore the subject further.

The second generally accepted theory, credited to von Mises and Hencky and others, states that yielding occurs when the octahedral shear stress¹¹ due to the general loading reaches the octahedral shear stress that occurs at the point of yielding in a uniaxial test specimen. This theory is exactly equivalent to the energy of distortion theory that says that yielding occurs when the energy per unit volume associated with the stresses of what is known as the *stress deviator matrix*¹² reaches the critical value of that distortion energy per

¹¹ See Section 2.8.

¹² The stress deviator matrix is the stress matrix less the scalar value of the average normal stress multiplied by the identity matrix, that is, it is $[\sigma] - \sigma_{av}[I]$, where $\sigma_{av} = \frac{1}{3}(\sigma_{xx} + \sigma_{yy} + \sigma_{zz})$. The average stress

unit volume as determined by a uniaxial tensile test. In other words, the energy of distortion and the stress deviator matrix relate plastic, flow entirely to changes in shape as opposed to changes in size; that is, yielding is due entirely to shear stresses and not at all to normal stresses. The von Mises–Hencky theory for ductile materials is often more accurate than the Tresca–St. Venant theory in relation to test data, but it can be a little nonconservative. The stress state plot for von Mises–Hencky theory corresponding to Fig. 5.14 is shown in Fig. 2.11(b). The ellipse of Fig. 2.11(b) encloses the hexagon of Fig. 5.14 with common points at the corners of the hexagon.

5.7 Simplifications of Material Behavior

Now that some of the complications of the behavior of real engineering materials have been outlined in the preceding discussion, it should be clear that any all-encompassing mathematical formula for material response (strain) would be a function of several stresses and stress and strain rates, as well as temperature and time. Moreover, since the response depends on the previous stress–strain history of the material, such a complete functional description would have to be multivalued rather than single-valued. The conditional tense is used in the previous sentence because no such functional description is known even for a uniaxial loading. It is necessary to first divide the problem into more manageable parts, and then make appropriate simplifications for the material behavior. The division of the material response problem into various parts has already been suggested by the discussion of such separate problems as the creep problem, the fatigue crack growth problem, and so on. Another division of material response problems is inherent in the various common simplifications of the stress–strain relations for engineering materials. A simplification of the stress–strain relations that the reader has undoubtedly already met is that of a rigid material. The rigid body simplification (zero strain regardless of the stress or traction values) is useful whenever the actual deformations of the body are an insignificant portion of the overall motion of the body. The rigid body simplification is also useful in structural analysis when approximating one portion of a structure that is far more stiff (deflects far less under given loadings) than the other portions of the structure. Rigid supports are an example of such a usage. A second use of rigid bodies in structural analysis is explained when the dynamic response of structures to time-varying loads is introduced in Chapter 23.

The more prominent of the simplifications for nonrigid materials are illustrated in Fig. 5.15 for uniaxial loadings. The *linearly elastic* or *Hookean* material model is one where $E_c = E$, and stress and strain are taken to be directly proportional to each other regardless of their values. Unloading paths and loading paths are one and the same. This mathematical model for material behavior is entirely adequate for many engineering materials as long as the maximum stress remains below the yield stress. The *linearly elastic, perfectly plastic* material model has the modification that once the stress reaches a certain maximum value, the strain increases without limit at a constant strain rate. In order to better approximate the actual material stress–strain curve, the maximum stress is taken to be the yield stress rather than the proportional or elastic limit. Unloading paths are always parallel to the initial loading line. The *linearly elastic, strain hardening plastic* material model is

is the magnitude of the normal stress on the octahedral plane, and it is exclusively associated with volume changes. The stress deviator stresses are those responsible for changes in shape. At the onset of plastic behavior, that is, at the start of material yielding, the material essentially only changes shape, while the volume remains very nearly constant. Hence the association of the octahedral shear stress with the matrix of deviator stresses.

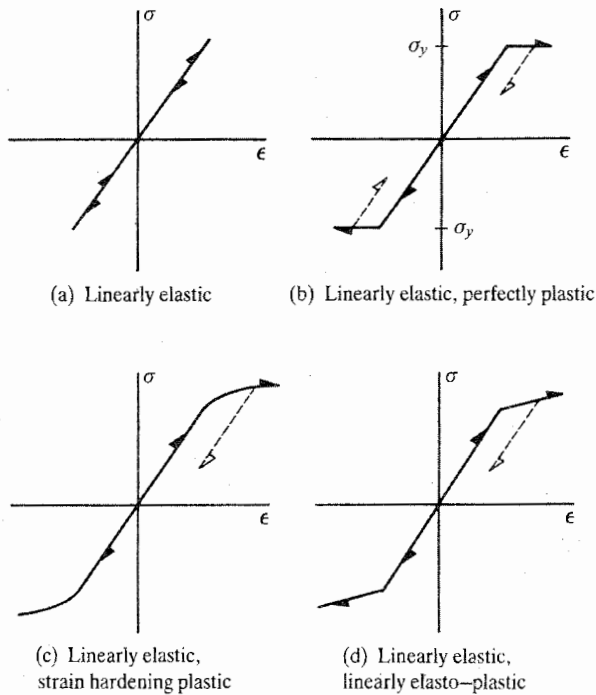


Figure 5.15. Four stress–strain mathematical models that can be used to approximate the load response behavior of structural materials.

one where plastic deformation occurs after the stress reaches a proportional limit. In this case, like most real materials, the plastic deformation is mixed with some continuing elastic deformation so as to produce a curved rather than flat path. A simpler form of the third material model is the *linearly elastic, linearly elasto-plastic* material model. This model is not to be confused with a bilinearly elastic material model where the unloading path is the same as the loading path. Note that few, if any, actual vehicular materials can be reasonably approximated by a bilinearly elastic material model, or any other type of nonlinear elastic model.

The mathematical treatment of the first two material models is straightforward. For the case of the linearly elastic material and uniaxial loading, the stress–strain relation is just $\sigma = E\epsilon$. For the linearly elastic, perfectly plastic model, there are simply limits of applicability imposed upon $\sigma = E\epsilon$. After the stress reaches the magnitude σ_y , where plastic flow begins, the stress can no longer increase, and then the additional strain equals the strain rate multiplied by time until rupture or unloading occurs. During unloading, the stress is equal to the modulus of elasticity multiplied by the difference between the total instantaneous strain and the plastic strain.

Over its loading portion, the linearly elastic, strain hardening plastic material model is often represented by a single equation of the form: $\epsilon = (\sigma/E) + \beta(\sigma/E)^n$. Again E in this equation is determined by the slope of the actual material's stress–strain curve at zero stress. The other two parameters, β and n are chosen so that the curve of the equation fits the experimental stress–strain curve at two points not far beyond the elastic limit. In the Ramberg–Osgood curve fit (Ref. [16]), the two parameters are chosen so that the formula coincides with the actual curve at secant modulus values of $0.85E$ and $0.7E$. Although

closer to the form of an actual stress–strain curve than these other simplified models, the Ramberg–Osgood method and other such formulations offer a nonlinear algebraic formula for the relation between strain and stress. As such, these formulations are quite cumbersome for use in the analyses discussed in this introductory text. One welcome feature of this formulation is that there is only one physically possible solution for the stress in terms of the strain; that is, only one positive root to the n th-order polynomial equation that arises when solving for the stress in terms of the strain.

Following the exercises, Endnote (1) presents a simple example involving linear elastic, perfectly plastic materials. The example is placed after the exercises because it is not important to an introduction to structural mechanics. However, it is included in this text because it illustrates, in the context of only the first of the more complicated material models, an application of the two subjects that have been emphasized in Chapters 1–4: (i) displacement continuity or strain compatibility and (ii) force equilibrium. Furthermore, this example is a simple illustration of the topic of *residual stresses*. Residual stresses are the stresses that remain in a structure after the loading, mechanical or thermal, is removed from the structure. This example can be applied directly to clad aluminums loaded beyond the yield stress of the cladding material. In general, residual stresses are difficult to estimate, as in the case of welded structures where residual stresses, sometimes as high as the material's yield stress, are created by the localized heating that accompanies the welding process.

After the above discussion of the complexities of material behavior, it should be no surprise that the material model that is used throughout this text is the linearly elastic model called Hooke's law. The value of the previous discussion lies in the awareness of some of the limitations on this model. If the reader is overly disappointed, he or she can take comfort in the thought that Chapter 6 demonstrates that even the linearly elastic material model, when extended to triaxial loadings, is not entirely without its complications. Further solace is available in the fact that the linearly elastic model can be considered as the first part of the other simplified models, and the fact that, as previously discussed, reusable vehicles are very seldom designed so as to allow plastic deformations. Thus the linearly elastic material model is well suited to vehicular structural mechanics.

Chapter 5 Exercises

- 5.1. Show that Eq. (5.1) is also valid for a rectangular cross-section of original dimensions a_0 by b_0 , and instantaneous dimensions a by b .
- 5.2. (a) Use Fig. 5.4(a) for AISI 4340 alloy steel, 200 ksi ultimate stress level, to calculate the Young's modulus, the offset yield stress, and the offset proportional limit for this material at room temperature.
(b) Use Fig. 5.4(b) for 2024-T42 aluminum alloy plate to calculate the tensile Young's modulus, the tensile offset yield stress, and the tensile offset proportional limit for this material for the L direction, at room temperature.
(c) Same as (b), but for compression.
- 5.3. Use Mil Handbook Five to determine the following three sets of material properties for the L direction for clad 7075-T6 aluminum sheet that is 0.32 cm thick.
(a) The A basis tensile and compressive yield stresses after a half hour at 400° F.
(b) The room temperature primary and secondary compressive Moduli of elasticity. Note that the existence of both a primary and secondary modulus of elasticity is due to the presence of a cladding covering the alloy core. When

the loading stresses the weaker cladding material beyond its yield stress, there is no increase in resistance (stress) to further loading on the part of the cladding. The core material has to fully shoulder all further increases in load. The core accepts higher stresses by straining more than it would if the cladding were also accepting increases in loading. This greater amount of straining per increase in stress causes a lower (secondary) modulus of elasticity after the cladding reaches its yield point. In many cases the differences between the two moduli are small enough to ignore in analysis.

- (c) Poisson's ratio and the weight density. (The reason why the value of the shear modulus is omitted is explained later.)
- (d) For a 7075-T6 extruded channel beam (an example of a "shape") that is 0.38 inches thick, determine the A basis compressive yield strength, longitudinal direction, after one-half hour at 350° F.

5.4. As previously stated, material selection for design requires consideration of many factors. However, there are some simple rules of thumb (derivable for simple cases (Ref. [16]) that provide initial guidance for minimizing weight. Some examples are: (i) the weight of a uniform rod subjected to a tensile load is minimized by selecting the material with the maximum value of the ratio of the yield stress to the mass density; (ii) the weight of a axially loaded uniform column is minimized by maximizing the ratio of the cube root of the modulus of elasticity to the mass density when the compressively loaded column has a specified length and end conditions, and a rectangular cross-section where the proportionality between the width and depth is fixed; and (iii) from Ref. [16], the weight of a thin-walled circular cylindrical shell of fixed radius and fixed length and variable thickness is minimized by maximizing the ratio of the square root of the modulus of elasticity to the density.

Given that 2024-T42 aluminum has a weight density of 0.100 lb/in³ for rods and columns $E = 10.5 \times 10^3$ ksi, $E_c = 10.7 \times 10^3$ ksi; for sheet and plate $E = 10.0 \times 10^3$ ksi, $E_c = 10.2 \times 10^3$ ksi; and that 4340 steel alloy (200 ksi ultimate) has a weight density of 0.283 lb/in³, and $E = E_c = 29.0 \times 10^3$ ksi for all forms; then on the basis of the above rules of thumb, which of these two materials is the better choice for the situations (i), (ii), and (iii) mentioned above? Use the yield stress values from Exercise 5.2 assuming that the compressive and tensile yield stresses are the same.

5.5. (a) Use the Palmgren–Miner theory to estimate whether there is a greater than, or less than, one-half probability of a fatigue failure for an unnotched, axial tensile specimen of wrought 7075-T6 aluminum alloy at room temperature in air, with a circular cross-section, if that material is subjected to the following load history where the two types of loading are randomly mixed:

Mean stress	Alternating stress	No. applied cycles
20 ksi	20 ksi	5 000 000
10 ksi	25 ksi	500 000

Hint: Use the constant life diagram to estimate the allowable number of cycles for both loading conditions, and convert the ratio of the above actual number of cycles to the allowable number of cycles into a percentage, and

then sum to estimate (roughly) the total percent fatigue damage. Remember that 100-percent damage accumulation implies a one-half probability of fatigue failure.

- (b) Same as above, but for bare 7075-T6 alloy sheet (longitudinal direction), 0.16 inches thick, with the following load history, where the sequence of load cycles is again without order:

Max. stress	Min. stress	No. load cycles
20 ksi	-20 ksi	1 000 000
40 ksi	0	100 000
30 ksi	-18 ksi	100 000

- (c) A piece of 7075-T6 aluminum sheet, 0.1 inch thick, is subjected to a total cyclic loading in its longitudinal direction that is composed of the following two unordered loadings:

Max. stress	Stress ratio	No. applied cycles
30 ksi	-1.0	30 000
40 ksi	0.0	50 000

If the theoretical stress concentration factor is 1.5, then use the Palmgren-Miner theory to determine whether the probability of a fatigue failure is less than or exceeds 50 percent.

- 5.6. (a) Explain why the area under a uniaxial tensile or compressive stress-strain curve is describable as work done upon the material per unit volume of material.
- (b) As (a) above, but this time for the stress-strain curve for a single shearing stress.

FOR THE EAGER

- 5.7. Consider a homogeneous bar of length L with rectangular cross-sectional dimensions b by h . Let the bar be stretched a small, finite distance ΔL . The cross-sectional dimensions are reduced by the amounts Δb and Δh . If the volume of the bar is the same after deformation as before, the case of perfect plasticity, what then is the Poisson's ratio for this perfectly plastic material? Note that here "small" means that $\Delta h/h$, $\Delta b/b$, $\Delta L/L \ll 1$, and thus their products may be discarded in comparison to the ratios themselves. (*Hint*: Equate the before and after volumes.)

FOR THE ESPECIALLY EAGER

- 5.8. As mentioned in Section 5.6, the maximum shearing stress as determined by three Mohr's circles can be used to establish the Tresca closed boundary for biaxial stress states that do not produce yielding (i.e., plastic behavior).
- (a) Actually show that this boundary between elastic and elasto-plastic behavior is a skewed hexagon on a stress state plot with two orthogonal axes where one stress axis is the stress in one of the two biaxial loading directions and

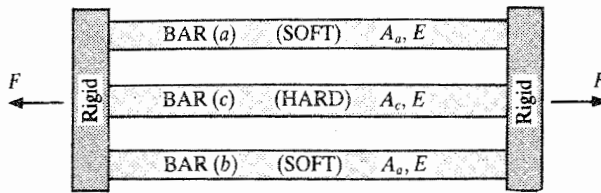


Figure 5.16. Example 5.3. A symmetrical three-bar structure.

the other stress axis is the stress in the other biaxial loading direction. *Hint:* The biaxial stresses are principal stresses, and the two biaxial stresses plot as points on their respective axes. Consider the maximum shearing stress associated with points (stress states) off the axes.

- (b) When that task is successfully accomplished, consider what three-dimensional surface serves the same purpose for a general triaxial loading. (The two-dimensional answer is a cross-section of the three-dimensional answer.)

Endnote (1) Residual Stress Example Problem

Example 5.3. Consider the symmetric, three-parallel-bar arrangement shown in Fig. 5.16. Each bar has the same length and a small cross-section. The two outer bars, bars *a* and *b* are a soft aluminum while bar *c*, the middle bar, is a hard aluminum with a yield stress that is twice that of the outer bars. All three aluminum bars have the same modulus of elasticity, *E*. At both the top and bottom of the three bars is a large hard steel fixture that transmits external loads to the three bars. The large steel fixtures can be modeled as rigid in comparison to the less stiff and weaker aluminum bars. The aluminum bars are to be modeled as linearly elastic, perfectly plastic.

Let the two-fixture, three-bar structural system be stretched in tension up to, but not beyond, the yield point of the center bar, and then let the force on the structural system then be reduced to zero. The two outer bars experience plastic deformation at half the applied load. As a result, when the externally applied load is reduced to zero, the outer bars are left with compressive residual stresses while the center bar remains in tension; see Fig. 5.17. The question is: What are the magnitudes of these residual stresses?

Solution. The rigid steel fixtures cause all three bars to have the same displacements and the same strains throughout the loading and after the loading has been removed. Thus the statement of strain compatibility is

$$\epsilon_a^f = \epsilon_b^f = \epsilon_c^f = \epsilon^f > 0$$

where the *a*, *b*, and *c* subscript refer to the bars, and the *f* superscript refers to the “final” equilibrium state.

To write the equation of force equilibrium, consider a free body diagram of one of the steel fixtures after the external loading is reduced to zero. The forces acting on the rigid fixture are equal and oppositely directed from the forces acting on the three bars. Since the two outer bars are the same, the force equilibrium equation becomes

$$2A_a\sigma_a^f + A_c\sigma_c^f = 0 \quad (\text{where } \sigma_a^f < 0)$$

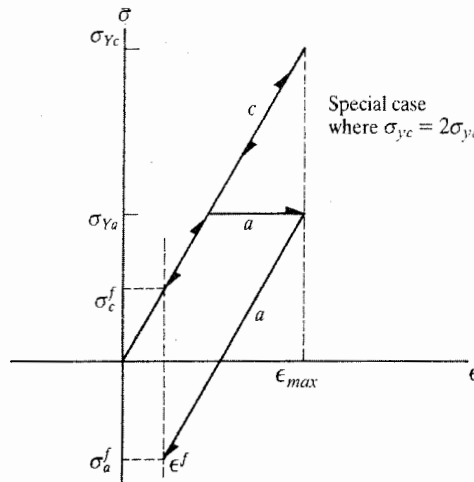


Figure 5.17. The loading and unloading curves for the three-bar structure of Example 5.3.

The stress–strain relations, when added to the compatibility and force equilibrium equations, completes the basic problem description. The stress–strain relations for the two types of bars are

$$\sigma_c^f = E\epsilon^f \quad \text{and} \quad \sigma_a^f = E\epsilon^f - \sigma_{ya}$$

where the y subscript is for yield, and from Fig. 5.17 it is possible to see that during unloading the stress in the outer bars is less than the stress in the center bar by the value of the yield stress in the outer bars.

Now it is a matter of combining the three basic equations. The compatibility equations stating that all the strains are the same have already been inserted into the stress–strain equations. Substituting the stress–strain relations into the force equilibrium equation and solving for ϵ^f yields

$$\epsilon^f = \frac{2A_a}{2A_a + A_c} \frac{\sigma_{ya}}{E}$$

Substituting the value of the final strain back into the stress–strain relations provides the solution for the residual stresses:

$$\sigma_c^f = +\frac{2A_a}{2A_a + A_c} \sigma_{ya}$$

$$\sigma_a^f = -\frac{A_c}{2A_a + A_c} \sigma_{ya}$$

Check that the units are correct. Note that if this model is used for clad aluminum where $A_c \gg A_a$, the stress in the core, area c is quite small. ■

Endnote (2) Crack Growth Example

Figure 5.18 shows a sketch of a fatigue failure surface. The failure surface is the cross-section of a round steel rod used to control a boat rudder. The failure surface is located along the shaft axis where the shaft exited the boat hull. There are two, nearly diametrically opposite, crack initiation points which appear to have resulted from the shaft

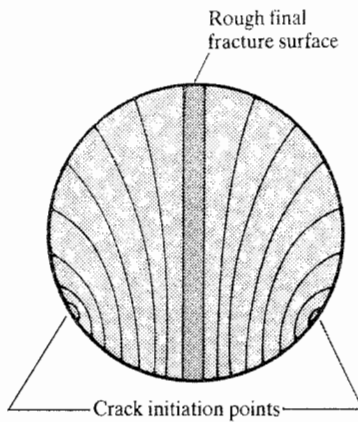


Figure 5.18. Beachmark pattern for crack growth in a certain circular shaft cross-section.

flexing and impacting against the boat hull. Presumably, the shaft-hull impacts scratched the shaft surface causing stress risers. Tensile stresses that resulted from continued shaft bending caused the twin cracks to grow inward. The thin strip of area along the vertical diameter is the area of the shaft cross-section that failed last. The relative smallness of this thin strip suggests that the average maximum tensile stresses acting on the failure surface were not very large. The origin of the many load cycles that caused this metal fatigue failure cannot be determined from inspection of the failure surface. Two possibilities are (i) a resonance with respect to the vibration caused by the boat engine, and (ii) water turbulence surrounding the rudder. The author thanks Mr. Jon Forst for bringing the broken shaft to his attention. Chapter 13 considers the theoretical stress concentration factor associated with a scratch on the polished surface of a circular shaft.

Linearly Elastic Materials

6.1 Introduction

Chapter 5 pointed out that the mechanical and thermal response of engineering structural materials is quite complex. Nevertheless, if a uniaxial stress value lies within the bounds of the compressive and tensile elastic/proportional limits, that complex behavior becomes relatively simple. Within those two limits, or as an approximation, slight extensions of those limits to the limits of the compressive and tensile yield stresses, there is very nearly a straight-line relation between stress and strain. Moreover, that straight-line relation is very nearly the same for both loading and unloading. That is, permanent set (plastic deformation) is negligible, and the relation between stress and strain is single-valued. In other words, the stress-strain relation no longer depends upon the previous load history. Under these circumstances materials are called *Hookean*, or *linearly elastic*. In summary, on the basis of extensive experimental evidence, engineering structural materials within the yield stress limits can be and are described by a mathematical model wherein the plot of stress versus strain is exactly a straight line, and this same straight line serves the dual purpose of being a loading line and an unloading line. Thus in this chapter the focus shifts from the complicated behavior of actual engineering materials to the justifications and implications of the relatively simple linearly elastic material model.

There are three important reasons to justify restricting almost all further studies within this text to stresses whose values are limited to being within the yield stress bounds of nearly linearly elastic behavior. The first reason is that, by allowing the adoption of the linearly elastic material model, the task of structural analysis is greatly simplified and hence more easily understood without the complications of a more mathematically elaborate material description. It is always good engineering practice when confronted with a new, difficult-to-understand problem, to first examine simplifications that will build understanding and that are likely to provide check points for any more advanced theory when that theory is developed. A second reason for restricting the stresses to lie within the bounds of elastic behavior is directly applicable to vehicular structures. That reason is that permanent deformations due to plastic strains unacceptably raise the possibility of problems that range from (i) degraded alignments that can disturb the dynamics and control of a vehicle, make maintenance more difficult, and increase wear on moving parts; to (ii) less efficient structure-fluid interactions such as increased drag in water or air, and, what is particularly important to flight vehicles, decreased lift; to even (iii) lowered esthetic values that interfere with customer satisfaction. A third reason for adopting the stress limits implicit in the linearly elastic material model, perhaps not as vital as the first two because of the possibility of detection through inspection of the permanent set caused by plastic behavior, but certainly not without importance, is that any permanent set reduces the loading path to structural failure. In many types of vehicles, almost any type of structural failure is quite likely to lower the satisfaction of the vehicle owners and especially the operators.

There are two distinct parts to the linearly elastic material model. The linear part of the linearly elastic material model is simply the previously noted statement of Hooke's law that

stress is equal to strain multiplied by the slope of the loading line, which is Young's modulus. Hooke's law refers to a single stress and its corresponding strain. However, Hooke's law and the Poisson effect are the basis for the equations that are developed later in this chapter to describe general triaxial loadings. Again, the elastic part of the linearly elastic material model is the part that says that the loading line and unloading line are exactly the same, and therefore there is no permanent set or other plastic behavior. There are broad implications to this part of the material model. Recall that the area under the stress-strain line represents work done per unit volume on the loaded material. Thus the recovery of all the area under the stress-strain line when unloading is completed can be interpreted as the complete recovery of all the work done on the material due to loading. From a work and energy point of view, the loading and unloading process of this material model is thus described as a reversible process. Therefore, an immediate implication of the elastic model is that no heat is generated, and thus lost, during the loading or unloading process. The inclusion of a no-heat-generation feature in the material model for actual engineering materials is experimentally justified¹ when the time duration of loading and unloading cycles within the elastic limits is measured in minutes or hours, rather than seconds or fractions thereof.

The lack of heat flow resulting from purely elastic material straining means, that for this elastic material model, there is no connection (called "coupling") between, on the one hand, the various equations involving stress and strain that have been, and are to be, developed in this text, and, on the other hand, the laws of thermodynamics and heat conduction. The lack of a connection between those two sets of equations does not mean that structural engineers have no use for the laws of thermodynamics and heat conduction. It just means that the laws of thermodynamics and heat conduction can be treated separately from the equations that govern stresses, strains, and displacements.

An important consequence of the simplification that no heat is generated when a structure is uniaxially stressed within the values of the yield stresses is that in the first law of thermodynamics, which is $dU = dW + dQ$, the differential of heat dQ , is zero. The conclusion that can be drawn from $dU = dW$ is that, when the structure is loaded, the incremental work done on the structure by the applied loads, dW , is stored within the structure as recoverable internal energy. This is so because U , the *strain energy*, is a point function, and dU is an exact differential. A simple illustration of this storage of recoverable energy, in a slightly more complicated context than uniaxial loading, is the compressed, elastic, coiled spring. The work done to compress the spring can be fully converted into kinetic energy, and thus recovered, by placing a small mass on the spring and then releasing the spring so as to impart a velocity to the small mass. The concepts of work and energy storage are quite important to structural analysts, and these concepts are applied to structures in later chapters starting with Chapter 15.

The above discussion of limitations on stress magnitudes is entirely in terms of uniaxial loadings. It might seem at first that for the situation of triaxial loading, the limitation necessary to accomplish (i) the same desired simplicity in the relations between stresses and strains and (ii) the same decoupling from the laws of thermodynamics would only be the

¹ A process, such as a loading process, during which no heat is gained or lost is called "adiabatic." The actual process of loading a real engineering structural material within the range of its elastic limits is a process that lies between the theoretical bounds of an adiabatic and an isothermal process. These two processes are very little different for a structural material subjected to those limited stresses. Since reversible adiabatic loading is part of the linearly elastic material model adopted herein, it is proved below that for this situation all the work done on the structural body is fully stored as elastic energy. In Ref. [3], the same is proved for the other bounding process, the reversible isothermal case.

requirement that all the principal stresses are to be bounded by their respective compressive and tensile yield stresses. Hopefully a recollection of the very brief discussion of the Tresca–St. Venant theory for the onset of biaxial or triaxial yielding is sufficient to discard such an initial thought. The way to get around having to choose between theories that predict the onset of yielding (i.e., the onset of plastic flow) and deal with the limits the chosen theory places on the principal stresses, is to simply require that the stresses in the structure do not cause plastic behavior. That is the limitation that is now adopted.

There are several general types of linearly elastic material models for triaxial loadings and temperature changes. The two material models that are most important in engineering practice are called orthotropic and isotropic materials. The following two sections define and explain these models. The orthotropic material model is examined first, and then specialized to the included form that is the isotropic material model. This is a labor saving procedure since the development of the equations that describe the two types of materials is essentially the same. Other types of linearly elastic material models are briefly mentioned at the end of the discussion on isotropic materials.

6.2 Orthotropic Materials

An *orthotropic material* is one where the material itself is so structured that the material has different physical and thermal characteristics in three orthogonal directions. Wood, with its grain, is an example of a natural material that fits this category. A man-made example is plywood, say with three plies at right angles to each other. Another man-made example is a single ply of a fiber composite material. As can be seen by these examples, the structure of the orthotropic material and the inherent orthogonal directions associated with that structure are often evident to the eye.² By far the simplest way to describe the material behavior of an orthotropic material is in terms of three orthogonal coordinate directions aligned with the structure of the material. Since wood, with its cylindrical grain geometry, is not a material of present concern, a Cartesian coordinate system is used throughout this chapter to label the three orthogonal directions of differing material properties that are inherent in the structure of an orthotropic material. Once those material directions are identified, the mathematical description of the material response to loads is just a matter of the repeated use of Hooke's law and Poisson's ratio.

The strain in the x direction that is caused by a stress in the x direction is the stress in the x direction divided by the Young's modulus for the x direction. In symbolic form this linear relation between strain and stress can be written as $\epsilon_{xx} = \sigma_{xx}/E_x$. From the previous discussion of shrinkage/expansion in the other two orthogonal directions when there is stretching/compression in the first orthogonal material direction, recall that Poisson's ratio, ν , is used to relate the interaction between the strains in orthogonal directions. For an orthotropic material, there are different Poisson's ratios for different coordinate direction interactions. For this reason, each Poisson's ratio for an orthotropic material carries two subscripts. The first of the two subscripts identifies the direction of the strain **from** which the effect is derived, while the second subscript identifies the direction **to** which the effect is

² If the internal structure of a material is not evident, and yet it is suspected that the material is orthotropic, that suspicion can be tested by loading the material in various directions and monitoring the displacement response. If it can be discovered that there are three orthogonal directions for which there is no shearing strain when a normal traction of constant magnitude is applied successively in those directions, and the longitudinal strains in those same directions are different, then the material is orthotropic with respect to those three orthogonal directions.

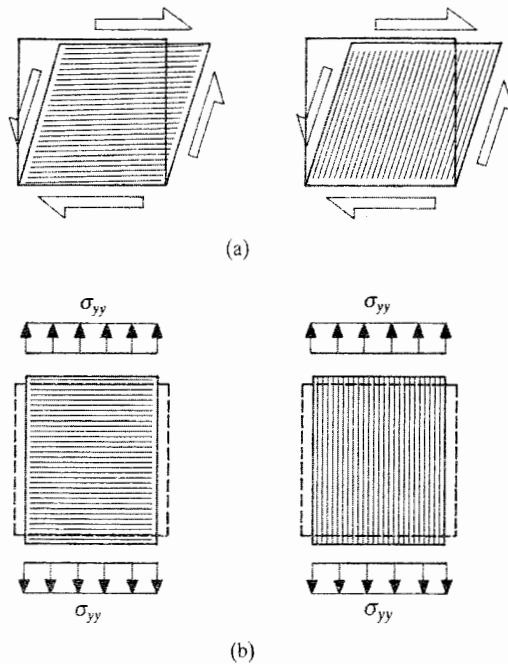


Figure 6.1. The effects of material symmetry: (a) shearing stress loadings aligned with the grain of the material; (b) normal stress loadings aligned with the grain of the material.

transferred.³ With this symbolism in place, it may be written that the additional strain in the x direction due solely to the positive strain in the y direction is $-v_{yx} \epsilon_{yy} = -v_{yx} \sigma_{yy}/E_y$. Similarly, the quantity $(-v_{zx} \sigma_{zz}/E_z)$ is the x direction strain due solely to the z direction stress. What is being done in this discussion is that each of the normal stresses is being treated as independent quantity. Each independent stress produces an independent increment in the x direction strain. Therefore, the total x direction strain is just the sum of all its components. Thus far,

$$\epsilon_{xx} = \frac{\sigma_{xx}}{E_x} - \frac{v_{yx} \sigma_{yy}}{E_y} - \frac{v_{zx} \sigma_{zz}}{E_z}$$

As can be seen from the above discussion, each of the normal stresses oriented with the material axes has a simple effect on each longitudinal strain oriented along another material axis. The shear stresses oriented with respect to the same material axes have no effect on the longitudinal strains. To see how that may be possible, see Fig. 6.1(a) where the lengths of the line segments aligned with the material axes and lying within the finite-sized rectangular parallelepiped are unaltered when the parallelepiped is sheared. The converse is also true. Consider the finite-sized parallelepiped of orthotropic material shown in Fig. 6.1(b). About the center of the parallelepiped, both the geometry of the parallelepiped and the structure of the material are symmetric. The normal traction and stress distribution is also symmetric. Thus the deformation response about the center axis of symmetry must be both symmetric and uniform. Since both a uniform positive and a uniform negative shearing strain would

³ Note that within the imposed stress limits, the various Young's moduli and the various Poisson's ratios are constants. Also note that the ordering of subscripts on Poisson's ratios in other texts is not always the same as adopted here.

result in a nonsymmetric deformation response, there cannot be any shearing strain. Thus it may be seen that normal stresses do not produce shearing strains, just as shearing stresses do not produce longitudinal strains when the normal stresses are oriented with respect to the material axes.

A shearing stress produces a shearing strain with respect to the same material axes. Since the properties of an orthotropic material are different in different directions, the shearing strains in the planes defined by the material axes are generally different even when the shearing stress in each plane is the same. Thus the linearly elastic relations generally have to have different proportionality constants between different pairs of shearing strains and stresses. That is, $\tau_{xy} = \sigma_{xy}/G_{xy}$, $\tau_{xz} = \sigma_{xz}/G_{xz}$, and $\tau_{yz} = \sigma_{yz}/G_{yz}$. The constants G_{ij} are, of course, called the shearing moduli of elasticity for the i, j plane. Note that there is no interaction between stresses and strains with different pairs of subscripts when the shearing stresses are oriented with respect to the material axes.

Since the orthotropic material being discussed is a linearly elastic material, any temperature change is independent of the normal and shearing stresses. Consider such a temperature change. A uniform temperature change throughout a differential rectangular orthotropic material parallelepiped produces a change in length, and thus another longitudinal strain increment, in each of the three orthogonal material directions of the parallelepiped. The x direction longitudinal strain due solely to a temperature change is related to the temperature change itself, symbolized as ΔT , by means of the x direction coefficient of thermal expansion, α_x . The relation is $\epsilon_{xx} = \alpha_x \Delta T$. Similar expressions hold for the other two temperature-induced orthogonal strains. A uniform temperature change throughout a rectangular parallelepiped does not produce any shearing strains in the parallelepiped. Again the reason for the lack of a shearing strain is the threefold symmetry of the material.

In order to avoid any questions regarding changes in the temperature change over the volume of an infinitesimal parallelepiped, the temperature change associated with the infinitesimal parallelepiped is taken to be the average value that exists at the geometric center of the infinitesimal parallelepiped. Since the distance between the geometric center and the corner point P is infinitesimal, and since the equations connecting stresses and strains and the heat conduction equations are uncoupled, this choice for the location of the point to which the temperature change is ascribed has no effect on either set of equations.

It is important to note that an implicit aspect of the simplicity of the above relationship between the temperature change and its induced strain is that this independent component of the total strain is always present regardless of any other factors, whenever there is a temperature change. In other words, the temperature change-induced portion of the total strain occurs entirely separately from the mechanically induced strains. In order to illustrate this fact, consider a uniform rod of length L that abuts rigid (i.e., unmoving) walls at both its ends. Let the bar be subjected to an increase in temperature. It may help to understand the resulting state of stress in the bar by first imagining that the right-hand rigid wall is temporarily removed, and the bar expands freely due to the temperature change-induced (positive) strain. Then let a compressive force be applied to the right-hand end of the bar. The compressive force produces a mechanically induced (negative) strain. Let the compressive force be made just large enough to push the bar back (without the bar buckling) the distance $\alpha_x \Delta T L$ that the right-hand end of the bar moved because of the temperature change. By this means the bar is restored to its original length, and the bar boundary conditions are again satisfied. Then the rigid wall is slipped back into its place in order to maintain that compressive force. In this case the mechanical strain is made just large enough to offset the thermal strain, thus making the *total* strain zero. The point is that, even from the view point of never having removed the right-hand wall, there is a thermal strain as well as a

mechanical strain. Only when the total strain is a known value, such as zero as is the case in this particular problem, is there a relation between the mechanical and thermal strain components of the total strain.

The stress in the above-discussed bar is the compressive force divided by the cross-sectional area of the bar. However, this scenario of removing and then reimposing boundary constraints is entirely unnecessary for determining the stresses induced by temperature change.⁴ The above scenario is presented because almost all persons new to structural analysis become confused at one time or another with regard to thermally induced stresses, and the above approach to the elementary bar problem is helpful for returning to the correct path. That correct path is what might be called the direct analytical approach to this same bar problem. This direct approach, which is suitable for much more complicated cases of thermal strain, proceeds in the manner explained in the example problem below.

Example 6.1. Let E_x be the modulus of elasticity of the above discussed bar in the direction of the length of the bar (the x direction). Then the equation for the strain in the x direction is

$$\epsilon_{xx} = \frac{\sigma_{xx}}{E_x} + \alpha_x \Delta T$$

Since every free body diagram shows that the stress on any cross-section is the same as that at any other cross-section, and since the temperature change is the same everywhere, the conclusion is that the strain is also a constant over the length of the bar. That is, since the right-hand side of the above equation is a constant, so too must the left-hand side be a constant. Since the ends of the bars do not displace, there is no change in length of the bar. Thus the constant strain ϵ_{xx} must be zero. Substituting this value for the strain into the above equation and solving for the stress yields the solution

$$\sigma_{xx} = -E_x \alpha_x \Delta T \quad \blacksquare$$

In subsequent chapters, emphasis is placed upon always identifying and then including in the analysis four pieces of information: (a) an equilibrium statement, either from a free body diagram (FBD) peculiar to the problem at hand, or from the general equilibrium equations derived from the FBD of the infinitesimal parallelepiped; (b) a strain compatibility or strain-displacement relation; (c) a relation between strains and stresses; and (d) boundary condition statements. In the simple analysis of the above example problem, three of these four statements have such simple forms that they might be overlooked. To avoid such an oversight, note that (a) is the statement that the stress is a constant; (b) is the information that the strain is a constant; and (d) identifies the strain as zero. Item (c) is the only equation in this example to have any substantial form. It is of course written out as the first equation of this example.

The coefficient of thermal expansion in actual structural materials is a nonlinear function of temperature. In some cases, this coefficient can approximately double over a thousand-degree temperature range. However, not many structures have nearly that great a temperature

⁴ Some analysts decry such phrases as “thermally induced stresses,” “thermal stresses,” “stresses due to temperature changes,” and the like. Their correct view is that temperature changes produce strains, and it is the constraints on the system, such as boundary conditions, or the indeterminacy of the structure itself that produce the stresses by prohibiting the free expansion of the material. However, using these phrases is a matter of common convenience at the expense of perhaps obscuring the actual origins of these stresses.

variation. Thus, when the temperature distribution is far less severe, it is almost always the case that the use of a constant coefficient of thermal expansion produces a negligible error. The constant coefficient to be used is, of course, the average value for the temperature range.

Finally, note that neither time nor stress rate nor strain rate have any place as variables in the description of the relation between strains and stresses for the linearly elastic, orthotropic material model. This fact, of course, restricts the use of this mathematical model to those situations where it is indeed possible to ignore those facets of the material problem. Now that all the contributions to the material model from stresses and temperature changes have been identified, these contributions can be combined together to form the complete *strain-stress equations* for the orthotropic material. When cast into matrix form, these equations in terms of coordinates aligned with the material axes are

$$\{\gamma\} = [S]\{\sigma\} + \Delta T\{\alpha\} \quad (6.1)$$

where

$$\begin{aligned} \{\gamma\}^t &= [\epsilon_{xx} \quad \epsilon_{yy} \quad \epsilon_{zz} \quad \gamma_{xy} \quad \gamma_{xz} \quad \gamma_{yz}] \\ \{\sigma\}^t &= [\sigma_{xx} \quad \sigma_{yy} \quad \sigma_{zz} \quad \sigma_{xy} \quad \sigma_{xz} \quad \sigma_{yz}] \\ \{\alpha\}^t &= [\alpha_x \quad \alpha_y \quad \alpha_z \quad 0 \quad 0 \quad 0] \end{aligned}$$

and

$$[S] = \begin{bmatrix} 1/E_x & -\nu_{yx}/E_y & -\nu_{zx}/E_z & 0 & 0 & 0 \\ -\nu_{xy}/E_x & 1/E_y & -\nu_{zy}/E_z & 0 & 0 & 0 \\ -\nu_{xz}/E_x & -\nu_{yz}/E_y & 1/E_z & 0 & 0 & 0 \\ \hline 0 & 0 & 0 & 1/G_{xy} & 0 & 0 \\ 0 & 0 & 0 & 0 & 1/G_{xz} & 0 \\ 0 & 0 & 0 & 0 & 0 & 1/G_{yz} \end{bmatrix}$$

Note that the upper right and lower left 3×3 submatrices are null. This is the mathematical statement that, as discussed above, there is no interaction (coupling) between the normal stresses and longitudinal strains on the one hand, and the shearing stresses and strains on the other hand, when the coordinates axes are the same as the material axes of symmetry.

The 6×6 matrix above is called the *compliance matrix* (Ref. [19]), or the material flexibility matrix. Within the compliance matrix there appear three Young's moduli, three shear moduli, and six Poisson's ratios for a total of a dozen material properties. However, there are three relations among these material properties. Hence there are nine independent material properties, or material constants, that define an orthotropic material without counting the three coefficients of thermal expansion. The three relations among the 12 material constants are a result of the necessary symmetry of the compliance matrix.⁵ That symmetry requires the following relations among the three moduli of elasticity and the six Poisson's ratios

$$\frac{\nu_{xy}}{E_x} = \frac{\nu_{yx}}{E_y} \quad \frac{\nu_{xz}}{E_x} = \frac{\nu_{zx}}{E_z} \quad \frac{\nu_{zy}}{E_z} = \frac{\nu_{yz}}{E_y} \quad (6.2)$$

There are no relations among the shear moduli.

⁵ The proof of the symmetry of the compliance matrix is best dealt with by first proving Betti's reciprocal theorem. Because of the lengths of these two proofs, and their peripheral relation to the objectives of this text, they are both relegated to Appendix A, Section 2.

The single matrix equation, Eq. (6.1) is equivalent to six linear, algebraic equations for the strains in terms of the stresses. These six equations can be solved simultaneously for the stresses in terms of the strains. Alternatively, matrix algebra can be used to accomplish the same goal. In order to determine the stresses in terms of the strains using matrix algebra, premultiply both sides of Eq. (6.1) by the inverse of the compliance matrix:

$$[S]^{-1}\{\gamma\} = [S]^{-1}[S]\{\sigma\} + [S]^{-1}\Delta T\{\alpha\}$$

Solving for $\{\sigma\}$:

$$\{\sigma\} = [S]^{-1}\{\gamma\} - \Delta T[S]^{-1}\{\alpha\}$$

Introducing the symbol $[E]$ for the inverse of the compliance matrix, that is,

$$[E] \equiv [S]^{-1}$$

allows the above equation to be rewritten as

$$\{\sigma\} = [E]\{\gamma\} - \Delta T[E]\{\alpha\} \quad (6.3)$$

Equations (6.3) are called the orthotropic *stress-strain equations*, and $[E]$ is called the *material stiffness matrix*. Another name for either the strain-stress equations Eq. (6.1), or the stress-strain equations above, Eq. (6.3), or both, is the *constitutive equations*. It is a straightforward matter to determine the elements of the 6×6 material stiffness matrix by inverting the compliance matrix. The results of the matrix inversion are

$$\begin{aligned} \mathcal{N}E_{11} &= E_x(1 - \nu_{xy}\nu_{yz}) & (\mathcal{N}E_{12} = \mathcal{N}E_{21}) &= E_x(\nu_{yx} + \nu_{zx}\nu_{yz}) \\ & & &= E_y(\nu_{xy} + \nu_{xz}\nu_{zy}) \\ \mathcal{N}E_{22} &= E_y(1 - \nu_{zx}\nu_{xz}) & (\mathcal{N}E_{13} = \mathcal{N}E_{31}) &= E_x(\nu_{zx} + \nu_{yx}\nu_{zy}) \\ & & &= E_z(\nu_{xz} + \nu_{xy}\nu_{yz}) \\ \mathcal{N}E_{33} &= E_z(1 - \nu_{xy}\nu_{yx}) & (\mathcal{N}E_{23} = \mathcal{N}E_{32}) &= E_y(\nu_{zy} + \nu_{xy}\nu_{zx}) \\ & & &= E_z(\nu_{yz} + \nu_{yx}\nu_{xz}) \end{aligned}$$

where

$$\mathcal{N} = 1 - \nu_{xy}\nu_{yx} - \nu_{xz}\nu_{zx} - \nu_{yz}\nu_{zy} - 2\nu_{xz}\nu_{zy}\nu_{yx}$$

and

$$E_{44} = G_{xy} \quad E_{55} = G_{xz} \quad E_{66} = G_{yz}$$

and all other elements of $[E]$ are zero. Remember that the above values for the elements of the material stiffness matrix, like those of the compliance matrix, are only valid when the Cartesian coordinate system is aligned with the axes inherent in the material.

6.3 Isotropic and Other Linearly Elastic Materials

An *isotropic material* is a material that has the same mechanical and thermal properties in all directions. In other words, all axes within the material are axes of material symmetry just as any diameter is an axis of symmetry for a circle. A metal casting would be an example of an isotropic material. Rolled metals usually have a slight degree of orthotropy. Hence the designations *L* (longitudinal) and *LT* (long transverse) for rolled sheet and plate products in Mil Handbook Five. However, the degree of orthotropy for the directional Young's moduli and Poisson's ratios is usually much less than the

differences between the tensile and compressive moduli of elasticity, and much less than the error in saying that strain is proportional to stress up to the yield stress rather than the proportional limit. Therefore, engineering practice is to model structural metals as isotropic materials. The constitutive equations for an isotropic material can be obtained from those for an orthotropic material simply by discarding all the directional subscripts attached to the material constants. Thus the isotropic compliance matrix and the isotropic material stiffness matrix involve but a single Young's modulus, shear modulus, and Poisson's ratio. Since it is convenient to have the isotropic strain-stress equations readily available, they are reproduced below. In matrix form they are

$$\begin{Bmatrix} \epsilon_{xx} \\ \epsilon_{yy} \\ \epsilon_{zz} \\ \gamma_{xy} \\ \gamma_{xz} \\ \gamma_{yz} \end{Bmatrix} = \begin{bmatrix} 1/E & -\nu/E & -\nu/E & 0 & 0 & 0 \\ -\nu/E & 1/E & -\nu/E & 0 & 0 & 0 \\ -\nu/E & -\nu/E & 1/E & 0 & 0 & 0 \\ \hline 0 & 0 & 0 & 1/G & 0 & 0 \\ 0 & 0 & 0 & 0 & 1/G & 0 \\ 0 & 0 & 0 & 0 & 0 & 1/G \end{bmatrix} \begin{Bmatrix} \sigma_{xx} \\ \sigma_{yy} \\ \sigma_{zz} \\ \sigma_{xy} \\ \sigma_{xz} \\ \sigma_{yz} \end{Bmatrix} + \Delta T \begin{Bmatrix} \alpha \\ \alpha \\ \alpha \\ 0 \\ 0 \\ 0 \end{Bmatrix} \quad (6.4)$$

or, as before,

$$\{\gamma\} = [S]\{\sigma\} + \Delta T\{\alpha\}$$

The stress-strain equations are sometimes written in another form because even when all the directional subscripts are deleted, the expressions for each matrix element still make for a crowded matrix. In the more compact terms of the Lamé constants λ and μ , the stress-strain equations are, where $e = \epsilon_{xx} + \epsilon_{yy} + \epsilon_{zz}$

$$\begin{aligned} \sigma_{xx} &= \lambda e + 2\mu\epsilon_{xx} - (3\lambda + 2\mu)\alpha\Delta T & \sigma_{xy} &= G\gamma_{xy} \\ \sigma_{yy} &= \lambda e + 2\mu\epsilon_{yy} - (3\lambda + 2\mu)\alpha\Delta T & \sigma_{xz} &= G\gamma_{xz} \\ \sigma_{zz} &= \lambda e + 2\mu\epsilon_{zz} - (3\lambda + 2\mu)\alpha\Delta T & \sigma_{yz} &= G\gamma_{yz} \end{aligned} \quad (6.5)$$

The Lamé constants are related to Young's modulus and Poisson's ratio by the following equations:

$$\begin{aligned} \lambda &= \frac{\nu E}{(1 + \nu)(1 - 2\nu)} & E &= \frac{\mu(3\lambda + 2\mu)}{\lambda + \mu} \\ \mu &= \frac{E}{2(1 + \nu)} & \nu &= \frac{\lambda}{2(\lambda + \mu)} \end{aligned} \quad (6.6)$$

For the record, the longitudinal strain-normal stress equations in terms of the Lamé constants are

$$\begin{aligned} 2\mu\epsilon_{xx} &= \sigma_{xx} - \lambda \frac{\sigma_{xx} + \sigma_{yy} + \sigma_{zz}}{3\lambda + 2\mu} + 2\mu\alpha\Delta T \\ 2\mu\epsilon_{yy} &= \sigma_{yy} - \lambda \frac{\sigma_{xx} + \sigma_{yy} + \sigma_{zz}}{3\lambda + 2\mu} + 2\mu\alpha\Delta T \\ 2\mu\epsilon_{zz} &= \sigma_{zz} - \lambda \frac{\sigma_{xx} + \sigma_{yy} + \sigma_{zz}}{3\lambda + 2\mu} + 2\mu\alpha\Delta T \end{aligned} \quad (6.7)$$

As previously noted, in the case of the orthotropic material model there are three relations between the material constants of the compliance matrix that are a result of the required symmetry of that matrix. The proof that the material stiffness matrix is also symmetric is

left as an exercise. The isotropic compliance and material stiffness matrices are identically symmetric, so there is nothing to be learned from matrix symmetry. Thus it appears that there are three material constants that are required to describe an isotropic material: either the set E , ν , and G , or the set λ , μ , and G . However, in actuality, there are only two independent material constants for an isotropic material. This may be proved as follows. Consider an arbitrarily shaped isotropic structural body subjected to an arbitrary set of loads and temperature changes. Choose a Cartesian coordinate system that is aligned with the axes of principal strain at the point under consideration. Then, from Eq. (4.9c) (or from Eq. (2.2) and the analogy between stresses and Green strains in all coordinate rotation equations), the shearing strain in any Cartesian coordinate system rotated with respect to the axes of the principal strains is

$$\gamma_{xy}^* = 2(\epsilon_{11} c_{xx} c_{yx} + \epsilon_{22} c_{xy} c_{yy} + \epsilon_{33} c_{xz} c_{yz})$$

where, again, numerical subscripts on stresses and strains indicate principal values. Now note, from Eq. (6.4), that for an isotropic material the axes for principal strains are always the same as the axes for principal stresses. Thus when the principal strains are inserted into the strain–stress equations, the stresses of these same strain–stress equations must be principal stresses. Extracting the first three strain–stress equations (rows) from the matrix equation, which is Eq. (6.4), and using them to substitute for the strains in the above equation leads to

$$\begin{aligned} \gamma_{xy}^* &= \frac{2}{E}(\sigma_{11} c_{xx} c_{yx} + \sigma_{22} c_{xy} c_{yy} + \sigma_{33} c_{xz} c_{yz}) \\ &\quad - \frac{2\nu}{E}[(\sigma_{22} + \sigma_{33}) c_{xx} c_{yx} + (\sigma_{11} + \sigma_{33}) c_{xy} c_{yy} + (\sigma_{11} + \sigma_{22}) c_{xz} c_{yz}] \\ &\quad + 2\alpha\Delta T(c_{xx} c_{yx} + c_{xy} c_{yy} + c_{xz} c_{yz}) \end{aligned}$$

The last expression, the one with the temperature change factor, can be shown to be zero by writing the dot product of $\mathbf{i}^* = c_{xx}\mathbf{i} + c_{xy}\mathbf{j} + c_{xz}\mathbf{k}$ and $\mathbf{j}^* = c_{yx}\mathbf{i} + c_{yy}\mathbf{j} + c_{yz}\mathbf{k}$ where each of these orthogonal unit vectors in the rotated coordinate system is written in terms of the direction cosines between the rotated and original coordinate systems. Having thus eliminated the third term, focus on the second term. One of the guides to successful algebraic manipulation is to seek symmetries of expression where these are readily available. The second term has three sums of pairs of the principal stresses. If the omitted principal stress is added to each of those pairs, the term becomes algebraically symmetric. To accomplish this goal, add the following expression that is *identically* zero to the right-hand side:

$$\begin{aligned} &\frac{2}{E}[\nu\sigma_{11} c_{xx} c_{yx} + \nu\sigma_{22} c_{xy} c_{yy} + \nu\sigma_{33} c_{xz} c_{yz} - \nu\sigma_{11} c_{xx} c_{yx} \\ &\quad - \nu\sigma_{22} c_{xy} c_{yy} - \nu\sigma_{33} c_{xz} c_{yz}] \end{aligned}$$

Grouping the positive parts of the above expression with the first of the two remaining parts of the equation for γ_{xy}^* , and the negative terms with the second part, leads to

$$\begin{aligned} \gamma_{xy}^* &= \frac{2(1+\nu)}{E}(\sigma_{11} c_{xx} c_{yx} + \sigma_{22} c_{xy} c_{yy} + \sigma_{33} c_{xz} c_{yz}) \\ &\quad - \frac{2\nu}{E}(\sigma_{11} + \sigma_{22} + \sigma_{33})(c_{xx} c_{yx} + c_{xy} c_{yy} + c_{xz} c_{yz}) \end{aligned}$$

The same zero sum of direction cosines eliminates the new second term. Now note that from Eq. (2.2), where the original axes in this case are principal axes, the stress and direction cosine terms within the parentheses sum to σ_{xy}^* . Thus

$$\gamma_{xy}^* = [2(1+\nu)/E]\sigma_{xy}^*$$

Moreover, for an isotropic material, the relation $\gamma_{xy}^* = \sigma_{yx}^*/G$ is also always true regardless of the orientation of the orthogonal coordinates. Equating these last two expressions for γ_{xy}^* yields the general isotropic relation between the three material constants

$$G = \frac{E}{2(1 + \nu)} \quad (6.8)$$

Hence the conclusion is that there are only two independent material constants for an isotropic material. From Eq. (6.6), it is apparent that the Lamé constant μ is the same as the shear modulus. Therefore, in terms of the Lamé constants, the two independent material parameters are λ and μ .

The final item of business for isotropic materials is to note that there are bounds on the possible values of Poisson's ratio. First of all, no homogeneous, isotropic material is known or imagined which expands in a direction perpendicular to the direction in which it is stretched, or that contracts in a direction perpendicular to the direction in which it is compressed [see Endnote (1)]. Thus it is concluded that Poisson's ratio cannot be a negative number. An upper bound for Poisson's ratio can be determined by considering a finite or differential-sized rectangular parallelepiped subjected to a state of hydrostatic pressure, P_0 , without any temperature change. Since there are no shear stresses, it should be clear that each principal stress has the value $-p_0$. Substituting these principal stress values into the isotropic strain-stress equations shows that there are no shear strains, and each principal strain has the value $-(1 - 2\nu)p_0/E$. If Poisson's ratio could take on the values equal to, or greater than $\frac{1}{2}$, then the rectangular parallelepiped would not be compressed by the hydrostatic pressure. Indeed, if the Poisson's ratio were greater than $\frac{1}{2}$, the material would expand under the action of the hydrostatic pressure. Since no known material behaves that way, it is concluded that $\frac{1}{2}$ is an upper bound for Poisson's ratio; that is, for isotropic materials,

$$0 \leq \nu \leq 0.5 \quad (6.9)$$

If the value of Poisson's ratio is $\frac{1}{2}$, the material is incompressible. When a metal undergoes mostly plastic deformation, the value of Poisson's ratio closely approaches $\frac{1}{2}$.

Note that the above bounds on Poisson's ratio only apply to an isotropic material. The values of the Poisson's ratios for orthotropic materials can and do exceed $\frac{1}{2}$ and even 1. It is also possible to develop bounds for the material constants of an orthotropic material based upon the observation that the compliance matrix has to be a positive definite matrix.⁶

Now that orthotropic and isotropic materials have been dealt with, the discussion of types of linearly elastic materials can be concluded by mentioning two other material models. An *anisotropic material* is one which has no axes or planes of material symmetry. This means that all stresses and strains interact with all other stresses and strains regardless of the coordinate axes chosen so that, in general, the compliance matrix has no zeros. Since the 6×6 compliance matrix is symmetric, there are 21 material constants that need to be determined in order to fully specify the behavior of such a material. No homogeneous material can be offered as an example of an anisotropic material. The usefulness of the

⁶ A positive definite matrix can be defined as a square matrix $[p]$ such that for all compatible vectors $\{x\}$, the triple product $\{x\}[p]\{x\} > 0$ whenever $\{x\}$ is not null. Two useful theorems pertaining to positive definite matrices, from Ref. [20], are that all their eigenvalues are positive, and the determinants of all sizes included within the matrix and centered upon the principal diagonal of the matrix are positive. This includes the individual elements on the principal diagonal, this latter theorem is the source of the inequalities for the orthotropic material constants.

concept of an anisotropic material is generally limited to that of being the most general case for a linearly elastic material. A *transversely isotropic material* is a material for which there is one plane where the mechanical and thermal properties are the same in all directions within that plane. This is merely a special case of an orthotropic material, where, for example, the properties in the x and y directions are the same, but are different in the z direction. The result of several bonded fiber composite plies with the same alignment, stacked on top of each other, is closely approximated by the transversely isotropic model. Five material constants are required to define such a model, and therefore five material tests are needed to determine the values of those five constants.

6.4 The Plane Stress Constitutive Equations

For the case of plane stress, the full three-dimensional orthotropic strain–stress equations for the coordinate axes of material symmetry reduce to the following matrix form:

$$\begin{Bmatrix} \epsilon_{xx} \\ \epsilon_{yy} \\ \gamma_{xy} \end{Bmatrix} = \begin{bmatrix} 1/E_x & -\nu_{yx}/E_y & 0 \\ -\nu_{xy}/E_x & 1/E_y & 0 \\ 0 & 0 & 1/G_{xy} \end{bmatrix} \begin{Bmatrix} \sigma_{xx} \\ \sigma_{yy} \\ \sigma_{xy} \end{Bmatrix} + \Delta T \begin{Bmatrix} \alpha_x \\ \alpha_y \\ 0 \end{Bmatrix} \quad (6.10)$$

with the auxiliary equations $\gamma_{xz} = \gamma_{yz} = 0$, and

$$\epsilon_{zz} = -\frac{\nu_{xz}}{E_x} \sigma_{xx} - \frac{\nu_{yz}}{E_y} \sigma_{yy} + \alpha_z \Delta T \quad (6.11)$$

The inversion of the above equations to obtain the stress–strain equations produces the result

$$\begin{Bmatrix} \sigma_{xx} \\ \sigma_{yy} \\ \sigma_{xy} \end{Bmatrix} = \frac{1}{(1 - \nu_{xy}\nu_{yx})} \begin{bmatrix} E_x & \nu_{yx}E_x & 0 \\ \nu_{xy}E_y & E_y & 0 \\ 0 & 0 & G_{xy}(1 - \nu_{xy}\nu_{yx}) \end{bmatrix} \begin{Bmatrix} \epsilon_{xx} \\ \epsilon_{yy} \\ \gamma_{xy} \end{Bmatrix} - \frac{\Delta T}{(1 - \nu_{xy}\nu_{yx})} \begin{Bmatrix} \alpha_x E_x + \alpha_y \nu_{xy} E_y \\ \alpha_y E_y + \alpha_x \nu_{yx} E_x \\ 0 \end{Bmatrix} \quad (6.12)$$

Again, the isotropic equations can easily be obtained from the orthotropic equations by the simple expedient of dropping all the directional subscripts. Since the orthotropic stress–strain equations stated above are a bit lengthy, the isotropic result is recorded as

$$\begin{Bmatrix} \sigma_{xx} \\ \sigma_{yy} \\ \sigma_{xy} \end{Bmatrix} = \frac{E}{1 - \nu^2} \begin{bmatrix} 1 & \nu & 0 \\ \nu & 1 & 0 \\ 0 & 0 & \frac{1}{2}(1 - \nu) \end{bmatrix} \begin{Bmatrix} \epsilon_{xx} \\ \epsilon_{yy} \\ \gamma_{xy} \end{Bmatrix} - \frac{E\alpha\Delta T}{1 - \nu} \begin{Bmatrix} 1 \\ 1 \\ 0 \end{Bmatrix} \quad (6.13)$$

In order to keep the number of symbols to a minimum, the plane stress compliance and matrix stiffness matrices are denoted with the same $[S]$ and $[E]$ symbols, respectively.

6.5 **Applications to Fiber Composites**

Recall that a fiber composite laminate is a stack of bonded plies, and a ply is a thin sheet of unidirectional fibers in a bonding material called the matrix. In other words, the

laminate is to the plies as plywood is to wood plies. The individual fiber composite plies of a laminate are generally modeled as being in a state of plane stress. The material axes of the individual plies are not necessarily rotationally aligned with the coordinate axes that are chosen to best represent the geometry of the laminate. In order to discuss Cartesian coordinate rotations for individual plies, let each ply axis be an "original" axis, and let the laminate axis be the "rotated" axis. Recall that the orthotropic constitutive equations stated above, Eqs. (6.10) and (6.11), are only valid for the material axes of the fiber composite plies. Thus, once again it is necessary to use the rotation equations developed initially in Chapter 2 in order to obtain the constitutive relations for the plies in terms of the laminate coordinate system. Casting Eqs. (2.6) into matrix form yields

$$\begin{Bmatrix} \sigma_{xx}^* \\ \sigma_{yy}^* \\ \sigma_{xy}^* \end{Bmatrix} = \begin{bmatrix} \cos^2 \theta & \sin^2 \theta & 2 \sin \theta \cos \theta \\ \sin^2 \theta & \cos^2 \theta & -2 \sin \theta \cos \theta \\ -\sin \theta \cos \theta & \sin \theta \cos \theta & (\cos^2 \theta - \sin^2 \theta) \end{bmatrix} \begin{Bmatrix} \sigma_{xx} \\ \sigma_{yy} \\ \sigma_{xy} \end{Bmatrix} \quad (6.14)$$

which can be written concisely as $\{\sigma^*\} = [R(\theta)]\{\sigma\}$

Recall that the angle θ is positive counterclockwise from the original material axes (without asterisks) to the laminate axes (with asterisks). The exact analogy between the rotation of the Green strains and the rotation of stresses, after converting from the Green shearing strains to the engineering shearing strains, produces the rotation equation for fiber composite strains as

$$\begin{Bmatrix} \epsilon_{xx}^* \\ \epsilon_{yy}^* \\ \gamma_{xy}^* \end{Bmatrix} = \begin{bmatrix} \cos^2 \theta & \sin^2 \theta & \sin \theta \cos \theta \\ \sin^2 \theta & \cos^2 \theta & -\sin \theta \cos \theta \\ -2 \sin \theta \cos \theta & 2 \sin \theta \cos \theta & \cos^2 \theta - \sin^2 \theta \end{bmatrix} \begin{Bmatrix} \epsilon_{xx} \\ \epsilon_{yy} \\ \gamma_{xy} \end{Bmatrix} \quad (6.15)$$

This equation can be written concisely as $\{\gamma^*\} = [r(\theta)]\{\gamma\}$, where γ is used to represent the 3×1 vector of strains in order to make clear that the shearing strain term is the engineering shearing strain rather than the Green shearing strain. Note that the differences between $[R]$ and $[r]$ are limited to factors of 2 between some of the off-diagonal terms, which of course are a result of the conversion from Green's strains to engineering strains. It is easy to observe that

$$[R(-\theta)]^t = [r(\theta)] \quad \text{and} \quad [r(-\theta)]^t = [R(\theta)]$$

It is necessary to obtain the inverse of the rotation matrix $[r(\theta)]$. The inverse relation between the two strain vectors is (see additional exercises)

$$\begin{Bmatrix} \epsilon_{xx} \\ \epsilon_{yy} \\ \gamma_{xy} \end{Bmatrix} = \begin{bmatrix} \cos^2 \theta & \sin^2 \theta & -\sin \theta \cos \theta \\ \sin^2 \theta & \cos^2 \theta & \sin \theta \cos \theta \\ 2 \sin \theta \cos \theta & -2 \sin \theta \cos \theta & \cos^2 \theta - \sin^2 \theta \end{bmatrix} \begin{Bmatrix} \epsilon_{xx}^* \\ \epsilon_{yy}^* \\ \gamma_{xy}^* \end{Bmatrix} \quad (6.16)$$

As might be expected by considering exactly what is accomplished by these rotation matrices, the inverse of the matrix $[r(\theta)]$ is equal to the matrix $[r(-\theta)] = [R(\theta)]^t$. The same thing is true for the $[R(\theta)]$ matrix, that is, its inverse equals $[R(-\theta)] = [r(\theta)]^t$. Thus Eq. (6.16) can be rewritten as

$$\{\gamma\} = [r(-\theta)]\{\gamma^*\} \quad (6.16a)$$

Equations (6.14) and (6.16a) can now be used to write the stress-strain equation for a fiber composite ply for any coordinate axes, and in particular, the coordinate axes of the laminate. Premultiplying Eq. (6.12) by $[R(\theta)]$, replacing $\{\gamma\}$ by $[r(-\theta)]\{\gamma^*\} = [R(\theta)]^t\{\gamma^*\}$,

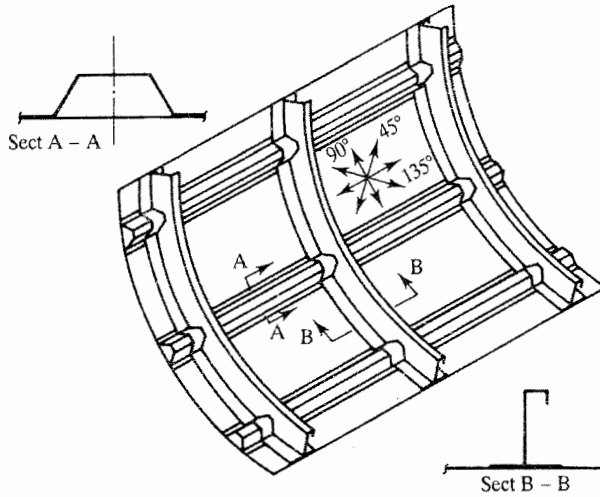


Figure 6.2. Structural design features for a central portion of a fuselage built of fiber composites. Courtesy of the Aerospace Structures Information and Analysis Center.

and noting Eq. (6.14), yields

$$\begin{aligned} \{\sigma^*\} &= [R(\theta)][E][R(\theta)]^t\{\gamma^*\} - [R(\theta)]\{A\}\Delta T \\ &= [E^*]\{\gamma^*\} - \{A^*\}\Delta T \end{aligned} \quad (6.17)$$

where the definitions of the material stiffness matrix and the thermal expansion matrix in the laminate (rotated) coordinates, $[E^*]$ and $\{A^*\}$ respectively, are obvious. Clearly the material stiffness matrix of this general stress–strain equation for an orthotropic material in a state of plane stress is one that is generally without zero elements. Similarly,

$$\begin{aligned} \{\gamma^*\} &= [r(\theta)][S][R(-\theta)]\{\sigma^*\} + [r(\theta)]\{\alpha\}\Delta T \\ &= [S^*]\{\sigma^*\} + \{\alpha^*\}\Delta T \end{aligned} \quad (6.18)$$

Note that $[S^*]$ is a symmetric matrix because

$$[S^*] = [r(\theta)][S][R(-\theta)] = [r(\theta)][S][r(\theta)]^t$$

The latter form clearly shows that $[S^*] = [S^*]^t$. Of course, this same conclusion may be drawn for $[E^*]$. The use of composite laminates to form a portion of an aircraft structure is illustrated in Fig. 6.2.

6.6 Summary

For a broad class of materials, this chapter establishes the mathematical link between stresses and strains. This link closes the chain connecting prescribed boundary tractions to stresses to strains to displacements to prescribed boundary displacements. That final link, called the constitutive equations, was forged by developing a linearly elastic material model that closely approximates the behavior of actual structural materials when the stresses are limited to values that do not produce appreciable plastic deformations. The first two features of the linearly elastic material model, (i) the straight-line relation between strain and stress, and (ii) the congruence of the loading and unloading paths, make the constitutive equations linear algebraic, and single-valued. The third and last feature of the

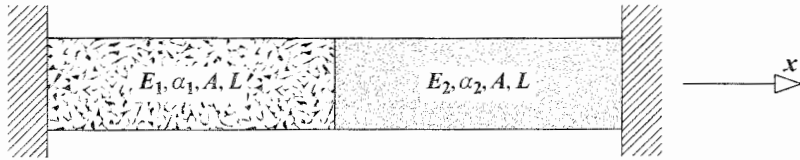


Figure 6.3. Example 6.2. A heated bimetallic bar.

linearly elastic material model, the storage of all work done on the material as elastic energy, is a result of the congruence of the loading and unloading paths and the absence of heat generation in the elastic stress range. This last feature has considerable importance and is developed further in Part IV.

There are only two important types of linearly elastic materials. These two types of materials are called orthotropic and isotropic. Orthotropic materials have a (usually clearly evident) material structure that consists of three orthogonal planes of symmetry. The intersections of these planes of symmetry are called the material axes. Orthotropic materials have different properties in the different material axis directions. The orthotropic constitutive equations are complicated by the presence of nine independent material constants, not counting the three coefficients of thermal expansion. In stark contrast, an isotropic material, which is a material that has the same properties in all directions, has only two independent material constants, plus a single coefficient of thermal expansion. The isotropic material constitutive equations can be developed exactly the same way as those equations are developed for an orthotropic material, or the orthotropic results can be converted to the isotropic case by removal of all directional subscripts on the material constants.

The things the reader needs to take away from this chapter are primarily (i) familiarity with the stress–strain and strain–stress equations, particularly those for plane stress; and (ii) the idea that thermal strains are always present whenever there is a temperature change.

Example 6.2. The bimetallic bar shown in Fig. 6.3 is heated so that it undergoes a uniform temperature change $+T_0$. If the ends of the bar are restrained from any axial movement, and the geometry of the bar is uniform, what then is the stress in the bar. Base your analysis on the assumption that the bar does not buckle. *Hint:* It is here necessary to write an equilibrium equation, material equations, and strain–displacement equations.

Solution. A free body diagram at the juncture of the two different materials shows that since the axial forces in the two halves are the same, and since the cross-sectional areas are the same, $\sigma_1 = \sigma_2 = \sigma$. Without any loss of generality, assume that $\alpha_1 > \alpha_2$. Then the juncture at $x = L$ moves to the right an unknown distance u_0 . Therefore, $\epsilon_1 = u_0/L$, and $\epsilon_2 = -u_0/L$. Since $\epsilon_1 = (\sigma/E_1) + \alpha_1 T_0$, and $\epsilon_2 = (\sigma/E_2) + \alpha_2 T_0$, from the relationship $\epsilon_1 = -\epsilon_2$, $(\sigma/E_1) + \alpha_1 T_0 = -(\sigma/E_2) - \alpha_2 T_0$. After solving this equation for the stress, the result is

$$\sigma = -\frac{E_1 E_2}{E_1 + E_2} (\alpha_1 + \alpha_2) T_0 \quad \blacksquare$$

Chapter 6 Exercises

- 6.1. Determine the strain–stress relations of an isotropic material for a cylindrical coordinate system.

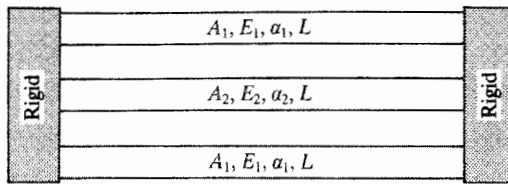


Figure 6.4. Exercise 6.5. A symmetrical three-bar structure.

- 6.2. (a) In Appendix A it is proved that the compliance matrix for an orthotropic material must be symmetric. The equations in this chapter reflect the symmetry of that compliance matrix and its inverse, the material stiffness matrix. Prove the general theorem that the inverse of any symmetric matrix is also symmetric. *Hint:* Given $[S] = [S]^t$, prove $[E] = [E]^t$ where $[E] = [S]^{-1}$. Start with the identity matrix $[I] = [S][E]$, and transpose this last expression. Then there are two more steps.
- (b) When are the directions of the principal stresses the same as the directions of the principal strains in an isotropic material?
- (c) When are the directions of the principal stresses the same as the directions of the principal strains in an orthotropic material?
- 6.3. For the case of plane stress, determine the expression for the strain ϵ_{zz} in terms of the other two longitudinal strains for the case of an isotropic material.
- 6.4. From the following data, determine the value of σ_{xy} . (Present your answer using the appropriate number of significant figures.) The material is isotropic. $\alpha \Delta T = 12 \times 10^{-4}$ in/in, $E = 10 \times 10^6$ psi, Poisson's ratio = 0.30, and $[\gamma] = [15. \ 1.5 \ 2.0 \ 10. \ 15. \ 3.0] \ 10^{-4}$.
- 6.5. Consider the simple structure composed of three isotropic bars capped by rigid fixtures as shown in Fig. 6.4. The rigid caps can move without rotation in the direction of the bar axes. At the original temperature of this structure, the structure was stress-free. What are the stresses in the bars when the three bars experience a uniform temperature change equal to the value T_0 ? Should and does your answer say that the stresses are zero when the two coefficients of thermal expansion are equal? *Hint:* Be sure to write equilibrium equations for the bars and the bar caps, a strain compatibility equation based upon the displacements of the system, and the two constitutive equations, one for each material. Then you will have sufficient equations to determine all unknowns.

FOR THE EAGER

- 6.6. One step in the calculation of the inverse of a square matrix is the determination of the determinant of the matrix. Calculate the determinant of the rotation matrix $[r(\theta)]$.
- 6.7. In the development of Eq. (6.17), the column matrices $\{A\}$ and $\{A^*\}$ appear. What are the elements of these matrices? What is $\{\alpha^*\}$ in Eq. (6.18)?
- 6.8. If the middle bar of the structure of Exercise 6.5 was miscut so that it is a distance $\delta \ll L$ longer than the twin outer bars, but is forced to fit into the structure with the outer bars, then what are the stresses in the bars? (The stress due to a misfit is one example of a "residual stress.")

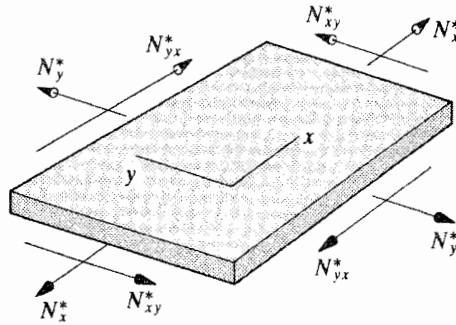


Figure 6.5. Exercise 6.11. The sign convention for in-plane stress resultants, that is, for in-plane normal and shearing forces per unit of edge length.

- 6.9. An isotropic material has the same properties in all directions. This may mean that the compliance matrix and the material stiffness matrix of the isotropic constitutive equations are exactly the same irrespective of the choice of orthogonal axes. To investigate the question, consider the case of plane stress where the material stiffness matrix is $[E]$. The material stiffness matrix for rotated axes is $[E^*] = [R(\theta)][E][r(-\theta)]$.
- (a) Should the isotropic material stiffness matrix be the same for any choice of coordinate axes, that is, $[E^*] = [E]$? If not, why not?
- (b) For the plane stress case cited above, is $[E^*]$ actually equal to $[E]$?
- 6.10. Confirm or deny that the plane strain $\sigma - \epsilon$ equations are

$$(1 - 2\nu)\sigma_{xx} = \frac{E}{1 + \nu}[(1 - \nu)\epsilon_{xx} + \nu\epsilon_{yy}] - E\alpha\Delta T$$

$$(1 - 2\nu)\sigma_{yy} = \frac{E}{1 + \nu}[\nu\epsilon_{xx} + (1 - \nu)\epsilon_{yy}] - E\alpha\Delta T$$

$$\sigma_{xy} = \frac{E\gamma_{xy}}{2(1 + \nu)}$$

FOR THE ESPECIALLY EAGER

- 6.11. Consider a laminate of $2N$ plies where the ply orientations and thicknesses are symmetric about the midplane of the laminate. Let the laminate be loaded in the plane of the laminate as shown in Fig. 6.5 where the quantities N_x , N_y , and $N_{xy} = N_{yx}$ are the forces per unit of edge length in the directions indicated. (Each force per unit of edge length is equal to the corresponding traction multiplied by the total thickness of the laminate.) Since the laminate is symmetric, the top half and bottom half equally share the uniformly applied loads, so that the laminate only stretches, or contracts, and shears, rather than bends or twists. Thus all the strains are the plane stress type strains of the 3×1 column matrix $\{\gamma\}$ previously discussed. Thus the equation of equilibrium becomes, summing the stresses over the thicknesses, t , of the $2N$ plies with the index p .

$$2 \sum_{p=1}^N t_p \{\sigma^{(p)*}\} = \{N^*\}$$

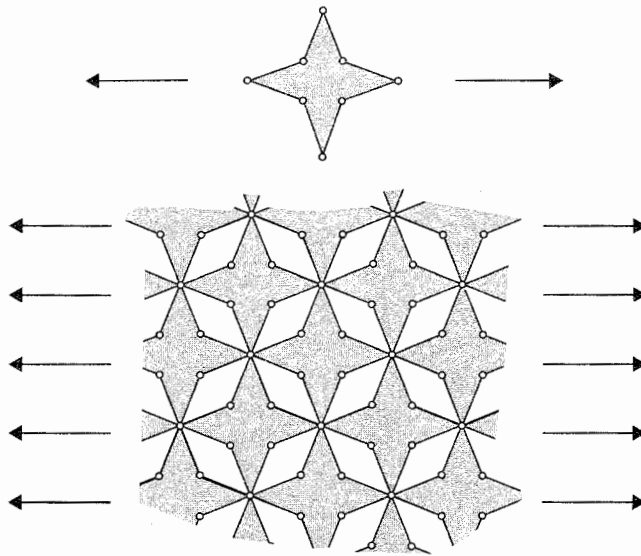
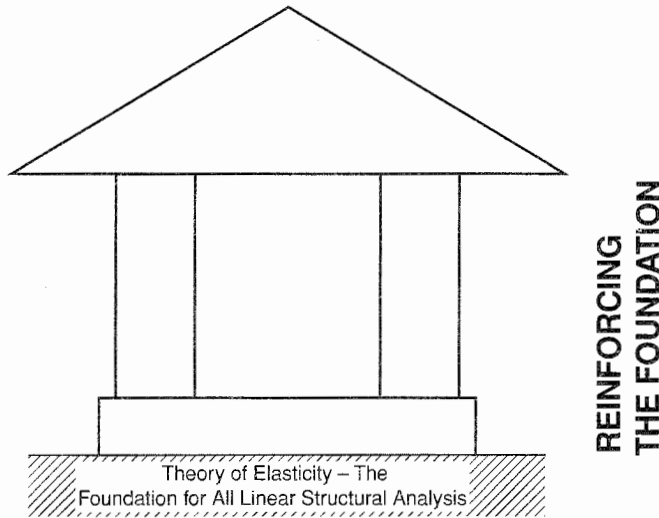


Figure 6.6. Visualization of a material microstructure as a series of hinged bar segments that require vertical expansion in response to a horizontal expansion.

where the asterisk indicates the laminate coordinate axes. Put this equilibrium equation together with the stress–strain matrix equations for each bonded ply in the laminate coordinate system. Then use appropriate strain compatibility equations to determine the stress in each ply in the ply coordinate system.

Endnote (1) Negative Poisson Ratios

As reported in the May 1989 issue of *Design News*, negative Poisson ratios (-0.1 to -0.7) have proved possible for polyurethane foams that have what is called a “reentrant” microarchitecture. A simple explanation of that three-dimensional microarchitecture can be based on the eight bar, pinned mechanism shown in Fig. 6.6. Forcing apart the outer left-hand and right-hand hinges straightens and thus expands the top and bottom links. The same happens to the links on the left and right sides. Hence there is expansion in the two orthogonal directions. This foam is not a homogeneous material. Thus there is no contradiction with the previous discussion.

****INTRODUCTION TO THE THEORY
OF ELASTICITY******II.1 Introduction**

There are only two chapters in this optional part of the textbook. Chapters 7 and 8 simply provide examples in different circumstances of putting together the four basic sets of equations for a stress formulation (the equilibrium equations, compatibility equations, the strain–stress material equations, and the stress boundary conditions) or a displacement formulation (the equilibrium equations, the stress–strain constitutive equations, the strain–displacement equations, and the displacement or stress boundary conditions).

This section is labeled optional for two reasons. The first and foremost reason is that the type of problems that are solved in Part II, particularly those of Chapter 8, in which the geometry of the structural element involves straight line (planar) boundaries, are more easily, indeed routinely, solved by the finite element method, which is presently the dominant approximate method of structural analysis. Only the very simple circular geometries of Chapter 7 offer a rare exception to the rule, which is to use the finite element method and forget the exact solutions offered in these two chapters and elsewhere. The second reason that this part of the textbook is optional is because it is expected that most, if not all, undergraduate curriculums cannot provide the time to consider this material, which, as mentioned, is far from the center of present engineering practice. Thus, the question arises as to why this material should be included at all. The first reason for its inclusion is that these exact solutions provide a basis for judging the accuracy of all the approximate methods of analysis that follow, including the finite element method. For example, the beam bending

solutions of Chapter 8 are referenced in Chapters 9 and 10. The second reason for including these exact solutions is that they possess a degree of elegance, and elegance is always to be appreciated.

Part II concludes with a series of fifty-six True–False questions intended as a review of the material of Parts I and II, but mostly Part I.

The Theory of Elasticity

7.1 Introduction

Chapters 1–6 developed (i) the general equilibrium equations from a free body diagram (FBD) of a differential rectangular parallelepiped taken from a structural body of any shape and material; (ii) the strain–displacement equations and the equivalent compatibility equations from the geometry of the deformations of the same parallelepiped; and finally (iii) the constitutive equations for the isotropic and orthotropic linearly elastic material models. Again, these three sets of equations, which apply over the interior of the structural body, are called the field or domain equations. The Cauchy equations, which relate the tractions and the stresses at the boundary, were also discussed at length, and mention was made of prescribed displacement equations that specify displacements at the boundary. Again, the Cauchy and the prescribed displacement equations are collectively called the boundary condition equations. Together, the three sets of field equations and the boundary condition equations form the four sets of equations that are the basis for what is called the *theory of elasticity*. This chapter demonstrates what can be done with these **four sets of equations**.

There are six unknown stresses, six unknown strains, and three unknown displacements throughout the domain (interior) of the structural body of interest. There are three equilibrium equations, six stress–strain equations, and six strain–displacement equations. Thus there are a total of 15 unknown stresses, strains, and displacements, and 15 independent equations relating those quantities. As is demonstrated later, another way of counting unknowns and equations is to use the compatibility equations in the tally, and thereby have no need to consider displacements. By this alternate approach there are the three equilibrium equations, the six strain–stress equations, and three (of six) independent compatibility equations. In other words, there are 12 independent equations (of 15 equations) for the 12 unknown stresses and strains. Thus, within the limits imposed on these equations (small displacements), it appears that the problem of determining the stresses, strains, and displacements is now completely formulated and open to solution. In the development below, this prospect is demonstrated to be fact. However, in broad classes of structural analysis problems, actually obtaining practical solutions for everyday structural engineering tasks may often require compromises as is seen in Part III.

There are two overall approaches that can be taken to formulating the theory of elasticity problem. The first approach is to combine the 15 equations in 15 unknown stress, strain, and displacement functions into a smaller number of equations with the same smaller number of unknowns. Combining equations is accomplished by substituting for, and thus eliminating, unknown functions. While such an approach generally makes more practical the simultaneous consideration of the resulting fewer number of equations, the value of this first approach is quite limited in the theory of elasticity. Some details of this first approach are considered in Endnote (1).

The second general approach to the theory of elasticity is simply to consider individually the four sets of equations of the first paragraph in some appropriate sequence. This second

approach is demonstrated in the next three sections of this chapter, where two relatively simple examples are presented. These example problems serve as a model for the individual application of each of the three sets of field equations and the boundary condition equations to any structural analysis problem. The advantage of this second approach is that it is often possible to simplify one or more of the four sets of equations by immediately tailoring those equation sets to the problem at hand. Chapter 8 provides additional example problem solutions in this same sequential analysis style in a different context.

7.2 A Theory of Elasticity Solution Using Stresses

The organization of the unknown stress, strain, and displacement functions for solution, in either a unified or sequential approach, is usually accomplished in just one of two mutually exclusive ways. These two formulations are known as the *stress formulation* and the *displacement formulation*. As the names imply, a stress formulation is a solution organized so that the remaining unknown functions are the stresses, while the displacement formulation uses the displacements as the remaining unknown functions. Both formulations require the use of stress equilibrium equations, but make different choices among the pairs of possibilities thereafter. Summaries showing how a problem can be formulated exclusively in terms of stresses or exclusively in terms of displacements follow.

The stress formulation builds upon:

1. The equilibrium equations in terms of stresses.
2. The compatibility equations in terms of strains.
3. The strain–stress equations.
4. Boundary conditions that only involve tractions. The tractions are related to the internal stresses via the Cauchy equations.

The solution process for the stress formulation is to use the strain–stress equations to substitute for the strains in the compatibility equations so as to obtain the combined equations entirely in terms of stresses. Then with the equilibrium and boundary condition equations that are already in terms of stresses, a solution for the stresses can be sought. This approach is limited to those circumstances where all the boundary conditions can be written entirely in terms of stresses, including zero valued-stresses.

The displacement formulation builds upon:

1. The equilibrium equations in terms of stresses.
2. The stress–strain equations.
3. The strain–displacement equations.
4. Boundary condition statements that involve either tractions, or prescribed displacements, or both.

The solution process for the displacement formulation is to use (i) the stress–strain equations to replace the stresses in the equilibrium equations with strains; (ii) the strain–displacement equations in order to write the combined equilibrium and constitutive equations in terms of displacements and thereby have the combined field equations entirely in terms of displacements; and (iii) use the same sequence of stress–strain and strain–displacement field equations to rewrite the traction boundary condition equations in terms of displacements. Then, with the prescribed displacement boundary conditions, all boundary condition equations, as well as the field equations, are in terms of displacements.

This section illustrates the individual, that is, the sequential use of all four sets of theory of elasticity equations in the solution of a problem where stresses are the unknown functions.

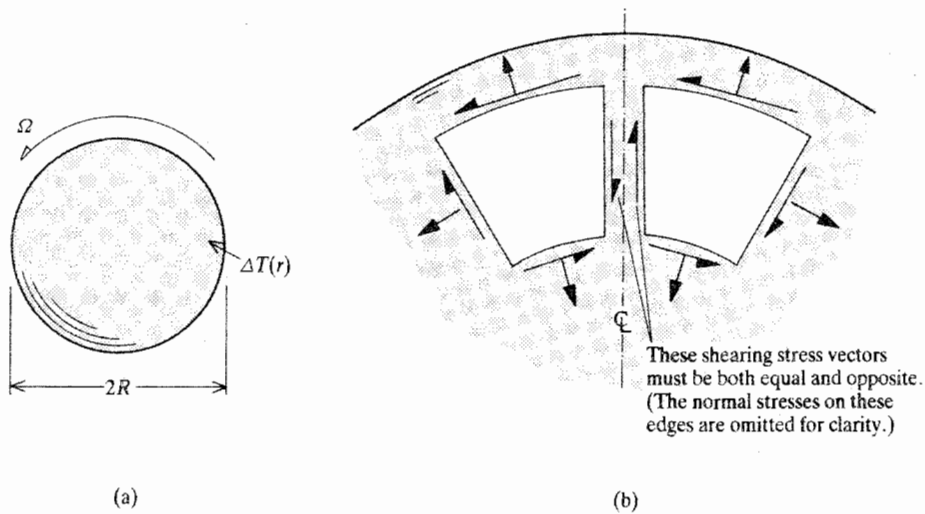


Figure 7.1. (a) The rotated and heated disk problem of Examples 7.1 and 7.2. (b) Example 7.1. A diagram of two side-by-side differential elements defined by cylindrical coordinates. This sketch is useful for deducing that the shearing stresses must everywhere be zero. In Example 7.2, a similar diagram of deformed, cylindrical coordinate, differential elements can be constructed to show that the shearing strains must everywhere be zero.

In the following section, the same problem is solved again using displacements as the unknown functions.

Example 7.1. Determine the stresses in a uniform, circular disk of radius R and thickness h that is rotating about its center at a constant angular velocity Ω , and is subjected to a temperature change that varies with radial distance only; see Fig. 7.1(a). Let the material of the disk be homogeneous, linearly elastic, and isotropic. Assume that the angular velocity, Ω , and the temperature change are sufficiently large that the effects of the body force due to the gravitational field are insignificant.

Comment. This problem can be regarded as a much simplified version of the problem of determining the stresses in a rotor disk of a turbine engine or the disk of a gyroscope. In particular, the geometry of the rotor or gyroscope disk, and the mechanical and thermal loading are greatly simplified. Such gross simplifications are often necessary in order to make it possible to obtain analytical solutions to the theory of elasticity equations. The solutions to such simplified problems can only serve as general guides to stress patterns in actual rotor disks. However, such guides are sometimes useful for design purposes, and such solutions also serve as guides for evaluating possible difficulties with approximate methods of analysis which can closely follow much more complicated geometries and loadings.

Solution. A stress formulation will be used to obtain the solution. The solution process can begin with the equilibrium equations in cylindrical coordinates. Cylindrical coordinates, of course, are appropriate for this geometry. The first thing to note is that there is no loading in the z direction, and neither the geometry nor the centrifugal loading nor temperature vary in the z direction. This permits the major simplification of recognizing this problem as a plane stress problem. Hence the solution begins by stating that $\sigma_{rz} = \sigma_{\theta z} = \sigma_{zz} = 0$. This is a tentative solution in the sense that it is now necessary to show that the remaining stresses

are capable of meeting all the solution requirements, such as all the boundary conditions. In this case they are able to do so. The equilibrium equations in polar coordinates are stated in Exercise 1.10 as two equations in terms of the three remaining stresses. Another vital simplification is obtained when the circular symmetry of the problem is recognized. That is, neither the geometry, nor the centrifugal loading, nor the temperature change vary with the angular coordinate, θ . The mathematical form of saying that nothing varies with θ is to say that all the partial derivatives with respect to θ are zero, and all unknown functions are only functions of the radial coordinate r . Hence the further conclusion that all the partial derivatives with respect to the radial coordinate are actually total derivatives. Thus the equilibrium equations reduce to the far less formidable form of the following two ordinary differential equations:

$$\begin{aligned} r \frac{d\sigma_{rr}}{dr} + \sigma_{rr} - \sigma_{\theta\theta} + r\rho B_r &= 0 \\ r \frac{d\sigma_{r\theta}}{dr} + 2\sigma_{r\theta}r\rho B_\theta &= 0 \end{aligned} \quad (7.1)$$

Clearly the next thing to do is determine the values of the body forces per unit mass (i.e., accelerations) B_r and B_θ . The centrifugal acceleration at any point on the disk is the product of the radial coordinate at that point and the square of the angular velocity, and of course, it is directed in the outward radial direction. Thus

$$B_r = r\Omega^2 \quad \text{and} \quad B_\theta = 0$$

Therefore the second equilibrium equation becomes

$$r \frac{d\sigma_{r\theta}}{dr} + 2\sigma_{r\theta} = 0$$

This latter ordinary differential equation is a rather simple one since it can be solved, for example, by separating the variables and integrating to obtain

$$\int \frac{d\sigma_{r\theta}}{\sigma_{r\theta}} = -2 \int \frac{dr}{r} + \text{constant}$$

or

$$\ln(\sigma_{r\theta}) = -2 \ln(r) + \ln(C_0)$$

or

$$\sigma_{r\theta}(r) = \frac{C_0}{r^2}$$

Thus the form of the solution for the shearing stress is known. The value of the constant of integration can be determined, as always, by referring to a boundary condition for the shearing stress. An obvious boundary condition, as discussed below, is that the shearing stress at the outer rim of the disk (i.e., at $r = R$) is zero. Substitution of the above solution for $\sigma_{r\theta}$ into this boundary condition establishes that the constant of integration, C_0 , must be zero. Therefore the shearing stress is zero throughout the disk. An experienced engineer always attempts to determine whether the mathematical result makes sense. To this end consider Fig. 7.1(b). In this case it is clear that the symmetry of the loading and geometry about any diameter of the disk requires that the shearing stresses on the two adjacent sides of two adjacent differential elements be equal in magnitude and act in the same direction. However, Newton's third law requires that these same shear stresses be equal and oppositely directed. The only way both of these requirements can be met is for these typical shear stresses to be zero.

Returning to the first equation of equilibrium, it is clear that the problem is indeterminate since there are two unknown stresses and only one remaining equilibrium equation:

$$r\sigma'_{rr} + \sigma_{rr} - \sigma_{\theta\theta} = -\rho r^2 \Omega^2 \quad (7.2)$$

The necessary additional equation in terms of the radial and hoop stresses is the equation of compatibility in cylindrical coordinates for the r, θ plane, called the primary compatibility equation. The general form of this compatibility equation in cylindrical coordinates is developed in Exercise 3.6. Endnote (3) briefly comments upon adapting this general equation form to this problem. A far better approach is to develop a compatibility equation for the special circumstances of this problem. This second approach is much superior because it produces a compatibility equation that contains derivatives of a lower order relative to the general compatibility equation. From Exercise 3.10, the three strain–displacement equations reduce to

$$\epsilon_{rr} = \frac{du}{dr} \quad \epsilon_{\theta\theta} = \frac{u}{r} \quad \gamma_{r\theta} = \frac{dv}{dr} - \frac{v}{r} \quad (7.3)$$

The first two strain–displacement equations involve the strains directly related via the strain–stress equations to the remaining unknown stresses. These two strain expressions can be combined so as to eliminate the displacement u . The result, as per Example 3.1, is the compatibility equation for this problem:

$$\epsilon_{rr} = \frac{d}{dr}(r\epsilon_{\theta\theta}) = r\epsilon'_{\theta\theta} + \epsilon_{\theta\theta}$$

For further comment on this compatibility equation, see Endnote (3).

Since cylindrical coordinates also form an orthogonal coordinate system, Hooke's law and the Poisson effect can be utilized with these coordinates just as they were utilized with Cartesian coordinates. Therefore the strain–stress equations for the Hookean, isotropic material are

$$\begin{aligned} E\epsilon_{rr} &= \sigma_{rr} - \nu\sigma_{\theta\theta} + E\alpha\Delta T \\ E\epsilon_{\theta\theta} &= \sigma_{\theta\theta} - \nu\sigma_{rr} + E\alpha\Delta T \end{aligned} \quad (7.4)$$

Substitution of the strain–stress equations into the compatibility equation, after some manipulation, yields the result

$$r\nu\sigma'_{rr} + (1 + \nu)\sigma_{rr} = r\sigma'_{\theta\theta} + (1 + \nu)\sigma_{\theta\theta} + rE\alpha\Delta T'(r) \quad (7.5)$$

This is the second equation in the two unknown normal stresses. The task now is to solve simultaneously Eq. (7.2), which contains the effects of the centrifugal acceleration, and Eq. (7.5), which contains the effect of the temperature change. An appropriate approach to their solution is to eliminate one of the two unknown stresses in order to work with one equation in one unknown. This can be accomplished by solving Eq. (7.2) for the hoop stress, $\sigma_{\theta\theta}$, and then substituting for the hoop stress in Eq. (7.5) to obtain an equation entirely in terms of the radial stress. After simplification, the result is

$$r^2\sigma''_{rr} + 3r\sigma'_{rr} = -rE\alpha\Delta T' - (3 + \nu)\rho r^2 \Omega^2 \quad (7.6)$$

The above differential equation, like its antecedents, has nonconstant coefficients. However, the reader may recognize that this equation has the special form that can be reduced to a differential equation with constant coefficients by means of the transformation $r = R \exp(s)$, where s is the new, nondimensional variable; see Exercise 7.9. If the reader

is not familiar with that standard procedure, note that multiplying both sides of Eq. (7.6) by the integrating factor r allows that equation to be rewritten as

$$\frac{d}{dr}(r^3\sigma'_{rr}) = -E\alpha r^2\Delta T'(r) - (3+\nu)\rho r^3\Omega^2$$

or, again using indefinite integration,

$$r^3\sigma'_{rr} = C_1 - E\alpha \int r^2\Delta T'(r) dr - \frac{1}{4}(3+\nu)\rho r^4\Omega^2$$

Integrating again after division by the cube of the radius produces the solution of the differential equation for the radial stress:

$$\begin{aligned}\sigma_{rr}(r) &= C_2 - \frac{C_1}{2r^2} - \frac{3+\nu}{8}\rho r^2\Omega^2 \\ &\quad - E\alpha \int \left(\frac{1}{r^3} \int r^2\Delta T'(r) dr \right) dr\end{aligned}\quad (7.7)$$

The solution for the hoop stress is obtained by substituting Eq. (7.7) into Eq. (7.2), that is,

$$\begin{aligned}\sigma_{\theta\theta}(r) &= \sigma_{rr} + r\frac{d\sigma_{rr}}{dr} + r^2\rho\Omega^2 \\ &= C_2 + \frac{C_1}{2r^2} - \frac{1+3\nu}{8}\rho r^2\Omega^2 \\ &\quad - E\alpha \frac{1}{r^2} \int r^2\Delta T'(r) dr \\ &\quad - E\alpha \int \frac{1}{r^3} \left(\int r^2\Delta T'(r) dr \right) dr\end{aligned}\quad (7.8)$$

In order to determine the two constants of integration in the two expressions for the stresses, it is now convenient to specify a particular temperature change, and it is necessary to mathematically describe the boundary conditions. Starting with the specification of the temperature change, note that a uniform temperature change has no effect on the stresses. To make the problem simple, let the temperature change be

$$\Delta T(r) = \frac{r}{R}T_0 \quad \text{or} \quad \Delta T'(r) = \frac{T_0}{R}$$

A constant could also easily be made part of the temperature change. In the chosen case, the temperature integrals can be evaluated as follows:

$$\begin{aligned}\frac{1}{r^2} \int r^2\Delta T'(r) dr &= \frac{T_0}{R} \frac{1}{r^2} \int r^2 dr = \frac{T_0 r}{3R} \\ \int \frac{1}{r^3} \left(\int r^2\Delta T'(r) dr \right) dr &= \frac{T_0}{R} \int \frac{1}{r^3} \left(\int r^2 dr \right) dr = \frac{T_0 r}{3R}\end{aligned}$$

The only remaining task is to discover and apply the boundary condition equations. Recall that the Cauchy (i.e., stress) boundary condition equations were previously derived from an equilibrium statement for a differential-sized portion of a structural body at a boundary of the body. An equally valid viewpoint, that is often more convenient as it is here, is that the tractions on the outer boundary are simply other names for the stresses on the exterior of the boundary. From this viewpoint, two boundary conditions for this problem are that the radial stress and shearing stress are both zero at the outer rim of the disk where $r = R$. The hoop stress is not a boundary stress for this geometry because $\sigma_{\theta\theta}$ does not

appear on the outer boundary of the disk. The shearing stress boundary condition has already been used to demonstrate that the shearing stress is zero everywhere throughout the disk. Thus there remains but one boundary condition for the two constants of integration. Note that if the disk were annular instead of solid, the second boundary condition for the radial stress would be found on the inner boundary of the annulus. This suggests that the center point of the disk is a degenerate boundary, and that the second boundary condition is to be found there. There are no concentrated forces acting at the center of the disk, nor are there any geometric irregularities there. Thus it may be deduced that the stresses at the center of the disk are finite quantities. However, if the radial coordinate, r , is set to zero in Eqs. (7.7) and (7.8), the stresses determined by those expressions become infinite unless the first constant of integration, C_1 , is set equal to zero.¹ Thus C_1 is set equal to zero. Using the previously discussed boundary condition that $\sigma_{rr}(r = R)$ is zero produces the result

$$C_2 = \frac{3 + \nu}{8} \rho R^2 \Omega^2 + \frac{1}{3} E \alpha T_0$$

and thus the final solutions for this particular temperature change are

$$\begin{aligned} \sigma_{rr}(r) &= \frac{3 + \nu}{8} \rho \Omega^2 (R^2 - r^2) + \frac{1}{3} E \alpha T_0 \left[1 - \frac{r}{R} \right] \\ \sigma_{\theta\theta}(r) &= \frac{1}{8} \rho R^2 \Omega^2 \left[(3 + \nu) - (1 + 3\nu) \left(\frac{r}{R} \right)^2 \right] + \frac{1}{3} E \alpha T_0 \left[1 - \frac{2r}{R} \right] \end{aligned} \quad (7.9)$$

Substitution of these two solutions into the equilibrium equations, the six general compatibility equations written in terms of stresses after use of the strain–displacement equations, and the boundary conditions shows that these two stress solutions satisfy all equations, and thus are the single valid solution. ■

The solution process for this plane stress problem was lengthy. However the procedure is as it always is for a plane stress formulation. That is, the primary compatibility equation in terms of strains is changed to a compatibility equation in terms of stresses by use of whatever strain–stress equations describe the material of the structural body. This differential equation and the differential equations of equilibrium are solved together to determine the stresses. (Clearly, skill in solving differential equations is important to these solution procedures.) The analytical solution to the ordinary differential field equations contains unknown constants of integration, which are evaluated by use of boundary condition equations that are particular to the problem at hand. Thus the boundary condition equations must be recognized and stated by the analyst. The replacement of the unknown constants of integration by their values as determined by the boundary conditions completes the problem solution.

The solutions for the radial and hoop stresses for the given linear temperature change, as provided in Eqs. (7.9) are confirmed in the next section. Solutions for these same stresses for an arbitrary temperature change in the radial direction are considered in the Chapter 7 exercises.

7.3 A Theory of Elasticity Solution Using Displacements

This section reconsiders exactly the same problem discussed in the previous section. This time the problem is solved using displacements as the unknown quantities.

¹ To ensure that neither of the two integral expressions in Eq. (7.8) are infinite when $r = 0$, it is sufficient to limit the temperature change to being an analytical function of r .

Example 7.2. Determine the displacements, and then the stresses in a uniform, circular disk of radius R and thickness h that is rotating about its center at a constant angular velocity Ω , and is subjected to a temperature change that varies with radial distance only; see Fig. 7.1(a). Let the material of the disk be homogeneous, linearly elastic, and isotropic. Assume that the angular velocity, Ω , and the temperature change are sufficiently large that the effects of the body force due to the gravitational field are insignificant.

Solution. Again the problem solution begins with the recognition that the rotating, heated disk is a plane stress problem. Zero values for shearing stresses σ_{rz} and $\sigma_{\theta z}$ and isotropic stress-strain relations mean that the shearing strains γ_{rz} and $\gamma_{\theta z}$ are also zero. The longitudinal strain ϵ_{zz} is dependent on the values of ϵ_{rr} and $\gamma_{\theta\theta}$ (see Exercise 6.3), and since those two strains are not zero, neither is ϵ_{zz} . The solution for ϵ_{zz} can be obtained when the other two longitudinal strains are determined. The displacements that are involved with the remaining nonzero strains, ϵ_{rr} , $\gamma_{r\theta}$, and $\epsilon_{\theta\theta}$, are only the two displacements $u(r, \theta)$ and $v(r, \theta)$, and thus they are the displacements that are used to formulate the problem and obtain its solution. The displacement $w(r, \theta)$ is of little importance, but it could be determined by integration of ϵ_{zz} when that strain is determined. In summary, the displacements that are sought for this, or any other plane stress problem, are u and v , which here, of course, are in the r and θ directions, respectively.

The solution proceeds as before with the recognition that the geometry and the physical and thermal loading are axisymmetric. Thus there are no changes in the θ coordinate direction. Hence (i) all stresses, strains, and displacements are only functions of the radial coordinate; (ii) all partial derivatives with respect to θ are zero; and (iii) all partial derivatives with respect to the radial coordinate are total derivatives. Furthermore, the axisymmetry of the problem requires that $\gamma_{r\theta}$ be zero. To understand why this is so, reconsider the differential-sized elements that are sketched in Fig. 7.1(b). This time consider these two elements from a geometric viewpoint. Since the shearing strain does not vary with θ , the two elements must have the same shearing deformation. Without loss of generality, assume that the two elements have a negative shearing strain in the plane of the paper. This means that the two elements elongate along diagonals running from the upper left to the lower right of each of the two elements, and shorten along the other diagonals. However, the fact that these two elements lie on opposite sides of an axis of symmetry, a diameter of the circle of the disk, means that the two elements have to elongate and shorten along opposite diagonals. The only way the two elements can meet both requirements of deforming in the same and opposite fashions is that neither element elongate or shorten along either diagonal, that is, that there be no shearing strain $\gamma_{r\theta}$. This conclusion leads to the further result from the last of Eqs. (7.3) that

$$\frac{dv}{dr} = \frac{v}{r}$$

The solution to this first order differential equation,

$$v(r) = C_0 r$$

with its constant of integration, C_0 , is easily obtained by separating the variables. In what is an unusual circumstance, there are no boundary conditions that can be used to determine the constant of integration, C_0 . However, when one door is closed, usually another is open. Consider Fig. 7.2, which shows a sketch of the displacement pattern represented by the above solution. Figure 7.2 clearly shows that these displacements are to be interpreted as just rigid body rotations of the disk. Since rigid body displacements have no effect on stresses or strains, and thus are of no structural interest, they can be ignored. That is, C_0 ,

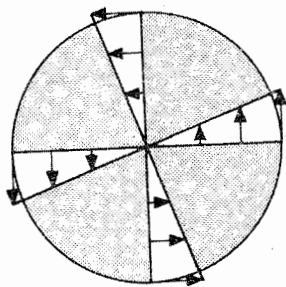


Figure 7.2. Example 7.2. The rigid body pattern of displacements in the θ direction.

and thus $v(r)$, can be set equal to zero with the interpretation that the elastic deformations in the θ direction are zero.

The major task remaining is to discover the values of the other displacement, $u(r)$. To this end, return to the strain–displacement equation stated in Eqs. (7.3)

$$\epsilon_{rr} = \frac{du}{dr} \quad \text{and} \quad \epsilon_{\theta\theta} = \frac{u}{r}$$

Following the same procedure used with all displacement formulations, these strain–displacement equations are substituted into the stress–strain equations, which in turn are substituted into the remaining equilibrium equation,² Eq. (7.2). The details of these steps are as follows. In terms of the displacement, the stress–strain equations become

$$\begin{aligned} \sigma_{rr} &= \frac{E}{1-\nu^2} \left(u' + \frac{\nu u}{r} \right) - \frac{E\alpha\Delta T}{1-\nu} \\ \sigma_{\theta\theta} &= \frac{E}{1-\nu^2} \left(\frac{u}{r} + \nu u' \right) - \frac{E\alpha\Delta T}{1-\nu} \end{aligned} \tag{7.10}$$

After substitution of the above stress–strain equations into the remaining equilibrium equation

$$r\sigma'_{rr} + \sigma_{rr} - \sigma_{\theta\theta} = -r^2\rho\Omega^2 \tag{7.2}$$

the result, after some simplification, is

$$r^2u'' + ru' - u = r^2(1+\nu)\alpha\Delta T'(r) - (1-\nu^2)\frac{r^3\rho\Omega^2}{E} \tag{7.11}$$

Again the final displacement formulation differential equation has the same pattern of non-constant coefficients as the corresponding stress formulation differential equation. However, in this case the zeroth derivative term is not missing. Since an initial integrating factor may not be readily apparent [see Endnote (2)], the complementary solution to this differential equation is obtained by replacing the independent variable r by means of the coordinate transformation $r = R \exp(s)$, where s is a temporary, nondimensional variable; see Exercise 7.9. The final result for the complementary solution, after a return to the use of the independent variable r is

$$u_c(r) = Ar + \frac{B}{r}$$

² Since the shearing strain is zero, so too is the shearing stress, and thus the second equilibrium equation disappears.

where A and B are the two constants of integration. This solution can easily be checked by direct substitution into the homogeneous differential equation. The particular solution for the centrifugal body force is obtainable by the method of undetermined coefficients. A brief review of that limited method for solving differential equations can be found in Section III.2. The result of the application of that or any other method is

$$u_p(r) = \frac{1 - \nu^2}{8E} r^3 \rho \Omega^2$$

which also can be checked by direct substitution into the nonhomogeneous differential equation. Obtaining a simple particular solution for the temperature loading requires specification of the temperature change. As in the case of the stress formulation, choose a linear temperature change such that

$$\Delta T = \frac{r}{R} T_0$$

where T_0 is an arbitrary constant. Then the additional particular solution, which is also obtainable by the method of undetermined coefficients, is

$$u_p(r) = \frac{1}{3} \left(\frac{r}{R} \right)^2 (1 + \nu) \alpha R T_0$$

Hence the total solution has the form

$$u(r) = Ar + \frac{B}{r} + \frac{r^2}{3R} (1 + \nu) \alpha T_0 - \frac{1 - \nu^2}{8E} r^3 \rho \Omega^2$$

It is now necessary to identify the boundary condition equations in terms of the displacement $u(r)$ and its derivatives, and apply those boundary conditions to the present solution in order to evaluate the two constants of integration, A and B . Again it is necessary to consider the center point of the disk as a boundary point where the displacement in the radial direction must be zero when disregarding rigid body motion. The second boundary condition is the familiar one that the radial stress, by σ_{rr} , at the outer boundary ($r = R$) is zero. The first of these two boundary conditions requires the elimination of the B/r term by requiring that B have the value zero.

The second boundary condition equation, $\sigma_{rr} = 0$, has to be written in terms of the displacement $u(r)$ and its first derivative, where r is then set equal to R . The procedure to accomplish this task is the same as it was for the field equation. That is, the stress-strain equations are used to replace the radial stress by strains, and the strain-displacement equations are used to replace the strains by the radial displacement. Thus the boundary condition equation $\sigma_{rr}(R) = 0$ becomes

$$u'(R) + \nu \frac{u(R)}{R} = (1 + \nu) \alpha T_0 \quad (7.12)$$

After substitution and some simplification, the solution for the remaining constant of integration is

$$A = \frac{1}{3} (1 - \nu) \alpha T_0 + (3 + \nu)(1 - \nu) \frac{\rho R^2 \Omega^2}{8E}$$

Thus the final solution for the radial displacement is

$$\begin{aligned} \frac{u}{R} = \frac{1}{3} & \left[(1 - \nu) \frac{r}{R} + (1 + \nu) \left(\frac{r}{R} \right)^2 \right] \alpha T_0 \\ & + (1 - \nu) \left[(3 + \nu) \frac{r}{R} - (1 + \nu) \left(\frac{r}{R} \right)^3 \right] \frac{\rho R^2 \Omega^2}{8E} \end{aligned} \quad (7.13)$$

Now that the displacements everywhere in the disk are known, the stresses in the disk are found simply by differentiating the displacements to obtain the strains, and then using the stress–strain equations to obtain the stresses. The results for the radial and hoop stresses by this route are exactly the same as those obtained when stresses were used as the unknown quantities in the field equation. ■

This concludes the example solutions where a specific temperature change was chosen in order to complete the problem. One of the more challenging exercises at the end of the chapter discusses the solution for this disk problem for an arbitrary temperature change in the radial direction.

The equations associated with this illustrative problem admit exact solutions containing a finite number of terms. Such analytical solutions are called *closed form solutions*. Exact solutions to other differential equations in the form of infinite series are called *open form solutions*. Open form solutions are just as useful for engineering purposes as closed form solutions. Indeed, many theory of elasticity problems are so challenging that any type of analytical solution is a major accomplishment.

7.4 Reprise

In order to provide one and a half more examples of the sequential use of the four sets of equations that comprise the theory of elasticity, this section presents two further example problems that can be solved using ordinary differential equations.

Example 7.3. Analyze a thin, annular disk where the only loading upon the disk is a uniform traction in the positive θ direction, T_θ , that acts at the outer disk edge where $r = b$. The inner edge, where $r = a$, is bonded to a rigid shaft. The disk has a constant thickness, and the disk material is homogeneous, isotropic, and Hookean. There is no temperature change.

Solution. Sketch the problem. The first thing to note is that this too is a plane stress problem, and again the same displacement conditions exist at all values of the angular coordinate, θ . That is, the stresses, and displacements do not vary with θ , and thus these quantities are only functions of the radial coordinate. Therefore all partial derivatives with respect to theta are zero, and all partial derivatives with respect to the radial coordinate are total derivatives.

The next things to note are the boundary conditions, where the boundaries of this elastic system are at the inner and outer radii. The displacement and traction boundary conditions are

$$\begin{aligned} u(r = a) = 0 \quad \sigma_{rr}(r = b) = 0 \\ v(r = a) = 0 \quad \sigma_{r\theta}(r = b) = +T_\theta \end{aligned}$$

These boundary conditions are “mixed”; that is, they involve both displacement and stress statements. Therefore, it is necessary to use a displacement formulation when analyzing this disk. The interior equations for a displacement formulation are, as always, the

equilibrium equations, the stress-strain equations, and the strain-displacement equations. The equilibrium equations for this particular problem are Eqs. (7.1) with both body forces per unit mass being zero. Therefore,

$$\begin{aligned} r\sigma'_{rr} + \sigma_{rr} - \sigma_{\theta\theta} &= 0 \\ r\sigma'_{r\theta} + 2\sigma_{r\theta} &= 0 \end{aligned}$$

Again, the second equilibrium equation is uncoupled from the first, and thus the two equations can be solved separately. The strain-displacement equations are Eqs. (7.3). Working first with the shearing terms, the shearing stress-strain equation is just

$$\sigma_{r\theta} = G\gamma_{r\theta} = G\left(v' - \frac{v}{r}\right)$$

Substitution into the second equilibrium equation would yield a second order differential equation in terms of the displacement $v(r)$. A better approach is to work with successive first order differential equations. Recall that r is an integrating factor for that equilibrium equation, and thus that equilibrium equation can be written as

$$\frac{d}{dr}(r^2\sigma_{r\theta}) = 0$$

or

$$\sigma_{r\theta} = \frac{C_1}{r^2}$$

which, from the above shearing stress-displacement equation, leads to the following first order differential equation in terms of the displacement:

$$rv' - v = \frac{C}{r} \quad \text{where} \quad C = \frac{C_1}{G}$$

This differential equation can be solved in many different ways. Writing the left-hand side as an exact differential requires first dividing both sides of the above equality by the integrating factor r^2 . Then

$$\frac{d}{dr}(v/r) = C/r^3$$

or

$$v(r) = Dr - \frac{C}{2r}$$

where D is another constant of integration. Now that the form of the solution for the displacement in the θ direction has been obtained, it is necessary to specialize it to this problem by applying the boundary conditions related to that displacement. First the boundary condition $\sigma_{r\theta}(b) = +T_\theta$ must be written in displacement form as

$$G\left[v'(b) - \frac{v(b)}{b}\right] = T_\theta$$

Using $v(a) = 0$ and the above boundary condition equation to determine the two constants of integration leads to the simultaneous equations

$$Da - \frac{C}{2a} = 0$$

and

$$D + \frac{C}{2b^2} - D + \frac{C}{2b^2} = \frac{T_\theta}{G}$$

whose solutions are $C = T_\theta b^2/G$ and $D = \frac{1}{2}(T_\theta/G)(b^2/a^2)$. Thus, for $0 < a \leq r \leq b$,

$$v(r) = \frac{T_\theta b^2}{2Ga} \left(\frac{r}{a} - \frac{a}{r} \right) \quad (7.14)$$

Clearly, the units are correct, $v(a) = 0$, and the θ direction displacement increases in the radial direction. From this solution the solutions for the shearing strain and shearing stress are easily obtained.

To complete the solution process it is necessary to determine $u(r)$ as well. For small displacements, it may be possible to guess that $u(r)$, and the radial and hoop strains and stresses, are zero. However, it is more satisfying to deduce that result. Substituting the first two strain-displacement equations $\epsilon_{rr} = u'$, and $\epsilon_{\theta\theta} = u/r$, into the two stress-strain equations again produces Eqs. (7.10), where, in this case, the temperature change is zero. Substituting the so modified Eqs. (7.10) into the first of the two equilibrium equations yields, after some simplification

$$r^2 u'' + r u' - u = 0$$

which is just a special case of Eq. (7.11). That previous work demonstrated that the solution to this differential equation is

$$u(r) = Ar + \frac{B}{r}$$

The boundary conditions in terms of displacements only are

$$u(a) = 0 \quad \text{and} \quad u'(b) + \frac{\nu}{b} u(b) = 0$$

where the latter equation is, of course, $\sigma_{rr}(b) = 0$ in terms of the displacement. Substituting the displacement solution into these two boundary condition equations yields

$$Aa + \frac{B}{a} = 0 \quad \text{and} \quad A - \frac{B}{b^2} + \frac{\nu}{b} \left(Ab + \frac{B}{b} \right) = 0$$

These are two homogeneous algebraic equations whose only solution is $A = B = 0$. Thus the conjecture that $u(r) = 0$ is fully confirmed. ■

In the mathematical model adopted for the above problem, the circular shaft upon which the disk is bonded is modeled as being rigid. This modeling is acceptable for this disk problem even when the shaft is far less stiff than the disk. This is so because the rotation of the shaft, which results from the torque transmitted from the disk to the shaft, is entirely irrelevant to this disk problem. The focus is upon the disk, not the shaft. The rotation of the shaft is wholly equivalent to a rigid body rotation of the disk, and rigid body rotations are without significance with respect to the deformations of the disk.

Do not confuse the above problem with the problem that is the twisting of a straight rod with an annular cross-section. The two problems have little in common because the geometries, disk and rod, are quite different. The only nonzero shearing stress of the rod torsion problem is $\sigma_{z\theta}$, while the only nonzero stress of this disk problem is $\sigma_{r\theta}$.

Example 7.4. A certain planet is orbited by a small, distant moon. That moon, which has a total radius of 500 miles, has an ice covering that is estimated to be 200 miles thick. The 300-mile radius core of the moon has a mass density that is only slightly greater than that of the ice covering. Thus let an average mass density ρ_0 be used to characterize the entire moon. Also let the following additional, tentative, approximations be accepted.

- i. The moon and its core are perfect spheres, and the ice and core material are sufficiently fractured that their weight is transmitted uniformly towards the interior of the moon.
- ii. The moon is spinning about its own axis at such a small angular velocity that all centripetal accelerations are negligible.
- iii. The gravitational pulls of the planet, all other moons of that planet, and nearby stars are negligible within the interior of the moon compared to its own gravitational effects.
- iv. In compression, the moon material is linearly elastic and isotropic.
- v. There is no atmospheric pressure.

Then, in the following three steps, prepare to estimate the pressures at the bottom of the ice ocean by estimating the pressures everywhere throughout the interior of the moon

- (a) Use the result of Exercise 1.16 to write that one equilibrium equation for the stresses everywhere within the interior of the moon; be sure to write the equilibrium equation in its simplest form.
- (b) Assume that the one indeterminate equilibrium equation of the previous step is the only nontrivial equilibrium equation, and then describe only in word form what it is that needs to be done next in order to obtain a stress formulation set of governing differential equations
- (c) Write the two stress boundary conditions for σ_{rr} .

Solution. (a) The spherical geometry mandates the use of spherical coordinates. The equilibrium equation for the spherical r direction is, from the solution to Exercise 1.16,

$$r \frac{\partial \sigma_{rr}}{\partial r} + 2\sigma_{rr} + \frac{\partial \sigma_{\phi r}}{\partial \phi} + \sigma_{\phi r} \cot \phi - (\sigma_{\phi\phi} + \sigma_{\theta\theta}) + \frac{\partial \sigma_{\theta r}}{\partial \theta} \csc \phi + \rho r B_r = 0$$

Because the depth of the ice ocean is a significant fraction of the total radius of the moon, it is necessary to account for the change in the magnitude of the acceleration of gravity with radial distance from the center of the moon by use of the formula

$$g(r) = g_0 \frac{r}{R} \quad (R = 500 \text{ miles})$$

where the moon surface value g_0 is a known constant with units of acceleration, and r is the radial distance. Since there are only negligible centrifugal accelerations,

$$B_r = -g(r) \quad B_\theta = B_\phi = 0$$

Furthermore, since the spin axis of the moon is unimportant, the moon geometry, material distribution, and loading are all spherically symmetric. Thus all shearing stresses are zero, and all partial derivatives with respect to θ and ϕ are zero, and $\sigma_{\phi\phi} = \sigma_{\theta\theta}$. Hence all partial derivatives with respect to r are total derivatives, and the equilibrium equation reduces to

$$r \frac{d\sigma_{rr}}{dr} + 2\sigma_{rr} - 2\sigma_{\theta\theta} - \rho_0 g_0 \left(\frac{r^2}{R} \right) = 0$$

This is, of course, one equation in two unknown stresses.

(b) The next thing to do to obtain a stress formulation of this problem is to write the strain compatibility equations in terms of spherical coordinates. The compatibility equations in terms of spherical coordinates can be obtained from a solid mechanics handbook such as Ref. [7], or, better yet, in the fashion of Example 7.1, use the similarly obtained spherical coordinate strain–displacement equations to develop a first order compatibility equation based upon the above comments regarding the three partial derivatives plus the spherical symmetry deduction that the deflections in the θ and ϕ directions, $u(r)$ and $w(r)$, are zero. Once the one strain compatibility equation in terms of ϵ_{rr} and $\epsilon_{\theta\theta}$ is determined, use the estimated strain–stress material equations to write the strain compatibility equation in terms of the two stresses σ_{rr} and $\sigma_{\theta\theta}$.

(c) Exactly analogously to the spinning disk problem, the boundary conditions are

$$\sigma_{rr}(r = R) = 0 \quad \text{and} \quad \sigma_{rr}(r = 0) = \text{finite} \quad \blacksquare$$

If the core of the moon had a mass density that was significantly different than that of the ice covering, then the problem solution would proceed as indicated in Exercise 6.

7.5 Summary

The first purpose of this chapter is to show the sequential use of the equilibrium equations, the constitutive equations, and the strain–displacement or compatibility equations. The second purpose is to illustrate the search for boundary conditions. In most theory of elasticity problems, the boundaries and the boundary conditions are readily apparent. The disk problem in this chapter shows what may be necessary when the boundaries and boundary conditions are not readily apparent. The third purpose of this chapter is to illustrate side by side a stress formulation solution and a displacement formulation solution for a problem that involves only one independent coordinate, in this case r . The dependence of all the unknown functions (displacements or stresses) on a single coordinate causes all the differential equations to be ordinary differential equations, and thus easier to solve. The exercises at the end of this chapter also only involve the single spatial coordinate r .

The next chapter presents analytical solutions, without derivation, to two selected problems in the theory of elasticity. Those problems are presented with a view towards further illustrating the writing and application of boundary conditions and providing the reader with a very small sample of some of the simpler theory of elasticity solutions that are presently available. Those plane stress problems are framed in terms of Cartesian coordinates, and they involve two independent spatial coordinates. Thus the field equations that are associated with these problems are partial differential equations. That is the reason why those solutions are simply presented rather than derived in this text. Be assured, however, that the use of a device called the Airy stress function, which is introduced in an optional section of Chapter 8, makes the derivation of these solutions quite manageable.

Chapter 7 Exercises

- 7.1. (a) Use Eq. (7.14) to calculate the shearing stress in the disk of Example 7.3 as a function of the radial coordinate, r . Check to see whether the shearing stress at the outer edge is actually equal to the applied traction at the outer edge.
- (b) Now write the expression for the shearing stress anywhere within the disk in terms of the total torque M acting upon the outer edge of the disk. Note

that this torque M results from the shearing stress traction that is applied to the outer disk edge.

- (c) Should and does the shearing traction at the inner circular edge of the disk have a greater value than the shearing traction at the outer edge, which value is T_0 ?
 - (d) Given that the radial displacement is zero, is it true that the only possible solution for the radial and hoop stresses is that they too are zero?
 - (e) If the boundary conditions at the inner edge of this disk were changed from displacement boundary conditions to those of a uniform shearing traction that equilibrated the torque at the outer edge, and a zero radial traction, what then would be the solutions for the two displacements?
- 7.2. Consider a thick spherical shell of inner radius a and outer radius b . Let this thick shell be a containment vessel for an intense pressure p_0 . The applicable equilibrium equation, from the solution to Exercise 1.17, is

$$r \frac{\partial \sigma_{rr}}{\partial r} + 2\sigma_{rr} + \frac{\partial \sigma_{\phi r}}{\partial \phi} + \sigma_{\phi r} \cot \phi - (\sigma_{\theta\theta} + \sigma_{\phi\phi}) + \frac{\partial \sigma_{\theta r}}{\partial \theta} \csc \phi + r \rho B_r = 0$$

- (a) Adapt this general equilibrium equation in spherical coordinates to this particular case of a thick spherical shell with an internal pressure by writing this equation in its simplest possible form.
 - (b) If you were to pursue this problem using a displacement formulation, which of the following sets of equations would you employ (A) the strain–stress equations in spherical coordinates; (B) the stress–strain equations in spherical coordinates; (C) the strain–displacement equations in spherical coordinates; and/or (D) compatibility equations in spherical coordinates?
 - (c) If you were to pursue this problem using a stress formulation, which of the above four sets of equations would you employ?
 - (d) For present purposes, assume that a stress formulation would only involve the stresses σ_{rr} and $\sigma_{\theta\theta}$ and their derivatives, and a displacement formulation would only involve the displacement in the r direction, $u(r)$, and its derivatives. In either case, one σ_{rr} stress BC is required at $r = a$, and another at $r = b$. State those BCs.
 - (e) In the case of a displacement formulation, the stress BCs need to be converted to equations that are written in terms of the displacement $u(r)$ and its derivatives, all localized to one boundary or the other. Describe, using words only, how that conversion can be affected.
 - (f) For spherical coordinates, write the six isotropic strain–stress equations, including the effects of temperature changes.
- 7.3. (a) For the disk of Example 7.1, where now $\Omega = 0$ and the temperature change has a constant value T_1 , use Eqs. (7.7) and (7.8) and the stress BC to determine the values of radial and hoop stresses within the disk.
- (b) Use the result given in Exercise 7.8(d) to again determine the radial and hoop stresses in the disk of Example 7.1 when $\Omega = 0$ and the temperature change has a constant value T_1 .
- (c) If the temperature change were described by the linear expression $(T_0r + T_1)$, would the solution be any different from the solution for a temperature change of just T_0r ?

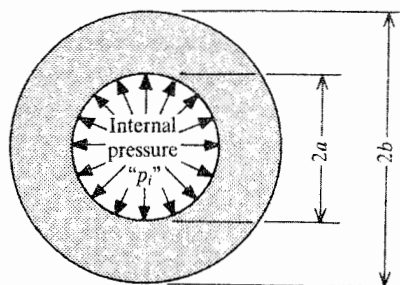


Figure 7.3. Exercises 7.4 and 7.5.

7.4. Consider a thin annular body of thickness h , inner radius a , and outer radius b ; see Fig. 7.3.

- (a) Let the only loading on this structural body be a compressive normal traction in the plane of the annulus. Let that traction be in the form of a pressure p_i acting on the surface of the inner radius. The stress formulation solutions that satisfy the equilibrium, constitutive, and compatibility equations for this plane stress problem can be shown from either Eqs. (7.7) and (7.8), or Ref. [21] to be

$$\sigma_{rr}(r) = \frac{A}{r^2} + B \quad \sigma_{\theta\theta}(r) = -\frac{A}{r^2} + B \quad \sigma_{r\theta} = 0$$

where $0 \leq a \leq r \leq b$ and A and B are constants of integration. Determine the values of the two constants of integration and thereby complete the solution for the stresses.

- (b) Is it true that in the situation of part (a) the radial stress is always compressive while the hoop stress is always tensile? Is this situation in accord with your expectations?
- (c) Where are the maximum values of the two stresses?
- (d) Repeat part (a) but change the traction to an inward acting pressure p_0 acting at the outer radius b . Note that changing the boundary conditions has no effect on the form of the field equation solutions.
- (e) Repeat part (a) but this time have both the inner and outer pressures acting on the annular body. Is the solution thus obtained the sum (i.e., superposition) of the solutions for parts (a) and (d)?
- (f) Note that the sum of these two normal stresses is always a constant. Therefore the strain ϵ_{zz} everywhere across the annular surface is also a constant. Therefore, since they would fit together perfectly, any number of these thin annular bodies could be stacked on top of each other to form a thick cylinder. Compare the above "thick cylinder" stress solutions to the "thin cylinder" solutions obtained from equilibrium considerations alone, which, from Section 1.4, are that σ_{rr} varies from zero at the outer boundary to a value of p_i at the inner boundary, and

$$\sigma_{\theta\theta} = \frac{\bar{R}}{t} P_i \quad \text{and} \quad \sigma_{r\theta} = 0$$

where \bar{R} is the mean radius, which is equal to $(a + b)/2$, and t is the thickness, which is equal to $(b - a)$.

- 7.5. Consider again the same thin annular body of the previous exercise. It is suggested that such an annulus can be heated and then slipped onto a cylinder whose outer diameter is nominally the same, or a trifle larger than the inner diameter of the annulus so that when the assembly cools, there will be a tight fit between the annulus and the cylinder. To investigate the relation between temperature and displacement implied by this suggestion, let the only loading on the annulus be that due to a constant temperature change, T_0 . The general solution for the radial displacements $u(r)$ for the annulus due to a temperature change T_0 is the same as that for the solid disk. That is, from either the solution to Eq. (7.11), which is $u(r) = A_1 r + A_2/r$, or from Exercise 7.8(a) below, where B_1 and B_2 are merely different constants of integration, and substitution of the constant T_0 for the temperature change is still required in the integral of this expression,

$$u(r) = \frac{1+\nu}{r} \int r \alpha \Delta T(r) dr + B_1 r + \frac{B_2}{r}$$

Note that just like the first offered solution for $u(r)$, this second solution for $u(r)$ contains one term directly proportional to r , and one term inversely proportional to r .

- (a) Write the boundary conditions for the inner and outer radial surfaces, and then determine the two constants of integration A_1, A_2 or B_1, B_2 when the temperature change has a constant value T_0 over the volume of the structural body. *Hint:* For example, $\sigma_{rr}(r = b) = 0$ implies

$$bu'(b) + \nu u(b) = (1 + \nu)b\alpha T_0$$

- (b) Determine whether or not the inner radius of the annulus increases when the constant temperature change is an increase in temperature.

FOR THE EAGER

- 7.6. Two steel tubes with the nominal dimensions shown in Fig. 7.4 are assembled into a single tube by heating the outer tube, cooling the inner tube, inserting the inner tube into the outer tube, and then letting the two tubes return to room temperature. If the outer radius of the inner tube is slightly oversized, while the inner radius of the outer tube is slightly undersized, then a firm bond will result. As a step towards determining the stresses in these tubes that result from the above-described bonding procedure, the shrinkage on the outer radius of the inner tube after assembly was measured to be 0.001 in by means of what was a difficult, and perhaps inaccurate measurement.
- (a) As a further step towards determining these stresses, write the two boundary conditions for each of the two tubes. (Note that these stresses will be the residual stresses of the assembly process, and when the tube assembly is subjected to other stresses, these assembly stresses are called initial stresses.) *Hint:* By Newton's third law, the radial stresses on each side of the common boundary between the two tubes are the same.
- (b) Note that, by symmetry, the tangential displacement is zero. The nontrivial equilibrium equation is the same for each tube. For either tube, write that equation in terms of the unknown stresses.
- (c) For either tube, write the stress-strain equations for the situation where the two tubes have returned to room temperature.

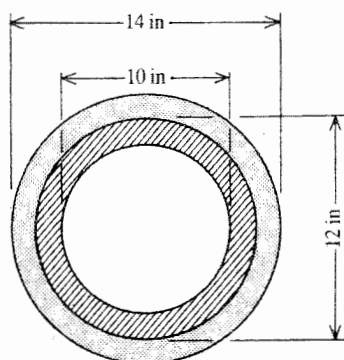


Figure 7.4. Exercise 7.6

- (d) Write the appropriate strain–displacement equations for either tube.
 (e) Obtain the differential equation for the radial displacement for either tube.
- 7.7. Follow the procedure outlined in Endnote (1) and derive any one of Eqs. (7.15) and any one of Eqs. (7.16). *Hint:* Recall, for example, that the first of Eqs. (7.15) is the equilibrium equation that deals with forces acting in the x coordinate direction.
- 7.8. The solution procedure used in Section 7.4 to solve Eq. (7.11) involved finding a complementary solution and two particular solutions to that ordinary differential equation. In order to simply determine a particular solution for the thermal term on the right-hand side, a linear temperature change was adopted. Such a specific choice was not really necessary. In way of general explanation, let the left-hand side of an ordinary differential equation in terms of the unknown function $u(r)$ have the form

$$a(r)u''(r) + b(r)u'(r) + c(r)u(r)$$

If the condition $(b/a)' = (c/a)$ is met, then this left-hand side can be rewritten as

$$a(r)\{f(r)[g(r)u(r)]'\}'$$

where the functions $f(r)$ and $g(r)$ are solutions to the equations

$$fg = 1 \quad \text{and} \quad \frac{f'}{f} = -\frac{b}{a} \quad \text{or} \quad \frac{g'}{g} = \frac{b}{a}$$

This form allows direct integration of the right-hand side with the result that both the complementary and particular solutions are generated. The application of this general theorem to Eq. (7.11) produces the result that

$$r^2u''(r) + ru'(r) - u(r) \equiv r^2 \frac{d}{dr} \left(\frac{1}{r} \frac{d}{dr} [ru(r)] \right)$$

This rewritten form of the left-hand side of the differential equations is in a form that allows two successive direct integrations.

- (a) Use the above rewritten form of Eq. (7.11) to obtain the following solution for that differential equation, and its first derivative:

$$u(r) = \frac{1+\nu}{r} \int r\alpha\Delta T(r)dr - (1-\nu^2)\frac{r^3\rho\Omega^2}{8E} + C_1r + \frac{C_2}{r}$$

$$u'(r) = -\frac{1+\nu}{r} \int r\alpha\Delta T(r)dr$$

$$+ (1+\nu)\alpha\Delta T(r) - 3(1-\nu^2)\frac{r^3\rho\Omega^2}{8E} + C_1 - \frac{C_2}{r^2}$$

- (b) Apply the boundary conditions $u(r=0) = 0$ and $\sigma_{rr}(r=R) = 0$ in order to determine the values of the constants of integration C_2 , which equals zero, and C_1 .
- (c) Substitute the above constants of integration into the solution for the displacement $u(r)$ in order to obtain the following solution for $u(r)$. (Recall $v(r) = 0$.)

$$u(r) = \frac{(1-\nu)\rho\Omega^2R^3}{8E} \left[(3+\nu)\frac{r}{R} - (1+\nu)\left(\frac{r}{R}\right)^3 \right]$$

$$+ \frac{1+\nu}{r} \int r\alpha\Delta T(r)dr + (1-\nu)\frac{r}{R^2} \left(\int r\alpha\Delta T(r)dr \right) \Big|_{r=R}$$

Then show that for $\Omega = 0$ and for a constant temperature change equal to T_0 , the solution for $u(r)$ is $\alpha T_0 r$.

- (d) Using the above expression for the displacement $u(r)$, determine the values of the radial and hoop stresses to be

$$\sigma_{rr} = (3+\nu)\rho\Omega^2\frac{R^2}{8} \left[1 - \left(\frac{r}{R}\right)^2 \right] + \frac{E}{R^2} \int r\alpha\Delta T(r)dr \Big|_{r=R}$$

$$- \frac{E}{r^2} \int r\alpha\Delta T(r)dr$$

$$\sigma_{\theta\theta} = \rho\Omega^2\frac{R^2}{8} \left[(3+\nu) - (1+3\nu)\left(\frac{r}{R}\right)^2 \right]$$

$$+ \frac{E}{r^2} \int r\alpha\Delta T(r)dr + \frac{E}{R^2} \left(\int r\alpha\Delta T(r)dr \right) \Big|_{r=R} - E\alpha\Delta T(r)$$

- (e) If the temperature change $\Delta T(r) = (r/R)T_0$, does the above general result reduce to the expressions set forth in Eqs. (7.9)?

7.9. As mentioned in Section 7.4, the homogeneous form of Eq. (7.11) can be reduced to an ordinary differential equation with constant coefficients by means of the coordinate transformation; $r = R \exp(s)$, or $s = \ln(r/R)$.

- (a) Use the chain rule for ordinary derivatives and carry out that transformation to obtain the corresponding homogeneous differential equation in terms of

$u(s)$ and its derivatives. *Hint:* The solution procedure begins by writing $du/dr = (du/ds)(ds/dr) = (1/r)(du/ds)$.

- (b) Solve that homogeneous equation for $u(s)$, and then transform it back so as to obtain $u(r) = Ar + B/r$, where, again, A and B are constants of integration.

Endnote (1) General Problem Formulations

There are two standard ways that the 15 equations of the theory of elasticity are combined in order to reduce the number of equations and the equal number of unknown functions, and thereby make the general theory of elasticity problem statement more compact. The first way is to eliminate all the unknowns but the three independent displacements. The first step towards achieving this displacement formulation is to substitute the stress–strain equations into the three independent equilibrium equations in order to eliminate the stresses. The result is three independent equations in terms of the six strains rather than the six stresses. The second step is to substitute the six strain–displacement equations into the above-modified three equations in order to eliminate the six strains. The result is three independent equations in terms of the three displacements. These equations, Eqs. (7.15), are called the *Navier equations* (Ref. [3]),³ or the *Navier–Cauchy equations* (Ref. [21]). They may be written for an isotropic material as

$$\begin{aligned}(\lambda + \mu) \frac{\partial}{\partial x} \left(\frac{\partial u}{\partial x} + \frac{\partial v}{\partial y} + \frac{\partial w}{\partial z} \right) + \mu \nabla^2 u - (3\lambda + 2\mu) \frac{\partial}{\partial x} (\alpha \Delta T) + \rho B_x &= 0 \\(\lambda + \mu) \frac{\partial}{\partial y} \left(\frac{\partial u}{\partial x} + \frac{\partial v}{\partial y} + \frac{\partial w}{\partial z} \right) + \mu \nabla^2 v - (3\lambda + 2\mu) \frac{\partial}{\partial y} (\alpha \Delta T) + \rho B_y &= 0 \\(\lambda + \mu) \frac{\partial}{\partial z} \left(\frac{\partial u}{\partial x} + \frac{\partial v}{\partial y} + \frac{\partial w}{\partial z} \right) + \mu \nabla^2 w - (3\lambda + 2\mu) \frac{\partial}{\partial z} (\alpha \Delta T) + \rho B_z &= 0\end{aligned} \quad (7.15)$$

where λ and μ are, again, the Lamé material constants, and ∇^2 (read “del squared”) in Cartesian coordinates is the following partial derivative operator

$$\nabla^2 = \nabla \cdot \nabla = \frac{\partial^2}{\partial x^2} + \frac{\partial^2}{\partial y^2} + \frac{\partial^2}{\partial z^2}$$

The boundary condition equations that are prescribed displacements are, of course, already in terms of displacements, and thus require no modification. The boundary condition equations that relate stresses to known tractions need to be rewritten in terms of the displacements rather than stresses. Exactly the same process outlined above that was used to formulate the equations for the interior in terms of displacements only is used for these equations for the boundaries. That is, stresses are replaced by strains, and then strains are replaced by displacements. The same process is possible because the stress–strain equations, and the strain–displacement equations are valid at the boundaries as well as in the

³ Louis Marie Henri Navier (1785–1836) published this result in 1821. Barré de Saint Venant was one of his pupils (Ref. [2]).

interior. The result for an isotropic material for that portion of the overall boundary for which tractions are prescribed, sometimes called surface one, or S_1 , is

$$\begin{aligned}
 & \lambda c_{nx} \left(\frac{\partial u}{\partial x} + \frac{\partial v}{\partial y} + \frac{\partial w}{\partial z} \right) + \mu \left(c_{nx} \frac{\partial u}{\partial x} + c_{ny} \frac{\partial u}{\partial y} + c_{nz} \frac{\partial u}{\partial z} \right) \\
 & \quad + \mu \left(c_{nx} \frac{\partial v}{\partial x} + c_{ny} \frac{\partial v}{\partial x} + c_{nz} \frac{\partial v}{\partial x} \right) = T_x + c_{nx}(3\lambda + 2\mu) \alpha \Delta T \\
 & \lambda c_{ny} \left(\frac{\partial u}{\partial x} + \frac{\partial v}{\partial y} + \frac{\partial w}{\partial z} \right) + \mu \left(c_{nx} \frac{\partial v}{\partial x} + c_{ny} \frac{\partial v}{\partial y} + c_{nz} \frac{\partial v}{\partial z} \right) \\
 & \quad + \mu \left(c_{nx} \frac{\partial u}{\partial y} + c_{ny} \frac{\partial v}{\partial y} + c_{nz} \frac{\partial v}{\partial y} \right) = T_y + c_{ny}(3\lambda + 2\mu) \alpha \Delta T \\
 & \lambda c_{nz} \left(\frac{\partial u}{\partial x} + \frac{\partial v}{\partial y} + \frac{\partial w}{\partial z} \right) + \mu \left(c_{nx} \frac{\partial w}{\partial x} + c_{ny} \frac{\partial w}{\partial y} + c_{nz} \frac{\partial w}{\partial z} \right) \\
 & \quad + \mu \left(c_{nx} \frac{\partial u}{\partial z} + c_{ny} \frac{\partial v}{\partial z} + c_{nz} \frac{\partial w}{\partial z} \right) = T_z + c_{nz}(3\lambda + 2\mu) \alpha \Delta T
 \end{aligned} \tag{7.16}$$

Obviously these are a formidable grouping of governing differential equations and boundary condition equations. General solutions to these partial differential equations are not known. There are particular solutions that may be found, for example, in Refs. [8] and [9]. Since all that is desired of the reader of this text is the knowledge of the existence of the Navier equations, these limited solutions are not pursued.

The alternative to the displacement formulation is the stress formulation. The unified stress formulation begins with the six strain compatibility equations, Eqs. (3.16). Recall that of these six equations only three are independent equations. The six strain–stress equations are used to replace the six strains in all six compatibility equations by the six unknown stresses. Then the three independent equilibrium equations, which of course are already in terms of the six stresses, are substituted into (i.e., combined with) each of the six compatibility equations in order to obtain six independent equations (three from the equilibrium equations, and three from the six compatibility equations) in terms of the six stresses. These final six equations are called the *Beltrami–Michell equations* (Ref. [3]). The main value that the Beltrami–Michell equations, and their attendant boundary condition equations, have is that they illustrate that there is a general stress formulation, and that sanctions the development of special-case stress formulations. The six Beltrami–Michell equations for an isotropic material can be written as

$$\begin{aligned}
 & (1 + \nu) \nabla^2 \sigma_{xx} + \frac{\partial^2}{\partial x^2} (\sigma_{xx} + \sigma_{yy} + \sigma_{zz}) - \nu \nabla^2 (\sigma_{xx} + \sigma_{yy} + \sigma_{zz}) \\
 & \quad = -2(1 + \nu) \frac{\partial \rho B_x}{\partial x} - E \alpha \left[\frac{\partial^2}{\partial x^2} \Delta T + \nabla^2 \Delta T \right] \\
 & (1 + \nu) \nabla^2 \sigma_{yy} + \frac{\partial^2}{\partial y^2} (\sigma_{xx} + \sigma_{yy} + \sigma_{zz}) - \nu \nabla^2 (\sigma_{xx} + \sigma_{yy} + \sigma_{zz}) \\
 & \quad = -2(1 + \nu) \frac{\partial \rho B_y}{\partial y} - E \alpha \left[\frac{\partial^2}{\partial y^2} \Delta T + \nabla^2 \Delta T \right] \\
 & (1 + \nu) \nabla^2 \sigma_{zz} + \frac{\partial^2}{\partial z^2} (\sigma_{xx} + \sigma_{yy} + \sigma_{zz}) - \nu \nabla^2 (\sigma_{xx} + \sigma_{yy} + \sigma_{zz}) \\
 & \quad = -2(1 + \nu) \frac{\partial \rho B_z}{\partial z} - E \alpha \left[\frac{\partial^2}{\partial z^2} \Delta T + \nabla^2 \Delta T \right]
 \end{aligned} \tag{7.17}$$

$$\begin{aligned}
 (1 + \nu)\nabla^2\sigma_{xy} + \frac{\partial^2}{\partial x\partial y}(\sigma_{xx} + \sigma_{yy} + \sigma_{zz}) &= -(1 + \nu)\left[\frac{\partial\rho B_x}{\partial y} + \frac{\partial\rho B_y}{\partial x}\right] - E\alpha\frac{\partial^2\Delta T}{\partial x\partial y} \\
 (1 + \nu)\nabla^2\sigma_{xz} + \frac{\partial^2}{\partial x\partial z}(\sigma_{xx} + \sigma_{yy} + \sigma_{zz}) &= -(1 + \nu)\left[\frac{\partial\rho B_x}{\partial z} + \frac{\partial\rho B_z}{\partial x}\right] - E\alpha\frac{\partial^2\Delta T}{\partial x\partial z} \\
 (1 + \nu)\nabla^2\sigma_{yz} + \frac{\partial^2}{\partial y\partial z}(\sigma_{xx} + \sigma_{yy} + \sigma_{zz}) &= -(1 + \nu)\left[\frac{\partial\rho B_y}{\partial z} + \frac{\partial\rho B_z}{\partial y}\right] - E\alpha\frac{\partial^2\Delta T}{\partial y\partial z}
 \end{aligned}$$

The stress formulation boundary condition equations are simply the Cauchy equations. The Cauchy equations are useful only where tractions are prescribed, which again is the surface designated by the symbol S_1 . If the total boundary surface also contains areas where displacements are prescribed, surface areas which are designated as S_2 , then a stress formulation is generally not at all convenient. Hence when the boundary is either in S_2 or mixed (i.e., in S_1 and S_2) the displacement formulation is usually the only practical selection. This is so because, as noted in Chapter 3, displacement-strain equations are not available, and thus displacements cannot be replaced by strains, and the strains replaced by stresses. In other words, at the boundary, it is possible to usefully replace stresses by the derivatives of displacements, but displacements cannot be usefully replaced by the integrals of stresses. The displacement formulation is also the preferred choice for structural dynamic problems; that is, those problems where the structural accelerations are not constants. The reason for this is that, of course, the accelerations (the body forces per unit mass) must first be written as time derivatives of the displacements, and again there are no displacement-strain equations that can be used to convert the displacement time derivatives into stress time derivatives.

The stress formulation for the special case of plane stress is worth special mention. In this case, to match the three unknown stresses, there are two independent equations of equilibrium, Eqs. (1.10), and one independent compatibility equation, Eq. (3.14a). However, this compatibility equation stands alone only in the case of plane strain. In the case of plane stress, the strain ϵ_{zz} is not zero. Thus Eq. (3.14a) is but one of four nontrivial compatibility equations. The other three compatibility equations require that the three second partial derivatives of ϵ_{zz} be zero. However, ϵ_{zz} , through the strain-stress equations, is a function of σ_{xx} and σ_{yy} (see Exercise 5.3 for the isotropic case). The usual procedure is to omit these latter three compatibility equations from the solution process, and then check to see whether these additional three compatibility equations are also satisfied. If those three equations cannot be satisfied, then the discrepancy is noted, and the solution is retained as an approximate solution. Such solutions that have been investigated experimentally have proved to be wholly satisfactory.

The above-mentioned two equilibrium equations and the one compatibility equation can, by means of a potential function for the three unknown stresses, called the Airy⁴ stress function, be reduced to the even more convenient form of a single partial differential equation in terms of that one unknown potential function. This particular stress formulation has led to numerous useful plane stress solutions (Ref. [21]), many of which could be developed in this introductory text. Again, the derivation and application of the Airy stress function formulation for plane stress problems is a very low-priority item, so it is left as an optional section in the next chapter. The device of using a potential function for stresses

⁴ George Biddell Airy (1801–1892), British astronomer and mechanic, introduced the stress function that bears his name in 1862. In three-dimensional problems, three independent potential functions are required, and thus the benefits of the potential function approach are fewer.

is nevertheless an important solution tool, and the technique is illustrated again when the theory of elasticity equations are specialized to the problem of the torsion of isotropic, prismatic bars in Chapter 12.

In summary, the three sets of interior or field equations of the theory of elasticity can be combined in two different ways to obtain governing differential equations of broad applicability. Again, the equilibrium equations, the stress–strain equations, and the strain–displacement equations are combined to form the three Navier equations, which are in terms of the three unknown displacements. The six Beltrami–Michell equations, which are in terms of the six unknown stresses, are obtained by combining the equilibrium, compatibility, and strain–stress equations. Again, engineers hardly ever work with either of these grand formulations.

Endnote (2) Another Solution to the Disk Displacement Equation

An integrating factor solution for Eq. (7.11), which is a bit more general than that obtained previously can be obtained as follows. By both adding and subtracting the term ru' , rewrite Eq. (7.11) as

$$\begin{aligned}(r^2u'' + 2ru') - (ru' + u) &= r^2(1 + \nu)\alpha\Delta T' - (1 - \nu^2)r^3\frac{\rho\Omega^2}{E} \\ \frac{d}{dr}(r^2u') - \frac{d}{dr}(ru) &= r^2(1 + \nu)\alpha\Delta T' - (1 - \nu^2)r^3\frac{\rho\Omega^2}{E}\end{aligned}$$

Multiplying through by dr , and carrying out an indefinite integration yields

$$r^2u' - ru = C_1 + (1 + \nu) \int r^2\alpha\Delta T' dr - (1 - \nu^2)r^4\frac{\rho\Omega^2}{4E}$$

To find the next integrating factor, note the minus sign that separates the two left-hand side terms. Recall that $(d/dr)(f/g) = (gf' - fg')/g^2$. Thus divide the above equation by r^3 , and let $f = u$, and $g = r$ so that

$$\frac{ru' - u}{r^2} = \frac{d}{dr}\left(\frac{u}{r}\right) = \frac{C_1}{r^3} + (1 + \nu)\frac{1}{r^3} \int r^2\alpha\Delta T' dr - (1 - \nu^2)r\frac{\rho\Omega^2}{4E}$$

Integrating, and then multiplying through by r yields

$$u(r) = C_2r - \frac{C_1}{2r} + r(1 + \nu) \int \frac{1}{r^3} \left(\int r^2\alpha\Delta T' dr \right) dr - (1 - \nu^2)r^3\frac{\rho\Omega^2}{8E}$$

With $A = C_2$ and $B = -\frac{1}{2}C_1$, and $\alpha T(r)$ given the same explicit value of rT_0/R , then the above answer is exactly the same as the previous solution for $u(r)$ with constants of integration. The reader is invited to carry out the integration of the temperature change term and verify that statement.

Endnote (3) Example 7.1 Compatibility Equation

The general form of the compatibility equation in cylindrical coordinates is set forth in Exercise 3.6 when the solutions for the three constants $A = C = -B = 1.0$ are entered. This equation can be adapted to Example 7.1 by setting all partial derivatives with

respect to θ equal to zero, and replacing all partial derivatives with respect to r by total derivatives with respect to r . Then the adapted compatibility equation reduces to

$$\epsilon'_{rr} = (r\epsilon_{\theta\theta})''$$

This equation can be immediately integrated once to obtain

$$\epsilon_{rr}(r) = [r\epsilon_{\theta\theta}(r)]' + C$$

where, of course, C is a constant of integration. The first two terms of the above equation are the entire compatibility equation that is derived from the adapted displacement terms. From that viewpoint, C is clearly zero. However, if that adapted displacement approach to the compatibility equation were not pursued, the fact that C is zero would not be evident at all. This constant of integration would have to be carried throughout all the remaining algebraic manipulations, and eventually determined to be zero from the boundary conditions. This should make clear the advantage of deriving compatibility equations from adapted displacement expressions where possible.

Plane Stress Theory of Elasticity Solutions

8.1 Introduction

Chapter 7 illustrated the direct approach to solving selected problems in structural mechanics. In that chapter solutions for structural displacements and stresses were obtained through the separate use of the four sets of equations that constitute the theory of elasticity. There were no major difficulties in solving the example problems of that chapter because the original three-dimensional problems were reduced to one-dimensional problems (i.e., problems involving only one independent spatial variable) by means of plane stress and symmetry concepts. More challenging problems are the theory of elasticity problems that involve two independent spatial variables, such as plane stress problems in general. The purpose of this chapter is to present two of the simplest of such problems and their solutions in order for the reader to obtain some familiarity with their characteristics. The selected example and exercise problem solutions of this chapter are sufficiently valuable to be referenced in succeeding chapters as proof of the accuracy of the approximations adopted in those chapters.

While the following theory of elasticity solutions provide valuable practice in all the essentials of structural engineering analysis, it is also important to know that from the point of view of everyday structural engineering practice, theory of elasticity solutions are rarely, if ever, referenced. The advent of modern digital computers and the development of modern numerical methods, particularly the finite element method that is explained in Part V of this textbook, have relegated theory of elasticity solutions to the role of mere curiosities. Such a trivial status is mostly due to the fact that there are so few useful plane stress theory of elasticity solutions, called *exact solutions*. Hence the practicing structural engineer faced with a plane stress problem would undoubtedly immediately resort to a finite element analysis without bothering to consider whether or not an exact solution would be possible, and would not suffer for neglecting such a possibility.

8.2 Solution Examples

Since general plane stress problems involve two spatial coordinates, their direct solution requires dealing with partial differential equations. However, the reader is not expected to know any of the various techniques for solving partial differential equations. Thus in the example solutions discussed in this and the next section, the style of the presentation is one where the stress solution results are verified rather than derived.

Example 8.1. Consider the uniformly thin rectangular sheet or slab of dimensions $2a$ by $2b$ shown in Fig. 8.1(a). Let this thin slab be in a state of plane stress, and let all the body forces be zero. Let the material be isotropic and let the stresses within the rectangle be as follows:

$$\sigma_{xx}(x, y) = -My/I \quad \text{and} \quad \sigma_{xy} = \sigma_{yy} = 0$$

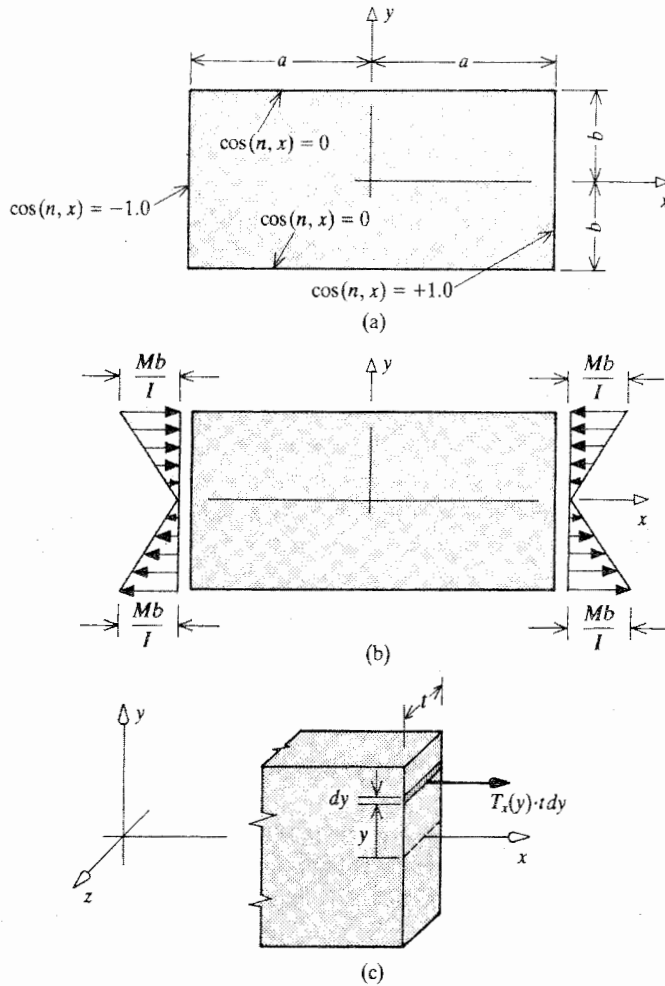


Figure 8.1. Example 8.1. (a) The geometry and coordinate system. (b) The required tractions. (c) The integration set-up for determining the forces and moments produced by the end tractions.

where M and I are constants to be discussed later. Let the tractions at the edges be determined later. Again, what is being done here is the inverse of the usual, direct task. That is, a geometry has been selected and a solution (a stress state) has been chosen. After verifying that it is a solution (i.e., that the necessary interior theory of elasticity equations are satisfied), then the problem (the loading) is determined. This approach of choosing the solution and then finding the problem it solves is both sufficiently common and important to the theory of elasticity to merit being named the *inverse method*.

The first task is to determine whether the above stress state actually does satisfy the three sets of interior (i.e., field) equations of the theory of elasticity. Since the approach taken here is that of a stress formulation, the three sets of field equations that need to be checked are the two plane stress equilibrium equations, the three plane stress constitutive equations for an isotropic material, and the compatibility equations. With the body forces being zero, the two equations of equilibrium, Eqs. (1.10), are satisfied identically. The constitutive equations

become

$$\begin{aligned}\epsilon_{xx} &= \frac{\sigma_{xx}}{E} = -\frac{My}{EI} & \gamma_{xy} &= 0 \\ \epsilon_{yy} &= -\frac{\nu\sigma_{xx}}{E} = +\frac{\nu My}{EI}\end{aligned}$$

When these strains are substituted into the primary plane stress compatibility equation, Eq. (3.14), it is evident that each term in the primary compatibility equation is zero, and thus that equation is also identically satisfied. The other five compatibility equations are also satisfied. Recall that the satisfaction of the compatibility equations makes it unnecessary to consider the strain–displacement equations.

All that remains to complete the verification of the given stresses as a stress solution is to demonstrate that these stresses are in accord with the traction boundary conditions at the edges of the rectangle. Since no tractions have been previously stated, this step simply becomes a matter of accepting as part of the problem definition whatever tractions are required by the Cauchy equations, Eqs. (1.11). In this case these boundary condition equations reduce to

$$T_x = \sigma_{xx} \cos(n, x) \quad \text{and} \quad T_y = 0$$

Using the direction cosines shown in Fig. 8.1(a), it can be seen that at the top and bottom edges where $y = +b$ and $y = -b$, both tractions must be zero. At the edges $x = +a$ and $x = -a$, the shearing tractions are zero while the normal tractions must be as illustrated in Fig. 8.1(b). Recall that the tractions are always positive in the direction of the positive coordinate axes.

Thus it is established that, for a thin, rectangular slab of an isotropic material subjected only to edge tractions as shown in Fig. 8.1(b), the stress distribution is as given above. Note that changing the origin of the coordinate system, or changing the shape of the boundary of the slab of material does not change the fact that the given stresses satisfy the equilibrium, constitutive, and compatibility equations, and hence are a solution in the interior of a structural body. However, changing the location of the origin of the coordinate system, or the shape of the boundary, changes the problem for which those stresses are a solution.

This solution becomes more useful to engineers when a slightly different view of the geometry of this structural body is adopted. Let the length a be larger than the length b . In this case, there is actually no restriction of any kind regarding the size of a relative to that of b . It is just a matter of having the thin, uniform slab look like a beam of rectangular cross-section,¹ with b only somewhat larger than the constant thickness t . From a beam point of view, it is clear that the tractions at each beam end cross-section do not produce either an axial force or a shear force. However, the tractions at both $x = +a$ and $x = -a$ do produce equal moments whose magnitude can be obtained by integrating (summing) all the infinitesimal moments produced by the tractions acting upon infinitesimal areas. For example, at the end cross-section $x = +a$, consider an infinitesimal area, $t \, dy$, of that cross-section at a distance y above the x axis; see Fig. 8.1(c). The infinitesimal force normal to that infinitesimal area is the quantity $(\sigma_{xx} t \, dy)$. The moment arm about the z axis is the

¹ This is a point of some importance. To be reasonably accurate, the approximate theory for beam stresses that is most frequently used by engineers, to be discussed in Part III, generally requires that the beam be “long,” that is, it requires that the beam length-to-depth ratio be approximately 10 to 1 or more.

distance y . Thus the total moment at the right-hand end of the beam is

$$M_z(x = a) = -t \int_{-b}^{+b} y \sigma_{xx} dy = + \frac{2Mb^3t}{3I}$$

where a minus sign is inserted to comply with a sign convention for beam moments in which moments that tend to curve the beam into a happy face smile are positive, and moments that produce the shape of frown are negative. Let the previously unspecified constant I be required to have the value $I = t(2b)^3/12$, which is the area moment of inertia of the beam cross-sectional area about an axis passing through the center of the beam cross-section and paralleling the z -axis. Then the above integral shows that the constant M is the value of the moment $M_z(x = a)$. Since the σ_{xx} stresses are independent of the variable x , so too is the bending moment. That is, the bending moment is the same at all beam cross-sections. Thus this stress solution is the solution for a long or short beam subjected to opposite bending moments at each end cross-section, if the tractions are applied as indicated in Fig. 8.1(b).

The approximate engineering solution for beam bending stresses, which is developed in later chapters, reproduces this particular theory of elasticity solution. Hence that approximate stress solution is called “exact” in the special circumstance of a beam loaded only by bending moments.

The strains calculated above can be integrated to obtain the following displacements relative to the center of the beam or slab. The result of the integrations is

$$u(x, y) = -\frac{M}{EI}xy \quad v(x, y) = \frac{M}{2EI}(x^2 + \nu y^2)$$

The $v(x, y)$ displacement solution shows that the beam does have positive curvature. The $u(x, y)$ displacement solution shows that, because of its linear change in the y direction, any plane cross-section of the beam (i.e., at a fixed value of x) deforms into a plane section that is rotated about an axis paralleling the z axis. This is mentioned because a fundamental approximation of the engineering beam bending theory to be discussed in later chapters is that “plane sections remain plane after deformation.” ■

The following example problem is only a bit more elaborate than the preceding example problem. Since the proposed solution in this case, as was true the previous case, is in terms of stresses, exactly the same four sets of equations require checking. The only variation here from the above is the adoption of a much more efficient combination form of the compatibility and strain–stress equations.

Example 8.2.² Consider the plane stress problem of the rectangular slab manufactured from an isotropic material that is illustrated in side view in Fig. 8.2. In this case, as in the latter part of the previous example, the geometric dimensions of $2a \times 2b$ by t are to be interpreted as those of a beam of length $2a$ with rectangular cross-sectional dimensions $2b \times t$. Note that in this case there is a partial specification of the boundary conditions. That is, there is a traction $T_y = +p$ acting on the bottom surface, $y = -b$. All that is said at present regarding the beam ends is that there are shear forces acting on the two faces $x = \pm a$ that equilibrate

² This example is taken from Ref. [21], which is an excellent source of information on many such problems.

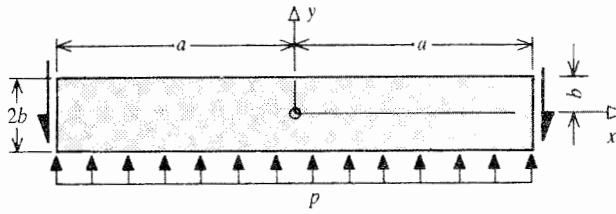


Figure 8.2. Example 8.2. A uniformly loaded, simply supported, uniform beam.

the traction acting at the bottom surface. The stress solution proposed for this problem is

$$\begin{aligned}\sigma_{xx}(x, y) &= \frac{3p}{4} \left\{ \left(\frac{a}{b}\right)^2 \left[1 - \left(\frac{x}{a}\right)^2\right] \left(\frac{y}{b}\right) + \left[\frac{2}{3} \left(\frac{y}{b}\right)^3 - \frac{2}{5} \left(\frac{y}{b}\right)\right] \right\} \\ \sigma_{xy}(x, y) &= -\frac{3p}{4} \frac{a}{b} \frac{x}{a} \left[1 - \left(\frac{y}{b}\right)^2\right] \\ \sigma_{yy}(x, y) &= -\frac{3p}{4} \left[\frac{1}{3} \left(\frac{y}{b}\right)^3 - \frac{y}{b} + \frac{2}{3}\right]\end{aligned}\quad (8.1)$$

It is not difficult to show that these stresses identically satisfy the plane stress equations of equilibrium, Eqs. (1.10), when the body forces are zero. Substitution of these stresses into the plane stress strain–stress equations in order to obtain the expressions for the strains, and then substitution of those strain expressions into the plane stress compatibility equation, Eq. (3.14), shows that the primary plane stress compatibility equation, and hence the constitutive equations, are satisfied. This process of testing a possible plane stress solution to determine whether it satisfies both the plane stress constitutive equations and the primary plane stress compatibility equation, is a process that recurs sufficiently frequently to make it desirable to simplify the process by condensing the relevant equations into a single equation. The condensation can be accomplished by using the general form of the plane stress, strain–stress equations, Eqs. (6.10), to rewrite the primary plane stress compatibility equation, Eq. (3.14a), in terms of stresses. Using, in order to simplify the result, the sum of the two plane stress equilibrium equations, Eqs. (1.10), each partially-differentiated to obtain the mixed partial derivative $2(\partial^2\sigma_{xy}/\partial x \partial y)$, the primary plane stress compatibility equation in terms of stresses becomes

$$\nabla^2(\sigma_{xx} + \sigma_{yy}) + E\nabla^2(\alpha\Delta T) + (1 + \nu) \left[\frac{\partial}{\partial x}(\rho B_x) + \frac{\partial}{\partial y}(\rho B_y) \right] = 0 \quad (8.2)$$

The two plane stress equilibrium equations and Eq. (8.2) are the usual choice of the three plane stress equations for the three unknown plane stresses. For steady-state conditions, that is, when the temperature distribution is not changing with respect to time (i.e. when the partial derivative of the temperature with respect to time is zero), the heat conduction equation requires that

$$\nabla^2(\Delta T) = 0$$

Equation (8.2) is also simplified if the body forces are constant over the area of the structure.

Now it is a simple matter to verify that the candidate stress expressions for this example, Eqs. (8.1), do indeed satisfy the combination of the constitutive equations and the primary

plane stress compatibility equation, which is Eq. (8.2).³ Since Eqs. (8.1) thus satisfy the equilibrium, constitutive, and compatibility equations, it is said that Eqs. (8.1) are a theory of elasticity solution.

It is now necessary to examine the boundaries of the rectangular slab to see whether the Cauchy boundary condition equations are satisfied. If the boundary condition equations are also satisfied, then, of course, the proposed solution is indeed *the* theory of elasticity solution for this problem. Repeating the plane stress Cauchy equations for easy reference:

$$T_x = \sigma_{xx} \cos(n, x) + \sigma_{xy} \cos(n, y)$$

$$T_y = \sigma_{xy} \cos(n, x) + \sigma_{yy} \cos(n, y)$$

At the top surface of the beam, where the variable y has the fixed value $+b$,

$$T_x = 0 \quad \sigma_{xx} = \dots \quad \sigma_{xy} = 0 \quad \cos(n, x) = 0$$

$$T_y = 0 \quad \sigma_{xy} = 0 \quad \sigma_{yy} = 0 \quad \cos(n, y) = +1$$

At the bottom surface of the beam where $y = -b$,

$$T_x = 0 \quad \sigma_{xx} = \dots \quad \sigma_{xy} = 0 \quad \cos(n, x) = 0$$

$$T_y = +p \quad \sigma_{xy} = 0 \quad \sigma_{yy} = -p \quad \cos(n, y) = -1$$

Substitution in turn of the above two sets of boundary values shows that the Cauchy boundary condition equations at the top and bottom surfaces are satisfied, that is, each Cauchy equation reduces to the identity zero equals zero. Since this is a plane stress problem, there are of course nothing but zero tractions and stresses at the front and back side surfaces.

The situation at the beam end surfaces is not as straight forward as at the top, bottom, and side beam surfaces. As mentioned previously, tractions are not initially specified on the two end surfaces. The only specification for the end surfaces is that the net result of the tractions acting on those surfaces is the two downward shearing forces which equilibrate the sum effect of the traction on the bottom surface, and nothing more. An investigation of the end surfaces begins with writing the tractions that must be present at both ends of the beam in order for the Cauchy equations to be satisfied. For example, at the end $x = +a$, where $\cos(n, x) = +1$, and $\cos(n, y) = 0$, the nonzero tractions are

$$T_x(a, y) = \sigma_{xx}(a, y) = \frac{3p}{4} \left[\frac{2}{3} \left(\frac{y}{b} \right)^3 - \frac{2}{5} \frac{y}{b} \right]$$

$$T_y(a, y) = \sigma_{xy}(a, y) = \frac{3p}{4} \frac{a}{b} \left[1 - \left(\frac{y}{b} \right)^2 \right]$$

(8.3)

The tractions at $x = -a$ are the same except for a sign change on T_x . Thus it may be stated that the initially stated stress expressions are an exact plane stress solution for a rectangular cross-section beam loaded by a pressure p acting along its bottom surface if the end supports are such as to provide exactly the end tractions specified above. Actual beam supports for such a beam are commonly a set of discrete connections such as nails, bolts, rivets, edge welds, and so forth. In such cases, it is quite unlikely that the traction distribution at the support surface would be that described by the above traction equations. Nevertheless, this stress solution may not be without value. Note that the integral of the above y direction traction

³ While the proposed plane stress solution of this example does satisfy the primary plane stress compatibility equation, Eq. (3.14), the proposed solution does not satisfy all the three-dimensional compatibility equations, unless the Poisson ratio is zero. The error is in equations that involve the strain ϵ_{zz} , and can be ignored.

over the end cross-sectional area at $x = +a$ yields a downward-directed force of magnitude pta , which, together with the equal downward reaction at the other end, equilibrates the upward pressure at the bottom surface. Furthermore, both the axial force and bending moment produced by the x direction traction, acting over either end area, have zero magnitudes. That is, from Eqs. (8.3), at $x = +a$:

$$\begin{aligned} \text{Equivalent downward vertical end force} &= -t \int_{-b}^{+b} T_y(a, y) dy = pta \\ \text{Equivalent horizontal end force} &= t \int_{-b}^{+b} T_x(a, y) dy = 0 \\ \text{Equivalent end bending moment} &= t \int_{-b}^{+b} yT_x(a, y) dy = 0 \end{aligned} \quad (8.4)$$

Again, if the actual beam end supports in some manner supplied the above overall reactions of equilibrating vertical forces but zero axial forces and bending moments, then perhaps, at least in some equivalent equilibrium sense, the above stress solution may still have value. Section 8.3 deals with this conjecture, and establishes it as being true. However, before proceeding with that development and leaving this example, there is an aspect of the above solution that is worthy of comment. The comment is that if the beam is long compared to its depth, that is, if $a^2 \gg b^2$, because of the presence of the factor a^2/b^2 , the first bracketed part of the expression for σ_{xx} is more important (bigger) than any other such part of any of the three stresses. The single bracketed part of σ_{xy} is the second largest such part. The simple, approximate methods for determining stresses in beams that are developed in later chapters are able to provide (i) this important first part of the x direction normal stress; and (ii) the total shear stress. The beam bending approximate method is not able to estimate the y direction normal stress, nor the remaining, less important parts of the x direction stress. Thus it will be said that the beam bending approximate stress solution is satisfactory when the beam is long, that is, when $a^2 \gg b^2$. When the beam is short, then either a numerical method of analysis which satisfies as many of the theory of elasticity equations as possible needs to be used, or a refined approximate beam bending theory needs to be used. The value in separating the components of the solution according to the presence of the factors of (a/b) or (b/a) also holds true for displacements as well as stresses. For example, the upward vertical displacement at the center of this beam relative to the center of the end cross-sections, is, according to Ref. [21],

$$v(0, 0) = \frac{5pa^4}{16Eb^3} \left[1 + \frac{12}{5} \left(\frac{b}{a} \right)^2 \left(\frac{4}{5} + \frac{\nu}{2} \right) \right] \quad (8.5)$$

The first and larger part of this two-part solution is obtainable by the simpler, approximate method of later chapters. The second part of the above solution, which is only important for short beams, is only obtainable by use of the theory of elasticity. ■

8.3 St. Venant's Principle

In the preceding paragraph it was pointed out that in order for a stress solution to be wholly accurate throughout the volume of the structural body, the actual supports must be such as to provide precisely those tractions that match the stress distribution at the support surfaces. It was further remarked that it is quite unlikely that an actual stress distribution at an actual support would closely approximate that deduced for the simplified type of supports that are convenient for analyses. Since the stress distribution at actual supports

can be expected to differ significantly from the theory of elasticity stress distribution, the question arises as to whether the actual stress distribution over the remainder of the body would also differ significantly from that calculated by use of the theory of elasticity.

The negative answer to this question is provided by *St. Venant's principle*, which states that *If the tractions (or forces and moments) acting upon a small portion of the surface of a compact elastic body are replaced on that small surface by another, statically equivalent, system of tractions (or forces and moments), then the change in loading has only a negligible effect on the stresses located away from that surface at linear distances that are larger than the largest dimension of the surface on which the forces were changed.* (Refs. [21, 37])

There are several points concerning St. Venant's principle that bear discussion. First of all, this principle is a powerful tool because the distance from the surface which bears the altered but equivalent loading, beyond which the changes in stress are negligible, is often as small as the largest dimension of the surface area under discussion. For example, in the case of the rectangular cross-section beam loaded with an upward pressure along its bottom surface discussed in the previous section, St. Venant's principle affirms that beyond a distance of $2b$ from each beam end there is no practical difference between the calculated and actual stresses in the beam whether or not the beam end support tractions are those of Eqs. (8.3), or any other set of tractions that produce the overall effects listed in Eqs. (8.4). If $a^2 \gg b^2$, then the stresses over the great majority of the beam volume are correctly calculated by the theory of elasticity solution.

For the distance outside of which the stresses for the equivalent loadings differ only negligibly, for that distance to be small, the body must be a compact, solid body. Reference [21] states that if "the body is not of a solid form, as for instance a beam with a very thin web, or a thin cylindrical shell, a self-equilibrating distribution of force on one end may make itself felt at distances many times the depth or diameter." Figure 8.3 provides a simple illustration of a slight variation on this caution. In Fig. 8.3(a) and (b), a long, simple two-dimensional, pin-jointed truss is shown. The truss is loaded over the depth of its end by two different, statically equivalent force systems having a zero moment about the center of the end section and a total resulting (tensile) force of magnitude N . It should be clear that with respect to the two different loading cases, the force distributions in the bars of the truss are not the same at any point in the truss, close or far from the end of the truss where the loadings are applied. If, however, the outside dimensions of the truss are fixed while the number of bars in the truss is increased uniformly over the area of the truss, and the number of supports at the left end is increased correspondingly, then the two force distributions away from the loaded end will become more alike as the number of bars increases. At the extreme end of the process of adding bars, the elastic body becomes a solid two-dimensional body of dimensions $2b$ by L . In this case the normal stresses in the direction of the concentrated tensile force N becomes virtually uniform (less than a 3 percent error) at a distance of only $2b$ from the loaded end of the solid structure. This diffusion of a concentrated force into a very nearly uniform stress distribution in such a short distance is a dramatic illustration of St. Venant's principle. A general proof of St. Venant's principle based upon energy considerations, which is credited to Goodier, is stated in Ref [21].

8.4 ** Review Problem**

This and the previous chapter have emphasized a checklist consisting of (i) equilibrium equations; (ii) constitutive equations; (iii) compatibility or strain displacement equations; and (iv) boundary condition equations. One- and two-dimensional plane stress

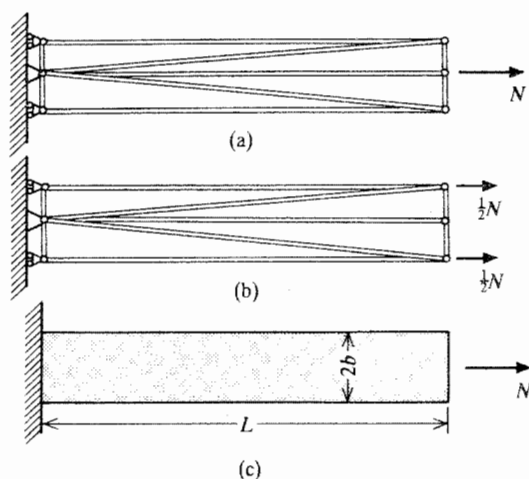


Figure 8.3. Two different loadings on a simple truss and a uniform slab, where the slab represents a limiting case for the truss as the number of pin joints and bars within the outer boundaries of the truss increase without limit.

problems have provided a basis for illustrating the application of this checklist. The following example problem, which is a variant of previous problems, demonstrates that the checklist of concepts that underlie those four sets of equations can be just as useful in structuring a solution to a structural analysis problem that bears little resemblance to a plane stress problem.

Example 8.3. Consider the structure pictured in Fig 8.4(a) in its exaggerated deformed state. The structure is composed of three, equal length, dissimilar bars that are attached by hinges to two end fixtures that are sufficiently stiff relative to the bars to be modeled as rigid. The structure is loaded by equal and opposite forces F . Determine the bar extensions and stresses.

Solution. The sequential use of the four sets of equations provides an **organized** approach to the solution of this problem. For convenience, and without loss of generality, assume that all the bars elongate as shown in Fig. 8.4(a), and thus it follows that the stresses in all bars are assumed to be tensile and all displacements are elongations. A negative solution for a displacement or stress, of course, means contraction or compression, respectively.

Start the analysis by noting that the entire structure is in a state of static equilibrium. FBDs of arbitrary portions of any of the three bars demonstrates that the axial stress in each bar is a constant along the length of the bar. A FBD of either end fixture, such as is shown for the left end fixture in Fig. 8.4(b) provides the following *equilibrium equations*:

$$\begin{aligned} \text{Summing forces: } & \sigma_a A_a + \sigma_c A_c + \sigma_e A_e = F \\ \text{Summing moments: } & (b + d) A_a \sigma_a + (d) A_c \sigma_c = 0 \end{aligned} \quad (8.6)$$

These equilibrium equations are two equations in the three unknown stresses. Thus the problem is indeterminate, and it is necessary to investigate the displacements. The next step is to write the *constitutive equations* for the elastic portions of the structural system. They are

$$\sigma_a = E_a \epsilon_a \quad \sigma_c = E_c \epsilon_c \quad \sigma_e = E_e \epsilon_e$$

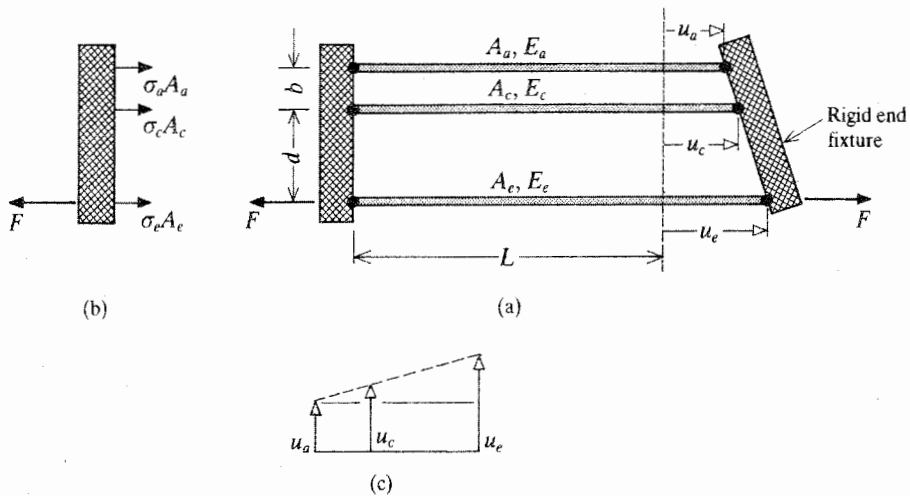


Figure 8.4. Example 8.3. A nonsymmetrical three-hinged bar structure: (a) the deformation pattern with all displacements transferred to the right-hand end; (b) free body diagram of the right end fixture; (c) diagram of the proportionality of the bar displacements.

Since the stresses are constants, so too are the strains. Hence the following *strain-displacement equations*:

$$\epsilon_a = \frac{u_a}{L} \quad \epsilon_c = \frac{u_c}{L} \quad \epsilon_e = \frac{u_e}{L}$$

The *boundary condition equations* for a problem with discrete structural elements, as in this case, are open to more than one interpretation to the extent of which equations are to be called the boundary condition equations. It could be argued that the Eqs. (8.6) are actually boundary condition equations while the interior equilibrium equations are those that establish the stresses as being constant along the length of the bars. In any event, there is additional information concerning the displacements at the edges of the elastic bars. These displacements are constrained by the rigid end fixture to form a straight-line pattern as shown in Fig. 8.4(c). From similar triangles,

$$\frac{u_c - u_a}{b} = \frac{u_e - u_a}{b + d} \tag{8.7}$$

This “third” boundary condition equation completes the analysis. Now it is a matter of choosing to replace the displacements in Eq. (8.7) by stresses, or choosing to replace the stresses in Eqs. (8.6) by displacements. By the first of these two options, Eq. (8.7) becomes, after use of the strain-displacement and constitutive equations,

$$(b + d) \left(\frac{\sigma_c}{E_c} - \frac{\sigma_a}{E_a} \right) = b \left(\frac{\sigma_e}{E_e} - \frac{\sigma_a}{E_a} \right) \tag{8.8}$$

Equations (8.6) and (8.8) are three equations that can be solved for the three unknown stresses. Once the stresses are known, it is a simple matter to calculate the strains and displacements.

The second option of substituting the stress–strain and strain–displacement equations into Eqs. (8.6) yields

$$\begin{aligned} E_a A_a u_a + E_c A_c u_c + E_e A_e u_e &= FL \\ (b + d)E_a A_a u_a + (d)E_c A_c u_c &= 0 \end{aligned} \quad (8.9)$$

Equations (8.7) and (8.9) are three equations that can be solved for the three unknown displacements. Again, once the displacements are known, then strains and stresses can be calculated. Since both solution options lead to a system of three simultaneous, algebraic equations, there is no advantage here to either the stress or the displacement formulation option. ■

8.5 Summary

The theory of elasticity solutions generally require mathematical analysis skills that are not expected of undergraduate students. Indeed, the total number of theory of elasticity solutions that have been solved by anyone is quite small compared to the number of different problems that could easily be posed. Nevertheless, the theory of elasticity is quite useful. Its solutions are the standard of accuracy for all other solutions. As demonstrated in the example problems, the foundations of the theory of elasticity are present in one form or another in all structural analyses. It was for these reasons that the theory of elasticity has been the sole object of study of Part II of this text. This chapter illustrates two theory of elasticity solutions that have practical use with respect to judging the accuracy of approximate solutions for beams. The direct application of theory of elasticity solutions themselves to actual problems, where possible, is facilitated by reference to St. Venant's principle.

The exercises that follow are intended to show the versatility of analytical solutions such as are found in this chapter, and give the reader an opportunity to further practice confirming such theory of elasticity solutions. A short description of the Airy stress function approach to plane stress problems is provided in the next section for those who are interested in what once was an important approach to plane stress problems but has been superseded by the finite element method of approximate analysis.

8.6 ****The Airy Stress Function****

The Airy stress function is a useful means of condensing the stress formulation of the plane stress problem down from two equilibrium equations, Eqs. (1.10), and one primary compatibility equation in terms of stresses, Eq. (8.2), to one, often simple, equation. The Airy stress function is an example of a potential function. A potential function is any function that, when differentiated, provides a quantity of interest that has a physical reality. The potential function itself often does not have a physical interpretation. A familiar example of a potential function is the gravitational potential function (the potential energy in the gravitational field). When differentiated, it provides the magnitude and direction of the weight force. Still other examples of potential functions that may be familiar to the reader are found in the study of two-dimensional fluid flows where the fluid velocities are determined from partial derivatives of a “stream function” when the flow is incompressible, and from partial derivatives of a “velocity potential function” when the nonviscous flow lacks vorticity. In a similar manner, for present purposes, a body force potential function

$V(x, y)$ can be defined for body forces per unit mass of the structural body. Let

$$\rho B_x = -V_{,x} \quad \text{and} \quad \rho B_y = -V_{,y} \quad (8.10)$$

where a comma following a function and preceding one or more independent variables as subscripts indicates partial differentiation of that function with respect to those independent variables. The Airy stress function $\Phi(x, y)$ is related to stresses by the following definitions in terms of Cartesian coordinates:

$$\Phi_{,xx} + V \equiv \sigma_{yy} \quad \Phi_{,yy} + V \equiv \sigma_{xx} \quad \Phi_{,xy} \equiv -\sigma_{xy} \quad (8.11)$$

Other examples of potential functions are found in later chapters of this text. The advantage of these definitions of the body force potential function and the Airy stress function is that when these definitions are substituted into the plane stress equilibrium equations, Eqs. (1.10), both of those equations reduce to $0 = 0$; that is the two equilibrium equations are identically satisfied. What this means is that the mere use of an Airy stress function is all that is necessary to satisfy the requirements of equilibrium. It is sometimes said that the Airy stress function and the body force potential function “integrate” the plane stress equilibrium equations. The only remaining field equation that needs to be satisfied is Eq. (8.2). Substitution of that Airy stress function and the body force potential into that compatibility and isotropic constitutive equation produces

$$\nabla^4 \Phi(x, y) = -E\alpha \nabla^2(\Delta T) - (1 - \nu) \nabla^2 V \quad (8.12)$$

where the biharmonic operator ∇^4 is the product of the harmonic operator with itself. That is, in Cartesian coordinates,

$$\nabla^4 = \nabla^2 \nabla^2 = \frac{\partial^4}{\partial x^4} + 2 \frac{\partial^4}{\partial x^2 \partial y^2} + \frac{\partial^4}{\partial y^4}$$

As mentioned previously, when the temperature change is not a function of time, and the body forces are constant over the mass of the structural body, the right-hand side of Eq. (8.12) is zero. In those circumstances the single field requirement that the Airy stress function must satisfy reduces to the very simple form

$$\nabla^4 \Phi(x, y) = 0 \quad (8.13)$$

There are many functions $\Phi(x, y)$ that satisfy the above equation. For example, there is an infinite number of polynomial expressions that fulfill this requirement. The difficulty with this approach lies with the boundary conditions (BC). Stress BCs can always be expressed by Eqs. (8.11) along with the Cauchy equations that then relate the plane stresses in terms of the Airy stress function to the given tractions at the boundary surface. However, finding by analytical means a function $\Phi(x, y)$ that satisfies both, say Eq. (8.13) and an arbitrarily chosen set of tractions on an irregular boundary, can be very difficult indeed. For numerical analyses, the boundary condition manipulations described in Ref. [16] are sometimes useful. The most common analytical approach is to take the approach of selecting a function $\Phi(x, y)$ that satisfies, say, Eq. (8.13), selecting a set of equations, $\Gamma(x, y) = 0$, that define a boundary for the plane stress structure and then use Eqs. (8.11) and the Cauchy equations to determine the tractions on that boundary. This is another example of the inverse method where the solution, $\Phi(x, y)$, and the boundary geometry are chosen and the problem statement that consists of the tractions acting on that boundary is deduced. This inverse approach has yielded many worthwhile solutions in both Cartesian and cylindrical coordinates, many of

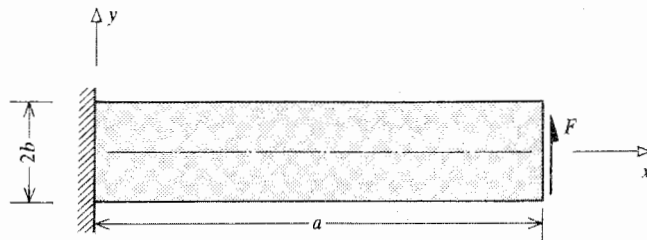


Figure 8.5. Exercise 8.3. A tip-loaded cantilevered beam.

which are detailed in Ref. [21]. For example, from that reference,

$$\Phi(x, y) = \frac{3F}{4b} \left(xy - \frac{xy^3}{3b^2} \right)$$

when used with a rectangular boundary of width L and depth $2b$, could be used to describe the stresses in a long or short beam loaded with a parabolically varying shearing traction at the left beam end at $x = 0$ that sums to a total force F . This applied force F is reacted at $x = L$ with an oppositely directed, but equal-magnitude shearing traction plus the counterclockwise, equilibrating moment FL that is produced by the linearly varying normal traction $T_x = \sigma_{xx}$ at $x = L$. In other words, this Airy stress function can be used to describe the stresses in a tip-loaded beam cantilevered at $x = L$. A modification to this problem, for the sake of a better challenge, is considered in Exercise 8.3.

Chapter 8 Exercises

- 8.1.** Show that Eqs. (8.1) do indeed satisfy the equations of equilibrium whenever the body forces per unit mass are negligible.
- 8.2. (a)** Let the rectangular sheet of Fig. 8.1(a) be composed of an isotropic material with material constants E , ν , G , and α . In this case, it is known by measurement that this sheet has been uniformly stretched a distance $2u_0$ in the x direction and a distance $2v_0$ in the y direction, and that there has been a uniform temperature change T_0 . That is, the values u_0 , v_0 , and T_0 are constants. It is also observed that the sheet is in a state of plane stress. Guess that the mathematical description of the displacement field throughout the sheet is

$$u(x, y) = \frac{x}{a} u_0 \quad \text{and} \quad v(x, y) = \frac{y}{b} v_0$$

and, on this basis, determine the tractions at edges $x = a$ and $y = b$, which, along with the temperature change, have stretched the sheet in the x and y directions.

- (b)** If (u_0/a) is not equal to (v_0/b) , is there a value of αT_0 for which the tractions at all four edges can be zero?
- 8.3.** Confirm that the following plane stress distribution is applicable to the problem of the cantilevered beam loaded by an end force F as shown in Fig. 8.5. There are no body forces. In the stress distribution, the constant c is to be determined so that all requirements are met. Note that there are no stress conditions to be met at $x = 0$; that is, there are only displacement requirements there, and they

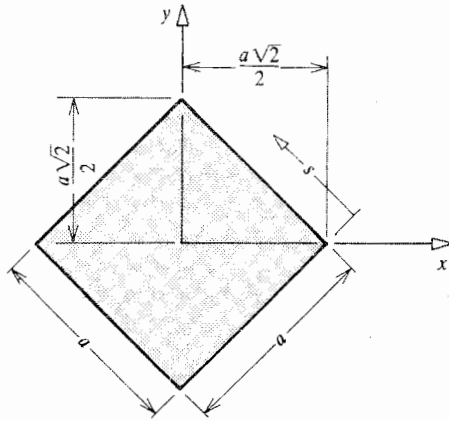


Figure 8.6. Exercise 8.4.

are not a matter of present concern.

$$\sigma_{xx} = -\frac{cFy(a-x)}{2tb^3} \quad \sigma_{yy} = 0$$

$$\sigma_{xy} = \frac{cF \left[1 - \left(\frac{y}{b} \right)^2 \right]}{4bt}$$

where t is the thickness of the slab or beam in the z direction.

- 8.4. Consider the square metal sheet and the Cartesian coordinate system shown in Fig. 8.6. The proposed plane stress solution is

$$\sigma_{xx} = \sigma_{yy} = \sigma_{xy} = \frac{\sigma_0}{a}(y-x)$$

- Determine whether or not the proposed plane stress solution is actually a solution within the interior of any homogeneous, isotropic, linearly elastic body.
 - Regardless of your answer to part (a), determine the tractions T_x and T_y on the upper right-hand edge surface where $x + y = \sqrt{2}a/2$. Your answer may be presented in terms of either Cartesian coordinate.
 - As above, but for the lower right edge.
 - Determine the *normal* and *shearing* tractions along the edge surface identified in part (b), again in terms of either Cartesian coordinate.
 - As above, but for the lower right edge.
 - Express the normal and shearing tractions along the upper right-hand edge in terms of the arc length coordinate s shown in the figure.
 - There is a straight line of zero stress. Locate it.
 - Is it now clear that this is the problem of the beam loaded only by bending moments, rotated 45° ?
- 8.5. (a) A certain structural body that is homogeneous, isotropic, and Hookean has a plane boundary surface that is defined by the equation $y = +b$. If the structural body is in a state of plane stress, rewrite the following two stress type boundary conditions in terms of the derivatives of the structural

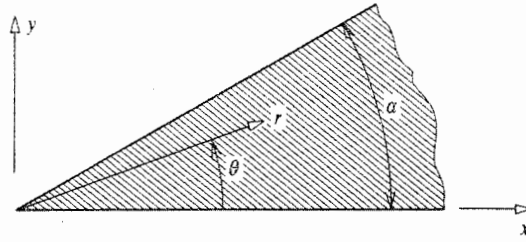


Figure 8.7. Exercise 8.6.

displacements at that one boundary: $T_x(x, b) = 0$, and $T_y(x, b) = -p_0$, where p_0 is a constant. *Hint:* Successively convert the traction statement to a stress statement to a strain statement to a displacement statement.

- (b) The structural body above also has a plane boundary surface at $x = -a$, which is subjected to a pressure of magnitude p_0 , that is, $T_x(-a, y) = +p_0$, $T_y(-a, y) = 0$. Write the corresponding deflection boundary conditions for this surface.

FOR THE EAGER

- 8.6. Consider the semiinfinite wedge shaped body with wedge angle α sketched in Fig. 8.7. This homogeneous, isotropic, linearly elastic body is in a state of plane stress. A proposed stress solution in polar coordinates is

$$\sigma_{rr}(\theta) = 2\sigma_0 \left[\alpha - \theta - \frac{1}{2} \sin 2\theta + (\cos 2\theta - \cos^2 \theta) \tan \alpha \right]$$

$$\sigma_{\theta\theta}(\theta) = \sigma_0 [2(\alpha - \theta) + \sin 2\theta - 2 \cos^2 \theta \tan \alpha]$$

$$\sigma_{r\theta}(\theta) = -\sigma_0 [-1 + \cos 2\theta + \sin 2\theta \tan \alpha]$$

where σ_0 is a constant with units of stress. Note that none of the above stresses is a function of the radial coordinate.

- (a) Determine whether the above stresses satisfy the equations of equilibrium everywhere within the interior of the wedge.
 (b) Determine whether or not these stresses satisfy the constitutive equations and the primary compatibility equation for plane stress. Note that in polar coordinates

$$\nabla^2 = \frac{\partial^2}{\partial r^2} + \frac{1}{r} \frac{\partial}{\partial r} + \frac{1}{r^2} \frac{\partial^2}{\partial \theta^2}$$

- (c) Determine the normal traction $-T_\theta \equiv -T_y$ and the shear traction $-T_r \equiv -T_x$ acting upon the wedge edge where $\theta = 0$.
 (d) Determine the normal traction $+T_\theta$, and the shear traction $+T_r$ acting upon the wedge edge where $\theta = \alpha$.
 (e) Provide a written description of the tractions acting upon the wedge edge surfaces.
 (f) Could this theory of elasticity problem be a basis for judging the accuracy of a strength of materials solution for a tapered, cantilevered beam with a uniform loading? One thing that is necessary to do before answering this question is to determine whether overall beam equilibrium requires a concentrated force at the beam tip. (Problem from Ref. [21].)

- 8.7.** Reconsider the semiinfinite structural body of Fig. 1.13(a) where the depth into the paper is an arbitrary finite value. Determine whether the plane stress state

$$\begin{aligned}\sigma_{xx} &= -\sigma_0 \exp\left(-\frac{\pi x}{2a}\right) \cos\left(\frac{\pi y}{2a}\right) \\ \sigma_{xy} &= -\sigma_0 \exp\left(-\frac{\pi x}{2a}\right) \sin\left(\frac{\pi y}{2a}\right) \\ \sigma_{yy} &= +\sigma_0 \exp\left(-\frac{\pi x}{2a}\right) \cos\left(\frac{\pi y}{2a}\right)\end{aligned}$$

- (a) satisfies the interior equilibrium equations, and requires equilibrating tractions similar to those shown in Fig. 1.13(b);
 (b) satisfies the compatibility equation, and thus is a valid solution for a long, thin sheet of material being pushed at one end while the pushing force is equilibrated by shearing forces at the top and bottom surfaces.
 (c) Suggest other theory of elasticity solutions for this geometry that can be superimposed upon this solution and provide interpretations for the combinations of solutions.
- 8.8.** Confirm that the following definitions for the Airy stress function in terms of polar coordinates identically satisfy the plane stress equilibrium equations and are thus valid definitions.

$$\begin{aligned}r^2\sigma_{rr} &= r\Phi_{,r} + \Phi_{,\theta\theta} + V & \sigma_{\theta\theta} &= \Phi_{,rr} + V \\ r^2\sigma_{r\theta} &= \Phi_{,\theta} - r\Phi_{,r\theta}\end{aligned}$$

Note that the Airy stress function equation for steady-state temperature changes and constant body forces is, of course, still the biharmonic equation:

$$\nabla^4\Phi(r, \theta) = 0$$

where again, for polar coordinates, the harmonic operator has the form

$$\nabla^2 = \frac{\partial^2}{\partial r^2} + \frac{1}{r} \frac{\partial}{\partial r} + \frac{1}{r^2} \frac{\partial^2}{\partial \theta^2}$$

- 8.9.** Given the following valid Airy stress functions and plane stress boundaries, determine the loading upon those boundaries in order to define the associated problem. Let all body forces be zero. Note that C has different units and values in each case.
- (a) $\Phi(x, y) = Cy^2$, rectangular boundary at $x = \pm a, y = \pm b$.
 (b) $\Phi(x, y) = Cy^3$, rectangular boundary at $x = \pm a, y = \pm b$.
 (c) $\Phi(x, y) = Cy^2$, circular boundary $x^2 + y^2 = R^2$.
 (d) $\Phi(x, y) = Cxy$, rectangular boundary at $x = \pm a, y = \pm b$.
 (e) $\Phi(x, y) = C \sin(\pi x/a) \sinh(\pi y/a)$, square boundary at $x = \pm a, y = \pm a$.
 (f) $\Phi(r, \theta) = Cr \sin \theta$, circular boundary $x^2 + y^2 = r^2$.
 (g) $\Phi(r, \theta) = Cr^2 \sin 2\theta$, circular boundary $x^2 + y^2 = r^2$.
- 8.10.** As mentioned, there are many functions that satisfy the biharmonic equation. Of course, any function that satisfies the harmonic equation also satisfies the

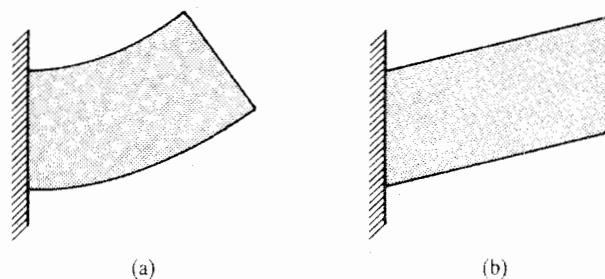


Figure 8.8. Exercise 8.11. (a) Bending deformations (right angles at all corners) without shearing deformations. (b) Shearing deformations (lack of right angles at all corners) without bending deformations.

biharmonic equation. Demonstrate that the following functions satisfy the harmonic equation.

- (a) $\Phi(r, \theta) = Cr^{-n} \cos n\theta$ where n is any real number.
 (b) $\Phi(r, \theta) = C \cos[n \ln(r/R)] \cosh n\theta$ where n is any real number.

- 8.11.** The deformations of a beam of length a and depth $2b$ that is loaded by a shearing force, such as the cantilevered beam of Exercise 8.3 can be thought of as having two parts. The first part of the deformations can be attributed to the bending of the beam that occurs as a result of the shearing force giving rise to a bending moment. The second part of the deformation can be ascribed to the shear force itself. That is, the total deformation can be thought of as having a portion due to bending distortion and a portion due to shearing distortion. The separate patterns of deformation are indicated in Fig. 8.8. From Ref. [21] or Endnote (1), the x and y direction displacements of the cantilevered beam are as follows:

$$u(x, y) = -\frac{3F}{2Et} \frac{y}{b} \left\{ \left(\frac{a}{b}\right)^2 \left[\frac{x}{a} - \frac{1}{2} \left(\frac{x}{a}\right)^2 \right] - \frac{1}{6}(2+\nu) \left(\frac{y}{b}\right)^2 \right\}$$

$$v(x, y) = +\frac{3F}{2Et} \left\{ (1+\nu) \left(\frac{b}{a}\right)^2 \frac{x}{a} + \frac{1}{2} \left(\frac{x}{a}\right)^2 - \frac{1}{6} \left(\frac{x}{a}\right)^3 + \frac{\nu a}{2b} \left(\frac{y}{b}\right)^2 \left[1 - \frac{x}{a} \right] \right\}$$

In contrast to the above results obtained by the theory of elasticity, the usual engineering theory of beam displacements assumes that the displacements in the x direction vary linearly with the y coordinate and that there is no shearing deformation. The displacement at the center of the loaded end cross-section, as calculated by the engineering theory of beam displacements, is

$$v(a, 0) = \frac{F}{2Et} \left(\frac{a}{b}\right)^3$$

- (a) Compare the theory of elasticity solution for the vertical displacement (v) at the center of the end cross-section with the above engineering beam theory solution that does not include shear deformations in order to determine the magnitude of the shear deformation; that is, write the exact theory of elasticity solution as the sum of two parts where the first part is the above engineering beam theory solution plus a second part that can be attributed to the shearing deformation of the cantilevered beam. Note that the shear force distribution is uniform along the length of the beam.

- (b) Consider $F/(\text{effective cross-sectional area in shear})$ to be the average shear stress anywhere along the length of the beam. Use this value of the average shear stress to obtain an average shear strain by dividing by the shearing modulus, and then use this average shear strain to obtain the corresponding tip displacement of the cantilevered beam by multiplying the average shear strain by the length of the cantilevered beam, a . Compare this result with the result obtained in part (a) for the shearing portion of the total tip displacement in order to determine the effective cross-sectional area in shear, and then the constant k that the actual cross-sectional area of $(2bt)$ must be multiplied by so as to determine this effective cross-sectional area for shearing deformations.
- (c) Finally, form the ratio of the bending tip displacement to the shearing tip displacement and show that for this cantilevered beam with a rectangular cross-section, for a length-to-depth ratio $(a/2b)$ of 10, the bending contribution to the total tip displacement is approximately one hundred times greater than the shearing contribution.

Endnote (1) An Example of Calculating Displacements from a Stress Solution

From the solution to Exercise 8.3, the stress distribution for the tip force loaded cantilevered beam of Fig. 8.5 is

$$\sigma_{xx} = -\frac{3F}{2b^3t}y(a-x) \quad \sigma_{yy} = 0 \quad \sigma_{xy} = \frac{3F}{4bt} \left(1 - \frac{y^2}{b^2}\right)$$

Hence, from Hooke's law, the three relevant strains are

$$\epsilon_{xx} = -\frac{3F}{2Eb^3t}y(a-x) \quad \epsilon_{yy} = \frac{3\nu F}{2Eb^3t}y(a-x) \quad \gamma_{xy} = \frac{3(1+\nu)F}{2Ebt} \left(1 - \frac{y^2}{b^2}\right)$$

The beam displacements are obtained by integrating the above strain expression using the linear strain-displacement equations $\epsilon_{xx} = \partial u/\partial x$, $\epsilon_{yy} = \partial v/\partial y$, and $\gamma_{xy} = \partial u/\partial y + \partial v/\partial x$. Hence

$$\begin{aligned} \frac{\partial u}{\partial x} = -\frac{3F}{2Eb^3t}y(a-x) &\rightarrow u(x, y) = -\frac{3F}{2Eb^3t}y \left(ax - \frac{x^2}{2}\right) + f(y) \\ \frac{\partial v}{\partial y} = \frac{3\nu F}{2Eb^3t}y(a-x) &\rightarrow v(x, y) = \frac{3\nu F}{4Eb^3t}y^2(a-x) + g(x) \end{aligned}$$

where $f(y)$ and $g(x)$ are functions of integration to be determined, in part, by substituting the above results for u and v into the above expression for the shearing strain. That result is

$$\begin{aligned} \gamma_{xy} &= (1+\nu) \frac{3F}{2Eb^3t}(b^2 - y^2) \\ &= \left[-\frac{3F}{2Eb^3t} \left(ax - \frac{x^2}{2}\right) + f'(y) \right] + \left[-\frac{3\nu F}{4Eb^3t}y^2 + g'(x) \right] \end{aligned}$$

Conceptually rearrange the second part of the above equation so that all the terms involving x are equal to all the terms involving y plus any constant terms. Change the value of x at will while y is held constant. The changing value of x does not affect the equality. The only

way that this is possible is for those terms involving x to be a constant, say C_0 . Making that replacement, the above equality can be written as the following two equalities:

$$-\frac{3F}{2Eb^3t} \left(ax - \frac{x^2}{2} \right) + g'(x) = C_0 \quad \text{or} \quad g(x) = C_0x + \frac{3F}{2Eb^3t} \left(a \frac{x^2}{2} - \frac{x^3}{6} \right) + C_1$$

and

$$(1 + \nu) \frac{3F}{2Eb^3t} (b^2 - y^2) - f'(y) + \frac{3\nu F}{4Eb^3t} y^2 = C_0$$

or

$$f(y) = C_2 - C_0y + (1 + \nu) \frac{3F}{2Eb^3t} b^2y - \frac{2 + \nu}{6} \frac{3F}{2Eb^3t} y^3$$

Thus the expressions for the two displacement components are as follows:

$$u(x, y) = -\frac{3F}{2Eb^3t} y \left(ax - \frac{x^2}{2} \right) + C_2 - C_0y + (1 + \nu) \frac{3F}{2Eb^3t} b^2y - \frac{2 + \nu}{6} \frac{3F}{2Eb^3t} y^3$$

$$v(x, y) = \frac{3\nu F}{4Eb^3t} y^2(a - x) + C_0x + \frac{3F}{2Eb^3t} \left(a \frac{x^2}{2} - \frac{x^3}{6} \right) + C_1$$

The above three constants of integration can be determined from three displacement boundary conditions. At the cantilevered end, let the displacements at the coordinate origin be zero. The third BC is chosen to be $\partial u / \partial y = 0$ at the coordinate axes origin in order to retain the perpendicular at the cantilevered end. This choice allows a shearing deformation at the cantilevered end. Applying these BCs

$$C_0 = (1 + \nu) \frac{3F}{2Eb^3t} b^2 \quad \text{and} \quad C_1 = C_2 = 0$$

Hence, the final expression for the displacements in this cantilevered beam is

$$u(x, y) = \frac{3F}{2Eb^3t} y \left(ax - \frac{x^2}{2} \right) - \frac{2 + \nu}{6} \frac{3F}{2Eb^3t} y^3$$

$$v(x, y) = \frac{3\nu F}{4Eb^3t} y^2(a - x) + (1 + \nu) \frac{3F}{2Eb^3t} b^2x + \frac{3F}{2Eb^3t} \left(a \frac{x^2}{2} - \frac{x^3}{6} \right)$$

Since $k = F/EI$ and $a = L$, the solution for the beam tip vertical deflection at $y = 0$ is

$$v(a, 0) = \frac{FL^3}{3EI} \left[1 + 3(1 + \nu) \frac{b^2}{a^2} \right]$$

where, again, only the first part of this solution is obtainable from a strength of materials analysis. The second part of this solution is very small for a beam whose length exceeds ten times its depth.

Parts I and II Review Questions

Part I. True or False?

(Answers at the end of this section)

1. The principal stress axes are always the same as the principal strain axes in an isotropic material.
2. The principal stress axes are always the same as the principal strain axes in an orthotropic material.
3. The equations of compatibility derived in this text, such as $\epsilon_{xx,yy} + \epsilon_{yy,xx} = \gamma_{xy,xy}$, are valid for large strains as well as small strains. (Recall that small strains are linear expressions involving the derivatives of displacements, while large strains further include quadratic expressions involving derivatives of the displacements.)
4. The coordinate rotation equation for stresses, that is, $[\sigma^*] = [c][\sigma][c]^t$, is valid for any material, not just an isotropic material.
5. The equations of equilibrium apply to a material undergoing plastic deformations as well as a material undergoing purely elastic deformations.
6. The line paralleling the linear portion of the stress–strain curve that defines an offset yield stress originates at a strain value of 0.01 in/in.
7. Not counting the coefficient of thermal expansion, there are three independent material constants that require specification for the linearly elastic, isotropic material model.
8. Young’s modulus is the same as the modulus of rigidity.
9. The Cauchy equations are a set of algebraic equations that relate the tractions to the internal stresses, but do not include the body forces.
10. Both the constitutive and strain–displacement equations for an isotropic material are different from those for an orthotropic material.
11. The Cauchy equations can be viewed as an application of Newton’s second law; that is, they are based upon a summation of forces.
12. The material stiffness matrix $[E]$ is the matrix transpose of the material compliance matrix $[S]$.
13. Although based on different concepts, as a practical matter, the proportional limit, the elastic limit, and the ultimate stress have practically indistinguishable values.
14. The percentage elongation is a measure of the ductility of a material.
15. If the stresses can be determined from use of equilibrium conditions alone, then the analysis is called statically determinate.
16. An elastic material has a negligible hysteresis curve for a small number of complete loading cycles if the maximum applied stress is less than the yield stress. (Here “loading cycle” means a loading followed by an unloading in either tension or compression or both.)
17. The slope of the stress–strain curve for compression is termed the compressive tangent modulus.

18. The modulus of elasticity in tension can be different from that in compression even for aluminum alloys.
19. In an orthotropic material, as in any material subjected to a state of stress, the plane of maximum shear stress is always at a 45° angle to two of the planes of the principal stress.
20. In the case of plane stress, the strain in the z direction can be determined from the strains in the other two orthogonal directions when the material is isotropic.
21. A homogeneous material is one that has the same material properties at every point in the body. Even an orthotropic material can be considered to be a homogeneous material, at least for pieces of material on a scale much larger than, say, the size of the fiber diameters, or the spacing between fibers, in the case of a fiber-reinforced composite.
22. An elastic material can experience a fatigue failure even though the maximum stress does not exceed half the elastic limit in tension.
23. In a metallic structural material, the modulus of elasticity and the ductility are likely to increase with decreasing temperature.
24. In structural engineering, stiffness and strength are two different names for the same material characteristic.
25. The compatibility equations can be derived from the strain–displacement equations.
26. The Palmgren–Miner law for fatigue can be properly described as a damage accumulation theory.
27. In an isotropic material, if the Poisson's ratio and the shearing modulus are known, then the Young's modulus may be calculated.
28. For an isotropic material, a structural body in a state of plane stress is also in a state of plane strain.
29. A viscoelastic material is one for which creep deformations are significant.
30. For a general stress state, at any point in the structure, the sum of all three shearing stresses ($\sigma_{xy} + \sigma_{xz} + \sigma_{yz}$) is the same regardless of the orientation of the Cartesian coordinate axes.
31. In three dimensions, the maximum normal stress vector is always oriented 90° from the minimum normal stress vector.
32. The maximum shear stress is always one-half the difference between the maximum and minimum principal stresses.
33. There is an isomorphism, that is, an exact analogy in form, between the Green strain coordinate axis rotations and stress coordinate axis rotations.
34. If it is known that a structural body is in a state of equilibrium, then the six compatibility equations can be solved for the six strains, and hence, by use of the constitutive equations, the six stresses.
35. In the case of plane strain, if the two displacements of interest are $u(\zeta, \xi) = C(4\zeta + 2)\sin(\pi\xi)$, and $v(\zeta, \xi) = C(\zeta - 3)(\xi - 2)$, then $\epsilon_{\xi\xi} = \pi C(4\zeta + 2)\cos(\pi\xi)$, where $\zeta = x/l$ and $\xi = y/L$ are two nondimensional, Cartesian coordinates.
36. "Strain hardening" is another name for the Bauschinger effect.
37. The matrix of direction cosines is a nonsymmetric matrix.
38. One of the six relations among the direction cosines is as follows:

$$c_{xx}^2 + c_{xy}^2 + c_{xz}^2 = 1.0$$

39. Equilibrium equations are always sufficient to determine all the stresses in a structural body in a state of plane stress, but are not always sufficient to determine all the displacements in that same structure.
40. The ultimate stress of a steel alloy can be estimated by a hardness test.
41. An A-basis tensile strength will be numerically greater than or equal to a B-basis tensile strength.
42. The creep characteristics of steels can be found on $S-N$ diagrams.
43. The mathematical solution for the strains that is obtained from the three independent measurements of a strain gauge rosette is an example of eigenvalue problem solution.
44. The Palmgren–Miner rule for estimating the percentage damage done to a structural component is most accurate when the magnitudes of the applied load cycles have a random order rather than a specific ordering such as by magnitude with the smallest magnitude load cycles occurring first.
45. The line paralleling the linear portion of the stress–strain curve that defines an offset yield stress originates at a strain value of 0.0001 in/in.
46. An elastic material can experience a fatigue failure when the principal stresses are compressive.
47. The compatibility equations derived in Chapter 3 are valid for an orthotropic material as well as an isotropic material.
48. In an orthotropic material, if the six Poisson's ratios and the three shearing moduli are known, then the three Young's moduli may be calculated.
49. The Green shearing strains have twice the value of the corresponding engineering shearing strains.
50. The linearly constitutive equations and the linear strain displacement equations are also valid for loads that vary slowly with time if they are valid for static loads whose magnitudes are equal to the maximum values of the time-varying loads.
51. The equations of equilibrium, which are derived in Chapter 1 for the interior of a body of general shape, do not apply to a material undergoing plastic deformations.

Part II. True or False?

52. If, in a displacement formulation analysis, the displacements in a structural body are described by continuous, single-valued mathematical functions, then there is no need to use the compatibility equations. In other words, the compatibility equations are not used in any displacement formulation of a theory of elasticity problem.
53. In general, stress boundary conditions can be expressed in terms of the displacements and/or their derivatives at the boundary, but displacement boundary conditions cannot be expressed in terms of stresses and/or their derivatives at the boundary.
54. St. Venant's principle states that, for linearly elastic materials, the strains in one orthogonal direction bear a fixed ratio to the strains in the other two orthogonal directions.
55. A displacement formulation of a theory of elasticity problem is usually unsuitable when there are mixed boundary conditions.
56. The strain–displacement equations are a necessary part of any theory of elasticity displacement formulation.

Answers

1. True. The planes perpendicular to the axes of principal stress are the planes of the differential-sized rectangular parallelepiped where there are no shearing stresses. For an isotropic material, each shearing strain is equal to the associated shearing stress divided by the shear modulus of elasticity, G . Therefore, if the shearing stresses are zero, so too are the shearing strains. Thus these planes are also the planes of principal strains.
2. False. The principal stress axes and the principal strain axes are the same in an orthotropic material only in the special case where those two sets of axes are also the material axes. For other than the material axes the material stiffness and compliance matrices are generally filled with nonzero elements that couple, for example, the normal stresses to the shearing strains. Therefore, the principal (normal) stresses can produce shearing strains whenever the principal stress axes are other than the material axes.
3. False. The cited compatibility equations are only valid for small strains such as $\epsilon_{xx} = \partial u / \partial x$ because such strain expressions are the basis of the derivation of the strain compatibility equations that are presented in Chapter 3.
4. True. All the equations involving the rotations of stresses, or strains, were deduced before any discussion of material properties. It is only when stresses are related to strains (forces to displacements) is there a need to describe the material. Since rotations of stresses, or strains, are accomplished without any reference to the relationships between stresses and strains, those results are valid for any material.
5. True. Again, the equilibrium equation derivations do not require any relationship between stress and strain. Therefore the equilibrium equations are valid for any material.
6. False. The offset line defining the yield stress originates at a strain value of 0.002.
7. False. Only two constants are required since $G = E/[2(1 + \nu)]$.
8. False. Young's modulus is E , while the modulus of rigidity, as it is called, is G . They are not the same, but have the relation cited above.
9. True. As the derivation shows, the body forces acting upon the infinitesimal-sized tetrahedron are infinitesimal compared to the forces associated with the stresses and tractions.
10. False. The constitutive equations differ, but the strain–displacement equations, which are only a matter of the geometry of deformation, are the same for the two types of material.
11. True. The Cauchy equations were indeed obtained by applying Newton's laws to that infinitesimal-sized tetrahedron framed by the three Cartesian directions.
12. False. The material stiffness matrix is the inverse, not the transpose, of the compliance matrix.
13. False. The proportional limit and the elastic limit usually have very much the same values, but the ultimate stress value is distinctly higher in value.
14. True. The greater the percent elongation, for a given loading, the more ductile the material. Cast iron, for example, is called a brittle material because it fails almost entirely without any plastic deformations. When cast iron was used to build railroad bridges in the nineteenth century, the result was those historic pictures we see today of collapsed railroad bridges bearing locomotives and coal cars. Ductile steel was the solution to this problem because steel does undergo considerable deformation before failing, and thus provides clear warning of an impending failure.

15. True. This is the definition of “statically determinate.”
16. True. If there are tens of thousands of load cycles, then there often is a slow accumulation of permanent elongations.
17. True. This is the definition of the compression tangent modulus. Of course, the tangent modulus is a constant for all the stress–strain points on the linear portion of the stress–strain curve, and varies thereafter.
18. True. However, the differences between the tensile modulus of elasticity and the compressive modulus of elasticity, for structural materials such as aluminum, are usually only a couple of percent. In that case, it is a difference that is ignored in most engineering analyses.
19. True. Again, all the stress rotation equations were derived without reference to any material properties. Therefore the 45° rule applies to any material.
20. True. This result is probably best established by doing a little algebra. Consider the isotropic strain–stress equations for the normal strains. Since this is a case of plane stress, begin by setting σ_{zz} equal to zero. Then solve the first two strain–stress equations simultaneously for the normal stresses in the x and y directions. Substitute those results for σ_{xx} and σ_{yy} into the third strain–stress equation, the equation for ϵ_{zz} obtaining

$$\epsilon_{zz} = -\frac{\nu}{1-\nu}(\epsilon_{xx} + \epsilon_{yy}) + \frac{(1+\nu)}{(1-\nu)}\alpha\Delta T$$

21. True. This is again a case of smoothing over small difficulties in order to achieve great simplifications in an analysis.
22. True. Steel is a material that generally will never experience a fatigue failure if the values of the mean stress and alternating stress are less than those values where the S – N curves become nearly horizontal as the number of cycles becomes very large. Aluminum S – N curves have no such horizontal asymptote. If enough load cycles are applied to an aluminum component, eventually there will be a failure.
23. False. Ductility in structural metals increases with increasing temperature.
24. False. The strength of a material is a measure of the stress the material can bear before the material fails in some way, such as by undergoing plastic yielding or rupture. The stiffness of a material is a measure of how much stress is required for a given strain. Thus the modulus of elasticity is a measure of structural stiffness, while a yield stress or an ultimate stress are measures of material strength. In other words, stiffness directly involves displacements or deformations, while strength need not. These two different concepts carry over to structures. The strength of a structure is measured by how much load the structure can support before some part of the structure yields, ruptures, or deflects too much. The stiffness of a structure is measured by the amount of loading that is required to produce a unit displacement. Thus the concept of stiffness at a single point on the structure, or in some more general sense, always involves a displacement.
25. True. This is how the compatibility equations were derived.
26. True. The idea that damage accumulates linearly is the basis of the Palmgren–Miner law.
27. True. The formula is

$$E = 2G(1 + \nu)$$

28. False. An isotropic body in a state of plane stress cannot truly also be in a state of plane strain since the σ_{xx} and σ_{yy} stresses cause a ϵ_{zz} strain. Note, however, that,

as is seen in later chapters, the common strength of materials approximation for beams (and plates and shells) contains this contradiction.

29. True. This is what is meant by a viscoelastic material.
30. False. At any interior point, the sum of the normal stresses ($\sigma_{xx} + \sigma_{yy} + \sigma_{zz}$) is coordinate-rotation invariant, not the sum of the shearing stresses. Consider the case of plane stress. In this case, the sum of the shearing stresses is simply σ_{xy} . This shearing stress varies from its maximum value to zero as the x and y coordinates are rotated.
31. True. In any material, the maximum and minimum valued normal stress vectors are two of the three principal stresses, and the principal stresses are always oriented 90° from each other.
32. True. This fact is established by simply examining the three Mohr's circles that describe the three-dimensional stress state at any geometric point within a loaded structure.
33. True. This fact can be established by noting that the rotation equations for stresses and strains have the same form only when Green's strains are used rather than engineering strains.
34. False. The six compatibility equations cannot be solved for the six strains since those six equations are not six independent equations.
35. False. First note that ζ and ξ are just nondimensional forms of x and y , respectively. Thus the normal strain in the ξ direction is just a variation on the normal strain in the y direction. Then the normal strain in the ξ direction is simply the partial derivative of the displacement in the y direction, which is v , partially differentiated with respect to ξ . Then

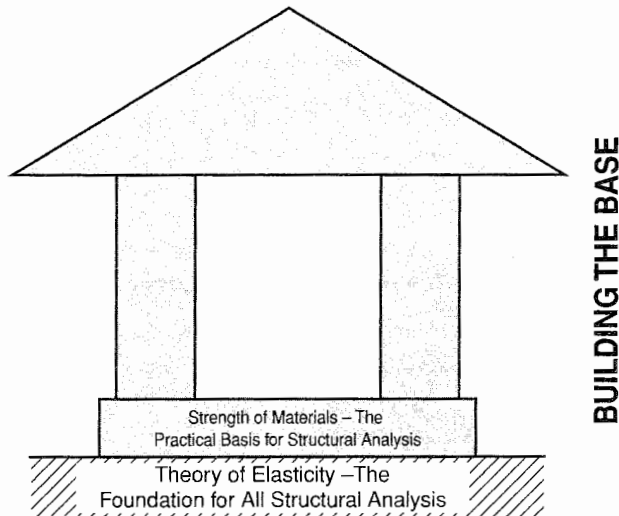
$$\epsilon_{\xi\xi} = \frac{\partial v}{\partial \xi} = C(\zeta - 3)$$

36. False. Strain hardening is the increase in the yield stress after: (i) the process of loading past the original yield stress; (ii) unloading; and (iii) then reloading. The Bauschinger effect is the decrease in the opposite yield stress (say, the compressive yield stress) after first loading beyond the yield stress with one type of loading (say, tension) and then reversing the direction of loading and proceeding to the yield stress of the reversed type of loading.
37. True. The matrix entry in the first row, second column, called the (1, 2) entry, is the cosine of the angle between the x^* axis and the y axis. The (2, 1) entry is the cosine of the angle between the y^* axis and the x axis. In a general case these angles are not the same. Therefore the two cosines are not the same, and therefore the matrix of direction cosines is not symmetric.
38. True. This identity can be confirmed by first writing the component form of the unit vector aligned with the x^* axis, which is $\mathbf{i}^* = c_{xx}\mathbf{i} + c_{xy}\mathbf{j} + c_{xz}\mathbf{k}$. Then it is only a matter of taking the dot product of this vector with itself.
39. False. In a state of plane stress, there are but two equilibrium equations, and these two equations involve three stresses. Hence, in general, there are an insufficient number of equilibrium equations, and neither the stresses nor the displacements can be determined from only equilibrium considerations. Such a problem is termed "indeterminate."
40. True.

41. False. Since the A-basis allowable strength is statistically more conservative than the corresponding B-basis value, it is associated with a lower numerical value than the B-basis value.
42. False. An $S-N$ plot provides information on fatigue strengths.
43. False. The strain gauge equations are a set of linear algebraic equations where the number of unknowns is the same as the number of equations. There is no trivial solution, and the equations can be solved by successive substitution to eliminate unknown quantities in order to arrive at a unique final solution.
44. True. For example, if a loading consisted of 100 000 load cycles of small amplitude, and another 100 000 load cycles of a larger amplitude, it can be expected that more damage would be done to the structural material if all the large amplitude load cycles were applied first, and then all the small amplitude load cycles. The explanation is that the large amplitude load cycles are more effective in opening up cracks than the small amplitude load cycles, but the small amplitude load cycles can then continue to “grow” (i.e., lengthen) the already created cracks. This is so because the longer the crack, the easier it is to extend the crack. If the order of loading were reversed, the small amplitude load cycles might not open up any cracks, and the following large amplitude load cycles would then encounter a basically undamaged material.
45. False. An offset strain of 0.002 is associated with offset yield stresses, while 0.0001 is for offset proportional limits.
46. False. After crack initiation, fatigue crack growth is dependent on the presence of tensile stresses. When the principal stresses are entirely compressive, there cannot be any tensile stresses.
47. True. The compatibility equations were derived without any reference to material properties.
48. False. First of all, the orthotropic shear moduli have no relation to the three orthotropic Young’s moduli or the six orthotropic Poisson’s ratios. The three relations between the three moduli just establish the proportionality of the three moduli. They do not allow a solution for their values. Another way of saying this is to say that those three equations are not independent.
49. False. The Green shearing strains are one-half the value of the corresponding engineering shearing strains; that is, $\epsilon_{ij} = \frac{1}{2}\gamma_{ij}$.
50. True. Slowly varying loads are no different than static loads. The meaning of “slowly varying” has not been explained in this textbook because it is related to what is called the “first natural period” of the structure, measured in seconds of time, which is a precise dynamic characteristic depending upon both the mass and the stiffness of the structure. A less precise, but useful, way of judging whether or not loads are “slowly varying” is to judge whether or not the loads create significant amounts of kinetic energy. Any structural dynamics textbook explains these concepts in more detail. The truth of the given statement relates more strongly to the linear constitutive equations, which cease being valid after the elastic limit or other plasticity boundary is reached. If the loads, slowly varying or static, are less than those that put the material at that boundary, then both sets of equations are valid.
51. False. The equilibrium equations are valid for all materials.
52. True. In a displacement type analysis, the strain–displacement equations are used instead of the compatibility equations.

53. True. Stress boundary condition statements can be expressed in terms of strains via the use of the material constitutive equations, and the strains can then be expressed in terms of the derivatives of the displacements. Thus the stress boundary conditions can be written in terms of displacements. The reverse is not true. The fixed values of the displacements generally cannot be differentiated to get strains at the boundary. For example, consider a three-dimensional body with a boundary plane that is aligned with the x, z plane. Hence the normal direction for this boundary plane is the y direction. For a stress formulation analysis, it would be necessary to replace the specification of the three displacements at that boundary with a specification of the normal stress, σ_{yy} , and the shearing stresses on this y plane in the x and z directions; three pieces of information for three other pieces of information. If for example, all three displacements at this planar boundary are specified to be zero, it is then also known that at that boundary the partial derivatives of all three displacements in the x and z directions are also zero. However, nothing would be known about partial derivatives with respect to the y direction. Thus there would be no information, for example, on the normal strain in the y direction, and therefore no possibility of specifying σ_{yy} .
54. False. This statement is a correct statement with respect to Poisson's ratio, not St. Venant's principle.
55. False. It is the stress formulation that is usually unsuited to a problem involving both displacement and stress type boundary conditions.
56. True. The strain-displacement equations are necessary to convert the equilibrium equations in terms of stresses, in the interior of the body or at its boundaries, to statements involving displacements.

ENGINEERING THEORY FOR STRAIGHT, LONG BEAMS



III.1 Aircraft and Other Vehicular Structures

The structure of a flight or marine vehicle usually has a dual function: (i) it transmits and resists the fluid and other forces that are applied to the vehicle; and (ii) it acts as a cover that provides an aerodynamic or hydrodynamic shape that protects the contents of the vehicle from the environment. This combination of roles is fortunate since, from the standpoint of structural weight, the most efficient location for the structural material is at the outer surface of the vehicle. Thus the structures of flight and marine vehicles, and some land vehicles, are essentially thin shells. If these shells are not reinforced by stiffening members, they are referred to as *monocoque*. When the cross-sectional dimensions of the shell are large, the wall of a monocoque structure must be relatively thick to resist bending, compressive, and torsional loads without buckling. In such cases a much more weight-efficient type of construction is one which contains stiffening members that permit a much thinner covering shell. Stiffening members may also be required to diffuse concentrated loads into the skin. (Most aircraft have “strong points” where the structure can be put on jacks or lifted by a crane.) Construction of this type is called semimonocoque. Typical segments of semimonocoque flight structures are sketched in Fig. III.1.

As is evident from the slightly simplified sketches in Fig. III.1, or from the drawings of an actual aircraft structure presented at the beginning of this textbook, there are basically three types of structural components that are combined to form a vehicular structure. The first type of component is the beam that runs in the lengthwise direction of the wing or fuselage or other major substructure. If the beam runs the length of a wing and its depth is

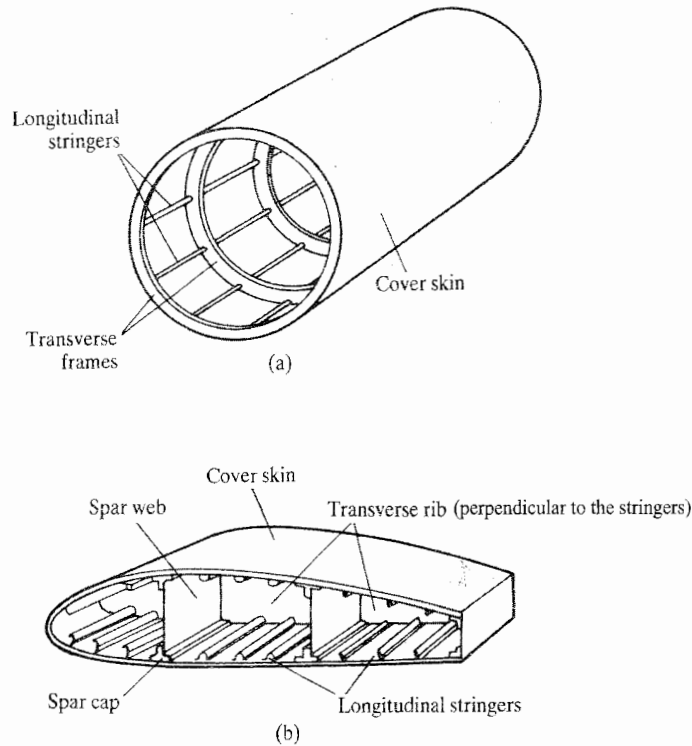


Figure III.1. Typical semimonocoque construction, from Ref. [16]. (a) Fuselage component. (b) Aerodynamic surface component.

the thickness of the wing, then that beam is called a spar. There are usually a minimum of two wing spars, the front spar and the back spar. If the beam runs along the length of the wing or fuselage, and does not extend through the depth of the wing or fuselage, then that beam is called a longitudinal stringer. Either way, beams are a prominent part of vehicular structures.

Part III (Chapters 9 through 14) is devoted to the study of beams subjected to static loads of all kinds. The first three of these chapters deals in a general fashion with the bending of beams, including an introduction to the buckling of beams. The next two chapters provide a general treatment of the twisting of beams. One major reason to have at least two spars in a wing is that, along with the skin covering those spars, they form a “torsion box” that greatly enhances the torsional stiffness of the wing. A torsionally flexible beam is open to failure due to such instabilities as divergence and flutter, as discussed in Chapter 23.

The second type of component is the rib in the wing, and the frame in the fuselage. The geometries of ribs and frames is not as simple as that of beams. Their analysis is discussed in Part V in connection with the introduction to the finite element method of analyzing structures. Chapter 19 in particular deals with these geometries, as does Chapter 22. The third type of component is the skin that covers the grid of ribs or frames and spars or stringers. The analysis of skins is also introduced in Chapters 19 and 22. In summary, from Ref. [16], in semimonocoque flight and marine structures the “cover” or “skin” has the following structural functions:

1. It transmits fluid forces to the longitudinal and transverse supporting members by plate and membrane action.
2. It develops shearing stresses that react the applied torsional moments and shearing forces.
3. It acts with the longitudinal members in resisting the applied bending and axial loads.
4. It acts with the longitudinals in resisting the axial load and with the transverse members in reacting the hoop or circumferential load when the structure is pressurized.

The "longitudinal stiffeners," or "stringers," serve the following purposes:

1. They resist bending and axial loads along with the skin.
2. They tend to divide the skin into small panels and thereby increase its buckling and compressive failure stresses.
3. They act with the skin in resisting axial loads caused by pressurization.
4. They act to arrest the growth of cracks in the skin by accepting tensile loads the skin can no longer carry.

The transverse members in body structures are called "frames," "rings," or, if they cover all or most of the cross-sectional area, "bulkheads." In aerodynamic surfaces they are referred to as "ribs." These members are used to

1. Maintain the cross-sectional shape.
2. Distribute concentrated loads into the structure and redistribute stresses around structural discontinuities.
3. Establish the column length and provide end restraint for the longitudinals to increase their column buckling stress.
4. Providing edge restraint for the skin panels and thereby increase the plate buckling stress of these elements.
5. Act with the skin in resisting the circumferential loads due to pressurization.

III.2 The Method of Undetermined Coefficients

The method of undetermined coefficients is an effective means of determining particular solutions to a nonhomogeneous ordinary differential equation with constant coefficients whenever the nonhomogeneous portion of the differential equation (i.e., the nonzero right-hand side) consists of one or more functions each of which has a finite number of distinct derivatives. For example, consider the ordinary differential equation with constant coefficients that determines the general form of the function $f(x)$:

$$f''(x) - 3f'(x) + 2f(x) = 4x^2 + 3 \sin(2x) + 5 \tan(x)$$

The first two of the three functions on the right-hand side of the above equation, x^2 and $\sin(2x)$, have a finite number of distinct derivatives. The zeroth, first, second, and third derivatives of the first function are x^2 , x , 1 , and 0 . All higher order derivatives are the same as the third derivative. Thus there are only four distinct derivatives of this function. The second function $\sin(2x)$ has only two distinct derivatives, which are $\sin(2x)$ and $\cos(2x)$. However, there are an infinite number of distinct derivatives of the function $\tan(x)$. For this last function the method of undetermined coefficients is inadequate, and a more powerful, but lengthy, method, such as the method of the variation of parameters, would have to be used to determine the particular solution corresponding to it.

Although it is quite possible to treat $4x^2$ and $3 \sin(2x)$ together, the explanation is clearer if they are attacked successively. Let $f_1(x)$ be the particular solution corresponding to $4x^2$. The method of undetermined coefficients begins with a trial function composed of all the distinct derivatives of x^2 multiplied by undetermined coefficients such as A, B, C, \dots . Here

$$f_1(x) = Ax^2 + Bx + C$$

so that

$$f_1' = 2Ax + B \quad \text{and} \quad f_1'' = 2A$$

Substituting these values into the left-hand side of the differential equation, and equating the result to the appropriate part of the right-hand side, which is $4x^2$, leads to

$$(2A) - 3(2Ax + B) + 2(Ax^2 + Bx + C) = 4x^2$$

The above equality can hold only if²

$$2A = 4 \quad 2B - 6A = 0 \quad \text{and} \quad 2C - 3B + 2A = 0$$

or

$$A = 2 \quad B = 6 \quad \text{and} \quad C = 7$$

Thus the particular solution corresponding to $4x^2$ is

$$f_1(x) = 2x^2 + 6x + 7$$

Similarly, to obtain the particular solution corresponding to $3 \sin(2x)$ let

$$f_2(x) = A \sin(2x) + B \cos(2x)$$

Substitution into the differential equation yields

$$\begin{aligned} [-4A \sin(2x) - 4B \cos(2x)] - 3[2A \cos(2x) - 2B \sin(2x)] \\ + 2[A \sin(2x) + B \cos(2x)] = 3 \sin(2x) \end{aligned}$$

Again equating coefficients of the sine and cosine functions yields

$$-2A + 6B = 3 \quad \text{and} \quad 6A + 2B = 0$$

Simultaneous solution produces $A = -0.15$ and $B = 0.45$. Thus the particular solution for this right-hand side is

$$f_2(x) = \frac{1}{20}[-3 \sin(2x) + 9 \cos(2x)]$$

The total particular solution is the sum of $f_1(x)$, $f_2(x)$, and the particular solution corresponding to $5 \tan(x)$. Of course, the total particular solution plus the complementary solution comprise the total solution.

² The validity of this statement rests upon the concept of linear independence, and the fact that the functions x^2 , x , and 1 are mutually linearly independent. See Section III.3.

III.3 Linear Independence

The reader may already be familiar with the concept of linear independence with respect to vectors in three-space, that is, vectors with three components. For example, if a certain vector \mathbf{A} is equal to the sum of two other vectors \mathbf{B} , and \mathbf{C} , with multiplicative constants (i.e., $\mathbf{A} = \alpha\mathbf{B} + \beta\mathbf{C}$), then the first vector is not linearly independent of the other two vectors. Furthermore, any four vectors in three-space must be linearly dependent; that is, any fourth vector can be written as the sum of the other three vectors with appropriate factors. One consequence of this latter fact is that any three-space vector can be described in terms of the unit vectors \mathbf{i} , \mathbf{j} , and \mathbf{k} . It is possible to extend that idea to functions because it is possible to think of functions as vectors with an infinite number of components. The definition of linear independence in terms of functions is as follows:

A set of functions F, G, H, \dots are *linearly independent* if, for the following equality to be true for all values of the variables in the arguments of the functions, the constants $\alpha, \beta, \gamma, \dots$ must be zero.

$$\alpha F + \beta G + \gamma H + \dots = 0$$

Thus, if there is any nonzero set of constants $\alpha, \beta, \gamma, \dots$ for which the equality holds, then the set of functions F, G, H, \dots are *linearly dependent*. For example, any combination of two or three, or all four of the following functions is linearly independent:³

$$\sin(x) \quad \cos(x) \quad \sin(2x) \quad \cos(2x)$$

That is, there is no set of constants α and β , for example, for which

$$\alpha \sin(x) + \beta \cos(x) = 0$$

for all values of x except for the constants $\alpha = \beta = 0$. Note that linear independence is not the same as independence. For example, while $\sin(x)$ and $\cos(x)$ are linearly independent, the two functions are not independent functions since $\sin(x)$ is the square root of $1 - \cos^2(x)$. An example of two linearly dependent functions could be $2x$ and $3x$ because in the equality

$$\alpha(2x) + \beta(3x) = 0$$

α can have the nonzero value -3 , while β can have the nonzero value $+2$. Other sets of linearly dependent functions, in this case three functions, can readily be inferred from the following identities:

$$\cos^2 x - \sin^2 x = \cos(2x) \quad \text{and} \quad \sinh(x) + \cosh(x) = \exp(x)$$

One way of ascertaining whether or not a set of N functions of a single variable are linearly independent is to calculate the corresponding $N \times N$ Wronskian determinant (Ref. [39]). The N elements of the first row of this determinant are the N functions themselves. The second row of this determinant is the N first derivatives of the N functions. The third row is the N second derivatives, and so on. If the Wronskian determinant is zero for any value of the single variable, then the set of functions is linearly dependent. For example,

³ The fact that these functions along with all other similar functions are linearly independent allows these functions to form a basis for trigonometric Fourier series. (Jean-Baptiste-Joseph Fourier, 1768–1830, French mathematician, is celebrated as well for his work on heat flow.)

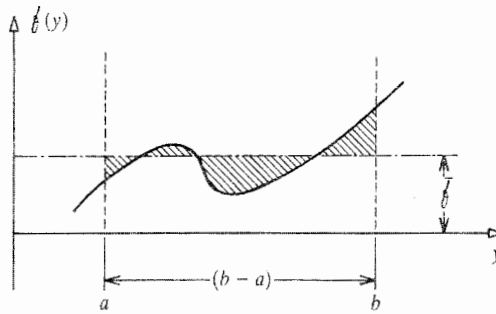


Figure III.2. The mean functional value for the interval (a, b) .

the value of the Wronskian determinant for the first cited functions $\sin x$, $\cos x$, $\sin 2x$, and $\cos 2x$ is $+1$ for all values of x . Hence these four functions are linearly independent.

III.4 The Mean Value Theorem

Consider the integrals

$$\iint_A y \, dA \quad \text{and} \quad \iint_A z \, dA$$

These two integrals are appropriately named the first moments of the area about the z axis and the y axis, respectively. Note which coordinate axis the moment is about. The evaluation of these integrals can be explained by reviewing the mean value theorem for a continuous function of a single variable, say $f(y)$. The mean value theorem states that for any continuous function over the interval $[a, b]$, there exists an "average value," symbolized as \bar{f} , such that

$$\bar{f}(b - a) = \int_a^b f(y) \, dy$$

See Fig. III.2, which indicates one path to proving this theorem (which also can be considered as simply a definition of the average value) when it is recalled that the basic definition of a definite integral is the area beneath a curve. On the same basis, the above integral relation can easily be extended to two dimensions. With y taking the place of f ,

$$\bar{y}A = \iint_A y \, dA$$

Bending and Extensional Stresses in Beams

9.1 Introduction

The theory of elasticity problems of Chapters 7 and 8 are restricted to plane stress problems. In most of those illustrative problems the elastic body has a simple geometry that is either a circular disk or a straight beam with a uniform, rectangular cross-section. In each of those example problems the loadings and material properties are also chosen to be mathematically simple. While there are many theory of elasticity solutions much more complex than those illustrated in Chapters 7 and 8, it may generally be said that almost all theory of elasticity solutions involve relatively simple geometries, simple material descriptions, and simple loadings. For example, there are no theory of elasticity solutions for straight beams with any of the efficient cross-sectional geometries usually used in engineering, such as I- or H-shaped cross-sections. Thus it is quite rare that a theory of elasticity solution is, in any precise sense, directly applicable to an everyday engineering problem. Nevertheless, the theory of elasticity problem is the problem to be solved in one manner or another.

One possible approach to actual engineering problems involving the common components (often called “elements”) of vehicular structures such as bars or beams, and plates or shells, is to seek what is called a *numerical solution* to all four sets of equations that comprise the theory of elasticity rather than seek an *analytical solution*. The solutions of Chapters 7 and 8 exemplify analytical solutions, that is, solutions expressed in terms of mathematically smooth functions. Analytical solutions have the advantage of clearly demonstrating how a solution, say for a stress value at any point within the structure, depends upon the geometric, material, and loading factors associated with the problem. A numerical solution is a solution that is limited to a set of discrete numerical values that describe, say, the individual stress components or displacement components at usually a small number of points within a structural body. Each numerical solution is limited to a single geometry, material state, and loading. The information provided by a numerical solution, which can be voluminous for a complicated problem, often must be plotted on drawings of the structure in order for the analyst to grasp the significance of the solution. These are minor drawbacks compared to the great advantage of numerical solutions, which is that, by use of modern digital computers, they are often routinely possible.

The other possible approach to using the theory of elasticity to solve actual engineering problems is to simplify the theory of elasticity by relaxing one of its various field requirements; that is, compromising either stress equilibrium, or material description, or displacement compatibility. While such a simplification cannot usefully be made in general, such a simplification is possible with structural elements that have restricted shapes such as beams, plates, and shells. It cannot be overemphasized that all such generally accepted simplifications in the form of approximations to either the stress or displacement field for such special geometries are well grounded upon extensive experimental evidence.

Engineering experience has revealed the usefulness of each of the above two means of circumventing the mathematical difficulties presented by the theory of elasticity in the

analysis of beams, plates, and shells. The first approach, the application of numerical methods to the full set of theory of elasticity equations, is much too costly for routine use. This approach is reserved for very unusual cases such as those where great accuracy is desired for a problem beyond analytical treatment, or as a test of a computer program or even a computer. Hence, the application of numerical methods to the full set of the equations of the theory of elasticity will receive no further attention in this textbook. On the other hand, compromised versions of the theory of elasticity, given the name "strength of materials" or "applied elasticity," are reasonably accurate, yet cheap, means of analyzing beams, plates, and shells. Thus strength of materials solutions for beams, plates, and shells are the routine approach to these basic structural elements. Keep in mind that cost-effective accuracy, rather than mathematical purity, is the goal of engineering analysis.

As effective as strength of materials analytical solutions are for individual beams, plates, and shells, and very small numbers of beams connected together, the usual strength of materials solution techniques are much too complicated for the analysis of entire vehicular structures since those structures are commonly modeled as consisting of large numbers of beams, plates, shells, and other elements. Present-day vehicular structural analyses almost always depend upon a combination of (i) numerical analysis techniques that allow consideration of large numbers of individual structural elements and (ii) strength of materials descriptions applied to simpler forms of individual structural elements. Clearly, even without the necessity of determining the applied loads, there are many topics that need to be explored before the reader is ready to undertake a complete vehicular structural analysis. The two interrelated tasks to be undertaken in Part III are (i) the thorough development of the concept of strength of materials/applied elasticity and (ii) the use of this applied elasticity approach for the analytical description of the response of beam elements to known applied thermal and mechanical loads. Numerical analyses techniques are introduced in Part V.

In summary, Part III introduces a cost-effective alternative to the theory of elasticity for beams. This alternative is based upon simplifying the theory of elasticity. The resulting approximate theory is called "strength of materials" or "applied elasticity." With the exception of one part of one chapter that is a temporary return to the full rigor of the theory of elasticity, the remainder of this text utilizes the type of approximations introduced here in both analytical and numerical solutions.

9.2 An Elaboration on the Scope of Strength of Materials

When the elastic body under study has one of several special geometries, then it is possible to make simplifying approximations to the theory of elasticity.¹ Elastic bodies that do have special geometries for which such simplifications are quite successful are (i) bars and beams, which are structural elements where two of the three orthogonal dimensions are at least three or four times smaller than the third dimension, which is the length of the bar or beam; and (ii) membranes, plates, and shells² where one dimension, the thickness, is at least several times smaller than the other two dimensions. In Part III, only *long* bars

¹ As is discussed later, there are qualifications. For example, the approximations to be made are generally not valid in the immediate vicinity of concentrated forces.

² A *beam* can either be a straight structural body, or it can be curved. Without qualification, it is always assumed that the beam is straight. A *bar* has the same geometry as a beam, but only experiences twisting and extensional deformations while a beam also experiences bending, and perhaps shearing deformations. An unloaded *plate* is a structural body that has a flat midplane between the two surfaces that define the thickness of the plate, while a *shell* has a curved midplane; for example, a spherical or cylindrical shell. Plates and shells bend, twist, extend (or contract), and perhaps shear. An unloaded

and *long* beams, and membranes, the simplest of these structural elements, are discussed.³ Even though the strength of materials theories for *thin* plates and *thin* shells are based upon essentially the very same simplifications used with long-beam theory, their resulting analytical theories can be nevertheless quite challenging. Chapter 22, following the same procedures of this chapter, introduces thin plate theory.

9.3 Stress Resultants

Preliminary to developing the approximation that permits the rapid analysis of beams within the limits of what is termed engineering accuracy,⁴ it is useful to introduce the concept of *stress resultants*. Stress resultants, such as bending moments and shear forces, are convenient for describing the loads transmitted by beams. (Sometimes the bending moments and shear forces can be easily calculated by writing moment and force equilibrium equations.) Stress resultants represent the stresses in the beam in an aggregate form. Thus it may be said that the stresses give rise to the stress resultants. It is also valid to take the viewpoint that the stress resultants cause the stresses. For example, as was seen in Example 8.1, the application of a bending moment to a beam causes σ_{xx} stresses. Both cause and effect viewpoints are useful in the work below.

In order to obtain a precise definition of the various stress resultants, consider Fig. 9.1(a), which shows a segment of a beam of arbitrary cross-section and material composition. The cross-section located at the coordinate value x is shown three times: once (in the middle) to establish the geometric relation between the point $O(x, 0, 0)$, where the x axis pierces the orthogonal cross-section, and an arbitrary point $P(x, y, z)$ on that same cross-section; once (to the right) to show the stresses of that same cross-section acting on an infinitesimal area of dimensions dy by dz extending from point P ; and once (to the left) to show the stress resultants for the entire cross-section acting at the point O that are about to be defined in terms of the stresses at point P . For the stress resultants, the symbol M indicates a moment, and its subscript indicates the coordinate axis about which the moment acts. However, rather than use the symbol M_x for a twisting (i.e., torsional) moment, where it is too easy to mistake the subscript x for a factor in later work, the symbol M_t is used instead. Note the use of a double-headed arrow (right-hand rule) to indicate a moment.⁵ The symbol V is used to designate shear forces and its subscript indicates which coordinate axis the shear force

membrane has the same geometry as an unloaded plate, but it is so thin as to have negligible resistance to bending. Taut aluminum foil is an example of a membrane.

³ The relative terms "long" applied to beams, and "thin" applied to plates and shells, mean that, under a general smooth loading, their bending deformations are much greater than their shearing deformations, with the result that the latter deformations can be ignored. Roughly, a long beam has a length at least ten times greater than its largest cross-sectional dimension. "Long" applied to bars means that the twisting of the bar can also be described by a simpler theory.

⁴ "Engineering accuracy" is a term that generally means within 5–7 percent of the experimental or theory of elasticity solution, in the unlikely case where the latter happens to be known. Note that, although such accuracy is always the goal, all useful engineering calculations are not that accurate. For example, in the airfoil flutter problem, an eigenvalue problem involving aerodynamic loads that arise from the motion of the aircraft, a calculated flutter speed may differ from a test value by more than 20 percent. Yet the calculation is made because of the importance of having some estimate of the actual flutter speed.

⁵ The action of the moment can be deduced from this symbol by imagining gripping the arrow with the right hand with the thumb pointing in the direction indicated by the double heads. The remaining fingers show the action of the moment.

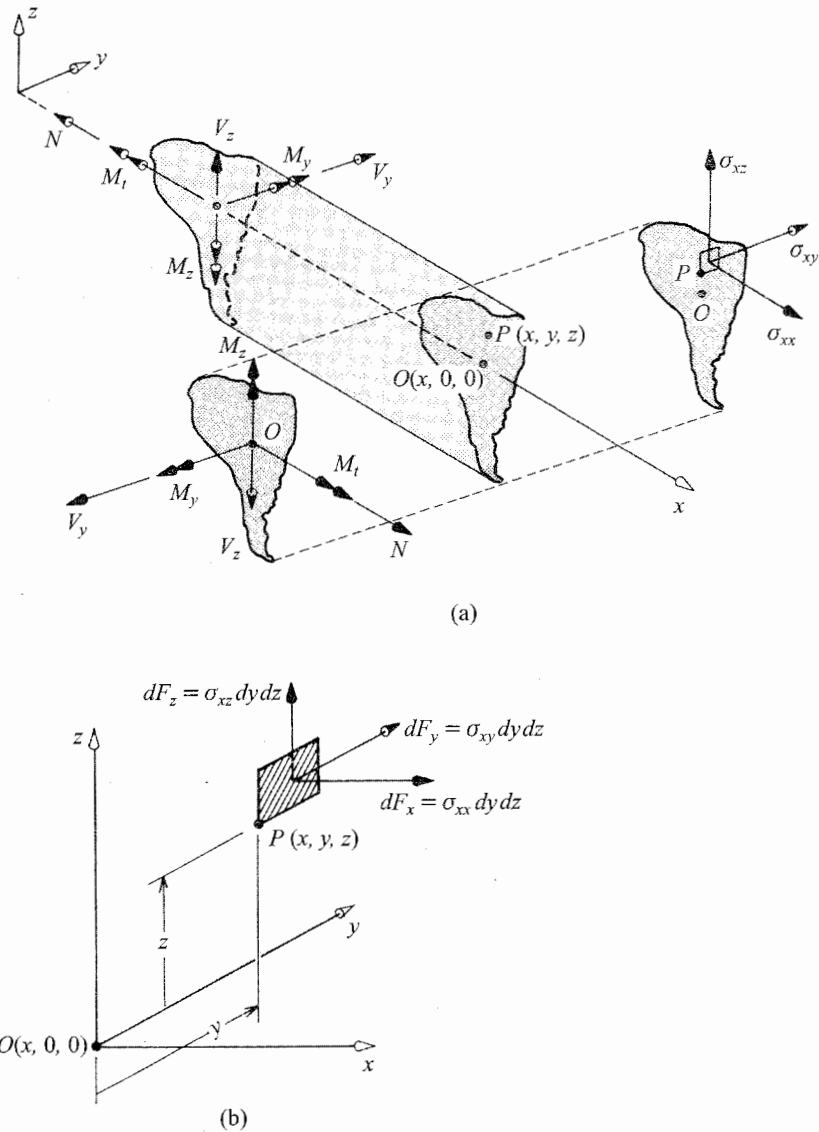


Figure 9.1. (a) The positive sign convention for all the beam stress resultants (internal bending and twisting moments, internal shearing and axial forces) at both a front face and a back face, which, since it is an arbitrary choice, must be memorized. (b) Differential forces acting upon the differential area at point P . The distances y and z from the x axis are the finite moment arms for these forces.

parallels. The symbol N , which does not require a subscript in the case of beams, indicates a tensile force, or a compressive force when N has a negative value.

The choice of the positive directions for the stress resultants is as shown in Fig. 9.1(a) for both the front and back face cross-sections (different values of x) of a finite-length beam segment. The choice of a stress resultant sign convention is an arbitrary choice, but of course, once made, it must be adhered to thereafter so as to avoid sign errors. Thus this sign convention for the stress resultants must be memorized in order to effectively use this

textbook. The moment convention may be remembered by associating it with a happy face smile; that is, the positive bending moments in both the y plane and the z plane bend the beam to produce a positive curvature.

Again, the intent here is to determine the stress resultants in terms of the stresses. The plan is to work with the two descriptions of the same stresses on the same x cross-section, where the stress resultants are one such description, and the stresses themselves are the other.⁶ Consider the stress resultant N . It is defined as the force created by the stresses σ_{xx} acting over the area of the cross-section. In other words, when all the differential axial forces $dF_x = \sigma_{xx} dy dz$ acting on the cross-section are added together (i.e., integrated), the result is N , see Fig. 9.1(b). Similarly, when all the differential shear forces $dF_z = \sigma_{xz} dy dz$ are added together the result is (the negative of) V_z . The minus sign that appears in the definition of V_z is solely a result of the shear stresses being positive in one direction, while the shear force is positive in the opposite direction. Minus signs are 180° turns. These and the other force-type stress resultant definitions can be expressed mathematically as

$$N(x) \equiv + \iint_A \sigma_{xx}(x, y, z) dy dz \quad (9.1a)$$

$$V_y(x) \equiv - \iint_A \sigma_{xy}(x, y, z) dy dz \quad (9.1b)$$

$$V_z(x) \equiv - \iint_A \sigma_{xz}(x, y, z) dy dz \quad (9.1c)$$

The differential forces at point P give rise to differential moments about the three coordinate axes. For example, the finite moment arm of the differential force dF_x for a moment about the y axis is the coordinate value z . All such differential moments can be summed to obtain the total moment about the y axis which is designated M_y . Thus, accounting for the two different sign conventions,

$$M_y(x) \equiv - \iint_A z \sigma_{xx}(x, y, z) dy dz \quad (9.1d)$$

$$M_x(x) \equiv - \iint_A y \sigma_{xx}(x, y, z) dy dz \quad (9.1e)$$

$$M_t(x) \equiv + \iint_A [y \sigma_{xz}(x, y, z) - z \sigma_{xy}(x, y, z)] dy dz \quad (9.1f)$$

Again, the derivation of the above stress resultant–stress equations depends upon recognizing that at the same cross-section, the one with coordinate value x , the stresses and the corresponding stress resultants are merely different ways of describing the same internal force distribution. These same stress resultant–stress equations can also be derived by means of a free body diagram of a differential length of beam with the stress resultants on the back face, and the stresses on the front face, or vice versa. See the exercises for the especially eager at the end of this chapter.

⁶ No differential stress increments are attached to the stresses on the differential area shown in Fig. 9.1(a) because that differential face is a back face for point $P(x, y, z)$.

The A subscript on the double integrals merely indicates that the area integration is to take place over the entire beam cross-sectional area A at the point x along the beam length. Thus this is a case of definite, rather than indefinite, integration. Hence the cross-sectional coordinate variables y and z , which are the variables of the integration, disappear when the integration limits are applied, and thus the stress resultants are only functions of the distance x along the length of the beam. This is similar to, say, any function of both x and y being singly integrated over x between two definite values of x , and thus producing a function of y alone. For example,

$$\int_1^2 (x + y)^{1/2} dx = \frac{2}{3} [(2 + y)^{3/2} - (1 + y)^{3/2}]$$

In this chapter and Chapters 10 and 11, only the bending moment and axial force stress resultants are considered. The effects on the beam produced by the internal torsional moment and the internal shear forces are considered in subsequent chapters.

The point $O(x, 0, 0)$ where the x axis pierces the plane of the cross-section is, of course, the origin for the y and z axes, and the y and z coordinates locate all points in the cross-section relative to that point. Since the moment arms for the stresses that produce the moment stress resultants are the y and z coordinates, then all of the above force and moment resultants act at point $O(x, 0, 0)$. This observation becomes important in later work, beyond the scope of this textbook, that involves the coupling of the finite bending and finite twisting deformations of beams. At present there are no restrictions on the location of the x axis in relation to the beam cross-section, but its location is soon to be fixed.

9.4 The Approximate Pattern for Beam Displacements

There are basically two general ways in which the theory of elasticity can be simplified in order to obtain a strength of materials theory for appropriate types of structural components. The first way is to make an approximation regarding the displacements of the body to be studied. The second way is to make an approximation regarding the stress field within the body.⁷ Both types of approximations are employed to solve different types of problems. (Never are both types of approximations made independently for the same part of any structural body.) In this chapter, which is devoted to analyzing the stresses that result from the bending and extension of beams, a standard **displacement** approximation is chosen. Then, following the procedures of the theory of elasticity, the consequent strain and stress approximations are determined.

Based upon experimental results and the evidence of those theory of elasticity solutions that are available, the long-beam displacements, under the action of bending moments, axial forces, shear forces, and even a general temperature change, are approximated by requiring that the deformations throughout the volume of the long beam be such that

- i. The planar cross-sections of the undeformed beam remain plane after deformation;
- ii. the planar cross-sections remain perpendicular to any axis along the length of the beam (in particular, remain normal to the [bent] x axis); and
- iii. the planar cross-sections retain their original size and shape after deformation.

⁷ Infrequently, strains are the chosen approximation, but for a linearly elastic material the choice of a strain approximation is only a variation on a stress approximation choice.

These approximations to the actual beam deformations are the basis of what is called the *engineering theory of beam bending*, or *Bernoulli–Euler beam theory*. If the second of these requirements for the beam deformation pattern is deleted, then the remaining requirements form the basis for a more complicated beam theory called Timoshenko beam theory⁸ that is sufficiently more accurate to be suitable for short beams. Timoshenko beam theory results differ very little from those of Bernoulli–Euler beam theory in the case of long beams, and thus Timoshenko beam theory is not further discussed in this text. Note that the third approximation essentially excludes Poisson effects from Bernoulli–Euler beam theory. That is, no matter how the beam is compressed or extended along its length, the approximation is that the beam cross-section is unaffected. Thus it may be expected that Poisson's ratio, having a zero value, has no part to play in the engineering theory of beam bending.

The above three postulated approximations have the effect that if the displacements (including the rotations) along the x axis are known, then the displacements at any point on a beam cross-section can be deduced. This is illustrated in side view with a y plane rotation in Fig. 9.2(a) where $O(x, 0, 0)$ is a point on the x axis, and $P(x, y, z)$ is an arbitrary point on the same cross-section. Fig. 9.2(b) illustrates the same fact in a three-dimensional view. With ϕ_y , being the right-hand rule rotation of the cross-section about the negative y axis, and ϕ_z being the rotation about the positive z axis (a seemingly weird, but common sign convention), the three displacement components at point $P(x, y, z)$ can be written as the following three equations:

$$\begin{aligned} u(x, y, z) &= u(x, 0, 0) - y\phi_z(x, 0, 0) - z\phi_y(x, 0, 0) \\ v(x, y, z) &= v(x, 0, 0) \\ w(x, y, z) &= w(x, 0, 0) \end{aligned} \tag{9.2}$$

where, in keeping with the reality of most vehicular beam rotations, the angles of rotation, ϕ_y and ϕ_z , are now limited to being so small that their cosines have the value 1.0, and their sines are equal to the value of the angles themselves expressed in radians. Note that this limitation regarding the size of the rotations, which thus becomes another constraint on the validity of the theory being developed, is a very loose constraint. For example, the error in the above assumption for an 11° angle is less than 2 percent for the cosine, and less than 1 percent for the sine. For an 8° angle, it is less than 1 percent for the cosine, and less than one-third of 1 percent for the sine. An 11° rotation (nearly $\frac{1}{5}$ radian) would be unusually large for the beam elements of vehicular structures in most circumstances.

Equations (9.2) encompass all three of the above-listed approximations for the beam deformations, and they are the basis for the estimation of the stresses in beams. The last two of these three equations are a direct result of the third assumption. Having made these approximations, the theory of elasticity is used hereafter to obtain an equation for the stresses in the beam. However, since the actual displacements are not quite as simple as those listed in Eqs. (9.2), contradictions can be expected. Before starting the process of determining the stresses from the assumed displacements, the notation of Eqs. (9.2) is

⁸ Jean Bernoulli (1667–1748), Swiss mathematician (the younger brother of Jacques, father to Daniel, and teacher of Euler), made many important contributions to pure and applied mathematics and mechanics (Ref. [2]). Leonhard Euler (1707–1783), Swiss mathematician, is considered the greatest mathematician of the eighteenth century. He was interested in the application of science to engineering (Ref. [2]). Stephen P. Timoshenko (1878–1972), born in Russia, became the most influential American educator in the field of structural mechanics.

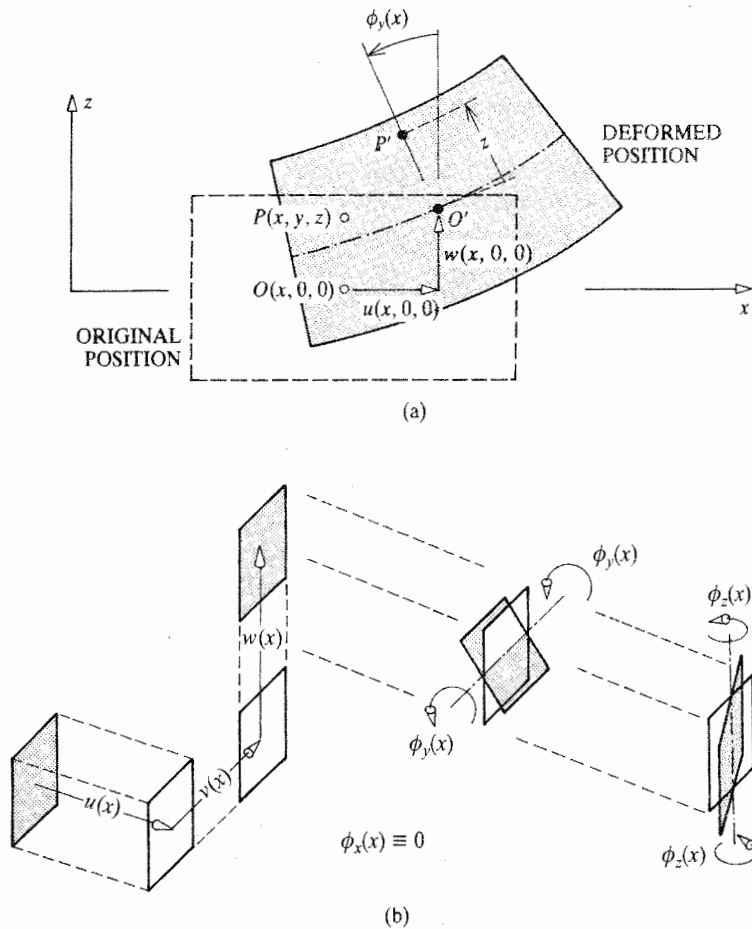


Figure 9.2. (a) The y direction side view of the Bernoulli–Euler beam displacement pattern showing the displacements u , w , and ϕ_y . (b) Isometric view of all five (exaggerated) displacements involved with beam bending and extension.

simplified. Change $u(x, 0, 0)$ to simply $u(x)$, $\phi_z(x, 0, 0)$ to $\phi_z(x)$, and so forth, in order to dispose of the unnecessary zeros. From this point on when discussing beams, u alone will be identical to $u(x)$, the displacement on the x axis in the x direction, and so on. The displacement components of the material points along the x axis, u , v , w , ϕ_y , and ϕ_z are henceforth called the beam “deflections.”

Since all displacements are fully described by the continuous, differentiable deflection functions of Eqs. (9.2), it is possible to calculate the six small displacement-induced strains using the strain–displacement equations, Eqs. (3.12). Note first, however, that the direct consequence of the second Bernoulli–Euler beam assumption is that

$$\gamma_{xy} = \gamma_{xz} = 0$$

and the third Bernoulli–Euler beam approximation requires that

$$\epsilon_{yy} = \epsilon_{zz} = \gamma_{yz} = 0$$

Combining the strain–displacement equations, Eqs. (3.12), with the above displacement–deflection equations, Eqs. (9.2), and then applying the above requirement that $\gamma_{xy} = \gamma_{xz} = 0$, leads to

$$\gamma_{xy}(x, y, z) = \frac{\partial u(x, y, z)}{\partial y} + \frac{\partial v(x, y, z)}{\partial x} = 0$$

or

$$0 = -\phi_z(x) + v'(x) \quad \text{or} \quad v' = \phi_z$$

where each prime on a function of x indicates a differentiation with respect to x , and

$$\gamma_{xz}(x, y, z) = \frac{\partial u(x, y, z)}{\partial z} + \frac{\partial w(x, y, z)}{\partial x} = 0$$

or

$$0 = -\phi_y(x) + w'(x) \quad \text{or} \quad w' = \phi_y$$

The Interpretation of these last two results is that for a deformed Bernoulli–Euler beam, the bending slopes are the same as their corresponding rotations.

The three equalities $\epsilon_{yy} = \epsilon_{zz} = \epsilon_{yz} = 0$ produce the identity that zero equals zero. Finally, using the first of Eqs. (9.2), and the strain–displacement equation for the sixth strain yields

$$\epsilon_{xx}(x, y, z) = \frac{\partial u(x, y, z)}{\partial x} = u'(x) - yv''(x) - zw''(x) \quad (9.3)$$

It is seen that the strain has, as well as the displacements, a linear or planar variation over the straight beam cross-section; that is, with x fixed, the strain varies linearly with y and z .

Now that the Bernoulli–Euler strains have been determined, it is possible to proceed to determine the Bernoulli–Euler stresses by use of the linearly elastic stress–strain equations. It is at this point that the contradictions inherent in the Bernoulli–Euler approximations become apparent. For example, one contradiction that stands out when considering the stress–strain equations is that although there may be shear forces, and thus shear stresses, acting on a beam cross-section, the approximation is that there are no corresponding shear strains. The easiest way to wiggle out of this and other mathematical contradictions is to treat the beam as having convenient, fictitious orthotropic material properties. On this basis, conclude from the second Bernoulli–Euler approximation and the fourth and fifth orthotropic strain–stress equations, Eqs. (6.1), that the shear moduli G_{xy} and G_{xz} must be infinite. From the third Bernoulli–Euler approximation and examination of the second, third, and sixth orthotropic strain–stress equations, conclude that E_y , E_z , and G_{yz} must also be infinite, and that α_y , and α_z must be zero for that basic approximation to be realized. The Poisson ratios with x , y and x , z subscripts must also be zero as a result of Eqs. (6.2). This fictitious orthotropicity of the Bernoulli–Euler beam can be viewed as a hidden, fourth approximation.⁹

⁹ The use of fictitious orthotropic material constants is not the only approach to arriving at the Bernoulli–Euler strain–stress equation. Endnote (1) offers a justification for concluding that the y and z direction normal stresses are typically much smaller than the x direction normal stress in an isotropic beam, and thus may be neglected so as to achieve the *same* strain–stress result for ϵ_{xx} deduced using fictitious material constants.

The nontrivial end result of this manipulation of the orthotropic material properties in order to have the Bernoulli–Euler approximations compatible to the strain–stress equations is, at any point on the beam cross-section

$$\epsilon_{xx} = \frac{\sigma_{xx}}{E_x} + \alpha_x \Delta T$$

After dropping the directional subscripts from the material properties because there is only one surviving modulus of elasticity and one surviving coefficient of thermal expansion, the results for the beam stresses are

$$\begin{aligned} \sigma_{xx} &= E(\epsilon_{xx} - \alpha \Delta T) \\ \sigma_{yy} &= \sigma_{zz} = \sigma_{yz} = 0 \\ \sigma_{xy}, \sigma_{xz} &\text{ to be discussed in Chapters 12, 13, and 14} \end{aligned} \quad (9.4a)$$

The first of the above results has the deceptive appearance of a simple one-dimensional stress–strain equation. Nevertheless, the above development establishes its applicability with respect to a beam subjected to bending in two orthogonal planes as well as extension. When the expression for the single nonzero strain from Eq. (9.3) is used, it is clear that the stress also varies with all three Cartesian coordinates. That is, at any point (y, z) on the cross-section located at the distance x along the length of the beam

$$\sigma_{xx} = E[u'(x) - yv''(x) - zw''(x) - \alpha \Delta T] \quad (9.4b)$$

This equation for the only nonzero or significant normal stress that arises due to bending and extension of the beam is not wholly satisfactory as a solution because the quantities u' , u'' , and w'' are not normally known at the start of a beam stress analysis. A more useful form of the solution for the above stress can be obtained by substituting Eq. (9.4b) into the expressions for N , M_y , and M_z in Eqs. (9.1). In order to make that substitution in the most general way, let the beam cross-section be nonhomogeneous. This means that the material properties E and α both vary with the cross-sectional coordinates y and z . Allowing this generality in no way contradicts any of the three approximations made earlier in this development. “Plane sections remain plane,” and so forth, are the approximations for a nonhomogeneous, orthotropic beam as well as a homogeneous, isotropic beam. Substituting Eq. (9.4b) into the expression for $N(x)$ yields

$$\begin{aligned} N(x) &= \iint_A E(y, z) u'(x) dy dz - \iint_A y E(y, z) v''(x) dy dz \\ &\quad - \iint_A z E(y, z) w''(x) dy dz - \iint_A E(y, z) \alpha(y, z) \Delta T(x, y, z) dy dz \end{aligned}$$

In order to have the convenience of a more natural set of units associated with the terms to be developed, a reference modulus of elasticity, E_0 , is now introduced. The constant value E_0 is used to normalize the various moduli of elasticity of the nonhomogeneous beam cross-section. Its value is arbitrary. For example, if a beam happened to be part steel ($E = 29.0 \times 10^6$ psi) and part aluminum ($E = 10.0 \times 10^6$ psi), it would be convenient (but not necessary) to choose E_0 as 10.0×10^6 psi because the value divides nicely into the other two values. The choice of a particular value for the reference modulus has no effect whatsoever on the final calculation of the axial stress, σ_{xx} , because the next step is to both multiply and divide the above right-hand side by E_0 . The above right-hand side can be further improved by noting that the deflections such as $u(x)$, which are only functions

of x , can be removed from inside the various integrals because they are unaffected by the integration over y and z . The result, where the product $dy dz$ is replaced by the more general term dA , is

$$N = E_0 \left(u' \iint_A \frac{E}{E_0} dA - v'' \iint_A y \frac{E}{E_0} dA - w'' \iint_A z \frac{E}{E_0} dA \right) - \iint_A E \alpha \Delta T dA \quad (9.5)$$

Consider the first integral in the above right-hand side. The modulus ratio (E/E_0) is nondimensional. Without this ratio the value of this integral would simply be the cross-sectional area, A . Thus the integral including this nondimensional ratio also has units of area. In this integral each infinitesimal area dA is adjusted, that is, "weighted," by the modulus ratio, making perhaps some dA factors expand and perhaps others contract. Thus it is reasonable to designate this integral as the *modulus weighted area*, A^* . That is, let

$$A^* \equiv \iint_A \frac{E}{E_0} dA \quad (9.6a)$$

Consider the second and third integrals in Eq. (9.5). These two integrals are called the two *first moments of the modulus weighted area*.¹⁰ Now recall that no conditions have been placed on the location of the x axis, that is, the origin of the y and z cross-sectional coordinates with respect to the geometry of the cross-section. Again, everything that has been done so far has been done for an arbitrary placement of the coordinate origin of those cross-sectional coordinates. At this point, however, for the sake of simplifying Eq. (9.5) and two later, similar equations, the origin of the y and z coordinate axes is chosen for each cross-section in such a manner that the second and third integrals of Eq. (9.5) are zero. In other words, requiring that these two integrals must always vanish determines the location of the origin of the y and z axes for each cross-section. Exactly how this is accomplished is discussed in detail in the section after the next section.

The fourth and last integral in Eq. (9.5) is the result of a temperature change. This integral has the units of force. Thus the fourth integral is called the equivalent thermal force, and is symbolized as $N_T(x)$. (Note that the subscript T is for "thermal," while the subscript t is for "torsion.") Hence Eq. (9.5) reduces to

$$N = E_0 A^* u' - N_T \quad (9.7a)$$

or

$$u' = \frac{N + N_T}{E_0 A^*} \equiv \frac{N^c}{E_0 A^*}$$

where for simplicity, the mechanical and thermal equivalent axial forces are combined into a total equivalent axial force, N^c .

Equation (9.7a) is the end result of substituting the x direction normal stress equation, Eq. (9.4b), into the equation for the axial force stress resultant, Eq. (9.1a). There are two other stress resultant equations that also involve the axial stress σ_{xx} . These are the equations for $M_y(x)$ and $M_z(x)$. The process of substituting σ_{xx} into those integral expressions proceeds

¹⁰ An integral containing a distance coordinate raised to the n th power is referred to as the n th moment of everything else in the integrand plus the differential term.

in very much the same way as it did for N^c . For example, for M_y ,

$$M_y(x) = -E_0 \left(u' \iint_A z \frac{E}{E_0} dA - v'' \iint_A uz \frac{E}{E_0} dA - w'' \iint_A z^2 \frac{E}{E_0} dA \right) + \iint_A z E \alpha \Delta T dA$$

The integral factor for $u'(x)$ is zero because this factor is the same as one of the two modulus weighted first moment integrals that was required to be zero in the above development for the axial force $N(x)$. Since the y and z coordinate axes were positioned to make both first moment integrals vanish (two conditions on the two coordinates), there is no further freedom of action to adjust the value of the *second* moment expressions that appear immediately above. Again, a second moment is an integral where there are coordinate factors in the integrand such as the products (yz) , (y^2) , or (z^2) . The three possible second moments are symbolized as follows:

$$I_{yy}^* \equiv \iint_A z^2 \frac{E}{E_0} dA > 0 \quad I_{zz}^* \equiv \iint_A y^2 \frac{E}{E_0} dA > 0 \quad (9.6b)$$

$$I_{yz}^* \equiv I_{zy}^* \equiv \iint_A yz \frac{E}{E_0} dA$$

The first two of the above integrals are called *modulus weighted (m.w.) area moments of inertia*, with the first of the two being about the y axis, and the second being about the z axis. When the beam cross-section is homogeneous, with the choice $E_0 = E$, these two terms are simply called area moments of inertia.¹¹ The third of the above integrals is called the *modulus weighted area product of inertia*. Shortened variations of these names, such as those obtained by dropping “modulus weighted” and “area,” are common, and are used extensively in this text and elsewhere. The two (m.w.) area moments of inertia are measures of the dispersion of the (m.w.) area of the beam cross-section away from its center, which is called the (m.w.) centroid. The further from the centroid, soon to be defined, the distribution of the cross-sectional area, the greater the values of the area moments of inertia. The greater the area moments of inertia, the stiffer and more efficient the beam cross-section, up to a point. If the area of the cross-section is so arranged that, in order to make the moments of inertia large, the cross-section consists of very thin webs and flanges, then such a cross-section would be prone to the local buckling of those thin webs and flanges. If such buckling does occur, at the very least, the cross-section would lose much of its efficiency, and the buckling might well lead to total beam failure. The product of inertia, as will soon be seen, is a measure of the lack of symmetry of the cross-section, and unlike the (m.w.) moments of inertia, the (m.w.) product of inertia can be zero or have negative values.

The last integral in the above expression for $M_y(x)$ has the units of a bending moment. It is symbolized as $-M_{yT}$, and, without the negative sign, it is called the equivalent thermal moment about the y axis. The reason for the negative sign is: (1) to maintain the same algebraic pattern found in the case of $N^c = N + N_T$, and (2) have the positive M_{yT} produce the same type of beam curvature that a positive M_y produces. To see that a positive M_{yT} does

¹¹ The name “moment of inertia” as used with cross-sectional areas is a misnomer. Its usage is due to the similarity of the second moment of area to the second moment of mass, which is truly a moment of inertia. It is, however, the only name used.

produce a beam curvature just like a mechanical moment, first note that constant values of ΔT and α produce no equivalent thermal moment (i.e., no effect) because when these constants are removed, the remaining integral is a first moment integral that has a zero value. Now, if the temperature change is such that there is an increase below the y axis and a decrease above the y axis, then from the viewpoint of thermal expansions and contractions, the beam will have a curvature exactly like that produced by positive bending moments, and M_{yT} will have a positive value. Inserting these symbols into the stress resultant equation yields

$$M_y + M_{yT} \equiv M_y^c = E_0 I_{yz}^* v'' + E_0 I_{yy}^* w'' \quad (9.7b)$$

Similarly, the stress resultant equation for $M_z(x)$ reduces to

$$M_z + M_{zT} \equiv M_z^c = E_0 I_{zz}^* v'' + E_0 I_{yz}^* w'' \quad (9.7c)$$

Note that if the product of inertia and the temperature change are zero, and the beam cross-section is homogeneous, then the relation between the bending moment and curvature in the x, z plane is just $M_y = E I_{yy} w''$, which will be familiar to those who have previously studied strength of materials. Finally, these two equations for the combined moments in terms of the curvatures can be solved simultaneously for the curvatures v'' and w'' in terms of M_y^c and M_z^c . The result is

$$E_0 \left[I_{yy}^* I_{zz}^* - (I_{yz}^*)^2 \right] w''(x) = M_y^c I_{zz}^* - M_z^c I_{yz}^* \quad (9.7d)$$

$$E_0 \left[I_{yy}^* I_{zz}^* - (I_{yz}^*)^2 \right] v''(x) = M_z^c I_{yy}^* - M_y^c I_{yz}^* \quad (9.7e)$$

The result for u' in terms of N^c obtained previously in Eq. (9.7a), and the solutions for the two deflection derivatives v'' , and w'' , in terms of the bending moments, Eqs. (9.7d, e), can now be inserted into the previous solution for the axial normal stress, Eq. (9.4b), to obtain

$$\sigma_{xx} = \frac{E}{E_0} \left\{ \frac{N^c}{A^*} - y \left(\frac{M_z^c I_{yy}^* - M_y^c I_{yz}^*}{I_{yy}^* I_{zz}^* - (I_{yz}^*)^2} \right) - z \left(\frac{M_y^c I_{zz}^* - M_z^c I_{yz}^*}{I_{yy}^* I_{zz}^* - (I_{yz}^*)^2} \right) \right\} - E\alpha \Delta T \quad (9.8)$$

See Endnote (2) for a proof that the denominator $I_{yy}^* I_{zz}^* - (I_{yz}^*)^2 > 0$. The presence of the factor $1/E_0$ outside the braces in the above equation results in the elimination of the arbitrary factor E_0 from the calculation of the (nonarbitrary) final value for σ_{xx} . This formula for the x direction normal stress that results from mechanical and thermal loading is useful because (i) the material properties E and α would be known quantities; (ii) the cross-sectional properties A^* , I_{zz}^* , and so forth, and the equivalent thermal loadings can be calculated as explained in the following sections; and (iii) if the beam is *statically determinate*, that is, if the moments M_y and M_z can be determined solely by use of equilibrium equations, the calculation of σ_{xx} for any point (y, z) on the beam cross-section becomes a simple matter of arithmetic. If the beam is *statically indeterminate*, that is, if the available force and moment equilibrium equations are not sufficient to calculate the bending moments at the cross-section of interest as a result of too many support reactions, then the calculation of the bending moments is a bit more involved. Chapters 10 and 11 present one possible approach for the indeterminate case, and later chapters present two other approaches.

Note that at any particular cross-section, that is, for a fixed value of the x coordinate, all the cross-sectional properties, and the combined forces and combined moments have fixed values. However, the material properties E and α , and the temperature change, can possibly

vary over the plane of the cross-section in any manner. Hence, for a nonhomogeneous cross-section, even in the absence of a temperature change of any kind and unlike the displacements and axial strain, the axial stress distribution over the area of the cross-section is not necessarily linear in the cross-sectional coordinates. Finally, note that Eq. (9.8) is subject to considerable simplification if some of the complications included in its scope are not actually present for the beam under study. For example, if the beam is homogeneous and subjected only to a bending moment, say M_y , and if the product of inertia is zero as it sometimes is, and if there is no temperature change, then Eq. (9.8) reduces simply to

$$\sigma_{xx} = -\frac{zM_y}{I_{yy}}$$

A great variety of partial simplifications are also possible and are left to the reader.

9.5 The Accuracy of the Beam Stress Equation

For most beams, the above-assumed pattern for the beam deformations (and its implied stress distribution) has been experimentally proved to be quite accurate for general mechanical and thermal loadings that vary gradually. When the spatial distribution of the mechanical loading varies rapidly, as for example in the vicinity of a large concentrated force, then normal stresses other than the axial stress are quite significant, and the Bernoulli–Euler beam theory is inadequate. St. Venant’s principle can be used to judge that the predicted stresses, Eq. 9.8, away from the concentrated load are reasonably accurate.

The variation in the thermal loading is determined by the variation in the temperature change. The above development imposes no restrictions on the form of the temperature change. However, the physics of heat conduction requires that the analytical form of any temperature change satisfy the heat conduction equation, which in its steady state (i.e., no changes with respect to time) form is

$$\nabla^2(\Delta T) = 0$$

In the work that follows, the temperature change variation over the beam cross-section is often modeled as piecewise constant; that is, like a staircase or a series of adjacent temperature plateaus. In a physical sense, such a steady-state temperature distribution is impossible. Heat would be transferred from the hotter to the colder portion of the beam, and the temperature discontinuities would be smoothed into a continuous temperature distribution that would satisfy the above equation when thermal equilibrium was achieved. Nevertheless, piecewise constant temperature change modeling is often used just as a convenient mathematical approximation to an actual temperature distribution.

For the same reasons that the Bernoulli–Euler beam theory is in error in the vicinity of a sharp change in the loading along the length of the beam, the stress equation, Eq. (9.8), is also in error wherever there is a change in beam geometry that gives rise to a stress concentration. For example, an abrupt change in the size of the beam cross-section would result in stresses that cannot be estimated by Bernoulli–Euler theory. Moreover, even without regard to stress concentrations, there are general combinations of loadings and beam cross-sectional geometries for which this theory is inadequate. The two major categories of beam cross-sections for which the above assumptions often do not produce acceptable solutions for stresses are (i) cross-sections that are not *compact*, and (ii) *multiconnected* cross-sections for which there is an appreciable temperature change. It is difficult to define compactness for this purpose. However, the beam cross-section of Fig. 9.1 is compact, while those illustrated in Figs. 9.3(a, b, c) are not compact. Figure 9.3(a) depicts in a much

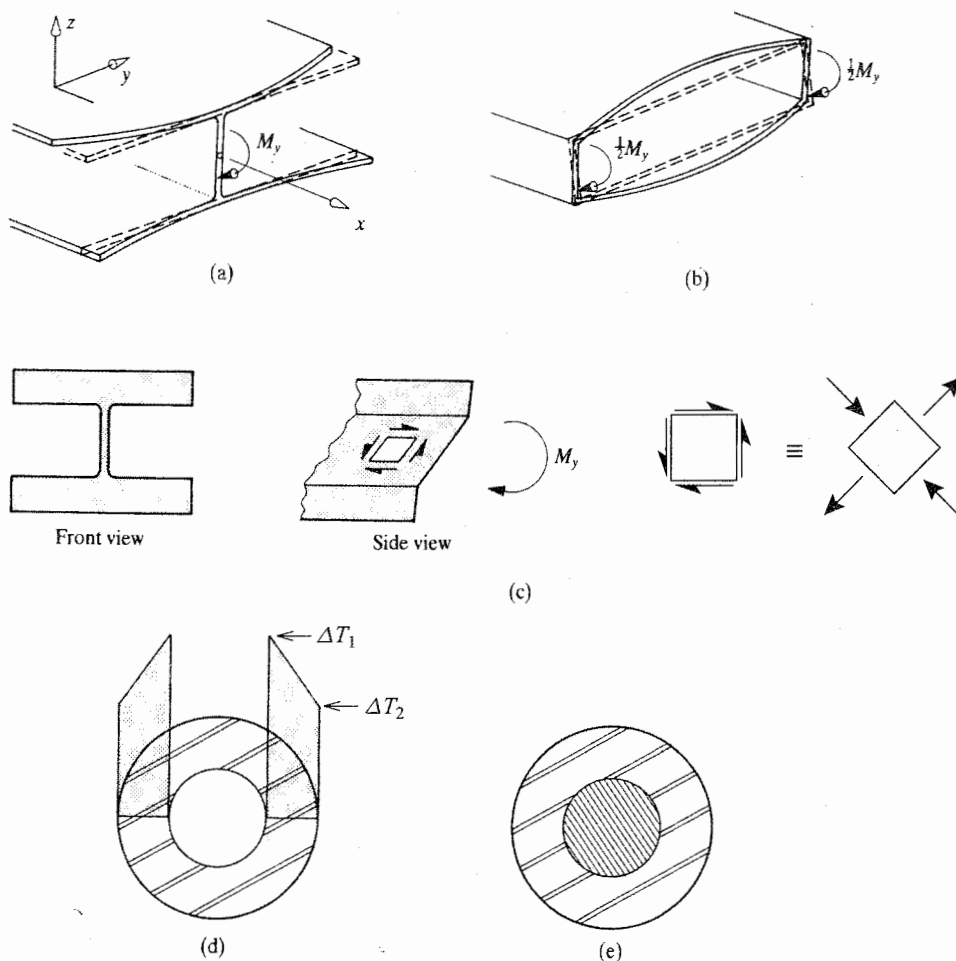


Figure 9.3. (a) The shear lag deformation pattern (much exaggerated) for a very wide flange beam as a result of web bending. (b) The shear lag deformation pattern (much exaggerated) for a box beam as a result of web bending, again showing that for noncompact beam cross-sections, plane cross-sections do not remain plane after bending. (c) A seemingly compact beam cross-section which does not remain plane after bending because the web is too weak. (d) A thick cylinder temperature change that varies in the radial direction that also negates the Bernoulli–Euler hypothesis. (e) A nonhomogeneous beam cross-section subjected to a uniform temperature change that can have substantial stresses other than axial stresses varying linearly over the beam cross-section.

exaggerated fashion the displacements of an H beam cross-section with very wide flanges that is subjected to a bending moment. The dashed lines illustrate the assumed Bernoulli–Euler displacement pattern, while the solid lines show the actual displacement pattern. The discrepancy is due to the accumulation of shearing deformations in the flanges, and this phenomena is known as *shear lag*. Note its potential presence in wide (relative to thicknesses) “box beam” cross-sections as well, as is shown in Fig. 9.3(b). The unusual H cross-section illustrated in Fig. 9.3(c), in front and side views after deformation due to an applied load, might appear to be fairly compact in some ordinary sense of the word. However, since the

web is so thin relative to the massive flanges, any bending moment that loads the flanges to their stress capacity will also cause large shearing deformations in even this shallow web, with the result that plane sections do not remain plane. Hence Eq. (9.8) does not provide an accurate stress solution in this case. (A further complication for such a cross-section is the potential for the thin web to buckle because at a 45° rotation to the orientation of the differential element shown in the sketch, the shear becomes compression as well as tension.) The usual approach to these three situations in themselves is to treat each of the three beams not as beams, but as structures consisting of several structural elements.

An entirely different type of situation for which Bernoulli–Euler beam theory is inadequate is shown in Figs. 9.3(d) and (e). It is possible to offer a mathematical definition pertaining to *simply connected* and *multiply connected* regions or cross-sections. A simply connected planar region is one where any closed curve wholly contained within the outer boundary of the region can be shrunk down to a point without piercing another boundary of the region. In other words, there are no inner boundaries that are not actually part of the outer boundary. The H, T, Z and rectangular cross-sections are examples of singly connected cross-sections. A region that is not singly connected is multiply connected to a degree equal to the number of distinct, closed inner boundaries within the outer boundary. From Ref. [16], Fig. 9.3(d) shows a commonplace situation of a doubly connected cross-section subjected to a nonuniform temperature change distribution. From previous work it should be clear that sizable radial and tangential stresses would occur, and Bernoulli–Euler beam theory cannot begin to describe those stresses because in the Bernoulli–Euler beam theory those nonaxial normal stresses have negligible values. Figure 9.3(e), also from Ref. [12], shows a nonhomogeneous cross-section, which, because of the different coefficients of thermal expansion, can also have sizable radial and hoop stresses even with a uniform temperature change. These latter two problems require either an analytical solution to the theory of elasticity equations or a numerical solution with or without approximations to the theory of elasticity equations.

After noting the above restrictions on the accuracy of Bernoulli–Euler beam theory, the reader can gain some confidence in this approximate beam displacement pattern for compact, homogeneous cross-sections by returning to the theory of elasticity displacements for a cantilevered beam with a rectangular cross-section as set forth in the Chapter 8 exercises. The displacement in the x direction, $u(x, y)$, consists of the sum of two parts. The first part varies linearly in the coordinate distance y , while the second part of the sum varies as the cube of y . The first term is much bigger than the second term because it includes the factor (a/b) squared, where again a is the beam length, b is half of the beam depth, and $a \gg b$. The point is that since the horizontal displacements $u(x, y)$ vary very nearly linearly with y , the original cross-section is very nearly displaced in a planar fashion, as is the general approximation for all Bernoulli–Euler beams.

In summary, each of the Bernoulli–Euler approximations stated at the beginning of Section 9.4, while not exact, is nevertheless quite accurate for the bending and extension of beams that have compact cross-sections. If the reader is fortunate enough to have available to him or her those education company supplied pieces of rubber shaped as beams (ten or more times longer than the largest of the cross-sectional dimensions) with, for example, a rectangular or circular cross-section (quite compact), then for the purposes of testing the accuracy of the Bernoulli–Euler approximations, the reader can easily bend those beams in various ways. The author is confident that even for bending deflections equal to, or even greater than, the depth of the beam (called large deflections), the reader, using his or her unaided eye, will see that the edges of the marked cross-sections will not exhibit any deviation from their original straight lines. The reader will also see for himself or herself that the edges of the marked cross-sections remain perpendicular to lines paralleling the

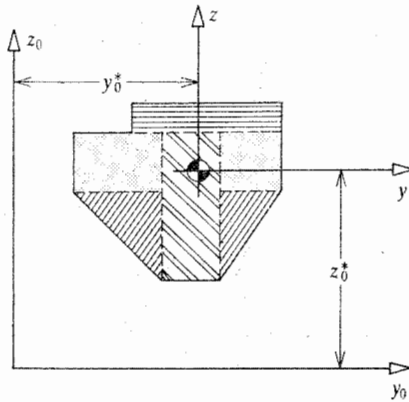


Figure 9.4. An arbitrarily shaped, nonhomogeneous beam cross-section approximated by simple geometries covering sub-areas of constant material properties.

beam axis. Finally, the reader will be able to estimate that each cross-section retains its original shape and area.

9.6 Calculation of the Area Properties of the Nonhomogeneous Cross-Section

The process of calculating the cross-sectional properties needed for the extensional and bending stress equation, Eq. (9.8), begins with the mathematical modeling of the nonhomogeneous beam cross-section. See Fig. 9.4, which shows an idealized (i.e., squared-off) cross-section of general shape and general material distribution divided into sub-areas. Each sub-area has a geometry that is simple enough to allow the quick calculation of its area and to allow the quick location of its individual sub-area centroid. Note that the material distribution of the nonhomogeneous beam cross-section is taken to be “piecewise constant,” that is, each sub-area is arranged so that it has constant material properties. This sort of mathematical model fits the situation where, for example, a flange of a built-up beam is made of steel, while the web is made of aluminum. It can also be made to fit the case, for example, of all-aluminum beam that is subjected to a temperature change that involves a steep temperature gradient. In this case the modulus of elasticity can vary appreciably in a continuous manner over the beam cross-section. This continuous variation in E can be approximated using a staircase set of constant values, which is this piecewise constant model. While this type of modeling of the cross-section is often the most suitable choice, the integrals to be evaluated can also be treated using any number of other numerical procedures, or even the calculus.

With this stepwise material distribution model, it is possible to proceed to efficiently calculate the modulus weighted area A^* on the basis that the integral over the entire cross-sectional area is nothing other than the sum of the integrals over all the sub-areas. This is exactly analogous to saying in one dimension that the integral from a to c is the integral from a to b plus the integral from b to c . Once the total area integral is divided into a sum of integrals over the homogeneous sub-areas, then the (E/E_0) factors of the sub-area integrands are constants and those factors can be removed from their individual integrals. What remains is only the integrals over the sub-areas, which evaluate as the sub-areas themselves. In mathematical form, this process proceeds as follows:

$$A^* = \iint_A \frac{E}{E_0} dA = \sum \iint_{A_i} \frac{E}{E_0} dA = \sum \left(\frac{E}{E_0} \right)_i \iint_{A_i} dA = \sum \frac{E_i}{E_0} A_i \quad (9.9a)$$

where, for brevity, the indices for summation are omitted from the summation symbol. Those indices are here and henceforth understood to run from 1 to the maximum positive integer that is the number of sub-areas, unless otherwise stated.

The first step in the calculation of the area moments and product of inertia, as set forth in Eqs. (9.6b), is the selection of a convenient pair of Cartesian coordinates, which are here called y_0 and z_0 . The chief purpose of the y_0, z_0 pair of coordinates is to locate the *modulus weighted centroid*. (With this, and all other such names, when the cross-section is homogeneous, the "modulus weighted" (m.w.) modifier is unnecessary.) The m.w. centroid is the origin of the y, z coordinate system, called the centroidal coordinate system. These centroidal coordinates enter directly into the stress calculation of Eq. 9.8 by locating the point on the cross-section for which the stress is being calculated, and they enter indirectly as a result of being the coordinates that are part of the previous definitions of the stress resultants, and the m.w. area moments and product of inertia. The two different sets of coordinate axes, as shown in Fig. 9.4, are separated by the distances y_0^* and z_0^* . Hence the coordinate transformations $y = y_0 - y_0^*$ and $z = z_0 - z_0^*$, which can be deduced by considering any point in the first quadrant. When these transformations are combined with the previous requirement that, when using the y, z coordinate system, both first moments of the m.w. area be zero, the results are

$$0 \equiv \iint_A y \frac{E}{E_0} dA = \iint_A (y_0 - y_0^*) \frac{E}{E_0} dA = \iint_A y_0 \frac{E}{E_0} dA - y_0^* \iint_A \frac{E}{E_0} dA$$

where the last integral is none other than A^* and, similarly,

$$0 = \iint_A z_0 \frac{E}{E_0} dA - z_0^* A^*$$

The strategy employed to locate the modulus weighted centroid is the same as that used to calculate A^* ; that is, each area integral is divided into a sum of integrals over sub-areas. For example, in the second case above, after transposing,

$$z_0^* A^* = \sum \iint_{A_i} z_0 \frac{E}{E_0} dA = \sum \left(\frac{E}{E_0} \right)_i \iint_{A_i} z_0 dA$$

When each of the sub-areas has a simple shape such as a rectangle, or perhaps a triangle, then the location of the centroid of each sub-area is known. Then, for such sub-areas, each of the integrals in the latter sum can be evaluated by resorting to the mean value theorem, which is briefly reviewed in Section III.4. With $(\bar{z}_0)_i$ being the distance from the y_0 axis to the centroid of sub-area i , the final result is then

$$z_0^* A^* = \sum \left(\frac{E}{E_0} \right)_i (\bar{z}_0)_i A_i \quad (9.9b)$$

Similarly,¹²

$$y_0^* = \frac{1}{A^*} \sum \left(\frac{E}{E_0} \right)_i (\bar{y}_0)_i A_i$$

The above calculation of y_0^* and z_0^* locates the modulus weighted centroid relative to the chosen coordinate axes, y_0 and z_0 . However, many times one or both of the calculations for

¹² The use of parentheses around quantities like y_0 in order to append another subscript like i is only for emphasis. Writing y_{0i} is entirely equivalent to $(y_0)_i$.

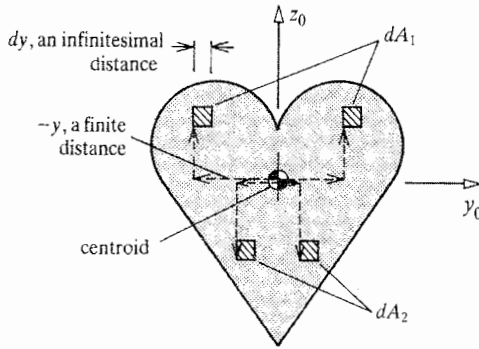


Figure 9.5. An area with one axis of symmetry demonstrating that the product of inertia for this area, and all such areas, has a zero value.

y_0^* and z_0^* are unnecessary because of the existence of an axis of symmetry with respect to both the geometry and material distribution of the cross-section. For the sake of discussion, assume there exists such an axis of symmetry. Then let, for example, the z_0 axis coincide with that axis; see Fig. 9.5. Consider the calculation for y_0^* in the form

$$y_0^* A^* = \iint_A y_0 \frac{E}{E_0} dA$$

As a result of symmetry of geometry and material distribution, there are an equal number of equally sized $(E/E_0) dA$ at equal distances from the z_0 axis. Thus for each $(E/E_0) dA$ with some positive moment arm value for y_0 , there is another $(E/E_0) dA$ with a negative moment arm, and the sum for this and all such pairs is zero. Thus it should be clear that y_0^* is zero. Furthermore, if there are two such axes of symmetry, then the modulus weighted centroid has to lie at their intersection.

The calculation of the modulus weighted moments and product of inertia can proceed in one of two ways. The first approach is to sum about the modulus weighted centroid, that is, to use only centroidal coordinates, while again employing the advantages of the sub-area model. From the definitions of Eqs. (9.6),

$$\begin{aligned} I_{yy}^* &\equiv \iint_A z^2 \frac{E}{E_0} dA = \sum \iint_{A_i} z^2 \frac{E}{E_0} dA = \sum \left(\frac{E}{E_0} \right)_i \iint_{A_i} z^2 dA \\ &= \sum \left(\frac{E}{E_0} \right)_i (I_{yy})_i = \sum \left(\frac{E}{E_0} \right)_i [\bar{I}_{yy} + (\bar{z})^2 A]_i \end{aligned} \quad (9.9c)$$

where the final form is a result of using the parallel axis theorem,¹³ and where all moments or products of inertia with an upper bar are about the centroid of the sub-area, and \bar{z}_i is the distance in the z direction from the modulus weighted centroid (of the entire cross-section) to the centroid of the sub-area. Similarly,

$$\begin{aligned} I_{zz}^* &= \sum \left(\frac{E}{E_0} \right)_i [\bar{I}_{zz} + (\bar{y})^2 A]_i \\ I_{yz}^* &= \sum \left(\frac{E}{E_0} \right)_i [\bar{I}_{yz} + \bar{y}\bar{z}A]_i \end{aligned} \quad (9.9d)$$

¹³ A derivation of the inclusive parallel axis theorem for a nonhomogeneous cross-section follows shortly.

The quantity \bar{I}_{yz} is always zero for a rectangular sub-area, or any homogeneous area or sub-area with at least one axis of symmetry. To understand why this is so, consider again an arbitrarily shaped, homogeneous area with one axis of symmetry such as is shown in Fig. 9.5. Recall that the integral definition of the product of inertia, in terms of y and z coordinates, can be interpreted as a sum where each term of the sum is the product of a rectangular differential area and the y and z direction centroidal coordinates to the corner of the infinitesimal area. With this in mind, consider either the upper or lower pair of infinitesimal areas shown in Fig. 9.5. The vertical distances from the centroid of the larger area to the corners of these infinitesimal areas is the same, while the horizontal distances have the same magnitudes but opposite signs. Thus the products of the differential areas $dy dz$ and the y and z directional distances for both of these infinitesimal areas together is zero. Thus it is easy to see that every infinitesimal area of the symmetric area (or sub-area) can be paired with another infinitesimal area so that, for the pair, the product of these areas and their two corner coordinates sum to zero. Obviously this same argument for a zero value for the area product of inertia can be extended to any nonhomogeneous cross-sectional shape that has the same axis of symmetry for the geometry of the cross-section and for the material property distribution when one of the coordinate axes is placed upon that axis of symmetry.

It is useful to look at a second approach to calculating the modulus weighted moments and product of inertia. This second approach uses the arbitrarily located, but convenient coordinate system y_0, z_0 . To do this is only a matter of convenience. The inconvenience of the first approach is that the location of the modulus weighted centroid is often such that it is tiresome calculating the distances from it to the centroids of the sub-areas. It is often much easier to calculate the distances from the convenient origin of this arbitrarily located coordinate system to the centroids of the sub-areas. The applicable formulas are based upon the previously developed relations between the centroidal and arbitrarily located coordinate systems, which again are $y = y_0 - y_0^*$ and $z = z_0 - z_0^*$. Now, for example, define the modulus weighted moment of inertia about the y_0 axis as

$$\begin{aligned} I_{y_0 y_0}^* &\equiv \iint_A z_0^2 \frac{E}{E_0} dA = \iint_A (z + z_0^*)^2 \frac{E}{E_0} dA \\ &= \iint_A z^2 \frac{E}{E_0} dA + 2z_0^* \iint_A z \frac{E}{E_0} dA + (z_0^*)^2 \iint_A \frac{E}{E_0} dA \end{aligned}$$

or

$$I_{y_0 y_0}^* = I_{yy}^* + 2(z_0^*)(0) + (z_0^*)^2 A^*$$

or

$$I_{yy}^* = I_{y_0 y_0}^* - (z_0^*)^2 A^* \quad (9.10a)$$

Similarly,

$$I_{zz}^* = I_{z_0 z_0}^* - (y_0^*)^2 A^* \quad (9.10b)$$

and

$$I_{yz}^* = I_{y_0 z_0}^* - y_0^* z_0^* A^* \quad (9.10c)$$

Equations (9.10) are the modulus weighted forms of the parallel axis theorems. These theorems allow the easy calculation of the modulus weighted moments and product of inertia at the m.w. centroid whenever the corresponding quantities are known with respect to the origin of the arbitrarily located coordinate system. If the second right-hand side term is transposed to the left-hand side, then they are formulas for calculating the moments and product of inertia at an arbitrarily chosen parallel axis in relation to a centroidal axis, such as that of a homogeneous sub-area. This latter idea is used immediately below. Keep in mind that at least one of the two axes must be a centroidal axis. Note further that the cross-sectional m.w. area moments and product of inertia are always a minimum about the centroid.

Using the parallel axis theorems, the m.w. moments and product of inertia about the arbitrary axes can be developed in exactly the same form as their counterparts were developed with respect to the m.w. centroidal axes. Thus the usual moment and product of inertia calculations begin with

$$\begin{aligned} I_{y_0 y_0}^* &= \sum \left(\frac{E}{E_0} \right)_i [\bar{I}_{yy} + (\bar{z}_0)^2 A]_i \\ I_{z_0 z_0}^* &= \sum \left(\frac{E}{E_0} \right)_i [\bar{I}_{zz} + (\bar{y}_0)^2 A]_i \\ I_{y_0 z_0}^* &= \sum \left(\frac{E}{E_0} \right)_i [\bar{I}_{yz} + \bar{y}_0 \bar{z}_0 A]_i \end{aligned} \quad (9.11)$$

The above equations complete the description of the process for determining those properties of a nonhomogeneous beam cross-section that are necessary for approximating the axial stress σ_{xx} in a beam when the beam undergoes bending and extension. (Again, the shear stresses that result from the twisting and shearing deformation of the beam are discussed in Chapters 13 and 14.) It is necessary to practice using these equations. In the first example, the cross-sectional properties are determined using the calculus so as to offer a reminder that there are some cross-sections for which the basic approach of the calculus is the best approach.

Example 9.1. Calculate the area moments of inertia of a homogeneous, solid, elliptical cross-section. Let a be the semimajor axis length, and b the semiminor axis length so that the equation for the boundary of the cross section is

$$\left(\frac{y}{a} \right)^2 + \left(\frac{z}{b} \right)^2 = 1$$

Solution. Since there are two axes of symmetry that intersect at the center of the ellipse, that is where the centroid lies. The existence of either axis of symmetry allows a zero value to be assigned immediately to the product of inertia. Since the location of the centroid is known, there is no need to calculate the area of the ellipse, which incidentally is πab . Since the ellipse is not easily approximated with a collection of rectangles and triangles, the solution for the two remaining moments of inertia will be obtained using double integration. The two-fold symmetry of the cross-section can be used to simplify the double integration by confining it to the area of the ellipse located in the first quadrant. This tactic leads to a result

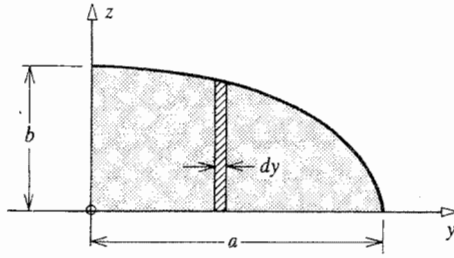


Figure 9.6. Example 9.1. One quarter of an elliptical beam cross-section.

that is one-fourth of the value of the solution for the entire cross-section; see Fig. 9.6. Thus

$$I_{yy} = 4 \iint_{A/4} z^2 dA = 4 \int_0^a \int_0^{b[1-(y/a)^2]^{1/2}} z^2 dz dy$$

or

$$I_{yy} = 4 \int_0^a \frac{1}{3} b^3 \left[1 - \left(\frac{y}{a} \right)^2 \right]^{3/2} dy$$

In order to evaluate this last integral, let $(y/a) = \cos \theta$, so

$$\left[1 - \left(\frac{y}{a} \right)^2 \right] = \sin^2 \theta \quad \text{and} \quad dy = -a \sin \theta d\theta$$

Substituting, where the lower limit becomes $\pi/2$, and the upper limit becomes 0, and then reversing the order of integration so as to eliminate the negative sign, yields

$$I_{yy} = \frac{4ab^3}{3} \int_0^{\pi/2} \sin^4 \theta d\theta = \frac{\pi ab^3}{4}$$

where the identities $\sin^2 \theta = \frac{1}{2}[1 - \cos 2\theta]$, and $\cos^2 \theta = \frac{1}{2}[1 + \cos 2\theta]$ are used to simplify the integrand by writing

$$\sin^4 \theta = \frac{3}{8} - \frac{1}{2} \cos 2\theta + \frac{1}{8} \cos 4\theta$$

The area moment of inertia about the z axis is obtained immediately by interchanging y and a for z and b to arrive at

$$I_{zz} = \frac{\pi a^3 b}{4} \quad \blacksquare$$

Example 9.2. The beam cross-section shown in Fig. 9.7 consists of two aluminum channels fastened to a steel plate. The moduli of elasticity are 29.9×10^6 psi for the steel, and 9.9×10^6 psi for the aluminum. The 5-inch deep channels have cross-sectional areas of 1.97 in². The steel plate is 7.0 in wide by 1.0 in thick. Use the y_0, z_0 axes shown in order to determine the location of the m.w. centroid. Note that the cross-sections of actual rolled (steel) or extruded (aluminum) channel beams, for reasons that are explained in later chapters, have rounded outer boundaries. In Fig. 9.7, and most of the other sketches of beam

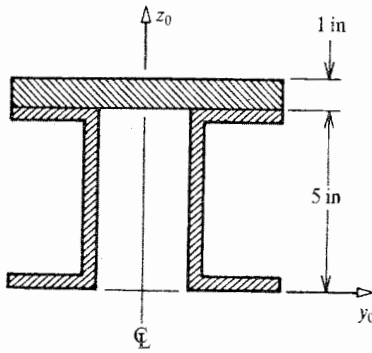


Figure 9.7. Example 9.2. An idealized, nonhomogeneous, symmetric beam cross-section.

cross-sections that follow, the rounded boundaries have been squared off for the purpose of facilitating the calculation.

Solution. The z_0 axis is an axis of both geometric and material symmetry. Therefore y_0^* is zero. Let E_0 be 9.9×10^6 psi. then

$$A^* = \sum \left(\frac{E}{E_0} \right)_i A_i = (29.9/9.9)(7.0 \text{ in}^2) + 2(1.97 \text{ in}^2) = 25.08 \text{ in}^2$$

(If the steel modulus were used as the reference modulus, then $A^* = 8.3 \text{ in}^2$.) Now

$$\begin{aligned} z_0^* A^* &= \sum \left(\frac{E}{E_0} \right)_i (\bar{z}_0)_i A_i = (29.9/9.9)(5.5 \text{ in})(7.0 \text{ in}^2) + 2(2.5 \text{ in})(1.97 \text{ in}^2) \\ &= 126.13 \text{ in}^3 \end{aligned}$$

Hence $z_0^* = 5.0 \text{ in}$ in which means that the m.w. centroid is on the z_0 axis, 5 inches above the y_0 axis. This same result for the m.w. centroid is obtained regardless of the chosen value of E_0 . Note further that the minimum number of significant digits present in the input data is two. Thus any final result should also be reported with two significant digits. However, it is important to retain at least two more significant digits with intermediate calculations. Again, the answer is not complete without the clear specification of the units. It is recommended that the units be included with each factor as illustrated above in order to provide a quick check on the consistency of those units. ■

Example 9.3. The beam cross-section shown in Fig. 9.8 is composed of a flat plate bonded to an angle section. The Young's moduli are indicated. Note again the idealization of the angle section. The rounded fillet on the inside of the juncture of the two legs has been ignored, and the rounded tips of the two legs have been squared off to facilitate the calculation. The m.w. centroid has the coordinate values $(y_0, z_0) = (-t, 7t)$ as shown in the sketch. Calculate I_{yy}^* and I_{yz}^* .

Solution. Since distances from the m.w. centroid to the sub-area centroids are conveniently calculated in terms of integer multiples of t , the moment and product of inertia about the m.w. centroid can easily be calculated directly. Recall that the area moment of inertia of a rectangle about an axis parallel to its base, at the rectangle's own centroid, is one-twelfth

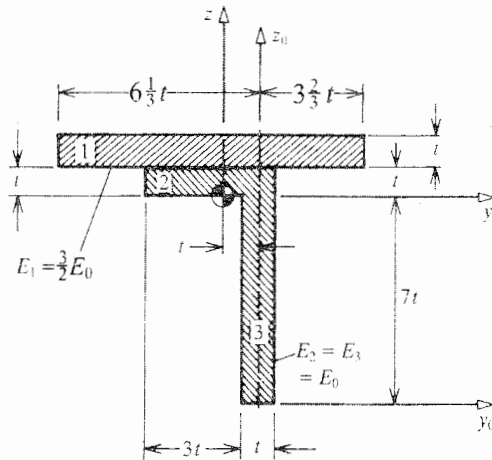


Figure 9.8. Example 9.3. A nonhomogeneous, nonsymmetric beam cross-section.

of the product of the base length multiplied by the height cubed. Thus

$$I_{yy}^* = \sum \left(\frac{E}{E_0} \right) [\bar{I}_{yy} + (\bar{z})^2 A]_i = (1.5)[(10t^4/12) + (1.5t)^2(10t^2)] + (1)[(3t^4/12) + (0.5t)^2(3t^2)] + (1)[(t)(8t)^3/12 + (-3t)^2(8t^2)]$$

$$I_{yy}^* = 151t^4 \quad \text{where the units are the units of } t$$

and

$$I_{yz}^* = \sum \left(\frac{E}{E_0} \right) [\bar{I}_{yz} + \bar{y}\bar{z}A]_i$$

where here $\bar{I}_{yz} = 0$, as is the case for all rectangles.

$$I_{yz}^* = (1.5)[(1.5t)(-t/3)(10t^2)] + (0.5t)(-t)(3t^2) + (-3t)(t)(8t^2) = -33t^4$$

Note again that the product of inertia can be positive or negative, but the moments of inertia must always be positive. In this, as in most cases, it is an easy matter to guess the sign associated with the product of inertia. Examining the sketch of the cross-section, it is seen that with respect to the y and z axes emanating from the m.w. centroid, the majority of the cross-section lies in the second and fourth quadrants where the (yz) products are all negative. Thus it is expected that in this case the (net) product of inertia should be negative and, of course, it is. For those who wish to investigate calculating the required quantities by first calculating their respective values about the arbitrary origin, note $A^* = 26t^2$, $I_{y_0y_0}^* = 1425t^3$, and $I_{y_0z_0}^* = -215t^4$. Of course, the same reasoning can be used to affirm the negativeness of this latter product of inertia. Prove to yourself that $I_{zz}^* = 140.6t^4 \approx 140t^4$. ■

Example 9.4. An H cross-section is idealized as shown in Fig. 9.9. As a result of high temperatures, Young's modulus in the top flange is reduced to six-tenths of its room temperature value, and in the web it is reduced to eight-tenths of its room temperature value. Calculate I_{yy}^* and I_{yz}^* .

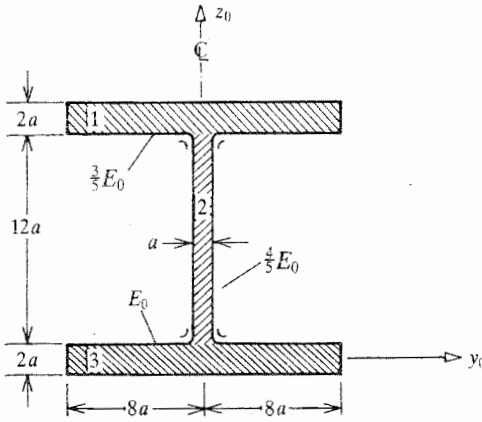


Figure 9.9. Example 9.4. Temperature-change-induced reductions in Young's modulus in an idealized beam cross-section.

Solution. It is generally best to select the arbitrary axes so that they pass through as many local centroids as possible in order to cause as many zero transfer distances as possible. Thus the choice of arbitrary axes shown in the sketch, which also has the merit of making the nonzero transfer distances positive values. The next step is to locate the m.w. centroid. By reason of symmetry, $y_0^* = 0$,

$$\begin{aligned} A^* &= (0.6)[(16a)(2a)] + (0.8)[12a^2] + (1)[32a^2] = 60.8a^2 \\ z_0^* A^* &= (0.6)[32a^2](14a) + (0.8)[12a^2](7a) + 0 = 336a^3 \\ z_0^* &= 5.53a \end{aligned}$$

and it makes sense that the m.w. centroid would lie below the geometric centroid because the cross-section has higher moduli at the bottom. In this example it is judged more convenient to calculate the moment of inertia about the centroid by first calculating that quantity about the arbitrary origin.

$$\begin{aligned} I_{y_0 y_0}^* &= \sum \left(\frac{E}{E_0} \right)_i \left[I_{yy} + (\bar{z}_0)^2 A \right]_i = (0.6)[(16a)(2a)^3/12 + (14a)^2(32a^2)] \\ &\quad + (0.8)[(a)(12a)^3/12 + (7a)^2(12a^2)] \\ &\quad + (1)[(16a)(2a)^3/12 + 0] = 3769a^4 + 586a^4 + 11a^4 = 4366a^4 \\ I_{yy}^* &= I_{y_0 y_0}^* - (z_0^*)^2 A^* = 4366a^4 - (5.53a)^2(60.8a^2) = 2500a^4 \end{aligned}$$

The product of inertia is zero because of the symmetry of both the geometry and the material distributions. ■

9.7 Calculation of Equivalent Thermal Loads

The same strategies used to calculate the m.w. area properties can be used to calculate the equivalent thermal loads. The sub-area approach using simple shapes (i.e., rectangles and possibly triangles) is emphasized in this section. Starting with the definition

$$N_T(x) = + \iint_A E(y, z) \alpha(y, z) \Delta T(x, y, z) dA$$

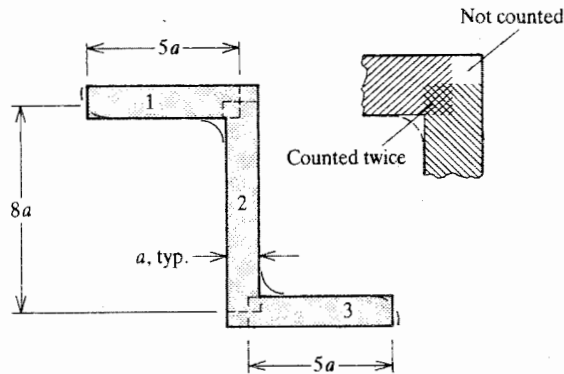


Figure 9.10. Example 9.5. Use of overlapping rectangles at beam cross-section corners in order to simplify calculations.

and recalling the mathematical meaning of any Riemann integral,¹⁴ the immediate result of using sub-areas each with a constant value of $E\alpha T$ is

$$N_T(x) = +E_0 \sum \left(\frac{E}{E_0} \right)_i [\alpha \Delta T A]_i \quad (9.12a)$$

$$M_{yT}(x) = -E_0 \sum \left(\frac{E}{E_0} \right)_i \bar{z}_i [\alpha \Delta T A]_i$$

$$M_{zT}(x) = -E_0 \sum \left(\frac{E}{E_0} \right)_i \bar{y}_i [\alpha \Delta T A]_i \quad (9.12b)$$

Note that the coordinates in the above equations are exclusively those originating at the m.w. centroid. It is entirely possible to develop a set of parallel axis theorems for these equivalent thermal loads in order to obtain the small convenience of first calculating the equivalent thermal stress resultants at an arbitrary location. While such equations are sometimes useful, it is left to the reader to develop those equations as an exercise.

Example 9.5. The Z section beam cross-section shown in Fig. 9.10 is subjected to a temperature change distribution that is approximated in a piecewise fashion where the temperature change in the upper flange is $2T_0$, in the web it is T_0 , and in the lower flange it is zero. If the Young's modulus and the coefficient of thermal expansion are not significantly affected by these temperature changes, what then are the values of N_T and M_{iT} ?

Solution. Note that when the cross-section is thin, there is very little error in using the centerline distances to define the rectangles that comprise the cross-section. This type of approximation is in keeping with those approximations that square off the cross-section tips and delete the fillets at the interior 90° angles. Using this geometric modeling,

$$N_T(x) = +E_0 \sum \left(\frac{E}{E_0} \right)_i [\alpha \Delta T A]_i = +E\alpha [(2T_0)(5a^2) + (T_0)(8a^2)] = 18a^2 E\alpha T_0$$

Note that the units check, that is, the answer has units of force. Note further that the answer is positive, and a positive axial force is one that extends the beam, which is exactly what

¹⁴ From Ref. [1], Bernhard Riemann, German mathematician (1826–1866), lay the groundwork for a general theory of integration.

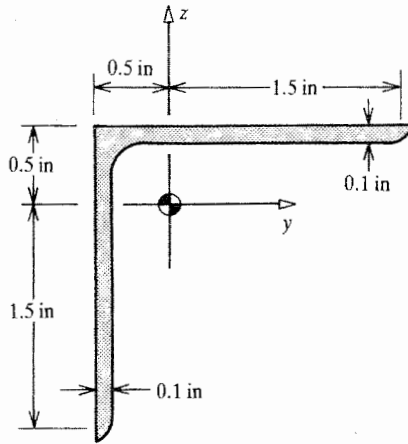


Figure 9.11. Example 9.6. A symmetric angle beam cross-section.

would be expected with a positive temperature change (i.e., an increase in temperature).

$$\begin{aligned} M_{zT}(x) &= -E_0 \sum \left(\frac{E}{E_0} \right)_i \bar{y}_i [\alpha \Delta T A]_i \\ &= -E\alpha [(-2.5a)(2T_0)(5a^2) + 0 + 0] = +25a^3 E\alpha T_0 \end{aligned}$$

Again the units check. Furthermore, the direction of the moment, which would cause the left side of the cross-section to rotate out of the paper about the centerline of the web, and the right side to rotate into the paper, is consistent with the given temperature change. ■

Example 9.6. The material of the $2 \times 2 \times \frac{1}{10}$ angle section shown in Fig. 9.11 is such that $E = 1.0 \times 10^7$ psi, and $\alpha = 1.0 \times 10^{-5}$ in/(in-°F). Assuming that these material properties are not appreciably altered by a temperature change that varies linearly in the z direction (i.e., $T(x, y, z) = (z/h)T_0$, where $h = 1$ in), calculate all three equivalent thermal loads given: $T_0 = 100$ °F, the location of the centroid, and the values $I_{yy} = I_{zz} = 0.1668$ in⁴, and $I_{yz} = +0.100$ in⁴.¹⁵

Solution.

$$N_T = \iint_A E\alpha \Delta T dA = \frac{E\alpha T_0}{h} \iint_A z dA = 0$$

where the (m.w. or not) first moment of the area about the (m.w. or ordinary) centroid is always zero. This should make sense to the reader in that (i) the centroid is the “balancing point” of the area, and (ii) since, in this case, the temperature change varies linearly from zero at the centroid, the net sum of the temperature change is zero.

$$\begin{aligned} M_{yT} &= - \iint_A z E\alpha \Delta T dA = - \frac{E\alpha T_0}{h} \iint_A z^2 dA \\ &= - \frac{E\alpha T_0}{h} I_{yy} = -1668 \text{ lb-in} \rightarrow -1700 \text{ lb-in} \end{aligned}$$

¹⁵ Information on rolled steel and extruded aluminum beam cross-sections can be found in a variety of handbooks; for example, Refs. [12] and [22].

Similarly,

$$M_{zT} = -\frac{E_{\alpha}T_0}{h}I_{yz} = -1000 \text{ lb-in}$$

9.8 Principal Axes for the Beam Cross-Section

The stress equation, Eq. (9.8), and other important equations to be derived in the following chapters, are simplified significantly if the m.w. product of inertia is zero. The m.w. product of inertia can be made to be zero with respect to a new set of centroidal axes by rotating these new centroidal axes counterclockwise from the y, z centroidal axes. The centroidal axes for which the area product of inertia is zero are called the *principal axes* of the cross-section, and the area moments of inertia about those axes are called the *principal moments of inertia*. Let the principal axes be designated as the Y and Z axes. To determine the angle θ , the angle of the counterclockwise rotation from the y and z axes to the principal axes, it is only necessary to adapt the coordinate rotation equation, Eq. (4.2), to the present, two-dimensional situation, and write $I_{YZ}^* \equiv 0$. That is,

$$y\mathbf{j} + z\mathbf{k} = Y\mathbf{j}^* + Z\mathbf{k}^*$$

which leads to

$$Y = y(\mathbf{j}^* \cdot \mathbf{j}) + z(\mathbf{j}^* \cdot \mathbf{k})$$

or

$$Y = +y \cos \theta + z \sin \theta$$

and, similarly

$$Z = -y \sin \theta + z \cos \theta$$

Then write

$$\begin{aligned} I_{YZ}^* \equiv 0 &= \iint_A YZ \frac{E}{E_0} dA = -\sin \theta \cos \theta \iint_A y^2 \frac{E}{E_0} dA + \sin \theta \cos \theta \iint_A z^2 \frac{E}{E_0} dA \\ &\quad + (\cos^2 \theta - \sin^2 \theta) \iint_A yz \frac{E}{E_0} dA \end{aligned}$$

or

$$0 = \frac{1}{2} \sin 2\theta [I_{yy}^* - I_{zz}^*] + \cos 2\theta I_{yz}^*$$

Solving for θ ,

$$\tan 2\theta = -\frac{2I_{yz}^*}{I_{yy}^* - I_{zz}^*} \quad (9.13)$$

Again, this $\tan 2\theta$ equation determines the value of θ that is the counterclockwise rotation to the principal axes from the original (usually horizontal and vertical) centroidal axes. If the same coordinate substitution process is used for the two m.w. area moments of inertia with respect to the Y and Z axes, then it is determined that

$$\begin{aligned} I_{YY}^* &= I_{yy}^* \cos^2 \theta + I_{zz}^* \sin^2 \theta - I_{yz}^* \sin 2\theta \\ I_{ZZ}^* &= I_{yy}^* \sin^2 \theta + I_{zz}^* \cos^2 \theta + I_{yz}^* \sin 2\theta \\ I_{YY}^* + I_{ZZ}^* &= I_{yy}^* + I_{zz}^* \end{aligned} \quad (9.14)$$

The form of these solutions is familiar. The solution for the counterclockwise angle θ that makes I_{yz}^* equal to zero is the same as the solution for the counterclockwise angle θ that makes σ_{xy}^* equal to zero, but for a negative sign. An isomorphism between the plane stress rotation equations and these moment of inertia rotation equations can be set up on the basis of a direct correspondence between stresses and moments of inertia, but with the negative of I_{yz}^* replacing σ_{xy} . The isomorphism confirms that one of the principal m.w. area moments of inertia is a maximum moment of inertia for the cross-section, when the other is a minimum. This maximum and minimum value information can usually be used to make a rough guess for the rotational orientation of the m.w. principal axes as a good check on the precise calculation of their orientation. Hence, in this circumstance, the use of an adaptation of Mohr's circle is not that helpful. It is much simpler to proceed directly to solve Eq. (9.13) for θ , then substitute that value into the first two of Eqs. (9.14), and then use the third of those equations as a further check. Practice with these familiar types of equations is left to the exercises.

The work involved in determining the principal axes plus the change from the use of the coordinate distances y and z to principal coordinate distances Y and Z in the stress equation, Eq. (9.8), usually fully offsets the simplification obtained in the form of the stress equation. The change to principal axes in the stress equation is not generally recommended for hand calculations. The topic of principal axes is introduced here because there are circumstances discussed later where the simplification obtained through the use of principal axes is quite helpful, and it is desired to make clear the distinction between the principal axes and another frequently mentioned term, the neutral axis. Note that the latter term is singular. The *neutral axis* is the line (straight line in Bernoulli–Euler theory) in the plane of the cross-section along which there is no axial stress σ_{xx} . The loci of the neutral axis is the neutral surface. The equation for the neutral axis is directly obtained by simply setting σ_{xx} equal to zero in the stress equation, Eq. (9.8). Whenever there is no temperature change, and there is no net axial force, the neutral axis must pass through the m.w. centroid. In any event, the advantage in locating the neutral axis is that, since the normal stress¹⁶ has a planar variation over the cross-section, points on the cross-section farthest from the neutral axis are the points of maximum normal stress.

Example 9.7. The homogeneous cross-section shown in Fig. 9.12 is subjected to a positive bending moment about the y axis of 300 kip-in. Determine the value of the maximum normal stress on the cross-section, and its point of location. Note that

$$I_{yy} = 240 \text{ in}^4 \quad I_{zz} = 135 \text{ in}^4 \quad I_{yz} = -108 \text{ in}^4$$

Solution. Define

$$R_{zz} \equiv [I_{yy}I_{zz} - (I_{yz})^2]/I_{zz}$$

$$R_{yz} \equiv [I_{yy}I_{zz} - (I_{yz})^2]/I_{yz}$$

¹⁶ Recall that all the mathematical developments in this chapter are limited in scope to the situation where all axial stresses are less than the yield stress(es). If the linearly elastic material model that is adopted in the derivation of the Bernoulli–Euler stress equation for all portions of the nonhomogeneous beam were to lead to normal stresses in excess of the yield stress(es), then that material model would have to be replaced by some other material model, for example, a linearly elastic, perfectly plastic material model. In the case of the linearly elastic, perfectly plastic material model, homogeneous beam cross-sections, and high stresses, a portion of the cross-sectional area would bear uniform normal stress values equal to a yield stress value, and the remainder of the cross-sectional area would bear normal stress values that decreased linearly from the yield stress value(s) to zero values at the neutral axis.

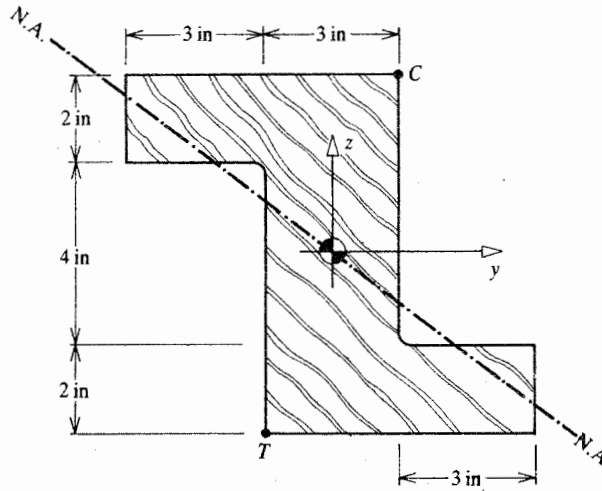


Figure 9.12. Example 9.7. The use of the neutral axis to locate points of maximum tensile and compressive stress.

Then, in this case, Eq. (9.8) becomes

$$\sigma_{xx} = -\frac{zM_y}{R_{zz}} + \frac{yM_y}{R_{yz}}$$

The given area data yields $R_{zz} = +153.6 \text{ in}^4$, $R_{yz} = -192 \text{ in}^4$. Substitution into the stress equation shows that

$$\sigma_{xx} = -1.953z - 1.563y \quad \text{ksi}$$

when the coordinates are in units of inches. Setting the normal stress equal to zero provides the equation for the neutral axis, which is $z = -0.8y$. This line is shown in the sketch. From the sketch it is clear that the maximum tensile stress is at point *T*, while the maximum compressive stress is at point *C*.

$$\text{At point } T: \quad y = -1.5 \text{ in}, z = -4.0 \text{ in and } \sigma_{xx} = +10.2 \text{ ksi}$$

$$\text{At point } C: \quad y = +1.5 \text{ in}, z = +4.0 \text{ in and } \sigma_{xx} = -10.2 \text{ ksi}$$

Substitution of other coordinate values in the above stress equations would yield lesser absolute values of stress. ■

9.9 Summary

This chapter marks an important departure from the previous treatment of the mechanics of engineering materials. Again, the rigorous treatment discussed in Part II is called “the theory of elasticity.” This chapter introduces the first of many simplifications that are the basis for the approximate theories which collectively go by the name of “strength of materials” or “applied elasticity.” The adoption of these approximations is well grounded upon both theoretical and experimental results. However, it is necessary to remember that there are limitations on the applicability of strength of material results. The subject area of strength of materials is introduced by means of one of the simplest of structural elements, the long, straight beam. Three approximations for the geometry of the deformed beam, plus an

assumption of peculiar orthotropic material behavior in order to overcome contradictions, leads to the Bernoulli–Euler equation for the axial stress in the beam when the beam is bent and extended. The other two normal stresses and the shear stress σ_{yz} are taken to have zero values. The other two shear stresses are dealt with in subsequent chapters. The great value of the Bernoulli–Euler theory is that the approximate solution for the axial stress has the form of an algebraic equation. This algebraic formulation, Eq. (9.8), stands in stark contrast to the partial differential equations of the theory of elasticity.

There are other differences between a strength of materials analysis and a theory of elasticity analysis. One stylistic difference, inherent in the approximations made, is the narrowing of the necessary description of the displacement field for the entire structural element. In the case of the bending and extension of a long beam, the displacements and stresses everywhere in the beam depend entirely upon the three displacements and the two bending rotations along the x axis of the beam, where the x axis is defined as the straight line loci of modulus weighted centroids. The displacements of the x axis are called the beam “deflections.” Another stylistic difference is that in a strength of materials analysis, the emphasis through all earlier stages of the analysis is on the various stress resultants rather than the stresses themselves. The definitions of the beam stress resultants require that they act at the m.w. centroids, or in other words, along the x axis.

The use of the Bernoulli–Euler beam stress equation requires the calculation of various geometric quantities and equivalent thermal stress resultants. The examples above and below, and the exercises below provide ample practice for those calculations. The mechanical stress resultants are determined from equilibrium considerations alone when the beam is statically determinate. When the beam is statically indeterminate, the continuity of the beam deflections is an additional consideration as discussed in several following chapters.

Example 9.8. A long beam whose nonhomogeneous cross-section is made up of an aluminum channel section, $E = E_0$, and a titanium cover plate, $E = 2.2E_0$, is shown in Fig. 9.13(a). An idealization of this cross-section is shown in Fig. 9.13(b). There is no appreciable mechanical loading on the beam ($N = M_y = M_z = 0$), but a temperature gradient through the cross-section of the beam can be approximated so that the thermal strain in the cover plate is $2\alpha_0 T_0$, while that throughout the channel is $1\alpha_0 T_0$. Calculate the thermally induced stress at: (i) the top of the cover plate; and (ii) at the bottom of the channel. Let the dimension $a = 11.8t$.

Solution. The task is to calculate axial stresses. The first thing to note is that the cross-section is symmetric with respect to both its geometry and material distribution. Therefore the m.w. centroid lies on the axis of symmetry, and $M_{zT} = I_{yz}^* = 0$. (If it is not clear that thermal moment is zero, its actual calculation would soon reveal that fact.) Therefore, with no mechanical loading, the form of Eq. (9.8) that applies in this situation is

$$\sigma_{xx} = \frac{E}{E_0} \left(\frac{N_T}{A^*} - z \frac{M_{yT}}{I_{yy}^*} - E_0 \alpha \Delta T \right)$$

This formula shows which quantities must be calculated. Calculating the cross-sectional properties first

$$A^* = \sum \frac{E_i}{E_0} A_i = (2.2)(2at) + 3at = 7.4at$$

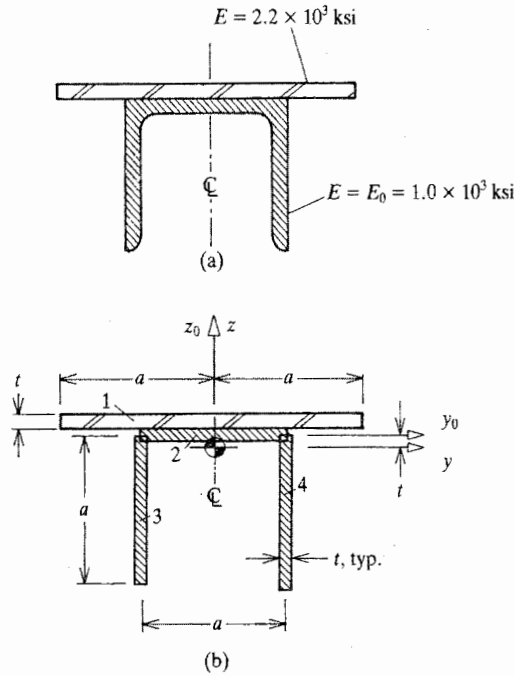


Figure 9.13. Example 9.8. Another example of idealizing a beam cross-section for calculation purposes.

again, $y_0^* = 0$ by symmetry, and with $a = 11.8t$,

$$z_0^* = \frac{1}{A^*} \sum \left[\bar{z}_{0i} \frac{E_i}{E_0} A_i \right] = (1/7.4at)[(2.2)(t)(2at) + 2(1)(-a/2)(at)] = -t$$

Of course, this negative answer for z_0^* places the m.w. centroid a distance t below the y_0 axis. Since the m.w. centroid is conveniently located, the m.w. moment of inertia is best calculated directly:

$$\begin{aligned} I_{yy}^* &= \sum \left(\frac{E}{E_0} \right)_i [\bar{I}_{yy} + (\bar{z}_0)^2 A]_i = (2.2)[(2at^3/12) + (2t)^2(2at)] \\ &\quad + (1)[(at^3/12) + t^2(at)] + 2(1)[(a^3t/12) + (t - 0.5a)^2(at)] \\ &= 212t^4 + 13t^4 + 840t^4 = 90.25at^3 \end{aligned}$$

Incidentally, $I_{zz}^* = 3370t^4 = 285.6at^3$, and again $I_{yz}^* = 0$. Now it is necessary to calculate the equivalent thermal stress resultants.

$$\begin{aligned} N_T(x) &= +E_0 \sum (E/E_0)_i [\alpha \Delta T A]_i = E_0[(2.2)(2\alpha_0 T_0)(2at) + (1)(\alpha_0 T_0)(3at)] \\ &= 11.8E_0\alpha_0 T_0 at \\ M_{yT}(x) &= -E_0 \sum \left(\frac{E}{E_0} \right)_i \bar{z}_i [\alpha \Delta T A]_i \\ &= -E_0[(2.2)(2t)(2\alpha_0 T_0)(2at) + (1)(t)(\alpha_0 T_0)(at) - 2(1)(4.9t)(\alpha_0 T_0)(at)] \\ &= -(18.6E_0\alpha_0 T_0 at^2 - 9.8E_0\alpha_0 T_0 at^2) = -8.8E_0\alpha_0 T_0 at^2 \end{aligned}$$

The fact that the equivalent thermal moment is negative makes sense because the thermal strains would give the beam a negative curvature, that is, cause the beam to bend downward. Now all the necessary quantities for calculating the thermal stress are available. At the top of the cover plate, $z = +2.5t$. Hence the axial stress there is

$$\begin{aligned}\sigma_{xx} &= (2.2) \left[(11.8E_0\alpha_0T_0at)/(7.4at) - (2.5t)(-8.8E_0\alpha_0T_0at^2)/(90.25at^3) \right. \\ &\quad \left. - 2.0E_0\alpha_0T_0 \right] \\ \sigma_{xx} &= -0.36E_0\alpha_0T_0\end{aligned}$$

It makes sense that the cover plate is in compression because, unrestrained by the channel, it would expand more than the channel. However, the channel partially restrains the cover plate from that greater expansion by compressing the cover plate. By the same reasoning, the top of the channel, above the y axis must be in tension, while below the y axis the remainder of the channel must be in compression. At the bottom of the channel, $z = -10.8t$. Therefore the axial stress there is

$$\begin{aligned}\sigma_{xx} &= (1.0) \left[(11.8E_0\alpha_0T_0at)/(7.4at) - (-10.8t)(-8.8E_0\alpha_0T_0at^2)/(90.25at^3) \right. \\ &\quad \left. - 1.0E_0\alpha_0T_0 \right] \\ \sigma_{xx} &= -0.46E_0\alpha_0T_0\end{aligned}$$

Finally, note that if mechanical loadings were also present, then these loadings would merely be combined with the equivalent thermal loadings so as to obtain the combined loadings, those with the superscripted lower-case letters c . ■

Example 9.9

- The homogeneous angle cross section shown in the idealized sketch of Fig. 9.14(a) is subject to the following mechanical loads: $N = 0$, $M_y = 2M_0$, and $M_z = M_0$. There are no temperature changes. Given the cross-sectional properties $R_{yy} = 268.6t^4$, $R_{zz} = 1,075t^4$, and $R_{yz} = 898.6t^4$, locate the point of maximum tensile stress and determine the magnitude of that stress.
- On the sketch of the angle cross-section, draw in your estimate of the location of the principal axes based only on your understanding of the meaning of principal axes as producing the maximum and minimum area moments of inertia rather than on the basis of a calculation.
- For the same angle cross-section, now let there be a temperature change of $+T_0$ over the entire flange, and $+2T_0$ over the entire web. Calculate only the one thermal bending moment M_{yT} . These temperature changes are not sufficient to appreciably affect the magnitude of the modulus of elasticity.

Solution. (a) The stress equation to be solved, Eq. 9.8, in term of the inertia ratios, is

$$\sigma_{xx}(y, z) = \frac{N^c}{A^*} - y \left[\frac{M_z^c}{R_{yy}^*} - \frac{M_y^c}{R_{yz}^*} \right] - z \left[\frac{M_y^c}{R_{zz}^*} - \frac{M_z^c}{R_{yz}^*} \right] - E \alpha \Delta T$$

Substituting the given values, and then setting the normal stress equal to zero, produce the neutral axis straight line equation $z = -2.0y$, which is plotted on the cross-section in Fig. 9.14(b). From that figure, it can be seen that there are two points to consider, but a quick substitution of y and z coordinates shows that point P is the extreme point for tension.

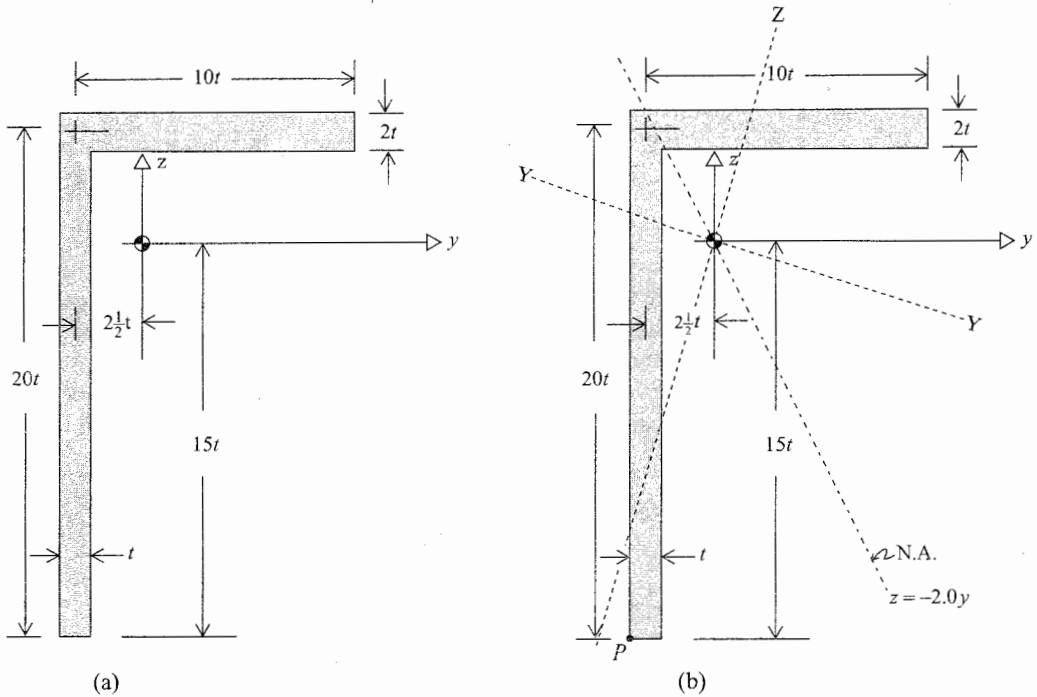


Figure 9.14. (a) Example 9.9. Idealized angle cross-section. Note all dimensions are centerline dimensions. (b) The located neutral axis and the estimated location of the principal axes.

Hence

$$\sigma_{xx}(-3t, -15t) = (3.0t) \left[\frac{M_0}{268.6t^4} - \frac{2M_0}{898.6t^4} \right] + (15t) \left[\frac{2M_0}{1054t^4} - \frac{M_0}{898.6t} \right] = 0.0157 \frac{M_0}{t^3}$$

(b) One way to estimate or check the location of the principal axes of a beam cross-section is to use the identity of form between mass and area moments of inertia, which is

$$\left. \begin{array}{l} \text{two-dimensional} \\ \text{mass moment of inertia} \end{array} \right\} = \iint y^2 d(\text{mass})$$

$$\text{while area moment of inertia} = \iint y^2 d(\text{area})$$

To this end, think of the cross-section as a piece of stiff sheet metal (something with mass), and then ask yourself where would you glue a stick (one of the principal axes) to the sheet metal cross-section so that you could spin the cross-section around the stick with the greatest angular velocity. (The greatest angular velocity would be associated with the least mass moment of inertia.) In this case the stick would be glued approximately where the Z - Z axis is drawn in Fig. 9.14(b). Of course, the other principal axis, Y - Y , is perpendicular to this minimum area moment of inertia axis, and would be the axis about which the area moment of inertia is greatest. As an aside, all engineers should develop as many checks on their work as possible because often the difference between an experienced engineer and the novice is that the experienced engineer seeks many checks on his or her work.

(c) The calculation for the equivalent thermal moment about the y axis is

$$M_{yT} = -\iint z E \alpha \Delta T dA = -[(-5t)E\alpha(2T_0)(20t^2) + (5t)E\alpha(T_0)(20t^2)] = 100E\alpha T_0 t^3$$

The Bernoulli–Euler beam stress equation is written in terms of m.w. centroidal Cartesian coordinates that have any convenient rotational orientation to the beam cross-section. However, there is one special rotational orientation of the cross-sectional coordinate axes, called the principal axes, that simplifies that stress equation. Unless the principal axes are evident upon inspection of the cross-sectional geometry, as they would be when there was an axis of symmetry, it is not worthwhile determining their rotational orientation for the sake of the stress calculation. However, for later deflection calculations, the use of principal axes can be an essential simplification. Remember that principal axes are only a matter of the cross-sectional geometry. On the other hand, the neutral axis depends on both the cross-sectional geometry and the loading. Therefore, in general, the two types of axes do not coincide.

Chapter 9 Exercises

- 9.1. (a) Determine the values of y_0^* and z_0^* for the selected coordinate axes and the nonhomogeneous cross-section shown in Fig. 9.15(a), where $E_1 = 3.0 \times 10^7$ psi, and $E_0 = E_2 = E_3 = 1.0 \times 10^7$ psi.
- (b) Determine the values of y_0^* and z_0^* for the selected coordinate axes and the nonhomogeneous cross-section shown in Fig. 9.15(b). Note the variation in Young's modulus due to temperature changes.
- (c) Calculate the values of y_0^* and z_0^* for the cross-section of Fig. 9.15(c).

- 9.2. (a) A long steel plate and an aluminum Z-section are bonded together to form a nonhomogeneous beam cross-section as shown in the idealized sketch of Fig. 9.16(a). For the selected coordinate axes shown, calculate the location of the m.w. centroid and the value of the m.w. product of inertia if the ratio of the Young's moduli for steel to that for aluminum is 3 to 1. Use the aluminum modulus of elasticity as the reference modulus.
- (b) Locate the centroid of the idealized angle iron shown in Fig. 9.16(b). Note that, due to a temperature change, T_0 , the Young's modulus for the (lower) flange is only $0.9 E_0$.

For this same cross-section, determine the values of I_{yy}^* and I_{yz}^* .

- (c) Consider the idealized, nonhomogeneous, straight beam cross-section shown in Fig. 9.16(c). Given that $A^* = 20.8 t^2$, and $z_0^* = 8.85 t$, complete the process of locating the modulus weighted centroid.

Calculate I_{yy}^* and I_{zy}^* (for future reference, $I_{zz} = 274 t^4$)

- 9.3. (a) A long flat plate ($E = E_0$) is bolted to an angle section ($E = 2E_0$) to form the beam cross-section shown in Fig. 9.17(a). Use the selected coordinate axes shown, and m.w. centroidal coordinates that are positive in the same directions as the selected coordinates, to determine I_{yy}^* and I_{yz}^* .
- (b) The top flange of the idealized channel section shown in Fig. 9.17(b) is heated to a temperature that reduces its Young's modulus by 20 percent. Determine only I_{zz}^* and I_{yz}^* . Use the room temperature Young's modulus, E , as the value of E_0 .

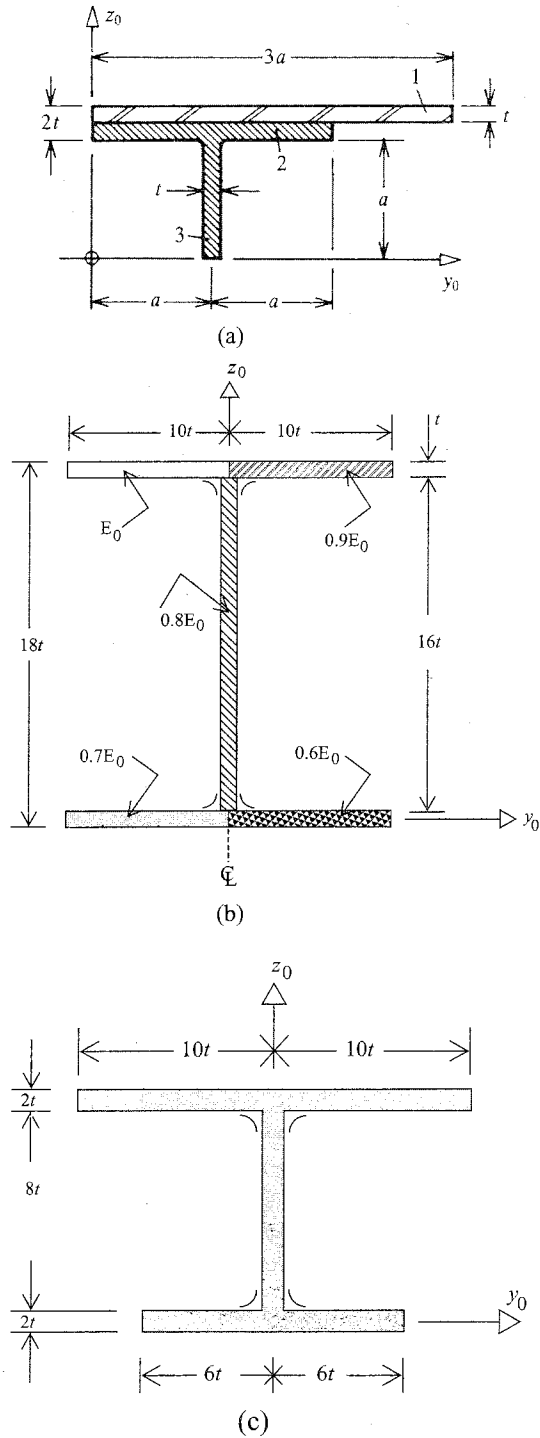


Figure 9.15. (a) Exercise 9.1(a). A nonhomogeneous cross-section. (b) Exercise 9.1(b). A nonhomogeneous wide flange ("H") beam. (c) Exercise 9.1(c). A homogeneous beam cross-section.

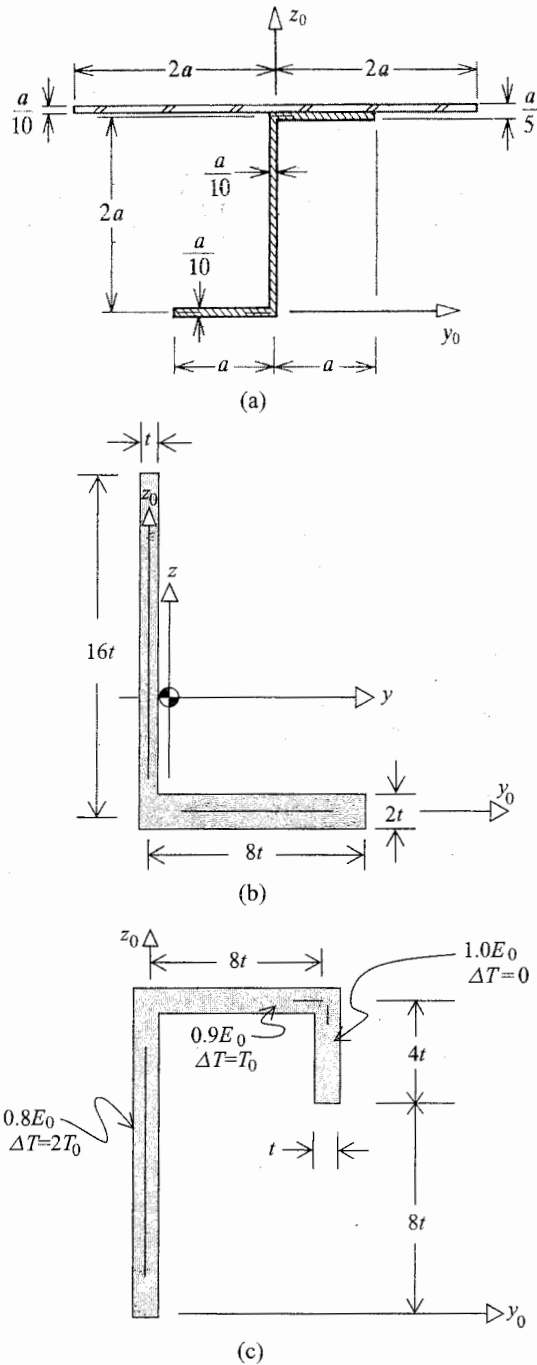


Figure 9.16. (a) Exercise 9.2(a). A nonhomogeneous cross-section. The z_0 axis runs along the centerline of the beam web. (b) Exercise 9.2(b). Nonhomogeneous angle beam cross-section. (c) Exercise 9.2(c). Nonhomogeneous channel beam cross-section.

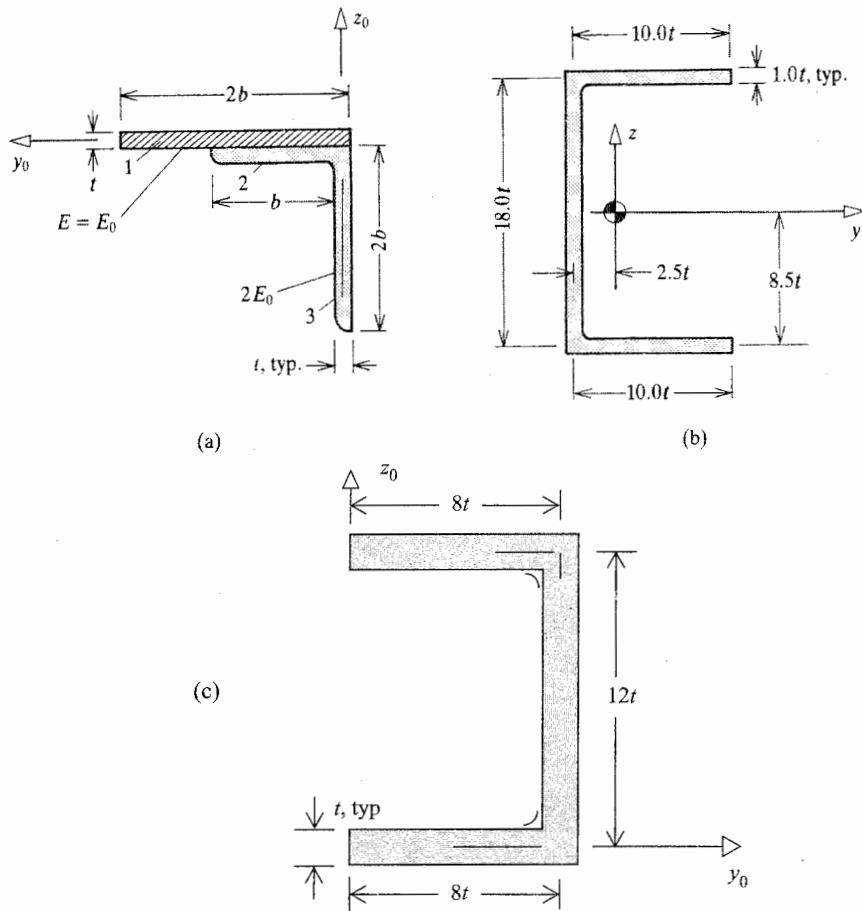


Figure 9.17. (a) Exercise 9.3(a). A nonhomogeneous cross-section. (b) Exercises 9.3(b) and 9.9(b). Note that, because of the temperature-induced change in Young's modulus, the channel beam cross-section no longer has an axis of symmetry. (c) Exercise 9.3(c). Within the top flange, $E = 0.8E_0$, and $\Delta T = 2T_0$. Within the web, $E = 0.9E_0$, and $\Delta T = T_0$. Within the bottom flange, $E = E_0$, and $\Delta T = 0$.

(c) Consider the idealized beam cross-section shown in Fig. 9.17(c). The simplified piece-wise constant temperature distribution shown leads to the indicated piece-wise constant variation in Young's modulus. Using this information

- (i) Locate the modulus weighted centroid.
- (ii) Calculate the area moment of inertia about the z axis.
- (iii) Determine the area product of inertia.

- 9.4.** (a) For the homogeneous angle section shown in Fig. 9.18(a), determine all moments of inertia including the product of inertia with respect to horizontal and vertical centroidal axes.
- (b) Repeat part (a) for the cross-section shown in Fig. 9.18(b).
- (c) Repeat part (a) for the cross-section shown in Fig. 9.18(c).

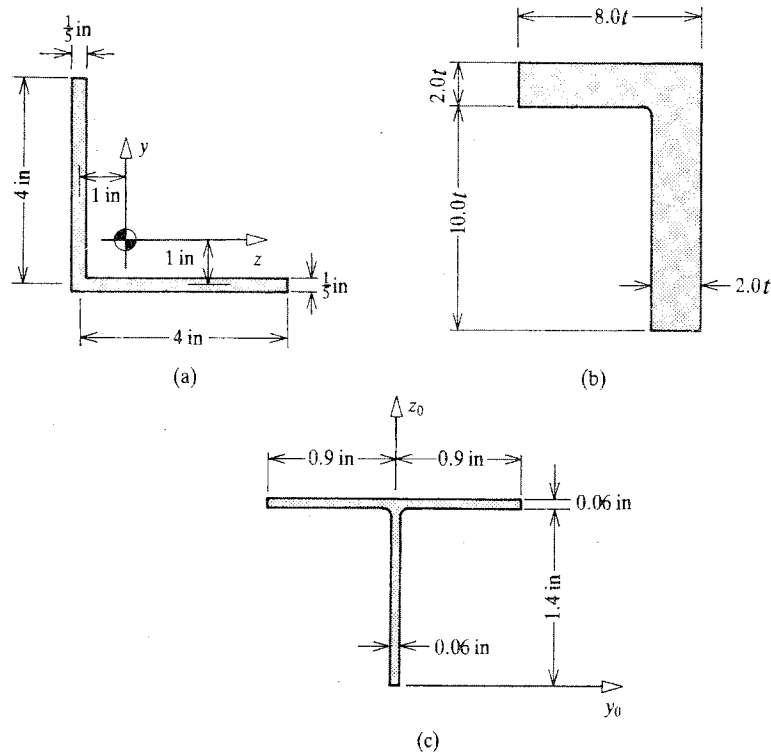


Figure 9.18. (a) Exercise 9.4(a). (b) Exercise 9.4(b). (c) Exercise 9.4(c).

- (d) Locate the principal axes and determine the values of the principal moments of inertia for the cross-section of part (a). Be sure to check that the sum of the principal moments of inertia equals the sum of the unrotated area moments of inertia.
- (e) As in part (d) for the cross-section of part (b).
- (f) As in part (d) for the cross-section of part (c).
- 9.5. For the nonhomogeneous cross-section shown in Fig. 9.19, determine the principal area moments of inertia.
- 9.6. (a) Determine the values for the area moments and product of inertia for the homogeneous, solid triangular cross-section shown in Fig. 9.20.
- (b) If $a = 3.00$ cm, $b = 6.00$ cm, what then are the principal moments of inertia.
- 9.7. Calculate I_{yz}^* and I_{zz}^* for the idealized built-up box beam shown in Fig. 9.21. It should be clear that all thicknesses have the dimension t .
- 9.8. (a) For the idealized nonhomogeneous beam cross-section shown in Fig. 9.22 (a), determine the values of I_{yy}^* and I_{yz}^* if the z_0 axis is along the web centerline, the idealized rectangles are numbered from top to bottom, and

$$E_1 = 2.1 \times 10^5 \text{ N/mm}^2 \quad E_0 = E_2 = E_3 = 0.7 \times 10^5 \text{ N/mm}^2$$

$$A^* = 160 \text{ mm}^2 \quad y_0^* = 12.8 \text{ mm} \quad z_0^* = 22.95 \text{ mm}.$$

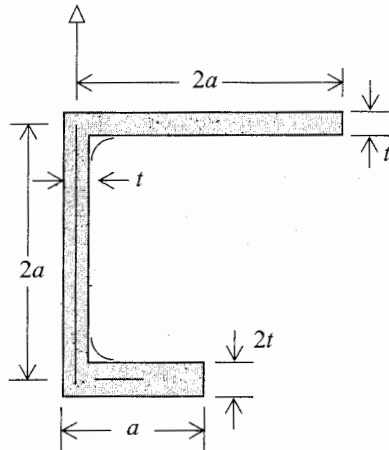


Figure 9.19. Exercise 9.5. Nonhomogeneous channel beam cross-section. Within the upper flange $E = E_0$, $\Delta T = 0$. Within the web, $E = 0.9E_0$, and $\Delta T = +T_0$. Within the lower flange, $E = 0.8E_0$, and $\Delta T = 2T_0$.

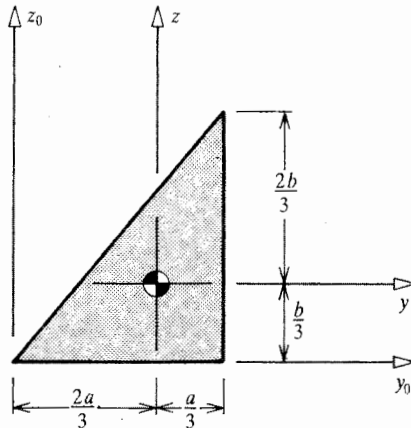


Figure 9.20. Exercise 9.6.

- (b) Calculate the area moments and product of inertia for the cross-section sketched in Fig. 9.22(b).
- 9.9. (a) Calculate the equivalent thermal moment M_{yT} for the cross-section of part (a) of the previous problem if the temperature changes associated with each of the respective idealized rectangles are such that

$$(\alpha \Delta T)_1 = -1.0 \times 10^{-3} \quad (\alpha \Delta T)_2 = 0 \quad (\alpha \Delta T)_3 = +1.0 \times 10^{-3}$$

- (b) If in the top flange of the idealized channel of Fig. 9.17(b) the thermal strain (the product of the coefficient of thermal expansion and the temperature change) is $\alpha_0 T_0$, what then is the magnitude of the equivalent thermal moment about the y axis?
- (c) Calculate M_{yT} for the cross-section of Fig. 9.17(c).

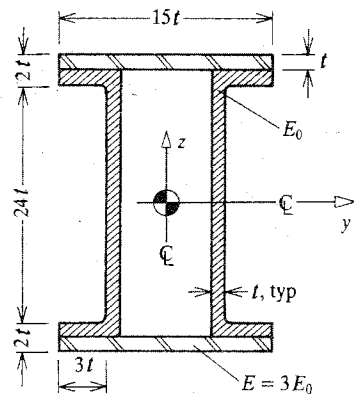


Figure 9.21. Exercise 9.7.

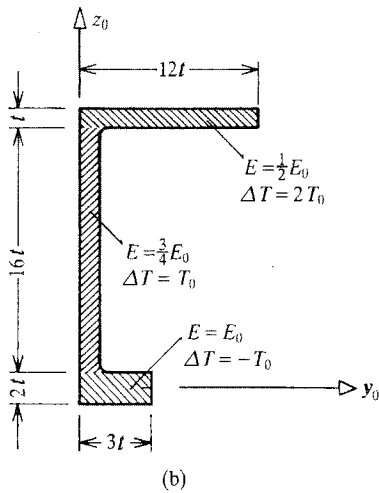
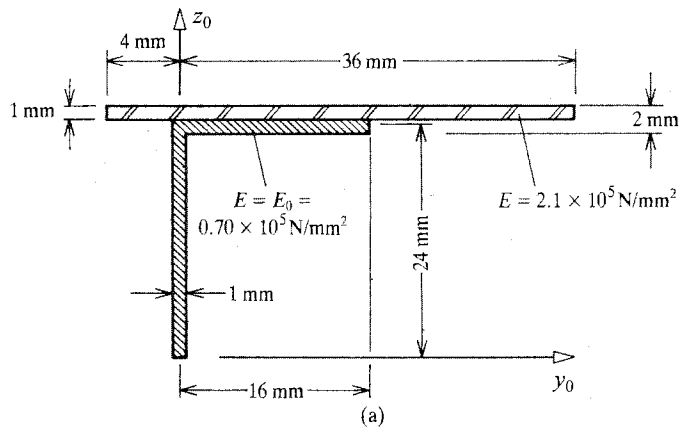


Figure 9.22. (a) Exercises 9.8(a) and 9.9(a). (b) Exercises 9.8(b) and 9.12(b).

- (d) Calculate N_T , M_{yT} , and M_{zT} for the cross-section of Fig. 9.19.
- (e) Calculate N_T and M_{zT} for the cross-section of Fig. 9.16(b).
- (f) Calculate N_T and M_{zT} for the cross-section of Fig. 9.16(c).
- 9.10. Develop a generally applicable parallel axis theorem for the equivalent thermal moment M_{yT} ; that is, develop the theorem that relates the two different values of this equivalent thermal moment at the y_0 and y axes.
- 9.11. Assuming that the Young's modulus and coefficient of thermal expansion are uniform over the cross-section, and the upper flange, web, and lower flange experience the temperature changes indicated in Fig. 9.23, what then is the value of M_{yT} ?
- 9.12. (a) The T cross-section shown in Fig. 9.24 experiences temperature changes that are multiples of T_0 as shown in the sketch. Determine the values of N_T , M_{yT} , and M_{zT} .
- (b) As above, but for the cross-section of Fig. 9.22(b).
- 9.13. Using the strength of materials approach, calculate the stresses in the simply supported, rectangular cross-section beam loaded as shown in Fig. 8.5. Compare this strength of materials solution to the theory of elasticity solution for the normal stresses as given in Exercise 8.2. In either case, are the σ_{yy} stresses of comparable magnitude to the σ_{xx} stresses?
- 9.14. (a) For the cross-section of Fig. 9.18(a), determine the magnitude of the stress at the point $y = -1.0$ in, $z = +3.0$ in for the loads given below.
- (b) For the cross-section of Exercise 9.4(b), determine the magnitude of the stress at the point $y = +7.2$ in, $z = 3.95$ in for the loads given below.
- (c) As above, but for the bottom of the web of the T section of Fig. 9.18(c).
- $$N = 1.0 \text{ kip} \quad M_y = 10.0 \text{ kip-in} \quad M_z = -6.0 \text{ kip-in.}$$
- (d) According to the "Manual of Steel Construction," a **W 14 × 109** homogeneous, doubly symmetric cross-section, shown in Fig. 9.25, has an area equal to 32 square inches, while $I_{yy} = 1240 \text{ in}^4$, and $I_{xz} = 447 \text{ in}^4$. If the only applied loads are a moment about the y axis of magnitude $2 M_0$, and a moment about the z axis of magnitude M_0 , determine the location and magnitude of the maximum **tensile** stress.
- 9.15. If $a = 8t$, and $I_{yy} = 750t^4$, and if the beam is free to expand or contract without constraint, then determine the stress in the beam of Exercise 9.12(a) at the top of the flange and at the bottom of the web if the temperature change is the only type of loading.

FOR THE EAGER

- 9.16. (a) Determine the location and magnitude of the maximum tensile and compressive stresses in Exercise 9.14(a).
- (b) As above, but for Exercise 9.14(b).
- (c) As above, but for Exercise 9.14(c).
- 9.17. Show that the stress at any point on an arbitrary, homogeneous, symmetric cross-section that results from a planar temperature change over the area of the cross-section is zero when the beam is free to expand or contract without restraint.

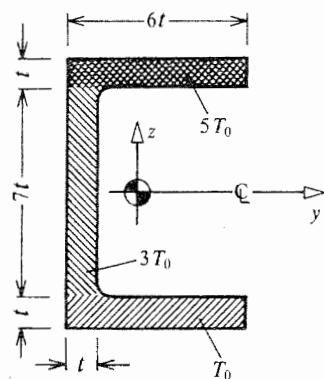


Figure 9.23. Exercise 9.11.

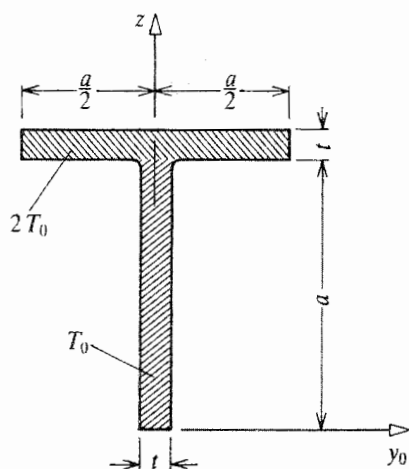


Figure 9.24. Exercise 9.12(a).

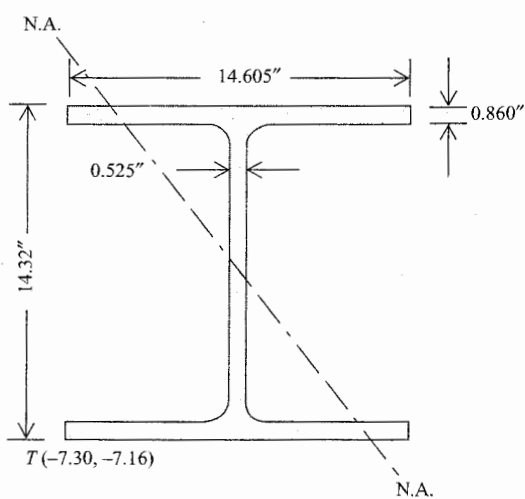


Figure 9.25. Exercise 9.14(d)

To that end, let the planar temperature change be represented by the following equation, where the T_i are arbitrary constants:

$$\Delta T(y, z) = T_1 + yT_2 + zT_3$$

- 9.18. Rederive Eqs. (9.1) by means of a free body diagram of a slice of beam of differential length dx where the back end is located at the coordinate value x . Does your solution change in any way if the beam cross-section varies smoothly along the length of the beam?

FOR THE ESPECIALLY EAGER

- 9.19. In the expression for the approximate displacement $u(x, y, z)$ stated in Eqs. (9.2), the effect of the translation $u(x)$ and the effects of the two rotations $\phi_y(x)$ and $\phi_z(x)$ were superimposed without any interaction between them. Another way of saying the same thing in this case is to say that the first of Eqs. (9.2) represents a vector addition of the three separate displacement components. Note again that the translational displacements are clearly vector quantities, and can be added as such. However, observation shows that if, for example, one rotates a die successively 90° in two different directions, the order of the two rotations affects the final orientation of the die. Thus the conclusion that large rotations (around 90°) do not add vectorially because the order of addition affects the value of the sum. In other words, these two large rotations interact. The question is then: Is this first of Eqs. (9.2) valid and, if so, in what sense? More specifically, is this equation a good approximation for small angles, and if so, how small is "small"?

Hint: An equation from spherical geometry, easily proved using three unit vectors, states that if the angles α , β , and ϕ that lie between the two intersecting planes, $PQRS$ and $PABC$, are as shown in Fig. 9.26, then

$$\tan \phi = \tan \alpha \cos \theta + \tan \beta \sin \theta$$

where the angle APC is a right angle, the angle θ is the angle APB , the angle α is the angle APQ , the angle ϕ is the angle BPR , and the angle β is the angle CPS . Prove this formula, and then consider the case where the angles ϕ , α , and β (but not θ) are sufficiently small that the tangents of these angles are equal to the angles themselves. Interpret the resulting formula as the decomposition of the vector ϕ into its vector components. Then draw a conclusion regarding the vector summation of "small" angles.

Endnote (1) The Predominance of the Normal Axial Stress

When considering a beam, the stress in which the analyst is usually most interested is the maximum normal stress. Consider a uniform, simply supported beam of length L loaded in the z plane by a uniform upward load per unit length, f_0 ; see Fig. 9.27(a), which shows the left half of this beam. Let the load per unit length arise from a pressure p acting upward over the bottom surface, which has a thickness into the paper of magnitude t ; that is, $f_0 = pt$. For simplicity of discussion, let the beam cross-section be rectangular with a total depth of magnitude B . A simple equilibrium calculation using this left-hand half of this beam as a free body diagram shows that the maximum internal moment acting upon this beam occurs at midspan. That internal moment has a magnitude of $(\frac{1}{8})f_0L^2$. The approximate

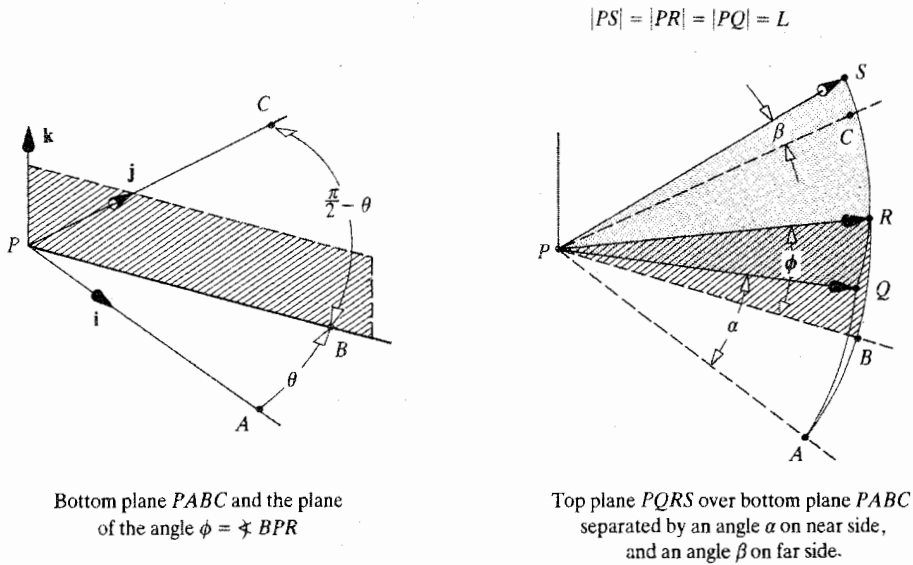


Figure 9.26. Exercise 9.19. A diagram for the discussion of the vector addition of small angles.

stress calculation shows that the normal axial stress is zero at the beam middepth, and varies linearly across the depth of the beam, as shown in Fig. 9.27(b). The resisting internal bending moment, in terms of the maximum axial stress σ_m , is $(\frac{2}{3}B)(\frac{1}{2}\sigma_m \frac{B}{2})t = (\frac{1}{6})B^2t\sigma_m$. Equating the magnitudes of the two equilibrating moments shows that, with $p = f_0/t$

$$\sigma_m = \frac{3}{4}p \frac{L^2}{B^2}$$

This maximum axial stress is a maximum value of σ_{xx} . The maximum value of σ_{yy} can be surmised to be of the order of magnitude p . With $10 = (L/B)$, it is clear that the maximum value of σ_{xx} is two orders of magnitude greater than that of the maximum value of σ_{yy} . Hence the indication that the normal stresses σ_{yy} and σ_{zz} can be ignored in preference to σ_{xx} . If a cantilevered beam were considered for this same analysis, the disparity between the sets of normal stresses would be twice as large.

The above approximate analysis for the simply supported beam is fully validated by the theory of elasticity solution found in Example 8.2. The results of that example problem show that the upward-acting pressure p acting on the bottom beam surface results in a normal stress $\sigma_{yy} = -p$ at the bottom surface (the maximum value), which tapers off to $\sigma_{yy} = 0$ at the top surface. The maximum values for σ_{xx} are at the top and bottom beam surfaces at the beam midspan. The magnitude of the maximum compressive stress is the same as the magnitude of the maximum tensile stress, which is

$$\sigma_{xx}|_{max} = \frac{3}{4}p \left[\left(\frac{L}{B} \right)^2 + \frac{4}{15} \right]$$

and the same conclusions apply.

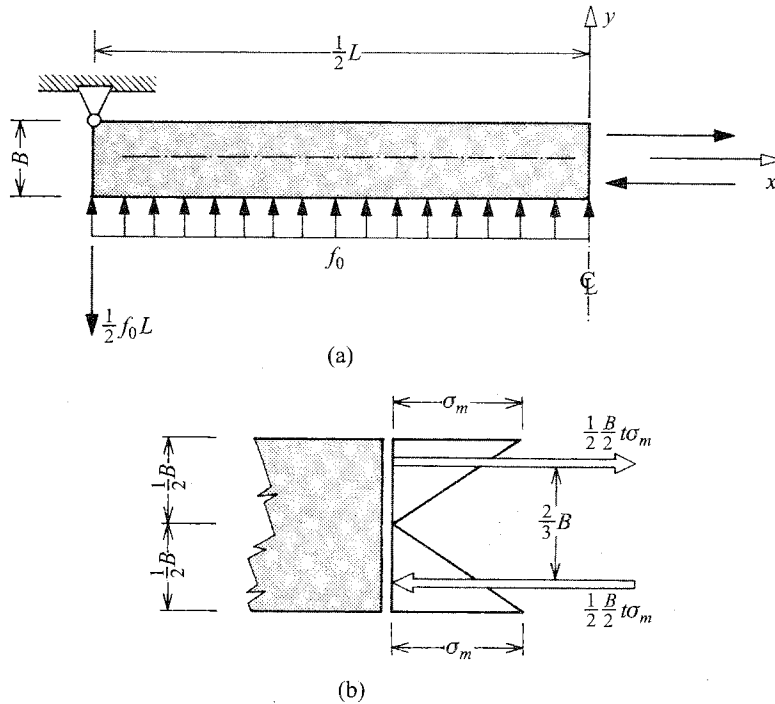


Figure 9.27. A diagram for the discussion of relative stress magnitudes.

Endnote (2) Schwartz's Inequality

The purpose of this endnote is to prove that the denominator $I_{yy}^* I_{zz}^* - (I_{yz}^*)^2$ of the beam normal stress equation, Eq. (9.8), is not only never zero, but to prove that this difference between these two positive quantities is always positive. To this end, consider the following integral over the entire area of an arbitrarily chosen, nonhomogeneous, beam cross-section

$$\iint (y + \beta z)^2 dA^* > 0$$

The integral is always greater than zero for any finite-sized cross-section because the integrand is always positive. Expand the integrand, and apply the definitions of the various m.w. area moments to get

$$\iint (y^2 + 2\beta yz + \beta^2 z^2) dA^* \geq I_{zz}^* + 2\beta I_{yz}^* + \beta^2 I_{yy}^* > 0$$

Picture the a plot of the quadratic polynomial function in beta: $\beta^2 I_{yy}^* + 2\beta I_{yz}^* + I_{zz}^*$. As the above inequality makes clear, this parabola would always lie above the beta axis. Therefore, this quadratic polynomial must have two imaginary roots. Since the two roots are imaginary, the discriminant of the quadratic must be negative. Therefore

$$4(I_{yz}^*)^2 - 4I_{yy}^* I_{zz}^* < 0 \quad \text{or} \quad I_{yy}^* I_{zz}^* > (I_{yz}^*)^2$$

Q.E.D. The above is a special case of Schwartz's inequality. The reader is invited to use a similar procedure to the above to prove the companion inequality $I_{yy}^* + I_{zz}^* \geq 2|I_{yz}^*|$.

Beam Bending and Extensional Deflections

10.1 Introduction

The use of Eq. (9.8), the strength of materials solution for the bending and extensional axial stress $\sigma_{xx}(x, y, z)$ in a long, straight beam, requires a knowledge of the internal axial force $N(x)$ and the internal bending moments $M_y(x)$ and $M_z(x)$. The difficulty is that a free body diagram (FBD) of a beam under study is often insufficient by itself to determine the axial force or bending moments at any point along the beam x -axis. As previously mentioned, whenever the equilibrium equations alone are insufficient to determine the internal stress resultants, the structure is called indeterminate. Most beams, or beam elements, that are parts of aerospace structures are indeterminate because these beams are mostly elements of beam grids and frames with, as much as possible, rigid connections. The grids and frames are often covered by thin sheeting, referred to as the vehicle skin. Thus there are many internal unknown reactions. One purpose of this type of construction is to make the structure, and hence individual beams, as stiff as possible within the constraint of least weight. Increased stiffness¹ has many advantages in a beam or a structure. For example, the stiffer the beam or structure, the higher the load required to buckle the beam or structure, and the lesser the chance of aeroelastic instabilities such as those discussed in Chapter 9. The stiffer the beam or structure, the higher its natural frequencies and the lesser the chance that gusts or control motions will stress the structure. The stiffer the structure, the lesser the chance that moving parts, such as those that are part of the control system, will experience interference from other parts of the structure.

In the same manner as is true in the theory of elasticity when equilibrium equations are inadequate for the purposes of determining the stresses, it is necessary to combine the Bernoulli–Euler displacement and material equations with the equilibrium equations in order to obtain sufficient equations so as to allow a solution for the stress resultants. This chapter makes that combination in a way that produces three equations for the three beam deflections. (Recall that “deflections” are the displacements and rotations at the x axis of the beam.) The advantage of having the final equations in terms of the deflections is that the solution process is the same whether or not the beam is statically indeterminate.

The next two sections concentrate on developing equilibrium equations in suitable stress resultant forms. Section 10.3 combines those equilibrium equations with the continuous deflections on the basis of the relations between the derivatives of the deflections and the axial force and bending moments that have been developed in the last chapter. The resulting three beam deflection differential equations are worthy of study not only for their own value, but also because there are close parallels between these beam equations and the similarly useful deflection equations for plates and shells. The beam equations also provide an opportunity for extensive practice in writing and using both rigid and elastic boundary conditions.

¹ Recall that “strength” refers to the magnitude of the loading a structure can bear without failing in some way, while “stiffness” refers to the loading required to deform the structure a given amount.

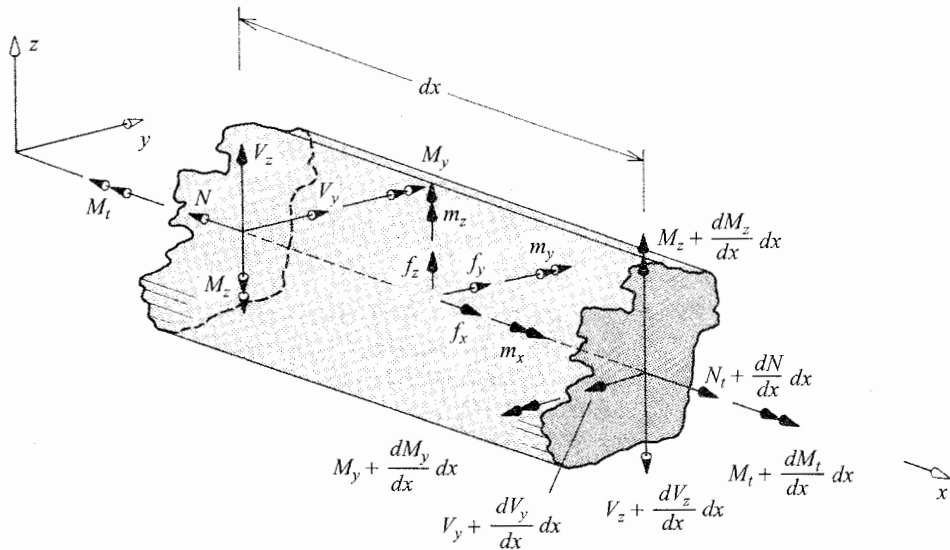


Figure 10.1. A free body diagram, using the undeformed geometry, for obtaining linear equilibrium equations. This diagram also introduces a sign convention for externally applied forces per unit of beam length and externally applied moments per unit of beam length, which must be committed to memory. Be sure to distinguish between M , a bending or twisting moment, and m , a bending or twisting moment per unit length.

10.2 The Small Deflection Beam Equilibrium Equations

Chapter 9 developed the stress resultant–stress equations, Eqs. (9.1), on the basis that the normal and shear stresses on a cross-section sum to forces and moments on that same cross-section. However, it was also pointed out that the same stress resultant–stress equations could be developed by writing equilibrium relations from a FBD consisting of a differential length of beam loaded by stresses on one cross-section and stress resultants on the opposite cross-section. Therefore, the requirements of equilibrium have been addressed, but only in part. Taking stock of the already developed equilibrium relations shows that the general stress-to-stress equilibrium relations are completed in Chapter 1, and the axial stress (σ_{xx}) to beam stress resultant (N , M_y , M_z), equations, and the reverse relation, are completed in Chapter 9. What remain to be investigated are the beam stress resultant to beam stress resultant equilibrium relations. These equilibrium relations have different levels of complexity, where the degree of complexity depends upon the range of equation applicability. There are the linear relations, which are the most limited in their range of applicability, and there are also the more broadly useful nonlinear relations at various levels of complexity. The linear relations are quickly derived in this section in order to (i) help clarify the derivation of the nonlinear equations that follow, since that latter derivation can be obscured by geometric details and various approximations, and (ii) emphasize the differences between the linear and nonlinear equations.

Consider the differential length of beam as shown in Fig. 10.1. Note the exaggeration of the differential length relative to the finite dimensions of the beam cross-sections for the sake of clarity in showing the *applied loads per unit length* at the center of the beam slice. Let f_x , f_y , and f_z , all functions of x only, symbolize the applied forces per unit length of the beam in the positive x , y , and z coordinate directions, respectively. Let $m_x(x)$, $m_y(x)$,

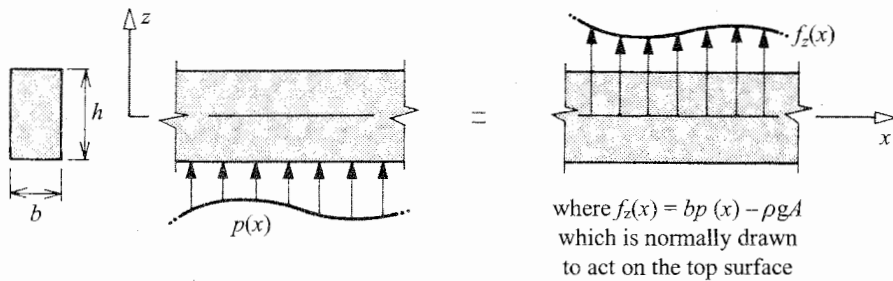


Figure 10.2. The usual representation for beam theory purposes of beam surface tractions and beam body forces as forces per unit of beam length.

and $m_z(x)$ represent the applied moments per unit length of the beam that are positive by the right-hand rule about the positive x , y and z coordinate axis directions, respectively. The mathematical functions that model the applied forces per unit length are required to be bounded, piecewise continuous functions, and the moments per unit length also must be piecewise differentiable functions. All the applied loads per unit length act along the x axis regardless of their origins. To be clear about the origins of these quantities, consider, for example, a homogeneous beam with a rectangular cross-section. Let there be an applied (normal) pressure on the bottom surface of the beam as shown in Fig. 10.2. Let the mass density of the beam be symbolized by ρ . Then the weight per unit length of the beam is $\rho g A$, where g is the acceleration of gravity. Then f_z , the force per unit length in the z direction at and along the x axis is $(pb - \rho g A)$. Clearly this load modeling is crude compared to the theory of elasticity, where the pressure would be treated as an external traction ($T_z = +p$) on the bottom surface ($z = -h/2$), and the weight of the beam would be treated as a body force per unit mass ($B_z = -g$). The reason for this relative crudeness is that it has very little effect upon the accuracy of the solution for either the beam deflections or the most important stress, which is σ_{xx} . Such a condensing of the loading is wholly in keeping with the other simplifications of beam theory.

Moments per unit length, while not overly common, are possible. For example, if, in the x, z plane, the top surface of a beam were subjected to a shearing traction in the positive x direction, while the lower surface were subjected to a shearing traction of equal magnitude in the negative x direction, then along the x axis there would be a moment per unit length about the y axis. A more common situation would be one where the beam stiffens a plate or shell that is twisted. The mechanics of the plate or shell are such that they would transmit a moment per unit length to the beam.

Return to Fig. 10.1. The use of a differential, rather than a finite length in this FBD for force and moment summations removes any ambiguity regarding what value of the applied load per unit length is to be used in load summations. For example, since the quantity f_x cannot have more than a differential change over the differential length dx , its value at the left-hand cross-section, $f_x(x)$, is an accurate representation of this force per unit length over the entire differential length dx . Now, a summation of forces in the x and z directions, respectively, yields

$$-N + (N + dN) + f_x dx = 0 \quad \text{or} \quad \frac{dN}{dx} = -f_x \tag{10.1a}$$

$$+V_z - (V_z + dV_z) + f_z dx = 0 \quad \text{or} \quad \frac{dV_z}{dx} = +f_z \tag{10.1b}$$

where the forces per unit length must be multiplied by the differential lengths in order to be properly part of a force summation. A summation of moments about the y axis at the right-hand end of the differential element yields

$$+M_y + V_z dx + f_z dx \left(\frac{dx}{2} \right) + m_y dx - (M_y + dM_y) = 0$$

or

$$\frac{dM_y}{dx} = V_z + m_y \quad (10.1c)$$

where, after division by dx , the term involving f_z is dropped because it contains a differential factor that makes that term infinitesimal compared to the other terms of the equality. Note that division by the quantity dx is wholly permissible because, although that quantity is infinitesimal, it is never zero. A similar shear and moment equation can easily be derived for the x, y plane. They and the similar twisting moment equation are

$$\frac{dV_y}{dx} = f_y \quad (10.1d)$$

$$\frac{dM_z}{dx} = V_y - m_z \quad (10.1e)$$

$$\frac{dM_t}{dx} = -m_t \quad (10.1f)$$

The above six results, which relate the various stress resultants to each other and to the loads per unit length, and which are clearly linear ordinary differential equations, can be encapsulated for present purposes as: (1) the change in a bending moment is a shear force (plus a moment per unit length if present); and (2) the change in the shear or axial force is a corresponding force per unit length. As will be seen in the next section, the reason that these results are linear ordinary differential equations is that the geometry of the differential beam element shown in Fig. 10.1 is only negligibly distorted by the applied loads. In other words, in this case there is no appreciable interaction between the loads and the geometry of the beam differential length. Specifically, the deformation of the beam element is so small that the lines of action of the stress resultants are essentially unaltered. This is exactly the same situation that prevailed throughout the discussion of the theory of elasticity once the nonlinear portions of the strain expressions were set aside. These linear equilibrium equations,² Eqs. (10.1), are fully adequate for a great many beam analyses. However, there are important categories of beam problems for which these equations are inadequate. One such category of problems is beam buckling problems, which are discussed in an introductory fashion in the next chapter. Since many vehicular structures consist in part of long beams, thin plates, and thin shells that are prone to buckle if not adequately stiffened, it is desirable to prepare for this important problem category by considering, in as simple a fashion as possible, the interaction between the loads and the geometry of the beam by analyzing a distorted beam element.

10.3 Nonlinear Beam Equilibrium Equations

The derivation of the stress resultant equilibrium equations in their simplest three-dimensional form for a beam segment with finite deflections is facilitated by first noting the

² These linear beam equilibrium equations are also called the "infinitesimal deflection beam equilibrium equations," and the "small deflection beam equilibrium equations."

following circumstances and conclusions regarding the relative size of both stress resultants and deflections:

1. Beams are very much stiffer in their axial direction than in their lateral direction. That is, for example, a flexible 6-inch (15-cm) plastic ruler is easily bent far from its original straight condition, but no person pulling on the usual such ruler can produce a perceptible change in length. A person attempting to compress the ruler may buckle and break the ruler, but the length of the ruler will not be perceptibly shortened when the pieces of the ruler are reassembled. Therefore, it is reasonable as a first step in dealing with the distorted geometry of a beam segment to consider significant (but limited) bending slopes and angles of twist, but make the approximation that there is no change in beam differential length sufficient to affect the orientation of the internal forces and moments.³
2. At the limits of the permitted bending deflections, from the above it should be clear that beam tensile axial forces can be very much larger than beam shearing forces. In long beams with cross-sectional shapes that are actually used in vehicular construction, the compressive axial forces limited by buckling are also generally much larger than the shearing forces that produce bending moments that in turn produce the limiting bending slopes. Again, for example, it is easy to manually flex a new pencil, but more difficult indeed to manually compress a new pencil⁴ to the point where it buckles. Hence the products of shearing forces multiplied by the small values of the limited bending slopes in units of radians (or their derivatives, which are taken to be of the same order of magnitude) are negligible in comparison with axial forces. Furthermore, any type of stress resultant multiplied by a limited bending slope or angle of twist in units of radians, or their derivatives, is a significantly smaller quantity than that same type of stress resultant not multiplied by a limited bending slope or angle of twist derivative.

Consider Fig. 10.3(a) where a beam segment of differential length dx is shown in its undistorted (unloaded) and distorted (loaded) configurations. In the distorted configuration, two new sets of unit vectors with tildes and carets define the individual rotations of the front and back cross-sections after the beam segment is translated and rotated from its undistorted position to its distorted position. Both sets of unit vectors are centered at the x axis. Therefore, all the stress resultant force and moment vectors shown in Figs. 10.3(b), which are drawn separately for clarity, coincide with one of the unit vectors with regard to origin and direction. The back cross-section and the corresponding unit vectors have rotated through the angle of twist ϕ_x ,⁵ and the two bending slopes ϕ_y and ϕ_z as shown in Fig. 10.3(c). The front cross-section, at a distance $x + dx$ along the x axis, has a twist and rotations that are differential increments to those on the back face; that is, the corresponding values are $\phi_x + d\phi_x$, $\phi_y + d\phi_y$ and $\phi_z + d\phi_z$. In order to examine the angles between the two sets of unit vectors of the distorted geometry, think of the second set being initially coincident with the first set. Then rotate the second set through one differential angle after another so as to obtain the final, second vector set, orientations. This sequencing is shown in Fig. 10.4(a), (b), and (c), with (d) as a summary. As discussed in Exercise 9.19, the order of these small rotations is totally immaterial. Now recall from Fig. 2.2 that all that is necessary

³ It is seen later, Eqs. (10.2), that the bending rotations are limited by the requirement that $\phi_y^2, \phi_z^2 \ll 1.0$, and small changes in axial length are considered when discussing axial strains.

⁴ Avoid the possibility of driving splinters through your hands.

⁵ Again, in the right-hand rule sense, the angle of twist ϕ_x is positive about the positive x axis, and the bending slopes ϕ_y and ϕ_z are positive about the negative y axis and the positive z axis, respectively.

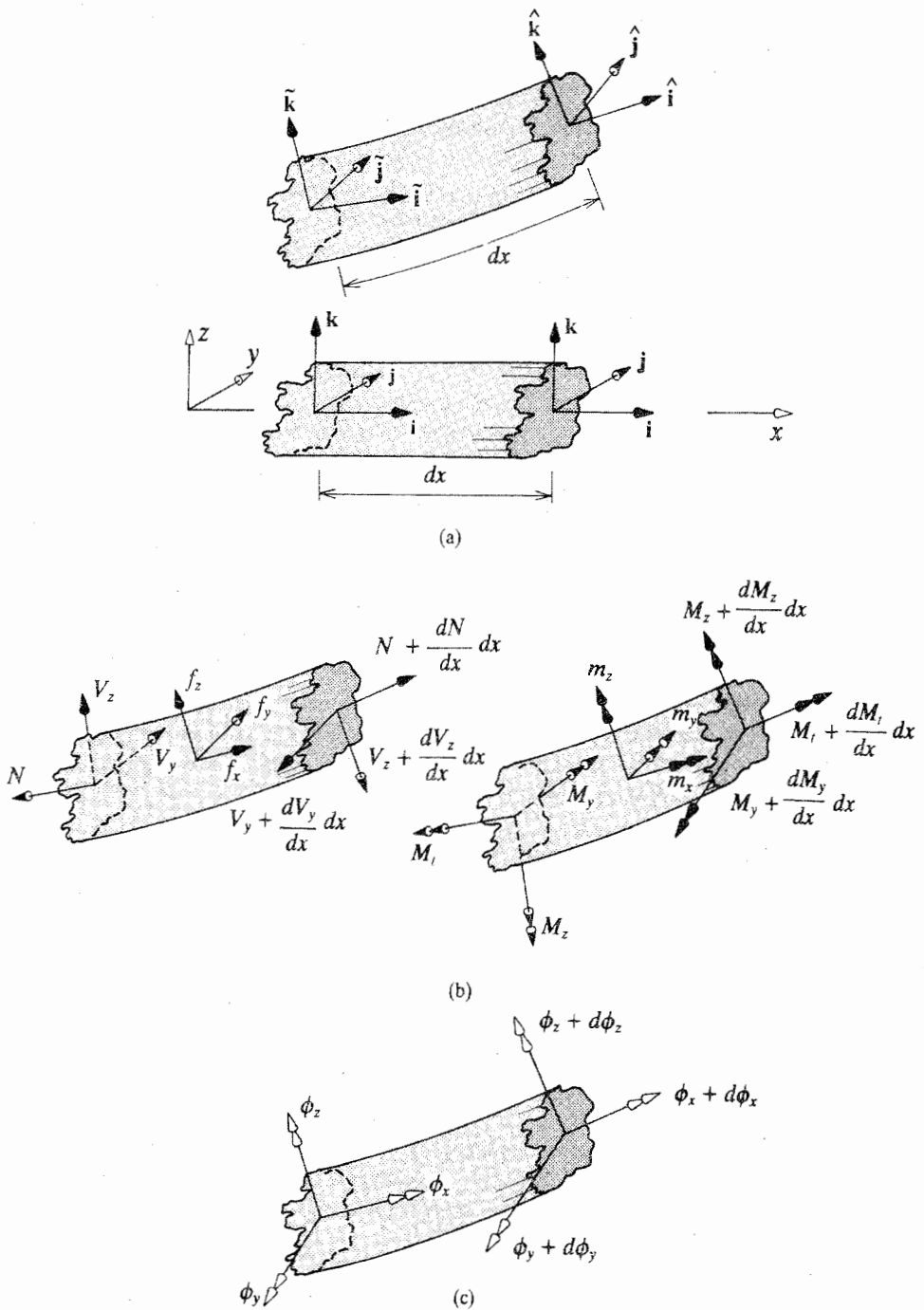


Figure 10.3. (a) The three sets of unit vectors that define the orientations of the front and back faces of the differential beam element before and after deformation. (b) One free body diagram of the forces and forces per unit length acting upon a differential length of beam, and for clarity, a separate FBD of the same free body for the moments and moments per unit length. (c) The changes in the differential beam element rotations from the back cross-section at x to the front beam cross-section at $x + dx$.

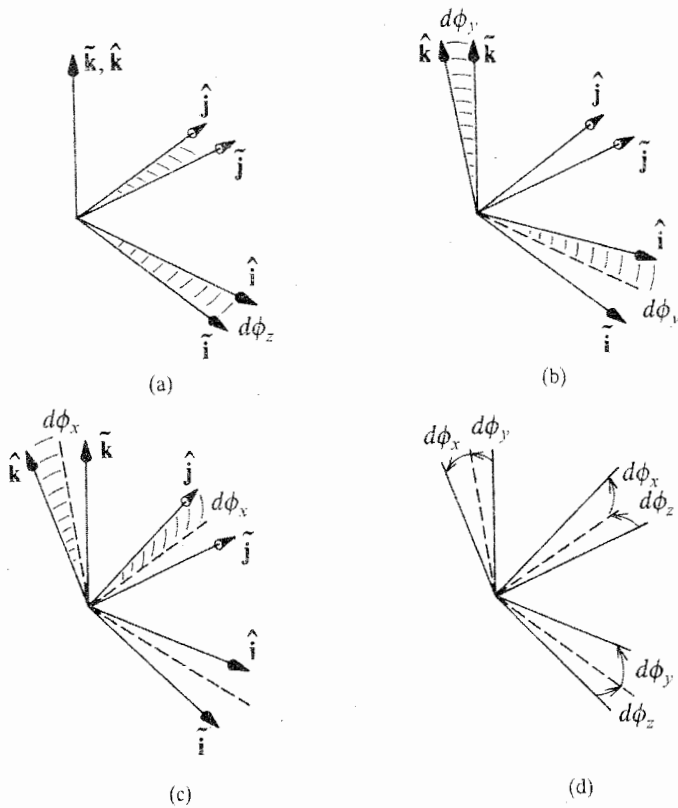


Figure 10.4. A sequencing of the rotations that distinguish the caret (or circumflex) unit vectors from the tilde unit vectors: (a) a first rotation about the z axis of magnitude $d\phi_z$; (b) a second rotation about the y axis of $d\phi_y$; (c) a third rotation about the x axis of magnitude $d\phi_x$; (d) a summary of all three rotations.

to obtain the magnitude of the component of one vector in the direction of another vector is simply to multiply the first vector by the cosine of the angle between the two vectors. To speed up the process of identifying the cosines between unit vectors, the following table is constructed from Fig. 10.4(d) on the basis that the cosine of any differential angle is 1.0; and

$$\cos [(\pi/2) + (\text{differential angle})] = -(\text{that differential angle})$$

$$\cos [(\pi/2) - (\text{differential angle})] = +(\text{that differential angle})$$

Cosines between Unit Vectors

	\hat{i}	\hat{j}	\hat{k}
\tilde{i}	1.0	$-d\phi_z$	$-d\phi_y$
\tilde{j}	$d\phi_z$	1.0	$-d\phi_x$
\tilde{k}	$d\phi_y$	$d\phi_x$	1.0

Now all is prepared to sum forces and moments on the distorted beam segment of length, dx . Consulting Figs. 10.3(b) and the above table, the result of summing forces in the \hat{i} direction is

$$(N + dN) - N(1.0) + V_y(+d\phi_z) + V_z(+d\phi_y) + f_x dx(1.0) = 0$$

where the other forces per unit length have two differential factors and are thus immediately identifiable as negligible. Summing forces in the \hat{k} direction in a similar manner yields

$$-(V_z + dV_z) + V_z(1.0) - N(-d\phi_y) + V_y(-d\phi_x) + f_z dx(1.0) = 0$$

There is a similar equation for the summation of forces in the \hat{j} direction that is left to the reader as an exercise. Summing moments in the \hat{i} direction (i.e., about the \hat{x} -axis) leads to

$$(M_t + dM_t) - M_t(1.0) + M_y(+d\phi_z) - M_z(+d\phi_y) + m_t dx(1.0) = 0$$

where the moments due to the offset of the shearing forces are second order differential quantities, and are therefore omitted along with the m_y and m_z terms, which are omitted for the same reason of having two differential factors. (Remember that the length of the beam is only dx , which is greatly exaggerated in the sketch.) Similarly, summing moments in the \hat{k} direction (i.e., about the \hat{z} -axis) leads to

$$(M_z + dM_z) - M_z(1.0) - M_t(-d\phi_y) + M_y(-d\phi_x) - V_y dx(1.0) + m_z dx(1.0) = 0$$

The summation of moments in the \hat{j} direction (i.e., about the \hat{y} axis) is left to the reader as an exercise. Dividing by dx , and otherwise simplifying the above four equations and the two similar undervived equations, and then dropping small terms (the products of shears and the derivatives of rotations) as previously discussed, results in six equations, five of which contain derivatives of the bending slopes. Before writing those six equations, consider Fig. 10.5, which shows an x, z plane side view of the distorted beam element that clearly

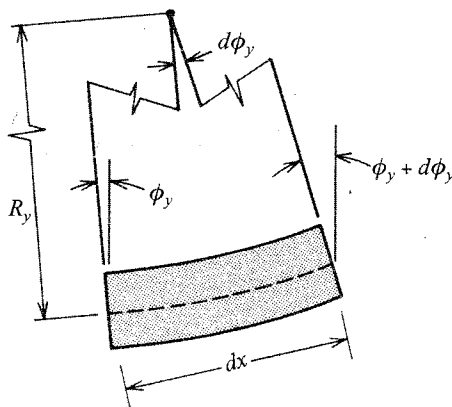


Figure 10.5. A y plane view of a differential length of beam showing the radius of curvature (compressed) and the associated rotations and change in the rotation between the beam length ends.

identifies the difference in rotations between the back and front cross-sections in that x, z plane, which is $d\phi_y$. The relation between any differential arc length such as dx and any corresponding differential angle such as $d\phi_y$ is always based on circular geometry. The relationship in terms of the radius of curvature R_y is

$$\frac{1}{R_y} = \frac{d\phi_y}{dx} \quad (\text{i.e., where } ds \equiv dx)$$

Recall from the calculus that

$$\frac{1}{R_y} = \frac{w''}{[1 + (w')^2]^{3/2}}$$

which is algebraically difficult to deal with. However, if the slope w' (and by analogy, v') are limited so that

$$(w')^2, (v')^2 \ll 1.0 \quad (10.2)$$

then the formula for the radius of curvature is greatly simplified to the point of being linear. In that case

$$\frac{d\phi_y}{dx} = w'' \quad \text{and} \quad \frac{d\phi_z}{dx} = v'' \quad (10.3)$$

which exactly correspond to the equations for v' and w' developed in Section 9.4 where the linear theory of elasticity strain–displacement equations are used to process the Bernoulli–Euler beam approximations. Having the rotations equal the slopes, the physical interpretation of the equations $\phi_y = w'$ and $\phi_z = v'$, ensures consistency between the equilibrium equations below and the beam stress equation, Eq. (9.8). Thus the linearizations that are Eqs. (10.2) and (10.3) are now adopted and Eqs. (10.2) are limits for the validity of these linearizations. However Eqs. (10.2) are rather weak limits in that even with a 6° slope for the deformed beam with respect to its undeformed position, there is only a 1 percent error. (A 6° slope associated with a beam deformation is quite noticeable, and in some vehicular structures and many civil structures, would be quite alarming.) Thus, finally, using Eqs. (10.3) with the previous simplifications leads to the following six *beam stress resultant equilibrium equations*:

$$\frac{dN}{dx} = -f_x \quad (10.4a)$$

$$\frac{dV_y}{dx} = +f_y + [Nv''] \quad (10.4b)$$

$$\frac{dV_z}{dx} = +f_z + [Nw''] \quad (10.4c)$$

$$\frac{dM_t}{dx} = -m_t + [M_z w'' - M_y v''] \quad (10.4d)$$

$$\frac{dM_y}{dx} = +V_z + m_y + [M_t v'' - M_z \phi'_x] \quad (10.4e)$$

$$\frac{dM_z}{dx} = +V_y - m_z + [M_y \phi'_x - M_t w''] \quad (10.4f)$$

Contrasting the above equations with the linear equilibrium equations, Eqs. (10.1), shows that the nonlinear terms are those enclosed within the brackets. The bracketed terms are

nonlinear because, as is evident for example in Eqs. (9.7), the bending moments of these products depend upon the second derivatives of the deflections, and vice versa. The nonlinear terms are not nearly as important as the linear terms when the beam deflections are small.⁶ In other words, the nonlinear terms may be totally disregarded unless the deflections are anticipated to be finite, as in the case of a buckled beam, or in the case of extensive interaction between bending and extension deflections or between bending and twisting deflections, as represented by the nonlinear terms. An example of a nonbuckling interaction is when a beam is bent by lateral loads, but the bending deflections are diminished by the presence of a large axial tensile force. A quantitative demonstration of this fact is presented in the next chapter.

The initial buckling of beams represents a situation where finite deflections are of the essence. Since it is desired to do no more in Part III of this textbook than introduce the topic of buckling, that is, to look only at the simplest type of buckling, which is the interaction of axial compressive forces and beam bending, then the bracketed terms in the last three equations which couple bending and twisting are no longer of interest. That is, bending and twisting are only considered separately in this text hereafter.⁷ Hence the bracketed twisting bending interaction terms are discarded from Eqs. (10.4e, f). Similarly, the bracketed term in Eq. (10.4d) likewise is eliminated since this bracketed quantity is of the same small order of magnitude as the bracketed twisting–bending interaction terms. Therefore, making these simplifications leaves only the bracketed terms in Eqs. (10.4b, c).

Having the desired equilibrium equations, it is now time to turn to the Bernoulli–Euler strain–deflection equation, Eq. (9.3). When that equation is combined with the Bernoulli–Euler stress–strain equation, the result is Eq. (9.4b). The forms of that equation that are most convenient for present use are Eqs. (9.7). Rewrite Eqs. (9.7b, c) as

$$M_y(x) = E_0 I_{yz}^* v''(x) + E_0 I_{yy}^* w''(x) - M_{yT}(x)$$

$$M_z(x) = E_0 I_{zz}^* v''(x) + E_0 I_{zz}^* w''(x) - M_{zT}(x)$$

Substitution of these equations into the equilibrium equations, Eqs. (10.4e, f), and then Eqs. (10.4b, c), along with the following thermal load definitions that mimic the mechanical load equilibrium equations, Eqs. (10.4)

$$M''_{yT}(x) \equiv V'_{zT}(x) \equiv f_{zT}(x) \quad \text{and} \quad f_z + f_{zT} \equiv f_z^c$$

$$M''_{zT}(x) \equiv V'_{yT}(x) \equiv f_{yT}(x) \quad \text{and} \quad f_y + f_{yT} \equiv f_y^c$$

⁶ Such descriptions as small/large or infinitesimal/finite are inadequate for describing beam bending deflections. Precision is best served by separate categorizations for strains and rotations. However, to keep this matter as simple as possible, the following terminology is adopted for this introductory text. Let “small” lateral beam deflections be those that are adequately estimated by the linear equations. Such lateral deflections are generally less than one-quarter the depth of the beam (Ref. [16]). Let “finite” deflections be those estimated by the equations of this chapter where the limitation is Eqs. (10.2). Let “large” describe any deflections greater than these.

⁷ An example of coupling between bending and twisting deflections is the situation where a beam with a very thin rectangular cross-section, such as some plastic rulers, is cantilevered at one end and subjected to a tip shearing force that initially tends to bend the beam about the undeflected centroidal axis with the much larger area moment of inertia. When the tip shearing force is made sufficiently large, the beam still bends very little about that first centroidal axis, but it twists and bends about the second centroidal axis considerably because such a beam is very flexible in torsion as well as bending about the second axis. Further discussion of the coupling between bending and twisting deflections can be found in Chapter 11 and in Ref. [23], which is highly recommended for this purpose.

after transposition, leads to the following form of the w and v deflection equations:

$$[E_0 I_{yy}^* w''(x)]'' + [E_0 I_{yz}^* v''(x)]'' - N w''(x) = f_z^c(x) + m_y'(x) \quad (10.5a)$$

$$[E_0 I_{zz}^* v''(x)]'' + [E_0 I_{yz}^* w''(x)]'' - N v''(x) = f_y^c(x) + m_z'(x) \quad (10.5b)$$

If the beam is uniform, then the two derivatives on each bracketed quantity act only on the curvature terms (the second derivatives of the deflections). Much use is made of these two fourth order ordinary differential equations.⁸ While these are the generally recommended beam deflection equations, they are not the only useful description of the beam deflections caused by loads. Eqs. (9.7d, e), which only involve second order derivatives, can also be used in all cases, but with unknown reactions as part of the moment expressions when the beam is statically indeterminate. In some cases, particularly statically determinate cases, this earlier second order differential equation form is a quicker route to a solution. Nevertheless, the emphasis here is entirely on the fourth order equations because they are more instructive, often more efficient (particularly with the more challenging problems), and to some extent less open to mistakes because they involve only the applied distributed loads rather than the derived moment expressions, and also because of the regularity of the associated boundary conditions. Before discussing the two fourth order equations further, it is necessary to derive the companion u deflection equation.

Early on in this section, the approximation was made that the arc length of the differential beam element before loading, dx , remained the same after loading. That is, in mathematical terms, $ds \equiv dx$. This was done for the sole purpose of sorting out the magnitudes of the relative changes in geometry of the bent beam element. Obviously, when considering displacements and strains along the x axis that result from the presence of an axial force $N(x)$, this approximation of relative distortion is too drastic. Reintroducing a strain along the x axis, that is, $\epsilon_{xx}(x) = u'(x)$, means returning to Eq. (9.7a),

$$N(x) = E_0 A^* u'(x) - N_T(x) \quad (9.7a)$$

and combining it with Eq. (10.4a). Defining

$$N_T'(x) \equiv -f_{xT}(x) \quad \text{and} \quad f_x(x) + f_{xT}(x) \equiv f_x^c(x)$$

leads to the following u deflection equation:

$$[E_0 A^* u'(x)]' = -f_x^c(x) \quad (10.5c)$$

Equations (9.7a) and (10.5c) are the two forms of the u deflection equation. An extended, third form is discussed briefly in Endnote (1). The same things said about the fourth order and second order derivative forms of the v and w deflection equations apply here to the second and first order forms of the u deflection equation; that is, Eq. (10.5c) is the recommended form.

The solution path for the three deflection equations is: (i) solve Eq. (10.5c), then (ii) determine $N(x)$ from Eq. (9.7a), then (iii) insert that value of $N(x)$ in the v and w deflection equations, Eqs. (10.5a, b), and then (iv) seek their solution. If the beam is uniform and the axial force $N(x)$ turns out to be a constant ($f_x = 0$), then the v and w deflection equations have the mathematical form of linear ordinary differential equations with constant coefficients. Then their complementary solution is always simple. However, the interaction

⁸ Remember that, while these two deflection equations do describe the interaction of beam bending and extension, they do not include the interaction of bending and twisting. Modifying them to include the latter is simply done by keeping the appropriate bracketed terms throughout the short derivation.

between a nonzero axial force N and lateral forces per unit length $f_y(x)$ and $f_z(x)$ is not truly linear even when N is a constant since superposition of these two differing types of loads is not valid. The original nonlinearity inherent in the use of the distorted geometry is manifested in this manner. In other words, the two bending equations allow the superposition of lateral loads, that is, those loads that appear on the right-hand side of the differential equation, but not the superposition of axial loads and lateral loads because the axial load interacts with the lateral deflections caused by the lateral loads. Mathematically, this interaction is represented by the product of the axial force and the curvature on the left-hand side of these two differential equations.

If $N(x)$ is other than a constant, then the solution of the deflection differential equations may require the use of numerical methods. Before proceeding to illustrate the solution process, it is useful to introduce the subject of boundary conditions. In order to have the u , v , and w differential equations restated close to the summaries of boundary conditions, Eqs. (10.5), are repeated here. Remember that A^* , I_{yy}^* , I_{zz}^* , and I_{yz}^* can also vary with the beam length variable x .

$$\begin{array}{l}
 u: \quad [E_0 A^* u'(x)]' = -f_x^c(x) \\
 v: \quad [E_0 I_{zz}^* v''(x)]'' + E_0 I_{yz}^* w''(x)'' - N v''(x) = f_y^c(x) + m_z'(x) \\
 w: \quad [E_0 I_{yy}^* w''(x)]'' + E_0 I_{yz}^* v''(x)'' - N w''(x) = f_z^c(x) + m_y'(x)
 \end{array} \quad (10.5)$$

10.4 Boundary Conditions and the Boundary Value Problem

In mathematical terms, the above beam deflection equations, Eqs. (10.5), are governing differential equations (GDEs) for the domain (open interval) $0 < x < \text{beam length}$. Since they are ordinary differential equations, their solution produces one constant of integration for each derivative of the highest order derivative in the equation. Hence integration of the u deflection equation produces two constants of integration, and integration of the v and w deflection equations produces four constants of integration for each of those two equations. As is the case with all differential equations with spatial domains, these unknown constants of integration are determined by means of additional information about the values of the u , v , and w deflections, or their derivatives, at the end or boundary points of the beam. The boundary points are the points on the x axis at the supports for the beam, or at the unsupported ends of the beam. These additional items of information concerning the deflections or the derivatives of the deflections at the end points are called the *boundary conditions*. The general form of the boundary conditions, or support conditions, are so important that they are often used to characterize the beam. For example, beams are referred to as cantilevered, or simply supported, or clamped-clamped, and so on. The boundary conditions (BCs) are as much a part of the problem statement as the loading, geometry, and material information.

The energy methods introduced in Part IV of this text are used to prove⁹ that the problem of solving the second order u deflection equation and the fourth order v and w deflection equations, by use of their attendant boundary conditions, falls into a special category of problems called *boundary value problems*. Like all boundary value problems, the problem

⁹ See Endnote (2), Chapter 15.

of integrating the three GDEs to determine the beam deflections, and from those deflections the beam stresses, has the following characteristics:

1. The highest order derivative of each GDE is an even number.
2. Half that even number of boundary conditions is always found at each boundary point.
3. The order of the highest order derivative appearing in the BCs is always at least one order of derivative less than the highest order derivative appearing in the GDE.
4. The BCs at a beam end point are always one, but never both, of a pair of possible BCs; for example, for the u deflection equation the single BC at each beam end must be a statement about either the u deflection itself or about the axial force N .

A complete listing in tabular form of these required alternative boundary condition statements is presented in Table 10.1 in detailed mathematical form for each of the three deflection equations. In the table, the notation $x = b$ is meant to indicate that the unknown function is evaluated at one of the two beam boundary points. As before, tilde (\sim) markings on deflection functions are meant to indicate known, fixed (from the problem statement) values of the quantity so modified. For example, the BCs $\tilde{v}(0) = \tilde{v}'(0) = 0$ indicate that in the x, y plane the beam is “clamped” against a lateral deflection and rotation at the end $x = 0$. Such markers are unnecessary for the force and moment quantities. The axial force and moment equations found in the “Or” column were previously derived as Eqs. (9.7a, b, c). As such, these axial and moment equations are true for any value of x . All that has been done to make them part of the BCs table is to specialize the value of x to be one of the boundary points. The same is true for the shearing force equations, which are obtained from Eqs. (10.4e, f) after substitution of the moment equations, Eqs. (9.7b, c).

This is how to use the first boundary condition table. For the u deflection equation, as mentioned above, at each beam end, the analyst must decide whether the axial (longitudinal) deflection at that end is known (usually zero), or the axial force is known. If the deflection is the known value, then that statement is made. For example, if a beam of original length L has been stretched a known distance, say 1.0 mm, by an unknown axial force, then the BC statements could be $u(0) = 0.0$ and $u(L) = 1.0$ mm; or, if the other end of the beam is used as reference, $u(0) = -1.0$ mm, and $u(L) = 0.0$. If, instead of the deflection, the axial force at $x = L$ is the known quantity, say 1×10^5 N, and there is no temperature change to produce an $N_T(L)$, then the BC statement is

$$E_0A^*(L)u'(L) = 100\,000\text{ N}$$

where the value of the axial stiffness coefficient E_0A^* at $x = L$ is substituted. If there were a temperature change that produced an equivalent thermal axial force evaluated at that end of, say, $N_T(L) = -50\,000$ N, then the above BC would have to be altered to

$$E_0A^*u'(L) - (-50\,000\text{ N}) = 100\,000\text{ N}$$

In every case the object is to write a statement about the u deflection or its first derivative evaluated at both end values of the independent variable, x . It is the same in the case of the v and w deflection equations.

For the sake of this discussion, let the end of the beam at $x = 0$ in the x, z plane be “simply supported.” That is, let the lateral (bending) deflection $w(0)$ be zero at that beam support, but let the beam be free to rotate without restraint at that support. Then the first line of the table for the w deflection equation says choose *either* a statement about the deflection value at that end *or* a statement about the externally applied shearing type force at that

Table 10.1. General boundary condition statements for beams where "b" is a beam end point

Differential Equation	Either	Or
u:	Axial deflection $u(b) = \bar{u}(b)$	Axial force $E_0 A^*(b)u'(b) - N_T(b) = N(b)$
v:	Lateral deflection $v(b) = \bar{v}(b)$	Shear force $[E_0 I_{zz}^*(b)v''(b)]' + [E_0 I_{yz}^*(b)w''(b)]' - V_{yT}(b) + m_z(b) = V_y(b)$
	Bending slope $v'(b) = \bar{v}'(b)$	Bending moment $E_0 I_{zz}^*(b)v''(b) + E_0 I_{yz}^*(b)w''(b) - M_{zT}(b) = M_z(b)$
w:	Lateral deflection $w(b) = \bar{w}(b)$	Shear force $[E_0 I_{yz}^*(b)v''(b)]' + [E_0 I_{yy}^*(b)w''(b)]' - V_{zT}(b) - m_y(b) = V_z(b)$
	Bending slope $w'(b) = \bar{w}'(b)$	Bending moment $E_0 I_{yz}^*(b)v''(b) + E_0 I_{yy}^*(b)w''(b) - M_{yT}(b) = M_y(b)$

end of the beam. In this discussion it is the deflection that is known to be zero; hence write $w(0) = 0$. Note that nothing is known a priori about the shearing force, which is the unknown force reaction at the support, other than it has the value necessary to make the end deflection zero. Note that it is taken for granted that the analyst has *not* employed force and moment equilibrium equations in order to calculate the support reactions even if the beam is statically determinate. More to the point, it is never necessary to calculate the support force and moment reactions whenever the task is the solution of *deflection* differential equations. It is for that reason it is presumed that the external shear force, that is, the lateral support reaction, is not known at the time of writing the BCs.

Continuing with the discussion of the simple support at $x = 0$, the second line of the Table 10.1 for the w deflection equation prompts the analyst to choose between making a statement *either* about the bending slope at that end, $w'(0)$, *or* about the externally applied bending moment at that end of the beam. In this case nothing is known a priori about the bending slope. Therefore there must be a statement to be made about the moment at that end. Without an externally applied bending moment at $x = 0$, and with an equivalent thermal moment value at $x = 0$ of, say, $+M_{th}$, the statement about the moment begins as simply $M_y(0) = 0$, which then, from the table, translates in terms of the unknown deflection functions into

$$E_0 I_{yz}^* v''(0) + E_0 I_{yy}^* w''(0) - M_{th} = 0$$

It is this equation, which is in terms of the unknown deflection functions that appear in the GDEs, that is the required BC, not $M_y(0) = 0$. If there had been an externally applied clockwise moment at $x = 0$ of magnitude, say, M_0 , then the right-hand side zero of the above equation would be replaced by $+M_0$. If, on the other hand, at this beam end, there is no externally applied moment, no thermal moment, a zero product of inertia, and a nonzero moment of inertia about the y axis, then this moment BC becomes just $w''(0) = 0$. It is quite important to always simplify BCs, as well as all other algebra, as much as possible.

The boundary condition that requires a bit more explanation is the one involving the shear force at the beam end. This BC is written whenever the end of the beam is unsupported; that is, when there is a (support) "free" end. (Another possibility, which is not discussed

until Chapter 11, is an elastic support at the beam end in question.) This BC in general form is

$$[E_0 I_{yz}^* v''(b)]' + [E_0 I_{yy}^* w''(b)]' - V_{zT}(b) - m_y(b) = V_z(b)$$

This BC has an additional feature, which is derivatives of products of the beam stiffness factors and the beam curvatures. If the beam is uniform, then the stiffness factors are constants, and this BC reduces to

$$E_0 I_{yz}^* v'''(b) + E_0 I_{yy}^* w'''(b) - V_{zT}(b) - m_y(b) = V_z(b)$$

Although it is usually best not to do so, if the stiffness factors are not constants, then the product rule for derivatives may be employed with the result that

$$E_0 I_{yz}^*(b) v''(b) + E_0 I_{yz}^*(b) v'''(b) + E_0 I_{yy}^*(b) w''(b) + E_0 I_{yy}^*(b) w'''(b) - V_{zT}(b) - m_y(b) = V_z(b)$$

10.5 Uncoupled Forms of the GDEs and the BCs

It is easy to see that when the product of inertia is not zero, then both the v and w differential equations, and the bending moment and shearing force BCs as stated above, mix or “couple” the two lateral deflection derivatives. This is algebraically tedious. There are two, limited, ways of avoiding that algebraic mess. The first way out is to simply rotate the centroidal axes so as to achieve principal axes. When the product of inertia is zero, all the coupling between deflection derivatives in the GDEs disappears. The problem with this direct approach is that if the BCs in the original x, z plane are different from those in the x, y plane, there will be a new coupling of the deflections through the BCs in the principal coordinate directions. Even if all the BCs were the same in the two orthogonal planes, it would also be necessary to vectorially resolve the applied loadings into the principal coordinate directions. That too can be messy. As a result, this first approach is not further considered except to say that *if an axial force must be included in the lateral deflection GDEs, then, regardless of any other difficulties, it is best (but not necessary) to work with principal centroidal coordinates.*

A second way out of this difficulty is to retain the original, convenient coordinate directions, and use forms of the GDEs and BCs that have already been solved simultaneously so as to separate the deflection derivatives. This approach is also limited to special circumstances.

The special circumstances that allow the decoupling of the GDEs and the bending moment and shear force BCs when the product of inertia is not zero are: (i) the derivatives of the beam stiffnesses (the various EI factors) are zero; (ii) all the bending moment terms and all the shearing force terms at the beam ends that enter into the BCs are known quantities; and (iii) *there are no appreciable axial forces.*

These circumstances are indeed limited, but not unusual. The advantage that is achieved by recognizing these circumstances is sufficient for the reader to keep in mind the possibility of decoupling the GDEs and the BCs. Furthermore, a nice aspect of this approach is that it is not necessary to remember the first of the above two conditions that are necessary to completely decouple a given problem. *It is best to proceed to decouple as many of the GDEs and BC equations as possible.* When decoupling is not possible, simply revert back to the GDEs and BC equations of the preceding section.

The most efficient way to decouple the various equations is, again, to use forms of the GDEs and BCs that have already been solved simultaneously so as to separate the deflection derivatives. To this end, it is convenient to reintroduce the following *ratio of inertia* definitions. Let

$$\begin{aligned} R_{yy}^* &\equiv \frac{I_{yy}^* I_{zz}^* - (I_{yz}^*)^2}{I_{yy}^*} \\ R_{zz}^* &\equiv \frac{I_{yy}^* I_{zz}^* - (I_{yz}^*)^2}{I_{zz}^*} \\ R_{yz}^* &\equiv \frac{I_{yy}^* I_{zz}^* - (I_{yz}^*)^2}{I_{yz}^*} \end{aligned} \quad (10.6)$$

Again Schwartz's inequality (Ref. [20]) demonstrates that the first two of the above ratios of inertia are always positive. Then the simultaneous solutions for the v and w deflection decoupled GDEs, which are limited in validity to the case where the beam is uniform and the axial force is zero, are then

$$\begin{aligned} E_0 R_{zz}^* w''''(x) &= [f_z^c(x) + m'_y(x)] - \frac{I_{yz}^*}{I_{zz}^*} [f_y^c(x) - m'_z(x)] \\ E_0 R_{yy}^* v''''(x) &= [f_y^c(x) + m'_z(x)] - \frac{I_{yz}^*}{I_{yy}^*} [f_z^c(x) + m'_y(x)] \end{aligned} \quad (10.7a,b)$$

(only for uniform beams and no axial forces N)

The bending moment BC equations in Table 10.1 are restatements of Eqs. (9.7b, c). Recall from Chapter 9 that if those two equations are solved simultaneously for the curvatures, then the result is Eqs. (9.7d, e). These two equations, with $x = b$, are the alternative BC forms listed in Table 10.2. Furthermore, if Eqs. (9.7d, e) are differentiated with respect to x , and use is made of Eqs. (10.4e, f), then alternative forms for the third derivatives are also possible.

The task of writing the BCs may look to be more daunting than it normally is because it is unusual for many of these complications to be present in the same beam problem, except, of course, in the case of final examinations. The next step is to gain confidence by practicing writing the GDEs and their solutions, and writing and using the BC equations.

10.6 Solutions for Beam Deflection Problems

This section presents a sequence of problem solutions that increase in complexity. Recall that the solution process always begins with the u deflection equation, and determining $N(x)$ is a necessary result of this first step. The solution for each deflection equation involves five distinct steps: (i) specializing the form of the left-hand side of each GDE to the problem at hand; (ii) writing the right-hand side expressions for each of the distributed loads; (iii) writing the BC equations appropriate to each GDE; (iv) integrating the completed GDEs; and (v) using the BCs to evaluate the constants of integration. After a bit of practice, the above steps (i) and (ii) are virtually immediate after determining the area moments of inertia, which may be done by computer program. Finally, remember that

Table 10.2. Alternative beam bending boundary condition equations

Either	Or	
		For all circumstances but elastic supports (next chapter)
$w'(b) = \bar{w}'(b)$	$E_0 w''(b) = \frac{M_y^c(b)}{R_{zz}^*(b)} - \frac{M_z^c(b)}{R_{yz}^*(b)}$	
$v(b) = \bar{v}(b)$	$E_0 v''(b) = \frac{M_z^c(b)}{R_{yy}^*(b)} - \frac{M_y^c(b)}{R_{yz}^*(b)}$	(9.7d,e)
		Uniform beams only, with or without an axial force
$w(b) = \bar{w}(b)$	$E_0 w'''(b) = \frac{V_z^c(b) + m_x(b)}{R_{zz}^*} - \frac{V_y^c(b) - m_z(b)}{R_{yz}^*}$	
$v(b) = \bar{v}(b)$	$E_0 v'''(b) = \frac{V_y^c(b) - m_z(b)}{R_{yy}^*} - \frac{V_z^c(b) + m_x(b)}{R_{yz}^*}$	(9.7d',e')

once the deflections are determined, the stress at any cross section can be determined via Eq. (9.4b) or, if preferred, Eq. (9.8).

Example 10.1. Determine the axial deflection at the right-hand end of the uniform, homogeneous bar shown in Fig. 10.6.

Solution. Since only a longitudinal (i.e., axial) deflection is sought, only the u deflection equation need be considered. Noting that $E_0 A^* = EA = \text{constant}$, and $f_x(x) = 0$, and there is no temperature change, then the GDE $[E_0 A^* u'(x)]' = -f_x^c(x)$ becomes simply $u''(x) = 0$. Its solution is

$$u(x) = C_1 x + C_2$$

where the C_i are the constants of integration. The boundary conditions are determined by inspecting the drawing of the bar. The hatched symbol on the left end indicates that the bar end cannot deflect. Therefore, $u(0) = 0$ is the first of the two BCs. Since the other BC must be found at the other end of the bar, that end is examined next. Since nothing is known a priori about the longitudinal deflection at that end, a statement must be made regarding the force acting there. In this case that statement is $N(L) = +N_0$. This statement must be converted to one involving the longitudinal deflection. Consulting the first line of the first BC table, and making the substitutions appropriate to this problem, leads to $u'(L) = N_0/EA$. Substitution of these BCs yields $C_2 = 0$, and $C_1 = N_0/E/A$, so that

$$u(x) = \frac{N_0 x}{EA} \quad \text{and} \quad u(L) = \frac{N_0 L}{EA}$$

It is worth remembering that the total deflection of a bar loaded by a constant axial force is equal to the (force) multiplied by the (length), divided by the axial stiffness coefficient (EA). ■

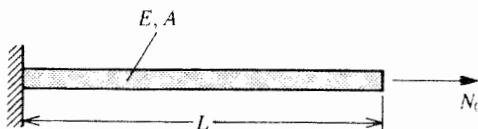


Figure 10.6. Example 10.1. A uniform, axially loaded bar.

Example 10.2. Solve the above problem without the axial force at the end, but with a uniform axial load per unit length of magnitude f_0 acting in the positive x direction.

Solution. Since $f_x(x) = +f_0$, the GDE and BCs in this case are

$$EAu''(x) = -f_0 \quad \text{where} \quad u(0) = 0 \quad \text{and} \quad u'(L) = 0$$

The latter boundary condition is the end result of $N(L) = 0$ and the use of the first line of the first BC table. Integrating the GDE leads to

$$EAu'(x) = -xf_0 + C_1 \quad \text{and} \quad EAu(x) = -\frac{1}{2}f_0x^2 + C_1x + C_2$$

Application of the BCs shows that $C_2 = 0$ and $C_1 = +f_0L$. Thus, in this case,

$$u(x) = \frac{f_0x}{EA} \left(L - \frac{x}{2} \right) \quad \text{and} \quad u(L) = +\frac{f_0L^2}{2EA}$$

If f_0L is set equal to N_0 , then it is seen that the distributed load is half as effective in producing an end deflection as the concentrated load positioned at the bar end. This is because the stress in the bar in the distributed load case diminishes from N_0/A at one end to zero at the other end of the bar, while it is a constant N_0/A in the concentrated load case. The same average stress of the distributed load case can be achieved by positioning the concentrated force at the center of the bar. This midbar positioning also produces the same end deflection. ■

Example 10.3. Repeat the first example problem, but this time with both the same constant axial force per unit length, f_0 , acting over the length of the bar, and the same axial force, N_0 , acting at the right-hand end of the bar.

Solution. This time the GDE and BCs are as follows:

$$EAu''(x) = -f_0 \quad \text{where} \quad u(0) = 0 \quad \text{and} \quad EAu'(L) = N_0$$

Integration of this same GDE of the second example produces the same result, namely,

$$EAu'(x) = -xf_0 + C_1 \quad \text{and} \quad EAu(x) = -\frac{1}{2}f_0x^2 + C_1x + C_2$$

the application of the present BCs causes $C_2 = 0$ and $C_1 = N_0 + f_0L$. Therefore,

$$u(x) = \frac{f_0x(L - x/2)}{EA} + \frac{N_0x}{EA} \quad \text{and} \quad u(L) = \frac{f_0L^2 + 2N_0L}{2EA}$$

It is evident that when the two right-hand side loadings (inputs to the system) are superimposed, the two previous deflection solutions (structural system outputs) are likewise superimposed. This is always true when the GDE system is mathematically linear. ■

The purpose of the next example is (i) to be a reminder that the beam deflection GDEs, as an adaptation from the theory of elasticity, are based on the premise that the material is free to expand or contract when its temperature is changed; and (ii) to illustrate that it is the BCs that establish the particular circumstances of the problem at hand.

Example 10.4. Consider the two bars shown in Fig. 10.7. The uniform, homogeneous bars are exactly the same. Both bars are subjected to a constant temperature change, T_0 , throughout their volume. Only their right-hand BCs differ. The bar in Fig. 10.7(a) is not free to expand, while the bar in 7(b) is wholly free to expand along its length. (Recall that

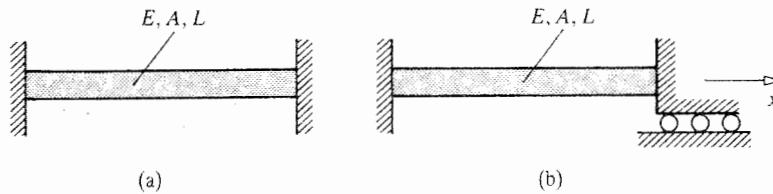


Figure 10.7. Example 10.4. (a) No axial deflection permitted at either beam end. (b) No resistance to axial deflections at the right-hand beam end.

Bernoulli–Euler theory disregards the expansion of the cross-section.) Determine the stress in both bars.

Solution. Since there are no mechanical loads, the preparatory work for both bars consists entirely of calculating the equivalent thermal force and moments.

$$N_T(x) = + \iint_A E(y, z) \alpha(y, z) \Delta T(x, y, z) dA = E\alpha T_0 A$$

because all values are constants. The thermal moments, which depend on the first area moments about the centroids, are zero. Since N_T is a constant, its derivative is zero. That is,

$$f_{xT}(x) = 0 \quad \text{and thus} \quad f_x^c(x) = 0$$

and the u deflection equation for both bars reduces immediately to $u''(x) = 0$. The result of the integration of that GDE is again

$$u(x) = C_1 x + C_2$$

where the C_i , as always, are constants of integration. To this point the analysis of each bar has been exactly the same. It is the BCs that distinguish between the two bars. Again the BCs are determined by inspection of the sketches. The BCs for bars (a) and (b) are

$$\begin{aligned} \text{(a)} \quad & u(0) = u(L) = 0 \\ \text{(b)} \quad & u(0) = 0, \quad \text{and} \quad N(L) = 0 \rightarrow EAu'(L) - N_T(L) = 0 \quad \text{or} \quad u'(L) = \alpha T_0 \end{aligned}$$

where use is made of the first BC table in order to write the force BC of case (b) in terms of the deflection derivatives at the bar end. The application of these BCs to the GDE solution produces the respective solutions

$$\begin{aligned} \text{(a)} \quad & u(x) = 0 \quad N(x) = -E\alpha T_0 A \\ \text{(b)} \quad & u(x) = \alpha T_0 x \quad N(x) = 0 \end{aligned}$$

where use is again made of Eq. (9.7a) which again is $N(x) = E_0 A^* u'(x) - N_i(x)$. These solutions, which state there are no longitudinal deflections in the case of bar (a) and there is no axial force in the case of bar (b), should be in accord with the reader's intuition. It should also be clear that, in the absence of bar buckling (to be discussed later), neither bar bends, that is, $v(x) = w(x) = 0$. However, at this learning stage, it is worthwhile checking to see how the bending equations provide that conclusion. For this purpose it is sufficient to consider only the w deflection equation for bar (a). For simplicity, let the product of inertia be zero. This GDE and its BCs are then

$$EIw'''(x) + E\alpha T_0 A w''(x) = 0 \quad w(0) = w'(0) = w(L) = w'(L) = 0$$

This differential equation and its attendant BCs all of which have a left-hand side that only involves the unknown function $w(x)$ and all of which have a zero right-hand side as well, is called a homogeneous system. Any such homogeneous boundary value problem has only the solution that the unknown function is zero. This fact is easily demonstrated in this case. If the temporary definition is made that

$$\beta^2 = \frac{\alpha T_0 A}{I}$$

then it may be verified that the solution to the above GDE is

$$w(x) = C_1 \sin \beta x + C_2 \cos \beta x + C_3 x + C_4$$

When the above four homogeneous BCs are applied to this solution, and the resulting four algebraic, simultaneous equations are solved by a process of canceling nonzero factors and eliminating unknowns, then the demonstration that $w(x) = 0$ is complete. Remember that for all the unknown functions to have a zero solution, both the GDE and the BCs must have zero right-hand sides, and the left-hand sides must only involve the unknown functions and known coefficients. Thus it may be concluded both mathematically and physically that in both cases the bending deflections are zero.

To complete the example problem by calculating the stresses, it is only necessary to use Eq. (9.4b), which is

$$\sigma_{xx} = E[u'(x) - yv''(x) - zw''(x) - \alpha \Delta T]$$

In case (a) $u' = 0$, and in case (b) $u' = \alpha T_0$. Then the stress result for case (a) is

$$\sigma_{xx} = E[0 - 0 - 0 - \alpha T_0] = -E\alpha T_0$$

and for case (b) it is

$$\sigma_{xx} = E[\alpha T_0 - 0 - 0 - \alpha T_0] = 0$$

which again are the expected results. The stress in case (a) is, of course, the compressive stress necessary to keep the beam within its original length. If, for example, the bar material is a commonly used alloy steel such as 4130, or 4140, or 4340 where the average α is approximately 7.6×10^{-6} per degree Fahrenheit over a temperature change from room temperature to 500 °F, and $E = 29 \times 10^6$, or 5 to 7 percent less at the higher temperatures, then the stress in the bar is nearly 100 ksi for a temperature change of 500 °F. Thus if the beam has a 1 in² cross-sectional area, then the rigid support would have to react a force of 100 kips without any appreciable movement. Not many supports are so rigid. Therefore it is clear that this mathematical model involving rigid beam supports is not realistic for such a bar and such a large temperature change. In such a case the replacement of the rigid support by a support that can move in response to a load, which in later discussions is called an elastic support, would be an important improvement in the mathematical model for bar (a) and its supports.

This has been a long exposition to arrive at the simple results for the two problems that

$$\begin{aligned} \text{(a) } u(x) &= 0 & \sigma_{xx} &= -E\alpha T_0 \\ \text{(b) } u(x) &= \alpha T_0 x & \sigma_{xx} &= 0 \end{aligned}$$

The process could have been speeded up significantly by first noting that there is neither a loading, nor a temperature change, nor a boundary condition to produce either a v or w bending deflection. Hence $v(x) = w(x) = 0$ can be stated without further justification. Writing the GDE as $u''(x) = 0$, and obtaining its solution $u(x) = C_1 x + C_2$ is quickly

done. The only item that requires careful attention is writing the one force BC; that is, first identifying that the axial force is zero at the right end in case (b), and then using the axial force formula to write that boundary condition in terms of $u'(L)$. After that, substitution of the BCs in the GDE solution and substitution into the stress equation completes the two problems. ■

Example 10.5. Determine the deflections in the homogeneous, uniform, clamped–clamped (fixed–fixed) beam sketched in Fig. 10.8. The product of inertia for this beam is zero.

Solution. The presumption is always that the deflections are small unless stated or discovered to be otherwise. Therefore there is no geometric (as opposed to external loading) interaction between the bending deflections and the axial deflection. The lack of such a coupling between deflections and the lack of an axial loading of any kind means that $u(x) = N(x) = 0$.

Only the x, z plane is sketched. The implication is that there is no loading in the x, y plane. Since the product of inertia is zero, there is no coupling between the v and w deflections. Hence $v(x) = 0$. This latter conclusion can be verified by noting that the GDE for that deflection is $v''''(x) = 0$ with BCs $v(0) = v'(0) = v(L) = v'(L) = 0$. Since all equations are homogeneous, the only solution is $v(x) = 0$.

The GDE for the w deflection is Eq. (10.5a), which, with the axial force and the product of inertia being zero, reduces to

$$[E_0 I_{yy}^* w''(x)]'' = f_z^c(x) + m_y'(x)$$

or Eq. (10.7a), which produces the same result. Similar to the v deflection equation, the left-hand side for this particular equation reduces to $EI_{yy} w''''(x)$. Since there is no temperature change nor moment per unit length mentioned, the right-hand side of the GDE reduces to just f_0 . Hence the GDE becomes simply

$$EI_{yy} w''''(x) = +f_0$$

Since a clamped (fixed) support admits neither a lateral deflection nor a bending slope, the w deflection BCs are

$$w(0) = w'(0) = w(L) = w'(L) = 0$$

Since not all these five equations are homogeneous, there is a unique, nonzero solution. Integration of the GDE leads to

$$EI_{yy} w'(x) = \frac{f_0 x^3}{6} + \frac{C_1 x^2}{2} + C_2 x + C_3$$

$$EI_{yy} w(x) = \frac{f_0 x^4}{24} + \frac{C_1 x^3}{6} + \frac{C_2 x^2}{2} + C_3 x + C_4$$

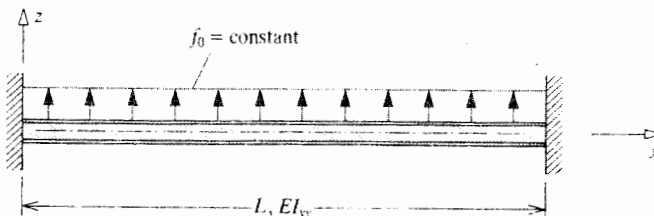


Figure 10.8. Example 10.5, and Exercises 10.9 and 10.11.

Note that at this point in the analysis there are four unknown constants of integration and four BCs with which to determine their values. Hence the uniqueness of this solution. The first two BCs show that $C_3 = C_4 = 0$. The latter two BCs lead to the simultaneous algebraic equations whose solutions are

$$C_1 = -\frac{f_0 L}{2} \quad \text{and} \quad C_2 = \frac{f_0 L^2}{12}$$

When these values for the constants of integration are inserted into the deflection solution, and that result is reorganized for greatest simplicity, it is seen that

$$u(x) = v(x) = 0 \quad \text{and} \quad w(x) = \frac{f_0 x^2}{24EI_{yy}}(L-x)^2$$

This solution is seen to have the symmetry about the point $x = L/2$ that must obviously be present in the actual beam deflections. That is, replacing x by $(L-x)$ yields exactly the same solution. ■

As a postscript to the above example, note that the above deflection solutions can be differentiated and those three results substituted into the stress equation:

$$\begin{aligned} \sigma_{xx} &= E[u'(x) - yv''(x) - zw''(x) - \alpha\Delta T] = -zEw''(x) & (9.4b) \\ &= -\frac{f_0 z}{12I_{yy}}(L^2 - 6Lx + 6x^2) \end{aligned}$$

Differentiating the axial stress with respect to x and setting that result equal to zero shows that the local maximum for the stress occurs at the beam midspan. This local maximum must be compared to the stress values at the beam ends to determine the absolute maximum. It turns out that the stresses at the beam ends are twice the stresses at midspan for this uniformly loaded clamped-clamped beam.

Example 10.6. Up to the point of determining the constants of integration, determine the deflections of the uniform, nonhomogeneous beam sketched in Fig. 10.9. The beam cross-sectional properties are A^* , I_{yy}^* , I_{zz}^* , and I_{yz}^* . Note that in this case the m.w. product of inertia is not zero.

Solution. Since there is no loading in the x direction, $u(x) = N(x) = 0$. The latter equality is easily verified by a FBD of any right-hand portion of the beam. The next question is: Which

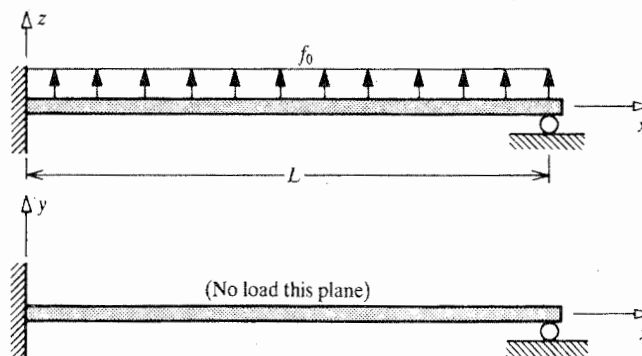


Figure 10.9. Example 10.6.

set of GDEs is the better choice for determining the bending (lateral) deflections? Since the axial force is zero and the beam cross-sectional properties are constant, it is certainly better to begin with the decoupled equations, Eqs. (10.7). In this case these equations reduce to

$$E_0 R_{zz}^* w''''(x) = f_0 \quad \text{and} \quad E_0 R_{yy}^* v''''(x) = -(I_{yz}^*/I_{yy}^*) f_0$$

The latter of the above two GDEs clearly shows that $v(x)$ is not zero when the product of inertia is not zero even though there is no loading in the y direction. The above GDEs are easily integrated to obtain their polynomial solutions. The remaining essential part of the solution process is completed by writing the BCs. Recall that since there are two fourth order GDEs, a total of eight BCs must be stated, and four of those BCs are found at each end of the beam. The four BCs for the left end, and two of the four for the right end are clearly¹⁰

$$w(0) = w'(0) = v(0) = v'(0) = w(L) = v(L) = 0$$

The remaining two BCs at the right-hand end are $M_y(L) = M_z(L) = 0$. As always, these last two BCs must be rewritten in terms of the deflection derivatives. Consulting the first two lines of the table of alternate boundary condition equations leads to the final BCs

$$w''(L) = v''(L) = 0$$

Again, decoupling the GDEs and BCs considerably simplifies the work necessary to evaluate the constants of integration. ■

Example 10.7. Repeat the problem above with the additional load of a counterclockwise moment of magnitude M_0 acting in the x, y plane at the right-hand end of the beam.

Solution. Since the additional applied loading is at a beam end, that loading is far better treated as being part of the BCs than as being part of a GDE. Thus the GDEs remain as they were. The first six BCs are also unchanged. The last two BCs are now $M_y(L) = 0$, and $M_z(L) = +M_0$. From the table of alternate boundary condition equations,

$$w''(L) = -\frac{M_0}{E_0 R_{yz}^*} \quad \text{and} \quad v''(L) = +\frac{M_0}{E_0 R_{yy}^*} \quad \blacksquare$$

Example 10.8. Repeat the problem above with the addition of a forced downward lateral deflection of the left-hand end of the beam in the x, y plane of magnitude v_0 , and a forced counterclockwise rotation at the same end in the same plane of magnitude r_0 .

Solution. All GDEs and BCs remain the same but for $v(0) = 0$, which is changed to $v(0) = -v_0$, and for $v'(0) = 0$, which is changed to $v'(0) = +r_0$ (Be sure to understand the sign convention for the rotations or slopes. For example, in the x, y plane, the deflection v is positive up, that is, in the positive y direction. The x coordinate is positive to the right. Thus dv and dx are positive in the same ways. Consider the right triangle created by the positive

¹⁰ The single roller symbol at the right end of the beam is to be understood to represent a roller on a rigid plane at both the bottom of the beam and at the top of the beam. Therefore the upwardly directed loading cannot lift the beam away from the right-hand support. Rollers and partial rollers (rockers) are frequently used support systems. They are often seen, for example, under one of the ends of highway bridges.

dx and positive dv where the hypotenuse is the deformed beam's loci of centroids. Thus a positive dv/dx defines a slope that is a counterclockwise rotation. See Endnote (1) in Chapter 11.) ■

Equations (10.7b), when applicable (uniform beam, known end loads, no appreciable axial force N), are an efficient basis for setting up the bending GDEs. The challenging aspect of writing the GDEs is describing the load per unit length. The following exercise concentrates on that aspect of the total problem.

Example 10.9. Write the GDEs and BCs for the uniform, nonhomogeneous beam shown in Fig. 10.10. The m.w. product of inertia is not zero. The equivalent thermal moments have been calculated to be as follows:

$$M_{yT}(x) = +M_0 \left[1 - \left(\frac{x}{L} \right)^2 \right] \quad \text{and} \quad M_{zT}(x) = +2M_0$$

Solution. Equations (10.7b,a) are applicable. The first task is to evaluate $f_z^c(x)$ and $f_y^c(x)$. Beginning with the equivalent thermal load per unit length, recall that

$$\begin{aligned} M_{yT}''(x) &\equiv V_{zT}'(x) \equiv f_{zT}(x) & \text{so} & \quad f_{zT}(x) = -\frac{2M_0}{L^2} \\ M_{zT}''(x) &\equiv V_{yT}'(x) \equiv f_{yT}(x) & \text{so} & \quad f_{yT}(x) = 0 \end{aligned}$$

(Note that if the x, z plane thermal moment varied linearly rather than quadratically, the equivalent thermal moments would not appear in either GDE. In that case they would only enter the analysis by means of the BCs.) For the mechanical component of the distributed loading it is necessary to write the analytical expressions that describe the loading sketched in Fig. 10.10. In the x, z plane the distributed loading decreases linearly from a magnitude

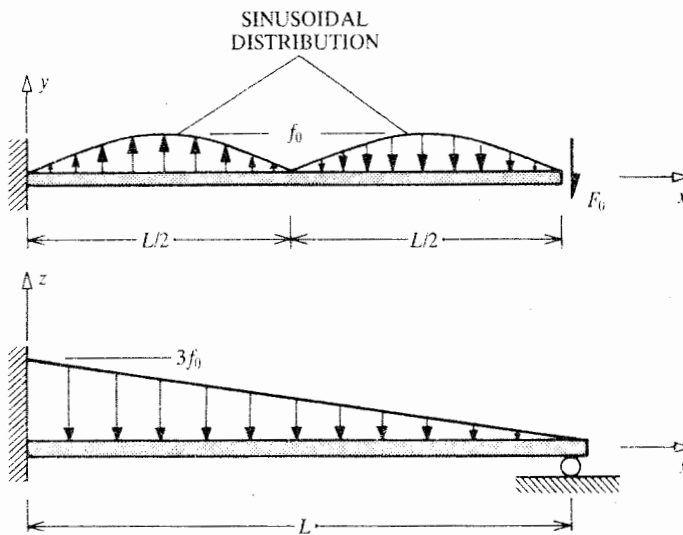


Figure 10.10. Example 10.9. (Do not overlook the concentrated force in the z plane at the beam tip.)

of $3f_0$ at $x = 0$ to zero at $x = L$. Fitting this information to the general form for a straight line yields

$$f_z(x) = -3f_0 \left[1 - \left(\frac{x}{L} \right) \right]$$

The sinusoidal distributed load in the x, y plane is described by

$$f_y(x) = +f_0 \sin \left(\frac{2\pi x}{L} \right)$$

which, while it can be deduced rationally, is probably best developed by experimentation. Now

$$f_z + f_{zT} \equiv f_z^c = -3f_0 \left(1 - \frac{x}{L} \right) - \frac{2M_0}{L^2}$$

and

$$f_y + f_{yT} \equiv f_y^c = +f_0 \sin \left(\frac{2\pi x}{L} \right)$$

As mentioned, in this case it is possible to use the ratio of inertia equations. These two equations become

$$E_0 R_{zz}^* w''''(x) = -3f_0 \left(1 - \frac{x}{L} \right) - \frac{2M_0}{L^2} - \frac{I_{yz}^*}{I_{zz}^*} [f_0 \sin(2\pi x/L)]$$

and

$$E_0 R_{yy}^* v''''(x) = f_0 \sin \left(\frac{2\pi x}{L} \right) + \frac{I_{yz}^*}{I_{yy}^*} \left[3f_0 \left(1 - \frac{x}{L} \right) + \frac{2M_0}{L^2} \right]$$

The indefinite integration of the above GDE is straightforward because each polynomial or sinusoidal function on the right-hand side is integrated separately. Turning now to the BCs, first note that the supports are not the same for both planes. Therefore it is not possible to decouple all the BCs. This means that solving for the constants of integration takes a bit more algebraic effort. The four BCs at the left-hand end are simply

$$w(0) = w'(0) = v(0) = v'(0) = 0$$

The sole deflection BC at the right end is $w(L) = 0$. The moment type BCs are $M_y(L) = M_z(L) = 0$, and the last BC is $V_y(L) = +F_0$. The last three BCs are converted into statements pertinent to the deflections as follows. From the table of alternative boundary condition equations, where

$$M_{yT}(L) = 0 \quad \text{and} \quad M_{zT}(L) = 2M_0$$

then

$$w''(L) = \frac{-M_z^c(L)}{E_0 R_{yz}^*} = -\frac{2M_0}{E_0 R_{yz}^*}$$

$$v''(L) = \frac{-M_z^c(L)}{E_0 R_{yy}^*} = +\frac{2M_0}{E_0 R_{yy}^*}$$

The BC equation for v'''' from the same table cannot be used because the value of $V_z(L)$ is not known, turning to the first BC table, it is necessary to adapt, with $V_{yT}(L) = 0$, the equation

$$[E_0 I_{zz}^* v''(L)]' + [E_0 I_{yz}^* w''(L)]' - V_{yT}(L) + m_z(L) = V_y(L)$$

which becomes

$$E_0 I_{zz}^* v'''(L) + E_0 I_{yz}^* w'''(L) = +F_0$$

This completes the statement of the required eight BCs. Again, the result of the last BC involving both bending deflection derivatives requires a bit more work in determining the constants of integration than would be necessary if all the BCs were uncoupled. ■

10.7 Summary

The challenge of a beam bending and/or extension problem is to simultaneously satisfy (i.e., solve) the GDEs and the BCs. (If the characteristics of the problem change with time, then initial conditions would also have to be met and there would be a mass–acceleration term added to the GDE.) The general form of the finite deflection beam equations, including thermal effects, is Eqs. (10.5a, b, c). When there is no appreciable axial force, and when the beam has a uniform geometry, then Eqs. (10.5a, b) can be significantly simplified as Eqs. (10.7b, a). These latter equations have the advantage that the two bending deflections are separated (decoupled) even when the m.w. product of inertia is not zero.

The general forms of the beam BC equations are presented in tabular form. In the case of the longitudinal (i.e., axial) deflections, at *each* beam end, *either* an axial deflection BC applies, *or* an axial force BC applies—never both. For the bending equations, it is always necessary to choose between (i) *either* a lateral deflection BC *or* a shearing force BC, and (ii) *either* a bending slope BC *or* a bending moment BC. The proof of this “either/or” pairing of boundary conditions must wait until Chapter 15 and is presented in Endnote (2) of that chapter. The deflection BCs are either stated or self-evident. The moment and force BCs require careful attention. The general expressions for moment and shearing force BCs are listed in the first BC table. In a second BC table the general moment and shearing force expressions are solved simultaneously for the deflection derivatives so that, whenever possible, the BC equations for the two bending deflections can be separated for the purpose of reducing the algebraic work necessary to determine the constants of integration. The exercises below and the following chapter provide many opportunities to practice solving beam equations in a variety of circumstances. Three final example problems, follow. They illustrate that (i) what occurs between the beam end points belongs in the GDEs and nowhere else; and (ii) what occurs at the beam end points belongs in the BC statements and nowhere else.

Example 10.10. Consider the unsupported beam end, where $x = \ell$, shown in Fig. 10.11. The force F_0 and the moment M_0 are externally applied loads. The product of inertia is zero, so the *tapered* beam as a whole is bending only in the plane of the paper. That is, $v(x) = 0$. Write the two boundary conditions for this beam end taking into account that

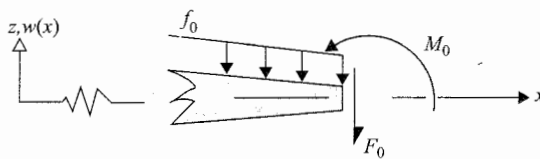


Figure 10.11. Example 10.10.

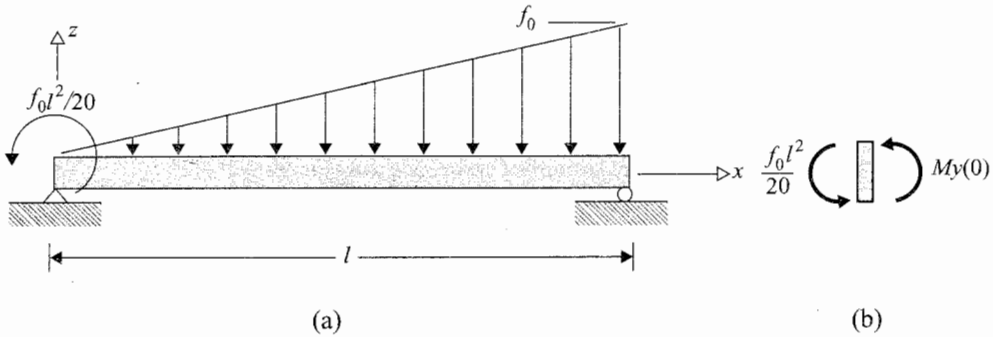


Figure 10.12. (a) Example 10.11. (b) FBD of the left beam end.

$EI_{yy}(x) = EI_0[1 - x/2\ell]$, so that $EI_{yy}(\ell) = EI_0/2$, and that there are temperature changes that cause the following equivalent bending moment in the plane of the paper:

$$M_{yT}(x) = 2M_0 \left[\frac{3x}{\ell} - 1 \right]$$

Solution. Since neither the deflection nor the bending slope is known at $x = \ell$, it is necessary to write a statement about the internal shear force and internal bending moment there. This task requires drawing a FBD of a differential length of beam at the beam end. By summing forces and moments there, the FBD provides the equations $M_y(\ell) = +M_0$, and $V_z(\ell) = +F_0$. The load per unit length acting over the differential length only produces an infinitesimal force, which, of course, is discarded. Noting $M_{yT}(\ell) = +4M_0$, and $V_{zT}(\ell) = +6M_0/\ell$, and using the first BC table, the bending moment boundary condition is

$$\frac{1}{2}EI_0w''(\ell) = 4M_0 + M_0 \quad \text{or} \quad w''(\ell) = \frac{10M_0}{EI_0}$$

Using the first BC table for the shearing force, taking into account that since the beam is tapered, the stiffness coefficient has a derivative as well as the deflection, and using the product rule for the derivative, lead to

$$\begin{aligned} EI'_{yy}(\ell)w''(\ell) + EI_{yy}(\ell)w'''(\ell) &= V_{zT}(\ell) + V_z(\ell) \\ \text{or} \quad -\frac{EI_0}{2\ell}w''(\ell) + \frac{EI_0}{2}w'''(\ell) &= 6\frac{M_0}{\ell} + F_0 \\ \text{or} \quad w''(\ell) - \ell w'''(\ell) &= \frac{-2F_0\ell}{EI_0} - \frac{12M_0}{EI_0} \quad \blacksquare \end{aligned}$$

Example 10.11. (a) The uniform, homogeneous, beam shown in Fig. 10.12 is loaded only in the x, z plane as shown. The beam cross-section is nonsymmetric, and its cross-sectional properties are

$$I_{yy} = 2I_0 \quad I_{zz} = 3I_0 \quad I_{yz} = -I_0$$

Write, but do NOT integrate, the two fourth-order, governing differential equations that describe the bending deflections of this beam.

(b) With the supports in the x, y plane being the same as those shown for the x, z plane, write the eight boundary conditions appropriate for this beam.

Solution.

$$(a) \quad 2EI_0 w''''(x) - EI_0 v''''(x) = -\frac{x}{l} f_0$$

$$-EI_0 w''''(x) + 3EI_0 v''''(x) = 0$$

or, after solving simultaneously, the simplified equations to be integrated are

$$EI_0 v''''(x) = -\frac{x f_0}{5l} \quad \text{and} \quad EI_0 w''''(x) = -\frac{3x f_0}{5l}$$

(b) The preliminary eight BC statements are

$$v(0) = w(0) = v(l) = w(l) = 0,$$

$$M_y(0) = -\frac{f_0 l^2}{20}, \quad M_z(0) = 0, \quad \text{and} \quad M_y(l) = M_z(l) = 0$$

Converting the latter four BCs to statements involving the derivatives of the deflections leads to

$$2EI_0 w''(0) - EI_0 v''(0) = -\frac{f_0 l^2}{20} \quad 2EI_0 w''(l) - EI_0 v''(l) = 0$$

$$-EI_0 w''(0) + 3EI_0 v''(0) = 0 \quad -EI_0 w''(l) + 3EI_0 v''(l) = 0$$

or, after solving the above four equations simultaneously, the simplest forms of these latter four BCs are

$$EI_0 w''(0) = -0.03 f_0 l^2 \quad w''(l) = 0$$

$$EI_0 v''(0) = -0.01 f_0 l^2 \quad v''(l) = 0$$

Example 10.12. For the loading and the uniform, homogeneous beam shown in Fig. 10.13: (a) write the lateral deflection GDEs and the corresponding BCs; write those equations in uncoupled form to the extent possible; and (b) integrate and apply the BCs so as to determine the continuous expressions for the deflections. The beam cross-section and the

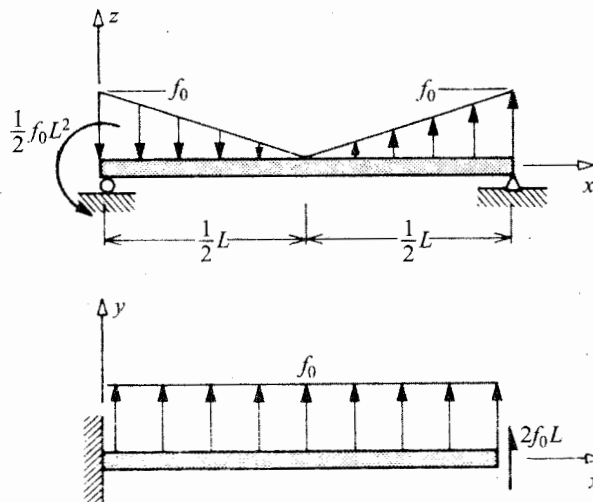


Figure 10.13. Example 10.12.

thermal loading are such that

$$I_{yy} = I_{zz} = 2I_0 \quad \text{and} \quad I_{yz} = -I_0$$

$$M_{yT}(x) = f_0L^2 \quad \text{and} \quad M_{zT}(x) = \frac{f_0L^2}{3} \left(3 - \frac{x}{L}\right)^2$$

Solution. (a) A FBD quickly establishes the fact that $N(x) = 0$. The other quantities necessary to write the GDEs are

$$R_{zz} = R_{yy} = \frac{3}{2}I_0 \quad R_{yz} = -3I_0 \quad V_{yT}(x) = -\frac{2}{3}f_0L \left(3 - \frac{x}{L}\right)$$

$$f_{yT}(x) = \frac{2}{3}f_0, \quad f_y(x) = f_0, \quad \text{and thus} \quad f_y^c(x) = \frac{5}{3}f_0$$

$$f_z(x) = f_z^c(x) = f_0 \left(\frac{2x}{L} - 1\right) \quad m_y(x) = m_z(x) = 0$$

Using Eqs. (10.7), which are the uncoupled forms of the GDEs, the result is

$$EI_0w''''(x) = \frac{4f_0x}{3L} - \frac{f_0}{9} \quad \text{and} \quad EI_0v''''(x) = \frac{2f_0x}{3L} - \frac{7f_0}{9}$$

The eight deflection BCs are

$$\text{(i-iv)} \quad w(0) = w(L) = v(0) = v'(0) = 0$$

The initial forms of the force-type BCs are, from FBDs of the beam ends,

$$\text{(v)} \quad M_y(0) = -\frac{1}{2}f_0L^2 \quad \text{(vi)} \quad M_y(L) = 0$$

$$\text{(vii)} \quad M_z(L) = 0 \quad \text{and} \quad \text{(viii)} \quad V_y(L) = -2f_0L$$

Equations (vi) and (vii) can be used together to write uncoupled BC equations for the second derivatives of the two deflections. From the second BC table, these two BC equations are

$$\text{(vi)} \quad EI_0w''(L) = \frac{2}{3}f_0L^2 + \frac{4}{9}f_0L^2 = \frac{10}{9}f_0L^2$$

$$\text{(vii)} \quad EI_0v''(L) = \frac{8}{9}f_0L^2 + \frac{1}{3}f_0L^2 = \frac{11}{9}f_0L^2$$

Since Eqs. (v) and (viii) cannot be paired with corresponding information in the other orthogonal plane, these two BC equations have to be written in coupled form. From the first BC table,

$$\text{(v)} \quad -\frac{1}{2}f_0L^2 = -EI_0v''(0) + 2EI_0w''(0) - f_0L^2$$

or

$$2EI_0w''(0) - EI_0v''(0) = \frac{1}{2}f_0L^2$$

or

$$\text{(viii)} \quad -2f_0L = 2EI_0v'''(L) - EI_0w''' + \frac{4}{3}f_0L$$

$$2EI_0v'''(L) - EI_0w'''(L) = -\frac{10}{3}f_0L$$

(b) Integrating the two field equations is straightforward. The results are

$$EI_0w(x) = \frac{f_0}{90L}x^5 - \frac{f_0}{216}x^4 + \frac{C_1}{6}x^3 + \frac{C_2}{2}x^2 + C_3x + C_4$$

$$EI_0v(x) = \frac{f_0}{180L}x^5 - \frac{7f_0}{216}x^4 + \frac{C_5}{6}x^3 + \frac{C_6}{2}x^2 + C_7x + C_8$$

Application of the BC equations $w(0) = v(0) = v'(0)$ immediately leads to the result that $C_4 = C_7 = C_8 = 0$. The BC $w(L) = 0$ and the four-force type BCs produce the following five simultaneous equations:

$$\begin{aligned} C_1 L^2 + 3C_2 L + 6C_3 &= -\frac{7}{180} f_0 L^3 \\ 2C_2 - C_6 &= \frac{9}{18} f_0 L^2 & C_1 L + C_2 &= \frac{17}{18} f_0 L^2 \\ C_5 L + C_6 &= \frac{13}{18} f_0 L^2 & 2C_5 - C_1 &= -\frac{90}{18} f_0 L \end{aligned}$$

The last four have to be solved together. The result is

$$\begin{aligned} C_1 &= -\frac{22}{18} f_0 L & C_2 &= \frac{39}{18} f_0 L^2 & C_5 &= -\frac{56}{18} f_0 L \\ C_6 &= \frac{69}{18} f_0 L^2 & \text{and then} & & C_3 &= -\frac{319}{360} f_0 L^3 \end{aligned}$$

Substitution of these constants of integration into the solutions for the deflections produces the result, where $\xi = x/L$,

$$\begin{aligned} w(x) &= \frac{f_0 L^4}{1080 EI_0} (12\xi^5 - 5\xi^4 - 220\xi^3 + 1170\xi^2 - 957\xi) \\ v(x) &= \frac{f_0 L^4}{1080 EI_0} [6\xi^5 + 35\xi^4 - 560\xi^3 + 2070\xi^2] \end{aligned}$$

It is not difficult to check and see that these two solutions satisfy the GDEs and the BCs. The second derivatives of these solutions substituted into Eq. (9.4b) can be used to study the stress distribution in the beam. ■

Endnote (4) presents one final example problem where the governing differential equation is integrated for a nonuniform beam.

Chapter 10 Exercises

- 10.1.** (a) Derive Eq. (10.1d).
 (b) Derive Eq. (10.1e).
 (c) Derive (10.1f).
 (d) Rederive Eq. 10.4(a) for the special circumstance of bending only in the x, z plane as shown in Fig. 10.14. Note that the differential length of beam has the shape of a circular arc with a radius of curvature R , and the infinitesimal angle subtended by the infinitesimal beam length is $d\theta_y \equiv dw' = \frac{dw'}{dx} dx = w'' dx$. Keep in mind $\sin(dw') = w'' dx$, and $\cos(dw') = 1.0$.
 (e) Use Fig. 10.14 to derive Eq. (10.4b).
- 10.2.** Using only the beam axial deflection equations, calculate the axial force $N(x)$ in the homogeneous, nonuniform bar shown in Fig. (10.15), where there is a uniform axial force per unit length in the positive x direction of magnitude f_0 , and
 (a) $EA(x) = EA_0[3 - (x/L)]$, and $N_T(x) = -N_0[(1/2) - (x/L)^2]$;
 (b) $EA(x) = EA_0[4 - 3(x/L)]$, and $N_T(x) = -N_0[(2) - (x/L)^2]$.
 (c) Calculate the axial tip deflection of a horizontal, uniform, cantilevered beam of length L that is rotating about a vertical axis at its clamped end with a constant angular velocity Ω . Let A_0 be the constant area of the beam cross-section, and ρ be the beam material mass density. *Hint:* The outwardly directed centrifugal force per unit length is $x\rho A_0\Omega^2$ where x is measured from the clamped beam end.

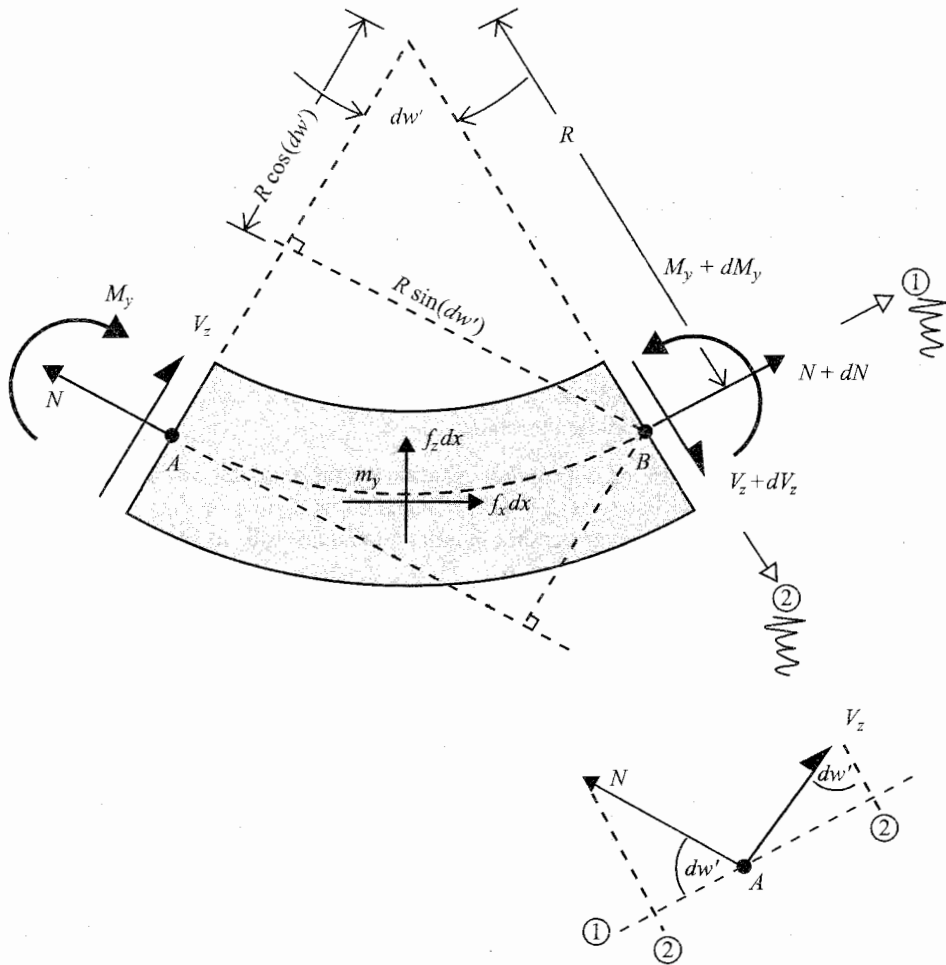


Figure 10.14. Exercises 10.1(d) and (e).

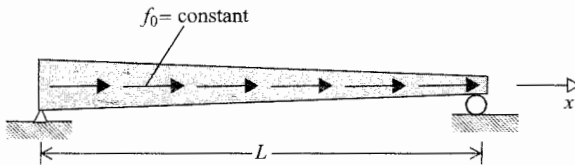


Figure 10.15. Exercise 10.2.

10.3. Calculate all three deflection functions for a uniform, homogeneous beam of length L that is cantilevered at the origin of the x coordinate axis and unsupported (free) at its other end, if the product of inertia is zero, and if the only loading is in the x, z plane, such that:

- (a) The loading is a lateral force per unit length in the positive z direction that varies linearly from a magnitude of f_0 at $x = 0$ to zero at $x = L$.

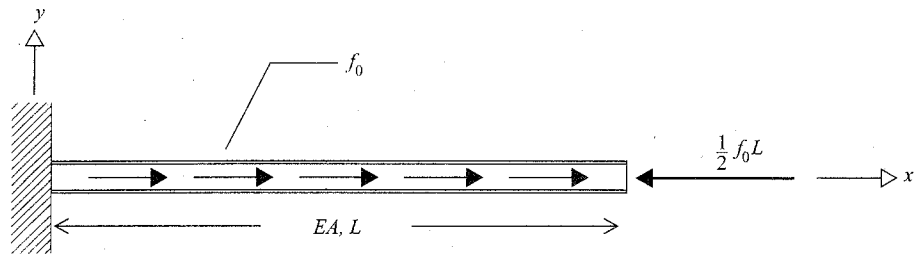


Figure 10.16. Exercise 10.4

- (b) The loading is both a concentrated force at the free end of magnitude F_0 acting upward, and a concentrated moment at the free end of magnitude M_0 acting in the counterclockwise direction.

- 10.4. (a) Write the governing differential equation for the axial deflections of uniform, homogeneous bar (i.e., $EA = \text{const.}$) loaded as shown in Fig. 10.16 with a constant axial loading per unit length and an end load. In addition, there is a thermal loading of magnitude

$$N_T = f_0 L \left(2 - \frac{x}{L} \right)$$

- (b) For the same beam and loading as above, write the axial deflection boundary conditions.
 (c) Determine $u(x)$.

- 10.5. Consider a tall, straight tower modeled as a beam. Let the tower height be L , the constant stiffness coefficient be EA , and the uniform weight per unit length of the tower be $\rho g A$. The tower supports a large weight Mg at its top. Let the axial coordinate x originate at the tower base. Determine the expression for the axial deflections of the tower, and the expression for the stress in the tower.

- 10.6. Consider the beam shown in Fig. 10.17 in both plan view and side view. The following data apply to this beam

$$E_0 = E \quad I_{yy}^* = 2I_0 \quad I_{zz}^* = 3I_0 \quad I_{yz}^* = -I_0 \quad N = N_T = 0$$

$$M_{yT} = \frac{f_0 L^2}{20} \left[2 - \frac{x^2}{L^2} \right] \quad M_{zT} = \frac{f_0 L^2}{30} \left[3 - \frac{x^2}{L^2} \right]$$

Write the *coupled* governing differential equations that describe the bending of this beam.

- 10.7. Consider the uniform, homogeneous beam shown in Fig. 10.18. There is neither a temperature change nor an axial loading. However the product of inertia is not zero, and because of a misfit the right-hand beam support is a distance d_0 above the otherwise undeformed beam axis. Determine the bending slope at $x = L$ by solving appropriate differential equations. (Note that unless otherwise specified, the support conditions, less enforced deflections, are the same in the x, y plane, and there is no loading in the x, y plane).

- 10.8. For the same beam of Exercise 10.7, discard the enforced deflection and replace the previous lateral force per unit length by one that acts in the negative z direction

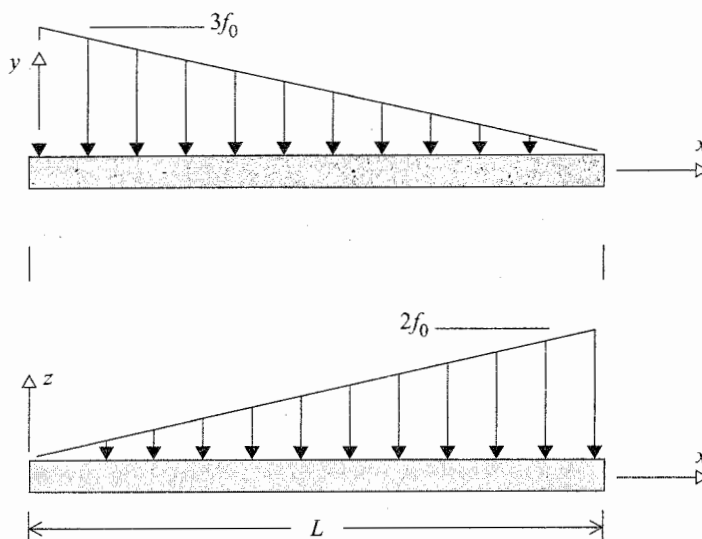


Figure 10.17. Exercise 10.6.

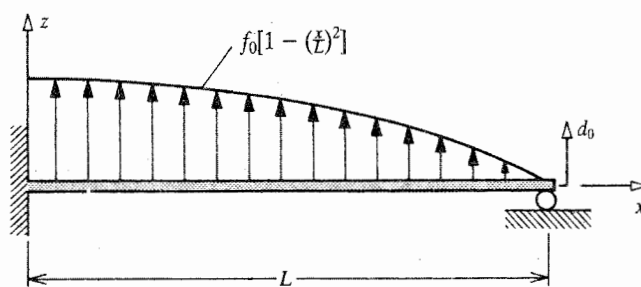


Figure 10.18. Exercises 10.7 and 10.8.

and varies linearly from a magnitude of f_0 at the fixed end to zero at the roller end, and a clockwise moment, M_0 , at the roller end, also in the x, z plane. Then calculate the deflection functions.

- 10.9.** Using the Bernoulli–Euler beam deflection theory, calculate the vertical deflection at the center of the simply supported beam shown in Fig. 8.2 and compare that result with Eq. (8.5). Note the BCs are at $x = -a$ and at $x = +a$. The uniform force per unit length, f_y , is the pressure p multiplied by the beam thickness, t . Recall that the beam cross-section is rectangular.
- 10.10.** (a) If a uniform, homogeneous, cantilevered beam of length L is subjected to a temperature change equal to $T_1x + T_2z$, where T_1, T_2 are constants with appropriate units, and the x axis originates at the fixed end, what then are the tip deflections $u(L), v(L)$, and $w(L)$? Let $I_{yy} = I$, and $I_{zz} = I_{yz} = I/10$, and let the modulus of elasticity be unchanged by the temperature change.
- (b) As above, but this time let $I_{yy} = 2I, I_{zz} = I$, and $I_{yz} = -I$.
- (c) As above, but this time let $I_{yy} = I, I_{zz} = I/2$, and $I_{yz} = -I/10$.

- (d) As in case (a), but this time the temperature change is $T_3(b^3 + z^3)$, where b is the half-depth of the beam.
- 10.11.** If a uniform, homogeneous, fixed–fixed beam of length L is loaded in the x, z plane by a uniform force per unit length of magnitude f_0 , as shown in Fig. 10.8, then determine the magnitudes of the bending moments at the center of the beam and at the clamped ends. This time let $I_{yy} = I$, and $I_{zz} = I_{yz} = I/10$.
- 10.12.** For the beam of Exercise 10.10, replace the equivalent thermal loading by a uniform force per unit length in the x, z plane of magnitude $2f_0$ in the positive z direction, and a uniform force per unit length in the x, y plane of magnitude f_0 the positive y direction, and again calculate the tip deflections. (Note that these two distributed loadings can be considered to be the vector components of one distributed loading.)
- 10.13.** Determine the deflections of the beam in Exercise 10.11 if the distributed loading is changed to:
- (a) A force per unit length in the x, z plane in the positive z direction that increases linearly from zero at the left end to a value of $3f_0$ at the right end, and again no load in the x, y plane.
- (b) A force per unit length in the z direction that increases sinusoidally from zero at both beam ends to its single maximum value of $2f_0$ at the beam center, and a force per unit length that has the same distribution in the y direction, but has only half that magnitude.

FOR THE ESPECIALLY EAGER

- 10.14.** Rederive Eqs. (10.5a, b) so as to include the bending and twisting interaction terms that were dropped in the original derivation.
- 10.15.** As opposed to the familiar rigid end beam supports, that is, supports that act at single points, an *elastic* or *Winkler foundation* is a distributed beam support that acts along the length of the beam. An elastic foundation is assigned a stiffness k (in units of force divided by length squared, that is, lateral force per unit of lateral deflection per unit of beam length). What this means is that the elastic foundation reacts to beam deflections in a linear fashion at any foundation supported point along the length of the beam with a lateral force per unit length at the point of deflection equal to k multiplied by the magnitude of the beam lateral deflection. The next paragraph illustrates mathematically how the Winkler foundation interacts with a beam. The Winkler foundation is conventionally symbolized by a very large number of independent, small coiled springs connecting, say, a beam bottom and a rigid plane beneath the beam. The “elastic foundation” is used as an imperfect model for elastic supports that are actually continuous (and thus the deflections of which are not truly independent of each other), because a truly continuous elastic support presents greater mathematical difficulties. Wooden railroad ties on a crushed rock bed that support the beams that are the railroad tracks, and, say, the epoxy matrix supporting a single, long carbon fiber against bending would be suitably modeled using this mathematical device.

Consider a simply supported beam of length L on a Winkler foundation. Let the y, z axes be principal axes, and let the only loading be a uniform distributed loading in the x, z plane acting in the positive z direction with a magnitude of f_0 . Then $u = v = 0$, and the remaining GDE and BCs are

$$EI_{yy}w''''(x) = f_0 - kw(x) \quad w(0) = w''(0) = w(L) = w''(L) = 0$$

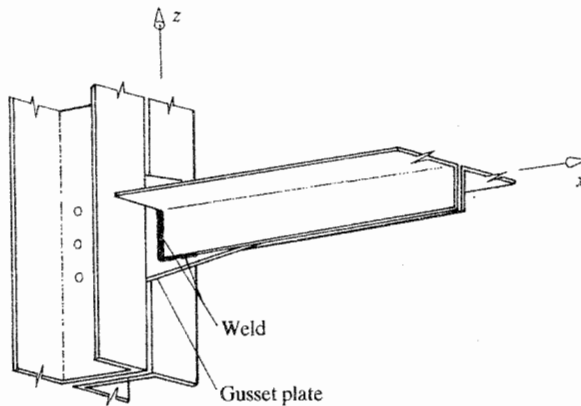


Figure 10.19. A possible origin for a clamped (or continuous) beam boundary condition within a structure.

The Winkler foundation is seen to provide a distributed reacting force per unit length along the length of the beam that is proportional to the beam deflection $w(x)$. The reader's task is to traverse the algebraic jungle in order to obtain the general solution for the bending deflection $w(x)$.

10.16. (a) Derive Eq. (10.4b).

(b) Derive Eq. (10.4e).

10.17. After the first integration in Exercise 10.2(b), the result is $EA(x)u'(x) = f_0(L - x) + N_T(x)$. Use the given values of $EA(x)$ and $N_T(x)$ to determine the solution for $u(x)$. Tables of integration formulas may be used if needed. Endnote (4) might also be helpful.

Endnote (1) Different BCs in Different Planes at the Same Beam End

Consider the double angle beam end shown in Fig. 10.19. This typical civil or marine engineering type of connection illustrates the first point of this endnote. Each of the two symmetrically arranged angle beams is welded at its top, end, and bottom (dark lines) to a gusset plate that in turn is well anchored to the remainder of the structure. Since the thin gusset plate is very stiff in bending about the y axis, but relatively easily bent about the z axis, and since the welded connection allows virtually no relative motion between the angle beams and the gusset plate, then it is reasonable to model this beam end as clamped to (i.e., continuous with) the remainder of the structure in the x, z plane and simply supported, with respect to the remainder of the structure, in the x, y plane. If rivets or bolts, rather than welds, were used to make the connection between the angle beams and the gusset plate, and the number of rivets or bolts were only two or three arranged in a single row, then the connection in the x, z plane might best be modeled as being a simple support too because of the clearances that are typical between a bolt or rivet shank and the bolt hole or rivet hole. If there were two rows of bolts and each row had, say, four bolts, then a fixed connection model between the beam and the column could be more appropriate. Thus it is quite possible to have different types of BCs in different planes at the same beam end.

A reasonable clamped-end model for an individual beam is uncommon, but can occur in the sort of situation sketched in Fig. 10.20. Because of the symmetry of the continuous beam and the loading, the rotation at the middle support must be zero. Hence this continuous

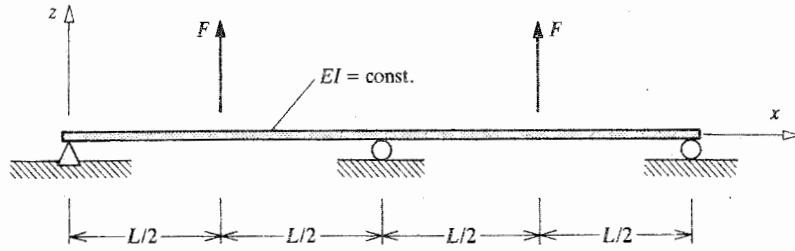


Figure 10.20. A possible source for a “clamped” boundary condition for a single beam.

beam of length $2L$ over three supports can be modeled as a single beam of length L over two supports by having the left half-length simply supported at $x = 0$, and clamped at $x = L$.

Deciding upon the mathematical description of the BCs of a beam depends partly upon what the analyst is attempting to do, as well as the manner in which the beam is attached to other parts of the structure. For example, if the analyst is investigating the natural wind dynamic response of a beam structure with riveted and bolted connections, the analyst would generally tend at first to describe the beam ends as being simply supported because then the beam structure would be less stiff, and hence more likely to respond dynamically (and hence detrimentally) to natural wind forces with their predominantly lower loading frequencies with respect to time. However, if the response of the same beam structure was being investigated when the loading was an earthquake loading consisting of relatively higher frequency components, then the analyst, in order to be properly pessimistic, would tend to first view the beam connections as fixed so that again the structure would be more likely to respond dynamically to the applied loading.

Endnote (2) The Nonlinear Form of the Axial Deflection Equation

There is a variety of Eq. (10.5c) that is worth mentioning to complete the loop of interactions between the axial (u) and the longitudinal (v, w) deflections. As Eq. (10.5c) stands there is no effect on the beam u deflection by the presence of v and w deflections. On the other hand, the v and w deflections are influenced by the presence of a u deflection through the agency of the axial force $N(x)$ which involves $u'(x)$. This interaction omission can be overcome by extending the formula for the axial strain to the nonlinear form of the axial strain stated in Eqs. (3.11) or, better yet, from (3.7) because of the small size of $u(x)$ and its derivatives relative to $v(x)$ and $w(x)$ and their derivatives. Thus, for this purpose, the Bernoulli–Euler nonlinear strain–deflection equation becomes

$$\epsilon_{xx}(x, y, z) = u' + \frac{1}{2}[(v')^2 + (w')^2] - yv'' - zw''$$

Substitution of the above into the Bernoulli–Euler stress–strain equation, Eq. (9.4b) leads to

$$\sigma_{xx}(x, y, z) = E \left\{ u' + \frac{1}{2} [(v')^2 + (w')^2] - yv'' - zw'' - \alpha \Delta T \right\}$$

Then using the fact that the axial force $N(x)$ is equal to the integral of σ_{xx} over the cross-sectional area, and the relation $N'(x) = -f_x(x)$, and the similar thermal definition, leads to

$$[E_0 A^* u'(x)]' + \frac{1}{2} \{ E_0 A^* [(v')^2 + (w')^2] \}' = -f_x^c(x)$$

which is, of course, the extension of Eq. (10.5c) to include the effects of the bending deflections upon the axial deflection. This equation is highly nonlinear and consequently difficult to

manage in almost all circumstances. However, a simple solution to a special case of this equation can be found, for example, in Ref. [16]. That solution suggests that the nonlinear terms of the above equation are only of importance when both (i) the beam ends are supported in a fashion that requires the beam to stretch when it bends, and (ii) the maximum lateral deflection is of a magnitude of approximately one-quarter to one-third of the beam depth or more.

Endnote (3) The Presence of the Moment per Unit Length Terms in the Shear Force Boundary Condition Expressions

It is quite easy to demonstrate that if a thin, rectangular sheet of cardboard or other flexible material is placed over a slightly smaller rectangular opening (so as to provide simple support boundary conditions for this rectangular plate) and the center of this rectangular plate is forced downward, then the corners of the rectangular plate tend to lift off the support. It is well known by those acquainted with thin plate theory that: (i) the equilibrating reaction along those parts of the support that remain in contact with the flat plate is in the form of an upward, varying force per unit of support length; and (ii) if the corners of the rectangular plate are attached to the support, and thus prevented from lifting off the support, intense reacting forces per unit of support length occur at the corners. The rise in intensity is so sharp as to virtually amount to having downward acting concentrated forces at the plate corners. Both a descriptive and a mathematical explanation for the origin of these concentrated plate corner forces, involving the twisting moments per unit of edge length acting upon the plate edges, can be found, for example, in Ref. [52] or Chapter 22 of this text. The point of this discussion is that the beam shear force BC equations derived in this chapter show that the beam moments per unit length at the beam ends produce the same effect upon the beam (end forces) as the twisting moments per unit length produce upon the plate (corner forces). In other words, the effect of the presence of the moment per unit length terms in the shear force BC equations for long beams is quite analogous to the perhaps better-known corner forces that act on thin plates.

Endnote (4) Exact Integrations for a Nonuniform Beam

It is infrequently the case that an engineer in industry or government finds it useful to integrate a GDE in the fashion described below because numerical techniques are the usual fare. However, such integrations are occasionally necessary, particularly when doing research. For this reason, this slightly more complicated integration is discussed.

Example 10.13. Write the GDE and BCs for the nonuniform bar of length L loaded as shown in Fig. 10.21. The axial stiffness factor and the equivalent thermal axial force are the following functions of x :

$$EA(x) = EA_0 \left(3 - \frac{x}{L}\right) \quad N_T(x) = f_0 L \left(2 - \frac{x}{L}\right)^2$$

Solution. The general GDE is $(d/dx)[EA(x)u'(x)] = -f_x(x) - f_{xT}(x)$. Here $f_x(x) = f_0[2 - (x/L)]$ and $f_{xT}(x) = -N_T'(x) = +2f_0[2 - (x/L)]$. Hence the specific GDE is

$$\frac{d}{dx} \left[EA_0 \left(3 - \frac{x}{L}\right) u'(x) \right] = -3f_0 \left(2 - \frac{x}{L}\right)$$

As is seen by examining the solution to this equation, it is best *not* to differentiate the product $EA(x)u'(x)$. The first BC is simply $u(0) = 0$. The second BC is $N(L) = +f_0L$.

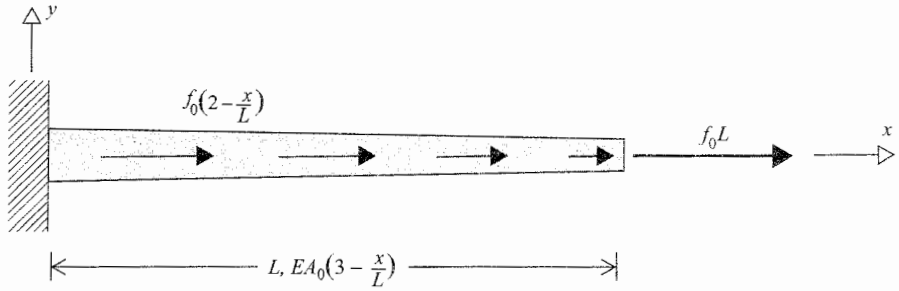


Figure 10.21. Example 10.13

Using the first BC table, and noting that $EA(L) = 2EA_0$ and $N_T(L) = f_0L$, this second BC can be written in terms of the deflection as

$$f_0L = 2EA_0u'(L) - f_0L \quad \text{or} \quad u'(L) = \frac{f_0L}{EA_0}$$

The first of the two integrations is quite simple. Multiply both sides of the GDE by dx . The left-hand side is then an exact differential. Then indefinite integration yields

$$EA_0 \left(3 - \frac{x}{L}\right) u'(x) = C_1 - 3f_0L \left[2\frac{x}{L} - \frac{1}{2}\left(\frac{x}{L}\right)^2\right]$$

Divide by $[3 - (x/L)]$ so as to isolate the unknown function $u'(x)$:

$$EA_0u'(x) = \frac{C_1}{3 - (x/L)} - \frac{3f_0L}{2} \frac{(x/L)^2 - 4(x/L)}{(x/L) - 3}$$

Again multiply both sides by dx to obtain an exact differential on the left-hand side. In the first term on the right-hand side, note that $dx = -Ld[3 - (x/L)]$. In the numerator of the second term on the right-hand side, add and subtract 3, and then factor. That is,

$$\begin{aligned} \left[\left(\frac{x}{L}\right)^2 - 4\left(\frac{x}{L}\right)\right] &= \left[\left(\frac{x}{L}\right)^2 - 4\frac{x}{L} + 3\right] - 3 \\ &= \left[\frac{x}{L} - 3\right]\left[\frac{x}{L} - 1\right] - 3 \end{aligned}$$

Then integrate indefinitely to obtain

$$EA_0u(x) = C_2 - C_1L \int \frac{d[3 - (x/L)]}{3 - (x/L)} - \frac{3f_0L}{2} \int \left(\frac{x}{L} - 1 + \frac{3}{[3 - (x/L)]}\right) dx$$

If the denominator were more complicated than it is in this case, the partial fractions technique can be used to simplify the integrand. Again writing $dx = -Ld[3 - (x/L)]$ in the last integral,

$$EA_0u(x) = C_2 - C_1L \ln\left(3 - \frac{x}{L}\right) - \frac{3f_0L^2}{4} \left[\left(\frac{x}{L}\right)^2 - 2\frac{x}{L} - 6 \ln\left(3 - \frac{x}{L}\right)\right]$$

Note that absolute values are not necessary for the logarithm because the minimum value for $3 - (x/L)$ is $+2$. Since there are two identical logarithm functions, it is convenient to

combine them into one term with a unknown constant. That is, let $C_3 = 9f_0L^2/2 - C_1L$, so that

$$EA_0u(x) = C_2 + C_3 \ln\left(3 - \frac{x}{L}\right) - \frac{3f_0L^2}{4} \left[\left(\frac{x}{L}\right)^2 - 2\frac{x}{L}\right]$$

This is the general form of the solution for $u(x)$ in terms of two constants of integration. Now it is only necessary to apply the two BCs: (i) $u(0) = 0$, and (ii) $EA_0u'(L) = f_0L$. The first BC yields

$$C_2 = -C_3 \ln 3$$

Then

$$EA_0u(x) = C_3 \ln\left(1 - \frac{x}{3L}\right) - \frac{3f_0L^2}{4} \left[\left(\frac{x}{L}\right)^2 - 2\frac{x}{L}\right]$$

with

$$EA_0u'(x) = -\frac{C_3/3L}{1 - (x/3L)} - \frac{3f_0L}{2} \left[\frac{x}{L} - 1\right]$$

the second BC yields $-2f_0L^2 = C_3$. Hence the final form of the solution, which satisfies the GDE and the BCs, is

$$EA_0u(x) = -2f_0L^2 \ln\left(1 - \frac{x}{3L}\right) - \frac{3f_0L^2}{4} \left[\left(\frac{x}{L}\right)^2 - 2\frac{x}{L}\right]$$

or

$$EA_0u(x) = +2f_0L^2 \ln\left(\frac{3L}{3L-x}\right) + \frac{3f_0L^2}{4} \left[2\left(\frac{x}{L}\right) - \left(\frac{x}{L}\right)^2\right]$$

Note that the second term is also a positive term for the range of x/L that applies here. ■

Additional Beam Bending Topics

11.1 Introduction

This chapter introduces three topics that expand the usefulness of the Bernoulli–Euler beam bending and extension equations developed in the previous chapter. The first topic is elastic beam end supports. The use of elastic end supports begins the process, developed further in Part V, of modeling beams that are parts (elements) of larger elastic structures. The second topic is partial span distributed loads, and concentrated loads acting at points other than the beam ends. Then, both as another form of loading, and as a prelude to the third topic, combined lateral and axial loading cases are also examined. The third topic is beam buckling. This chapter provides only a brief introduction to beam buckling theory. However, some of the complexities of the topic are mentioned without being explored mathematically. The mathematical differences between the one standard type of buckling analysis introduced here and all the other beam analyses of this chapter and Chapter 10 are underscored. Additional aspects of beam and plate buckling theory are provided in Part VI.

Before proceeding to these three topics, it is worthwhile mentioning again a limitation on the scope of the beam bending theory developed in Chapter 10 which is retained in this chapter. That limitation is that the bending deflections are small. Thus it is possible to confine the axial and bending interactions to the bending equations, and to deal with the bending and twisting deflections separately, without regard for any interaction between them. Chapter 10 discusses this limitation with respect to axial and bending deflections. Endnote (4) at the end of this chapter elaborates upon this limitation with regard to bending and twisting deflections.

11.2 The Concept of Elastic Boundary Conditions

In all the problems of the previous chapter, the beam end supports were either “rigid” or, in the case of a free end, nonexistent. When the supports are modeled as rigid, either the deflection or rotation or both have a fixed value, usually zero, that is entirely independent of the magnitude of the applied loading. There are often circumstances when a better model for a beam support is one that, like the beam itself, also deflects in response to the applied load. After all, no object is truly rigid. The so-called rigid support is only an approximation for a support that either deflects considerably less than the structure it supports, or whose deflected position is simply a convenient datum from which to reference the deflections of the supported structure. When a support does have a significant deformation that is best counted as part of total deflection, but does not dissipate energy, it is called an *elastic support*. The BCs associated with elastic supports are, of course, called *elastic boundary conditions*.

Before discussing elastic supports themselves, it is necessary to first discuss the structural element that is used to represent (i.e., mathematically model) all elastic supports. That structural element, the linear coiled spring, is the simplest of all structural elements. Aside

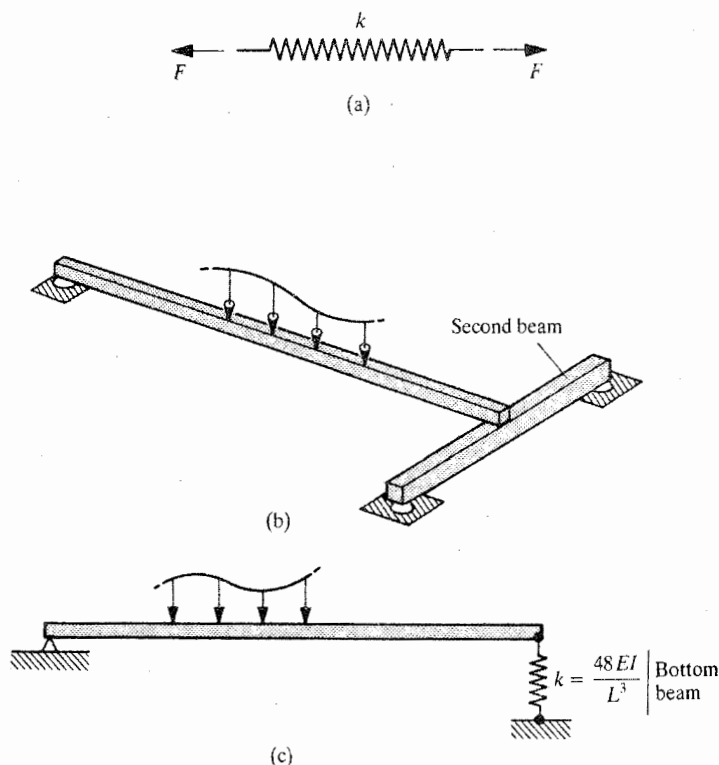


Figure 11.1. (a) The coiled (or helical) spring element as a replacement for any more complicated structure loaded at a single point. (b) A two-beam structure that can be simplified by introducing an equivalent coiled spring for the second beam. (c) The single beam (in-plane) mathematical model for the original two-beam structure.

from some suspension systems, coiled springs as physical realities are rarely if ever structural components of vehicular structures. However, coiled springs are often used to represent parts (called substructures) of a larger structure, and when the substructure is viewed as a support for the beam or other component under study, the substructure is called an elastic support. Linear springs are chosen for this modeling role because their force–deflection description is the very simple algebraic relation

$$F = ku$$

where k is the spring stiffness factor, which is analogous to EI in a beam or EA in a bar; F is an arbitrary force in the spring axis direction, positive when tensile as shown in Fig. 11.1(a); and u is the relative deflection of the two spring ends. When one spring end is fixed against motion, then of course u is the total deflection of the other spring end.

The spring shown in Fig. 11.1(a) is specifically a rectilinear spring since the transmitted force and the associated deflection act in a straight line. A rotational spring is exactly like a rectilinear spring except that where the rectilinear spring is a device for forces and rectilinear deflections, the rotational spring relates moments and rotational deflections according to the formula

$$M = K\theta$$

The following two paragraphs provide a simple example where one beam can be modeled as an elastic support for another beam by use of one or more linear springs. Consider the top beam shown in Fig. 11.1(b) which has a rigid support at its left end, and at its right end rests on a second beam, at that bottom beam's midspan, without having a firm connection (such as that produced by extensive welding or several bolts or rivets) between the two beams. Since the bottom beam is simply supported and has a zero product of inertia, the relation between the downward force F_b transmitted from the top beam to the bottom beam midspan, and the lateral midspan deflection of the bottom beam, w_b , can be shown to be¹

$$F_b = \frac{48EI_b}{L_b^3} w_{max} = k_b w_b$$

Thus, an equivalent rectilinear spring of stiffness $48EI_b/L_b^3$ can be used to replace the bottom beam in the analysis model for the top beam, as shown in Fig. 11.1(c), because both the bottom beam and the rectilinear spring have the same effect upon the top beam in every respect. That is, the top beam has the same deflections and stresses with either the bottom beam support or the linear spring support. This example therefore illustrates the use of a linear spring to model what is essentially a three-dimensional beam configuration in the much more convenient arrangement of two dimensions.

If now the two beams are firmly attached so that not only their lateral deflections at the joint are the same, but their rotations at the joint are also the same (called a rigid joint), then the bottom beam would have to twist as the top beam developed a bending slope at its right-hand end. Since, in this adjusted circumstance, the top beam's bending slope is inhibited by the elastic torsional stiffness of the bottom beam, the analysis model of the top beam in Fig. 11.1(c) needs now to be augmented by the inclusion of a rotational spring as well as the original rectilinear spring at the right-hand end of the top beam. (The torsional characteristics of beams are discussed in the chapters that immediately follow this one.) A spiral form, such as is shown in Fig. 11.2(a), is used as the symbol for a rotational spring (from the form of such springs as the main springs of the wholly mechanical wristwatches of yesteryear).

11.3 Elastic Support Boundary Conditions

Having indicated the origin of springs in the mathematical models of beams, and a little bit about how the stiffnesses of such springs can be evaluated, it is now necessary to explain how to deal with the BCs created by the springs. For this purpose, consider Fig. 11.2(a). This figure shows the x, z plane view of the right-hand end of a beam that has every possible complication. Specifically, in this case there is both a rectilinear and a rotational spring, an externally applied end force, F_2 , a bending moment, M_2 , a temperature change, and a nonzero product of inertia. The development of the two bending BCs in the x, z plane begins with the understanding that there cannot be a prior knowledge of the values of the beam end lateral translation, $w(L)$, or bending slope, $w'(L)$. Thus, following the BC pairing rules discussed in the last chapter, the BC statements must be statements concerning the end moment and end shearing force. Therefore it is necessary to prepare a free body diagram (FBD) of the beam end. As per usual, in this FBD it is necessary *always* to use positive directions for the stress resultants $M_y(L)$ and $V_z(L)$. Figure 11.2(b)

¹ To verify this bottom beam relation at this point, use the second order relation $EI_{yy}w''(x) = M_y(x)$, the half-span BC $w(0) = 0$, and the symmetry condition $w'(L/2) = 0$; or wait to study Section 11.4 where concentrated loads are discussed.

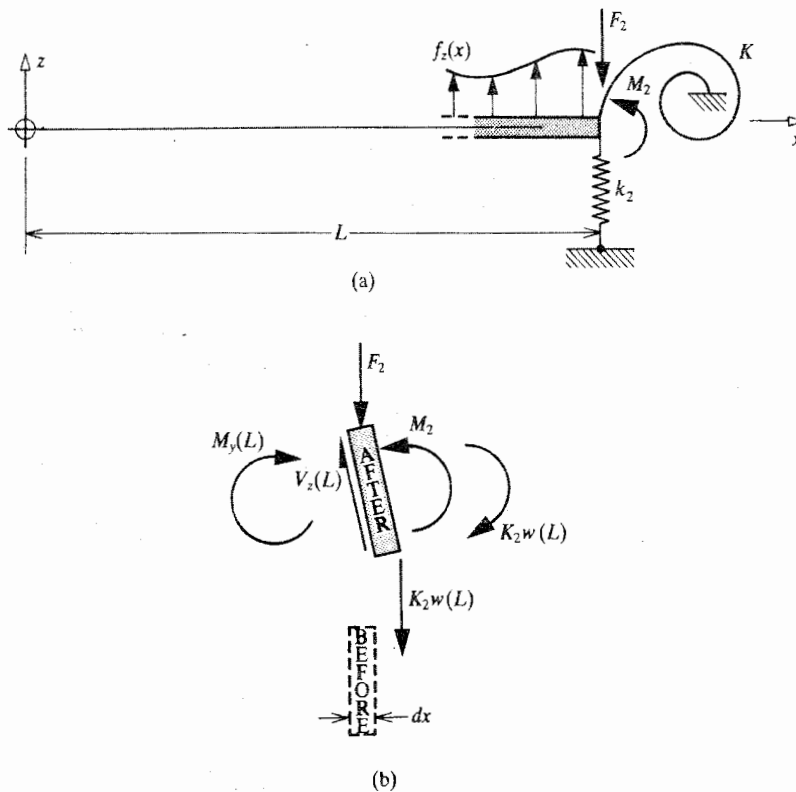


Figure 11.2. (a) An example boundary condition at $x = L$. (b) A free body diagram of a deflected beam slice of length dx at $x = L$. Just as the internal shearing forces and internal bending moments must be placed upon the FBD according to their positive sign conventions, the deflections that give rise to spring forces and spring moments must be drawn in their positive directions *regardless of the actual loading* so that the correctly directed deflection-opposing spring reactions also can be added to the free body diagram. There is no need for a sign convention for the external concentrated forces and moments.

shows the details of that FBD, and the position of the beam end before loading and its *assumed* position after loading. Since the spring forces depend upon the deflections, it is essential that the positive directions of all unknown deflections, including bending slopes, *always* be used whenever they are part of the BCs, as is the case here. In other words, it does not matter what the actual deflections and slopes are expected to be in response to the applied loadings. Like any derivation involving force and deflection quantities in general terms, those quantities must be used in their positive sense according to the adopted sign convention. To have positive lateral deflections, the beam end is shown as having moved upward, and having rotated counterclockwise. See Endnote (1) for a discussion of the bending slope sign convention. The two springs are stretched accordingly. The upward movement of the beam end causes a downward spring force on the beam end as illustrated in the FBD. In exactly the same fashion, the moment applied to the beam end by the rotational spring resists the counterclockwise beam end rotation, and is thus clockwise in the FBD of the beam end. *Springs always oppose deflections.* Now it is simply a matter of summing forces and moments. Note that the distributed forces and moments per unit length only act

over a differential length, and thus produce negligible forces and moments with respect to this summation. Hence

$$V_z(L) - k_2 w(L) = F_2 \quad \text{and} \quad M_y(L) + K_2 w'(L) = M_2$$

As ever, the stress resultants need to be converted into expressions involving the derivatives of the deflections. Unfortunately, in the case of elastic end supports, the BCs cannot be decoupled when the product of inertia is not zero. The results, after referencing the shearing force and bending moment expressions of the first BC table (in Chapter 10) are

$$\begin{aligned} [E_0 I_{yz}^* v''(L)]' + [E_0 I_{yy}^* w''(L)]' - V_{zT}(L) - m_y(L) - k_2 w(L) &= F_2 \\ E_0 I_{yz}^* v''(L) + E_0 I_{yy}^* w''(L) - M_{yT}(L) + K_2 w'(L) &= M_2 \end{aligned} \quad (11.1)$$

where, again, a lower-case m is a moment per unit length. If it so happened that the same types of elastic supports existed in the x, y plane, then the BCs for the x, y plane would have exactly the same form as those above if $(v, w, y, z, 2)$ are replaced by $(w, v, z, y, 1)$ respectively, provided that the externally applied force F_1 , is in the negative y direction, and the externally applied moment M_1 is, with respect to the right-hand rule, about the positive z axis. Example problems involving spring BCs at both the left and right ends of beams are presented below with additional applications discussed in later sections.

Equation (11.1) could be used as a template for any beam right-hand end. However, it is strongly recommended that once this equation is understood, it be ignored as a template. It is far better to draw FBDs specific to the problem at hand because the skill of drawing FBDs, which is so basic to structural analysis, should be much more available to the reader than Eqs. (11.1) ever could be. To that end, simply recall the requirement that the force and the moment that springs apply to a beam end are always opposite to the positive deflections of the beam end.

Example 11.1. Write the bending, that is, w and v deflection BCs, for the beam end at $x = L$ shown in Fig. 11.3(a). The beam is uniform, and the product of inertia, the distributed moment, and the temperature change are zero.

Solution. FBDs for the x, z and x, y planes are shown in Fig. 11.3(b), where the length of the beam end segment is infinitesimal. Summing forces and moments in each case leads to the following preliminary equations:

$$\begin{aligned} V_z(L) - k_z w(L) &= -F_0 & V_y(L) - k_y v(L) &= 0 \\ M_y(L) &= 0 & M_z(L) + K_y v'(L) &= 0 \end{aligned}$$

Note again that the springs always produce “snap-back” reactions to the positive spring deflections. Now it is necessary to write these preliminary BC equations entirely in terms of deflection derivatives and the externally applied loads. With the product of inertia being zero, it makes no difference which of the two BC tables are used, but the first one is less cumbersome in this case. The above equations become, respectively,

$$\begin{aligned} E_0 I_{yy}^* w'''(L) - k_z w(L) &= -F_0 & E_0 I_{zz}^* v'''(L) - k_y v(L) &= 0 \\ E_0 I_{yy}^* w''(L) &= 0 & E_0 I_{zz}^* v''(L) + K_y v'(L) &= 0 \end{aligned}$$

which are the four required equations in the form necessary for the determining constants of integration. If the beam were not uniform as stated, then the two shear equations would

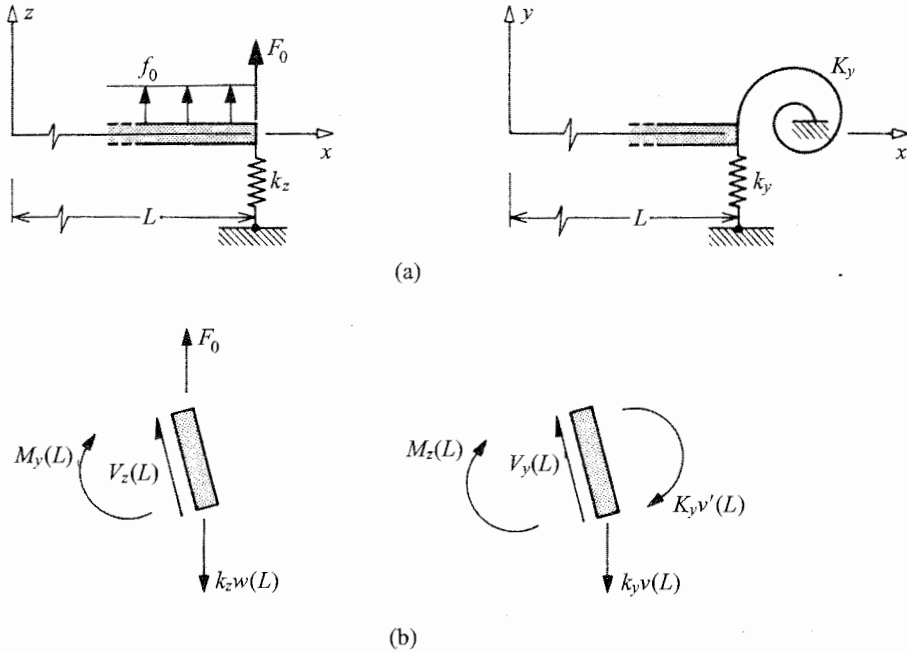


Figure 11.3. (a) Example 11.1. Boundary conditions at $x = L$. (b) Corresponding beam end free body diagrams showing spring reactions to positive values of $w(L)$, $v(L)$, and $v'(L)$.

have to be altered so as to involve both the moments of inertia and their first derivatives evaluated at $x = L$, as per the first of Eqs. (11.1). ■

Example 11.2. If the product of inertia is not zero, what then are the BCs for the beam end at $x = 0$ shown in Fig. 11.4(a) given that

$$M_{zT}(x) = M_0 \left(1 - \frac{x}{L} \right) \quad M_{yT}(x) = M_0 \left(5 - \frac{3x}{L} \right)$$

Solution. The FBDs for the two views of the beam end slice are shown in Fig. 11.4(b). Summing forces and moments leads to the following preliminary equations:

$$\begin{aligned} V_y(0) + kv(0) &= 0 & V_z(0) &= F_0 \\ M_z(0) &= M_0 & M_y(0) - Kw'(0) &= 0 \end{aligned}$$

If the first BC table is used, the results are, respectively,

$$\begin{aligned} E_0 I_{zz}^* v'''(0) + E_0 I_{yz}^* w'''(0) + kv(0) &= -\frac{M_0}{L} \\ E_0 I_{zz}^* v''(0) + E_0 I_{yz}^* w''(0) &= 2M_0 \\ E_0 I_{yz}^* v'''(0) + E_0 I_{yy}^* w'''(0) &= F_0 - 3\frac{M_0}{L} \\ E_0 I_{yz}^* v''(0) + E_0 I_{yy}^* w''(0) - Kw'(0) &= 5M_0 \end{aligned}$$

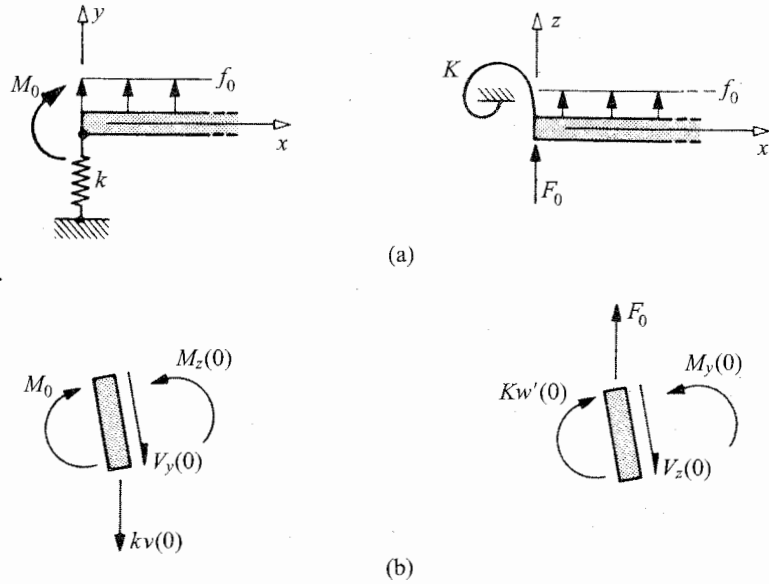


Figure 11.4. (a) Example 11.2. Boundary conditions at $x = 0$. (b) Corresponding beam end free body diagrams showing spring reactions to positive values of $v(0)$ and $w'(0)$.

If the second BC table is used, the final BC equations are, respectively,

$$E_0 R_{yy}^* v'''(0) + kv(0) = -\frac{M_0}{L} - \left(F_0 - \frac{3M_0}{L} \right) \left(\frac{I_{yz}^*}{I_{yy}^*} \right)$$

$$E_0 R_{yy}^* v''(0) + \frac{I_{yz}^*}{I_{yy}^*} K w'(0) = M_0 \left(2 - 5 \frac{I_{yz}^*}{I_{yy}^*} \right)$$

$$E_0 R_{zz}^* w'''(0) - \frac{I_{yz}^*}{I_{zz}^*} kv(0) = F_0 - \frac{M_0}{L} \left(3 - \frac{I_{yz}^*}{I_{zz}^*} \right)$$

$$E_0 R_{zz}^* w''(0) - K w'(0) = M_0 \left(5 - 2 \frac{I_{yz}^*}{I_{zz}^*} \right)$$

Since the second and third of the above BC equations still couple the v and w deflections, the extra effort required by the use of the second table of BCs is questionable. In the context of the total problem, it is probably still worth that extra effort because the other two of the above equations are uncoupled. ■

In summary, the use of spring elements is frequently convenient for the substitute representation of various parts of an elastic structure. Writing spring BCs is no different than writing other force-type BCs.

11.4 Concentrated and Partial Span Loads

The physical reality of a “concentrated force” is that of a particularly intense pressure acting over a relatively small axial length in the case of a beam, or a small surface area in the case of a plate, shell, or structural potato. For example, in Fig. 11.1(b), the top

beam applies, in this sense, a concentrated force acting downward on the bottom beam. If the joint between the two beams is rigid, then the top beam also applies a concentrated torsional moment to the bottom beam. Sometimes it is mathematically convenient to consider that the concentrated force acts at a point. For example, in rigid body dynamics, the logical consequence of an infinite pressure and infinite stress is of no concern in the analysis of the motion of a rigid body. In this study of linearly elastic beams, which concentrates on the use of the fourth order beam equations that have distributed loads as the input quantities, the idealization of a point force is not at all convenient. Since beam distributed loads are best described by suitable functions of the independent spatial variable x , the preference here is to model concentrated loads as (intense) distributed loads using a suitable function of x . Hence the choice of the following mathematics, which is also useful in the study of the dynamics of structures. For present purposes, consider the following somewhat restricted definition of the *Dirac delta function*, whose standard symbol is $\delta(x - x_0)$. In the argument of the delta function, the variable is x , and x_0 is the parameter. A parameter is a constant without any set value. Refer to Fig. 11.5 and define the Dirac delta function² in three steps as follows:

- (i) $\delta(x - x_0)$ is everywhere differentiable, and it is an even function about x_0
- (ii) $\delta(x - x_0) = 0$ for all x not in the interval $(x_0 - \epsilon/2, x_0 + \epsilon/2)$, where ϵ is vanishingly small
- (iii) $\int_{-\infty}^{+\infty} \delta(x - x_0) dx = \int_{x_0 - \frac{1}{2}\epsilon}^{x_0 + \frac{1}{2}\epsilon} \delta(x - x_0) dx = 1.0$

Note that, from the third part of the definition, the units that must be associated with the Dirac delta function in this usage are the inverse of length. The next thing to do is not to confuse the Dirac delta function with other “deltas.” For example, in Part IV of this text, a variational operator symbolized by δ is used extensively. However, it is an operator, that is, it has no value in itself. Therefore it is not anything like a function. Another delta symbol, one that always has two subscripts attached to it, is the Kronecker delta. The Kronecker delta is a tensor that is somewhat like a unit matrix. It has no use in this textbook. The Dirac delta function is undefined³ in the vanishingly small interval $(x_0 - \epsilon/2, x_0 + \epsilon/2)$. This is deliberately done in order to allow the delta function to model any smooth curve within a relatively small interval that is: (i) symmetric about the center of the interval; (ii) zero at either end of the interval; and (iii) can be adjusted to have a unit area between the smooth curve and the x axis. Thus one possible form for the delta function within that small interval is a triangular spike with slightly rounded vertices, a base length of ϵ , and a height of $2/\epsilon$. Note that since ϵ is a very small number, the height of this triangle is a very large number. Mathematically, it would be called “unbounded.” Another such possibility which has much the same characteristics as the rounded triangular form is the function $(2/\epsilon) \cos^2[\pi(x - x_0)/\epsilon]$ when confined to the interval of length ϵ centered at x_0 . There are many more such possibilities. See appendix V of Ref. [53].

Clearly the Dirac delta function has a shape that is well suited for describing any distributed quantity of very high intensity that acts over a very short length. Thus expressions of the type $f(x) = F_0 \delta(x - x_0)$ and $m(x) = M_0 \delta(x - x_0)$, with their respective units of

² Paul A. M. Dirac (1902–1984), British theoretical physicist and Nobel prize winner (Ref. [71]). The more general definition of the Dirac delta function involves an arbitrary, continuous function of the variable x in the two integrals of the third part of the definition.

³ The lack of precisely defined values for the Dirac delta function in the neighborhood of x_0 means that the Dirac delta function is not actually a function. Its more flexible definition puts it into the classification of what mathematicians call a “distribution.”

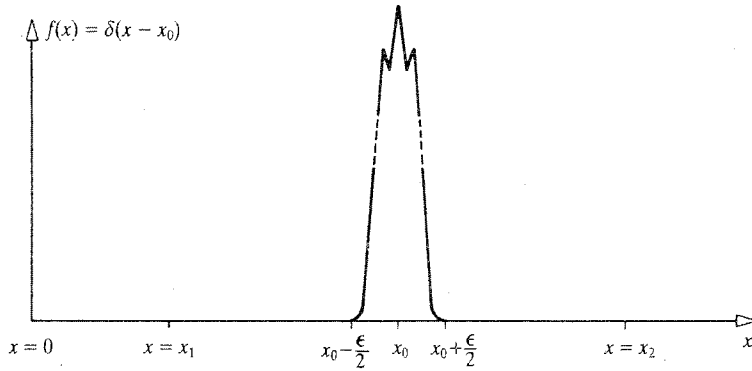


Figure 11.5. A sketch of one possible form of the Dirac delta function acting at $x = x_0$.

force per length and moment per length, can be used to describe intense distributed forces and moments. The integration of these continuous functions shows that their sum effect is the same as that of a concentrated force F_0 and a concentrated moment M_0 , respectively. These concentrated loads are, of course, located at $x = x_0$. As is seen below, these types of expressions for force and moment loads per unit length can be used in the beam equations in exactly the same way that any other distributed load expressions are used.

When the beam equations are integrated, the Dirac delta function must also be integrated. The third part of its definition specifies the value of definite integrals of the delta function. However, the previous integrations of the beam equations have, to this point, always been indefinite integrals. The way to retain the greater simplicity of indefinite integrals, and yet use the third part of the delta function definition, is to use definite integration with a variable limit. Specifically, for training purposes, all integrations will be from $x = 0$ to an arbitrary value of x less than $x = L$. Consider Fig. 11.5 and the value of the integral

$$I(x) = \int_{\hat{x}=0}^{\hat{x}=x} \delta(\hat{x} - x_0) d\hat{x}$$

where \hat{x} is the “dummy” variable of integration. When x , the upper limit of the integral, equals x_1 , or any such value between zero and $(x_0 - \epsilon/2)$, $I(x)$ being the area under the curve obviously equals zero. Furthermore, $I(x_0) = 1/2$, and when \hat{x} is in the interval $(x_0 + \epsilon/2, L)$, $I(x) = 1.0$. This three-part result can be well organized by defining the *Heaviside step function*, or the *unit step function*, symbolized here as $\text{stp}(x - x_0)$. Its two-part definition is

- (i) $\text{stp}(x - x_0) - 0.5$ is everywhere differentiable, and an odd function⁴ about $x = x_0$.
(ii) $\text{stp}(x - x_0) = \begin{cases} 0 & \text{whenever } x < x_0 - \epsilon/2 \\ 1 & \text{whenever } x > x_0 + \epsilon/2 \end{cases}$

⁴ Recall that an even function is one where $E(x) = E(-x)$, and odd function is one where $O(x) = -O(-x)$. Examples of even functions about $x = 0$ are x^4 and $\cos x$. Examples of odd functions about $x = 0$ are x^3 and $\sin x$. The function $(x + 1)$ is odd about -1 , but is neither even nor odd about zero. It, $(x + 1)$, is the sum of an even and an odd function. If a function can be expanded into a power series, clearly it too can be considered to be a sum of an even and an odd function. Can you show that the derivative of an even function is odd, and vice versa?

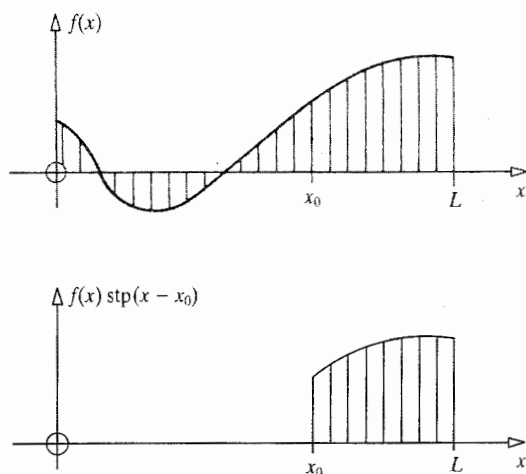


Figure 11.6. Effect on an arbitrary function $f(x)$ defined over the interval $0 \leq X \leq L$ when multiplied by the Heaviside step function with parameter x_0 .

In simple terms, the Heaviside⁵ step function has the value one whenever its argument is positive, and the value zero whenever its argument is negative, and has a smooth transition between zero and one. From the above discussion it should be clear that

$$\int_{\hat{x}=0}^{\hat{x}=x} \delta(\hat{x} - x_0) d\hat{x} = \text{stp}(x - x_0)$$

and

$$\frac{d}{dx} \text{stp}(x - x_0) = \delta(x - x_0)$$

The Heaviside step function, like the Dirac delta function, but for the center point of the interval, is not precisely defined in the interval $(x_0 - \epsilon/2, x_0 + \epsilon/2)$, and there are an infinite number of smooth ways that the transition from zero to one can take place in that very small interval.

The Heaviside step function is useful in its own right as a means of describing partial span loadings. For example, if there is a lateral force of magnitude $f_0(x)$ in the positive z direction over the second half of a beam length, then that loading can be described as $f_z(x) = f_0(x) \text{stp}(x - L/2)$. If, instead, that same loading were over the first half of the span, then the description would be either $f_0(x) \text{stp}(L/2 - x)$ or $f_0(x)[1 - \text{stp}(x - L/2)]$. Even though the second expression is obviously more cumbersome, it will be preferred for the sake of standardization until the use of this step function is totally familiar. It should be clear that the Heaviside step function can be used as a perfect mathematical band filter so as to retain undisturbed any function over one interval while wholly suppressing that same function outside of the desired interval. See Fig. 11.6. Similarly, the Dirac delta function is a mathematical “point” filter when used as a factor in an integrand of a definite integral.

The integration of the Heaviside step function, which is the same as the second integral of the Dirac delta function, is approached directly. Consider the integration of an arbitrary bounded function $f(x)$ multiplied by the step function with parameter x_0 . The integral from zero to x of that product can be divided into the integral from zero to $x_0 - \epsilon/2$, plus the integral from $x_0 - \epsilon/2$ (now shortened to x_0^-) to $x_0 + \epsilon/2$ (i.e., x_0^+) plus the integral from

⁵ Oliver Heaviside (1850–1925), English electrical engineer (Ref. [71]).

x_0^+ to x , regardless of the relative values of x and x_0 . That is,

$$\int_0^x f(\hat{x}) \text{stp}(\hat{x} - x_0) d\hat{x} = \int_0^{x_0 - \frac{1}{2}\epsilon} f(\hat{x}) \text{stp}(\hat{x} - x_0) d\hat{x} + \int_{x_0^-}^{x_0^+} f(\hat{x}) \text{stp}(\hat{x} - x_0) d\hat{x} + \int_{x_0^+}^x f(\hat{x}) \text{stp}(\hat{x} - x_0) d\hat{x} = \text{stp}(x - x_0) \int_{x_0}^x f(\hat{x}) d\hat{x} \quad (11.2)$$

In the way of an explanation, in the interval $(0, x_0^-)$ the step function has the value zero. Therefore the first integral of the first right-hand side is also zero. The interval of integration of the second integral of the first right-hand side is the minute length ϵ . The value for this second right-hand side integral is bounded by the product of the infinitesimal ϵ and the maximum value of $f(x)$ in that minute interval. This product is negligibly small because the maximum value of $f(x)$ must be a finite value. In the third integral of the first right-hand side the step function has the constant value one. Hence the step function can be factored out of the integrand. Recognize that the Heaviside step function must multiply the final form of the integral in order to limit the values of x for which the solution is valid. That is, the original integral shows that the applicability of the nonzero solution is limited to the interval $x_0 \leq x \leq L$ because the answer must be zero everywhere else. Therefore the final integral must be multiplied by that step function in order to achieve that limitation. By comparing the original integral to the last of the above integral expressions, the result can be summarized by saying that the bi-constant step function passes out of the definite integral while appropriately altering the limits of integration as it does so. Common uses of the above theorem are

$$\int_0^x \text{stp}(\hat{x} - x_0) d\hat{x} = \text{stp}(x - x_0) \int_{x_0}^x d\hat{x} = (x - x_0) \text{stp}(x - x_0)$$

which is a special case of

$$\int_0^x (\hat{x} - x_0)^n \text{stp}(\hat{x} - x_0) d\hat{x} = \frac{1}{1+n} (x - x_0)^{(n+1)} \text{stp}(x - x_0) \quad (11.3)$$

where n is any number greater than or equal to zero. With the use of the formulas of Eqs. (11.2) and (11.3), any partial span load expressions can be integrated nearly as easily as they would be integrated without the presence of the Heaviside step function as a factor.

11.5 Partial Span and Concentrated Load Example Problems

The following example problems illustrate the writing of the beam GDEs when concentrated loads and partial span loads are present. Further practice writing BCs when there are elastic end supports is also provided.

Example 11.3. Write the two beam bending GDEs and the bending BCs for the uniform, homogeneous beam with a symmetric cross-section shown in Fig. 11.7. Integrate the v deflection GDE, and apply the BCs so as to determine the constants of integration. State the deflection solution in a well organized form. Integrate the w deflection GDE, but do not determine the constants of integration.

Solution. Since the product of inertia and the axial force $N(x)$ are zero, the GDEs are

$$EI_{zz}v''''(x) = +F_0\delta\left(x - \frac{L}{3}\right) + f_0\left[\text{stp}\left(x - \frac{L}{3}\right) - \text{stp}\left(x - \frac{2L}{3}\right)\right]$$

$$EI_{yy}w''''(x) = +M_0\delta'\left(x - \frac{L}{3}\right) - \frac{3f_0}{L}\left(x - \frac{2L}{3}\right)\text{stp}\left(x - \frac{2L}{3}\right)$$

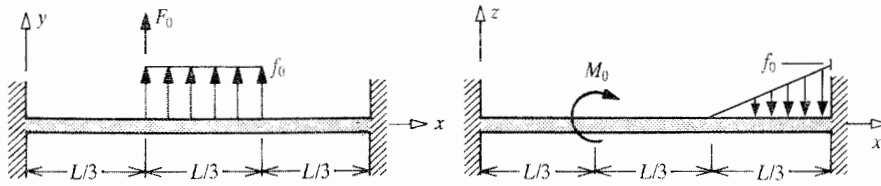


Figure 11.7. Example 11.3.

where the first right-hand side term of the second equality is the derivative of the distributed moment, $m_y(x) = +m_0\delta(x - L/3)$. Recall that the Dirac delta function is everywhere differentiable, and therefore placing a prime on the function is sufficient to indicate its derivative. In the same quantity, be sure to note the relation of M_0 and the positive y axis. In the x, z plane view because all Cartesian coordinate systems follow the right-hand rule, the y axis is into the paper. Thus the sign assigned to this term.

The required eight BCs are especially simple. They are

$$w(0) = w'(0) = v(0) = v'(0) = w(L) = w'(L) = v(L) = v'(L) = 0$$

The four definite integrations between the limits $(0, x)$ for the first GDE follow. However, first note that the definite integral between the limits of $(0, x)$ of, say, $[dv'''(x)/dx] dx$, which is clearly an exact differential after canceling the two dx 's, produces $[v'''(x) - v'''(0)]$. If the constant quantity $v'''(0)$ were known from the BC equations, its value could be substituted immediately. In this case, its value is not known before obtaining the final solution. Hence it is an unknown constant, that is, exactly the same as a constant of integration. Therefore, for the sake of brevity, the usual C_i notation is used for these constants of integration. Thus

$$\begin{aligned} EI_{zz}v'''(x) &= C_1 + F_0 \operatorname{stp}\left(x - \frac{L}{3}\right) \\ &\quad + f_0 \left[\left(x - \frac{L}{3}\right) \operatorname{stp}\left(x - \frac{L}{3}\right) - \left(x - \frac{2L}{3}\right) \operatorname{stp}\left(x - \frac{2L}{3}\right) \right] \\ EI_{zz}v''(x) &= C_2 + C_1x + F_0 \left(x - \frac{L}{3}\right) \operatorname{stp}\left(x - \frac{L}{3}\right) \\ &\quad + \frac{f_0}{2} \left[\left(x - \frac{L}{3}\right)^2 \operatorname{stp}\left(x - \frac{L}{3}\right) - \left(x - \frac{2L}{3}\right)^2 \operatorname{stp}\left(x - \frac{2L}{3}\right) \right] \\ EI_{zz}v'(x) &= C_2x + \frac{C_1x^2}{2} + \frac{F_0}{2} \left(x - \frac{L}{3}\right)^2 \operatorname{stp}\left(x - \frac{L}{3}\right) \\ &\quad + \frac{f_0}{6} \left[\left(x - \frac{L}{3}\right)^3 \operatorname{stp}\left(x - \frac{L}{3}\right) - \left(x - \frac{2L}{3}\right)^3 \operatorname{stp}\left(x - \frac{2L}{3}\right) \right] \\ EI_{zz}v(x) &= \frac{C_2x^2}{2} + \frac{C_1x^3}{6} + \frac{F_0}{6} \left(x - \frac{L}{3}\right)^3 \operatorname{stp}\left(x - \frac{L}{3}\right) \\ &\quad + \frac{f_0}{24} \left[\left(x - \frac{L}{3}\right)^4 \operatorname{stp}\left(x - \frac{L}{3}\right) - \left(x - \frac{2L}{3}\right)^4 \operatorname{stp}\left(x - \frac{2L}{3}\right) \right] \end{aligned}$$

where the v deflection BCs at $x = 0$ immediately eliminate the third and fourth constants of integration that are identical to $EI_{zz}v'(0)$ and $EI_{zz}v(0)$, respectively. (Be sure to satisfy yourself that the stated solutions for the y direction lateral deflection and bending slope do indeed satisfy the BCs at $x = 0$.) The v deflection BCs at $x = L$ and the third and fourth of the above expressions can now be used to determine the first two constants of integration.

Substituting the v deflection BCs at $x = L$ leads to

$$0 = C_2L + \frac{C_1L^2}{2} + \frac{2F_0L^2}{9} + \frac{f_0L^3}{6} \left[\frac{8}{27} - \frac{1}{27} \right]$$

$$0 = \frac{C_2L^2}{2} + \frac{C_1L^3}{6} + \frac{4F_0L^3}{81} + \frac{f_0L^4}{24} \left[\frac{16}{81} - \frac{1}{81} \right]$$

multiplying the first of the above by 54 and the second by 162 produces

$$54C_2 + 27C_1L = -12F_0L - \frac{28}{12}f_0L^2$$

$$81C_2 + 27C_1L = -8F_0L - \frac{15}{12}f_0L^2$$

which yields the solutions

$$C_2 = +\frac{4}{27}F_0L + \frac{13}{324}f_0L^2$$

$$C_1 = -\frac{20}{27}F_0 - \frac{1}{6}f_0L$$

These constants provide as a final solution for the v deflection

$$EI_{zz}v(x) = \frac{2}{81}F_0x^2(3L - 5x) + \frac{f_0Lx^2}{648}(13L - 18x)$$

$$+ \frac{f_0}{24} \left[\left(x - \frac{L}{3} \right)^4 \text{stp} \left(x - \frac{L}{3} \right) - \left(x - \frac{2L}{3} \right)^4 \text{stp} \left(x - \frac{2L}{3} \right) \right]$$

$$+ \frac{F_0}{6} \left(x - \frac{L}{3} \right)^3 \text{stp} \left(x - \frac{L}{3} \right)$$

Hence, for example

$$EI_{zz}v \left(\frac{L}{3} \right) = \frac{2F_0}{81} \left(\frac{L^2}{9} \right) \left(\frac{4L}{3} \right) + \frac{f_0L^3}{9(648)}(7L) + \frac{f_0}{24}[0] + \frac{F_0}{6}(0)$$

Integration of the z direction deflection equation proceeds in the same manner:

$$EI_{yy}w'''(x) = C_5 + M_0\delta(x - L/3) - \frac{3f_0}{2L} \left(x - \frac{2L}{3} \right)^2 \text{stp} \left(x - \frac{2L}{3} \right)$$

$$EI_{yy}w''(x) = C_5x + C_6 + M_0 \text{stp} \left(x - \frac{L}{3} \right) - \frac{f_0}{2L} \left(x - \frac{2L}{3} \right)^3 \text{stp} \left(x - \frac{2L}{3} \right)$$

$$EI_{yy}w'(x) = \frac{C_5x^2}{2} + C_6x + M_0 \left(x - \frac{L}{3} \right) \text{stp} \left(x - \frac{L}{3} \right) - \frac{f_0}{8L} \left(x - \frac{2L}{3} \right)^4 \text{stp} \left(x - \frac{2L}{3} \right)$$

$$EI_{yy}w(x) = \frac{C_5x^3}{6} + \frac{C_6x^2}{2} + \frac{M_0}{2} \left(x - \frac{L}{3} \right)^2 \text{stp} \left(x - \frac{L}{3} \right)$$

$$- \frac{f_0}{40L} \left(x - \frac{2L}{3} \right)^5 \text{stp} \left(x - \frac{2L}{3} \right)$$

and the same process as was used for the y direction deflection equation could be used to determine this last pair of constants of integration. ■

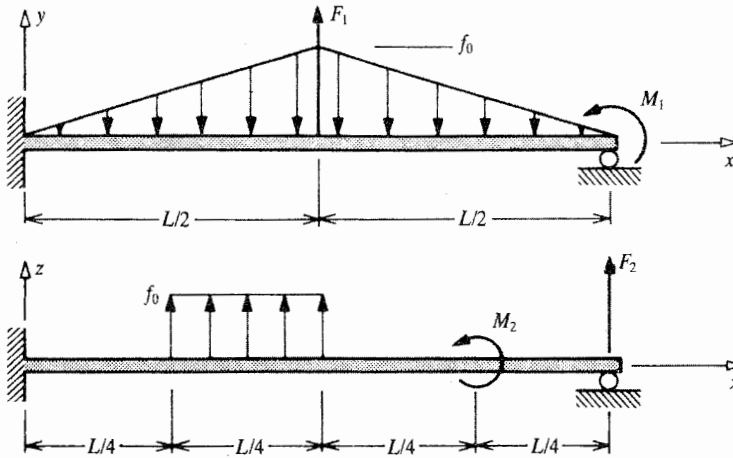


Figure 11.8. Example 11.4.

Example 11.4. Write the beam bending GDEs and BCs for the uniform, homogeneous, nonsymmetric beam shown in Fig. 11.8. Do not integrate the GDEs.

Solution. Since the rigid supports are the same in both orthogonal planes, the v and w deflection BCs can be wholly decoupled even though the product of inertia is not zero. The decoupled form of the GDEs are Eqs. (10.7). Without temperature effects, these two equations are

$$ER_{zz}w''''(x) = [f_z(x) + m'_y(x)] - \frac{I_{yz}}{I_{zz}}[f_y(x) - m'_z(x)]$$

$$ER_{yy}v''''(x) = [f_y(x) - m'_z(x)] - \frac{I_{yz}}{I_{yy}}[f_z(x) - m'_y(x)]$$

In this case,

$$f_z(x) = +f_0 \left[\text{stp} \left(x - \frac{L}{4} \right) - \text{stp} \left(x - \frac{L}{2} \right) \right]$$

$$m'_y(x) = -M_2 \delta' \left(x - \frac{3L}{4} \right) \quad m'_z(x) = 0$$

and

$$f_y(x) = F_1 \delta \left(x - \frac{L}{2} \right) - \frac{2f_0x}{L} \left[1 - \text{stp} \left(x - \frac{L}{2} \right) \right] + 2f_0 \left(\frac{x}{L} - 1 \right) \text{stp} \left(x - \frac{L}{2} \right)$$

where separate expressions for each half-span are written for the linearly varying applied force per unit length in the x, y plane. There is a somewhat less cumbersome way of expressing the linearly varying force per unit length. The underlying thought is to consider that the left-hand linearly varying load extends over the entire length of the beam and, at half-span, there begins an oppositely directed, linearly varying load at twice the rate (i.e., slope) of the first distributed load. The net effect is the subtraction of the double slope from the original slope to produce the triangular loading desired, in the slightly simpler form

$$f_y(x) = F_1 \delta \left(x - \frac{L}{2} \right) - \frac{2f_0x}{L} - 2f_0 \left(1 - \frac{2x}{L} \right) \text{stp} \left(x - \frac{L}{2} \right)$$

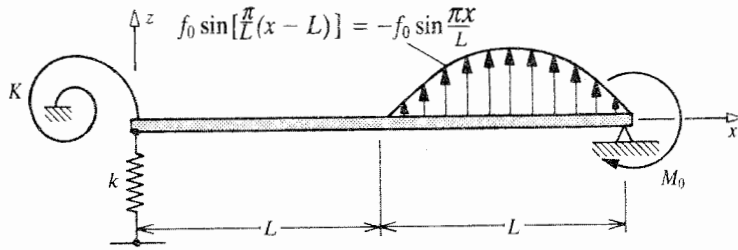


Figure 11.9. Example 11.5.

Another advantage of this form is that it can quickly be put into the highly advantageous form of Eq. (11.3) by factoring $-2/L$ out of the bracketed term. That is, in preparation for integration the last term can be rearranged as

$$-2f_0 \left(1 - \frac{2x}{L}\right) \text{stp} \left(x - \frac{L}{2}\right) = +4\frac{f_0}{L} \left(x - \frac{L}{2}\right) \text{stp} \left(x - \frac{L}{2}\right)$$

The reader can be assured of the correctness of any of these expressions for the triangular portion of $f_y(x)$ by checking its values, say, at $x = 0$ and $L/4$, and at $3L/4$ and L . (It is also correct at $x = L/2$). Since these are linear relations, if each half-span load checks at two points, it checks everywhere.

Substitution of the above f_y and f_z and m'_y expressions completes the statement of the GDEs. The statement of the BCs is

$$w(0) = w'(0) = v(0) = v'(0) = w(L) = v(L) = 0$$

and the preliminary equations are $M_y(L) = 0$, and $M_z(L) = +M_1$. Using the second BC table leads quickly to

$$ER_{yz}w''(L) = -M_1 \quad \text{and} \quad ER_{yy}v''(L) = +M_1$$

The force F_2 does not enter into either the GDEs or the BCs because it is entirely reacted by the right-hand support, and thus, with respect to the present approximate theory, has no effect upon the beam. ■

Example 11.5. Seek the deflection functions for the homogeneous, uniform, symmetric beam of length $2L$, loaded and supported as shown in Fig. 11.9. The distributed force per unit length acting upon the right half of the beam has a sinusoidal distribution. Expressed in terms that simplify the algebra, let the spring stiffnesses and the end moment terms be

$$k = \alpha \frac{EI_{yy}}{L^3} \quad K = \beta \frac{EI_{yy}}{L} \quad M_0 = 2\mu \frac{EI_{yy}}{L}$$

where α , β , and μ are convenient nondimensional constants. The temperature change is such that $N_T = M_{zT} = 0$, and

$$M_{yT}(x) = \mu \frac{EI_{yy}}{L} \left(1 - \frac{x}{L}\right)$$

Solution. Since there are no mechanical or thermal loadings in the x or y directions, and since there is no coupling between the v and w deflections, it is clear that $u(x) = v(x) = N(x) = 0$.

The remaining GDE is simply

$$EI_{yy}w''''(x) = -f_0 \sin\left(\frac{\pi x}{L}\right) \text{stp}(x - L)$$

where the negative sign for the positively directed distributed force is the result of the sine function being negative in the interval $L < x < 2L$. Note that regardless of the BCs, the deflection solution for this beam, as well as those of the preceding examples of this section, is better approached using fourth order differential equations rather than second order differential equations. From a FBD (left to the reader) of the left end of the beam,

$$Kw'(0) = M_y(0) = EI_{yy}w''(0) - M_{yT}(0)$$

and

$$kw(0) + V_z(0) = kw(0) + EI_{yy}w'''(0) - M'_{yT}(0) = 0$$

or, using the temporary nondimensional constants defined above, these two equations become, respectively

- (i) $\beta w'(0) - Lw''(0) = -\mu$
- (ii) $\alpha w(0) + L^3w'''(0) = -\mu L$

For the right-hand end of the beam, the lateral deflection at the knife edge is zero and, from a FBD, again left to the reader,

$$-M_0 = M_y(2L) = EI_{yy}w''(2L) - M_{yT}(2L)$$

That is,

- (iii) $w(2L) = 0$

and

- (iv) $Lw''(2L) = -2\mu - \mu = -3\mu$

Successively integrating the GDE between the limits $(0, x)$ leads to

$$\begin{aligned} EI_{yy}w''''(x) &= C_1 + \frac{f_0L}{\pi} \left[1 + \cos\left(\frac{\pi x}{L}\right) \right] \text{stp}(x - L) \\ EI_{yy}w'''(x) &= C_1x + C_2 + \frac{f_0L}{\pi}(x - L) \text{stp}(x - L) + \left(\frac{f_0L^2}{\pi^2}\right) \sin\left(\frac{\pi x}{L}\right) \text{stp}(x - L) \\ EI_{yy}w''(x) &= \frac{C_1x^2}{2} + C_2x + C_3 + \frac{f_0L}{2\pi}(x - L)^2 \text{stp}(x - L) \\ &\quad - \frac{f_0L^3}{\pi^3} \left[1 + \cos\left(\frac{\pi x}{L}\right) \right] \text{stp}(x - L) \end{aligned}$$

and

$$\begin{aligned} EI_{yy}w(x) &= \frac{C_1x^3}{6} + \frac{C_2x^2}{2} + C_3x + C_4 + \frac{f_0L}{6\pi}(x - L)^3 \text{stp}(x - L) \\ &\quad - \frac{f_0L^3}{\pi^3}(x - L) \text{stp}(x - L) - \frac{f_0L^4}{\pi^4} \sin\left(\frac{\pi x}{L}\right) \text{stp}(x - L) \end{aligned}$$

There are of course, four constants of integration and four BCs by which they may be determined. It is almost always better to begin with the BCs at $x = 0$, even when those BCs

are as messy as they are in this case. As a preliminary step note that because $\text{stp}(x - L)$ is a factor for each term that does not involve a constant of integration,

$$\begin{aligned} EI_{yy}w(0) &= C_4 & EI_{yy}w'(0) &= C_3 \\ EI_{yy}w''(0) &= C_2 & EI_{yy}w'''(0) &= C_1 \end{aligned}$$

Hence the first two BCs become

$$\begin{aligned} \beta C_3 - LC_2 &= -\mu EI_{yy} \\ \alpha C_4 + L^3 C_1 &= -\mu LEI_{yy} \end{aligned}$$

The last two BCs become

$$\begin{aligned} \frac{4C_1L^3}{3} + 2C_2L^2 + 2C_3L + C_4 &= -\frac{f_0L^4}{6\pi} + \frac{f_0L^4}{\pi^3} \\ 2C_1L^2 + C_2L &= -\frac{f_0L^3}{\pi} - 3\mu EI_{yy} \end{aligned}$$

which are four simultaneous equations in the four unknown constants of integration. Examination of these four equations indicates that using the first two in order to eliminate the third and fourth constants is an efficient solution approach. In this way the third of the above four equations becomes

$$C_1L^2 \left(\frac{4}{3} - \frac{1}{\alpha} \right) + 2C_2L \left(1 + \frac{1}{\beta} \right) = \mu EI_{yy} \left(\frac{2}{\beta} + \frac{1}{\alpha} \right) + f_0L^3 \left(\frac{1}{\pi^3} - \frac{1}{6\pi} \right)$$

Now it is just a matter of (i) using the one equation immediately above, which is a combination of the first, second and third equations, simultaneously with the fourth equation so as to determine C_1 and C_2 ; (ii) determining C_3 and C_4 from the first two equations; and then (iii) substituting these four constants into the integrated form for $EI_{yy}w(x)$. This solution process is straightforward, but slightly messy without numerical values for α and β . For example, the solution for C_1 is

$$\begin{aligned} C_1 \left(\frac{8}{3} + \frac{4}{\beta} + \frac{1}{\alpha} \right) &= -\frac{\mu EI_{yy}}{L^2} \left(6 + \frac{8}{\beta} + \frac{1}{\alpha} \right) \\ &\quad - \frac{f_0L}{\pi} \left(\frac{11}{6} + \frac{2}{\beta} + \frac{1}{\pi^2} \right) \end{aligned}$$

which is more easily obtained than it might appear. Of course, this solution is easily compacted if, for example, $\alpha = 2$, $\beta = 4$. The solution for the remaining constants of integration are also not difficult to obtain as

$$\begin{aligned} C_2 \left(\frac{8}{3} + \frac{4}{\beta} + \frac{1}{\alpha} \right) &= +\frac{\mu EI_{yy}}{L} \left(4 + \frac{4}{\beta} - \frac{1}{\alpha} \right) + \frac{f_0L^2}{\pi} \left(1 - \frac{1}{\alpha} + \frac{2}{\pi^2} \right) \\ \beta C_3 \left(\frac{8}{3} + \frac{4}{\beta} + \frac{1}{\alpha} \right) &= +\mu EI_{yy} \left(3 + \frac{4}{\beta} - \frac{1}{\alpha} \right) + \frac{f_0L^3}{\pi} \left(1 - \frac{1}{\alpha} + \frac{2}{\pi^2} \right) \\ \alpha C_4 \left(\frac{8}{3} + \frac{4}{\beta} + \frac{1}{\alpha} \right) &= +\mu EI_{yy}L \left(5 + \frac{8}{\beta} + \frac{1}{\alpha} \right) + \frac{f_0L^4}{\pi} \left(\frac{11}{6} + \frac{2}{\beta} + \frac{1}{\pi^2} \right) \end{aligned}$$

If μ were now made some factor of (f_0L^3/EI_{yy}) , then substitution of the above constants of integration into the solution for $w(x)$ would be a matter of simple algebra. ■

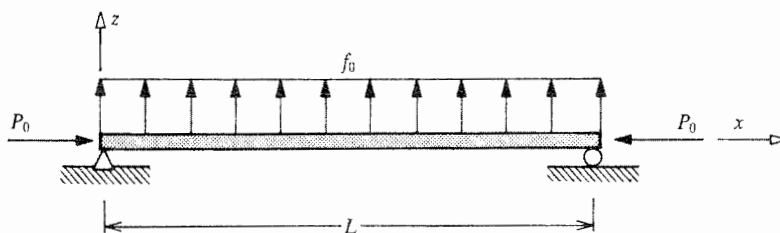


Figure 11.10. Example 11.6.

All previous examples dealt with beam loading situations where there were either axial loadings or lateral loadings, but not both. Furthermore, all the chosen boundary conditions allowed the beam to bend without stretching. Thus in all the previous examples there was no interaction between the axial and lateral deflections. The following example considers the case where a beam bears an axial as well as a lateral loading. This is a more intricate example than the preceding examples even though concentrated lateral forces, and so forth, have been omitted for the sake of simplicity.

Example 11.6. Consider the simply supported, uniform, homogeneous beam-column shown in Fig. 11.10, where P_0 and F_0 are known loads of fixed magnitude. As per usual, the absence of an x, y plane diagram indicates no loading and the same BCs in that plane. Let the temperature change and the product of inertia be zero, and let the moment of inertia about the y axis be I_0 . Calculate the lateral deflection of the beam.

Solution. Since the constant axial force is compressive, it must be assigned a negative value; that is, $N(x) = -P_0$. Thus the beam bending GDE reduces to

$$EI_0 w''''(x) + P_0 w''(x) = f_0$$

The zero deflection and zero moment BCs reduce to

$$w(0) = w(L) = w''(0) = w''(L) = 0$$

Define the known nondimensional parameter $\mu^2 \equiv (P_0 L^2)/(EI_0)$. Then the GDE may be rewritten as

$$w''''(x) + \frac{\mu^2}{L^2} w''(x) = \frac{f_0}{EI_0}$$

There are many ways to arrive at the complementary solution for this linear, ordinary differential equation with constant coefficients. For example, the trial function solution

$$w_c(x) = C \exp\left(\frac{rx}{L}\right)$$

where r is a nondimensional factor, *always* produces a complementary solution for this type of equation – a linear, ordinary differential equation with constant coefficients. Substitution of the trial solution into the homogeneous form of the GDE produces the result

$$C \exp\left(\frac{rx}{L}\right) [r^4 + \mu^2 r^2] = 0$$

The above equation is the zero product of three factors. One or more of the three factors must be zero for the equality to hold. The factor C cannot be zero because, if it were, there would not be any complementary solution. Then the deflection function would consist

entirely of the particular solution. This is not possible because the particular solution alone cannot satisfy the BCs. The exponential function is never zero, even when the argument is a complex number, because, when $r = a + bi$, then

$$\exp\left(\frac{rx}{L}\right) = \exp\left(\frac{ax}{L}\right) \left[\cos\left(\frac{bx}{L}\right) + i \sin\left(\frac{bx}{L}\right) \right]$$

The exponential function of a real argument is never zero, and the sine and cosine function are never simultaneously zero. Therefore, the quantity $[r^4 + \mu^2 r^2]$ must be zero. The resulting characteristic equation $[r^4 + \mu^2 r^2] = 0$ has the roots

$$r_1 = r_2 = 0 \quad r_3 = i\mu \quad r_4 = -i\mu$$

Substituting each of these four roots into the trial solution makes it possible to write the complementary solution as the sum of the four trial solutions, that is,

$$w_c(x) = C_1 + C_2 x + \tilde{C}_3 \exp\left(+\frac{i\mu x}{L}\right) + \tilde{C}_4 \exp\left(-\frac{i\mu x}{L}\right)$$

in which use is made of the usual procedure for repeated roots of replacing the second of the repeated zero root terms, $\exp(0)$, by that same term multiplied by the independent variable, x . This formulation for the deflection $w(x)$, which of course must be a real value, is a bit awkward. It can be simplified by again using the relation $\exp(i\theta) = \cos(\theta) + i \sin(\theta)$ and combining like terms to obtain a better form of the complementary solution as

$$w_c(x) = C_1 + C_2 x + C_3 \sin\left(\frac{\mu x}{L}\right) + C_4 \cos\left(\frac{\mu x}{L}\right)$$

where

$$C_3 = i(\tilde{C}_3 - \tilde{C}_4) \quad \text{and} \quad C_4 = (\tilde{C}_3 + \tilde{C}_4)$$

Since this solution is real valued for any values of length, beam stiffness, axial load, and spanwise coordinate, let $\mu x/L$ successively have the values 0 , $\frac{1}{2}\pi$, π , and $-\pi$. Then it is clear that these latter constants of integration also must be real numbers. Hence the original third and fourth constants, those with tildes, must be complex conjugates.

The particular solution to the GDE is simply $w_p(x) = f x^2 / (2P_0)$. Thus the total solution is

$$w(x) = C_1 + C_2 x + C_3 \sin\left(\frac{\mu x}{L}\right) + C_4 \cos\left(\frac{\mu x}{L}\right) + \frac{f_0 x^2}{2P_0}$$

The use of the four BC equations to determine the four constants of integration is routine. The two BCs at $x = 0$ yield

$$0 = C_1 + C_4 \quad \text{and} \quad 0 = -\left(\frac{\mu}{L}\right)^2 C_4 + \frac{f_0}{P_0}$$

or

$$-C_1 = C_4 = \frac{f_0 L^2}{P_0 \mu^2} = \frac{f_0 L^4}{EI_0 \mu^4}$$

The two BCs at $x = L$ yield

$$0 = -\frac{f_0 L^4}{EI_0} \frac{1}{\mu^4} + C_2 L + C_3 \sin \mu + \frac{f_0 L^4}{EI_0} \frac{1}{\mu^4} \cos \mu + \frac{1}{2} \frac{f_0 L^4}{EI_0} \frac{1}{\mu^2}$$

$$0 = -C_3 \left(\frac{\mu}{L}\right)^2 \sin \mu - \frac{f_0 L^4}{EI_0} \frac{1}{\mu^4} \left(\frac{\mu}{L}\right)^4 \cos \mu + \frac{f_0}{P_0}$$

The last equation can be solved for C_3 , and then the next to last equation can be solved for C_2 . The result for C_2 can be simplified to $C_2 = -f_0 L / (2P_0) = -(1/2L)(f_0 L^4 / EI_0)(1/\mu^2)$. Obviously simplifying all expressions is of great importance in cases like this. After substitution of the constants of integration, and some algebraic and trigonometric manipulation, the analytical solution for the deflection becomes

$$w\left(\frac{x}{L}\right) = \frac{f_0 L^4}{EI_0 \mu^4} \left[\frac{\sin \mu(x/L) + \sin \mu(1-x/L)}{\sin \mu} - 1 - \frac{\mu^2 x}{2L} \left(1 - \frac{x}{L}\right) \right]$$

In this form it is clear that this deflection function and its second derivatives are indeed zero at both $x = 0$ and at $x = L$, and this solution satisfies the original differential equation. The primary advantage of this form is that it is also evident that the solution for the deflection w is symmetric in (x/L) and $[1 - (x/L)]$, and therefore is symmetric about the midspan as it must be. Examination of this solution shows that the deflection increases directly with the magnitude of f_0 , but it changes in a much more complicated fashion with respect to the axial force P_0 which is embedded in μ . The reason for this is that the axial force appears in the GDE multiplying a deflection term, and thus is essentially part of a nonlinear component of the GDE even though the complete GDE has degenerated to the form of a mathematically linear differential equation. Although it is not at all evident, the lateral deflection increases with increasing P_0 . Endnote (2) contains further comment upon these and other aspects of this problem as well as the process of solving differential equations of this sort. ■

11.6 Introduction to Beam Buckling

Structures are designed to transmit loads, including compressive loads. Beams are often chosen to transmit compressive forces along their axes. Such beams are often referred to as a “beam-columns,” or simply “columns.” Such a beam-column might be a push-rod of a mechanical control system, or a member of a vehicular truss with or without a thin covering skin. (The thin skin serves to effectively eliminate beam buckling within the plane of the skin, but has only a limited effect normal to that plane.) The discussion in this section is mostly limited to the problem of the buckling of a simply supported beam-column, without an attached skin. This selection is suitable for pointing out the many facets of the type of buckling analysis to be discussed, while keeping the mathematical complexities to a minimum.

Figure 11.11 shows an initially straight, simply supported beam-column loaded by a compressive axial force whose magnitude is whatever is necessary to make the beam-column begin to bend away from its initial, straight form. The primary object of any buckling analysis is to deduce the magnitude of the loading that causes the structure or structural element to so bend. That is, in buckling analyses the magnitude of the compressive force is always an *additional unknown* along with the unknown deflections. Just as with analyses where the axial force of *known* magnitude is compressive, as in Example 11.6, the symbol P , rather than the equivalent $-N(x)$, is ordinarily used for the compressive force in the beam buckling problem.

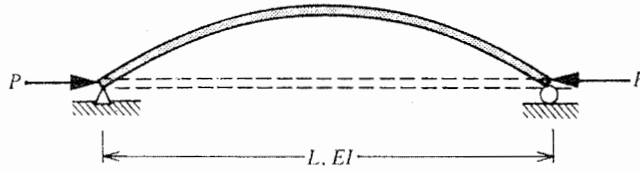


Figure 11.11. A buckled simply supported beam. The perfect beam, perfectly loaded, could buckle up or down. This is an example of a (essentially) nonlinear equation not having a unique solution.

In order to simplify the analysis by ensuring no interaction between the bending and torsional deflections, and by excluding the latter, the beam-columns discussed here are limited to those with doubly symmetric cross-sections.⁶ In this case, as is evident from experimenting with a plastic ruler, the beam buckles about the cross-sectional axis with the smaller of the two principal area moments of inertia, which is here symbolized by I . Choosing the x, z plane to be the buckling plane, the GDE and the zero end displacement and zero end moment BCs for this simply supported beam-column problem are, from Eq. (10.5a) and either BC table,

$$EIw''''(x) + Pw''(x) = 0$$

$$w(0) = w''(0) = w(L) = w''(L) = 0 \quad (11.4)$$

Note again that there is but one GDE, and it contains the two unknowns $w(x)$ and P . To begin the solution process for the GDE, divide the GDE by the quantity EI , and then define

$$\lambda^2 \equiv (P/EI)$$

There is no significance to the fact that in the previous similar example problem the corresponding parameter μ was made to be nondimensional, while here λ has the dimensions of the inverse of length. While nondimensional terms are normally preferred, in this case the dimensional term λ shortens the argument for the trigonometric functions that are seen to be part of the solution that is now sought.

It is perhaps worthwhile to review the standard procedure for determining the complementary solution to this linear GDE with constant coefficients. In this case the complementary solution is the total solution. The GDE coefficients are constant because the value of P that buckles the beam-column is a fixed value depending only on the fixed geometry and material of the beam-column. The complementary solution begins with the introduction of the always successful trial solution

$$w(x) = C \exp(rx)$$

where C is seen to be a constant of integration, and r is a parameter whose value is to be determined. Then

$$w''(x) = r^2 C \exp(rx) \quad \text{and} \quad w''''(x) = r^4 C \exp(rx)$$

The GDE becomes

$$[r^4 + r^2 \lambda^2] C \exp(rx) = 0 \quad (11.5)$$

⁶ Actually, a bit more is required to totally ensure the exclusion of torsional buckling in a doubly symmetric cross-section. However, it is uncommon for a beam to be so torsionally flexible yet stiff in bending for this additional requirement not to be met. See Ref. [23], Eq. (2.114).

Equation (11.5) is the zero product of three factors. At least one of those three factors has to be zero. If C were zero, then the total solution for the bending deflections of the buckled beam would and be zero. Unlike the last example problem, in this buckling problem the function $w(x) \equiv 0$ satisfies both the GDE and the BCs. This solution function is called the “trivial solution.” The trivial solution corresponds to the physical situation where the beam remains straight at any value of P , even one which could cause the beam to buckle. This latter situation is the case where the compressive force is perfectly oriented and located at the cross-sectional centroid, and the beam is perfectly uniform, perfectly straight, and perfectly insulated from all perturbations. It is not possible for any actual compressively loaded beam to remain straight for long whenever the compressive force exceeds the buckling force. In this circumstance the beam is said to be “unstable.” Hence the possibility of C being zero is discarded as no further interest. Furthermore, as is seen in Example 11.6, the exponential factor, $\exp(rx)$ is never zero. Therefore the only source of a useful zero in Eq. (11.5) is

$$r^2[r^2 + \lambda^2] = 0 \quad (11.6)$$

which, again, is an example of an algebraic “characteristic equation” for the parameter r . Since Eq. (11.6) is a fourth order polynomial equation, there are four roots, which are

$$r_1 = 0 \quad r_2 = 0 \quad r_3 = +i\lambda \quad r_4 = -i\lambda$$

The first two roots are a double root. Hence the two constant solutions that the two zero roots would individually imply when inserted back into the trial solution are changed to a single constant term and a single linear term. Again, the latter two solutions are transformed into a more convenient form as follows:

$$C_3 \exp(i\lambda x) + C_4 \exp(-i\lambda x) = (C_3 + C_4) \cos(\lambda x) + i(C_3 - C_4) \sin(\lambda x)$$

As discussed in Example 11.6, each of the two terms on the above right-hand side must be a real quantity. Since λx is a real quantity, so too are the sine and cosine of λx . Therefore the coefficients of the sine and cosine terms must also be real quantities, which means that C_3 and C_4 are complex conjugates. Therefore, in terms of a new set of real constants of integration, the solution for $w(x)$ is

$$w(x) = A + Bx + C \sin(\lambda x) + D \cos(\lambda x) \quad (11.7)$$

The reader is urged to verify that Eq. (11.7) is the complementary and total solution by direct substitution into the original GDE.

Now it is a matter of substituting into the BC equations. Again, it is more convenient to begin with the BCs at $x = 0$. Those two BC equations lead to

$$A + D = 0 \quad \text{and} \quad -\lambda^2 D = 0$$

Since it is simpler, first examine the second of these two equations. Since λ^2 is not zero because P is not zero, then D must be zero. Since D is zero, then so too must A be zero. The last two BC equations become

$$BL + C \sin(\lambda L) = 0 \quad \text{and} \quad -\lambda^2 C \sin(\lambda L) = 0$$

Again start with the simpler, second equation. Note again that λ^2 is not zero. If C is zero, then so too is B by the preceding equation. Having A , B , C , and D be zero leads to the rejected trivial solution of $w(x)$ being everywhere zero. Therefore the factor C cannot be allowed to be zero. The only remaining possible zero factor is

$$\sin(\lambda L) = 0$$

This choice forces B to be zero, but that is no matter since C is not zero. The only way this sine term can be zero is for

$$\lambda L = \pm n\pi$$

Sense can be made of this infinite number of possibilities by returning to the definition of λ . Substituting that definition in the above solution leads to

$$P = n^2 \pi^2 \frac{EI}{L^2} \quad (11.8)$$

which is an infinite number of solutions for P . Clearly the lowest value for P , which corresponds to $n = 1$, is the most significant because the higher force values corresponding to higher values of n cannot be gradually applied to the beam-column without first applying this lowest magnitude of compressive force that causes the beam-column to buckle.⁷ This lowest force value is called the *critical force value* or the *Euler buckling force value*. That is,

$$P_{cr} = \pi^2 \frac{EI}{L^2} \quad (11.9)$$

Using this solution for the magnitude of P produces the following solution for the deflection:

$$w(x) = C \sin\left(\frac{\pi x}{L}\right) \quad (11.10)$$

which shows that the buckling shape for the simply supported, uniform beam is sinusoidal, but gives no information regarding the magnitude of the maximum deflection. All the BCs have been used, and there are no other conditions available to evaluate this last constant of integration, C . This problem result is unlike all the other beam deflection problem results previously considered. Without getting into detailed mathematical definitions of the two problem classifications (for which one may see, e.g., Refs. [16, 25]), all prior beam deflection problems were, as previously labeled, examples of boundary value problems. They all had fully specified loadings and unique, fully defined solutions that are never zero for a nonzero loading. On the other hand, this buckling problem with its initially unknown applied force magnitude is an example of an *eigenvalue problem* in differential equation form. In a buckling eigenvalue problem, the unknown compressive loading is always the essential part of the eigenvalue.

In review, any differential equation eigenvalue problem always has (i) a GDE that includes both an unknown factor, the eigenvalue, and an unknown function of the independent variable, which in this case is $w(x)$, for a total of two unknowns in the one equation; (ii) a trivial (i.e., a datum (zero)) solution for the function of the independent variable regardless of the magnitude of the eigenvalue, which in this case is proportional to the applied force; (iii) distinct, as opposed to continuous, solutions for the eigenvalue corresponding to generally different solutions for the function of the independent variable, like Eq. (11.8); and (iv) solutions for the function of the independent variable, called the eigenfunctions, that always contain an unknown, multiplicative constant, like Eq. (11.10). This fourth item is a result of the first item, that is, of there being only one equation and two unknowns. Note that the indeterminate final constant of integration can be either positive or negative. This means physically that the perfectly straight beam is equally likely to buckle upward or buckle downward

⁷ Since the GDE does not make allowances for inertia forces, the loading must be considered to be applied sufficiently slowly so as to avoid the structure developing kinetic energy.

in Fig. 11.11 (in the absence of gravity). Thus, unlike all the linear differential equations considered previously, this essentially nonlinear equation does not have a unique solution.

The eigenvalue analysis for a beam-column with other than simple support BCs proceeds in the same fashion as the above case. Since the GDE is the same for any single, uniform beam-column subjected only to axial forces applied at its ends, it is only a matter of writing and applying the different BCs, reasoning which constants of integration must have fixed values, and arriving at, and solving, a single equation for the eigenvalue, and hence the critical force. The last two example problems and the exercises provide several problems that involve other BCs. Keep in mind that in any buckling problem, it is unwise to simply cancel any factor that arises from any aspect of the buckling problem solution without careful consideration.

The type of buckling described by the above analysis is called *Euler beam buckling*. It is a form of buckling where the stresses are entirely within the elastic range. It is the type of buckling that is prevalent for columns that are “long” with respect to their depth in the plane of bending. Few unreinforced beam-columns are designed to be so relatively long because the result would be unacceptably low buckling forces. The buckling of the more common, less slender, beam-columns involves either (i) local elastic buckling (e.g., the crimping of a flange in the case of thin cross-sections), or (ii) plastic deformations. Neither possibility is mathematically treatable using the beam equations derived in the previous chapter. Nevertheless, the above simply supported beam analysis is an introduction to these more advanced topics which are considered in the next to last chapter.

To elaborate on the above comments, be sure to understand that inherent in the above beam-column analysis is the linearly elastic stress-strain relation, Eq. (9.4a). Thus, at the very least, the above analysis is not applicable to a situation where the value of the Euler buckling load divided by the beam cross-sectional area exceeds the material stress-strain proportional limit. Indeed, when the axial load is less than the critical load, and the value of the increasing axial load divided by the cross-sectional area reaches the value of the yield stress, the perfectly straight column subjected to a perfectly aligned axial load does not buckle. Instead, such a beam-column undergoes ordinary compressive yielding. Thus there is limit to the applicability of the Euler buckling equation to the perfectly constructed and perfectly loaded beam-column. In the case of actual beams with common loadings, neither of which are ever perfect, in addition to being compressed, the beams are also always bent. That bending causes the stresses at the outer portions of the beam to exceed the proportional limit sooner than those nearer the centroid. This situation is, of course, not accounted for in the simple Euler analysis presented above. Therefore, for actual beams there is a smooth transition from short beams that fail by plastic yielding under the action of a compressive load at approximately the yield stress, to long, slender beams that buckle at the Euler buckling load (i.e., buckling stress).

There are various analyses that account for the axial load-induced nonelastic beam bending that occurs in shorter beams when P/A approaches the yield stress; see Ref. [64]. In such analyses the tangent modulus and secant modulus material properties play prominent parts. However, the more common engineering approach to the buckling of shorter beam-columns is to use an empirical formula that takes into account, by means of thorough testing, the usual eccentricities of loads and beam-column axes for beam-columns that are: (i) nominally straight; and (ii) nominally loaded parallel to the beam's unloaded axis at the centroids of the beam end cross-sections. These empirical formulas are to be used in place of the Euler critical load (or critical stress) equation when the beam's nondimensional slenderness ratio $S = (L^2 A/I)^{1/2}$ is less than the S values for which the Euler equation is valid. The least value of the slenderness ratio for which the Euler equation is a good

description of the beam-column buckling load or buckling stress is called the transition slenderness ratio, S_t .

The most famous of the empirical formulas for less slender beams is J. B. Johnson's parabolic formula. Johnson's parabola (Ref. [66]) in terms of the nondimensional axial stress is generally taken to have the form $P/(\sigma_y A) = 1 - C[S^2/(\pi^2 E/\sigma_y)]$ where again $S^2 = (L^2 A/I)$, and C is a constant. The constant C is usually determined by requiring that the above parabolic formula, as a function of the slenderness ratio, have the same $P/(\sigma_y A)$ value and the same slope as the Euler equation curve at the value of the transition slenderness ratio, S_t . Note that in terms of the slenderness ratio, the Euler buckling load equation, Eq. (11.9), can be written as $P/(\sigma_y A) = (\pi^2 E/\sigma_y)/S^2$. Equating these two formulas for $P/(\sigma_y A)$ and equating their slopes yields the result that the constant C has the value $\frac{1}{4}$, and the transition point between the two formulas is $S_t^2 = 2\pi^2 E/\sigma_y$.

In the case of beams with other than simple support BCs, the same empirical formulas can be used if the length of the beam is changed from the actual length to an effective length for those BCs according to the Euler analysis solution for those BCs. For example, Exercise 11.12 shows that the Euler buckling load for a clamped-clamped beam is $P_{cr} = 4\pi^2 EI/L^2$. This solution can be put into the form of the solution for the simply supported beam by rewriting this solution as $\pi^2 EI/(\frac{1}{2}L)^2 \equiv \pi^2 EI/(L^*)^2$ where the effective length for the clamped-clamped beam is $L^* = \frac{1}{2}L$. In the case of aluminum beams, also see Ref. [48].

11.7 ** Additional Comments on Beam Buckling **

Reconsider Eq. (11.9), the Euler beam buckling, lateral deflection, solution for the simply supported beam. That equation states that the deflected shape of the buckled beam is $w(x) = C \sin(\pi x/L) = w(L/2) \sin(\pi x/L)$. The physical interpretation of the nonspecific factor $w(L/2) \equiv w_{max}$ in Eq. (11.10) is that, associated with the unique value of the critical load, there is no unique value for the maximum (i.e., midspan) amplitude. This range of possible amplitudes starts with zero and extends to some value at which the basic finite beam-column deflection equation is at its limit of applicability. However, a more advanced buckling analysis, found for example in Ref. [3], tells a different story. That type of nonlinear analysis shows that while the analysis result of the previous section is very close to being true for maximum deflections extending to nearly one-tenth of the beam-column length, there is actually a very small increase in load required for increases in the maximum deflection within that range of deflections. Maximum deflections beyond that one-tenth of the length value require more substantial increased loadings. In other words, there is a (nearly) unique axial force versus lateral midspan deflection relationship for all values of the midspan deflection. The sole ambiguity is in the sign of the deflection, that is, the direction in which the perfectly loaded perfect beam deflects. Buckling a thin, flat plastic ruler can easily confirm the result of the more advanced analysis for larger maximum deflections, but it takes sensitive fingers to sense the P versus w_{max} relation for the lesser finite deflections.

The higher-valued buckling loads associated with higher values of the integer n in the original $(n\pi)^2 EI/L^2$ buckling load solution are only possible in the sense of describing stable beam deflections if additional constraints on the beam deflections are applied to the beam-column. For example, if the beam has an additional roller support at its midspan, then the deflection shape of Eq. (11.9) does not satisfy this additional deflection constraint condition, and thus is not a solution for this modified circumstance. However, the deflection shape $w(x) = C' \sin(2\pi x/L)$ does satisfy this new internal condition as well as the old BCs. Of course, this deflection shape also satisfies the GDE. Therefore $w(x) = C' \sin(2\pi x/L)$ is the deflection solution for the beam-column with the additional midspan roller support.

Since the integer n in this modified deflection solution has the value 2, the critical force value, or Euler buckling force value, for this modified problem is

$$P_{cr} = 4\pi^2 \frac{EI}{L^2}$$

See the first part of Endnote (6) for the case where the additional roller constraints are not located at points on the beam axis where $x = L/n$.

Another prominent example of a beam differential equation eigenvalue problem is the one that describes lateral beam vibrations in the absence of applied loads. In this "free vibration" case, the natural frequencies of the beam are the essential parts of the eigenvalue, and the eigenfunctions are again the lateral deflection functions. Exercise 11.17 addresses the related problems of the forced axial vibrations of a beam as well as the forced lateral vibrations of a beam.

The buckling problems discussed in this text are restricted to the situation where all compressive end forces P , and axial forces per unit length, retain their original orientation in space after beam buckling. This is the sort of behavior exhibited, for example, by forces due to gravity. It is possible to have applied compressive end forces that, rather than remain parallel to the undeformed beam axis, follow the rotation of the beam ends. These types of forces are often referred to as "body-fixed" forces. This innocuous appearing distinction turns out to be one difference between conservative and nonconservative forces. This distinction is rather important to the complexity of the necessary buckling analysis, and to the magnitude of the corresponding buckling load. The beam-column buckles under a lesser, sometimes a much lesser, force in the conservative case, and the conservative force analysis is also much simpler. Further comment on this matter is left to more advanced texts such as Refs. [23, 24].

The method of buckling analysis presented in the previous section is based on the beam equations derived in the preceding chapter. Those equations were derived for a beam-column bent to the extent of finite bending deflections from its original straight-line position. The original straight-line position is the only stable equilibrium position when (i) the beam-column loading is restricted to a compressive force whose magnitude is less than that of the buckling force and (ii) there are no lateral loads. When the magnitude of the applied compressive force is increased to the value of the buckling force, it is observed that the straight beam-column undergoes finite bending deflections that bring it into a bent equilibrium position. That is, the compressive buckling force (and higher magnitudes of such compressive forces), can retain (in the face of perturbations) a finite deflection bent form as an equilibrium configuration for the entire beam-column. Again, experiments with a thin, flat plastic ruler will confirm the above statements. The straight equilibrium configuration is unstable once the compressive load equals or exceeds the critical load.

For the reason that the beam equations of the preceding chapter describe a (stable) bent equilibrium configuration close to the (unstable) straight equilibrium configuration, for the same buckling force, the use of those beam equations is one aspect of a broad approach to buckling problems often referred to as the "adjacent equilibrium method." The adjacent equilibrium method is just one of four distinct approaches to the elastic buckling problem. See Ref. [24] for information on the "imperfection method," the "energy method," and the "dynamic analysis method," and the occasional need to combine these methods. Endnote (2), in the course of discussing the Example 11.6 boundary value problem, presents a variation upon the imperfection method wherein a lateral loading is used to indirectly "unstraighten," and thus make imperfect, a mathematically straight beam.

There are adjacent equilibrium problems that describe the interaction of applied fluid forces and structural deflections that are of particular interest to flight vehicle engineers. The simplest is the subsonic, unswept airfoil section torsional *divergence* problem. In some publications, the entire class of adjacent equilibrium problems is named divergence problems. See Exercise 11.16 and the last chapter for further information on the airfoil divergence problem. Furthermore, continuing with aircraft terminology, any stability problem involving the accelerating masses of a dynamic analysis is sometimes called a *flutter* problem, regardless of whether or not the structure includes airfoils or an aerodynamic origin for the time-varying loading.

11.8 Summary

The usefulness of the beam bending equations of Chapter 10 can sometimes be extended to the analysis of beams that are an individual element of a surrounding beam structure by modeling the beam end supports as having appropriate elastic stiffnesses. When the beam structure is limited to a very small number of other beams, it is sometimes not too much handwork to accurately estimate the beam end equivalent spring stiffnesses. However, the computer-based method discussed in Part V, the finite element method, is generally a much more appropriate approach to analyzing a beam that is part of a larger structure. The analysis of single beams as discussed here promotes an understanding of the treatment of beams within a finite element analysis.

The use of elastic supports in mathematical beam models can be combined with the use of the Dirac delta function and the Heaviside step function. These two mathematical distributions permit all manner of concentrated and distributed loads to be described in terms suitable for the analytical integration of the beam bending equations. A series of review example problems follows.

Example 11.7. Consider the elastically supported bar shown in Fig. 11.12(a). The bar is subjected to a constant temperature increase, T_0 . Recall previous comment that such a bar loading can deliver large forces to the supports at the ends of the bar. For example, for a steel bar experiencing only a 20 °F temperature increase, with $E = 29. E + 6$, and $\alpha = 6. E - 6$, the reaction at each of the supports is 3500 psi of beam cross-sectional area. Therefore modeling the supports as rigid may well be unrealistic. In this example the end supports are modeled as springs. The task at hand is (a) to determine the deflections of this bar; and (b) determine the stresses in the bar.

Solution. Since there is no mechanical loading, and the temperature change is a constant, the combined axial force per unit length is zero. Hence the GDE and its solution are simply

$$(d/dx)[EA u'(x)] = 0 \quad \text{and} \quad u(x) = C_1 x + C_2$$

From the free body diagrams of thin slices at the ends of the bar, the preliminary boundary conditions are $k_1 u(0) = N(0)$, and $k_2 u(L) = -N(L)$. The important point here is that the deflections, regardless of how obvious is the physical reality, must, like the stress reactions, always be drawn according to their sign convention. Since the spring forces act oppositely to the deflections, they have the directions shown in Fig. 11.12(b). Since $N(x) = EA u'(x) - N_T(x)$, and $N_T(x) = EA\alpha T_0$, these two BCs become

$$EA u'(0) - k_1 u(0) = EA\alpha T_0 \quad \text{and} \quad EA u'(L) + k_1 u(L) = EA\alpha T_0$$

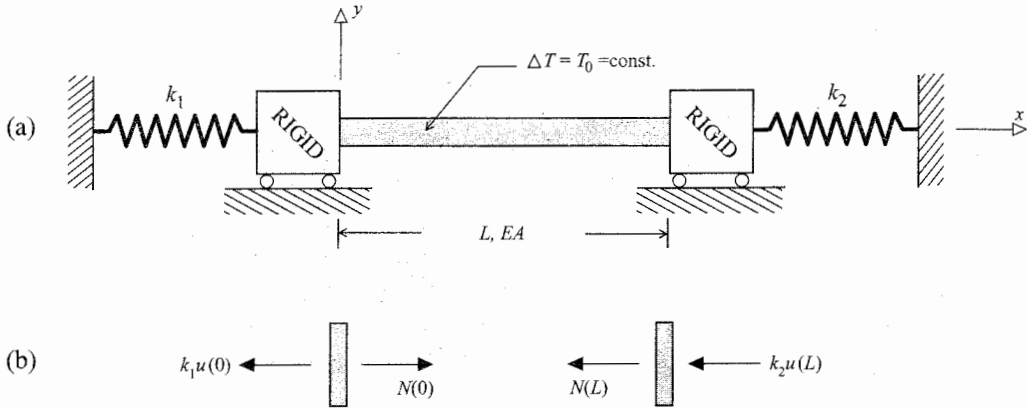


Figure 11.12. (a) A uniform beam with elastic supports subjected to a constant temperature increase. (b) Free body diagrams of the beam ends.

In order to simplify the algebra, let $K_1/EA = \beta$, and $K_2/EA = \gamma$, where β and γ have units of one over length. Substituting the deflection solution into the two BCs leads to the deflection solution

$$u(x) = \alpha T_0 \frac{(\beta + \gamma)x - \gamma L}{\beta + \gamma + \beta\gamma L} = \alpha T_0 \frac{\beta x - \gamma(L - x)}{\beta + \gamma + \beta\gamma L}$$

Note that in the case of rigid supports, both β and γ approach infinity. Then the deflection approaches zero. In the case of no supports, both beta and gamma approach zero, and the midspan deflection becomes zero, while the left end has a deflection of $-\frac{1}{2}L\alpha T_0$ and the right-hand bar end has a deflection of $+\frac{1}{2}L\alpha T_0$. Furthermore, if β is zero while γ is infinite, then $u(x) = -(L - x)\alpha T_0$. If β is infinite while γ is zero, then $u(x) = -(L - x)\alpha T_0$. Thus these four special cases have outcomes that are exactly as would be expected.

$$\sigma_{xx} = -E\alpha T_0 \frac{\beta\gamma L}{\beta + \gamma + \beta\gamma L}$$

Again it is possible to look at special cases. For example, if β and γ become infinite, then the axial stress is simply a compressive $E\alpha T_0 L$, as it should be. ■

Example 11.8. The nonuniform beam shown in Fig. 11.13 is subjected to various distributed and concentrated loadings as well as a temperature change that produces the following thermal moments

$$M_{yT}(x) = M_0 \left(2 - \frac{x}{L}\right) \quad M_{zT} = M_0 \left(3 - \frac{x}{L}\right)$$

Write the functions of x that are, respectively,

$$(a) f_y^c(x) \quad (b) f_z^c(x) \quad (c) m_y'(x) \quad (d) m_z'(x)$$

Then integrate the expression for $f_z(x)$ once only between the limits zero and x .

Solution. Because the equivalent lateral thermal loads per unit length are zero (the result of two derivatives of the given thermal moments), the combined lateral loads per unit length

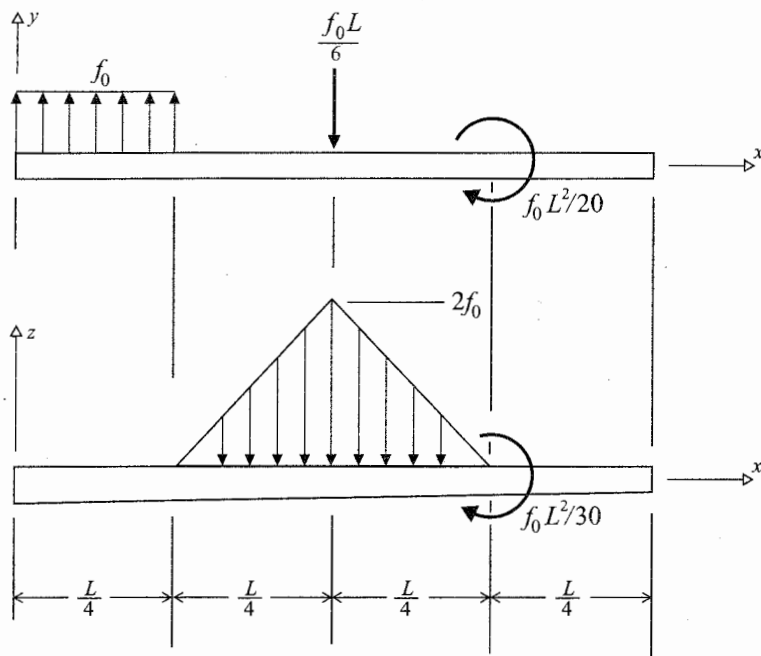


Figure 11.13. Example 11.8.

are the same as the mechanical applied lateral loads per unit length. They, and the derivatives of the moments per unit length, are

$$(a) f_y(x) = f_0 \left[1 - \text{stp} \left(x - \frac{L}{4} \right) \right] - \frac{f_0 L}{6} \delta \left(x - \frac{L}{4} \right)$$

$$(b) f_z(x) = +2f_0 \left(1 - \frac{4x}{L} \right) \left[\text{stp} \left(x - \frac{L}{4} \right) - \text{stp} \left(x - \frac{L}{2} \right) \right] \\ - 2f_0 \left(3 - \frac{4x}{L} \right) \left[\text{stp} \left(x - \frac{L}{2} \right) - \text{stp} \left(x - \frac{3L}{4} \right) \right]$$

$$(c) m'_y(x) = +\frac{f_0 L^2}{30} \delta' \left(x - \frac{3L}{4} \right)$$

$$(d) m'_z(x) = -\frac{f_0 L^2}{20} \delta' \left(x - \frac{3L}{4} \right)$$

By multiplying out the products and combining the second and third terms, the lateral force per unit length in the z direction can be rewritten in a form quite convenient for integration as

$$f_z(x) = -\frac{8f_0}{L} \left(x - \frac{L}{4} \right) \text{stp} \left(x - \frac{L}{4} \right) + \\ \frac{16f_0}{L} \left(x - \frac{L}{2} \right) \text{stp} \left(x - \frac{L}{2} \right) - \frac{8f_0}{L} \left(x - \frac{3L}{4} \right) \text{stp} \left(x - \frac{3L}{4} \right)$$

Hence

$$\int_0^x f_z(x) dx = -\frac{4f_0}{L} \left(x - \frac{L}{4} \right)^2 \text{stp} \left(x - \frac{L}{4} \right) + \\ \frac{8f_0}{L} \left(x - \frac{L}{2} \right)^2 \text{stp} \left(x - \frac{L}{2} \right) - \frac{4f_0}{L} \left(x - \frac{3L}{4} \right)^2 \text{stp} \left(x - \frac{3L}{4} \right)$$

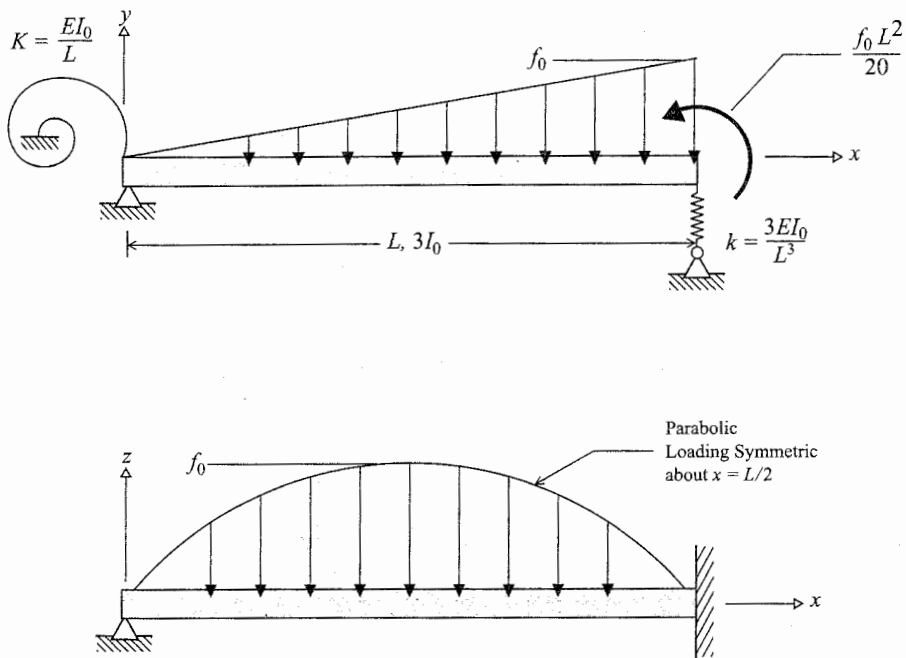


Figure 11.14. Example 11.9.

Example 11.9. (a) Write the UNCOUPLED governing differential equations for bending for the uniform beam shown in Fig 11.14. Let the beam properties and thermal loading be $N_T = 0$, and

$$E_0 = E \quad I_{yy}^* = 2I_0 \quad I_{zz}^* = 3I_0 \quad I_{yz}^* = +I_0 \quad M_{yT} = \frac{f_0 L^2}{20} \left(2 - \frac{x}{L}\right) \quad M_{zT} = \frac{f_0 L^2}{20} \left(2 - \frac{x^2}{L^2}\right)$$

(b) Do not integrate. Write the boundary conditions entirely in terms of the lateral deflection functions.

Solution. The parabolic expression for $f_z(x)$ can be determined either by trial and error, or by fitting the general form for a parabola to the case at hand. By the latter approach, write

$$f_z(x) = ax^2 + bx + c \quad \text{where} \quad f_z(0) = f_z(L) = 0 \quad \text{and} \quad f_z\left(\frac{L}{2}\right) = f_0.$$

Substituting the general form for the parabola into $f_z(0) = 0$ immediately produces the result $c = 0$. The simultaneous solution of the second and third conditions yields the result stated below.

The determination of the boundary conditions in the x, y plane must start with drawing free body diagrams of each beam end. It is wise to draw the FBDs large enough to clearly see how to sum forces and moments. Remember, of course, that each rigid support provides an unknown force, and perhaps a moment, reaction. These unknown reactions are never part of BC statements. Instead, there is always some type of a beam end deflection statement to be made. If the rigid support supplies an unknown moment, then there is always a known

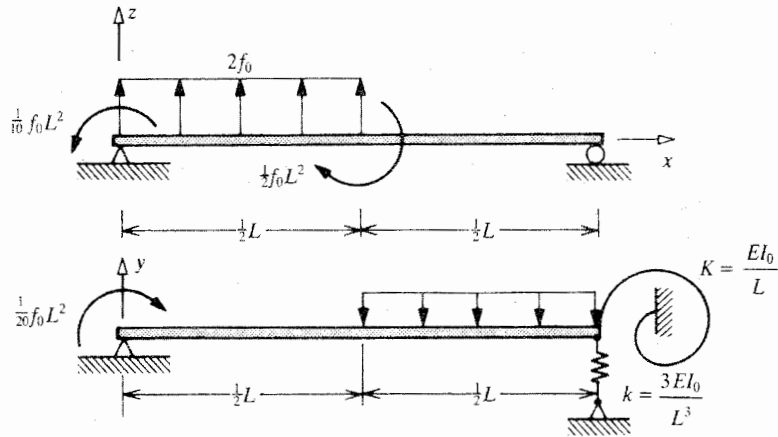


Figure 11.15. Example 11.10.

bending slope. If the rigid support supplies an unknown force reaction, then there is always a known lateral deflection.

$$(a) \quad R_{zz} = \frac{(3I_0)(2I_0) - I_0^2}{3I_0} = \frac{5}{3}I_0 \quad R_{yy} = \frac{5I_0^2}{2I_0} = \frac{5}{2}I_0 \quad R_{yz} = 5I_0$$

$$f_z = 4f_0 \left(\frac{x^2}{L^2} - \frac{x}{L} \right), \quad f_y = -f_0 \frac{x}{L}, \quad f_{zT} = 0, \quad f_{yT} = -\frac{f_0}{10}, \quad m_y = m_z = 0$$

$$\therefore \frac{5}{3}EI_0 w''''(x) = -4f_0 \frac{x}{L} + 4f_0 \frac{x^2}{L^2} - \frac{I_0}{3I_0} \left[-f_0 \frac{x}{L} - \frac{f_0}{10} \right] = f_0 \left(4 \frac{x^2}{L^2} - \frac{11x}{3L} + \frac{1}{30} \right)$$

$$\frac{5}{2}EI_0 v''''(x) = -f_0 \frac{x}{L} - \frac{f_0}{10} - \frac{1}{2} \left[-4f_0 \frac{x}{L} + 4f_0 \frac{x^2}{L^2} \right] = f_0 \left(-2 \frac{x^2}{L^2} + \frac{x}{L} - \frac{1}{10} \right)$$

$$\text{or } 5EI_0 w''''(x) = f_0 \left(12 \frac{x^2}{L^2} - 11 \frac{x}{L} + \frac{1}{10} \right) \quad 5EI_0 v''''(x) = f_0 \left(-4 \frac{x^2}{L^2} + 2 \frac{x}{L} - \frac{1}{5} \right)$$

$$(b) \text{ Deflection BCs: } v(0) = 0 \quad \text{and} \quad v(0) = w(0) = w(L) = w'(L) = 0$$

$$\text{Force BCs from FBDs: } (1) M_z(0) - \frac{EI_0}{L} v'(0) = 0 \quad (2) M_z(L) = f_0 L^2 / 20$$

$$(3) V_y(L) - \frac{3EI_0}{L^3} v(L) = 0 \quad (4) M_y(0) = 0$$

In this case, it is not beneficial to use the second BC table

$$(1) \quad 3EI_0 v''(0) + EI_0 w''(0) - \frac{EI_0}{L} v'(0) = M_{zT}(0) = \frac{f_0 L^2}{10}$$

$$(2) \quad 3EI_0 v''(L) + EI_0 w''(L) = M_{zT}(L) + \frac{f_0 L^2}{20} = \frac{f_0 L^2}{10}$$

$$(3) \quad 3EI_0 v'''(L) + EI_0 w'''(L) - \frac{3EI_0}{L^3} v(L) = M'_{zT}(L) = -\frac{f_0 L}{10}$$

$$(4) \quad EI_0 v''(0) + 2EI_0 w''(0) = M_{yT}(0) = \frac{f_0 L^2}{10}$$

Example 11.10. Consider the homogeneous, uniform beam of length L that is shown in Fig. 11.15. (a) Without actually integrating, write in a form suitable for integration (i.e., simplify as much as possible) the two uncoupled GDEs for beam bending. (b) In terms of the bending deflections and their derivatives, write the BCs in uncoupled form to the extent

possible. Let

$$I_{yy} = 2I_0 \quad I_{zz} = 4I_0 \quad I_{yz} = I_0$$

and

$$M_{yT}(x) = -\frac{f_0 L^2}{20} \left(2 - \frac{x}{L}\right) \quad M_{zT}(x) = \frac{f_0 L^2}{20} \left(3 - \frac{x}{L}\right)$$

Solution. (a)

$$R_{yy} = \frac{7}{2}I_0 \quad R_{zz} = \frac{7}{4}I_0 \quad R_{yz} = 7I_0 \quad m_z(x) = 0 \quad f_{zT}(x) = f_{yT}(x) = 0$$

and therefore

$$f_z^c(x) = 2f_0 \left[1 - \text{stp} \left(x - \frac{1}{2}L\right)\right] \quad m_y(x) = +\frac{1}{2}f_0 L^2 \delta \left(x - \frac{1}{2}L\right) \quad f_y^c(x) = -f_0 \text{stp} \left(x - \frac{1}{2}L\right)$$

After multiplying through by the leading fraction and simplifying the right-hand side of each GDE, the results are

$$EI_0 w''''(x) = \frac{8}{7}f_0 - f_0 \text{stp} \left(x - \frac{1}{2}L\right) + \frac{2}{7}f_0 L^2 \delta' \left(x - \frac{1}{2}L\right)$$

$$EI_0 v''''(x) = -\frac{2}{7}f_0 - \frac{1}{14}f_0 L^2 \delta' \left(x - \frac{1}{2}L\right)$$

(b) Eight BCs are necessary. The three deflection BCs are simply $v(0) = w(0) = w(L) = 0$. Since at $x = 0$ the beam has the same simple support in both Cartesian planes, it is possible to decouple the bending moment BCs at $x = 0$:

$$\begin{aligned} M_z(0) &= +\frac{1}{20}f_0 L^2 & M_{zT}(0) &= +\frac{3}{20}f_0 L^2 & M_z^c(0) &= +\frac{1}{5}f_0 L^2 \\ M_y(0) &= -\frac{1}{10}f_0 L^2 & M_{yT}(0) &= -\frac{1}{10}f_0 L^2 & M_y^c(0) &= -\frac{1}{5}f_0 L^2 \end{aligned}$$

Using the BC forms from the second BC table, the fourth and fifth BCs are

$$\begin{aligned} w''(0) &= \left(\frac{4}{7} \left(-\frac{1}{5}\right) - \frac{1}{7} \frac{1}{5}\right) \frac{f_0 L^2}{EI_0} = -\frac{1}{7} \frac{f_0 L^2}{EI_0} \\ v''(0) &= \left(\frac{2}{7} \frac{1}{5} - \frac{1}{7} \left(-\frac{1}{5}\right)\right) \frac{f_0 L^2}{EI_0} = \frac{3}{35} \frac{f_0 L^2}{EI_0} \end{aligned}$$

Since the supports in the two Cartesian planes at $x = L$ are not the same, it is not possible to decouple both of the moment BCs at this end. Using the BC form from the first BC table for the moment in the x, z plane leads to a sixth BC:

$$M_y(L) = 0 \quad M_{yT}(L) = M_y^c(L) = -\frac{1}{20}f_0 L^2$$

whence

$$v''(L) + 2w''(L) = -\frac{1}{20} \frac{f_0 L^2}{EI_0}$$

The seventh and eighth BCs are obtained from drawing a FBD of the beam end slice at $x = L$ in the x, y plane. The resulting two equilibrium equations are

$$M_z(L) + \frac{EI_0}{L} v'(L) = 0 \quad \text{and} \quad V_y(L) - \frac{3EI_0}{L^3} v(L) = 0$$

With $M_{zT}(L) = (1/10)f_0L^2$ and $V_{yT}(L) = -(1/20)f_0L$, and then using the BC forms from the first BC table, leads to the following form of the seventh and eighth BCs:

$$4Lv''(L) + Lw''(L) + v'(L) = +\frac{1}{10}\frac{f_0L^3}{EI_0}$$

$$4L^3v'''(L) + L^3w'''(L) - 3v(L) = -\frac{1}{20}\frac{f_0L^4}{EI_0}$$

The above answers for the BCs are entirely satisfactory. However, it turns out that in this particular problem there is an advantage to using the BC forms from the second BC table for the moment expressions at $x = L$. One of the BC equations turns out to be uncoupled while, of course, the second remains coupled. The collected data required for these moment equations are

$$M_z(L) = -Kv'(L) \quad M_{zT}(L) = +\frac{1}{10}f_0L^2 \quad M_z^c(0) = +\frac{1}{10}f_0L^2 - Kv'(L)$$

$$M_y(L) = 0 \quad M_{yT}(L) = -\frac{1}{20}f_0L^2 \quad M_y^c(0) = -\frac{1}{20}f_0L^2$$

The moment equation alternate forms for the sixth and seventh of the above BC equations from the second BC table are then

$$7Lw''(L) - v'(L) = -\frac{3}{10}\frac{f_0L^2}{EI_0}$$

$$7Lv''(L) + 2v'(L) = +\frac{1}{4}\frac{f_0L^2}{EI_0}$$

In this form of the sixth and seventh BC equations, there is also the advantage of one less deflection term. Lastly, note that in this special case it is also possible to use the second BC table for the shearing forces at $x = L$, which are summed in the eighth BC equation, because the beam is statically determinate in the x, z plane, and therefore the vertical reaction at $x = L$ can be calculated. This alternative is not overly advantageous. It is merely mentioned to support the comment that with linear problems there usually are a variety of ways to solve a given problem. ■

In Example 11.10 the partial span loads are described using Heaviside step functions where, as in all previous such descriptions, the coordinate variable appears first in the argument. Since this is slightly inefficient in some cases, an example problem illustrating the alternate use of the Heaviside step function may be found in Endnote (4).

The one topic of this chapter that is profoundly different from all previous beam problems is beam-column buckling. The reason why this topic is so different is that all the previous beam analyses, with one exception, did not involve the coupling (interaction) of any of the deflections with any of the applied loads. In the beam-column buckling problem there is an interaction between the lateral deflections and the axial compressive force. The effect of that interaction is essentially nonlinear, despite the mathematically linear appearance of the GDE. The buckling problem is an example of a structural feedback problem. To understand how the loading and deflections interact, focus upon the center of the deflected beam in Fig. 11.11. A FBD of either half of the beam shows that the internal midspan bending moment is equal to the axial force at the beam end multiplied by the midspan deflection. From experiment, and from a more accurate analysis than the analysis presented here, it is known that the midspan deflection increases as the applied axial force

increases. As the deflection increases, the bending moment at midspan also increases. This in turn increases the beam midspan curvature, ($M \rightarrow w''$), which geometrically requires a greater midspan deflection, which in turn increases the midspan bending moment, which increases the midspan deflection, and so on. These interrelated changes in beam curvature and axial force can only be described by a differential, as opposed to an algebraic, equation.

In this textbook, the problem of estimating a beam axial buckling force is approached primarily from the perspective of the adjacent equilibrium method. The adjacent equilibrium method always produces an eigenvalue problem. Depending upon the problem formulation, the eigenvalue problem can be either a differential equation eigenvalue problem, or an algebraic eigenvalue problem. The adjacent equilibrium beam buckling analysis presented above is, of course, a differential equation eigenvalue problem. See Example 11.11 below. Chapter 23 presents an adjacent equilibrium beam buckling analysis using beam finite elements. The finite element matrix formulation leads to an algebraic eigenvalue problem. Chapter 23 also briefly introduces the energy approach to elastic stability problems. Chapter 22 introduces the plate buckling problem from the adjacent equilibrium perspective.

Example 11.11. Determine the Euler buckling load for a uniform beam that is clamped at $x = 0$, and simply supported at $x = L$.

Solution. The Euler buckling GDE and its solution are, *as always*, $EIw''''(x) + Pw''(x) = 0$, and $w(x) = C_1 + C_2x + C_3 \sin(\lambda x) + C_4 \cos(\lambda x)$ where $\lambda^2 \equiv P/(EI)$. As usual, the principal axes for the cross-section are used, and the x, z plane is chosen to be the plane with the smaller bending stiffness. It is the boundary conditions that distinguish one Euler buckling problem from another. The BCs in this case are $w(0) = w'(0) = w(L) = w''(L) = 0$. Substituting the solution to the GDE into each of the four BC equations, and arranging those four results in matrix form, yields, after discarding nonzero factors;

$$\begin{bmatrix} 1 & 0 & 0 & 1 \\ 0 & 1 & \lambda & 0 \\ 1 & L & \sin(\lambda L) & \cos(\lambda L) \\ 0 & 0 & \sin(\lambda L) & \cos(\lambda L) \end{bmatrix} \begin{Bmatrix} C_1 \\ C_2 \\ C_3 \\ C_4 \end{Bmatrix} = \begin{Bmatrix} 0 \\ 0 \\ 0 \\ 0 \end{Bmatrix}$$

Since this is a homogeneous matrix equation, the only possibility⁸ for a nontrivial solution (i.e., one other than where all the constants of integration are zero) is to require that the determinant of the coefficient matrix be zero. Expanding that determinant by minors⁹ of the first row leads to

$$[\sin(\lambda L) \cos(\lambda L) - \lambda L \cos(\lambda L) - \sin(\lambda L) \cos(\lambda L)] - [-\sin(\lambda L)] = 0$$

or $\tan(\lambda L) = \lambda L$. This transcendental equation can be solved in any number of ways. Perhaps the easiest is to use either Newton's method or a trial-and-error approach with a hand calculator after using a sketch of the tangent function and the straight line to determine that they cross at approximately $\lambda L = 4.5$. The solution, to five significant figures, is $\lambda L = 4.4934$. From this result, the Euler buckling load is $P_{cr} = 20EI/L^2$, which is approximately twice that of the simply supported beam.

⁸ See Section 2.6.

⁹ Recall that expanding a determinant by multiplying along diagonals of the determinant is *not* valid for determinants whose size is larger than 3×3 .

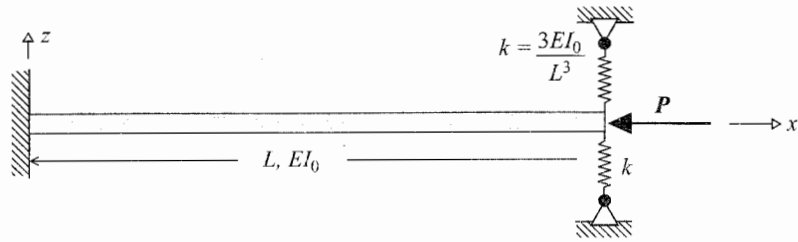


Figure 11.16. Example 11.12.

While it usually is of little importance, the shape of the buckled beam can be determined once the value of the eigenvalue is established. This objective is met by returning to the original matrix equation and solving for three of the constants of integration in terms of the fourth constant—the constant of integration that forever remains unspecified. In this case the result is

$$w(x) = C_1 \left[1 - 0.9973 \frac{x}{L} + 0.2219 \sin \left(4.4934 \frac{x}{L} \right) - \cos \left(4.4934 \frac{x}{L} \right) \right] \quad \blacksquare$$

Example 11.12. (a) The uniform beam shown in Fig. 11.16 is of length L , and is such that $EI_0 = EI_{yy} < EI_{zz}$. Therefore the beam will buckle first in the x, z plane. The beam is clamped at the left end ($x = 0$). At $x = L$, the beam is supported laterally by two translational springs each with stiffness factors $k = 3EI_0/L^3$. Determine the homogeneous, transcendental equation that can be used to determine the Euler buckling load for this beam when it is subjected to a compressive, axial load.

Solution. The GDE for this beam, and its solution, are, as always

$$EI_0 w''''(x) + Pw''(x) = 0, \quad w(x) = C_1 + C_2 x + C_3 \sin \lambda x + C_4 \cos \lambda x, \quad \text{where } \lambda^2 = \frac{P}{EI_0}.$$

The next task is to write the BC equations, and then use those equations to solve for the lowest valued eigenvalue, λ , from which the lowest value of P is determined. The two BCs at the beam tip are acquired from drawing a FBD. All four BCs *might seem to be*

$$w(0) = w'(0) = w''(L) = 0, \quad \text{and} \quad EI_0 w'''(L) - 2 \frac{3EI_0}{L^3} w(L) = 0$$

When these four equations are cast in matrix form, and the determinant is expanded, the resulting equation to be solved for the eigenvalue is

$$(\lambda L^3) - 6(\lambda L) \cos(\lambda L) - 6 \sin(\lambda L) = 0$$

Clearly zero is a root for this equation. A search for positive roots reveals that there is just one rather than an infinite number of such roots. That one positive root is $\lambda L = 1.68624$, or $P_{cr} = 2.84 \frac{EI}{L^2}$. The stiffer the boundary conditions, the higher the value for the critical axial force. This solution for $P_{cr} = 2.84 EI/L^2$ is a much lower critical axial load value than that determined for the simply supported beam, which was approximately $10 EI/L^2$. It was also determined above that the clamped–simply supported beam had a critical axial load value of approximately $20 EI/L^2$. A fully clamped beam has a critical value of nearly $40 EI/L^2$. The low value of this solution, and the absence of more than one positive solution to the eigenvalue transcendental equation should arouse grave suspicion, and that suspicion is indeed justified. The reason that this initial solution is **wrong** is that this type of analysis should be an *adjacent equilibrium* analysis. That is, the derivation of the beam equation

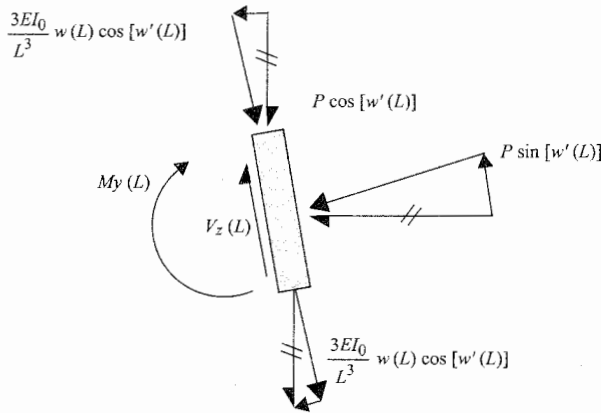


Figure 11.17. Example 11.12. Free body diagram of the elastically supported beam tip with all force components either parallel to, or perpendicular to the beam cross-section. It is important to remember that all Euler buckling analyses require energy conservative forces. This means that the axial force P retains its line of action, that is, remains horizontal as the beam deflects upward.

used here, $EI w''''(x) + Pw''(x) = 0$, was accomplished with a deflected (bent) differential beam length. The beam of Fig. 11.16 is not drawn as deflected. It represents the trivial solution where $w(x) = 0$, and this beam is not at an adjacent equilibrium state. To achieve an adjacent equilibrium state, the beam has to be deflected according to the positive sign conventions. In this case the beam has to be deflected upward, and the bending slopes have to be positive slopes. Hence the free body diagram of a very thin slice of the beam at the beam end should look like that of Fig. 11.17. Note that the axial force and the two spring forces have been resolved into components perpendicular and parallel to the internal shear force for easy summation. Since the bending slope at the beam tip is small, the cosine of that slope can be approximated as 1.0, while the sine of the bending slope can be approximated as the bending slope, $w'(L)$. Therefore the shear correct force boundary condition becomes

$$EI_0 w'''(L) + Pw'(L) = 2 \frac{3EI_0}{L^3} w(L)$$

The last BC equation can be simplified by dividing by EI_0 to get

$$L^3 w'''(L) + L^3 \lambda^2 w'(L) - 6w(L) = 0$$

The resulting matrix equation, whose coefficient matrix has a zero determinant, is

$$\begin{bmatrix} 1 & 0 & 0 & 1 \\ 0 & 1 & \lambda & 0 \\ 0 & 0 & -\lambda^2 \sin \lambda L & -\lambda^2 \cos \lambda L \\ 6 & L(6 - \lambda^2 L^2) & 6 \sin \lambda L & 6 \cos \lambda L \end{bmatrix} \begin{Bmatrix} C_1 \\ C_2 \\ C_3 \\ C_4 \end{Bmatrix} = \begin{Bmatrix} 0 \\ 0 \\ 0 \\ 0 \end{Bmatrix}$$

Expanding the determinant of the coefficient matrix leads to, where $x = \lambda L$

$$x^3 \cos x - 6x \cos x + 6 \sin x = 0 \quad \text{or} \quad \tan x = x - \frac{x^3}{6}$$

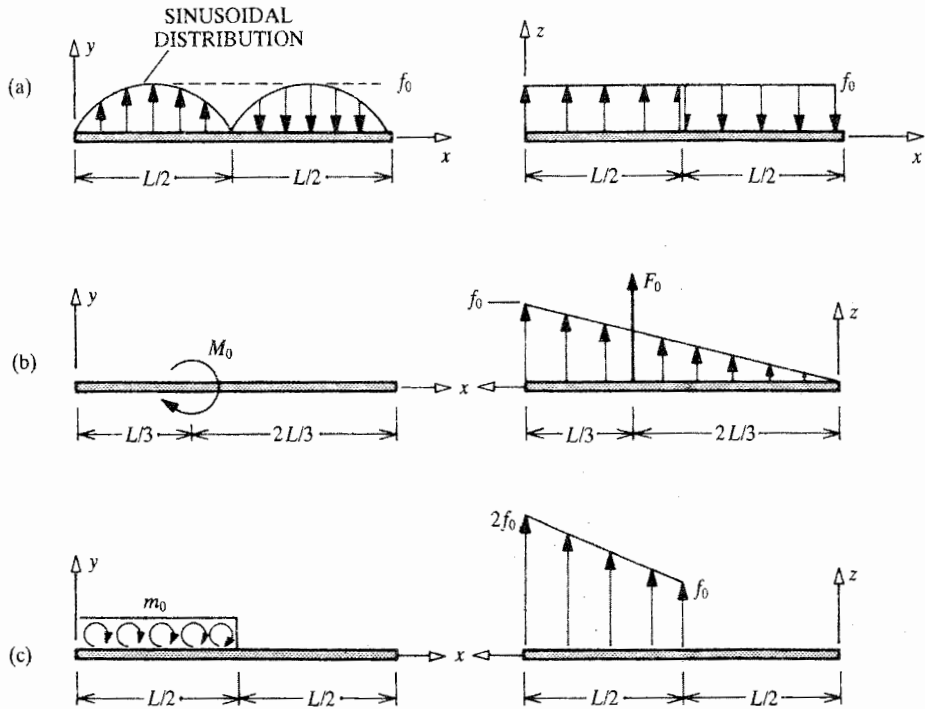


Figure 11.18. Exercise 11.2. Note that the direction of the x axis varies from sketch to sketch.

The solution to this transcendental equation from *Mathematica* is $x = 2.672$. Hence, with λ equaling the square root of P/EI_0 ,

$$P_{cr} = 7.13 \frac{EI_0}{L}$$

Chapter 11 Exercises

11.1. If a and b are constant values of the lengthwise coordinate x , integrate the following expressions twice with respect to x , between the limits of zero and x . Don't be concerned about constants of integration.

- (a) $\delta'(x - a)$ (b) $x \delta(x - b)$ (c) $(x - a) \text{stp}(x - b)$ (d) $(x - a)^2 \text{stp}(x - b)$

Integrate the following GDEs (from zero to x) so as to determine only the second derivative of the deflection function in terms of the two unknown integration constants.

- (e) $EIw''''(x) = f_0[1 - (2x/L)] \text{stp}(x - \frac{1}{2}L)$
 (f) $EIw''''(x) = f_0[1 + (2x/L)] \text{stp}(x - \frac{1}{2}L)$
 (g) $ERv''''(x) = M_0\delta'(x - a) + m_0\delta(x - b) + f_0 \text{stp}(x - c)$
 (h) $EIw''''(x) = (f_0/\sqrt{L})\sqrt{(x - c)} \text{stp}(x - c)$

11.2. Write the force per unit length and moment per unit length expressions for each of the beam lengths shown in (a) Fig. 11.18(a); (b) Fig. 11.18(b); (c) Fig. 11.18(c). There are no equivalent thermal loads in this case.

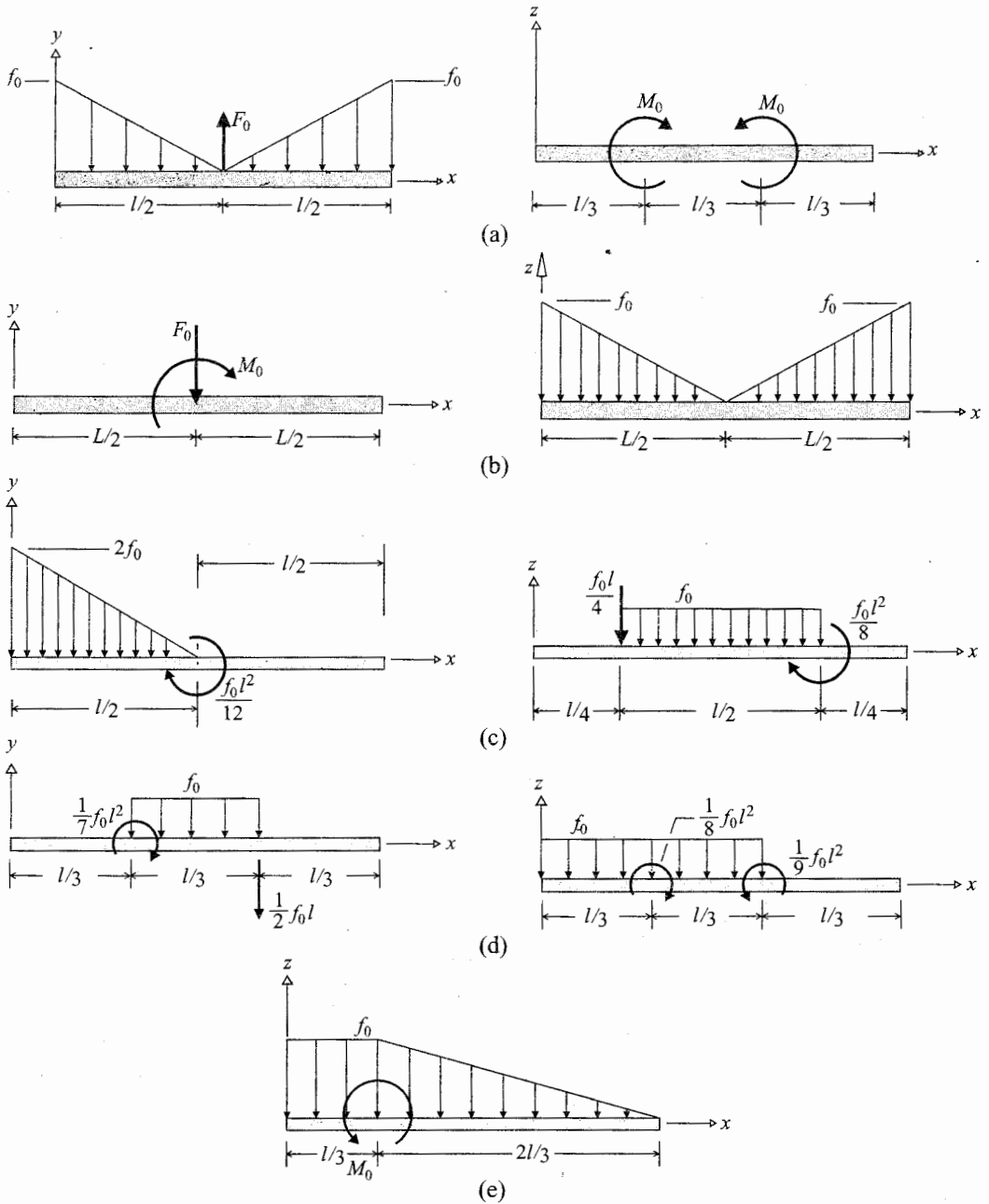


Figure 11.19. Exercise 11.3.

- 11.3. (a) Write the governing differential equations for the uniform beam and lateral loading shown in Fig. 11.19(a). Let the y and z axes be principal axes. Let the temperature change be zero. Ignore the boundary conditions.
- (b) For the beam and loading shown in Fig. 11.19(b), write analytic expressions for $f_y(x)$, $f_z(x)$, $m_y(x)$, and $m_z(x)$. Be sure to pay attention to the applicable sign conventions.

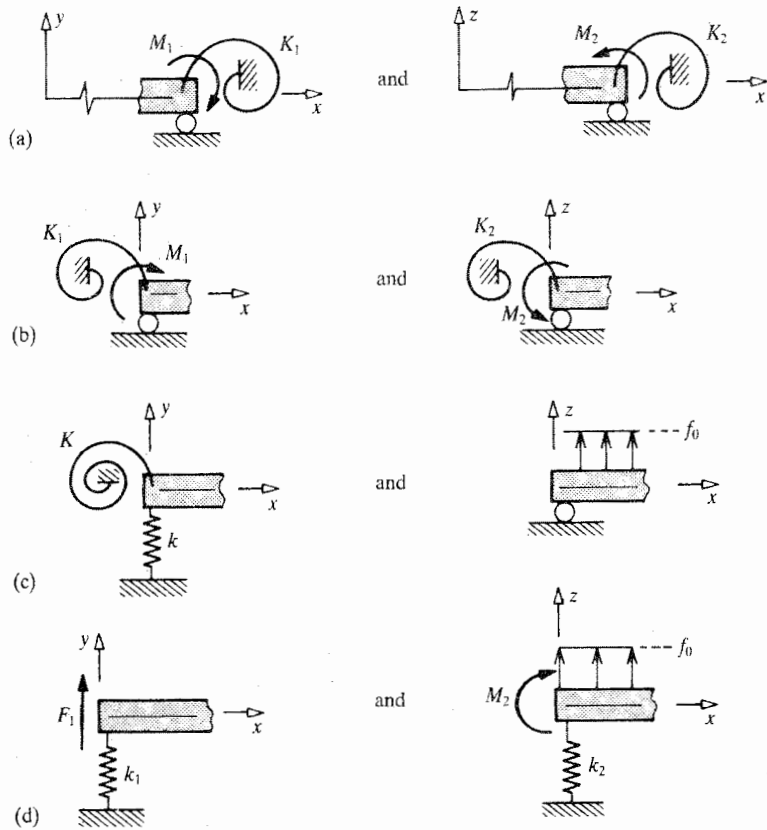


Figure 11.20. Exercise 11.4

(c) As above, but for the beam of Fig. 11.19(c).

(d) As above, but for the beam of Fig. 11.19(d).

(e) For the beam in Fig. 11.19(e), write the expression for $f_z(x) + m'_y(x)$, and then integrate that expression twice.

11.4. Draw FBDs as necessary, and write the final forms of the BCs for the beam end conditions shown in (a) Fig. 11.20(a); (b) Fig. 11.20(b); (c) Fig. 11.20(c); (d) Fig. 11.4(d). In each case let the product of inertia be other than zero, and let both orthogonal thermal moments have the value $+M_0[2 - (x/L)]$.

11.5. (a) Write the four boundary conditions in ready-to-use form (i.e., in terms of only the deflections and their derivatives) that are applicable to the end of the uniform, homogeneous, linearly elastic beam that is shown in Fig. 11.21(a). Note that

$$I_{yy} = 3I_0 \quad I_{zz} = 2I_0 \quad I_{yz} = 0 \quad \Delta T = 0$$

(b) In terms of the lateral deflections, write all the relevant boundary conditions for lateral deflections for the beam end shown in Fig. 11.21(b). Make all substitutions and differentiations, but here it is not necessary to further

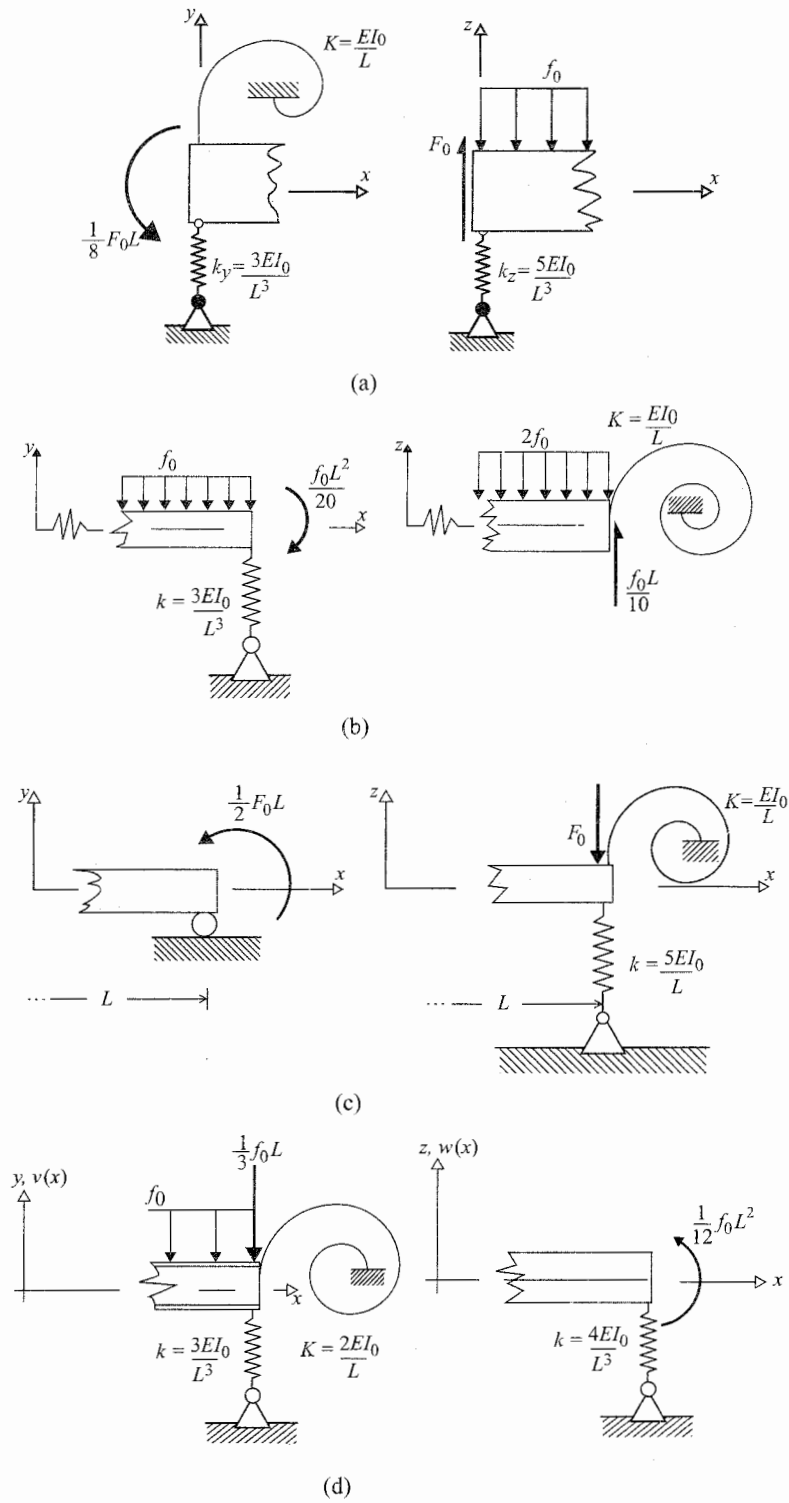


Figure 11.21. (a) Beam end at $x = 0$. (b) Beam end at $x = L$. (c) Beam end at $x = L$. (d) Beam end at $x = L$.

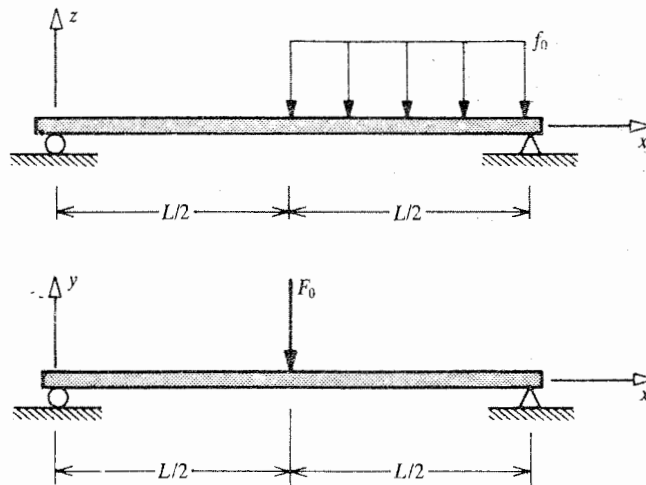


Figure 11.22. Exercise 11.6

simplify your answers. Note that this tapered beam is subjected to a thermal loading and

$$\begin{aligned}
 E_0 I_{yy}(x) &= 2EI_0 \left(3 - \frac{x}{L}\right) & E_0 I_{yz}(x) &= EI_0 \left(3 - \frac{x}{L}\right) \\
 E_0 I_{zz}(x) &= EI_0 \left(3 - \frac{x}{L}\right) & M_{yT} &= \frac{f_0 L^2}{50} \left(4 - \frac{2x}{L}\right) \\
 & & M_{zT} &= \frac{f_0 L^2}{50} \left(2 - \frac{x}{L}\right)
 \end{aligned}$$

Hint: Since beam boundary conditions are never integrated, it is necessary to carry out any differentiations required by the boundary conditions.

- (c) Write the *coupled* boundary conditions for the beam end shown in Fig. 11.21(c) entirely in terms of the applied mechanical and thermal loading, and the unknown deflection functions and their derivatives. The beam is uniform and homogeneous with the following, cross-sectional properties

$$\begin{aligned}
 I_{yy}^* &= 2I_0 & I_{zz}^* &= 3I_0 & I_{yz}^* &= -I_0 & M_{yT} &= F_0 L \left(1 + \frac{x}{L}\right) \\
 & & & & & & M_{zT} &= F_0 L \left(1 - \frac{x}{L}\right)
 \end{aligned}$$

- (d) Write the coupled boundary conditions for the beam end model at $x = L$ shown in Fig. 11.21(d). The cross-sectional properties and thermal loading for the uniform beam are as follows:

$$\begin{aligned}
 I_{yy}^* &= 2I_0 & I_{zz}^* &= 4I_0 & I_{yz}^* &= 2I_0 \\
 M_{yT}(x) &= \frac{f_0 L^2}{8} \left[2 - \frac{x}{L}\right] & M_{zT}(x) &= \frac{f_0 L^2}{8} \left[3 - \frac{x}{L}\right]
 \end{aligned}$$

- 11.6.** Write the GDE and BCs for the beam shown in Fig. 11.22 subject to the following conditions:

- (a) The product of inertia is zero, and the temperature change is zero.

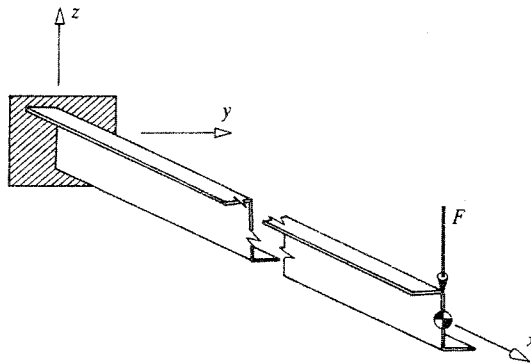


Figure 11.23. Exercise 11.10.

- (b) The product of inertia is not zero, and the temperature change is such that

$$M_{yT}(x) = M_0 \left(3 - \frac{x}{L}\right)^2 \quad \text{and} \quad M_{yT}(x) = 2M_0 \left(3 - 4\frac{x}{L}\right)$$

- 11.7. (a) Calculate the deflection function for a uniform, homogeneous, simply supported beam of length L subjected to a uniform lateral force per unit length of $f_z(x) = +f_0$, and an upward concentrated force in the same plane of magnitude f_0L that acts at the beam midspan. Use that solution to determine the beam midspan deflection.
- (b) Could that same midspan deflection be determined by solving the same problem first for the concentrated force and secondly, separately, for the distributed load, and then superimposing those, two results?
- 11.8. Apply the given BCs below to the deflection solution

$$ERw(x) = (x - L/2)^3 \operatorname{stp} \left(x - \frac{L}{2}\right) + C_1x^3 + C_2x^2C_3x + C_4$$

up to the point of developing the number of algebraic equations necessary to solve for the constants of integration in terms of the nondimensional constants α , β , and μ . Do *not* bother to actually solve the simultaneous equations.

$$w(0) = w(L) = 0 \quad \alpha Lw''(0) - \beta w'(0) = \mu \quad w''(L) = 2\mu$$

- 11.9. Determine the deflection functions of a uniform, homogeneous, symmetric, simply supported beam of length $L = a + b$ that is loaded with a concentrated force of magnitude F_0 acting downward at $x = a$ ($x = 0$ at the left beam end).
- 11.10. Determine the horizontal and vertical components of the tip deflection of the homogeneous, uniform, cantilevered beam with a Z cross-section as viewed from the free end (i.e., with $I_{yz} < 0$), when the beam is loaded with a downward acting, concentrated force of magnitude F_0 located at the beam tip; see Fig. 11.23.
- 11.11. The long, straight, homogeneous beam shown in top and side views in Fig. 11.24 is of length $2L$. Its uniform cross-sectional properties are $I_{yy} = 2I_0$, $I_{zz} =$

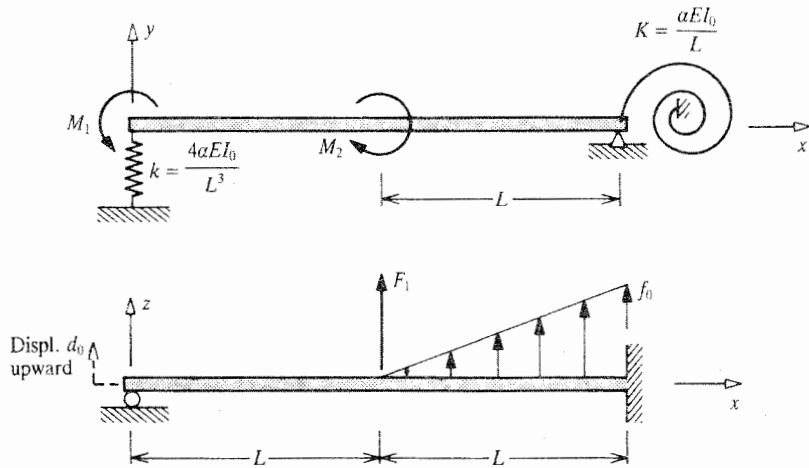


Figure 11.24. Exercise 11.11.

$3I_0$, and $I_{yz} = +I_0$. The spring constants are shown on the diagram in terms of the nondimensional constant α . The left beam end in the x, z plane is forced through an upward displacement of magnitude d_0 , the temperature change is such that $N_T = 0$, and

$$M_{yT}(x) = \frac{\beta EI_0}{L} \left(1 - \frac{2x}{L} \right) \quad M_{zT}(x) = \frac{\beta EI_0}{L} \left(3 - \frac{x}{L} \right)$$

- (a) For the loadings shown in the diagram, set up the uncoupled GDE for the two lateral displacements.
- (b) Create a summary listing of all BCs in simplest terms, that is, decouple the BCs wherever possible, and of course convert all stress resultants into terms involving the deflection derivatives. Let $\gamma/L = M_1/5EI_0$ for algebraic simplicity.
- (c) Integrate the uncoupled differential equation relevant to the x, y plane to the point of obtaining the deflection equation. Do *not* bother to determine the constants of integration.

11.12. The long, straight, homogeneous beam shown in top and side views in Fig. 11.25 is of length L . Its uniform cross-sectional properties are $I_{yy} = 4I_0$ and $I_{yz} = -I_0$. The spring constant is shown on the diagram in terms of the nondimensional constant α . The right beam end in the x, z plane is forced through a clockwise rotation of magnitude r_0 , the temperature change is such that $N_T = 0$, and

$$M_{yT}(x) = \frac{\beta EI_0}{L} \left(3 - \frac{2x}{L} \right) \quad M_{zT}(x) = \frac{\beta EI_0}{L} \left(2 - \frac{x}{L} \right)^2$$

(Be sure to notice the exponent on the quantity in parentheses in the expression for the second thermal moment.)

- (a) For the loadings shown in the diagram, plus the equivalent thermal loadings, set up the uncoupled GDE for the two lateral displacements.
- (b) List all BCs in simplest possible form.

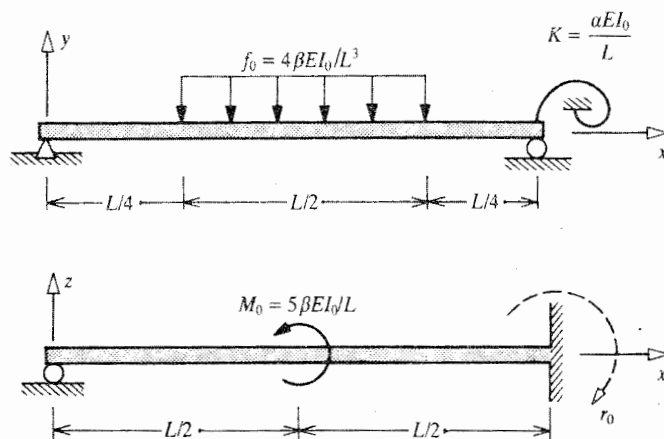


Figure 11.25. Exercise 11.12.

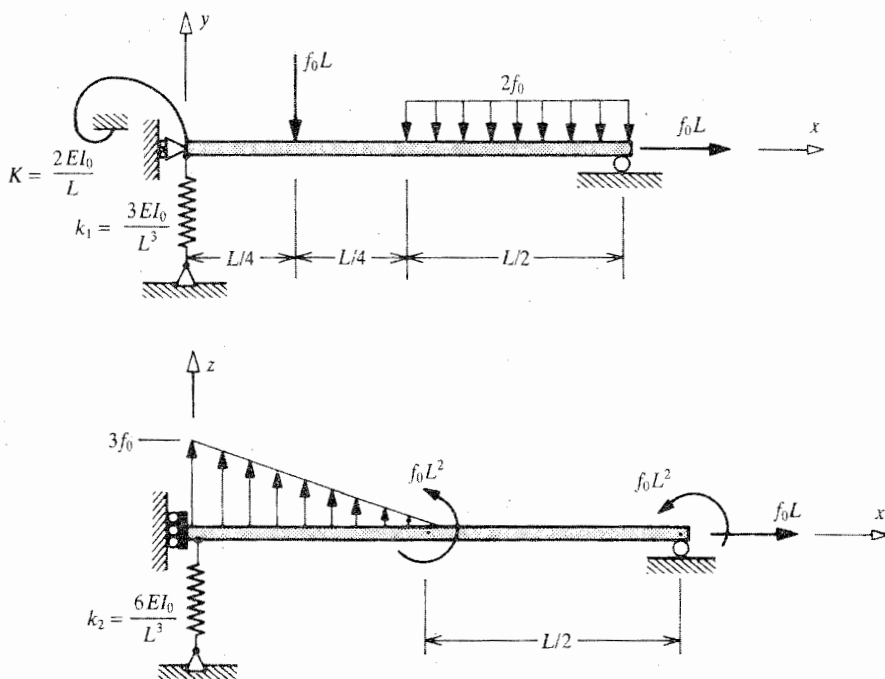


Figure 11.26. Exercise 11.13.

- 11.13. (a) Write the beam bending GDEs for the beam shown in Fig. 11.26. The long straight beam is such that $I_{yy} = 2I_0$, $I_{zz} = 3I_0$, and $I_{yz} = +I_0$. The thermal loading is such that

$$M_{yT}(x) = f_0L^2 \left(1 + \frac{x}{L}\right) \quad M_{zT}(x) = f_0L^2 \left(2 - \frac{x}{L}\right)^2$$

The left hand BC in the x, z plane is one where there is no bending slope, but only the spring resists lateral deflections at that end. Be sure to note the presence of the axial force. Do *not* integrate the GDEs.

- (b) Write the beam bending BCs for the beam of Fig. 11.26. For the sake of uniformity, use the first BC table at $x = 0$, and use the second BC table at $x = L$. Put all answers in terms of the quantity $(f_0 L^4 / EI_0)$, and place this known factor on the right-hand side of your BC equations. Place only the unknown deflection functions, and their derivatives, on the left-hand side of your BC equations.
- 11.14.** (a) Determine the critical buckling force and the deflected shape of a long, buckled beam-column with a uniform, symmetric cross-section and clamped-clamped BCs. In order that there may be an axial force acting at the beam end, picture the right-hand support as a very large, nonrotating, rigid mass that is clamped onto the beam extension into the mass, and which rides on frictionless rollers in the direction of the beam axis, as per Fig. 10.7(b). Then let the compressive axial force transmitted from the rigid mass to the beam have the magnitude P .
- (b) Reconsider the clamped-clamped beam of part (a). This time let the two clamped ends be totally immobile. Determine the critical value of αT_0 , the thermal strain due to a uniform temperature change throughout the beam, that will cause the beam to buckle.
- (c) Again, as in part (a), determine the critical buckling force and the deflected shape of a long, buckled beam-column with a uniform symmetric cross-section and clamped-clamped BCs, but where this time the right-hand support can now move laterally (i.e., in the y direction) without shear force resistance between the beam and the wall while maintaining a zero bending slope at that beam end. A spring with stiffness factor $k = 2EI/L^3$ opposes the lateral motion of the beam tip as shown in Fig. 11.27(a).
- (d) For the circumstance of beam bending, represent the simple frame of Fig. 11.27(b) as a single beam when the only loading acting upon the frame is F_1 , a load of unspecified magnitude. Fully detail your analysis model. Note that $L \neq l_1 \neq l_2$. From the point of view of beam bending, is your beam model one that leads to an eigenvalue problem or a boundary value problem?
- (e) For the circumstance of beam bending, represent the simple frame of Fig. 11.27(b) as a single beam when the only loading acting upon the frame is F_2 . Fully detail your analysis model. From the point of view of beam bending, is your beam model one that leads to an eigenvalue problem or a boundary value problem?
- 11.15.** (a) Determine the Euler buckling load for a long, uniform beam-column that is cantilevered at $x = 0$. Let the beam length be L , the stiffness factor in the plane of buckling be EI , and let the beam tip at $x = L$ be laterally supported in the plane of buckling by two translational springs, each with a stiffness factor of $k = 2EI/L^3$.
- (b) A uniform, symmetric beam-column is simply supported at both of its ends. In addition to the simple supports, at both beam ends there is also a rotational spring support. See Fig. 11.28(a). Determine the transcendental equation to be solved for the Euler buckling force for this beam with this combination of rigid and elastic supports.

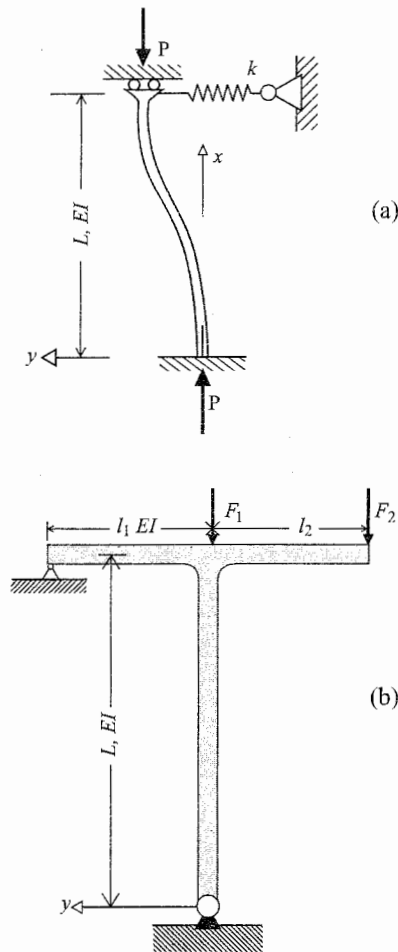


Figure 11.27. (a) Exercise 11.14(c). (b) Exercise 11.14(d, e).

- (c) The axially loaded beam shown in Figure 11.28(b) has the following relevant cross-sectional properties and a zero temperature change:

$$I_{yy} = 2I_0 \quad I_{zz} = I_0 \quad I_{yz} = 0$$

If the axial force remains horizontal as the beam deflects, write the transcendental equation whose solution provides the magnitude of the buckling force.

- (d) When the uniform beam of Fig. 11.28(c) buckles, it buckles in the x, z plane. This beam has a length L and a stiffness coefficient for the x, z plane of EI . Since the length l of the short link pinned to its support and to the end of the beam is much shorter than the length L , the short link can easily be modeled as rigid for the purpose of determining the buckling load for the beam. Using the sketches of the geometry of the deflected beam, and the accompanying FBD, write the GDE and the boundary conditions that describe the buckling of the beam.

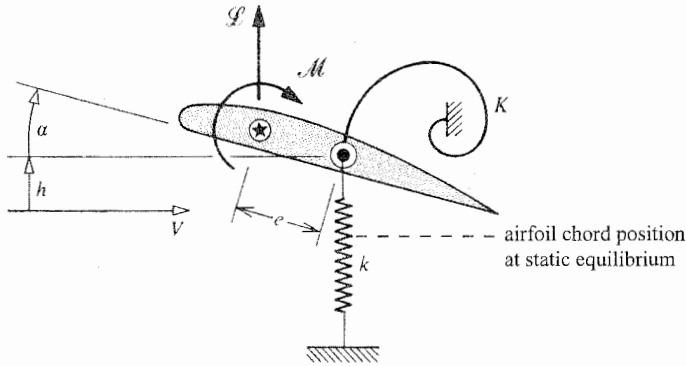


Figure 11.29. Exercise 11.16.

- (a) The rigid airfoil *section* divergence problem is a simplistic view of the divergence of an actual airfoil which normally has at least geometric and aerodynamic properties that vary along the airfoil span. Of course, the deflections of the airfoil also vary over the span length, and sometimes there is also significant deflection variation in the chordwise direction as well. Despite these problem limitations, for instructional purposes, examine the rigid airfoil section of Fig. 11.29. The rigid airfoil section is supported by linear springs that represent the total elastic properties of the airfoil structure. The applied loads are the “lift” force and the aerodynamic moment. The lift is equal to the product of the dynamic pressure q , the airfoil section planform area, and a lift coefficient that can be written as the product of the derivative of the lift coefficient with respect to the angle between the airfoil chord line and the direction of the air flow, and that angle itself. That is, $\mathcal{L} = qSC_{\ell\alpha}(\alpha + \alpha_0)$. This $C_{\ell\alpha}(\alpha + \alpha_0)$ representation is valid when α , which is called the angle of attack, is typically less than $\pm 10^\circ$. The quantity α_0 is due to the curvature of the airfoil. When, of course, $\alpha = -\alpha_0$, there is no lift. The aerodynamic moment is roughly independent of the angle of attack for such small α . The task for the reader is to write the moment equilibrium equation, solve that equation for the angle of attack, and then determine the value of the dynamic pressure which causes the angle of attack to become infinite.
- (b) The above approach is not an adjacent equilibrium approach, but can be made to be such by the following logic. The above moment equilibrium equation represents equilibrium at one particular deflection configuration, the one at α , and at the corresponding dynamic pressure. Investigate the possibility that at the dynamic pressure that causes divergence there are adjacent equilibrium states (neutral stability) where the angle of attack is $\alpha + d\alpha$, where $d\alpha$ is an arbitrary, small increment in the angle of attack. That is, replace α by $(\alpha + d\alpha)$ in the moment equilibrium equation. Use the two adjacent equilibrium states to solve for $d\alpha$ and obtain the result that $d\alpha$ multiplied by (“factor”) = 0. Since $d\alpha$ is not zero, the “factor” is zero. This conclusion again provides a solution for the divergence dynamic pressure that is independent of the angle of attack. Divergence is discussed in more realistic terms in Chapter 23.

- 11.17.** The most convenient way to use Newton's second law when applying it to a vibrating beam (i.e., a beam responding to time-varying loads) is to transpose the product of the mass and acceleration terms to the force side of that equation, and treat that product as an inertia force per unit length. (Recall the discussion in Chapter 1.) For example, in preparation for writing the differential equation that describes the one axial vibration of a homogeneous beam of mass density ρ , cross-sectional area A , and an axial acceleration that is the second time derivative of the axial deflection $u(x, t)$, note that the axial inertia force per unit length is

$$i_x(x, t) = -\rho g A \ddot{u}(x, t)$$

Without temperature changes, but with a time-varying applied axial force per unit length $f_x(x, t)$, the beam equation of motion becomes

$$[EA(x)u'(x, t)]' = -[-\rho g A(x)\ddot{u}(x, t) + f_x(x, t)]$$

or

$$[EA(x)u'(x, t)]' - \rho g A(x)\ddot{u}(x, t) = -f_x(x, t)$$

Clearly, with both spatial and temporal derivatives, the above equation is a partial differential equation. If the one right-hand side term were, contrary to normal form, transposed to the left-hand side and if each of the three terms were multiplied by dx , then the above equation would represent the sum of the elastic force, inertia force, and applied force as applied to a differential segment of beam length. Since the differential element is in "dynamic" equilibrium, this sum of all the forces is, as stated, zero.

The task for the reader is to write a similar partial differential equation for beam lateral vibrations. Do so both from the perspective of (i) the beam equations of Chapter 10, and (ii) directly from a FBD of a differential slice of beam. For simplicity, use principal centroidal axes, and do not include either rotary inertia effects produced by the changing beam bending slopes which have been demonstrated to be insignificant, or temperature effects, or an axial force. (Ignoring the rotary inertia effect means only summing forces while ignoring the moments acting on the differential slice of beam.) Confine your description to the x, z plane, and let the time-varying applied load per unit length for the x, z plane be $f_z(x, t)$.

The solution of such partial differential equations with arbitrary time-varying applied loads per unit length is often based upon the "normal mode method," oftentimes in combination with the numerical methods introduced in Part V.

- 11.18.** The same roller support is both the right-hand support for beam A and the left hand support for beam C. In other words, at that mutual support, both beams have a zero deflection. As shown in Fig. 11.30, in the gap between the two beam ends there is a torsional spring of stiffness K . Write the four BCs at this support if there are no temperature changes, and both products of inertia are zero.

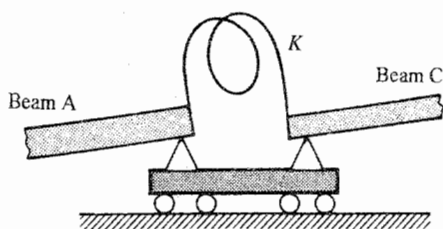


Figure 11.30. Exercise 11.18.

Endnote (1) The Bending Slope Sign Convention

The sign convention associated with the derivatives of a deflection function depend upon the sign convention of the deflection function and the positive direction of the spatial coordinate used to form the derivatives. Hence the sign convention for $w'(x)$, for example, depends not only upon that of $w(x)$, but also upon the selected positive direction for x . In order to illustrate how to determine the positive direction of the slope $w'(x)$, let the coordinate x be positive to the right, and the lateral deflection w be positive upward. Thus positive values of dx and dw are also to the right and upward, respectively. Put these differential quantities together in vector form according to their positive directions as shown in Fig. 11.31. From this diagram it is clear that the slope dw/dx is positive counterclockwise at all points along the beam axis, including both beam ends.

Endnote (2) Combined Beam Axial and Lateral Loadings

The first purpose of this endnote is to comment further upon the problem solution for the simply supported, uniform, homogeneous beam sketched in Fig. 11.10, where P_0 and F_0 are known loads of fixed magnitude, and the temperature change and the product of inertia are zero. As explained previously in Example 11.6, the bending GDE reduces to

$$EI_0 w''''(x) + P_0 w''(x) = f_0$$

while the zero deflection and zero moment BCs are

$$w(0) = w(L) = w''(0) = w''(L) = 0$$

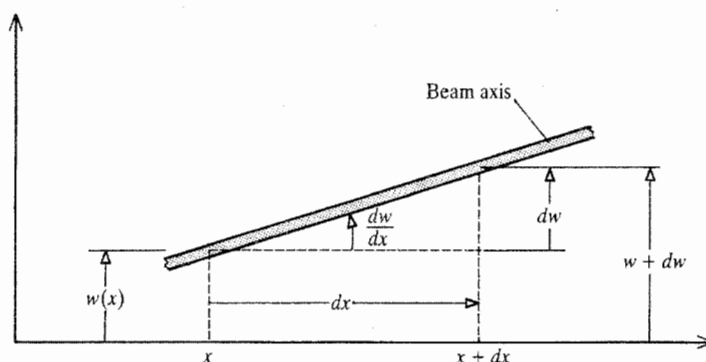


Figure 11.31. Determination of the direction of a positive ending slope.

This is a somewhat lengthy problem to solve, and it takes even more time to interpret the solution. For this reason, it is advisable to nondimensionalize the GDE and the BCs. First of all, let $\xi = x/L$. Note, by use of the chain rule, that

$$\frac{dw}{dx} = \left(\frac{dw}{d\xi}\right) \left(\frac{d\xi}{dx}\right) = \frac{1}{L} \frac{dw}{d\xi}$$

In other words, derivatives with respect to x can be replaced by derivatives with respect to ξ if the result is divided by L once for each order of derivative. Nondimensionalizing w itself is easily done by dividing the GDE by, say, the depth of the beam. To this end let $W(\xi) = w(\xi)/h$. Finally, recall the definition of the nondimensional parameter $\mu^2 \equiv (P_0 L^2)/(EI_0)$. Then, after dividing by EI_0 , the GDE may be rewritten as

$$W''''(\xi) + \mu^2 W''(\xi) = \frac{f_0 L^4}{h E I_0} \equiv f$$

Where here primes denote differentiation with respect to ξ , and each quantity in the above equation is nondimensional. The corresponding BCs become $W(0) = W(1) = W''(0) = W''(1) = 0$, where of course, in the BCs primes mean differentiation with respect to ξ .

The first point to make is that only two parameters, both of which are known quantities, appear in the problem statement that is the GDE and the BCs. Thus the solution for the deflection can only depend upon these two parameters. Rewriting that solution in terms of those two quantities, which makes it easier to comprehend and work with,

$$W(\xi) = \frac{f}{\mu^4} \left[\frac{\sin \mu \xi + \sin \mu(1 - \xi)}{\sin \mu} - 1 - \frac{\mu^2}{2} \xi(1 - \xi) \right]$$

As noted before, this solution identically satisfies both the GDE and the BCs, and it is evident that it is symmetric about the midspan of the beam.

The second point of this endnote is the interpretation of this solution. Since μ is directly proportional to P_0 , at first glance it would seem that the smaller P_0 became, the larger the deflection! If that were truly the mathematical result, it would obviously be wrong. The way to investigate this apparent paradox is calculate the midspan deflection, which is obviously the maximum deflection, as $\mu \rightarrow 0$. Understand that the parameter μ cannot be zero because that would alter the left-hand side of the differential equation, and hence change the basic form of the solution. This observation prompts the further observation that the above limit has to be the midspan deflection calculated for the same beam without the axial loading, which is $W(1/2) = 5f/384$. Now examine what happens to the midspan deflection as P_0 and μ become small:

$$\lim_{\mu \rightarrow 0} W(1/2) = \lim_{\mu \rightarrow 0} \frac{f}{\mu^4} \left[\frac{2 \sin(\mu/2)}{\sin \mu} - 1 - \frac{\mu^2}{8} \right]$$

Since the ratio of the bracketed term to μ^4 produces a zero over zero limit, this limit is treatable using L'Hôpital's rule. The use of L'Hôpital's rule in this case is a lengthy task since it must be applied four times with some trigonometric simplifications at each step, plus checking that the zero over zero limiting ratio persists after each step but the last. In the last step the ratio is 5:384, as it should be. Truncating both sine series expansions after μ^5 leads to the same result. Thus the fear that the midspan deflection becomes larger as the axial force becomes smaller is unfounded.

The third point is, as is obvious from either the expression for $W(\xi)$ or that for $W(1/2)$, that the parameter μ cannot exceed the value π without these deflections first being unbounded. The parameter μ reaches the value π when

$$P_0 = \frac{\pi^2 EI_0}{L^2} = P_{cr}$$

Thus, since the value of f_0 is wholly immaterial to this observation, it should be clear that this type of boundary value problem is also a way to determine the buckling load for a beam. Since this approach involves much more work than the comparable eigenvalue problem approach, there may be a temptation to dismiss this approach. That temptation is only half justified. Using a lateral load to slightly deform the structure as it is also loaded by (an increasing) compressive force is indeed an inefficient method of determining a buckling load. However, this approach is closely akin to the "imperfection method," which is one of the four basic approaches to determining buckling loads. More information on the imperfection approach can be found, for example, in Ref. [24].

The final purpose of this endnote is to make clear that Dirac delta and Heaviside step functions are *not* very useful when dealing with combined axial and lateral loadings that involve concentrated forces or moments. For this purpose, consider the following example problem.

Example 11.13. Consider a uniform, homogeneous, clamped-clamped beam of length L . Let the x axis originate at the left-hand fixed support. Let the z axis be a principal axis. Let the loading consist of three concentrated forces that are: (i) a lateral force F_0 at $x = L/3$; (ii) a lateral force βF_0 at $2L/3$; and (iii) an axial force αF_0 also at $x = 2L/3$. The two lateral forces are in the positive z direction, and the axial force is in the positive x direction. Up to the point of evaluating the constants of integration, prepare to determine the solution for the lateral deflection $w(x)$ over the beam length.

Solution. Since there is no symmetry and the beam is indeterminate, the most general small-deflection, differential equation approach will be used. Since the deflections are assumed to be small, the uncoupled axial equation can be solved first. That equation is

$$EAu''(x) = -f_x(x) = -\alpha F_0 \delta\left(x - \frac{2L}{3}\right)$$

Thus

$$EAu'(x) = -\alpha F_0 \text{stp}\left(x - \frac{2L}{3}\right) + C_0$$

and

$$EAu(x) = -\alpha F_0 \left(x - \frac{2L}{3}\right) \text{stp}\left(x - \frac{2L}{3}\right) + C_0 x + C_1$$

The BCs $u(0) = u(L) = 0$ establish that $C_1 = 0$ and $C_0 = \alpha F_0/3$. Thus the axial deflection and axial force solutions are

$$EAu(x) = \alpha F_0 \left[\frac{x}{3} - \left(x - \frac{2L}{3}\right) \text{stp}\left(x - \frac{2L}{3}\right)\right]$$

and

$$N(x) = \alpha F_0 \left[\frac{1}{3} - \text{stp}\left(x - \frac{2L}{3}\right)\right]$$

or, for $0 \leq x \leq 2L/3$, $N = \alpha F_0/3$, and for $2L/3 \leq x \leq L$, $N = -2\alpha F_0/3$. (As is discussed in the finite element chapters, the applied axial load is diffused into the beam in proportion to the axial stiffnesses of the first and second beam intervals; that is, since the first two-thirds of the beam has half the axial stiffness (EA/L) of the last third of the beam, it gets only half the axial load that is borne by the last third of the beam.)

The lateral bending differential equation, with $I_{yz} = 0$ and $I_{yy} = I$, can be written as

$$EIw''''(x) - \alpha F_0 \left[\frac{1}{3} - \text{stp} \left(x - \frac{2L}{3} \right) \right] w''(x) = F_0 \delta \left(x - \frac{L}{3} \right) + \beta F_0 \delta \left(x - \frac{2L}{3} \right)$$

In its present form of the above equation, the coefficient of $w''(x)$ is sufficiently nonconstant to make direct integration difficult. If this equation is merely divided into two differential equations so as to have constant N coefficients, then the analyst must confront, for the first two-thirds of the beam length, in one form or another, the differential equation

$$EIw''(x) - \frac{\alpha F_0}{3} w(x) = F_0 \left(x - \frac{L}{3} \right) \text{stp} \left(x - \frac{L}{3} \right)$$

The difficulty here is finding a particular solution. The trial solution $w_p(x) = (3/\alpha)(x - L/3) \text{stp}(x - L/3)$ does not work because $w_p''(x) = (3/\alpha)\delta(x - L/3)$, and this term is not offset by any other. In addition, it makes no physical sense for the total curvature, $w''(x)$, to have a singularity at $x = L/3$. Thus the best, but tedious, differential equation approach to this problem is to divide the beam length into three lengths $L/3$, let the nondimensional parameter $\mu^2 = \alpha F_0 L^2 / EI$, and write for

$$\begin{aligned} 0 \leq x \leq \frac{L}{3} & \quad w_1''''(x) - \frac{1}{3} \left(\frac{\mu}{L} \right)^2 w_1''(x) = 0 \\ \frac{L}{3} \leq x \leq \frac{2L}{3} & \quad w_2''''(x) - \frac{1}{3} \left(\frac{\mu}{L} \right)^2 w_2''(x) = 0 \\ \frac{2L}{3} \leq x \leq L & \quad w_3''''(x) + \frac{2}{3} \left(\frac{\mu}{L} \right)^2 w_3''(x) = 0 \end{aligned}$$

This approach puts all the concentrated forces at beam interval boundary points where they are easily dealt with. The solutions to these three differential equations are

$$\begin{aligned} 0 \leq x \leq \frac{L}{3} & \quad w_1(x) = C_2 + C_3 x + C_4 \cosh \left(\frac{\mu x}{3L} \right) + C_5 \sinh \left(\frac{\mu x}{3L} \right) \\ \frac{L}{3} \leq x \leq \frac{2L}{3} & \quad w_2(x) = C_6 + C_7 x + C_8 \cosh \left(\frac{\mu x}{3L} \right) + C_9 \sinh \left(\frac{\mu x}{3L} \right) \\ \frac{2L}{3} \leq x \leq L & \quad w_3(x) = C_{10} + C_{11} x + C_{12} \cos \left(\frac{2\mu x}{3L} \right) + C_{13} \sin \left(\frac{2\mu x}{3L} \right) \end{aligned}$$

Since there are 12 constants of integration, 12 BCs are needed. The BCs at the ends of the complete beam are simply

$$w_1(0) = w_1'(0) = 0 \quad \text{and} \quad w_3(L) = w_3'(L) = 0$$

Continuity of deflections and bending slopes at the third points requires that

$$w_1\left(\frac{L}{3}\right) = w_2\left(\frac{L}{3}\right) \quad w_2\left(\frac{2L}{3}\right) = w_3\left(\frac{2L}{3}\right)$$

$$w_1'\left(\frac{L}{3}\right) = w_2'\left(\frac{L}{3}\right) \quad w_2'\left(\frac{2L}{3}\right) = w_3'\left(\frac{2L}{3}\right)$$

From free body diagrams of beam slices at $x = L/3$ and at $x = 2L/3$, summation of moments about the y axis and summation of forces in the z direction leads to

$$w_1''\left(\frac{L}{3}\right) = w_2''\left(\frac{L}{3}\right) \quad w_2''\left(\frac{2L}{3}\right) = w_3''\left(\frac{2L}{3}\right)$$

$$w_1''\left(\frac{L}{3}\right) + \frac{1}{\alpha}\left(\frac{\mu}{L}\right)^2 = w_2''\left(\frac{L}{3}\right)$$

$$w_2''\left(\frac{2L}{3}\right) + \frac{\beta}{\alpha}\left(\frac{\mu}{L}\right)^2 = w_3''\left(\frac{2L}{3}\right)$$

These 12 BCs determine the values of the 12 constants of integration.

As an exercise, the reader is invited to confirm that the lateral deflection function for the left-hand half of a uniform, simply supported beam loaded at its midspan by a lateral force F_0 and everywhere loaded by an axial force N_0 , is

$$w(x) = \frac{1}{2}\left(\frac{F_0}{N_0}\right)x - \frac{\frac{1}{2}F_0}{\mu N_0 \cosh(\mu/L)} \sinh\left(\frac{\mu x}{L}\right) \quad \blacksquare$$

Endnote (3) Heaviside Step Function Additional Comments

The expressions for partially distributed loads can often be simplified when the argument of the Heaviside step function is also used with the spanwise coordinate x following a span length term. This interchange in positions does not alter the properties of the Heaviside step function. The function is still zero when the argument is negative, and still has the value +1 when the argument is positive. Consider the beam shown in Fig. 11.32 where the product of inertia is zero, and there is no temperature change. The load factors α and β are constants. Following the previous approach with the Heaviside step function, the GDEs after simplification, and for the purpose of a later comparison their first definite integrals from zero to x , are

$$EI_{yy}w''''(x) = \frac{6f_0x}{L} - 3f_0 - \frac{6f_0}{L}(x - \frac{1}{2}L) \text{stp}(x - \frac{1}{2}L) - \beta f_0 L^2 \delta(x - \frac{1}{2}L)$$

$$EI_{yy}w''''(x) = C_1 + \frac{3f_0x^2}{L} - 3f_0x - \frac{3f_0}{L}(x - \frac{1}{2}L)^2 \text{stp}(x - \frac{1}{2}L) - \beta f_0 L^2 \text{stp}(x - \frac{1}{2}L)$$

$$EI_{zz}v''''(x) = f_0 \text{stp}(x - \frac{1}{2}L) + \alpha f_0 L^2 \delta'(x - \frac{1}{2}L)$$

$$EI_{zz}v''''(x) = C_5 + f_0(x - \frac{1}{2}L) \text{stp}(x - \frac{1}{2}L) + \alpha f_0 L^2 \delta(x - \frac{1}{2}L)$$

The alternative is to write $f_z(w) = (6f_0/L)(\frac{1}{2}L - x) \text{stp}(\frac{1}{2}L - x)$, which leads to two fewer terms in the expression for w'''' ; that is, now

$$EI_{yy}w''''(x) = \frac{6f_0}{L}(\frac{1}{2}L - x) \text{stp}(\frac{1}{2}L - x) - \beta f_0 L^2 \delta(x - \frac{1}{2}L)$$

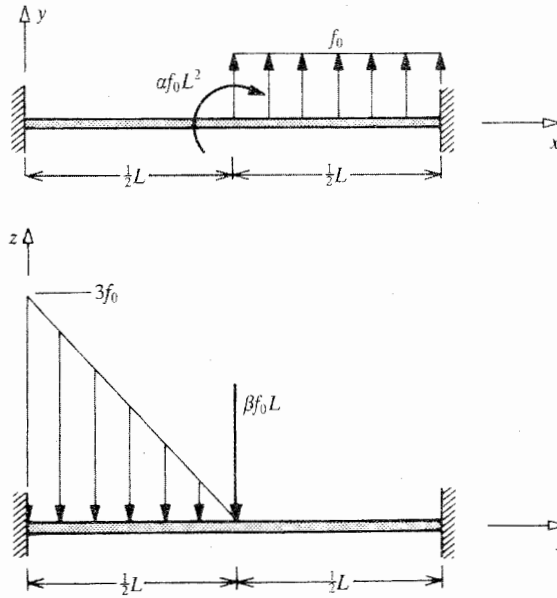


Figure 11.32. Endnote (3).

The point to note is that the definite integration of this form of the GDE is better done by integrating from x to L . In order to carry out this integration for the above GDE, first consider the general integral

$$I(x) = \int_{\hat{x}=x}^{\hat{x}=L} f(\hat{x}) \text{stp}(x_0 - \hat{x}) d\hat{x}$$

The value of x can range from zero to L . Regardless of the position of x relative to x_0 , the integral with limits (x, L) can be written as the sum of the two integrals with limits (x, x_0) and (x_0, L) . The step function obliterates the second of those integrals, and that, as before, leads to

$$I(x) = \text{stp}(x_0 - \hat{x}) \int_{\hat{x}=x}^{\hat{x}=x_0} f(\hat{x}) d\hat{x}$$

On this basis,

$$\int_x^L \frac{6f_0}{L} (x - \frac{1}{2}L) \text{stp}(\frac{1}{2}L - x) dx = \frac{3f_0}{L} (\frac{1}{2}L - x)^2 \text{stp}(\frac{1}{2}L - x)$$

and therefore

$$EI_{yy}w'''(x) = \hat{C}_5 + \frac{3f_0}{L} (\frac{1}{2}L - x)^2 \text{stp}(\frac{1}{2}L - x) - \beta f_0 L^2 \text{stp}(x - \frac{1}{2}L)$$

Clearly this alternate approach is little different from the original approach.

Endnote (4) Combined Bending and Torsional Loadings

As is learned when the shearing stresses due to lateral shearing forces are studied in Chapter 14 there is another axis of importance besides the x axis, that is, besides the m.w. centroidal axis. This other axis is called the beam *elastic axis*. The elastic axis is the locus

of those points on each beam cross-sections called the *shear center*. The significance of the shear center is that for small, as opposed to finite, deflections:

1. Lateral beam loads applied at the elastic axis do not cause any twisting of the cross-section.
2. Torques do not cause any bending of the elastic axis.

Hence the small beam bending deflections and the small torsional deflections at the shear center are the small deflections that are physically independent of each other. In other words, being physically uncoupled when both bending and twisting occur, the use of elastic axis deflections permits the beam bending and beam twisting to be treated wholly separately by means of differential equations each of which deals with just one of these two types of deflections. That is not possible using the m.w. centroidal axis deflections.

Thus, in order to obtain the advantage of uncoupled deflections, it is implicitly, assumed in all the problems and discussions in this and the preceding chapter that all externally applied lateral bending loads are applied along the elastic axis. When twisting is discussed in subsequent chapters, all torques are about the elastic axis. (The elastic axis and centroidal axis coincide when the beam cross-section has two axes of symmetry.)

The derivation of the beam deflection equations included the bending rotations about the y and z axes, but torsional rotations were explicitly omitted. This fact, coupled with the approximation that the beam cross-sectional shape is unchanged by loading, means that, in the absence of twisting, throughout the preceding derivations the lateral deflections of the shear centers are the same as those of the m.w. centroids. Hence the previously derived lateral deflection differential equations are still correct in the presence of twisting if the lateral deflections $v(x)$ and $w(x)$ are those of the elastic axis rather than the m.w. centroidal axis.

It also can be shown that if the *finite* deflections of the shear center are used instead of those of the m.w. centroid, then the beam bending equations, Eqs. (10.5a,b), when supplemented by the nonlinear bonding-twisting coupling terms of Exercise 10.14, retain exactly the same form, provided again that the bending and twisting moments are those about the beam elastic axis and the distributed lateral loads also act at the beam elastic axis. When the beam deflections are finite, even bending loads placed at the shearing center can produce twists. Since analytical approaches to the nonlinear beam bending and twisting equations are left to more advanced texts such as Ref. [23], the following short discussion is entirely in physical terms for the purpose of alerting the reader to these interactions, which are surprising if only the linear (i.e., small deflection) equations are kept in mind.

To that end, first consider a uniform, homogeneous, cantilevered beam with a thin Z cross-section as viewed from the free end; see Fig. 11.23. Let the Z section flange areas be the same size and shape. Let the only loading be a shearing force in the negative z direction, at the beam tip shear center, which in this case happens to be at the same location as the centroid. Since the product of inertia with respect to the y and z axes is negative, the beam tip will move downward and to the left, that is, in the negative z and y axis directions; see Exercise 11.10. Now, in this discussion (as opposed to the exercise) the loading is taken to be sufficiently large that the two tip bending deflections are finite. The tip deflection to the left creates a finite horizontal moment arm for the shearing force, which produces a torsional moment at the fixed end of the cantilevered beam, and to a lesser extent, all the cross-sections in between the fixed and free ends. Since a thin Z cross-section is rather weak in torsion, these torques, which are only a result of the shearing force, twist the beam quite noticeably.

Twisting of torsionally weak cross-sections can occur even when the beam cross-section product of inertia is zero. Consider another cantilevered beam which is oriented the same way as the above cantilevered beam, and which is also loaded with a vertical, downward tip force. In this case, let the beam cross-section be that of a very deep and narrow I beam. Since such a cross-section is doubly symmetric, its shear center and centroid coincide. Let the magnitude of the tip force be such that there is only a very small, downward vertical tip deflection. If the geometry of the beam is without the slightest irregularity, the shearing force is perfectly aligned so as to lie on the z axis of the cross-section, and there are never any perturbations, then that very small vertical deflection is all that will happen in the way of deflections. However, if the tip force is slightly rotated off its expected alignment, then the shearing force will have a small horizontal force component. Since the deep I cross-section is such that $I_{zz} \ll I_{yy}$, the deflection in the horizontal direction can be much greater than the vertical deflection. This horizontal deflection, exactly as discussed in the previous paragraph, produces a small moment arm for the larger vertical component of the total tip force. Again, the result is a small twisting moment acting on a series of cross-sections that are very weak in torsion. Again, sizable twists and shearing stresses result. This is essentially the reason why such cross-sections are seldom used in preference to, say, an H cross-section, where there is far less disparity between the two area moments of inertia.

In summary, there is no interaction between the bending and twisting deflections of the elastic axis when the two types of deflections are small. In order to facilitate the study of the elastic axis deflections, all applied lateral loads and twisting moments need to be resolved so that the lateral loads act along the beam elastic axis. When the bending and torsional loads cause deflections that are finite, significant interaction between bending and twisting can be expected, particularly when the beam is very flexible in torsion. Vehicular construction often uses beams which are weak in torsion because such beams are generally easier to attach as reinforcements to bulkheads, outer skins, and so forth, and are easier to inspect afterward.

Endnote (5) Beams Continuous over Several Supports

Consider a differential equation approach to a beam that is continuous over rigid supports such as that sketched in Fig. 11.33(a). For the purposes of analysis, this one continuous beam can be divided into several beams, each with ends defined by the rigid knife-edge or roller supports. The BCs at the first, left-hand support have already been discussed. Consider the BCs at the second support. For the sake of simplicity, let the product of inertia and the temperature change be zero, and let the discussion be limited to the x, z plane. When treating beam A as continuous with beam C, at the second support it is necessary to have for the two beams a total of four x, z plane BCs in terms of the z direction deflection and its derivatives. Let $w_a(x)$ and $w_c(x)$ be the respective deflection functions for beam A and beam C. Then the four required BCs are

$$w_a(x_a = L_a) = 0 \quad w_c(x_c = 0) = 0 \quad w'_a(x_a = L_a) = w'_c(x_c = 0) \\ M_{y_a}(x_a = L_a) = M_{y_c}(x_c = 0)$$

The third of the above BCs simply says that since the beam is continuous over the rigid support, the beam bending slopes on both sides of the support have to be the same. (If the beam were not continuous over the support—if, for example, there were a hinge in the beam itself—then there would be no interaction between beams A and C and each beam could then be treated separately by writing separate zero moment equations.) The fourth BC is

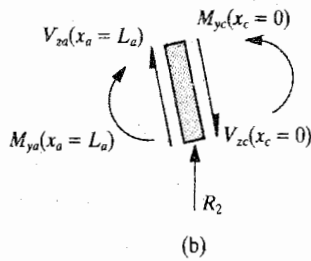
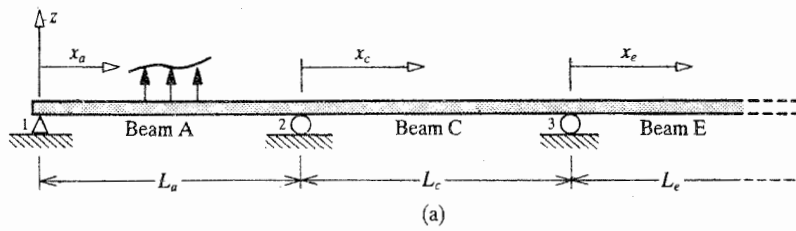


Figure 11.33. Endnote (5): (a) a beam continuous over several roller supports; (b) a free body diagram of the beam differential length at roller 2.

the result of summing the moments acting on the ends of the slice of beam centered at the second support as shown in the FBD of Fig. 11.31). Since the vertical force reaction at the second support is unknown, there is not information to be gained by summing forces. In this case where the area product of inertia and the temperature change are zero, the last BC becomes

$$(E_0 I_{yy})_a w''_a(x_a = L_a) = (E_0 I_{yy})_c w''_c(x_c = 0)$$

The third and fourth BCs couple the solution for beam A to that for beam C, and the BCs at the third support couple the solution for beam C to that for beam E, and so on. Then, in general, some of the constants of integration for each of the beams have to be determined simultaneously with other constants from all the other beams. Hence this approach is not at all appealing if there are more than two beams. This approach is not pursued further here.

There are several other ways of dealing with a beam grid or frame structure. An effective approach to a very small number of beams (the unit load method) and an effective approach for a large number of beams (the finite element method) are discussed at some length in Part V.

Uniform Torsion of Beams

12.1 Introduction

To a close approximation, when a beam bends and extends, each planar cross-section translates in each of the three Cartesian coordinate directions, and rotates about the y and z axes. The one motion that is excluded from those approximations is the twisting of the beam cross-section about the x axis, called ϕ_x . The primary reason for separating this one motion from the other five is that its inclusion substantially complicates the treatment of *finite* beam bending deflections. However, for *small* deflections, there is no interaction between the twisting motion and the other five motions. Thus by limiting the discussion of this chapter and Chapter 13 to the situation where the beam bending deflections, if present, are small, the following discussion of twisting deflections and torsional loadings can proceed without taking any notice at all of the extensional and bending deflections caused by axial and shearing forces and bending moments.

Recall that a bar is a beam that is loaded only in extension or torsion. Since only twisting deflections are to be discussed in this chapter and Chapter 13, here the terms beam and bar can be, and are, used interchangeably. Consider a bar with a noncircular cross-section. When the bar is twisted, the bar cross-section of arbitrary shape does not remain plane after twisting. On the contrary, the cross-section warps out of its original plane in apparently complicated ways. Thus there is no available complete characterization of the twisting deformations of a bar cross-section, precise or approximate, like that embodied in Eqs. (9.2) for beam bending and extension. Hence it is not possible to proceed from a fully defined deflection assumption to a complete set of strains, and then stresses and stress resultants, as is done for beam bending and extension. In other words, a strength of materials solution for a bar with a noncircular cross-section is not going to be possible.

While it is not possible to provide a complete, prior description of the twisting deformations of a beam with an arbitrary cross-section, it is possible to make some limited observations. Note that, because the warping deflections are small, after twisting the size and shape of the projection of a warped cross-section on its original plane are very much the same size and shape as that of the original cross-section. It turns out that this approximation, plus leaving the matter of the warping deformations of the cross-section to whatever description is provided by the relevant equations, is all that is necessary for a successful displacement formulation of the beam torsion problem by means of the theory of elasticity; see, for example, Ref. [16]. However, it also turns out that there is a better way. As discussed previously, the alternative to any displacement formulation is a stress formulation. It so happens that the stress formulation provides generally more tractable equations than the displacement formulation. Therefore, it is the approach to be developed here.

12.2 The Stress Formulation for Uniform Torsion

When approaching a new problem, it is sometimes best to take a broad, general view of the problem because the adopted generality saves the repetition associated with various subcases, and may even suggest a solution technique that might not be apparent in a limited view of the problem. Unfortunately, that is not the case for the torsion of beams. It is necessary to attack the beam torsion problem on an incremental basis, starting with the simplest useful problem statement. The problem that is first to be discussed is limited to that of a uniform, homogeneous, isotropic, Hookean beam loaded only by a twisting moment on one end cross-section and an equal and opposite twisting moment (or torsional moment or torque) acting on the other beam end cross-section. Moreover, it is required that there be no restraints against the warping of the originally plane beam cross-sections at either beam end. This limited situation is called *uniform torsion*, where the adjective “uniform” is derived from the cross-sectional geometry, and, as is seen below, the constancy of the torque and warping deformations.

With the first stipulation of only equal and opposite torsional moments acting at the beam ends, a simple freebody diagram (FBD) makes it clear that each cross-section, and each included length of the beam, supports the same torque. This, taken with the second stipulation that there is no warping restraint (i.e., each beam segment has the same boundary condition) leads to the conclusion that any two equal lengths of the same uniform beam must have the same twist. Thus it may be concluded that the twist per unit length is the same everywhere along the length of the beam. This constant value of twist per unit length, in units of rad/m or rad/in, is symbolized by θ .

From the second stipulation that the beam ends are free to warp without any form of restraint, it is reasonable to conclude that any two beam segments with the same length and uniform cross-section subjected to the same torque (and twist) would undergo the same warping of their end cross-sections. If all cross-sections of a beam undergo the same warping as the beam is twisted, then it is possible to guess that any two lines within the beam that are parallel to the x axis before the beam is twisted, and an equal distance from the axis of rotation, deform into exactly the same helix. From this point it is possible to speculate that these two helices, and for that matter all the helices from originally straight lines paralleling the x axis, do not change length. This speculative leap is not really so long because, as is shown in Fig. 12.1, without the effect of the rotation of the cross-section it would be quite clear that equal warping of originally plane cross-sections might not affect axial lengths. Rather than undertake a lengthy and difficult investigation of the helical and warped geometry, it is simply *tentatively* guessed that the lengths originally paralleling the x axis remain unchanged after twisting.

The tentative observation of no change in the projected cross-section size and shape for small angles between the warped and original cross-section can be quantified by writing $\epsilon_{yy} = \epsilon_{zz} = \gamma_{yz} = 0$. The tentative guess that the helices retain their original length can be described by writing $\epsilon_{xx} = 0$. Ignoring temperature changes because they never result in the twisting of a beam, and confining the analysis to linearly elastic, homogeneous, isotropic beams, leads to the tentative guess that

$$\sigma_{xx} = \sigma_{yy} = \sigma_{zz} = \sigma_{yz} = 0 \quad (12.1)$$

Since the overall approach to uniform torsion is to be a stress formulation, rather than build Eqs. (12.1) on questionable displacement conclusions, as is done above, it is much tidier to forget the tentative displacement conclusions that lead to Eqs. (12.1) (which all turn out to be true for small twists), and make Eqs. (12.1) the starting point of the uniform torsion

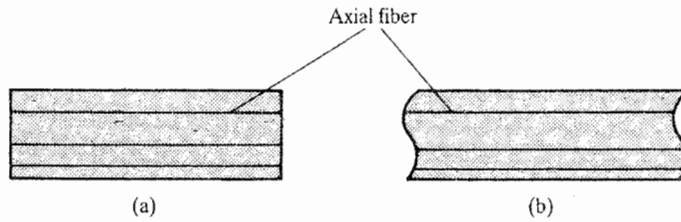


Figure 12.1. The exaggerated warping of a twisted uniform beam segment: (a) side view before twisting; (b) side view after twisting where the spiral shape of the axial fibers has been omitted for clarity.

analysis. Equations (12.1) are thus proposed as a *tentative*, partial solution to the uniform torsion problem in that Eqs. (12.1) are four of the six stress solutions being sought. In other words, Eqs. (12.1) become the set of assumptions to be *tested* by the various equations of the theory of elasticity. Another, more complete viewpoint is to say that Eqs. (12.1) are the beginning of an inverse problem for which they represent a partial solution, and now it is a matter of discovering whether this partial solution, along with the remaining two wholly unknown shearing stresses, can be fashioned into the uniform torsion problem.

The simplest place to begin the process of testing whether or not the proposed partial stress solution fits the uniform torsion problem is with the general equations of equilibrium, Eqs. (1.6a, b). In this situation, where body forces are excluded, because they never cause a beam to twist, the general equilibrium equations reduce to

$$\frac{\partial \sigma_{xy}}{\partial y} + \frac{\partial \sigma_{xz}}{\partial z} = 0 \quad \frac{\partial \sigma_{xy}}{\partial x} = 0 \quad \frac{\partial \sigma_{xz}}{\partial x} = 0 \quad (12.2)$$

where σ_{xy} and σ_{xz} are the two remaining stresses whose description is still open. The last two of these equations show that neither σ_{xy} nor σ_{xz} is a function of the x coordinate. The conclusion that these shearing stresses are the same for all cross-sections is in harmony with the previously discussed expectation that neither the torque nor warping nor twist per unit length vary with the x coordinate. In the style of solving partial differential equations, this information from (i.e., the solution of) the second and third equilibrium equations is stated as

$$\sigma_{xy} = \sigma_{xy}(y, z) \quad \text{and} \quad \sigma_{xz} = \sigma_{xz}(y, z) \quad (12.3)$$

The first of the above three equilibrium equations remains to be dealt with. This first equation will be satisfied (i.e., solved) by the introduction of a potential function. A potential function is simply an ordinary function, which may or may not have a physical interpretation, that when differentiated provides a quantity of interest. For example, a differentiation with respect to height above a datum, h , of the gravitational potential energy (mgh) provides the gravitational force ($-mg$), where m is the mass of the object, and g is the acceleration of gravity. The Airy stress function is an example of another potential function in solid mechanics, and the stream function for fluid velocities is an example of a potential function from fluid dynamics. Thus, for the purpose of satisfying all the equilibrium equations, define

$$\sigma_{xy} \equiv \frac{\partial \Psi(y, z)}{\partial z} \quad \text{and} \quad \sigma_{xz} \equiv -\frac{\partial \Psi(y, z)}{\partial y} \quad (12.4)$$

where $\Psi(y, z)$ is the potential function that when differentiated as indicated above provides the two shearing stresses sought. According to Ref. [21], this potential function Ψ was first

introduced by L. Prandtl. It is commonly referred to as the Prandtl stress function. Substitution of these two definitions into the three equilibrium equations shows that those equations are identically satisfied. In other words, it does not matter what specific functional form the Prandtl stress function may have. Its two-part definition as a function of the Cartesian coordinates y and z alone guarantees that all internal equilibrium requirements are met. In other words, merely including Eqs. (12.4) in the uniform torsion analysis is sufficient to satisfy the equations of equilibrium. The satisfaction or solving of the equilibrium equations by the Prandtl stress function is sometimes spoken of as the "integration" of the equilibrium equations by the Prandtl stress function.

Now it is necessary to turn to the two remaining internal aspects of the theory of elasticity, which are the material and compatibility equations. For the sake of simplicity, the previous limitation of the analysis to the case of homogeneous, isotropic, Hookean materials is reaffirmed. Thus the strain–stress equations are merely

$$\gamma_{xy} = \frac{1}{G}\sigma_{xy} = +\frac{1}{G}\frac{\partial\psi}{\partial z} \quad \gamma_{xz} = \frac{1}{G}\sigma_{xz} = -\frac{1}{G}\frac{\partial\psi}{\partial y}$$

Substitution of the strain–stress equations into the six compatibility equations, Eqs. (3.14), yields zero-equals-zero identities in the first, second, third, and sixth equations, and

$$\frac{\partial}{\partial z}[\nabla^2\psi] = 0 \quad \text{and} \quad \frac{\partial}{\partial y}[\nabla^2\psi] = 0 \quad \text{where} \quad \nabla^2 \equiv \frac{\partial^2}{\partial y^2} + \frac{\partial^2}{\partial z^2}$$

for the fourth and fifth equations, respectively. Since in this analysis there are only two Cartesian coordinates being used as analysis variables, ∇^2 is only the sum of the second partial derivative operator with respect to y and the second partial derivative operator with respect to z . The conclusion to be drawn from the above two equations is that $\nabla^2\psi$ is not a function of any of the spatial coordinates. Since there are no other independent variables, $\nabla^2\psi$ must be equal to an unknown constant of integration which is temporarily designated as C . Thus

$$\nabla^2\psi(y, z) = C \tag{12.5}$$

is the form of the field equation that results from the trial solution that is Eqs. (12.1).

It is still necessary to show that Eq. (12.5) is relevant to the uniform torsion problem. To this end, consider the boundary conditions (BCs). In order to consider the BCs, it is necessary to be more specific about the general characteristics of the geometry of what until now has been an entirely arbitrary beam cross-section. In order to deal with vehicular structures, it is necessary to deal with multiply connected beam cross-sections. However, multiply connected bar cross-sections complicate some of the proofs that follow, and that interferes with an understanding of the overall development. Therefore, for the sake of simplicity, after the groundwork of the next few paragraphs, the development in this section is limited to the simply connected cross-section. However, the full proofs for multiply connected cross-sections are included in Appendix A, and the results for multiply connected cross-sections are discussed after the derivations for the singly connected bar cross-section.

The boundary surfaces of a uniform, singly connected beam are its outer cylindrical surface and its two end cross-sections where the torques are applied. If the beam cross-section is multiply connected, then there are also inner cylindrical surfaces that link the voids of the uniform cross-sections. Consider the cylindrical surfaces first. In the case of uniform torsion, there are no tractions on either the outer or any existing inner cylindrical surfaces, and the direction cosine of the right angle between a normal to those surfaces and

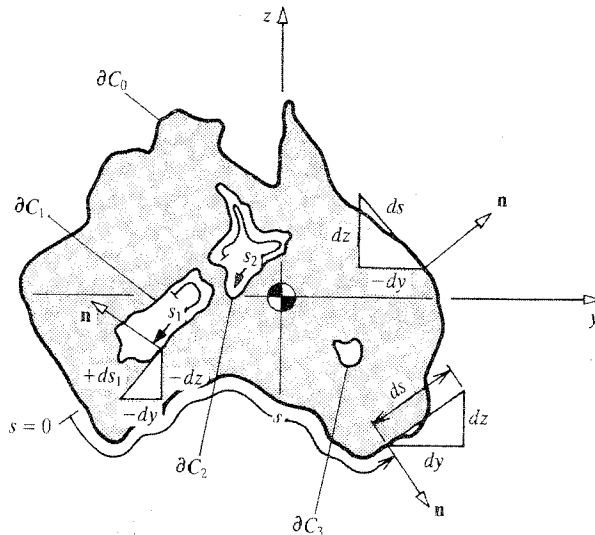


Figure 12.2. Multiply connected beam cross-section with outward normal vectors at the exterior boundary (∂C_0) and at the interior boundaries (∂C_i).

the x axis is always zero. Therefore, from Cauchy's equations, Eqs. (1.9), the BCs for both these outer and inner cylindrical surfaces reduce to the single equation

$$0 = \sigma_{xy} \cos(n, y) + \sigma_{xz} \cos(n, z)$$

or

$$0 = \frac{\partial \Psi(y, z)}{\partial z} \cos(n, y) - \frac{\partial \Psi(y, z)}{\partial y} \cos(n, z) \quad (12.6)$$

Be sure to note that because the variable x has no part in this BC equation, this BC equation is valid at all cross-sections. In the above form, the cylindrical surface BC appears to be a bit complicated because both terms vary from point to point on the curves that define the cylindrical boundary. Fortunately, this BC equation can be simplified greatly. Consider the multiply connected cross-section shown in Fig. 12.2, where there are three representative inner cylindrical surfaces. In the case of the unit normal vector on the outer boundary in the fourth quadrant, it is clear that the cosines of the angles between the positive direction of the normal vector and the positive directions of the y and z axes are

$$\cos(n, y) = \frac{dz}{ds} \quad \text{and} \quad \cos(n, z) = -\frac{dy}{ds} \quad (12.7)$$

where s , called the arc length coordinate, is the single counterclockwise coordinate that is sufficient to uniquely locate any point on the outer boundary relative to an arbitrary origin. The negative sign attached to the second direction cosine is a result of the corresponding angle being greater than 90° while the quantity dy is positive for positive ds in this quadrant. In the case of the unit normal vector on the outer boundary that is shown in the first quadrant, a positive value of ds creates a positive value of dz , but a negative value of dy . That is, as drawn, a positive change in the s coordinate value for that point on the outer boundary, leads to a negative change in the y coordinate value of that same boundary point. Thus the differential length, a positive quantity, is $-dy$. In this case where the angles between the normal vector and the coordinate axes are less than 90° , exactly the same results for the

direction cosines are obtained as those of Eqs. (12.7). The same would be true for boundary points located in the second and third quadrants. The same result can also be obtained for any inner boundary by having its arc length coordinate increase in a clockwise fashion as illustrated for the two beam cross-section openings on the left (South and North Islands).

Substitution of Eqs. (12.7) into the BC equations, Eq. (12.6), leads to a new form of the cylindrical surface BC equation, which is

$$0 = \frac{\partial \Psi}{\partial z} \frac{dz}{ds} + \frac{\partial \Psi}{\partial y} \frac{dy}{ds} = \frac{d\Psi(y, z)}{ds}$$

To fully understand this application of the chain rule and the meaning of the last derivative, note that on either the inner or outer boundaries, as opposed to the interior of the cross-section, the y and z coordinates are not independent of each other. Indeed, on the boundary there have to exist functional relations of the form $y = y(s)$ and $z = z(s)$ where s , the boundary arc length coordinate, can be viewed as a parameter that links and determines the two Cartesian coordinates when those two coordinates specify a boundary point. This is why, for example, dz/ds is a total derivative rather than a partial derivative. On this same basis, *on the boundary*, the Prandtl stress function is also only a function of the coordinate s , and its derivative with respect to s is also a total derivative. Of course, the conclusion to be drawn from the above equation is that the Prandtl stress function is a constant on the outer boundary and a (different) constant on each inner boundary. Since the Prandtl stress function is a potential function, and since the addition of a constant value to the Prandtl stress function in no way alters the physically real values of the stresses, then, for the sake of convenience, let the constant value of the Prandtl stress function on the outer boundary be zero. Of course, the constant values on the inner boundaries also have to be adjusted by the same additive amount, but since those values are unknown at this point, it makes no difference. Using the unambiguous symbols ∂C_0 and ∂C_i to designate the outer and i th inner boundary curves,¹ respectively, the BC equations are then

$$\Psi(s) = 0 \text{ on } \partial C_0 \quad \text{and} \quad \Psi(s) = \Psi_i \text{ on } \partial C_i \quad (12.8)$$

The adoption of Eqs. (12.8) is the first step linking the previous analysis, which lead to Eq. (12.5), to the specific problem of uniform torsion.

The two-dimensional GDE, which again is $\nabla^2 \Psi(y, z) = C$, and the above BCs have the welcome attribute of having quite simple forms. One remaining difficulty is that it is still necessary to learn more about the values of the various unknown constants that appear in the GDE and the BCs. The other remaining difficulty is that it is still necessary to complete the process of establishing that the above development is relevant to the uniform torsion problem. For this latter purpose, recall again that this entire development is an application of the inverse method wherein (i) four of the six stresses are taken to be zero; (ii) the equilibrium, linearly elastic material, and compatibility equations are used to define the conditions that need to be placed on the remaining two shearing stresses; and (iii) the complete stress solution is used along with the chosen beam geometry to define the applied loadings at the beam boundary surfaces. The first two steps have been completed. The first part of the third step, requiring zero tractions on the outer and inner cylindrical surfaces has also been completed.

¹ The symbol pair ∂C is unambiguous because there is no such thing as a partial differential. That is, a total derivative can be viewed as the ratio of two differentials, but a partial derivative cannot be so viewed.

Now it is necessary to investigate what information can be deduced from the only remaining boundary surfaces, the beam end cross-sections. Specifically, as the concluding effort of this inverse method approach, it is necessary to investigate whether or not the nonzero shearing stresses $\sigma_{xy} = \partial\Psi(y, z)/\partial z$ and $\sigma_{xz} \equiv -\partial\Psi(y, z)/\partial y$ actually produce the applied torques of the uniform torsion problem, and yet do not produce shearing forces that have no place in the uniform torsion problem. If equal and opposite torques are the only result of the two nonzero shearing stresses, then the assumed stress solution, Eqs. (12.1) along with the x plane shearing stress values that are a consequence of Eqs. (12.5) and (12.8), are the correct stress solutions for the uniform torsion problem.

To begin the task of determining the stress resultants at the beam end cross-sections, it is necessary to adapt the stress resultant–stress equations, Eqs. (9.1), to the present circumstances. Since it is proposed that $\sigma_{xx} = 0$ at either beam end, $N = M_y = M_z = 0$ and

$$V_y = \iint_A \frac{\partial\Psi}{\partial z} dA \quad V_z = + \iint_A \frac{\partial\Psi}{\partial y} dA$$

and

$$M_t = - \iint_A \left(y \frac{\partial\Psi}{\partial y} + z \frac{\partial\Psi}{\partial z} \right) dA$$

where A is the beam cross-sectional area that supports stresses, that is, A does not include any voids. The Green–Gauss theorem, which is reviewed in Section IV.2, can be used to evaluate the shearing force integrals. Doing so leads immediately to

$$V_y = + \oint \Psi dy = 0 \quad \text{and} \quad V_z = + \oint \Psi dz = 0$$

The values of these line integrals are zero because for a cross-sectional area without any interior boundaries and a piecewise smooth exterior boundary, $\Psi(s)$ has a zero value everywhere on the boundary path. The same zero result for the shearing force components is obtained in Appendix A, Section 3, for the multiply connected cross-section.

In order to evaluate the integral for the torque, rewrite that integral as the identical expression

$$M_t = - \iint_A \left(\frac{\partial(y\Psi)}{\partial y} + \frac{\partial(z\Psi)}{\partial z} \right) dA + 2 \iint_A \Psi dA$$

In this form the first integral can be evaluated by again using the Green–Gauss theorem. The result is

$$M_t = - \oint (y\Psi dz - z\Psi dy) + 2 \iint_A \Psi dA$$

Again, on the outer boundary $\Psi(s) = 0$. Therefore the above line integral for a singly connected cross-section is also zero. Thus

$$M_t = 2 \iint_A \Psi(y, z) dy dz \quad (12.9)$$

Hence, to have a nonzero torque, it need only be required that the above area integral not vanish. Hence, with this requirement, the hoped for result of having only the torque loading

associated with the uniform torsion problem has been verified, and therefore the stress solution is as described above.

A result similar to Eq. (12.9) is obtained for the multiply connected cross-section. For the multiply connected case, the torque is again twice the volume between the $\Psi = \Psi(y, z)$ surface and the y, z plane, but the integral of $\Psi(y, z)$ over the cross-section surface includes the internal voids over which $\Psi(y, z)$ is taken to have the constant values Ψ_i , the values of the Prandtl stress function at the edges of the voids, as is stated in Eq. (12.8). Thus, again, the adopted stress solution proves to be the theory of elasticity solution for the uniform torsion problem regardless of whether the beam cross-section is singly or multiply connected.

The final task is the specification of the constant C that appears in Eq. (12.5) and the constants Ψ_i that appear in Eq. (12.8). The latter set of constants are discussed in the next chapter. The determination of the constant C is achieved by calculating θ , the twist per unit length of the uniform beam in response to the applied torques. This deflection calculation is best done by use of the unit load method, which is described in Chapter 20. Since the unit load method has yet to be explained, that calculation is relegated to Appendix A, Section 4, where it can be understood after study of Chapter 20. The result of that calculation, for both the singly and multiply connected beam cross-sections is $C = -2G\theta$, where G is the constant shear modulus. Hence the summary statement of the uniform torsion problem is

$$\sigma_{xx} = \sigma_{yy} = \sigma_{zz} = \sigma_{yz} = 0 \quad (12.1)$$

$$\sigma_{xy} \equiv \frac{\partial \Psi(y, z)}{\partial z} \quad \text{and} \quad \sigma_{xz} \equiv -\frac{\partial \Psi(y, z)}{\partial y} \quad (12.4)$$

where $\Psi(y, z)$ is to be determined, in part, from the solution to the following GDE² and BCs

$$\boxed{\nabla^2 \Psi(y, z) = -2G\theta} \quad (12.10a)$$

$$\boxed{\Psi(s) = 0 \quad \text{on} \quad \partial C_0 \quad \text{and} \quad \Psi(s) = \Psi_i \quad \text{on} \quad \partial C_i} \quad (12.10b)$$

Since the GDE for this stress formulation relates the stress quantity Ψ to the deflection quantity θ rather than the applied load M_t , there is a need for the *auxiliary equation* that ties the stresses to the loading, which is, again

$$M_t = 2 \iint_A \Psi(y, z) dy dz \quad (12.9)$$

Clearly the function $\Psi(y, z)$ directly ties together the stresses and the twist per unit length, as well as the stresses and the applied torque. To tie together the constant value of the applied torque and the constant value of the twist per unit length, define "St. Venant's constant for uniform torsion," or simply the "torsion constant," symbolized by J , as

$$J \equiv \frac{M_t}{G\theta} \quad (12.11)$$

Like all other quantities of importance in this analysis, St. Venant's constant for uniform torsion also can be expressed in terms of the Prandtl stress function. Using the above

² The partial derivative operator ∇^2 is often called the "harmonic operator."

relations to substitute for M_t and $G\theta$ yields

$$J = -\frac{4}{\nabla^2\psi} \iint_A \psi \, dA$$

The importance of this quantity lies in the fact that GJ plays much the same role in beam twisting that EI plays in beam bending. Note that like area moments of inertia, St. Venant's constant for uniform torsion has units of length to the fourth power, and is generally different for different cross-sections.

12.3 Further Properties of the Prandtl Stress Function

Picture the surface above the y, z cross-sectional plane defined by the functional relation $\Psi = \Psi(y, z)$ as a hill or dome. That is, Ψ is the measure of height above the base plane. The base of the $\Psi(y, z)$ hill is the outer boundary of the beam cross-section where $\Psi(y, z)$ is zero. Lines of constant elevation for any hill or valley are called "contour lines." Geometrically, contour lines for the $\Psi(y, z)$ hill are defined by the intersection of the hill surface and planes paralleling the y, z plane. All contour lines are closed curves, and they are invariably drawn for equal increments in elevation. Thus the closer together the contour lines appear in an overhead view (a map), the steeper the slope of the hill. Of course, the mathematical description of contour lines is simply $\Psi(y, z) = \text{constant}$. For reasons soon to be revealed, the contour lines related to Ψ are called *lines of shearing stress*. They possess the properties that: (i) the total shearing stress vector, for which σ_{xy} and σ_{xz} are the Cartesian components, is everywhere tangent to these lines; and (ii) the magnitude of the total shearing stress vector is equal to the slope normal to the lines of shearing stress, that is, the magnitude of the gradient. Therefore, to picture the lines of shearing stress is to picture the complete shearing stress solution.

To prove the above two stated properties of the lines of shearing stress, it is convenient to introduce a local rotated coordinate system at each point along each contour line $\Psi(y, z) = \text{constant}$. Let that rotation be from the fixed y, z coordinates to the local coordinates n, s , where n is always in the direction of the outer normal vector for the particular line of shearing stress under discussion, and s is always tangent to that same line of shearing stress. Let s be positive in the counterclockwise direction; see Fig. 12.3. Clearly, at any fixed point, n, s constitute a right-handed, Cartesian coordinate system. This s coordinate is a slightly more general case of the s coordinate used previously for the outer boundary of the cross-section in that it is not confined to one, specific closed curve. Thus the need for the second coordinate, n , and thus derivatives here are partial derivatives. The rotation relations between the n, s and y, z coordinates can be determined precisely as was done in Eqs. (4.5), that is, with the use of unit vectors. The results in terms of the counterclockwise angle β between the y and n coordinate directions are

$$\begin{aligned} y &= n \cos \beta - s \sin \beta \\ z &= n \sin \beta + s \cos \beta \end{aligned}$$

The similar³ rotation formulas for the stress components are

$$\begin{aligned} \sigma_{xn} &= +\sigma_{xy} \cos \beta + \sigma_{xz} \sin \beta \\ \sigma_{xs} &= -\sigma_{xy} \sin \beta + \sigma_{xz} \cos \beta \end{aligned} \quad (12.12)$$

³ In this case the relations between the two pairs of shearing stresses can be based upon vector algebra because both pairs of shearing stresses act in the same plane, the x plane.

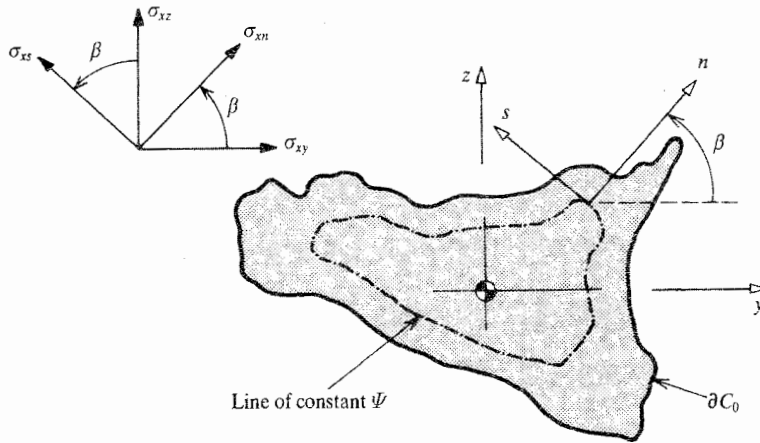


Figure 12.3. A solid beam cross-section showing a single contour line for the Prandtl stress function.

Since the n, s coordinate system was established so that $\Psi(n, s) = \text{constant}$ in the s coordinate direction for all values of n and s , then the derivative of the Prandtl stress function with respect to s must be zero. That is, using the chain rule,

$$0 = \frac{\partial \Psi}{\partial s} = \frac{\partial \Psi}{\partial y} \frac{\partial y}{\partial s} + \frac{\partial \Psi}{\partial z} \frac{\partial z}{\partial s}$$

The use of Eqs. (12.4), extended forms of Eqs. (12.7), and the first of Eqs. (12.12) shows that this last equation may be rewritten as

$$0 = \sigma_{xz} \sin \beta + \sigma_{xy} \cos \beta = \sigma_{xn}$$

Since σ_{xn} is always zero, σ_{xs} is the total shearing stress vector and, of course, it is tangent to the line of shearing stress. Indeed, this result justifies the name “lines of shearing stress” for the Prandtl stress function contour lines. The magnitude of σ_{xs} can be determined by considering the other orthogonal derivative

$$\frac{\partial \Psi}{\partial n} = \frac{\partial \Psi}{\partial y} \frac{\partial y}{\partial n} + \frac{\partial \Psi}{\partial z} \frac{\partial z}{\partial n}$$

Rewriting the above expression,

$$\frac{\partial \Psi}{\partial n} = -\sigma_{xz} \cos \beta + \sigma_{xy} \sin \beta = -\sigma_{xs}$$

This equation shows that σ_{xs} is the negative of the downhill slope of the Prandtl stress function surface normal to the lines of shearing stress.

The two interpretations that the total shearing stress vector is always tangent to the $\Psi(n, s)$ contour lines and equal to the negative of the normal slope $\partial \Psi / \partial n$, are valid for a multiply connected cross-section as well as a singly connected cross-section because nowhere in the development of this section was there any reference to anything but local points within the beam cross-section. These two interpretations take on added weight when combined with the results of Section 12.4.

The inner and outer cross-section boundaries are just special cases of lines of shearing stress because at those boundaries the Prandtl stress function has constant values. These

boundaries illustrate the fact that the shearing stress component normal to such a $\Psi(n, s)$ contour line, σ_{xn} , is zero. These boundaries are formed, of course, by the intersection of the plane of the beam cross-section and the beam cylindrical surfaces. Consider a differential-sized rectangular parallelepiped with one of its edges at and along such a cross-section boundary. A moment equilibrium equation about a central parallelepiped axis parallel to the edge that coincides with the cross-section boundary demonstrates that there is no stress component perpendicular to the boundary in the plane of the cross-section because there is none on the adjacent cylindrical surface.

12.4 The Membrane Analogy

This section establishes a remarkable analogy, due to Prandtl (Ref. [21]), between the lateral displacements of a taut membrane and the torsional stresses acting upon a beam cross-section. A *membrane* is defined as a flat, thin rubber sheet type body for which the thickness is very small relative to its other two linear dimensions. A membrane is so thin that there is only negligible internal resistance by the membrane to its being bent. In more familiar terms, a beam has internal resistance to being bent, but a piece of string, taut or not, does not. Like a piece of string, for which the membrane is a two-dimensional analog, the membrane must deflect in order to support (equilibrate) a lateral loading acting upon its surface area. That is, only by developing finite surface slopes can a horizontal membrane develop vertical tensile force components that oppose a vertical (lateral) loading. A sheet of paper, aluminum foil, or even a soap bubble are possible examples of membranes. A thicker sheet of aluminum would have significant bending stiffness, and would be called a *plate*. A plate is the two-dimensional analog of a beam.

Consider a taut membrane of arbitrary planar geometry in the y, z plane. Let the membrane have a constant thickness, and let it be fixed against all three deflection components at its outer boundary. Let there be a lateral pressure of magnitude $p(y, z)$ acting normal to the membrane surface that is positive in the same general direction as the positive x axis. The lateral pressure $p(y, z)$ causes an additional stretching of the membrane beyond that stretching which causes the membrane to be taut in its undeflected, planar position. Thus the membrane tensile forces that cause the membrane to be initially taut are increased as the membrane undergoes lateral deflections. The key assumption in the analysis that follows is that the lateral deflections are sufficiently limited that the resulting increases in the membrane tensile in-plane strains and in-plane forces are negligible relative to the initial tensile strains and forces that make the laterally undeflected membrane taut. This limitation is not overly restrictive because the increase in the membrane internal tensile strains and forces is proportional to the square of the membrane slopes (in units of radians, of course). See Exercise 12.11.

In order to describe the balance of in-plane forces within the membrane, let the initial internal in-plane forces be the result of the application along the outer edges of the membrane of tractions that parallel the plane of the membrane. Since the membrane has no bending stiffness, the stresses in the membrane are constant throughout the depth of the membrane. Thus there is no ambiguity in multiplying the outer edge tractions by the membrane thickness to obtain forces per unit of edge length. Let the tensile forces per unit of edge length be applied to a membrane of arbitrary planform in the manner suggested in Fig. 12.4, where the tensile forces per unit length are first applied to a rectangular boundary that encloses the eventual, actual boundary of the membrane. On the boundaries parallel to the y axis, let the tensile forces per unit length act only in the z direction and be symbolized as N_z , while those normal forces per unit length acting on the edges that parallel the z axis are

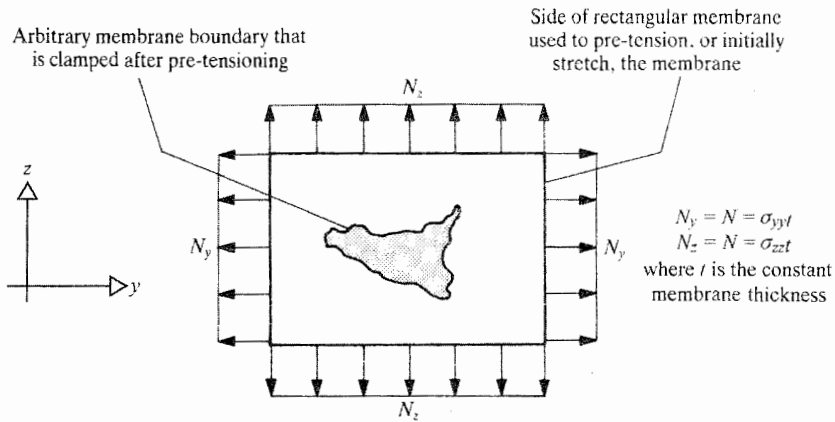


Figure 12.4. Plan view of a stretched membrane of arbitrary shape.

called N_y . Note that here no shearing forces per unit of edge length have been placed upon the rectangular membrane boundary. Now let $N_y = N_z = N$ a positive constant. Then there are no shearing stresses or shearing forces per unit length in any direction anywhere in the membrane. Furthermore, the normal force per unit length in any direction has the magnitude N . These two facts are examined in the first exercise.

Consider the FBD of a rectangular portion of the membrane where the in-surface dimensions are dy by dz as shown in Fig. 12.5. Note that, as usual, the size of the free body differential lengths is greatly exaggerated relative to the membrane's finite thickness for the sake of clarity. Also note that all the displacements, slopes, and changes in slope are drawn as positive quantities. Summing forces in the vertical x direction, where the cosine of the small angle between the pressure vector and the x direction is taken to be 1.0, and the sines of the slope angles are taken to be the angles themselves, leads to the result

$$\begin{aligned}
 -Ndy \frac{\partial u}{\partial z} + Ndy \left(\frac{\partial u}{\partial z} + \frac{\partial^2 u}{\partial z^2} dz \right) - Ndz \frac{\partial u}{\partial y} \\
 + Ndz \left(\frac{\partial u}{\partial y} + \frac{\partial^2 u}{\partial y^2} dy \right) + p(y, z) dy dz = 0
 \end{aligned}$$

After canceling offsetting terms and the subsequent common factors $dy dz$,

$$N\nabla^2 u = -p \quad (12.13)$$

Summing forces in the either the y or z direction leads by a more difficult route to this same result. The single BC for the membrane is simply

$$u(s) = 0 \quad \text{on} \quad \partial C_0$$

If, as shown in a side view section in Fig. 12.6, a right cylinder of arbitrary cross-section is brought into contact with the membrane so as to push the membrane above the y, z plane in such a manner that the membrane is flat over the top surface of the right cylinder, a distance h_1 above the y, z plane, then there is the additional BC on the inner membrane boundary, whose shape is defined by the cylinder cross-sectional shape, that

$$u(s) = h_1 = \text{constant on} \quad \partial C_1$$

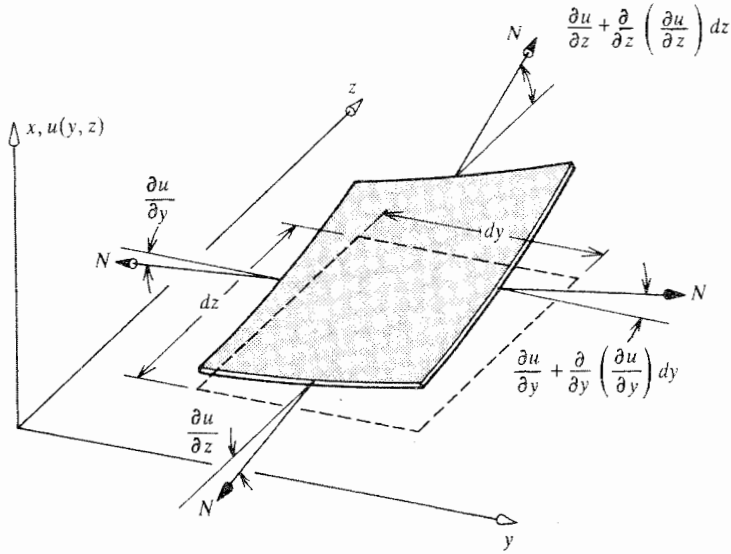


Figure 12.5. A free body diagram of a differential-sized membrane element subjected to a uniform tension. The pressure vector is omitted for clarity. The finite slopes of the membrane are limited only by the accuracy of the approximation that $\sin \theta \approx \theta$. Finite slopes are required so that the vertical components of the tensile forces can equilibrate the applied pressure.

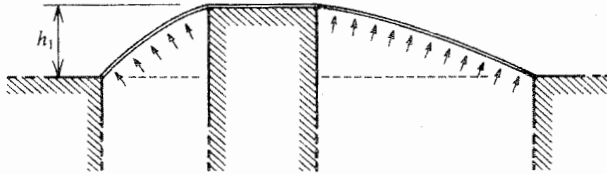


Figure 12.6. A sectioned side view of a uniform pressure-loaded membrane further raised by contact with a right angle cylinder.

There would of course be similar BCs for other such cylinder-induced boundaries. In addition, the following equation can be written for twice the volume between the membrane and the y, z plane

$$\text{Double Volume} = 2 \iint_A u(y, z) dy dz$$

A comparison of Eq. (12.13) for a constant pressure, these BCs, and this double volume equation on one hand with Eqs. (12.10) and the auxiliary torque equation, Eq. (12.9), on the other hand shows an exact mathematical analogy between the beam uniform torsion problem statement and the membrane lateral deflection problem statement. Such an exact analogy is often called an “isomorphism.” Thus a solution of the membrane problem for the lateral deflections $u(y, z)$ provides the same solution as the Prandtl stress function $\Psi(y, z)$ for a beam cross-section that has the same singly or multiply connected boundaries as the membrane. The usefulness of the isomorphism is not in solving one problem to get the solution to the other, because the two problems are equally difficult. Rather the usefulness

lies in the common experience of playing with balloons. That is, it is not difficult to imagine the deflected shape of a rubber membrane sheet loaded by a net, constant gas pressure when the inner and outer edges of the sheet are clamped along the same curves that form the inner and outer boundaries of a beam cross-section. The image of the contour lines of the deflected membrane is the image of the lines of shearing stress. The image of the membrane slopes, which is facilitated by the image of the contour lines, and vice versa, is the image of the shearing stress magnitudes. Thus, while it may be difficult, or even impossible, to get analytical solutions for many beam cross-sections, it is usually a simple matter to get a good, general sense of the shearing stress solution by just picturing the corresponding deflected membrane. This imaging can be used to estimate the location of the maximum torsional shearing stresses, or the relative torque carrying capacity of a cross-section.

Consider Fig. 12.7(a) which is the first in a short series of top and side view sketches of membranes deflected by a constant pressure. The membrane, hence Prandtl stress function, for the solid circular cross-section is easily imagined as the axisymmetric dome shown. Thus it is clear that (i) the lines of torsion shearing stress are circles; (ii) the maximum slopes, that is, maximum stresses, are at the outer boundary; and (iii) the shearing stress decreases to zero at the center of the cross-section. The hollow pipe cross-section of Fig. 12.7(b) is quite similar, with the *minimum* shearing stress at the inner diameter. Figure 12.7(c) shows a circular cross-section modified by the presence of a keyway. This cross-section represents an opportunity to demonstrate the power of the membrane analogy. Think of the air pressure reaching the bottom side of the membrane through a small, centrally located, vertical passageway rather than the broad opening that is drawn for the other cross-sections. Then think of pushing your finger into the membrane so as to flatten it against the y, z plane. Then it should be evident from your experience of pushing your finger into a balloon that the greatest membrane slopes are at the tip of your finger, and those fingertip boundary slopes can be significantly greater than the boundary slopes on the opposite side of the cross-section. The membrane sketch in Fig. 12.7(d) shows that the maximum torsional shearing stresses for a solid rectangular cross-section are also at the outer boundary points that are *closest* to the beam center. This commonplace result,⁴ which may be unexpected, helps highlight one of the differences between the solution for beam bending about an axis of symmetry and beam torsion solutions. Chief among these differences are that (i) while the maximum normal stress for a symmetric cross-section is always at one of the outer boundary points farthest from the cross-section centroid, the closest outer boundary points are often the location of the maximum shearing stress; and (ii) while there is one strength of materials beam bending stress solution for all compact beam cross-sections, each different compact cross-sectional geometry in the uniform beam torsion problem requires a distinctly different theory of elasticity solution.

Since the torque acting on a cross-section is proportional to the volume under the membrane, the greater that volume for a given slope, the greater the torque carrying capacity of the cross-section for a given stress. Reversing the thought process used with Fig. 12.7(c), it is clear, for example, that adding thin vanes to the circular cross-section of Fig. 12.7(a) to get that of Fig. 12.7(e) does very little to augment the torque carrying capacity of the cross-section. The torque carrying capacity of the cross-section in Fig. 12.7(f) is clearly

⁴ There are exceptions. For example, picture two oppositely oriented valentine hearts joined symmetrically at their widened tips by a narrow isthmus so as to make one figure eight type cross-sectional shape. Thus there is a finite cross-section thickness at the centroid. If the interior cusps of the valentine hearts drive deeply and sharply into the center of each valentine heart area, then the maximum membrane slope is at the tips of those cusps rather than at the outer boundary points closest to the centroid.

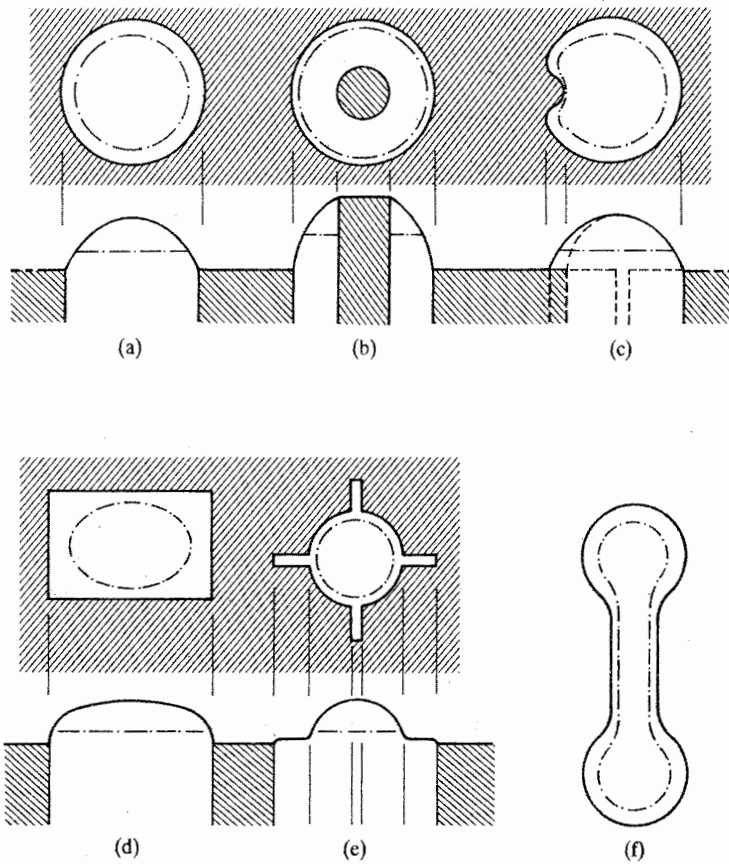


Figure 12.7. Membrane images for various beam cross-sectional shapes showing a single contour line in each case.

greater, but not much greater, than that of the two circular cross-sections and the one rectangular cross-section treated separately (particularly if the approximation of the next chapter is used with the rectangle). Thus, such a separate breakdown would provide a useful, conservative estimate of the torque carrying capacity for that cross-section.

Finally, from Ref. [32], Figs. 12.8(a, b) show detailed, experimentally determined membrane contour lines for portions of cross-sections of particular engineering importance. These diagrams show: (i) the need for rounded fillets in order for the stresses at internal corners to have magnitudes similar to those elsewhere on the cross-section edges; and (ii) the membrane bulge, that is, the additional volume, that occurs at the junctures of rectangular portions of the beam cross-section. The membrane analogy is used frequently throughout the remainder of the beam torsion discussion.

12.5 Closed Form Beam Torsion Analytical Solutions

There are very few exact solutions, involving only a finite number of terms, for the beam torsion problem of Eqs. (12.10). In order to become more familiar with these theory of elasticity beam torsion equations, this section presents two such solutions as examples. Before proceeding to those examples, it is worthwhile to briefly discuss the solution process

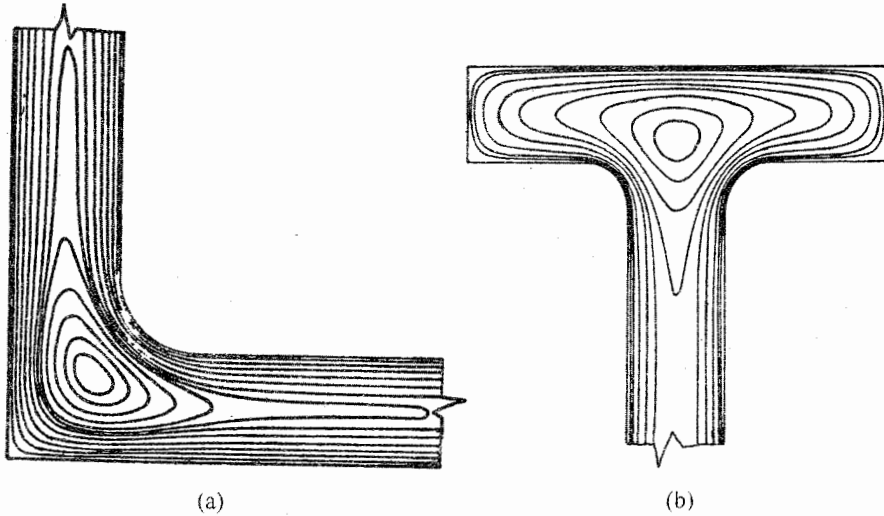


Figure 12.8. Experimentally obtained membrane contour lines at flange-web junctures from Ref. [32].

in general terms. The usual direct approach to the solution of any boundary value problem begins with the GDE, which in this case is

$$\left[\frac{\partial^2}{\partial y^2} + \frac{\partial^2}{\partial z^2} \right] \Psi(y, z) = -2G\theta \quad (12.10a)$$

Therefore what is sought are functions $\Psi(y, z)$ that, when subjected to the harmonic operator, yield a constant. There are many such terms but, as will be seen, few are useful for defining boundaries of engineering interest. The place to find the simplest solutions to the above second order GDE is in the field of polynomials. Brief experimentation shows that, when the general second order polynomial expression

$$\Psi_2(y, z) = C_1 + C_2y + C_3z + C_4y^2 + C_5yz + C_6z^2$$

is subjected to the harmonic operator, the result is the constant $2(C_4 + C_6)$, which may be equated to the constant $-2G\theta$ in the same way as done in Example 12.1. below. This is useful information because when this function $\Psi_2(y, z)$ is set equal to zero in order to define the outer boundary of the cross-section where the BC of $\Psi_2 = 0$ must hold true, the general result is the four conic sections. Therefore, it may now be expected that a solution can be found for beam cross-section whose symmetrically located inner and outer boundaries are circles and ellipses. Single parabolas and hyperbolas cannot, of course, be the sole descriptions of beam cross-sections because such cross-sections would never end.

The next thing to note is that any function $H(y, z)$ such that

$$\left[\frac{\partial^2}{\partial y^2} + \frac{\partial^2}{\partial z^2} \right] H(y, z) = 0$$

can be added to the above second order polynomial $\Psi_2(y, z)$ without affecting the previous outcome of the application of the harmonic operator; that is,

$$\left[\frac{\partial^2}{\partial y^2} + \frac{\partial^2}{\partial z^2} \right] [\Psi_2(y, z) + H(y, z)] = \text{the same constant}$$

There are many such functions, called harmonic functions. Harmonic functions can be higher order polynomials such as

$$H(y, z) = C_9(y^4 - 6y^2z^2 + z^4) + C_{10}(yz)(y^2 - z^2) \quad (12.14a)$$

or transcendental functions such as

$$H(y, z) = C \sin\left(\frac{\pi y}{a}\right) \sinh\left(\frac{\pi z}{a}\right) \quad (12.14b)$$

where a is a fixed length. Unfortunately, very few of these harmonic functions, when added to the above second order polynomial, are helpful in defining a beam cross-section boundary of engineering interest.⁵ Since it appears that defining a useful boundary is a major difficulty, it is sometimes efficient to concentrate on that aspect of the problem by putting it first.⁶ That is, in order to seek a direct solution to the uniform torsion problem for a given beam cross-section, first use the equation(s) of the boundary, $\Gamma(y, z) = 0$, to satisfy the BCs, and then seek to satisfy the GDE. The following two example problems illustrate this approach.

Example 12.1. Determine the Prandtl stress function solution, the value of the St. Venant constant for uniform torsion, and the magnitude of the maximum shearing stress in terms of the applied torque, for the solid elliptical beam cross-section of Fig. 12.9.

Comment. An alternate approach to the solution of this problem is presented in Endnote (3).

Solution. The equation for the boundary of the ellipse, in terms of centroidal coordinates, is

$$\Gamma(y, z) = 1 - \left(\frac{y}{a}\right)^2 - \left(\frac{z}{b}\right)^2 = 0$$

Thus any candidate function $\Psi(y, z)$ that contains the above $\Gamma(y, z)$ as a factor has the value zero at the boundary of the ellipse, and thus satisfies that required BC. Since $\Gamma(y, z)$ is already a second order polynomial, choose the following trial solution, where C_0 is a constant whose value is to be determined,

$$\Psi(y, z) = C_0 \left[1 - \left(\frac{y}{a}\right)^2 - \left(\frac{z}{b}\right)^2 \right]$$

Substituting this trial solution into Eq. (12.10a) yields

$$\left[\frac{\partial^2}{\partial y^2} + \frac{\partial^2}{\partial z^2} \right] \Psi(y, z) = -2C_0 \left(\frac{1}{a^2} + \frac{1}{b^2} \right) = -2G\theta$$

or

$$C_0 = G\theta \frac{a^2 b^2}{a^2 + b^2}$$

That is, as expected, the harmonic operator acting upon the trial solution does produce a constant that can be adjusted so that Eq. (12.10a) is satisfied. Thus

$$\Psi(y, z) = G\theta \frac{a^2 b^2}{a^2 + b^2} \left[1 - \left(\frac{y}{a}\right)^2 - \left(\frac{z}{b}\right)^2 \right]$$

⁵ Reference [21] states that St. Venant showed that the even-order terms of the polynomial of Eq. (12.14a) can be used in conjunction with second order polynomial terms and a constant term so as to closely approximate a square cross-section.

⁶ More precisely, it is not difficult to write expressions that satisfy the GDE, and it is not difficult to write expressions that satisfy the BCs. What is difficult is to do both simultaneously.

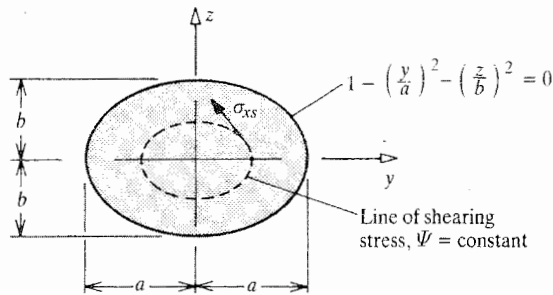


Figure 12.9. Example 12.1. A solid elliptical beam cross-section.

is the Prandtl stress function that satisfies both the GDE and the BC, and hence is the theory of elasticity solution. However, this solution cannot as yet provide the solution for the shearing stresses in terms of the applied torque because this solution is in terms of the twist per unit length. To make the conversion from $G\theta$ to M_t/J , write

$$\begin{aligned} M_t &= 2 \iint_A \Psi(y, z) \, dy \, dz \\ &= 2G\theta \iint_A \frac{a^2b^2}{a^2 + b^2} \left[1 - \left(\frac{y}{a}\right)^2 - \left(\frac{z}{b}\right)^2 \right] \, dy \, dz \\ &= 2G\theta \frac{a^2b^2}{a^2 + b^2} \left(\iint_A dA - \frac{1}{a^2} \iint_A y^2 dA - \frac{1}{b^2} \iint_A z^2 dA \right) \end{aligned}$$

The first of the three integrals of the last line is simply the area of the ellipse, πab , while the second and third are the area moments of inertia that are calculated in Chapter 9. Since $I_{zz} = (\frac{1}{4}) \pi a^3b$ and $I_{yy} = (\frac{1}{4}) \pi ab^3$, the solution for the torque in terms of the twist is $M_t = \pi G\theta [a^3b^3 / (a^2 + b^2)]$. Therefore, since $M_t = GJ\theta$,

$$J = \pi \frac{a^3b^3}{(a^2 + b^2)} \leq I_p = \frac{1}{4} \pi ab(a^2 + b^2)$$

where I_p is the polar moment of inertia for the ellipse. (The polar moment of inertia is mentioned because when $a = b$, and the ellipse becomes a circle, the torsion constant is the same as the polar moment of inertia. However, the circle and the annulus are the only cross-sections for which that is true.) Now it is possible to rewrite the Prandtl stress function in its desired form as

$$\Psi(y, z) = \frac{M_t}{\pi ab} \left[1 - \left(\frac{y}{a}\right)^2 - \left(\frac{z}{b}\right)^2 \right]$$

Now it is possible to relate the stresses to the applied torque. From Eqs. (12.4),

$$\sigma_{xy} = -\frac{2M_t z}{\pi ab^3} \quad \text{and} \quad \sigma_{xz} = +\frac{2M_t y}{\pi a^3 b}$$

Finally, from the membrane analogy, the maximum value of the stress is at $(y, z) = (0, \pm b)$, and has the magnitude

$$(\sigma_{xs})_{max} = \frac{2M_t}{\pi ab^2}$$

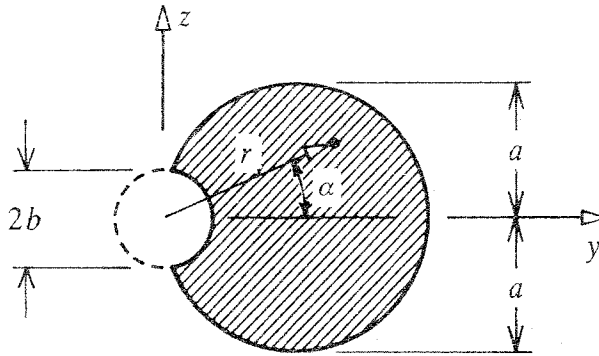


Figure 12.10. Example 12.2. A solid circular beam cross-section with a circular groove, called a keyway.

In summary, the equation for the elliptical boundary was fashioned into a trial function that first satisfied the single BC and then was made to successfully satisfy the GDE. The use of the auxiliary torque equation allowed writing the Prandtl stress function solution in terms of the applied torque. Then partial differentiation supplied the solutions for the stresses. ■

As mentioned earlier, the above results for the ellipse can be specialized to the circle by putting $a = b$. The circular cross-section has the unique property that its warping deflections are zero, even when the diameters of the beam cross-sections vary along the length of the beam (Ref. [12]). The assumption of that unique property of plane cross-sections remaining plane allows the simplified analysis for circular cross-sections found in introductory strength of materials textbooks.

Example 12.2. Consider the solid circular cross-section with a circular groove (keyway) shown in Fig. 12.10. The equation for the boundary of the larger circle is $r = 2a \cos \alpha$, and that for the smaller circular boundary is $r = b$, where r, α are polar coordinates. Hence, among others, the candidate Prandtl stress function

$$\Psi(r, \alpha) = C_0(r^2 - b^2) \left(1 - \frac{2a}{r} \cos \alpha \right)$$

satisfies the required BC of $\Psi = 0$ on the boundary of the cross-section. (a) Show that this candidate function is a valid Prandtl stress function, and in so doing, determine the required value of the constant C_0 in terms of the twist per unit length. (b) State where the maximum shear stress is to be found, and calculate its magnitude in terms of the twist per unit length. (c) If the maximum shearing stress in a circular bar without a groove is $Ga\theta$, what then is the ratio of the maximum stress in a scratched bar (i.e., where $b \rightarrow 0$) to the maximum stress in an unscratched bar?

Solution. (a) To be a valid Prandtl stress function, in addition to satisfying the BC, this function $\Psi(r, \alpha)$ must also satisfy

$$\nabla^2 \Psi(r, \alpha) = \left[\frac{\partial^2}{\partial r^2} + \frac{1}{r} \frac{\partial}{\partial r} + \frac{1}{r^2} \frac{\partial^2}{\partial \alpha^2} \right] \Psi(r, \alpha) = -2G\theta$$

where the polar coordinate form of the harmonic operator is shown. After the indicated partial differentiation, and some simplification, the left-hand side reduces to the constant $4C_0$. Therefore, the candidate function is certified as being a true Prandtl stress function when $C_0 = -G\theta/2$.

(b) As previously discussed, the maximum shearing stress is at the centerline of the groove, that is, at $(r, \alpha) = (b, 0)$. Thus the maximum shearing stress, which acts in the z direction, is the partial derivative of the Prandtl stress function with respect to r , evaluated at $r = b, \alpha = 0$, because along this line $y \equiv r$. The result is

$$(\sigma_{xs})_{max} = G\theta(2a - b)$$

(c) As $b \rightarrow 0$, the value of the maximum shearing stress approaches $2G\theta a$, and the ratio of the scratched to unscratched maximum shearing stresses approaches 2:1. This makes clear the importance of a well-polished surface finish for avoiding crack initiation due to shear slippage. ■

As commentary on the above result, and as a review of material from earlier chapters, note that part (c) shows that a simple scratch acts as a stress riser for torsion with a theoretical stress intensity factor of $K_t = 2.0$. The region on the cross-section of high stress values is quite limited as can be seen by noting that the z direction shearing stresses vary along the y axis according to the formula: $G\theta\{a[1 + (b/r)^2] - r\}$, and, if necessary, differentiating this result r . Thus if the scratched bar is subjected to a torque equal to a bit more than half the elastic torque capacity of the unscratched shaft (as might be routine use with a design factor of safety of 2), then there will be a very small region on the cross-section around the scratch where the shearing stresses equal or slightly exceed the yield stress. These circumstances are far from threatening an immediate failure of the shaft, but do set the stage for an eventual fatigue failure if, as usual, the torque undergoes changes in magnitude. The calculation of the integral of the auxiliary torque equation for this cross-section is briefly discussed in Endnote (1).

A final comment upon Example 12.2 is that it should be noted that the coordinate system (r, α) used throughout the solution is not a centroidal coordinate system. The use of non-centroidal orthogonal coordinates is permissible because nowhere in the theory of elasticity derivation of the uniform torsion equations, Eqs. (12.10a, b), is use made of the beam bending equations requirements that the first moments of area be zero and that the second moments be the area moments of inertia as set forth in Eqs. (9.6b). In another view of this important point, return to the formulation of the uniform torsion problem in terms of Cartesian coordinates as set forth by Eqs. (12.10a, b). Consider a second Cartesian coordinate system y_0, z_0 that is simply a translated coordinate system relative to the y, z coordinate system. Then, for example, $y_0 = y + \text{const.}$, and $\partial\Psi/\partial y = (\partial\Psi/\partial y_0)(\partial y_0/\partial y)$. But $\partial y_0/\partial y = 1$, and thus it is clear that the GDE is wholly unaffected by the choice of an orthogonal coordinate system. Coordinate rotations need not be considered because there has never been any restriction on the angular directions of y, z . As for the BCs, they only involve the function $\Psi(s)$, whose values along the boundary must be unaffected by any coordinate transformation. Thus the conclusion is that the analyst can use any convenient, orthogonal coordinate system.

12.6 Open Form Uniform Beam Torsion Solutions

The use of infinite series to satisfy either a GDE or a set of BCs, or both, is a common analytical practice. Nevertheless, such series are used in introductory textbooks,

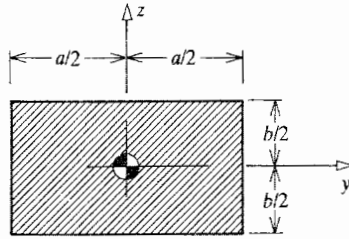


Figure 12.11. Example 12.3. A solid rectangular beam cross-section of dimensions a by b .

such as this, only if the analysis result is particularly important to the further development of required material. That is the present case. In order to logically develop the torsion constants and maximum stress values for H, I, T, channel, angle, and other such cross-sections of engineering importance, it is first necessary to develop the uniform torsion solution for the solid, rectangular cross-section.

Example 12.3. For a solid, rectangular cross-section of dimensions a by b shown in Fig. 12.11, determine the Prandtl stress function, the value of the St. Venant constant for uniform torsion, and the value of the maximum stress.

Solution. Trials of the usual simple functions and combinations of such functions shows that they do not satisfy both the BCs and the GDE. The next step is to consider an infinite series. In a manner very similar to that of the previous example problems, the procedure adopted here is to choose a series⁷ where each term satisfies the BCs identically, and then proceed to manipulate the unknown constant coefficients of the chosen series terms in order to satisfy the GDE. In addition to being zero on the boundaries $y = \pm a/2$ and $z = \pm b/2$, the symmetry of the membrane image indicates the series terms must be symmetrical (i.e., even functions) with respect to both coordinates. There are many such series. For example, each term in the following infinite series of simple, even-powered, polynomial terms, and each term in the infinite series of cosine terms, meets the symmetry requirement and the requirement of being zero at each point on the rectangular boundary. (Cosines with even indices do not have zero values on the rectangular boundary, and thus are excluded from the chosen series.)

$$\Psi(y, z) = (4y^2 - a^2)(4z^2 - b^2)[c_1 + c_2y^2 + c_3z^2 + c_4y^4 + \dots]$$

$$\Psi(y, z) = \sum_{\substack{m \\ \text{odd}}} \sum_{\substack{n \\ \text{odd}}} c_{mn} \cos\left(\frac{m\pi y}{a}\right) \cos\left(\frac{n\pi z}{b}\right)$$

(where, e.g., m odd of course means $m = 1, 3, 5, 7, \dots$). Polynomial series are advantageous when rapid calculation is important, but this particular series lacks the exceedingly valuable property of *orthogonality*. As is seen below, the orthogonality property allows the determination of each unknown series coefficient individually, that is, without solving a large array of simultaneous equations. There are several well-known polynomial series that do possess the orthogonality property, but they cannot be made to satisfy these BCs term-by-term. Hence it is appropriate here to forget the simplicity of polynomial series and choose as a trial solution the second of the above two series, which is (i) a complete orthogonal series for even functions, and (ii) zero at each point on the four sides of the rectangular boundary

⁷ The chosen series must have the property of being "complete," that is, able to represent any differentiable function satisfying the given BC.

because each term of the series has that property. Endnote (2) is a brief extension of this discussion on the concept of orthogonality and related matters.

Again, since the selected cosine series satisfies the BCs, all that remains is to choose values for the coefficients c_{mn} so that this infinite trial series also satisfies the GDE. First, subject to later confirmation, assume that the cosine series obtained after the partial differentiations required by the GDE converge. Then substituting the original cosine series into the GDE yields the requirement that

$$\sum_{\substack{m \\ \text{odd}}} \sum_{\substack{n \\ \text{odd}}} c_{mn} \left[\left(\frac{m\pi}{a} \right)^2 + \left(\frac{n\pi}{b} \right)^2 \right] \cos \left(\frac{m\pi y}{a} \right) \cos \left(\frac{n\pi z}{b} \right) = 2G\theta$$

In order to isolate and thus determine the unknown constant coefficients, c_{mn} , it is first necessary to multiply both sides of the above equality by the quantity

$$\frac{4}{ab} \cos \left(\frac{r\pi y}{a} \right) \cos \left(\frac{s\pi z}{b} \right)$$

where both r and s are arbitrary positive integers. Since the arbitrary integer indices r and s are entirely independent of the two summation indices m and n , the pair of factors $\cos(r\pi y/a) \cos(s\pi z/b)$ can be inserted inside the double summation. In other words, these two factors multiply every term in the double summation. Next, integrate over the cross-sectional area, that is, integrate both sides of the equality over the intervals $-a/2 \leq y \leq +a/2$ and $-b/2 \leq z \leq +b/2$. At this point, with the integrals in iterated form, the equality looks like

$$\begin{aligned} & \sum_{\substack{m \\ \text{odd}}} \sum_{\substack{n \\ \text{odd}}} c_{mn} \left[\left(\frac{m\pi}{a} \right)^2 + \left(\frac{n\pi}{b} \right)^2 \right] \frac{2}{a} \int_{-a/2}^{+a/2} \cos \left(\frac{m\pi y}{a} \right) \cos \left(\frac{r\pi y}{a} \right) dy \\ & \times \frac{2}{b} \int_{-b/2}^{+b/2} \cos \left(\frac{s\pi z}{b} \right) \cos \left(\frac{n\pi z}{b} \right) dz \\ & = 2G\theta \frac{4}{ab} \int_{-a/2}^{+a/2} \cos \left(\frac{r\pi y}{a} \right) dy \int_{-b/2}^{+b/2} \cos \left(\frac{s\pi z}{b} \right) dz \end{aligned} \tag{12.15}$$

The orthogonality property of the cosine functions is embodied in the following integral formulas whose verification is left to the reader as an exercise:

$$\frac{2}{a} \int_{-a/2}^{+a/2} \cos \left(\frac{m\pi y}{a} \right) \cos \left(\frac{r\pi y}{a} \right) dy = \begin{cases} 0 & \text{if } r \neq m \\ 1 & \text{if } r = m \end{cases} \tag{12.16}$$

and

$$\frac{2}{b} \int_{-b/2}^{+b/2} \cos \left(\frac{s\pi z}{b} \right) \cos \left(\frac{n\pi z}{b} \right) dz = \begin{cases} 0 & \text{if } s \neq n \\ 1 & \text{if } s = n \end{cases}$$

The significance and joy of these integral results with respect to the left-hand side of Eq. (12.15) is that these integrals sweep into oblivion all terms in the double series except the one term where $m = r$ and $n = s$. Thus, by means of the orthogonality property of the cosine functions on the intervals of the cross-section, the double summation is reduced to a single term involving the single unknown coefficient. The two integrals on the right-hand side can be evaluated by the use of the formula

$$\int_{-a/2}^{+a/2} \cos \left(\frac{r\pi y}{a} \right) dy = \frac{2a}{\pi r} (-1)^{(r-1)/2} \tag{12.17}$$

and its z variable analog. Substitution of these results into Eq. (12.15) yields

$$c_{rs}\pi^2 \left[\left(\frac{r}{a}\right)^2 + \left(\frac{s}{b}\right)^2 \right] = \frac{32G\theta}{\pi^2 rs} (-1)^{(r+s-2)/2}$$

which provides the value of each coefficient c_{rs} (or c_{mn}) that is necessary to make the trial series satisfy the GDE. Note that the exponent factor $(r + s - 2)/2$ is never a fraction, but always an integer. Switching the names of the integers from r, s to m, n allows the Prandtl stress function solution to be written as

$$\Psi(y, z) = \frac{32G\theta}{\pi^4} \sum_{\substack{m \\ \text{odd}}} \sum_{\substack{n \\ \text{odd}}} (-1)^{(m+n-2)/2} \frac{\cos(m\pi y/a) \cos(n\pi z/b)}{mn[(m/a)^2 + (n/b)^2]} \quad (12.18)$$

Integrating the value of the Prandtl stress function over the cross-sectional area leads, by way of the torque, to the St. Venant constant for uniform torsion. Differentiation leads to the value of the maximum stress. Equation (12.17) can be used to carry out the integration over the area of the cross-section. The result of the integration, after recognizing that -1 raised to the power $(m + n - 2)$ has the value $+1$ for all the odd values of those two indices, is

$$M_t = \frac{256}{\pi^6} abG\theta \sum_{\substack{m \\ \text{odd}}} \sum_{\substack{n \\ \text{odd}}} \frac{1}{m^2 n^2 [(m/a)^2 + (n/b)^2]}$$

The solution for the St. Venant constant for uniform torsion is again taken from the relation $M_t = GJ\theta$. It is

$$J = \beta ab^3 \quad (12.19)$$

where as a function of the aspect ratio a/b the nondimensional factor beta is

$$\beta \left(\frac{a}{b}\right) = \frac{256}{\pi^6} \sum_{\substack{m \\ \text{odd}}} \sum_{\substack{n \\ \text{odd}}} \frac{1}{m^2 n^2 [m^2 (b/a)^2 + n^2]}$$

Calculating the approximate values of $\beta(a/b)$ is not difficult. It is a matter of selecting a series of values for the aspect ratio of the rectangle, such as $a/b = 1, 2, 3, \dots$, and then, for each aspect ratio, choosing a finite upper limit for the indices m, n such as 21. (Here 21 is used to approximate infinity because it takes too long a time to sum an infinite number of terms.) Then it is just a matter of summing the 121 terms of the double summation using the chosen a/b value. Next choose a greater value for the maximum index, say 31, and sum those 256 terms. If the difference between the results for the two different maximum indices is within the desired accuracy, then the $\beta(a/b)$ value for the greater of the two indices can be used as the approximation for $\beta(a/b)$. If not, choose a still larger maximum index until there is convergence to the desired accuracy. Obviously, a simple digital computer program is suitable for this summation process. Figure 12.12 is a computer-generated graph of various calculated values of $\beta(a/b)$.

The maximum stress value is located at the center of either of the long sides of the rectangular cross-section, that is, at $y = 0, z = \pm b/2$. To obtain the magnitude of the maximum stress, it is only necessary to: (i) partial differentiate with respect to the direction normal to the boundary at that point, that is, with respect to z ; (ii) substitute $y = 0$ and $z = \pm b/2$; and (iii) take the absolute value of the result, that is, discard any negative sign since only the magnitude of the stress is of current interest. The result is

$$(\sigma_{xs})_{\max} = \frac{1}{\alpha} \frac{M_t}{ab^2}$$

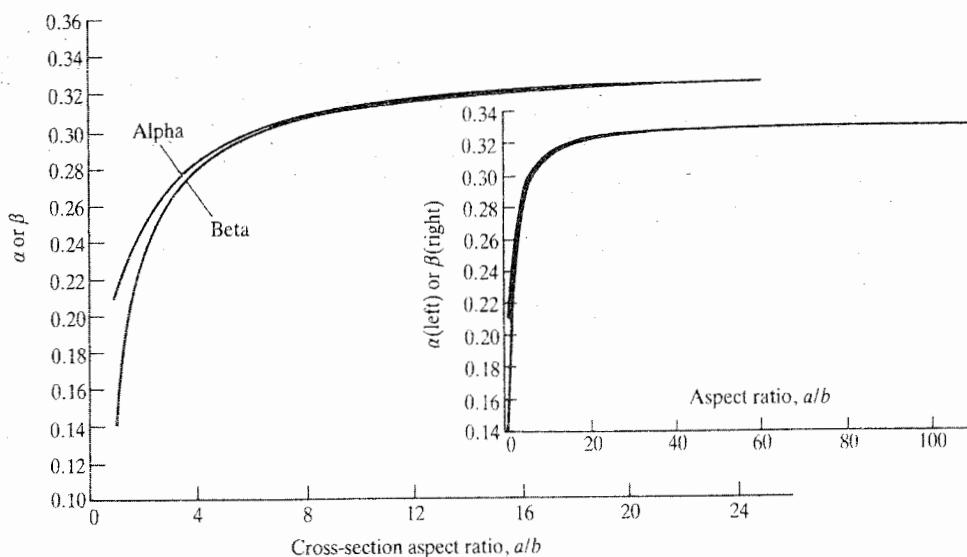


Figure 12.12. A plot of stress (α) and stiffness (β) parameters versus cross-section aspect ratio for twisted bars of rectangular cross-section. Courtesy of Ms. M. Godwin, Mr. S. Pujia, and Mr. R. Willingham.

where the nondimensional factor alpha is

$$\frac{1}{\alpha} = \frac{32}{\beta\pi^3} \sum_{\substack{m \\ \text{odd}}} \sum_{\substack{n \\ \text{odd}}} \frac{(-1)^{(m-1)/2}}{m[m^2(b/a)^2 + n^2]}$$

A graph of the values of α as a function of aspect ratio is also shown in Fig. 12.12. ■

12.7 Summary

The bending of a beam through small deflections does not significantly warp beam cross-sections, but the twisting of a beam, other than a beam with a circular or annular cross-section, does significantly warp the cross-section. Thus, while it is possible to accurately proceed on the basis that plane sections remain plane in the case of beam bending and extension, there is no such easy strength of materials entrée to the uniform torsion problem. The uniform torsion problem requires a solution to the equations of the theory of elasticity. Fortunately, it is possible to correctly guess that four of the six stresses are zero. The determination of the remaining two stresses, the x plane shearing stresses, of the uniform torsion problem requires a solution of Eqs. (12.9) and (12.10) for each cross-sectional shape. While these equations have a simple form, known analytical solutions are limited to a very few simple shapes. One more example problem is presented below.

Since the successful analytical application of St. Venant's uniform torsion theory is limited to simple cross-sectional shapes, its application to the usual beam cross-sections of actual vehicular structures might appear to depend entirely upon the use of numerical solution techniques. However, the combination of the membrane analogy, which is shown to be valid for singly and multiply connected cross-sections, and the exact solution for the rectangle, make possible the wide variety of simple, approximate beam torsion solutions that are discussed in Chapter 13.

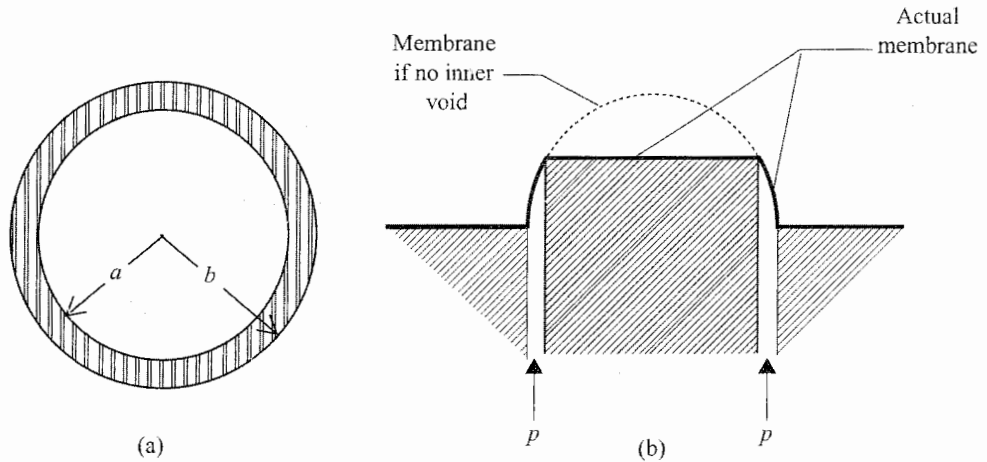


Figure 12.13. Example 12.4. (a) Annular cross-section. (b) Side view of corresponding membrane with plateau covering the internal void of radius “ a .”

It is well to remember that a condition for all the results of this chapter is that the beam is unrestrained with respect to the warping of the cross-section. This unrestrained beam warping BC is seldom fully present in actual vehicular construction. However, when this BC is present, unlike the beam bending solutions, the uniform torsion solutions are valid for all lengths of beam. The matter of warping constraint is further considered briefly in Chapter 13.

Example 12.4. Determine if the trial Prandtl stress function $\Psi(r) = (\frac{1}{2})G\theta(b^2 - r^2)$ meets the requirements for a uniform torsion solution for the annular cross-section shown in Fig. 12.13(a). If so, then determine the maximum shearing stress value due to twisting and the St. Venant constant for uniform torsion for this annular cross-section. Compare these two answers with the corresponding values provided by elementary strength of materials which are

$$\sigma_{shear} = M_t b / I_{polar} \quad \text{and} \quad J = I_{polar} = \iint_A r^2 dA$$

Note that these elementary strength of material values are based upon the unique knowledge that for annular and circular bar cross-sections, the planar cross-sections remain plane after the bar is twisted, and radii remain straight.

Solution. The first thing to do is to determine if the trial Prandtl stress function satisfies the uniform torsion GDE and the annular cross-section BCs. Substituting the given function into $\nabla^2 \Psi(r, \alpha) = -2G\theta$ shows that the GDE is indeed satisfied. At the outer cross-section boundary, where $r = b$, the trial function is indeed zero as it should be. At the inner boundary, the trial Prandtl stress function has the value $\Psi(a) = \frac{1}{2}G\theta(b^2 - a^2)$, which is the same positive constant everywhere on the inner boundary. Therefore all requirements have been met, and the trial function is accepted as correct. From a mental image of the membrane representing this valid Prandtl stress function, as shown in Fig. 12.13(b), the maximum stress value is at the outer edge of the cross-section where the slope perpendicular to the lines of constant shearing stress is greatest, and that perpendicular direction is simply the r direction. Therefore

$$\max \sigma_{shear} = \partial \Psi(b) / \partial r = G\theta b = M_t b / J$$

where the value of J is to be determined by calculating the relationship between the applied torque and the twist per unit length, θ . This task is accomplished by calculating the double volume under the membrane covering the actual cross-section plus the double volume under the membrane covering the central plateau, i.e., covering the central void. That is

$$M_t = 2 \int_0^{2\pi} \int_a^b \frac{1}{2} G\theta(b^2 - r^2)(r dr d\theta) + 2(\pi a^2) \left(\frac{1}{2} G\theta(b^2 - a^2)\right)$$

$$M_t = \frac{1}{2} \pi G\theta(b^2 - a^2)^2 + \pi G\theta(a^2 b^2 - a^4) = \frac{1}{2} \pi G\theta(b^4 - a^4)$$

Therefore the conclusion is that $J = (\frac{1}{2})\pi(b^4 - a^4)$. To complete the comparison to the values provided by elementary strength of materials, it is necessary to compute the polar moment of inertia.

$$I_{polar} = \int_0^{2\pi} \int_a^b r^2 (r dr d\alpha) = \frac{1}{2} \pi(b^4 - a^4)$$

This completes the validation of the elementary strength of materials formulas for annular cross-sections. In order to prepare to validate an approximation to be made in the next chapter, note that the shearing stress anywhere on the annular cross-section has the value $\partial\Psi(r)/\partial r = M_t r/J$, and in particular, the value of the shearing stress at the centerline of a thin annular cross-section is $\sigma_{xs}(r = (a+b)/2) = M_t(a+b)/[\pi(b^4 - a^4)]$, or $(b-a)\sigma_{xs} = M_t/[\pi(b^2 + a^2)]$, where the quantity $(b-a)$ is the thickness of the cross-section.

Further note that when a is only slightly less than b (a thin cross-section), then the stress of the inner boundary is only slightly less than the stress at the outer boundary, and neither differs much from their average value, the centerline stress. ■

Example 12.5. A uniform beam cross-section bounded by two circular arcs is sketched in Fig. 12.14(a). By rounding off the left-hand cusp as is illustrated in the sketch, the cross-section is an approximation to a uniform turbine blade. Consider the two candidate Prandtl stress functions listed below. (a) Determine whether or not they satisfy the circular arc BCs (i.e., for this purpose, ignore the rounding off of the turbine blade leading edge). (b) Determine whether or not the candidate Prandtl stress functions satisfy the GDE. (c) Calculate the maximum stress for this turbine blade cross-section as a function of the twist per unit length. (d) Determine the St. Venant constant for uniform torsion, J .

$$\Psi_1(r, \alpha) = \frac{1}{2} G\theta ab \left[1 - \left(\frac{r}{b}\right)^2 \right] \left[\left(\frac{r}{a}\right)^2 - 2 - 2 \cos 2\alpha \right]$$

$$\Psi_2(r, \alpha) = \frac{1}{2} G\theta b^2 \left[1 - \left(\frac{r}{b}\right)^2 \right] \left[1 - 2\frac{a}{r} \cos \alpha \right]$$

Solution. (a) In order to determine whether or not the candidate Prandtl stress functions are zero along both circular arcs that define the approximate cross-section, it is first necessary to write equations for those circular arcs in terms of the polar coordinates r, α . Directly from the diagram, the inner circular arc (the lower beam cylindrical surface) has the equation $r = b$. An equation for the outer circular arc can be obtained by drawing a radial line (length r) from the coordinate origin to a typical point on the outer arc; See Fig. 12.14(b). Since the outer arc is part of a circle whose diameter has the value $2a$, the right triangle

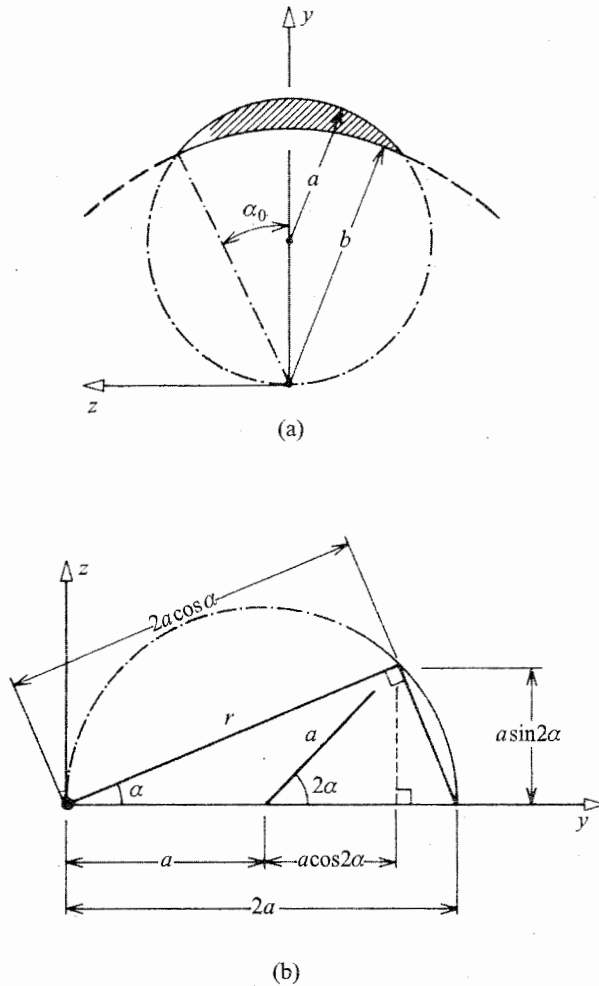


Figure 12.14. (a) Example 12.5 where circular arcs are used to approximate the majority of the boundary of a cambered airfoil. Note the orientation of the coordinate axes. (b) Geometry of the boundary arcs in terms of the polar coordinates (r, α) .

formed by the diameter and by the radial line yields the relation $r = 2a \cos \alpha$. Another equation for the outer arc can be obtained by drawing a line from the center of the outer arc circle to the same arbitrary point on the outer arc. Then the Pythagorean theorem yields $r^2 = (a + a \cos 2\alpha)^2 + (a \sin 2\alpha)^2 = 2a^2 + 2a^2 \cos 2\alpha$. Still another formula would be $a + a \cos 2\alpha = r \cos \alpha$. Of course, it is possible to go from any one of these formulas to the others by means of trigonometric identities. Now that the polar coordinate equations that designate the inner and outer arcs have been formulated, it is simply a matter of substituting them into the candidate Prandtl stress functions in order to test whether or not the zero value BCs are met. Substituting $r = b$ into the two candidate functions shows that both candidate functions are zero on the lower boundary. Thus that BC is met. Substituting the second of the upper arc formulas into the first candidate function, and substituting the first upper arc formula into the second candidate function shows that the two candidate functions are both

zero on the upper boundary arc. Thus both candidate functions satisfy the uniform torsion boundary conditions.

(b) The GDE that must be satisfied is

$$\frac{\partial^2 \Psi}{\partial r^2} + \frac{1}{r} \frac{\partial \Psi}{\partial r} + \frac{1}{r^2} \frac{\partial^2 \Psi}{\partial \alpha^2} = -2G\theta$$

Carrying out the partial differentiation shows that the first candidate function fails to satisfy the GDE, while the second function does satisfy the GDE. Only one candidate Prandtl stress function can satisfy any one set of BCs and the GDE because the solution to such a set of linear equations must be unique. By now it should be clear that the proper Prandtl stress function of this example problem is nothing more than a very slight variation on the Prandtl stress function of Example 12.2.

(c) The membrane analogy suggests that the maximum stress occurs at the point where $r = b, \alpha = 0$. To calculate the value of the stress at that point, note that the normal direction to the outer boundary at that point is the r direction. Thus, again

$$\sigma|_{max} = \left. \frac{\partial \Psi}{\partial r} \right|_{r=b, \alpha=0} = G\theta(2a - b)$$

For the sake of comparison, note that the stress at $(2a, 0)$ is

$$\sigma(2a, 0) = \left. \frac{\partial \Psi}{\partial r} \right|_{r=2a, \alpha=0} = \frac{1}{2}G\theta \left[2a - b \left(\frac{b}{2a} \right) \right]$$

It is easy to show that the latter stress value is never greater than the first stress value.

(d) Equation (12.9), $M_t = GJ\theta$, is used here to calculate the St. Venant constant for uniform torsion. In this case,

$$\begin{aligned} M_t &= 2 \iint_A \Psi_2(r, \alpha) r \, dr \, d\alpha \\ &= 2 \left(\frac{1}{2} \right) G\theta \int_{-\alpha_0}^{\alpha_0} \int_b^{2a \cos \alpha} (b^2 - r^2) \left(1 - \frac{2a}{r} \cos \alpha \right) r \, dr \, d\alpha \\ &= G\theta \int_{-\alpha_0}^{\alpha_0} \int_b^{2a \cos \alpha} [b^2 r - r^3 - 2(ab^2 - ar^2) \cos \alpha] \, dr \, d\alpha \\ &= G\theta \int_{-\alpha_0}^{\alpha_0} \left(\frac{2}{3} [2ab^3 \cos \alpha - 3a^2 b^2 \cos^2 \alpha + 2a^4 \cos^4 \alpha] - \frac{1}{4} b^4 \right) d\alpha \end{aligned}$$

At this point it is necessary to use trigonometric identities in order to put the cosine squared and cosine to the fourth power terms in a form suitable for direct integration. In particular,

$$\cos^2 \alpha = \frac{1}{2}(1 + \cos 2\alpha) \quad \text{and} \quad \cos^4 \alpha = \frac{1}{4}(1 + 2 \cos 2\alpha + \cos^2 2\alpha)$$

or

$$\cos^4 \alpha = \frac{1}{8}(3 + 4 \cos 2\alpha + \cos 4\alpha)$$

Hence from $M_t = G\theta(J)$

$$\begin{aligned} J &= \int_{-\alpha_0}^{\alpha_0} \left[\frac{4}{3} ab^3 \cos \alpha - \left(a^2 b^2 - \frac{2a^4}{3} \right) \cos 2\alpha + \frac{a^4}{6} \cos 4\alpha \right. \\ &\quad \left. + \frac{1}{4} (2a^4 - 4a^2 b^2 - b^4) \right] d\alpha \end{aligned}$$

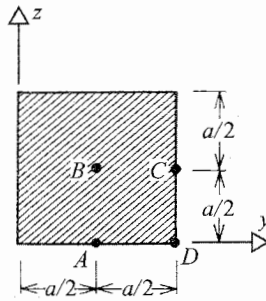


Figure 12.15. Exercise 12.3. A solid, square, bar cross-section.

Finally,

$$J = \frac{8}{3}ab^3 \sin \alpha_0 - \left(a^2b^2 - \frac{2a^4}{3} \right) \sin 2\alpha_0 + \frac{a^4}{12} \sin 4\alpha_0 + \frac{1}{2}(2a^4 - 4a^2b^2 - b^4) \alpha_0$$

This answer reduces to $J = (\pi/2)a^4$, the value for the full circular cross-section, when the interconnected constants $b = 0$ and $\alpha_0 = \pi/2$. On the basis of the membrane analogy, the St. Venant constant for a uniform turbine blade whose cross-sectional geometry is approximated by the two circular arcs can be approximated as a large percentage of the above answer. ■

Chapter 12 Exercises

- 12.1.** For the case where $N_y = N_z = N$, and $N_{yz} = 0$, on a rectangular boundary such as shown in Fig. 12.4, prove that the membrane shearing force per unit length is zero for any set of rotated Cartesian coordinate axes anywhere in the plane of the membrane, and that the tensile force per unit length is equal to N in any direction in the plane of the membrane. *Hint:* Recall that, by the definition of a membrane, the membrane bending stresses are wholly negligible. Thus the in-surface normal and shearing stresses σ_{yy} , σ_{yz} , and σ_{zz} are constant throughout the membrane thickness h . Thus $N_y = h\sigma_{yy}$, $N_{yz} = h\sigma_{yz}$, and $N_z = h\sigma_{zz}$. Since $N_y = N_z = N$, the normal stresses are equal, and hence from Mohr's circle, and so on.
- 12.2.** (a) Consider a rectangular cross-section of dimensions a horizontally by b vertically. Choose a y_0, z_0 Cartesian coordinate system that originates at the lower left corner of the rectangle. Using this coordinate system, construct a suitable candidate Prandtl stress function in the form of a double infinite series using only sine functions and unknown constant coefficients. Be sure that your candidate $\Psi(y_0, z_0)$ satisfies the uniform torsion BCs, which are $\Psi(0, z_0) = \Psi(a, z_0) = \Psi(y_0, 0) = \Psi(y_0, b) = 0$.
- (b) Would using the sine series of part (a) to obtain a complete uniform torsion solution be essentially different from using the cosine series solution set forth in Example 12.3 for the same purpose?
- 12.3.** A uniform beam with a solid, square cross-section, as shown in Fig. 12.15 is subjected to a constant torque M_t .
- (a) What is the magnitude and direction of the shearing stress at all four indicated points?
- (b) What is the magnitude of the St. Venant constant for uniform torsion?

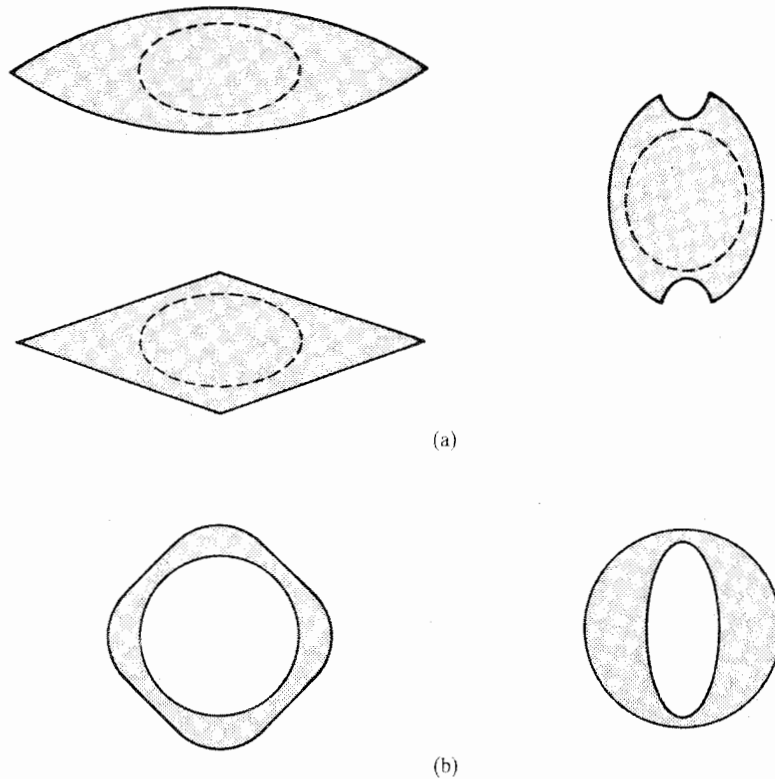


Figure 12.16. Exercise 12.5.

- 12.4.** Verify the integral formulas of (a) Eqs. (12.16) and (b) Eq. (12.17). *Hint:* For part (a), combine the trigonometric identities for $\cos(\alpha + \beta)$ and $\cos(\alpha - \beta)$ to obtain an expression for the product of two cosines as the sum of those two directly integrable cosine terms. Note that it is necessary to consider the cases of $r = m$ or $s = n$ separately.
- 12.5.** (a) If the membrane contour lines have the general shapes indicated by the dashed lines on the solid beam cross-sections shown in Fig. 12.16(a), then indicate the location on the cross-section where the maximum shearing stress due to twisting can be expected to be found.
- (b) Using your own estimate of the membrane contour lines, indicate where the maximum shearing stress due to twisting can be found for the cross-sections of Fig. 12.16(b).
- 12.6.** Using only the membrane analogy for the two rectangular cross-sections of equal areas shown in Fig. 12.17 determine:
- (a) For a given maximum stress, which cross-section could bear the greater torque.
- (b) For a given torque, which cross-section would bear the greater stress.
- 12.7.** (a) Determine whether or not the trial Prandtl stress function

$$\Psi(y, z) = G\theta(y^2 - a^2)(y + z^2 - R^2)$$

is a valid Prandtl stress function for the clipped circular cross-section shown in Fig. 12.18 by first checking the BC, and then checking the GDE.

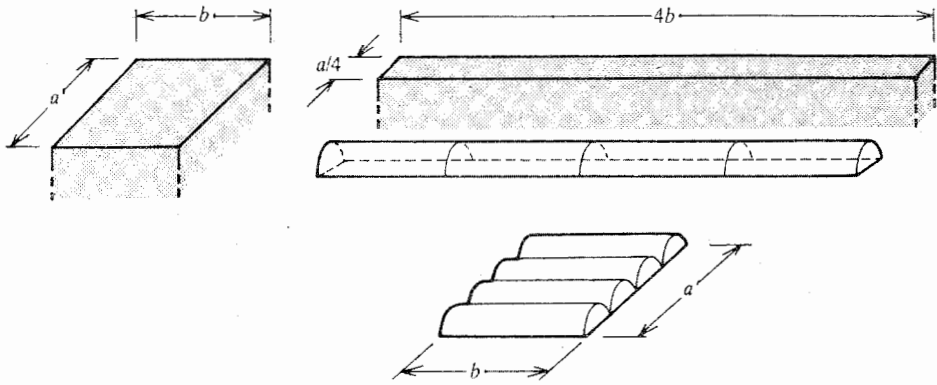


Figure 12.17. Exercise 12.6. Membrane image comparisons.

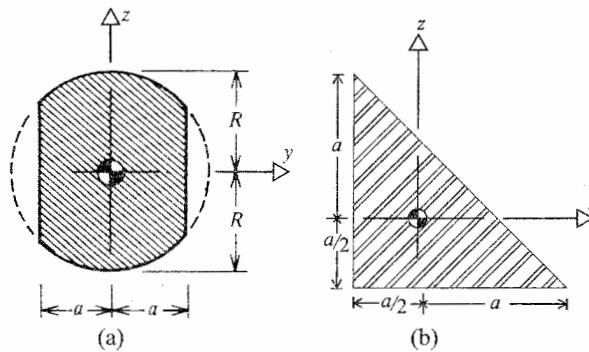


Figure 12.18. Exercise 12.7(a). A solid, clipped circular bar cross-section.

- (b) Given that the ∇^2 operator in polar coordinates has the form

$$\nabla^2 = \frac{\partial^2}{\partial r^2} + \frac{1}{r} \frac{\partial}{\partial r} + \frac{1}{r^2} \frac{\partial^2}{\partial \alpha^2}$$

determine whether or not the candidate Prandtl stress function

$$\Psi(r, \alpha) = G\theta \left[r^2 - \left(\frac{R^4}{r^2} \right) \right] \sin 2\alpha$$

satisfies the uniform torsion BCs and GDE for a solid bar cross-section that is a quarter-circle of radius R that is positioned on the Cartesian axes in the first quadrant.

- (c) Determine whether or not the candidate Prandtl stress function

$$\Psi(y, z) = G\theta [a^2(a + y + z) - 2a(y^2 + z^2) - 4yz(y + z)]$$

satisfies the uniform torsion problem BCs for the right angle, isosceles triangle cross-section shown in Fig. 12.18(b).

- (d) Does the candidate Prandtl stress function of part (c) satisfy the uniform torsion GDE?

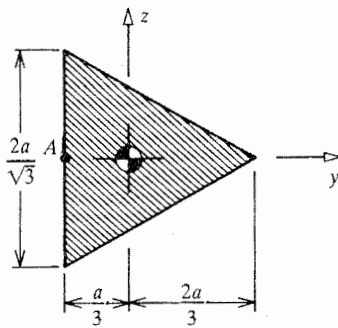


Figure 12.19. Exercise 12.8. A solid, equilateral triangle bar cross-section.

- 12.8. (a) Determine if the trial Prandtl stress function

$$\Psi(y, z) = G\theta \left(\frac{y^3 - 3yz^2}{2a} - \frac{y^2 + z^2}{2} + \frac{2a^2}{27} \right)$$

is a valid Prandtl stress function for the equilateral triangle cross-section shown in Fig. 12.19. That is, check its compliance with both the uniform torsion GDE and the BCs.

- (b) For this same equilateral triangular cross-section, locate the point of maximum shearing stress and calculate its magnitude in terms of the twist per unit length θ .
- (c) Evaluate the double integral that relates the torque to the twist.
- 12.9. The following trial Prandtl stress function, one of many, does satisfy the uniform torsion GDE.

$$\Psi(y, z) = (G\theta/a^2)(y^4 - 6y^2z^2 + z^4) - 1/2G\theta(y^2 + z^2)$$

Using a computer if desired, determine if $\Psi(y, z) = 0$ is a closed curve that can be construed as the outer boundary (or an outer boundary and one or more inner boundaries) of a bar cross-section.

- 12.10. (a) Determine the requirements to be placed upon the constant coefficients of the general third order polynomial function for that polynomial function to be “harmonic.” (Do not bother to investigate possible boundaries for this function by itself or in conjunction with any other function.)
- (b) Verify that the expressions of Eqs. (12.14a, b) are truly harmonic functions.

FOR THE EAGER

- 12.11. The taut string is the one-dimensional analog of the two-dimensional taut membrane. Prove that the increase in the large initial force in the (initially straight) taut string is proportional to the square of the slope of the cable. Note that, just as is the case with the membrane, gravitational effects on the string are being ignored so that when the string lacks a lateral load it is straight. (This exercise is used as a justification for a similar statement in Section 12.4 regarding the taut membrane.)
- 12.12. Why is the membrane deflection equation, Eq. (12.13), valid not only for small displacements, but also for finite lateral displacements limited by the accuracy of the approximation $\sin \theta \approx \theta$?

Endnote (1) A Comment on the Solution for a Circular Shaft with a Keyway

The auxiliary torque equation, in analytical form, for the circular shaft with the circular keyway, is

$$M_t = 2 \int_{\alpha = -\arccos(b/2a)}^{\alpha = +\arccos(b/2a)} \int_{r=b}^{r=2a \cos \alpha} \Psi(r, \alpha) r dr d\alpha$$

where, of course, $\Psi(r, \alpha) = -(G\theta/2)(r^2 - b^2)[1 - (2\alpha/r) \cos \alpha]$. In the above form the final answer includes arccosines. A more convenient approach is to define a new parameter, the limiting angle α_0 where $\cos(\alpha_0) = b/2\alpha$, just as is done in Example 12.4. Carrying out the above integration is generally easier than resorting to a numerical integration scheme. If the value of b is much less than a , the membrane analogy would justify using the J value for the perfect circle, or a large percentage thereof.

Endnote (2) Orthogonality

The focus of this endnote is upon the concept of orthogonality and the series of cosine terms that is used in this text to solve the uniform torsion problem for the rectangular cross-section. The orthogonality of vectors is a simple matter. Two vectors \mathbf{A} and \mathbf{B} are orthogonal (perpendicular) if $\mathbf{A} \cdot \mathbf{B} = \mathbf{B} \cdot \mathbf{A} = 0$. A 1×3 row matrix $\{A\}$ and a 3×1 column matrix $\{B\}$ are similarly orthogonal if $\{A\}\{B\} = \{B\}\{A\} = 0$. When the vectors \mathbf{A} and \mathbf{B} are written in terms of their Cartesian components as $\mathbf{A} = A_x\mathbf{i} + A_y\mathbf{j} + A_z\mathbf{k}$ and $\mathbf{B} = B_x\mathbf{i} + B_y\mathbf{j} + B_z\mathbf{k}$, then it is clear that the vector dot product and the matrix product are exactly the same thing. Hence it is possible to talk about the orthogonality of row and column matrices. This concept of the orthogonality of row and column matrices can be extended to the case where the matrices have n components (elements) rather than just 3, by simply attaching the orthogonality label to any such zero matrix product between a row matrix and a multiplicably compatible column matrix. The vector dot product and the matrix product of a row matrix and a column matrix both produce a scalar result. A scalar is a level of mathematical complexity below that of either the row matrix or the vector. A product between any two similar mathematical entities that yields a less complex result is termed an "inner product."

Consider $f(x)$ and $g(x)$ to be two continuous, bounded functions on the interval $[a, b]$. These two functions can be regarded as being row matrices or vectors with an infinite number of components, that is, having one component for each value of (the index) x . The inner product over the interval $[a, b]$ of these two functions is the definite integral of their ordinary product:

$$\int_a^b f(x) g(x) dx = \int_a^b g(x) f(x) dx$$

Again the order of multiplication is immaterial, and the result is a constant. Thus, when this inner product is zero, the two functions are said to be orthogonal to each other over the interval $[a, b]$. From the integral formulas of Eqs. (12.16), it is clear that the cosine functions, which are symmetrical about the origin, qualify as orthogonal functions over the indicated intervals.

The cosine series used in the solution for the rectangular cross-section is a special form of a (double) Fourier series. Since even the rudiments of Fourier⁸ series theory take several

⁸ Jean-Baptiste-Joseph Fourier (1768–1830), French physicist and mathematician.

pages of discussion, the reader is referred to other texts for an explanation of this powerful tool. All that is mentioned here is that there is an underlying assumption that the Prandtl stress function is twice differentiable over the area of the cross-section. If this is so, and the smoothness of membranes gives such confidence, then Fourier series theory guarantees that the cosine series converges to the correct Prandtl stress function. This type of double cosine series, sometimes called a Navier series, is not the most efficient choice of a successful trial function. Reference [21] presents the results of using a single cosine series in the variable y where the coefficients of the cosine terms are unknown functions of z . Such a series is sometimes called a Lévy series. One consequence of that choice is that the series to be summed to determine the St. Venant constant for uniform torsion is a rapidly converging, single sum rather than the double sum that the double cosine series produces.

Information on the four most common orthogonal polynomial series, those of Legendre, Tschebycheff, Laguerre, and Hermite, can be found in many texts dealing with mathematical analysis, such as Ref. [20].

Endnote (3) A Separation of Variables Approach to Example 12.1

A discussion of the various techniques for solving partial differential equations, and even the various classifications of partial differential equation solutions, must be left to other textbooks. However, there is one technique that is so often useful in solving the partial differential equations that confront engineers that it merits special mention. This technique is called the “separation of variables” technique. In order to explain this technique, consider a single, linear, partial differential equation that is written in terms of the unknown function $F(x, y, z, \dots)$. As its name suggests, the separation of variables technique involves using a trial solution, which is typically

$$F(x, y, z, \dots) = f(x)g(y)h(z) \cdots$$

For quick demonstration of this technique, consider a typical free vibration partial differential equation of the form

$$A \left(\frac{\partial^4 F(x, t)}{\partial x^4} \right) + B \left(\frac{\partial^2 F(x, t)}{\partial t^2} \right) = 0$$

where A and B are positive constants. Writing the solution as $F(x, t) = X(x)T(t)$ and substituting into the above equation yields, where primes indicate derivatives with respect to x , and dots with respect to t ,

$$AX''''(x)T(t) + BX(x)\ddot{T}(t) = 0$$

Rearrange the above equation as

$$\frac{X''''}{X} = -\frac{B}{A} \frac{\ddot{T}}{T}$$

The above left-hand side is solely a function of the independent variable x , while the right-hand side is solely a function of the independent variable t . Thus, for example, the variable t can be run through a range of values on the right-hand side, while the variable x is held constant. In this way it is evident that no matter how t is changed, the left-hand side, and thus also the right-hand side, is a constant. Let that constant be called p^2 . Thus it is possible to write

$$\ddot{T}(t) + \frac{Ap^2}{B} T(t) = 0$$

and

$$X''''(x) - p^2 X(x) = 0$$

Now the one partial differential equation has been reduced to two ordinary differential equations. Thus the independent variables of the original partial differential equation have been successfully separated. As an aside, the constant value p^2 was chosen to ensure a positive constant in these equations dealing with real quantities. A positive constant is chosen in anticipation of desiring a bounded solution for the function $T(t)$; that is, having sines and cosines rather than hyperbolic sines and hyperbolic cosines in the solution expression for $T(t)$.

With the above introduction of the separation of variables technique in place, now consider applying that technique to the Poisson equation and BCs of Example 12.1. Since writing $\Psi(y, z) = Y(y)Z(z)$ does not work in this case, try $\Psi(y, z) = Y(y) + Z(z)$. Substituting into Eq. (12.10a) yields

$$Y''(y) + Z''(z) = -2G\theta$$

The same argument that varies one independent variable while the other is held fixed may be used here to conclude that each of the two left-hand side terms in the above equation are constants. Let $Y''(y) = -2G\theta\Gamma$, where Γ is an unknown constant. Then $Z''(z) = +2G\theta(\Gamma - 1)$. Thus there are again two separate, ordinary differential equations for the functions of the independent variables. Integrating these two equations leads to

$$Y(y) = -G\theta[\Gamma y^2 + C_1]$$

and

$$Z(z) = -G\theta[(1 - \Gamma)z^2 + C_2]$$

Note that the linear terms in y and z have been omitted in recognition of the fact that the solutions must be symmetric about the y and z axes. Thus the Prandtl stress function may be written as

$$\Psi(y, z) = -G\theta \left[a^2\Gamma \left(\frac{y}{a}\right)^2 + b^2(1 - \Gamma) \left(\frac{z}{b}\right)^2 + C_0 \right]$$

where $C_0 = C_1 + C_2$. It is an easy matter to check that this solution does indeed satisfy the GDE. Now that task is to satisfy the BC that

$$\Psi(y, z) = \Psi \left(y, b \left[1 - \left(\frac{y}{a}\right)^2 \right]^{1/2} \right) = 0$$

This goal is achieved by first substituting $z = b[1 - (y/a)^2]^{1/2}$ into the Prandtl stress function solution, and then setting that result equal to zero. Their mutual linear independence (see Section III.3) allows separately setting the resulting y -squared term and the resulting constant term equal to zero. Those two new equations are

$$a^2\Gamma - b^2(1 - \Gamma) = 0 \quad \text{and} \quad b^2(1 - \Gamma) + C_0 = 0$$

When the solutions $\Gamma = b^2/(a^2 + b^2)$, $(1 - \Gamma) = a^2/(a^2 + b^2)$, and $C_0 = a^2b^2/(a^2 + b^2)$ are substituted into the above Prandtl stress function, the result of Example 12.1 is obtained anew.

Beam Torsion Approximate Solutions

13.1 Introduction

This chapter examines the standard engineering approaches to beam twisting used with those types of beam cross-sections that are commonly used in vehicular structures. These analytical approaches are far simpler than the theory of elasticity approach of Chapter 12, which requires the satisfaction of a second order partial differential equation and, in general, the satisfaction of a simple boundary condition on a difficult boundary. The basis of these approaches is the division of engineering beam cross-sections into two categories. The first category is that of thin-walled “open cross-sections” and the second category is that of thin walled “closed cross-sections.” A closed cross-section encloses one or more voids. A thin-walled pipe, or better yet, a thin-walled box beam built up from two oppositely facing channel cross-sections (i.e., C or Z) connected by top and bottom plates so as to produce a rectangular or roughly rectangular interior void, are examples of closed cross-sections. On the other hand, an open cross-section does not have any interior voids. A single channel beam, or an H or I beam are examples of open cross-section beams.

Thin open section beams are generally more efficient than equally strong closed section beams when bending moments and shearing forces are the only significant loadings. That is, in those circumstances, thin open section beams generally weigh less than thin closed section beams. Open cross-section beams also have the advantage that they are easier to connect to other structural components, and inspect for damage. The major disadvantage of open section beams, as is seen below, is that they are very weak in torsion. Hence the torsion analysis for thin open cross-sections is particularly important. On the other hand, closed section beams are relatively very stiff and strong in torsion, while possessing almost equally good bending properties. However, as indicated above, they are generally more costly to manufacture, connect, and inspect. Since their excellent torsional strength and stiffness properties are often vital to a vehicular component design, an accurate torsion analysis of closed section beams is also of great importance. For example, high aspect ratio wings are generally built around a “box beam” of skin and spars, which is a closed cross-section with a roughly rectangular void.

Aircraft wings are examples of vehicular components for which torsional stiffness can be particularly important. Anyone who has stuck his or her flattened hand out of an automobile window into a speed-limit wind stream, and rotated the hand up or down, has experienced the lift forces on the flattened hand that tend to both twist and bend one’s arm up or down. The same twisting effect occurs with wings, and this effect is briefly described at the point of static instability in Exercise 11.16. Of course, the inherent torsional stiffness of the wing is the major means of resisting this rotational static instability phenomenon called wing “divergence.” The reason almost all high-speed metal wings are swept back rather than swept forward is to lessen the possibility of wing divergence. The reduction of the divergence threat by rearward sweep does not do away with the need for torsional stiffness. A lack of torsional stiffness would also promote the possibilities of control surface reversal phenomena and the dynamic instability called airfoil flutter. Both of these phenomena are

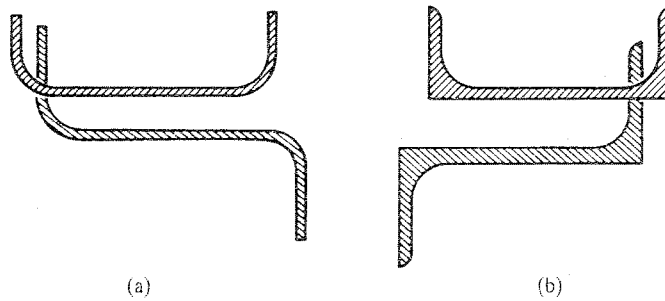


Figure 13.1. Contrasting thin, open beam cross-sections: (a) bent sheet metal channel and Z cross-sections; (b) extruded or rolled channel and Z cross-sections.

also strongly influenced by the torsional stiffness of the wing. Wing flutter is a wind stream-induced vibration that can be unstable; that is, the wing deflections can grow with time. When the deflections grow larger, so too do the strains and stresses. Failure can be very rapid with bad effects on aircrew and passenger morale. These aeroelastic phenomena, which are also possible in hydrofoils, are discussed in Refs. [28, 29] and in Chapter 23.

13.2 Open Cross-Section Beam Torsion

There are basically two different types of thin, open cross-section beams used in vehicular structures. The first type is manufactured by bending long pieces of sheet metal, usually aluminum. In this case the cross-section is essentially a bent rectangle where the bends have ample radii of curvature. Figure 13.1(a) illustrates a channel section and a Z-section bent from sheet metal. The second type of open cross-section is usually manufactured by either a (steel) rolling or an (aluminum) extrusion process. These rolled and extruded cross-sections differ from the first type in that the thickness of the cross-section always varies greatly at the junctions of the flanges and web. In this case, it is also possible that the flange thickness varies along the length of the flange, and, even if it is mostly constant, the flange thickness may be different from the web thickness; see Fig. 13.1(b). The open cross-section discussion begins with the constant thickness, bent sheet metal cross-section.

Figure 13.2(a) shows the Prandtl stress function or membrane surface for a high aspect ratio rectangular cross-section. The mathematical description of that membrane surface is the infinite double sum of Eq. (12.18). Note that except near the left and right ends of the cross-section, the membrane cross-section is very much the same over the length of the rectangle. Figure 13.2(b) shows an approximation to the actual membrane surface. In the approximation, the same membrane cross-section is used over the entire rectangle. It is advantageous to think of the approximate membrane surface as the central portion of the actual membrane surface of a rectangular cross-section where the short edges are an infinite distance apart. Clearly, with respect to calculating the maximum value of the stress at the center of the long side, this approximate membrane is virtually the same as the actual membrane. There is a small difference in the two volumes under the membranes as a result of the actual boundary condition (BC) of zero membrane elevation at the left and right edges of the finite rectangle. At large aspect ratios, this small volume difference can be offset, if desired, by simply reducing the long edge length by a couple of thicknesses at each end. Thus, in every important way, the approximate membrane that has a constant membrane cross-section in the y direction, call it $u(z)$ or $\Psi(z)$, is a very close approximation to the actual membrane, $u(y, z)$ or $\Psi(y, z)$.

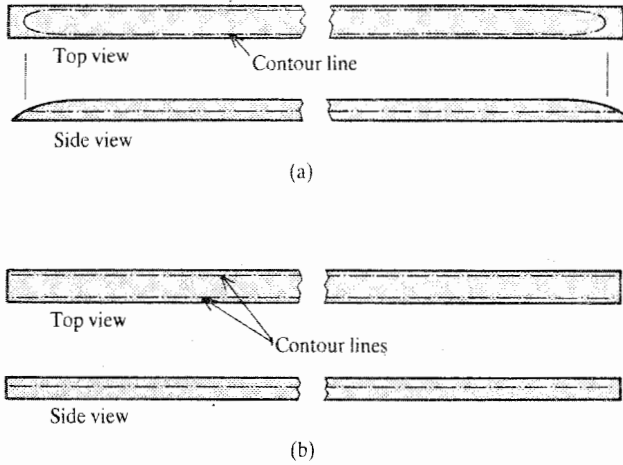


Figure 13.2. Membrane images for long, thin rectangular bar cross-sections: (a) actual membrane; (b) approximate membrane.

A mathematical description for $\Psi(z)$ is easily obtained from Eq. (12.10). In the case of an infinitely long rectangular cross-section, there is no variation of the Prandtl stress function in the y coordinate direction. Therefore, that governing differential equation (GDE) reduces from a partial differential equation to simply

$$\frac{d^2\Psi(z)}{dz^2} = -2G\theta$$

with the only BCs being $\Psi(z) = 0$ at $z = \pm b/2$. Direct integration and use of the two BCs yields

$$\Psi(z) = -G\theta \left[z^2 - \left(\frac{b}{2} \right)^2 \right] \quad (13.1)$$

Thus it is clear that the approximate membrane cross-section, or, what is the same thing, the actual membrane cross-section for a rectangle of infinite aspect ratio, is a parabola. St. Venant's constant for uniform torsion can be determined by use of eqs. (12.9) and (12.11), as usual. The result is easily obtained as

$$J = \frac{1}{3}ab^3 \quad (13.2)$$

where the factor of $\frac{1}{3}$ is, of course, the same as that given by Fig. 12.12 for an infinite aspect ratio. Replacing $G\theta$ by M_t/J , the maximum stress value is

$$(\sigma_{xs})_{max} = \frac{M_t b}{J} \quad (13.3)$$

Now consider the effect on the membrane image of bending the rectangle that is the sheet metal cross-section into the channel or Z shape of Fig. 13.1(a). If the radii of the bends are generous, as they should be, then the effect of the bends upon the membrane is minimal. In that case, all the above equations for the rectangular cross-section still apply. Of course the dimensions a and b of the bent cross-sections that are to be used in those equations are the length and thickness of the thin rectangle before it is bent.

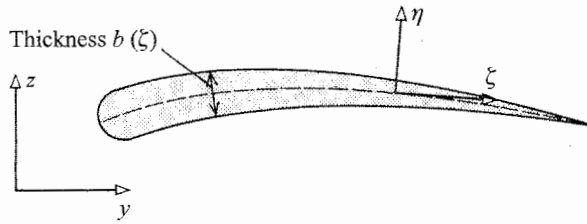


Figure 13.3. A thin, open cross-section with a variable thickness.

The above approximate approach can be extended to thin open cross-sections where the thickness varies along the centerline length a of the thin cross-section. Important examples of such thin cross-sections are those of propeller and turbine blades as shown in Fig. 13.3. Note that, since this new approximation is an extrapolation from the above theory for the infinite rectangle, there is still the requirement that $a \gg b$, or at least $a^2 \gg b^2$.¹ The extension of the infinite rectangle theory to a cross-section with a nonconstant thickness is made by assuming that the membrane cross-section in the thickness direction, at any point along the length of the cross-section centerline, is the same sort of inverted parabola that is used in the approximation for a rectangle of constant thickness. The justification for this assumption as an acceptable approximation rests on two observations. The first and more important observation is simply that the membrane experiments roughly support this approach. The second observation is closer to the reader's experience. It is that the parabolic cross-section is the exact solution for some of the rather disparate beam cross-sections for which exact solutions are known. In addition to the infinite rectangle, the parabola is the membrane cross-section for the ellipse, and even the equilateral triangle in the z direction, which, unlike the y direction, can be taken as a thickness direction for a straight centerline (the y axis).

The mathematical statement of this assumption is accomplished by: (i) setting up a right-handed, orthogonal coordinate system as shown in Fig. 13.3, where ζ is everywhere tangent to the centerline of the cross-section and thus η is everywhere in the thickness direction; and (ii) modifying Eq. (13.1) to allow the thickness b to vary with the ζ coordinate. Then the approximate Prandtl stress function is

$$\Psi(\zeta) = -G\theta \left[\eta^2 - \frac{1}{4}b^2(\zeta) \right] \quad (13.4)$$

The integration of this Prandtl stress function as per Eq. (12.9) and the use of Eq. (12.11) determines the approximate St. Venant constant for uniform torsion. From Eq. (12.9),

$$M_t = -2G\theta \int_{\zeta=0}^{\zeta=a} \left[\int_{\eta=-b(\zeta)/2}^{\eta=+b(\zeta)/2} \left[\eta^2 - \frac{1}{4}b^2(\zeta) \right] d\eta \right] d\zeta$$

or

$$M_t = \frac{1}{3}G\theta \int_{\zeta=0}^{\zeta=a} b^3(\zeta) d\zeta$$

where the additional approximation is made that the centerline of the thin open cross-section is close to being straight. If the centerline has significant curvature, it is then necessary to introduce into the above integrand the Jacobian of the fixed Cartesian coordinates y and z

¹ For example, this approximation scheme would not work at all well for a square cross-section viewed as a diamond shape. The error would be nearly 120 percent.

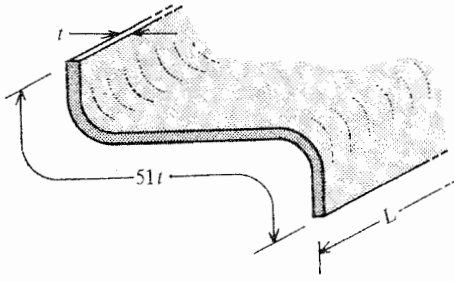


Figure 13.4. Example 13.1. A bent sheet metal Z-shaped bar cross-section.

with respect to the ζ , η coordinates, or the equivalent relation between differential areas in terms of the two coordinate systems. Then, without the Jacobian,

$$J = \frac{1}{3} \int_0^a b^3(\zeta) d\zeta \quad (13.5)$$

The membrane image clearly indicates that the maximum shearing stress occurs at the cross-section boundary. The derivative of the Prandtl stress function with respect to η , the coordinate perpendicular to the centerline, shows that the shearing stress in the ζ direction is a maximum where η is greatest, that is, at the point of maximum thickness. Even though the η coordinate is not everywhere perpendicular to the boundary, the η coordinate is often the normal coordinate at the point of maximum thickness when the boundary is a smooth curve. *In those cases*, it is proper to write

$$(\sigma_{xs})_{max} = \frac{M_t b_{max}}{J} \quad (13.6)$$

Again, the more accurate and flexible alternative to this approximation technique, at the expense of greater effort, is a numerical solution to the theory of elasticity torsion equations (Ref. [4]).

Example 13.1. A piece of sheet metal of dimensions $L \times 51t \times t$, is bent into a Z-section beam of length L as shown in Fig. 13.4. If this beam is loaded without warping constraint by a uniform torque of magnitude M_t , what then is the total twist ϕ , and what is the maximum stress on the cross-section assuming that the radii of curvature of the bends are an order of magnitude greater than the thickness t ?

Solution. The solution plan is, in turn, to calculate (i) J ; (ii) the maximal stress; (iii) the twist per unit length; and finally, (iv) the total twist. St. Venant's constant for uniform torsion and the maximum stress are obtained from Eqs. (13.2) and (13.3), respectively.

$$J = \frac{1}{3} ab^3 = \frac{1}{3} (51t)t^3 = 17t^4$$

$$(\sigma_s)_{max} = \frac{M_t b}{J} = \frac{M_t}{17t^3}$$

The twist per unit length is determined from the general formula $\theta = M_t/GJ$, and the total twist, ϕ , is simply the twist per unit length multiplied by the length, $L\theta$. Thus

$$\theta = \frac{M_t}{17Gt^4} \quad \phi = \frac{M_t L}{17Gt^4}$$

■

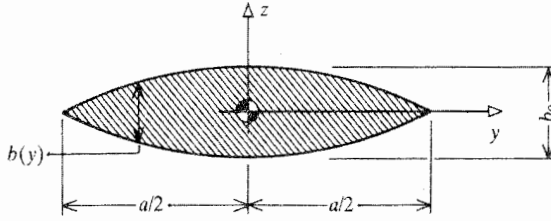


Figure 13.5. Example 13.2. A thin airfoil bar cross-section.

Example 13.2. Determine the approximate torsional constant J and the approximate maximum stress magnitude for a thin, solid cross-section whose two boundaries, as shown in Fig. 13.5, consist of two parabolas so that the cross-section thickness is described by the formula

$$b(y) = b_0 \left[1 - \left(\frac{2y}{a} \right)^2 \right]$$

The cross-section is without warping constraint, and it is subjected to a uniform torque of magnitude M_t .

Solution. Note that the coordinate system used to describe the cross-sectional thickness is not the same as the coordinate system used in the derivation for the St. Venant constant for this type of cross-section. Hence it is necessary to adjust the limits of integration in Eq. (13.5), the centerline integral of the cube of the thickness. In this case

$$\begin{aligned} J &= \frac{1}{3} \int_{y=-a/2}^{y=+a/2} b^3(y) dy \\ &= \frac{b_0^3}{3} \int_{-a/2}^{+a/2} \left[1 - 12 \left(\frac{y}{a} \right)^2 + 48 \left(\frac{y}{a} \right)^4 - 64 \left(\frac{y}{a} \right)^6 \right] dy \\ &= \frac{b_0^3}{3} \left(a - a + \frac{3a}{5} - \frac{a}{7} \right) \\ &= \frac{16ab_0^3}{105} \end{aligned}$$

Equation (13.6) is the formula to be used to calculate the maximum stress:

$$(\sigma_s)_{\max} = \frac{M_t b_{\max}}{J} = \frac{105M_t}{16ab_0^2}$$

The exercises at the end of the chapter provide further practice with these equations. ■

Example 13.3. Reference [41] provides the following data for the thickness $b(x)$ of an NACA 0008-34 airfoil of chord length c in terms of distance along the chord length x :

x	$0.05c$	$0.1c$	$0.2c$	$0.3c$	$0.4c$	$0.5c$	$0.6c$	$0.7c$	$0.8c$	$0.9c$
$50b/c$	1.66	2.44	3.40	3.87	4.00	3.88	3.55	2.99	2.21	1.24

The centerline of this symmetric airfoil cross-section is a straight line, and, of course, the thickness of the airfoil is zero at the leading edge ($x=0$) and the trailing edge ($x=c$). Calculate J , the uniform torsion constant, for a solid NACA 0008-34 cross-section of arbitrary chord length c . Then compute J when $c = 5$ inches.

Solution. Since there is no analytical expression for the thickness distribution readily at hand, the simplest approach is to carry out the integration of Eq. (13.5) numerically. The simplest numerical procedure is the trapezoidal rule, but a better answer would be obtained using Simpson's rule² over most parts of the airfoil cross-section, that is, the leading edge section, and the central section up to $0.9c$. Recall that Simpson's rule requires an even number of intervals n , (i.e., $n + 1$ subdivision points), and can be stated in general form as

$$\int_a^b F(x) dx = \frac{\Delta x}{3} [F_0 + 4F_1 + 2F_2 + 4F_3 + 2F_4 + \cdots + 4F_{n-1} + F_n]$$

In the first application of Simpson's rule at the leading edge where the thickness is changing rapidly, use $\Delta x = 0.05c$ and only two intervals. Call this first contribution to the total uniform torsion constant J_1 . In any part of the calculation for the total J , a convenient way of dealing with the cube of the thickness (the F in the above general formula) is, for example, to write $b(0.1c) = 2(1.66/100)c$. Therefore, $b^3(0.1c) = (8)(0.0166c)^3$, and thus

$$\begin{aligned} J_1 &= \frac{1}{3}(0.05c/3)(8)[(1)(0.0) + (4)(0.0166c)^3 + (1)(0.0244c)^3] \\ &= 1.46c^4 \times 10^{-6} \end{aligned}$$

In the second application, use $\Delta x = 0.1c$ and the eight intervals between $0.1c$ and $0.9c$:

$$\begin{aligned} J_2 &= \frac{8}{3}(0.1c/3)[(1)(0.0244c)^3 + (4)(0.0340c)^3 + (2)(0.0387c)^3 \\ &\quad + \cdots + (1)(0.0124c)^3] \\ &= 8.339c^4 \times 10^{-5} \end{aligned}$$

Use the trapezoidal rule with a single interval to cover the last interval between $0.9c$ and $1.0c$. The result is $J_3 = 2.54c^4 \times 10^{-7}$. Completing the above plan leads to $J = J_1 + J_2 + J_3 = 8.510c^4 \times 10^{-5} \rightarrow 8.5c^4 \times 10^{-5}$ where at most two significant figures is appropriate to the given data. If $c = 5$ inches, as it might for the solid cross-section of a remotely piloted model airplane, then $J = 0.053 \text{ in}^4$. ■

Rolled and extruded cross-sections, like all H, I, and T sections, are different from cross-sections made from bent sheet metal primarily because of the presence of fillets (the circular arc portions of the boundary curves between the straight line boundaries of the webs and flanges). As illustrated in Fig. 12.8, even small fillets result in large bulges in the membrane next to the fillets. These bulges mean significant additional torque carrying capacity for that single beam. On the other hand, the bulges also increase membrane slopes and thereby promote the possibility that the maximum torsional shearing stress occurs at the fillet rather than at the center of a web or flange. An empirical formula developed by Trefftz (Ref. [30]) in 1922 for the maximum stress at a fillet, σ_f , states that

$$\sigma_f = 1.74\sigma_{max} \left(\frac{t}{R} \right)^{1/3} \quad \text{where} \quad \sigma_{max} = \frac{M_t t_{max}}{J}$$

where t_{max} is the larger of the two adjacent thicknesses, and R is the radius of the fillet. Another estimate for this same maximum fillet stress can be found, for example, in Ref. [3].

A semiempirical method developed by Trayer and March (Ref. [31,32]) can be used to estimate the individual torsion constants for rolled and extruded cross-sections. This method is outlined in Endnote (1). In the case where the rolled or extruded beam is part of a

² Thomas Simpson (1710–1761), English mathematician.

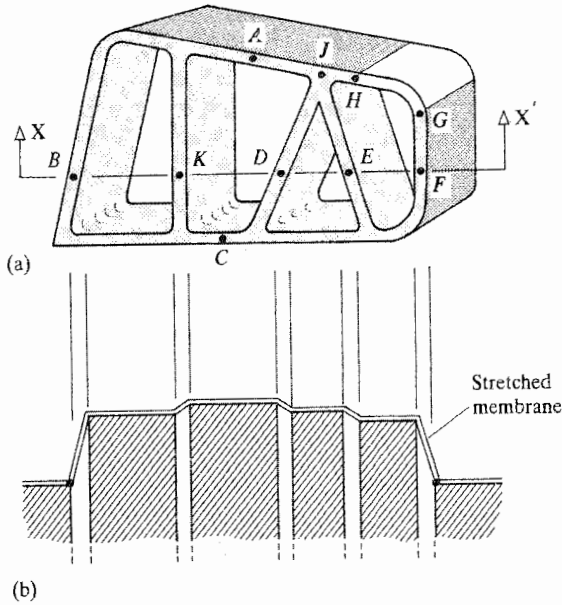


Figure 13.6. A multiply connected, closed beam cross-section: (a) typical geometry with identifying points; (b) membrane image at section $X-X'$.

large structure where the torsional stiffness of the structure as a whole involves the bending as well as twisting of beams, the extra effort of the Endnote (1) recipe would probably not be cost-effective. Generally, the use of one-third the sum of the centerline lengths multiplied by their respective thicknesses raised to the third power would be a satisfactory estimate.

13.3 Closed Section Beam Torsion

Figure 13.6(a) is an isometric view of a representative thin-walled, closed cross-section. In Fig. 13.6(b) section $X-X'$ shows a side view of the membrane or Prandtl stress function surface for this cross-section. Recall that the membrane analogy for multiply connected cross-sections requires that the membrane elevation over the inner voids correspond to the Prandtl stress function BC of Eq. (12.8) for the inner boundaries. This means that the membrane must form a plateau above the plane of the outer boundary over each inner void. All other features of the membrane analogy for a multiply connected cross-section are the same as that for a singly connected cross-section. In particular: (i) the torque is equal to twice the volume between the membrane surface and the plane of the outer boundary, including the volume above the voids; and (ii) the total shearing stress vector is directed along the membrane contour lines with a magnitude equal to the slope normal to the contour lines. (Note that over the areas of the plateaus above the voids, the membrane slope, and thus the cross-section shearing stress, is zero, as it should be.) The membrane image of Fig. 13.6 shows that unlike the open cross-section, the stress vectors in any thin wall of the closed cross-section all act in the same direction. Figure 13.7 further illustrates this membrane analogy conclusion. Furthermore, it is clear from the membrane sketch of Fig. 13.6 that the magnitudes of the shearing stresses have an average value at the center of the thin wall. The departure from that average value of the magnitudes of the shearing stresses at

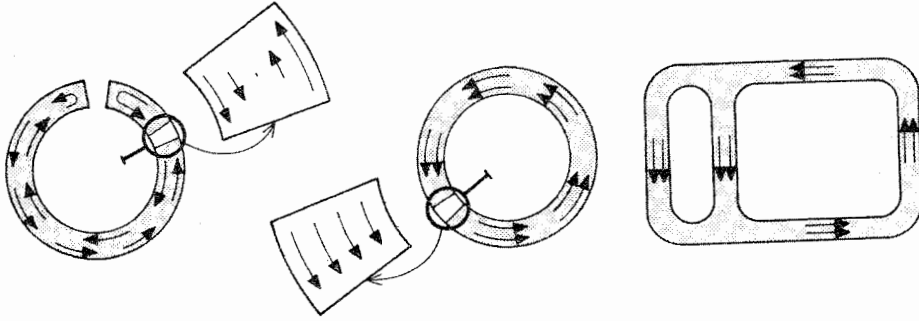


Figure 13.7. A magnifying glass comparison of the shearing stress distribution across the skin thickness of typical open and closed cross-sections.

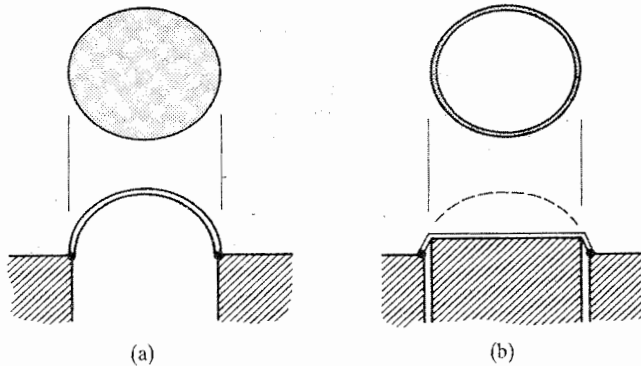


Figure 13.8. The near linearity of a membrane over a thin wall thickness even when the membrane curvatures are much exaggerated.

other points across the thickness of the thin wall is the subject of the following argument based on membrane images.

If the thin walled structure is momentarily viewed as a solid cross-section with its membrane covering the area defined by the outer boundary, as in Fig. 13.8(a), and then is viewed as the same cross-section with its original center cut out to form the thin walled cross-section, as shown in Fig. 13.8(b), then it should be clear that the shape of the thin-walled membrane outside the plateau does not differ much from that of the lower portion of the solid cross-section membrane. Since it is evident from the membrane image that the slopes of the lower portion of the membrane for the solid cross-section vary little through the thickness of the thin wall, it is concluded that the average stress along the centerline of the thin wall closely represents all stresses throughout the thickness of the thin wall. This argument is supported by the results of Example 12.4.

The differences in stress magnitude across the thin wall thickness are sufficiently small that they are easily and customarily ignored by introducing a quantity called the *shear flow*. The shear flow is defined as being equal to the product of the shear stress at the thin wall centerline and the thin wall thickness t . The shear flow is symbolized as q . Thus,

$$q = \sigma_{xs}t \quad (13.7)$$

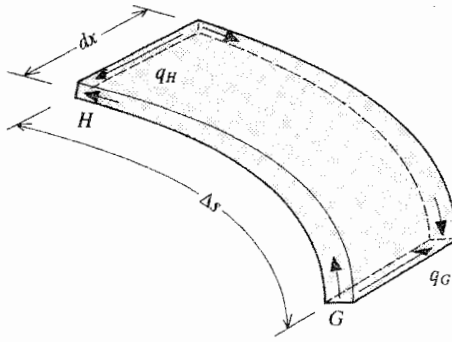


Figure 13.9. A thin-walled segment free body diagram from the closed cross-section of Fig. 13.6 where the length Δs is exaggerated and the thin wall thickness varies from point G to point H .

The reason for the selection of the name “shear flow” for this quantity is made clear later. The units of shear flow are force per unit of length along the thin wall centerline. The reason for the use of this quantity is that the torsional shear flow has the important characteristic for a closed cross-section that it is constant over any wall segment between centerline junctures.³ To prove this and related statements, first consider a FBD of the segment of the closed beam cross-section of Fig. 13.6 lying between points G and H . Again, a series of arc length coordinates s is used to locate positions along the thin wall centerlines. As redrawn in Fig. 13.9, let the finite distance between the two selected points be Δs , and let the x direction length of the uniform beam FBD be dx . For the sake of generality, let the wall thickness vary with the arc length coordinate. The head-to-head and toe-to-toe feature of the shearing stresses makes it evident that summing forces in the y and z directions leads to the forces on the back face canceling the forces on the front face, and thus to the identity that zero equals zero. However, summing forces in the x direction, after canceling dx from both terms, yields

$$q_G = q_H$$

which means that the shear flow in either an inner or outer wall segment is a constant between wall junctions. Now create another FBD of depth dx by cutting the closed cross-section of Fig. 13.6 at points A and C as shown in Fig. 13.10. After canceling the common factor dx , the sum of the external forces in the x direction yields

$$q_A = q_C$$

These results are in agreement with the membrane analogy. Refer to Fig. 13.11, which is for the same A to C section. From the definition of slope being the rise divided by the run, it is clear that the product of the shearing stress (the slope) and the thickness (the run) equals the shear flow (the rise). Thus, for this closed, thin cross-section, the shear flow is equal to the constant plateau height Ψ_i . This, incidentally, is one, limited, interpretation of the quantities Ψ_i . A similar conclusion using the membrane analogy can be drawn for the shear flow acting upon an inner wall, but again the result is the same as that from an equilibrium

³ The conclusions regarding the distribution at the unknown shear flows around the cross-sectional voids, which are to be drawn from FBDs and the writing of equilibrium equations, can be obtained more quickly and much more elegantly simply using the membrane analogy. The equilibrium approach is presented as a means of further validating this use of the membrane analogy.

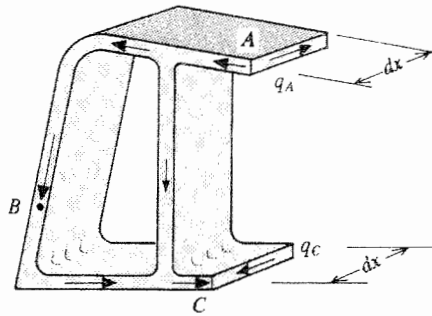


Figure 13.10. A free body diagram of another portion of the thin, multiply connected cross-section of Fig. 13.6. Again dx is greatly exaggerated.

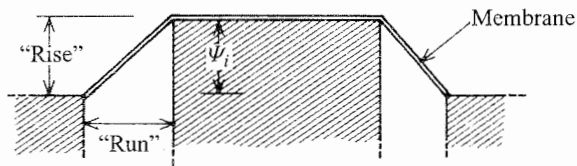


Figure 13.11. The membrane image of Fig. 13.6 along the unmarked line AC for the purpose of discovering the relationship between the shear flow and the value of the Prandtl stress function at interior boundaries of thin, closed cross-sections.

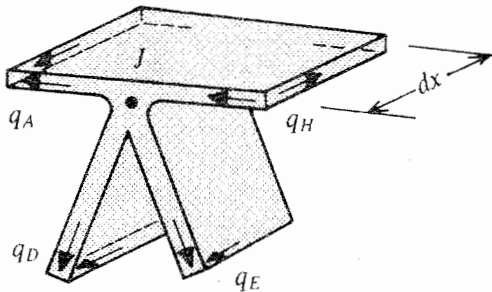


Figure 13.12. Free body diagram of the juncture at point J of the cross-section of Fig. 13.6.

argument. Consider wall junction J as redrawn in the FBD in Fig. 13.12. Summing forces in the x direction yields

$$q_H = q_A + q_D + q_E$$

Similarly,

$$q_A = q_B + q_K$$

These equations can be interpreted as saying that the shear flow into any junction is equal to the shear flow out of the junction. This observation coupled with the constancy of the shear flow between junctions makes it obvious that the shear flow has the same characteristics as those of an incompressible, inviscid fluid circulating endlessly in channels defined by the wall edges. Hence the name “shear flow.”

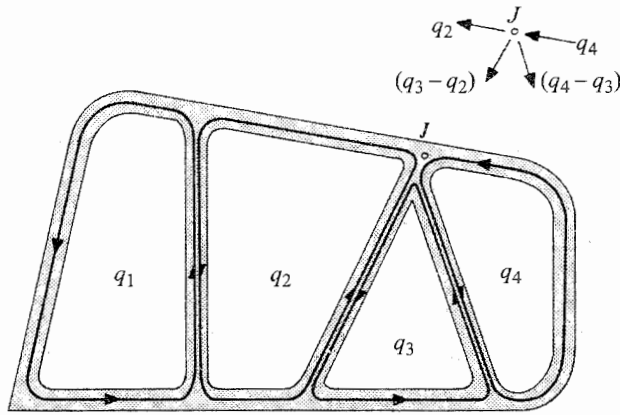


Figure 13.13. The efficient way of representing the shear flows acting upon a thin, multiply connected cross-section.

All three sets of equilibrium results can be concisely organized if the above cumbersome alphabetic shear flow notation is now replaced by that of Fig. 13.13, where a separate shear flow makes a complete loop around each internal void, or “cell.” For example, the shear flow in the internal web containing the point K is $(q_1 - q_2)$, upwardly directed, or $(q_2 - q_1)$ downwardly directed. Notice that this notation, without adding any other features, fully accommodates the shear flow constancy properly between junctions and at the opposite outer sides of voids, and correctly describes the “shear flow in equals the shear flow out” junction requirement. Since this arrangement of the numerical subscripted shear flows fully satisfies all previously derived shear flow equilibrium equations, and since those shear flows are still unknown, the task ahead is to find sufficient equations to determine the values of these unknown shear flows around each cell.

Consider an arbitrary segment of a typical, single shear flow loop as sketched in Fig. 13.14(a). In order to obtain the beam stress resultants associated with this shear flow, consider only the shear flows on the cross-section nearest the viewer. From Fig. 13.14(a), the total shearing force acting on a length ds along the centerline of the loop is $q ds$. Its vertical component is $(q ds) \sin \beta$, which can also be written as $(q ds)(dz/ds) = q dz$. Thus the sum of the differential forces in the z direction on the front face between points L and N is

$$\hat{V}_z = \int_L^N q dz = q \int_L^N dz = q \Delta z$$

When the integration is over the entire loop, that is, when N reaches L , then Δz , and hence \hat{V}_z , is zero. By a similar argument, the beam shearing force component in the y direction resulting from one or more of these shear flow loops is also seen to be zero. It is worth repeating that there are no shear forces arising from complete shear flow loops.

Now consider the moment stress resultant about an arbitrary moment center that is produced by the shear flow of that same loop segment. The moment produced by the shearing force $q ds$ is equal to that force magnitude multiplied by the perpendicular distance between the line of action of the force and the arbitrary moment center, r . That is,

$$\hat{M}_t = \int_L^N q r(s) ds = q \int_L^N r(s) ds$$

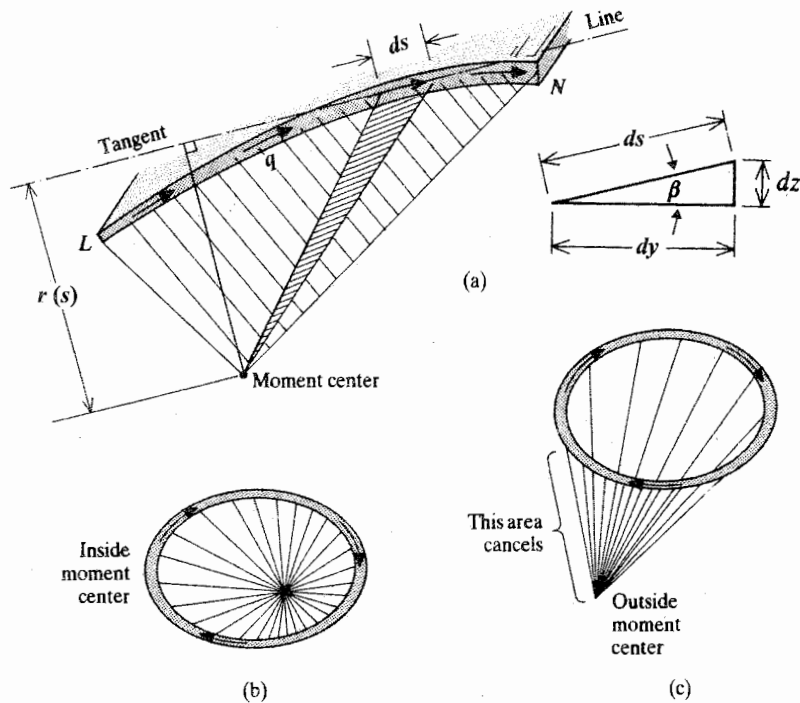


Figure 13.14. Calculating the shearing forces and twisting moments that result from the constant shear flow of a thin, single-cell cross-section.

The last line integral has a simple geometric interpretation. Since $r(s)$ is the height of the heavily hatched triangle in Fig. 13.14(a), and ds is its base length, the quantity $r(s) ds$ is twice the area of the heavily hatched triangle. Thus the total line integral is just the sum of all such triangles between L and N , which is twice the shaded area. If the arbitrary moment center is within the complete loop, as shown in Fig. 13.14(b), the line integral is twice the area enclosed by the loop centerline. The same result holds if the arbitrarily located moment center lies outside the complete loop of the centerline. In this case, it is necessary to carefully consider the direction of the moment contributed by each centerline segment, because some segments give rise to a counterclockwise moment while other segments give rise to a clockwise moment about the arbitrary moment center. When that fact is taken into account, it becomes clear that the total area outside the loop and between the tangents to the loop from the moment center is counted once for a clockwise moment and once for a counterclockwise moment, and hence cancels, leaving only the area within the closed centerline loop; see Fig. 13.14(c). In order to distinguish (i) the area enclosed within a centerline loop from (ii) the area of the beam cross-section material, the symbol \hat{A}_i is used for the area enclosed within the i th loop. Do not confuse these two very different beam areas. Then, for a beam with a single cell, $(2\hat{A})q = M_t$, or

$$q = \frac{M_t}{2\hat{A}} \quad (13.8a)$$

and, because the counterclockwise moments for each loop of a beam with more than one cell add together to form a total moment,

$$M_t = 2 \sum q_i \hat{A}_i \quad (13.8b)$$

The approximate solution of Eq. (13.8a) provides a good estimate of the exact centerline shearing stress value for a thin, circular cross-section. If R is the centerline radius of the thin annular cross-section, and t its thickness, then the difference between the approximate and exact solutions is the difference between R^2 and $R^2 + \frac{1}{4}t^2$. The difference between centerline stress and the corresponding maximum stress is the difference between b and $(\frac{1}{2})(b + a)$, which as discussed is negligibly small for a thin cross-section. Also see Exercise 13.3(e, f).

Equation (13.8a) is all that is necessary to determine the shear flow, and hence the uniform torsion shearing stress, in a single-cell beam of any cross-sectional shape. Furthermore, since Eqs. (13.8) are equilibrium equations, they are valid for any type of material. In the case of a beam with N cells, the equilibrium equation that is Eq. (13.8b) is inadequate by itself to determine the N shear flows. The problem is statically indeterminate. An additional $(N - 1)$ deflection equations, involving the twists per unit length of each cell, are required. From Section 5 of Appendix A, the twist per unit length for the i th cell is

$$\theta_i = \frac{1}{2G_0\hat{A}_i} \oint_{\partial C_i} \frac{q}{t^*} ds \quad (13.9)$$

where

$$t^*(s) = \frac{G}{G_0} t(s)$$

and s is the arc length coordinate running counterclockwise around the centerline of the wall surrounding the i th cell, $t = t(s)$ is the thin wall thickness, and G_0 is the arbitrary reference shear modulus that plays a role similar to that played by E_0 in bending theory. When the closed cross-section is sufficiently compact or sufficiently supported by x plane bulkheads (or "ribs" in the case of glider or other very high-aspect-ratio aircraft wings), so that the thin-walled cross-section retains its original shape as it twists, then the additional $(N - 1)$ equations are

$$\theta_1 = \theta_2 = \theta_3 = \dots = \theta_N \quad (13.10)$$

The example problems that follow illustrate the use of these uniform torsion equations. Before proceeding to the example problems, it is well to summarize the various results in one place. The equations to be solved for a single-cell, closed cross-section beam subjected to uniform torsion without warping constraint, are

single cell	
$\sigma_{xs}(s) = \frac{M_t}{2\hat{A}t(s)}$ $\theta = \frac{M_t}{4(\hat{A})^2 G_0} \oint \frac{1}{t^*} ds$ $J^* = \frac{4\hat{A}^2}{\oint \frac{1}{t^*} ds}$	(13.11)

and from $M_t = G_0 J^* \theta$,

The equations to be solved for the multicell closed cross-section in terms of the N shear flows are Eqs. (13.8b) and (13.10), using Eq. (13.9) to provide the details of Eq. (13.10). This set of equations is called *Bredt's equations* (Ref. [16]) or the Bredt–Batho equations (Ref. [65]).

Example 13.4. A lengthwise-slit annular tube and a closed annular tube have the same mean diameter D (from center of thickness to center of thickness) and same tube thickness t , where $D = 16t$. If both tubes are subjected to the same torque, what then is the ratio of the angles of twist per unit length, and the ratio of the approximate maximum cross-sectional stresses?

Solution. For both the slit (open), and the closed, thin circular cross-section, and all other cross-sections, $\theta = M_t/GJ$. Thus

$$\frac{\theta_s}{\theta_c} = \frac{J_c}{J_s}$$

where

$$J_s = \frac{ab^3}{3} = \frac{\pi Dt^3}{3}$$

and

$$J_c = \frac{4(\hat{A})^2}{\oint (1/t) ds} = 4 \frac{(\pi D^2/4)^2}{\pi D/t} = \frac{\pi D^3 t}{4}$$

where the thickness has a constant value, and hence can be factored out of the line integral. That step leaves only the line integral of the differential arc length, which, since it is just the sum of all the differential pieces of arc length, is always the total length of the path of integration. Therefore,

$$\frac{\theta_s}{\theta_c} = \frac{3D^2}{4t^2} = 192$$

The maximum stress in the slit tube is $M_t t/J$, while that for the closed tube is $M_t/(2t\hat{A})$. Thus

$$\begin{aligned} \frac{\sigma_s}{\sigma_c} &= \frac{2t\hat{A}}{J_s/t} = \frac{2(\pi D^2/4)t^2}{\pi Dt^3/3} \\ &= \frac{3D}{2t} = 24 \end{aligned}$$

The closed tube is clearly much stiffer and stronger than the slit or open tube. Short lengths of open, thin cross-sections are unavoidable whenever it is necessary to have access to the interior of a tubular structure, such as a submarine hull, or aircraft fuselage. Otherwise, vehicular structures are generally closed containers because twisting loads on vehicular structures are commonplace.

Example 13.5. The doubly symmetric nonhomogeneous box beam idealized in Fig. 13.15 has titanium top and bottom plates ($G = 6.2 \times 10^6$ psi), and aluminum channels ($G = 3.9 \times 10^6$ psi). The uniform box beam is without warping constraint, and it is subjected to a

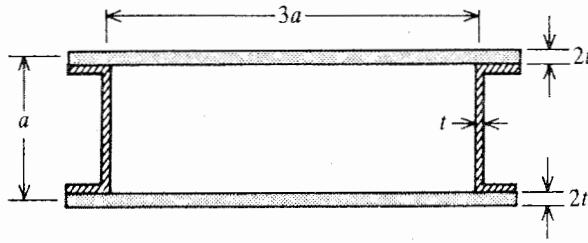


Figure 13.15. Example 13.5. An idealized thin box beam cross-section.

torque of magnitude M_t . Calculate: (a) the torsion shearing stress in the top and bottom plates, and in the web of the channels; (b) the modulus weighted St. Venant constant for uniform torsion; and (c) the twist per unit length.

Solution. (a) Since this is a single-cell beam cross-section, Eqs. (13.11) are applicable thus, with a_l designating aluminum, and t_i for titanium

$$\hat{A} = 3a^2 \quad \sigma_{al} = \frac{M_t}{6a^2t} \quad \sigma_{ti} = \frac{M_t}{12a^2t}$$

(b)

$$J^* = \frac{4(\hat{A})^2}{\oint \frac{1}{t^*} ds} \quad \text{where} \quad t^* = \frac{G}{G_0}t$$

Begin the J^* calculation by choosing G_0 to be the modulus of rigidity for aluminum. Arbitrarily choose to begin the line integral of the inverse of the local m.w. thickness around the perimeter of the rectangle of the box beam by starting the arc length coordinate, and hence the line integration, at the upper right corner. Recall that the arc length coordinate is positive in a counterclockwise direction. The modulus weighted thickness for the top plate is $(6.2/3.9)(2t) = 3.18t$, a constant over the entire centerline length of the top plate. Therefore, the value of the line integral over the full length of the centerline of the top plate is $3a/3.18t = 0.94a/t$. The portion of the line integral that results from proceeding with the arc length coordinate down the left-hand side web, where the m.w. thickness has the constant value t , is just a/t . The bottom plate and right-hand side web yield the same results as their symmetric opposites. Hence the total value for the line integral is

$$\oint \frac{1}{t^*} ds = [0.94 + 1 + 0.94 + 1](a/t) = 3.88 \frac{a}{t}$$

Therefore

$$J^* = \frac{4(9a^4)}{3.88a/t} = 9.3a^3t$$

(Note that if the orientation of the channel sections were reversed from “[]” to “[],” the approximate nature of these calculations suggests that the additional *thickness* provided by the aluminum flanges of the channel sections could be either ignored, or converted to an equivalent thickness of titanium by multiplying this flange thickness by the ratio of the aluminum to titanium shear moduli. Then the top plate would have three constant thickness segments.)

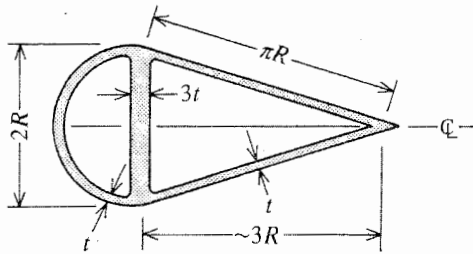


Figure 13.16. Example 13.6.

(c) The twist per unit length is $\theta = M_t/G_0J^*$, so

$$\theta = \frac{M_t}{9.3G_0a^3t}$$

which, of course, is an answer that, despite its appearance, is wholly independent of the choice of the value for G_0 . ■

Example 13.6. The cross-section of a uniform, aluminum rudder tab is sketched in Fig. 13.16. Set up, but do not bother to solve, the simultaneous equations necessary to determine the shear flows on the cross-section due to a uniform torque M_t .

Solution. Let q_1 be the counterclockwise shear flow around the left-hand side cell ($\hat{A}_1 = \pi R^2/2$), and q_2 be the counterclockwise shear flow around the triangular cell ($\hat{A}_2 \approx 3R^2$). There are thus two unknown shear flows requiring two simultaneous equations. The first of these equations is the equilibrium equation

$$M_t = 2\hat{A}_1q_1 + 2\hat{A}_2q_2 = \pi R^2q_1 + 6R^2q_2$$

The second equation necessary for a solution for the shear flows is the twist continuity equation $\theta_1 = \theta_2$. Recall Eq. (13.9). To evaluate θ_1 , start the counterclockwise line integral at the upper corner of the semicircle perimeter of the first cell. It does not matter where the integration begins. It is only necessary to begin somewhere. Around the semicircle, the thickness has the constant value t and the shear flow has the constant value q_1 . Thus this part of the line integral around the first cell is $(\pi R/t)q_1$. The final portion of that line integral results from proceeding up the center stiffener where the thickness has the constant value $3t$ and the shear flow has the constant value $(q_1 - q_2)$. The signs associated with the two shear flows are determined on the basis of the derivation which says that positive shear flows are in the positive direction of the local arc length coordinate. Therefore,

$$\oint_{\partial A_1} \frac{q}{t} ds = \frac{\pi R}{t} q_1 + \frac{2R}{3t} (q_1 - q_2)$$

Similarly,

$$\oint_{\partial A_2} \frac{q}{t} ds = \frac{2\pi R}{t} q_2 + \frac{2R}{3t} (q_2 - q_1)$$

Then, after canceling the factor $1/2G$, the second equation that started as $\theta_1 = \theta_2$ becomes

$$\frac{1}{\hat{A}_1} \left(\frac{\pi R}{t} q_1 + \frac{2R}{3t} (q_1 - q_2) \right) = \frac{1}{\hat{A}_2} \left(\frac{2\pi R}{t} q_2 + \frac{2R}{3t} (q_2 - q_1) \right)$$

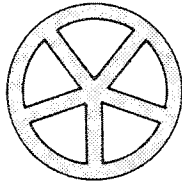


Figure 13.17. Example 1.7.

which reduces to just $12.47q_1 = 12.92q_2$ or $q_1 = 1.04q_2$. When substituted into the equilibrium equation, the above relation provides the solution for the two shear flows. As is the case here, the shear flows for cells bordering the outer boundary are usually of comparable magnitude, which means that the shear flows over interior webs are usually relatively small. ■

The exercises provide additional practice in solving multicell torsion problems. Note again that if the cross-section consisted of three cells, then the three equations for determining the three shear flows would be the one equilibrium equation and, when the cross-section is sufficiently stiff, the two continuity equations $\theta_1 = \theta_2$ and $\theta_1 = \theta_3$. The determination of the torsion constant for a multicell cross-section is accomplished by substituting the solutions for the shear flows into any one of the twist per unit length equations in order to determine the value of $\theta = \theta_i$. Then the torsion constant is determined simply from the general relation $M_t = GJ\theta$.

Example 13.7. Determine the uniform torsion shear flows for the five-cell cross-section shown in Fig. 13.17 where each cell has exactly the same geometry as the other cells.

Solution. The rotational symmetry of the cross-section means that all five shear flows are equal. Therefore their differences, the shear flow on the spokes of the wheel-shaped cross-section, must be zero. Thus the shear flow pattern is that of a single cell, and Eqs. (13.11) apply. Hence,

$$q_i = \frac{M_t}{2\pi R^2} \quad i = 1, 2, \dots, 5 \quad \blacksquare$$

13.4 Accuracy of the Uniform Torsion Theory

The uniform torsion theory is predicated upon the assumption that the torque and the cross-sectional geometry are constant, there is no warping restraint, and the end torques are applied in the form of end cross-section shearing tractions that duplicate the distribution of the predicted internal stresses. If the torque and cross-section vary gradually, the theory is still applicable. The case of gradually varying torque (and cross-section) is considered in the next section. Endnote (2) is a brief explanation of why a varying torque produces warping constraints.

If the end torques are not the result of shearing tractions that duplicate the predicted shearing stresses, then the pattern of the actual shearing stresses will differ from the predicted shear flows for several bar depths away from the bar ends. The presence of concentrated torques also disrupts the predicted stress patterns in the case of thin-walled beams, particularly closed cross-section beams, for distances along the length of such beams equal to several depths of the beam cross-section, much like the disruption of the predicted bending stress pattern caused by a concentrated force. As a further caution, it is also well to bear in

mind that multicell, built-up cross-sections of nominally the same geometry and material sometimes have somewhat different stiffnesses.

The effect of warping constraint is to stiffen the beam against twisting. A general theory for the uniform torsion of thin, open cross-sections with warping constraints at the beam ends was developed by Timoshenko (Ref. [33]). That theory shows that the effect from warping constraint at the beam ends upon the total twist, for the case of uniform torque, is negligible for long beams. Reference [4] provides the details of a solution for the particularly important special cases of I, Z, and channel cross-sections. The general thin-walled, open section, Timoshenko theory introduces an open cross-section warping constant Γ or C_w , with units of length to the sixth power. Like an area moment of inertia, the warping constant depends exclusively on the geometry of the beam cross-section. Certain open cross-sections (e.g., a cross-section shaped like a right-angled cross) have a zero warping constant. Thus their twist is unaffected by warping constraint. The warping constraint of closed, thin-walled cross-sections is a more complicated matter. Some solutions have been developed by von Karman and Chien, and Smith et al. (Ref. [4]).

13.5 Beams Subjected to a Variable Torque

The entire preceding theory was developed upon the basis of a constant torque and, thus, a constant twist per unit length, θ , which, in that circumstance, is equal to the total twist, $\phi \equiv \phi_x$, divided by the beam length. When a beam is subjected to a variable torque, the twist per unit length is also variable. In this case the twist per unit length is still equal to the twist divided by length. However, in order to have a unique value of this ratio at any point along the length of the beam, $\theta(x)$ must be written as the ratio of the differential increment in twist to the differential increment in distance along the length of the beam. That is, it is now necessary to write

$$\theta(x) = \frac{d\phi(x)}{dx} \quad (13.12)$$

Then the relation between the torque and twist per unit length becomes

$$M_t(x) = G_0 J^* \phi'(x) \quad (13.13)$$

The beam twisting equilibrium equation has been derived as Eq. (10.4d). Discarding the nonlinear terms, this equilibrium equation reduces to simply

$$M_t'(x) = -m_t(x)$$

Substitution of Eq. (13.13) into the above equation yields the linear beam governing differential equation for variable torque, which is

$$[G_0 J^* \phi']' = -m_t(x) \quad (13.14)$$

This second order GDE is a part of a boundary value problem. The corresponding single BC at each beam end is *either* the twist ϕ has a fixed value, usually zero, *or* the torque $M_t = G_0 J^* \phi'$ has a fixed value equal to the applied torque at that end, which also could be zero. (Recall that temperature changes never produce a twist.) Since this GDE and the corresponding BCs are much like the extension equations that were developed in preceding chapters, this boundary value problem does not require much further comment beyond three examples and some exercises. (Again, when Eq. (13.14) is applied to short thin, open cross-section beams, the effect of warping constraint can be included by adding the fourth order term $-[E\Gamma\phi'']'$ to the left-hand side of Eq. (13.14), doubling the number of BCs to

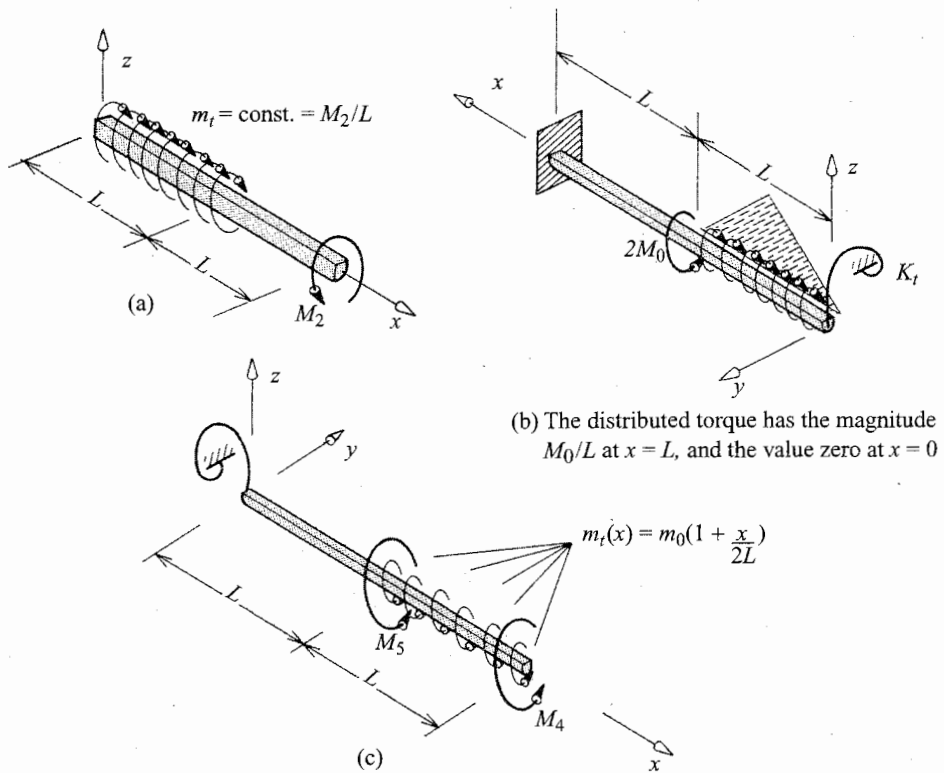


Figure 13.18. (a) Example 13.8. (b) Example 13.9. (c) Example 13.10.

two at each end, and including the warping normal stresses and warping displacements in those BC statements. See the last paragraph of Section 13.4 and Ref. [42].)

Example 13.8. Calculate the twist $\phi(2L)$ relative to the twist $\phi(0)$ for the homogeneous, uniform beam shown in Fig. 13.18(a). Note that the beam is in a state of static equilibrium, and that there is no constraint against either twisting or warping at either end of the beam.

Solution. Since $m_t = -M_2/L$, where M_2 is of fixed magnitude, the GDE becomes

$$GJ\phi''(x) = +\frac{M_2}{L}[1 - \text{stp}(x - L)]$$

with the required two BCs derived from Eq. (13.13). The BCs are

$$(i) \phi'(0) = 0 \quad \text{and} \quad (ii) GJ\phi'(2L) = +M_2$$

Performing the usual definite integration between the limits of zero and x first yields

$$GJ\phi'(x) = GJ\phi'(0) + x\frac{M_2}{L} - \frac{M_2}{L}(x - L)\text{stp}(x - L)$$

where the first right-hand side term drops out as a consequence of the first BC. Integrating again provides

$$GJ\phi(x) = GJ\phi(0) + x^2\frac{M_2}{2L} - \frac{M_2}{2L}(x - L)^2\text{stp}(x - L)$$

Setting $x = 2L$ produces the desired result:

$$\phi(2L) - \phi(0) = \frac{2LM_2 - LM_2/2}{GJ} = \frac{3M_2L}{2GJ} \quad \blacksquare$$

Note that boundary condition (ii) was not explicitly used to determine the total twist. In any problem where relative deflections are sought, the number of the BCs that are redundant equals the number of reference deflections. In this case, there is one reference deflection, $\phi(0)$, and one redundant BC.

Example 13.9. The uniform bar of length $2L$ shown in Fig. 13.18(b) is clamped at its left end and is constrained against twisting by a torsional spring of stiffness K_t at its right end. Set up the GDE and BCs for this problem.

Solution. Since the right-hand end has the more complicated BC, and since the description of the distributed torque would also be simplified, choose the origin of the x axis to be at the right-hand end. Then the GDE becomes

$$GJ\phi''(x) = +2M_0\Delta(x - L) - \frac{M_0}{L} \frac{x}{L} [1 - \text{stp}(x - L)]$$

It is worth mentioning that definite integration between the limits $(0, x)$ of the second of the above right-hand side terms is greatly facilitated if that expression is multiplied out and the x factor for the step function is converted to an $(x - L)$ factor by the simple expedient of adding and subtracting the quantity $L \text{stp}(x - L)$. The final result is

$$GJ\phi''(x) = +2M_0\Delta(x - L) - \frac{M_0}{L^2} [x - (x - L) \text{stp}(x - L) - L \text{stp}(x - L)]$$

The left-hand BC is simply $\phi(2L) = 0$. The BC at $x = 0$ requires a FBD where the beam slice is given a positive twist. Using the positive convention for the internal torque leads to the preliminary equation

$$M_t(0) - K_t\phi(0) = 0 \quad \text{then} \quad GJ\phi'(0) - K_t\phi(0) = 0 \quad \blacksquare$$

Example 13.10. Write, in a ready-to-use form, the GDE and BC equations for the uniform beam of length $2L$ which is loaded as shown in Fig. 13.18(c). The torsional spring at $x = 0$ has the spring constant K .

Solution. Since each term of the twist per unit length is positive, the GDE is written as

$$GJ\phi''(x) = -M_5\Delta(x - L) - m_0 \left(1 + \frac{x}{2L}\right) \text{stp}(x - L)$$

Again the second right-hand side term should be rewritten to facilitate definite integration between the limits $(0, x)$. The result is

$$GJ\phi''(x) = -M_5\Delta(x - L) - \frac{3}{2}m_0 \text{stp}(x - L) - \frac{m_0}{2L}(x - L) \text{stp}(x - L)$$

The two BC equations are obtained from FBDs of beam slices at each beam end. The results are

$$\begin{aligned} K\phi(0) = M_t(0) \quad \text{or} \quad GJ\phi'(0) - K\phi(0) &= 0 \\ M_t(2L) = +M_4 \quad \text{or} \quad GJ\phi'(2L) &= M_4 \end{aligned} \quad \blacksquare$$

13.6 Summary

The analysis of the twisting of the thin beam cross-sections used in vehicular construction begins with classifying the thin cross-section as either open or closed. If the thin cross-section is open, then the cross-sectional properties are simply estimated on the basis of the solution for the solid rectangular cross-section and the membrane analogy which connects the actual cross-section to the rectangular cross-section. If the open beam cross-section is that of a rolled or extruded beam, then the beam cross-section is likely to have significant fillets. Then, depending upon the importance of the accuracy of the estimate for the individual beam twisting stiffness factor J , the semiempirical approach of Endnote (1) may be employed for a more accurate estimate of the torsion constant, J , than is supplied by the standard thin open cross-section formula, which states that $J = \left(\frac{1}{3}\right) ab^3$.

Thin, open cross-sections are easily twisted and, as a result, can be subjected to high shearing stress values relative to similar closed cross-sections loaded by the same torque. Nevertheless, thin cross-sections usually have the advantage of being easier to connect to other structural members by means of rivets or bolts. Furthermore, access requirements may make openings in otherwise closed beam cross-sections unavoidable.

The analysis of twisted thin, closed beam cross-sections is based upon the equilibrium result, or more quickly, the membrane analogy result (see Exercise 13.13) that the shear flow in any thin-walled circuit around a single void of the closed cross-section is a constant. This information permits the calculation of the stresses in any single-cell, closed beam cross-section on the basis of equilibrium considerations alone. When there is more than one cell, and when the thin cross-section is quite compact, it is possible to say that all cells twist the same amount. This amounts to the required additional compatibility equations that are necessary to determine the shear flow in all parts of the cross-section. If the cross-section is not very compact, it may be best to use the structural analysis techniques introduced in Chapter 16. The following brief example reviews the twisting analysis of the various types of cross-sections.

Example 13.11. Calculate the St. Venant constant for uniform torsion for each of the beam cross-sections sketched in Fig. 13.19. All thin cross-sectional dimensions are centerline dimensions. Let the dimension c be much greater than the dimension t . Treat the cross-section of part (d) as compact.

Solution. (a) The rectangular cross-section is not thin. The exact solution for the rectangle should be used where $J = \beta ab^3$, and the value of β is that for the ratio a/b equal to 4. At that aspect ratio, from Fig. 12.2, $\beta = 0.28$. Thus

$$J = 0.28(8c)(2c)^3 = 18c^4$$

(b) For this thin, open cross-section, J is approximately equal to $\left(\frac{1}{3}\right) ab^3$. Thus

$$J = \left(\frac{1}{3}\right) (7c)(t)^3 = 2.3ct^3$$

(c) For this thin, homogeneous, single-cell, closed cross-section, the third of Eqs. (13.11) applies where $t^* = t$. The area enclosed by the thin wall centerline, \hat{A} , equals $6c^2$. The line integral around the thin wall centerline is equal to $10(c/t)$. Thus

$$J = 4(6c^2)^2/[10(c/t)] = 14c^3t$$

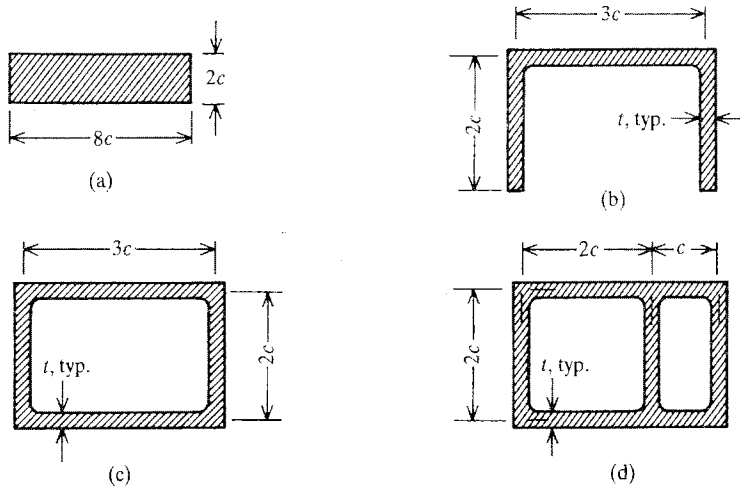


Figure 13.19. Example 13.11, where $c \gg t$ for all thin cross-sections.

(d) Since there are two cells to this thin-walled closed structure, there is no simple formula for the torsion constant. The torsion constant is determined by first calculating the two constant shear flows in the two-cell cross-section, and then calculating the twist per unit length. The torsion constant can be determined from the solution for the twist per unit length.

In order to calculate the two shear flows, first write the equilibrium equation

$$M_t = \sum (2\hat{A}q)_i = 8c^2q_1 + 4c^2q_2$$

With the value 2 being the ratio of the enclosed areas, the equality of the two twists per unit length of the two cells leads to the equation

$$q_1(6c) + (q_1 - q_2)(2c) = 2[q_2(6c) - q_1(2c)]$$

or

$$12q_1 = 14q_2$$

Substituting this latter result into the above equilibrium equation yields

$$q_1 = 0.0875 \frac{M_t}{c^2} \quad \text{and} \quad q_2 = 0.075 \frac{M_t}{c^2}$$

Now Eq. (13.9) can be used to calculate the twist per unit length in either cell. The result is

$$\begin{aligned} G\theta &= \frac{1}{8c^2t} \left[8c \left(0.0875 \frac{M_t}{c^2} \right) - 2c \left(0.075 \frac{M_t}{c^2} \right) \right] \\ &= \frac{1}{8c^2t} [0.55M_t/c] = \frac{M_t}{J} \end{aligned}$$

Thus

$$J = 14.5c^3t$$

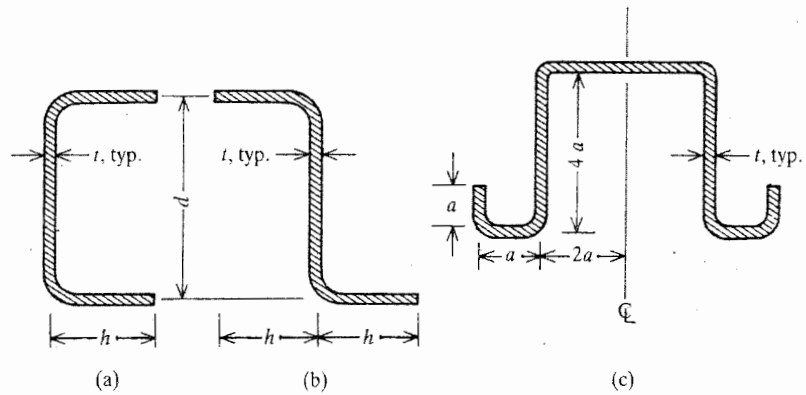


Figure 13.20. Exercise 13.1. Bent sheet metal open cross-sections.

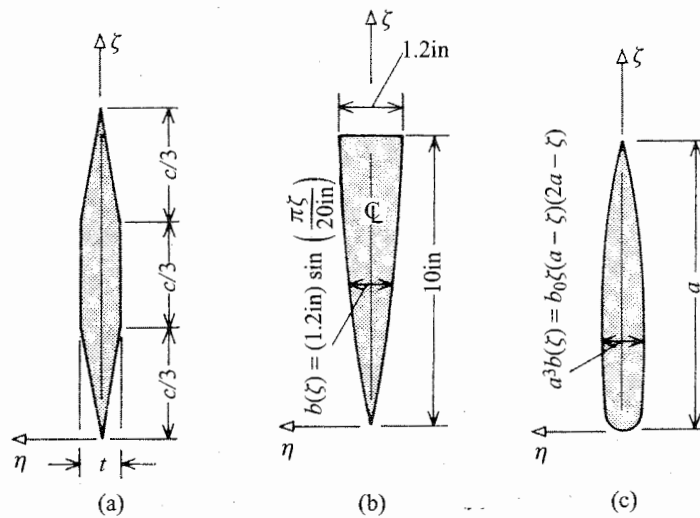


Figure 13.21. Exercise 13.2. Thin, open bar cross-sections of variable thickness.

Chapter 13 Exercises

- 13.1. In the case of no warping constraint, a uniform torque M_t , and a homogeneous material, determine the twist per unit length and maximum stress for each of the bent sheet metal cross-sections of Fig. 13.20.
- 13.2. (a) Calculate an approximate St. Venant constant for uniform torsion for the thin, solid cross-sections shown in Fig. 13.21(a). Also estimate the maximum stress.
 (b) As above for Fig. 13.21(b). Here, of course, the maximum stress is not at the point of maximum thickness.
 (c) As above for Fig. 13.21(c).
- 13.3. (a) What is the approximate value of the shear flow due to the uniform torque M_t shown, the corresponding maximum stress, and the m.w. St. Venant constant for uniform torsion for the closed, uniform cross-section shown in Fig. 13.22(a).

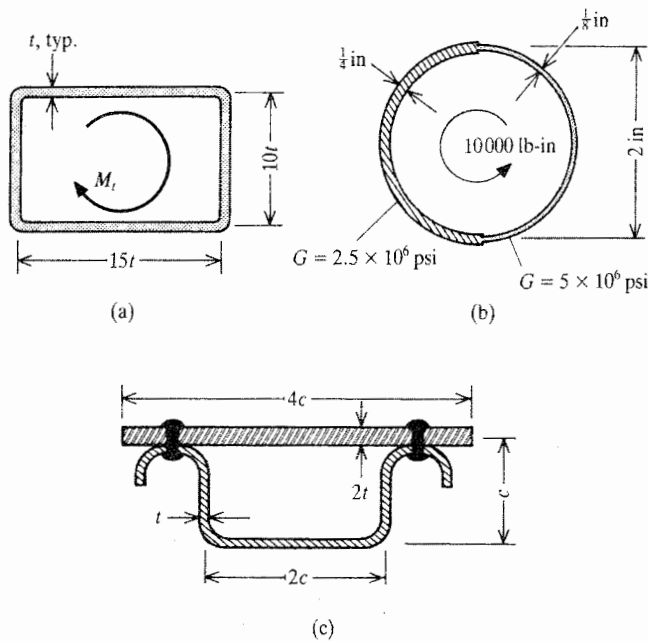


Figure 13.22. Exercise 13.3. Thin, single-cell cross-sections.

- (b) As above for the torque and the nonhomogeneous cross-section of Fig. 13.22(b).
- (c) As above for the torque and the nonhomogeneous cross-section of Fig. 13.22(c). Let $c \gg t$, and let the shear modulus of the top plate be $2G_0$ while that of the “hat” section is G_0 .
- (d) Consider a closed, thin, rectangular cross-section of centerline dimensions $8c$ by $2c$ and thickness $0.2c$. Show that the thin cross-section, with one-quarter of the area of a solid rectangular cross-section of dimensions $8c$ by $2c$, has a torsion constant that is slightly more than 57 percent of that for the solid cross-section.
- (e) For an annular cross-section where the inner radius, the radius of the void, is nine-tenths of the outer radius, show that the difference between the approximate solution for the centerline shearing stress and the exact maximum stress at the outer edge is 4.7 percent.
- (f) For the above annular cross-section, show that the percent error between the approximate solution and the exact solution for J is one-quarter of 1 percent.
- 13.4.** Ignoring the additional stiffness contributed by the fillets at the junctures of webs and flanges, calculate an approximate St. Venant constant for uniform torsion for the similar open and closed cross-sections sketched in Fig. 13.23.
- 13.5.** (a) Calculate the shear flows over the surface of the homogeneous, uniform cross-section shown in Fig. 13.24(a), for a constant torque M_t . Each curved portion is a circular arc and there is no significant warping constraint. Also calculate the value of the St. Venant constant for uniform torsion.
- (b) As above, for Fig. 13.24(b).

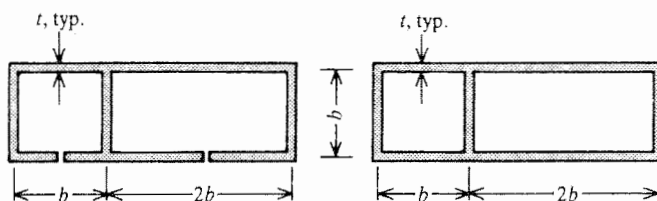


Figure 13.23. Exercise 13.4. An open and a closed, two cell bar cross-section.

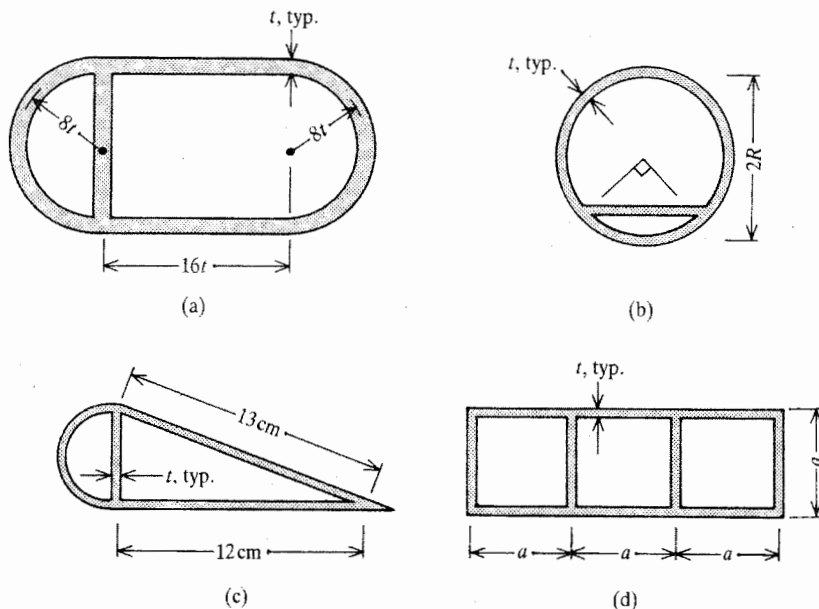


Figure 13.24. Exercise 5. Various multiply connected cross-sections.

- (c) As above, for Fig. 13.24(c).
 (d) As above, for Fig. 13.24(d).
- 13.6. (a) Calculate the tip rotation of a uniform, cantilevered beam of length L subjected to a constant torque per unit length of magnitude m_0 .
 (b) Calculate the tip rotation of a uniform, cantilevered beam of length L subjected to an end torque of magnitude M_0 .
 (c) Calculate the rotation at $x = L$ of a uniform beam of length L cantilevered at $x = 0$. The beam is subjected to a concentrated torque of magnitude $m_0 L$ at $x = L/2$, and a torque per unit length of magnitude m_0 acting over the outboard half ($\frac{1}{2}L \leq x \leq L$) in the direction opposite to that of the concentrated torque.
 (d) Do part (a) when $GJ(x) = GJ_0[2 - (x/L)]$.
 (e) Do part (b) when $GJ(x) = GJ_0[2 - (x/L)]$.
 (f) Do part (a) when $GJ(x) = GJ_0[2 - (x/L)]$, and $m_t(x) = m_0[2 - (x/L)]$.
- 13.7. A circular bar of length L is supported at its ends by frictionless ball bearings. With the x coordinate originating at one end of the bar, the torque per unit length is described by $m_t(x) = m_0 \sin(2\pi x/L)$. Calculate the total twist between ends.

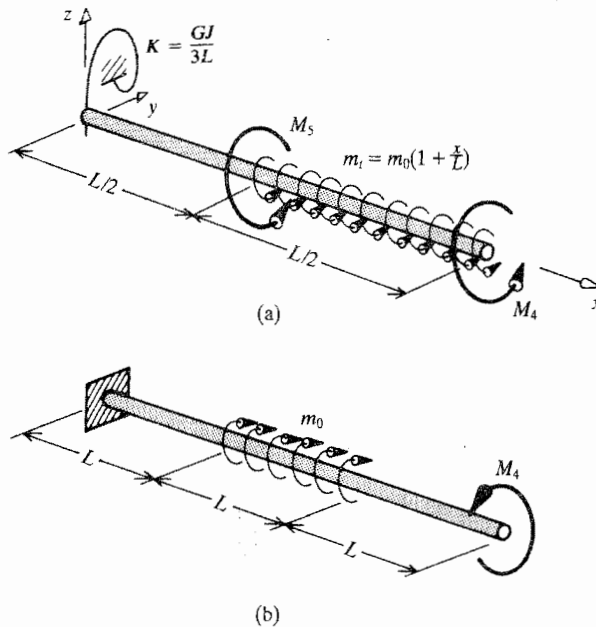


Figure 13.25. Exercise 13.8. Beams subjected to variable torques.

- 13.8. (a) Obtain analytical expressions for the twist $\phi(x)$ for the uniform bar with stiffness coefficient GJ shown in the sketch of Fig. 13.25(a).
 (b) As above, for Fig. 13.25(b).
- 13.9. It is suggested that the solution for the twist for the beam and loading discussed in Example 13.10 is

$$GJ\phi(x) = \left(x + \frac{GJ}{K}\right) \left(M_4 + M_5 + \frac{7}{4}m_0L\right) - M_5(x-L) \operatorname{stp}(x-L) - m_0L^2 \left[\frac{1}{12}\left(\frac{x}{L}\right)^3 + \frac{1}{2}\left(\frac{x}{L}\right)^2 - \frac{5}{4}\left(\frac{x}{L}\right) + \frac{2}{3}\right] \operatorname{stp}(x-L)$$

Determine why this solution is correct or incorrect.

FOR THE EAGER

- 13.10. In the case of the homogeneous, uniform, rolled or extruded sections sketched in Fig. 13.26, determine the value of the torsion constant using the recipe of Endnote (1).
- 13.11. Discuss the relative merits of building a box beam by use of top and bottom plates for flanges and a pair of channels for webs where in the first case the channels face inward (i.e.,]]) and in the second case the channels face outward (i.e.,] [). Can you suggest means suitable to a vehicular structure for overcoming the manufacturing difficulty inherent in first case?
- 13.12. Determine the equation for the twist for a beam cantilevered at $x=0$ and free at its opposite end, $x=L$. Let the beam be loaded with a positively directed, uniform torque per unit length of magnitude m_0 , and let the torsional stiffness factor $GJ(x)$ be equal to $GJ_0[1 - (x/L)]$. Note that at the beam's free end

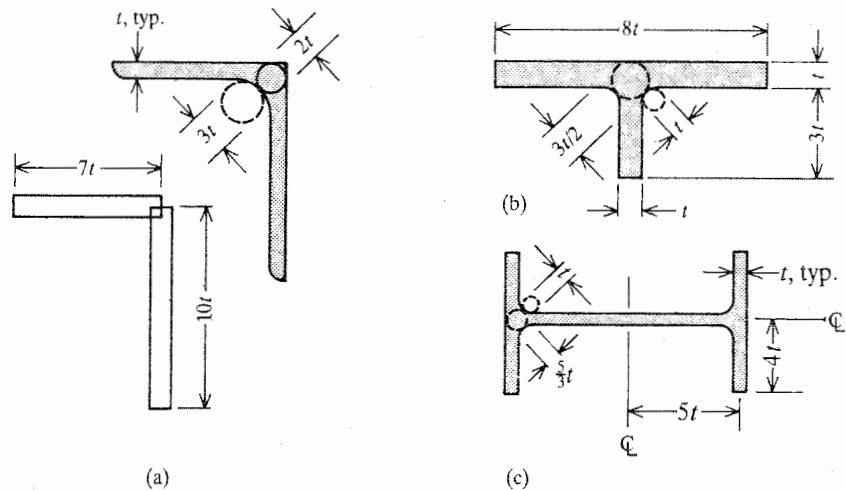


Figure 13.26. Exercise 13.10. Rolled or extruded bar cross-sections.

the stiffness factor drops to a zero value; that is, the beam has diminished to a point. *Hint:* Momentarily set aside the beam BCs, and proceed to integrate the GDE

$$\frac{d}{dx} \left[GJ_0 \left(1 - \frac{x}{L} \right) \frac{d\phi}{dx} \right] = -m_0$$

After obtaining the general solution with two constants of integration, which is

$$GJ_0\phi(x) = (m_0L^2 - C_1L) \ln \left(1 - \frac{x}{L} \right) - m_0L^2 \left(1 - \frac{x}{L} \right) + C_2$$

apply the first BC, $\phi(0) = 0$. Note that the apparent second BC that $M_t(L) = 0$ is useless because it degenerates to zero equals zero. Since no statement can be made about the value of $\phi'(L)$, consider what can be said about $\phi(L)$, and the result of that expectation.

- 13.13. Using the membrane analogy exclusively, justify the n -cell shear flow mathematical model where there is generally a different shear flow around each void as shown, for example, in Fig. 13.13.

Endnote (1) Torsion Constants for Rolled and Extruded Beams

The rectangular portions of a rolled or extruded beam cross-section are classified according to the three categories shown in Fig. 13.27(a, b, c). Note that “webs” are central rectangles whose corresponding membranes are open at both ends of the web rectangle. Flanges are classified according to whether the opening to their membrane is at an end, or at the center of their rectangle. The total St. Venant constant for uniform torsion for the entire rolled or extruded cross-section is taken to be the sum of component torsion constants for each flange and web of the cross-section, plus additional terms for the bulges at each of the fillets. That is,

$$J = \sum J_j$$

This approach is justified on the basis that the St. Venant constant for uniform torsion is proportional to the total volume under the membrane. The total volume under the membrane

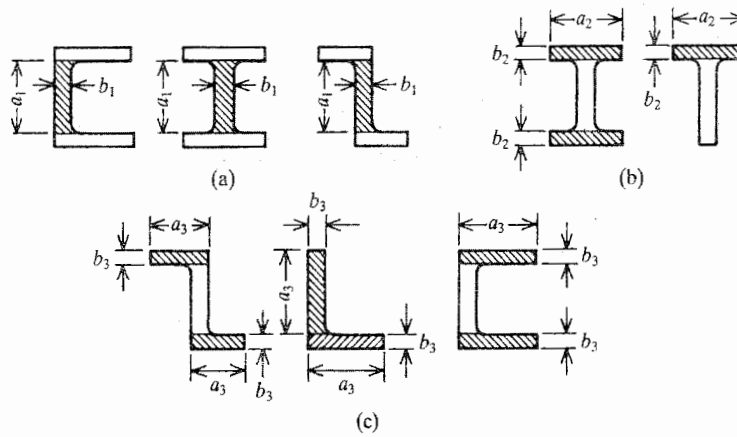


Figure 13.27. Endnote (1). From Ref. [32], rolled or extruded bar cross-sections that identify (a) webs, (b) flanges with a center juncture, and (c) flanges with an end juncture.

is the sum of the volumes under each segment of the membrane, that is, the sum of the volumes over each rectangle, plus the additional volumes attributable to the bulges. This approach is quantified as follows.

When the bulges at the junctures are temporarily ignored, it can be said that the membrane shape for a web is similar to that for an infinite rectangle. Thus the contribution to the total sum from the webs is taken to be

$$J_1 = \frac{1}{3} a_1 b_1^3$$

For flanges whose membranes are open at the sides, and thus held down at the short edges, as shown in Fig. 13.27(b), the usual formula for any rectangle is appropriate. That is, take

$$J_2 = \beta \left(\frac{a_2}{b_2} \right) a_2 b_2^3$$

where the β coefficient is taken from Fig. (12.12). Similarly, for flanges whose membranes is open at one end, where therefore the membrane has a slightly greater volume at the end, take as the torsion constant contribution the torsion constant of a rectangle with twice the aspect ratio of the actual rectangle. That is, take

$$J_3 = \beta \left(\frac{2a_3}{b_3} \right) a_3 b_3^3$$

To account for the bulges at the junctures of flanges and webs, include in the sum

$$J_4 = \alpha D^4$$

where this coefficient α is read from the graphs of Fig. 13.28, where D is the diameter of the largest circle that can be inscribed within the web-flange juncture. The sum $J = \sum J_i$ is the sum of the above component torsion constants as appropriate to the cross-section being analyzed. For example, a rolled H beam sum would have one J_1 , two J_2 , and two J_4 but no J_3 to account for its one web, two flanges, and two web-flange junctures, respectively. Similarly, an extruded channel section sum would have one J_1 , two J_3 , and two J_4 , but no J_2 , and an angle beam cross-section sum would only involve two J_3 and one J_4 .

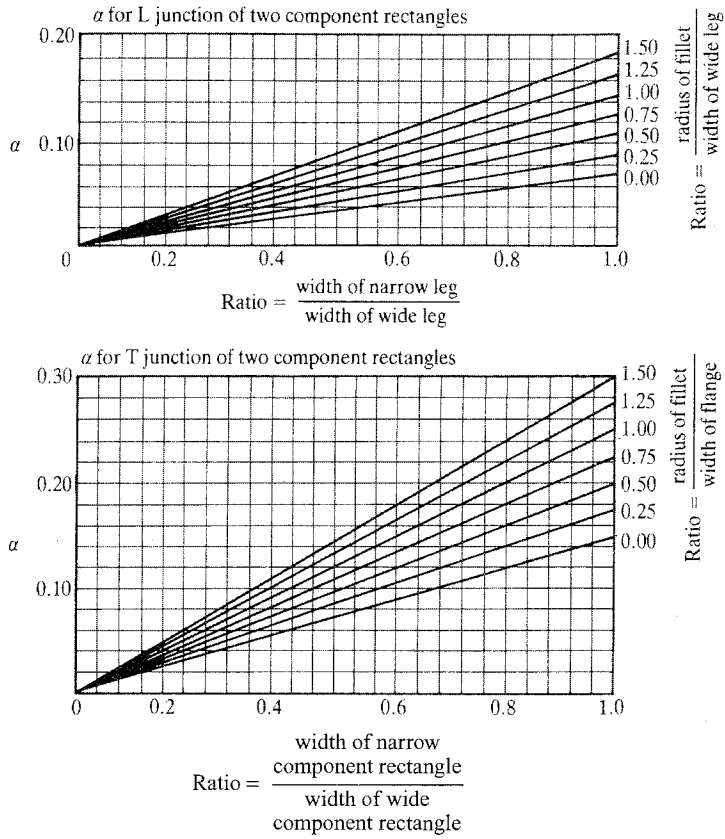


Figure 13.28. Endnote (1). From Ref. [32], the coefficient α that is used to determine the value of J_4 in the estimation of the St. Venant constant for the rolled or extruded cross-section.

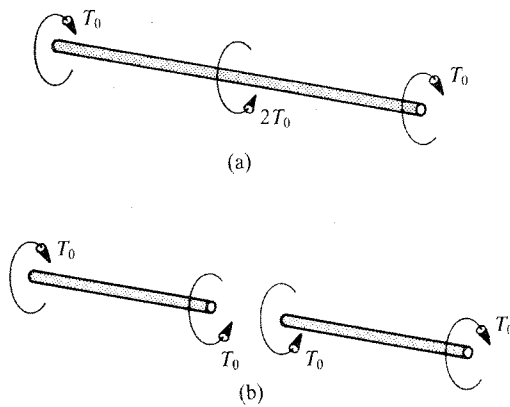


Figure 13.29. Endnote (2). Nonuniform warping and warping constraint.

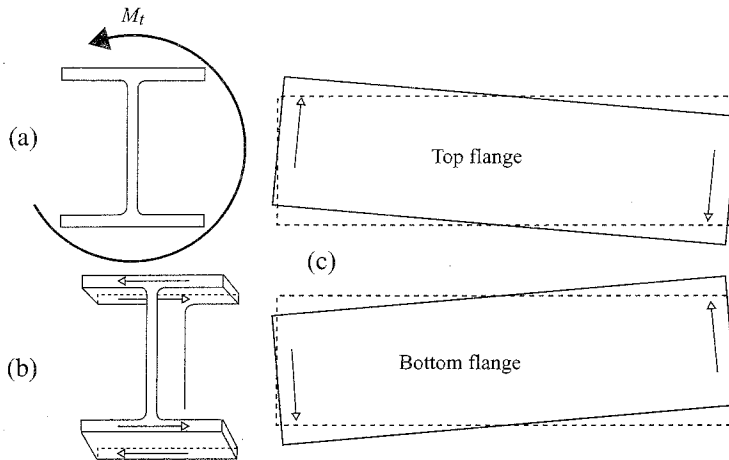


Figure 13.30. Endnote (2). (a) Applied torque. (b) Deflection of flanges in response to the torque, front view. (c) Top and bottom view of the flange deflections where the leftmost cross-section corresponds to the cross-section in part (b). The motion of the flanges makes the warping evident.

Endnote (2) Warping Constraint due to Varying Torque

To illustrate that a varying torque results in warping constraints, consider Fig. 13.29(a). In this figure, each half of the bar is twisted in different directions by the actions of the end torques and the centrally located concentrated torque. The Fig 13.29(b) FBDs of each half of the bar show that the total torques acting on each bar half are oppositely directed. The warping patterns for each bar half would therefore also be opposite to each other if the two bar halves were not connected to each other. Since the bar halves are connected at the bar center, there must be continuity of the warping displacements over the entire midspan cross-section. Since the only way the warping displacements can be both oppositely directed and the same at the midspan is for them to be zero. Zero warping displacements are one form of warping constraint.

To conclude the discussion of cross-section warping, Fig. 13.30 shows the warping pattern of a wide flange beam subject to a uniform torque. As the cross-section twists, and there is little or no axial strain, the flanges move as in part (b) of this figure, and as is more easily understood, as in part (c).

Beam Bending and Torsion Review Questions

Part III. True or False?

(Answers at the end of this section)

1. A basic difference between the theory of elasticity and strength of materials (“applied elasticity”) is that strength of materials solutions are based upon an approximation of either the stress field or the displacement field, while the theory of elasticity uses neither approximation.
2. Even for a nonhomogeneous beam, in Bernoulli–Euler straight beam bending theory both the displacements and the strains vary linearly in both centroidal coordinate directions over a compact beam cross-section.
3. Even for a nonhomogeneous beam, in Bernoulli–Euler beam bending theory the stresses vary linearly in both centroidal coordinate directions over the compact beam cross-section.
4. The number of Prandtl stress function BCs equals the number of internal boundaries plus one BC for the external boundary.
5. The membrane analogy for uniform torsion is based upon the extension of the Bernoulli–Euler beam bending approximations to membrane bending theory.
6. The membrane analogy for uniform torsion is useful for visualizing the torsional shearing stress distribution for both compact singly connected and compact multiply connected, beam cross-sections.
7. The equations that are useful for the analysis of a uniformly twisted, multicell, closed bar cross-section, with a sufficiently stiffened cross-sectional shape, are those deflection equations that say that the twist per unit length of each individual cell is the same, and those equilibrium equations that say that the resisting torque for each cell is the same.
8. For uniform torsion, the maximum shearing stress may occur at a fillet, but always occurs at an outer boundary point of the open, that is, singly connected, cross-section.
9. For an open beam cross-section, a greater fillet radius not only may lower the magnitude of the maximum shearing stress, but it also increases the magnitude of the St. Venant constant for uniform torsion, J .
10. The St. Venant constant for uniform torsion for a rectangular cross-section of edge dimensions $a \times b$ is $(\frac{1}{3})ab^3$ regardless of the relative magnitudes of the edge dimensions.
11. The torsional shearing stress distribution for a thin-walled, *open* cross-section is very nearly constant across the thickness, while that for a thin-walled *closed* cross-section varies from a maximum at one edge to zero at the center of the wall thickness to an oppositely directed maximum at the other edge of the thin wall.
12. The Prandtl stress function identically satisfies (or “integrates”) the equations of strain compatibility in terms of stresses for the uniform torsion problem.

(13–15) Among the approximations of Bernoulli–Euler beam theory are:

13. After bending deformation, the planar cross-sections remain perpendicular to any axis along the length of the beam.
14. The shearing stresses in the plane of the cross-section are zero even in the presence of shear forces.
15. There is no Poisson effect on the geometry of the cross-section (i.e., the cross-section retains its size and shape) as different parts of the beam are compressed and extended.
16. “Shear lag” is a term that describes the out-of-plane shearing deformations of a beam cross-section that otherwise remains plane after beam bending, and shear lag is only significant for beam cross-sections that are not at all compact.
17. The neutral axis is the axis for which the product of inertia is zero.
18. For a homogeneous beam cross-section, the principal area moments of inertia depend entirely upon the cross-section geometry and not at all upon the applied loading.
19. The principal area moments of inertia have the same rotation equation solution form in terms of the moments and product of inertia as the plane stress principal stresses have in terms of the normal stresses and the shearing stress.
20. When “finite” bending deflections are deflections that exceed one-quarter or one-third of the beam depth, and “small” bending deflections are anything smaller, then it is correct to say that *when* the beam equilibrium equations are derived taking into account the finite bending and twisting deflections of the beam, *then* there is coupling between the bending and twisting moments and the bending and twisting displacements.
21. An invariable rule for boundary conditions in any linear problem (not just boundary value problems) is that the number of boundary conditions equals the order of the highest spatial derivative in the GDE, and half that number of BCs is found at each boundary point.
22. The BCs for the fourth order beam bending equations must always follow the pattern that a statement must be made about either the bending slope or the bending deflection at each beam end, and another statement about either the bending moment or the shearing force at each end.
23. What have been called beam “elastic” boundary conditions are just more extensive forms of bending moment and shearing force boundary conditions.
24. The order of derivatives found in boundary condition equations must always be at least one less than the highest-order derivative found in the corresponding governing differential equation.
25. The Bernoulli–Euler beam bending equations of Chapters 9, 10, and 11 are not applicable to fiber composite and wood beams because fiber composites and wood are orthotropic materials.
26. The beam torsion equations of Chapters 12 and 13 are not applicable to uniform beams made from orthotropic materials.
27. The Heaviside step function can be written as the definite integral of the Dirac delta function with a lower limit of $-\infty$ and an upper limit of x .
28. One requirement for the validity of the uniform torsion theory for all lengths of bars is that there be nothing at the beam end cross-sections that prevents warping displacements.

29. The area moments of inertia for an entire beam cross-section with respect to axes at the centroid are a minimum compared to area moments of inertia for parallel axes at any other point in the plane of the cross-section, and the first moments of the total area about the centroid are zero regardless of the rotational orientation of the axes.
30. The Dirac delta function never has units of measurement associated with it, but the Heaviside step function always has units associated with it.
31. The membrane equilibrium equation derivation, because it did not involve distortions of the differential-sized membrane element, is valid only for small membrane deflections.
32. The governing differential equation for uniform beam torsion can be adjusted to account for warping restraints by the addition (with correct sign) of a term that is the product of the fourth order derivative of the twist and a coefficient that depends upon Young's modulus and the cross-section geometry.
33. The finite deflection "adjacent equilibrium" type of beam buckling analysis has solutions that are limited to (i) a trivial solution of zero deflection, and (ii) a series of nonzero deflection patterns associated with distinct compressive loads of increasing magnitude, of which only the deflection pattern associated with the smallest compressive force has any practical meaning.
34. In a manner that closely parallels the development of the Bernoulli–Euler beam bending equations, the development of the general beam torsion equations assumes that plane sections remain plane.
35. In the finite deflection buckling problem described by the finite deflection beam bending equation $EIw''''(x) + Pw''(x) = 0$, the compressive force is part of the eigenvalue while the corresponding eigenfunction is called the buckling mode shape.
36. In the above-described uniform buckling problem, the eigenfunctions depend upon the beam BCs, but the eigenvalue is wholly independent of the beam BCs.
37. If, in addition to a known compressive axial load, lateral loads are also present, then (i) the beam deflection problem is a boundary value problem and not an eigenvalue problem, and (ii) there is a specific deflection magnitude associated with specific magnitudes of the lateral and compressive loads.
38. The advantage of the membrane analogy is that it is simpler to mathematically solve membrane problems than to solve beam uniform torsion problems.
39. The St. Venant constant for uniform torsion, J , has units of length to the sixth power.
40. In the case of uniform torsion, each individual membrane contour line indicates the direction of the total shearing stress vector, and the lateral spacing between contour lines of equal height increments indicates the magnitude of the total shearing stress vector.
41. The fourth order differential deflection equations for beam bending that involve forces per unit length are merely variations on the second order differential deflection equations for beam bending that involve moments, and if the moment expressions can easily be written, then the second order deflection equations save two integrations.
42. The strain ϵ_{yz} is approximated as zero in both the engineering theory of beam bending and the engineering theory for the nonuniform torsion of beams.

43. The partial derivative of the Prandtl stress function Ψ in any coordinate direction on the plane of the beam cross-section yields the shearing stress in the coordinate direction that is orthogonal to the coordinate direction of the derivative.
44. To the state of present knowledge, the exact solution for the lateral deflections of a rectangular, thin membrane stiffened by a normal edge loading per unit length, N , that is constant in every direction, and loaded by a constant lateral pressure p , requires an infinite series.
45. The beam bending equation $EIw''''(x) = f_z(x)$ is, mathematically, a linear ordinary differential equation. One consequence of this linearity is that if both sides of this equation are multiplied by 2, and the factor 2 on the left-hand side is grouped with the deflection $w(x)$, it is easy to see that doubling the applied loading per unit length doubles the deflection. (The reader is assured that the preceding statement is true.) Now consider the mathematically linear ordinary differential equation $EIw''''(x) - Nw''(x) = f_z(x)$. Is it true or false that this ordinary differential equation reflects its nonlinear origin in that if the externally applied forces and externally applied lateral forces per unit length are doubled, the lateral deflection $w(x)$ is not doubled?
46. The beam twisting GDE $[GJ\phi'(x)]' = -m_t(x)$ is equally valid for short beams as it is for long beams.

Questions 47 through 50 refer to Fig. III.3.

47. The product of inertia for this homogeneous angle beam is $I_{yz} = -128t^4$, approximately.
48. If, in the top flange of length $16t$, there is a temperature change of magnitude T_0 , which is small enough not to appreciably affect the material constants of the angle beam, and there is no temperature change in the web of length $8t$, then the equivalent thermal moment about the y axis is $32\alpha T_0 t^3$, and that about the z axis is $64\alpha T_0 t^3$.
49. If now there is no temperature change, and if the only loadings acting upon the cross-section are certain bending moments M_y and M_z , and if the neutral axis passes through the point A , then the point C has the maximum stress value for the cross-section.
50. Among the labeled points only, that is, ignoring the vicinity of the fillet, the maximum shearing stress due to uniform torsion occurs at point B .
51. If the temperature change in a simply supported, uniform, homogeneous beam is a constant throughout the beam, then the axial stress is zero.
52. The deflections predicted by the Bernoulli–Euler beam theory are greater than the actual beam deflections, particularly if the beam length is short.
53. The neutral axis must always be a straight line passing through the beam cross-section centroid.
54. A cross-section of a straight beam twists about the centroid.
55. The first moment of area is not necessarily zero if the beam cross-section contains voids.
56. The Bernoulli–Euler beam theory sums the stress resultants at the centroid of each beam cross-section. That is, the two shearing forces pass through the cross-section's centroid, and the bending and twisting moments act about the Cartesian axes originating at the centroid. However, the three beam deflections and their rotations are measured at the shear center.

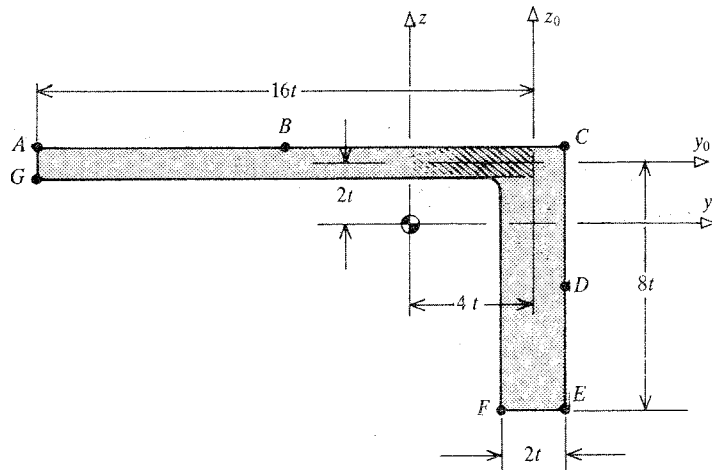


Figure III.3. Angle beam cross-section.

Answers

1. True. The only approximation incorporated into the theory of elasticity as presented here is that there are no significant body moments, which leads to the conclusion that the order of the subscripts on the stresses is without significance. On the other hand, simply to avoid the mathematical challenge presented by the theory of elasticity, strength of materials always involves a significant approximation based on a special geometry. For example, engineering beam theory postulates that plane sections remain plane after bending and extension, and so on.
2. True. The direct result of the first Bernoulli–Euler approximation that “plane sections remain plane” is that the displacements vary linearly with values of the centroidal coordinates. In a straight beam, the single strain—the axial strain—also varies linearly with the centroidal coordinates because that axial strain is obtained by differentiating with respect to the axial coordinate, not the in-plane centroidal coordinates.
3. False. In the Bernoulli–Euler straight beam theory, the displacements and strains vary linearly with respect to y and z over the nonhomogeneous cross-section, regardless of the presence of different material properties for the sub-areas of the cross-section. However, the bending stress $\sigma_{xx} = E\epsilon_{xx}$ and, for a nonhomogeneous beam, even E in its simplest mathematical form is only piecewise constant. Therefore, the linearly varying strain multiplied by a nonconstant E results in a nonlinear stress distribution. In the case of a piecewise constant E , the stress distribution is piecewise linear.
4. True. The Prandtl stress function is assigned a zero value at the outer boundary of the beam cross-section, and has an unknown constant value at the edges of all interior voids.
5. False. The membrane analogy for torsion is based upon the fact that the membrane deflection GDE and BC equations for the lateral deflection u are identical in form to the uniform torsion GDE and BC equations for the Prandtl stress function Ψ , plus the knowledge that the shearing stress vectors are everywhere tangent to lines of constant Ψ , and their magnitude is everywhere proportional to the slopes perpendicular to those contour lines. The derivation of the membrane GDE, unlike

- the plate bending GDE, in no way involves a Bernoulli–Euler type assumption of linearly varying in-plane membrane displacements.
6. True. As long as the shape of the cross-section is unaltered by the twisting, both the Prandtl stress function equations and the corresponding membrane equations, with their visual insight, are valid for any beam cross-section.
 7. False. The single equilibrium equation is that the sum of all the resisting torques for all the cells is equal to the torque applied to the uniform beam at the cross-section.
 8. True. For an open beam cross-section, the largest membrane slope is always at some point on the outer boundary, be that point at a fillet or elsewhere.
 9. True. If the maximum stress of an open cross-section is at a fillet, then increasing the fillet radius lessens the membrane slope and increases the volume under the membrane “bulge.”
 10. False. $J = (\frac{1}{3})ab^3$ is valid only if $a \gg b$. Otherwise $J = \beta ab^3$, where $\beta = \beta(a/b)$ is determined by a series summation or taken from a plot of that summation for different values of a/b .
 11. False. This statement is true if the words “open” and “closed” are interchanged.
 12. False. The Prandtl stress function identically satisfies the equilibrium equations for uniform torsion.
 13. True. This is the second of the three approximations. Its effect, along with the third approximation that the shape of the cross-section is unaltered by bending, is that all the shearing strains are zero valued, that is, are negligibly small.
 14. False. Since statement (13) is truly one of the Bernoulli–Euler assumptions, its immediate consequence is that in the Bernoulli–Euler theory there are no shearing strains due to shear forces. However, the presence of shearing stresses due to shear forces is not prohibited even though this causes a contradiction with respect to the strain–stress equations.
 15. True. Poisson’s ratio does not appear in engineering beam theory because in that theory, as a result of the third approximation, there are no strains in the y, z plane, and hence there is no Poisson effect.
 16. True. Engineering beam theory, which disregards shearing strains, is only valid for compact cross-sections. The effect of the shearing strains that, of course, are actually present becomes evident when the beam cross-section has, for example, very wide flanges. The small shearing strains accumulate over the very wide flanges to the point that it is no longer valid to say that the original plane cross-section remained plane after bending. See Fig. 9.3.
 17. False. The product of inertia is zero for principal axes. That is, the neutral axis is the line of zero stress in the plane of the cross-section. Hence the location of the neutral axis depends on the applied loading as well as the geometry of the cross-section, while the location of the principal axes depends only upon the cross-section geometry. Hence the additional dependence of the neutral axis upon the loading means that the neutral axis can have any relation to the principal axes, and hence any relation to any product of inertia.
 18. True. Principal or not, the area moments of inertia are second moments of area, and area alone. Thus they are determined by the cross-section geometry without any reference to applied loads.
 19. True. Comparing Eqs. (2.6) and Eqs. (9.14) shows that σ_{xx} corresponds to I_{yy} , σ_{yy} corresponds to I_{zz} , but a σ_{xy} corresponds to the negative of I_{yz} .
 20. True. This coupling for finite-sized deflections is evident in Eqs. (10.4).

21. False. The highest-order derivative in the differential equation must be the result of an even number of derivatives for this statement to be true. Another part that makes this statement false is the part that states that half the boundary conditions are always found at each boundary point. This is true for boundary value problems, but is not generally true. For example, when the product of inertia is zero, one of the two second order beam bending equations is, from before Eq. (10.5a, b)

$$E_0 I_{zz}^*(x) v'' = M_z^c(x)$$

In the case of a cantilevered beam, the two BC equations of zero deflection and zero slope would both be at the fixed beam end.

22. False. The correct pairing is (i) bending slopes or bending moments and (ii) lateral deflections or shearing forces. Again, this can be proved by the use of the principle of the minimum value of the total potential energy, and is done so in the third endnote of Chapter 15.
23. True. The reactions produced by the springs that provide elastic boundary conditions are shear forces and bending or twisting moments. As such, they must be summed along with the appropriate internal shear forces and internal moments and whatever external forces and external moments that are applied at the beam ends.
24. True. This is generally true for all structural engineering problems whether or not they fit the mold of a boundary value problem.
25. False. The beam bending equations are valid for any material whose stress-strain equations are, from Eq. (9.4a) and the preceding equation, $\sigma_{xx} = E_x (\epsilon_{xx} - \alpha \Delta t)$, and all other stresses are zero; that is, when all strains but ϵ_{xx} are zero. Before small fractures begin to accumulate in composite materials and wood, the stress-strain relations of those types of materials are as well approximated by that simple linear relation as the stress-strain relations of isotropic materials. Thus the beam bending equations are also valid for orthotropic beams as long as one of the orthotropic axes coincides with the beam axis. (On the other hand, the torsion equations as derived in this text are limited to isotropic materials.)
26. True. Unless G_{xy} equals G_{xz} , which would be more or less true, for example, for a fiber composite beam where all the fibers were aligned with the beam axis, the fourth and fifth compatibility equation would not simplify sufficiently to allow these G 's to cancel. See Section 12.2.
27. True. From Section 11.4.

$$\int_{\xi=0}^{\xi=x} \delta(\xi - x_0) d\xi = \text{stp}(x - x_0)$$

If $x_0 > 0$, then extending the lower limit to minus infinity has no effect.

28. True. The derivation of the beam torsion equations requires zero warping constraint at the beam ends. If there were warping constraints, then there would certainly be a significant nonzero σ_{xx} , which would not allow the Prandtl stress function by itself to satisfy the equilibrium equations. In long beams, the warping constraints can be ignored.
29. True. Eqs. (9.10), the parallel axis theorems, make clear that the moments of inertia about the centroid are a minimum compared to those about any parallel axes. The requirement that first moments of the total area are always zero was adopted to simplify the axial force and bending moment equations of, for example, Eq. (9.5).

30. False. The Dirac delta function always has units that are the inverse of its argument; for example, $\delta(x)$ has units of the inverse of length. The units of the Heaviside step function are always radians, which is considered to be no units (dimensionless).
31. False. The membrane equilibrium equation derivation did involve finite membrane slopes, and therefore it is valid for finite membrane deflections up to the point where those finite deflections cause significant increases in the size of the constant internal force per unit of edge length.
32. True. This matter was discussed in Section 13.4.
33. True. Since the beam buckling problem is an eigenvalue problem, there is (i) a trivial solution and (ii) a series of nontrivial solutions involving eigenvalues associated with the compressive loading, and eigenfunctions that detail the shape of the deflected beam. Only the lowest valued compressive force and its associated deflection pattern have meaning because it is not possible to increase the loads to reach those other solutions without applying rigid constraints to the beam.
34. False. In general, beam cross-sections warp when beams are subjected to torsional loads. Hence an assumption that the cross-section remains plane would be incorrect. Furthermore, no assumptions are made with regard to the general torsion problem with respect to either displacements or stresses. That is, although it is tentatively stated that four of the six stresses are zero as part of an inverse process to find the uniform torsion problem, this tentative assumption is confirmed as part of the theory of elasticity solution to the uniform torsion problem.
35. True. Specifically, the eigenvalue squared is P/EI . Since the deflection solution associated with the eigenvalue always contains an unknown multiplicative constant, the absolute magnitudes of the deflections cannot be determined, only their relative magnitudes; i.e., only their "shape."
36. False. Both the eigenvalue that contains the critical compressive load, and the corresponding buckling mode shape (deflection pattern) depend upon substituting the GDE solution into the beam BCs.
37. Both parts of the statement are true. Unlike a compressive axial force, the smallest lateral loading or bending moment causes the beam to bend. Therefore the question is not how large must the compressive force be to bend the beam (the eigenvalue problem), but how much the beam will bend due to the combination of axial and lateral loads (the boundary value problem).
38. False. Since the governing partial differential equation and BC equations are the same for the uniform torsion problem and the membrane deflection problem, neither is easier to solve than the other.
39. False. The St. Venant constant for uniform torsion, J , has units of length to the fourth power, while the warping constant has units of length to the sixth power.
40. True. These properties of the Prandtl stress function, as interpreted through the membrane analogy, are derived in Section 12.3.
41. True. For example, in simplest terms, twice differentiating the basic second order beam bending equation $EI_{zz}v''(x) = M_z(x)$ leads to $[EI_{zz}v''(x)]'' = M_z(x)'' = V_y(x)' = f_y(x)$.
42. True. The strain ϵ_{yz} is assigned a zero value by the third approximation of engineering beam bending theory: the approximation that beam cross-sections retain their (size and) shape after bending. The strain ϵ_{yz} has a zero value in uniform torsion theory because only σ_{xz} and σ_{xy} have nonzero values, and $\epsilon_{yz} = \sigma_{yz}/G$.
43. True. From Eqs. (12.4), for example, $\partial\Psi/\partial z = \sigma_{xy}$, where the z direction can be selected arbitrarily.

44. True. This is a matter of reversing the membrane analogy. That is, the rectangular membrane lateral deflection problem is analogous to the uniform twisting of a rectangular beam cross-section. As detailed in Section 12.6, the latter problem has only a series solution.
45. True. If both sides of the equation $EIw'''' - Nw'' = f_z$ are multiplied by the factor two, the result is $EI(2w)'''' - (2N)(1w)'' = (2f_z)$. Clearly, while the deflection function in the first term is doubled, the deflection function in the second term is not doubled. Therefore this equation does not really represent a linear load-response system.
46. False. The validity of the GDE $[GJ\phi'(x)]' = -m_t(x)$ requires that the effect on the angle of twist ϕ of the restraint against cross-section warping caused by nonuniform (i.e., nonconstant) torques be small. This effect is small in long bars, but it can significantly influence the solution for $\phi(x)$ in short bars. As discussed, the GDE for short bars is as above modified by the addition to its left-hand side of the term $-[E\Gamma\phi''(x)]''$, where E is Young's modulus and Γ is a property of the cross-sectional geometry with units of length to the sixth power.
47. False. The approximate value of I_{yz} is $-256t^4$.
48. False.

$$M_{yT} = - \sum (zE\alpha\Delta TA)_i = -2t(E\alpha T_0)(16t^2) = -32E\alpha T_0 t^3.$$

$$M_{zT} = - \sum (yE\alpha\Delta TA)_i = +4t(E\alpha T_0)(16t^2) = +64E\alpha T_0 t^3.$$

49. False. Since the only loading at the cross-section is that of mechanical bending moments, the neutral axis must pass through the centroid of the cross-section. See Eq. (9.8) for confirmation of this fact. A straight line drawn through the point A and the centroid shows that the point F lies further from the neutral axis than any other point on the cross-section. Thus the maximum stress value occurs at point F . The information provided is not sufficient to determine whether that maximum stress is tensile or compressive.
50. False. The overall maximum shearing stress due to a twisting moment is likely to occur at the inside edge of the fillet. However, among the labeled points, the points A , C , E , F , and G have a zero value for the uniform torsional shearing stress because they are all external corner points. (Recall the argument that since the uniform torsion solution requires that there be no shearing stresses anywhere on cylindrical sides of the beam, which sides are seen in edge view in Fig. III.3, then at an external corner point such as C , moment equilibrium of an infinitesimal parallelepiped at C requires that both orthogonal components of total shear stress be zero on the face of the parallelepiped that is coincident with the plane of the cross-section.) Since points B and D are away from the corner of the angle cross-section, the uniform torsion shearing stress at B and D can be estimated on the basis of the membrane analogy and the approximate variable thickness open cross-section solution, Eq. (13.6). Since the thickness at D is greater than that at B , the uniform torsion shearing stress at D is greater than that at B .

Note that it would be *incorrect* to estimate the maximum stress results for the separate rectangles of the flange and web using the rectangular beam stress solution as detailed in the equation following Eq. (12.18). That is, it is wrong to write the equations, from Fig. 12.12, that

$$\sigma(B) = M_t / [(0.32)(16t)t^2] \quad \text{and} \quad \sigma(D) = M_t / [(0.25)(8t)2t^2]$$

These two equations are wrong because the torsional moment in the above two equations is not the same. That is, the stress equation following Eq. (12.19) requires the value of the total torque acting upon the rectangular cross-section, or portion of the cross-section, in question. The total torque acting upon angle cross-section is not divided evenly between the two rectangular components of the total cross-section. Since $M_t = GJ\theta$, the total applied torque acting upon the angle cross-section is divided among the parts of the cross-section according to contributions of the various parts of the cross-section to the total stiffness coefficient GJ . The various components of the total J for the cross-section are discussed in Endnote (1) of Chapter 13.

51. True. The axial stress answer can be obtained from Eq. (9.8) by setting all the mechanical loads to zero, and evaluating and substituting the equivalent thermal loads.
52. False. The three Bernoulli–Euler hypotheses impose artificial constraints on the mathematical description of the beam deflections. Therefore, these three hypotheses stiffen the beam model, making its deflection less than those of the actual beam. The disparity is particularly notable when the beam is short. In a short beam the shearing deflections become a significant part of the total deflections. In the Bernoulli–Euler beam model, there are no allowances for shearing deflections. The Timoshenko beam theory allows shear deflections.
53. False. If there is an axial force as well as bending moments, then the neutral axis will not pass through the centroid. If there is a complicated temperature change, then the neutral axis will not be a straight line.
54. False. The cross-section of a straight beam twists about its shear center.
55. False. The first moment of area was chosen to be zero in all circumstances. It is this selection that permits the location of the cross-section's centroid.
56. True, for both parts. Since the beam's elastic axis (the loci of the shear centers) is the torsion axis for the beam, it is the only place where the two (small) lateral deflections $v(x)$ and $w(x)$ are not coupled with the twisting rotation. Hence, this is where the beam lateral and twisting deflections are measured. If centroid and shear center are different points on the cross-section, and if the lateral deflections were measured at the centroid, a pure (twisting) moment about the elastic axis would result in small lateral deflections without the presence of either shear forces or bending moments.

Beam Shearing Stresses Due to Shearing Forces

14.1 Introduction

Applied lateral forces acting upon beams produce interior shearing force stress resultants and shearing stresses. If the beam is statically determinate, then the interior shearing forces are easily calculated from force equilibrium equations. If the beam is statically indeterminate, then the shearing force stress resultants can be calculated by either the methods of analysis discussed in Part V, or, if necessary, from the Chapter 10 result for the shear forces at the cross-section centroid:

$$V_y(x) = [E_0 I_{zz}^* v''(x)]' + [E_0 I_{yz}^* w''(x)]' - V_{yT}(x) + m_z(x)$$

$$V_z(x) = [E_0 I_{yy}^* w''(x)]' + [E_0 I_{zy}^* v''(x)]' - V_{zT}(x) - m_y(x)$$

The deflection functions $v(x)$ and $w(x)$ are determined using the methods discussed in Chapters 10 and 11. Hence this chapter presumes that the shearing forces are known at whichever beam cross-section is the subject of discussion.

The objective of this chapter is to discuss techniques by which the beam shearing stresses can be calculated from a knowledge of the beam shearing force stress resultants. The process of using the beam shearing forces to calculate the beam shearing stresses parallels using the beam bending moments to calculate the beam normal stress σ_{xx} . Recall from Eqs. (9.1b, c), that the reverse task of calculating shear force stress resultants (acting at the beam centroid) from shearing stresses is a straightforward matter of integrating over the beam cross-section.

The shearing stresses in beams are seldom of any importance except when the beam has a thin cross-section, open or closed. In a thin cross-section, shearing forces can result in diagonal buckling, usually in the beam web. It is fortunate that shearing stresses are rarely important in a thick cross-section because the governing differential equation (GDE) and the boundary condition (BC) equation that specify the magnitudes and directions of the shearing stresses acting upon a thick cross-section are quite similar to, but even more complicated than, the corresponding torsion shearing stress equations (Ref. [21]). As a result, there are few solutions to that GDE and the corresponding BC equations.

In addition to safeguarding against shear buckling in beam webs, another reason for studying shear force-induced shearing stress distributions over thin beam cross-sections is that such distributions identify the *point* on the beam cross-section where, for small deflections, the application of the shearing force does not cause the cross-section to twist. This unique point is called the *shear center*, and the locus of this point for all cross-sections is called the beam *elastic axis*. See Endnote (4) of Chapter 11 for a discussion of related matters.

14.2 Thin-Walled Open Cross-Sections

Consider a differential-sized segment of a beam length that has an arbitrary shaped thin-walled cross-section. This beam segment can be from either an open or closed cross-section as is shown in Fig. 14.1(a, b). As usual, the x direction is along the length of the beam, while the s direction is along the centerline of the thin wall. Let the beam be uniform

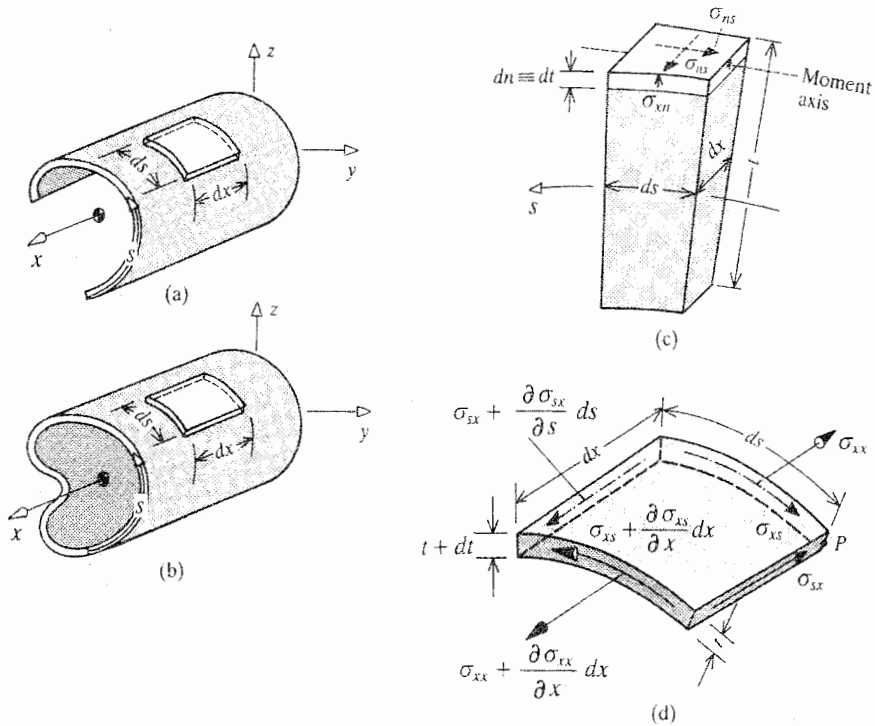


Figure 14.1. (a) Differential element of exaggerated size subjected to shearing stresses as part of a thin, open cross-section. (b) The same, but for a thin, closed cross-section. Note that the cross-section thickness can vary with the coordinate value s . (c) A demonstration that the total shearing stress at either cross-section edge has no component perpendicular to the edge. (d) The deduced free body diagram for the differential elements of parts (a) and (b).

in the x direction, but let the cross-section have a varying thickness and varying material properties. That is, let the thickness and material properties be functions of s , but not x . The differential-sized segment of Fig. 14.1(d) illustrates the variable, finite thickness, which for clarity is drawn smaller than the differential lengths dx and ds . Since the beam is subjected to applied shear forces, the bending moments are not constant. Thus the beam normal stress σ_{xx} varies over the length of the beam segment, that is, in the x direction, and is labeled accordingly. Since the linearly varying normal stress varies but slightly over the small thickness of any thin wall cross-sectional segment, then the normal stress at the centerline of the thin wall is both the average normal stress and a fair representation of the normal stress everywhere across the thickness. Thus a single normal stress vector can be used on each x face. There are no normal stresses on the s faces because in the Bernoulli–Euler beam theory, σ_{yy} and σ_{zz} are zero.

Now similarly consider the change in the magnitude and direction of the shearing stress over the thickness of the thin wall. As preparation for that undertaking, it is now required that the beam cylindrical surface tractions that produce the lateral forces per unit length $f_x(x)$, $f_y(x)$ and $f_z(x)$ and the moments per unit length $m_y(x)$ and $m_z(x)$ be zero. The now required absence of bending moments per unit length is only a minor limitation on the development below. The additional required absence of the forces per unit length means that the development below, to be wholly accurate within the confines of Bernoulli–Euler

beam theory, is limited to only those cases where the shearing forces $V_z(x)$ and $V_y(x)$ are constants. However, just as was true in the previous discussion of the accuracy of the beam normal stress equation, the accuracy of the derived shearing stress equation is satisfactory whenever the shearing forces vary gradually.

As a second step towards describing the change in the shearing stress across the finite thickness of the thin-walled cross-section, consider the moment equilibrium of a differential parallelepiped at the edge between the beam cross-section and the cylindrical surface of the beam. Such a parallelepiped, and the moment axis in question, are illustrated in Fig. 14.1(c) where the finite thickness is shown in better proportion to the differential distances. Since, by the limitations of the prior paragraph, there are no shearing tractions (analogous to σ_{nx}) in the x direction acting upon the cylindrical surfaces of the beam, then moment equilibrium reveals that σ_{xn} is also zero. Thus the total shear stress vector at the cross-section edge does not have a component perpendicular to the cross-section edge. The direction of the total shearing stress vector acting upon the beam cross-section at the cross-section edge has to be parallel to that edge. (As previously noted in Chapter 12, this deduction regarding shearing stress direction is, of course, also true for the shearing stresses due to uniform twisting moments.) If the thickness of the thin material is constant, then the total shear stress vector at the cross-section edge also parallels the centerline of the thin material. If the thickness varies, then the average direction of the top and bottom edge shear stresses parallels the direction of the centerline of the thin wall.

At this point these conclusions regarding the direction of the total shearing stress vector are extended over the entire thickness of the differential element. That is, it is hypothesized that the shearing stress, on average, parallels the s axis because the observed lack of distortion of the geometry of the cross-section shows that the thinness of the cross-section does not permit substantial cross-thickness shearing stresses to develop. Moreover, it is hypothesized that, like the normal stress magnitude, the shearing stress magnitude varies little over the thickness of the thin cross-section. Thus the shearing stress at the centerline of the material is representative of the shearing stress everywhere throughout the thickness. These conclusions are supported by the membrane analogy for shearing (Ref. [21]). Hence Fig. 14.1(d) has a single, representative shearing stress vector acting at and along the centerline on each of the four interior surfaces of the differential element. Note that moment equilibrium requires that $\sigma_{sx} = \sigma_{xs}$. However, since there is no reason to presume that the shearing stress does not vary in the s direction, such a change is included in the diagram.

Now that Fig. 14.1(d) has been justified, equilibrium equations for the s and x directions can be written. Since it has been accepted as a limitation of this development that there are no tractions on the upper and lower surfaces of the differential element, the s direction equilibrium equation produces the conclusion $\partial\sigma_{xs}/\partial x = 0$, which means that the shearing stress does not vary in the x direction, which is, of course, in keeping with the original limitation that the shear force does not vary in the x direction. Hence the shearing stress is only a function of the centerline coordinate s , and partial derivatives of the shearing stress with respect to the centerline coordinate become total derivatives. The x direction equilibrium equation is

$$\left(\sigma_{xx} + \frac{\partial\sigma_{xx}}{\partial x} dx\right)\left(t + \frac{1}{2}dt\right) ds - \sigma_{xx}\left(t + \frac{1}{2}dt\right) ds + (\sigma_{sx} + d\sigma_{sx})(t + dt) dx - \sigma_{sx}t dx = 0$$

The above equation simplifies to

$$\frac{\partial\sigma_{xx}}{\partial x}t ds + \sigma_{sx} dt + d\sigma_{sx}t = 0 \quad (14.1)$$

The second and third terms of Eq. (14.1), along with the constancy of the shear stress over the thickness of the thin wall, suggest reintroducing the convenient shear flow definition

$$q(s) \equiv \sigma_{xs}(s)t(s) \quad \text{so that} \quad dq = t d\sigma_{sx} + \sigma_{sx} dt$$

Therefore, after replacing the second and third terms of Eq. (14.1), by dq , and then dividing by ds , the equilibrium equation becomes

$$\frac{dq}{ds} = -t \frac{\partial \sigma_{xx}}{\partial x} \quad (14.2)$$

In order to determine the shear flow, it is necessary to integrate both sides of Eq. (14.2) with respect to the centerline coordinate between $s = 0$, and a typical value of s . After multiplying both sides by ds , and so integrating, the left-hand side of Eq. (14.2) becomes

$$\int_0^s dq = q(s) - q(0) \equiv q(s) - q_0$$

The evaluation of the integral of the right-hand side of Eq. (14.2) requires a knowledge of σ_{xx} . The only available expression for σ_{xx} is that provided by Eq. (9.8). Of course, Eq. (9.8) is a solution based upon the Bernoulli–Euler approximation that plane sections remain plane, undistorted, and perpendicular to the beam axis after bending. The shearing strains that accompany shear stresses, and the Poisson effect, certainly contradict the Bernoulli–Euler approximation. Nevertheless, as stated previously, those small effects do not undermine the general excellence of the Bernoulli–Euler approximation for long beams with compact beam cross-sections. Thus Eq. (9.8) is accepted for use here along with its requirements such as the y and z axes must be centroidal coordinates, and its limitations as discussed in Section 9.5. Recall in particular that Eq. (9.8) is not valid near a concentrated force loading or an abrupt change in beam geometry. Furthermore, the accuracy of Eq. (9.8) depends upon the bending moments only changing gradually over the span of the beam.

Adapting Eq. (9.8) to the case where there are no forces or bending moments per unit length acting along the length of the beam, that is, the shearing forces are constant along the length of the uniform beam,

$$\frac{\partial \sigma_{xx}}{\partial x} = \frac{E}{E_0} \left\{ \frac{(N^c)'}{A^*} - y \left[\frac{(M_z^c)'}{R_{yy}^*} - \frac{(M_y^c)'}{R_{yz}^*} \right] - z \left[\frac{(M_y^c)'}{R_{zz}^*} - \frac{(M_z^c)'}{R_{yz}^*} \right] - E_0 \alpha \Delta T' \right\}$$

or

$$\frac{\partial \sigma_{xx}}{\partial x} = \frac{E}{E_0} \left[-\frac{f_x \Gamma}{A^*} - y \left(\frac{V_y^c}{R_{yy}^*} - \frac{V_z^c}{R_{yz}^*} \right) - z \left(\frac{V_z^c}{R_{zz}^*} - \frac{V_y^c}{R_{yz}^*} \right) - E_0 \alpha \Delta T' \right]$$

Substituting the above equation into the integral from $s = 0$ to $s = s$ of Eq. (14.2) yields

$$\begin{aligned} q(s) &= q_0 - \int_0^s \frac{\partial \sigma_{xx}}{\partial x} t ds \\ q(s) &= q_0 + \frac{f_x \Gamma A^*(s)}{A^*} + \left(\frac{V_y^c}{R_{yy}^*} - \frac{V_z^c}{R_{yz}^*} \right) Q_z^* \\ &\quad + \left(\frac{V_z^c}{R_{zz}^*} - \frac{V_y^c}{R_{yz}^*} \right) Q_y^* + \int_0^s E_0 \alpha \Delta T' t ds \end{aligned} \quad (14.3)$$

where

$$A^*(s) = \int_0^s \frac{E}{E_0} t ds \quad Q_y^* = \int_0^s z \frac{E}{E_0} t ds \quad Q_z^* = \int_0^s y \frac{E}{E_0} t ds$$

The quantity $A^*(s)$ is the modulus weighted area between the origin of the centerline arc length coordinate and the point s on the thin cross-section centerline where the shear flow is being evaluated. The quantities Q_y^* and Q_z^* are the first moments of this m.w. area about the y and z axes respectively. These same first moments over the entire cross-section have a zero value because, due to the use of Eq. (9.8), the coordinates y and z must originate at the m.w. centroid. The same sub-area approach used so extensively in Chapter 9 for sub-areas chosen so as to have constant moduli leads to the following equations that are convenient for calculating the above three quantities. If A_i is such a constant modulus sub-area between $s = 0$ and $s = s$, then

$$\begin{aligned} A^*(s) &= \sum \frac{E_i}{E_0} A_i & Q_y^* &= \sum \bar{z}_i \frac{E_i}{E_0} A_i \\ Q_z^* &= \sum \bar{y}_i \frac{E_i}{E_0} A_i \end{aligned} \quad (14.4)$$

When there is no temperature change, the solution for the shear flow simplifies to

$$q(s) = q_0 + \left(\frac{V_y}{R_{yy}^*} - \frac{V_z}{R_{yz}^*} \right) Q_z^* + \left(\frac{V_z}{R_{zz}^*} - \frac{V_y}{R_{yz}^*} \right) Q_y^* \quad (14.5)$$

If the cross-section is open, and if the origin of the arc length coordinate s is placed at one end of the cross-section centerline, then $q_0 = t\sigma_{xs}(s=0) = 0$ because on the traction-free cylindrical side of the beam at $s = 0$, $\sigma_{sx} = 0$, and $\sigma_{xs} = \sigma_{sx}$. The following five example problems illustrate the use of Eqs. (14.5). The fourth of these examples shows that an open cross-section with a T junction is no problem because a different arc length coordinate can be started at each end of the cross-section away from the junction.

14.3 Thin-Walled Open Cross-Section Example Problems

The first example problem does not involve an idealized form of a beam cross-section that is used in vehicular construction. It is chosen only because it most simply illustrates the calculation of the first partial area moment, $Q_y(s)$. All other example problems are merely variations upon this simplest example. Let it be understood that all beam cross-section drawings show front faces. Therefore, in those drawings, positive shear force directions are opposite to the positive coordinate directions.

Example 14.1. Calculate the induced shear flow in the thin rectangular cross-section of thickness t and depth $2a$ which is shown in Fig. 14.2, when that cross-section is loaded by the shear force shown.

Solution. In this case the Cartesian coordinates are obviously principal axes. The shear forces are $V_z = +F$ and $V_y = 0$. Thus the shear flow formula reduces to

$$q = \frac{FQ_y}{I_{yy}}$$

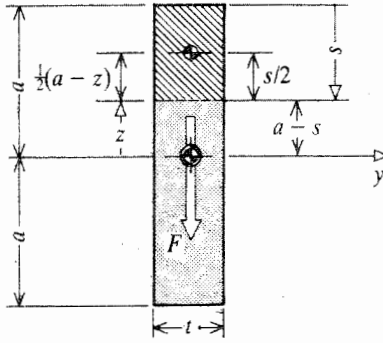


Figure 14.2. Example 14.1.

where $Q_y(s) = \bar{z}(s) A(s)$, and $I_{yy} = (1/12)t(2a)^3 = (2/3)a^3t$. The only task is to calculate the first moment of the partial area for the entire depth of the cross-section. For the sake of comparison, Q_y will be calculated first using the standard arc length centerline coordinate s , whose origin is at the top of the cross-section as indicated in the figure, and then it will be calculated again using the Cartesian coordinate z .

$$\begin{aligned} 0 \leq s \leq 2a \quad Q_y(s) &= (a - s + \frac{1}{2}s)st = (a - \frac{1}{2}s)st \\ &= ats - \frac{1}{2}ts^2 \end{aligned}$$

which, of course is zero at $s = 0$ and $s = 2a$. The maximum value of this partial area moment is $\frac{1}{2}a^2t$ which occurs at $s = a$. Now, doing the same calculation in terms of the Cartesian coordinate z ,

$$\begin{aligned} -a \leq z \leq a \quad Q_y(z) &= [z + \frac{1}{2}(a - z)](a - z)t = \frac{1}{2}(a + z)(a - z)t \\ &= \frac{1}{2}(a^2 - z^2)t \end{aligned}$$

This calculation could have been shortened by the amount of the first equality by noting that the distance from the y axis to the centroid of the area $A(s)$ is the average value of the distances a and z , that is, $\frac{1}{2}(a + z)$. In this case the parabolic form of Q_y , and hence the parabolic form of the shear flow and the shear stress, is a bit easier to interpret in terms of the Cartesian coordinate. Substituting for the induced shear flow

$$-a \leq z \leq a \quad q(z) = \frac{3}{4} \frac{F}{a^3} (a^2 - z^2)$$

and

$$\sigma_{xz} = -\frac{3}{4} \frac{F}{a^3 t} (a^2 - z^2)$$

The theory of elasticity infinite series solution for this cross-section shows that this approximate maximum shearing stress value of $(3/4)(F/at)$ is well within engineering accuracy across the width of the rectangular cross-section whenever $a > t$. Furthermore, this approximate solution is only about 10 percent off for a square cross-section, which of course, is not much like a thin cross-section.

For the sake of a quick comparison, the first area moments are now recomputed with the partial area starting at the bottom of the cross-section. That is, with $s = 0$ at the bottom of the cross-section centerline,

$$Q_y(s) = (a - \frac{1}{2}s)st = ast - \frac{1}{2}s^2t$$

which of course is no different from the previous calculation in terms of the arc length coordinate that originates at the top of the centerline. The calculation that requires careful attention is the one using the Cartesian coordinate z . When the partial area is at the bottom of the cross-section, the coordinate z has a negative value, making $-z$ a positive distance. Thus the partial area has the value

$$A(z) = [a - (-z)]t = (a + z)t$$

The distance to the centroid of this partial area is the average value of a and $-z$, which is $\frac{1}{2}(a - z)$. Therefore,

$$Q_y(z) = \frac{1}{2}(a - z)(a + z)t = \frac{t}{2}(a^2 - z^2)$$

just as before. ■

Example 14.2. A shearing force with orthogonal components F_y and F_z is applied to the juncture of the centerlines of the two flanges of the angle beam shown in Fig. 14.3(a) (It is soon to be discovered that that juncture is the one location on the cross-section where the shearing force can be applied without causing the cross-section to rotate.) If $a^2 \gg t^2$, calculate the shear flow in each leg of the idealized cross-section.

Solution. First it is necessary to calculate the characteristics of the homogeneous cross-section. To this end note that $A = 8at$, and from either flange centerline

$$\bar{y}_0 = \bar{z}_0 = \frac{1}{A} \sum \bar{z}_i A_i = \frac{2a(4at)}{8at} = a$$

Then

$$I_{yy} = I_{zz} = \sum (\bar{I}_{yy} + \bar{z}_i^2 A_i) = 13.333a^3t$$

and

$$I_{yz} = \sum \bar{y}_i \bar{z}_i A_i = 2(+a)(-a)(4at) = -8a^3t$$

Therefore,

$$R_{yy} = R_{zz} = 8.5333a^3t \quad \text{and} \quad R_{yz} = -14.222a^3t$$

When the arc length coordinate is started at either flange tip, q_0 is zero, and the equation for the shear flow, from Eq. (14.5) becomes

$$q(s) = \left(\frac{V_y}{R_{yy}} - \frac{V_z}{R_{yz}} \right) Q_z + \left(\frac{V_z}{R_{zz}} - \frac{V_y}{R_{yz}} \right) Q_y$$

where $V_y = -F_y$ and $V_z = -F_z$. In this case, because the flanges parallel either the y or z axis, it is better to write the first moments of the partial areas in terms of the y and z coordinates rather than arc length coordinates. Thus with

$$Q_y = \sum \bar{z}_i A_i \quad \text{and} \quad Q_z = \sum \bar{y}_i A_i$$

for the vertical flange, that is, for $-a \leq z \leq 3a$ (with $y = -a$),

$$Q_y = (3a - z)t \left(z + \frac{3a}{2} - \frac{z}{2} \right) = \frac{t}{2}(9a^2 - z^2)$$

$$Q_z = (3a - z)t(-a) = -at(3a - z)$$

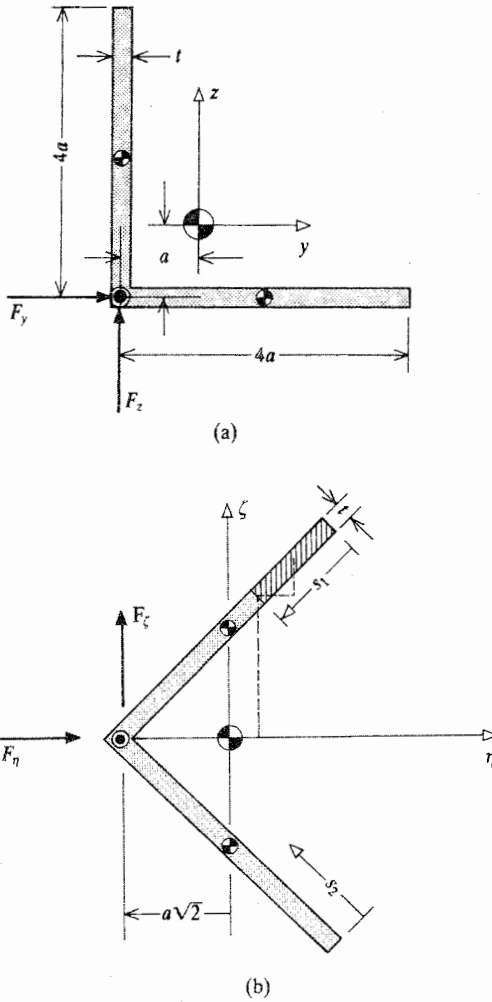


Figure 14.3. (a) Example 14.2. (b) Example 14.3.

For $-a \leq y \leq 3a$, it is simply a matter of interchanging y and z , that is,

$$Q_y = -at(3a - y)$$

$$Q_z = \frac{t}{2}(9a^2 - y^2)$$

Substituting these values into the shear flow equation, and simplifying yields the following result:

$$\begin{aligned} -a \leq z \leq 3a \quad q(z) &= (F_z/a)[0.0586(z/a)^2 - 0.0703(z/a) - 0.3164] \\ &\quad + (F_y/a)[0.0352(z/a)^2 - 0.1172(z/a) + 0.0352] \end{aligned}$$

$$\begin{aligned} -a \leq y \leq 3a \quad q(y) &= (F_y/a)[0.0586(y/a)^2 - 0.0703(y/a) - 0.3164] \\ &\quad + (F_z/a)[0.0352(y/a)^2 - 0.1172(y/a) + 0.0352] \end{aligned}$$

Note that these solutions provide zero values at the flange tips, that is, where the z or y coordinates have the value $3a$.

The direction of a positive shearing stress σ_{xs} or shear flow $q(s)$ is always in the direction of the arc length coordinate. In this case, the two arc length coordinates start at the flange tips and proceed towards the point $(-a, -a)$. Thus, for example, the shearing stress, induced by the force component F_z alone, at the midpoint of the vertical flange, where $z = +a$, is upward. This is not unexpected since this shearing force F_z also acts in the upward direction. When both F_z and F_y are present, then again the shear flow sum at that point is negative, indicating that the shear flow is upward along the flange centerline.

Be warned that besides the “induced” shearing stress, there is also the “reacting” shearing stress, which is the same as the induced shearing stress, but is oppositely directed. The advantage of the reacting shearing stress is that if the shearing stress results are superimposed upon a sketch of the cross-section along with the applied shearing force, then it is apparent and aesthetically pleasing that the shearing force and the reacting shearing stresses equilibrate each other. This makes for a more satisfactory presentation of the final result. Since there are two arbitrarily valued load components in this case, no such sketch is attempted in this exercise. However, such a sketch is presented in the third exercise. The reacting shearing stresses are also more convenient for calculating the location of the shear center. ■

Example 14.3. Redo the previous example problem, but this time use the principal axes ζ and η , which, of course, are aligned with the axis of symmetry as shown in Fig. 14.3(b). For ease of calculation, resolve the total applied shear force into components in the ζ and η directions.

Solution. Use of the rotation equations for area moments of inertia found in Chapter 9 produces the result

$$I_{\eta\eta} = 21.33a^3t \quad \text{and} \quad I_{\zeta\zeta} = 5.333a^3t$$

Obviously the area moment of inertia about the η axis must be greater than that about the ζ axis. Again, since both shear forces acting on this front face are in the positive coordinate directions, they both are negative; that is,

$$V_\eta = -F_\eta \quad \text{and} \quad V_\zeta = -F_\zeta$$

The shear flow equation in this case simplifies to

$$q = \frac{V_\zeta Q_\eta}{I_{\eta\eta}} + \frac{V_\eta Q_\zeta}{I_{\zeta\zeta}}$$

For the upper flange, let the arc length coordinate s_1 start, as usual, at the flange tip. Thus ζ and η have the respective values $(1/\sqrt{2})(4a - s_1)$ and $(1/\sqrt{2})(2a - s_1)$.

$$\begin{aligned} Q_\eta &= s_1 t \left(\zeta + \frac{s_1}{2\sqrt{2}} \right) = (4a - \sqrt{2}\zeta)t \left(\zeta + \frac{4a - \sqrt{2}\zeta}{2\sqrt{2}} \right) \\ &= \frac{t}{\sqrt{2}}(8a^2 - \zeta^2) \end{aligned}$$

and

$$\begin{aligned} Q_\zeta &= s_1 t \left(\eta + \frac{s_1}{2\sqrt{2}} \right) = (2a - \sqrt{2}\eta)t \left(\eta + \frac{2a - \sqrt{2}\eta}{2\sqrt{2}} \right) \\ &= \frac{t}{\sqrt{2}}(2a^2 - \eta^2) \end{aligned}$$

Thus

$$q(s_1) = - \left(\frac{F_\zeta [8 - (\zeta/a)^2]}{30.17a} + \frac{F_\eta [2 - (\eta/a)^2]}{7.54a} \right)$$

and similarly for the lower flange where s_2 is the arc length coordinate:

$$q(s_2) = - \left(\frac{F_\zeta [8 - (\zeta/a)^2]}{30.17a} + \frac{F_\eta [2 - (\eta/a)^2]}{7.54a} \right)$$

On the basis of these last two examples it appears to be somewhat easier to use conveniently oriented axes rather than principal axes, even when the directions of the principal axes are evident. ■

Example 14.4. (a) Determine the shear stress distribution and thus the magnitude and location of the maximum shear stress due to the shear force F_v shown acting on the idealized wide-flange (i.e., H) cross-section shown in Fig. 14.4(a).

(b) Do the same when the cross-section is a built-up cross-section of the same general geometry, but with steel flanges and an aluminum web as shown in Fig. 14.4(b). The ratio of the steel modulus to that of the aluminum is 3:1. Use the aluminum modulus, E_0 , as the reference modulus. Let the area and relevant moment of inertia of the aluminum angle beams used to connect the flanges to the web be $32t^2$ and $100t^4$ respectively. *Hint:* When calculating the partial first moment of the area for the web, consider the effect of the angle beam cross-sections to become suddenly and totally effective at the centroid of the angle beams, and do not bother making a calculation for the small part of the web between web top (or bottom) and the angle centroids.

Solution. (a) In both problem parts $I_{yz} = 0$, and there is only one shear force component. That is, $V_z = -F_v$. A quick calculation shows that for the homogeneous cross-section $I_{yy} = 108480t^4$, where the number of significant figures is reduced in the final solution. As ever, starting the arc length coordinate at a terminus of a flange centerline makes $q_0 = 0$. Thus the shearing stress equation in part (a) reduces to

$$\sigma_{xs}(s) = \frac{q(s)}{t} = \frac{F_v Q_y(s)}{I_{yy} t(s)}$$

Applying Eq. (14.4),

$$Q_y^* = \sum \bar{z}_i \frac{E_i}{E_0} A_i$$

to the left-hand side of the upper flange where $s_1 = 18t + y$, $\bar{z}_i = 25t$, and $A_i(s_1) = 2t s_1 = 2t(18t + y)$, the result is

$$Q_y = 50t^2 s_1 = 50t^2(18t + y)$$

Doing the same for the right-hand side of the upper (or lower) flange produces the similar result

$$Q_y = 50t^2 s_2 = 50t^2(18t - y)$$

In both halves of the top flange, with $F_v/(I_{yy}t)$ being a constant, the shearing stress increases linearly from zero at the flange tips to the flange maximum value of

$$\sigma_{xs} = 900 \frac{F_v t^3}{I_{yy}(2t)} = 0.0041 \frac{F_v}{t^2}$$

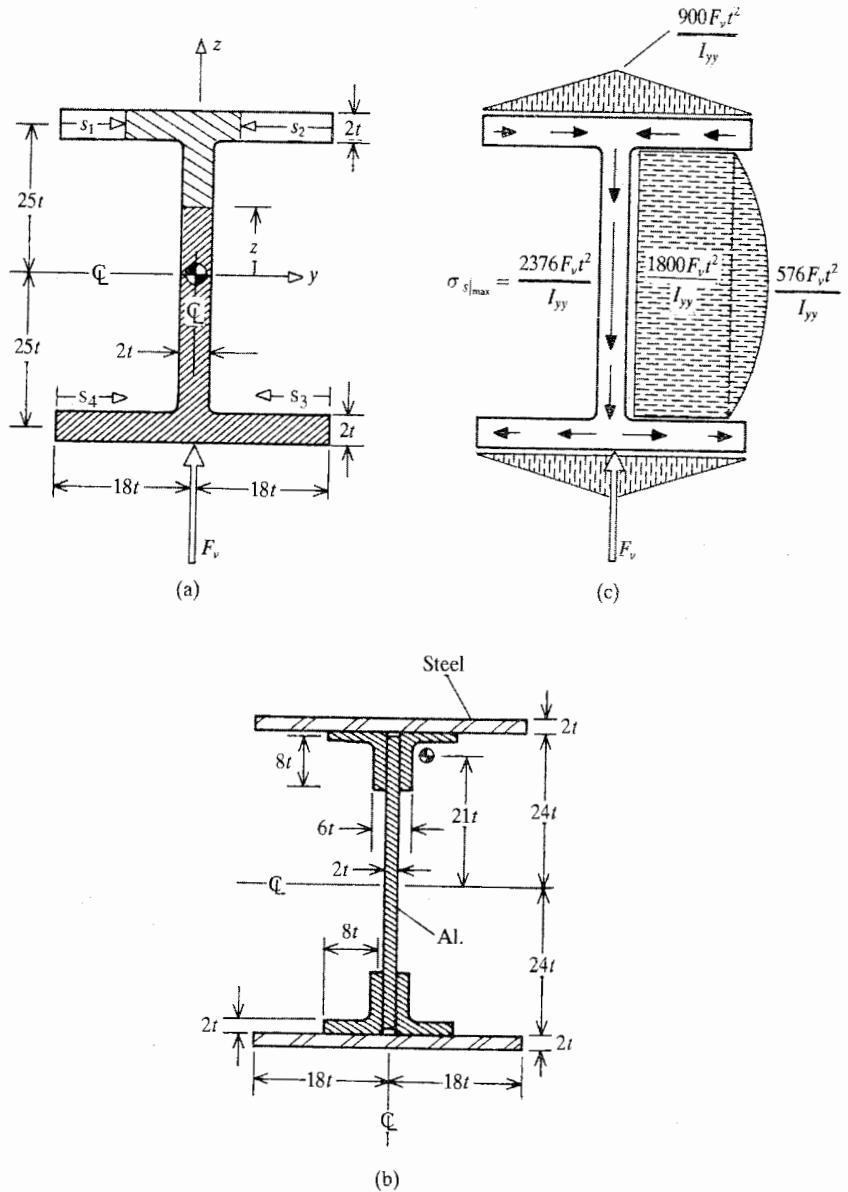


Figure 14.4. Examples 14.4: (a) homogeneous example, where all thicknesses are exaggerated; (b) nonhomogeneous (built-up) cross-section; (c) reacting shear stress diagram for the homogeneous case.

Proceeding from the web–flange juncture down the web with the arc length coordinate, that is, considering both the lightly hatched and plain areas of the cross-section,

$$\begin{aligned}
 Q_y(s) &= 25t(72t^2) + \left[z + \frac{1}{2}(24t - z) \right] (2t)(24t - z) \\
 &= 1800t^2 + t(576t^2 - z^2)
 \end{aligned}$$

Clearly the overall maximum value of the shearing stress occurs at the center of the web where $z = 0$. At the centroid

$$\sigma_{xs}|_{max} = 2376 \frac{t^3 F_v}{I_{yy}(2t)} = 0.011 \frac{F_v}{t^2}$$

Figure 14.4(c) shows a representation of the reacting shearing stresses.

(b) In this variation on part (a), the shearing stress equation becomes

$$\sigma_{xs}(s) = \frac{q(s)}{t} = \frac{F_v Q_y^*(s)}{I_{yy}^* t(s)}$$

and it is only necessary to adjust to the difference in the cross-section materials and the presence of the angle beams that provide the means of connecting the flanges to the web. In the right-hand side of the above equation, for the steel flange, for example, the calculation of the partial area moment becomes

$$Q_y^* = 3(50t^2)(s_2) = 150t^2(18t - y)$$

In this case I_{yy}^* also has a larger value, which is $288\,576t^4$ for the cross-section without the aluminum angles, plus $12\,900t^4$ for the aluminum angles, for a total of $301\,476t^4$. Thus the calculation for the maximum shearing stress in the top flange is

$$\sigma_{xs} = 2700 \frac{F_v t^3}{I_{yy}^* 2t} = 0.0045 \frac{F_v}{t^2}$$

which is little different from that of the homogeneous section, be it all-aluminum or all-steel. Proceeding to the web, past the centroid of the two angle beams,

$$\begin{aligned} Q_y^*(s) &= 3(25t)(72t^2) + 2(20t)(32t^2) \\ &\quad + \left[z + \frac{1}{2}(24t - z) \right] (2t)(24t - z) \\ &= 7320t^3 + t[576t^2 - z^2] \end{aligned}$$

Thus the maximum shearing stress is

$$\sigma_{xs}|_{max} = 7896 \frac{F_v t^3}{I_{yy}^* 2t} = 0.013 \frac{F_v}{t^2}$$

which again is little different from the previous result. ■

Example 14.5. Calculate the shearing stress distribution on the channel cross-section shown in Fig. 14.5(a), for positive values of both V_y and V_z . Let $a \gg t$, so then $I_{yy} = (8/3)a^3t$ and $I_{zz} = (5/12)a^3t$.

Solution. The induced shearing stress for this open cross-section beam reduces to

$$\begin{aligned} \sigma_{xs} &= \frac{V_z Q_y}{I_{yy} t} + \frac{V_y Q_z}{I_{zz} t} \\ &= \frac{3V_z}{8a^3 t^2} Q_y(s) + \frac{12V_y}{5a^3 t^2} Q_z(s) \end{aligned}$$

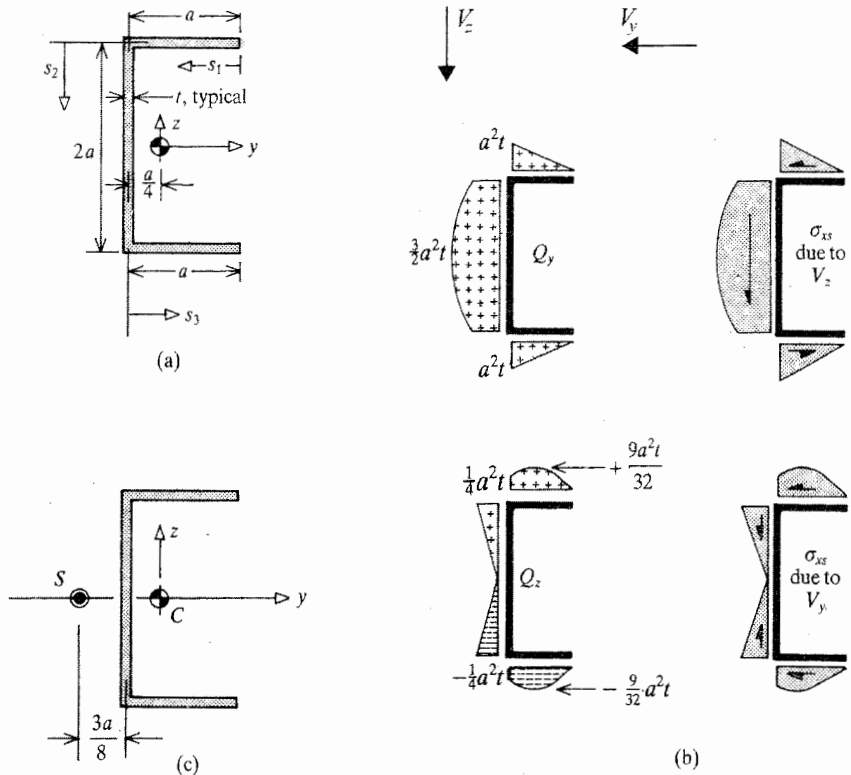


Figure 14.5. Examples 14.5 and 14.6: (a) cross-section and the various coordinates; (b) the first moments of the cross-sectional area and the corresponding induced stresses; (c) the shear center location.

Along the upper flange, $z = a$ and $s_1 = (3a/4) - y$. Therefore,

$$Q_y(y) = at \left(\frac{3a}{4} - y \right)$$

$$Q_z(y) = \left[y + \frac{1}{2} \left(\frac{3a}{4} - y \right) \right] t \left(\frac{3a}{4} - y \right) = t \left(\frac{9a^2}{32} - \frac{y^2}{2} \right)$$

Along the web, $s_2 = a - z$ and $y = -a/4$. Therefore,

$$Q_y(z) = a^2t + \left[z + \frac{1}{2}(a - z) \right] t(a - z) = \frac{t}{2}(3a^2 - z^2)$$

$$Q_z(z) = \frac{a^2t}{4} - \frac{a}{4}(a - z)t = \frac{atz}{4}$$

Along the lower flange, $z = -a$ and $s_3 = y + \frac{1}{4}a$. Therefore,

$$Q_y(y) = a^2t - a \left(y + \frac{1}{4}a \right) t = \frac{3a^2t}{4} - ayt$$

$$Q_z(y) = -\frac{a^2t}{4} + \left(\frac{y}{2} - \frac{a}{8} \right) \left(y + \frac{1}{4}a \right) t = \frac{t}{2} \left[y^2 - (3a/4)^2 \right]$$

Sketches of Q_y and Q_z and the shearing stresses induced by the two components of the total shear force are shown in Fig. 14.5(b). Note that these sketches are for induced shearing stresses rather than reacting shearing stresses. ■

14.4 The Open Section Shear Center

Recall that: (i) the shear center is defined as that unique point on the beam cross-section where the application of a shearing force does not produce a beam twist; and (ii) the locus of shear centers is called the elastic axis. Again, the further significance of the elastic axis is that it is also the axis of twist for the beam when a twisting moment is applied to the beam. See Endnote (1) for a proof of the latter statement.

The definition of the shear center, as the point where the application of a shear force does not cause a twisting rotation of the beam cross-section, provides all the information necessary to locate the shear center. Since any twisting moment causes a twist, it is simply a matter of placing the shear force at a point on the cross-section where the shear force and the *reacting* shear flow combine to produce a zero torsional moment about all points on the plane of the beam cross-section. This is the same as saying that the twisting moment about any point on the cross-section caused by the reacting shear stresses must be offset by the twisting moment about the same point caused by the applied shear force. For example, in order to calculate the distance e_y paralleling the y axis between the shear center and an arbitrarily selected moment center on the beam cross-section, it is only necessary to write the following moment equilibrium equation for the shear force resultant V_z and its reacting shearing stresses

$$V_z e_y = \oint r(s) \sigma_{xs}(V_z, s) t(s) ds \quad (14.6a)$$

where r is the perpendicular distance from the arbitrary moment center to each reacting stress vector σ_{xs} . Similarly, the vertical distance, e_z , from any arbitrary moment center (not necessarily the same one used to determine the horizontal location of the shear center) is determined from the moment equilibrium equation

$$V_y e_z = \oint r(s) \sigma_{xs}(V_y, s) t(s) ds \quad (14.6b)$$

Note that since reacting shear stresses are used in these two calculations, a summation of forces also produces a zero result. However, that summation only serves as a check upon the reacting shearing stress calculation. The following examples illustrate the process of locating the shear center for open cross-sections.

Example 14.6. Calculate the location of the shear center for the channel cross-section discussed in Example 14.5.

Solution. The first thing to do is to select a convenient moment center. A convenient moment center is one that causes as many as possible of the reacting shearing stresses, or reacting shear flows, along the cross-section centerline to have a zero moment arm, $r(s)$. The centerline point at either corner of the channel cross-section would cause those shearing stresses in the web and those in one of the flanges to have a zero moment arm, and thus would be a good choice. Another good choice for a moment center is that point where the beam cross-section axis of symmetry, the y axis, intersects the web centerline. In this latter case, only the shearing stresses in the web have a zero length moment arm, but because of the

symmetry, the moments about this middle point created by the shear flow in each flange have equal magnitudes. Thus the number of calculations is no more than if a corner point were chosen to be the moment center. In this example, the middle of the web centerline will be used as the arbitrary moment center for calculating both the horizontal and vertical offset of the shear center from that point on the cross-section.

To calculate the horizontal offset e_y of the shear center from the middle of the centerline of the channel web, it is of course necessary to work with the reacting shear flow that balances V_z . Using the reverse of the induced shear flow solution for V_z pictured in Fig. 14.5(b), where $I_{yy} = (8/3)a^3t$, and noting that the total reacting shearing force in each flange that results from the triangular shearing stress distribution is

$$\frac{V_z \left(\frac{1}{2}\right) (at^3)(a)}{\left(\frac{8}{3}a^3t\right) (t)} = \frac{3}{16} V_z$$

and that each of these reacting shearing forces has a moment arm of length a from the moment center, then the moment equation, Eq. (14.6a), becomes

$$V_z e_y = 2a \left(\frac{3}{16}\right) V_z$$

or

$$e_y = \frac{3a}{8}$$

The calculation of the vertical offset of the shear center from the selected moment center is even simpler. It is clear from the reacting shear stress diagram for V_y that, due to symmetry, there is no shearing stress-created moment about the chosen moment center. Thus the moment about the moment center created by the applied shear force, V_y , must also be zero. The only way that moment can be zero is for the vertical offset, e_z , to be zero. Hence the shear center is as pictured in Fig. 14.5(c). Note again that when the lines of action of the shearing stress resultants pass through the shear center, there is no moment about any point on the plane of the cross-section due to the shearing force and its reacting shearing stresses. ■

Example 14.6 illustrates the fact that whenever there is a geometric and material axis of symmetry, the reacting shearing stresses, due only to a shear force paralleling the axis of symmetry, also have to be symmetrically distributed. Thus that shear force must act along the axis of symmetry if there is to be no twisting moment acting upon the cross-section as a result of the application of that shear force to the beam cross-section. This argument, that the shear center is found on an axis of symmetry, applies equally well to closed as well as open cross-sections. Of course, centroids are also found on axes of symmetry. Therefore, if there happen to be two axes of symmetry for the cross-section, both the centroid and the shear center are located at their intersection, and are thus coincident. Hence the shear center for the rectangular cross-section of Example 14.1, and the shear centers for the two H cross-sections of Example 14.4 are coincident with the centroids of those cross-sections. The shear center for a circular pipe or a thin rectangular box cross-section would also lie at the cross-section centroid.

Using similar arguments to those above, it is possible to locate the shear center for many nonsymmetrical cross-sectional shapes without actually doing a mathematical calculation. For example, consider an angle beam cross-section where the flanges are oriented vertically

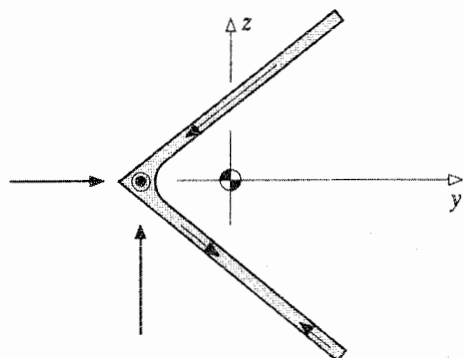


Figure 14.6. Example 14.7.

and horizontally. Let the two flanges be of different lengths and thicknesses. Place a vertical force at the corner of the angle beam cross-section. Since the reacting shear flow is always along the flange centerlines, then equilibrium in the horizontal direction requires that the shear flow in the horizontal flange must sum to a zero-valued horizontal force. Similarly, the reacting shear flow in the vertical flange must sum to a force that is equal and opposite to the applied shear force. Since the two vertical forces are colinear, they produce no twisting moment. Therefore the corner centerline point is the shear center.

Example 14.7. Locate the shear center for an equal-leg, angle cross-section where the smaller angle between the flanges is 78° rather than a right angle.

Solution. This cross-section has one axis of symmetry, which is selected to be the y coordinate axis. As Fig. 14.6 shows, this axis passes through the centroid and the corner of the angle. The shear center lies somewhere on that axis. Interestingly, this information is not needed in this case. It is only necessary to select the corner point where the centerlines of the two legs intersect as the moment center. With this moment center, regardless of the form of the shear flow distribution along the centerline of the angle legs, the reacting shearing stresses do not produce a moment about that moment center. Therefore, if the applied shearing forces also pass through that moment center, then the total moment on the cross-section about this moment center is zero. Thus, by definition, this particular moment center is the cross-section shear center. ■

14.5 Shear Flows in Thin-Walled Closed Cross-Sections

All that is additionally necessary to calculate the shear flow in a single-cell, closed, thin cross-section is to write the twisting moment equilibrium equation for the applied shear force and the reacting shear flows (or reacting shearing stresses). In the single-cell cross-section case, the reacting shear flow has two distinct parts that add together to form the total reacting shear flow. The first part of the total shear flow is $q_0 \equiv q(s = 0)$, which is the constant part of the shear flow everywhere along the centerline loop of the single cell. In the case of a closed cross-section, the constant q_0 term of Eq. (14.5) must be retained because there is, in general, no point on the closed centerline path where the total reacting shear flow is clearly zero. As was proved in Chapter 13, this constant shear flow around any closed

loop sums to a zero shearing force, but does produce a contribution to the twisting moment equilibrium equation of magnitude $2\hat{A}q_0$. The purpose of the twisting moment equilibrium equation is to determine the magnitude and direction of q_0 .

The second part of the total shear flow is the part involving the right-hand side terms in Eq. (14.5) other than q_0 ; that is, the part of the shear flow that would be the sole shear flow if the closed cross-section were cut open at the point $s = 0$. Of course, this part of the reacting shear flow produces a shearing force that equilibrates the applied shearing force. The moment contribution of this second part of the total shear flow to the torsional moment equilibrium equation is calculated in exactly the same way its moment is calculated in the process of locating the shear center of an open cross-section. The following example illustrates the solution process of writing the moment equilibrium equation for the purpose of calculating q_0 with sufficient generality to be a model for all such cross-sections.

Example 14.8. For the indicated shearing force, determine the shear flow along the centerline of the single-cell, thin, closed, triangular beam cross-section shown in Fig. 14.7(a). The indicated dimensions are, as usual, centerline dimensions.

Solution. The shear flow along the centerline of the thin cross-section is described by the following form of Eq. (14.5):

$$q(s) = q_0 + \frac{V_z Q_y(s)}{I_{yy}}$$

where, again, $q_0 = q(s = 0)$. Start the arc length coordinate at the right-hand apex. At this point $s = 0$, $Q_y = 0$, and q_0 is the total shear flow.

The first task is to calculate I_{yy} . This moment of inertia about the y axis is the sum of the contribution made by the left-hand web and twice the contribution made by the top flange. The top flange contribution is its moment of inertia at its own centroid about an axis parallel to the y axis plus the transfer term to the cross-section y axis. To obtain the top flange moment of inertia at its own centroid parallel to the y axis, use is made of the area moment of inertia axis rotation equations, Eqs. (9.14). In the rotation equation that determines I_{yy} , the moment of inertia of the top flange about its own centerline is completely neglected because it is such a small term. Therefore, the moment of inertia for the entire cross-section at its centroid is

$$\begin{aligned} I_{yy} &= (1/12)(t)(30t)^3 + 2[(1/12)(t)(39t)^3 \sin^2(22.62^\circ) \\ &\quad + (7.5t)^2(39t^2)] \\ &= 2250t^4 + 2[731.25t^4 + 2193.75t^4] = 8100t^4 \end{aligned}$$

Now, for the first moment of the partial area,

$$0 \leq s \leq 39t \quad Q_y(s) = (1/2)(15s/39)(st) = (15/78)s^2t$$

$$\text{and} \quad Q_y(39t) = 292.5t^3$$

$$\begin{aligned} 0 \leq z \leq 15t \quad Q_y(z) &= 292.5t^3 + t(15t - z) \left[z + \frac{1}{2}(15t - z) \right] \\ &= 405t^3 - \frac{1}{2}z^2t \end{aligned}$$

There is no need to go further since the first moment of area is symmetric about the y axis, returning to a zero value at the right-hand apex. Now all is ready to write the torsional

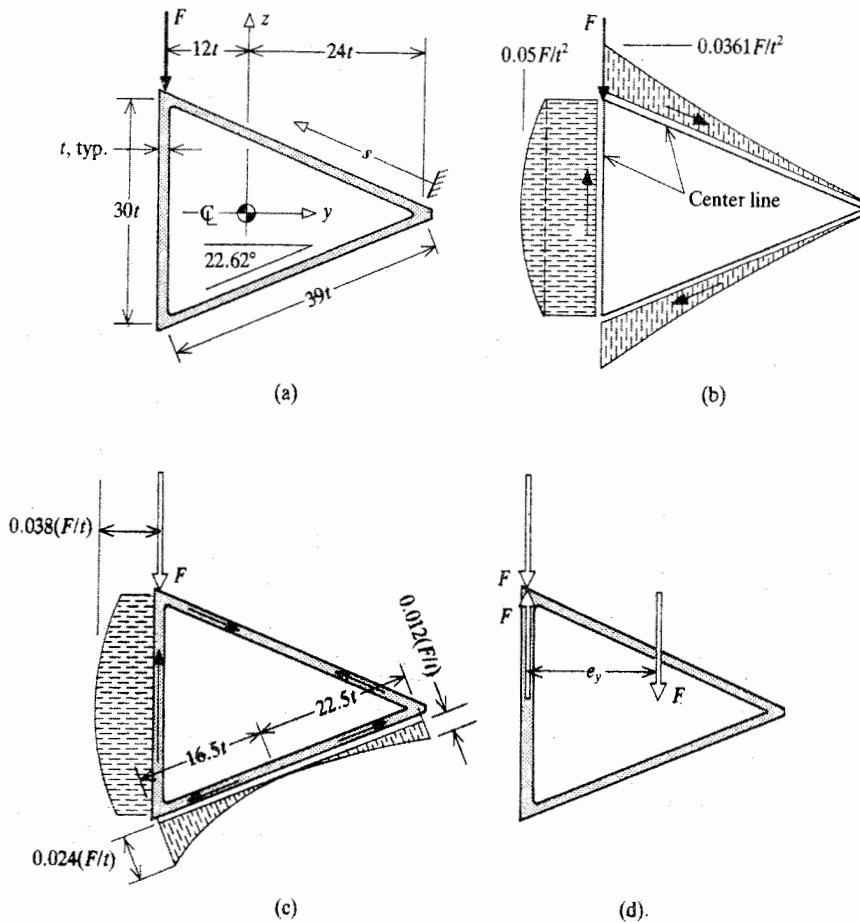


Figure 14.7. Example 14.8 and 14.9: (a) cross-section geometry, coordinates, and loading; (b) reacting open section shear stress distribution for opening at $s = 0$ (an equilibrium check: horizontal forces clearly sum to zero; upward web force is $1.361F$, while the downward component of both total flange forces is $0.361 F$, and thus there is vertical force equilibrium; yet there is no moment equilibrium because these open section shear stresses are only one part of the total solution); (c) the actual reacting shear flow as the sum of the open and closed cross-section shear flows; (d) the scheme to locate the closed section shear center by applying a torque so as to make the twist equal to zero.

moment equilibrium equation. The selected moment center is at $s = 0$, which eliminates the moment terms associated with the open section reacting shear flow of the two slanting flanges. There is a moment term for the applied shear force, F , a moment term for the first part of the reacting shear flow, q_0 , around the entire centerline, and a moment term for the open section reacting shear flow at the web. Again, from Eq. (13.8), the torque produced by the constant shear flow is $2q_0\hat{A}$. The torque due to the second part of the reacting shear flow, $V_z Q_y(s)/I_{yy}$, has to be integrated just as it was for the shear center calculation. Hence, with counterclockwise moments as positive, and the reacting shear flows oppositely directed to the arc length coordinate, the moment equilibrium equation for the purpose of determining

the unknown value of q_0 is

$$\begin{aligned}
 0 &= F(36t) - 2q_0(15t)(36t) - \oint r(s)q(s) ds \\
 0 &= 36Ft - 1080q_0t^2 - 2\frac{F(36t)}{8100t^4} \int_{z=0}^{15t} (405t^3 - \frac{1}{2}z^2t) dz \\
 0 &= 36Ft - 1080q_0t^2 - \frac{F(72t)}{8100t^4} [(405t^3)(15t) - (1/6)(15t)^3(t)] \\
 0 &= 36Ft - 1080q_0t^2 - \frac{F(72t)}{8100t^4} (5512.5t^4) \\
 0 &= 36Ft - 1080q_0t^2 - 49Ft
 \end{aligned}$$

Hence the solution for q_0 is

$$q_0 = -0.01204 \frac{F}{t}$$

where the negative sign indicates that this reacting shear flow is counterclockwise. This solution for the reacting q_0 needs only to be added to the second part of the total reacting shear flow to complete the solution for the total reacting shear flow, which is $q(s) - 0.01204(F/t)$. When the two oppositely directed reacting shear flows are combined as indicated, the point on the upper flange where the two shear flows cancel each other can be determined to be at the value s where $FQ_y/I_{yy} = q_0$, or

$$s^2 = (78/15)(0.01204)(I_{yy}/t^2)$$

or

$$s = 22.5t$$

Thus a sketch of the total reacting shear flow directions is as shown in Fig. 14.7(c). ■

The calculation of the location of the shear center for the above triangular cross-section can be accomplished by loading the cross-section with a moment of magnitude $e_y F$, such as that shown in Fig. 14.7(d). The quantity e_y , and hence the location of the shear center, is to be determined on the basis that: (i) the original downward load F is canceled by the upward force of the fictitious moment loading, and (ii) with the downward force of the fictitious moment loading acting at the shear center, the triangular cross-section does not twist. The key step of this scheme, setting the cross-sectional twist equal to zero, rests upon the fact that the derivation for the beam twist per unit length, θ , presented in Appendix A, Section 5, is applicable to variable shear flows as well as constant shear flows. Repeating Eq. (13.9),

$$\theta = \frac{1}{2G_0\hat{A}} \oint_{\delta C} \frac{q_r}{t^*} ds = 0$$

where $q_r = q_r(s)$ is the total reacting shear flow. Here the total reacting shear flow is equal to the sum of the previously calculated counterclockwise reacting shear flow q_0 , the clockwise open section reacting shear flow $q(s)$, and the counterclockwise reacting shear flow due to the introduction of the moment $e_y F$, whose shear flow magnitude is $e_y F/(2\hat{A})$.

Example 14.9. Calculate the location of the shear center of the thin, triangular cross-section of Example 14.8.

Solution. The shear center lies somewhere on the axis of symmetry, which is the y axis. To take advantage of the results of Example 14.8, introduce the additional straightening moment $e_y F$ as shown in Fig. 14.7(d). The equation to be solved for e_y is the zero twist equation, which reduces in this case to the line integral of the total shear flow around the triangle equals zero. Here $2\hat{A} = 1080t^2$, so

$$\int \left(q_0 - q(s) + \frac{e_y F}{1080t^2} \right) ds = 0$$

After transposing the second term, the equality becomes

$$\begin{aligned} 0.01204 \frac{F}{t} (108t) + \frac{108te_y F}{1080t^2} \\ = +2 \frac{F}{I_{yy}} \int_{z=0}^{z=39t} \frac{15}{78} s^2 t ds \\ + 2 \frac{F}{I_{yy}} \int_{z=15t}^{z=0} \left(405t^3 - \frac{1}{2} z^2 t \right) (-dz) \end{aligned}$$

$$\text{or} \quad 1.3003 + 0.1(e_y/t) = 0.9389 + 1.5 - 0.1389$$

$$\text{or} \quad e_y = 10t$$

which places the shear center slightly to the left of the centroid. ■

The application of this form of analysis to multicell cross-sections is quite possible, but not particularly recommended because of shear lag and cross-section distortion effects. Nevertheless, the procedure is briefly outlined as follows for those few multicell cross-sections which, while still thin, are also sufficiently compact that shear lag and distortional effects are minimal.

Imagine “cuts” in the thin outer walls of each cell of the closed cross-section. These “cuts” convert the closed cross-section to one that is now open. The second part of the total shear flow can now be calculated upon the basis that the cross-section is open. However, at each “cut” there is actually an unknown shear flow; that is, a q_0 for each cell. Call these constant shear flows q_i , where $i = 1, 2, \dots$. Thus for a cross-section with n cells, there are n unknown shear flow values. Of course these unknown shear flow values have to be added to the “open” section part of the shear flow to obtain the total shear flow. The n equations that determine the q_i , and thus complete the calculation of the total shear flow, are (i) one torsional equilibrium equation just like the one equation that was the crux of Example 14.8, and (ii) the $n - 1$ equations that say that the angles of rotation of the n cells are equal. Again, Eq. (13.9) is to be used to calculate the angles of rotation of each cell. Once the q_i are determined by simultaneous solution of the n equations, then the rotation of the cross-section, the same as that of any cell, is open to a quick calculation since the rotation per unit length equations were used to determine the q_i .

The shear center of the compact, thin, multicell cross-section can be located by using the second of Eqs. (13.11) in order to calculate the torque acting on any one cell that is necessary to counterbalance the actual twist per unit length calculated above. That torque can be equated to $e_y F$ is done in the above example.

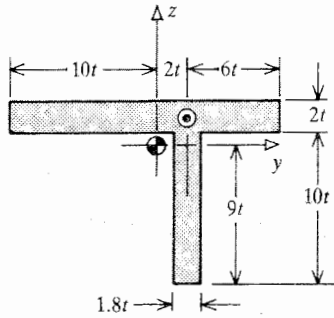


Figure 14.8. Example 14.10. An unsymmetrical, idealized T cross-section.

14.6 Summary

The calculation of shear flows that arise from the application of shearing forces to thin beam cross-sections is useful for the purposes of (i) insuring against shear buckling in individual beam webs, and (ii) locating shear centers for open cross-sections and single-cell, closed cross-sections. The importance of the shear center is that its locus is the beam axis of twist. Hence the shear center is the unique point on the cross-section where the bending and twisting deflections do not interact for small deflections. Therefore the bending and twisting degrees of freedom (to be discussed) are located along the loci of shear centers, which, again, is called the beam elastic axis. The shear center is located for an open cross-section by merely writing an appropriate twisting moment equilibrium equation. The shear center for a closed section additionally requires setting the twist per unit length equal to zero.

The following two example problems provide further instruction in calculating shear flows and locating shear centers for open and closed cross-sections. The exercises that follow provide further practice.

Example 14.10. Consider the idealized, homogeneous, open cross-section shown in Fig. 14.8. The area moments of inertia are as follows: $I_{yy} = 594t^4$, $I_{zz} = 1085t^4$, and $I_{yz} = -216t^4$. (a) Calculate Q_y and Q_z at every point along the cross-section centerline. (b) Calculate the magnitude of the reacting shearing stress at the centerline point $y = +2t$, $z = -2t$ in response to a positive (i.e., downward) shearing force of magnitude F_0 acting at the cross-section's shear center. (c) Without making a calculation, justify the assertion that the cross-section's shear center is at the intersection of the flange and web centerlines, that is, at the point $y = +2t$, $z = +2t$.

Solution. (a) The partial area moments are as follows:

$-10t \leq y \leq 2t$	$Q_y(y) = 2t(10t + y)(2t) = 4t^2(10t + y)$
area to left	$Q_z(y) = 2t(10t + y) \left[-\frac{1}{2}(10t - y) \right] = -t(100t^2 - y^2)$
$2t \leq y \leq 8t$	$Q_y(y) = 2t(8t - y)(2t) = 4t^2(8t - y)$
area to right	$Q_z(y) = 2t(8t - y) \left[-\frac{1}{2}(8t + y) \right] = t(64t^2 - y^2)$
$-9t \leq z \leq t$	$Q_y(z) = 1.8t(9t + z) \left[-\frac{1}{2}(9t - z) \right] = -0.9t(81t^2 - z^2)$
area below	$Q_y(z) = 1.8t(9t + z)(2t) = 3.6t^2(9t + z)$

It is, of course, not necessary to work inward from the ends of the centerlines. For example, again for the right-hand portion of the flange and for the web,

$$\begin{array}{ll}
 2t \leq y \leq 8t & Q_y(y) = 4t^2(10t + y) - 72t^3 \\
 \text{area to left} & Q_z(y) = 36t^3 - t(100t^2 - y^2) \\
 -9t \leq z \leq t & Q_y(z) = 72t^3 + 0.9t(t^2 - z^2) \\
 \text{area above} & Q_z(z) = 3.6t^2(t - z) - 36t^3
 \end{array}$$

Note that the above two alternate solutions are the negative of the first stated solutions. The sign difference is a result of the fact that the implicit centerline coordinate s , and hence the positive direction of the reacting shearing stress, is oppositely directed in the original and alternate cases. Note further that because the flange is nonsymmetric, the values of the partial area moments for the left- and right-hand parts of the flange do not match at the web centerline where $y = +2t$. Finally note that the latter two pairs of partial area moments go to zero at the end of their course.

(b) The applied loading at the cross-section is such that $V_z = +F_0$. Thus the formula for the shear flow is

$$q(s) = -\frac{V_z Q_z(s)}{R_{yz}} + \frac{V_z Q_y(s)}{R_{zz}}$$

The ratios of inertia are $R_{yz} = -2768t^4$, and $R_{zz} = 551t^4$. Thus, using the first listed values for the partial area moments, those where the area is below the point where the partial area moment is calculated, leads to

$$\begin{aligned}
 \sigma_{xs}(2t, -2t) &= \frac{F_0}{1.8t} \left(+\frac{3.6t^2(7t)}{2768t^4} - \frac{0.9t(77t^2)}{551t^4} \right) \\
 &= -0.065 \frac{F_0}{t^2}
 \end{aligned}$$

Since the s coordinate for this calculation is going up the web centerline, the above negative sign means that the induced shearing stress, as would be expected, is downward at the selected centerline point. Thus the reacting shearing stress is upward with the magnitude $0.065 F_0/t^2$.

(c) The total shear force acting upon the beam cross-section has to be in equilibrium with the reacting shear flow. Thus the total upward force produced by the reacting shear flow has to counterbalance the downward applied shear force F_0 . The upward force produced by the reacting shear flow is entirely a result of the shear flow in the web. This is so because the shear flow in the flange is everywhere approximated as horizontal and thus cannot produce a vertical force. In order for there to be moment equilibrium between the applied shear force and the reacting shear flow, the force produced by the reacting shear flow in the web must be colinear with the applied shear force. In other words, the applied shear force must act along the centerline of the web to avoid a net moment upon the cross-section. Thus the shear center must lie somewhere along the centerline of the web, or its extension. Note further that the shear flows in the flange have to sum to a zero magnitude horizontal force.

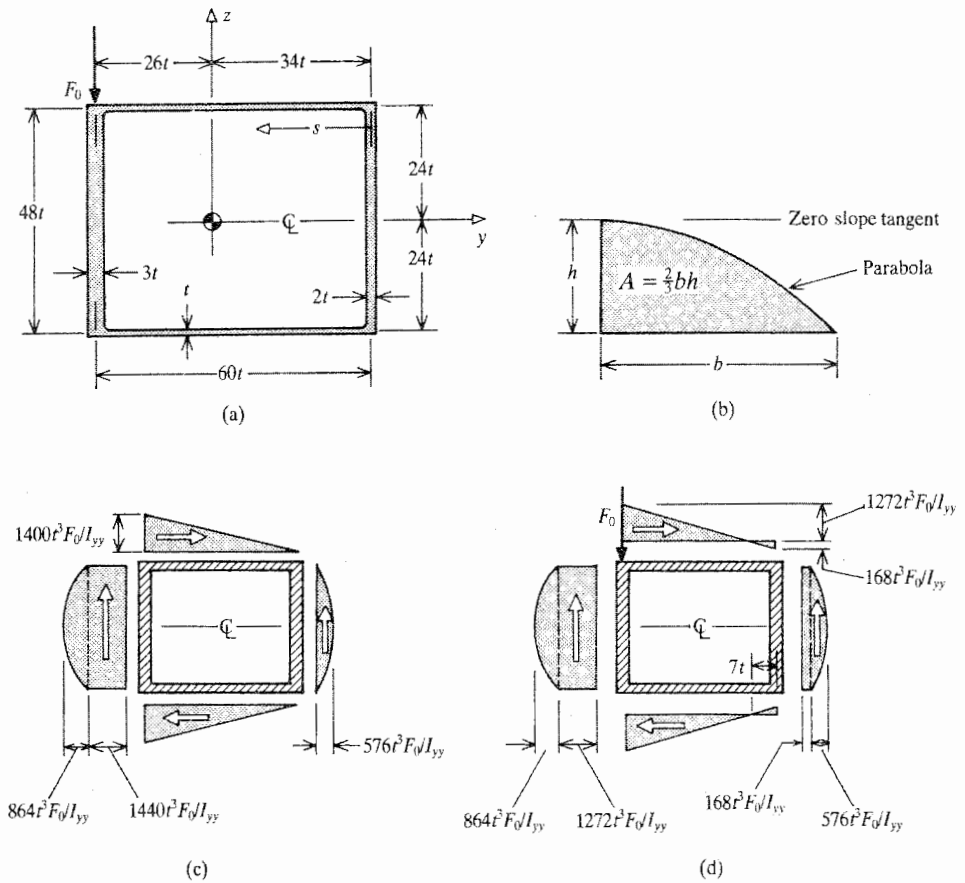


Figure 14.9. Example 14.11. (a) idealized box beam geometry and loading; (b) useful parabolic area formula; (c) reacting open section shear flow; (d) total reacting shear flow.

Now repeat the above style of argument for a horizontally directed applied shear force acting upon the cross-section. The conclusion is that for a zero net moment, that horizontally applied shear force has to be colinear with the flange centerline. Hence the shear center lies at the juncture of the flange and web centerlines. ■

Example 14.11. (a) Calculate and sketch the shear flow in the idealized, single-cell, closed cross-section shown in Fig. 14.9(a), where all dimensions are centerline dimensions. The total shear force acting on the cross-section has the magnitude F_0 and its point of application is the upper left corner of the cross-section. (b) Locate the shear center for this cross-section.

Solution. (a) In this case $V_y = 0$ and $V_z = +F_0$, and, because of the one axis of symmetry, the area product of inertia is zero. Thus Eq. (14.5) reduces to

$$q(s) = q_0 + \frac{F_0 Q_y}{I_{yy}}$$

A straightforward calculation shows that $I_{yy} = 115\,200t^4$. The calculation of the partial area moments begins with selecting a starting point for the centerline coordinate s . The upper

right-hand corner is chosen for the origin of the s coordinate, and, as always, it proceeds counterclockwise. With that choice, the relevant partial area moments are as follows:

$$\begin{aligned}
 \text{Top flange} \quad Q_y(y) &= t(34t - y)(24t) = 24t^2(34t - y) \\
 \text{Left web} \quad Q_y(z) &= 1440t^3 + 3t(24t - z) \left[\frac{1}{2}(24t + z) \right] \\
 &= 1440t^3 + 1.5t(576t^2 - z^2) \\
 \text{Bottom flange} \quad Q_y(y) &= 1440t^2 + t(26t + y)(-24t) \\
 &= 1440t^3 - 24t^2(26t + y) \\
 \text{Right web} \quad Q_y(z) &= 0 + 2t(24t + z) \left\{ - \left[24t - \frac{1}{2}(24t + z) \right] \right\} \\
 &= -t(576t^2 - z^2)
 \end{aligned}$$

Note that the partial area moments return to zero at the other end of the centerline, as they must. The next step is to calculate q_0 , the shear flow at $s = 0$. The value of q_0 is determined by the requirement that the total moment acting upon the cross-section about any moment center must be zero. A convenient moment center is the bottom left-hand corner. At that point the moment arms for the applied force, the shear flow in the left web, and the shear flow in the bottom flange are zero. There are two things to recall when writing this moment equation. The first thing is the result from Chapter 13 that the moment due to a constant shear flow such as q_0 is $2\hat{A}q_0$. The second thing, easily proved, is that the area under a parabolic segment which has a zero slope at its apex, as shown in Fig. 14.9(b) is two-thirds of the product of the base and the height. Therefore, after assuming (*incorrectly*) that the constant reacting shear flow q_0 is clockwise, and referring to Fig. 14.9(c), which is a plot of the reacting "open section" shear flows, which of course are proportional to the partial area moments, the moment equilibrium equation is

$$0 = \frac{F_0}{I_{yy}} \left[\frac{1}{2}(1440t^3)(60t)(48t) - \frac{4}{3}(576t^3)(24t)(60t) \right] + 2(60t)(48t)q_0$$

or

$$q_0 = -168t^3 \frac{F_0}{I_{yy}} = -(1.4583 \times 10^{-3}) \frac{F_0}{t}$$

where the negative sign indicates that the reacting q_0 is actually counterclockwise. Figure 14.9(d) is a sketch of the total reacting shear flow, $(q_0 + F_0 Q_y / I_{yy})$. Obviously, the net horizontal force produced by this total shear flow is zero, and it may be verified that the net upward vertical force produced by this reacting shear flow has the value $+F_0$.

(b) To determine the location of the shear center for this single-cell cross-section, first note that the shear center lies on the y axis because that is an axis of symmetry. To locate the vertical axis of the shear center, picture placing another downward shear force of magnitude F_0 at the unknown location of the shear center, a distance e_y to the right of the left web centerline. Also place an upward shear force of magnitude F_0 at the left web centerline. This latter force equilibrates the original applied shear force, and at the same time forms a twisting moment of magnitude $e_y F_0$ with the new downward F_0 . The moment arm e_y is to be adjusted so that the twist per unit length created by this newly applied twisting moment offsets the oppositely directed twist per length created by the original (actual)

applied loading. Using Eq. (13.9) to set the total twist per unit length equal to zero leads to the following reacting shear flow equation:

$$0 = \oint \frac{q_r(s)}{t(s)} ds$$

where

$$q_r(s) = q_0 + \frac{F_0 Q_y(s)}{I_{yy}} - \frac{e_y F_0}{2\hat{A}}$$

The calculation is a bit lengthy, but straightforward. First substitute $q_0 = -168 F_0 t^2 / I_{yy}$, and then transpose the "open cross-section" portion of the shear flow. Using the geometric areas sketched in Fig. 14.9(c) to carry out the integration of the open cross-section shear flow leads to

$$\begin{aligned} & -\frac{168 F_0 t^3}{I_{yy}} \left(\frac{2(60t)}{t} + \frac{48t}{3t} + \frac{48t}{2t} \right) \\ & - \frac{e_y F_0}{2\hat{A}} \left(\frac{2(60t)}{t} + \frac{48t}{3t} + \frac{48t}{2t} \right) \\ = & -\frac{F_0}{I_{yy}} \left(\frac{2(1/2)(1440t^3)(60t)}{t} + \frac{(1440t^3)(48t)}{3t} \right. \\ & \left. + \frac{(2/3)(864t^3)(48t)}{3t} - \frac{(2/3)(576t^3)(48t)}{2t} \right) \end{aligned}$$

or

$$\begin{aligned} & \frac{168(160)}{115\,200} + \frac{e_y}{t} \frac{120}{5760} \\ = & \frac{86\,400 + 23\,040 + 9216 - 9216}{115\,200} \end{aligned}$$

or

$$e_y = 34.4t$$

Thus the shear center lies on the weak side of the cross-section, slightly farther to the right of the geometric center than the centroid is to the left of the geometric center. ■

The cross-sections of Examples 14.9 and 14.10 differ not only in that the former is open while the latter is closed, but also in that the former, T cross-section is relatively compact, while the latter, box, cross-section is not at all compact. The lack of compactness of the box cross-section calls into serious question the accuracy of the shear flow solution for this cross-section. If the width and depth of the cross-section were, say, one-third of the dimensions specified, then the above analysis would be credible. As those dimensions are, the above analysis for the shear flows has to be considered to be nothing more than an estimate. See Exercise 14.8.

The above example demonstrates that care must be taken with the signs of the shear flow. In order to simplify the task of keeping track of the correct signs, the reader should consistently adhere to using only reacting shear flows or only induced shear flows. Finally, if the analyst only desires to locate a shear center, then the suggested procedure is to apply

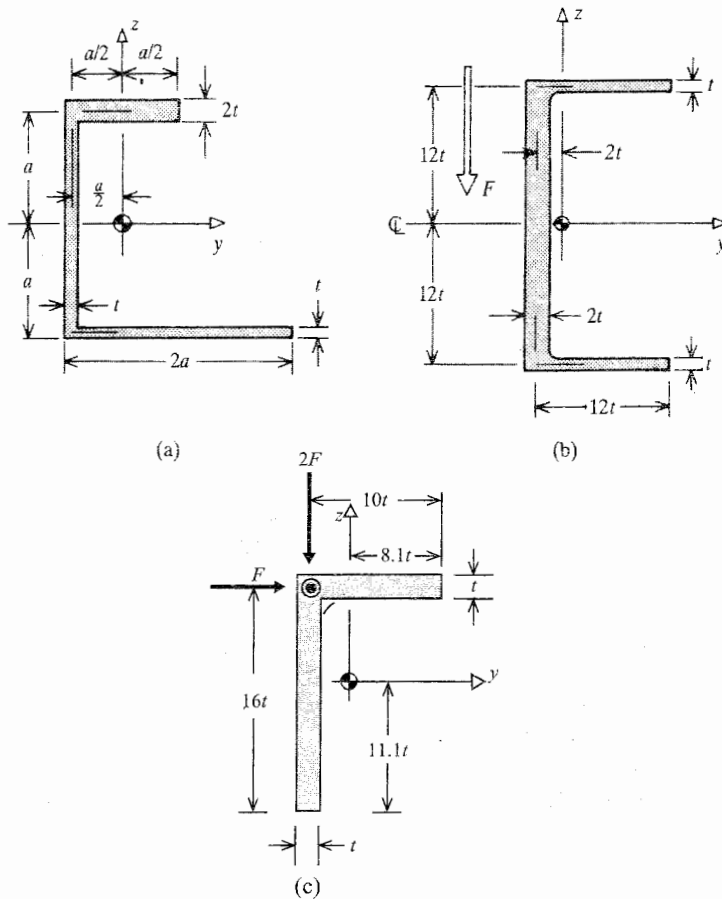


Figure 14.10. (a) Exercise 14.1(a, b). (b) Exercise 14.1(c, d). (c) Exercise 14.1(e).

a shear force of arbitrary magnitude at any convenient point on the cross-section, and then proceed as illustrated in the above triangular and rectangular, thin cross-sections.

Chapter 14 Exercises

- 14.1. (a) Calculate both Q_y and Q_z at all points along the material centerline of the homogeneous, nonsymmetrical, channel cross-section shown in Fig. 14.10(a). Express both area moments only in terms of the y and z centroidal coordinates. Be sure to simplify your answers.
- (b) Describe in words only how you would go about calculating the shearing stress distribution over this cross-section that would result from a resultant shearing force with arbitrary horizontal and vertical components.
- (c) Calculate the shear stresses in the channel cross-section sketched in Fig. 14.10(b) due to the vertical shear force shown.
- (d) Calculate the shear stresses in the channel cross-section of Fig. 14.10(b) if now the applied shear force is a horizontal force acting along the axis of symmetry.

- (e) Consider the idealized, homogeneous, cross-section shown in Fig. 14.10(c). The two components of the shearing force acting upon the cross-section are shown in the sketch. The approximate geometric parameters for this cross-section are as follows:

$$I_{yy} = 736t^4 \quad I_{yz} = 246t^4 \quad I_{zz} = 238t^4$$

$$\therefore R_{yy} = 156t^4 \quad R_{yz} = 466t^4 \quad R_{zz} = 482t^4$$

Since $V_y = -F$, and $V_z = 2F$, the expression for the shear flow due to these two shearing force components is

$$q = \frac{F}{t^4}(0.0063 Q_y - 0.0107 Q_z)$$

Write the expressions for Q_y and Q_z as functions of the centroidal coordinates.

- 14.2.** (a) Calculate the shear flow in the T cross-section of Fig. 9.18(c) if a vertical shearing force of magnitude F is applied to the cross-section shear center.
 (b) As above, for a horizontal shearing force of magnitude F applied to the cross-section shear center.
 (c) Locate the shear center of this T cross-section.
 (d) Using only words, not equations, explain how you would estimate the maximum shearing stress in the T cross-section (away from the fillets at the T juncture) if the vertical force F were applied at the left tip of the T cross-section rather than at the shear center.
- 14.3.** (a) Without a temperature change, calculate the shear flow in the channel cross-section of Fig. 9.17(b) due to a vertical shear force F applied at the cross-section shear center.
 (b) Repeat part (a), but this time include the effect of the indicated temperature change that is constant with respect to beam length. Note that the temperature change not only affects the Young's modulus of the top flange, but now Eq. (14.3) needs to be employed rather than Eq. (14.5).
- 14.4.** Calculate the shear flow in a thin, (closed) circular pipe of mean radius R and thickness t when it is subjected to a vertical shear force of magnitude F at the cross-section shear center, which, of course, is the same point as the centroid. *Hint:* By reason of the one axis of symmetry of loading and geometry, the total shear flow at the points on the material centerline intersected by the line of action of the shearing force (the z axis) is zero. Thus, in effect, this is an "open" cross-section. Use the counterclockwise coordinate $\alpha = s/R$ to locate points on the cross-section, with $\alpha = 0$ at $z = R$. Use the counterclockwise coordinate β such that $0 \leq \beta \leq \alpha$ for the purpose of carrying out the integration necessary to obtain the partial area first moment.
- 14.5.** (a) Locate the shear center of a thin semicircular cross-section of mean radius R and thickness t . Let the y axis be the axis of symmetry of the geometry, and use the angular coordinates of the previous exercise.
 (b) Locate the shear center of a thin, full circular cross-section with a single cut of negligible width at $y = R$. Note that the cut makes the cross-section an open cross-section. Use the coordinate α measured counterclockwise from the y axis, and β as described in the previous problem.

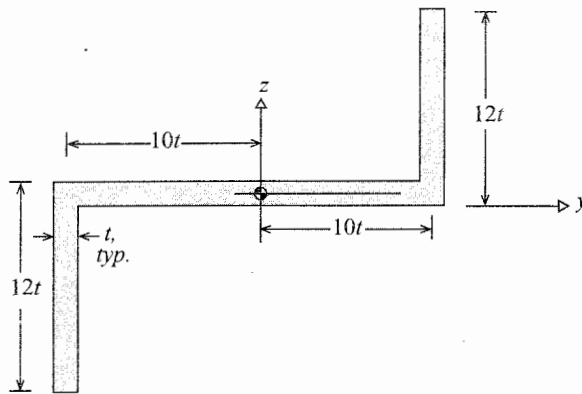


Figure 14.11. Exercise 14.6.

- (c) Locate the shear center of a thin circular cross-section of mean radius R and thickness t that only covers a sector of 240° . Note that with $R^2 \gg t^2$, I_{yy} , the moment of inertia about the axis of symmetry, is $[(2\pi/3) - (\sqrt{3}/4)]R^3t$.
- (d) As in part (c) above, locate the shear center of a thin circular cross-section that covers a sector of 270° .
- 14.6. (a) Determine the first moments of partial area for the Z cross-section shown in Fig. 14.11.
- (b) Write the expression for, and sketch the reacting shear flow distribution when the only applied load is $V_z = F$. For your information, $I_{yy} = 1154t^4$, $I_{zz} = 3069t^4$, and $I_{yz} = 1440t^4$.
- (c) Locate the shear center for the Z cross-section.
- 14.7. (a) Calculate the shear flow in the Z cross-section with equal length flanges of Fig. 9.10 if a vertical shearing force of magnitude F is applied to the cross-section shear center. Use a constant Young's modulus.
- (b) As above, for a horizontal shearing force of magnitude F .
- (c) Locate the shear center of this Z cross-section.
- 14.8. Calculate the shear flow in the reinforced angle cross-section of Fig. 9.18 if a vertical shearing force of magnitude F is applied to the cross-section shear center. *Hint:* Eq. (14.5) is wholly adequate to this task everywhere except where two materials together make up the cross-section thickness. If the materials had much different moduli in that region, an engineering solution would be to ignore the weaker material. In this case, the moduli are close in value. In this case the engineering solution is to use the actual m.w. centroid and moments of inertia, but use an average modulus where the two materials together make up the cross-section thickness for the calculation of the partial area first moments. This approximation is of little consequence because in this part of the cross-section the thickness is greater than any other part, and $\sigma_{xs} = q/t$.

FOR THE EAGER

- 14.9. (a) Locate the shear center of the thin, single-cell cross-section whose centerline geometry is like the letter D, that is, it is a semicircle of radius R closed along its diameter. The thickness is everywhere t .

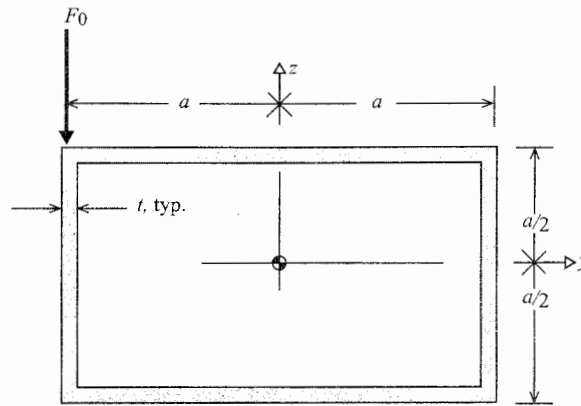


Figure 14.12. Exercise 14.11.

- (b) As above, but for the cross-section of Fig. 14.9(a) with the alteration that the centerline depth of the cross-section is changed from $48t$ to $24t$. *Hint:* The centroid is now a distance $27t$ from the centerline of the left web. (Note that the results of this exercise may be beyond the fringe of accuracy, but these dimensions put the location of the centroid at an integer distance from the left web.)
- (c) A depth and width for the geometry of Fig. 14.9(a) that would allow reasonable solution accuracy are $16t$ and $10t$ respectively. With this depth and width, and the same thicknesses, locate the shear center. The cross-sectional area is $100t^2$, and the centroid is located at $4.2t$ to the right of the left web centerline.

- 14.10.** The orientations of the cross-sections of the previous examples and exercises were chosen to avoid the inconvenience of having to deal immediately with negative moment arms for the calculation of the first moments of partial area. The channel section shown in Fig. 14.12 is different from the previous cross-sections in that respect. The simplest thing to do is just turn the cross-section upside down (i.e. reverse the directions of the coordinate axes) to have the familiar case of being able to begin with positive-valued moment arms. If for some reason that switch of coordinate directions would not be desirable, then it would be necessary to face up to challenge of negative moment arms. Therefore, calculate the first moments of partial area for the coordinate axes as shown. If there was a burning desire to calculate the shear flow too, then $I_{yy} = 2670t^4$, $I_{zz} = 420t^4$, and $I_{yz} = 0$.
- 14.11.** Accurately sketch the *resisting* shear flow in the thin rectangular cross-section due to the shearing force acting on the left web as shown in Fig. 14.12. *Hint:* Replace the given load by a shearing force of the same magnitude acting at the shear center, plus a moment, so that the new load system is statically equivalent to the original load. That is, let

$$\downarrow \square = \downarrow \square + \uparrow \square + \square \downarrow$$

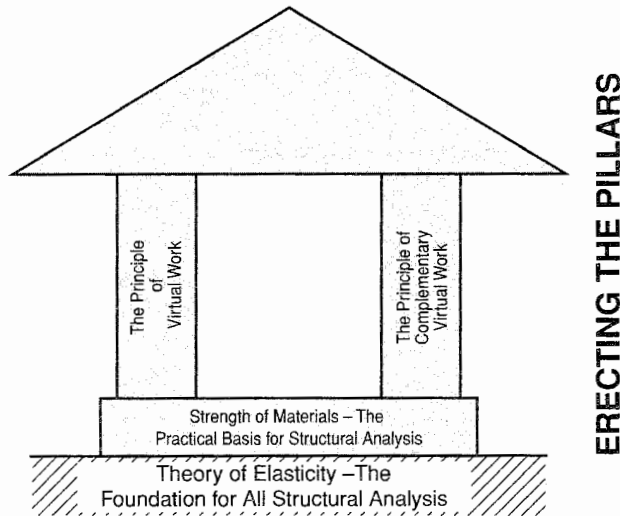
and then deal separately with the shear force and the moment.

Endnote (1) The Shear Center as the Center of Twist

The fact that the shear center is also the center of twist for an arbitrary cross-section is easily established by use of Maxwell's reciprocity theorem, which is discussed in Section 20.11, and demonstrated in Exercise 19.4. Restated in a form that is most useful here, Maxwell's reciprocity theorem¹ says that the work done by a first force or moment moving through the displacement caused by a second force or moment is equal to the work done by the second force or moment moving through the displacement caused by the first force or moment. Let the first load be an arbitrary shearing force acting at the shear center. Call it V . This force produces a bending deflection, call it v but, by definition, does not produce a rotation. Let the second load be an arbitrary moment about the shear center, M_t . This load produces a rotation, ϕ , and perhaps a bending deflection at the elastic axis, \hat{v} . Then the work done by the force V going through the bending deflection caused by the moment, $W_{12} = V\hat{v}$, is equal to the work done by the moment M_t going through the rotation caused by the shearing force, $W_{21} = M_t \cdot 0 = 0$. Since V is not zero, then \hat{v} must be zero. Hence the elastic axis does not bend as the result of the application of a twisting moment. Therefore the elastic axis is the center of twist.

¹ James Clerk Maxwell (1831–1879), Scottish physicist, developer, among other contributions, of the electromagnetic theory of light and Maxwell's equations, which describe the basic laws of electricity and magnetism in a unified fashion.

WORK AND ENERGY PRINCIPLES

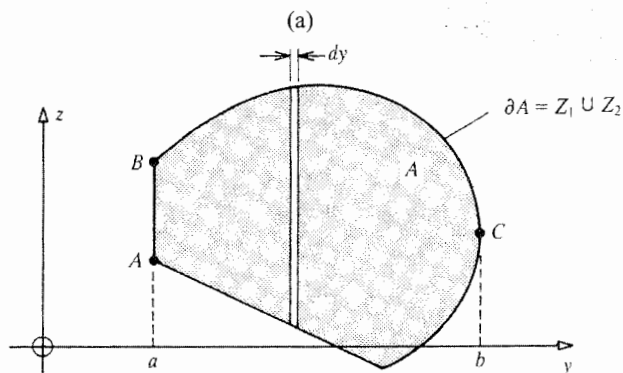


IV.1 Preface

There is only one chapter in Part IV so as to emphasize the important role work and energy principles play in modern structural analysis. Every chapter past this one depends upon the material of this chapter. The content of this chapter admittedly will be challenging to all those who have not had any previous experience with this material. For the student, the concept of work is not likely to have had a particularly prominent place in prior studies. The concept of potential energy is likely to have made a previous appearance only in relation to the gravitational potential. The calculus of variations, a key aspect of this chapter, is likely to be entirely new to the student (be sure to read Endnote (1)). Obviously in this chapter there are abundant opportunities for intellectual growth. In order to take advantage of those opportunities, the Green–Gauss theorem must be mastered. The next section provides a review of that theorem.

IV.2 The Green–Gauss Theorem

Consider a closed area A on an x plane such as shown in Fig. IV.1(a). Let this area be such that any line paralleling the z axis cuts ∂A , the piecewise smooth boundary of A , only twice. Let the various boundary segments that comprise the total boundary be divided into a lower and upper curve which meet at the points $y = a$ and $y = b$, where those points are the minimum and maximum y values on the boundary. In the case illustrated in Fig. IV.1, The “point” $y = a$ is actually a line segment. This possible alternate geometry does not alter



Between points A and C, the boundary is described by $Z_1(y)$; and between B and C by $Z_2(y)$

(b)

(c)

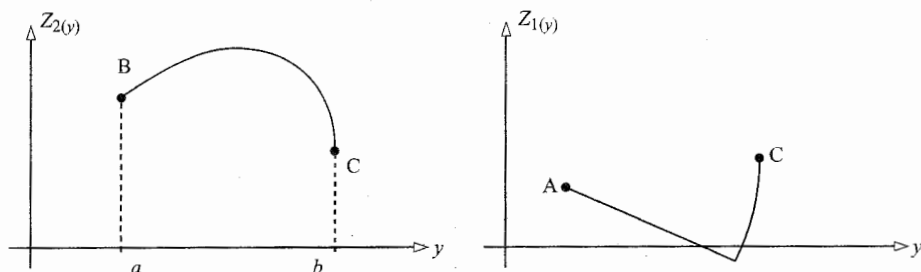


Figure IV.1. (a) A typical singly connected area over which the area integration first proceeds in the z direction. (b, c) The boundary curves $Z_1(y)$ and $Z_2(y)$, which together form ∂A .

the discussion. Let the respective equations of the lower and upper curves be grouped under the single-valued relations

$$z = Z_1(y) \quad \text{and} \quad z = Z_2(y)$$

where $Z_1(y)$ describes the values of z between point A and point C, while $Z_2(y)$ describes the values of z between point B and point C. See Fig. IV.1(b, c). For any differentiable function $F(y, z)$, consider the following double integral over the area A:

$$I_1 = \iint_A \frac{\partial F}{\partial z} dy dz = \int_{y=a}^{y=b} \left(\int_{z=Z_1(y)}^{z=Z_2(y)} \frac{\partial F}{\partial z} dz \right) dy$$

where the double integral, as is customary, has been viewed as a sum of a very large number of single integration z variable integrals multiplied by widths dy so as to form very thin vertical strips of area. Since integration is the inverse of partial differentiation, the interior integral of the above double integral can be evaluated as $F(y, z)$ where z is replaced by its limiting values. Thus

$$I_1 = \int_a^b \{F[y, Z_2(y)] - F[y, Z_1(y)]\} dy$$

Now consider the line integral with respect to y of the same function $F(y, z)$ counterclockwise around the closed boundary ∂A of the area A :

$$I_2 = \oint F(y, z) dy = \int_a^b F(y, z) dy + \int_b^a F(y, z) dy$$

Note that the line integral over the vertical line $B \rightarrow A$ is zero because dy is zero on that interval. Reversing the order of integration for the second integral, and inserting the constrained values of the variable z appropriate to each of the two integration paths, leads to

$$I_2 = \int_a^b F[y, Z_1(y)] dy - \int_a^b F[y, Z_2(y)] dy$$

A comparison of the final expressions for I_1 and I_2 shows that they are the negatives of each other. Hence,

$$\iint_A \frac{\partial F}{\partial z} dA = - \oint F dy$$

A very similar development for an area with a boundary that is only intersected twice by lines paralleling the y axis shows that

$$\iint_A \frac{\partial G}{\partial y} dA = + \oint G dz$$

When the above two results are combined into single area and single line integrals, that combination is called Green's theorem or Gauss's theorem, or the Green–Gauss¹ theorem. A variation on the Green–Gauss theorem is achieved when Eqs. (12.5) are used to replace dy and dz respectively by $-\cos(n, z) ds$ and $+\cos(n, y) ds$, as shown below where “ n ” is a linear coordinate in the direction of the outer normal unit vector at the outer boundary, ∂A .

$$\iint_A \left[\frac{\partial F}{\partial z} + \frac{\partial G}{\partial y} \right] dA = \oint [F \cos(n, z) + G \cos(n, y)] ds$$

The single interval requirement that any line paralleling the y and/or z axis intersect the area boundary only twice is a bit more stringent than just an hypothesis of being singly connected, in that it excludes certain, but not all, concavities. If a semicircular arc concavity replaced the vertical line $A-B$, there would be a violation with respect to lines paralleling the z axis but not for lines paralleling the y axis. Often, but not always, a region such as a multiconnected region that violates the single interval requirement can be divided into several subregions each of which satisfies the single interval requirement for both coordinate directions. See, for example, Fig. IV.2. In this case the integral over the entire area is simply treated as the sum of the integrals over several sub-areas where the Green–Gauss theorem does apply. Notice that the line integrals over the interior paths between the outer and inner boundaries of the area always occur in pairs that proceed in opposite directions. Thus those portions of the line integrals always cancel each other, and so the sum of all the line integrals reduces to just the line integral over the outer and inner boundaries. Note that the direction of integration around an inner boundary is opposite to that around the outer boundary.

¹ Karl Friedrich Gauss (1777–1855), German mathematician and astronomer. (For Green, see footnote 5 of Chapter 3.)

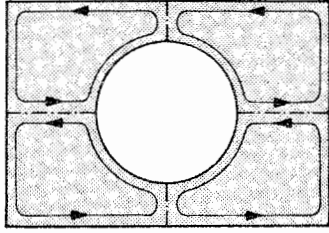


Figure IV.2. A division of a multiply connected region into y and z direction single interval subregions. Note that just two regions, no matter how constituted, would not be single interval regions in both orthogonal directions.

There is a three-dimensional version of the Green–Gauss theorem. It relates a volume integral to a surface area integral. Its proof proceeds in much the same fashion as the above proof. The result is (Ref. [3])

$$\iiint_V \left[\frac{\partial P}{\partial x} + \frac{\partial Q}{\partial y} + \frac{\partial R}{\partial z} \right] dV = \iint_S \{ P \cos(n, x) + Q \cos(n, y) + R \cos(n, z) \} dS$$

In the way of brief comments on the omitted derivation, note that if the $(\partial P/\partial x)$ term of the volume integral is to be integrated, then the strip of width dy of the previous area integration is here replaced by a long, thin cylinder of rectangular cross-sectional dimensions dy by dz . The shape of the volume boundary must be such that this long, thin cylinder intersects the volume boundary only twice. The two infinitesimal surface areas defined by those two intersections are the limits of this first integration. Hence the equations that represent the limits of integration for this inner integral are equations for a surface in space rather than a planar curve. In addition, the equations that equate, for example, $\{dy, dz\}$ to $\{dS \cos(n, x)\}$, are slightly more general forms of the equations derived for the Chapter 1 surface tetrahedron. They too may be derived in the fashion of Exercise 1.5.

Work and Potential Energy Principles

15.1 Introduction

In Parts I and III, equilibrium equations are established via Newton's laws by summing the forces and moments acting on isolated (free) bodies. Equilibrium equations assure continuity of forces and moments. Continuity of displacements is established by requiring either that (i) the orthogonal displacement or deflection components are described by differentiable functions in the case of a displacement formulation, or (ii) the strain compatibility equations are satisfied in the case of a stress formulation. Since the stresses acting upon fixed surfaces are vector quantities, and the displacement and deflection components are also vector quantities, the methods of Parts I, II, and III are often called "vector methods." This chapter introduces an alternate approach to vector methods. This alternate approach, called "energy methods," is often analytically superior to vector methods, particularly for complex problems. Energy methods have the same bases as vector methods. That is, just like vector methods, energy methods can be based upon Newton's laws and the same geometric description of structural deformations. However, energy methods involve scalar quantities such as work and potential energy. The shift from vector quantities to work and potential energy results in four important advantages.

The first advantage of energy methods is that the work or energy statements permit the choice of any coordinate system without a change in form for the basic equations. To illustrate this advantage in general terms at this beginning point in the topic development, consider Newton's second law of motion for a body of mass m , written for motion in a Cartesian x coordinate direction and then for motion in a cylindrical r coordinate direction.¹ These two equations are, respectively, using the usual rigid body dynamics symbols,

$$F_x = m \frac{d^2x}{dt^2} \quad \text{and} \quad F_r = m \frac{d^2r}{dt^2} - mr \left(\frac{d\theta}{dt} \right)^2$$

Note that the two vector component equations have different forms in the two different coordinate systems. Any statement of Newton's second law in a coordinate system other than a Cartesian coordinate system leads to a more complicated form of that equation. Another example of a change in the form of equilibrium equations with a change in coordinate system is seen in Chapter 1 where the two plane stress, internal equilibrium equations are derived for Cartesian and cylindrical coordinates. These two sets of stress equilibrium equations are, of course, only specialized examples of Newton's second law. As such, it is not surprising that, again, each of the two cylindrical coordinate equations has one or two more terms than the corresponding Cartesian coordinate equations.

In contrast to Newton's second law in terms of three force vector components or stress vector components, Newton's second law in terms of energy quantities has exactly the

¹ Note that, as is often the notation for rigid body motion, here the symbols x and r are center-of-mass displacements that are functions of time, rather than specifications of geometric location within an undeformed body.

same form regardless of the coordinate system. This has the advantage that the correct equation form is always immediately known regardless of which coordinate system is most convenient. In terms of (i) the kinetic energy of the mass, T ; (ii) the total potential energy of the deformable mass, Π , which can incorporate the effect of all or part of the conservative forces acting upon the body; and (iii) Q_i , a certain sum of all the forces not represented in the potential energy term, conservative or not,² Newton's second law for the time-varying i th coordinate $q_i(t)$ is

$$\frac{d}{dt} \left(\frac{\partial T}{\partial \dot{q}_i} \right) - \frac{\partial T}{\partial q_i} + \frac{\partial \Pi}{\partial q_i} = Q_i \quad (15.1)$$

where an upper dot is differentiation with respect to time. The meaning of q_i is explained in detail in Section 17.2. This more convenient form of Newton's second law is called the *Lagrange equation of motion*. Lagrange's equation is derived in Exercise 9. The importance of this equation is such that, in different forms, from this point through the majority of Chapters 16–21, the emphasis is on understanding just the last term on the left-hand side, and the right-hand side term. The first two terms of the Lagrange equation, which correspond to the *ma* of Newton's second law, are discussed briefly at the end of Chapter 19.

In the study of rigid body dynamics, the total potential energy is generally that associated with force fields such as the gravitational force field. In the study of deformable bodies, the potential energy is more complicated in that there is generally additional potential energy that is created by the applied forces having additional motions associated with the structural deformations. This chapter introduces the concepts that explain that additional potential energy. In summary, the first advantage to energy methods is that they allow a standardization of form for the required equations of deformable bodies while allowing the use of any coordinate system.

The second advantage for using energy methods is that work and energy methods often allow an analyst to use simpler geometric reasoning, and to avoid force-type interactions between components of a structure in favor of simpler displacement type interactions.

A third advantage for energy methods is simply that they provide another way of viewing physical phenomena, and thus add further insight into a phenomenon and an alternate analytical formulation. An illustration of the first point is as follows. The Lagrange equation, even though it is expressed in energy derivatives, is a summation of forces just like Newton's second law. Hamilton's principle (see Exercise 15.8), restates the Lagrange equation in a form that says that the motion of a mechanical system subjected to conservative or nonconservative forces must be such that the sum of the kinetic energy of, and the work done on, any mechanical system has to be a minimum. In other words, Hamilton's principle interprets the motion of a mechanical system from the viewpoint of minimizing the work and kinetic energy of the structural system, while the Lagrange equation speaks of a summation of forces.

An important historical controversy illuminates the second point concerning an alternate analytical formulation. There is a fourth order (biharmonic) partial differential equation for thin plate bending that very closely corresponds to the fourth order ordinary differential equation for long beam bending. When the thin plate fourth order governing differential equation was first developed, it was developed, as is done in Chapter 22, using vector methods to write the thin plate equilibrium equations. Those equilibrium equations involve the following stress resultants per unit length along the edge of any plate segment: a bending

² The difference between conservative and nonconservative forces is explained in Section 15.2.

moment, a twisting moment, and a lateral shear force. Reference [16] states that Poisson suggested that at an unsupported (i.e., force-free) plate edge, the boundary conditions should be that all three of these stress resultant quantities are zero. This seems, at first glance, to be an obvious requirement. However, for a clamped plate edge, there are only two deflection boundary conditions, and thus an apparent disparity in the number of boundary conditions. It was not until Kirchhoff developed the same fourth order thin plate bending deflection equation *and* simultaneously the associated boundary conditions using an energy method that the contradiction was overcome, and the two true force-type plate boundary conditions were discovered.

A fourth advantage for energy methods is that when using certain approximate methods of analysis that involve mathematical functions chosen by the analyst in order to approximate an unknown deflection or stress, an energy approach requires fewer conditions to be met by the selected approximating functions, and requires fewer derivatives of the approximating functions. These are important advantages because they make it easier to find suitable approximating functions.

In summary, energy methods for deformable bodies have exactly the same bases of force and displacement continuity as vector methods. However, energy methods are a more, sometimes a much more, convenient formulation of these bases. In fact, it is impossible to fully understand modern methods in structural analysis without understanding energy methods. In order to facilitate the introduction of energy methods, the general concepts of work and potential energy, and virtual work and virtual potential energy, are reviewed. Then the concept of the variational operator is explained so that full, confident use may be made of the virtual work and virtual potential energy concepts when applied to deformable bodies. Then the four basic energy method principles are derived for small displacements in varying degrees of completeness. These four basic principles are called the Principle of Virtual Work, the Principle of the Total Potential Energy, the Principle of Complementary Virtual Work, and the Principle of Complementary Total Potential Energy. The reader may have encountered limited forms of the first two principles because they are useful in dealing with problems in rigid body statics and dynamics.

15.2 Work and Potential Energy

Work is defined in differential terms. With W symbolizing work, \mathbf{F} representing a force resultant acting on a body, and \mathbf{r} being the position vector that locates the point of application of the force acting on the body, the definition of *the work done on the body by the force \mathbf{F}* is

$$dW \equiv \mathbf{F} \cdot d\mathbf{r} \quad (15.2a)$$

Clearly work is a scalar quantity. The right-hand side of the above definition can be rewritten in various equivalent forms. For example, if the force resultant and the position vectors are written in terms of their Cartesian coordinate components, that is, using the symbols commonly used for rigid body dynamics

$$\mathbf{F} = F_x \mathbf{i} + F_y \mathbf{j} + F_z \mathbf{k} \quad \text{and} \quad \mathbf{r} = x \mathbf{i} + y \mathbf{j} + z \mathbf{k}$$

then

$$dW = F_x dx + F_y dy + F_z dz \quad (15.2b)$$

Soon, when the subject is not that of rigid bodies but is that of deformable bodies, the Cartesian coordinates x , y , and z will no longer represent displacements but will be used

only to identify a material point in the deformable body. When the subject is deformable bodies, then $u = u(x, y, z)$, $v = v(x, y, z)$, and $w = w(x, y, z)$ will be the symbols that will denote the displacement components of the total displacement vector \mathbf{D} . In that case,

$$dW = \mathbf{F} \cdot d\mathbf{D} = F_x du + F_y dv + F_z dw. \quad (15.2c)$$

Of course, whatever the choice of symbols, work is done by a force moving through a displacement.

The work done on the body by the force can be integrated (summed) if the path followed by the force is known. That integral is a line integral, and the work done generally depends on the path followed. Another way of saying the same thing is to say that dW is not always an exact differential.

A simple illustration of this path dependency can be had by considering the work done by the dry friction force f_0 acting on a rectangular block of material that is slowly sliding along a curved path on the top of a table. Note that it is the friction force and the work that the friction force does upon the block that is being discussed, and not the other forces that cause the block to move or stay on the table top. The friction force is very nearly constant, and it is always directed opposite to the direction of motion. Therefore the friction force is everywhere tangent to the curved path followed by the block. Thus there is always a 180° angle between the friction force f_0 and ds , which is always tangent to the curved path and in the direction of the motion. Hence the total work done by the friction force on the block is just the negative of the product of the magnitude of the friction force and the path length. That is, where ds is the scalar magnitude of $d\mathbf{D}$, or dr ,

$$dW = -\oint f_0 ds = -f_0 \oint ds$$

Thus the longer the path, the more work is done on the block by the friction force. The work done on the block by the friction force is partly consumed in polishing the bottom of the block, and it is partly lost in heat generation and noise.

There is a class of forces that do work on material bodies, where the work done by those forces depends only upon the locations of the initial and final points of the path and not at all on the length or location of the path followed by the body. In mathematical terms, there are occasions where the right-hand side of Eq. (15.2a) is an exact differential. When the right-hand side is an exact differential, it may be integrated as an ordinary definite integral, and the value of that integral depends exclusively upon the limiting points on the integration path. To illustrate this type of force, consider the weight force acting on a block of material that is moving along a curved path in a three-dimensional space containing a constant gravity field. Again the focus is on a particular force, the weight force, and there is no present interest in the other forces that contribute to the motion of the block. Adopt a Cartesian coordinate system with the z axis directed opposite to the direction of the constant acceleration of gravity vector. Then the weight force \mathbf{F} is describable as $-mg\mathbf{k}$. Using common rigid body dynamics symbols for the last time, the differential tangent vector that is an increment in the length of the arbitrary path followed by the weight force is $d\mathbf{r} = dx\mathbf{i} + dy\mathbf{j} + dz\mathbf{k}$. Thus, after carrying out the dot product, the work done by the weight force on the block as it moves from point $A(x_a, y_a, z_a)$ to point $B(x_b, y_b, z_b)$, is

$$W(A; B) = \int_A^B dW = -mg \int_A^B dz = -mg(z_b - z_a)$$

Clearly the second integral is that of an exact differential, dz , which always integrates to z . In this case, only the z components of the initial and final positions affect the amount of

work done by the force acting upon the body. Notice that if the initial and final elevations are the same, no work at all is done by the weight force on the block. Another way of looking at this special result for the case where the weight returns to the initial elevation is to say that no work done by the weight force was lost, or, all the work done by the weight force was conserved. The constant, weight force is an example of what is called an (energy) “conservative” force, which is one where all work is recoverable by returning by *any* path to the original point of departure.

The case where dW is an exact differential, and thus the work done is independent of path, is of sufficient importance to have that exact differential be denoted by $dW = -dV$. The introduction of a new symbol is for the sake of clearly identifying this important simplifying circumstance. The quantity V is called the *potential energy*. The minus sign is included in the definition $dW = -dV$ in order that the potential energy associated with the weight force discussed above is a positive quantity when there is an increase in the elevation of the block.

Once again, since an exact differential is always integrable, the result of the integration of the exact work differential depends only on the initial and final points on the path. Again, the forces associated with the exact work differential are called conservative. Using the chain rule for exact differentials, it is possible to write

$$dW = -dV = -\left(\frac{\partial V}{\partial u}du + \frac{\partial V}{\partial v}dv + \frac{\partial V}{\partial w}dw\right) = -\nabla V \cdot d\mathbf{D}$$

Comparing this equation with Eq. (15.2c), and noting the independence of the factors du , dv , and dw , leads to the conclusion that the components of any conservative force are linked to a potential energy point function by the relations

$$F_x = -\frac{\partial V}{\partial u} \quad F_y = -\frac{\partial V}{\partial v} \quad F_z = -\frac{\partial V}{\partial w}$$

and the total value of any conservative force may be written as

$$\mathbf{F}_c = -\nabla V$$

This latter relation can be used as the basis for a test to determine whether or not a force that is mathematically describable in terms of coordinate position is conservative. From the vector identity $\nabla \times \nabla \Phi = 0$ for an arbitrary function $\Phi(x, y, z)$, it can be seen that $\nabla \times \mathbf{F}_c = 0$. This is both a necessary and sufficient condition for $\mathbf{F}_c = -\nabla V$, and thus a necessary and sufficient condition for a force being a conservative force.

In summary, Eq. (15.2a) defines what is meant by the work done by any force acting upon a body. When the work done on the body by a particular force is independent of the path followed by the body, that is, when dW is an exact differential, then the force doing the work is termed conservative. The negative of the finite work done by a conservative force is called the positive change in the potential energy of the body. Potential energy can be viewed as stored work, available to be recovered. Potential energy functions are not only associated with gravitational fields. A potential energy function can be associated usefully with the internal forces and displacements of elastic bodies.

15.3 Virtual Work and Virtual Potential Energy

Work and energy concepts are very useful in rigid body dynamics because, via Newton's second law, work can be directly related to changes in kinetic energy. The question

arises as to how these fundamental concepts of work and energy can be applied to deformable structural bodies, particularly when they have reached a state of static equilibrium. The answer to this question lies in broadening the work concept by introducing the concept of virtual work.

As in the discussion of actual work, consider any one of several actual forces acting on a structural mass in a state of static equilibrium.³ As before, if the point of application of the force on the mass were to undergo an actual infinitesimal motion, $d\mathbf{D}$, there would be an infinitesimal amount of actual work done by the force on the body. However, with the body in a state of static equilibrium, there is no actual motion. To broaden the work concept, now consider all possible infinitesimal motions of the point of force application from its actual static equilibrium position. Do so without regard for the actual forces, moments, or tractions acting upon the structural mass, and without any concern for how these possible motions might come to pass. The meaning here of “possible motions” is those motions that do not violate displacement constraints, such as displacement boundary conditions or other constraints on the actual displacements. For example, consider a block of material at rest on a table top. If all contemplated actual forces were such that the block would only move from one position on the table top to another, then for analysis purposes, the block is constrained to remain on the table top. Then all possible motions of the block would parallel the table top. Motions into the table top or off the table top are to be considered outside the realm of possible motions.

Since the above possible motions are unrelated to the actual loads, these motions exist only in the imagination of the analyst. In order to preserve the symbol $d\mathbf{D}$ as one representing an infinitesimal portion of an actual motion, a new symbol is introduced in order to represent any possible infinitesimal motion for the point of application of the force under consideration. That new symbol is $\delta\mathbf{D}$. The possibly fictitious displacement $\delta\mathbf{D}$ is called a *virtual displacement*.⁴

Define the work done by an actual force as that force moves through a virtual displacement as *virtual work*. In mathematical form:

$$\delta W \equiv \mathbf{F} \cdot \delta\mathbf{D} \quad (15.3)$$

Note again that the above applied force is the same applied force of the actual work discussion. Thus again, if this force is a conservative force, then this force can be derived from a potential function such that $\mathbf{F} = -\nabla V$. In this special case

$$\delta W = -\nabla V \cdot \delta\mathbf{D} \quad (15.4)$$

Just as is true for actual work, it is advantageous to identify the virtual work associated with a conservative force by the special symbol $-\delta V$. Hence the virtual potential energy is

$$\delta V = +\nabla V \cdot \delta\mathbf{D} \quad (15.5)$$

³ The limitation to static equilibrium is deliberate. The previous viewpoint of implicitly grouping all inertial forces with the body forces could easily have been retained in the development of the virtual work and virtual energy principles of this chapter. However, it is an important advantage of work and energy methods that the explicit description of the general form of the inertial loads is simply stated as one additional term to be added to the Principle of Virtual Work to form what is known as Hamilton's principle, named after Sir William Rowan Hamilton, Irish physicist (1805–1865) (Ref. [2]). See Exercise 8.

⁴ The adjective virtual means being so in essence or effect, but not being so in actual fact or name; for example, “although we have met, he is a virtual stranger.”

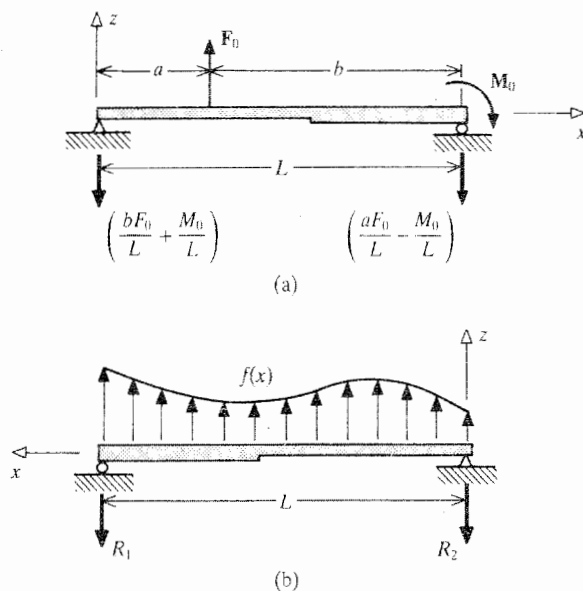


Figure 15.1. Example 2. (a) A typical concentrated force and a typical concentrated moment acting upon a nonuniform beam. (b) A general force per unit length acting upon a nonuniform beam.

Example 15.1. A rigid block rests on a table top that is inclined at an angle θ . Calculate the virtual work done by the gravity force mg on the rigid block for a virtual displacement δs that is (a) down the incline, (b) up the incline, and (c) horizontal on the incline. (d) If the coefficient of static friction is μ , calculate the virtual work done by the *static* friction force as a result of the three different motions of parts (a) through (c).

Solution. The component of the gravity force in the plane of the table top is $mg \sin \theta$. This force acts in the direction that is down the incline. Therefore, (a) $\delta W = +mg \sin \theta \delta s$; (b) $\delta W = -mg \sin \theta \delta s$; (c) $\delta W = 0$ because the actual force and the virtual displacement are perpendicular to each other. (d) Similarly, $\delta W = -\mu mg \cos \theta \delta s$ for the virtual displacement δs down the incline, $+\mu mg \cos \theta \delta s$ up the incline, and zero in the horizontal direction, because the static friction force is directed up the incline. In order to fully understand these answers, note that no virtual displacement creates or alters an actual force. In particular, the upwardly directed static friction force is not altered in either its magnitude or its direction by any virtual displacement. Furthermore, since there is no actual movement of the block, there is no dynamic friction force to be considered. ■

Example 15.2. Calculate the virtual work done by the actual loads acting upon the beams shown in Figs. 15.1(a, b).

Solution. In this case, the structure is a flexible beam rather than a rigid block. When a body is rigid, all material points in the body must necessarily move together. Thus one virtual displacement symbol can describe the virtual displacement of every material point in the rigid body. On the other hand, the points along the beam axis are able to move relative to each other. Thus it is possible to have different virtual deflections at each point along the beam axis. Since the loads are in the x, z plane, the virtual deflection components that will result in virtual work also lie in the x, z plane. Mimicking the actual deflection in the x, z

plane, $w(x)$, the symbol $\delta w(x)$ is used to describe the positive upward virtual deflection of the beam axis at the point x . Similarly, virtual deflections which are the rotations of the beam axis in the x, z plane at the point x are symbolized as $\delta w'(x)$. Like the virtual deflections, the virtual rotations follow the sign convention used with the actual rotations. (In order to conform with the constraint that all possible beam deflections, including the virtual deflections, must be very smooth functions of x , $\delta w(x)$ and $\delta w'(x)$ must be differentiable functions of x .) Then

- (a) $\delta W = F_0 \delta w(a) - M_0 \delta w'(L)$. The negative sign before the moment term indicates that the actual applied moment M_0 is in the opposite direction to the positive virtual bending slope. Note that the support reactions do no virtual work because the supports are constrained against any motion regardless of the loads that act upon the beam and the motions in the interior of the beam.
- (b) Since the force acting on the infinitesimal interval starting at any point x is $f(x) dx$, and since $\delta w(x)$, the virtual deflection at the point x , is a very good description of the virtual deflection everywhere along the infinitesimal interval dx starting at point x , then the virtual work done along the infinitesimal interval is $f(x) dx \delta w(x)$. (Hereafter the interval starting at point x is referred to, in short, as the point x .) Then the total virtual work is the sum of the virtual work done by all the forces acting upon the structure, which is

$$\delta W = \int_0^L f(x) \delta w(x) dx$$

Again, the support reactions, which are constrained against vertical motion, have no virtual deflections and hence do not do any virtual work. In the above integral, $\delta w(x)$ is just another function of the variable x . As such it can be integrated just like any other function if a specific form were chosen for this function. Do note that if there is a δ on one side of an equality, there must also be a δ on the other side of the equality too. ■

Understand that the above integration is not integration over a path of fictitious deflections. Rather, it is a summing up over the length of the beam of the virtual work done by each real force $f(x) dx$ at the point x moving only as far as the small virtual deflection at the same point, $\delta w(x)$. Since all real forces always have fixed values as they move through a virtual displacement, there is never a need to integrate over the path of a virtual displacement.

15.4 The Variational Operator

Again, using the notation u, v, w for the structure's Cartesian displacement components at the point of force application, the differential of the total displacement vector is

$$d\mathbf{D} = du \mathbf{i} + dv \mathbf{j} + dw \mathbf{k}$$

Similarly, the virtual displacement vector can be written in terms of its components as

$$\delta\mathbf{D} = \delta u \mathbf{i} + \delta v \mathbf{j} + \delta w \mathbf{k}$$

where, of course, δu , and so on, are the magnitudes of the Cartesian components of the total virtual displacement, $\delta\mathbf{D}$. If the above expression for $\delta\mathbf{D}$ is substituted into Eq. (15.5), and

if the various dot products are carried out, then the result for a conservative force is

$$\delta V = \frac{\partial V}{\partial u} \delta u + \frac{\partial V}{\partial v} \delta v + \frac{\partial V}{\partial w} \delta w \quad (15.6)$$

The form of Eq. (15.6) is striking. It is exactly the same form as that of the first order differential of a function $V(u, v, w)$. That is, comparing Eq. (15.6) with the chain rule expansion

$$dV(u, v, w) = \frac{\partial V}{\partial u} du + \frac{\partial V}{\partial v} dv + \frac{\partial V}{\partial w} dw$$

suggests that the δ of such expressions as δD and $\delta \mathbf{D}$ can be considered as an operator acting upon V and \mathbf{D} with a separate identity, just as the differential operator d can be separated from the quantities V and \mathbf{D} in the respective exact differentials dV and $d\mathbf{D}$. Moreover, since there are no restrictions on the point function V , the analogy of form suggests that the δ can be considered as a new mathematical operator on all point functions just as d can be considered as the differential operator for all point functions. It is useful to have this enlarged concept of the delta symbol as an operator. Hence the operator nature of δ is now adopted and patterned after the differential operator solely on the basis of the above similarity of form. Keep in mind that the differential quantity dW , when it relates to nonconservative forces is not an exact differential. Then, for such work, neither the d nor the δ can be separated from the W in the dW or δW expressions, respectively.

Further consideration shows that it is useful to make a distinction between the δ and d operators. Consider the general mathematical expression for the differential of a point function V of the arbitrary functions u , v , and w , where each of these three functions is in turn a function of x , y , z . Then, first of all, as written above, $dV(u, v, w)$ depends upon the differentials du , dv , and dw . By the same chain rule, each of these three differentials can be expressed in terms of the differentials of the variables upon which u , v , and w depend. For example,

$$du(x, y, z) = \frac{\partial u}{\partial x} dx + \frac{\partial u}{\partial y} dy + \frac{\partial u}{\partial z} dz$$

This expression quantifies the generally small change in the function $u(x, y, z)$ over the generally very short distances dx , dy , and dz . The quantity δu also can, and generally does, vary from material point to material point as was discussed in Example 15.2 for the case of $\delta w(x)$ for a beam. That is, in general, δu is also a function of x , y , and z . However, in the context of virtual work it makes no sense to apply the chain rule to δu , as is done above for du , and talk of a δx or a δy or a δz , because *in this context* the quantities x , y , and z only name the material point at which the virtual displacement $\delta \mathbf{D}$ is taking place. That is, changes in the spatial coordinates themselves play no part in the evaluation of the virtual work at the point (x, y, z) , or any other point. The spatial coordinates only identify the point at which the actual force is applied. Only the actual forces and the virtual displacements δu , δv , and δw affect the value of the virtual work. Another way of saying the same thing is to say that at the material location where each virtual work producing force is applied, the quantities x , y , z have fixed values that do not permit a variation.

For these reasons, for any point function, define the *variational operator* δ as having the same properties as the familiar differential operator d , except that the variation, as it is called, of all independent variables, such as any of the Cartesian coordinates, is defined always to be zero. All dependent functions, subject to the comments of this paragraph, have variations. For example, the displacements, which are functions of the spatial coordinates,

are dependent functions and thus have variations. However, dependency is not the only requirement for a function to have a nonzero variation. The dependent function must also have an arbitrary or unknown functional form, at least before the completion of the analysis. Thus, for example,

- i. The variation of the implicit functional $F(u, v, w)$ where u, v, w are unknown functions of x, y, z , is $\delta F = (\partial F/\partial u)\delta u + (\partial F/\partial v)\delta v + (\partial F/\partial w)\delta w$; and in particular
- ii. The variation of an explicit function of unknown functions, such as $V(u, v, w) = C_1u^2 + C_2\sqrt{v} + C_3w$, where again u, v, w are unknown functions of the independent variables x, y, z , and the C_i are constants, is $\delta V(u, v, w) = 2C_1u\delta u + \frac{1}{2}(C_2/\sqrt{v})\delta v + C_3\delta w$; but in contrast
- iii. The variation of the function $f(u, v, w) = uvw(u + v + z)$ is zero if it is known that $u = x \sin y$, $v = \sqrt{y}$, and $w = z \cos x$, because this $f(u, v, w)$ is then an explicit, known function of only the independent spatial variables and there is no way to have a variation.

Endnote (1) contains further comment upon the differences between variations, differentials, and derivatives.

Using the above definition of the variational operator, reconsider the definition of virtual work as it is expressed in Eq. (15.3) when the resultant force is conservative. In the present notation, that equation is

$$\delta W = \delta(W) = \mathbf{F} \cdot \delta \mathbf{D} \quad (15.3)$$

Since the application of the variational operator to the work function is taken to be the product of a force function and a variation of a displacement function, then it is clear from this expression that for the purposes of calculating virtual work by the product rule for differentiation, force-type quantities are to be regarded as independent variables; that is, they possess a zero variation. The interpretation of Eq. (15.3) is simply that, from the point of view of virtual work, the force system (the independent variables) causes the structural displacement field (the dependent variables). Concentrated and distributed forces and moments are not the only physical variables that must be classified as independent variables in all expressions related to the virtual work of deformable bodies. Time and temperature changes also must always be classified as independent variables.

Example 15.3. If $G(u, v; x, y) = uy \sin v + xu^2$, determine δG if $u = u(x, y)$ and $v = v(x, y)$ are unknown functions of arbitrary functional form.

Solution. The variational operator behaves according to Eq. (15.6) exactly like a differential operator limited to dependent variables when applied to point functions. Therefore, all the familiar rules of ordinary calculus for point functions carry over to the calculus of variations. In this case, u and v are meant to be identified as dependent variables, and x and y as independent variables. Hence,

$$\delta G = (y \sin v + 2xu)\delta u + (uy \cos v)\delta v \quad \blacksquare$$

There are two more properties of the variational operator that require mentioning.

Property 1

$$\delta \left(\frac{\partial u}{\partial x} \right) = \left(\frac{\partial}{\partial x} \right) \delta u$$

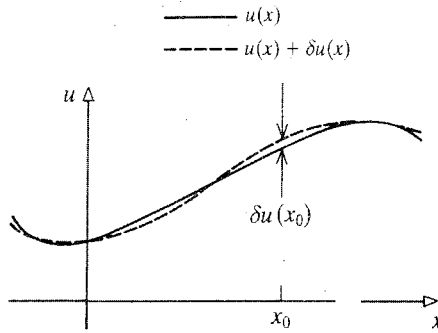


Figure 15.2. A typical function $u(x)$ and its varied path, the function $u(x) + \delta u(x)$, where the variation upon the function $u(x)$ is constrained to be smooth at every point x .

Discussion. This property involves, for example, the partial derivative of the unknown, dependent variable $u(x, y, z)$ with respect to the independent variable x , that is, $\partial u/\partial x$. In order to discuss this quantity, fix the values of the other two variables, y and z , and focus on the change in the function u with respect to x , which is indicated in an arbitrary fashion by the solid line in Fig. 15.2. Consider the function $u(x) + \delta u(x)$, which is called the “varied path.” Let the varied path, which is represented by the dashed line in the same figure, be everywhere “close” to the original path, $u(x)$. Now the function $\partial u/\partial x$, not shown in the sketch, can, like any function, also have a close varied path which in this case is denoted by $\partial u/\partial x + \delta(\partial u/\partial x)$. It is now required, *by definition*, that the slope of the varied path of the original function $u(x)$, that is, $(\partial/\partial x)[u(x) + \delta u(x)]$, be the same as varied path of the slope function, that is, $\partial u/\partial x + \delta(\partial u/\partial x)$. This is formally called the case of the weak variation, which is the only variation required for this text. That required equality immediately produces the important relation stated above that $\delta(\partial u/\partial x) = (\partial/\partial x)\delta u$. In other words, it is required that the order of the application of the variational operator and the partial or total derivative operator be irrelevant. In other words, using the basic mathematical term, it is required that the two operators be “commutative.”

Note from the above paragraph that in addition to variations on the basic function $u(x, y, z)$, there are as a matter of course, variations on the derivatives of $u(x, y, z)$. Each different derivative of a dependent function is another dependent function. Thus if there were a function of the basic function and some of its derivatives, (i.e., a functional), such as $F(x, u, u_x, u_{zz})$, where the subscripted commas that indicate partial differentiation⁵ are omitted only when they are within the arguments of functionals so that the independent variable subscripts by themselves indicate partial differentiation, then that functional’s variation would be as follows:

$$\delta F(x, u, u_x, u_{zz}) = \frac{\partial F}{\partial u} \delta u + \frac{\partial F}{\partial u_x} \delta u_x + \frac{\partial F}{\partial u_{zz}} \delta u_{zz}$$

Each different partial (or total) derivative is just another chain rule dependent variable, and in light of property 1, there is no ambiguity attached to δu_x because the order of $\partial/\partial x$ and δ is immaterial.

⁵ For example, the notation $u_{,y} \equiv \partial u/\partial y$; $F_{x,y} \equiv \partial F_x/\partial y$; and $F_{y,zz} \equiv \partial^2 F_y/\partial z^2$.

Example 15.4. (a) If $u = u(x, y, z)$, calculate the variation of the functional $f(y, u, u_z) = uy \cos(u_z)$. (b) If $v = v(x, y)$, and if $G(x, y, v, v_x, v_y) = v + y(\partial v/\partial x) + x(\partial v/\partial y)$, calculate δG in terms of δv and its derivatives.

Solution. (a) $\delta f = [y \cos(u_z)] \delta u - [uy \sin(u_z)] \delta u_z$. (b) $\delta G = \delta v + y \delta v_x + x \delta v_y = \delta v + y(\partial/\partial x) \delta v + x(\partial/\partial y) \delta v$ ■

Property 2. Definite integration over independent variables and the variational operator are commutative. For example, where the empty parentheses below indicate any argument containing one or more unknown dependent variables and/or their derivatives, and possibly one or more independent variables,

$$\delta \iiint_{\text{Vol.}} F() dx dy dz = \iiint_{\text{Vol.}} \delta F() dx dy dz$$

The proof of this proposition is set forth in Endnote (1).

15.5 The Principle of Virtual Work

Consider an arbitrarily shaped body such as that pictured in Fig. 1.6 subjected to an arbitrary set of surface tractions (which might include concentrated forces and moments) and body forces, neither of which vary with time. Let the loads be limited so that all deflections are sufficiently small that the nonlinear portions of the strain–displacement equations can be neglected without a loss of accuracy. The deformable body’s boundary surface defines the limits of the structural system. Everything outside the body surface is “external,” and everything inside is “internal.” Thus the loads applied to the outside of the boundary surface are classified as “external.” Since the body forces arise from external force fields, they too are classified as “external.” The virtual work done on the arbitrary body by the all external loads can be summed in the following two expressions, where S_1 signifies the surface (skin) area where forces are prescribed.

$$\delta W_{ex} = \iint_{S_1} (T_x \delta u + T_y \delta v + T_z \delta w) dS + \iiint_{\text{Vol.}} \rho (B_x \delta u + B_y \delta v + B_z \delta w) d(\text{Vol.}) \quad (15.7a)$$

and where $\delta u = \delta u(x, y, z)$, $\delta v = \delta v(x, y, z)$, $\delta w = \delta w(x, y, z)$ are arbitrary small virtual displacements that do not violate the constraints placed upon the structural system. The above equality may be explained by first noting that, for example, $T_x dS$ is a force on the body surface in the x direction. When this force is multiplied by the x direction component of the total virtual displacement, δu , at the point of application of the force $T_x dS$, the product is the virtual work done on the body by that differential-sized force component. When the virtual work of all such differential forces is summed, that is, integrated over the total surface area, the result is the total virtual work accomplished by the actual tractions acting on the body as they move through the selected virtual displacements.⁶ Similar reasoning applies to the differential body forces per unit mass, multiplied by the mass density, and their corresponding virtual displacements throughout the volume of the body.

⁶ This is a reminder that the total surface area S is divided into two separate and distinct parts, S_1 and S_2 . On the surface area S_2 , where displacements are prescribed (i.e., have fixed values), all virtual displacements (i.e., variations on those constant values) are necessarily zero. Therefore the equality of Eq. (15.7a) is unaltered by replacing the limits of integration S_1 by the total surface area S .

Now that the sum of the above surface integral and the above volume integral have been identified as the total external virtual work, this development begins with the *identity*

$$\begin{aligned} & \iint_S (T_x \delta u + T_y \delta v + T_z \delta w) dS + \iiint_{\text{Vol.}} \rho (B_x \delta u + B_y \delta v + B_z \delta w) d(\text{Vol.}) \\ &= \iint_S (T_x \delta u + T_y \delta v + T_z \delta w) dS + \iiint_{\text{Vol.}} \rho (B_x \delta u + B_y \delta v + B_z \delta w) d(\text{Vol.}) \end{aligned} \quad (15.7b)$$

Since this starting point is an identity, then the result is also an identity. This means that the conclusion is valid for all forces and displacements, that is, all structural analyses confined to small displacements.

To work effectively with Eq. (15.7b) it is best to be concise. Hence, rewrite the right-hand side of that equation in matrix form as

$$\iint_S [\delta u] \{T\} dS + \iiint_{\text{Vol.}} \rho [\delta u] \{B\} d(\text{Vol.}) \quad (15.7c)$$

where, of course $[\delta u] = [\delta u \ \delta v \ \delta w]$, $\{T\} = [T_x \ T_y \ T_z]$, and so on. Temporarily call the first of the above two integrals I_1 , and the second I_2 . Since the first integral, I_1 involves the tractions at the surface, those tractions can be replaced by the stresses on the inside of the boundary surface by means of the Cauchy equation, Eq. (1.9), which is $\{T\} = [\sigma] \{v\}$ with the result that

$$I_1 = \iint_S [\delta u] [\sigma] \{v\} dS$$

where again $\{v\} = [\cos(n, x) \ \cos(n, y) \ \cos(n, z)]$. Since the product of a 1×3 matrix and a 3×3 matrix is a 1×3 matrix, then the matrix product $[\delta u] [\sigma]$ may temporarily be named $[P \ Q \ R] \equiv [P]$, where the row matrix elements P , Q , and R are

$$P = \sigma_{xx} \delta u + \sigma_{xy} \delta v + \sigma_{xz} \delta w$$

$$Q = \sigma_{xy} \delta u + \sigma_{yy} \delta v + \sigma_{yz} \delta w$$

$$R = \sigma_{xz} \delta u + \sigma_{yz} \delta v + \sigma_{zz} \delta w$$

Use of the three-dimensional form of the Green–Gauss equation from the last equation of Section IV.2 allows this surface integral

$$I_1 = \iint_S [P] \{v\} dS \equiv \iint_S [v] \{P\} dS$$

to be rewritten as the following volume integral:

$$I_1 = \iiint_{\text{Vol.}} \left(\frac{\partial P}{\partial x} + \frac{\partial Q}{\partial y} + \frac{\partial R}{\partial z} \right) d(\text{Vol.})$$

The next step is to carry out each indicated differentiation. Note, for example, that using the rule for the derivative of a product, $(\partial/\partial x)(\sigma_{xx} \delta u) = (\partial \sigma_{xx} / \partial x) \delta u + \sigma_{xx} \delta u_{,x}$ where, in the latter term of these two terms, the partial derivative operator and the variational operator have been interchanged. When, similarly, all nine derivatives that compose the sum that is the integrand of the above volume integral are expanded into their 18 component terms, and

that result is added to the three terms of the volume integral I_2 , the total can be arranged as

$$\begin{aligned}
 \text{right-hand side} = & \iiint_{\text{Vol.}} \left\{ \left[\frac{\partial \sigma_{xx}}{\partial x} + \frac{\partial \sigma_{xy}}{\partial y} + \frac{\partial \sigma_{xz}}{\partial z} + \rho B_x \right] \delta u \right. \\
 & + \left[\frac{\partial \sigma_{xy}}{\partial x} + \frac{\partial \sigma_{yy}}{\partial y} + \frac{\partial \sigma_{yz}}{\partial z} + \rho B_y \right] \delta v \\
 & + \left[\frac{\partial \sigma_{xz}}{\partial x} + \frac{\partial \sigma_{yz}}{\partial y} + \frac{\partial \sigma_{zz}}{\partial z} + \rho B_z \right] \delta w \\
 & + [\sigma_{xx} \delta u_{,x} + \sigma_{xy} \delta v_{,x} + \sigma_{xz} \delta w_{,x}] \\
 & + [\sigma_{xy} \delta u_{,y} + \sigma_{yy} \delta v_{,y} + \sigma_{yz} \delta w_{,y}] \\
 & \left. + [\sigma_{xz} \delta u_{,z} + \sigma_{yz} \delta v_{,z} + \sigma_{zz} \delta w_{,z}] \right\} d(\text{Vol.}) \quad (15.8a)
 \end{aligned}$$

The first three bracketed terms are recognized as the left-hand sides of the general equilibrium equations, Eqs. (1.6). It is possible to write these complete general equilibrium equations in matrix form as

$$[\partial][\sigma] + \rho[B] = [0] \quad (1.6)$$

where
$$[\partial] = \begin{bmatrix} \frac{\partial}{\partial x} & \frac{\partial}{\partial y} & \frac{\partial}{\partial z} \end{bmatrix}$$

is the row vector of partial derivative operators, and, of course,

$$[B] = [B_x \ B_y \ B_z]$$

(Note that the partial derivative sign ∂ has no meaning by itself as an operator, that is, it must be part of a larger symbol like the above matrix symbol; and the scalar term $\partial f(x, y, z)$ has no meaning because there are no partial differentials, only partial derivatives.) With respect to the last three bracketed terms of Eq. (15.8a), let the *virtual strains* that result from the single-valued, differentiable virtual displacements be required to satisfy the strain-displacement equations as a *precondition* of this development. Then, for example, $\delta u_{,x} = \delta(\partial u / \partial x) = \delta \epsilon_{xx}$, and the two σ_{xy} terms can be grouped together as $\sigma_{xy} \delta \gamma_{xy}$, and so on. Then the last three bracketed terms can be rewritten as $[\sigma]\{\delta \gamma\}$, where

$$[\sigma] = [\sigma_{xx} \ \sigma_{yy} \ \sigma_{zz} \ \sigma_{xy} \ \sigma_{xz} \ \sigma_{yz}]$$

is the 1×6 row matrix of the six actual stresses, and

$$\begin{aligned}
 \{\delta \gamma\} &= \delta \left[\frac{\partial u}{\partial x} \ \frac{\partial v}{\partial y} \ \frac{\partial w}{\partial z} \ \frac{\partial u}{\partial y} + \frac{\partial v}{\partial x} \ \frac{\partial u}{\partial z} + \frac{\partial w}{\partial x} \ \frac{\partial v}{\partial z} + \frac{\partial w}{\partial y} \right]^t \\
 &= [\delta \epsilon_{xx} \ \delta \epsilon_{yy} \ \delta \epsilon_{zz} \ \delta \gamma_{xy} \ \delta \gamma_{xz} \ \delta \gamma_{yz}]^t \quad (15.9)
 \end{aligned}$$

is the 6×1 vector of the virtual engineering strains that are the consequence of the virtual displacements throughout the volume of the structural body. Note that there should be no confusion between $[\sigma]$, the 3×3 symmetric matrix, and $[\sigma] = \{\sigma\}^t$, the 1×6 matrix. Both stress matrices convey the same information. Making these substitutions yields

$$\text{right-hand side} = \iiint_{\text{Vol.}} ([\partial][\sigma] + \rho[B])\{\delta u\} d(\text{Vol.}) + \iiint_{\text{Vol.}} [\sigma]\{\delta \gamma\} d(\text{Vol.}) \quad (15.8b)$$

which is the desired form. Now for the final step. When a state of (static) equilibrium exists for the general body under consideration, the first integral of the above expression vanishes. Then the final result may be stated as

$$\boxed{\iint_{S_1} [\delta u]\{T\} dS + \iiint_{\text{Vol.}} \rho[\delta u]\{B\} d(\text{Vol.}) = \iiint_{\text{Vol.}} [\sigma]\{\delta\gamma\} d(\text{Vol.})} \quad (15.10a)$$

Clearly Eq. (15.10a), called the *Principle of Virtual Work*, is true only when the general body is in a state of equilibrium⁷ that is, when there is equilibrium at the boundary in the form of Cauchy's matrix equation, and when there is equilibrium in the interior in the form of Eqs. (1.6). By essentially reversing the above mathematical process, and by again using, virtual strains compatible with the virtual displacements, it is not difficult to begin with the Principle of Virtual Work, as stated in Eq. (15.10a), and derive the Cauchy boundary equilibrium equations and the general interior equilibrium equations. This proof is presented in Endnote (2). Based on that proof, and the above result, it can be said that the Principle of Virtual Work (PVW) is both a necessary and sufficient condition for equilibrium. In other words, *the PVW requires the use of virtual displacements and virtual strains that satisfy the strain–displacement equations that are part of Eq. (15.9), and which are the equivalent of the compatibility equations, and then enforces the boundary and interior equilibrium equations for the real externally applied forces and their corresponding internal stresses.*

The PVW is valid for all selected virtual displacements without the slightest regard for the applied loads, be they conservative or nonconservative. Note again that it is the expressions for small strains that are used in this derivation. Therefore, for this reason, the above derivation is limited to small displacements. See Ref. [3] for a discussion of the PVW for finite strains.

In summary, if the analyst chooses virtual displacements and virtual strains that are compatible among themselves, then the PVW assures equilibrium. The only set of equations that have not been involved in this development are the stress–strain or the strain–stress equations. The absence from the derivation of these constitutive equations means that the PVW is valid for any type of material, including rigid bodies. When the material is *rigid*, Eq. (15.10a) reduces to

$$\delta W_{ex} = 0$$

This is so because in a rigid body there are no actual internal relative displacements, and hence no actual internal strains. Since all virtual displacements, including virtual relative displacements, are not permitted to violate the system constraints, the virtual strains must also be zero. As above, zero virtual strains cause the right-hand side of the PVW to be zero. The following two elementary examples indicate that the use of the PVW with compatible deflections yields the system equilibrium equations.

Example 15.5. Reconsider the rigid rectangular block of Example 15.1 that is resting upon an inclined table top. Use the PVW to write the equilibrium equation for the direction up or down the incline. Again μ is the coefficient of static friction.

Solution. Give the rigid block a virtual displacement δs down the incline. In this case the compatibility of all deflections is trivial. It is represented by having both the static

⁷ Again, static equilibrium is assumed only because time-varying inertial forces are best described in terms of kinetic energy.

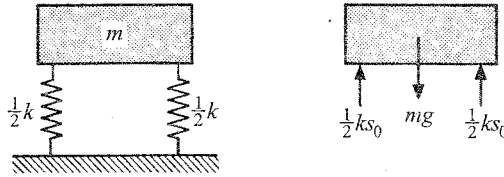


Figure 15.3. Example 15.6. Two springs supporting a mass m .

friction force and the in-plane weight component have the same virtual displacement. The virtual work of the forces external to the block is $\delta W_{ex} = +mg \sin \theta \delta s - \mu mg \cos \theta \delta s$. As discussed above, since the block is rigid, $\delta W_{ex} = 0$. Deleting the arbitrary factor δs yields the equilibrium equation $mg \sin \theta = \mu mg \cos \theta$. A virtual displacement δs directed up the incline only leads to $\delta W_{ex} = -mg \sin \theta \delta s + \mu mg \cos \theta \delta s$, and the same equilibrium equation results. A virtual displacement in any other direction on the incline again alters the external virtual work by a common factor which is the cosine of the angle between the downward direction and the direction of the virtual displacement, but does not alter the equilibrium equation. ■

As a comment on the above elementary example, note that if, in contradiction to the definition that all virtual displacements have to comply with all constraints associated with the mathematical model of the structural system, the rectangular rigid block is given a virtual displacement perpendicular to the plane of the incline, then, with N being the normal component of the force that the incline exerts upon the block.

$$\delta W_{ex} = 0 = N \delta s - mg \cos \theta \delta s$$

This equality provides a solution for the force that maintains the constraint that keeps the block from penetrating the table top. This illustrates the fact that virtual displacements that oppose the system constraints can be used to calculate the forces that maintain those constraints. However, from this point on, as originally defined, all virtual displacements will again comply with all constraints. Nevertheless, this aside has the value that it permits repeating the point that regardless of the direction of a virtual displacement, even if it is in a direction forbidden by the constraints, the magnitudes of the actual forces are always unchanged throughout the virtual displacement, even when those forces would change greatly in even a very small actual distance. The next section elaborates upon this point.

Example 15.6. Consider the spring-mounted rigid mass shown in Fig. 15.3. Write the vertical equilibrium equation for the rigid mass.

Solution. Define the structural system as the rigid mass alone. This choice avoids having to deal with the complexities of the coiled springs, responds to the problem statement, and reduces the PVW to simply $\delta W_{ex} = 0$. Give the mass an upward virtual displacement δs from its static equilibrium position. The static equilibrium position of the mass is an unknown downward vertical distance s_0 from the position of the top of the uncompressed, (i.e., unloaded) springs. Since each spring has been compressed a downward vertical distance s_0 , each spring exerts an upward force of magnitude $\frac{1}{2}ks_0$. Thus

$$\delta W_{ex} = 0 = -mg \delta s + \left(\frac{1}{2}ks_0 + \frac{1}{2}ks_0 \right) \delta s \quad \text{or} \quad ks_0 = mg$$

which is an equilibrium equation that can be solved for the distance s_0 through which the springs are compressed. ■

Equation (15.10a), the Principle of Virtual Work, can be written more compactly. As before, the left-hand side of this identity is δW_{ex} . The next section shows that the right-hand side of Eq. (15.10a) can be identified as the negative of the internal virtual work, which is denoted as $-\delta W_{in}$. The presence of the negative sign is explained below.

15.6 Internal Virtual Work

As shown in Fig. 15.4(a), consider a differential, rectangular parallelepiped subjected to a general stress state. The present purpose is to calculate the virtual work done by all the indicated stresses and body forces acting externally upon the infinitesimal parallelepiped as a result of *all* the virtual displacements that are possible for this deformable, infinitesimal body. The possible virtual displacements are three rigid body virtual translations, three rigid body virtual rotations, a virtual change in volume, and a virtual change in shape. The virtual change in volume can be achieved by having virtual longitudinal strains. The virtual change in shape is accomplished by having virtual shearing strains.

Consider the situation where the differential-sized parallelepiped undergoes an arbitrary rigid body rectilinear displacement in the x direction of magnitude δu . The resulting work done by the stresses acting upon the differential-sized parallelepiped is identified as $d(\delta W)$, where this d is the same d used in the term $d(\text{Vol.})$. The sum of the products of the corresponding forces and virtual displacements is

$$\begin{aligned} d(\delta W_{ex}) = & -\sigma_{xx} dy dz \delta u + \left(\sigma_{xx} + \frac{\partial \sigma_{xx}}{\partial x} dx \right) dy dz \delta u \\ & -\sigma_{yx} dx dz \delta u + \left(\sigma_{yx} + \frac{\partial \sigma_{yx}}{\partial y} dy \right) dx dz \delta u \\ & -\sigma_{zx} dx dy \delta u + \left(\sigma_{zx} + \frac{\partial \sigma_{zx}}{\partial z} dz \right) dx dy \delta u \\ & + \rho B_x dx dy dz \delta u \end{aligned}$$

After simplification, the result is the first general equilibrium equation, Eq. (1.6a), multiplied by the arbitrary common factor δu and the differential of volume. Thus if the parallelepiped is in equilibrium, the virtual work done on the parallelepiped as the result of a uniform virtual displacement is zero, and vice versa. In a similar manner, it is a simple matter to show that for a large or small rigid body rotation about Cartesian coordinates axes through the centers of the faces of the parallelepiped, zero virtual work implies the moment equilibrium equations $\sigma_{xy} = \sigma_{yx}$, and so on, and vice versa. Thus the conclusion that the virtual work associated with any virtual rigid body motion is zero when the differential-sized body is in equilibrium, and vice versa.

Now consider one step in a change in the volume of the differential parallelepiped. With a view towards an eventual superposition of deformations, let there first be a virtual strain $\delta \epsilon_{xx}$, and no other virtual strains. Without any loss of generality, let this virtual strain be the result of the back x face being stationary while the front x face moves in the positive x direction a distance $\delta \epsilon_{xx} dx$ as shown in Fig. 15.4(b). The distance the front x face moves has this value because the virtual strain, like any small strain, is the change in the original length divided by the original length. When the strain is multiplied by the original length,

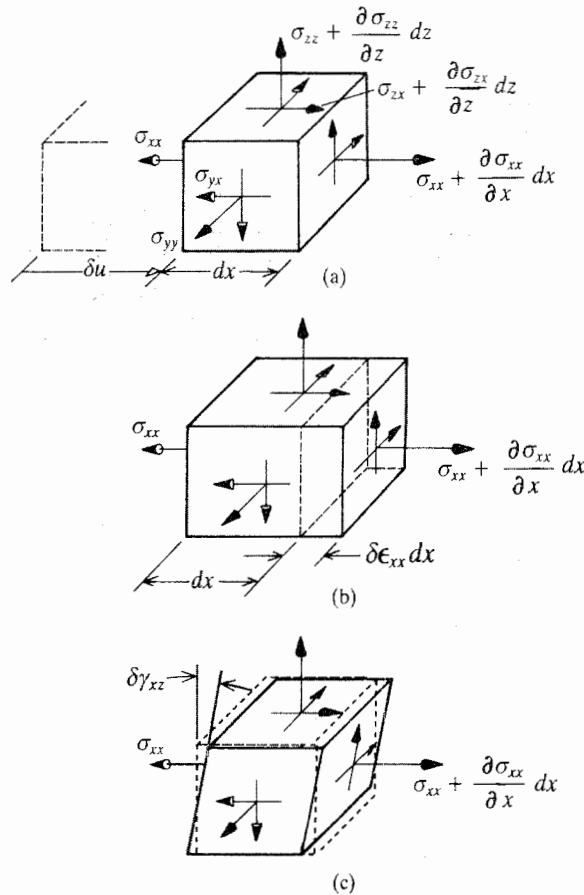


Figure 15.4. Figures for evaluating the virtual work done by the actual internal stresses acting throughout a loaded structure when the structure undergoes general virtual displacements that include rigid body components, and different types of deformations. (a) A representative virtual rigid body motion, δu . (b) A typical virtual change in size. (c) A typical virtual change in shape.

which in this case is dx , the result is the desired change in length. Another important point to recognize is that when the parallelepiped undergoes this or any other virtual deformation, the magnitudes of the actual stresses are unchanged. This lack of linkage between the actual stresses and the virtual strains parallels the lack of a linkage between the actual force and the virtual displacement in the definition of virtual work.

Now the preparations are complete for the calculation of the virtual work done by all the stresses acting upon the parallelepiped when only the front x face undergoes a virtual displacement that results in the single virtual strain $\delta \epsilon_{xx}$. These stresses are external to the boundary surface of the parallelepiped. From that point of view, they are tractions. The work done by the tractions on the back x face is zero since there is no displacement at that face. The work done by the front face traction is $[\sigma_{xx} + (\partial \sigma_{xx} / \partial x) dx] dy dz \delta \epsilon_{xx} dx$. The work done by the stresses/tractions on the other four faces depends upon how far the centers of those faces move when the x face moves the distance $\delta \epsilon_{xx} dx$. To be perfectly general, let $0 \leq \beta \approx \frac{1}{2} \leq 1$, and let the distance that these four side face centers move be $\beta \delta \epsilon_{xx} dx$.

Then the work done by remaining stresses is

$$\begin{aligned} & \left[-\sigma_{xy} + \left(\sigma_{xy} + \frac{\partial \sigma_{xy}}{\partial y} dy \right) \right] dx dz \beta \delta \epsilon_{xx} dx \\ & + \left[-\sigma_{xz} + \left(\sigma_{xz} + \frac{\partial \sigma_{xz}}{\partial z} dz \right) \right] dx dy \beta \delta \epsilon_{xx} dx + \rho B_x dx dy dz \beta \delta \epsilon_{xx} dx \end{aligned}$$

Hence, after subtracting and adding $\beta(\partial \sigma_{xx}/\partial x)\delta \epsilon_{xx} dz$, the total work done by the stresses/tractions on the differential parallelepiped can be written as

$$\begin{aligned} d(\delta W) = & \left[\sigma_{xx} \delta \epsilon_{xx} + (1 - \beta) \frac{\partial \sigma_{xx}}{\partial x} \delta \epsilon_{xx} dx \right] dx dy dz \\ & + \beta \left[\frac{\partial \sigma_{xx}}{\partial x} + \frac{\partial \sigma_{xy}}{\partial y} + \frac{\partial \sigma_{xz}}{\partial z} + \rho B_x \right] dx dy dz \delta \epsilon_{xx} dx \end{aligned}$$

The second bracketed quantity is zero because it is the left-hand side of the first general equilibrium equation, and it is required that the parallelepiped be in a state of static equilibrium. The second term of the first bracketed quantity is infinitesimal compared to the first term, and thus may be discarded. Hence, the virtual work done by the stresses/tractions external to the parallelepiped is $d(\delta W) = \sigma_{xx} \delta \epsilon_{xx} dx dy dz$ for this virtual strain. Similar expressions can be derived for the two other normal virtual displacements $\delta \epsilon_{yy} dy$ and $\delta \epsilon_{zz} dz$, and the three virtual shearing strains, where one of the three is pictured in Fig. 15.4(c). When all these terms are summed, the result is

$$\begin{aligned} d(\delta W) = & [\sigma_{xx} \delta \epsilon_{xx} + \sigma_{yy} \delta \epsilon_{yy} + \sigma_{zz} \delta \epsilon_{zz} + \sigma_{xy} \delta \gamma_{xy} + \sigma_{xz} \delta \gamma_{xz} \\ & + \sigma_{yz} \delta \gamma_{yz}] dx dy dz = [\sigma] \{\delta \gamma\} d(\text{Vol.}) \end{aligned}$$

which is exactly the same as the right-hand side of Eq. (15.10a). On the basis of Newton's third law, for each of the external stresses acting upon the parallelepiped, such as are shown in Fig. 15.4, there are equal and oppositely directed stresses within the parallelepiped. These internal stresses may be thought of as acting on the inside of the six faces of the parallelepiped in the same way as the above-discussed stresses/tractions act on the outside faces. The work done by those internal stresses differs from the above only in sign. Thus, on this basis, the right-hand side of Eq. (15.10a) is identified as the negative of the total internal virtual work, $-\delta W_{in}$. After transposing the right-hand side of Eq. (15.10a) to the left-hand side the PVW, Eq. (15.10a), can be written succinctly as

$$\boxed{\delta W_{ex} + \delta W_{in} = \delta W = 0} \quad (15.10b)$$

With this clarification of the meaning of δW_{in} , it is now possible to begin to illustrate the application of the PVW to deformable bodies. However, most applications of the PVW are postponed to Chapter 17 in order to allow the uninterrupted discussion of another closely related work principle and the brief discussion of two closely related energy principles. Endnote (3) provides one type of application of the PVW which proves the previously mentioned pairing of beam bending boundary conditions.

15.7 Complementary Virtual Work

In the above development of the Principle of Virtual Work (PVW), certain choices were made with regard to what were the dependent variables and what were the independent variables. There are many such principles as the PVW, and now is the time to make a

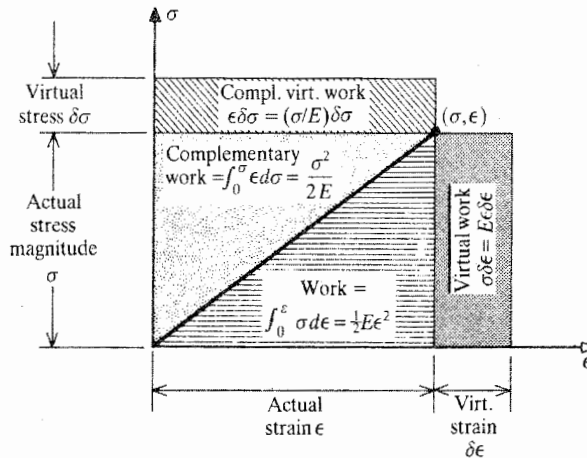


Figure 15.5. In the case of a linearly elastic material, the relationship between real (i.e., actual) work, complementary actual work, virtual work, and complementary virtual work, for one (internal) stress and its corresponding strain.

general statement regarding the classification of variables. Regardless of the principle, spatial coordinates, time, and temperature are identified as independent variables. After that, it is the choice of the analyst. In the derivation of the PVW, all applied loads and their related quantities, such as stresses, are independent quantities, while the displacements, and their related quantities, like strains, are dependent variables. In other words, the adopted viewpoint for the PVW is that the strains and displacements depend upon the applied loads. It is equally valid to take the viewpoint that the loads depend upon the displacements and strains. For example, as is seen by the equivalent relations

$$F = \frac{48EI}{L^3} w \left(\frac{L}{2} \right) \quad \text{and} \quad w \left(\frac{L}{2} \right) = \frac{FL^3}{48EI}$$

that the force acting at the center of a uniform, simply supported, symmetric beam depends upon the midspan deflection just as much as the midspan deflection depends upon the force. In other words, forces require displacements or deflections, just as much as displacements or deflections require forces or moments.

On the above basis, the opposite viewpoint to that which was adopted in the derivation of the PVW is now adopted in this section. That is, in this section the choice is made that the displacements and the strains are among the independent variables. The tractions, body forces, and stresses are here regarded as functions of the displacements or strains, and are the only dependent quantities. Thus the tractions, body forces, and stresses are the only functions that are to be varied.

Recall that the work done on a structural body, per unit volume, is the area under the curve of the stress–strain plot. Figure 15.5 shows a stress–strain plot for a uniaxially loaded, linearly elastic, uniform rod. Note that the actual work done per unit volume, the area between the straight-line loading path and the strain axis, is $\frac{1}{2}\sigma\epsilon$. In this simple case, as well as the nonlinearly elastic case, the virtual work per unit volume is simply $\sigma\delta\epsilon$. Now consider the area on the other side of the stress–strain curve. The area between the stress–strain curve and the stress axis is called the *complementary work* per unit volume. In the linearly elastic case, the complementary work has exactly the same value as the actual work. However, the *complementary virtual work* per unit volume has the value $\epsilon\delta\sigma$ for

both linearly and nonlinearly elastic materials. Again, in the case of complementary virtual work, the stresses and the applied forces are the dependent variables, and hence are varied, while the displacement-type quantities are chosen to be independent variables, and hence are not varied.

It is useful to now constrain the fictitious virtual loads and virtual stresses. Like actual load systems, all virtual applied loads are required to be in a state of equilibrium among themselves and with the internal virtual stresses. For example, from the first Cauchy equation and the first general equilibrium equation, it is required that the x direction components of the total virtual traction and the total virtual body force be such that

$$\delta T_x = \delta \sigma_{xx} \cos(n, x) + \delta \sigma_{xy} \cos(n, y) + \delta \sigma_{xz} \cos(n, z)$$

and

$$\frac{\partial(\delta \sigma_{xx})}{\partial x} + \frac{\partial(\delta \sigma_{xy})}{\partial y} + \frac{\partial(\delta \sigma_{xz})}{\partial z} + \rho \delta B_x = 0$$

After stipulating these preliminary requirements for equilibrium among the virtual forces and stresses, the derivation of the Principle of Complementary Virtual Work (PCVW) begins with the identity

$$\begin{aligned} \iint_{S_2} (u \delta T_x + v \delta T_y + w \delta T_z) dS + \iiint_{\text{Vol.}} \rho (u \delta B_x + v \delta B_y + w \delta B_z) d(\text{Vol.}) &\equiv \\ \iint_{S_2} (u \delta T_x + v \delta T_y + w \delta T_z) dS + \iiint_{\text{Vol.}} \rho (u \delta B_x + v \delta B_y + w \delta B_z) d(\text{Vol.}) &= I_{\text{surf}} + I_{\text{Vol.}} \end{aligned}$$

Once again, it must be emphasized that since the starting point is an identity, so too will be the end result which is the PCVW. Again, this will mean that the PCVW will be valid in all circumstances (of small displacements). Working only with the two integrals on the right-hand side of the above identity, begin with the surface integral here called I_{surf} . The first thing to do is extend the limits of integration from S_2 where displacements are prescribed, and since the tractions are unknown, they can be varied as is seen above. Extend this limit to include S_1 without changing the value of the integral. This is possible because on S_1 forces are prescribed, and hence their variation must be zero. Using the virtual Cauchy equations, I_{surf} can be written as

$$\begin{aligned} I_{\text{surf}} = \iint [u(\delta \sigma_{xx} v_x + \delta \sigma_{xy} v_y + \delta \sigma_{xz} v_z) + v(\delta \sigma_{xy} v_x + \delta \sigma_{yy} v_y + \delta \sigma_{yz} v_z) \\ + w(\delta \sigma_{xz} v_x + \delta \sigma_{yz} v_y + \delta \sigma_{zz} v_z)] dS \end{aligned}$$

Using the Green–Gauss theorem, I_{surf} can be converted into the volume integral

$$\begin{aligned} I_{\text{surf}} = \iiint_{\text{Vol.}} \left[\frac{\partial}{\partial x} (u \delta \sigma_{xx}) + \frac{\partial}{\partial y} (u \delta \sigma_{xy}) + \frac{\partial}{\partial z} (u \delta \sigma_{xz}) + \frac{\partial}{\partial x} (v \delta \sigma_{xy}) + \frac{\partial}{\partial y} (v \delta \sigma_{yy}) \right. \\ \left. + \frac{\partial}{\partial z} (v \delta \sigma_{yz}) + \frac{\partial}{\partial x} (w \delta \sigma_{xz}) + \frac{\partial}{\partial y} (w \delta \sigma_{yz}) + \frac{\partial}{\partial z} (w \delta \sigma_{zz}) \right] d(\text{Vol.}) \end{aligned}$$

Combining this surface integral result with the original volume integral on the right-hand side of the original identity, leads to

$$\begin{aligned}
 I_{surf} + I_{Vol.} = & \iiint_{Vol.} [u(\rho\delta B_x + \delta\sigma_{xx,x} + \delta\sigma_{xy,y} + \delta\sigma_{xz,z}) + v(\rho\delta B_y + \delta\sigma_{xy,x} + \delta\sigma_{yy,y} + \delta\sigma_{yz,z}) \\
 & + w(\rho\delta B_z + \delta\sigma_{xz,x} + \delta\sigma_{yz,y} + \delta\sigma_{zz,z})] d(Vol.) + \\
 & \iiint_{Vol.} [u_{,x}\delta\sigma_{xx} + v_{,y}\delta\sigma_{yy} + w_{,z}\delta\sigma_{zz} + (u_{,y} + v_{,x})\delta\sigma_{xy} \\
 & + (u_{,z} + w_{,x})\delta\sigma_{xz} + (v_{,z} + w_{,y})\delta\sigma_{yz}] d(Vol.) \quad (15.11)
 \end{aligned}$$

It is at this point that the other precondition, that of the general equilibrium of the virtual stresses and the virtual body forces is introduced, and the first of the above two volume integrals is eliminated. The next step is to both add and subtract the following integral from the above result

$$\iiint_{Vol.} [\epsilon_{xx}\delta\sigma_{xx} + \epsilon_{yy}\delta\sigma_{yy} + \epsilon_{zz}\delta\sigma_{zz} + \gamma_{xy}\delta\sigma_{xy} + \gamma_{xz}\delta\sigma_{xz} + \gamma_{yz}\delta\sigma_{yz}] d(Vol.)$$

and regroup terms to get for the original right-hand side

$$\begin{aligned}
 I_{surf} + I_{Vol.} = & \iiint_{Vol.} \left[\left(\frac{\partial u}{\partial x} - \epsilon_{xx} \right) \delta\sigma_{xx} + \left(\frac{\partial v}{\partial y} - \epsilon_{yy} \right) \delta\sigma_{yy} + \left(\frac{\partial w}{\partial z} - \epsilon_{zz} \right) \delta\sigma_{zz} \right. \\
 & + \left(\frac{\partial u}{\partial y} + \frac{\partial v}{\partial x} - \gamma_{xy} \right) \delta\sigma_{xy} + \left(\frac{\partial u}{\partial z} + \frac{\partial w}{\partial x} - \gamma_{xz} \right) \delta\sigma_{xz} \\
 & + \left. \left(\frac{\partial v}{\partial z} + \frac{\partial w}{\partial y} - \gamma_{yz} \right) \delta\sigma_{yz} \right] d(Vol.) \\
 & + \iiint_{Vol.} [\epsilon_{xx}\delta\sigma_{xx} + \epsilon_{yy}\delta\sigma_{yy} + \epsilon_{zz}\delta\sigma_{zz} + \gamma_{xy}\delta\sigma_{xy} + \gamma_{xz}\delta\sigma_{xz} + \gamma_{yz}\delta\sigma_{yz}] d(Vol.)
 \end{aligned}$$

The last step is to now introduce the strain–displacement equations for the actual strains and displacements. This step cancels the first of the above integrals, and leads to the final result

$$\begin{aligned}
 & \iint_S (u\delta T_x + v\delta T_y + w\delta T_z) dS + \iiint_{Vol.} \rho(u\delta B_x + v\delta B_y + w\delta B_z) d(Vol.) \\
 & = \iiint_{Vol.} (\epsilon_{xx}\delta\sigma_{xx} + \epsilon_{yy}\delta\sigma_{yy} + \epsilon_{zz}\delta\sigma_{zz} + \gamma_{xy}\delta\sigma_{xy} + \gamma_{xz}\delta\sigma_{xz} + \gamma_{yz}\delta\sigma_{yz}) d(Vol.) \quad (15.12)
 \end{aligned}$$

In other words, given the strain–displacement equations, obtain the PCVW, which is Eq. (15.12). In this case the reverse procedure of starting with the PCVW, Eq. (15.12), and obtaining the strain–displacement equations is quite straightforward, and left to the reader. With that result in hand, it can be said that the PCVW is necessary and sufficient for (the same thing as) the strain–displacement equations. In other word, simply writing this equation for any structural system enforces continuity of displacements and strain compatibility in that system.

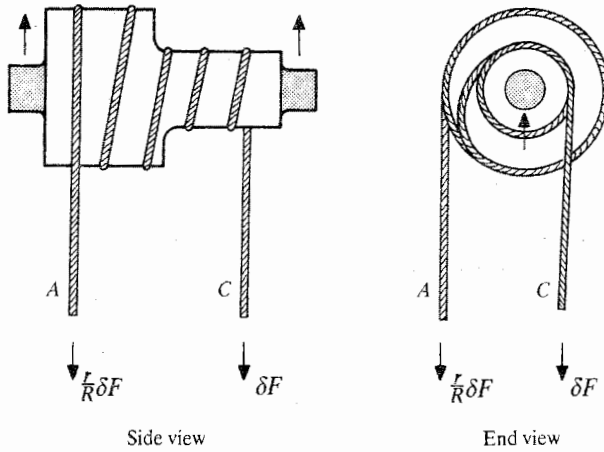


Figure 15.6. Example 15.7. The analysis of a pulley using complementary virtual work.

The Principle of Complementary Virtual Work can be written in more concise matrix form as

$$\boxed{\iint_{S_2} [u] \{\delta T\} dS + \iiint_{\text{Vol.}} \rho [u] \{\delta B\} d(\text{Vol.}) = \iiint_{\text{Vol.}} [\gamma] \{\delta \sigma\} d(\text{Vol.})} \quad (15.12a)$$

or in still more concise form, $\delta W_{ex}^* = -\delta W_{in}^*$, or

$$\boxed{\delta W_{ex}^* + \delta W_{in}^* = \delta W^* = 0} \quad (15.12b)$$

Just as is the case for the PVW, the PCVW makes no reference to constitutive equations. Thus the PCVW is valid for a structure composed of any material including one that is rigid. When the structure is rigid, the PCVW reduces to $\delta W_{ex}^* = 0$. However, there are very few rigid body problems for which the PCVW sheds much light. One such problem is offered in Example 15.7. Nevertheless, the PCVW is very useful for elastic structures, be they linearly elastic or nonlinearly elastic. Chapters 20 and 21 are devoted to examining the application of the PCVW to elastic structures. Endnote (4) of this chapter uses the PCVW to rederive the uniform torsion equations in terms of the Prandtl stress function.

Example 15.7. Determine the travel of the inner inextensional rope of the one-stage, compound, rigid pulley shown in Fig. 15.6 relative to the travel of the outer inextensional rope.

Solution. Disregard the actual tensile forces in the inner and outer ropes at points A and C. Since the PCVW requires that all virtual forces equilibrate each other, place virtual forces at points A and C that are in moment equilibrium about the axis of the pulley as shown in the figure. Then, with the downward vertical deflection of the rope at point A being u_a and

the downward vertical deflection at point C being u_c , the calculation of the complementary virtual work is

$$\delta W_{ex}^* = 0 = \frac{r}{R} \delta F u_a + \delta F u_c \quad \text{or} \quad u_c = -\frac{r}{R} u_a \quad \blacksquare$$

In summary, just as the PVW is based upon virtual displacements that are continuous and virtual strains that are compatible, the PCVW is based upon virtual stresses, virtual tractions, and virtual body forces that are in equilibrium. Just as the PVW is a statement that is wholly equivalent to the vector equations of interior and exterior equilibrium, the PCVW is a statement that is a necessary and sufficient condition for the geometric strain–displacement equations. Neither the PVW nor the PCVW involve any relation between the actual stresses and actual strains. Therefore, both the PVW and the PCVW apply to structural bodies with any constitutive relations whatsoever. However, both principles because they involve the small displacement strain–displacement equations, are limited to small strains only. Finally, using tensor notation, it is easy to prove that the products $[\sigma] \{\delta \gamma\}$ and $[\gamma] \{\delta \sigma\}$ are unaltered by rotations of the Cartesian coordinate system.

15.8 **Energy and Other Principles**

The internal and external loads acting upon a structural system are conservative whenever the material of the structure is reasonably describable by an elastic material model, the external loads retain their original line of action irrespective of the deformation of the structure, and in certain other cases (Ref. [34]). When the forces are conservative, so too is the actual and virtual work accomplished by those forces. Like any conservative work expression, that work can be equated to the negative of a corresponding potential energy. Therefore, for conservative forces, from the negative of the external virtual work expression, the virtual potential energy of the external loads is written as

$$\delta V = - \iint_S [\delta u] \{T\} dS - \iiint_{\text{Vol.}} \rho [\delta u] \{B\} d(\text{Vol.})$$

Like any potential function, the external virtual potential energy of the external loads, V , is a point function. Therefore, the δ can be treated as an operator acting upon this potential energy function. Hence

$$\delta(V) = -\delta \left[\iint_S [u] \{T\} dS + \iiint_{\text{Vol.}} \rho [u] \{B\} d(\text{Vol.}) \right] \quad (15.13)$$

where the quantity within the square brackets is, of course, the *potential energy of the external loads*. Since this expression is a potential for work rather than complementary work, here the loads are considered to be independent variables and are to be treated as if they were constants when subject to the variational operator.

Just as there is a potential function for conservative external loads, there is also a potential function for the accompanying conservative internal loads. Consider the virtual internal potential energy that is the result of actual stresses moving through virtual strains. It is here symbolized as δU . Again, like any conservative work and potential energy relationship,

the virtual internal potential energy, called the *virtual strain energy*, is the negative of the internal virtual work. Hence it is possible to write from Eq. (15.10a, b) that

$$\delta U = \iiint_{\text{Vol.}} [\sigma] \{\delta \gamma\} d(\text{Vol.})$$

Introducing the linearly elastic stress-strain relations (without temperature change effects for the moment) yields

$$\delta U = \iiint_{\text{Vol.}} [\gamma] [E] \{\delta \gamma\} d(\text{Vol.}) = \frac{1}{2} \iiint_{\text{Vol.}} \delta [\gamma] [E] \{\gamma\} d(\text{Vol.})$$

where the reader can verify that the variation of the quadratic form $(1/2)[\gamma][E]\{\gamma\}$ is indeed $[\gamma][E]\{\gamma\}$ because $[E]$ is a symmetric matrix (see the exercises.) Interchanging the order of the integration and the variation leads to

$$\delta U = \delta \frac{1}{2} \iiint_{\text{Vol.}} [\gamma] [E] \{\gamma\} d(\text{Vol.}) = \delta(U) \quad (15.14)$$

where, of course,

$$U = \frac{1}{2} \iiint_{\text{Vol.}} [\gamma] [E] \{\gamma\} d(\text{Vol.})$$

The internal potential energy that is a result of strains, U , is, of course, called the (actual) *strain energy*. Replacing the external and internal virtual work expressions of the PVW by their respective potentials, and multiplying through by -1 , yields

$$\delta U + \delta V = \delta(U + V) = \delta \Pi = 0 \quad (15.15)$$

where $\Pi \equiv U + V$, is called the *total potential energy*. Since the variation of the total potential energy is zero, Eq. (15.15) is called the (*principle of the stationary value of the total potential energy*). The Principle of the Stationary⁸ Value of the Total Potential Energy differs from the PVW in that (i) it is limited to conservative external forces and elastic internal forces, and (ii) as such, it involves a specific constitutive relation. What is gained by the use of this limited, special form is the knowledge that the stationarity is at the minimum of the total potential energy (Ref. [3]). The fact that the total potential energy is a minimum for compatible displacements when the force system is required to be in equilibrium is important to the use of this principle with approximate methods of analysis. This principle is also called the *principle of the minimum value of the total potential energy*.

To consider potential functions for complementary work quantities, first consider the product of stress and strain. Since, for an elastic material, both stress and strain are single-valued point functions, so too is their product a single-valued point function. Consider a stress-strain plot for an elastic material such as is shown in Fig. 15.5, which is for a linearly elastic material. The actual loading path terminates at some unique pair of values (ϵ, σ) . Consider the rectangle whose sides parallel the stress and strain axes and where one diagonal runs from $(0, 0)$ to (ϵ, σ) . Since the area of this rectangle is the product of the final stress and strain values, this rectangular area represents the point function $\sigma \epsilon$. When the loading

⁸ The meaning of "stationary" in this context is taken from the circumstance of a tangent having a zero slope, such as it would at a local maximum, local minimum, or inflection point. At a point where the slope of the tangent is zero, the function is neither increasing nor decreasing, that is, it is "stationary."

is such that the actual internal work, the part of the rectangle below the stress–strain path is also a point function (i.e., when the internal work is conservative), then the remaining area, which is the complementary internal work, is the difference between the two point functions, and thus must also be a point function. In other words, when the actual work is conservative, so too is the complementary work. When the actual internal complementary work is conservative, then it can be represented as the negative of a potential function U^* , which is called the *complementary strain energy*.

In a similar fashion, it can be reasoned that whenever the external loads do conservative work, the complementary external work is also conservative. In that case a potential energy can be associated with the complementary external work, which is called the *complementary potential energy of the external loads*, V^* . Thus, under the same conditions that permit the principle of the minimum value of the total potential energy, there is the *principle of the minimum value of the total complementary potential energy*, which is

$$\delta U^* + \delta V^* = \delta(U^* + V^*) \equiv \delta \Pi^* = 0 \quad (15.16)$$

where

$$U^* = \frac{1}{2} \iiint_{\text{Vol.}} [\sigma][S]\{\sigma\} d(\text{Vol.})$$

and

$$V^* = V = - \iint_S [u]\{T\} dS - \iiint_{\text{Vol.}} \rho [u]\{B\} d(\text{Vol.})$$

Note that while $V = V^*$, the variations of these two quantities are quite different because with V only the displacements are varied, while with V^* , only the traction and body force components are varied. Note further that while the integrand of U , often referred to as *the strain energy density* and symbolized as U_0 , is always written as a function of the strains, the integrand of U^* , *the complementary strain energy density*, U_0^* , is always written as a function of the stresses. In exactly the same fashion as the PCVW, this principle, the principle of the minimum value of the total complementary potential energy, when used with a force system in equilibrium, enforces strains compatible with the strain–displacement equations.

The last four sections have set forth the essentials of the four basic principles, the PVW, the PCVW, the principle of the minimum value of the total potential energy, and the principle of the minimum value of the total complementary potential energy. In keeping with this pattern of increasing brevity of discussion, it is appropriate to just mention that there are still other principles. One distinguishing characteristic of these other principles is that they involve a different set of dependent variables. For example, the Hellinger–Reissner principle and the Reissner principle treat both the stresses and strains over the interior as dependent quantities. Hence both stresses and strains are varied in these two closely related principles.

15.9 **Modifications for Temperature Changes**

The presence of temperature changes complicates the writing of potential energy functions. Consider Figs. 15.7(a, b), which represent two different uniaxial loading stress–strain paths to the same final point on the stress–strain plot. In the first case, the mechanical loads are applied first, and then the temperature change. In the second case, the order of the

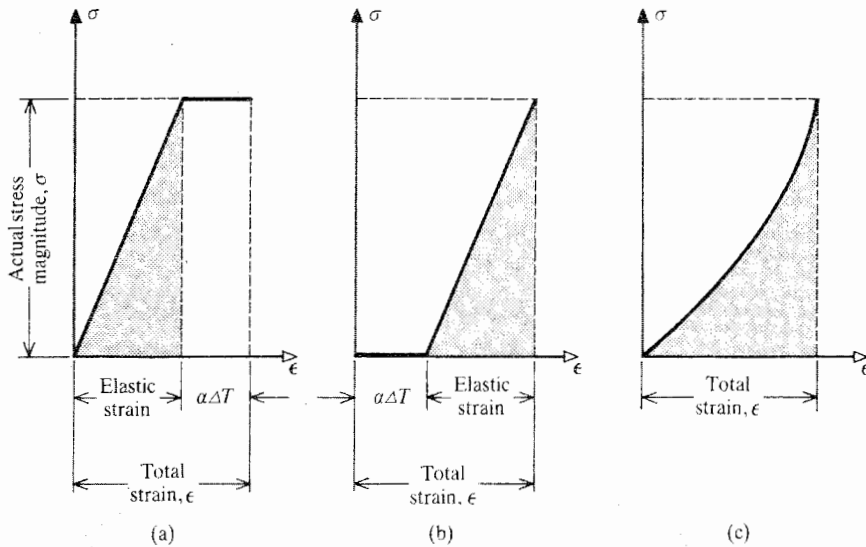


Figure 15.7. Stress–strain curves for an unconstrained, linearly elastic material subjected to different orderings of the same mechanical and thermal loadings leading to the same final stress and strain values. (a) The mechanical loading first. (b) The thermal loading first. (c) The simultaneous application of the mechanical and thermal loadings.

mechanical and thermal strains is reversed. Note, as before, the viewpoint is adopted that with regard to the stress–strain relations, each differential parallelepiped is wholly free to expand in response to a temperature change, and whatever actual *internal* constraints are present are imposed by the strain–displacement and equilibrium equations, and the *external* constraints are imposed by the displacement and force-type boundary conditions. Hence these diagrams show no increase in stress due to the thermal expansion. As before, the area under the curve is the work done per unit volume on the differential-sized parallelepiped. Clearly, the work done per unit volume is not the same in these two cases. Thus, when there is a temperature change, the work is path-dependent or nonconservative even for a linearly elastic material. Hence no potential function can be ascribed to either quantity of work. However, there is one portion of the total work that is the same in both cases (i.e., independent of path) and is thus eligible to be called conservative and have an associated potential function. That invariant portion of the total work is represented by the shaded triangular portion $[\frac{1}{2}(\epsilon - \alpha \Delta T)]$, where ϵ is the total strain, and $(\epsilon - \alpha \Delta T)$ is the elastic strain, that is, the strain that results solely from the action of the conservative external forces acting upon the linearly elastic material. Thus the integrand of the volume integral for the strain energy, the strain energy density, for this uniaxial loading case with a temperature change becomes

$$U_0 = \frac{1}{2} \sigma (\epsilon - \alpha \Delta T) = \frac{1}{2} E (\epsilon - \alpha \Delta T)^2$$

Again, the product $\sigma \epsilon$ is path-independent, so then too is $(\sigma \epsilon - U_0) \equiv U_0^*$. Carrying out this last bit of algebra shows that

$$U_0^* = \frac{1}{2} \sigma (\epsilon + \alpha \Delta T) = \frac{1}{2} \sigma^2 + \sigma \alpha \Delta T$$

In a manner similar to the previous internal virtual work calculations of Section 15.6, it can be shown that, when all six stresses are present, and each strain is considered in turn,

$$U_0 = \frac{1}{2}[\sigma_{xx}(\epsilon_{xx} - \alpha \Delta T) + \sigma_{yy}(\epsilon_{yy} - \alpha \Delta T) + \sigma_{zz}(\epsilon_{zz} - \alpha \Delta T) \\ + \sigma_{xy}\gamma_{xy} + \sigma_{xz}\gamma_{xz} + \sigma_{yz}\gamma_{yz}]$$

where there is no effect from the temperature changes on the work done by the shearing stresses and strains. In matrix form, with the use of Eq. (6.3) for an isotropic material, that is, by use of $\{\sigma\} = [E]\{\gamma\} - \Delta T [E]\{\alpha\}$,

$$U_0(\gamma) = \frac{1}{2}[\gamma]\{\sigma\} - \frac{1}{2}\alpha \Delta T(\sigma_{xx} + \sigma_{yy} + \sigma_{zz}) \\ = \frac{1}{2}[\gamma][E]\{\gamma\} - \frac{1}{2}\Delta T([\gamma][E]\{\alpha\} + \alpha(\sigma_{xx} + \sigma_{yy} + \sigma_{zz})) \\ = \frac{1}{2}[\gamma][E]\{\gamma\} - E\alpha \Delta T \frac{(\epsilon_{xx} + \epsilon_{yy} + \epsilon_{zz})}{1 - 2\nu} \\ + \frac{(3E/2)(\alpha \Delta T)^2}{1 - 2\nu}$$

Recall that when the variation operator is applied to $U_0(\gamma)$, the third term in the final expression for U_0 disappears. Similar expressions can be written for the complementary strain energy density. Using Eq. (6.1) for an isotropic material, then

$$U_0^*(\sigma) = \frac{1}{2}[\sigma]\{\gamma\} + \frac{1}{2}\alpha \Delta T(\sigma_{xx} + \sigma_{yy} + \sigma_{zz}) \\ = \frac{1}{2}[\sigma][S]\{\sigma\} + \alpha \Delta T(\sigma_{xx} + \sigma_{yy} + \sigma_{zz})$$

While the above strain and complementary strain energy expressions are a bit lengthy, they are seldom needed beyond the reduced form of plane stress.

15.10 Summary

$$\text{Virtual Work: } \delta W \equiv \mathbf{F} \cdot \delta \mathbf{D} \quad \text{CVW: } \delta W^* \equiv \mathbf{D} \cdot \delta \mathbf{F}$$

There is one pair of basic work principles, and another pair of basic potential energy principles. Each pair of principles closely parallels the other pair. The pair of potential energy principles are particularly convenient when working with elastic materials. The more general work principles are valid for nonconservative as well as conservative loads and materials. (Again, an example of a nonconservative material is an elasto-plastic material that is both loaded and unloaded.)

The PVW enforces equilibrium of the actual stresses when its use begins with varied strains that are compatible with the continuous virtual displacements. The PCVW enforces compatible actual strains when it begins with varied loads that are in equilibrium. The PVW corresponds to a displacement formulation, while the PCVW corresponds to a stress formulation. Both principles are desirable because it is always desirable to have more than one way to approach a problem. As is generally true for the corresponding two types of formulations, the PVW is easier to use in large, complex problems, because identifying the unknown deflection quantities is much easier than identifying unknown internal forces, while the PCVW is easier to use in small problems in the sense that generally there are fewer unknown quantities to be determined.

Students are sometimes confused by the presence of the factor one-half in front of some work and energy expressions and its absence from other such expressions. The factor

one-half is a flag that indicates that work or energy expression is for actual work done, or energy stored, by real, not virtual, forces acting upon a linearly elastic material. The reason for this is that only in the case of real forces and real displacements do the stress and the strain increase together. When, as in Fig. 15.5, the force–displacement curve is a straight line, then a triangular shape is created under that curve. Then the factor one-half is necessary to describe the area of that triangle under the force–displacement curve, which is the work done upon the material body. When the forces are fully developed, as is always the case with virtual displacements, then the forces do not vary with the displacement, and the work done is simply the force multiplied by the virtual displacement, and thus there is no factor of one-half. A factor other than one-half in front of a nonvirtual energy expression would indicate a nonlinearly elastic material.

Example 15.8. Let $f(x, y, u, v, u_x) = yu + xv + x^2u_x$. (a) If $u = u(x, y)$ and $v = v(x, y)$, what then is δf ? (b) If $u = x\sqrt{y}$, and $v = y\sqrt{x}$, what then is δf ?

Solution. (a) Using the ordinary differential calculus, but restricting the use of the variation operator to the dependent functions u and v and their derivatives, leads to $\delta f = y\delta u + x\delta v + x^2\delta u_x$. The last of these three terms could be written as $x^2(\partial/\partial x)\delta u$. (b) $\delta f = 0$, because now $f = f(x, y)$ is a known function of the independent variables x and y . ■

Chapter 15 Exercises

- 15.1.** (a) Show that the force $\mathbf{F}_1 = (F_0/L)(y\mathbf{i} + x\mathbf{j})$ is conservative, and the force $\mathbf{F}_2 = (F_0/L)(y\mathbf{i} - x\mathbf{j})$ is nonconservative by taking their curl (i.e., by calculating $\nabla \times \mathbf{F}$).
- (b) Calculate the work done by each force between the points $(0, 0)$ and (a, b) along each of the three paths: (i) a dogleg up the y axis to the point $(0, b)$ and then paralleling the x axis to (a, b) ; (ii) along a straight line between $(0, 0)$ and (a, b) ; and (iii) a dogleg paralleling first the x axis and then the y axis.
- 15.2.** Take the variation of the following functions where it is understood that u and v are dependent variables of unknown form while x and y are independent variables
- (a) $(u + xy)^2v$
 (b) $u + yu_x$
 (c) $G(x, u_x, v_x)$
 (d) $u \sin(u_x)$
- 15.3.** (a) Consider Fig. 15.8. The externally applied forces F_1 and F_2 have known values. The beam reactions are designated by R_i , $i = 1, 2, 3$. Note that the right-hand end of the beam is forced to undergo an upward (actual) deflection of magnitude d_0 . Calculate the external virtual work.
- (b) As in part (a), calculate the external complementary virtual work.
- (c) Consider a uniform traction T_r , acting at the outer edge of a flat plastic disk of radius R and uniform thickness h . This disk is in a state of plane stress where the actual displacements are only functions of r , and not of θ . Thus it is appropriate to also limit the virtual displacements throughout the disk to being only functions of the radial distance. On this basis, calculate the external virtual work done by the traction at the outer disk boundary.
- (d) Calculate the virtual work done by the gravitational force acting upon a pendulum bob of mass m when, at the typical instant in time for which this calculation is to be made the pendulum is at an angle θ to the vertical, static equilibrium

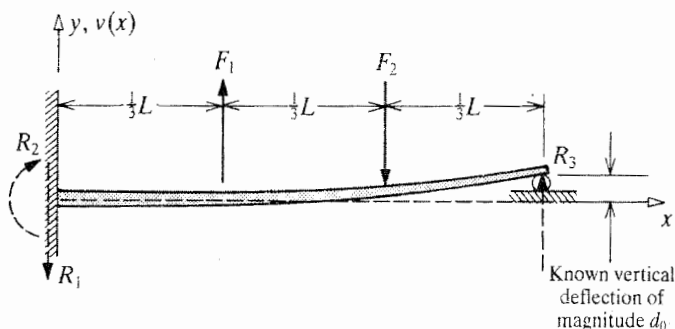


Figure 15.8. Exercise 15.3 (a, b). A beam loaded by forces and enforced deflections.

position of the pendulum. Let L be the distance from the axis of rotation to the center of mass of the bob.

(e) Calculate the complementary external virtual work at the circular boundary of part (c).

15.4. Verify that $\delta(\frac{1}{2}[\gamma][E]\{\gamma\})$ is indeed $[\gamma][E]\{\delta\gamma\}$ in the case of plane strain by actually carrying out the matrix multiplication, and then applying the variational operator. Hopefully the reader will then see that what is true for this case where the column vector is 3×1 is true regardless of the size of the column vector.

15.5. (a) Write the expression for the virtual external work in cylindrical coordinates for a single, actual, external force \mathbf{F} of arbitrary magnitude when u , v , and w are the unknown displacements at the point of application of the force in the r , θ , and z directions.

(b) Write the expression for the complementary virtual work of the circumstances of part (a). Here, of course, the magnitude of the force is unknown.

FOR THE EAGER

15.6. Explain why the previously developed expressions for U_0 and U_0^* hold true even when the temperature change and the mechanical loads are applied simultaneously as shown in Fig. 15.7(c).

15.7. From the PVW, derive the first of the three theory of elasticity equilibrium equations by letting $\delta u(x, y, z) = \text{const.}$, and $\delta v(x, y, z) = \delta w(x, y, z) = 0$. Use the Green–Gauss theorem.

15.8. Derive *Hamilton's principle* which is, where T is the kinetic energy, t is time, and $t_1 < t_2$ are arbitrary values of time,

$$\int_{t_1}^{t_2} (\delta T + \delta W) dt = 0$$

Hint: Start again with Eq. (15.7a), which still fully describes the virtual external work. Now, however, the tractions and body forces are functions of time as well as the spatial coordinates. Again use the Cauchy equation, Eq. (1.9) and the Green–Gauss theorem as before to obtain the same result, which is Eq. (15.8b). The first difference in the derivation occurs at this point in the right-hand side of Eq. (15.8b).

Now, rather than write zero as the value for the first integral on the right-hand side, as was done in the static case, Newton's second law is written as

$$[\partial][\sigma] + \rho[B] = \rho \left[\frac{d^2u}{dt^2} \quad \frac{d^2v}{dt^2} \quad \frac{d^2w}{dt^2} \right] = \rho[\ddot{u}]$$

where, of course, $[\ddot{u}]$ is a row vector of accelerations of the infinitesimal parallelepipeds (points) of the structural mass. These latter accelerations are in addition to the first set of accelerations $[B]$. The difference between the two sets of accelerations is now that those accelerations that do not vary with time are conveniently placed in the first set, $[B]$, while those that do vary with time are placed in the second set. In other words, write Eq. (15.8b), which is

$$\delta W_{ex} = \iiint_{\text{Vol.}} ([\partial][\sigma] + \rho[B])\{\delta u\} d(\text{Vol.}) + \iiint_{\text{Vol.}} [\sigma]\{\delta \gamma\} d(\text{Vol.})$$

as

$$\delta W_{ex} = + \iiint_{\text{Vol.}} \rho[\ddot{u}]\{\delta u\} d(\text{Vol.}) + \iiint_{\text{Vol.}} [\sigma]\{\delta \gamma\} d(\text{Vol.})$$

After transposing the second integral on the right-hand side to the left-hand side,

$$\delta W_{ex} + \delta W_{in} = \delta W = \iiint_{\text{Vol.}} \rho[\ddot{u}]\{\delta u\} d(\text{Vol.})$$

Now integrate both sides of the above equality with respect to time over the arbitrary time interval (t_1, t_2) . After interchanging the order of integration, which is wholly valid since both definite integrals have finite intervals of integration, and there are no singularities in either the accelerations or the virtual displacements, the result for the right-hand side is

$$\iiint_{\text{Vol.}} \int_{t_1}^{t_2} \rho[\ddot{u}]\{\delta u\} dt d(\text{Vol.})$$

Now the typical term of the above three-part volume integrand is

$$\frac{d\dot{u}}{dt} \delta u dt = d\dot{u} \delta u = d(\dot{u} \delta u) - \dot{u} d(\delta u) = d(\dot{u} \delta u) - \dot{u} \delta \dot{u} dt$$

Substitute and carry out the time integration. The first term is an exact differential, so it integrates to $(du/dt) \delta u$ which must be evaluated at the values of the arbitrary time limits of integration. Since the varied displacement δu is arbitrary, it is convenient to require that $\delta u(x, y, z; t_1) = \delta u(x, y, z; t_2) = 0$, that is, require that the varied displacement components always be zero at the end points of any time interval of interest. Then this first integral vanishes. A typical term of the second integrand can be rewritten as

$$-\rho \dot{u} \delta \dot{u} = -\delta \left[\frac{1}{2} \rho \dot{u}^2 \right] = -\delta T$$

The remaining steps of the derivation are left to the reader. As a final remark, a similar principle can be derived for the complementary virtual work. However, complementary work principles do not seem to be nearly as advantageous in structural dynamics as they are for static problems.

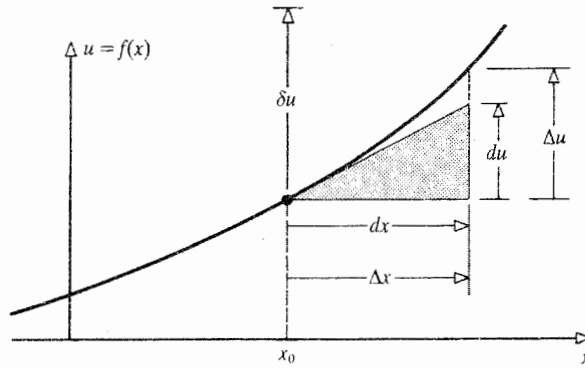


Figure 15.9. A sketch illustrating the differences between du , δu , and Δu , where the latter quantity is the total change in the function $u(x)$ in response to a change in the independent variable, Δx . When dx is small and equal to Δx , then du is a close approximation to Δu . Note that δu is only associated with the point x ; that is, in no way is it tied to any change in the independent variable x .

15.9. Use Hamilton's principle to derive the Lagrange equation of motion, Eq. (15.1). Note that the Lagrange equation can be derived without a full explanation of the meaning of the coordinate set $\{q\}$ for which q_i is the i th term. These coordinates, called "generalized coordinates," are explained in Section 17.2. *Hint:* In its most general form, the kinetic energy is a function both of time and the generalized displacements as well as of the generalized velocities; that is, in general, $T = T(dq_i/dt, q, t)$. In its most general form, the virtual work (and its corresponding virtual potential energy) is at most a function of the generalized displacements. Also note that by definition, the virtual work can always be written as $\delta W = \sum Q_i \delta q_i$, where the coefficients of the virtual displacements are called the "generalized forces."

15.10. What are the generalized forces of Exercise 15.5(a) associated with δu , δv , and δw .

Endnote (1) Further Explanation of the Variational Operator

It was previously explained that for a dependent function $f(x)$ of unknown functional form, δf is not tied to a δx as df is tied to dx , because, by definition, all variations of independent variables such as x are zero (i.e., they do not exist). In order to contrast differentials and variations, consider Fig. 15.9, which shows a graph of an arbitrary dependent variable $u = u(x, y, z)$ where, for clarity of discussion, the coordinates y and z are fixed. In other words, for the moment, consider only changes in $u(x, y, z)$ with respect to x . At point x_0 , a differential change in x produces a like change in $u(x)$ according to the definition for the differential at the point $x = x_0$; that is, $du = f'(x_0)dx$. The geometric interpretation of the first derivative at $x = x_0$ as the tangent to the curve $u = f(x)$ at $x = x_0$ shows that the bigger dx , the bigger the magnitude of du . Note in passing that the total change in u , here called Δu , that results from a change in the independent variable, $\Delta x \equiv dx$, is not, in general, the same as du but is very closely approximated by du when dx is required to become vanishingly small. In contrast to du and Δu , δu stands by itself. That is, δu does not depend in any way on either a variation of the independent variable x , which of course does not exist, or the values of the function $u = u(x)$ at $x = x_0$ or elsewhere. It is a totally arbitrary value, positive or negative, at any particular point $x = x_0$. The function

$\delta u(x)$, however, should always have properties that parallel those of the function $u(x)$; that is, $\delta u(x)$ should be equally continuous and differentiable. Again, the sum $u(x) + \delta u(x)$ is called the “varied path.”

Consider the analytical functional⁹ $F(x, y, u, u_x)$ of the unknown function $u = u(x, y)$, and its partial derivative $u_x = u_x(x, y)$. This is a limited choice for the argument of F , but it is sufficient to illustrate all the necessary concepts. Also consider the functional value when its dependent variables are augmented by their respective variations, that is, also consider $F(x, y, u + \delta u, u_x + \delta u_x)$. Another way of saying the same thing is to say consider the original functional and the functional of the varied paths. Define the difference between these two functionals as the *total variation* of the functional, which is written as

$$\delta^t F = F(x, y, u + \delta u, u_x + \delta u_x) - F(x, y, u, u_x)$$

If the four quantities of the argument of the functional $F(x, y, u, u_x)$ are formally treated as any four variables, and the functional $F(x, y, u + \delta u, u_x + \delta u_x)$ is treated formally as the same function evaluated at somewhat different values of the four variables, then it is possible to write a Taylor’s series expansion for the functional with respect to the varied coordinates. The Taylor’s series result is (see the multivariable expansion description in Section I.2)

$$\begin{aligned} F(x, y, u + \delta u, u_x + \delta u_x) &= F(x, y, u, u_x) + \delta u \frac{\partial F}{\partial u} + \delta u_x \frac{\partial F}{\partial u_x} \\ &+ \frac{1}{2} \left[(\delta u)^2 \frac{\partial^2 F}{\partial u^2} + 2\delta u \delta u_x \frac{\partial^2 F}{\partial u \partial u_x} + (\delta u_x)^2 \frac{\partial^2 F}{\partial u_x^2} \right] \\ &+ \frac{1}{3!} \left[(\delta u)^3 \frac{\partial^3 F}{\partial u^3} + 3(\delta u)^2 \delta u_x \frac{\partial^3 F}{\partial u^2 \partial u_x} + \dots \right] + \dots \end{aligned}$$

or

$$\delta^t F = \left\{ \frac{\partial F}{\partial u} \delta u + \frac{\partial F}{\partial u_x} \delta u_x \right\} + \left\{ \frac{1}{2} \left[\frac{\partial^2 F}{\partial u^2} (\delta u)^2 + 2 \frac{\partial^2 F}{\partial u \partial u_x} \delta u \delta u_x + \frac{\partial^2 F}{\partial u_x^2} (\delta u_x)^2 \right] \right\} + \dots$$

where, of course, $(\delta u)^2 = \delta u \delta u$, for example. Since there are no increments, or varied path for the x, y variables, there are no partial derivatives with respect to those variables. The last expression can be rewritten, just as is done for differentials, as

$$\delta^t F = \delta F + \frac{1}{2} \delta^2 F + \frac{1}{3!} \delta^3 F + \dots$$

where $\delta^2 F = \delta[\delta F]$, $\delta^3 F = \delta[\delta^2 F]$, and so on. In words, the above equation says that the total variation is equal to the sum of the first variation plus the second variation plus the third variation and so on. To verify that $\delta^2 F = \delta[\delta F]$, note that

$$\delta \left[\frac{\partial F}{\partial u} \delta u + \frac{\partial F}{\partial u_x} \delta u_x \right] = \frac{\partial}{\partial u} \left[\frac{\partial F}{\partial u} \delta u + \frac{\partial F}{\partial u_x} \delta u_x \right] \delta u + \frac{\partial}{\partial u_x} \left[\frac{\partial F}{\partial u} \delta u + \frac{\partial F}{\partial u_x} \delta u_x \right] \delta u_x$$

which is exactly the same result that is called $\delta^2 F$ above.

When the variations on the arbitrary dependent variables are required to be very small, each succeeding term in the series for the total variation is very much smaller than the preceding term, and can be neglected if all preceding terms are not required to be zero.

With this information in place, it is now possible to proceed to prove that the first variation (i.e., the variational operator) and definite integration with respect to independent

⁹ A functional is simply a function of one or more other functions.

variables are commutative. Consider the following representative definite integral I over a fixed volume

$$I = \iiint_{\text{Vol.}} F(x, u, u_x) dx dy dz$$

and what is now defined as

$$I + \delta^t I = \iiint_{\text{Vol.}} F(x, u + \delta u, u_x + \delta u_x) dx dy dz$$

Since the limits of integration for the two integrals above are exactly the same, the first integral can be subtracted from the second. That is,

$$\delta^t I = \iiint_{\text{Vol.}} \delta^t F(x, u, u_x) dx dy dz$$

If the higher-order variational terms are discarded on both sides of the equality after requiring, as always, that all variations of the arbitrary functions be very small, the result is that the total variations become first variations, and

$$\delta \iiint_{\text{Vol.}} F dx dy dz = \iiint_{\text{Vol.}} \delta F dx dy dz$$

which completes the proof.

Note again that in order for the dependent function to have a variation, its functional form must be unknown. Examples of famous functions (Ref. [3]) that are unknown before analysis, but whose explicit form can be determined using the variational operator are: (i) the function $y(x)$ that describes the path taken by a particle as it moves, solely under the influence of a constant gravitational field acting in the negative y direction, from one point in space, (x_1, y_1) , to another point in space at a lower elevation, (x_2, y_2) , in the least elapsed time; (ii) the shortest path between two points on a given surface geometry; and (iii) the curve between two fixed points in the x, y plane which, when revolved about the x axis, produces a surface of revolution with the minimum surface area. The calculus of variations, as it is called, is a powerful tool for dealing with problems where a function (like that which defines a path in a plane) is sought that minimizes or maximizes a characteristic associated with the function (like elapsed travel time). A single simple example of this type of application of the calculus of variations is presented below.

Consider a functional of the known form $F(x, u, u', u'')$ where $u(x)$ is an unknown function. Consider minimizing or maximizing the integral

$$I(u) = \int_{x_1}^{x_2} F(x, u, u', u'') dx$$

In order to obtain the form of the function $u(x)$ which renders the integral $I(u)$ a minimum or maximum, apply the variational operator to both sides of the definition of $I(u)$, and set $\delta I(u)$ equal to zero. Setting $\delta I(u) = 0$ is similar to setting a derivative equal to zero so as to obtain a maximum or a minimum. Then

$$\begin{aligned} 0 &= \int_{x_1}^{x_2} \delta F(x, u, u', u'') dx \\ &= \int_{x_1}^{x_2} \left[\frac{\partial F}{\partial u} \delta u + \frac{\partial F}{\partial u'} \delta u' + \frac{\partial F}{\partial u''} \delta u'' \right] dx \end{aligned}$$

Since the variations δu and $\delta u'$ are not independent of each other, it is necessary to integrate by parts in order to have a single varied function in the integrand in preparation for a concluding argument in the next paragraph. Therefore, repeatedly integrating by parts,

$$0 = \int_{x_1}^{x_2} \left[\frac{\partial F}{\partial u} - \frac{d}{dx} \left(\frac{\partial F}{\partial u'} \right) + \frac{d^2}{dx^2} \left(\frac{\partial F}{\partial u''} \right) \right] \delta u \, dx \\ + \left[\frac{\partial F}{\partial u'} - \frac{d}{dx} \left(\frac{\partial F}{\partial u''} \right) \right] \delta u \Big|_{x_1}^{x_2} + \frac{\partial F}{\partial u''} \delta u' \Big|_{x_1}^{x_2}$$

It is now required that the variation be such that both boundary terms are individually equal to zero. The result is that the above integral is also equal to zero. The above integral can be zero for all arbitrarily selected functional values of $\delta u(x)$ only if the remainder of the integrand is zero. Hence the conclusion

$$\frac{\partial F}{\partial u} - \frac{d}{dx} \left(\frac{\partial F}{\partial u'} \right) + \frac{d^2}{dx^2} \left(\frac{\partial F}{\partial u''} \right) = 0 \quad (15.17)$$

This is one form of the *Euler–Lagrange equation*. Other forms depend upon the functions that appear in the argument of the functional. The solution of this differential equation, the unknown function $u(x)$, is the function that minimizes or maximizes, depending upon the application, the original integral $I(u)$. A simple clarifying illustration of the use of the Euler–Lagrange equation is as follows.

Example 15.9. Everyone knows that the shortest distance on a plane between two points is a straight line. Prove it. (See Ref. [3] for the solution when the surface is that of a sphere.)

Solution. Without loss of generality, let the two end points, P_1 and P_2 , lie in the plane $z = 0$. Then let the coordinates of the two end points be (x_1, y_1) and (x_2, y_2) , respectively. In this case the line between the end points, curved or straight, can be described by the function $y(x)$, where, of course, here y is the dependent variable. Then the distance between the two end points is described by the following line integral:

$$\text{Distance} = \oint ds = \oint [(dx)^2 + (dy)^2]^{1/2} = \int_{x_1}^{x_2} [1 + (y')^2]^{1/2} dx$$

where the ratio of the differentials, dy/dx , is now interpreted as the derivative $y'(x)$. The distance is minimized by requiring that its variation be zero, or equivalently, solving the Euler–Lagrange equation for $y(x)$ where the functional $F = [1 + (y')^2]^{1/2}$. Since the functional is only a function of $y'(x)$, the Euler–Lagrange equation reduces to $(d/dx)(\partial F/\partial y') = 0$, or $\partial F/\partial y' = C_0$. Since $\partial F/\partial y' = y'/[1 + (y')^2]^{1/2}$, it is necessary to solve

$$y' = C_0 [1 + (y')^2]^{1/2}$$

After squaring both sides, and solving for $y'(x)$,

$$y'(x) = \left[\frac{C_0^2}{1 - C_0^2} \right]^{1/2} \equiv m$$

where m is just another positive or negative constant. The unique solution for $y'(x) = m$ is $y(x) = mx + b$, which, of course, is a general equation for a straight line in the z plane. Thus the straight line is the shortest distance between two points on a plane. ■

Endnote (2) Proof That the Principle of Virtual Work Is a Sufficient Condition for Equilibrium

The task is to start with Eq. (15.10a) and derive both the general equilibrium equations and the Cauchy equations of the first chapter. Before beginning, it is worth noting that it is a general mathematical judgement that matrices are a superior organizing algebra when the subject is ordinary differential equations, but Cartesian tensors are a superior organizing algebra when partial derivatives are involved, as they are here. As an example of this general observation, the present task is quite awkward and clumsy using matrices, but would be quite direct and simple using Cartesian tensors. Since Cartesian tensors have not been explained, and thus are not available, the next best thing is simply to write out what would be very compact using the index notation that is Cartesian tensors. Writing out all the terms makes the proof somewhat lengthy, but there is really no other satisfactory option.

Begin with Eq. (15.10a). The first step is to again recognize that on S_2 , where displacements are prescribed, all virtual displacements are necessarily zero. Therefore extending the surface integral over $S_2 + S_1 = S$ does not alter the value of this first integral. Thus the PVW can be written out as

$$\begin{aligned} & \iint_S (T_x \delta u + T_y \delta v + T_z \delta w) dS + \iiint_{\text{Vol.}} \rho (B_x \delta u + B_y \delta v + B_z \delta w) d(\text{Vol.}) \\ &= \iiint_{\text{Vol.}} (\sigma_{xx} \delta \epsilon_{xx} + \sigma_{yy} \delta \epsilon_{yy} + \sigma_{zz} \delta \epsilon_{zz} + \sigma_{xy} \delta \gamma_{xy} + \sigma_{xz} \delta \gamma_{xz} + \sigma_{yz} \delta \gamma_{yz}) d(\text{Vol.}) \end{aligned}$$

Consider the six strain–displacement equations $\epsilon_{xx} = \partial u / \partial x$, and so on. The second step in this proof is to introduce the basic requirement of the PVW, which is that everywhere in the structural system the virtual displacements (which are arbitrary and small) and the virtual strains satisfy the six virtual strain–virtual displacement equations. Applying the variational operator to both sides of the strain–displacement equations provides the virtual strain–virtual displacement equations $\delta \epsilon_{xx} = \delta(\partial u / \partial x) = \delta u_{,x}$, and so on. Then the above right-hand side can be written as

$$\begin{aligned} & \iiint_{\text{Vol.}} [\sigma_{xx} \delta u_{,x} + \sigma_{yy} \delta v_{,y} + \sigma_{zz} \delta w_{,z} + \sigma_{xy} (\delta u_{,y} + \delta v_{,x}) + \sigma_{xz} (\delta u_{,z} + \delta w_{,x}) \\ & \quad + \sigma_{yz} (\delta v_{,z} + \delta w_{,y})] d(\text{Vol.}) \end{aligned}$$

To this right-hand side add the zero quantity

$$\begin{aligned} & \iiint_{\text{Vol.}} (\sigma_{xx,x} \delta u + \sigma_{yy,y} \delta v + \sigma_{zz,z} \delta w + \sigma_{xy,y} \delta u + \sigma_{xy,x} \delta v + \sigma_{xz,z} \delta u + \sigma_{xz,x} \delta w \\ & \quad + \sigma_{yz,z} \delta v + \sigma_{yz,y} \delta w) d(\text{Vol.}) - \iiint_{\text{Vol.}} (\text{same integrand}) d(\text{Vol.}) \end{aligned}$$

The first and second of these three right-hand side integrals can be combined so that the right-hand side has the form

$$\begin{aligned} & \iiint_{\text{Vol.}} [(\sigma_{xx}\delta u)_{,x} + (\sigma_{yy}\delta v)_{,y} + (\sigma_{zz}\delta w)_{,z} + (\sigma_{xy}\delta u)_{,y} + (\sigma_{xy}\delta v)_{,x} + \cdots \\ & + (\sigma_{yz}\delta w)_{,y}] d(\text{Vol.}) - \iiint_{\text{Vol.}} [(\sigma_{xx,x} + \sigma_{xy,y} + \sigma_{xz,z})\delta u + (\sigma_{xy,x} + \sigma_{yy,y} \\ & + \sigma_{yz,z})\delta v + (\sigma_{xz,x} + \sigma_{yz,y} + \sigma_{zz,z})\delta w] d(\text{Vol.}) \end{aligned}$$

The first of these now two volume integrals on the right-hand side can be transformed into a surface integral via the Green–Gauss theorem. Doing that, and then transposing the two right-hand side integrals to the left-hand side yields.

$$\begin{aligned} & \oint_S [(T_x - \sigma_{xx}v_x - \sigma_{xy}v_y - \sigma_{xz}v_z)\delta u + (T_y - \sigma_{xy}v_x - \sigma_{yy}v_y - \sigma_{yz}v_z)\delta v \\ & + (T_z - \sigma_{xz}v_x - \sigma_{yz}v_y - \sigma_{zz}v_z)\delta w] dS + \iiint_{\text{Vol.}} [(\rho B_x + \sigma_{xx,x} + \sigma_{xy,y} + \sigma_{xz,z})\delta u \\ & + (\rho B_y + \sigma_{xy,x} + \sigma_{yy,y} + \sigma_{yz,z})\delta v + (\rho B_z + \sigma_{xz,x} + \sigma_{yz,y} + \sigma_{zz,z})\delta w] d(\text{Vol.}) = 0 \end{aligned}$$

Since the virtual displacements are arbitrary, temporarily require the virtual displacements at the surface to have zero values. This temporary step causes the surface integral to have a zero value. Also let $\delta v = \delta w = 0$ in the interior. Then let the remaining virtual displacement throughout the interior, δu , vary in all manner of ways. No matter how this interior virtual displacement varies, the value of the volume integral remains zero. The only way that is possible is for the remainder of the integrand to be zero. Hence the first of the general equilibrium equations is obtained. Doing the same thing in turn with δv , and then δw , produces the other two general equilibrium equations. Now that the general equilibrium equations have been established, they can be used to evaluate the final volume integral as zero. With the volume integral gone, return to the surface integral which also now clearly has the value zero in all circumstances. The surface values of the virtual displacements can be now be chosen so that two of the three are zero while the third is arbitrary. Since the volume integral is gone, nothing need be said about its virtual displacements at this point in the proof other than they must be continuous with those on the surface. This same procedure used with the volume integral leads to each of the three Cauchy equations. Therefore, starting with the PVW, both the general equilibrium equations and the boundary condition equilibrium equations have been obtained. Thus, this development, coupled with the previous development of the PVW based on the employment of the Cauchy equations and the general equilibrium equations, proves that the PVW is a necessary and sufficient condition for equilibrium everywhere in the structural system. This conclusion means that if the PVW is used in an analysis, no summing of forces or moments or any other type of equilibrium equation need be written. Equilibrium is assured simply by using the PVW. Again, this was all done without writing any material equations of any kind. Therefore the PVW is applicable to any material.

Endnote (3) Proof of the Pairing of BCs for the Beam Fourth Order Bending Equations and the Second Order Extension Equations

The proof proceeds most conveniently from the PVW or the principle of the minimum value of the total potential energy, which are $\delta W_{ex} + \delta W_{in} = 0$ and $\delta(U + V) = 0$, respectively. For clarity of development, let the beam be homogeneous, the cross-sectional product of inertia zero, and let there be no temperature change. The removal of any or all of these three restrictions would not significantly alter the style of the proof that follows. The external work or energy expressions for loadings per unit length along the beam axis, using the notations of Part III are

$$\delta W_{ex} = -\delta V = \int_0^L [f_x(x) \delta u(x) + f_y(x) \delta v(x) + f_z(x) \delta w(x) - m_y(x) \delta w'(x) + m_z(x) \delta v'(x)] dx$$

Since all the other bending and extensional (actual) strains are zero, the internal virtual work and strain energy expressions for a Bernoulli-Euler beam are

$$-\delta W_{in} = +\delta U = \int_0^L \iint_A [\sigma_{xx} \delta \epsilon_{xx} dA] dx$$

where zero actual strains means zero virtual strains. From Eqs. (9.3, 4b)

$$\begin{aligned} \epsilon_{xx} &= u' - yv'' - zw'' \\ \sigma_{xx} &= E(u' - yv'' - zw'') \\ \delta \epsilon_{xx} &= \delta u' - y\delta v'' - z\delta w'' \end{aligned}$$

Hence, substituting into the internal work or strain energy expression leads to

$$\begin{aligned} \delta U = \int_0^L E \left[u' \delta u' \iint_A dA + v'' \delta v'' \iint_A y^2 dA + w'' \delta w'' \iint_A z^2 dA \right. \\ \left. - [u' \delta v'' + v'' \delta u'] \iint_A y dA - [u' \delta w'' + w'' \delta u'] \iint_A z dA \right. \\ \left. + [w'' \delta v'' + v'' \delta w''] \iint_A yz dA \right] dx \end{aligned}$$

Since all first moments about the beam cross-section centroid are zero, and since in this simplified case, the product of inertia is also zero, the last three integrals disappear. The first three integrals are the cross-sectional area, A , and the two area moments of inertia I_{zz} and I_{yy} , respectively. Combining the work or energy expressions leads to the one identity

$$\begin{aligned} 0 = \int_0^L [EAu' \delta u' + EI_{zz} v'' \delta v'' + EI_{yy} w'' \delta w'' - f_x \delta u - f_y \delta v - f_z \delta w \\ + m_y \delta w' - m_z \delta v'] dx \end{aligned} \quad (15.18)$$

Weak variations such as δw , $\delta w'$, and $\delta w''$ are not independent of each other. Rather, $\delta w'$ is the derivative of δw , and so on. It is necessary to put all variations on the same basis by integrating by parts. For example,

$$\int_0^L EAu' \delta u' dx = \int_0^L EAu' \frac{d(\delta u)}{dx} dx = (EAu') \delta u \Big|_0^L - \int_0^L (EAu')' \delta u dx$$

Similarly,

$$\int_0^L m_z \delta v' dx = m_z \delta v \Big|_0^L - \int_0^L m'_z \delta v dx$$

and

$$\int_0^L EI_{zz} v'' \delta v'' dx = (EI_{zz} v'') \delta v' \Big|_0^L - \int_0^L (EI_{zz} v'')' \delta v' dx$$

and

$$\int_0^L (EI_{zz} v'')' \delta v' dx = (EI_{zz} v'')' \delta v \Big|_0^L - \int_0^L (EI_{zz} v'')'' \delta v dx$$

From Eqs (9.7a), where the axial force $N = EAu'$, and (9.7b, c) where $M_z = EI_{zz} v''$ and $M_y = EI_{yy} w''$, and Eqs. (10.4), where, for example, $V_z = M'_y - m_y = (EI_{yy} w'')' - m_y$, Eq. (15.18) becomes

$$\begin{aligned} 0 = & - \int_0^L [(EAu')' + f_x] \delta u dx + \int_0^L [(EI_{zz} v'')' - f_y + m'_z] \delta v dx \\ & + \int_0^L [(EI_{yy} w'')' - f_z + m'_y] \delta w dx + N \delta u \Big|_0^L + M_z \delta v' \Big|_0^L \\ & + M_y \delta w' \Big|_0^L - V_y \delta v \Big|_0^L - V_z \delta w \Big|_0^L \end{aligned} \quad (15.19)$$

Equation (15.19) is an identity. This equation holds true for all variation functions $\delta u(x)$, $\delta v(x)$, and $\delta w(x)$. Each of the variations δu , δv , and δw is wholly independent of the other two. For the moment, fix the values of all three of these variations at the end points of the interval $(0, L)$, and let each of these three variations, *in turn*, take on arbitrary values over the interval $(0, L)$ while the other two variation functions are fixed in their values over that interval. In this way, all of the terms in Eq. (15.18) are fixed but one. For the sake of definiteness, let the first of the three integrals over the beam length be the one where the variation function is changed arbitrarily, say from $\delta u_1(x)$ to $\delta u_2(x)$. Since Eq. (15.18) holds true for both δu_1 and δu_2 , these two forms of Eq. (15.18) can be subtracted from each other in order to obtain

$$0 = \int_0^L [(EAu')' + f_x] (\delta u_2 - \delta u_1) dx$$

The value of this integral is always zero regardless of the values of the arbitrary function $(\delta u_2 - \delta u_1)$. It is easy to prove, by way of contradiction, that the only way this integral can always be zero is for the quantity in square brackets to be zero. Hence the governing differential equation for beam extension, Eq. (10.5c). The other two integrals yield the linear forms (i.e., the forms without the coupling with the axial force) of the two beam bending governing differential equations, Eqs. (10.5a, 10.5b). Now that the three integrals of Eq. (15.19) are identified as always being zero, consider the functions evaluated at the beam

boundaries. While it is not true over an interval, it is true *at the single points* that are the boundary points that the variations δu , δv , δw , $\delta u'$, $\delta v'$, and $\delta w'$ are independent of each other. Hence, using the same argument which begins with making four of these five arbitrary terms zero, each of the last five terms of Eq. (15.19) is also individually zero. Therefore, for example, the term

$$N \delta u \Big|_0^L = 0$$

means that at both boundary points, either the axial force N must be zero, or the axial deflection u must be a constant. Similarly for the other four terms. This completes the proof of the either/or pairing of the boundary conditions. The pairing of an even number of possible boundary conditions and an even order GDE, all of which are able to be derived from an work or energy expression, constitutes a *boundary value problem*.

Endnote (4) Derivation of the Uniform Torsion Beam Equations Using the Principle of Complementary Virtual Work

Consider a uniform, homogeneous, linearly elastic beam subjected to equal but oppositely applied (real) torques acting at the ends of the beam. For the sake of simplicity, let the beam cross-section be singly connected. In order to apply the Principle of Complementary Virtual Work, it is necessary to have a useful virtual load system that is in equilibrium. To that end for equilibrium of the virtual loads at the surface of the beam, apply equal and oppositely directed virtual moments, δM_t , at the end cross-sections of the beam. In order to obtain internal equilibrium for the virtual loads first recall that the general form of the internal equilibrium equations for real stresses is satisfied by requiring that (i) all stresses but the shearing stresses on the x plane (beam cross-section) be zero; and (ii) the two nonzero shearing stresses be related to the Prandtl stress function Ψ as follows:

$$\sigma_{xy} = \frac{\partial \Psi}{\partial z} \quad \text{and} \quad \sigma_{xz} = -\frac{\partial \Psi}{\partial y}$$

Therefore internal equilibrium of the virtual stresses is satisfied by requiring all the virtual stresses but the virtual shearing stresses acting upon the beam cross-section be zero, and the those shearing stresses be related to the virtual Prandtl stress function by the relations

$$\delta \sigma_{xy} = \frac{\partial(\delta \Psi)}{\partial z} \quad \text{and} \quad \delta \sigma_{xz} = -\frac{\partial(\delta \Psi)}{\partial y}$$

Thus the virtual equilibrium requirements of the PCVW have been met. In this circumstance, where L is the length of the beam, and $L\theta$ is the relative twist between the two ends of the beam, the PCVW, $\delta W_{ex}^* = -\delta W_{in}^* = +\delta U^*$, reduces to the statement

$$\delta M_t L \theta = \int_L \iint_A (\epsilon_{xy} \delta \sigma_{xy} + \epsilon_{xz} \delta \sigma_{xz}) dA dx$$

Using Hooke's law to write the strains as the stresses divided by the shearing modulus, the above equation becomes

$$\delta M_t L \theta = \int_L \iint_A \frac{1}{G} \left[\frac{\partial \Psi}{\partial z} \delta \left(\frac{\partial \Psi}{\partial z} \right) + \frac{\partial \Psi}{\partial y} \delta \left(\frac{\partial \Psi}{\partial y} \right) \right] dA dx$$

or, since $\Psi = \Psi(y, z)$ is not a function of x ,

$$G\theta\delta M_t = \iint_A \left[\frac{\partial\Psi}{\partial y} \frac{\partial(\delta\Psi)}{\partial y} + \frac{\partial\Psi}{\partial z} \frac{\partial(\delta\Psi)}{\partial z} \right] dA$$

This integral can be conveniently rewritten as

$$\begin{aligned} G\theta\delta M_t &= \iint_A \left[\frac{\partial}{\partial y} \left(\frac{\partial\Psi}{\partial y} \delta\Psi \right) + \frac{\partial}{\partial z} \left(\frac{\partial\Psi}{\partial z} \delta\Psi \right) \right] dA - \iint_A \left[\frac{\partial^2\Psi}{\partial y^2} + \frac{\partial^2\Psi}{\partial z^2} \right] \delta\Psi dA \\ &= \oint \delta\Psi \left(\frac{\partial\Psi}{\partial y} dz - \frac{\partial\Psi}{\partial z} dy \right) - \iint_A \nabla^2\Psi \delta\Psi dA \end{aligned}$$

where the Green–Gauss theorem has been used to convert the first area integral into a line integral. To complete this process it is necessary to tie together the external virtual loading with the internal virtual stresses. From the relationship between the torque at a cross-section and the shearing stresses at that cross-section, as derived in Chapter 10,

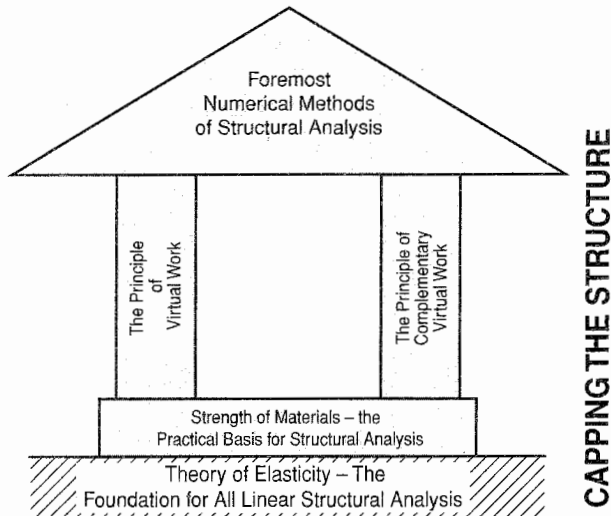
$$\begin{aligned} \delta M_t &= \iint_A (y\delta\sigma_{xz} - z\delta\sigma_{xy}) dA = - \iint_A \left[y \frac{\partial(\delta\Psi)}{\partial y} + z \frac{\partial(\delta\Psi)}{\partial z} \right] dA \\ &= - \iint_A \left[\frac{\partial}{\partial y} (y\delta\Psi) + \frac{\partial}{\partial z} (z\delta\Psi) \right] dA + 2 \iint_A \delta\Psi dA \\ &= - \oint \delta\Psi (y dz - z dy) + 2 \iint_A \delta\Psi dA \end{aligned}$$

Substituting this identity for the virtual torque into the previous PCVW identity, and transposing terms, leads to

$$0 = \oint \delta\Psi \left[\left(\frac{\partial\Psi}{\partial y} + G\theta y \right) dz - \left(\frac{\partial\Psi}{\partial z} + G\theta z \right) dy \right] - \iint_A \delta\Psi (\nabla^2\Psi + 2G\theta) dA$$

Again, start with temporarily requiring the arbitrary function $\delta\Psi$ be zero around the outer boundary of the cross-section. Then the above area integral is also zero for this particular choice for the arbitrary function $\delta\Psi$ while having nonzero, continuous values over the interior of the cross-section. If the area integral is zero regardless of the choice of values for the arbitrary function $\delta\Psi$ over the area of the cross-section, then the quantity in parentheses must be zero in all circumstances. Hence the uniform torsion GDE. With the area integral eliminated, the line integral must be zero in all circumstances. Therefore, on the outer boundary, either the Prandtl stress function must be a constant, or the quantity in brackets must be zero. The unfamiliar quantity in brackets is related to derivatives of a quantity called the warping function, and is of no present interest. Hence the boundary condition that Ψ equals a constant (selected to be zero) on the outer boundary of the cross-section. Since $\delta\Psi$ is zero on the outer boundary, the question may arise as to why $\delta\Psi$ equals zero cannot be an acceptable reason for the area integral being zero. If $\delta\Psi$ were zero over the interior of the cross-section, then that would make Ψ a constant over the interior, which in turn would mean that the actual shearing stresses on the cross-section are zero. This lack of stresses would contradict the presence of an applied torque, and thus is rejected.

ENERGY-BASED NUMERICAL SOLUTIONS



V.1 Preface

In Chapters 16–21, the focus shifts from solving differential equations to employing the Principle of Virtual Work, or the Principle of Complementary Virtual Work, or, for those who prefer them, the corresponding energy principles. The goal remains the same: to solve larger and more complicated structural analysis problems. The shift in focus is more stylistic than fundamental. As the last chapter's endnotes demonstrate, the beam differential equations follow from either the Principle of Virtual Work, in the case of bending and extension, or the Principle of Complementary Virtual Work, in the case of twisting. Although not demonstrated here, the reverse path from differential equations to a work or energy principle is also possible when the differential equation meets certain requirements as described by Ref. [3], p. 158. Hence it is essentially a matter of convenience whether a differential equation or a work principle is the starting point of an analysis. If the structure contains more than a couple of structural elements, it is usually, if not always, the work or energy principles that are most convenient. Indeed, one particular application of the Principle of Virtual Work – the finite element method – coupled with modern digital computers, permits the routine analysis of structures with many thousands of structural elements. The finite element method is a numerical method that is unperturbed by geometric or material complexity, and it allows the analyst to minutely model (and thus analyze) one part of a structure while getting by with a crude model of other parts of the structure. Hence this part of the textbook emphasizes the finite element method. Chapter 16

introduces the Rayleigh–Ritz method, which can be viewed as the origin of the finite element method. Chapters 17 and 18 introduce the finite element method in the simple context of beams and bars. Chapter 19 presents a brief survey of more advanced applications to membranes and solids. The use of the finite element method with plate elements and the use of the finite element method in stability problems are topics that are introduced, respectively, in Chapters 22 and 23.

The finite element method is not the only method an analyst needs for general competence. Analysis methods that flow from the Principle of Complementary Virtual Work, and there are many such methods, also need attention. There are limited circumstances where these methods are more convenient than the finite element method. Indeed, one of these analysis methods is convenient for deriving the finite element method equations for a curved beam. See Ref. [72], p. 146. Hence there are two chapters, Chapters 20 and 21, to cover these types of analyses.

*****Precursor Numerical Analyses*******16.1 Introduction**

Routine analyses of structures whose mathematical models contain more than two or three structural elements (e.g., beams, plates, springs) are accomplished today using one or another of the commercially available, large or small capacity, standard structural analysis digital computer software packages. The larger commercially available structural analysis programs have become so inclusive, that few types of analyses are beyond their reach. In addition to producing what is called a numerical analysis of the structure's mathematical model, such software packages, perhaps in combination with auxiliary programs, are also commonly used in creating a structure's mathematical model, and in simplifying the interpretation of the analysis results. The basis for the large majority, if not all, of these general use software packages is a numerical analysis technique called the finite element method, which is introduced in Chapter 17.

The essence of any numerical analysis is the replacement of a collection of partial or ordinary differential equations (or sometimes integral equations) by a much larger set of simultaneous, algebraic equations. The set of algebraic equations involve an equal number of algebraic variables that, in one sense or another, are used to approximate the continuous, unknown functions of the differential equations being replaced by the algebraic equations. In almost every case, the differential equations are those obtained from strength of materials. If the differential equations are nonlinear, so too are the algebraic equations. The capacity of a structural analysis software program refers to the number of such approximating algebraic equations the program can assemble and then solve. The greater the capacity, the greater the number of algebraic variables that can be used to detail a structural model. The greater the number of algebraic variables actually used in a particular analysis, the greater the cost of that analysis.

16.2 Numerical Methods of Note

In marked contrast to human beings, digital computers excel at compiling and solving simultaneous, algebraic equations. Thus the rise in the use and development of numerical analysis techniques since the 1950s and 1960s has been closely tied to the parallel development of the digital computer. The advent of the modern digital computer has not only made numerical analyses the routine choice of structural analysts, but the digital computer has profoundly influenced the types of numerical analyses that are selected for use. At one time there were a great many types of numerical analyses under development. Most of those numerical analysis techniques were limited in scope, such as those limited to structures whose governing differential equations can be reduced to differential equations having only one independent spatial variable (Ref. [43]), or numerical techniques that are limited to a very small number of structural elements involving more than one independent spatial variable (Ref. [45]). This rich diversity of numerical methods was, in itself, a drawback. No matter how much more elegant or accurate a particular numerical technique of limited scope

might be within its range of applicability compared to other numerical techniques, it was generally impractical for analysts to devote their efforts to learning the nuances of all those limited methods. What was needed was one or two well-developed numerical methods that were applicable to almost all types of structures.

Before focusing on the finite element method, the one general numerical method of structural analysis almost exclusively used today, it is worth mentioning first that there are two older, broadly applicable, generally successful methods of numerical analysis. These two methods long predate the advent of digital computers. The two older general numerical methods are the finite difference method (Refs. [16, 46]) and the Rayleigh–Ritz method (Refs. [25, 47]). The finite difference method is still much used outside of structural analysis in such fields as fluid dynamics and heat transfer. Within the field of structural analysis, the finite difference method is still generally preferred for analyses where the structure's equilibrium position is not determined by reference to an unloaded position, as is true, for example, in the case of a cable towed from a ship or airplane. The finite difference method is sometimes preferred for structural shell analyses.

The finite difference method is very well suited to modern digital computers because the unknown quantities are always large numbers of discrete values of the unknown functions. To better understand how the finite difference method involves discrete values of the unknown functions, the following sample is provided. Consider either an energy expression or a differential equation that contains a second partial derivative with respect to x of the unknown function $F(x, y)$. The finite difference technique is to first replace the continuous region over which the energy expression or partial differential equation applies with a grid of (generally) regularly spaced points. The idea is to solve the differential equation or evaluate the work or energy integral at each of the discrete grid points. If the grid is made to be sufficiently dense, then the discrete solution approximates the continuous solution over the region where the equations apply. (That region is called the “domain” of the equations.) In order to facilitate the analysis, these discrete points are numbered. In this sample, let the numbers of three adjacent points lying along a line paralleling the x axis be $i - 1$, i , and $i + 1$. Let the distance between these three points be h . Call the unknown values of the function $F(x, y)$ at these three points F_{i-1} , F_i and F_{i+1} , respectively. The next step is to approximate the derivatives of the differential equation by use of the discrete values of the unknown function. For example, for an error that depends upon the square of the ratio of h to a characteristic length of the domain in the x direction, the second partial derivative with respect to x at point i has the approximation (Ref. [16])

$$\left(\frac{\partial^2 F}{\partial x^2}\right)_i = \frac{1}{h^2} (F_{i-1} - 2F_i + F_{i+1})$$

This approximation, and other partial derivative approximations are conveniently derived using Taylor's series expansions.

One strength of the finite difference method is that it is no more difficult to set up the finite difference equations for nonlinear problems than it is for linear problems. It is also a relatively simple matter to estimate the errors associated with the finite difference type of numerical analysis. In the analysis of structures subjected to time-varying loads, finite difference techniques, while not often chosen to describe derivatives of the unknown functions with respect to the spatial variables, are often chosen to represent changes in the structural variables with respect to time. The main drawbacks to the use of the finite difference method in structural analysis are that (i) usually more equations have to be solved than with other methods and (ii) some boundary geometries and some boundary and corner conditions are not easily automated or even correctly written.

In contrast to the “brute force” of the finite difference method, the Rayleigh–Ritz¹ method, sometimes called the Ritz method, is quite elegant. Its major strength is the relatively small number of equations that need to be solved. Thus the original form of the Rayleigh–Ritz method (RRM) benefited relatively far less from the advent of the modern digital computer than numerical methods like the finite difference method. The major difficulty with the RRM is that it is limited in its application to relatively simple structures, although those structures need not be limited only to beams. Specifically, the structure can certainly involve a dozen or two structural elements of any kind. The application of the RRM to static and dynamic structural analyses is not as routine as many applications of the finite difference method. The RRM requires the analyst to be intimately involved in the analysis through the choice of specific functions that should meet possibly difficult requirements. This aspect of the RRM, that these selected functions are particular to each analysis, is the main impediment to automating the RRM for solutions utilizing a digital computer. Another drawback to the RRM is that the RRM is sometimes best served by the analyst hand calculating definite integrals or using a general mathematics program to carry out the integration. If orthogonal functions (see Chapter (12), Endnote (2)) can be used, then it is possible that the evaluation of the integrals may be a simple matter.

When the techniques of the RRM are applied to a set of governing differential equations and boundary conditions, rather than to energy expressions, the method is then called (one or another variety of) the Galerkin method. Only a few examples of the Rayleigh–Ritz technique are provided here because, in one sense, the finite element method, the focus of the next three chapters, is merely a special case of the RRM. In the finite element method, the selected functions are chosen during the course of the derivation of the finite element, and thus these same selected functions are used for all applications of that type of finite element.

Example 16.1. Using only two, nonpolynomial, selected functions of the spatial coordinate x , perform a RRM analysis for the center deflection of a uniform beam of length L that is clamped at both beam ends. The beam is loaded by an upward uniform force per unit length of magnitude f_0 which acts across the entire beam length. Choose the x coordinate origin to be at the beam center so that the fixed beam ends are located at $x = -L/2$ and $x = +L/2$. The beam has a symmetric cross-section.

Comment. From the solution to the beam bending differential equation, the exact strength of materials solution for the beam axis deflections is the following quartic:

$$384EIw(x) = f_0(16x^4 - 8x^2L^2 + L^4) \quad \text{so that} \quad EIw(0) = \frac{f_0L^4}{384}$$

If the selected approximating functions for the RRM analysis were those of the above polynomial² then the above exact solution would be the RRM result. However, nonpolynomial functions are purposely chosen for this example analysis in order to demonstrate the fact that any functions that satisfy the deflection boundary conditions (BCs), if taken in sufficient number (which usually is a small number), can be used to obtain a very good approximation to the exact solution.

Furthermore, a good approximation is not the only information obtained from a RRM analysis. When the RRM analysis meets all deflection-type BC requirements, it is known

¹ John Strutt, third Baron Rayleigh (1842–1919), English physicist, published *Theory of Sound* in 1877. Walter Ritz (1878–1909), Swiss physicist.

² When dealing with polynomials, it is usually more convenient to integrate from zero to L . In terms of that spatial coordinate x , the differential equation deflection solution is $24EIW(x) = f_0x^2(L-x)^2$.

that the RRM analysis solution is either an upper or lower bound for the true solution. For example, in this case, the RRM deflection solution must be less than the above-stated strength of materials deflection solution. This is so because the use of a (complete) infinite series solution in a RRM analysis would always provide an exact solution, and a RRM finite series solution is an infinite series constrained to having all but a relatively few terms equal to zero. Any constraint stiffens a structure. For example, if the deflection at $x = 21L/50$, close to the right-hand support, were constrained to be zero, then the beam would deflect less under the action of a given loading. The constraints on the infinite series work the same way. A situation where a RRM analysis solution provides an upper bound is a case where the RRM is used to estimate a structure's natural frequencies. The stiffer the structure, the higher the natural frequencies of vibration. Thus the RRM natural frequency estimates (except the highest) are always higher than the "exact" strength of materials natural frequencies (Ref. [61]). The fact that strength of materials theory also introduces constraints via its approximations to the element deflections means that both the RRM and strength of materials natural frequencies are higher than the true experimental natural frequencies.

Solution. The RRM is often coupled with one of the energy principles. However, since in this text the focus is upon the very closely related work principles, the PVW is chosen to obtain the approximate solution for the midspan deflection. Thus, the analysis is based upon Eqs. (9.3), (9.4b), and the following form of $\delta W_{ex} = -\delta W_{in} = \delta U$:

$$\delta W_{ex} = \int_{-L/2}^{+L/2} f_0 \delta w(x) dx \quad \text{and} \quad \delta U = \int_{-L/2}^{+L/2} \iint_A \sigma_{xx} \delta \epsilon_{xx} dA dx$$

For a Bernoulli–Euler beam, the only beam strain $\epsilon_{xx} = -z w''(x)$. Hence $\delta \epsilon_{xx} = -z \delta w''(x)$, and $\sigma_{xx} = -z E w''(x)$. Substituting these strain and stress expressions into the above equation for δU yields

$$\delta U = \int_{-L/2}^{L/2} E w''(x) \delta w''(x) \left[\iint_A z^2 dA(y, z) \right] dx$$

so that $\delta W_{ex} = \delta U$ becomes

$$\int_{-L/2}^{+L/2} f_0 \delta w(x) dx = \int_{-L/2}^{+L/2} E I w''(x) \delta w''(x) dx \quad (16.1)$$

Following the example problem statement, write the approximate beam axis lateral deflections $w(x)$ using two selected functions as

$$w(x) = q_1 f_1(x) + q_2 f_2(x) \quad (16.2)$$

where q_i are unknown parameters to be determined. Understand that these weighting factors are not functions of x . The analyst must choose the twice-differentiable functions $f_1(x)$ and $f_2(x)$ so that: (i) together in the above weighted sum they generally provide the deflection pattern expected by the analyst; and (ii) they individually satisfy the deflection BCs

$$w(-L/2) = w'(-L/2) = w(+L/2) = w'(+L/2) = 0$$

because the enforcement everywhere of the strain–displacement equations is a requirement for the validity of the PVW. Of course there are many functions that provide the expected deflection shape and meet this BC constraint. For example, the functions

$$f(x) = \cos^2(\pi x/L), \quad \cos^3(\pi x/L), \quad \text{etc.}$$

meet these two requirements. However, since in the PVW these functions must be multiplied together and integrated, the choice of functions can have a considerable impact on the amount of work required of the analyst. The analyst first prefers to use orthogonal functions if possible. Failing that, the analyst chooses functions that are easy to integrate. In this case, choose

$$f_1(x) = 1 + \cos(2\pi x/L) \quad \text{where} \quad f_1'(x) = -\frac{2\pi}{L} \sin(2\pi x/L)$$

$$f_2(x) = 1 + \cos(6\pi x/L) \quad \text{where} \quad f_2'(x) = -\frac{6\pi}{L} \sin(6\pi x/L)$$

The first function approximates the expected deflection shape while the second function is viewed as modifying the first function so as to make it closer still to the correct solution. Thus the value of q_2 should be much less than the value of q_1 if these functions are well chosen. Of course, both functions satisfy the deflection BCs and are symmetric about $x = 0$.

The best way to find suitable functions is to make sketches of the functions that come to mind. Quite often, the sketching process will suggest still more possible functions. Sketches are a superior means of checking that candidate functions do indeed approximate the expected deflection pattern. In particular, sketches are useful for checking that the candidate functions satisfy the analysis BCs. In this case, sketches of, for example, the even functions: $\cos(\pi x/L)$; $1 + \cos(\pi x/L)$; $1 + \cos(3\pi x/L)$; $1 + \cos(4\pi x/L)$; $1 + \cos(5\pi x/L)$; and so on, would show that these functions do not have both zero values and zero slopes at $x = +\frac{1}{2}L$ and at $x = -\frac{1}{2}L$, and thus cannot be used to satisfy the beam BCs. Of course the above selected functions, $f_1(x)$ and $f_2(x)$, do have both zero values and zero slopes at $x = +\frac{1}{2}L$ and at $x = -\frac{1}{2}L$, and thus do satisfy the beam BCs.

Now, with respect to the first integral of Eq. (16.1),

$$\delta w(x) = \delta q_1[1 + \cos(2\pi x/L)] + \delta q_2[1 + \cos(6\pi x/L)]$$

where, again, there is no variation of the functions of the independent variable when their form is known as is the case here. Carrying out the first integration between the limits $-L/2$ and $+L/2$ leads from Eq. (16.17), to

$$\delta W_{ex} = f_0 L (\delta q_1 + \delta q_2)$$

With respect to the second integral of Eq. (16.1), the integral for the negative of the internal virtual work uses

$$w''(x) = -q_1 \frac{4\pi^2}{L^2} \cos(2\pi x/L) - q_2 \frac{36\pi^2}{L^2} \cos(6\pi x/L)$$

$$\delta w''(x) = -\delta q_1 \frac{4\pi^2}{L^2} \cos(2\pi x/L) - \delta q_2 \frac{36\pi^2}{L^2} \cos(6\pi x/L)$$

Substituting and carrying out the integration by use of Eq. (12.16) leads to

$$-\delta W_{in} = EI \left(q_1 \delta q_1 \frac{16\pi^4 L}{L^4} \frac{1}{2} + q_2 \delta q_2 \frac{1296\pi^4 L}{L^4} \frac{1}{2} \right)$$

Equating the coefficients of the arbitrary factors δq_i leads to the immediate solutions

$$q_1 = \frac{f_0 L^4}{8\pi^4 EI} \quad q_2 = \frac{f_0 L^4}{648\pi^4 EI}$$

Substituting the above solution into Eq. (16.2), and setting $x = 0$ yields the following approximation to the midspan deflection:

$$w(0) = 2(q_1 + q_2) = \frac{164 f_0 L^4}{648 \pi^4 EI} = \frac{f_0 L^4}{(384.88) EI}$$

which is a one-quarter of one percent error. As expected, this RRM deflection solution is less than the exact strength of materials solution. Obviously this was more work for an inexperienced analyst than a straightforward solution of the beam differential equation. However, since the RRM involves single integrals rather than higher-order differential equations, the RRM is particularly suited to beams or other structural elements that have varying or discontinuous stiffnesses and loadings involving concentrated loads or other discontinuous loads. The RRM is an especially effective means of approximating natural frequencies of vibration because, even if the deflections are not well approximated, it can be proved that the natural frequencies are well approximated (Refs. [25, 61]). ■

Example 16.2. Redo the previous example involving the uniform clamped–clamped beam subjected to a constant, upward loading per unit length of magnitude f_0 . This time select two polynomial functions.

Comment. This problem is sufficiently simple that one well-selected polynomial function should be adequate. However, to demonstrate that the fact that if one function proves to be exact, the finite series weighting factors q_j for all other functions turn out to be zero.

Solution. Since the selected functions are to be polynomials, let the spanwise coordinate x run from zero to L in order to simplify the application of the limits of integration. Again, the boundary conditions required to be met by all the selected functions to be used in the Rayleigh–Ritz series are

$$w(0) = w'(0) = w(L) = w'(L) = 0$$

The first two BCs can be met if each selected function has x^2 as a factor. The latter two BCs can be met if each term has $(L - x^2)$ as a factor. Furthermore, each selected function needs to be symmetric about midspan. For these reasons, let the two-term, approximating series be

$$w(x) = q_1 x^2 (L - x)^2 + q_2 x (L - x) x^2 (L - x)^2$$

or
$$w(x) = q_1 (x^2 L^2 - 2Lx^3 + x^4) + q_2 (x^3 L^3 - 3L^2 x^4 + 3Lx^5 - x^6)$$

So
$$\delta w(x) = \delta q_1 (x^2 L^2 - 2Lx^3 + x^4) + \delta q_2 (x^3 L^3 - 3L^2 x^4 + 3Lx^5 - x^6)$$

First evaluate the external virtual work. Since the only applied loading is the constant, upward force per unit length, f_0 ,

$$\begin{aligned} \delta W_{ex} &= \int_0^L f_0 \delta w(x) dx \\ &= f_0 \delta q_1 \int_0^L (x^2 L^2 - 2Lx^3 + x^4) dx + f_0 \delta q_2 \int_0^L (x^3 L^3 - 3L^2 x^4 + 3Lx^5 - x^6) dx \\ &= \delta q_1 \left(\frac{f_0 L^5}{30} \right) + \delta q_2 \left(\frac{f_0 L^7}{140} \right) \end{aligned}$$

The next step is to evaluate the negative of the internal virtual work, which, in this case where the structure is elastic, is the same as the virtual strain energy. Again, since the subject is a beam, the strain energy expression is

$$\delta U = \int_0^L EI w''(x) \delta w''(x) dx$$

Differentiating the selected finite series yields

$$w''(x) = q_1(2L^2 - 12Lx + 12x^2) + q_2(6L^3x - 36L^2x^2 + 60Lx^3 - 30x^4)$$

and
$$\delta w''(x) = \delta q_1(2L^2 - 12Lx + 12x^2) + \delta q_2(6L^3x - 36L^2x^2 + 60Lx^3 - 30x^4)$$

Substituting these two second derivative expressions into the virtual strain-energy expression, carrying out the multiplications either by hand or by computer, and then completing the integration, yield

$$\delta U = q_1 \delta q_1 \left(\frac{4EIL^5}{5} \right) + (q_1 \delta q_2 + q_2 \delta q_1) \left(\frac{6EIL^7}{35} \right) + q_2 \delta q_2 \left(\frac{2EIL^9}{35} \right)$$

Now equate the virtual external work to the virtual strain energy. Since δq_2 and δq_1 are arbitrary functions subject to the whims of the analyst, let δq_2 be zero while δq_1 remains arbitrary. Then reverse this procedure by letting δq_1 be zero while δq_2 remains arbitrary. The result is the following two simultaneous equations to be solved for q_1 and q_2 :

$$\frac{f_0 L^5}{30} = q_1 \left(\frac{4EIL^5}{5} \right) + q_2 \left(\frac{6EIL^7}{35} \right)$$

and
$$\frac{f_0 L^7}{140} = q_1 \left(\frac{6EIL^7}{35} \right) + q_2 \left(\frac{2EIL^9}{35} \right)$$

After clearing fractions and solving, the result is

$$q_1 = \frac{f_0}{(24EI)} \quad \text{and} \quad q_2 = 0$$

Hence
$$w(x) = \frac{f_0 x^2(L-x)^2}{24EI} \quad \text{and} \quad w(L/2) = \frac{f_0 L^4}{384EI}$$

which confirms that the first of the two functions is the exact Bernoulli–Euler answer, and makes clear why the second weighting function is zero. ■

Example 16.3. Using a virtual work formulation, obtain a one term Rayleigh–Ritz solution for the deflections of a simply supported beam whose nonuniform stiffness coefficient varies along the span of length L according to the formulas

$$EI(x) = EI_0 \left(1 + \frac{2x}{L} \right) \quad \text{for } 0 \leq x \leq \frac{L}{2}$$

and
$$EI(x) = EI_0 \left(3 - \frac{2x}{L} \right) \quad \text{for } \frac{L}{2} \leq x \leq L$$

Note that the piecewise linear stiffness coefficient $EI(x)$ is symmetric about the midspan point, where the stiffness coefficient has its maximum value. Let the applied loading again be a uniform force per unit length acting upward of magnitude f_0 .

Comment. This problem could be solved using the fourth-order beam bending differential equation taking into account the discontinuity at midspan in the expression for the stiffness

coefficient. It is left to the reader to decide if the differential equation approach or the Rayleigh–Ritz approach is more appealing.

Solution. Since a linear polynomial has been employed to describe the variation in the stiffness coefficient, ease of integration suggests selecting approximating functions that are also polynomials. Since the exact strength of materials solution is not available, caution would suggest using more than one suitable function. In addition to being symmetric about the midspan point, the selected functions need to satisfy the deflection type boundary conditions. Since the beam is simply supported, those BCs in this case are only two in number: $w(0) = w(L) = 0$. Two polynomial functions that meet these requirements are $f_1 = x(L - x)$ and $f_2 = x^2(L - x)^2$. Note that sine functions are also possible selections. With these preliminaries settled, it is now a matter of writing the integral expressions for the external virtual work and the virtual strain energy, and then equating the two. Since both the loading and the geometry of the beam are symmetric about midspan, the integration can be simplified by just integrating over the interval $(0, L/2)$ and doubling the result. Hence, with

$$w(x) = q_1(xL - x^2) + q_2(x^2L^2 - 2x^3L + x^4)$$

$$\text{and } w''(x) = -2q_1 + q_2(2L^2 - 12xL + 12x^2)$$

$$\text{then } \delta W_{ex} = 2 \int_0^{L/2} f_0[\delta q_1(xL - x^2) + \delta q_2(x^2L^2 - 2x^3L + x^4)] dx$$

$$\text{or } \delta W_{ex} = \left(\frac{f_0L^3}{6}\right) \delta q_1 + \left(\frac{f_0L^5}{60}\right) \delta q_2$$

Note that the varying stiffness factor does not complicate the virtual work expression. After substituting the linear polynomial expression for the stiffness coefficient, and those for $w''(x)$ and $\delta w''(x)$, and carrying out the necessary multiplications, the result for the virtual strain energy expression is

$$\delta U = 2 \left(\frac{EI_0}{L}\right) \int_0^{L/2} [q_1\delta q_1(4L + 8x) - (q_2\delta q_1 + q_1\delta q_2)(4L^3 - 16L^2x - 24x^2L + 48x^3) + q_2\delta q_2(4L^5 - 40L^4x + 96x^2L^3 + 96x^3L^2 - 432x^4L + 288x^5)] dx$$

$$\delta U = 2 \left(\frac{EI_0}{L}\right) \left[q_1\delta q_1(3L^2) - (q_2\delta q_1 + q_1\delta q_2) \left(-\frac{L^4}{4}\right) + q_2\delta q_2 \left(\frac{11L^6}{20}\right) \right]$$

After equating the virtual external work to the virtual strain energy, first setting δq_2 equal to zero, and then in turn setting δq_1 equal to zero, obtain the simultaneous equations

$$\begin{aligned} \frac{f_0L^3}{6} &= 2 \left(\frac{EI_0}{L}\right) \left[q_1(3L^2) + q_2 \left(\frac{L^4}{4}\right) \right] \\ \frac{f_0L^5}{60} &= 2 \left(\frac{EI_0}{L}\right) \left[q_1 \left(\frac{L^4}{4}\right) + q_2 \left(\frac{11L^6}{20}\right) \right] \end{aligned}$$

The solution to these two simultaneous equations is $q_1 = 0.02755905(f_0L^2/EI_0)$ and $q_2 = 0.00262467(f_0/EI_0)$. Substituting this solution into the original two-term approximating series provides the differentiable solution for the beam deflections. The fact that the first weighting factor is about ten times the value of the second weighting factor suggests that the choice of the first approximating function was a good one. ■

Before proceeding to another variety of a RRM analysis involving beams, one involving beam buckling, it is necessary to provide a brief explanation of the external work done by

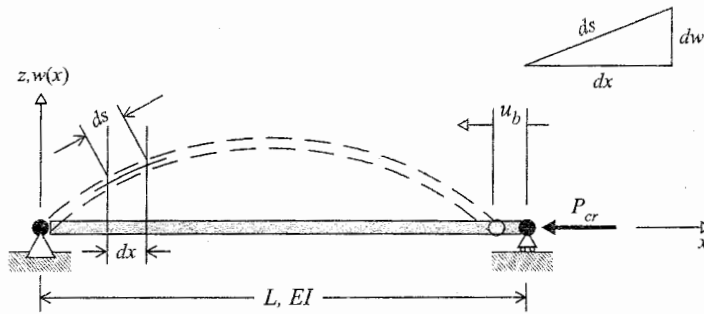


Figure 16.1. Diagram showing the deflections of a buckled beam and the consequent work done by the critical value of the compressive axial load.

the compressive axial force P acting on a beam-column when the beam buckles. The beam buckles when the beam moves from its straight, static equilibrium configuration to a slightly bent, static equilibrium configuration. As fully explained, for example, in Refs. [3] and [23], in both of these “adjacent equilibrium” configurations, to an exceedingly close approximation, the compressive force has the same value P_{cr} . Figure 16.1 shows both the (exaggerated) bent and the straight adjacent equilibrium configurations, and the small but finite axial distance u_b through which the constant compressive force P_{cr} moves when the beam buckles, thus doing positive work. Since the axial force acting upon both the straight and bent beams is the same, the axial length of the two beam configurations is the same. Thus the magnitude of u_b can be written as

$$u_b = \int_0^L ds - \int_0^L dx$$

The first part of the integral over ds , the part over the curved beam length, simply provides the length of the beam, L , and the latter part, where ds is the same as dx , provides the length u_b . The second integral, the one over dx , which is over the straight form of the beam, simply provides the length L . From the same figure it can be seen that $ds = [(dx)^2 + (dw)^2]^{1/2} = [1 + (dw/dx)^2]^{1/2} dx$. Substituting this expression for ds into the above equation, and approximating the upper limit of the second integral by simply L , lead to

$$W_{ex} = P_{cr} u_b = P_{cr} \int_0^L \left\{ \left[1 + \left(\frac{dw}{dx} \right)^2 \right]^{1/2} - 1 \right\} dx = 1/2 P_{cr} \int_0^L \left(\frac{dw}{dx} \right)^2 dx$$

where the binomial theorem was used to expand the above square root. Therefore

$$\delta W_{ex} = P_{cr} \int_0^L \frac{dw}{dx} \delta \left(\frac{dw}{dx} \right) dx = P_{cr} \int_0^L w'(x) \delta w'(x) dx$$

A more rigorous derivation of the virtual work expression can be found in Ref. [3], pp. 467–470. This derivation also shows that the compression of the beam before buckling is immaterial to the buckling analysis. To further cement confidence in the above expression for external virtual work, note if this virtual work expression is coupled with the virtual strain energy integral

$$\delta U = \int_0^L EI w''(x) \delta w''(x) dx$$

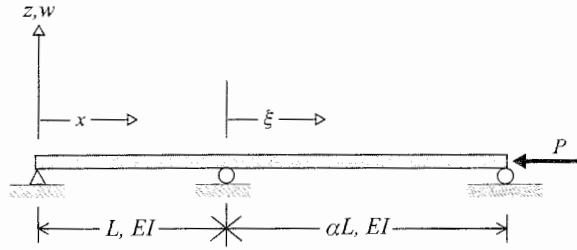


Figure 16.2. Example 16.4

and both integrals are integrated by parts, the result is the familiar Euler buckling equation $EIw''''(x) + P_{cr}w''(x) = 0$.

Example 16.4. Using the RRM and a work/energy formulation, determine the Euler buckling load of the continuous beam over three supports shown in Fig. 16.2. Note that for convenience, two spanwise coordinates are used: x over the left-hand beam, and ξ over the right-hand beam.

Comment. Since the stiffness coefficient is a constant, this problem could be solved using a differential equation approach. The two beams would have to be tied together by writing the following four boundary conditions at the interior support

$$w(x = L) = w(\xi = 0) = 0 \quad w'(x = L) = w'(\xi = 0)$$

and $w''(x = L) = w''(\xi = 0)$

Note that no shearing force boundary condition can be written at the interior support because of the presence of the unknown reaction force.

Solution. The use of single sine functions for both uniform spans appears to be a good starting point. Before using the PVW, it is necessary that the sine functions satisfy the zero deflection conditions at the three supports, and that the two sine functions have continuous slopes at the interior support. The two functions that satisfy these requirements are easily determined to be

$$w(x) = (q/\alpha) \sin\left(\frac{\pi x}{L}\right) \quad \text{and} \quad w(\xi) = -q \sin\left(\frac{\pi \xi}{\alpha L}\right)$$

where $w'(x) = \left(\frac{\pi q}{\alpha L}\right) \cos\left(\frac{\pi x}{L}\right)$ and $w'(\xi) = -\left(\frac{\pi q}{\alpha L}\right) \cos\left(\frac{\pi \xi}{\alpha L}\right)$

and $w''(x) = -\left(\frac{\pi^2 q}{\alpha L^2}\right) \sin\left(\frac{\pi x}{L}\right)$ and $w''(\xi) = \left(\frac{\pi^2 q}{\alpha^2 L^2}\right) \sin\left(\frac{\pi \xi}{\alpha L}\right)$

First calculate δU .

$$\begin{aligned} \delta U = & - \int_0^L EI \left(\frac{\pi^2 q}{\alpha L^2}\right) \sin\left(\frac{\pi x}{L}\right) \left(\frac{\pi^2 \delta q}{\alpha L^2}\right) \sin\left(\frac{\pi x}{L}\right) dx \\ & + \int_0^{\alpha L} EI \left(\frac{\pi^2 q}{\alpha^2 L^2}\right) \sin\left(\frac{\pi \xi}{\alpha L}\right) \left(\frac{\pi^2 \delta q}{\alpha^2 L^2}\right) \sin\left(\frac{\pi \xi}{\alpha L}\right) d\xi \end{aligned}$$

or
$$\begin{aligned} \delta U = & EI \left(\frac{\pi^4 q \delta q}{\alpha^2 L^4}\right) \int_0^L \sin\left(\frac{\pi x}{L}\right) \sin\left(\frac{\pi x}{L}\right) dx \\ & + EI \left(\frac{\pi^4 q \delta q}{\alpha^4 L^4}\right) \int_0^{\alpha L} \sin\left(\frac{\pi \xi}{\alpha L}\right) \sin\left(\frac{\pi \xi}{\alpha L}\right) d\xi \end{aligned}$$

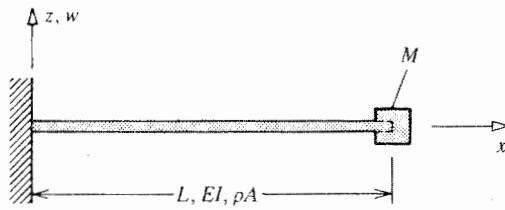


Figure 16.3. A cantilevered beam undergoing force free, bending vibrations in the plane of the paper.

The value of the first of the above two integrals is $L/2$, and that of the second integral is $\alpha L/2$. Therefore

$$\delta U = \frac{1}{2} EI \left(\frac{\pi^4 q \delta q}{L^3} \right) \left(\frac{1}{\alpha^2} + \frac{1}{\alpha^4} \right)$$

Now turn to the evaluation of

$$\begin{aligned} \delta W_{ex} &= P_{cr} \int w'(x) \delta w'(x) dx = P_{cr} \int \left(\frac{\pi^2 q \delta q}{\alpha^2 L^2} \right) \cos \left(\frac{\pi x}{L} \right) \cos \left(\frac{\pi x}{L} \right) dx \\ &\quad + P_{cr} \int \left(\frac{\pi^2 q \delta q}{\alpha^2 L^2} \right) \cos \left(\frac{\pi \xi}{\alpha L} \right) \cos \left(\frac{\pi \xi}{\alpha L} \right) d\xi \end{aligned}$$

or
$$\delta W_{ex} = \frac{1}{2} P_{cr} \left(\frac{\pi^2 q \delta q}{L} \right) \left(\frac{1}{\alpha^2} + \frac{1}{\alpha} \right)$$

Equating the virtual strain energy to the virtual work leads to the solution for the critical load

$$P_{cr} = \pi^2 (EI/L) \left[\frac{(1 + \alpha^2)}{\alpha^2(1 + \alpha)} \right]$$

As a check on this answer, note that if α is equal to one, which means that the two beams have the same length, then the critical axial load here is the same as that for two simply supported beams of length L , end to end, subjected to an axial force P_{cr} , or the same as that for a single simply supported beam, with a midspan support, because its buckling shape is the same as that of the second buckling mode of such a beam without a midspan support: $4\pi^2 EI/(2L)^2$. ■

Very briefly, in preparation for the next example problem, understand that any elastic system, once set in motion and in the absence of further applied loads, will soon vibrate back and forth at a fixed number of vibratory cycles per second. That constant frequency of vibration is called the *first natural frequency*. Here the word “natural” means that the structural system is free of externally applied loads. Just like beam buckling, where there are many buckling load solutions, there are many natural frequency solutions. Unlike the beam buckling problem, the second, third, and higher natural frequencies generally do matter, but the first natural frequency is almost always the more important frequency of vibration.

Example 16.5. For vibrations in the plane of the paper, use the RRM to estimate the first natural frequency of the cantilevered, uniform, symmetric beam and discrete mass sketched in Fig. 16.3. The beam has a mass per unit length of ρA , and its stiffness factor is EI . Let the total mass of the beam, ρAL , be less than that of the tip mass, M . Define the mass ratio as $\mu = M/(\rho AL)$.

Comment. The “exact” strength of materials solution for this problem proceeds from the beam GDE, where the only applied load per unit length is the inertial load per unit length.

(Recall from previous discussion that any inertial load has the form of a mass multiplied by the negative of the mass's acceleration.)

$$EIw''''(x, t) = f_z(x, t) = -\rho A\ddot{w}(x, t)$$

with BCs $w(0, t) = w'(0, t) = M_y(L, t) = 0$, and $V_z(L, t) = M\ddot{w}(L, t)$. The last BC is obtained by noting that the deflection of the tip mass is positive upward. Hence the velocity and the acceleration of the tip mass are also positive upward. Hence the resulting tip mass inertia force acts downward because all inertia forces are opposite to the direction of the acceleration, and therefore have negative signs. Since all load-free vibrations of linearly elastic systems are sinusoidal (called harmonic) in time, the deflection of any point along the length of the beam can be written as $w(x, t) = W(x) \sin(2\pi ft)$, where f is the frequency of vibration in units of cycles per second (i.e., Hz). Substituting, and canceling the sine term produces the following time-invariant GDE and BCs:

$$W''''(x) - \lambda^4 W(x) = 0 \quad \text{where} \quad \lambda^4 = \frac{4\pi^2 f^2 \rho A}{EI}$$

and

$$W(0) = W'(0) = W''(L) = 0 \quad \text{and} \quad w'''(L) + \lambda^4 \mu L W(L) = 0$$

The solution to the GDE in terms of four unknown constants of integration and the unknown eigenvalue λ is

$$W(x) = A \sin(\lambda x) + B \cos(\lambda x) + C \sinh(\lambda x) + D \cosh(\lambda x)$$

Substitution of this solution into the four homogeneous BCs, and then expanding the 4×4 determinant of the coefficient matrix of the vector of constants of integration, with careful attention to signs, yields the following transcendental characteristic equation for all values of the eigenvalue in terms of the mass ratio μ

$$1 + \cos(\lambda L) \cosh(\lambda L) = \lambda L \mu [\sin(\lambda L) \cosh(\lambda L) - \cos(\lambda L) \sinh(\lambda L)]$$

A numerical solution to this transcendental equation is best achieved by use of a digital computer. The difficulty is that each such numerical solution requires a specific value for the parameter μ and the total solution is a plot of λ , or f , versus μ . An approximate solution to this equation for a general value of μ can be sought for small values of λL by using the following approximations to the transcendental functions which are obtained from their respective Taylor series expansions: $\sin \theta = (\theta - \theta^3/6)$, $\cos \theta = (1 - \theta^2/2 + \theta^4/24)$, $\sinh \theta = (\theta + \theta^3/6)$, and $\cosh \theta = (1 + \theta^2/2 + \theta^4/24)$. Then, with $\theta = \lambda L$,

$$1 + \left(1 - \frac{\theta^2}{2} + \frac{\theta^4}{24}\right) \left(1 + \frac{\theta^2}{2} + \frac{\theta^4}{24}\right) = \theta \mu \left[\left(\theta - \frac{\theta^3}{6}\right) \left(1 + \frac{\theta^2}{2} + \frac{\theta^4}{24}\right) - \left(1 - \frac{\theta^2}{2} + \frac{\theta^4}{24}\right) \left(\theta + \frac{\theta^3}{6}\right) \right]$$

or, after discarding fifth and higher powers of θ ,

$$1 + 1 - \frac{\theta^4}{4} + \frac{\theta^4}{12} = \mu \theta \left(\theta + \frac{\theta^3}{2} - \frac{\theta^3}{6} - \theta + \frac{\theta^3}{2} - \frac{\theta^3}{6} \right)$$

or

$$2 - \frac{\theta^4}{6} = \frac{2\mu\theta^4}{3} \quad \text{or} \quad \theta^4 = (\lambda L)^4 = \frac{12}{1 + 4\mu}$$

or

$$\dot{f}^2 = \frac{3}{\pi^2} \left(\frac{EI}{4ML^3 + \rho AL^4} \right) \quad (\text{units check})$$

The above process is time-consuming. Contrast the above lengthy differential equation solution to the following, comparatively simple RRM energy-based solution which takes far less time when the analyst is familiar with the procedure.

Solution. In any RRM analysis, in order to obtain roughly the same accuracy of solution, the analyst can either choose a small number of carefully chosen, generally more complicated, approximating functions or a larger number of simple approximating functions. In this hand-calculated solution the former choice is made. (An exercise examines the latter approach.) Examples of carefully chosen approximating functions for the dynamic deflections of the beam-mass system are the static deflections of the beam-mass system due to appropriate static loads. An appropriate static load for the case where $M \gg \rho AL$ is that of a concentrated force F at the beam tip where the discrete mass M is located. An appropriate static load for the case where $\rho AL \gg M$ is a uniform load per unit length over the length of the beam. In the present case where simply $M > \rho AL$, the concentrated tip load is still appropriate because those masses where the vibration amplitudes are largest are more important to the natural frequency solution than those masses where the vibration amplitudes are smallest. Thus, while a better answer could be obtained using both static deflection functions with different weighting factors, q_j for the sake of simplicity, with very little loss of accuracy, the single static deflection function from the tip-loaded beam is chosen as the approximating function for this RRM analysis.

The static deflection function is obtained from the second order beam equation $EIw''(x) = M(x) = F(L - x)$. The solution is $EIw(x) = (1/2)FLx^2 - (1/6)Fx^3$ or $w(x) = (1/2)w(L)[3(x/L)^2 - (x/L)^3]$. Thus write for the RRM approximate analysis

$$w(x, t) = q(t) \left[3 \left(\frac{x}{L} \right)^2 - \left(\frac{x}{L} \right)^3 \right]$$

where $q(t)$ is the single generalized coordinate that defines the amplitude of the vibration, while $[3(x/L)^2 - (x/L)^3]$ defines the approximate shape of the beam vibration in its first vibratory mode. Rather than use the force-based fourth order beam ordinary differential equation $W''''(x) - \lambda^4 W(x) = 0$ developed above for the RRM analysis, use will be made of the corresponding work and energy terms. Since there are no applied loads, the work done by external loads is zero. There is only the strain energy of the flexing beam, and the kinetic energy of the system mass. The total kinetic energy of the system is

$$\begin{aligned} T &= \frac{1}{2} M \dot{w}^2(L, t) + \frac{1}{2} \int_0^L \rho A \dot{w}^2(x, t) dx \\ T &= 2M\dot{q}^2(t) + \frac{1}{2} \int_0^L \rho A \dot{q}^2(t) \left[3 \left(\frac{x}{L} \right)^2 - \left(\frac{x}{L} \right)^3 \right]^2 dx \\ T &= 2M\dot{q}^2(t) + \frac{6}{35} \rho AL \dot{q}^2(t) \end{aligned}$$

Since this structure is linearly elastic,

$$U = \frac{1}{2} \int_0^L EI [w''(x, t)]^2 dx$$

Since the rigid mass has no strain energy, it makes no contribution to the above equation. Substituting for $w(x, t)$ and carrying out the above integration leads to the result

$$U = \frac{6EI}{L^3} q^2(t)$$

There is no potential energy to include in this analysis, other than the above strain energy. The gravitational forces are entirely offset by elastic forces that are not included in the above strain–energy expression. Only those deflections that are measured from the position the beam takes in response to its own weight contribute to the above strain energy.

Since this is a case where the beam is undergoing a vibratory motion, the plan is to use the energy form of Newton’s second law, which is called the Lagrange equation.³ Using the Lagrange equation $(d/dt)(\partial T/\partial \dot{q}) - \partial T/\partial q + \partial U/\partial q = 0$ (see Exercise 15.9) leads to

$$\left(4M + \frac{12}{35}\rho AL\right) \ddot{q}(t) + \frac{12EI}{L^3} q(t) = 0$$

The solution to the above ordinary differential equation is

$$q(t) = C \sin(2\pi f t + \phi)$$

where C and ϕ are constants of integration that depend on the initial conditions, which are of no interest here. Substituting the above solution into the above differential equation shows that the first natural frequency of vibration is

$$f^2 = \frac{3}{\pi^2} \left(\frac{EI}{4ML^3 + (12/35)\rho AL^4} \right)$$

which is a slightly higher value than the previous solution $f^2 = (3/\pi^2)[EI/(4ML^3 + \rho AL^4)]$, which was obtained above when the “exact” characteristic equation was approximated in order to locate its smallest root. Again, this is the approximate first natural frequency because the selected dynamic deflection function only approximates the first mode shape. Again, a Rayleigh–Ritz solution for a first natural frequency is always greater than the exact solution for the first natural frequency. ■

Example 16.6. Consider the rectangular slab of uniform thickness h sketched in Fig. 16.4. The slab material is homogeneous, linearly elastic, and isotropic. As shown in the sketch, where σ_0 is a constant, the loading is parabolically distributed tractions on the left- and right-hand sides of the rectangle, and these tractions do not vary over the thickness of the slab edge. The slab therefore is in a state of plane stress, and is in a state of external equilibrium. Use the RRM along with the Principle of Complementary Virtual Work (PCVW) to approximate the internal stress distribution.

Comment. All the previous example problems, as all the exercises, employ the Principle of Virtual Work (PVW) with displacement unknowns to obtain a RRM approximate solution. The reason for that choice is that the finite element method, which is a form of a RRM analysis employing the PVW, is clearly the dominant method of structural analysis today. However, the unit load method, which is also a necessary part of any structural analyst’s repertoire, and the subject of Chapters 20 and 21, employs the PCVW. Hence the PCVW cannot be neglected. Thus the inclusion of this example problem which also serves as a

³ In the Lagrange equation, the weighting factor q is called a *generalized coordinate*. Generalized coordinates are further explained in the first part of Chapter 17. An alternate approach to the use of the Lagrange equation is to argue that the maximum value of the kinetic energy is equal to the maximum value of the strain energy.

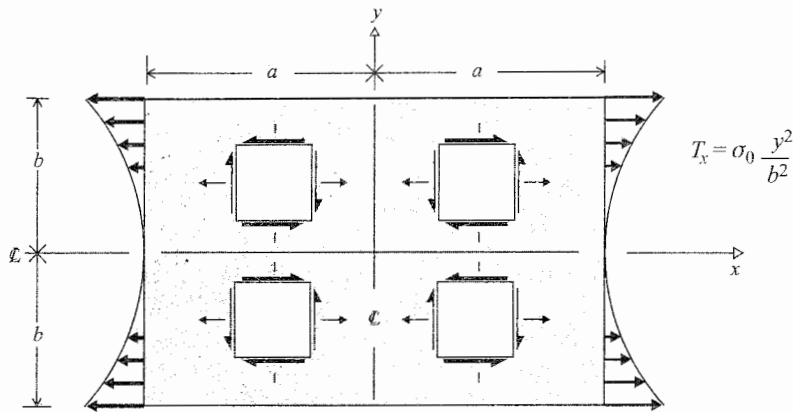


Figure 16.4. Example 16.6. Slab/plate with in-plane loading.

reminder of the basic plane stress equations. While this problem is lengthy, be assured that the unit load problem and any of the other closely related PCVW based methods are easy to apply within their realm of application.

Solution. The first task is to decide upon the approximating functions for the three nonzero stresses σ_{xx} , σ_{yy} , and σ_{xy} . Since the applied traction is a polynomial, and for ease of integration, polynomial expressions are chosen. Start the selection of the approximating functions with the unknown function σ_{xx} . Since the PCVW requires equilibrium and enforces continuity, the chosen polynomial for σ_{xx} will have to have the value $+\sigma_0(y/b)^2$ where $x = \pm a$. Since the loading, geometry and material have both the x and the y axes as axes of symmetry, only even valued polynomial terms are appropriate selections, and these additional series terms must be zero at $x = \pm a$. Keeping in mind St. Venant's principle, it can be guessed that while σ_{xx} is parabolic at the edges, it will tend to a more uniform distribution at the slab center. The last consideration is that a short series is satisfactory here because the main purpose of this example problem is to be illustrative. Thus choose the somewhat brief approximation

$$\sigma_{xx} = \sigma_0(y/b)^2 + (a^2 - x^2)(p_1 + p_2y^2 + p_3y^4 + p_4x^2 + p_5x^2y^2)$$

where, like the q 's used as weighting factors for RRM selected deflection functions, the p 's are weighting factors for the stress function finite series terms. (The switch in symbols is made because later the q 's will, while serving the same purpose, take on an expanded meaning that will not include the p 's.) Now turn to selecting an approximating polynomial for σ_{xy} . As shown in Fig. 16.4, the double symmetry requires that if the shearing stresses are positive, as illustrated, in the first quadrant, they must also be positive in the third quadrant and negatively valued in the second and fourth quadrants. This means that σ_{xy} needs to be described by odd-valued polynomials. Furthermore, the shearing stress must have a zero value at all four edges. Therefore select the following approximating function:

$$\sigma_{xy} = (a^2 - x^2)(b^2 - y^2)(p_6xy)$$

Similarly the normal stress σ_{yy} requires even valued polynomial terms, which must be zero at the top and bottom plate edges. Hence choose

$$\sigma_{yy} = (b^2 - y^2)(p_7 + p_8x^2 + p_9y^2 + p_{10}x^2y^2)$$

Note that even in this brief analysis there are ten parameters to be determined. (An original attempt started with nine parameters, but was adjusted to ten so that the equilibrium equations could be satisfied. Failures require adjustments.) The next step is to require that these stresses meet the requirements of the plane stress, general equilibrium equations. The first of these two equations is $\partial\sigma_{xx}/\partial x + \partial\sigma_{xy}/\partial y = 0$. Substituting the above chosen functions leads to

$$(-2p_1 + 2p_4 + p_6a^2b^2)x + (-2p_2 + 2p_5a^2 - 3p_6a^2)xy^2 + (4p_4 + p_6b^2)x^3 - 2p_3xy^4 + (-4p_5 + 3p_6)x^3y^2 = 0$$

Since this equation has to be true for all values of x and y , this equation is an identity. That means like terms on the left hand side of this equation have to match like terms on the right hand side of this equation; that is, the collective coefficients of each polynomial term have to be zero. Another way of saying this with more authority is to say that the linear independence (see Section III.3) of each polynomial term requires that each of their collective coefficients must be zero. Solving the resulting four simultaneous equations, which is easily done, reveals that $p_1 = (1/4)p_6a^2b^2$, $p_2 = -(3/4)p_6a^2$, $p_3 = 0$, $p_4 = -(1/4)p_6b^2$, and $p_5 = (3/4)p_6$. Substituting these solutions in the assumed forms for σ_{xx} and σ_{xy} gives

$$\sigma_{xx} = \sigma_0(y/b)^2 + (p_6/4)(a^2 - x^2)(a^2b^2 - b^2x^2 - 3a^2y^2 + 3x^2y^2)$$

and

$$\sigma_{xy} = p_6xy(a^2 - x^2)(b^2 - y^2)$$

Substituting the above expression for the shearing stress and the original form for the normal stress $\sigma_{yy} = (b^2 - y^2)(p_7 + p_8x^2 + p_9y^2 + p_{10}x^2y^2)$ into the second of the plane stress equilibrium equations, $\partial\sigma_{xy}/\partial x + \partial\sigma_{yy}/\partial y = 0$, and again using linear independence to equate the coefficients of like terms, leads to

$$\sigma_{yy} = (p_6/4)(b^2 - y^2)(a^2b^2 - 3b^2x^2 - a^2y^2 + 3x^2y^2)$$

While it was lengthy, the development of the approximating functions is now complete, and now equilibrium is assured. The next step is to apply the PCVW, $\delta W_{ex}^* = -\delta W_{in}^* = \delta U^*$, and thereby determine the value of the unknown parameter p_6 . Starting with the surface integral for the external complementary virtual work, it simplifies to

$$\delta W_{ex}^* = h \oint \delta T_x u \, ds = 0$$

The above integration over the four edge surfaces of the rectangular parallelepiped and its top and bottom surfaces reduces to the line integral around the perimeter of the rectangle because on most surfaces, both T_x and T_y are zero, and on the edge surfaces of depth h , the differential of surface area is $h \, ds$. The value of the line integral is zero because on the left and right hand edges, the traction T_x is a fixed quantity, and thus does not allow a variation. (When the unit load method is studied, there will be examples where variations on force quantities on S_2 will not be zero.) Turn now to the complementary virtual strain energy which for plane stress is

$$\delta U^* = \iiint_{\text{Vol.}} [\epsilon_{xx}\delta\sigma_{xx} + \epsilon_{yy}\delta\sigma_{yy} + \gamma_{xy}\delta\sigma_{xy}] \, dA \, dh$$

While the strain energy is written in terms of displacement type quantities, the complementary strain energy is written entirely in terms of stress type quantities. To accomplish that task, it is necessary to utilize the plane stress constitutive (i.e., material) equations, which

are (i) $E \epsilon_{xx} = \sigma_{xx} - \nu \sigma_{yy}$; (ii) $E \epsilon_{yy} = \sigma_{yy} - \nu \sigma_{xx}$; and (iii) $E \gamma_{xy} = 2(1 + \nu) \sigma_{xy}$; where ν is Poisson's ratio. Making these substitutions

$$\delta U^* = (h/E) \iint_A [(\sigma_{xx} - \nu \sigma_{yy}) \delta \sigma_{xx} + (\sigma_{yy} - \nu \sigma_{xx}) \delta \sigma_{yy} + 2(1 + \nu) \sigma_{xy} \delta \sigma_{xy}] dA$$

Hence $\delta W_{ex}^* = \delta U^*$ becomes

$$0 = \int_{-a}^a \int_{-b}^b [(\sigma_{xx} - \nu \sigma_{yy}) \delta \sigma_{xx} + (\sigma_{yy} - \nu \sigma_{xx}) \delta \sigma_{yy} + 2(1 + \nu) \sigma_{xy} \delta \sigma_{xy}] dx dy$$

From applying the variational operator to the actual stress expressions

$$\begin{aligned} \delta \sigma_{xx} &= (\delta p_6/4)(a^2 - x^2)(a^2 b^2 - b^2 x^2 - 3a^2 y^2 + 3x^2 y^2) \\ \delta \sigma_{xy} &= \delta p_6 x y (a^2 - x^2)(b^2 - y^2) \\ \delta \sigma_{yy} &= (\delta p_6/4)(b^2 - y^2)(a^2 b^2 - 3b^2 x^2 - a^2 y^2 + 3x^2 y^2) \end{aligned}$$

After substituting the actual and varied stress expressions into the complementary virtual strain energy equation above

$$\begin{aligned} 0 = \int_{-a}^a \int_{-b}^b & \{ [\sigma_0(y/b^2) + (p_6/4)(a^2 - x^2)(a^2 b^2 - b^2 x^2 - 3a^2 y^2 + 3x^2 y^2) - \nu(p_6/4)(b^2 - y^2) \\ & * (a^2 b^2 - 3b^2 x^2 - a^2 y^2 + 3x^2 y^2)] [(\delta p_6/4)(a^2 - x^2)(a^2 b^2 - b^2 x^2 - 3a^2 y^2 + 3x^2 y^2)] \\ & + [(\delta p_6/4)(b^2 - y^2)(a^2 b^2 - 3b^2 x^2 - a^2 y^2 + 3x^2 y^2) - \nu \sigma_0(y/b^2) + \nu(p_6/4)(a^2 - x^2) \\ & * (a^2 b^2 - b^2 x^2 - 3a^2 y^2 + 3x^2 y^2)] [(\delta p_6/4)(b^2 - y^2)(a^2 b^2 - 3b^2 x^2 - a^2 y^2 + 3x^2 y^2)] \\ & + 2(1 + \nu)[p_6 x y (a^2 - x^2)(b^2 - y^2)] [\delta p_6 x y (a^2 - x^2)(b^2 - y^2)] \} dx dy \end{aligned}$$

Note that the arbitrary factor δp_6 cancel. This leaves one equation to be solved for p_6 in terms of the known quantity σ_0 . There is little point in carrying out the above definite integration. However, once p_6 has been determined, all three stresses are also determined, and the problem is concluded. ■

A bit of perspective is in order. The above problem was lengthy for a textbook problem, even without completing the last time consuming step of carrying out the definite integration in order to determine the one unknown parameter. Based upon on a comparison with earlier example problems in this chapter dealing with beams, the reader might get the *false* impression that the use of the PCVW with unknown stresses (again, called a stress formulation) is an inferior approach to the use of the PVW with displacement type unknowns. The fundamental reason that this problem was much lengthier is that, in contrast to the earlier beam problems, there are no useful strength of materials approximations that can be used with a slab (i.e., plate) loaded in its own plane. Thus the need to here use the plane stress theory of elasticity equations with their attendant complexity. A second point in favor of using the PCVW is that the above stress formulation solution is not as efficient as it could be. It could have been somewhat simplified by the use of the Airy⁴ stress function, $\Phi(x, y)$, a potential function for stresses much like the Prandtl stress function. Employing the Airy

⁴ The Airy stress function is explained in the optional section 8.6. From Ref. [21], George B. Airy introduced this potential function in a *Brit. Assoc. Advancement Sci. Rept.*, 1862.

stress function would have allowed one finite polynomial series to be used for all three stresses.

The desirability of the above hand calculation has to be judged against the other hand calculation possibilities. The effort required to complete, for example, a RRM displacement approach would not be much different from that expended in the above analysis. There would be the very slight simplification that the selected displacement functions would not have to meet any boundary condition requirements because, in this case, there are no displacement boundary conditions. Choosing the selected displacement functions would, perhaps, be a bit more difficult. Judging from the above selected stress formulation series that contain terms such as $x^2 y^4$ and $x^4 y^2$, and the fact that the displacements have to be differentiated to obtain the strains and stresses, then it can be concluded that the selected displacement functions would have to involve some seventh order polynomial terms to achieve the same accuracy as this stress formulation. It is safe to say that there is no other displacement formulation *hand* calculation technique that would be superior to a displacement RRM analysis for this problem. The situation changes completely if a digital computer and finite element software are available. Such a computer based finite element analysis would not be any sort of burden because the machine would set up the solution pattern and solve for the large number of discrete displacement unknowns in the blink of an eye. Thus the reader can appreciate what a revolution occurred with the dual development of the finite element method and the digital computer. Chapter 19 explains this finite element process for plane stress problems along with other types of problems that are not accessible through strength of materials approximations. Chapters 20 and 21 show the case of using a stress formulation and the PCVW with small beam frame and grid problems.

In addition to the older, finite difference method and the RRM, there is continuing competitor to the dominant finite element method that is called the boundary element method; see Refs. [67, 68]. The particular advantage of the boundary element method is that the number of unknowns, and hence the number of equations necessary to determine those unknowns, for the same accuracy, can be many times less than the number of unknowns required by the finite element method. This is so because the nodal points used by the boundary element method, also called the boundary integral method, cover only the boundary surfaces of the object being analysed, rather than both the surface and interior as is necessary with the finite element method. The drawback that is most serious for this sophisticated method with respect to the analysis of vehicular structures is that, by itself, it is restricted to linear, static problems. Today the boundary element method is being applied to problems in fracture mechanics and plasticity. Other, less successful, general methods that a reader of the older technical literature will frequently encounter have the names: (i) collocation method or point matching method (see Endnote (1) of Chapter 19); (ii) the least-squares method; (iii) Kantorovitch's method; and (iv) the Trefftz-Morely method.

16.3 Summary

There are all manner of ways of classifying numerical analyses. Some classifications are particular to the solution technique of the numerical analysis itself, and some classifications merely reflect the options of any type of structural analysis, analytical or numerical. Starting with the latter, a numerical analysis method can be classified as either a deflection method, or a stress method, or a mixed method. The "finite element method" is a deflection method because the unknown variables of that method are the structure's deflections at discrete points throughout the volume and on the boundary surface of the structure. However, when the present deflection finite element method in all its diversity

was first being developed, there was considerable competition between it and another finite element method using internal forces and moments as unknowns. The finite element stress formulation soon came to a dead end, and the finite element method is today exclusively a deflection method.⁵

Other general methods seem to be equally useful in the form of either a stress or a deflection formulation. The RRM is such a method. However, just as is true for analytical solutions, the stress formulation of the RRM is limited to those situations where the problem BC equations are exclusively stress or traction equations. RRM solutions for structural dynamics problems, as most but not all numerical methods, are generally limited to deflection formulations because of the necessity of dealing with accelerations. An example of a numerical method that requires the use of both deflections and stress resultants is the transfer matrix method (Ref. [43]). Generally speaking, a numerical method using a stress formulation will provide a more accurate solution for the stresses than the deflections, while a deflection-based numerical analysis will provide a more accurate solution for the deflections than the stresses.

A second way of classifying numerical methods is by whether they exactly satisfy either the governing differential equations (GDEs), or the BCs, or neither. For example, the selected deflection functions that form the basis for a RRM deflection formulation must exactly satisfy the deflection BCs. After the choice is made for the deflection functions that exactly satisfy the deflection BCs, then the GDEs are satisfied approximately. A nontraditional form of the RRM is to reverse the above approach by first selecting functions that exactly satisfy the GDEs, and then using those selected functions to approximate the BCs. The finite difference and finite element methods exactly satisfy neither the GDEs nor the BC equations. This is one reason that these two methods can be applied so easily and generally. Another basic choice that is closely related to the choice of what equations, if any, are to be exactly satisfied, is the choice of whether to base the numerical method on energy formulations or differential equations. The use of energy formulations is often the more convenient, or even the only practicable choice. The advantages of the work or energy formulation include: (i) there are fewer BCs and continuity conditions to be satisfied; and (ii) the coefficient matrices of the unknown quantities are often symmetrical, an important advantage, when a work or energy method is used, while often they are not symmetrical when a differential equation is the basis of the approximation.

A third classification of numerical methods is whether the method is based upon finite series approximations to the unknown functions, or whether the method is based upon a singularity solution. In structural analysis, finite series solutions are by far the most prevalent. The RRM, the finite difference method, the finite element method, and a host of others are examples of series solutions. (In the finite difference case, the approximations to the derivatives can be derived from a Taylor's series.) The boundary element method is the only prominent numerical method for structural analysis that is a singularity method. It is based upon the analytical solution for a concentrated force acting upon a point within the volume of the structure (Ref. [9]). It is called a singularity solution because the concentrated force, of course, causes an infinite stress at its point of application. Note that singularity solutions are much more common in fluid dynamics, where the singularities are such things as point sources of fluid entering the fluid flow from outside the flow field and point "sinks" that drain fluid from the flow field.

⁵ There are so many research papers whose subjects are the development and testing of new finite elements that it is not really possible to be categorical about any aspect of finite element theory or usage. Finite elements using derivatives of deflections have been proposed but have not achieved popularity.

Chapter 16 Exercises

- 16.1.** (a) Re-solve the beam deflection problem of Example 16.1 using as the sole selected approximating function $f(x) = 16x^4 - 8x^2L^2 + L^4$, and obtain the exact strength of materials solution; *or* use a lengthwise coordinate x that starts at the left end of the beam, and the selected function $f_1 = x^2(L-x)^2$ to obtain the exact strength of materials solution.
- (b) As in part (a), but now let the stiffness factor vary symmetrically about midspan so that for $0 \leq x \leq \frac{1}{2}L$, $EI(x) = (2EI/L)(L-x)$.

- 16.2.** (a) Suggest two polynomial functions for a RRM analysis that are suitable for calculating the deflections of a uniform beam of length L that is cantilevered at $x = 0$. At the free end where $x = L$ there is an upward force of magnitude F_0 .

(b) Redo part (a), but this time suggest two nonpolynomial functions.

- 16.3.** (a) Redo Example 16.5 but this time actually use the single, simple function $(x/L)^2$ to describe the shape of the vibrating beam as it vibrates in its first natural mode.

(b) As above, but this time write

$$w(x, t) = q_1(t) \left(\frac{x}{L}\right)^2 - q_2(t) \left(\frac{x}{L}\right)^3$$

or write

$$w(x, t) = q_1(t) \left(\frac{x}{L}\right)^2 + q_2(t) \left(\frac{x}{L}\right)^3$$

The only difference between these two, two-term series approximations is that their respective solutions for q_2 will differ in sign only.

- 16.4.** Consider a simply supported, uniform, symmetric beam of length L and mass per unit length ρA which supports a rigid, discrete mass of magnitude M at its centerspan. Calculate the first natural frequency of this beam-mass system by

(a) using as the approximate dynamic deflection shape for this beam-mass system the first vibration mode shape when there is no rigid mass at the centerspan, that is, when $w(x, t) = q_1(t) \sin(\pi x/L)$

(b) using, as would be appropriate when the rigid mass exceeds the mass of the beam, the static deflection shape that results when a concentrated static force is applied at the beam centerspan. (Note that if the mass of the beam is much less than that of the discrete mass, then the beam can be replaced by a massless spring having a stiffness equal to the centerspan beam stiffness, that is, having $k = 48EI/L^3$. Then with the natural frequency of any spring-mass system being $4\pi^2 f^3 = k/M$ in this case $f^2 = (12/\pi^2)(EI/ML^3)$.)

- 16.5.** (a) Use the RRM to determine the buckling load of a simply supported beam of length L whose simplified stiffness coefficient description is the constant value $2EI$ over the outer one-thirds of the beam, and $3EI$ over the inner one-third of the beam. (The greater stiffness is at the center because that is where the greater bending moment due to the axial force occurs.) Use a single approximating function.

- (b) Use the RRM to determine the buckling load of a cantilevered beam of length L whose simplified stiffness coefficient description is $3EI$ over the half of the beam at the clamped end, and $2EI$ over the half of the beam closest to the free end. Use a single approximating function.
- (c) Use the RRM to determine the buckling load of a uniform, simply supported, beam of length L with stiffness coefficient EI , when the compressive loading over the left half of the beam is $2P$, while that over the right half of the beam is P . Use a single approximating function.
- (d) Use the RRM to determine the buckling load of a uniform, cantilevered beam of length L with stiffness coefficient EI , when the compressive force acting on the half of the beam nearest the clamped end has the magnitude $2P$, while that over the other half of the beam is merely P . Use a single approximating function.
- (e) Determine the buckling load of a simply supported beam whose left half has a stiffness coefficient $2EI$, and bears a compressive force $2P$, while the right half has a stiffness coefficient of EI , and bears a compressive force of magnitude P . Use a single approximating function.
- (f) Combine the cantilevered beam stiffnesses of part (b) and the loadings of part (d), and determine the buckling load. Use two approximating functions.

16.6. (a) Calculate the center, lateral bending deflection of a thin, rectangular plate of length a in the x direction, and length b in the y direction. The plate is simply supported at all four sides, and subjected to a uniform lateral pressure in the (upward) z direction of magnitude p_0 . Understand that the lateral loading of this problem makes it quite different from the plate problem of Example 16.6, which features an in-plane loading. Therefore, in this case, the virtual external work is

$$\delta W_{ex} = \int_0^a \int_0^b p_0 \delta w(x, y) dx dy$$

The bending strain energy for a thin plate, from Ref. [16], p. 379, is

$$U = 1/2 \int_0^a \int_0^b D [(w_{,xx} + w_{,yy})^2 - 2(1 - \nu)(w_{,xx} w_{,yy} - w_{,xy} w_{,xy})^2] dx dy$$

where, again, subscript coordinates following a comma indicate partial derivatives with respect to that coordinate, D is a plate stiffness factor comparable to EI for beams, and, again, ν is Poisson's ratio. Use the RRM and the single approximating function $w(x, y) = q \sin(\pi x/a) \sin(\pi y/b)$ to obtain the plate center lateral deflection.

- (b) As above, but this time also use a second approximating function that is also symmetric about the plate center, $q_3 \sin(3\pi x/a) \sin(3\pi y/b)$. When doing so, it is important to recognize the orthogonality of the sine functions on these intervals of integration. This orthogonality greatly simplifies the integration.
- (c) In light of the orthogonality of these sine functions, would it be practical to use an infinite series of such approximating functions $q_n \sin(n\pi x/a) \sin(n\pi y/b)$, where n is an odd integer?

- 16.7. Consider a uniform, simply supported, circular plate of radius R , and thickness h . The plate is loaded by a concentrated force at its center. Propose a series of approximating functions to be used in a RRM analysis for the purpose of determining the center deflection. Write the virtual work expression.

FOR THE EAGER

- 16.8. (a) Reconsider the thin slab of Fig. 16.4. This time let $T_x(y)$ vary linearly along the left and right plate edges in the manner that it has the value $+\sigma_0$ at the top of the slab, and the value $-\sigma_0$ at the bottom of the slab, and, of course, a zero value at the x axis. Select appropriate finite series for each of the three stresses of this case of plane stress. *Hint:* One term of the σ_{xx} series has to be $\sigma_0(y/b)$ in order to satisfy the Cauchy equilibrium equations. Further consideration of the σ_{xx} stress pattern suggest that it must be even function in x , and an odd function in y . What to do about the other two stresses is less clear, but can be surmised from the fact that differentiating an even function produces an odd function, and vice versa. This suggests that, from the first general equilibrium equation, that the shearing stress, σ_{xy} , should be odd in x , and even in y ; and that the normal stress σ_{yy} should be even in x , and odd in y .
- (b) Assume that the solution to Example 16.6 was fully obtained along with the solution of part (a) of this exercise. Would it be valid to superimpose the two solutions? Would it be valid to rotate the part (a) problem and solution 90° so that $T_x(y)$ above became $T_y(x)$, and each (a, x) of the solution was replaced by (b, y) ?
- 16.9. (a) Reconsider the previous exercise. This time choose to use the RRM with the PVW. Select finite series expansions for the displacement functions $u(x, y)$ and $v(x, y)$. Plan how to complete the remainder of the problem.
- (b) Consider the same $2a$ by $2b$ by h rectangular parallelepiped of part (a) of the previous exercise. This time let the top and bottom edges be fixed against all displacements. Since the boundary conditions involve displacements, recall that a displacement formulation is now necessary. How should the selected finite deflection series of part (a) be modified for this set of boundary conditions?
- (c) As in part (b), now let the top and bottom edges be fixed against displacements only in the x direction, but are constrained to be linear in the y direction.

Introduction to the Finite Element Method

17.1 Introduction

The finite element method introduced in this chapter is the routine choice for the analysis of structures in government and industry, large companies and small. The finite element method is especially useful in the aerospace sciences and all related fields. For engineering applications, the finite element method was introduced to the engineering community by aerospace structural dynamicists in Ref. [49]. It is not the only useful, or necessary-to-know, method (one other method requires discussion), but it dominates because it is the only method suitable for large, complicated structures such as airplanes, helicopters, ships, and land vehicles, as well as the small redundant structures discussed here. It is particularly broad in scope. As a mathematical concept the finite element method is applicable to a wide variety of problems including such diverse problems as those of fluid dynamics, heat transfer, electromagnetic fields, and electrical circuits. As a mathematical concept, it is an adaptation of the Rayleigh–Ritz method. In this adaptation, instead of the requirement for choosing approximation functions for each new analysis, a finite element analysis can be computer programmed because the same functions are repeatedly used for the same type of structural element. Instead of using the complicated functions that are sometimes necessary to meet boundary condition requirements of complicated structures, this adaptation uses simple functions, almost exclusively polynomial terms for quick computer processing. These simple functions can accurately approximate the complicated solution functions by approximating those complicated functions one small segment at a time rather than over the entire domain as is done in a Rayleigh–Ritz analysis. Indeed, from a mathematician’s point of view, the finite element method is a Rayleigh–Ritz method applied to small “subdomains.” These two aspects, simple functions and subdomains, are the source of the enormous success of the finite element approach.

A major drawback of the finite element method (FEM) is the necessity of solving large numbers of algebraic equations. Thus it is necessary to acknowledge the importance of modern digital computers to the success of the FEM.

All of the preceding chapters were preparation for the presentation of the finite element method in this chapter and Chapters 18 and 19. The theory of elasticity chapters prepared the way for the development of the Principle of Virtual Work (capital letters for emphasis), and the strength of materials chapters prepared the way for the practical implementation of the Principle of Virtual Work. The use of the Principle of Virtual Work indicates that the finite element method today is a stiffness/deflection based method. In its early development, there was a flexibility/force finite element method, but it did not prove to be useful for large structures, and consequently eventually disappeared. Since (independent) deflections are used to characterize a finite element structural model, they are a key aspect of the method, and are the next topic to be discussed.

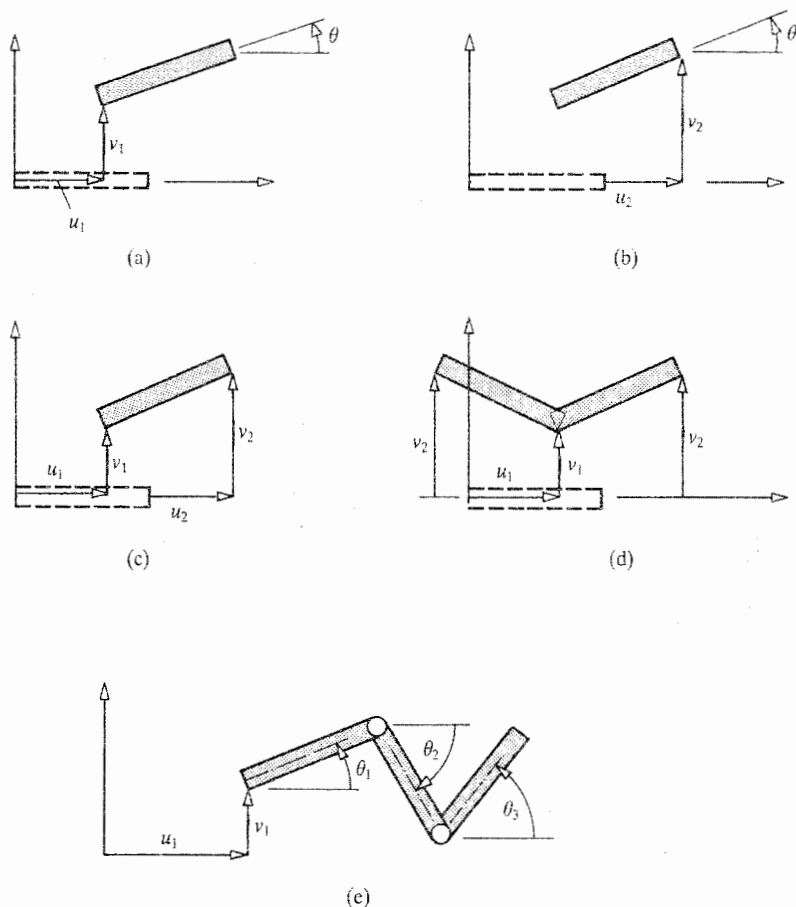


Figure 17.1. The rigid body motion in a plane by one or more connected rods. Examples of valid and invalid generalized coordinates.

17.2 Generalized Coordinates

The finite set of independent deflections that unambiguously determine (perhaps in an approximate way) the deflections of every material point in a structural body is called the set of *generalized coordinates*, or the *degrees of freedom*, of the structural system. Note that by definition these “coordinates” determine deflections in a specified direction at a specified material point rather than merely locate (i.e., name) a material point as cartesian coordinates locate a material point before (or after) displacement. Thus there is no similarity between generalized coordinates which measure deflections and the familiar point-locating coordinates of, say, cartesian and cylindrical coordinate systems.

The simplest way to begin an explanation of, and to complete the definition of, generalized coordinates is to return to rigid body dynamics. Consider the situation where a rigid rod of length L is free to move in a given plane like a flat ruler sliding on a table top. Thus the rigid rod is not permitted to rotate about an axis along its own length, and of course, the rod is not permitted to leave the plane. See Fig. 17.1, where the original position of the rod is outlined while the deflected position of the rod is shaded. The generalized coordinates that locate the deflected position of the material points of the rod are the *minimum* number of measured values of any kind that are required to uniquely specify the deflected

position of the rigid flat rod given the restraints on the motion of the rod. Figure 17.1(a) shows one set of three values that uniquely define the deflected position of the flat rod. The three values are the horizontal and vertical deflection of one end of the rod and the counterclockwise rotation of the rod from the horizontal. Nothing less than three measured values is sufficient to define the deflected position. However, the three values of Fig. 17.1(a) are not, by any means, the only possible three generalized coordinates. Figure 17.1(b) shows another possible set of three generalized coordinates that happen to be associated with the other end of the rod. Other sets of three generalized coordinates can be based upon the horizontal and vertical deflection of any specific point on the rod centerline, and, of course, the deflection of that point on the rod axis does not have to be measured with horizontal and vertical components. Generalized coordinates similar to polar coordinates could also be used.

Figure 17.1(c) shows four rectilinear coordinates locating the deflected position of the rod, which of course is one more than the set of generalized coordinates allows. This situation can be corrected by introducing one equation of constraint upon the four coordinates. Since the length of the rigid rod is fixed, the equation of constraint for these four deflection coordinates is

$$L = [(u_2 - u_1)^2 + (v_2 - v_1)^2]^{1/2}$$

With this equation of constraint, any three of the four deflection coordinates can now be accepted as generalized coordinates, while the remaining one of the four is understood to be a dependent quantity, and thus, not a generalized coordinate. Note that not any set of three coordinates is satisfactory. Figure 17.1(d) shows that the candidate set (u_1, v_1, v_2) is unsatisfactory because for given values of those three coordinates there are in general two possible deflected positions for the rod. The same would be true of the sets (u_1, u_2, v_1) or (u_1, u_2, v_2) . Figure 17.1(e) shows that if additional rigid rods are linked to the original rod with hinges, only one additional generalized coordinate is required for each additional link. Some other examples of generalized coordinates for bodies with only rigid components are as follows.

Example 17.1. A rigid airplane moving in three-dimensional space requires six generalized coordinates. One possible choice for the six generalized coordinates is the three rectilinear displacements and three rotations that are: (i) the change in altitude of the center of mass of the rigid airplane; (ii) the northward change in the center of mass position (iii) the eastward change in the center of mass position; (iv) the rotation of the rigid airplane about an east–west axis; (v) the rotation of the rigid airplane about a north–south axis; and (vi) the rotation of the rigid airplane about a vertical axis. If the rotation angles are small ($\tan \theta \approx \theta$ as per Exercise 9.19), then the order of the rotations is unimportant. ■

Example 17.2. A rigid pendulum constrained to move in a single plane and whose pivot point is attached to the end of another rigid pendulum constrained to move in the same plane and whose pivot point is free to move horizontally on a monorail requires three generalized coordinates. The generalized coordinate set (u, θ_1, θ_2) shown in Fig. 17.2 is a good choice for a vibration (i.e., a time-varying motion) analysis. In this double-pendulum case, the three horizontal rectilinear deflections of the upper pivot point, the upper bob, and the lower bob, (u, u_1, u_2) , are also possible generalized coordinates because the vertical motion of each bob is determined by the horizontal motion. ■

The above examples using rigid bodies should make clear that any set of generalized coordinates is the minimum number of measurable quantities required to unambiguously

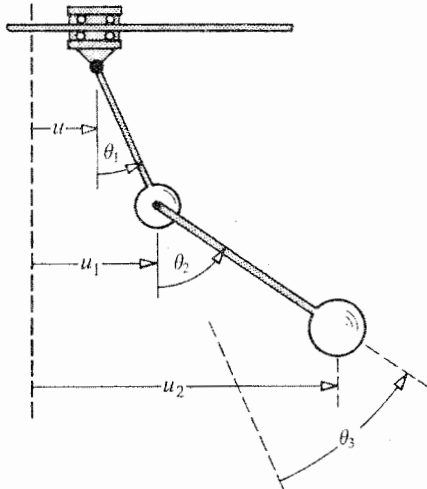


Figure 17.2. Possible generalized coordinates for describing the motion of a rail supported double pendulum, with rigid components, moving in a single plane.

locate the displaced position of all material points of the body under study relative to the body's undisplaced position or any other known position. The minimum number of generalized coordinates, which is also called the number of degrees of freedom (DOF) of the body under study, is independent of the choice of the quantities selected to be the generalized coordinates (or DOF).

As an example of a generalized coordinate whose reference position is not an undisplaced position, consider again the double pendulum of Fig. 17.2. Another valid set of generalized coordinates is (u, θ_1, θ_3) , where θ_3 is the relative rotation of the lower pendulum with respect to the arm of the upper pendulum. Finally note that generalized coordinates do not have to be rectilinear or curved distances or angles of rotation. A pathological, but possible, choice for the two generalized coordinates required for locating the displaced center of mass position of a nonmagnetic marker on a rectangular plane of finite dimensions is as follows. Cover the plane with light refracted through a prism so that one end of the visible light spectrum is at one side of the rectangle, and the other end of the visible spectrum is at the other end of the rectangle. Then create a strong electrostatic field whose lines of constant electrostatic intensity are roughly perpendicular to the lines of constant color. Then the displaced position of the marker can be described by a change in light wavelength and a change in electrostatic field intensity.

Generalized coordinates have exactly the same purpose when used with flexible bodies. However, the situation with flexible bodies is a bit more complicated. Consider a beam of length L that is simply supported at its two ends. Consider the lateral deflections in the z direction of points along the beam axis. Let points along the beam axis be identified in the usual way by an x coordinate axis that originates at one beam end and proceeds towards the other beam end. Using generalized coordinates in exactly the same fashion as they were used in relation to rigid bodies, one generalized coordinate would be needed to describe the lateral deflection at the beam midspan, that is, to describe $w(x = \frac{1}{2}L)$. That discrete generalized coordinate could be called $w(L/2)$. If any load can be applied to the beam, then the description of the lateral deflections at $x = L/4$ and at $x = 3L/4$ would require two more generalized coordinates. In the presence of a totally arbitrary lateral beam

loading, the measurement of the lateral deflections at $x = L/8, 3L/8, 5L/8,$ and $7L/8$ would require four more generalized coordinates. This distance halving and doubling of the required number of generalized coordinates can go on indefinitely with the conclusion that an infinite number of discrete generalized coordinates are necessary to describe the deflections of a beam subjected to an arbitrary loading. Since it takes much too long to even count an infinite number of generalized coordinates, no less use them productively, then the use of generalized coordinates for the analysis of flexible bodies requires a compromise. Two types of compromises have been widely used. The first of these two common compromises is to replace discrete coordinates by a finite number of “distributed” coordinates that are capable of very closely approximating the lateral deflection of every point along a beam axis when the beam is subjected to an arbitrary loading. This is the approach of the Rayleigh–Ritz method as it is generally used. This distributed coordinate approach can also be viewed as an application of generalized Fourier series. Endnote (1), a very brief description of this process using polynomials, is all that need be said here about distributed generalized coordinates.

The second of the two generally accepted compromises is to reject the possibility of an arbitrary loading in favor of only two types of permitted loadings, which are: (i) concentrated forces, and (ii) concentrated moments. This is the compromise used by the FEM for the sake of being able to use a finite number of generalized coordinates to describe the deflected form of flexible bodies. In this fashion, the concentrated forces and moments become an approximation to whatever actual loading acts upon the structure to be analyzed. This approximation is not as crude as it may at first appear, particularly if the structural loading is represented by a large number of concentrated forces and moments. In order to illustrate how an actual distributed loading is replaced by a series of concentrated loads, consider, for example, a single beam as an entire structure. Let that beam be loaded by a uniformly distributed force over its entire length. In the FEM, that uniform force per unit length is replaced typically by a set of equally spaced, statically equivalent, concentrated forces. The magnitude of each concentrated force is simply the magnitude of the force per unit length multiplied by the length between the equally spaced concentrated forces. Both the style and the accuracy of this distributed force approximation, which allows only concentrated forces and moments as the loads acting upon the flexible beam, is examined briefly in Endnote (2). Be sure to examine Endnote (2). Exercise 17.2(b) examines the similar question of replacing a triangularly shaped force per unit length between two points with concentrated forces at those two points. Exercise 17.7 considers an alternate approach to converting the distributed load to discrete forces and moments.

In order to understand how the above limitation on allowable types of loads permits a finite number of generalized coordinates to completely describe the deflected position of a flexible body, consider the bending of a uniform beam segment of length l that lies between two points where, concentrated loads are applied to an overall beam of length L , see Fig. 17.3(a). For the sake of simplicity, let the single plane in which the beam segment bends be the plane of the principal cross-sectional coordinate z , and x . Let the lateral deflections at the segment ends be

$$w(0) = w_1 \quad w(l) = w_2 \quad w'(0) = \theta_1 \quad w'(l) = \theta_2 \quad (17.1)$$

Figure 17.3(b) illustrates positive values of these four deflections. Note that the bending slope rotations are positive counterclockwise. Figure 17.3(c) shows the same information in the usual FEM fashion. The four integers in the latter diagram refer to the selected ordering of the deflections when these deflections are arranged in a matrix vector. As is seen later, that same ordering is used for the shear forces and bending moments corresponding to these lateral deflections and bending slopes. Thus Fig. 17.3(c) serves a dual purpose.

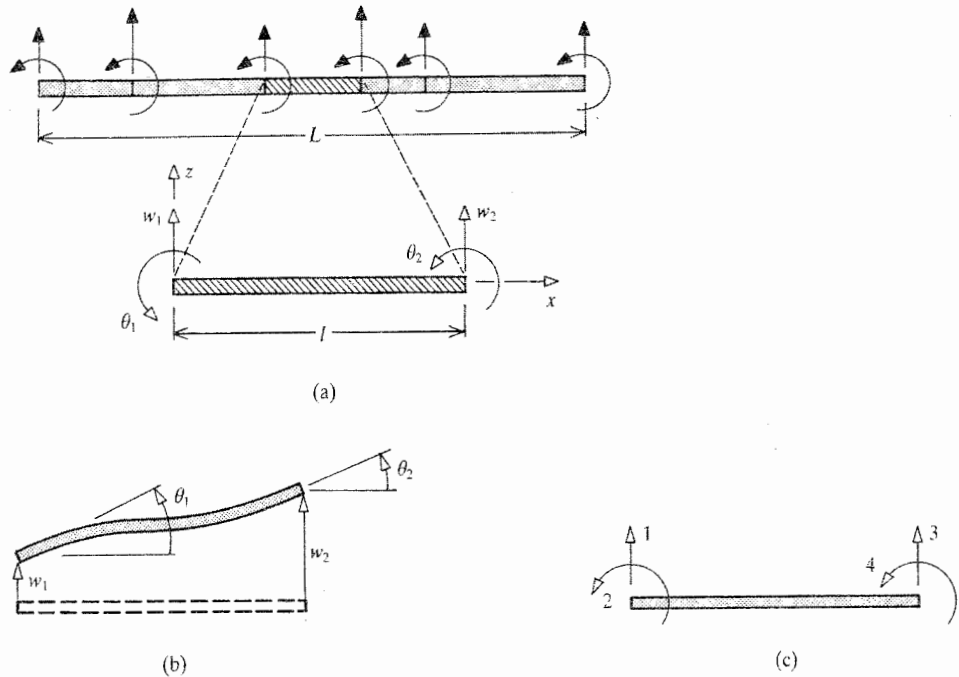


Figure 17.3. The beam bending finite element. (a) The overall beam where the loading is represented solely by concentrated forces and moments, and an excerpted element of that beam showing the controlling end deflections of that element. (b) A diagram clarifying the meaning of the beam element generalized coordinates. (c) The standard representation of the positive sign convention for the four beam bending generalized coordinates and their associated shearing forces and bending moments.

The short development below proves that, with the above load limitation provision, the four end point deflections are the generalized coordinates for this beam segment. Consider the beam segment fourth order beam bending governing differential equation which, because of the lack of an axial force and the lack of a distributed loading, reduces to

$$EIw''''(x) = 0 \quad (17.2)$$

The solution to Eq. (17.2) is

$$w(x) = C_1x^3 + C_2x^2 + C_3x + C_4 \quad (17.3a)$$

The deflection boundary conditions (BCs) for this solution are Eqs. (17.1). Substitution of the beam bending deflection solution into those BC equations, after some algebraic manipulation, yields the solution

$$w(x) = [2(w_1 - w_2) + (\theta_1 + \theta_2)l] \left(\frac{x}{l}\right)^3 - [3(w_1 - w_2) + (2\theta_1 + \theta_2)l] \left(\frac{x}{l}\right)^2 + [\theta_1 l](x/l) + w_1 \quad (17.3b)$$

Since the deflection at any point along the x axis is entirely determined by the beam segment end deflections, the contention that those end deflections are the generalized coordinates for the beam bending in one plane is now proved. Similarly, when there is no loading between the ends of the beam segment in the other principal plane, the bending of the

beam segment in that other principal plane is completely determined by the end deflections and end rotations in that plane. As will be seen shortly, the twist of a beam segment and the extension of a beam segment, if there are no interior loads, are similarly and respectively determined by the twists and axial deflections at the beam segment ends. Thus it can be expected that in general a small number of deflections at the boundaries of a structural segment can be used as the generalized coordinates for the deflections everywhere throughout the structural segment whenever suitable restrictions are placed on the applied loading.

17.3 The Beam Bending Finite Element

The derivation of the matrix equation that describes the bending of a beam segment in finite element form begins with a reorganization of Eq. (17.3b). If Eq. (17.3b) is organized on the basis of the generalized coordinates rather than on the basis of the powers of the axial coordinate x , and if (x/l) is symbolized as ξ , then Eq. (17.3b) becomes

$$w(\xi) = (2\xi^3 - 3\xi^2 + 1)w_1 + l(\xi^3 - 2\xi^2 + \xi)\theta_1 \\ + (-2\xi^3 + 3\xi^2)w_2 + l(\xi^3 - \xi^2)\theta_2 \quad (17.4a)$$

or

$$w(\xi) = N_1(\xi)w_1 + N_2(\xi)\theta_1 + N_3(\xi)w_2 + N_4(\xi)\theta_2 \quad (17.4b)$$

or

$$w(\xi) = \sum N_i(\xi)q_i = [N(\xi)]\{q\} \quad (17.4c)$$

where q_i is the symbol for the i th generalized coordinate; for example, $q_4 = \theta_2$. The functions N_i are called "shape functions." The shape functions have a fundamental role in the development of any deflection-based finite element. To aid in examining the four shape functions, note that

$$\text{Beam slope} = w'(x) = \frac{dw}{dx} = \frac{dw}{d\xi} \frac{d\xi}{dx}$$

Since $d\xi/dx = (d/dx)(x/l) = 1/l$, then the bending slope is

$$w'(x) = (6\xi^2 - 6\xi)\frac{w_1}{l} + (3\xi^2 - 4\xi + 1)\theta_1 \\ + (-6\xi^2 + 6\xi)\frac{w_2}{l} + (3\xi^2 - 2\xi)\theta_2 \quad (17.4d)$$

Examining Eqs. (17.4a) and (17.4d) it is clear that when $x = \xi = 0$, then $w(0) = w_1$ and $w'(0) = +\theta_1$, and when $x = l$ or $\xi = 1$ then $w(x = l) = w_2$ and $w'(x = l) = +\theta_2$. Figure 17.4 shows a plot of each of the four shape functions. These four plots show the above characteristics for the deflections and bending slopes at the beam segment ends. Moreover, the four plots illustrate the fact deducible from Eqs. (17.4a) that each shape function describes the shape of the beam segment if its corresponding generalized coordinate has the value +1 while the other three generalized coordinates have the value zero.

Once the relation between the relevant deflection and the generalized coordinates via the shape functions is established, as it is in this case in the form of Eq. (17.4c), the derivation

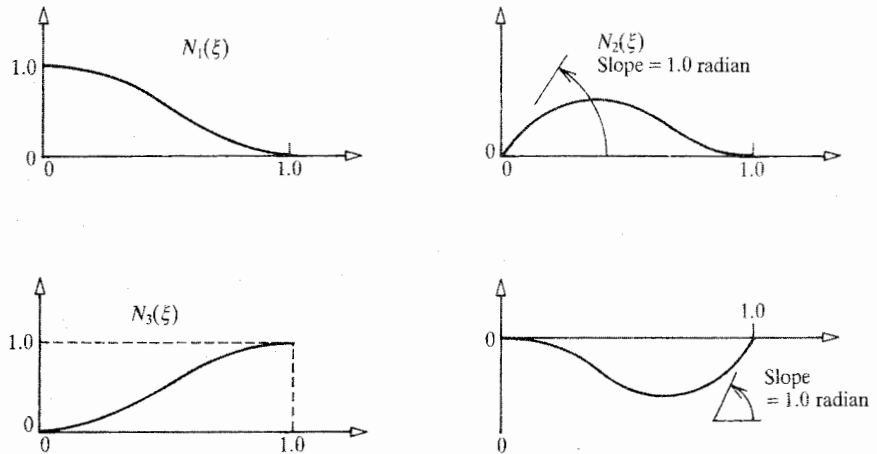


Figure 17.4. Plots of the four bending shape functions for a beam finite element. (Note that similar symbols are used for all shape functions and the wholly unrelated axial forces.)

of the finite element matrix equation for the structural segment is most often just a matter of applying the Principle of Virtual Work (PVW). From Chapter 15, the PVW can be restated in general as

$$\delta W_{ex} = \delta U = \iiint_{\text{Vol.}} \{\sigma\} \{\delta\gamma\} d(\text{Vol.}) \quad (17.5)$$

When applied to the beam segment, the left-hand side, the virtual work of the loads external to the beam segment, is simply the product of (i) the shear force and bending moment stress resultants at the beam segment ends and (ii) the corresponding virtual displacements at the beam segment ends. To be wholly clear on exactly which concentrated moments and shears are being referred to, examine Figs. 17.5(a, b). Figure 17.5(a) shows the FEM sign convention for these stress resultants, which, while being internal to the overall beam, are external to the beam segment under discussion. Again, this sign convention selection mimics the sign convention for the generalized coordinates. On the other hand, the concentrated loads acting upon the beam that were used to define the length of the beam segment are external to the overall structural system. These concentrated loads are viewed as acting at points, called “nodes,” located between the beam segments. See Fig. 17.5(b), which focuses upon the k th node, which lies between the i th and the j th beam segment. In that figure the external applied force and applied moment are temporarily called F_k and M_k respectively, and no sign convention for these external loads is implied by the figure. With this arrangement it should be clear that all the internal stress resultants acting at a node, that is, the bending moments and shearing forces at the ends of each beam segment adjacent to the node, sum to the external loads acting at the node. These equilibrium relationships between the internal stress resultants and the externally applied loads are established later by application of the PVW. In the meantime, for any beam bending segment,

$$\begin{aligned} \delta W_{ex} &= V_1 \delta w_1 + M_1 \delta \theta_1 + V_2 \delta w_2 + M_2 \delta \theta_2 \\ &= \{\delta q\} \{Q\} \end{aligned} \quad (17.6)$$

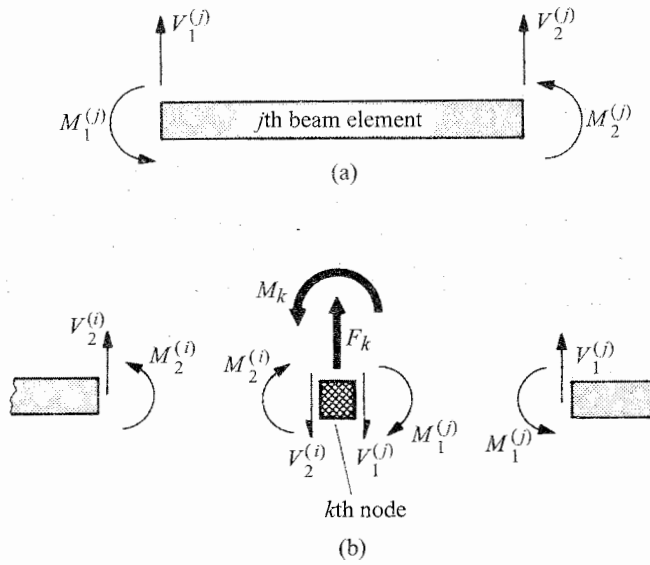


Figure 17.5. (a) The internal shearing forces and moments that act at the ends of the j th beam finite element. (b) A FBD illustrating how the internal stress resultants at the beam finite ends relate to the applied loads at the selected nodes of the structure. Note that there is no sign convention for the externally applied loads M_k and F_k . The virtual work done by the two applied loads is positive or negative according to the selected positive directions of the nodal/structural/system/global degrees of freedom.

where the generalized force vector is

$$[Q] = [V_1 \quad M_1 \quad V_2 \quad M_2]$$

As for the right-hand side of the virtual work statement of Eq. (17.5), recall that the only strain permitted in a (bent) Bernoulli–Euler beam is ϵ_{xx} . Hence the only nonzero stress that needs to be considered is σ_{xx} , which is related to ϵ_{xx} by Eq. (9.4). Hence Eq. (17.5) reduces to

$$[\delta q]\{Q\} = \iiint_{\text{Vol.}} E(\epsilon_{xx} - \alpha \Delta T) \delta \epsilon_{xx} d(\text{Vol.}) \tag{17.7a}$$

Adapting Eq. (9.3), which describes the axial normal strain ϵ_{xx} in terms of the derivatives of the deflections, to the present circumstance where $w(x)$ is the only beam deflection being considered (the other deflections, $v(x)$ and $u(x)$ are considered separately later), leads to

$$\epsilon_{xx}(x, y, z) = -zw''(x) \quad \text{and} \quad \delta \epsilon_{xx} = -z \delta w''(x)$$

Substituting these strain and virtual strain expressions into Eq. (17.7a) yields

$$[\delta q]\{Q\} = \iiint_{\text{Vol.}} E[z w''(x) + \alpha \Delta T][z \delta w''(x)] d(\text{Vol.})$$

Again the above integral over the volume of the beam can be written as the combination of an integral over the beam length and an integral over the cross-sectional area. Doing that,

and factoring out those quantities from the interior area integrals that are not functions of the centroidal coordinates, leads to

$$\begin{aligned} [\delta q]\{Q\} &= \int_l \left(\iint_A E z^2 dA \right) w''(x) \delta w''(x) dx \\ &\quad + \int_l \left(\iint_A z E \alpha \Delta T dA \right) \delta w''(x) dx \end{aligned}$$

Permitting Young's modulus to vary over the cross-section again calls for the introduction of a reference value of Young's modulus, E_0 . Multiplying and dividing the first of the above integrals by the constant E_0 makes the first quantity in brackets $E_0 I_{yy}^*$. The second quantity in brackets is recognized from Eq. (9.7b) as $-M_{yT}(x)$. Thus the above equation becomes

$$[\delta q]\{Q\} = E_0 I_{yy}^* \int_l w''(x) \delta w''(x) dx - \int_l M_{yT}(x) \delta w''(x) dx \quad (17.7b)$$

In this introductory exposition, the second integral is now simplified by choosing an average value of $M_{yT}(x)$ over the length of the beam segment, which is here called M_T . See Exercise 17.9 for a comment on this step. The next step is to introduce Eq. (17.4b) into the above integrals. Note

$$\begin{aligned} w''(x) &= \frac{1}{l^2} w''(\xi) = \frac{1}{l^2} [N_1''(\xi) w_1 + N_2''(\xi) \theta_1 + N_3''(\xi) w_2 + N_4''(\xi) \theta_2] \\ &= \frac{1}{l^2} [N''(\xi)] \{q\} \\ \delta w''(x) &= \frac{1}{l^2} \delta w''(\xi) = \frac{1}{l^2} [N_1''(\xi) \delta w_1 + N_2''(\xi) \delta \theta_1 + N_3''(\xi) \delta w_2 + N_4''(\xi) \delta \theta_2] \\ &= \frac{1}{l^2} [\delta q] \{N''(\xi)\} \end{aligned}$$

where

$$N_1'' = 12\xi - 6 \quad N_2'' = l(6\xi - 4) \quad N_3'' = -12\xi + 6 \quad N_4'' = l(6\xi - 2)$$

Substituting the latter parts of the above equalities for $w''(x)$ and $\delta w''(x)$ into the above virtual work equality, and recognizing that the row and column vectors of the generalized coordinates and their variations are not functions of x , or any other spatial coordinate, yields

$$\begin{aligned} [\delta q]\{Q\} &= E_0 I_{yy}^* \int_l \delta w''(x) w''(x) dx - M_T \int_l \delta w''(x) dx \\ [\delta q]\{Q\} &= \frac{E_0 I_{yy}^*}{l^4} [\delta q] \int_l \{N''(\xi)\} [N''(\xi)] dx \{q\} \\ &\quad - \frac{M_T}{l^2} [\delta q] \int_l \{N''(\xi)\} dx \end{aligned}$$

or

$$\begin{aligned} [\delta q]\{Q\} &= \frac{E_0 I_{yy}^*}{l^3} [\delta q] \int_0^1 \{N''(\xi)\} [N''(\xi)] d\xi \{q\} \\ &\quad - \frac{M_T}{l} [\delta q] \int_0^1 \{N''(\xi)\} d\xi \end{aligned}$$

Consider the first integral in the above equality. The product of the 4×1 column matrix and the 1×4 row matrix is a 4×4 square matrix. That square matrix is

$$\begin{bmatrix} 36(4\xi^2 - 4\xi + 1) & 12(6\xi^2 - 7\xi + 2)l & -36(4\xi^2 - 4\xi + 1) & 12(6\xi^2 - 5\xi + 1)l \\ 12(6\xi^2 - 7\xi + 2)l & 4(9\xi^2 - 12\xi + 4)l^2 & -12(6\xi^2 - 7\xi + 2)l & 4(9\xi^2 - 9\xi + 2)l^2 \\ -36(4\xi^2 - 4\xi + 1)l & -12(6\xi^2 - 7\xi + 2)l & 36(4\xi^2 - 4\xi + 1) & -12(6\xi^2 - 5\xi + 1)l \\ 12(6\xi^2 - 5\xi + 1)l & 4(9\xi^2 - 9\xi + 2)l^2 & -12(6\xi^2 - 5\xi + 1)l & 4(9\xi^2 - 9\xi + 1)l^2 \end{bmatrix}$$

Recall that the integral of a matrix is the matrix of the integrals of the elements of the matrix. Carrying out both integrations in the above equality leads to

$$[\delta q]\{Q\} = [\delta q][k^*]\{q\} - M_T[\delta q]\{\Lambda\} \quad (17.8)$$

where

$$[k^*] \equiv \frac{E_0 I_{yy}^*}{l^3} \begin{bmatrix} 12 & 6l & -12 & 6l \\ 6l & 4l^2 & -6l & 2l^2 \\ -12 & -6l & 12 & -6l \\ 6l & 2l^2 & -6l & 4l^2 \end{bmatrix} \quad \{\Lambda\} \equiv \begin{Bmatrix} 0 \\ -1 \\ 0 \\ +1 \end{Bmatrix}$$

The arbitrary matrix of virtual deflections, $[\delta q]$ can be eliminated from Eq. (17.8) by the following logic. Rewrite that equality as

$$[\delta q] (\{Q\} - [k^*]\{q\} + M_T\{\Lambda\}) = 0$$

The left-hand side of the above equality is the zero product of a 1×4 row matrix and a 4×1 column matrix. That product produces the zero sum of four terms regardless of the arbitrary values of the virtual deflections. In other words, changing the value of one of the virtual deflections does not alter the value of the sum, which is zero. The only way that result is possible is for the coefficient of the changed virtual deflection to be zero. Thus, all four of the coefficients of the virtual deflections are zero. Thus

$$\{Q\} - [k^*]\{q\} + M_T\{\Lambda\} = \{0\}$$

or

$$\{Q\} + M_T\{\Lambda\} = [k^*]\{q\}$$

letting $M_T\{\Lambda\} \equiv \{Q_T\}$, and $\{Q\} + \{Q_T\} \equiv \{Q^c\}$, then the final beam segment bending equation for one plane only is obtained as

$$\boxed{\{Q^c\} = [k^*]\{q\}} \quad (17.9)$$

Equation (17.9) is the culmination of using: (i) the generalized coordinates and the individual associated deflection patterns that are embodied in the shape functions; (ii) Bernoulli–Euler small-deflection beam theory to relate the strain ϵ_{xx} to the curvature w'' , and hence to the deflections; and (iii) the PVW to enforce equilibrium. As such, the deflection boundary conditions at the beam segment ends are incorporated into this algebraic relation. The beam segment is described by an algebraic equation because the engineering beam theory derivative relations were integrated in the PVW.

At this point, to comply with universal usage, the beam segment is henceforth referred to as a beam finite element. It is called a finite element to distinguish it from a differential element. The square matrix $[k^*]$ is called the (single plane) beam (bending) stiffness matrix for a nonhomogeneous beam element. The element stiffness matrix gets its name from the stiffness factor of the spring force–deflection relation $F = ku$, which parallels

Eq. (17.9) because $\{Q^e\}$ is the vector of equivalent generalized forces, and $\{q\}$ is the vector of generalized deflections in the x, z plane.

Of course, the finite element description for beam bending in the x, y plane has exactly the same form as Eq. (17.9), where the shearing forces, moments, moment of inertia, and deflections of the x, z plane are replaced by the corresponding quantities of the x, y plane. Since the beam element may have a rather short length, the above stiffness matrix slightly overestimates the element stiffness because the shearing flexibility (flexibility is the reverse of stiffness) of the element becomes significant relative to the bending flexibility as the beam length becomes short. Specifically, when γGA is close in value to EI/l^2 , then the shearing flexibility is approximately 10 percent of the bending flexibility, and the effects of shearing deformation should be included in the stiffness matrix along with the above effects of bending deformation. This matter is treated in an exercise for the eager.

There is a feature of these 4×4 beam element bending stiffness matrices that may be surprising. The element stiffness matrix is singular to the second degree. Examining the details of the matrix in Eq. (17.8), it is easily seen that the first and third rows are the negatives of each other, which makes the determinant of the stiffness matrix zero. Further note that, following the usual procedures of manipulating determinants without changing their value, multiplication of the first row by -1 , and adding that result to the second row makes the second row the negative of the fourth row. This double singularity is explained by the fact that in the plane, the beam element by itself has two rigid body degrees of freedom. In other words, for the beam element by itself, for example, w_1 and θ_1 can be given arbitrary values, and when $w_2 = w_1 + l\theta_1$ and $\theta_2 = \theta_1$, then there are no internal strains, and therefore no internal work. Thus it is impossible to invert the beam element bending stiffness matrix and solve for specific deflections. This singularity characteristic is or should be present in all element stiffness matrices.

17.4 The Bar and Spring Element Stiffness Matrix Equations

The development of the beam element bending stiffness matrix equation of the previous section was somewhat lengthy. All the features of that derivation can be reviewed in the following much simpler derivation of the bar matrix stiffness equation. To achieve the greatest possible simplicity in the development of the bar element matrix equation, the effect of a temperature change is omitted. The effect of a temperature change is considered in an exercise and discussed in some detail in the next chapter.

Consider the bar element shown in Fig. 17.6(a). Once again, since the generalized coordinates that control the axial deflections of the element, and the axial force stress resultants, are chosen to have the same sign convention, there is no need to label the diagram arrows

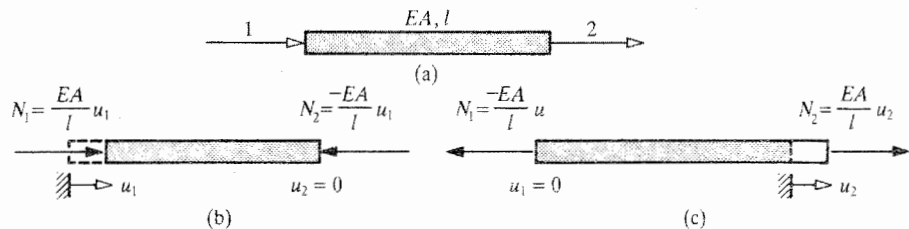


Figure 17.6. The bar finite element. (a) The deflection and axial force sign convention. (b) The equilibrated forces necessitated by the deflection u_1 . (c) The equilibrated forces necessitated by the deflection u_2 .

beyond numbering the order of the degrees of freedom or generalized forces in their respective vectors. Solution of the beam axial deflection equation $E_0A^*u''(x) = 0$, with $\xi = x/l$, and BCs $u(0) = u_1$, and $u(\xi = 1) = u_2$, leads to

$$u(x) = (1 - \xi)u_1 + \xi u_2$$

or

$$u(x) = \begin{bmatrix} (1 - \xi) & \xi \end{bmatrix} \begin{Bmatrix} u_1 \\ u_2 \end{Bmatrix} = [N(\xi)]\{q\} \quad (17.10)$$

where it is necessary to distinguish carefully between the $N(\xi)$ of the shape functions and the N of the axial force stress resultants, which like the shape functions always bear subscripts when written individually. After the above preparation, the derivation of the bar finite element equation is completed by applying the PVW, which is

$$\delta W_{ex} = \iiint_{\text{Vol.}} [\sigma]\{\delta\gamma\} d(\text{Vol.}) \quad (17.5)$$

The left-hand side of the PVW is again written in terms of the axial force stress resultants because they are the two forces external to the bar element. The left-hand side is then

$$\delta W_{ex} = [\delta u_1 \quad \delta u_2] \begin{Bmatrix} N_1 \\ N_2 \end{Bmatrix} = [\delta q]\{N\} \quad (17.11)$$

Once again, since the longitudinal strain is the only Bernoulli–Euler strain, the vectors in the right-hand side of the PVW reduce to the scalar product $\sigma_{xx} \delta\epsilon_{xx}$. This strain is obtained from the deflection $u(x) = [N(\xi)]\{q\}$ by differentiating with respect to x . The result is

$$\begin{aligned} \epsilon_{xx} &= \left[-\frac{1}{l} \quad +\frac{1}{l} \right] \{q\} \quad \text{and} \quad \delta\epsilon_{xx} = \left[-\frac{1}{l} \quad +\frac{1}{l} \right] \{\delta q\} \\ &= [\delta q] \begin{Bmatrix} -1/l \\ +1/l \end{Bmatrix} \end{aligned}$$

Then, with $\sigma_{xx} = E\epsilon_{xx}$, the PVW becomes

$$\delta W_{ex} = \int_0^l \iint_A \sigma_{xx} \delta\epsilon_{xx} dA dx = \int_0^l \iint_A \delta\epsilon_{xx} E\epsilon_{xx} dA dx$$

Substituting,

$$[\delta q]\{N\} = [\delta q] \int_0^l E_0A^* \begin{Bmatrix} -1/l \\ +1/l \end{Bmatrix} \begin{bmatrix} -1/l & +1/l \end{bmatrix} dx \{q\}$$

After carrying out the matrix product and the integration, the result is

$$[\delta q]\{N\} = [\delta q][k^*]\{q\}$$

which leads to

$$\boxed{\{N\} = [k^*]\{q\}}$$

which in expanded form is

$$\begin{Bmatrix} N_1 \\ N_2 \end{Bmatrix} = \frac{E_0A^*}{l} \begin{bmatrix} +1 & -1 \\ -1 & +1 \end{bmatrix} \begin{Bmatrix} u_1 \\ u_2 \end{Bmatrix} \quad (17.12)$$

Equation (17.12) is of course the desired nonhomogeneous, uniform bar, matrix stiffness equation. The simplicity of this equation prompts an investigation into whether this matrix equation could have been obtained even more simply than by means of the above derivation. Consider a new derivation of Eq. (17.12) merely upon the basis of matrix algebra and the familiar general uniform bar deflection–force relation, which is $u = Nl/EA$. Referring to Fig. 17.6(b), consider fixing the u_2 degree of freedom at a zero value, while requiring that u_1 take on an arbitrary positive value. The result would be the compression (without buckling) of the uniform bar. The axial forces required to accomplish this situation would be $N_1 = +(E_0A^*/l)u_1$ and $N_2 = -(E_0A^*/l)u_1$. If this result is arranged in matrix form, then

$$\begin{Bmatrix} N_1 \\ N_2 \end{Bmatrix} = \frac{E_0A^*}{l} \begin{bmatrix} +1 & \\ & -1 \end{bmatrix} \begin{Bmatrix} u_1 \\ u_2 \end{Bmatrix}$$

If u_1 is held at a zero value while u_2 is given an arbitrary positive value, as shown in Fig. 17.6(c), the second column of the above matrix equation can be filled in to rederive the element stiffness matrix of Eq. (17.12).

The usefulness of the above matrix algebra approach is evident when the matrix stiffness equation for an elastic spring element is sought. When an actual coiled spring is extended along its axis, the curved beams of the coiled spring both bend and twist, making its analysis slightly lengthy. However, using the above approach in exactly the same way that is used for the bar, the result for the elastic spring matrix stiffness equation is

$$\begin{Bmatrix} N_1 \\ N_2 \end{Bmatrix} = k \begin{bmatrix} +1 & -1 \\ -1 & +1 \end{bmatrix} \begin{Bmatrix} u_1 \\ u_2 \end{Bmatrix} \quad (17.13)$$

where, of course, k is the spring stiffness factor.

This approach of determining, in turn, the end forces (and moments where applicable) that result from a single element end displacement can be extended to other one-dimensional finite elements. For example, Example 21.12 and Exercise 21.16 indicate how the beam bending finite element stiffness matrix of Eq. (17.9) can be so derived using a force/flexibility method. However, this approach is *not* useful for developing the element stiffness matrices of two-dimensional finite elements, such as a plate bending finite element.

17.5 Assembling the System Matrix Equation

At this point the development of matrix element stiffness equations for different finite elements is interrupted so that the utility of those matrix equations that have already been developed can be demonstrated. Before the individual finite element matrix equations can be useful, it is necessary to understand how the stiffness matrices for individual finite elements can be “assembled” so as to describe the structural system created by the joining together of the individual structural elements.

To this end, consider creating a FEM model of the structure shown in Fig. 17.7(a). In order to convert that ordinary mathematical model into a finite element analysis model it is only necessary to choose node points that define the end points of each beam element and the spring element. Remember that the beam finite elements developed so far require that the element area and area moments of inertia be uniform throughout the length of the element, and that there be no loading between the nodes. The first of these two requirements leads to the selection of the five node points shown in Fig. 17.7(b), where the node points are indicated by little square boxes and circles that enclose the number assigned to the node. The second requirement results in the replacement of the distributed force over the

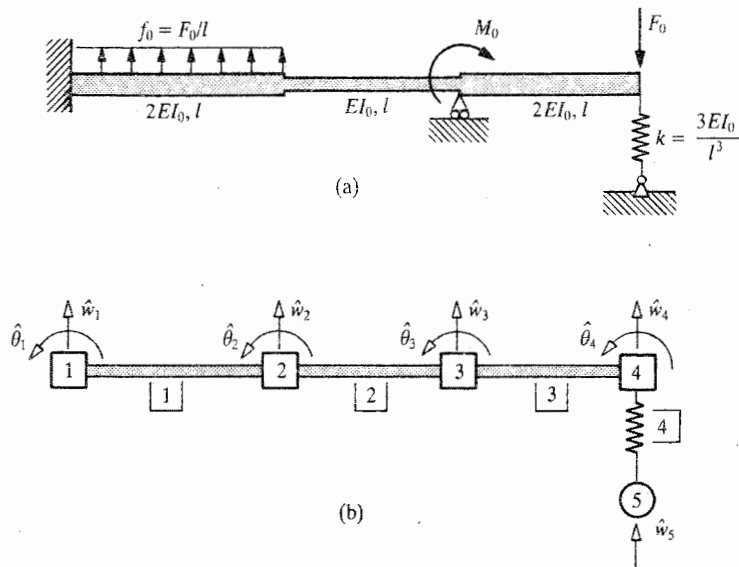


Figure 17.7. The formulation of a finite element model from the mathematical model of the structure. (a) A typical analysis model. (b) The corresponding finite element model with numbered nodes and numbered structural elements.

left-hand beam segment by statically equivalent concentrated forces at each end of that beam segment. In this case the left-hand one of those two concentrated forces is simply absorbed by the rigid support. While this crude treatment of the distributed loading, f_0 , would not be good modeling technique for a structure the analyst really cared about, it is suitable for these example problems.

A second step in the preparation of the finite element model for a structural system is the selection of a set of generalized coordinates *for the structure as a whole*. These “global generalized coordinates” or “global degrees of freedom,” which are always located at nodes, fully describe the structural system deflections in exactly the same fashion as the element coordinates describe the element deflections. There is no sign convention for the global coordinate system, but the use of a regular pattern in their selection is a great benefit when it comes to interpreting analysis results. The nine global coordinates selected for this four-element structural system are shown in Fig. 17.7(b). The global DOF are distinguished from the various element generalized coordinates by the addition of a circumflex ($\hat{\cdot}$) to the usual deflection symbol. The vector form of the global coordinates is therefore symbolized as $\{\hat{q}\}$.

The types of global generalized coordinates selected for the structural system necessarily reflect the types of DOF that are used to describe the deflections of the structure’s finite elements. Thus at each node located at a beam end there is a lateral deflection and a bending rotation. Note that node 5 is only connected to a spring end. Thus only an axial deflection coordinate is used there. Indeed, it would be incorrect to place a global rotation coordinate at node 5 because spring ends only translate in the direction of the spring axis and never offer resistance to a rotation. In other words, spring connections are always hinge connections. When all the structural elements at a node have a hinged connection at that node, then, rather than use the usual square to signify the node, a circle suggestive of a hinge is used instead.

The object of the present work is to use the local element stiffness matrices to assemble a system or global stiffness matrix. To this end consider the individual element stiffness matrices for the three beams and the one spring of Fig. 17.7(b). For the given values of l and EI_{yy} , the element stiffness matrix and associated element deflection vector for beam element 1 is

$$[k_1]\{q^{(1)}\} = \frac{2EI_0}{l^3} \begin{bmatrix} 12 & 6l & -12 & 6l \\ 6l & 4l^2 & -6l & 2l^2 \\ -12 & -6l & 12 & -6l \\ 6l & 2l^2 & -6l & 4l^2 \end{bmatrix} \begin{Bmatrix} w_1^{(1)} \\ \theta_1^{(1)} \\ w_2^{(1)} \\ \theta_2^{(1)} \end{Bmatrix}$$

The stiffness matrix and generalized deflection vector for beam 3 is the same as the above except that the subscript upon the stiffness matrix symbol is a 3 instead of a 1, and the superscripts upon the deflection terms are likewise altered. The stiffness matrix and deflection vector for beam 2 are similarly identified. Notice that in the case of beam 2, however, the multiplicative factor for the stiffness matrix is EI_0/l^3 rather than twice that quantity. The element stiffness matrix and element deflection vector for the spring in terms of the given data are

$$[k_4]\{q^{(4)}\} = \frac{3EI_0}{l^3} \begin{bmatrix} +1 & -1 \\ -1 & +1 \end{bmatrix} \begin{Bmatrix} u_1^{(4)} \\ u_2^{(4)} \end{Bmatrix}$$

Now that the standard forms for the element stiffness matrices have been adapted to the data for the elements of the given structure, it is necessary to combine the element stiffness matrices and deflection vectors in order to create the structural system stiffness matrix, with its associated global deflection vector. To this end, recall that the external and internal virtual work for the entire structure is merely the sum of the external and internal virtual work of all the components (i.e., elements) of the structure. That is,

$$\delta W_{ex} = \sum_i \delta W_{ex}^{(i)} \quad \text{and} \quad \delta W_{in} = \sum_i \delta W_{in}^{(i)}$$

Rather than actually use the first summation, which would be nothing more than writing the sort of equilibrium equations that are obtainable from the FBD of "node k " as illustrated in Fig. 17.5(b), it is *always* preferable to do for the global virtual deflections what was done for the element virtual deflections. That is, write

$$\delta W_{ex} = \sum \hat{Q}_i \delta \hat{q}_i = [\delta \hat{q}][\hat{Q}] \quad (17.14a)$$

where the virtual work that results from a positive value of each virtual deflection is considered in turn while all other virtual deflections are held to zero values. This process for obtaining the generalized forces $\{\hat{Q}\}$ is amply illustrated in this and subsequent examples.

The second summation, $\delta W_{in} = \sum \delta W_{in}^{(i)}$, is the key to assembling the system stiffness matrix from the element stiffness matrices. Consider the i th finite element of the total system. Setting aside temperature change considerations for the moment, its individual internal virtual work statement is known from Eq. (17.8) to have the form

$$\delta W_{in}^{(i)} = -[\delta q^{(i)}][k_i]\{q^{(i)}\} \quad (17.14b)$$

Now consider the relationship that exists between the local coordinates of the i th element and the global coordinates of the total structure. The second beam element is chosen to

illustrate this matter. Inspection of the global coordinate system definitions in Fig. 17.7(b) shows the following relations between the global and second element DOF:

$$\begin{aligned} w_1^{(2)} &= \hat{w}_2 & \text{and} & & \theta_1^{(2)} &= \hat{\theta}_2 \\ w_2^{(2)} &= \hat{w}_3 & \text{and} & & \theta_2^{(2)} &= \hat{\theta}_3 \end{aligned} \quad (17.15a)$$

These relations can be cast in matrix form as follows:

$$\begin{Bmatrix} w_1^{(2)} \\ \theta_1^{(2)} \\ w_2^{(2)} \\ \theta_2^{(2)} \end{Bmatrix} = \begin{bmatrix} 0 & 0 & \cdots & 1 & 0 & 0 & 0 & \cdots & 0 & 0 & 0 \\ 0 & 0 & \cdots & 0 & 1 & 0 & 0 & \cdots & 0 & 0 & 0 \\ 0 & 0 & \cdots & 0 & 0 & 1 & 0 & \cdots & 0 & 0 & 0 \\ 0 & 0 & \cdots & 0 & 0 & 0 & 1 & \cdots & 0 & 0 & 0 \end{bmatrix} \begin{Bmatrix} \hat{w}_1 \\ \hat{\theta}_1 \\ \hat{w}_2 \\ \hat{\theta}_2 \\ \hat{w}_3 \\ \hat{\theta}_3 \\ \hat{w}_4 \\ \hat{\theta}_4 \\ \hat{w}_5 \end{Bmatrix}$$

or, in the compact matrix form,

$$\{q^{(2)}\} = [T_2]\{\hat{q}\} \quad (17.15b)$$

Similar DOF transformation matrix equations can be written easily for each of the other two beam elements and the one spring element. Applying the variational operator to both sides of the above relation yields

$$\{\delta q^{(2)}\} = [T_2]\{\delta \hat{q}\}$$

where of course only the deflection terms receive a variation. Substituting these two DOF transformation equations into the internal virtual work expression for element 2, which is

$$\delta W_m^{(2)} = -[\delta q^{(2)}][k_2]\{q^{(2)}\}$$

yields

$$\begin{aligned} \delta W_m^{(2)} &= -[\delta \hat{q}][T_2]^t[k_2][T_2]\{\hat{q}\} \\ &= -[\delta \hat{q}][K_2]\{\hat{q}\} \end{aligned}$$

where of course,

$$[K_2] \equiv [T_2]^t[k_2][T_2]$$

Note that $[K_2]$ is a nine by nine square matrix, and as such, it is multiplicatively compatible with the nine by one global DOF vector $\{\hat{q}\}$. The matrix $[K_2] = [T_2]^t[k_2][T_2]$ is the contribution of the second beam element to the total stiffness matrix. This is so because what is true for the second structural element is true for all the structural elements that compose the structure, and in general,

$$\begin{aligned} \delta W_m &= \sum \delta W_m^{(i)} = - \sum [\delta q^{(i)}][k_i]\{q^{(i)}\} \\ &= - \sum [\delta \hat{q}][T_i]^t[k_i][T_i]\{\hat{q}\} \end{aligned}$$

Thus

$$\begin{aligned} \delta W_m &= -[\delta \hat{q}] \left(\sum [T_i]^t[k_i][T_i] \right) \{\hat{q}\} \\ &= -[\delta \hat{q}][\hat{K}]\{\hat{q}\} \end{aligned}$$

where of course

$$[\hat{K}] = \sum [T_i]^t [k_i] [T_i] = \sum [K_i] \quad (17.16)$$

The nine by nine matrix $[\hat{K}]$, which includes the stiffness contributions from all the structural elements, is called the assembled stiffness matrix.

A simpler way of amassing the structure's stiffness matrix from the element stiffness matrices is now explored in detail. Again using the second beam element to illustrate the process, consider matrix multiplication in submatrix form of the triple product

$$[T_2]^t [k_2] [T_2] = \begin{bmatrix} 0 \\ \dots \\ \mathbf{I} \\ \dots \\ 0 \end{bmatrix} [k_2] \begin{bmatrix} 0 & \vdots & \mathbf{I} & \vdots & 0 \end{bmatrix}$$

where, in $[T_2]^t$, the top zero submatrix is 2×4 , the identity submatrix is 4×4 , and the bottom zero submatrix is 3×4 . The multiplication of compatible submatrices is accomplished in exactly the same way that ordinary matrix elements are multiplied. That is, the above matrix triple product involving submatrices can be carried out as if it were the ordinary triple product of a 3×1 matrix multiplying a 1×1 matrix multiplying a 1×3 matrix. Of course, as in all matrix products, the matrix order must be maintained. Hence the result in submatrix form is

$$[K_2] = [T_2]^t [k_2] [T_2] = \begin{bmatrix} 0 & 0 & 0 \\ 0 & k_2 & 0 \\ 0 & 0 & 0 \end{bmatrix}$$

Expanding $[K_2]$ from submatrix form as below reveals that the DOF transformation matrix $[T_2]$ positions the 4×4 $[k_2]$ matrix in the structure's 9×9 stiffness matrix according to the correspondences of Eq. (17.15a) and, of course, in accordance with the order of the global DOF in the $\{\hat{q}\}$ vector. In expanded form,

$$[K_2] = \frac{EI_0}{l^3} \begin{bmatrix} 0 & 0 & 0 & 0 & 0 & 0 & 0 & 0 & 0 \\ 0 & 0 & 0 & 0 & 0 & 0 & 0 & 0 & 0 \\ 0 & 0 & 12 & 6l & -12 & 6l & 0 & 0 & 0 \\ 0 & 0 & 6l & 4l^2 & -6l & 2l^2 & 0 & 0 & 0 \\ 0 & 0 & -12 & -6l & 12 & -6l & 0 & 0 & 0 \\ 0 & 0 & 6l & 2l^2 & -6l & 4l^2 & 0 & 0 & 0 \\ 0 & 0 & 0 & 0 & 0 & 0 & 0 & 0 & 0 \\ 0 & 0 & 0 & 0 & 0 & 0 & 0 & 0 & 0 \\ 0 & 0 & 0 & 0 & 0 & 0 & 0 & 0 & 0 \end{bmatrix}$$

In other words, the DOF transformation matrices do nothing more than position the 4×4 beam element stiffness matrix in the 9×9 stiffness matrix according to the rows and columns of the global DOF at the nodes of the beam element.

Similarly, the use of the DOF transformation matrix $[T_1]$ for the first beam element positions the terms of that element stiffness matrix, $[k_1]$, in the first four rows and columns

of $[K_1]$. That is, the expanded element stiffness matrix for the first beam element (i.e., the element stiffness matrix for the first beam element in relation to the global DOF) is, where the factor 2 has been placed inside the matrix,

$$[K_1] = \frac{EI_0}{l^3} \begin{bmatrix} 24 & 12l & -24 & 12l & 0 & 0 & 0 & 0 & 0 \\ 12l & 8l^2 & -12l & 4l^2 & 0 & 0 & 0 & 0 & 0 \\ -24 & -12l & 24 & -12l & 0 & 0 & 0 & 0 & 0 \\ 12l & 4l^2 & -12l & 8l^2 & 0 & 0 & 0 & 0 & 0 \\ 0 & 0 & 0 & 0 & 0 & 0 & 0 & 0 & 0 \\ 0 & 0 & 0 & 0 & 0 & 0 & 0 & 0 & 0 \\ 0 & 0 & 0 & 0 & 0 & 0 & 0 & 0 & 0 \\ 0 & 0 & 0 & 0 & 0 & 0 & 0 & 0 & 0 \\ 0 & 0 & 0 & 0 & 0 & 0 & 0 & 0 & 0 \end{bmatrix}$$

Similarly, the nonzero terms of expanded element matrix $[K_3]$ are the 16 terms that occupy its fifth, sixth, seventh, and eighth rows and columns. Those rows and columns correspond to the global coordinates at the nodes of the third beam element. Finally, the spring element stiffness matrix, $[K_4]$, in terms of the global DOF, is

$$[K_4] = \frac{EI_0}{l^3} \begin{bmatrix} 0 & 0 & 0 & 0 & 0 & 0 & 0 & 0 & 0 \\ 0 & 0 & 0 & 0 & 0 & 0 & 0 & 0 & 0 \\ 0 & 0 & 0 & 0 & 0 & 0 & 0 & 0 & 0 \\ 0 & 0 & 0 & 0 & 0 & 0 & 0 & 0 & 0 \\ 0 & 0 & 0 & 0 & 0 & 0 & 0 & 0 & 0 \\ 0 & 0 & 0 & 0 & 0 & 0 & 0 & 0 & 0 \\ 0 & 0 & 0 & 0 & 0 & 0 & 3 & 0 & -3 \\ 0 & 0 & 0 & 0 & 0 & 0 & 0 & 0 & 0 \\ 0 & 0 & 0 & 0 & 0 & 0 & -3 & 0 & 3 \end{bmatrix}$$

where the terms of the 2×2 spring stiffness matrix are again positioned in the rows and columns corresponding to the global coordinates at the spring element nodes. The final step to obtaining the structure's stiffness matrix is, in accordance with Eq. (17.16), to add all the expanded element stiffness matrices. The result is

$$[\hat{K}] = \frac{EI_0}{l^3} \begin{bmatrix} 24 & 12l & -24 & 12l & \cdots & 0 & 0 & 0 & 0 & 0 \\ 12l & 8l^2 & -12l & 4l^2 & \cdots & 0 & 0 & 0 & 0 & 0 \\ -24 & -12l & \boxed{36} & \boxed{-6l} & \cdots & \boxed{-12} & \boxed{6l} & \cdots & 0 & 0 & 0 \\ 12l & 4l^2 & \boxed{-6l} & \boxed{12l^2} & \cdots & \boxed{-6l} & \boxed{2l^2} & \cdots & 0 & 0 & 0 \\ \cdots & \cdots \\ 0 & 0 & \boxed{-12} & \boxed{6l} & \cdots & \boxed{36} & \boxed{6l} & \cdots & \boxed{-24} & \boxed{12l} & 0 \\ 0 & 0 & \boxed{6l} & \boxed{2l^2} & \cdots & \boxed{6l} & \boxed{12l^2} & \cdots & \boxed{-12l} & \boxed{4l^2} & 0 \\ \cdots & \cdots \\ 0 & 0 & 0 & 0 & \cdots & \boxed{-24} & \boxed{-12l} & \cdots & \boxed{27} & \boxed{-12l} & \boxed{-3} \\ 0 & 0 & 0 & 0 & \cdots & \boxed{12l} & \boxed{4l^2} & \cdots & \boxed{-12l} & \boxed{8l^2} & 0 \\ \cdots & \cdots \\ 0 & 0 & 0 & 0 & \cdots & 0 & 0 & \cdots & \boxed{-3} & 0 & \boxed{3} \end{bmatrix}$$

The chief conclusion of this section is that since the effect of the DOF transformation matrices can easily be predicted for each element in every circumstance, there is no need to use such transformation matrices. Assembling the structure stiffness matrix is seen to be merely a matter of positioning the individual element stiffness matrix terms of each structural component within the larger confines of the stiffness matrix for the entire structural system. The positioning of the element stiffness terms proceeds according

to the rows and columns associated with the global coordinates that match the element DOF of each individual structural element. This structure consisting of three beams and one spring illustrates the assembling process for obtaining the assembled stiffness matrix in a particularly straightforward manner. Here the beam element stiffness matrices are positioned in order down the main diagonal of the system stiffness matrix in the overlapping fashion indicated. In this example, only the spring element demonstrates the common necessity of separately entering the individual terms of an element stiffness matrix in their proper position. More extended examples of assembling structure stiffness matrices follow.

The assembled stiffness matrix $[\hat{K}]$ has several characteristics worth noting. First of all, the assembled stiffness matrix, like all element stiffness matrices, must be symmetric. See Appendix A, Section 2. Another characteristic is that the more elements that connect at a node, the more individual stiffness terms there are that need to be added together.¹ This agrees with the physical observation that the more structural elements connected together at a particular location, the more stiff the structure is at that location (i.e., the more difficult it is to cause a deflection there). A common assembled stiffness matrix characteristic which is illustrated in this case is that the upper right and lower left corners of the assembled stiffness matrix are populated only by zeros. If there were a fourth, fifth, sixth, etc., beam connected in the same serial manner as the first three beams, then the element stiffness matrices for those additional beams would follow the same pattern of having successive, overlapping positions on the extended main diagonal of the assembled stiffness matrix. Then the “banding” of the assembled stiffness matrix nonzero terms along the main diagonal of the matrix, and the population of zeros in the upper right and lower left corners would be much more prominent. It would also be the case that the total number of zero entries would soon well exceed the number of nonzero entries. Thus the assembled matrix for a long string of serially connected beams, as is the case for most large structures, would be called “sparse.” If the long series of beams looped around to form a closed loop, then the stiffness matrix would still be sparse. However, since the first and last beams are connected together, there would be nonzero entries in the upper right and lower left corners of the assembled stiffness matrix because the DOF of the first and last rows and columns would be common to both of those connected end beams.

Another characteristic of the assembled stiffness matrix is less obvious. Be aware that the effect of the supports of the three beam and one spring structure have not been as yet introduced into the structure stiffness matrix. Therefore, just like the element stiffness matrices, the structure’s assembled stiffness matrix is singular to the degree of the number of rigid body motions that are possible for the structure. A simple rigid body motion for this unsupported structure is an up or down translation where all the w ’s have the same value and all the θ ’s are zero. This leads immediately to the observation that the determinant of the assembled stiffness matrix has an all-zero column if, following the rules of determinants, the first, third, fifth, seventh, and ninth columns, which correspond to the lateral deflection terms, w , are all multiplied by the same number and added together. Of course, an all-zero column makes the determinant zero and the matrix singular.

A fifth characteristic of any stiffness matrix is that its terms can be nondimensionalized. The nondimensionalization of a structure’s assembled stiffness matrix can be illustrated by nondimensionalizing the element beam bending stiffness matrix. This latter

¹ When adding terms from different stiffness matrices, be sure that all terms of the sum have consistent units. For example, if the sum appears to be $4l^2 + 6l$, then an error has been made.

nondimensionalization can be accomplished by factoring out an l from the second and fourth columns and dividing the second and fourth rows by l . The result for beam element j is

$$\begin{Bmatrix} V_1 \\ M_1/l \\ V_2 \\ M_2/l \end{Bmatrix}^{(j)} = \frac{EI_0}{l^3} \begin{bmatrix} 12 & 6 & -12 & 6 \\ 6 & 4 & -6 & 2 \\ -12 & -6 & 12 & -6 \\ 6 & 2 & -6 & 4 \end{bmatrix} \begin{Bmatrix} w_1^{(j)} \\ l\theta_1^{(j)} \\ w_2^{(j)} \\ l\theta_2^{(j)} \end{Bmatrix}$$

It is immaterial whether the superscript j is placed upon the entire vector, as on the right-hand side, or placed on the individual terms of the vector, as is done with $\{q\}$.

The final step in writing the assembled matrix equation $\{\hat{Q}\} = [\hat{K}]\{\hat{q}\}$ is detailing the generalized force vector. Recall that

$$\delta W_{ex} = \{\delta\hat{q}\}[\hat{Q}]$$

Also recall the discussion that the generalized force vector terms are just those *external* forces and moments acting upon the structural system that do virtual work when each of the global generalized coordinates are varied *in turn*. To illustrate this process, return to Figs. 17.7(a, b). Taking each of the global DOF in turn, first consider a positive variation upon w_1 with zero variations for all the other generalized coordinates. The virtual work done by *all* the external forces acting upon this structural system is the product of the force reaction at the left-hand support and δw_1 . Let all support reactions, regardless of whether they are forces or moments, be symbolized by a generic R . Be sure to understand that, in general, all the terms symbolized simply by R are not usually the same. Precisely what R stands for is deduced from its position in $\{\hat{Q}\}$. Then $\delta W_{ex} = R \delta\hat{w}_1$, and $Q_1 = R$. Similarly,

$$\begin{aligned} \delta W_{ex} &= R \delta\hat{\theta}_1 & \delta W_{ex} &= \frac{1}{2} F_0 \delta\hat{w}_2 & \delta W_{ex} &= 0 \delta\hat{\theta}_2 & \delta W_{ex} &= R \delta\hat{w}_3 \\ \delta W_{ex} &= -M_0 \delta\hat{\theta}_3 & \delta W_{ex} &= -F_0 \delta\hat{w}_4 & \delta W_{ex} &= 0 \delta\hat{\theta}_4 & \delta W_{ex} &= R \delta\hat{w}_5 \end{aligned}$$

Then the generalized force vector (written in row transpose form to save space) is

$$\{\hat{Q}\} = [R \quad R \quad \frac{1}{2} F_0 \quad 0 \quad R \quad -M_0 \quad -F_0 \quad 0 \quad R]^t$$

This concludes the detailed explanation for this illustrative example of each of the three parts of the assembled stiffness matrix equation $\{\hat{Q}\} = [\hat{K}]\{\hat{q}\}$.

17.6 Solving the System Matrix Equation

Solving the above assembled matrix equation $\{\hat{Q}\} = [\hat{K}]\{\hat{q}\}$ for static loads requires some comment. The first step in the solution process is the insertion of the deflection BCs into the vector of generalized coordinates $\{\hat{q}\}$. The force BCs (i.e., the support reactions) have already been entered as R 's into the generalized force vector. In the case of the previous illustrative example, inspection of Fig. 17.7(a) reveals that the deflection BCs are

$$\hat{w}_1 = \hat{\theta}_1 = \hat{w}_3 = \hat{w}_5 = 0$$

A simple check on the correct insertion of the deflection BCs in $\{\hat{q}\}$ and the proper insertion of the reaction entries (the R 's) into $\{\hat{Q}\}$ is that on any row where there is an unknown reaction

R there must also be a known deflection (usually, but not necessarily, zero); and on any row where there is a known generalized force there must also be a unknown deflection. Inserting the above four BCs into the assembled matrix equation yields the following generalized coordinate vector:

$$\{\hat{q}\} = \{0 \quad 0 \quad \hat{w}_2 \quad \hat{\theta}_2 \quad 0 \quad \hat{\theta}_3 \quad \hat{w}_4 \quad \hat{\theta}_4 \quad 0\}^t$$

The postmultiplication of this global DOF vector, with its zero entries, with the assembled stiffness matrix $[\hat{K}]$ results in the elimination of the first, second, fifth, and ninth columns of the system stiffness matrix. Removing those columns from the system stiffness matrix and at the same time removing the zero terms from the global DOF vector leads to

$$\begin{Bmatrix} R \\ R \\ \frac{1}{2}F_0 \\ 0 \\ R \\ -M_0 \\ -F_0 \\ 0 \\ R \end{Bmatrix} = \frac{EI_0}{l^3} \begin{bmatrix} -24 & 12l & 0 & 0 & 0 & 0 \\ -12l & 4l^2 & 0 & 0 & 0 & 0 \\ 36 & -6l & 6l & 0 & 0 & 0 \\ -6l & 12l^2 & 2l^2 & 0 & 0 & 0 \\ -12 & -6l & 6l & -24 & 12l & 0 \\ 6l & 2l^2 & 12l^2 & -12l & 4l^2 & 0 \\ 0 & 0 & -12l & 27 & -12l^2 & 0 \\ 0 & 0 & 4l^2 & -12l & 8l^2 & 0 \\ 0 & 0 & 0 & -3 & 0 & 0 \end{bmatrix} \begin{Bmatrix} \hat{w}_2 \\ \hat{\theta}_2 \\ \hat{\theta}_3 \\ \hat{w}_4 \\ \hat{\theta}_4 \end{Bmatrix}$$

The next step is to set aside all those equations of the above nine algebraic equations that contain an unknown reaction in the generalized force vector. Thus the first, second, fifth, and ninth rows that are set aside exactly correspond to the columns that were deleted. This correspondence will always exist. The remaining matrix equation is, in general,

$$\{\tilde{Q}\} = [\tilde{K}]\{\tilde{q}\} \quad (17.17)$$

and in particular,

$$\begin{Bmatrix} \frac{1}{2}F_0 \\ 0 \\ -M_0 \\ -F_0 \\ 0 \end{Bmatrix} = \frac{EI_0}{l^3} \begin{bmatrix} 36 & -6l & 6l & 0 & 0 \\ -6l & 12l^2 & 2l^2 & 0 & 0 \\ 6l & 2l^2 & 12l^2 & -12l & 4l^2 \\ 0 & 0 & -12l & 27 & -12l^2 \\ 0 & 0 & 4l^2 & -12l & 8l^2 \end{bmatrix} \begin{Bmatrix} \hat{w}_2 \\ \hat{\theta}_2 \\ \hat{\theta}_3 \\ \hat{w}_4 \\ \hat{\theta}_4 \end{Bmatrix}$$

The above *global* or *system* matrix equation is fully equivalent to five simultaneous equations in five unknowns. This system of equations can now be solved for the unknown deflections in any number of ways. Once the unknown deflections are determined, they can be inserted into the set aside equations in order to evaluate the unknown reactions. In this case, and in all other cases, obtaining the support reactions is simply a matter of multiplication. In matrix form, from the set aside rows, that multiplication to obtain the reactions is

$$\begin{Bmatrix} R \\ R \\ R \\ R \end{Bmatrix} = \frac{EI_0}{l^3} \begin{bmatrix} -24 & 12l & 0 & 0 & 0 \\ -12l & 4l^2 & 0 & 0 & 0 \\ -12 & -6l & 6l & -24 & 12l \\ 0 & 0 & 0 & -3 & 0 \end{bmatrix} \begin{Bmatrix} \hat{w}_2 \\ \hat{\theta}_2 \\ \hat{\theta}_3 \\ \hat{w}_4 \\ \hat{\theta}_4 \end{Bmatrix}$$

Finally, recall that once all the global DOF are known, then the nodal deflections for each beam element are easily calculated, if necessary by $\{q^{(i)}\} = [T_i]\{\hat{q}_i\}$. Once the beam element DOF are known, the deflections, strains, and stresses anywhere within the beam element can be determined using the shape functions

$$\begin{aligned} w(x) &= \sum N_i(x)q_i = [N(x)]\{q\} \\ \epsilon_{xx}(x, y, z) &= -zw''(x) \\ \sigma_{xx}(x, y, z) &= E(\epsilon_{xx} - \alpha \Delta T) \end{aligned} \quad (17.4c)$$

17.7 Example Beam Frame and Grid Problems

It is necessary to practice the concepts discussed above. Two example problems are presented. The first example is very little different from the above. The second example breaks new ground in that the global DOF are not quite as conveniently associated with the element DOF, and the small twisting and small bending deflections have to be considered simultaneously.

Example 17.3. Set up, but do not solve, the simultaneous equations in matrix form necessary to determine the nodal deflections of the two-beam-two-spring structure shown in Fig. 17.8.

Solution. Using, as always, the same sign convention for the beam bending element where lateral nodal deflections are positive up, and bending slopes are positive counterclockwise, the beam element stiffness matrices and the beam element generalized coordinate vectors are

$$[k_{21}]\{q^{(21)}\} = \frac{EI_0}{l^3} \begin{bmatrix} 12 & 6l & -12 & 6l \\ 6l & 4l^2 & -6l & 2l^2 \\ -12 & -6l & 12 & -6l \\ 6l & 2l^2 & -6l & 4l^2 \end{bmatrix} \begin{Bmatrix} w_1^{(21)} \\ \theta_1^{(21)} \\ w_2^{(21)} \\ \theta_2^{(21)} \end{Bmatrix}$$

$$[k_{22}]\{q^{(22)}\} = \frac{EI_0}{l^3} \begin{bmatrix} 24 & 12l & -24 & 12l \\ 12l & 8l^2 & -12l & 4l^2 \\ -24 & -12l & 24 & -12l \\ 12l & 4l^2 & -12l & 8l^2 \end{bmatrix} \begin{Bmatrix} w_1^{(22)} \\ \theta_1^{(22)} \\ w_2^{(22)} \\ \theta_2^{(22)} \end{Bmatrix}$$

$$\begin{Bmatrix} N_1 \\ N_2 \end{Bmatrix}^{(41)} = [k_{41}]\{q^{(41)}\} = \frac{EI_0}{l^3} \begin{bmatrix} +7 & -7 \\ -7 & +7 \end{bmatrix} \begin{Bmatrix} u_1 \\ u_2 \end{Bmatrix}^{(41)}$$

$$\begin{Bmatrix} N_1 \\ N_2 \end{Bmatrix}^{(42)} = [k_{42}]\{q^{(42)}\} = \frac{EI_0}{l^3} \begin{bmatrix} +23 & -23 \\ -23 & +23 \end{bmatrix} \begin{Bmatrix} u_1 \\ u_2 \end{Bmatrix}^{(42)}$$

Let the global DOF be upward \hat{w}_i 's and counterclockwise $\hat{\theta}_i$'s at node i where the index i runs from 1 through 4. Let a positive upward \hat{w}_5 be the sole DOF at node 5. Since only a spring element connects to node 5, there is no rotational DOF required at node 5. If a rotational degree of freedom were used at node 5, then there would be no stiffness associated with that DOF because all spring ends are always hinged ends, and there is no resistance

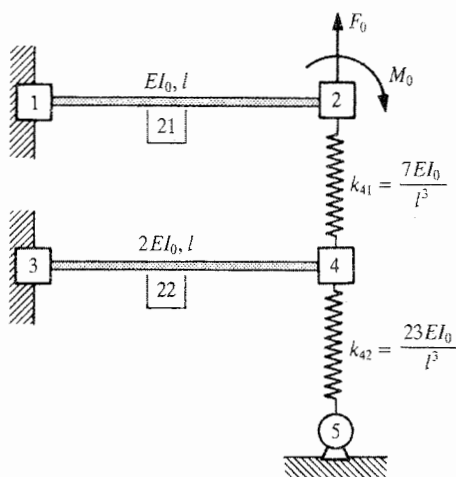


Figure 17.8. Example 17.3. A beam-spring finite element model.

to rotation at a hinge. Thus there would be nonzero entries in the system stiffness matrix along the rows and columns corresponding to that superfluous rotational DOF. Since such rows and columns of zeros must be eventually deleted so that the global stiffness matrix, $[\tilde{K}]$, can be used for a solution for the unknown DOF, it is best never to enter them in the first place.

The next step is to write all the element stiffness matrices and generalized coordinate vectors in terms of the global (system) DOF. One way of accomplishing this task is visualizing placing the standard spring element or beam element DOF diagrams upon each of the spring or beam elements of the structural system, and then noting the correspondences between the element coordinates and the global coordinates. For example, when this superposition is done for springs number 41 and 42 the result is

$$[k_{41}]\{\hat{q}\} = \frac{EI_0}{l^3} \begin{bmatrix} +7 & -7 \\ -7 & +7 \end{bmatrix} \begin{Bmatrix} \hat{w}_4 \\ \hat{w}_2 \end{Bmatrix}$$

$$[k_{42}]\{\hat{q}\} = \frac{EI_0}{l^3} \begin{bmatrix} +23 & -23 \\ -23 & +23 \end{bmatrix} \begin{Bmatrix} \hat{w}_5 \\ \hat{w}_4 \end{Bmatrix}$$

Hand assembly of the system stiffness matrix is facilitated when the global DOF are in the same order in all element stiffness matrices. Therefore, it is convenient to interchange the rows of the above two matrix equations. The columns must also be interchanged so that they are multiplied by the correct factor from the deflection vector. The results of that double interchange are

$$[k_{41}]\{\hat{q}\} = \frac{EI_0}{l^3} \begin{bmatrix} +7 & -7 \\ -7 & +7 \end{bmatrix} \begin{Bmatrix} \hat{w}_2 \\ \hat{w}_4 \end{Bmatrix}$$

$$[k_{42}]\{\hat{q}\} = \frac{EI_0}{l^3} \begin{bmatrix} +23 & -23 \\ -23 & +23 \end{bmatrix} \begin{Bmatrix} \hat{w}_4 \\ \hat{w}_5 \end{Bmatrix}$$

It is clear that the reordering of the global DOF for a spring element has no effect whatsoever, upon the spring element stiffness matrix. Therefore, no further concern need be paid to the ordering of spring global DOF. The very same conclusion would be arrived at if the

spring element diagram were placed so that its positive deflection vectors were opposite in direction to the positive directions of the chosen global generalized coordinates. Sign differences between the element and global generalized coordinates for beam elements are discussed at length later.

The stiffness matrix and the two column matrices of the assembled matrix equation $\{\hat{Q}\} = [\hat{K}]\{\hat{q}\}$ (i.e., the system equation before the reduction in size that follows the insertion of the deflection BCs) are shown below. The assembled stiffness matrix is symmetric, as it should be. Notice that the single physical connection between the upper and lower beams in the form of spring number 41 is reflected in the system stiffness matrix terms (3, 7) and (7, 3). These matrix terms provide the corresponding mathematical connection (called coupling) between the data of the upper beam, which is located in the first four rows and columns, and the data of the lower beam, which is located in the next group of four rows and columns.

$$[\hat{K}] = \frac{EI_0}{l^3} \begin{bmatrix} 12 & 6l & -12 & 6l & 0 & 0 & 0 & 0 & 0 \\ 6l & 4l^2 & -6l & 2l^2 & 0 & 0 & 0 & 0 & 0 \\ -12 & -6l & 19 & -6l & 0 & 0 & -7 & 0 & 0 \\ 6l & 2l^2 & -6l & 4l^2 & 0 & 0 & 0 & 0 & 0 \\ 0 & 0 & 0 & 0 & 24 & 12l & -24 & 12l & 0 \\ 0 & 0 & 0 & 0 & 12l & 8l^2 & -12l & 4l^2 & 0 \\ 0 & 0 & -7 & 0 & -24 & -12l & 54 & -12l & -23 \\ 0 & 0 & 0 & 0 & 12l & 4l^2 & -12l & 8l^2 & 0 \\ 0 & 0 & 0 & 0 & 0 & 0 & -23 & 0 & 23 \end{bmatrix}$$

and

$$\begin{aligned} \{\hat{Q}\} &= [R \quad R \quad F_0 \quad -M_0 \quad R \quad R \quad 0 \quad 0 \quad R]^t \\ \{\hat{q}\} &= [0 \quad 0 \quad \hat{w}_2 \quad \hat{\theta}_2 \quad 0 \quad 0 \quad \hat{w}_4 \quad \hat{\theta}_4 \quad 0]^t \end{aligned}$$

Note again the correspondences between the known deflection DOF and the unknown generalized forces, and vice versa. Discarding all assembled stiffness matrix columns multiplied by zero, and setting aside the corresponding rows, leads to the system matrix equation to be solved for the unknown deflections. That equation is

$$\begin{Bmatrix} F_0 \\ -M_0 \\ 0 \\ 0 \end{Bmatrix} = \frac{EI_0}{l^3} \begin{bmatrix} 19 & -6l & -7 & 0 \\ -6l & 4l^2 & 0 & 0 \\ -7 & 0 & 54 & -12l \\ 0 & 0 & -12l & 8l^2 \end{bmatrix} \begin{Bmatrix} \hat{w}_2 \\ \hat{\theta}_2 \\ \hat{w}_4 \\ \hat{\theta}_4 \end{Bmatrix}$$

In order to comment on the above solution, first recall that the system matrix equation, which is obtained after the insertion of the deflection BCs and the setting aside of the equations that determine the support reactions, is symbolized as $\{\tilde{Q}\} = [\tilde{K}]\{\tilde{q}\}$. Then the solution for the deflection vector can be *formally* written as

$$\{\tilde{q}\} = [\tilde{K}]^{-1}\{\tilde{Q}\} = [f]\{\tilde{Q}\}$$

where $[f]$ is called the flexibility matrix (short for flexibility influence coefficient matrix) because of the general meaning of "flexibility" being the reverse of "stiffness." There are no zeros in this and most flexibility matrices. As opposed to the above approach of inverting the stiffness matrix to obtain the flexibility matrix, a force approach such as the unit load

method which is introduced in Chapter 20, can be taken to directly calculate the terms of the flexibility matrix. See Exercise 17.10. The procedure is simply to first apply a single unit magnitude force or moment, whichever corresponds to the n th generalized coordinate, at the corresponding node of the structure and in the direction of that one generalized coordinate. Then calculate all the resulting deflections at that node and all other nodes. The ordered deflections are then the columns of the flexibility matrix. This approach is far less practical if the structure is statically indeterminate. While touching upon the subject of static determinacy and indeterminacy, note again that since the FEM is a deflection method, its application is exactly the same regardless of whether the structure is statically determinate or indeterminate.

Example 17.4. Set up, but do not solve, the system finite element matrix equation $\{\bar{Q}\} = [\bar{K}]\{\bar{q}\}$ for the two-beam structure and loading shown in Fig. 17.9(a). Note that the two ends of the structure are clamped. The material and geometric data for the two uniform, homogeneous, linearly elastic beams are

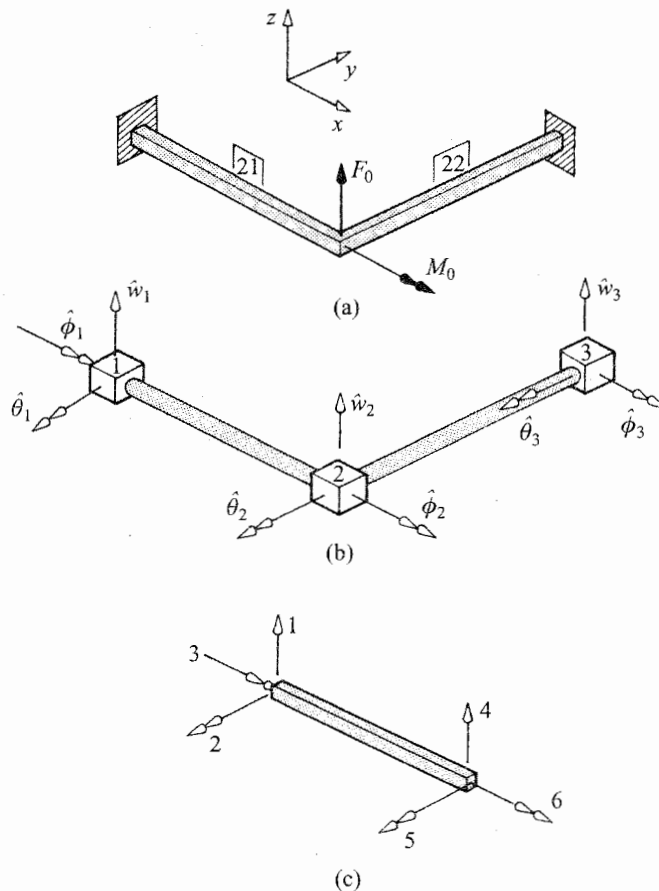


Figure 17.9. Example 17.4. A simple beam grid. (a) The mathematical model. (b) The finite element model showing the global degrees of freedom. (c) The selected ordering of the element degrees of freedom.

	Beam 21	Beam 22
Length	l	l
Bending stiffness	$2EI_0$	$4EI_0$
Torsional stiffness	$GJ_0 = 3EI_0$	$GJ_0 = 5EI_0$

Solution. Since both beams are twisted as well as bent, it is necessary to use the global DOF shown in Fig. 17.9(b). Note that in the case of the global DOF, all the rotations described by a ϕ are rotations about the x axis, while all rotations symbolized by a θ are rotations about the negative y axis. This consistency allows easier interpretation of numerical results, especially with larger problems. Let the global deflection matrix be ordered as

$$\{\hat{q}\} = [\hat{w}_1 \quad \hat{\theta}_1 \quad \hat{\phi}_1 \quad \hat{w}_2 \quad \hat{\theta}_2 \quad \hat{\phi}_2 \quad \hat{w}_3 \quad \hat{\theta}_3 \quad \hat{\phi}_3]^t$$

Of course, the global load matrix has a corresponding ordering. As ever, the global stiffness matrix is built from the element stiffness matrices. In this case, where each beam is twisted as well as bent, it is necessary to use both the one plane, beam element bending stiffness matrix with its four DOF and the beam element twisting stiffness matrix with its two DOF. The latter generic matrix is developed in Exercise 17.2. The result of that exercise, where as usual M_i is a torque and ϕ is a twist, is

$$\begin{Bmatrix} M_{r1} \\ M_{r2} \end{Bmatrix} = \frac{GJ}{l} \begin{bmatrix} +1 & -1 \\ -1 & +1 \end{bmatrix} \begin{Bmatrix} \phi_1 \\ \phi_2 \end{Bmatrix}$$

For small deflections there is no interaction (“coupling”) between beam bending and twisting. Thus, the *element* stiffness matrix for both bending and twisting is merely the result of combining the bending matrix with the twisting matrix using zeros for the matrix terms that couple bending to twisting. The way the two generic matrices are combined depends upon the ordering for the six DOF. See Fig. 17.9(c) for this case. Then simply interspace the rows and columns of the two matrices according to that order. For example, using the above listed data for beam 21, the product of the beam element stiffness matrix and the element deflection vector for beam 21 is

$$[k_{21}]\{q^{(21)}\} = \frac{EI_0}{l^3} \begin{bmatrix} 24 & 12l & 0 & -24 & 12l & 0 \\ 12l & 8l^2 & 0 & -12l & 4l^2 & 0 \\ 0 & 0 & 3l^2 & 0 & 0 & -3l^2 \\ -24 & -12l & 0 & 24 & -12l & 0 \\ 12l & 4l^2 & 0 & -12l & 8l^2 & 0 \\ 0 & 0 & -3l^2 & 0 & 0 & 3l^2 \end{bmatrix} \begin{Bmatrix} w_1^{(21)} \\ \theta_1^{(21)} \\ \phi_1^{(21)} \\ w_2^{(21)} \\ \theta_2^{(21)} \\ \phi_2^{(21)} \end{Bmatrix}$$

Again note that, for small deflections, the rows that pertain to bending moments and shearing forces always have zeros as factors for the twists, and the rows for the twisting moments always have zeros as factors for the lateral deflections and bending slopes. In other words, reflecting the lack of a mechanical interaction, the two sets of deflections are mathematically decoupled.

Since the global coordinates were selected to harmonize with the element coordinates of beam 21, the above relationship in terms of the global coordinates is simply

$$[k_{21}]\{\hat{q}\} = \frac{EI_0}{l^3} \begin{bmatrix} 24 & 12l & 0 & -24 & 12l & 0 & 0 & 0 & 0 \\ 12l & 8l^2 & 0 & -12l & 4l^2 & 0 & 0 & 0 & 0 \\ 0 & 0 & 3l^2 & 0 & 0 & -3l^2 & 0 & 0 & 0 \\ -24 & -12l & 0 & 24 & -12l & 0 & 0 & 0 & 0 \\ 12l & 4l^2 & 0 & -12l & 8l^2 & 0 & 0 & 0 & 0 \\ 0 & 0 & -3l^2 & 0 & 0 & 3l^2 & 0 & 0 & 0 \\ 0 & 0 & 0 & 0 & 0 & 0 & 0 & 0 & 0 \\ 0 & 0 & 0 & 0 & 0 & 0 & 0 & 0 & 0 \\ 0 & 0 & 0 & 0 & 0 & 0 & 0 & 0 & 0 \end{bmatrix} \begin{bmatrix} \hat{w}_1 \\ \hat{\theta}_1 \\ \hat{\phi}_1 \\ \hat{w}_2 \\ \hat{\theta}_2 \\ \hat{\phi}_2 \\ \hat{w}_3 \\ \hat{\theta}_3 \\ \hat{\phi}_3 \end{bmatrix}$$

At this point it is well to note that including the additional rows and columns of zeros that correspond to global coordinates that are not associated with the structural element in question adds very little to the information conveyed by the element stiffness matrix written in terms of the global coordinates. Therefore, from this point onward, the element stiffness matrices in terms of the global coordinates are written in truncated form where only those global coordinates having nonzero factors in the stiffness matrix are listed.

The bookkeeping problem for beam 22 is a bit more complicated. Aligning the element coordinate system of Fig. 17.9(c) with beam 22 in such a manner that the left end of the element is at node 2 (always the preferred option) while the right end is at node 3 leads to the following relations:

$$\begin{aligned} w_1^{(22)} &= \hat{w}_2 & \theta_1^{(22)} &= \hat{\phi}_2 & \phi_1^{(22)} &= -\hat{\theta}_2 \\ w_2^{(22)} &= \hat{w}_3 & \theta_2^{(22)} &= \hat{\phi}_3 & \phi_2^{(22)} &= -\hat{\theta}_3 \end{aligned}$$

with a similar set of relations for the corresponding load terms. The next step is to proceed to write the element stiffness matrix $\{Q^{(22)}\} = [k_{22}]\{q^{(22)}\}$ in terms of the global coordinates while (1) conforming with the accepted ordering of the global coordinates and the corresponding load vector terms, and (2) doing so in terms of the positive values of the global DOF and generalized forces. Step (1) is accomplished by noting that the second, third, fifth, and sixth of the above relations, and their load counterparts, require interchanging the order of the second and third rows and columns, and the fifth and sixth rows and columns of the original element stiffness matrix which followed the (w, θ, ϕ) ordering. The second step is accomplished by detaching the -1 factor from $\hat{\theta}_2$ and $\hat{\theta}_3$ and applying it instead to the terms of the (now) second and fifth columns. After this half-step the sign changes in the element stiffness matrix look like

$$\begin{array}{cccccc} + & - & + & + & - & + \\ + & - & + & + & - & + \\ + & - & + & + & - & + \\ + & - & + & + & - & + \\ + & - & + & + & - & + \\ + & - & + & + & - & + \end{array}$$

Removing the minus sign from the moments about the negative y axis so as to obtain the positive sign convention for those quantities is accomplished by multiplying the

second and fifth equations (rows) by -1 . Therefore the final sign change pattern in this case is

$$\begin{array}{cccccc}
 + & - & + & + & - & + \\
 - & + & - & - & + & - \\
 + & - & + & + & - & + \\
 + & - & + & + & - & + \\
 - & + & - & - & + & - \\
 + & - & + & + & - & +
 \end{array}$$

Note that there are never any sign changes (or negative signs) along the main diagonal of the matrix. While this bookkeeping is a bit tedious to do by hand, it is the sort of thing a digital computer program does very quickly and flawlessly. Thus the (truncated) element stiffness for beam 22 in terms of the global coordinates is then

$$[K_{22}]\{\hat{q}\} = \frac{EI_0}{l^3} \begin{bmatrix} 48 & 0 & 24l & -48 & 0 & 24l \\ 0 & 5l^2 & 0 & 0 & -5l^2 & 0 \\ 24l & 0 & 16l^2 & -24l & 0 & 8l^2 \\ -48 & 0 & -24l & 48 & 0 & -24l \\ 0 & -5l^2 & 0 & 0 & 5l^2 & 0 \\ 24l & 0 & 8l^2 & -24l & 0 & 16l^2 \end{bmatrix} \begin{Bmatrix} \hat{w}_2 \\ \hat{\theta}_2 \\ \hat{\phi}_2 \\ \hat{w}_3 \\ \hat{\theta}_3 \\ \hat{\phi}_3 \end{Bmatrix}$$

Putting these two element stiffness matrices into the assembled stiffness matrix leads to

$$\begin{Bmatrix} R \\ R \\ R \\ +F_0 \\ 0 \\ +M_0 \\ R \\ R \\ R \end{Bmatrix} = \frac{EI_0}{l^3} \begin{bmatrix} 24 & 12l & 0 & -24 & -12l & 0 & 0 & 0 & 0 \\ 12l & 8l^2 & 0 & -12l & 4l^2 & 0 & 0 & 0 & 0 \\ 0 & 0 & 3l^2 & 0 & 0 & -3l^2 & 0 & 0 & 0 \\ -24 & -12l & 0 & 72 & -12l & 24l & -48 & 0 & 24l \\ 12l & 4l^2 & 0 & -12l & 13l^2 & 0 & 0 & -5l^2 & 0 \\ 0 & 0 & -3l^2 & 24l & 0 & 19l^2 & -24l & 0 & 8l^2 \\ 0 & 0 & 0 & -48 & 0 & -24l & 48 & 0 & -24l^2 \\ 0 & 0 & 0 & 0 & -5l^2 & 0 & 0 & 5l^2 & 0 \\ 0 & 0 & 0 & 24l & 0 & 8l^2 & -24l & 0 & 16l^2 \end{bmatrix} \begin{Bmatrix} \hat{w}_1 \\ \hat{\theta}_1 \\ \hat{\phi}_1 \\ \hat{w}_2 \\ \hat{\theta}_2 \\ \hat{\phi}_2 \\ \hat{w}_3 \\ \hat{\theta}_3 \\ \hat{\phi}_3 \end{Bmatrix}$$

Application of the deflection BCs ($\hat{w}_1 = \hat{\theta}_1 = \hat{\phi}_1 = \hat{w}_3 = \hat{\theta}_3 = \hat{\phi}_3 = 0$) and the setting aside of the equations that determine the values of the reacting shear forces and moments at the clamped supports leads to $\{\bar{Q}\} = [\bar{K}]\{\bar{q}\}$, that is,

$$\begin{Bmatrix} +F_0 \\ 0 \\ +M_0 \end{Bmatrix} = \frac{EI_0}{l^3} \begin{bmatrix} 72 & -12l & 24l \\ -12l & 13l^2 & 0 \\ 24l & 0 & 19l^2 \end{bmatrix} \begin{Bmatrix} \hat{w}_2 \\ \hat{\theta}_2 \\ \hat{\phi}_2 \end{Bmatrix}$$

As before, the above matrix equation can, of course, be solved for the three unknown deflections, and those three results can be used to determine the magnitudes of the reactions at the clamped ends. The stresses and deflections can then be determined anywhere along the beam elements. ■

It needs to be emphasized that this two-beam example problem would be far less work if the analyst were familiar with, and had available to him or her, any one of the various commercial FEM digital computer programs, which would automatically compose element stiffness matrices and assemble the structure's stiffness matrix while deducing and keeping track of all relations between the element and global DOF. The purpose then of these detailed expositions is for the analyst to understand the underlying logic of any FEM digital

computer program so as to be better prepared to use such a program, and to be better prepared to determine his or her own (undoubtedly infrequent) errors in the use of that FEM program.

It may occur to the reader that a lot of hand work could be saved if the global deflection vector $\{\hat{q}\}$ were skipped in preference to proceeding directly to $\{\bar{q}\}$. Skipping over $\{\hat{q}\}$ would save writing those terms of the element stiffness matrices that are going to be deleted once the BCs are applied to $\{\hat{q}\}$ with the result that the analyst would be moving around smaller matrices. While this is true, keeping the $\{\hat{q}\}$ step in this exposition has the value that doing so follows the procedure of most commercial FEM programs. Most programs follow that procedure because, for a large structure, the number of DOF situated away from the supports of the structure greatly exceeds the number of DOF at the structure's supports. Therefore, the savings in program storage and running time achieved by bypassing $\{\hat{q}\}$ are minimal. The advantage of keeping the $\{\hat{q}\}$ step in a commercial program is that it becomes a very simple matter to investigate the effects of changing the BCs. This is of importance because the BCs are seldom so simple as to be well described by such simplifications as "simply supported" or "clamped."

17.8 More Extensive Example Problems

The next example problem contains only marginally new considerations. However, since there are three beam elements in this example, there is considerably more hand work. In order to make the example problem more manageable, it is divided into several parts.

Example 17.5. For the planar, portal frame structure and loading shown in Fig. 17.10(a), let each uniform, linearly elastic, homogeneous beam have the same length l and the same bending stiffness factor EI_0 , and the same axial stiffness factor EA_0 . Let the axial stiffness of each beam be such that $EA_0/l = 100EI_0/l^3$. Let both spring stiffness factors have the value $3EI_0/l^3$.

- (a) Set up an appropriate global deflection vector for the system finite element matrix equation before the application of BCs; that is, choose a $\{\hat{q}\}$ for the matrix equation $\{\hat{Q}\} = [\hat{K}]\{\hat{q}\}$.
- (b) Write the (truncated) element stiffness matrix for the lintel beam, beam 31, for the generalized coordinates of the global DOF vector chosen above.
- (c) For the chosen global DOF, write both truncated and the nontruncated element stiffness matrix for beam 21, the left-hand post.
- (d) Write the (truncated) element stiffness matrix for spring element 51 in terms of the global generalized coordinates.
- (e) Write the structure's global matrix equation after imposition of the BCs. That is, detail $\{\bar{Q}\} = [\bar{K}]\{\bar{q}\}$.

Solution. (a) Without boundary supports, and with only the given loading, 14 DOF are necessary to describe the deflections of the three-beam–two-spring structural system; see Fig. 17.10(b). (If there were, say, an additional concentrated lateral load at the center of one of the two posts, that is, at the center of one of the two vertical beams, then another node and another three DOF would be necessary for the FEM mathematical model.) In this situation for the sake of brevity of notation, the nodes are numbered with single digits. With the use of a commercial FEM program, where brevity is never an important consideration, it is advisable to use nonsequential integers for the nodes, such as 10, 20, 30, 40, and so on,

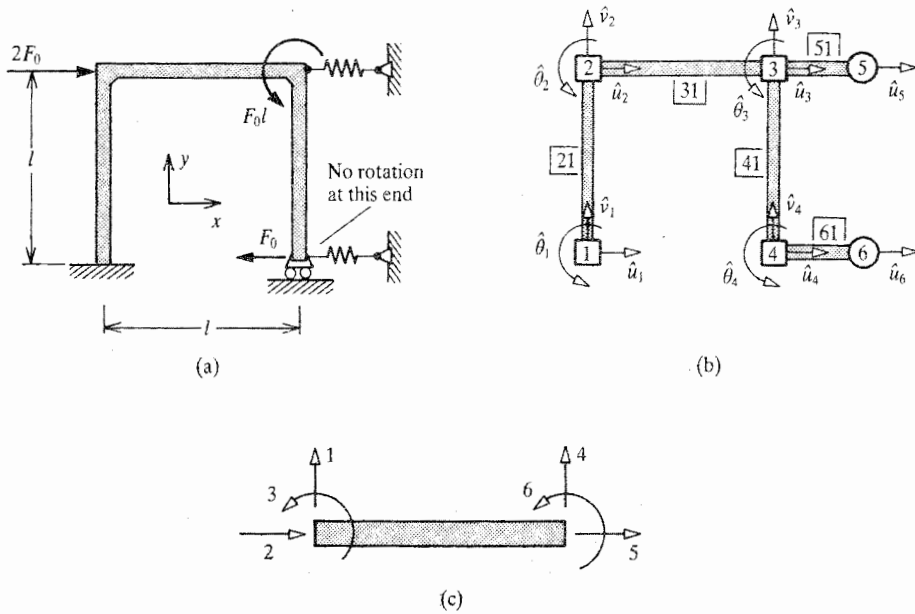


Figure 17.10. Example 17.5. (a) The mathematical model. (b) The finite element model with the global DOF. (c) The ordering of the element DOF.

rather than 1, 2, 3, 4, and so on. Such a choice allows later insertion of new nodes for new loadings or design changes while still keeping neighboring integers for neighboring nodes. While there is a small numerical advantage to numbering the nodes from the most flexible part of the structure towards the stiffest part of the structure, the reverse order was used for this small structure. Let the global DOF vector here be ordered as

$$\{\hat{q}\} = [\hat{u}_1 \quad \hat{v}_1 \quad \hat{\theta}_1 \quad \hat{u}_2 \quad \hat{v}_2 \quad \hat{\theta}_2 \quad \hat{u}_3 \quad \dots \quad \hat{\theta}_4 \quad \hat{u}_5 \quad \hat{u}_6]^t$$

Putting the terms of the vector in alphabetical and numerical order simply makes the vector easier to remember. With all the \$u_i\$ positive to the right, and all the \$v_i\$ positive upward, and all the \$\theta_i\$ positive counterclockwise, the deflection solution, when obtained, is easier to interpret.

(b) Turning now to the element stiffness matrix relations, note that for this structure and loading it is necessary to consider both the axial and lateral deflections of each beam. Again the externally applied loading is limited to the situation where the system deflections are sufficiently small that there is no interaction between lateral and axial deflections and loads. Therefore, it is only necessary to merge the existing small deflection axial and lateral stiffness matrices. For example, using the combined beam element DOF diagram of Fig. 17.10(c) the element matrix equation for beam 31 is

$$\begin{Bmatrix} V_1 \\ N_1 \\ M_1 \\ V_2 \\ N_2 \\ M_2 \end{Bmatrix}^{(31)} = \frac{EI_0}{l^3} \begin{bmatrix} 12 & 0 & 6l & -12 & 0 & 6l \\ 0 & 100 & 0 & 0 & -100 & 0 \\ 6l & 0 & 4l^2 & -6l & 0 & 2l^2 \\ -12 & 0 & -6l & 12 & 0 & -6l \\ 0 & -100 & 0 & 0 & 100 & 0 \\ 6l & 0 & 2l^2 & -6l & 0 & 4l^2 \end{bmatrix} \begin{Bmatrix} w_1 \\ u_1 \\ \theta_1 \\ w_2 \\ u_2 \\ \theta_2 \end{Bmatrix}^{(31)}$$

where the superscripts on the load and deflection vectors are applied to all the elements in those two vectors. Notice that paralleling the previous bending–twisting example problem, there are no lateral and axial coupling terms in the stiffness matrix, that is, there are no nonzero terms that multiply the lateral deflections along the rows for the axial forces, and there are no nonzero terms multiplying the axial deflections along the rows for the bending moments and shearing forces. Thus, as it must be, the lack of physical coupling between the two types of small deflections is reflected in the mathematical statement of the element stiffness matrix.

The next step is to replace the deflection vector $\{q^{(31)}\}$ by the truncated form of the global DOF vector $\{\hat{q}\}$. That term-by-term equality is easily written as

$$\{q^{(31)}\} = [\hat{v}_2 \quad \hat{u}_2 \quad \hat{\theta}_2 \quad \hat{v}_3 \quad \hat{u}_3 \quad \hat{\theta}_3]^t$$

The problem with this is that the terms of the above global deflection vector are not in the prescribed order of the overall global deflection vector. It is necessary to interchange the two pairs of u 's and v 's. Doing so causes the first and second rows and columns to be interchanged, and the fourth and fifth rows and columns to be interchanged. The final result, with the truncated global DOF vector in its chosen order, is

$$\{Q^{(31)}\} = \frac{EI_0}{l^3} \begin{bmatrix} 100 & 0 & 0 & -100 & 0 & 0 \\ 0 & 12 & 6l & 0 & -12 & 6l \\ 0 & 6l & 4l^2 & 0 & -6l & 2l^2 \\ -100 & 0 & 0 & 100 & 0 & 0 \\ 0 & -12 & -6l & 0 & 12 & -6l \\ 0 & 6l & 2l^2 & 0 & -6l & 4l^2 \end{bmatrix} \begin{Bmatrix} \hat{u}_2 \\ \hat{v}_2 \\ \hat{\theta}_2 \\ \hat{u}_3 \\ \hat{v}_3 \\ \hat{\theta}_3 \end{Bmatrix}$$

which amounts to nothing more than just recombining the original beam element extension matrix and beam element bending matrix in the order of the global coordinates rather than the order of the element coordinates. Again, the global form of the generalized force vector is to be written after the assembly of the structure's stiffness matrix.

(c) In the case of beam 21, fitting the local DOF diagram of Fig. 17.10(c) to the global DOF of diagram Fig. 17.10(b) can be done in either one of two ways. Here the choice has been made to orient the local diagram vertically such that $w_1^{(21)} = -\hat{u}_1$, $u_1^{(21)} = +\hat{v}_1$, and so on; that is, choosing to rotate the local diagram 90° counterclockwise and superimpose it on beam 21. Thus beginning with

$$\begin{Bmatrix} V_1 \\ N_1 \\ M_1 \\ V_2 \\ N_2 \\ M_2 \end{Bmatrix}^{(21)} = \frac{EI_0}{l^3} \begin{bmatrix} 12 & 0 & 6l & -12 & 0 & 6l \\ 0 & 100 & 0 & 0 & -100 & 0 \\ 6l & 0 & 4l^2 & -6l & 0 & 2l^2 \\ -12 & 0 & -6l & 12 & 0 & -6l \\ 0 & -100 & 0 & 0 & 100 & 0 \\ 6l & 0 & 2l^2 & -6l & 0 & 4l^2 \end{bmatrix} \begin{Bmatrix} w_1 \\ u_1 \\ \theta_1 \\ w_2 \\ u_2 \\ \theta_2 \end{Bmatrix}^{(21)}$$

the next step is to replace the element DOF vector by the global DOF vector. That is, write

$$\{q^{(21)}\} = [-\hat{u}_1 \quad \hat{v}_1 \quad \hat{\theta}_1 \quad -\hat{u}_2 \quad \hat{v}_2 \quad \hat{\theta}_2]^t$$

Now the negative signs have to be stripped from the \hat{u}_1 and \hat{u}_2 terms and placed in the element stiffness matrix. Following the explanation of the previous example, the result is the sign change pattern

$$\begin{array}{cccccc} + & - & - & + & - & - \\ - & + & + & - & + & + \\ - & + & + & - & + & + \\ + & - & - & + & - & - \\ - & + & + & - & + & + \\ - & + & + & - & + & + \end{array}$$

which leads to

$$\{Q^{(21)}\} = \frac{EI_0}{l^3} \begin{bmatrix} 12 & 0 & -6l & -12 & 0 & -6l \\ 0 & 100 & 0 & 0 & -100 & 0 \\ -6l & 0 & 4l^2 & 6l & 0 & 2l^2 \\ -12 & 0 & 6l & 12 & 0 & 6l \\ 0 & -100 & 0 & 0 & 100 & 0 \\ -6l & 0 & 2l^2 & 6l & 0 & 4l^2 \end{bmatrix} \begin{Bmatrix} \hat{u}_1 \\ \hat{v}_1 \\ \hat{\theta}_1 \\ \hat{u}_2 \\ \hat{v}_2 \\ \hat{\theta}_2 \end{Bmatrix}$$

Note that the symmetry of the element stiffness matrix is preserved through all sign alterations. Once again, the analyst normally does not have to bother with these coordinate transformations. The commercial digital computer program attends to all this bookkeeping. As a review, the nontruncated global form for beam 21 is

$$\begin{Bmatrix} \hat{V}_1 \\ \hat{N}_1 \\ \hat{M}_1 \\ \hat{V}_2 \\ \hat{N}_2 \\ \hat{M}_2 \\ \hat{V}_3 \\ \vdots \\ \hat{M}_4 \\ \hat{N}_5 \\ \hat{N}_6 \end{Bmatrix} = \frac{EI_0}{l^3} \begin{bmatrix} 12 & 0 & -6l & -12 & 0 & -6l & \dots & 0 & 0 \\ 0 & 100 & 0 & 0 & -100 & 0 & \dots & 0 & 0 \\ -6l & 0 & 4l^2 & 6l & 0 & 2l^2 & \dots & 0 & 0 \\ -12 & 0 & 6l & 12 & 0 & 6l & \dots & 0 & 0 \\ 0 & -100 & 0 & 0 & 100 & 0 & \dots & 0 & 0 \\ -6l & 0 & 2l^2 & 6l & 0 & 4l^2 & \dots & 0 & 0 \\ 0 & 0 & 0 & 0 & 0 & 0 & \dots & 0 & 0 \\ \vdots & \vdots & \vdots & \vdots & \vdots & \vdots & \dots & \vdots & \vdots \\ 0 & 0 & 0 & 0 & 0 & 0 & \dots & 0 & 0 \\ 0 & 0 & 0 & 0 & 0 & 0 & \dots & 0 & 0 \\ 0 & 0 & 0 & 0 & 0 & 0 & \dots & 0 & 0 \end{bmatrix} \begin{Bmatrix} \hat{u}_1 \\ \hat{v}_1 \\ \hat{\theta}_1 \\ \hat{u}_2 \\ \hat{v}_2 \\ \hat{\theta}_2 \\ \hat{u}_3 \\ \vdots \\ \hat{\theta}_4 \\ \hat{u}_5 \\ \hat{u}_6 \end{Bmatrix}^{(21)}$$

(d) Just as for beam element 31, the element stiffness matrix for spring element 51, in terms of the global coordinates, can be written immediately in truncated form because of the positive one-to-one correspondence between the element and global coordinates. The result is

$$\{Q^{(51)}\} = \frac{EI_0}{l^3} \begin{bmatrix} +3 & -3 \\ -3 & +3 \end{bmatrix} \begin{Bmatrix} \hat{u}_3 \\ \hat{u}_5 \end{Bmatrix}$$

(e) The element stiffness matrix for beam element 41 would be an exact duplicate of that for beam element 21 if the beam DOF diagram of Fig. 17.10(c) were applied to it in the same way that DOF diagram was applied to beam element 21, and if the node numbers 3 and 4 were interchanged. Since the nodes numbering is as it is, the easier thing to do is to rotate clockwise the DOF diagram so that the node i of the DOF diagram is placed at

node 3. Then the sign changes for the element stiffness matrix are only applied to the four axial stiffness terms. This amounts to no sign changes at all. Thus

$$\{Q^{(41)}\} = \frac{EI_0}{l^3} \begin{bmatrix} 12 & 0 & 6l & -12 & 0 & 6l \\ 0 & 100 & 0 & 0 & -100 & 0 \\ 6l & 0 & 4l^2 & -6l & 0 & 2l^2 \\ -12 & 0 & -6l & 12 & 0 & -6l \\ 0 & -100 & 0 & 0 & 100 & 0 \\ 6l & 0 & 2l^2 & -6l & 0 & 4l^2 \end{bmatrix} \begin{Bmatrix} \hat{u}_3 \\ \hat{v}_3 \\ \hat{\theta}_3 \\ \hat{u}_4 \\ \hat{v}_4 \\ \hat{\theta}_4 \end{Bmatrix}$$

The element stiffness matrix for spring element 61 is the same as that for spring element 51, but of course, the DOF are \hat{u}_4 and \hat{u}_6 .

From Fig. 17.10(a), the BCs for the assembled frame structure are

$$0 = \hat{u}_1 = \hat{v}_1 = \hat{\theta}_1 = \hat{v}_4 = \hat{\theta}_4 = \hat{u}_5 = \hat{u}_6$$

Deleting the corresponding columns and setting aside the corresponding rows of the *element* stiffness matrices, and then assembling the structure stiffness matrix, produces the final result

$$\begin{Bmatrix} 2F_0 \\ 0 \\ 0 \\ 0 \\ 0 \\ F_0l \\ -F_0 \end{Bmatrix} = \frac{EI_0}{l^3} \begin{bmatrix} 112 & 0 & 6l & -100 & 0 & 0 & 0 \\ 0 & 112 & 6l & 0 & -12 & 6l & 0 \\ 6l & 6l & 8l^2 & 0 & -6l & 2l^2 & 0 \\ -100 & 0 & 0 & 115 & 0 & 6l & -12 \\ 0 & -12 & -6l & 0 & 112 & -6l & 0 \\ 0 & 6l & 2l^2 & 6l & -6l & 8l^2 & -6l \\ 0 & 0 & 0 & -12 & 0 & -6l & 15 \end{bmatrix} \begin{Bmatrix} \hat{u}_2 \\ \hat{v}_2 \\ \hat{\theta}_2 \\ \hat{u}_3 \\ \hat{v}_3 \\ \hat{\theta}_3 \\ \hat{u}_4 \end{Bmatrix}$$

where the vector of generalized forces was again written by calculating the virtual work done by the external forces and moments when each generalized coordinate is, in turn, given a virtual displacement. ■

The above problem is particularly lengthy. None of the exercises are nearly that lengthy. The value of this example is that it provides more of an appreciation for what a commercial FEM digital computer program does routinely for any static load problem. There are two aspects of the above example problem that bear comment. The first comment is that in this small example problem, with its seven DOF in the $\{\hat{q}\}$ vector, it makes little difference in which order the nodes are numbered. The cost of the computer analysis would vary only insignificantly from that of the above analysis if the nodes were numbered in a random order; that is, if the node at the upper spring right-hand end were called node 1, if the node at the bottom of the left post were called node 2, and so on. Such is not the case if the number of DOF of the $\{\hat{q}\}$ vector is several hundred. Then it is cost-effective, to the extent possible, to keep to a numbering scheme where adjacent nodes have adjacent nodal numbers. Such a procedure promotes having the nonzero elements of the stiffness matrix cluster along the main diagonal of the stiffness matrix. This in turn allows for a quicker solution of the simultaneous equations represented by $\{\hat{Q}\} = [\hat{K}]\{\hat{q}\}$. There are commercial subroutines that do nothing but reorder the DOF to make the solution process less costly in terms of computer time.

The second comment is that if the ratio of the beam axial stiffnesses to the beam bending stiffnesses were not just $EA_0/l = 100EI_0/l^3$, but were, say, $EA_0/l = 10\,000EI_0/l^3$, then there would be a marked imbalance in the relative magnitudes of the terms of the $[\hat{K}]$ matrix. Such disparities in the relative stiffnesses of different parts of the structure often leads to

what is called matrix ill-conditioning. Matrix ill-conditioning interferes with the accurate solution of the final matrix equation for the deflection vector $\{\tilde{q}\}$. One way of avoiding such gross disparities and the consequent matrix ill-conditioning is to approximate as rigid those parts of the structure which are relatively much, much stiffer than other parts of the structure. This approach has the added advantage of simplifying the mathematical model. For example, if, in the above example problem, $EA_0/l = 10\,000EI_0/l^3$, then it would be proper to approximate each beam axial stiffness as infinite. Then \hat{v}_2 and \hat{v}_3 would necessarily be zero. It also would be necessary that $\hat{u}_2 \equiv \hat{u}_3$. The consequences of this change upon the above $\{\tilde{Q}\} = [\tilde{K}]\{\tilde{q}\}$ matrix equation can be deduced by going back to the idea of writing a DOF transformation matrix relationship. That is, write the relation that $\{\tilde{q}_{old}\} = [\tilde{T}]\{\tilde{q}_{new}\}$. The details of this transformation relation are as follows:

$$\begin{Bmatrix} \hat{u}_2 \\ \hat{v}_2 \\ \hat{\theta}_2 \\ \hat{u}_3 \\ \hat{v}_3 \\ \hat{\theta}_3 \\ \hat{u}_4 \end{Bmatrix}^{old} = \begin{bmatrix} 1 & 0 & 0 & 0 \\ 0 & 0 & 0 & 0 \\ 0 & 1 & 0 & 0 \\ 1 & 0 & 0 & 0 \\ 0 & 0 & 0 & 0 \\ 0 & 0 & 1 & 0 \\ 0 & 0 & 0 & 1 \end{bmatrix} \begin{Bmatrix} \hat{u}_2 \\ \hat{\theta}_2 \\ \hat{\theta}_3 \\ \hat{\theta}_4 \end{Bmatrix}^{new}$$

Taking the variation of both sides of this equality and transposing matrices leads to $[\delta\tilde{q}_{old}] = [\delta\tilde{q}_{new}][\tilde{T}]^t$. Now write the virtual work expressions

$$\delta W_{ex} = [\delta\tilde{q}_{new}]\{\tilde{Q}_{new}\} = [\delta\tilde{q}_{old}]\{\tilde{Q}_{old}\}$$

Substituting $[\delta\tilde{q}_{old}] = [\delta\tilde{q}_{new}][\tilde{T}]^t$ into the equality $[\delta\tilde{q}_{new}]\{\tilde{Q}_{new}\} = [\delta\tilde{q}_{old}]\{\tilde{Q}_{old}\}$ leads to

$$[\delta\tilde{q}_{new}]\{\tilde{Q}_{new}\} = [\delta\tilde{q}_{new}][\tilde{T}]^t\{\tilde{Q}_{old}\}$$

or

$$\{\tilde{Q}_{new}\} = [\tilde{T}]^t\{\tilde{Q}_{old}\}$$

Similarly, making the substitutions $[\delta\tilde{q}_{old}] = [\delta\tilde{q}_{new}][\tilde{T}]^t$ and $\{\tilde{q}_{old}\} = [\tilde{T}]\{\tilde{q}_{new}\}$ in the internal virtual work expression,

$$\delta W_{in} = -[\delta\tilde{q}_{old}][\tilde{K}_{old}]\{\tilde{q}_{old}\}$$

produces the new structural system stiffness matrix

$$[\tilde{K}_{new}] = [\tilde{T}]^t[\tilde{K}_{old}][\tilde{T}]$$

Thus the details of the new system matrix equation in this situation are

$$\begin{Bmatrix} 2F_0 \\ 0 \\ F_0l \\ -F_0 \end{Bmatrix} = \frac{EI_0}{l^3} \begin{bmatrix} 27 & 6l & 6l & -12 \\ 6l & 8l^2 & 2l^2 & 0 \\ 6l & 2l^2 & 8l^2 & -6l \\ -12 & 0 & -6l & -15 \end{bmatrix} \begin{Bmatrix} \hat{u}_2 \\ \hat{\theta}_2 \\ \hat{\theta}_3 \\ \hat{u}_4 \end{Bmatrix}$$

As a partial check, the (1, 1) term of the new system matrix can be verified by noting that for a nonzero value of \hat{u}_2 , and zero values for the other three DOF, beam 21 and beam 41 each contribute a $(12EI_0/l^3)\hat{u}_2$ resisting force, and spring 51 contributes a $(3EI_0/l^3)\hat{u}_2$ resisting force. Spring 61 contributes nothing since, with the other DOF having zero values, it is not deflected at all. Similarly, with respect to this one term, beam 31 only undergoes a rigid

body motion as an undeformed beam, and thus also does not provide an elastic resisting force.

Note that if there were an externally applied horizontal force F_1 acting to the left at node 3, then the generalized force corresponding to δu_2 , calculated directly from the virtual work expression, would be $(2F_0 - F_1)$ since both concentrated forces would do virtual work in response to such a virtual deflection.

Again, using DOF transformation matrices is a most inefficient use of computer storage space. It is necessary to investigate how the above revised system matrix equation can be written by starting with a FEM model that postulates beam axial rigidity.

Example 17.6. Redo Example 17.5, but this time, from the beginning of the analysis, model the beam axial stiffnesses as being infinite, that is, let the beams be axially rigid.

Solution. Referring to Fig. 17.10(b), axial rigidity and the BCs in this case mean from the beginning that $\hat{v}_1 = \hat{v}_2 = \hat{v}_3 = \hat{v}_4 = 0$. In other words, instead of saying that the stiffness is infinite, what is stated mathematically is that the deflections \hat{v}_2 and \hat{v}_3 are zero. Omitting these four DOF from the element matrix equations (i.e., deleting their rows and corresponding columns) leads to the following truncated element stiffness matrices for beams 21 and 41 in terms of the remaining global DOF

$$\{Q^{(21)}\} = \frac{EI_0}{l^3} \begin{bmatrix} 12 & -6l & -12 & -6l \\ -6l & 4l^2 & 6l & 2l^2 \\ -12 & 6l & 12 & 6l \\ -6l & 2l^2 & 6l & 4l^2 \end{bmatrix} \begin{Bmatrix} \hat{u}_1 \\ \hat{\theta}_1 \\ \hat{u}_2 \\ \hat{\theta}_2 \end{Bmatrix}$$

$$\{Q^{(41)}\} = \frac{EI_0}{l^3} \begin{bmatrix} 12 & 6l & -12 & 6l \\ 6l & 4l^2 & -6l & 2l^2 \\ -12 & -6l & 12 & -6l \\ 6l & 2l^2 & -6l & 4l^2 \end{bmatrix} \begin{Bmatrix} \hat{u}_2 \\ \hat{\theta}_3 \\ \hat{u}_4 \\ \hat{\theta}_4 \end{Bmatrix}$$

Note that because beam element 31 is axially rigid, DOF \hat{u}_2 replaces \hat{u}_3 in the matrix equation for element 41 in order to have only independent DOF in the final equations. For beam 31 there are only two nonzero global DOF, and after deleting the other four rows and columns, the condensed element stiffness matrix is

$$\{Q^{(31)}\} = \frac{EI_0}{l^3} \begin{bmatrix} 4l^2 & 2l^2 \\ 2l^2 & 4l^2 \end{bmatrix} \begin{Bmatrix} \hat{\theta}_2 \\ \hat{\theta}_3 \end{Bmatrix}$$

The two spring matrix equations are unaffected by the change in the modeling of the beams. Their truncated element matrix equations in terms of the global DOF remain as

$$\{Q^{(51)}\} = \frac{EI_0}{l^3} \begin{bmatrix} +3 & -3 \\ -3 & +3 \end{bmatrix} \begin{Bmatrix} \hat{u}_3 \\ \hat{u}_5 \end{Bmatrix}$$

and

$$\{Q^{(61)}\} = \frac{EI_0}{l^3} \begin{bmatrix} +3 & -3 \\ -3 & +3 \end{bmatrix} \begin{Bmatrix} \hat{u}_4 \\ \hat{u}_6 \end{Bmatrix}$$

Assembling the $\{\hat{Q}\} = [\hat{K}]\{\hat{q}\}$ system matrix equation is done in the usual way. Care must be exercised in the placement of the individual terms of the first row and first column of the beam 41 element stiffness matrix since the corresponding global DOF is \hat{u}_2 , not \hat{u}_3 .

accomplished by equating the element DOF to the corresponding global or structure's DOF, and then physically placing the element stiffness matrix entries in the rows and columns of the structure's stiffness matrix that correspond to the global DOF. In this way the stiffnesses of all the elements are added at each node to which an element is connected. The generalized force vector is detailed by calculating the virtual work done by all the applied loads when each DOF in turn is given a virtual displacement while all other DOF are fixed. The next to last step in the static load analyses discussed here is the introduction of the deflection boundary conditions. When the deflection BCs are zero values for certain DOF, then the introduction of those BCs eliminates columns of the global stiffness matrix $[\hat{K}]$. When the corresponding rows of $[\hat{K}]$ are also set aside in order to later calculate the support reactions, the result is the square matrix $[\hat{K}]$. Now there are as many equations as there are unknown nodal deflections, and the simultaneous solution of those equations can be accomplished in any number of ways. The solution for the nodal deflections permits the calculation of the stresses or stress resultants in any of the finite elements used to model the structure. The following example problems illustrate the above outlined procedure in its totality.

Example 17.7. In the introductory study of structural vibrations, the mathematical models of the simple structures to be analyzed are often such that the stiffness properties of the structure are exclusively represented by springs, while the distributed mass of the structure (much like applied, distributed loads) is concentrated into discrete (lumped), rigid masses. In other words, all the structure's elastic properties are concentrated in the massless springs, while all the structure's mass properties are concentrated in the inflexible masses. A typical simple model is shown in Fig. 17.11(a). In this case there are no externally applied loads, so the vibration of this structure is called *free vibration*, as in "free of applied loads or natural vibration." The free vibration analysis of this structure requires the use of the structural mass matrix and the same structural stiffness matrix that is used for static analyses. It is, of course, that same stiffness matrix that is the focus of our attention here. In order to focus upon the stiffness matrix, consider the following static load problem: (a) If a static, horizontal force of magnitude F , acting to the right, is applied to node 2 (mass m_1), use the finite element model of Fig. 17.11(b) in order to determine the form of the structural stiffness matrix equation; and (b) calculate the forces in each of the four springs in response to the applied load F .

Solution. (a) The five structural DOF, \hat{u}_1 through \hat{u}_5 are shown in Fig. 17.11(b). Each spring element stiffness matrix has the form

$$[k_i] = \begin{bmatrix} +k_i & -k_i \\ -k_i & +k_i \end{bmatrix} \quad \text{where } i = 1, 2, 3, 4, 5$$

Writing the virtual work expression in terms of the global DOF, and assembling the global stiffness matrix from the five individual element stiffness matrices, that is, using the element stiffness matrices to connect global DOF, leads to

$$\{Q\} = [R \quad F \quad R \quad 0 \quad R]$$

and

$$[\hat{K}\{\hat{q}\}] = \begin{bmatrix} +k_1 & -k_1 & & & \\ -k_1 & k_1 + k_2 + k_3 & -k_2 & -k_3 & \\ & -k_2 & +k_2 & & \\ & -k_3 & & k_3 + k_4 & -k_4 \\ & & & -k_4 & +k_4 \end{bmatrix} \begin{Bmatrix} \hat{u}_1 \\ \hat{u}_2 \\ \hat{u}_3 \\ \hat{u}_4 \\ \hat{u}_5 \end{Bmatrix}$$

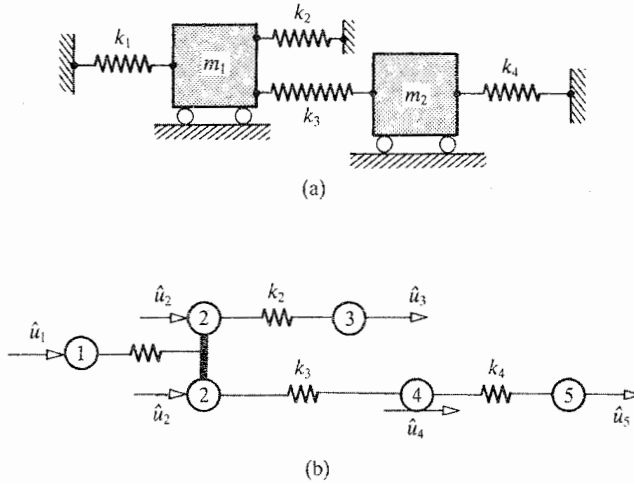


Figure 17.11. Example 17.7. (a) A common vibration analysis mathematical model of a structure where the mass and elasticity of the structure have been separately concentrated in discrete mass and spring elements. (b) The finite element model of the same structure.

Insertion of the boundary conditions that $\hat{u}_1 = \hat{u}_3 = \hat{u}_5 = 0$ leads to the following structural stiffness matrix relation

$$\{\tilde{Q}\} = [\tilde{K}]\{\tilde{q}\} \quad \text{or} \quad \begin{Bmatrix} F \\ 0 \end{Bmatrix} = \begin{bmatrix} k_1 + k_2 + k_3 & -k_3 \\ -k_3 & k_3 + k_4 \end{bmatrix} \begin{Bmatrix} \hat{u}_2 \\ \hat{u}_4 \end{Bmatrix}$$

where, again, $Q_1 = F$ and $Q_2 = 0$ are obtained from calculating the external virtual work done by all the applied loads (just F in this case) during separate virtual deflections δu_2 and δu_4 while all other virtual deflections are zero.

(b) The above global stiffness matrix equation can be solved to obtain the following two positive solutions:

$$\hat{u}_2 = \frac{F(k_3 + k_4)}{k_0^2} \quad \hat{u}_4 = \frac{Fk_3}{k_0^2}$$

where

$$k_0^2 = (k_1 + k_2 + k_3)(k_3 + k_4) - k_3^2 = (k_1 + k_2)(k_3 + k_4) + k_3k_4$$

Substituting these two solutions (and the BCs) into the element stiffness matrices provides the solutions for the spring forces, f_i . Those solutions are

$$\begin{aligned} f_1 &= F \frac{k_1(k_3 + k_4)}{k_0^2} & f_2 &= -F \frac{k_2(k_3 + k_4)}{k_0^2} \\ f_3 &= -F \frac{k_3k_4}{k_0^2} & f_4 &= -F \frac{k_3k_4}{k_0^2} \end{aligned}$$

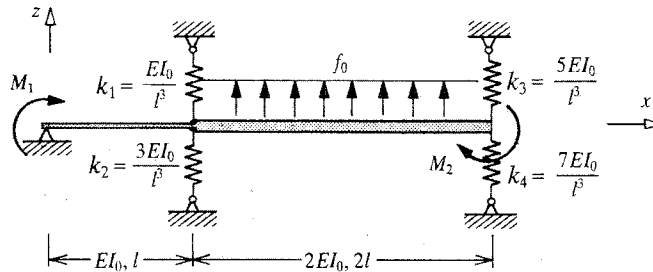
Clearly, each spring only shoulders a portion of the total applied force F . Furthermore, equilibrium requires that the static forces in springs 3 and 4 be equal. ■

Example 17.8.

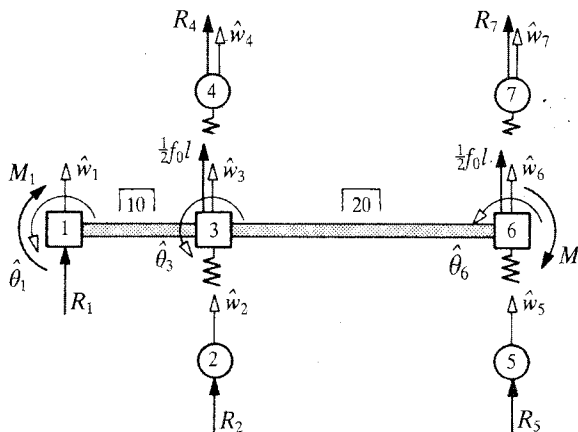
- Create a finite element structural model from the mathematical structural model shown in Fig. 17.12(a). Use the fewest possible number of finite elements.
- Set up the global finite element matrix equation $\{\hat{Q}\} = [\hat{K}]\{\hat{q}\}$, the relation that can be used to solve for the unconstrained global DOF. For this purpose, let $k_1 = EI_0/L^3$, $k_2 = 3EI_0/L^3$, $k_3 = 5EI_0/L^3$, $k_4 = 7EI_0/L^3$.
- Given the solution to the global matrix equation, determine all the reactions.
- Determine the algebraic expressions for the bending stresses everywhere in the right-hand beam in terms of the beam spatial coordinates x and z .

Solution. (a) Figure 17.12(b) shows the simplest finite element model that can be used with this structure and loading. The model could be refined by replacing beam element 20 by two or more beam elements and proportioning the distributed load accordingly. Since beam element 10 is unloaded over its length, no advantage is obtained by replacing it by more than one beam element. The simple model of Fig. 17.12(b) is used in this example.

(b) The stiffness matrices for the springs and beam element 10 are the standard element stiffness matrices. The stiffness matrix for beam element 20 has to be altered to account for



(a)



(b)

Figure 17.12. Example 17.8. (a) The mathematical model. (b) The finite element model showing the global generalized coordinates, the applied loading, and the support reactions.

the fact that the stiffness coefficient is $2EI_0$ rather than just EI_0 and the length is $2L$ rather than just L . Note that $2L$ must replace L in the bending stiffness matrix template inside the matrix as well as in the EI/L^3 factor outside the matrix. As would be expected, the longer the beam, the less stiff the beam. The beam element 20 stiffness matrix is

$$\{k_{20}\}\{q^{(20)}\} = \frac{EI_0}{L^3} \begin{bmatrix} 24/8 & 12L/4 & -24/8 & 12L/4 \\ 12L/4 & 8L^2/2 & -12L/4 & 4L^2/2 \\ -24/8 & -12L/4 & 24/8 & -12L/4 \\ 12L/4 & 4L^2/2 & -12L/4 & 8L^2/2 \end{bmatrix} \{q^{(20)}\}$$

The assembly of the two beam stiffness matrices and the four spring stiffness matrices leads to the following 10×10 system stiffness matrix $[\hat{K}]$ and deflection vector $\{\hat{q}\}$

$$\frac{EI_0}{L^3} \begin{bmatrix} 12 & 6l & & -12 & 6L & & & & & & \\ 6L & 4L^2 & & -6L & 2L^2 & & & & & & \\ & & 3 & -3 & & & & & & & \\ -12 & -6L & -3 & 19 & -3L & -1 & & -3 & 3L & & \\ 6L & 2L^2 & & -3L & 8L^2 & & & -3L & 2L^2 & & \\ & & & -1 & & 1 & & & & & \\ & & & & & & 7 & -7 & & & \\ & & & -3 & -3L & & -7 & 15 & -3L & -5 & \\ & & & 3L & 2L^2 & & & -3L & 4L^2 & & \\ & & & & & & & -5 & & 5 & \end{bmatrix} \begin{Bmatrix} \hat{w}_1 \\ \hat{\theta}_1 \\ \hat{w}_2 \\ \hat{w}_3 \\ \hat{\theta}_3 \\ \hat{w}_4 \\ \hat{w}_5 \\ \hat{w}_6 \\ \hat{\theta}_6 \\ \hat{w}_7 \end{Bmatrix}$$

The virtual work equation for this structure is

$$\begin{aligned} \delta W = R_1 \delta \hat{w}_1 - M_1 \delta \hat{\theta}_1 + R_2 \delta \hat{w}_2 + \frac{1}{2} f_0 L \delta \hat{w}_3 + 0 \delta \hat{\theta}_3 + R_4 \delta \hat{w}_4 \\ + R_5 \delta \hat{w}_5 + \frac{1}{2} f_0 L \delta \hat{w}_6 - M_2 \delta \hat{\theta}_6 + R_7 \delta \hat{w}_7 \end{aligned}$$

After inserting the BCs $\hat{w}_1 = \hat{w}_2 = \hat{w}_4 = \hat{w}_5 = \hat{w}_7 = 0$, eliminating the corresponding columns of $[\hat{K}]$, and setting aside the corresponding rows, the global stiffness matrix equation is

$$\begin{Bmatrix} -M_1 \\ \frac{1}{2} f_0 L \\ 0 \\ \frac{1}{2} f_0 L \\ -M_2 \end{Bmatrix} = \frac{EI_0}{L^3} \begin{bmatrix} 4L^2 & -6L & 2L^2 & 0 & 0 \\ -6L & 19 & -3L & -3 & -3L \\ 2L^2 & -3L & 8L^2 & -3L & 2L^2 \\ 0 & -3 & -3L & 15 & -3L \\ 0 & 3L & 2L^2 & -3L & 4L^2 \end{bmatrix} \begin{Bmatrix} \hat{\theta}_1 \\ \hat{w}_3 \\ \hat{\theta}_3 \\ \hat{w}_6 \\ \hat{\theta}_6 \end{Bmatrix}$$

In order to obtain a digital computer solution to this set of five simultaneous equations, let the magnitude of the applied moment M_1 be $(1/4)f_0L^2$, and that of the applied moment M_2 be $(1/5)f_0L^2$. Furthermore, in order to have a stiffness matrix that contains only numerical values, divide the first, third, and fifth of the above simultaneous equations by L , and factor out an L from the first, third, and fifth columns, placing this latter L into the DOF vector. In this way the rotation DOF are now multiplied by L , and $[\tilde{Q}] = f_0L[-1/4 \ 1/2 \ 0 \ 1/2 \ -1/5]$. Then the solution, which is temporarily stated to seven significant figures for the purpose of retaining numerical accuracy in the remaining calculations, is

$$[\tilde{q}] = \frac{f_0L^3}{EI_0} [-0.0163 \ 1944 \ 0.0506 \ 2501L \ 0.0595 \ 139 \ 0.0374 \ 3056L \ -0.0896 \ 5279]$$

(c) Retrieving the set aside rows, the solution for the reactions is

$$\begin{Bmatrix} R_1 \\ R_2 \\ R_4 \\ R_5 \\ R_7 \end{Bmatrix} = \frac{EI_0}{L^3} \begin{bmatrix} 6L & -12 & 6L & 0 & 0 \\ 0 & -3 & 0 & 0 & 0 \\ 0 & -1 & 0 & 0 & 0 \\ 0 & 0 & 0 & -7 & 0 \\ 0 & 0 & 0 & -5 & 0 \end{bmatrix} \frac{f_0 L^3}{EI_0} \begin{Bmatrix} -0.0163 \ 1944 \\ 0.0506 \ 2501L \\ 0.0595 \ 1390 \\ 0.0374 \ 3056L \\ -0.0896 \ 5279 \end{Bmatrix}$$

Multiplication of the two matrices of the above right-hand side yields

$$[R] = f_0 L [-0.35 \quad -0.15 \quad -0.05 \quad -0.26 \quad -0.19]$$

where the negative signs indicate that all five reactions are directed downward. Note that the sum of the five reactions is $-f_0 L$, as is should be.

(d) One way of calculating the stress at any point (x, z) of beam element 20 is to first calculate the shearing forces and moments at the ends of the beam element. This first step may be accomplished by returning to the element 20 stiffness matrix set forth at the beginning of part (b) of this example problem. Substituting the appropriate global DOF for the element DOF yields

$$\begin{Bmatrix} V_1 \\ M_1 \\ V_2 \\ M_2 \end{Bmatrix}^{(20)} = \frac{EI_0}{L^3} \begin{bmatrix} 24/8 & 12L/4 & -24/8 & 12L/4 \\ 12L/4 & 8L^2/2 & -12L/4 & 4L^2/2 \\ -24/8 & -12L/4 & 24/8 & -12L/4 \\ 12L/4 & 4L^2/2 & -12L/4 & 8L^2/2 \end{bmatrix} \begin{Bmatrix} \hat{w}_3 \\ \hat{\theta}_3 \\ \hat{w}_6 \\ \hat{\theta}_6 \end{Bmatrix}$$

The bending moment at any place along the length of the beam element can be calculated in terms of the element 20 generalized forces as $M(x) = xV_1 - M_1 = M_2 + (2L - x)V_2$. Then, from Chapter 9, the stress is simply $\sigma_{xx} = -zM(x)/I_{yy}$.

A second way of calculating the stress at any point (x, z) in beam element 20 is to return to the derivation of the beam bending finite element, and recall that

$$\begin{aligned} \sigma_{xx} &= -zEw''(x) = -z \left(\frac{E}{l^2} \right) \left[N'' \left(\frac{x}{l} \right) \right] \{q\} \\ &= -z \frac{E}{l^2} \left[\left[12 \left(\frac{x}{l} \right) - 6 \right] \quad l \left[6 \left(\frac{x}{l} \right) - 4 \right] \quad - \left[12 \left(\frac{x}{l} \right) - 6 \right] \quad l \left[6 \left(\frac{x}{l} \right) - 2 \right] \right] \{q\} \end{aligned}$$

where, here $l = 2L$, and as above, the element DOF are replaced by the appropriate global DOF. This second approach requires many fewer multiplications, but the first approach may be easier to remember. ■

The preceding problems involving the bending of beam frames and the bending and twisting of beam grids were both lengthier and more extensive than they had to be as hand work. This was so because (i) the transition from element to system degrees of freedom occupied attention; and (ii) following the usual programming choice, the deflection boundary conditions were not entered into the problem solution until the next to last step. Since the emphasis is presently on hand calculations for the purpose of understanding processes followed by commercial finite element programs, and since all the basics of the solution process have been covered, it is time to become more efficient writing out these solutions. From this point on, for these hand calculations, the global generalized coordinates and their associated boundary conditions are entered into the individual element equations as

soon as possible. Hence the element generalized coordinates do not appear again in setting up the $\{Q\} = [K]\{q\}$ global equations. Therefore, as a matter of notation, for the sake of efficiency, it is no longer necessary to place circumflexes on the system degrees of freedom to distinguish them from the element degrees of freedom, and the tildes can be dropped from the final stiffness matrix equation. When these simplifications are adopted, then writing $\{Q\} = [K]\{q\}$ for small structural system can be done efficiently and relatively quickly after a bit of practice.

The next example problem follows the above shortcuts, and also deals with one of the frequently occurring remaining complications that often arise in finite element modeling. That complication is the modeling of very stiff bending elements. Previously, in recognition of the fact that the axial extension stiffnesses of beams are very much greater than their lateral bending stiffnesses, it was decided to routinely model beams as axially rigid whenever beam bending and extension occur in the same structure. In the same spirit, consider a beam element that has a length L , and another with a length $(L/10)$. Since stiffness is a measure of required force per given deflection, and since, for example, the relationship between a lateral concentrated force at the midspan of a simply supported beam and the lateral deflection at the same point is $F = (48EI/L^3)w(L/2)$, or for another example, the relationship between the lateral tip deflection of a cantilevered beam and the lateral tip force is $F = (3EI/L^3)w(L)$, it is clear that the beam whose length is one-tenth that of the other beam is, in the case of such loadings, one thousand times stiffer. With other loadings, the difference is even greater. Hence, to avoid ill-conditioning in large stiffness matrices, beams that are a lot shorter than others are routinely modeled as rigid. That is done in the next example. Other complications that have yet to be addressed are enforced deflections and equivalent loads due to temperature changes. These are simpler matters, left to Chapter 18.

Example 17.9. Write the stiffness matrix equation $\{Q\} = [K]\{q\}$ for the elongated beam grid shown in Fig. 17.13. Let $GJ = \frac{1}{2}EI$. Note that, for convenience, the directions of the system generalized coordinates have been chosen to be in agreement with the beam element degree of freedom sign convention.

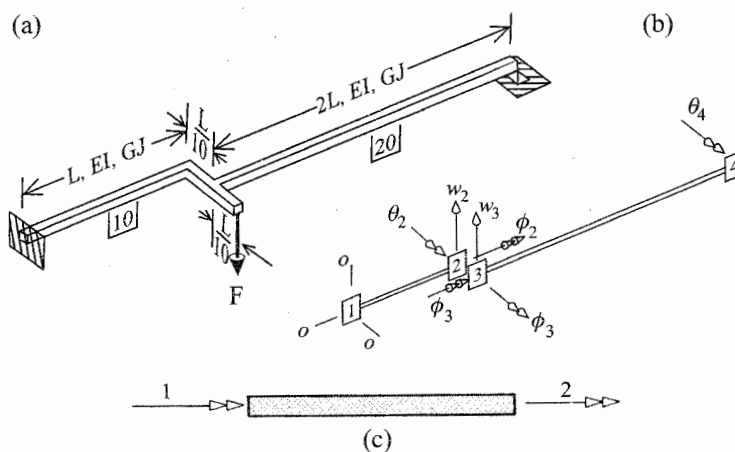


Figure 17.13. Example 17.9. (a) analysis model. (b) finite element model. (c) Reminder of the finite element sign convention for beam/bar twisting.

Solution. After applying the fixed boundary conditions at node one, the bending portion of the beam ten stiffness matrix is the two by two matrix equation

$$[k_{10}]\{q\} = \frac{EI}{L^3} \begin{bmatrix} 12 & -6L \\ -6L & 4L^2 \end{bmatrix} \begin{Bmatrix} w_2 \\ \theta_2 \end{Bmatrix}$$

After application of the boundary condition that ϕ one equals zero, the twisting matrix equation reduces to the 1×1 matrix equation $[k_{10}]\{q\} = (GJ/L)[+1]\{\phi_2\} = \frac{1}{2}(EI/L^3)[+L^2]\{\phi_2\}$. Combining these two matrices yields

$$[k_{10}]\{q\} = \frac{EI}{L^3} \begin{bmatrix} 12 & -6L & 0 \\ -6L & 4L^2 & 0 \\ 0 & 0 & 0.5L^2 \end{bmatrix} \begin{Bmatrix} w_2 \\ \theta_2 \\ \phi_2 \end{Bmatrix}$$

After entering $2L$ for every L in the standard beam bending matrix template, and combining the bending and twisting matrices as above, the result is

$$[k_{20}]\{q\} = \frac{EI}{L^3} \begin{bmatrix} 1.5 & 1.5L & 0 & 1.5L \\ 1.5L & 2L^2 & 0 & L^2 \\ 0 & 0 & 0.25L^2 & 0 \\ 1.5L & L^2 & 0 & 2L^2 \end{bmatrix} \begin{Bmatrix} w_3 \\ \theta_3 \\ \phi_3 \\ \theta_4 \end{Bmatrix}$$

where the support symbol at node four is meant to indicate a simple support where the beam end can neither deflect laterally nor twist, but can have a bending slope. Now the task is to introduce the (short beam) rigid link between beams 10 and 20. Modeling that short beam as rigid creates a relationship between the degrees of freedom at node 2 and those at node 3. Since the beam 10 matrix is slightly smaller, choose to replace the node 2 DOF with those at node 3. From the geometry of that connection, $w_2 = w_3 + 0.1L\phi_3$, $\theta_2 = \theta_3$, $\phi_2 = \phi_3$, so

$$\begin{Bmatrix} w_2 \\ \theta_2 \\ \phi_2 \end{Bmatrix} = \begin{bmatrix} 1 & 0 & 0.1L \\ 0 & 1 & 0 \\ 0 & 0 & 1 \end{bmatrix} \begin{Bmatrix} w_3 \\ \theta_3 \\ \phi_3 \end{Bmatrix}$$

Writing the above DOF transformation as $\{q_2\} = [T]\{q_3\}$, and recalling Eq. (17.14),

$$\delta U = [\delta q_2][k_{10}]\{q_2\} = [\delta q_3][T]^t[k_{10}][T]\{q_3\} = [\delta q_3][k_{10}]\{q_3\}$$

which shows that in order to associate the beam 10 stiffness matrix with the node 3 generalized coordinates, the original matrix must be premultiplied by the transpose of the transformation matrix, and postmultiplied by the transformation matrix. Note that the result must also be a symmetric matrix. Doing that matrix multiplication is a simple matter, and the result is

$$[k_{10}]\{q\} = \frac{EI}{L^3} \begin{bmatrix} 12 & -6L & 1.2L \\ -6L & 4L^2 & -0.6L^2 \\ 1.2L & -0.6L^2 & 0.62L^2 \end{bmatrix} \begin{Bmatrix} w_2 \\ \theta_2 \\ \phi_2 \end{Bmatrix}$$

Writing the generalized force vector from a virtual work calculation, and assembling the beam 10 and beam 20 stiffness matrices, produce the final result

$$\begin{Bmatrix} -F \\ 0 \\ 0.1FL \\ 0 \end{Bmatrix} = \frac{EI}{L^3} \begin{bmatrix} 13.5 & -4.5L & 1.2L & 1.5L \\ -4.5L & 6L^2 & -0.6L & L^2 \\ 1.2L & -0.6L & 0.87L^2 & 0 \\ 1.5L & L^2 & 0 & 2L^2 \end{bmatrix} \begin{Bmatrix} w_3 \\ \theta_3 \\ \phi_3 \\ \theta_4 \end{Bmatrix}$$

Of course, when a commercial finite program is used, all the analyst has to do is either code a rigid link between nodes 2 and 3, or code the relationship between the DOF. Then the program does the rest with no further effort on the part of the analyst. ■

The new aspect of the following example is that it shows how to deal with beams for which I_{yz} is not zero. Another worthwhile aspect of this example is the further treatment of a more extensive case involving a rigid finite element.

Example 17.10. Consider the two-beam structure of Fig. 17.14. Each of the identical beams is of length L . The cross-sectional properties of each beam are $I_{yy} = 3I_0$, $I_{zz} = 2I_0$, $I_{yz} = I_0$, and $GJ = EI_0$. As Fig. 17.14 shows, the tips of the cantilevered beams are connected by a thin plate that is relatively rigid in its own plane, but offers insufficient resistance by its own bending or twisting to link the bending slope degrees of freedom θ_1 to θ_2 , or ψ_1 to ψ_2 . However, preliminarily assume that the thin plate does not buckle, with the result that the beam tip y and z direction lateral deflections and ϕ_1 and ϕ_2 are linked together. Write the final finite element matrix equation for this structural system.

Comment. When a beam element is bent in both the x, y plane and the x, z plane, then the same 4×4 beam element bending stiffness matrix needs to be used for both planes with their respective generalized coordinates and respective area moments of inertia. Thus, when the y and z axes are principal axes, as has been the case in all the previous examples, the 8×8 stiffness matrix for this beam element has the form

$$\begin{bmatrix} (EI_{zz}^*/L^3)[k'] & [0] \\ [0] & (EI_{yy}^*/L^3)[k'] \end{bmatrix} \begin{Bmatrix} q_{z \text{ plane}} \\ q_{y \text{ plane}} \end{Bmatrix}$$

where $[k']$ is meant to represent just the 4×4 element bending matrix without its pre-multiplying stiffness factor. From either using the full bending strain equation $\epsilon_{xx} = -yw''(x) - zw''(x)$ in Eq. (17.7) or from Ref. [72], p. 125, when the y and z axes are *not* principal axes, the above 8×8 stiffness matrix is modified by replacing both off-diagonal

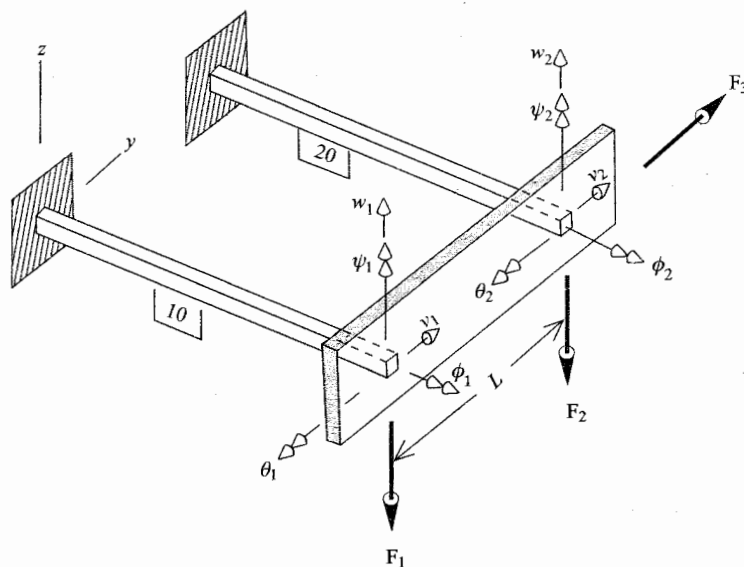


Figure 17.14. Example 17.10.

transformation matrix between the ten constrained generalized coordinates and the seven unconstrained DOF is

$$\begin{Bmatrix} w_1 \\ \theta_1 \\ v_1 \\ \psi_1 \\ \phi_1 \\ w_2 \\ \theta_2 \\ v_2 \\ \psi_2 \\ \phi_2 \end{Bmatrix} = \begin{bmatrix} 0 & 0 & 1 & 0 & 0 & 0 & -L \\ 1 & 0 & 0 & 0 & 0 & 0 & 0 \\ 0 & 0 & 0 & 0 & 1 & 0 & 0 \\ 0 & 1 & 0 & 0 & 0 & 0 & 0 \\ 0 & 0 & 0 & 0 & 0 & 0 & 1 \\ 0 & 0 & 1 & 0 & 0 & 0 & 0 \\ 0 & 0 & 0 & 1 & 0 & 0 & 0 \\ 0 & 0 & 0 & 0 & 1 & 0 & 0 \\ 0 & 0 & 0 & 0 & 0 & 1 & 0 \\ 0 & 0 & 0 & 0 & 0 & 0 & 1 \end{bmatrix} \begin{Bmatrix} \theta_1 \\ \psi_1 \\ w_2 \\ \theta_2 \\ v_2 \\ \psi_2 \\ \phi_2 \end{Bmatrix}$$

or $\{q_{unc}\} = [T]\{q_{con}\}$, where the zeros have been entered to just aid in locating the few nonzero terms. Recognizing that the bottom right 5×5 submatrix is an identity matrix, as it should be, simplifies the matrix multiplication. The next step is to form the triple matrix product $[T]^t[k][T]$, which yields the symmetric 7×7 system matrix incorporating the rigid element at the beam tips. This requires a few minutes, but it is not at all difficult to do by hand. The result is

$$\frac{EI_0}{L^3} \begin{bmatrix} 12L^2 & 4l^2 & -18L & & 6L & & 18L^2 \\ 4L^2 & 8L^2 & -6L & & -12L & & 6L^2 \\ -18L & -6L & 72 & -18L & 24 & -6L & -36L \\ & & -18L & 12L & -6L & 4L^2 & \\ -6L & -12L & 24 & -6L & 48 & -12L & -12L \\ & & -6L & 4L^2 & -12L & 8L^2 & \\ 18L^2 & 6L^2 & -36L & & -12L & & 38L^2 \end{bmatrix} \begin{Bmatrix} \theta_1 \\ \psi_1 \\ w_2 \\ \theta_2 \\ v_2 \\ \psi_2 \\ \phi_2 \end{Bmatrix}$$

Now every degree of freedom is coupled to every other degree of freedom. The last step is to acquire the corresponding generalized force vector by writing the expression for the virtual work. Again, the generalized force vector corresponding to the 7×1 coordinate vector can be developed directly from the external virtual work expression if the three equations of constraint are kept in mind. A less thoughtful and lengthier alternative way of doing this is to first write the virtual work expression in terms of the ten unconstrained generalized coordinates, and then make the above transformation to the constrained generalized coordinates. That is,

$$\delta W = [\delta q_{unc}]\{Q_{unc}\} = [\delta q_{con}][T]^t\{Q_{con}\}$$

The transpose of the 10×1 , unconstrained generalized force vector is

$$\{Q_{unc}\}^t = [-F_1 \quad 0 \quad 0 \quad 0 \quad 0 \quad -F_2 \quad 0 \quad F_3 \quad 0 \quad 0]$$

After the $[T]^t\{Q_{con}\}$ multiplication, the result for the seven-by-one system generalized force vector is

$$\{Q_{con}\} = [0 \quad 0 \quad -(F_1 + F_2) \quad 0 \quad F_3 \quad 0 \quad LF_1]$$

At this point all the components of the force-deflection interaction of the structural system model are fully described. ■

Chapter 17 Exercises

- 17.1. Identify two different sets of generalized coordinates for:
- A pair of rigid scissors lying flat on a table top.
 - A bird with a rigid body of finite dimensions to which two rigid wings are hinged as a door is hinged to a door frame.
 - The three rigid links of Fig. 17.1(e) moving in a plane if the two ends of the three-piece system are constrained to move along a single, horizontal straight line.
 - A rigid bead moving along a rigid wire with an arbitrary shape in three-dimensional space.
 - The rigid hour hand of an otherwise rigid watch on a person's wrist if the hour hand is disconnected from its drive mechanism.
 - The three links of part (c) if each end of the three links is constrained to move along one of two closeby parallel lines.
- 17.2. (a) Use matrix algebra and the known torque-twist relation $\phi = M_l l / GJ$ to show that the matrix stiffness equation for the twisting of a uniform bar with the sign convention of Fig. 17.9(c) is

$$\begin{Bmatrix} M_{l1} \\ M_{l2} \end{Bmatrix} = \frac{GJ}{l} \begin{bmatrix} +1 & -1 \\ -1 & +1 \end{bmatrix} \begin{Bmatrix} \phi_1 \\ \phi_2 \end{Bmatrix}$$

- What would be the finite element discretization of a linearly distributed, lateral force per unit length which had the value f_0 at the left end of the beam bending finite element, and the value zero at the right end of the beam bending finite element of length l ?
 - Why are all the entries along the main diagonal of any stiffness matrix, global or element, always positive quantities?
- 17.3. (a) Starting with the mathematical model of the structure shown in Fig. 17.15(a), establish a corresponding finite element model using the minimum number of finite elements that allows a description of the essential features of the structure and loading. Select nodes and global DOF that apply to the unconstrained structure.

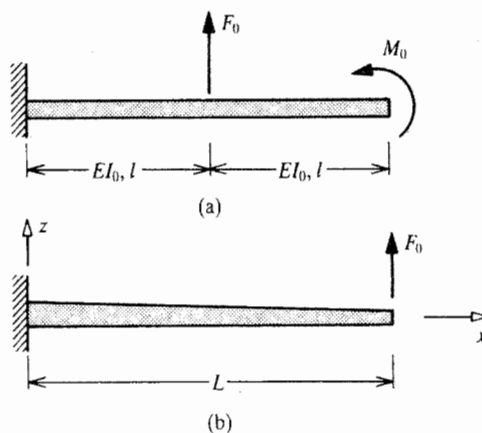


Figure 17.15. Exercise 17.3. Mathematical models to be converted to finite element models.

- (b) As above, for the structural mathematical model shown in Fig. 17.15(b), where the beam stiffness coefficient decreases uniformly from $5EI_0$ at $x = 0$ to $1EI_0$ at $x = L$.
- (c) Consider a uniform, linearly elastic, homogeneous beam of length $2L$ that is clamped at $x = 0$ and at $x = 2L$. Let a lateral concentrated force of magnitude F_0 act at $x = L$. Set up an appropriate FEM mathematical model for this beam structure and write the final matrix equation $\{\tilde{Q}\} = [\tilde{K}]\{\tilde{q}\}$.
- (d) Repeat the above problem, but this time modify the structure by inserting a frictionless hinge at $x = L$. *Hint:* At the node at the hinge there is one global lateral deflection, but since there is no continuity of bending slopes at the hinge, there are two bending slope rotations, one for each beam end adjacent to the hinge.
- 17.4.** Use the indicated finite element model, if given, or select a FEM model with the fewest possible DOF for each of the structures cited below, and then write the global matrix equation $\{\tilde{Q}\} = [\tilde{K}]\{\tilde{q}\}$. If necessary, replace the distributed loads by the simplest possible statically equivalent concentrated forces.
- (a) The structure sketched in Fig. 17.16.
- (b) The structure sketched in Fig. 17.17.
- (c) The structure sketched in Fig. 17.18.
- (d) The structure sketched in Fig. 17.19, where $GJ_0 = \beta EI_0$.
- (e) The structure of Fig. 17.20, each beam length is L .
- (f) The structure of Fig. 17.21(a).
- (g) The structure of Fig. 21.27.
- (h) The structure of Fig. 21.6.
- (i) The structure of Fig. 20.7(a).
- (j) The structure of Fig. 20.20.
- (k) The structure of Fig. 21.9(a).
- (l) The structure of Fig. 21.22(a).
- (m) The structure of Fig. 21.11(a).
- (n) The structure of Fig. 21.2.
- (o) The structure of Fig. 21.30, where the FEM model is as shown in Fig. 17.21. Again let $GJ_0 = \beta EI_0$.
- (p) The structure of Example 17.4, but this time let beam 21 have a length $2L$ and stiffness coefficients $2EI_0$ and $2GJ_0$, while beam 22 has a length L and stiffness coefficients EI_0 and GJ_0 . Let $GJ_0 = \frac{1}{2}EI_0$.
- 17.5.** (a) Consider the FEM model of the planar, two-story frame structure sketched in Fig. 17.22. If the axial stiffnesses of all beams and columns are modeled as being infinite, then choose appropriate DOF for this FEM model. Do *not* develop the stiffness matrix for this structure.
- (b) Select a FEM mathematical model for the structure shown in Fig. 21.12, which uses two beam elements each of length l for the horizontal beam. Model each of the three beam elements as being axially rigid. Then write the structure matrix equation $\{\tilde{Q}\} = [\tilde{K}]\{\tilde{q}\}$.
- (c) Reconsider the portal frame of Fig. 17.10(a). In this case, delete both spring elements, and clamp the right-hand column foot as well as the left-hand column foot. Use \hat{u}_2 , $\hat{\theta}_2$, and $\hat{\theta}_3$ as the generalized coordinates. If all axial stiffnesses are infinite, what then is the matrix $[\tilde{K}]$?
- (d) Redo Example 17.6, but this time have all the horizontal DOF positive to the left.

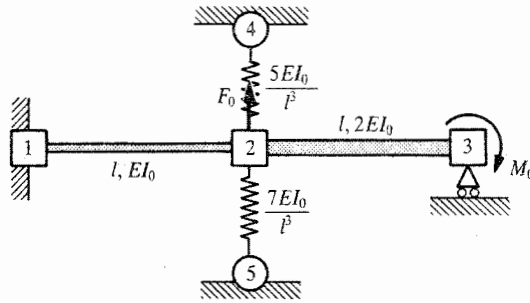


Figure 17.16. Exercise 17.4(a). A partial finite element model.

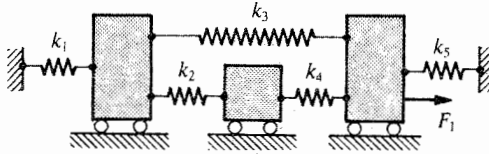
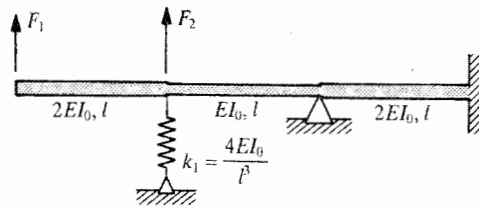
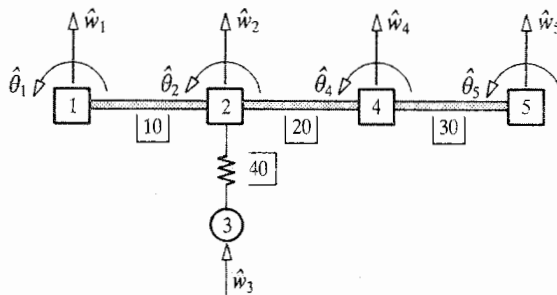


Figure 17.17. Exercise 17.4(b). A partial finite element model involving linear springs and rigid masses.



(a)



(b)

Figure 17.18. Exercise 17.4(c). (a) An analysis model. (b) A finite element model.

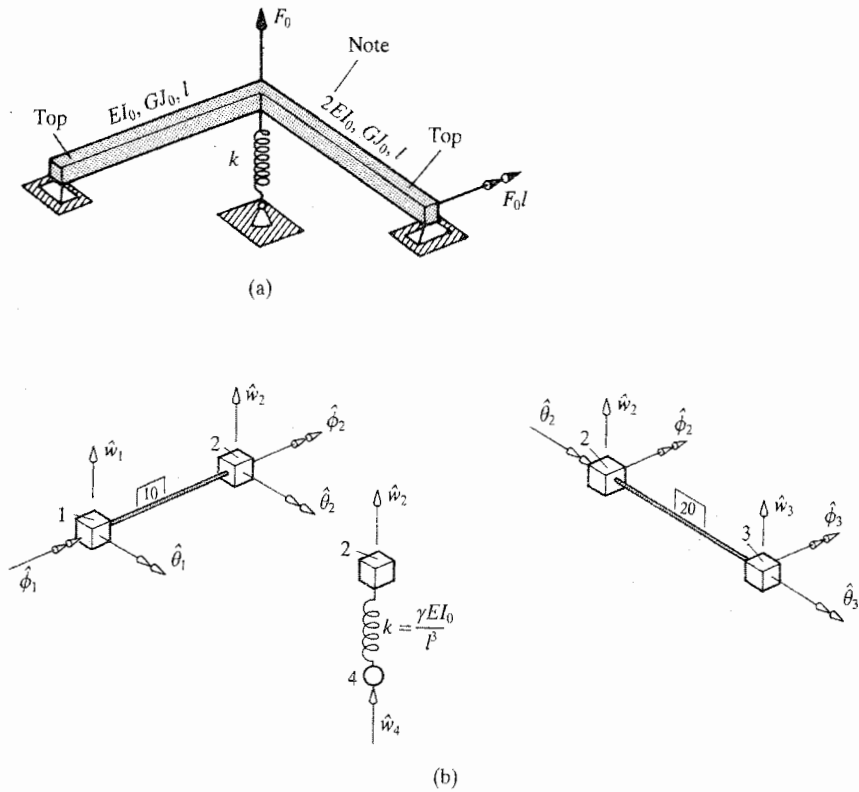


Figure 17.19. Exercise 17.4(d). (a) An analysis model. (b) An exploded view of the global DOF for each structural component. This is meant to be a reminder that once the global DOF have been calculated, the element DOF are known, and thus the element stresses can be calculated.

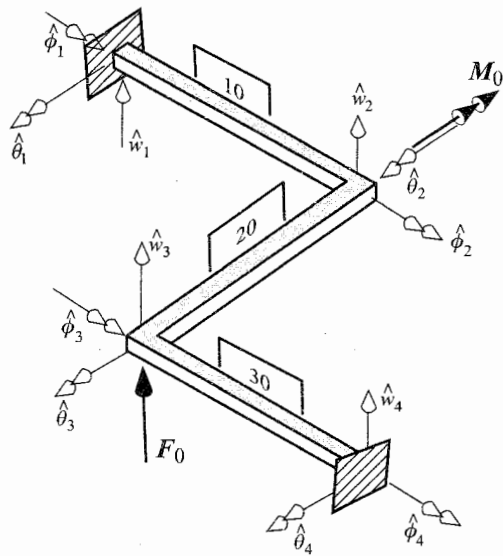


Figure 17.20. Exercise 17.4(e). Three beams at right angles forming a beam grid. Note $EI_{10} = EI_{30} = EI_0$, $GJ_{10} = GJ_{30} = \frac{1}{2}EI_0$, $EI_{20} = 2EI_0$, and $GJ_{20} = EI_0$.

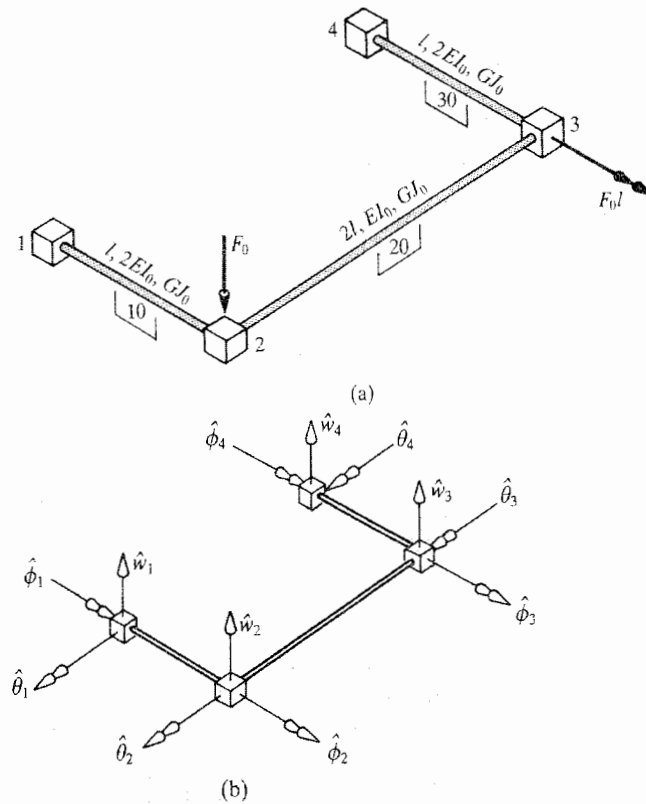


Figure 17.21. Exercise 17.4(o). (a) The loading. (b) The global DOF.

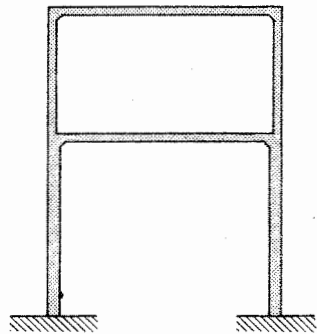


Figure 17.22. Exercise 17.5.

FOR THE EAGER

- 17.6. Derive the axial stiffness matrix equation for a homogeneous bar when, in addition to mechanical loads, there is a temperature change that is:
- A constant T_0 throughout the bar element. *Hint:* Remember to use Eq. (9.4a).
 - A linear function of the axial coordinate: $(x/L)T_1$.
- 17.7. (a) In the FEM, when an external distributed load acts along the length of a one-dimensional finite element or over the surface of a two- or three-dimensional

structural element, that distributed load is generally replaced by both equivalent external discrete forces and discrete moments at the nodes. As mentioned earlier, the usual approach is to simply use forces that are statically equivalent to the distributed load. A more elegant and consistent approach is to use forces and moments that produce the same virtual work as the distributed load. Even though tests have shown little difference in the accuracy associated with these two approaches, many commercial FEM programs give the analyst a choice between the two approaches. For this reason, develop the equivalent virtual work generalized force vector for a uniform lateral load per unit length f_0 applied over the total length of a beam element for beam bending in one plane. As before, let the beam element have a uniform geometry, and let the bending plane be a plane defined by a cross-section principal axis.

- (b) As above, but for a distributed load that is zero at $x = 0$, and which increases linearly to f_0 at $x = l$.

- 17.8. Develop a modification for the x, z plane beam bending stiffness matrix in order to approximate the effect of beam shearing deformation in that plane. *Hint:* Approximate the shearing deflections, as shown in Fig. 17.23, as

$$w_s(\xi) = (1 - \xi)w_1 + \xi w_2 = [N(\xi)]\{q\}$$

so that

$$\gamma_{xz}(\xi) = -(w_1/l) + (w_2/l) \quad \text{and} \quad \sigma_{xz} = G\gamma_{xz}$$

Then use the PVW to derive additional stiffness matrix terms for the first and third rows and columns of the bending stiffness matrix. Follow the guidance of Section 20.5 when integrating over the cross-sectional area by attaching the shearing stress, cross-section shape factor to the area value (i.e., write γA instead of plain A) in recognition of the fact that the shearing strain and shearing stress are not uniform over the cross-section as is suggested in the above approximations for those quantities.

- 17.9. Comment upon the accuracy of replacing $M_{yT}(x)$ by its average value, M_T , in Eq. (17.7b). *Hint:* As an intermediate and quickly arrived at step, establish the general conclusion that the definite integral over x of the arbitrary, smooth function $f(x)$ multiplied by the arbitrary, smooth function $g(x)$, over the interval (a, b) , is equal

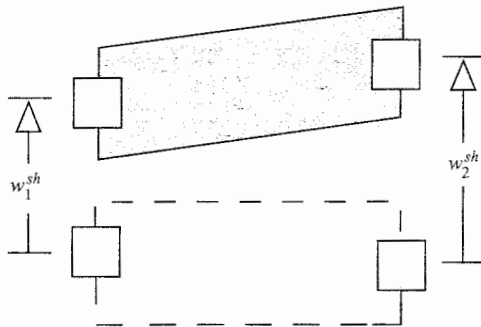


Figure 17.23. Exercise 17.8. Shearing deflections in a beam element where the beam element deforms like a stack of vertically oriented playing cards. Contrast this purely shearing deformation with the purely bending deformation shown in Fig. 9.2(a).

to the average value of the product $f(x)g(x)$ multiplied by the factor $(b - a)$. Then show that if the average value of the product $f(x)g(x)$ is equal to the product of the (separate) average values of $f(x)$ and $g(x)$, then there is no difficulty with the treatment of the equivalent thermal moment. However, if, in general, the average value of the product is not equal to the product of the average values, then can restrictions that are reasonable in the finite element context be applied to the equivalent thermal moment that permit this treatment of the equivalent thermal moment as an approximation? For example, note that the chosen algebraic steps are wholly correct for an equivalent thermal moment that is constant over the length of the beam finite element.

Endnote (1) Distributed Coordinates

Consider an unrestrained beam of length $2l$ that has an arbitrarily bent shape where all the beam deflections from the beam's undeformed position are small. Then, as usual, the lateral deflections of the unstretched beam do not induce any noteworthy axial deflections or forces. Identify points along the beam (deformed or undeformed) axis by the coordinate $\xi = x/l$ that originates at the center of the beam span. Thus one end of the beam is at $\xi = -1$, while the other end is at $\xi = +1$; see Fig. 17.24. The arbitrarily bent shape of the deformed beam, $w(\xi)$, can be constructed step by step in the following way. As is apparent from the figure, there is an average value for $w(\xi)$. Call that average value w_0 . Then w_0 is a crude approximation to $w(\xi)$. In order to improve the approximation, note that for the deflection sketched in the figure, the deflection function generally slopes from the lower left to the upper right. Then the approximation to $w(\xi)$ can be improved by writing

$$w(\xi) = w_0 + w_1\xi$$

where, in some sense, the constant value w_1 is some average magnitude of the slope. The parameters w_0 and w_1 are *distributed generalized coordinates* because they locate (crudely so far) all the material points of the deformed beam as a whole rather than individually. On the other hand, generalized coordinates that refer to specific, that is, individual geometric points are called *discrete* generalized coordinates. The approximation to the deflection function $w(\xi)$ can be vastly improved by adding more terms to the above two-term polynomial series. Instead of just adding the product of different constants and the values of ξ^2 , ξ^3 , and so on, consider

$$w(\xi) = w_0 + w_1\xi + \frac{1}{2}w_2(3\xi^2 - 1) + \frac{1}{2}w_3(5\xi^3 - 3\xi) + \frac{1}{8}w_4(35\xi^4 - 30\xi^2 + 3) + \frac{1}{8}w_5(63\xi^5 - 70\xi^3 + 15\xi) + \dots$$

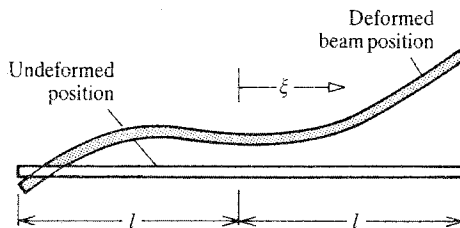


Figure 17.24. Endnote (1). An arbitrary beam element deflection pattern.

where the polynomial terms of order 2 and above begin the process of approximating the curvatures of the bent beam. This power series can be rewritten in summation form, where $i = 0, 1, 2, \dots$ as

$$w(\xi) = \sum_i w_i P_i(\xi) \quad (17.5)$$

where, of course, for example, $P_0(\xi) = 1$, and $P_1(\xi) = \xi$, etc. The apparently strange choice of polynomial terms is now explained. The polynomial terms $P_i(\xi)$ are called Legendre polynomials. Ref. [39] They have many special properties. For present purposes, their most important property is that the integral from $\xi = -1$ to $\xi = +1$ of the product $P_i(\xi)P_j(\xi)$ is zero whenever $i \neq j$, and has the value $2/(2j + 1)$ whenever $i = j$. This orthogonality property permits the quick determination of the values of the series constants w_i whenever $w(\xi)$ is specified. From the above information it is easy to show by multiplying both sides of Eq. (17.18) by $P_j(\xi)$ that

$$w_j = \left(\frac{2j + 1}{2} \right) \int_{-1}^{+1} w(\xi) P_j(\xi) d\xi$$

Now it is clear how the series coefficients w_i are determined by $w(\xi)$. Note again by referring to Eq. (17.18) that the reverse viewpoint that the series coefficients w_i determine $w(\xi)$ is also valid because the $P_i(\xi)$ terms are always of fixed form. If the series is infinite, then the function $w(\xi)$ is precisely described by the series. If the series is finite, then the function $w(\xi)$ is approximated by the series. It turns out that very good approximations can be obtained by a couple of dozen series terms. Even better approximations often can be obtained using Tschebycheff polynomials, or Fourier trigonometric series. Since small numbers of series terms are adequate for describing deflected forms, the use of distributed coordinates is quite practical for the purposes of structural analysis. As previously mentioned, this approach is at the heart of the usual Rayleigh–Ritz analysis.

Endnote (2) Accuracy of the Concentrated Load Approximation

At first thought, the restriction to concentrated forces and moments must seem to be a very crude approximation, for example, to a smooth distributed loading along the length of a beam. Indeed, it may be a crude approximation if just a few concentrated forces and moments are used to make the load approximation, and the entire structure consists of only a few beams. In order to illustrate the error associated with this one aspect of the FEM with respect to engineering beam theory, consider a single uniform beam of length L with a symmetric cross-section where the area moment inertia about the bending axis is I and the beam depth is $2c$. Let the only loading be a uniform lateral load per unit length of magnitude f_0 acting over the entire length of the beam. The solution to the beam bending differential equation shows that the lateral deflection at the center of the beam is

(i) for the simply supported beam:

$$w\left(\frac{L}{2}\right) = \frac{5f_0L^4}{384EI} = 0.01302 \frac{f_0L^4}{EI}$$

(ii) for the clamped–clamped beam:

$$w\left(\frac{L}{2}\right) = \frac{f_0L^4}{384EI} = 0.002604 \frac{f_0L^4}{EI}$$

The magnitude of the maximum bending stress at the center of the beam is

- (i) for the simply supported beam:

$$\sigma_m \left(\frac{L}{2} \right) = \frac{f_0 L^2 c}{8I} = 0.1250 \frac{f_0 L^2}{I}$$

- (ii) for the clamped-clamped beam:

$$\sigma_m \left(\frac{L}{2} \right) = \frac{f_0 L^2 c}{24I} = 0.04167 \frac{f_0 L^2}{I}$$

A short series of four FEM analyses for this beam using two, four, six, and finally eight beam segments shows the following results, courtesy of Dr. Suresh Chander:

- (i) For the simply supported beam

No. beam segments	Midspan deflection $f_0 L^4 (EI)$	Percent error	Midspan stress $f_0 L^2 c / I$	Percent error
2	1.042×10^{-2}	20	1.25×10^{-1}	None
4	1.237×10^{-2}	5	1.25×10^{-1}	None
6	1.273×10^{-2}	2.2	1.25×10^{-1}	None
8	1.286×10^{-2}	1.2	1.25×10^{-1}	None

- (ii) For the clamped-clamped beam

No. beam segments	Midspan deflection $f_0 L^4 (EI)$	Percent error	Midspan stress $f_0 L^2 c / I$	Percent error
2	2.604×10^{-3}	None	6.250×10^{-2}	50
4	2.604×10^{-3}	None	4.688×10^{-2}	12.5
6	2.604×10^{-3}	None	4.398×10^{-2}	5.5
8	2.604×10^{-3}	None	4.297×10^{-2}	3.1

It is clear that both the FEM deflection and stress solutions are within engineering accuracy for this single beam with simple support or clamped BCs if six beam segments are used to represent the beam, or, to the present point, five concentrated forces are used to represent the uniform load per unit length. Moreover, the FEM is at best when applied to the analysis of structures composed of a large number of structural elements. Then even a relatively crude approximation for the estimated loads on individual beams is satisfactory for that one small part of the total structure, even when the loads on all small parts of the total structure are so approximated.

Endnote (3) The Reason for the Name “Generalized Coordinates”

The location of the material point $P(x, y, z)$ of the deformable body shown in Fig. 17.25, prior to the deformation of that body, is fully identified by the set of cartesian coordinates x, y, z . In the figure, the undeformed position of that body is indicated by the dashed boundary line. With respect to cartesian coordinate axes fixed in space, after deformation, that same material point moves to the position $P'(x + q_1, y + q_2, z + q_3)$. Thus the set of generalized coordinates q_1, q_2, q_3 are coordinates in the sense that they locate position in the same way that ordinary coordinates “name” a point of the undeformed

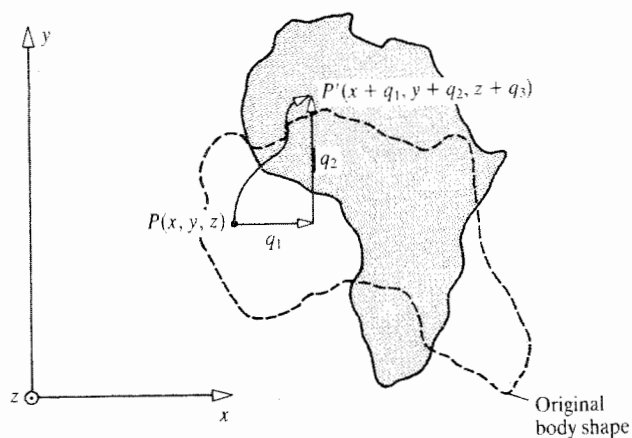


Figure 17.25. The generalized coordinates as descriptions of the displacements of a deformable structural body.

body. It should also be clear that the generalized coordinates also fully describe a motion and the possible ways that motion can take place. That is, the very nature of these three generalized coordinates is such that they describe three orthogonal translations. For this reason, the full set of generalized coordinates are also the degrees of freedom of the body in question.

Finite Element Truss Problems

18.1 Introduction

The use of a separate chapter for truss problems is prompted by the convenience of using the simpler bar element, as opposed to the beam element, as a means of illustrating the following topics that are less vital to an overall understanding of the basics of the FEM: (i) bars (or beams, or whatever) that are neither horizontally nor vertically oriented so that the element DOF are rotated relative to the global DOF; (ii) the equivalent loads that arise from enforced boundary deflections; and (iii) the equivalent loads that arise as a result of temperature changes or other initial strains. For the sake of simplicity, the developments of this chapter will be kept within the confines of planar trusses. The only slightly more complicated geometry of three-dimensional structures, which is available in all major commercial programs, is not necessary to the development of the reader's understanding of the concepts to be explored here. However, the bar element in three dimensions is adequately introduced in Exercise 18.10(b).

Bar elements do not differ much from beam elements. A distinction is usually made in a commercial FEM program between a beam and a bar in order to use the simpler bar element formulation wherever possible. It can be expected that any such program offers a beam element that includes the axial deformation properties of a bar. That is, there is always available a beam element with six DOF at each beam end, for a total of 12 DOF. These six DOF at each beam end are the three rectilinear deflections (u , v , w) and the three rotations, (ϕ , w' , v'). The inclusion in the set of beam DOF of the deflections u_1 , ϕ_1 , and u_2 , ϕ_2 is, of course, what makes the beam behavior include the bar behavior. Again, the 12 DOF, small-deflection, beam element stiffness matrix is nothing other than the uncoupled merging of the axial, the twisting, and the two lateral bending beam element stiffness matrices discussed separately in Chapter 17.

18.2 The Rotated Bar Element

Consider the bar element sketched in Fig. 18.1. Note that a lateral DOF has been added to each bar end. For small deflections, the bar has *no stiffness* associated with these lateral deflections. That is, for example, the bar rotation that is described by the lateral deflection v_2 , when u_1 , u_2 , and v_1 are held to zero values, is presumably sufficiently small that, geometrically speaking, there is no appreciable difference between the circular path followed by the right-hand end of the fixed-length bar and the straight-line path followed by the right-hand end of the stretching bar as that right-hand end follows the rectilinear track of v_2 . In other words, as before, the lateral deflections are presumed sufficiently small so as not to induce appreciable axial forces.¹ Thus, from Eq. (17.12), the linear form of the bar

¹ It is easy to show that in these circumstances the axial stretch (ΔL) in the beam is almost exactly $\frac{1}{2}v_2^2/L$. If the lateral deflection $v_2 = 0.1$ in, $L = 50$ in, $E = 10^7$ psi, $A = 1$ in², then the axial force due to the induced stretch has the negligible value $N = \frac{1}{2}(10^7 \text{ psi})(1 \text{ in}^2)(0.1 \text{ in})^2/(50 \text{ in})^2 = 20$ lbs, which is the order of magnitude of the weight force of approximately 5 lbs.



Figure 18.1. The bar finite element augmented with lateral DOF.

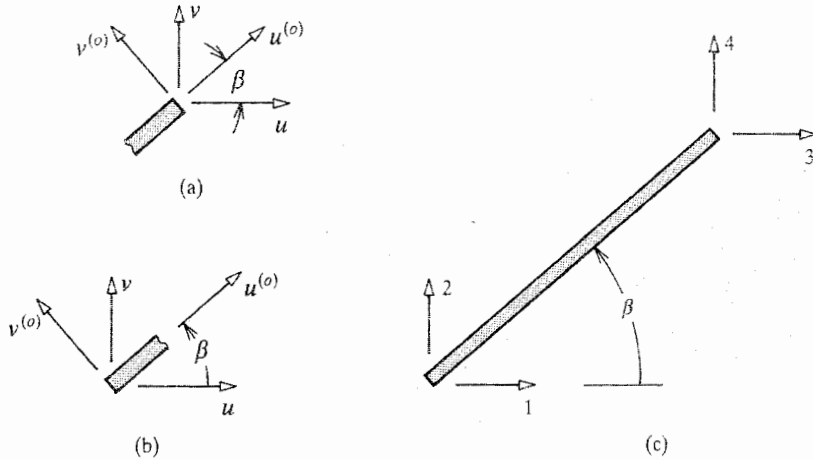


Figure 18.2. The four horizontal and vertical finite element DOF for the arbitrarily rotated bar.

element matrix stiffness equation, when expanded to accommodate these two new DOF, is as shown below, where there are only zeros occupying the rows and columns associated with the two lateral deflections

$$\begin{Bmatrix} N_1 \\ V_1 \\ N_2 \\ V_2 \end{Bmatrix} = \frac{E_0 A^*}{l} \begin{bmatrix} 1 & 0 & -1 & 0 \\ 0 & 0 & 0 & 0 \\ -1 & 0 & 1 & 0 \\ 0 & 0 & 0 & 0 \end{bmatrix} \begin{Bmatrix} u_1 \\ v_1 \\ u_2 \\ v_2 \end{Bmatrix}$$

The above matrix equation in its present form is only suitable for horizontal or vertical bars in a planar truss. Since not all the bars of a truss can be either horizontal or vertical, it is necessary to consider bars that are, say, rotated through a counterclockwise angle β from the horizontal. Of course, the four element DOF of the above matrix equation rotate with the bar. However, especially in the case of large trusses, for the sake of uniformity in interpreting results, it is most convenient to have global DOF that are horizontal and vertical. The assembly of the global stiffness matrix from the bar element stiffness matrices is greatly facilitated if the bar element DOF are also horizontal and vertical. Figures 18.2(a, b) show that the old DOF, now superscripted with an *o* for old, or "original orientation," which are fixed in their relation to the bar axis, bear the same relation to the new, horizontal and vertical DOF regardless of which bar end is discussed. Using the rotation

relations of Eq. (4.6), the old set of element DOF are related to the new set of element DOF by the matrix relation

$$\begin{Bmatrix} u_1 \\ v_1 \\ u_2 \\ v_2 \end{Bmatrix}^{(o)} = \begin{bmatrix} \cos \beta & \sin \beta & 0 & 0 \\ -\sin \beta & \cos \beta & 0 & 0 \\ 0 & 0 & \cos \beta & \sin \beta \\ 0 & 0 & -\sin \beta & \cos \beta \end{bmatrix} \begin{Bmatrix} u_1 \\ v_1 \\ u_2 \\ v_2 \end{Bmatrix} \quad (18.1a)$$

The above coordinate transformation may be written concisely as

$$\{q\}^o = [T_o]\{q\} \quad (18.1b)$$

Returning to the PVW, the internal virtual work for the bar element can be written as

$$-\delta W_{in} = [\delta q^o][k_o]\{q^o\} = [\delta q][T_o]^t[k_o][T_o]\{q\}$$

or

$$-\delta W_{in} = [\delta q][k]\{q\}$$

where the new element stiffness matrix for the rotated bar is the result of carrying out the above indicated triple matrix product $[T_o]^t[k_o][T_o]$. The details of the result are

$$[k^*] = \frac{E_0 A^*}{l} \begin{bmatrix} \cos^2 \beta & \cos \beta \sin \beta & -\cos^2 \beta & -\cos \beta \sin \beta \\ \cos \beta \sin \beta & \sin^2 \beta & -\cos \beta \sin \beta & -\sin^2 \beta \\ -\cos^2 \beta & -\cos \beta \sin \beta & \cos^2 \beta & \cos \beta \sin \beta \\ -\cos \beta \sin \beta & -\sin^2 \beta & \cos \beta \sin \beta & \sin^2 \beta \end{bmatrix} \quad (18.2)$$

Figure 18.2(c) pictures the bar element for which the above matrix is the element stiffness matrix. Now it is just a matter of assembling these matrices so as to obtain the matrix equation for any planar, statically loaded truss under study. The two example problems that follow are sufficient to illustrate that process.

Example 18.1. Write the matrix stiffness equation for the five-bar truss sketched in Fig. 18.3. The stiffness factor for each bar is $E_0 A^*/L$.

Solution. The counterclockwise angles of rotation of bars 20, 25, 30, 35, and 40 are, respectively, 0° , 30° , 45° , 60° , and 90° . Following the derivation of the above stiffness matrix, the bar rotation is determined by imagining a horizontal line passing through the lower numbered node, and extending to the right. Therefore the element stiffness matrices are

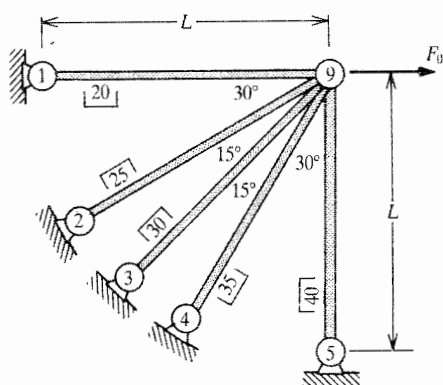
$$[k_{20}]\{q\}^{(20)} = \frac{E_0 A^*}{L} \begin{bmatrix} 1 & 0 & -1 & 0 \\ 0 & 0 & 0 & 0 \\ -1 & 0 & 1 & 0 \\ 0 & 0 & 0 & 0 \end{bmatrix} \begin{Bmatrix} u_1 \\ v_1 \\ u_9 \\ v_9 \end{Bmatrix}$$

$$[k_{25}]\{q\}^{(25)} = \frac{E_0 A^*}{L} \begin{bmatrix} 3/4 & \sqrt{3}/4 & -3/4 & -\sqrt{3}/4 \\ \sqrt{3}/4 & 1/4 & -\sqrt{3}/4 & -1/4 \\ -3/4 & -\sqrt{3}/4 & 3/4 & \sqrt{3}/4 \\ -\sqrt{3}/4 & -1/4 & \sqrt{3}/4 & 1/4 \end{bmatrix} \begin{Bmatrix} u_2 \\ v_2 \\ u_9 \\ v_9 \end{Bmatrix}$$

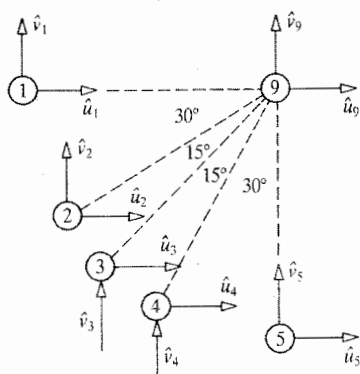
$$[k_{30}] \{q\}^{(30)} = \frac{E_0 A^*}{L} \begin{bmatrix} 1/2 & 1/2 & -1/2 & -1/2 \\ 1/2 & 1/2 & -1/2 & -1/2 \\ -1/2 & -1/2 & 1/2 & 1/2 \\ -1/2 & -1/2 & 1/2 & 1/2 \end{bmatrix} \begin{Bmatrix} u_3 \\ v_3 \\ u_9 \\ v_9 \end{Bmatrix}$$

$$[k_{35}] \{q\}^{(35)} = \frac{E_0 A^*}{L} \begin{bmatrix} 1/4 & \sqrt{3}/4 & -1/4 & -\sqrt{3}/4 \\ \sqrt{3}/4 & 3/4 & -\sqrt{3}/4 & -3/4 \\ -1/4 & -\sqrt{3}/4 & 1/4 & \sqrt{3}/4 \\ -\sqrt{3}/4 & -3/4 & \sqrt{3}/4 & 3/4 \end{bmatrix} \begin{Bmatrix} u_4 \\ v_4 \\ u_9 \\ v_9 \end{Bmatrix}$$

$$[k_{40}] \{q\}^{(40)} = \frac{E_0 A^*}{L} \begin{bmatrix} 0 & 0 & 0 & 0 \\ 0 & 1 & 0 & -1 \\ 0 & 0 & 0 & 0 \\ 0 & -1 & 0 & 1 \end{bmatrix} \begin{Bmatrix} u_5 \\ v_5 \\ u_9 \\ v_9 \end{Bmatrix}$$



(a)



(b)

Figure 18.3. Example 18.1. (a) An equal bar length planar truss. (b) The selected global DOF.

Assembling the global stiffness matrix and then applying the BCs that $u_1 = v_1 = u_2 = v_2 = \dots = u_5 = v_5 = 0$ yields the easily solved matrix equation

$$\begin{Bmatrix} F_0 \\ 0 \end{Bmatrix} = \frac{E_0 A^*}{L} \begin{bmatrix} 2.500 & 1.366 \\ 1.366 & 2.500 \end{bmatrix} \begin{Bmatrix} u_9 \\ v_9 \end{Bmatrix} \quad (18.3)$$

It is interesting to note that this type of truss is one of the very few where the number of deflection unknowns using a deflection method can be less than the number of force unknowns (redundants) when a force-type analysis is used.

Example 18.2. Develop the global matrix equation to be solved for the nonzero deflections of nodes 2, 3, and 4 of the planar truss sketched in Fig. 18.4. The material and geometric properties of the bars are

Bar number	10	11	12	13	14	15
EA_0 coeff.	2	2	2	2	1	1
Length	L	$\sqrt{3}L$	L	$\sqrt{3}L$	$2L$	$2L$

Solution. Again, to save hand work and space from this point onward, the BCs are inserted into the element stiffness matrices after they are written in terms of the global coordinates. The BCs in this case are $u_1 = v_1 = v_2 = 0$. The rotation angle for each bar is, based on the lower of the two nodal numbers

Bar number	10	11	12	13	14	15
β (degrees)	0	90	0	90	120	60

Therefore the bar stiffness matrices in terms of the unknown DOF are

$$[K_{10}] \{q\}^{(10)} = \frac{EA_0}{L} [2] u_2$$

$$[K_{11}] \{q\}^{(11)} = \frac{EA_0}{L} \begin{bmatrix} 0 & 0 & 0 \\ 0 & 0 & 0 \\ 0 & 0 & 2/\sqrt{3} \end{bmatrix} \begin{Bmatrix} u_2 \\ u_4 \\ v_4 \end{Bmatrix}$$

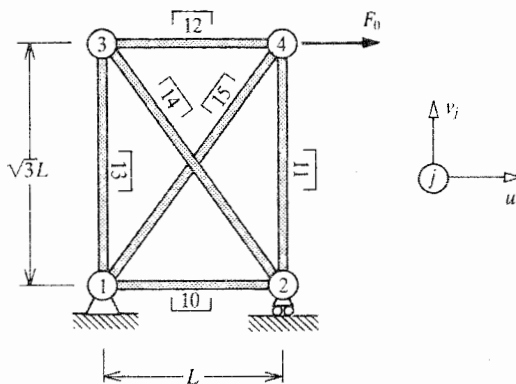


Figure 18.4. Example 18.2. A planar truss and the selected global DOF.

$$[K_{12}]\{q\}^{(12)} = \frac{EA_0}{L} \begin{bmatrix} 2 & 0 & -2 & 0 \\ 0 & 0 & 0 & 0 \\ -2 & 0 & 2 & 0 \\ 0 & 0 & 0 & 0 \end{bmatrix} \begin{Bmatrix} u_3 \\ v_3 \\ u_4 \\ v_4 \end{Bmatrix}$$

$$[K_{13}]\{q\}^{(13)} = \frac{EA_0}{L} \begin{bmatrix} 0 & 0 \\ 0 & 2/\sqrt{3} \end{bmatrix} \begin{Bmatrix} u_3 \\ v_3 \end{Bmatrix}$$

$$[K_{14}]\{q\}^{(14)} = \frac{EA_0}{L} \begin{bmatrix} 1/8 & -1/8 & \sqrt{3}/8 \\ -1/8 & 1/8 & -\sqrt{3}/8 \\ \sqrt{3}/8 & -\sqrt{3}/8 & 3/8 \end{bmatrix} \begin{Bmatrix} u_2 \\ u_3 \\ v_3 \end{Bmatrix}$$

$$[K_{15}]\{q\}^{(15)} = \frac{EA_0}{L} \begin{bmatrix} 1/8 & \sqrt{3}/8 \\ \sqrt{3}/8 & 3/8 \end{bmatrix} \begin{Bmatrix} u_4 \\ v_4 \end{Bmatrix}$$

The assembly of the above bar element stiffness matrices leads to the following system stiffness matrix equation in terms of the horizontal and vertical global DOF:

$$\begin{Bmatrix} 0 \\ 0 \\ 0 \\ F_0 \\ 0 \end{Bmatrix} = \frac{EA_0}{24L} \begin{bmatrix} 51 & -3 & 3\sqrt{3} & 0 & 0 \\ -3 & 51 & -3\sqrt{3} & -48 & 0 \\ 3\sqrt{3} & -3\sqrt{3} & (9 + 16\sqrt{3}) & 0 & 0 \\ 0 & -48 & 0 & 51 & 3\sqrt{3} \\ 0 & 0 & 0 & 3\sqrt{3} & (9 + 16\sqrt{3}) \end{bmatrix} \begin{Bmatrix} u_2 \\ u_3 \\ v_3 \\ u_4 \\ v_4 \end{Bmatrix}$$

Note that if element stiffness matrices of the diagonal bars of the above six-bar truss were not assembled with those of the other four bars, then the global stiffness matrix would be singular. This again illustrates the fact that singular stiffness matrices are associated with structures that can undergo rigid body motions.

18.3 Equivalent Thermal Loads

Any discussion of the bars of trusses involves the implicit limitation that the bars are bars; that is, they do not bend and thus do not exhibit beam action. To work within this limitation requires that the temperature changes in the bars do not bend the bars. If the bars are nonhomogeneous, and the cross-section material layout is nonsymmetric, then even a temperature change that is constant over the bar cross-section can produce an equivalent thermal bending moment.² Therefore, in this chapter, while the bars are permitted to be nonhomogeneous, the material distribution of the bar cross-sections must be such that a temperature change that is constant over the cross-section does not produce an equivalent thermal moment M_{zT} or M_{yT} .

² With a temperature change that is constant over the cross-section, the integral for the thermal moment about the z -axis, for example, reduces to the integral over the area of the quantity $yE\alpha$. The definition of the m.w. centroid only requires that the integral over the area of yE be zero. Differences in the values of α therefore can produce a thermal moment for a constant temperature change.

A temperature change that is only a function of the axial coordinate x is a temperature change that is a constant over every bar cross-section. Let that type of temperature change be symbolized as $\Delta T = T(x)$. Again applying the PVW, $\delta W_{ex} = -\delta W_{in}$, but this time including temperature change effects, yields

$$\delta W_{ex} = \iiint_{\text{Vol.}} \sigma_{xx} \delta \epsilon_{xx} d(\text{Vol.}) = \int_0^L \iint_A \delta \epsilon_{xx} E [\epsilon_{xx} - \alpha T(x)] dA dx$$

From the development of the bar element shape functions in the previous chapter, the expression for the total strain is

$$\epsilon_{xx} = u'(x) = [N'(x)] \{q\} = \frac{1}{L} [-1 \quad +1] \{q\}$$

and

$$\delta \epsilon_{xx} = \frac{1}{L} [-1 \quad +1] \{\delta q\} = \frac{1}{L} [\delta q] \begin{Bmatrix} -1 \\ +1 \end{Bmatrix}$$

Thus

$$\begin{aligned} \delta W_{ex} = & \left([\delta q] \begin{Bmatrix} -1 \\ +1 \end{Bmatrix} [-1 \quad +1] \right) \frac{E_0}{L^2} \int_0^L \iint_A \frac{E}{E_0} dA dx \{q\} \\ & - \left([\delta q] \begin{Bmatrix} -1 \\ +1 \end{Bmatrix} \right) \frac{E_0 \alpha_0}{L} \int_0^L \iint_A \frac{E}{E_0} \frac{\alpha}{\alpha_0} T(x) dA dx \end{aligned}$$

where values of the reference modulus E_0 have been inserted for convenience. The second area integral above is also simplified by the introduction of a reference value of the coefficient of thermal expansion in a manner that is wholly analogous to the introduction of the reference value of Young's modulus. The first area integral is A^* . Let the second area integral, after the factoring out of that integral the function $T(x)$, which is not affected by the area integration, be defined as A^{**} . Since both these weighted areas are constants for a uniform bar, they can be factored out of their respective length integrals. Then the value of the first length integral is merely L . The second length integral is

$$\frac{1}{L} \int_0^L T(x) dx = T_{av}$$

the average temperature change along the length of the bar. Thus

$$\delta W_{ex} = [\delta q] \frac{E_0 A^*}{L} \begin{bmatrix} +1 & -1 \\ -1 & +1 \end{bmatrix} \{q\} - [\delta q] E_0 \alpha_0 A^{**} T_{av} \begin{Bmatrix} -1 \\ +1 \end{Bmatrix}$$

or

$$[\delta q] \{Q\} = [\delta q] [k^*] \{q\} - [\delta q] \{Q_T\}$$

or

$$\boxed{\{Q^c\} = \{Q\} + \{Q_T\} = [k^*] \{q\}} \quad (18.4)$$

Just as is the case with all other equivalent thermal loads, the FEM equivalent thermal forces are added to mechanical forces.

From the above result, the bar element matrix stiffness equation in terms of both the two axial and two lateral, originally oriented (i.e., old) DOF, as shown in Fig. 18.1, can be written as before as

$$\{Q^o\} = \frac{E_0 A^*}{L} \begin{bmatrix} 1 & 0 & -1 & 0 \\ 0 & 0 & 0 & 0 \\ -1 & 0 & 1 & 0 \\ 0 & 0 & 0 & 0 \end{bmatrix} \begin{Bmatrix} u_1 \\ v_1 \\ u_2 \\ v_2 \end{Bmatrix}^{(o)} - E_0 A^{**} \alpha_0 T_{av} \begin{Bmatrix} -1 \\ 0 \\ +1 \\ 0 \end{Bmatrix}$$

or in more concise terms as $\{Q^o\} = [k_o] \{q^o\} - \{Q_T^o\}$, where again the matrix superscript or subscript o stands for “old” or “original orientation.” Recall the DOF rotation relation between the old and the new bar end DOF developed in the previous section:

$$\{q^o\} = [T_0] \{q\} \quad (18.1b)$$

(Avoid confusion between the above symbol for the coordinate transformation matrix and the frequently used symbol for a constant temperature change.) As above the external and internal virtual work for the bar element can be written as

$$\delta W_{ex} = [\delta q^o] [k_o^*] \{q^o\} - [\delta q^o] \{Q_T^o\}$$

Applying the DOF transformation relation of Eq. (18.1b), the external virtual work becomes

$$\delta W_{ex} = [\delta q] [T_0]^t [k_o^*] [T_0] \{q\} - [\delta q] [T_0]^t \{Q_T^o\}$$

or

$$[\delta q] \{Q\} = [\delta q] [k^*] \{q\} - [\delta q] \{Q_T\}$$

which directly leads to the familiar form

$$\{Q\} + \{Q_T\} \equiv \{Q^c\} = [k^*] \{q\}$$

where now

$$\{Q_T\} = E_0 A^{**} \alpha_0 T_{av} \begin{Bmatrix} -\cos \beta \\ -\sin \beta \\ \cos \beta \\ \sin \beta \end{Bmatrix}$$

Example 18.3. Redo Example 18.1 where in addition to the mechanical force shown in Fig. 18.3 there is a uniform temperature change of magnitude T_0 in bar 35, and a uniform temperature change of magnitude $2T_0$ in bar 40. For simplicity, let all the bars now be homogeneous.

Solution. The rotation angles for bars 35 and 40 are, again, 60° and 90° , respectively. Therefore the complete thermal force vectors for these two bars are

$$\{Q_T\}^{(35)} = EA\alpha T_0 \begin{Bmatrix} -1/2 \\ -\sqrt{3}/2 \\ 1/2 \\ \sqrt{3}/2 \end{Bmatrix} \quad \{Q_T\}^{(40)} = EA\alpha T_0 \begin{Bmatrix} 0 \\ -2 \\ 0 \\ 2 \end{Bmatrix}$$

The BCs of this truss require the setting aside of the first two rows of both of the above equivalent force vectors because those rows correspond to the zero deflections at nodes 4

and 5. The result of adding these two equivalent force vectors to the original mechanical force vector in Eq. (18.3), with of course no effect on the stiffness matrix, is then

$$\{Q^e\} = \begin{Bmatrix} F_0 + \frac{1}{2}EA\alpha T_0 \\ \frac{1}{2}(4 + \sqrt{3})EA\alpha T_0 \end{Bmatrix} = \frac{EA}{L} \begin{bmatrix} 2.500 & 1.366 \\ 1.366 & 2.500 \end{bmatrix} \begin{Bmatrix} u_9 \\ v_9 \end{Bmatrix}$$

Note that, as would be expected, the major portion of the total equivalent applied thermal force is clearly in the positive v_9 direction. ■

It is worthwhile to recall that once the two deflection components at node 9 of the previous example problem are determined from the solution of the above matrix equation, the bar element horizontal and vertical force components are calculated from the element matrix equation. For example, for bar 35

$$\{Q\}^{(35)} = [k_{35}]\{q\}^{(35)} - \{Q_T\}^{(35)}$$

The horizontal and vertical components of $\{Q\}^{(35)}$ then have to be resolved in the direction of the bar axis in order to obtain the axial force. The bar stresses are then just the bar axial forces divided by the homogeneous area. An alternate approach for obtaining the bar element stresses is to first rotate the element global DOF solutions back to the original element axial and lateral directions, using Eq. (18.1) and then write

$$\sigma_{xx} = E(\epsilon_{xx} - \alpha T_0) = \frac{E}{L}(u_2^0 - u_1^0) - E\alpha T_0$$

As is implicit in all these truss analyses, it is assumed that the bars do not buckle under the action of compressive forces, just as it is assumed the bars do not yield or experience a brittle failure under the action of either compressive or tensile forces. If a bar in a two-dimensional truss did buckle by bending in the plane of the truss, then the force transmitted by that beam to the rest of the structure would be essentially limited to the buckling force in that beam. That is, the force in the buckled beam would remain nearly the same, while that of the other bars would increase in response to an increase in the external set of forces. If a beam buckled out of the plane of the truss, then, given the usual types of actual joint connections, it would cause the other beams to also leave the unloaded plane of the truss, with the result that any postbuckling analysis would be more complicated.

18.4 Other Initial Strains

Once again, consider the five-bar truss of Fig. 18.3. This time, let there be neither a mechanically applied load nor a temperature change. Instead, let bar 35 be cut slightly too long, while the other four bars have their correct length. Nevertheless, let it be that all five bars were forced into position so that the connection at node 9 was accomplished despite the misfit of bar 35. Let the ratio of the extra length to the correct length, a small number, be called ϵ_0 . This strain symbol is appropriate because the ratio of the extra length to the correct length parallels the change in length over length definition of a direct engineering strain, and of course, the units (mm/mm, or in/in) are the same. The forcing of bar 35 to make the connection at node 9 compresses bar 35 and stretches the other four bars. Thus there are what are called *initial strains* or *initial stresses* or initial axial forces within the truss before any external mechanical forces or temperature changes are applied to the truss. If the magnitude of the misfit, ϵ_0 , is known or is stipulated as a design parameter, then the

initial forces in the truss can be calculated in one of two ways. The first way is to return to the original derivations and write, for example, that

$$\sigma_{xx} = E(\epsilon_{xx} - \alpha T_0 - \epsilon_0)$$

where, in an exact analogy to the treatment of temperature changes, the misfit strain is also to be subtracted from the total strain in order to obtain the (additional) elastic strain that results from the applied loads. The second approach is to use the thermal load approach previously discussed in conjunction with a fictitious constant temperature change T_f that is such that $\alpha T_f = \epsilon_0$. Using this latter approach produces the following system stiffness matrix equation, which is only a slight variation on the previous example problem. From

$$\{Q_0\}^{(35)} = EA\epsilon_0 \begin{Bmatrix} -1/2 \\ -\sqrt{3}/2 \\ 1/2 \\ \sqrt{3}/2 \end{Bmatrix}, \quad \text{and all other } \{Q_0\} = \{0\}$$

$$\{Q\} = \begin{Bmatrix} \frac{1}{2}EA\epsilon_0 \\ (\sqrt{3}/2)EA\epsilon_0 \end{Bmatrix} = \frac{EA}{L} \begin{bmatrix} 2.500 & 1.366 \\ 1.366 & 2.500 \end{bmatrix} \begin{Bmatrix} \hat{u}_9 \\ \hat{v}_9 \end{Bmatrix}$$

18.5 Enforced Deflections

Enforced deflections result in another type of equivalent load vector. Consider the six-bar truss of Fig. 18.4 where now the right-hand support is no longer a roller support but rather a fixed hinge support. Furthermore, let the new right-hand support be forced to move horizontally to the right a distance u_0 . (Note that an enforced vertical motion of the right-hand support would only tilt the entire truss through the same rotation for all bars, and there would not be any induced forces in the bars.) Notice that the enforced deflection of node 2 of magnitude u_0 causes axial forces in all the bars regardless of whether bar 10 is present or not. Also note that the axial force in bar 10 can be calculated immediately as $N_{10} = 2EA_0u_0/L$ because in this one case, both axial end deflections are known. The approach to calculating the axial forces in the remaining bars of the truss is best explained by returning to the practice of writing the system stiffness matrix equation in terms of all the system DOF, that is, including those with known boundary values. In this case $\{\hat{Q}\} = [\hat{K}]\{\hat{q}\}$ is first reduced by applying the homogeneous BCs $u_1 = v_1 = v_2 = 0$, and thus eliminating the first, second, and fourth columns. The intermediate result from Example 18.2, after adjusting the generalized force corresponding to u_2 to an R to account for the change in BCs from that original example problem, is

$$\begin{Bmatrix} R \\ 0 \\ 0 \\ F_0 \\ 0 \end{Bmatrix} = \frac{EA_0}{24L} \begin{bmatrix} 51 & -3 & 3\sqrt{3} & 0 & 0 \\ -3 & 51 & -3\sqrt{3} & -48 & 0 \\ 3\sqrt{3} & -3\sqrt{3} & (9 + 16\sqrt{3}) & 0 & 0 \\ 0 & -48 & 0 & 51 & 3\sqrt{3} \\ 0 & 0 & 0 & 3\sqrt{3} & (9 + 16\sqrt{3}) \end{bmatrix} \begin{Bmatrix} \hat{u}_2 \\ \hat{u}_3 \\ \hat{v}_3 \\ \hat{u}_4 \\ \hat{v}_4 \end{Bmatrix}$$

Since, $u_2 = u_0$, which is not zero, the first column of the above stiffness matrix is not eliminated. Instead, proceed with the matrix reduction process by partitioning the above stiffness matrix into two matrices which are the 5×1 matrix of the former first column and the 5×4 matrix of the former second through fifth columns. This partition and matrix

multiplicative consistency requires the vector of the former first column to be multiplied by u_0 , while the 5×4 rectangular matrix is multiplied by

$$\{q\} = [\hat{u}_3 \quad \hat{v}_3 \quad \hat{u}_4 \quad \hat{v}_4]^t$$

As before, setting aside the first row, which contains an unknown reaction, leads to

$$\begin{Bmatrix} 0 \\ 0 \\ F_0 \\ 0 \end{Bmatrix} - \frac{EA_0 u_0}{24L} \begin{Bmatrix} -3 \\ 3\sqrt{3} \\ 0 \\ 0 \end{Bmatrix} = \frac{EA_0}{24L} \begin{bmatrix} 51 & -3\sqrt{3} & -48 & 0 \\ -3\sqrt{3} & (9 + 16\sqrt{3}) & 0 & 0 \\ -48 & 0 & 51 & 3\sqrt{3} \\ 0 & 0 & 3\sqrt{3} & (9 + 16\sqrt{3}) \end{bmatrix} \begin{Bmatrix} \hat{u}_3 \\ \hat{v}_3 \\ \hat{u}_4 \\ \hat{v}_4 \end{Bmatrix}$$

In concise form, the above equation can be written as

$$\{Q\} + \{Q_d\} = \{Q_{total}\} = [K]\{q\}$$

and solved for $\{q\}$ as usual. Then the horizontal reaction at the fixed right-hand support can be calculated just as any reaction can be calculated. Specifically, from the set aside u_2 row,

$$R = \frac{EA_0}{24L} (51u_0 - 3\hat{u}_3 + 3\sqrt{3}\hat{v}_3)$$

This result makes obvious the fact that the horizontal support reaction at node 2 not only depends upon the horizontal motion at that node (through the agency of the force induced in bar 10), but it also depends upon the motion of node 3, which influences the force induced in bar 14. The vertical bar 11 has no effect upon that horizontal support reaction because it cannot offer any resistance to a small lateral deflection at its end.

18.6 Summary

The planar rotation treatment for bars developed in this chapter is also directly applicable to beams and all other types of finite elements whose DOF are rotated in a plane relative to the global DOF. When the bar or beam is situated in three-dimensional space, then Eq. (4.6) is the applicable rotation equation not only for the rectilinear DOF but also for the angular DOF treated as the vector quantities they are whenever those angular deflections are small in the sense discussed in Exercise 9.19. The truss examples of this chapter make clear the usefulness of having the rotated forms of the element stiffness matrices available for the purpose of assembling the system stiffness matrix.

Once again, because of their indeterminacy, the treatment of equivalent thermal loads is of considerable importance to the analysis of vehicular structures. The bar element has served as a detailed example of how the equivalent thermal forces are derived even when the element is nonhomogeneous, and how those equivalent thermal forces are utilized. Recall that Section 17.3 offers a similar derivation of equivalent thermal bending moments for the beam element. The method of treating trusses subjected to enforced deflections also can be used without any modification for composing that type of equivalent load for structures composed of beams and other finite elements; see Exercise 18.8. The first two remaining pinned truss examples review the detailed treatment of equivalent thermal and equivalent enforced deflection loadings within a single truss problem. Example 18.6 returns to the previous chapter's task of constructing $\{Q\} = [K]\{q\}$ for a frame where there is now an enforced deflection.

Example 18.4. Each of the seven bars of the pin-jointed planar truss shown in Fig. 18.5(a) has the same length L and the same axial stiffness coefficient EA_0 . The three upper bars

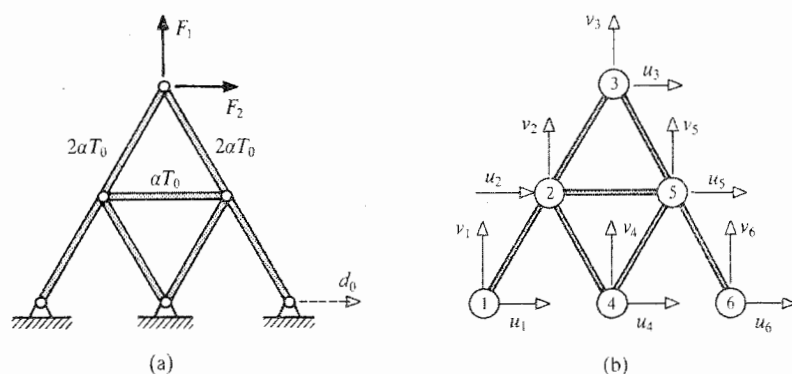


Figure 18.5. Example 18.4. (a) The mechanical, thermal, and enforced displacement loading. (b) The finite element model.

experience the labeled average temperature change strains, and there is an enforced lateral deflection d_0 at joint number 6. Use the DOF shown in Fig. 18.5(b) to write the FEM matrix equation $\{Q\} = [K]\{q\}$ for this truss.

Solution. Name the bars by means of the bar end joint numbers. Then the rotations of each bar axis can be described as follows:

Bar	12	23	45	25	24	35	56
Angle	60°	60°	60°	0°	-60°	-60°	-60°

The element stiffness matrices and corresponding DOF vectors, after application of the structural BCs, are

$$[k_{23}]\{q\} = \frac{EA_0}{4L} \begin{bmatrix} 1 & \sqrt{3} & -1 & -\sqrt{3} \\ \sqrt{3} & 3 & -\sqrt{3} & -3 \\ -1 & -\sqrt{3} & 1 & \sqrt{3} \\ -\sqrt{3} & -3 & \sqrt{3} & 3 \end{bmatrix} \begin{Bmatrix} u_2 \\ v_2 \\ u_3 \\ v_3 \end{Bmatrix}$$

$$[k_{12}]\{q\} = \frac{EA_0}{4L} \begin{bmatrix} 1 & \sqrt{3} \\ \sqrt{3} & 3 \end{bmatrix} \begin{Bmatrix} u_2 \\ v_2 \end{Bmatrix} \quad [k_{45}]\{q\} = \frac{EA_0}{4L} \begin{bmatrix} 1 & \sqrt{3} \\ \sqrt{3} & 3 \end{bmatrix} \begin{Bmatrix} u_5 \\ v_5 \end{Bmatrix}$$

$$[k_{24}]\{q\} = \frac{EA_0}{4L} \begin{bmatrix} 1 & -\sqrt{3} \\ -\sqrt{3} & 3 \end{bmatrix} \begin{Bmatrix} u_2 \\ v_2 \end{Bmatrix}$$

$$[k_{25}]\{q\} = \frac{EA_0}{4L} \begin{bmatrix} 4 & 0 & -4 & 0 \\ 0 & 0 & 0 & 0 \\ -4 & 0 & 4 & 0 \\ 0 & 0 & 0 & 0 \end{bmatrix} \begin{Bmatrix} u_2 \\ v_2 \\ u_5 \\ v_5 \end{Bmatrix}$$

$$[k_{56}]\{q\} = \frac{EA_0}{4L} \begin{bmatrix} 1 & -\sqrt{3} & -1 \\ -\sqrt{3} & 3 & \sqrt{3} \end{bmatrix} \begin{Bmatrix} u_5 \\ v_5 \\ +d_0 \end{Bmatrix}$$

where the known value d_0 is inserted for u_6 , and

$$[k_{35}]\{q\} = \frac{EA_0}{4L} \begin{bmatrix} 1 & -\sqrt{3} & -1 & \sqrt{3} \\ -\sqrt{3} & 3 & \sqrt{3} & -3 \\ -1 & \sqrt{3} & 1 & -\sqrt{3} \\ \sqrt{3} & -3 & -\sqrt{3} & 3 \end{bmatrix} \begin{Bmatrix} u_3 \\ v_3 \\ u_5 \\ v_5 \end{Bmatrix}$$

Then the assembled structural stiffness matrix and DOF vector are

$$[K]\{q\} = \frac{EA_0}{4L} \begin{bmatrix} 7 & \sqrt{3} & -1 & -\sqrt{3} & -4 & 0 \\ \sqrt{3} & 9 & -\sqrt{3} & -3 & 0 & 0 \\ -1 & -\sqrt{3} & 2 & 0 & -1 & \sqrt{3} \\ -\sqrt{3} & -3 & 0 & 6 & \sqrt{3} & -3 \\ -4 & 0 & -1 & \sqrt{3} & 7 & -\sqrt{3} \\ 0 & 0 & \sqrt{3} & -3 & -\sqrt{3} & 9 \end{bmatrix} \begin{Bmatrix} u_2 \\ v_2 \\ u_3 \\ v_3 \\ u_5 \\ v_5 \end{Bmatrix}$$

The total generalized force vector is the sum of the mechanical load vector plus the equivalent enforced deflection load vector plus the equivalent thermal load vector, that is, $\{Q\} = \{Q\} + \{Q_d\} + \{Q_T\}$, where

$$\{Q\} = \begin{Bmatrix} 0 \\ 0 \\ F_2 \\ F_1 \\ 0 \\ 0 \end{Bmatrix} \quad \{Q_d\} = \frac{EA_0 d_0}{4L} \begin{Bmatrix} 0 \\ 0 \\ 0 \\ 0 \\ 1 \\ -\sqrt{3} \end{Bmatrix} \quad \{Q_T\} = EA_0 \alpha T_0 \begin{Bmatrix} -1 & -1 \\ -\sqrt{3} & \\ 1 & -1 \\ \sqrt{3} & +\sqrt{3} \\ & 1 & +1 \\ & & -\sqrt{3} \end{Bmatrix}$$

where the three columns of values of the thermal load vector, which need to be combined to obtain the final value in each row, correspond to beams 23, 25, and 35, respectively. Now all the components of the final matrix equation $\{Q\} = [K]\{q\}$ have been specified. Note that only the thermal strain in element 25 should cause any internal forces or stresses in the bars 12, 24, 25, and 56, while there should be no temperature change-induced stresses from any source in bars 23 and 35. Similarly, bars 23 and 35 should not have any internal forces or stresses as a result of the enforced deflection. ■

Example 18.5. Write the global matrix equation $\{Q\}^c = [K]\{q\}$ for the four-bar planar truss sketched in Fig. 18.6. Note that the two left-hand bars are subjected to a temperature change, and the bottom right support has experienced a upward deflection of magnitude d_0 . The stiffness coefficients of each bar are indicated in the figure.

Solution. Determining the contributions of each bar to the global stiffness matrix equation is simply a matter of using the element stiffness matrix template and the thermal load template. For bar 1–3, where the rotation angle is $+45^\circ$, the result is

$$\frac{2EA_0}{\ell} \begin{bmatrix} 0.5 & 0.5 \\ 0.5 & 0.5 \end{bmatrix} \begin{Bmatrix} u_3 \\ v_3 \end{Bmatrix} - 2EA_0 \alpha T_0 \begin{Bmatrix} 0.7071 \\ 0.7071 \end{Bmatrix}$$

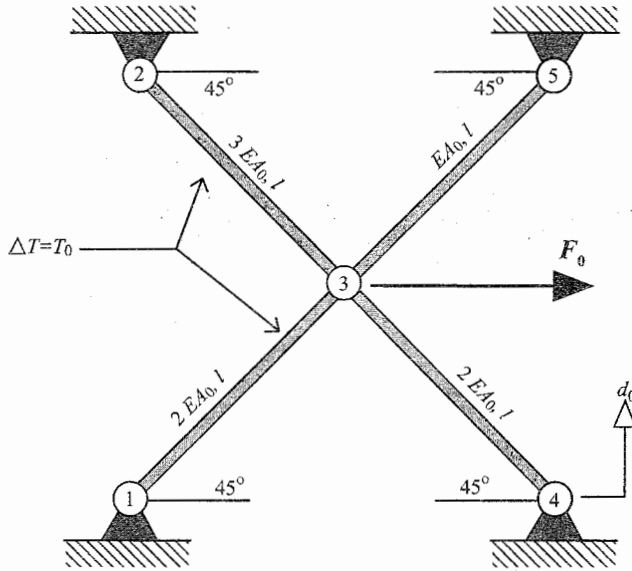


Figure 18.6. Example 18.5. A four-bar truss subjected to a mechanical loading and equivalent loadings due to temperature changes and a support motion.

For bar 2–3, where the rotation angle is -45° , the result is

$$\frac{3EA_0}{\ell} \begin{bmatrix} 0.5 & -0.5 \\ -0.5 & 0.5 \end{bmatrix} \begin{Bmatrix} u_3 \\ v_3 \end{Bmatrix} - 3EA_0\alpha T_0 \begin{Bmatrix} 0.7071 \\ -0.7071 \end{Bmatrix}$$

For bar 3–4, where the rotation angle is -45° , the result, including the enforced deflection, is

$$\frac{2EA_0}{\ell} \begin{bmatrix} 0.5 & -0.5 & 0.5 \\ -0.5 & 0.5 & -0.5 \end{bmatrix} \begin{Bmatrix} u_3 \\ v_3 \\ d_0 \end{Bmatrix}$$

For bar 3–5, where the rotation angle is $+45^\circ$, the result is

$$\frac{EA_0}{\ell} \begin{bmatrix} 0.5 & 0.5 \\ 0.5 & 0.5 \end{bmatrix} \begin{Bmatrix} u_3 \\ v_3 \end{Bmatrix}$$

Assembling the four matrices after separating out the enforced deflection leads to

$$\begin{Bmatrix} F_0 \\ 0 \end{Bmatrix} + \frac{\sqrt{2}}{2}EA_0\alpha T_0 \begin{Bmatrix} 5 \\ -1 \end{Bmatrix} + EA_0\frac{d_0}{\ell} \begin{Bmatrix} -1 \\ 1 \end{Bmatrix} = \frac{EA_0}{\ell} \begin{bmatrix} 4 & -1 \\ -1 & 4 \end{bmatrix} \begin{Bmatrix} u_3 \\ v_3 \end{Bmatrix}$$

which can easily be solved for the two unknown deflections. ■

Example 18.6. Set up the matrix equation $\{Q\} = [K]\{q\}$ for the two-bay planar frame shown in Fig. 18.7(a). Each of the five beams has the same length L and the same bending stiffness coefficient EI_0 . Model the axial stiffness of each beam as being rigid. Use the nodal DOF shown in Fig. 18.7(b). Note the two enforced deflections at the left-hand support.

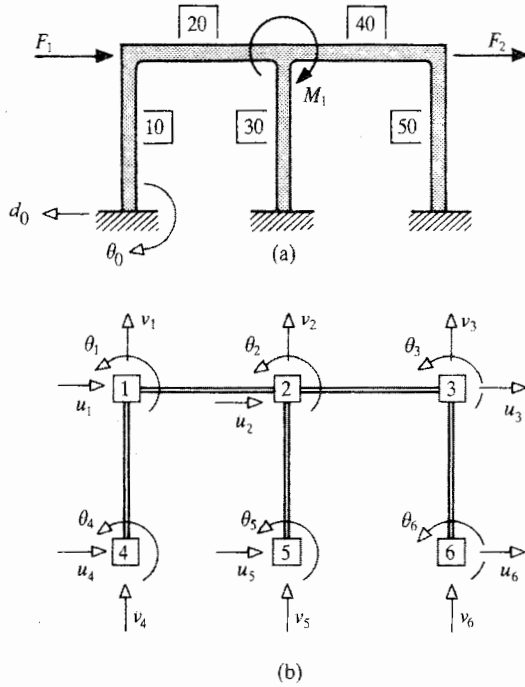


Figure 18.7. Example 18.6. (a) The analysis model with beam element numbering. (b) The remainder of the finite element model.

Comment. Note that with the support boundary conditions being modeled as clamped, it turns out that there are fewer deflection unknowns using the FEM than there would be force and moment unknowns using any force method of analysis. If, on the other hand, the three support BCs were changed to those of simple support, then there would only be one redundant force and, hence, just a single force method equation to solve.

Solution. The structural BCs require that $u_4 = v_4 = \theta_4 = u_5 = v_5 = \theta_5 = u_6 = v_6 = \theta_6 = 0$. The axial rigidity means that

$$v_1 = v_2 = v_3 = 0 \quad \text{and} \quad u_1 = u_2 = u_3 = u$$

Hence the element stiffness matrices, using u as the lateral DOF, are

$$[k_{10}] \{q\} = \frac{EI_0}{L^3} \begin{bmatrix} 12 & 6L \\ 6L & 4L^2 \end{bmatrix} \begin{Bmatrix} u \\ \theta_1 \end{Bmatrix} + \frac{EI}{L^3} \begin{bmatrix} -12 & 6L \\ -6L & 2L^2 \end{bmatrix} \begin{Bmatrix} -d_0 \\ -\theta_0 \end{Bmatrix}$$

$$[k_{30}] \{q\} = \frac{EI_0}{L^3} \begin{bmatrix} 12 & 6L \\ 6L & 4L^2 \end{bmatrix} \begin{Bmatrix} u \\ \theta_2 \end{Bmatrix}$$

$$[k_{50}] \{q\} = \frac{EI_0}{L^3} \begin{bmatrix} 12 & 6L \\ 6L & 4L^2 \end{bmatrix} \begin{Bmatrix} u \\ \theta_3 \end{Bmatrix} \quad [k_{20}] \{q\} = \frac{EI_0}{L^3} \begin{bmatrix} 4L^2 & 2L^2 \\ 2L^2 & 4L^2 \end{bmatrix} \begin{Bmatrix} \theta_1 \\ \theta_2 \end{Bmatrix}$$

and

$$[k_{40}] \{q\} = \frac{EI_0}{L^3} \begin{bmatrix} 4L^2 & 2L^2 \\ 2L^2 & 4L^2 \end{bmatrix} \begin{Bmatrix} \theta_2 \\ \theta_3 \end{Bmatrix}$$

Thus the final FEM matrix equation is

$$\begin{Bmatrix} +F_1 + F_2 \\ 0 \\ -M_1 \\ 0 \end{Bmatrix} = \frac{EI_0}{L^3} \begin{bmatrix} 36 & -6L & -6L & -6L \\ -6L & 8L^2 & 2L^2 & 0 \\ -6L & 2L^2 & 12L^2 & 2L^2 \\ -6L & 0 & 2L^2 & 8L^2 \end{bmatrix} \begin{Bmatrix} u \\ \theta_1 \\ \theta_2 \\ \theta_3 \end{Bmatrix} \\ + \frac{EI}{L^3} d_0 \begin{Bmatrix} 12 \\ 6L \\ 0 \\ 0 \end{Bmatrix} - \frac{EI}{L^3} \theta_0 \begin{Bmatrix} 6L \\ 2L^2 \\ 0 \\ 0 \end{Bmatrix}$$

The problem setup is complete when the equivalent load vectors on the right-hand side are transposed to the left-hand side and combined with applied forces and moment. It should be apparent that modeling beam elements as axially rigid, which is usually appropriate, greatly simplifies the matrix equation for a frame or grid undergoing small deflections. ■

If this original planar frame were enlarged by repetition of the original frame in two other planes parallel to the original plane of the frame, so that there were now nine beam-columns paralleling the v DOF direction, six beams in the u DOF direction, and another connecting six beams in the w DOF direction (so as to form a square “roof” structure), then this three dimensional frame would not be appreciably more complicated than the original planar frame. The routine difference would be that the three-dimensional frame would require more DOF. Specifically, the three-dimensional frame with axially rigid beams would require three rotational DOF at each of the nine roof nodes, but only three u direction DOF, and only three w direction DOF. The point is that it is not much of a step from two dimensions to three dimensions. This and related matters are considered further in Exercise 18.10.

Chapter 18 Exercises

- 18.1.** Set up, but do not bother to solve, the system stiffness matrix equation for the homogeneous truss of
- Fig. 20.4(a)
 - Fig. 20.22
 - Fig. 21.10(a)
 - Fig. 21.29
 - Fig. 21.25(a)
 - Fig. 21.25(b)
 - Fig. 21.25(c)
- 18.2.** (a) Redo Example 18.6 where now the only enforced deflection is at the center support, is upward, and has a magnitude of d_1 .
- As above, but the upward deflection is at the right-hand support, and has a magnitude d_2 .
 - Can the results of parts (a) and (b) be superimposed?

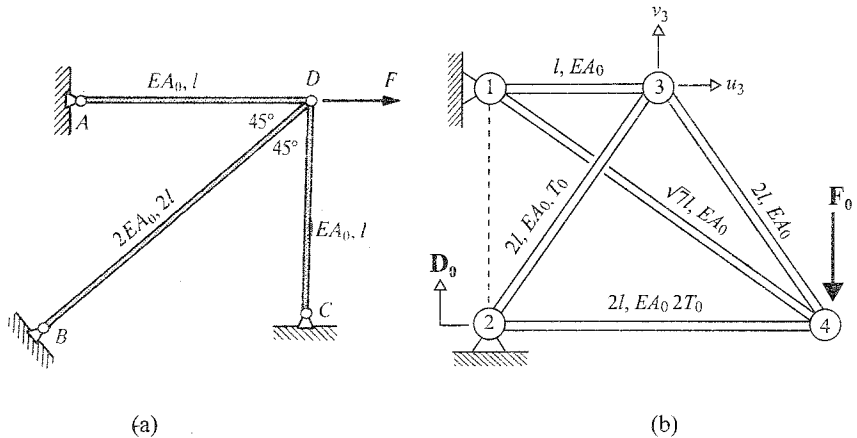


Figure 18.8. Exercise 18.3 (a). Exercise 18.3 (b).

- 18.3. (a) Use the finite element method to determine the force in bar AD of the simple truss sketched in Fig. 18.8(a).
 (b) Write the FEM matrix equation $\{Q^c\} = [K]\{q\}$ for the five-bar, pin-jointed truss shown in Fig. 18.8(b). Note that two bars have average temperature changes, and joint 2 is forced upward a small distance D_0 .
- 18.4. Write the system stiffness matrix equation $\{Q\} = [K]\{q\}$ for the six-bar, homogeneous truss of Fig. 18.4 when the same force F_0 acts upon the truss and there is a uniform temperature change of magnitude
 (a) T_0 in bar 13
 (b) $2T_0$ in bar 12
 (c) T_0 in bar 13 and $2T_0$ in bar 12
- 18.5. Write the system stiffness matrix equation $\{Q\} = [K]\{q\}$ for the planar truss of Fig. 21.10(a) when there are no applied mechanical loads but there is a uniform temperature change of magnitude T_0 only (a) in bar 1; (b) in bar 2; (c) in bar 3; (d) in bar 4.
- 18.6. Write the system stiffness matrix equation $\{Q\} = [K]\{q\}$ for the planar truss of Fig. 21.29 when top bar BC experiences a steady-state temperature change that varies in a bilinear fashion over the length of the bar in such a way that the temperature change is zero at joints B and C , and rises in a linear fashion from both bar ends to a maximum value of T_0 at the center of the bar.
- 18.7. Write the system stiffness matrix equation $\{Q\} = [K]\{q\}$ for the planar truss of Fig. 21.10(a) when there is no applied mechanical loading, but there is a small enforced vertical deflection of magnitude v_0 at: (a) joint B ; (b) joint C ; (c) joint D ; (d) joint E .
- 18.8. Write the FEM matrix equation $\{Q\} = [K]\{q\}$ for the continuous, uniform beam supported by four equally spaced knife-edge and roller supports that is shown in Fig. 18.9, when the third support from the left is forced downward a distance w_0 . The deformed shape of the beam is indicated by the dashed line. The beam bending stiffness coefficient is EI_0 .

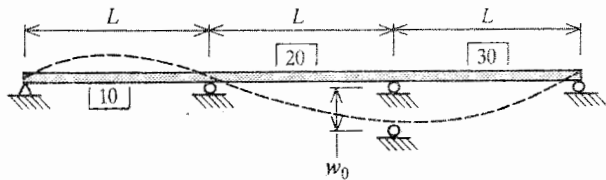


Figure 18.9. Exercise 18.8. A three span continuous beam subjected to an enforced displacement.

- 18.9. Write the system stiffness matrix equation $\{Q\} = [K]\{q\}$ for the planar truss of Fig. 21.10(a) when there is no applied mechanical loading, but there is a small initial strain of magnitude ϵ_0 (a) in bar BA ; (b) in bar CA ; (c) in bar DA ; or (d) in bar EA .

FOR THE EAGER

- 18.10. (a) Determine the six DOF stiffness matrix for a *beam* bending element for bending in a single plane that is rotated through a counterclockwise angle β within the plane of the paper. Do not bother to carry out any matrix multiplications. *Hint:* Consider Eqs. (18.1a, b) which is the bar DOF rotation equation for the same rotation in a plane. Note that the beam rotational DOF are unaffected by the change in beam orientation in the plane. (As per usual, the beam element is to be considered to be axially rigid.)
- (b) Determine the DOF rotation matrix for a *bar* element in three dimensions, and write the triple matrix product (i.e., without actually carrying out the matrix product) that is the stiffness matrix for a bar element in three dimensions. *Hint:* Consider the applicability of Eq. (4.6) as a basis for a DOF rotation matrix for the bar element which now has three rectilinear DOF at each of the two bar ends.
- Comment:* Once the element stiffness matrix for the bar element in three dimensions is available, structural finite element models such as that shown in the computer drawing that is Fig. 18.10 are readily attainable with a sufficiently large computer, or with a smaller computer coupled with a technique called "substructuring." The substructuring technique is briefly outlined in Endnote (1).
- (c) In three-dimensional space, can the same relation that exists between the *rectilinear* beam end deflection DOF in the rotated cartesian coordinate system and the original cartesian coordinate system be used with the beam end *rotational* DOF referenced to the same two coordinate systems?

- 18.11. Consider a truss where the material of all of the bars is to be described by a single stress-strain plot which is multilinear; that is, the stress-strain plot is approximated by a series of connected straight lines starting at the origin. In particular, let the slope of the loading path from zero strain to the strain value ϵ_1 , be E_1 the slope from ϵ_1 to ϵ_2 be E_2 , and so on. Note that for this material model to closely approximate actual material behavior, the truss' external loads must be applied so that none of these bars is unloaded appreciably during the load application. Describe in general terms how a digital computer could process the bars of such a loaded truss

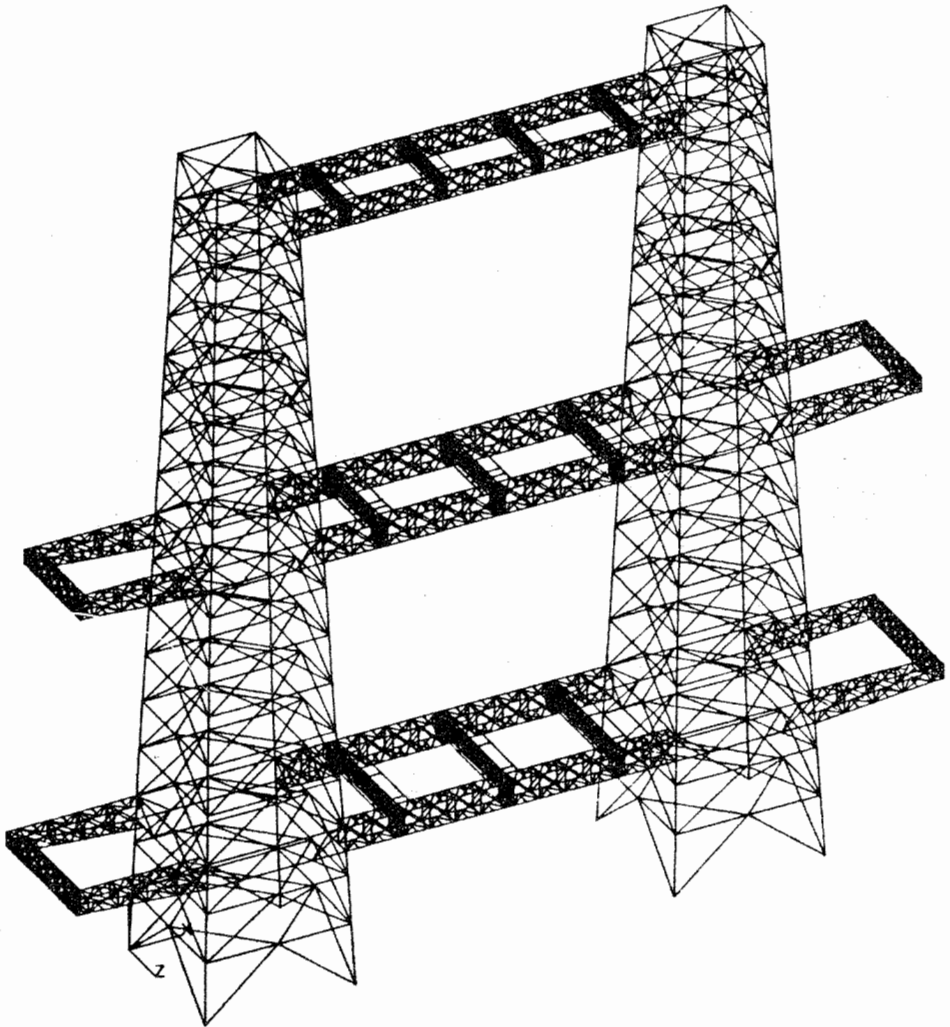


Figure 18.10. A computer drawing of a finite element model using a very large number of beam and bar finite elements. Courtesy of Dr. Frank Chang.

undergoing small deflections when the material behavior of those bars is described by this multilinear description.

Endnote (1) Substructuring in Static Analyses

Sometimes the available computer cannot manage the large number of DOF the analyst believes is necessary to describe a given structure. In that case the analyst can opt to divide that large structure into several substructures that can be partially processed, in order to reduce their individual number of DOF, before the substructures are linked together to form the final matrix equations for the total structure. The cost to be paid for this option is the expenditure of more computer running time. Consider, for example, the top platform of the tower structure shown in Fig. 18.10. Let that platform be one of several substructures of the total structure. The top platform can be modeled as a single, extended finite element.

The procedure for a static load case is as follows. Let all the bars and beams of the top platform be assembled in the usual manner to form $[\hat{K}]$ for the top platform with a corresponding $\{\hat{q}\}$. Divide $\{\hat{q}\}$ into two sets of DOF. Let the first set be those DOF that are to be retained in the analysis, and let the second set be those DOF that are to be omitted. Designate these two sets as $\{q_r\}$ and $\{q_0\}$, respectively. The retained coordinate set must include those DOF of the top platform elements that describe the deflections of the top platform where the top platform is joined to the two towers that support the top platform. The retained set may include other DOF sufficient to provide a sparse representation of the total top platform deflections. Order the generalized coordinate vector so that $[\hat{q}] = [q_r \ q_0]$. Then the matrix equation for the top platform becomes, in submatrix form,

$$\begin{Bmatrix} Q_r \\ \dots \\ Q_0 \end{Bmatrix} = \begin{bmatrix} K_{rr} & \dots & K_{ro} \\ \dots & \dots & \dots \\ K_{ro}^t & \dots & K_{oo} \end{bmatrix} \begin{Bmatrix} q_r \\ \dots \\ q_0 \end{Bmatrix} \quad (18.5)$$

The load vector $\{Q_0\}$ is composed entirely of known loads. The load vector $\{Q_r\}$ contains both the unknown reactions that act between the top platform and the towers, and possibly some known or zero-valued forces as well. The stiffness submatrices on the main diagonal are, of course, square matrices. Multiplying out the first and second rows of the above matrix equation yields

$$\begin{aligned} \{Q_r\} &= [K_{rr}]\{q_r\} + [K_{ro}]\{q_0\} \\ \{Q_0\} &= [K_{ro}]^t\{q_r\} + [K_{oo}]\{q_0\} \end{aligned} \quad (18.6)$$

The second of the above matrix equations can be solved for $\{q_0\}$:

$$\{q_0\} = [K_{oo}]^{-1}(\{Q_0\} - [K_{ro}]^t\{q_r\})$$

Substituting into the first of Eqs. (18.6) so as to eliminate $\{q_0\}$ leads to

$$[K_{rr} - K_{ro}K_{oo}^{-1}K_{ro}^t]\{q_r\} = \{Q_r - K_{ro}K_{oo}^{-1}Q_0\}$$

or

$$[\bar{K}_{rr}]\{q_r\} = \{\bar{Q}_r\} \quad (18.7)$$

The submatrix $[K_{oo}]$ is always invertible because when the DOF of the interfaces between the top platform substructure and the remainder to the total structure, which must be assigned to $\{q_r\}$, are arbitrarily fixed, then there is no possible rigid body motion of the substructure. The substructure equation, Eq. (18.7), is of exactly the same form as an element stiffness equation. That is, there is a column matrix of unknown deflections $\{q_r\}$; there is a square coefficient matrix of fully specified terms; and there is a load vector of known and unknown loads. Sometimes the substructure is referred to as a "super" finite element because of the generally larger number of DOF that are associated with it. Now it is just a matter of assembling these super elements in the usual manner to form the total structure.

It may appear that the obvious drawback to this procedure is that the inversion of $[K_{oo}]$ could be, for a large number of DOF, an expensive operation with regard to computer time. The inversion of $[K_{oo}]$ is not actually necessary. In order to justify this statement, write the coordinate transformation

$$\begin{Bmatrix} q_r \\ q_0 \end{Bmatrix} = \begin{bmatrix} I \\ -K_{oo}^{-1}K_{ro}^t \end{bmatrix} \{q_r\} + \begin{Bmatrix} 0 \\ K_{oo}^{-1}Q_0 \end{Bmatrix} = \begin{bmatrix} I \\ T \end{bmatrix} \{q_r\} + \begin{Bmatrix} 0 \\ Q_c \end{Bmatrix} \quad (18.8)$$

Substituting the above right-hand side for $\{q\} = \{q_r \quad q_0\}$ into Eq. (18.5), and premultiplying by $[I \quad T]$, after some algebraic simplification, reproduces Eqs. (18.7). Now return to Eq. (18.5) and initiate the standard Gauss–Jordan elimination process starting with the last DOF of $\{q_0\}$. After the Gauss–Jordan process is completed for $\{q_0\}$, and before starting with $\{q_r\}$, what was Eq. (18.5) now has the appearance

$$\begin{Bmatrix} ? \\ \dots \\ ? \end{Bmatrix} = \begin{bmatrix} ? & \vdots & 0 \\ \dots & \dots & \dots \\ ? & \vdots & I \end{bmatrix} \begin{Bmatrix} q_r \\ \dots \\ q_0 \end{Bmatrix} \quad (18.5a)$$

The lower row of question marks can be determined by referring to the lower row of Eq. (18.8), which may be rewritten as

$$-[T]\{q_r\} + \{q_0\} = \{Q_c\}$$

The upper row of question marks can be identified by reference to Eq. (18.7), that is,

$$[\bar{K}_{rr}]\{q_r\} + [0]\{q_0\} = \{\bar{Q}_r\}$$

Putting the latter two equations into Eq. (18.5a), the result is

$$\begin{Bmatrix} \bar{Q}_r \\ \dots \\ Q_c \end{Bmatrix} = \begin{bmatrix} \bar{K}_{rr} & \vdots & 0 \\ \dots & \dots & \dots \\ -T & \vdots & I \end{bmatrix} \begin{Bmatrix} q_r \\ \dots \\ q_0 \end{Bmatrix} \quad (18.5b)$$

Thus the cost-efficient Gauss–Jordan procedure, rather than a matrix inverse, can be used to obtain the $[\bar{K}_{rr}]$ matrix as well as the transformation matrix $[T]$ and the vector $\{Q_c\}$, which can be used to recapture the values of the $\{q_0\}$ vector after solution for the $\{q_r\}$ vector. This procedure is credited to R. J. Guyan, and is sometimes called Guyan reduction or static condensation (Ref. [69]).

Basic Aspects of Multidimensional Finite Elements

19.1 Introduction

Beams and bars alone do not a vehicular structure make. Vehicular structures are typically beam frames and grids enveloped in a thin skin. See, for example, the illustrations in the front of this textbook, or the illustration in Endnote (2) of this chapter, which discusses the function of the thin skin, the stringers, and the frames. Characteristically, the skin thickness is much smaller than the distances between the beams that support the skin. In order to extend the finite element method to analytical models of vehicular structures, it is now necessary to begin to consider the analysis of thin skins in combination with the beam grids and frames that provide support for the skin. For the sake of simplicity, the discussion of thin skins in this introductory chapter is restricted to those that have a midsurface that parallels a single plane.

There are two distinct load cases for a planar, thin skin. In the first load case the edge traction vectors and the internal stress vectors parallel the plane of the skin, and are constant across the small thickness dimension of the skin. Furthermore, in this plane stress case, the skin is thick enough, or the lateral beam supports are sufficiently close to each other, that the skin does not buckle. Thus the deflection vectors also parallel the unloaded skin midsurface. The purpose of this chapter is to introduce a finite element-based deflection formulation to this plane stress problem. Doing so illustrates on an elementary level one general approach to creating finite elements beyond the one-dimensional beam and bar finite elements discussed in Chapters 17 and 18.

In the second external load case the flat skin is loaded so that after deformation the skin is no longer planar. This would be the case (i) if the in-plane, externally applied, mechanical or thermal loading varied across the outer edge thickness of the skin in such a manner as to cause bending or twisting moments; or (ii) if there were a loading lateral to the plane of the skin that causes bending or twisting moments. Analogously to the bending of beams, if the lateral deflection of the skin is less than one-quarter the skin thickness, then the skin behavior is described by linear plate theory. If the lateral deformations are several times greater than the skin thickness, then membrane theory is suitable. If the lateral deformations are on the same order of magnitude as the skin thickness, then the nonlinear, von Kármán plate theory is appropriate. Plate bending and twisting are discussed in the next to last chapter of this textbook.

In addition to introducing the deflection approach to the plane stress problem via the finite element method (FEM), this chapter also provides a brief introduction to three-dimensional finite elements and the use of the FEM when the applied loads vary with time.

19.2 A Rectangular Plane Stress Finite Element

Recall that in the FEM, beams, uniform or not, with general lateral loadings, are analyzed by approximating them by a sequence of finite length, uniform beam segments. Similarly, a thin skin in a state of plane stress can be approximated by a collection of

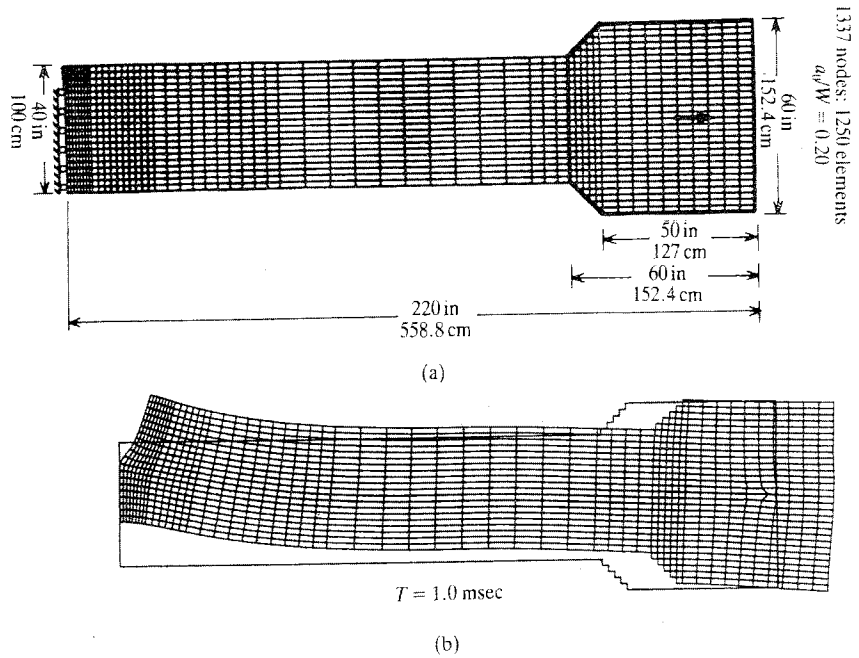


Figure 19.1. A typical finite element mesh using many simple finite elements for the sake of numerical accuracy. The model is that of a dynamic fracture test specimen. Only one half of the test specimen is modeled due to symmetry. Courtesy of Professor Charles Schwartz.

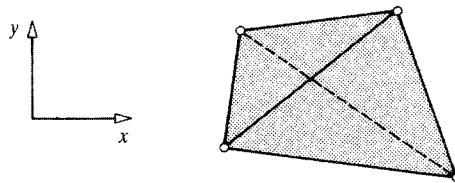


Figure 19.2. A plane stress quadrilateral finite element formed from two pairs of half thickness triangular plane stress finite elements, one pair superimposed upon the other pair.

constant thickness skin segments with finite dimensions. See Fig. 19.1, which shows a computer plot of a typical finite element arrangement for a structure that happens to be a dynamic fracture test specimen. The undeformed shape of the finite elements in Fig. 19.1 is rectangular. In most commercial finite element digital computer programs, the available simple shapes for skin segment finite elements are quadrilateral and triangular shapes. The quadrilateral-shaped finite element is often created by putting together two pairs of half thickness triangular finite elements superimposed upon each other as shown in Fig. 19.2. The triangular and quadrilateral shapes have the advantage of allowing a straight-line segment approximation to any skin geometry.

Since the first purpose of this chapter is limited to introducing the plane stress finite element, the specific geometry of the element is of lesser importance than the ideas upon which the element is based. Therefore, rather than tackle the more difficult geometry of the triangular plane stress finite element, the simpler, but less practical, rectangular plane stress finite element is chosen to illustrate the concepts that underlie two- and three-dimensional

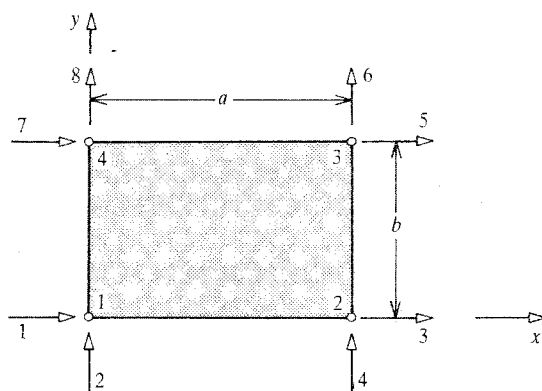


Figure 19.3. The coordinate system, geometry, and ordering of the DOF for a rectangular plane stress finite element.

finite elements. The triangular plane stress finite element is discussed briefly in the following section in order to show the parallels between its development and the development of the rectangular finite element.

Consider the plane stress rectangular finite element pictured in Fig. 19.3. The first question to be answered is what are the degrees of freedom (DOF) of the rectangular finite element. The previously discussed beam and bar elements provide only limited guidance. As with the beam and bar elements, it would seem that the rectangular element DOF are best placed at the element boundary for ease of joining one element with another. It would also seem to be true that the number of such DOF should be as small as possible because each additional DOF requires the solution of an additional simultaneous equation. The above two guidelines do have important exceptions. However, those two guidelines are a useful basis for an initial development of a plane stress finite element. Algebraic experimentation shows that, as illustrated in Fig. 19.3, placing two DOF at each corner of the rectangle is a satisfactory approach. The eight in-plane DOF of the rectangular plane stress finite element are thus selected to be $q_1 = u_1$, $q_2 = v_1$, $q_3 = u_2$, $q_4 = v_2$, $q_5 = u_3$, and so on.

Once again, the element stiffness matrix is to be developed using the Principle of Virtual Work (PVW). In order to use the PVW in the same successful fashion as was done with the beam and bar finite elements, the deflections everywhere within the rectangular finite element have to be uniquely and continuously defined by the eight deflection components at the four corners. In other words, equations that parallel the beam and bar shape function equations, Eqs. (17.4) and (17.10), have to be developed for the rectangular plane stress finite element. However, unlike the one-dimensional beam and bar elements, there is no concise deflection solution for the plane stress rectangle given the deflections at the four corners. Moreover, even if such a solution were available, it would not be particularly useful because it would necessarily conflict with the PVW requirement that the displacements everywhere along the outer boundaries of the element (i.e., in and between the several adjacent finite elements) be continuous. Another, and therefore approximate, means of relating the corner deflections and the finite element's internal and boundary deflections is appropriate.

The internal deflections can be represented exactly in a general form by writing their functional representation in terms of complete infinite series for which there is an arbitrary coefficient attached to each term of the series. In this, as in any given set of circumstances, some series expansions are more convenient than others. In this case a power (polynomial) series

is chosen to represent the internal, in-plane, deflections. A power series is a cost-efficient choice for a numerical analysis application such as that pictured in Fig. 19.1 because the polynomial terms of the power series are much more quickly calculated by a digital computer than those of, say, a trigonometric series. Other vital advantages are discussed below. A power series with nonnegative exponents is a "complete" series in that it is capable of representing a wide class of well-behaved functions called "analytic" functions. Indeed the definition of an analytic function depends upon that function being representable by the power series called a Taylor series (Ref. [1]).

Let the power series for the two in-plane deflection components be written as

$$\begin{aligned}u(x, y) &= \alpha_0 + \alpha_1x + \alpha_2y + \alpha_3x^2 + \alpha_4xy + \alpha_5y^2 + \dots \\v(x, y) &= \beta_0 + \beta_1x + \beta_2y + \beta_3x^2 + \beta_4xy + \beta_5y^2 + \dots\end{aligned}$$

where the unknown α and β coefficients need to be determined. The only deflection information available to determine these coefficients is the set of corner deflections. The corner deflections only comprise four pieces of information for each of the two deflection components, $u(x, y)$ and $v(x, y)$. Hence only four α and four β coefficients can be determined this way without introducing more deflection conditions. Thus it becomes a question of which are the four most important terms in the two power series. Only those eight terms are to be retained, while all others are to be discarded. While exceptions can always be found, the more important terms of a series expansion are usually those terms with the lowest exponents in the case of a polynomial series, or with the lowest indices in the case of a trigonometric series. This general guide is true in this case. The reasons specific to this finite element are as follows. Without the constant term of each of the two series, there would be no way to represent an in-plane rigid body (i.e., zero strain) motion of the rectangular finite element without introducing false strains into the rectangular element. See Endnote (1) for a detailed explanation of this point. Similarly, without the two pairs of linear terms, there would be no way to represent a state of constant strain throughout the rectangular element. Since the constant strain case is as basic as the rigid body motion case, the first three terms of each deflection expansion are selected for use.

The fourth term selected for inclusion in the two deflection series must provide, as much as possible, for (i) an appropriate change in strain across the element; and (ii) continuity between elements. This latter requirement is necessary for the valid application of the PVW, which requires the satisfaction of the strain-displacement equations so that it can enforce equilibrium internally and at the nodal connections between adjacent elements. The three quadratic terms x^2 , y^2 , and xy are now considered as candidates for that fourth and last position in the two finite series approximations for the displacement components. First consider x^2 for the u series expansion, and y^2 for the v series expansion. One major problem with this choice is that, for example, at the upper edge of the plane stress rectangle, where $y = b$, the displacement in the u direction would vary parabolically. At the bottom of the adjacent rectangular plane stress element, where for that element, $y = 0$, the horizontal displacement would also vary parabolically. However, there can be no assurance that the two variations would be the same because there are only two nodes connecting these two elements while it takes three constraints to define a parabola. Hence there would not be complete interelement compatibility. Another major problem would be that the two normal strains, $\partial u/\partial x$ and $\partial v/\partial y$, would vary linearly within the rectangular element while the shearing strain $\partial v/\partial x + \partial u/\partial y$ would be a constant. From the plane stress, stress-strain equations, Eqs. (6.12) or (6.13), the normal stress would vary linearly while the shearing stress would be a constant. This situation would violate the general equilibrium equations within the element.

Similarly, if the choice was made to use y^2 in the series expansion for $u(x, y)$, and x^2 in the $v(x, y)$ expansion, then within the element the shearing stress would vary linearly in both directions while the two normal stresses would be constant. This too would violate the general equilibrium equations within the element. This possible choice would also have the unacceptable defect that it produces a parabolic variation in the $u(0, y)$ and $u(a, y)$ deflections, that is, the deflections along the left- and right-hand boundaries. Therefore these deflections would not be continuous with the boundary deflections of the adjacent rectangular elements. There would be gaps and/or overlaps between the adjacent elements. Thus this choice must also be disqualified. The remaining possibility is the xy term for both displacements, making those two series have exactly the same form and the same behavior in the x and y directions. With this choice, the normal strain ϵ_{xx} would vary linearly in the y direction, and ϵ_{yy} would vary linearly in the x direction; γ_{xy} would vary linearly in both directions. While not perfect, this would allow the three stresses to vary linearly. Finally, there would be no problem at any element edge because both displacements would vary linearly at those edges, and the two common nodes of adjacent elements would provide the two common parameters that would make those linear variations the same for both adjacent elements. Thus this choice of the xy term provides inter-element compatibility and thus allows the use of the PVW.

Therefore let the chosen series expansions for this four-node plane stress element be

$$\begin{aligned} u(x, y) &= \alpha_0 + \alpha_1 x + \alpha_2 y + \alpha_3 xy \\ v(x, y) &= \beta_0 + \beta_1 x + \beta_2 y + \beta_3 xy \end{aligned} \quad (19.1)$$

The above two plane stress deflection equations correspond to the beam equation which is Eq. (17.3a). The similarities are that: (i) Eqs. (19.1) and Eq. (17.3a) are truncated polynomial series descriptions of deflections suitable to that type of finite element; and (ii) both descriptions contain unspecified constants. That is, the four constants of integration of Eq. (17.3a), C_1 through C_4 , correspond to the α 's and β 's of Eq. (19.1). The difference between Eqs. (19.1) and Eq. (17.3a) is that the cubic polynomial of Eq. (17.3a) is the exact solution to the applicable strength of materials beam bending equation, Eq. (17.2), while Eqs. (19.1) are only approximations to the actual deflections within a finite rectangular portion of a plane stress continuum when the element is relatively small. In general, the larger the finite element, the cruder the approximation. If each of the many rectangles is reasonably small with respect to the in-plane lengths associated with the structure and the loading, such as is shown in Fig. 19.1, then the above linear approximation in each rectangle forms an accurate straight-line segment approximation to the actual deflection pattern.

In Eqs. (17.3b) and (17.4a), the four constants of integration are replaced by their equivalent values in terms of the bending deflections and bending slopes at the beam element ends. To obtain a pair of equations corresponding to Eqs. (17.4a), the eight parameters of Eq. (19.1) now need to be determined in terms of the eight corner deflections. This is accomplished by simply substituting the cartesian coordinates of each of the corners into Eqs. (19.1), and solving simultaneously. That is, starting with

$$\begin{aligned} u_1 &= \alpha_0 & v_1 &= \beta_0 \\ u_2 &= \alpha_0 + \alpha_1 a & v_2 &= \beta_0 + \beta_1 a \\ u_3 &= \alpha_0 + \alpha_1 a + \alpha_2 b + \alpha_3 ab & v_3 &= \beta_0 + \beta_1 a + \beta_2 b + \beta_3 ab \\ u_4 &= \alpha_0 + \alpha_2 b & v_4 &= \beta_0 + \beta_2 b \end{aligned}$$

an easy simultaneous solution leads to

$$\begin{aligned} \alpha_1 &= (u_2 - u_1)/a & \alpha_2 &= (u_4 - u_1)/b & \alpha_3 &= (u_1 + u_3 - u_2 - u_4)/ab \\ \beta_1 &= (v_2 - v_1)/a & \beta_2 &= (v_4 - v_1)/b & \beta_3 &= (v_1 + v_3 - v_2 - v_4)/ab \end{aligned}$$

or, after rearranging,

$$\begin{aligned}
 u(x, y) &= \left(1 - \frac{x}{a} - \frac{y}{b} + \frac{xy}{ab}\right) u_1 + \frac{x}{a} \left(1 - \frac{y}{b}\right) u_2 \\
 &\quad + \left(\frac{xy}{ab}\right) u_3 + \frac{y}{b} \left(1 - \frac{x}{a}\right) u_4 = \sum N_i(x, y) u_i \\
 v(x, y) &= \left(1 - \frac{x}{a} - \frac{y}{b} + \frac{xy}{ab}\right) v_1 + \frac{x}{a} \left(1 - \frac{y}{b}\right) v_2 \\
 &\quad + \left(\frac{xy}{ab}\right) v_3 + \frac{y}{b} \left(1 - \frac{x}{a}\right) v_4 = \sum N_i(x, y) v_i
 \end{aligned} \tag{19.2}$$

where $i = 1, 2, 3, 4$. Thus the shape functions for the plane stress rectangle are now identified. Note that, like all shape functions, they have the value 1.0 at the spatial coordinate values corresponding to the DOF for which they are a coefficient in the deflection expressions, and they have the value 0.0 at the spatial coordinate values where all other DOF are located. See Section 19.5 for a discussion of how this shape function characteristic aids the determination of the required shape functions.

With the shape functions for the approximate deflections in hand, it is now a routine matter to use the strain–deflection equations and the stress–strain equations of the theory of elasticity in order to evaluate the element internal virtual work on the right-hand side of Eq. (17.5). For conciseness, let $(x/a) = X$, and $(y/b) = Y$. Then

$$\begin{aligned}
 \{\gamma\} &= \begin{Bmatrix} \epsilon_{xx} \\ \epsilon_{yy} \\ \gamma_{xy} \end{Bmatrix} = \begin{Bmatrix} \partial u / \partial x \\ \partial v / \partial y \\ (\partial u / \partial y) + (\partial v / \partial x) \end{Bmatrix} = [B]\{q\} \\
 &= \begin{bmatrix} -(1-Y)/a & 0 & (1-Y)/a & 0 \\ 0 & -(1-X)/b & 0 & -X/b \\ -(1-X)/b & -(1-Y)/a & -X/b & (1-Y)/a \\ & & Y/a & 0 & -Y/a & 0 \\ & & 0 & X/b & 0 & (1-X)/b \\ & & X/b & Y/a & (1-X)/b & -Y/a \end{bmatrix} \begin{Bmatrix} u_1 \\ v_1 \\ u_2 \\ v_2 \\ u_3 \\ v_3 \\ u_4 \\ v_4 \end{Bmatrix} \tag{19.3}
 \end{aligned}$$

Now all is ready for use of the PVW as applied to the structural body that is a single rectangular finite element. For that element, the external virtual work is merely the eight in-plane force components multiplied by their respective virtual displacements. Again see Fig. 19.4(a). That is, because there are no body forces acting upon this finite element, and all the external boundary loads are required to act at the corners of the finite element where the nodes of the global DOF are to be located,

$$\begin{aligned}
 \delta W_{ex} &= F_{x1} \delta u_1 + F_{y1} \delta v_1 + F_{x2} \delta u_2 + \cdots + F_{y4} \delta v_4 \\
 &= [\delta q] \{Q\}
 \end{aligned} \tag{19.4}$$

The negative of the internal virtual work for this plane stress finite element reduces to

$$-\delta W_{in} = \iiint_{\text{Vol.}} [\delta \epsilon_{xx} \quad \delta \epsilon_{yy} \quad \delta \gamma_{xy}] \begin{Bmatrix} \sigma_{xx} \\ \sigma_{yy} \\ \sigma_{xy} \end{Bmatrix} d(\text{Vol.})$$

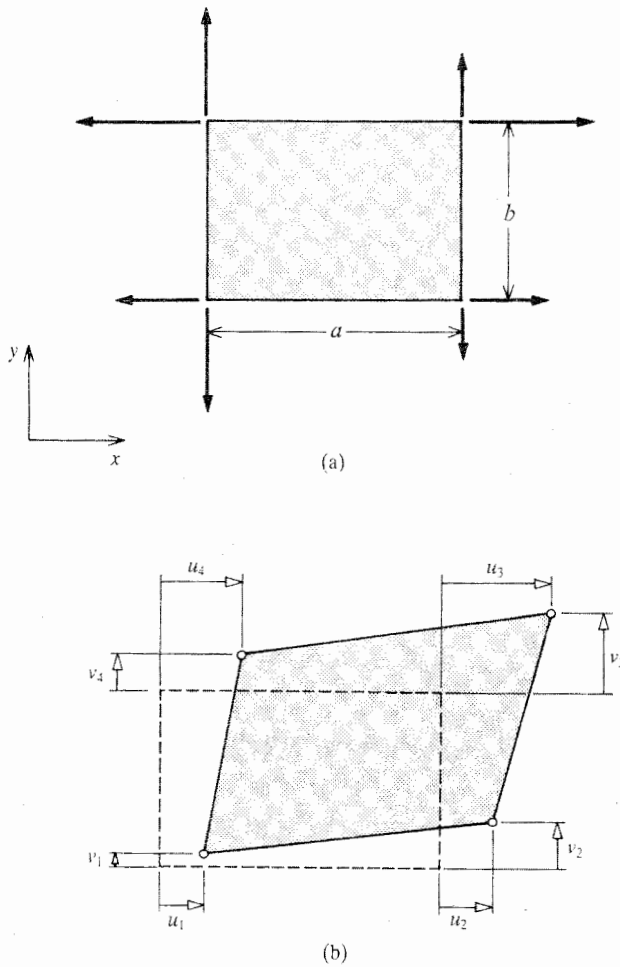


Figure 19.4. (a) Typical corner (nodal) forces for a discussion of possible deflections and strains in a rectangular plane stress finite element. (b) The nonrigid body deflection pattern (much exaggerated) for the rectangular plane stress finite element.

or

$$-\delta W_{in} = h \int_0^a \int_0^b [\delta\epsilon_{xx} \quad \delta\epsilon_{yy} \quad \delta\gamma_{xy}] \begin{Bmatrix} \sigma_{xx} \\ \sigma_{yy} \\ \sigma_{xy} \end{Bmatrix} dx dy$$

where h is the thickness of the skin. Taking the variation of both sides of Eq. (19.3) leads to $\{\delta\gamma\} = [B]\{\delta q\}$, or

$$[\delta\gamma] = [\delta q][B]^t$$

In this case of plane stress, the 3×1 stress vector for an isotropic material is that set forth in Eq. (6.13). Equation (6.13) can be written as

$$\begin{Bmatrix} \sigma_{xx} \\ \sigma_{yy} \\ \sigma_{xy} \end{Bmatrix} = \frac{E}{1-\nu^2} \begin{bmatrix} 1 & \nu & 0 \\ \nu & 1 & 0 \\ 0 & 0 & \frac{1}{2}(1-\nu) \end{bmatrix} \begin{Bmatrix} \epsilon_{xx} \\ \epsilon_{yy} \\ \gamma_{xy} \end{Bmatrix} - \frac{E\alpha \Delta T}{1-\nu} \begin{Bmatrix} 1 \\ 1 \\ 0 \end{Bmatrix}$$

or, in more concise form,

$$\{\sigma\} = [D]\{\gamma\} - \Delta T \{\gamma_T\} \quad (6.13a)$$

Substituting $\{\gamma\} = [B]\{q\}$ into Eq. (6.13) provides the stresses as functions of the generalized coordinates

$$\{\sigma\} = [D][B]\{q\} - \Delta T \{\gamma_T\} \quad (6.13b)$$

Now the PVW can be developed as

$$\begin{aligned} [\delta q]\{Q\} &= [\delta q]h \int_0^a \int_0^b [B]^t [D][B] dx dy \{q\} \\ &\quad - [\delta q]h T_{av} \int_0^a \int_0^b [B]^t \{\gamma_T\} dx dy \end{aligned}$$

where, for simplicity in this development, T_{av} , an average temperature change is used for the entire finite element. This choice of an average temperature change is reasonable when the finite elements are used in sufficient numbers to reasonably approximate the actual temperature change with a series of constant values, as would likely be the case in a finite element model such as that shown in Fig. 19.1. Following the usual argument so as to remove the arbitrary row vector of virtual displacements from both sides of the above equation leads to

$$\{Q\} = h \int_0^a \int_0^b [B]^t [D][B] dx dy \{q\} - h T_{av} \int_0^a \int_0^b [B]^t \{\gamma_T\} dx dy$$

Since the first integral is a symmetric, square matrix, and the second integral is a column vector, the above result can be written more concisely as

$$\{Q\} = [k]\{q\} - \{Q_T\}$$

or even more simply as

$$\{Q\} + \{Q_T\} \equiv \{Q^c\} = [k]\{q\} \quad (19.5)$$

As explained in Chapter 18, the equivalent thermal load vector $\{Q_T\}$ is not limited to initial strains due to temperature changes, but that vector can be adjusted to include all types of initial strains.

It is clear now what needs to be done to obtain the element stiffness matrix $[k]$. It is necessary to actually carry out the matrix multiplication $[B]^t [D][B]$, and then the double integration of that 8×8 result. This is a lengthy, but routine, process that is not worth duplicating here. The final result is given below in terms of the following space-saving, nondimensional, quantities. Let

$$\begin{aligned} k_0 &\equiv +(1/3)[(b/a) + \frac{1}{2}(1-\nu)(a/b)] \\ k'_0 &\equiv +(1/3)[(a/b) + \frac{1}{2}(1-\nu)(b/a)] \\ k_1 &\equiv -(1/6)[2(b/a) - \frac{1}{2}(1-\nu)(a/b)] \\ k'_1 &\equiv -(1/6)[2(a/b) - \frac{1}{2}(1-\nu)(b/a)] \\ k_2 &\equiv -(1/6)[(b/a) + \frac{1}{2}(1-\nu)(a/b)] \\ k'_2 &\equiv -(1/6)[(a/b) + \frac{1}{2}(1-\nu)(b/a)] \\ k_3 &\equiv +(1/6)[(b/a) - (1-\nu)(a/b)] \\ k'_3 &\equiv +(1/6)[(a/b) - (1-\nu)(b/a)] \\ n_0 &\equiv (1/8)(1+\nu) \quad \text{and} \quad n_1 \equiv (1/8)(3\nu-1) \end{aligned}$$

Then the rectangular plane stress finite element stiffness matrix can be written as

$$[k] = \frac{Eh}{1-\nu^2} \begin{bmatrix} k_0 & n_0 & k_1 & n_1 & k_2 & -n_0 & k_3 & -n_1 \\ n_0 & k'_0 & -n_1 & k'_3 & -n_0 & k'_2 & n_1 & k'_1 \\ k_1 & -n_1 & k_0 & -n_0 & k_3 & n_1 & k_2 & n_0 \\ n_1 & k'_3 & -n_0 & k'_0 & -n_1 & k'_1 & n_0 & k'_2 \\ k_2 & -n_0 & k_3 & -n_1 & k_0 & n_0 & k_1 & n_1 \\ -n_0 & k'_2 & n_1 & k'_1 & n_0 & k'_0 & -n_1 & k'_3 \\ k_3 & n_1 & k_2 & n_0 & k_1 & -n_1 & k_0 & -n_0 \\ -n_1 & k'_1 & n_0 & k'_2 & n_1 & k'_3 & -n_0 & k'_0 \end{bmatrix} \quad (19.6)$$

The equivalent thermal force vector is easily evaluated. The result is

$$\{Q_T\}^t = \frac{1}{2} \frac{Eh\alpha T_{av}}{1-\nu} [-b \quad -a \quad b \quad -a \quad b \quad a \quad -b \quad a] \quad (19.7)$$

where, again, the temperature change is the average temperature change for the finite element.

Now that the rectangular plane stress finite element is fully detailed, it can be used to create finite element structural models in exactly the same fashion as the beam and bar finite elements.

Example 19.1. (a) Prepare by hand a finite element analysis of (i.e., write $\{\bar{Q}\} = [\bar{K}]\{\bar{q}\}$ for) the symmetric structure shown in Fig. 19.5(a). The only applied loading is the force F which acts in the plane of the structure. The thickness of the skin is h . The cross-sectional area of the reinforcing bar is $36h^2$. The Young's modulus for both the bar and the skin is E . The Poisson's ratio for the skin is $1/3$. As usual, assume that the shearing stresses in the skin do not produce skin buckling.

(b) After obtaining a solution for the global DOF, calculate the magnitude of the axial force at the left end of the central bar.

Comment. This small structure is representative of vehicular structures because it involves both a skin and a beam or bar stiffener to which concentrated loads can be applied. The skin stiffener is often called a "longitudinal stringer," or just a "stringer."

Solution. (a) Since this small beam and skin structure is only loaded in its own plane, only bar and plane stress finite elements are necessary to produce a finite element model for this structure. The next thing to note is that the symmetry of the structure and loading allows the analysis to be limited to the top half of the structure. The number of finite elements to be used to describe the skin and bar depends heavily on whether or not the small structure stands alone or is actually just one part of a larger structure. If this small structure stands alone, then a reasonable, but minimum number of rectangular plane stress and bar finite elements is shown in Fig. 19.5(b). Note that the rectangular geometry requires that all adjacent rectangular elements have the same edge dimensions. This is unfortunate because the finite element arrangement shown in Fig. 19.5(b) gives equal attention, on the one hand, to those parts of this small structure where the stresses, strains, and deflections change only gradually, and, on the other hand, to those parts of the structure where the changes are not at all gradual. A much more reasonable arrangement using commercially

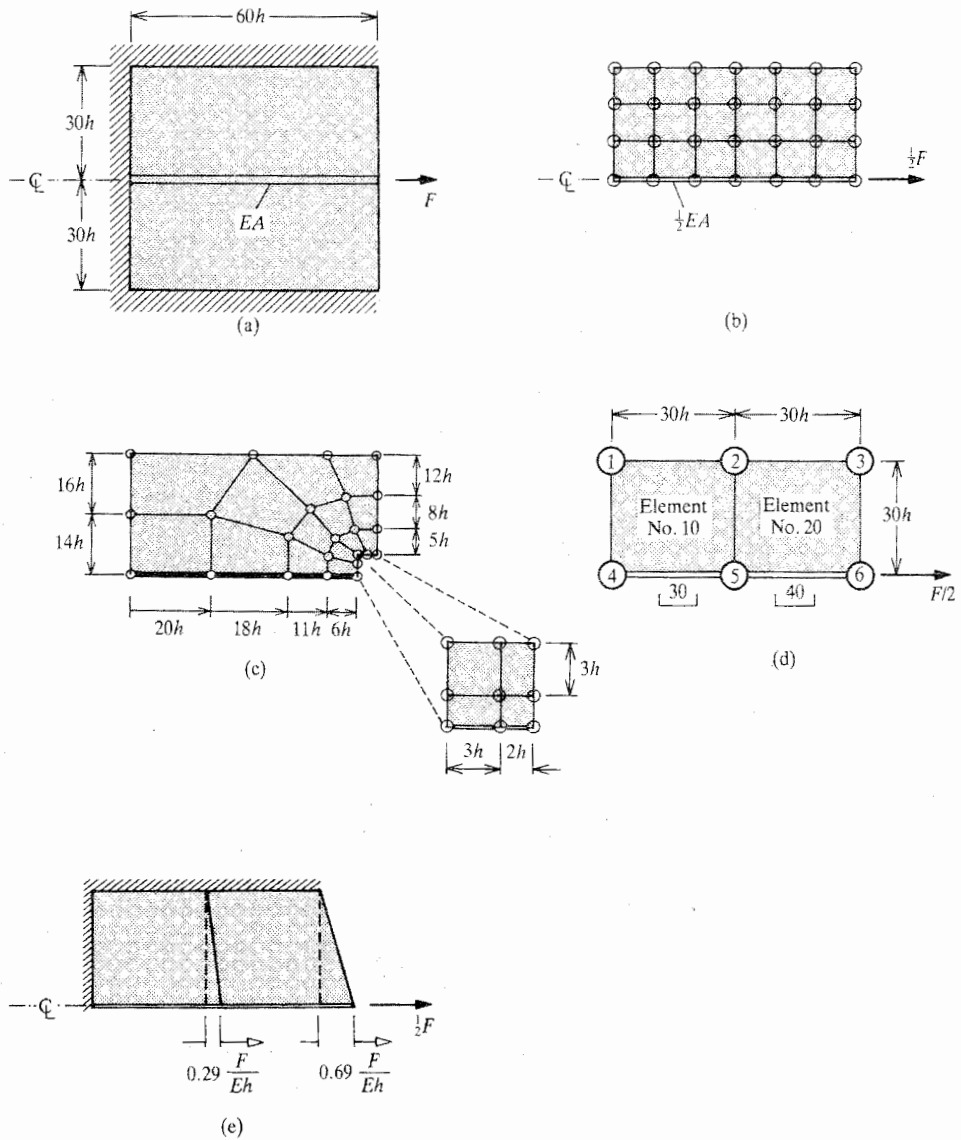


Figure 19.5. Example 19.1. (a) The analysis model of the sheet-beam structure. (b) A finite element model of the same structure using 18 rectangular plane stress finite elements and 6 bar elements for a total of 56 DOF. (c) A finite element model using the same number of plane stress and bar elements as the previous model, but one which will produce much more accurate numerical results near the point of application of the load which is where the deflections and stresses vary more rapidly with distance. This second finite element model illustrates another shortcoming of finite elements limited to a rectangular geometry. (d) The finite element model used for the hand calculation. (e) A plot of the deflection results.

available quadrilateral finite elements is shown in Fig. 19.5(c). In that figure the linearly changing finite elements are concentrated where the greatest changes in strain are expected so as to better approximate those changes.

If this small structure were part of a much larger structure, budget and computer storage limitations would generally not allow so many degrees of freedom for a small portion of the overall structure, unless of course there was something particularly important about this small part. If this small structure is a noncritical part of a much larger structure, the top half of this structure would likely be modeled with as few as two plane stress elements and two bar elements, or even one of each. (The approximate, linearly varying deflections chosen for this finite element work best when the ratio of the edge lengths, a/b , equals 1.0, which would be the case here if two rectangular elements were used.) Since this solution is to be done by hand, the latter view is now adopted. Consequently, the selected finite element model of nodes and elements is as shown in Fig. 19.5(d).

The skin finite element stiffness matrices are relatively large. Therefore, in order to save space and time, the procedure of first applying the BCs to the element stiffness matrices is the procedure used in this example. In this example, the global DOF BCs are particularly simple. The constraints on all motion at the top and left boundaries of the structure leads to

$$u_1 = v_1 = u_2 = v_2 = u_3 = v_3 = u_4 = v_4 = 0$$

The symmetry of the structure and loading means that none of the nodes on the centerline of the structure move up or down. Therefore

$$v_5 = v_6 = 0$$

Thus the only nonzero plane stress DOF are u_5 and u_6 , which are also the only necessary DOF for the two bar elements. Hence, after applying the BCs, the stiffness matrices for the two bar elements in terms of the two nonzero DOF are, where only half the bar area is used due to the symmetry,

$$[k_{30}]\{q^{30}\} = \frac{1}{2} \frac{EA}{l} u_5 \quad \text{and} \quad [k_{40}]\{q^{40}\} = \frac{1}{2} \frac{EA}{l} \begin{bmatrix} +1 & -1 \\ -1 & +1 \end{bmatrix} \begin{Bmatrix} u_5 \\ u_6 \end{Bmatrix}$$

where

$$\frac{1}{2} \frac{EA}{l} = \frac{18Eh^2}{30h} = 0.6Eh$$

For both plane stress finite elements, the ratios $a/b = b/a = 1.0$, $k_0 = 4/9$, $k_1 = -5/18$, and $Eh/(1 - \nu^2) = 1.125Eh$. The correspondences between the element and global DOF are $u_2^{(10)} = u_5$ for element 10, and $u_1^{(20)} = u_5$ while $u_2^{(20)} = u_6$ for element 20. Thus the two skin stiffness matrices reduce to

$$[k_{10}]\{q^{10}\} = 1.125Eh(4/9)u_5$$

and

$$[k_{20}]\{q^{20}\} = 1.125Eh \begin{bmatrix} 4/9 & -5/18 \\ -5/18 & 4/9 \end{bmatrix} \begin{Bmatrix} u_5 \\ u_6 \end{Bmatrix}$$

Assembling the two matrices of size 1×1 and the two matrices of size 2×2 produces the final matrix equation:

$$\begin{Bmatrix} 0 \\ 0.5F \end{Bmatrix} = Eh \begin{bmatrix} (0.6 + 0.6 + 0.5 + 0.5) & -(0 + 0.6 + 0 + 0.3125) \\ -(0 + 0.6 + 0 + 0.3125) & (0 + 0.6 + 0 + 0.5) \end{bmatrix} \begin{Bmatrix} u_5 \\ u_6 \end{Bmatrix}$$

or

$$\begin{Bmatrix} 0 \\ 0.5F \end{Bmatrix} = Eh \begin{bmatrix} 2.20 & -0.9125 \\ -0.9125 & 1.10 \end{bmatrix} \begin{Bmatrix} u_5 \\ u_6 \end{Bmatrix}$$

The solution to the above simultaneous equations is easily found to be $u_5 = 0.29F/Eh$, and $u_6 = 0.69F/Eh$. A plot of the solution for the two DOF looks like that shown in Fig. 19.5(e).

(b) Once the above two simultaneous equations are solved for u_5 , the force in bar element 30 can be obtained from the bar element 30 stiffness matrix equation. Of course it is necessary to remember that the total force in bar element 30 is that for both halves of the bar cross-sectional area. In other words, the total force at node 4 is

$$\frac{EA}{l}u_5 = \frac{36Eh^2}{30h}u_5 = 0.35F$$

Clearly, since only one-third of the applied force reaches the end of the stringer, two-thirds of the applied force is diffused through the skin of the small structure to the skin's rigid supports. ■

Example 19.2. Discuss in words only how the solution procedure for Example 19.1 would change if the direction of the applied force F were changed so that it was now directed out of the plane of the paper at the same location. Again, assume small deflections.

Solution. The load out of the plane of the paper causes bending of both the central beam and the skin. Therefore, bar elements are no longer suitable. Beam elements are now necessary. Similarly, plane stress elements are no longer suitable. Rectangular plate bending elements (to be developed in the next to last chapter) are now needed. Closely analogous to the beam bending finite element, the typical commercially available quadrilateral plate bending finite element has three DOF at the four corners. The three DOF are the lateral deflection and the bending slope rotations about two cartesian coordinate axes. Also see, for example, Ref. [50], chapter 10.

The selection of the number of plate bending elements proceeds on nearly the same basis as before. However, for a crude grid, the number of plate bending elements should be at least as large as the number of plane stress elements. If the grid pictured in Fig. 19.5(c) were used in this case also, the clamped end BCs for the plate and beam, and the symmetry conditions mean that the four nonzero DOF for this case would be the lateral deflections and beam bending slopes at nodes 5 and 6. (The beam twisting DOF required by the plate finite elements are required to be zero because of the structural and loading symmetry.) ■

As a final comment on the rectangular plane stress element, recall that this element is derived above for the special case of an isotropic material. Developing a plane stress rectangular finite element for an orthotropic material would only require using Eq. (6.12) instead of Eq. (6.13) for the stress-strain relationship. Of course, the resulting algebra would be considerably more tedious, not only because there are five material constants to keep track of, rather than just two, but because in order to achieve generality it is necessary to

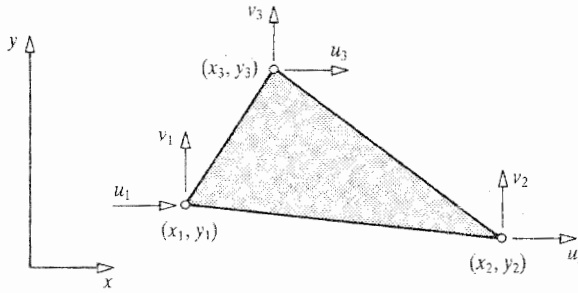


Figure 19.6. The coordinate system and the selected element DOF for the triangular plane stress finite element.

consider the possibility that the material axes of the finite element are not aligned with edges of the finite element. Therefore, when using a commercial finite element digital computer program for an orthotropic material, expect to input the angle of rotation of the material axes from some specified coordinate axes or element edge.

19.3 A Triangular Plane Stress Element in Brief

The more geometrically useful plane stress triangular finite element can be derived in exactly the same way that the rectangular finite element was derived in the above discussion or, alternately, by more elegant means (Refs. [50, 54]). Without the burden of the algebra, the highlights of the straightforward derivation are as follows. The truncated series expansions for the deflections are

$$u(x, y) = \alpha_0 + \alpha_1 x + \alpha_2 y$$

$$v(x, y) = \beta_0 + \beta_1 x + \beta_2 y$$

Just as before, these six parameters, α_0 through β_2 , can be determined in terms of the corner deflections, which are the element DOF. See Fig. 19.6 for an illustration of the element DOF. Just as before, linking the six truncated series parameters and the element DOF is accomplished by specializing the cartesian coordinates to the corner locations; for example,

$$u_1 = \alpha_0 + \alpha_1 x_1 + \alpha_2 y_1$$

$$u_2 = \alpha_0 + \alpha_1 x_2 + \alpha_2 y_2$$

and so on, and solving simultaneously. After regrouping the results in terms of the element DOF, the matrix equation $\{u\} = [N]\{q\}$ is obtained, where $[u] = [u(x, y) \ v(x, y)]$. Of course, the three distinct shape functions are linear functions of the x and y coordinates. Therefore, just as is true for the rectangle, the deflections along any edge of the triangle vary linearly from one corner to another, and are completely controlled by the corner deflections. Hence the edge deflections of one plane stress triangular finite element are exactly the same as those of any adjacent plane stress triangular (or plane stress rectangular) finite element. Therefore intra- and interelement deflection continuity is present with the result that this formulation meets the continuity requirement of the PVW.

Once the deflections everywhere within the triangle and along its borders are described in terms of the nodal deflections (analogous to element BCs), the remaining procedure is exactly the same as that for the rectangle. That is, the next step is to differentiate the deflections in order to obtain the strain vector. The use of the appropriate material stiffness

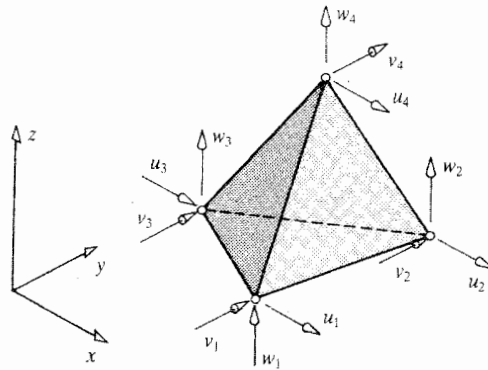


Figure 19.7. The coordinate system and element DOF for the constant strain tetrahedron unite element.

matrix provides the stress vector. Varying the strain vector is the final preparatory step. Substituting $[\delta\epsilon]$ and $\{\sigma\}$ into the PVW satisfies the general force equilibrium requirement, and provides the details of the 6×6 element stiffness matrix. The integration over the volume of the triangular element that is required by the PVW is particularly simple in this case. This is so because the deflections are linear functions of the spatial coordinates. Therefore the stresses and strains and their products are constants. Since these constants can be factored out of the volume integral, the volume integral that remains can be evaluated as simply the area of the triangular element multiplied by its depth.

One small difference between these rectangular and triangular plane stress finite elements is that, since the stresses within the triangular element are constants, those stresses satisfy the intraelement equilibrium equations, Eqs. (1.6). On the other hand, the four-node rectangular element utilizes linearly varying stresses that do not satisfy Eq. (1.6). On balance, there is little to choose between these two plane stress elements with respect to accuracy. This can be understood by viewing the deflection series expansions for these two different elements as Taylor's series without the remainder terms. The remainder terms encompass the error for the deflection series expansions for the two elements. The remainders, and hence the errors, for each Taylor's series expansion involve the polynomial terms of the order greater than the last complete polynomial order of the expansion. The last complete polynomial order in both element expansions is the first. The single quadratic term xy in the rectangular element expansion is, of course, incomplete because it lacks the companionship of the x^2 and the y^2 terms. Thus the errors in both element expansions involve the squares of the lengths of the element sides normalized by a characteristic length of the skin that is being analyzed.

19.4 Three-Dimensional Finite Elements

The constant strain finite element with a solid shape that has the same geometric adaptability as the plane stress triangular element is the tetrahedron element. Such an element with its 12 DOF is shown in Fig. 19.7. Its deflection series expansions are simply

$$u(x, y, z) = \alpha_0 + \alpha_1 x + \alpha_2 y + \alpha_3 z$$

$$v(x, y, z) = \beta_0 + \beta_1 x + \beta_2 y + \beta_3 z$$

$$w(x, y, z) = \gamma_0 + \gamma_1 x + \gamma_2 y + \gamma_3 z$$

The procedure to be followed for this element to the point of application of the PVW is, of course, exactly the same as it is for the two plane stress elements discussed above. Again, since the strain and stress quantities are constants, the volume integration required by the PVW is a relatively simple matter.

Since the geometry of a grouping of tetrahedrons is sometimes difficult to picture, commercial software packages often offer “brick elements” that are composed of five tetrahedrons so as to produce a rectangular parallelepiped (or near rectangular parallelepiped) geometry. Filling the bulk of a given volume with bricks is a much more manageable task. See Figs. 19.8(a, b).

Another aspect of the problem of visualizing the finite element model concerns inadvertently omitting a two- or three-dimensional finite element from the overall model. In an ordinary computer plot of the finite element model for the structure, or that part of the structural model that involves only that one type of finite element, it is not clear whether a given space is filled by an element or not. A computer plot where the geometry of the nodes is at one scale while the elements are drawn smaller immediately reveals whether there are any missing elements. See Fig. 19.9 for an illustration of such a plot, which clearly shows that no elements have accidentally been omitted.

19.5 Refined Finite Elements of Simple Shapes

A two- or three-dimensional finite element's generalized coordinates need not only be positioned at element corners. For example, a rectangular plane stress element can be developed that has eight pairs of element DOF as pictured in Fig. 19.10(a). One reason to consider having more DOF associated with a two- or three-dimensional finite element can be understood by considering the triangular plane stress finite element discussed above. That triangular finite element is a constant strain-type element. With other than the simplest types of loadings, each adjacent three-node, six-DOF triangular plane stress finite element in the finite element model can be expected to have a different constant strain value. In other words, the strain values would have a stair-step type pattern over the area of the model, as shown in Fig. 19.10. Although the linearly varying intraelement deflection pattern of the three-node element can produce a good approximation to the actual deflections, this stair-step pattern for the strains would not be as good a representation for the actual strains. Since the stresses are proportional to the strains, their solution values also would be inferior to the deflection solution.¹ One way to improve the stress solution is to have a triangular plane stress element in which the strains vary linearly, instead of having just constant values. This can be accomplished by increasing the number of polynomial terms in each of the two truncated series expansions for the in-plane deflection functions so as to include the x^2 , xy , and y^2 polynomial terms. This increase in the number of terms to a total of six in each of the two series requires tying each set of six series parameters to six points on the element boundary. Thus is born the 12-DOF triangular plane stress element with a pair of generalized coordinates at each corner and at each edge center. Again, this alternate type of finite element form is not illustrated with the triangular geometry because of its greater algebraic complexity. Rather it is illustrated in the discussion below for a finite element with a rectangular boundary.

¹ Typically, deflection-based approximate methods of analysis provide inferior stress solutions while stress-based approximations provide inferior deflection solutions.

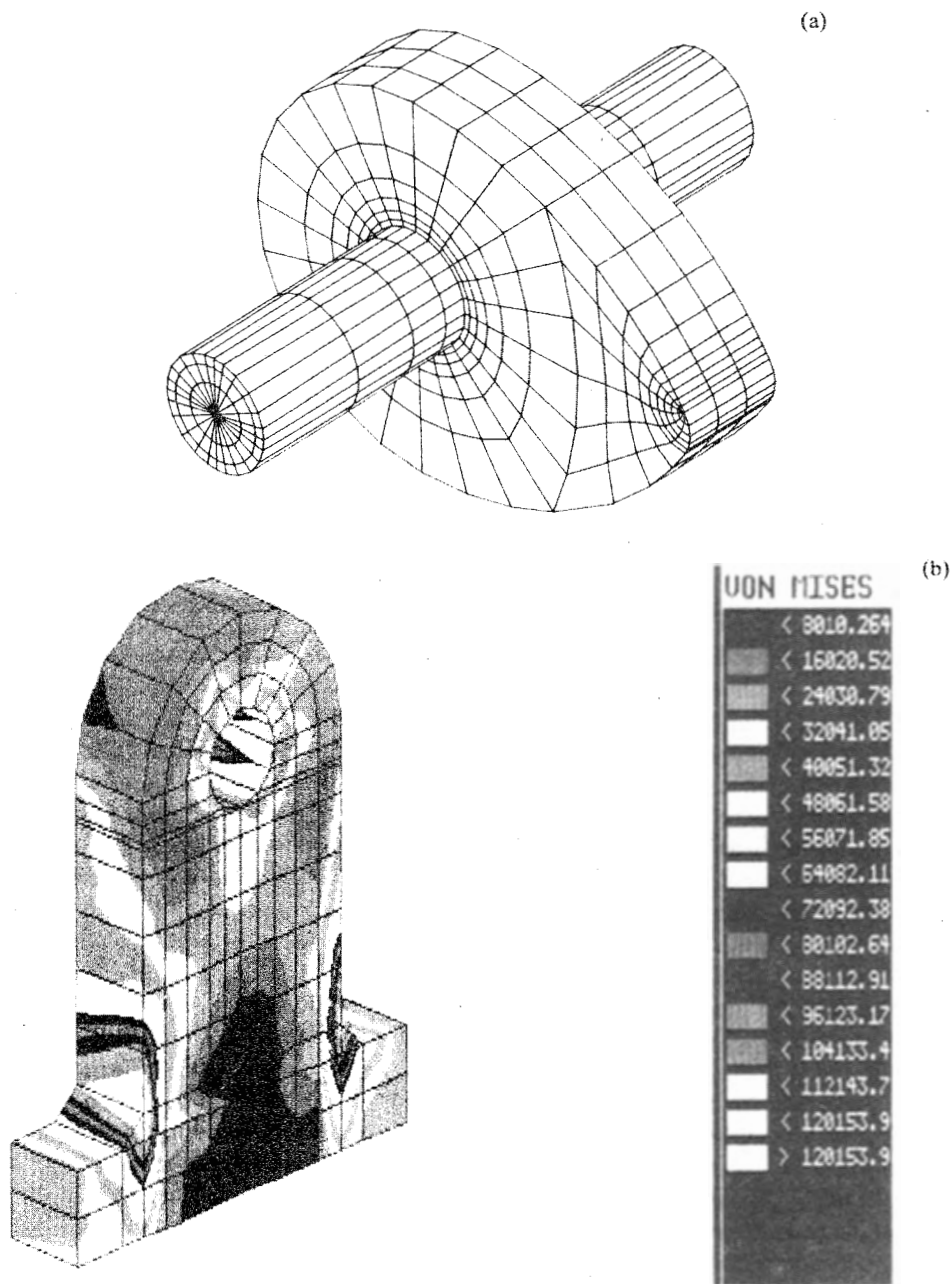


Figure 19.8. Example models using three-dimensional (solid) finite elements. (a) A shaft segment with cam, courtesy of Mr. Jeffrey Meeker. (b) A trunnion bracket, courtesy of Mr. Scott Buie. The multihued pattern (originally in full color) superimposed on the trunnion bracket finite element model is that of the stress ranges indicated in the accompanying key. Computer graphics, of which these diagrams are examples, are often the only practical way of making manageable the large quantities of numerical analysis data that are commonplace when the FEM analysis involves large numbers of DOF.

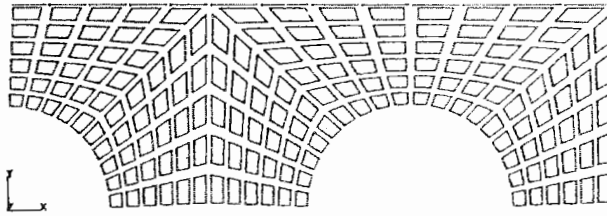


Figure 19.9. A computer drawing of a doubly symmetric, two-dimensional finite element model where the dimensions of the individual elements have been decreased in order to check that no elements have been omitted inadvertently. Courtesy of Mr. Paul Van Gulik.

Consider again the plane stress rectangular finite element sketched in Fig. 19.11(a). Since for this element there are, for example, eight v_i DOF, the truncated series expansion for $v(x, y)$ would be

$$v(x, y) = \beta_0 + \beta_1x + \beta_2y + \beta_3x^2 + \beta_4xy + \beta_5y^2 + \beta_6x^2y + \beta_7xy^2 \quad (19.8)$$

It is immediately evident that solving simultaneously for the β_i parameters in terms of the v_i , $i = 1, 2, 3, \dots, 8$, is considerably more work than when there were three or four terms in the truncated series deflection expansion. At this point, and certainly when considering even more DOF for a given geometry, it is worth considering the alternate approach of directly writing the shape functions that relate the deflections at any point in the interior of the element, or at the element boundary, to the element DOF. It turns out that writing the shape functions directly can sometimes be quite simple. Recall that any shape function

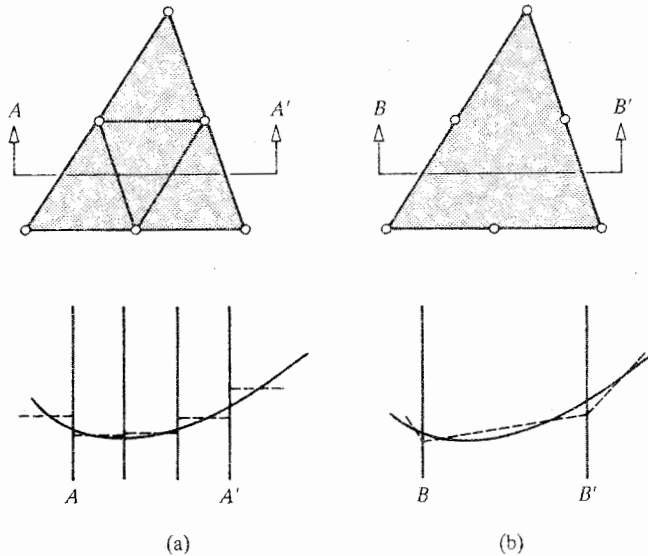


Figure 19.10. A comparison of the strain fields for (a) a group of four unrefined finite elements and (b) one refined finite element. The refined element has the same number of DOF as the four unrefined elements, and covers the same area. The solid line represents the actual strain distribution of the structure along the horizontal line. The dashed lines represent the finite element approximations to the actual strain, and in these figures it is presumed that these approximations are close to the average values of the actual strain.

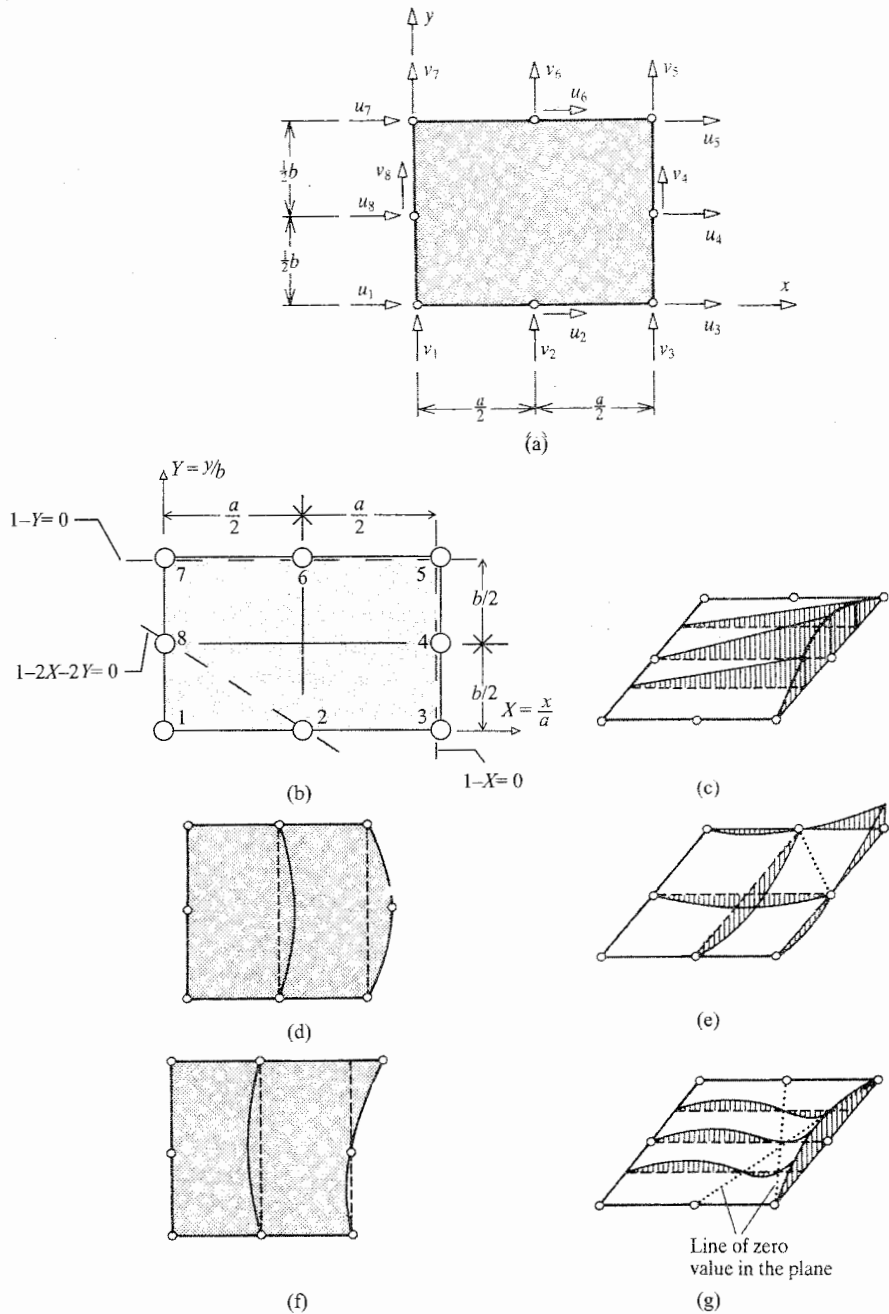


Figure 19.11. A refined rectangular plane stress finite element. (a) The element coordinate system and the element DOF. (b) The lines of zero value used to create the shape function for node number one. (c) The values of the shape function $N_4(X, Y)$ plotted as ordinates above the x, y plane. (d) The shape function $N_4(X, Y)$ interpreted as an induced deflection pattern resulting from a u_4 deflection. (e) The values of the shape function $N_5(X, Y)$ plotted as ordinates above the x, y plane. (f) The shape function $N_5(X, Y)$ interpreted as an induced deflection pattern resulting from a u_5 deflection. (g) The values of the less desirable shape function $F_4(X, Y)$ plotted as ordinates above the x, y plane. The function $F_4(X, Y)$ has the required shape function values at all corner points and edge centers. However, its associated deflection pattern is more remote from physical reality than that of $N_4(X, Y)$, and is one reason why $F_4(X, Y)$ is rejected.

has the essential characteristics that: (i) at the spatial coordinate values of the associated DOF, the shape function has the value +1; and (ii) at the spatial coordinate values of any other DOF, the shape function has the value zero. With, again, $X = x/a$, and $Y = y/b$, the following functions, called “serendipity”² shape functions, are suitable as shape functions for the 16-DOF rectangular finite element pictured in Fig. 19.11(a):

$$\begin{aligned} N_1(X, Y) &= (1 - X)(1 - Y)(1 - 2X - 2Y) & N_2(X, Y) &= 4X(1 - X)(1 - Y) \\ N_3(X, Y) &= X(1 - Y)(2X + 2Y - 1) & N_4(X, Y) &= 4XY(1 - Y) \\ N_5(X, Y) &= XY(2X + 2Y - 3) & N_6(X, Y) &= 4XY(1 - X) \\ N_7(X, Y) &= (1 - X)Y(2Y - 2X - 1) & N_8(X, Y) &= 4(1 - X)Y(1 - Y) \end{aligned}$$

The origin of the shape function $N_1(X, Y)$ for node one is illustrated by the three dashed lines of Fig. 19.11(b). This shape function needs to have the value zero at nodes two through eight. Together, the three dashed lines, $1 - Y = 0$, $1 - 2X - 2Y = 0$, and $1 - X = 0$, pass through all of these seven nodes. Simply using the left-hand sides of these equations for these three lines as factors creates $N_1(X, Y)$. In this case, no adjustment is necessary to obtain a unit value at $X = Y = 0$. Of course, the other seven shape functions are determined in the same manner using only three lines. Note that if the products contained in these eight shape functions are multiplied out, the result in each case would be polynomial terms limited to the set $1, x, y, x^2, xy, y^2, x^2y$, and xy^2 , which is complete through the second order.

The shape functions with even-numbered subscripts are for the DOF pairs located at the centers of the edges. They are a nice set of shape functions in that they have somewhat the sort of shape that the deflections would have if their respective edge center were forced to have a positive unit deflection while all the other corners and edge centers were restrained against deflection. See Fig. 19.11(c) for a plot of the shape function $N_4(X, Y)$ which is associated with the two generalized coordinates at the center of the right-hand edge. Note that this plot is the conventional type plot for a function with two cartesian type variables, rather than as in Fig. 19.11(d), which is a sketch of the same function interpreted as an in plane deflection pattern. This version of $N_4(X, Y)$ is not the only possible version. Another function that has the value 1 at the center of the right-hand edge and zero values at all four corners and the three other edge centers is, for example,

$$F_4(X, Y) = 4X(2X - Y - 1)(2X + Y - 2)$$

First, by itself, this function is less desirable because its much more complicated shape, as pictured in Fig. 19.11(g), bears less resemblance to the actual deflection pattern that results from these deflection constraints. However, this function’s major difficulty is that it introduces an X^3 term into the truncated polynomial series expansions for the two deflections; see Eq. (19.8). Since no other polynomial terms would be deleted, there would then be nine polynomial terms with only the eight constraints imposed by the four corners and four edge centers. If the other shape functions were also altered so that other polynomial terms were deleted to make room for X^3 , (and Y^3 for balance), then one difficulty would be, as discussed below, that the resulting rectangular elements would not possess interelement continuity as called for by the PVW. Therefore $F_4(X, Y)$ is an example of an unsatisfactory candidate shape function.

The shape functions with odd-numbered subscripts are for the corner DOF. As Figs. 19.11(d, f) show, these functions do not have quite the desirable characteristic of

² A word coined by Horace Walpole from a fairy tale concerning three princes of Serendip (now Sri Lanka) to describe a state of regularly making interesting, accidental discoveries.

being approximately the deflection pattern if a corner were given a horizontal or vertical deflection while all other corners and edge centers were constrained against deflections. Nevertheless, these are the selected shape functions because they contain only the polynomial terms of Eq. (19.8), and there are no better competitors that also contain only those polynomial terms. Having only those polynomial terms is important because, along any edge of the rectangle, the deflections can only vary quadratically. For example, along the top edge where $Y = 1$, the series expansion for $v(x, b)$ is a parabola in terms of X . The exact shape of that parabola with its three coefficients is fully controlled by the values of the three corner and edge center DOF v_5 , v_6 , and v_7 . Since the corners and edges of the adjacent rectangle have exactly the same nodal deflections, the lower edge of the adjacent rectangle has exactly the same deflections as the top edge of the rectangle under discussion. Thus, as called for by the PVW, the eight-node rectangular finite elements that compose the finite element model have continuous deflections across their boundaries as well as in their interiors.

Now that the shape functions of the 16-DOF rectangular plane stress element have been fully qualified, the remainder of the development is routine. Again the deflections are written as

$$u(X, Y) = \sum N_i(X, Y) u_i \quad \text{and} \quad v(X, Y) = \sum N_i(X, Y) v_i$$

Then the above deflections are differentiated according to the theory of elasticity equations in order to obtain the strains. The stress expressions are obtained from the constitutive equations. Then the PVW enforces equilibrium in a general sense with a result that leads directly to the element stiffness matrix $[k]$.

Further basic aspects of the FEM are discussed in Chapters 22 and 23. Nevertheless, many facets of the FEM are left to FEM textbooks.

19.6 ****The Finite Element Method with Time-Varying Loads****

In engineering practice, one of the more challenging aspects of a structural analysis is deciding what loads are appropriate to the analysis. The loads acting upon a vehicle arise from many sources. For example, for a flight vehicle the loads are first of all the weight loads, the steady-state³ lift and drag components of the net aerodynamic force, the aerodynamic moment, and the loads produced by the thrust provided by the power plant. However, the largest loads are likely to be the inertia loads that result from gusts, maneuvering, landing, or, in the case of a rocket launch, the vibrations that result from the turbulence of the rocket exhaust. Landing loads are of course of special concern, especially for wire-arrested landings upon aircraft carriers. In order to illustrate the pervasiveness of inertia loads, note that the critical loads for certain aircraft wings have been the inertia loads associated with taxiing over rough taxiways. All these inertial loads have magnitudes that depend upon the motion, in particular the accelerations, of the flight vehicle. The reverse is also true. The motion of the flight vehicle depends upon the inertia and other loads applied to the vehicle. Therefore a differential equation, rather than an algebraic equation, is needed to describe the interaction between the inertia loads and the vehicle's time-varying deflections.

The differential equation that describes the load-deflection interaction is nothing more than the equilibrium statement that the sum of the inertia loads, plus the elastic loads, plus the applied loads, plus the damping friction loads, equals zero. Continuity and boundary conditions are accounted for by writing this differential equation in terms of generalized

³ "Steady-state" means unchanging with respect to time.

coordinates that assure continuous deflections throughout the structure and at the supports. The material equations are incorporated in the description of the elastic loads. Thus the differential equation that describes the load–deflection interaction, in the approximate sense of strength of materials, accounts for all four of the concerns of any structural analysis: equilibrium, deflection continuity, material behavior, and boundary conditions.

The form of that differential equation, partial or ordinary, depends upon how the structure is mathematically modeled. If the structure is modeled as having continuously distributed mass and continuously distributed elastic properties, as is the case for every actual structure, then the equilibrium statement has the form of one or more partial differential equations. See, for example, Exercise 11.14. The general engineering approach to solving a partial differential equation is, when possible, to first reduce it to a set of ordinary differential equations by one of various mathematical techniques. An alternate approach, verified over many years, is to model the structure as a collection of interconnected discrete masses and discrete elastic elements. In this mathematical model, the elastic elements have no mass, and the mass elements have no elasticity; that is, the mass elements are rigid bodies. In this case the equilibrium statement, called the equation(s) of motion, is immediately in the form of a set of ordinary differential equations. This is the engineering approach most often used because (i) the continuum model is especially cumbersome when the structure consists of more than a very few structural elements; (ii) the discrete elastic elements are conveniently described as finite elements; and (iii) the description of the inertial loads is easily obtained for discrete masses. The following example offers a brief review of the discretization process.

Example 19.3. Set up a finite element model for a simply supported, uniform beam of length L , stiffness coefficient EI , mass per unit length ρA , which is subjected to a uniform lateral force per unit length of magnitude $f_z(t)$. Ignore damping forces of all kinds.

Solution. Since the single-beam structure is subjected to a time-varying load, it is necessary to model both the elastic and inertial properties of the beam. Since the modeling of the elastic properties of a structure requires more careful attention, that is, more refinement, than the modeling of the inertial properties, the elastic modeling is best done first. Being guided by the results of Endnote (2) of Chapter 17 let this beam be divided into six identical parts of length $L/6$. Let each of these beam segments be represented by a beam finite element of that length; see Fig. 19.12. In recognition of the symmetry of the structure and loading, and in keeping with the present procedure of immediately applying all deflection BCs, the beam bending slope DOF at the center of the beam is omitted because it must have a zero value. The deflection DOF at the beam support is also omitted for the same reason.

The magnitudes of the discrete or “lumped” masses are determined by evenly dividing the distributed beam mass between the various node points. Since the lumped mass of magnitude $\rho AL/12$ at the beam support can have no motion, and thus cannot load the beam, it is omitted. Note that only discrete mass values have been placed at the nodes. That is, in this case, the lumped masses have been assigned zero mass moment of inertia. This is so because it has been amply demonstrated that the mass moments of inertia of the beams themselves have much less effect on the motion of the beam than the mass of the beams.⁴ Therefore, in this case, there are mass terms associated with the lateral deflections but not with the bending slopes.

⁴ Mass moments of inertia of *nonstructural* masses typically supported by beams in vehicular structures can have significant impact upon vibrations.

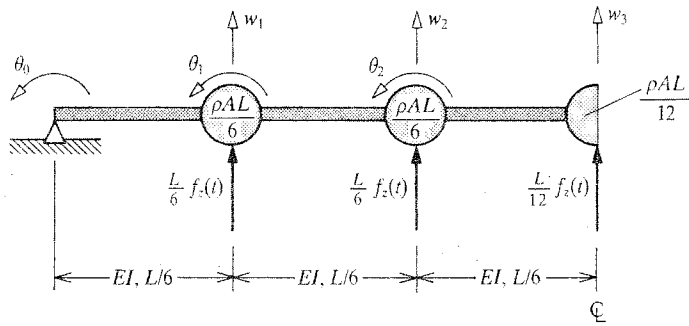


Figure 19.12. Example 19.3. A finite element structural dynamics model containing discrete masses without elasticity, and beam elements without mass. Time-varying loads are applied to the “lumped” masses.

As before, the uniform lateral load is discretized in exactly the same fashion as the distributed mass. That is, concentrated forces are applied at the node points. Thus the structural model is a collection of “lumped” masses that have no flexibility and which are (i) connected to each other by elastic finite elements that have no mass and (ii) acted upon by the discretized loads. ■

Having introduced the type of finite element model that is the basis for the type of structural dynamics analysis discussed here, it is time to discuss in turn the inertial, elastic, applied, and damping forces and moments that comprise the equilibrium statement. However, before doing so, it is necessary to note a change in viewpoint that is reflected in the finite element model of the above example. Since the basis of any equilibrium statement is, as always, Newton’s second law, the four types of forces and moments that are to be discussed have to be those loads that act upon the discrete masses of the structure. That is, all previous finite element discussions focus upon forces and moments that act upon the elastic elements. By Newton’s third law, the elastic forces and moments that act upon the discrete masses that are positioned at the structure’s nodes are equal and opposite to the forces and moments that act upon the elastic elements. Thus all the elastic forces and moments that act upon the discrete masses are concisely described by the matrix product $-[K]\{q\}$.

Inertial forces, as discussed in Section are always the product of -1 , a mass term, and an acceleration term; See Eq. (1.5). When there is more than one mass, the corresponding matrix form is $-[M]\{\ddot{q}\}$, where $[M]$ is called the mass matrix or the inertia matrix. Of course, the column vector is called the acceleration vector, or generalized acceleration vector. A rigorous derivation of the elements of the mass matrix always can be obtained from writing the kinetic energy expression for the structural system, and then putting that expression in matrix form as

$$T = \frac{1}{2} \{\dot{q}\} [M] \{\dot{q}\}$$

This kinetic energy form is valid whenever the kinetic energy is only a function of the system velocities, and not the system deflections, which is always the case when structures undergo small deflections with respect to fixed frames of reference. Whenever the accelerations of the structural system are easily discerned, the use of the kinetic energy expression is

unnecessary. Such is the case for the beam of Example 19.3. For that beam, the inertial forces associated with the three lumped masses are simply

$$-\frac{\rho AL}{6}\ddot{w}_1 \quad -\frac{\rho AL}{6}\ddot{w}_2 \quad -\frac{\rho AL}{12}\ddot{w}_3$$

Therefore the inertia matrix $[M]$ corresponding to the acceleration vector

$$[\ddot{q}(t)] = [\ddot{w}_1(t) \quad \ddot{w}_2(t) \quad \ddot{w}_3(t) \quad \ddot{\theta}_0(t) \quad \ddot{\theta}_1(t) \quad \ddot{\theta}_2(t)]$$

is a diagonal matrix where all the off-diagonal terms are zero, the first three diagonal terms are $(\rho AL/6)$, $(\rho AL/6)$, and $(\rho AL/12)$ respectively, and the last three diagonal terms are also zero. The reason for grouping together in the above acceleration vector all the accelerations that multiply nonzero mass matrix terms, and then all the accelerations that multiply only zero mass matrix terms, is explained in Endnote (2).

The third set of loads are the external concentrated loads that are applied at the nodes of the finite element model. These loads are symbolized as $\{Q\}$, and they are individually functions of time. In general they are nonconservative forces. In certain circumstances, as discussed in the last chapter, the applied loads may also depend upon the generalized coordinates $\{q\}$, the generalized velocities $\{\dot{q}\}$, and the generalized accelerations $\{\ddot{q}\}$.

Similar to the inertia and elastic loads, the damping (i.e., velocity-dependent) forces are often written as $-[C]\{\dot{q}\}$. Damping forces are usually much more mathematically complicated than is indicated here, where they are simply described as linear functions of the generalized velocities. The form of the damping forces used here is that for "equivalent viscous damping forces." Viscous damping forces are of interest primarily because they are the only damping forces that admit a linear mathematical description. Other damping forces, which are either nonlinear or have a more complicated phase relationship to the other forces, are made equivalent to viscous damping forces on the basis of equal work dissipated per vibration cycle. There is no need in this textbook to be concerned about detailing the constant elements of the symmetric damping matrix, $[C]$.

Now that the four different types of forces that make up the equations of motion have been discussed briefly, these forces can be summed to zero (dynamic equilibrium). After placing all the terms involving the generalized coordinates on the left-hand side, the result of the summation of forces is

$$[M]\{\ddot{q}\} + [C]\{\dot{q}\} + [K]\{q\} = \{Q\} \quad (19.9)$$

A more rigorous derivation of the above equation can be obtained from use of the Lagrange equation of motion, Eq. (16.1). As stated above, the kinetic energy expression used in that equation defines the mass matrix. The stiffness matrix is developed from the same static force-deflection considerations used to assemble any FEM stiffness matrix,⁵ after the DOF have been selected for the structure. More than any other consideration, the DOF are selected to ensure a reasonable mathematical description of the elastic components of the structure. As always, the generalized forces $\{Q\}$ are determined from a virtual work statement.

The type of problem described by Eq. (19.9) depends upon the type of time-varying loading that is applied to the structure. If, for example, the applied load vector is a set of known (i.e., estimated) time-varying loads, or $\{Q\}$ is composed of equivalent loads dependent upon the *known* motion of the structural system supports (i.e., the known system boundary

⁵ In parallel to the kinetic energy expression, the stiffness matrix can also be defined by writing the strain energy expression for the entire structure, which is $U = \frac{1}{2}\{q\}[K]\{q\}$.

deflections, velocities, and accelerations), then the problem is a “structural vibration problem” akin to an ordinary boundary value problem. If the applied load vector depends upon the unknown motion of the structural system, then Eq. (19.9) is a mathematical description of a dynamic instability problem in the form of an eigenvalue problem. Airfoil (or hydrofoil) flutter is an example of a dynamic instability fully described by the above equation. Flutter is a vibration where, once a certain fluid velocity (and Mach number in the case of air) have been exceeded, the vibration deflection and stress amplitudes can increase with time, sometimes very rapidly, until structural failure occurs. Since the phasing (i.e., sequencing of the maximum and minimum values) of the fluid loads and the structural response is critical to the flutter phenomenon, complex algebra is used in the eigenvalue analysis, which predicts the fluid velocity and Mach number at which the vibration amplitudes neither decrease (i.e., are damped out) nor increase. See Chapter 23 for a more detailed description of this phenomenon.

An equally complicated situation is the case where the most economical approach to describing the applied loads leads to use of probabilistic descriptions of the loads themselves. Such loads are called “random” loads. Specifically, random loads differ from “deterministic” loads in that the magnitude and direction of a random load, is described only in terms of probabilities. Only deterministic loads are considered in this textbook. For the sake of contrast, recall that statistics play a part in all load selections, random and deterministic. For example, in the design of the landing gear and wings of an aircraft, the designer cannot afford to make the landing gear and wings so strong (and thus so heavy) that they can withstand any hard landing. The procuring agency or the designers choose a design vertical descent speed that they statistically estimate will be only exceeded infrequently by well-trained aviators. That is, a certain crash risk is accepted on the basis that the total probable crash cost in terms of lives and money is less than what would have been the cost of the lost performance due to greater weight.

The selection of a maximum design descent speed pushes the statistical basis for that selection into the background, simplifying the landing load analysis. This is called an “envelope” approach. It is often a suitable approach for load related quantities that can be modeled as time-invariant, such as a vertical descent speed. However, there are many instances where the use of one or a series of maximum values for a time-varying loading would greatly overstate the load. For example, this would be the case if an applied oscillating load were such that its constant magnitude could be well estimated, but its frequency was random. That is, say, the load occurs at just one frequency that continuously changes with time, but that frequency can only be described in terms of a probability of occurrence. If such a load were to be treated as if it dwelled at each of the lower natural frequencies of the structure (a near worst case, envelope approach), then the natural frequency resonant effect would possibly require the structure to be greatly strengthened to the point where the structure’s natural frequencies were then outside of the range of the frequencies of the applied loading. A far more weight-conscious point of view would be one that took into account the engineered low probability of the loading frequency falling within the half-power frequency points bracketing each of a structure’s natural frequencies for a significant time period, and the consequent (possibly) low probability of structural damage. Whether or not the probability for structural damage is low, the structural response can be characterized by a probability statement. Thus, at the conclusion of the analysis, the decision can be made as to whether or not the probability of the response exceeding some safe level is acceptable.

There is one other important aspect of the applied dynamic load vector that is simple to explain. The applied load vector can be divided into two parts. The first part is the vector of all the applied *static* loads, $\{Q_s\}$. Examples of such loads for a flight vehicle would be the

weight loads and the steady-state aerodynamic loads. The remainder of the total load vector is the vector of all the time-varying loads, $\{Q_r(t)\}$. Let the solution for the generalized deflections due to the static load vector $\{Q_s\}$ be the vector $\{q_s\}$. That is, let

$$[K]\{q_s\} = \{Q_s\} \quad (19.10)$$

Since the applied load vector and the stiffness matrix are matrices that are composed of time-invariant quantities, so too is the response vector $\{q_s\}$. Therefore, all the time derivatives of $\{q_s\}$ are zero. Let the deflections $\{q_r(t)\}$ be the difference between the total deflections $\{q\}$ and the static deflections $\{q_s\}$. That is, let $\{q\} = \{q_s\} + \{q_r(t)\}$. Then the generalized coordinates $\{q_r\}$ must be measured from the static equilibrium position established by the static generalized coordinates $\{q_s\}$ in response to the static loads. Substituting

$$\{q\} = \{q_s\} + \{q_r(t)\}, \quad \{\dot{q}\} = \{\dot{q}_r(t)\}, \quad \{\ddot{q}\} = \{\ddot{q}_r(t)\} \quad (19.11)$$

into Eq. (19.9), and then subtracting Eq. (19.10) yields

$$[M]\{\ddot{q}_r(t)\} + [C]\{\dot{q}_r(t)\} + [K]\{q_r(t)\} = \{Q_r(t)\} \quad (19.12)$$

Since the linear equations for the dynamic and static deflections can be stated separately as Eqs. (19.10) and (19.12), their solutions can be obtained separately. Again, as evidenced by the first of Eqs. (19.11), when the static deflections are obtained or merely envisioned, the static deflections become simply a datum for the dynamic deflections. Just as importantly, as indicated by Eq. (19.12), the static deflections and static forces, such as weight, lift, drag, and so on, have no effect whatever upon the dynamic deflections $\{q(t)\}$ when those deflections are small enough that the response equations are linear. Again, the direct integration and modal solution techniques that are used to solve Eq. (19.12) are left to textbooks on structural dynamics (Refs. [25, 38, 72]).

Example 19.4. Write the matrix equation of motion for the simple elastic structure and applied loading pictured in Fig. 19.13(a). The appropriate part of the mass of the now massless beam has been included in the rigid mass at the beam tip. For the sake of algebraic convenience, let $EI = 2GJ$. Ignore damping effects. Note that the mass moments of inertia of the tip mass are $I_x = (5/16)ML^2$ and $I_y = ML^2/16$, and these mass moments of inertia about the mass center have no connection to I , the beam area moment of inertia. Also note that the idealized system has no motion in the y direction or rotation about the z axis.

Solution. The mathematical model of the structure already embodies all the required features of a discrete model in that the mass and elastic properties of the structure have been separated for ease of treatment. The next step is therefore to select a set of generalized coordinates. The generalized coordinates can be selected either to make the description of the elastic forces as simple as possible or to make the description of the inertial forces as simple as possible. Since the elastic forces are almost always the more complicated of the two, it is better to choose the DOF so as to simplify the description of the elastic forces. The required three DOF are pictured in Fig. 19.13(b). The system stiffness matrix is constructed in the usual way from parts of the beam bending and beam twisting element stiffness matrices. The result is

$$[K]\{q\} = \frac{EI}{L^3} \begin{bmatrix} 12 & -6L & 0 \\ -6L & 4L^2 & 0 \\ 0 & 0 & 0.5L^2 \end{bmatrix} \begin{Bmatrix} w \\ \theta \\ \phi \end{Bmatrix}$$

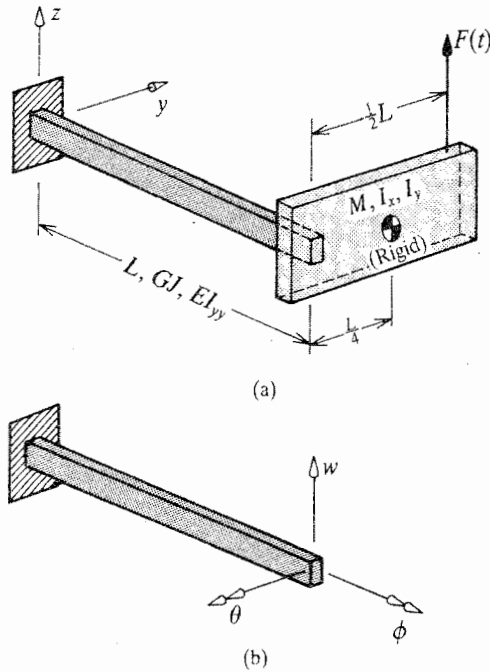


Figure 19.13. Example 19.4. (a) The coordinate system, geometry, and the time-varying loading. Note that here an “ I ” with two or no subscripts is an area moment of inertia, while an “ I ” with one subscript is a mass moment of inertia. (b) The nonzero three global DOF.

Since the inertial forces are not altogether obvious, in this case the mass matrix will be determined by writing the kinetic energy expression for this structure. Remember: (i) the kinetic energy of any system depends entirely upon the motion of the mass of the system; and (ii) the possible motions of the system can be deduced from the possible deflections of the system. The most general upward deflection of the rigid mass center of mass is $w + (L/4)\phi$. Thus the general expression for the velocity in the z direction is just the time derivative of this quantity. Hence the system kinetic energy is

$$T = \frac{1}{2}M[\dot{w} + (L/4)\dot{\phi}]^2 + \frac{1}{2}I_x\dot{\phi}^2 + \frac{1}{2}I_y\dot{\theta}^2$$

The next step is to expand the first term and then factor this expression into the matrix form $\frac{1}{2}[\dot{q}][M]\{\dot{q}\}$ so as to obtain the mass matrix.

The generalized force vector is, as always, obtainable from the expression for virtual work. Here

$$\delta W_{ex} = F\delta w + 0\delta\theta + \frac{L}{2}F\delta\phi = [\delta q]\{Q\}$$

Thus the matrix equation of motion is

$$\frac{M}{16} \begin{bmatrix} 16 & 0 & 4L \\ 0 & L^2 & 0 \\ 4L & 0 & 6L^2 \end{bmatrix} \begin{Bmatrix} \ddot{w} \\ \ddot{\theta} \\ \ddot{\phi} \end{Bmatrix} + \frac{EI}{L^3} \begin{bmatrix} 12 & -6L & 0 \\ -6L & 4L^2 & 0 \\ 0 & 0 & \frac{1}{2}L^2 \end{bmatrix} \begin{Bmatrix} w \\ \theta \\ \phi \end{Bmatrix} = \begin{Bmatrix} F \\ 0 \\ \frac{1}{2}FL \end{Bmatrix}$$

where the (3, 3) term of the mass matrix is the sum of I_x and $ML^2/16$. Note that the w and ϕ coordinates are coupled (i.e., mathematically connected) by means of the off-diagonal

terms of the mass matrix, while the w and θ coordinates are coupled by means of the off-diagonal terms of the stiffness matrix. What this means physically is that, for example, a w motion (which activates the first columns) produces an inertial moment about the x axis of magnitude $ML\ddot{w}/4$ (from the third row). This twisting moment in turn produces the twisting deflection ϕ . Thus w and ϕ are inertially coupled. ■

19.7 Summary

This chapter provides just a glimpse into the possibilities of small-deflection finite element analyses for both static and dynamic loads. There are many, many more types of more versatile linear finite elements than are discussed in this brief introduction. (The chapter on plate theory, Chapter 22, introduces a simple plate bending finite element.) Nonlinear finite element analyses for finite deflections and corresponding stresses are also well established. Fortunately, the reader can choose between numerous textbooks that treat the subject, not only with respect to structural mechanics, but with respect to such disciplines as fluid dynamics and heat transfer. Finite element analysis is likely to remain the generally preferred approach for detailed analyses in almost all geometrically complex structures for quite some time to come.

When the applied loads vary significantly with time, the finite element stiffness matrix becomes only one part of the equation of motion. At a minimum, a mass matrix is also required. In this chapter, the mass matrix is determined by first discretizing the structural model so that the structure's elastic elements contain no mass, while the structure's mass elements are rigid (i.e., contain no flexibility). The discretizing procedure used here is a simple static balance type division of the mass in each structural element between the system nodes to which that element is connected. It is also possible to take the more sophisticated approach of apportioning the mass of each structural element on the basis of the shape functions used to describe the deflections of that structural element. This latter technique has not led to greater solution accuracy, and thus is left undiscussed. After the structural system is discretized, the mass matrix is deduced either from the inertia forces acting upon the structural masses as the structure accelerates, or from writing the system kinetic energy expression. The latter approach guarantees a symmetric mass matrix. As discussed in Chapter 23, symmetric mass and stiffness matrices greatly simplify solution processes.

Writing the linear equations of motion often requires a bit more than developing the mass and stiffness matrices. If damping forces have an appreciable effect on the motion of the system, they too need to be included in the equations of motion. When linearized, the damping forces are represented by the product of a square, symmetric matrix of constants, called the damping matrix, and the generalized velocity vector. There are too many aspects to this often ignorable damping matrix for it to be discussed in this introduction. However, the damping matrix can be developed in exactly the same way the applied load vector is developed. The applied load vector is determined, as usual, by writing a virtual work expression for all the external forces and moments acting upon the structural system. (The external loads are all the loads not included in the inertial loads associated with the mass matrix or the elastic loads associated with the stiffness matrix, or the damping matrix if this latter matrix has already been developed by other means.) The validity of this procedure is based upon Hamilton's principle, which is derived in Exercise 16.8.

As is usually the case with engineering equations, writing the linear (finite element) equations of motion is less strenuous than solving those same equations. This section focuses upon writing the finite element linear equations of motion in order to prepare the reader for the material of Chapter 23. Solution techniques for the complete

linear equations of motion are left to textbooks that are devoted to that single topic (Refs. [38, 72]).

Chapter 19 Exercises

- 19.1.** The simple structure shown in Fig. 19.14 is four pinned end bars interconnected by a thin sheet of thickness h . (The thin sheet serves approximately the same structural purpose that diagonal bars would serve.) All five structural elements have the same Young's modulus. The Poisson's ratio for the thin sheet is $1/3$. If $a = 20h$, $b = 15h$, and the cross-sectional area of the four bars is $12h^2$, then using a single rectangular plane stress finite element to model the skin, write $\{Q\} = [K]\{q\}$ for:
- The loading shown in the sketch.
 - A loading where there is only a single horizontal force of magnitude F acting at node 4.
 - Redo part (a), but this time remove the roller supports at nodes 2 and 4, and, in place of the previous loading, let an applied force of magnitude F act vertically at node 2. Assume that the skin does not buckle.
- 19.2.** (a) Write the 6×1 applied load vector for the beam structure of Example 19.13
- Write the undamped equations of motion for the spring and lumped mass system of Example 17.7. Let the only force acting upon this spring mass system be the static force mentioned in the example, which is now a time-varying force.
 - Write the undamped equations of motion for the spring and lumped mass system of Exercise 17.4(b). Let a time-varying force of magnitude $F_1(t)$ act to the right upon the right-hand mass. Number the masses from left to right.
 - Write the mass matrix and the applied load vector for the structure of Example 17.3 and Fig 17.8 if the springs have negligible mass, the beams have a uniform mass density and a total mass of magnitude M for the top beam and $2M$ for the bottom beam. Let the applied force F_0 and the applied moment M_0 now be functions of time. Use the simplest possible discrete mass model.

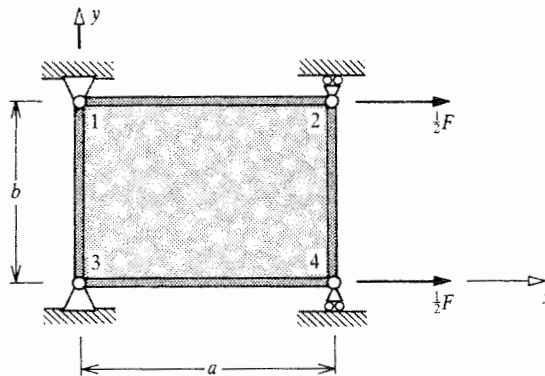


Figure 19.14. Exercise 19.1.

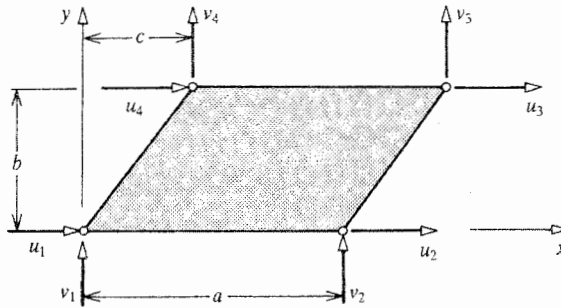


Figure 19.15. Exercise 19.4.

- (e) As in part (d), but this time for the structure of Fig. 17.16. Let the total mass of the left-hand beam be M while that of the right-hand beam is $2M$.
- (f) How would the mass matrix of part (e) be altered if a large, nonstructural mass of magnitude $9M$ and mass moment of inertia ML^2 were at the right-hand support?
- 19.3. Show by means of a series of sketches that five tetrahedrons are required to form a rectangular parallelepiped. *Hint:* Go about the solution in reverse order; that is, begin by drawing the rectangular parallelepiped; then draw oppositely directed diagonals on two opposite faces; then one at a time remove (erase) the outline of one tetrahedron involving an outer corner until the only tetrahedron left is a centrally located tetrahedron two of whose edges are the oppositely directed diagonals mentioned above.
- 19.4. (a) Determine the suitability of the deflection expansion $u(x, y) = \alpha_0 + \alpha_1 x + \alpha_2 y + \alpha_3 [xy - (c/b)y^2]$ for the parallelogram-shaped plane stress finite element sketched in Fig. 19.15.
- (b) Suggest an appropriate expansion for $v(x, y)$.
- (c) Utilizing the deflection expansions of the first two parts of this problem, is this element in a state of internal equilibrium?

FOR THE EAGER

- 19.5. Consider a nine-node rectangular plane stress finite element where four of the element nodes are at the corners, four of the element nodes are at the edge midpoints, and the ninth node is at the center of the rectangle. Suggest a shape function for a DOF positioned at
- The lower left-hand corner ($x = 0, y = 0$).
 - The upper left-hand corner ($x = 0, y = b$).
 - The lower right-hand corner ($x = a, y = 0$).
 - The upper right-hand corner ($x = a, y = b$).
 - The middle of the lower edge ($x = \frac{1}{2}a, y = 0$).
 - The middle of the upper edge ($x = \frac{1}{2}a, y = b$).
 - The middle of the left edge ($x = 0, y = \frac{1}{2}b$).
 - The middle of the right edge ($x = a, y = \frac{1}{2}b$).
 - The center of the element ($x = \frac{1}{2}a, y = \frac{1}{2}b$).
- 19.6. Consider a finite element model of an unconstrained rectangular slab which is composed of grid of plane stress elements where there are 24 rectangular

finite elements along each edge. The only loading experienced by the slab is a temperature change that is symmetric about the vertical centerline of the rectangle. Along any row of finite elements, the temperature change decreases from a maximum average value of $10T_0$ at the center (the twelfth and thirteenth columns), to a value of $9T_0$ at the eleventh and fourteenth column, to a value of $8T_0$ at the tenth and fifteenth columns, and so on, to a value of T_0 at the third and twenty-second column, and to where the temperature change is zero in the outer two columns of rectangular elements.

- (a) In words only, describe the steps that would be necessary to determine the nodal deflections due to the equivalent thermal loading. The dimensions of each element are a by b .
- (b) How is the induced stress in any finite element determined?
- 19.7. (a) Using the strength of materials beam bending theory of Chapter 11, write the partial differential equation for the mathematical function $w(x, t)$ that describes the lateral motion of the continuous beam with distributed mass (not discrete masses) considered in Example 19.3. *Hint:* Positive lateral forces per unit length and positive lateral deflections are upward, that is, in the z direction. Since deflections are positive upward, then velocities and accelerations are also positive upward. The part of the total lateral force per unit length caused by the motion of the beam (i.e., the inertia force per unit length) is then $-\rho A[\partial^2 w(x, t)/\partial t^2]$.
- (b) If the y and z axes are principal axes, what then are the boundary conditions for this beam?
- (c) Show that a variable separate solution to the homogeneous portion of this partial differential equation is possible by writing and substituting $w(x, t) = W(x)T(t)$, where $W(x)$ and $T(t)$ are functions to be determined.
- (d) Reason on physical grounds that the function $T(t)$ cannot be zero, and then rewrite the BCs for this same homogeneous solution.
- (e) Apply the BCs of part (d) to the solution for $W(x)$.
- (f) Having obtained a solution to the homogeneous part of the partial differential equation, now consider obtaining the particular solution for the general function $f_z(t)$ by writing as the additional portion of the total solution

$$w(x, t) = \sum_n g_n(t) \sin(n\pi x/L)$$

where $g_n(t)$ is a set of functions to be determined. After substituting the above trial solution, how could the orthogonality of the eigenfunctions $\sin(n\pi x/L)$ be used to obtain a series of uncoupled ordinary differential equations each of which can be solved for one of the functions $g_n(t)$? Note that this trial particular solution, by construction, satisfies the beam boundary conditions.

- 19.8. There is little, if any, advantage to having a refined bar element. Nevertheless, for the sake of practicing obtaining shape functions, show that the axial deflection of a uniform bar of length l in terms of three shape functions and the three axial DOF u_1 at $x = 0$, u_2 at $x = l/2$, and u_3 at $x = l$ (all DOF positive in the positive x direction), is

$$u(\xi) = N_1(\xi)u_1 + N_2(\xi)u_2 + N_3(\xi)u_3$$

where

$$\xi = \frac{x}{l}, \quad \text{and} \quad N_1(\xi) = 2\xi^2 - 3\xi + 1$$

$$N_2(\xi) = 4(\xi - \xi^2), \quad \text{and} \quad N_3(\xi) = 2\xi^2 - \xi$$

Hint: Three DOF uniquely determine a parabolic deflection pattern over the length of the element. Therefore, begin with $u(x) = Ax^2 + Bx + C$.

Endnote (1) An Explanation for Rigid Body Motion-Induced False Strains

In order to better understand why the omission of either of the two constant terms in the Eq. (19.1) series expansions for the in-plane deflections of the rectangular plane stress finite element would result in the calculation of nonexistent strains within the element, consider one of the two approximate deflection series without the constant term. Let, for the sake of establishing its deficiency, the y direction deflections within the rectangle be represented by the truncated series expansion

$$v(x, y) = \beta_1 x + \beta_2 y + \beta_3 x^2 + \beta_4 xy + \beta_5 y^2 \quad (?)$$

This expansion can be investigated without any concern for the number of element nodes to be assigned to the rectangular element. The y direction strain within the rectangle is then

$$\epsilon_{yy} = \frac{\partial v}{\partial y} = \beta_2 + \beta_4 x + 2\beta_5 y$$

Now, let there be a vertical rigid body motion of magnitude v_0 . Since this rigid body motion is just another y direction deflection, it must fit the general form for the deflection approximation; that is, the following must be *approximately* true for all values of x and y :

$$v_0 = \beta_1 x + \beta_2 y + \beta_3 x^2 + \beta_4 xy + \beta_5 y^2$$

where here the β coefficients have specific values for this specific deflection. The desire for approximate fidelity in the above equation is based upon the realization that complete fidelity is impossible, for example, at the corner point $x = 0, y = 0$.

It is possible to solve for the five unknown betas by choosing five distinct points within the rectangle and thereby writing five independent equations for that purpose. The difficulty is that every choice of five different points within the rectangle yields a different solution for the five β 's, which means that the strain ϵ_{yy} will not only not be zero as it should be for this rigid body motion, but be different from point to point within the rectangle. The hopelessness of this task is evident when it is realized that because the above deflection equation should hold for all values of x and y , that equation is an identity. Therefore, from the viewpoint of linear independence, all the β 's must be zero for an obvious contradiction. Hence it is not possible to omit the constant term from the deflection series and even approximate a rigid body motion.

Endnote (2) Reducing the Number of DOF in a Dynamic Analysis

In a typical large, discrete mass and discrete elastic element structural model, far fewer mass elements than elastic elements are needed for good analytic accuracy. Therefore the usual economic structural model for a structural dynamics analysis is one for which there are a large number of DOF for which there are no associated mass terms. The beam model of Example 19.3 illustrates this point in that fifty percent of the DOF, all the bending slopes,

have no associated mass terms. This situation offers an opportunity to reduce the number of DOF present in the analysis. It is usually very important to reduce the number of DOF in a structural dynamics analysis because the solution process can be very much more computer time-consuming than a comparable static analysis. The process of reducing the number of DOF is very similar to that set forth in Endnote (1) of Chapter 18. In order to demonstrate the process with dynamic equations, consider the following undamped equations of motion:

$$\begin{bmatrix} M & 0 \\ 0 & 0 \end{bmatrix} \begin{Bmatrix} \ddot{q}_a \\ \ddot{q}_o \end{Bmatrix} + \begin{bmatrix} K_{aa} & K_{ao} \\ K_{oa} & K_{oo} \end{bmatrix} \begin{Bmatrix} q_a \\ q_o \end{Bmatrix} = \begin{Bmatrix} Q_a \\ Q_o \end{Bmatrix}$$

The mass matrix is organized into four submatrices so that all the zero mass terms are associated with the generalized coordinates designated as $\{q_o\}$. For the structural system of Example 19.3, $[q_a] = [w_1 \ w_2 \ w_3]$, and $[q_o] = [\theta_0 \ \theta_1 \ \theta_2]$. The subscripts a and o may be thought of as suggesting "analysis" and "omitted." The stiffness matrix is also partitioned into submatrices in order to match the partitioning of the mass matrix. When the matrix products of the submatrices are written out, the result is

$$[M] \{\ddot{q}_a\} + [K_{aa}] \{q_a\} + [K_{ao}] \{q_o\} = \{Q_a(t)\}$$

and

$$[K_{oa}] \{q_a\} + [K_{oo}] \{q_o\} = \{Q_o(t)\}$$

The latter equation can be solved for

$$\{q_o\} = -[K_{oo}]^{-1} [K_{oa}] \{q_a\} + [k_{oo}]^{-1} \{Q_o(t)\}$$

and that solution substituted into the first equation. The result is

$$[M] \{\ddot{q}_a\} + [K_{aa} - K_{ao} K_{oo}^{-1} K_{oa}] \{q_a\} = \{Q_a\} - \{K_{ao} K_{oo}^{-1} Q_o\}$$

The size of this equation of motion is the size of $\{q_a\}$. By means of a judicious choice of where to lump masses, and of how many masses are necessary for the accuracy desired, this process can be used to eliminate as much as 80 percent, or even 90 percent, of the original number of DOF. There is, of course, a price to be paid for this important advantage. It is necessary either to invert the submatrix $[K_{oo}]$ and carry out three matrix multiplications, or to follow the Guyan reduction procedure discussed briefly at the end of Endnote (1) of Chapter 18. It is worth this computational price in almost all circumstances. Note that since $[K_{oo}]$ is a square submatrix of a nonsingular matrix, it is always invertible. Also note that the new stiffness matrix $[K_{aa} - K_{ao} K_{oo}^{-1} K_{oa}]$ is symmetric because $[K_{ao}]$ is the transpose of $[K_{oa}]$. The importance of the symmetry of the mass and stiffness matrices is discussed in Chapter 23.

The Unit Load Method for Determinate Structures

20.1 Introduction

This chapter introduces just one of the many applications of the Principle of Complementary Virtual Work (PCVW). There are many small variations on this one application. The unit load method, the dummy load method, the virtual load method, the Maxwell–Mohr method, (Ref. [16]) the Muelier-Breslau method, (Ref. [16]) and the complementary virtual work method are all names given to what is essentially this same procedure. Since, in the case of linearly elastic materials, these same methods of analysis can also be derived from the PVW, (Ref. [16]) this same procedure is sometimes even called the method of virtual work. For the time being, the general form of this basic PCVW analysis procedure is called the unit/dummy/virtual load method. Later, the slight distinctions between the unit load method, the dummy load method, and the virtual load method are described, and the unit load method is chosen for full development.

To add to the confusion of names, there is an equally popular method based upon the Principle of the Minimum Value of the Total (Complementary) Energy that is only stylistically different from the unit/dummy/virtual load method. This method is called Castigliano's second theorem.¹ About half of the engineering students in the United States are first taught the unit/dummy/virtual load method, while the other half are first taught Castigliano's second theorem. There is very little advantage to one of these methods with respect to the other. Castigliano's second theorem may have the advantage of requiring a little less thought in its application to many problems, but the unit/dummy/virtual load method is perhaps a little easier to fully understand and apply in more complicated cases. The unit/dummy/virtual load method is presented here primarily because it is an offshoot from the PCVW, while Castigliano's second theorem is best developed from the Principle of the Minimum Value of the Complementary Total Potential Energy.²

The unit/dummy/virtual load method is a "force" or "flexibility" method; that is, it falls within the general category of stress formulations. This method is generally useful *only* for structures composed of a relatively few structural elements (called "modest" structures), and even then those structural elements must be of the simplest types. There are other types of force/flexibility analyses that are more practical for structures that include greater numbers of, and more complicated, structural elements. However, again, displacement formulations ("displacement" or "stiffness" methods) have proved to be more practical for the digital computer analysis of such structures.

The justifications for studying the unit/dummy/virtual load method are: (i) it is possible to use the unit/dummy/virtual load method for the analysis of small structures without the benefit of computers and computer programs because this approach generally involves

¹ Castigliano's first theorem and other techniques based directly upon the PVW are discussed in Chapter 17. Castigliano, an Italian engineer, published in 1873. Engesser, a German engineer, established the second theorem in its present form in 1889.

² The integrals employed in Castigliano's second theorem can also be derived immediately from the integrals of Eq. (20.5), which are used with the unit/dummy/virtual load method.

significantly fewer unknown quantities, and hence fewer simultaneous equations requiring solution, than any displacement method; (ii) for the same reasons, for modest or simplified problems, the unit/dummy/virtual load method can be quicker to use and easier to document than using a structural analysis computer program even with pre- and post-processors for inputting data and presenting analysis results; (iii) the unit/dummy/virtual load method is not a numerical method like the finite element method, and therefore its solutions permit the easier identification of the effects of changes in design parameters in simplified design models; and (iv) there are a small number of problems, for example, those involving curved beams, for which the unit/dummy/virtual load method will provide more accurate answers than most standard finite element programs unless a great many finite elements are used in the mathematical model of the structure, which can be much more costly. It is also worth noting that the analyses of modest structures for which the unit/dummy/virtual load method is well suited are not necessarily simple problems. For example, the unit/dummy/virtual load method accommodates, with relative ease, such complications as nonuniform geometries and nonlinear, elastic material behavior. However, analyses of modest structures which involve geometric (as opposed to material) nonlinearities, such as beam buckling problems, are best approached by means of displacement formulations. See (Ref. [3]).

20.2 External Complementary Virtual Work in the Unit Load Method

The unit/dummy/virtual load method is fundamentally a means of calculating actual deflections due to actual loads. Its basis is the Principle of Complementary Virtual Work. Recall from Chapter 15 that the PCVW can be stated as $\delta W_{ex}^* + \delta W_{in}^* = 0$, and that complementary virtual work (CVW), external or internal, is the work typically done by virtual forces moving through actual deflections, and virtual moments moving through actual rotations. External CVW is simply the CVW done by virtual loads whose origins are external to the boundaries of the structural system under consideration. External CVW is detailed in its most general form by the left-hand side of Eq. (15.12a), and of course the negative of the internal CVW is detailed in its most general form by the right-hand side of Eq. (15.12a).

$$\iint_{S_2} [u] \{ \delta T \} dS + \iiint_{\text{Vol.}} \rho [u] \{ \delta B \} d(\text{Vol.}) = \iiint_{\text{Vol.}} [\gamma] \{ \delta \sigma \} d(\text{Vol.}) \quad (15.12a)$$

Consider a structural body of general shape subjected to an arbitrary temperature change and an arbitrary general mechanical loading, as shown in Fig. 20.1. Consider the use of external and internal CVW in relation to, for example, the calculation of the actual displacement of this structural body in the z direction at the internal or boundary point P . For that use, this adaptation of the PCVW employs a set of virtual loads that includes a concentrated, virtual force δF_z of arbitrary magnitude that acts in the z direction at point P . Let the other virtual forces and the virtual moments be *any* set of convenient reactions at the rigid supports that equilibrates the virtual force δF_z .³ In addition to equilibrating the external virtual force at point P , the external virtual forces and moments at the rigid supports must be selected

³ In contrast to this fictitious (virtual) load system, any actual load system not only has to be in a state of equilibrium, but it also has to be such that it produces displacements and strains that are compatible, and stresses that are related to the strains by the material constitutive equations.

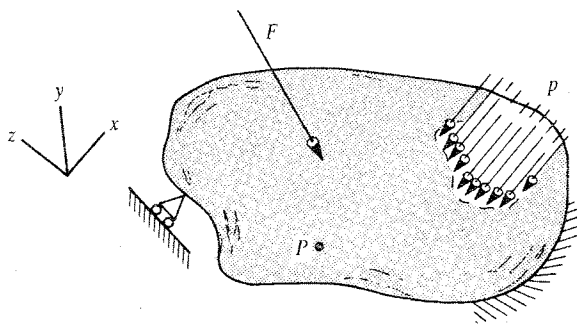


Figure 20.1. A general deformable body supported by unmovable rigid supports and subjected to a general loading system.

so that they do a known amount (usually zero) of CVW.⁴ Note that the virtual load system does not have to bear any resemblance to the actual load system. Designating the z direction displacement at point P as $w(P)$, then the total external complementary virtual work done by the imposed virtual load system is just the product $w(P)\delta F_z$ plus the known value of the CVW that is done at the rigid supports.

Recall that a structure is called “statically determinate” if all its support and internal reactions can be determined by simply writing static equilibrium equations. If the structural body is statically determinate, the exclusive circumstance of this chapter, then any actual motion of one or more of the supports results in a rigid body motion of both the structure and the virtual loads that the structure bears. If, for a virtual load system, u is an actual rigid body translation, and θ is a rigid body rotation, then the CVW done by the virtual forces and the virtual moments is $\sum u\delta F$ and $\sum \theta\delta M_i$. Since the constant values of u and θ can be factored out of the summations, it becomes clear that all rigid body motions of any equilibrated virtual load system produce zero CVW. Thus, when present, support motions for statically determinate structures, or other rigid body motions such as those of flight vehicles, can be totally ignored because such motions have no effect upon the CVW produced by the actual deformations and the virtual forces. That is, the total CVW involves only the deformations of the structure, not its rigid body motions, and the total CVW in this statically determinate case is just $w(P)\delta F_z$. (Chapter 21 discusses rigid support motion in the case of statically indeterminate structures.)

As an aside, it is instructive to note that the value $w(P)\delta f_z$ for the total external complementary virtual work for this statically determinate situation can also be obtained from the previously developed general integral expressions for the external complementary virtual work. From Eq. (16.12a)

$$\delta W_{ex}^* = \iint_{S_2} \{u\} \{\delta T\} dS + \iiint_{Vol.} \rho \{u\} \{\delta B\} d(Vol.)$$

Again, S_2 is the boundary surface area of the structure where displacements are prescribed. For the sake of definiteness, let point P lie on the boundary of the body. Since there are no chosen virtual body forces in this case, the second of the above integrals disappears. The

⁴ There is a choice of how, at the rigid supports, to equilibrate the virtual force that is placed at the point and in the direction of the desired displacement, only if, as is discussed in Chapter 21, the structure is statically indeterminate.

concentrated virtual force δF_z placed at point P can only be regarded as the result of an intense traction, δT_z , acting over a very small area dS , which surrounds the point P . In other words, the integral by itself of the intense traction δT_z over the very small area dS is equal to δF_z . The area dS at the point P is so small that the displacement $w(P)$ is essentially a constant over that area. Hence the first of the above integrals reduces to

$$\delta W_{ex}^* = w(P) \iint_{S_2} \delta T_z dS = w(P) \delta F_z$$

which, of course, is the same result as previously obtained.

Clearly, the same sort of result can be obtained for the displacement at any surface point P in any of the three original coordinate directions, or any rotated coordinate direction. A similar argument can be made for an intense internal virtual force $\rho \delta B_z d(\text{Vol.})$. Thus in general, by the use of a single virtual force of arbitrary magnitude, δF , which is applied at the point and in the direction of the desired displacement u , and which is reacted at unmoving rigid supports, the total external complementary virtual work can be written as simply

$$\delta W_{ex}^* = u \delta F \quad (20.1)$$

20.3 Internal CVW for Beam Bending and Extension

The internal complementary virtual work involves the virtual stresses and the actual strains. For a body of general shape, it is rather difficult to determine the actual strains or even choose useful virtual stresses that internally equilibrate the selected external virtual load system. In order to cope with the internal CVW in a simple way, it is necessary to greatly restrict the geometry of the general body. Therefore, in what follows, the development of internal complementary virtual work expressions is limited to such relatively simple structural elements as beams, bars, coiled spring representations of other structural elements, and to the simple structures that consist of small numbers of these structural elements. See Endnote (1). Combinations of bars and in-plane shear membrane elements are discussed in (Ref. [16]).

Since the expressions for the internal complementary virtual work for beam bending and extension are fairly simple, yet as complicated as those of any of the structural elements that are suitable for use with the unit/dummy/virtual load method, these expressions are derived first. Again, the negative of the internal CVW is the integral over the volume of the entire structure of the virtual stresses multiplied by their respective actual strains, as in Eq. (15.12a). When beam bending and extension are described by use of the Bernoulli–Euler approximate beam bending and extension theory, then the only strain that results from the action of axial loads, shear forces, and bending moments is ϵ_{xx} . Therefore, for the volume of one or more beams,

$$-\delta W_{in}^* = \iiint_{\text{Vol.}} \epsilon_{xx} \delta \sigma_{xx} d(\text{Vol.}) \quad (20.2)$$

From Eq. (9.4)

$$\epsilon_{xx} = \frac{\sigma_{xx}}{E} + \alpha \Delta T$$

For the sake of simplicity, rather than use Eq. (9.8) for the x direction normal stress in its nonprincipal axis form, now let the y and z axes be the principal axes of the beam cross-section. Furthermore, to accommodate those readers who skipped over Chapter 9's treatment

of nonhomogeneous beams and temperature changes, let the beam be homogeneous and let there be no temperature changes.⁵ With these additional simplifications, Eq. (9.8) reduces to

$$\sigma_{xx} = \frac{N}{A} - y \frac{M_z}{I_{zz}} - z \frac{M_y}{I_{yy}}$$

Substitution of the above stress expression into the previous strain expression yields the stress/force formulation for the actual strain:

$$\epsilon_{xx} = \frac{N}{EA} - y \frac{M_z}{EI_{zz}} - z \frac{M_y}{EI_{yy}} \tag{20.3}$$

The expression for the virtual stress is obtained directly from the above stress expression by simply noting that this stress expression is valid for any set of applied loads, and therefore is valid for the virtual load system. Since there is no virtual change in temperature,

$$\delta\sigma_{xx} = \frac{\delta N}{A} - y \frac{\delta M_z}{I_{zz}} - z \frac{\delta M_y}{I_{yy}} \tag{20.4}$$

This same result can also be obtained by applying the delta operator to both sides of the above stress expression while recalling that with the Principle of Complementary Virtual Work, only force-type quantities are varied. Substituting Eqs. (20.3) and (20.4) into Eq. (20.2) yields

$$-\delta W_{in}^* = \iiint_{\text{Vol.}} = \left(\frac{\delta N}{A} - y \frac{\delta M_z}{I_{zz}} - z \frac{\delta M_y}{I_{yy}} \right) \left(\frac{N}{EA} - y \frac{M_z}{EI_{zz}} - z \frac{M_y}{EI_{yy}} \right) d(\text{Vol.})$$

Carrying out the indicated multiplications leads to

$$\begin{aligned} -\delta W_{in}^* = \iiint_{\text{Vol.}} & \left\{ \left(\frac{N \delta N}{EA^2} \right) + y^2 \left(\frac{M_z \delta M_z}{EI_{zz}^2} \right) + z^2 \left(\frac{M_y \delta M_y}{EI_{yy}^2} \right) \right. \\ & - y \left(\frac{N \delta M_z}{EA I_{zz}} + \frac{\delta N M_z}{EA I_{zz}} \right) - z \left(\frac{N \delta M_y}{EA I_{yy}} + \frac{\delta N M_y}{EA I_{yy}} \right) \\ & \left. + yz \left(\frac{M_y \delta M_z + M_z \delta M_y}{EI_{yy} I_{zz}} \right) \right\} d(\text{Vol.}) \end{aligned}$$

Let the integration over the volume of the beam proceed first by integrating over a typical cross-sectional area of each beam, and then by integrating over the length of each beam. With respect to the integration over each beam area, each of the above quantities within parentheses is a constant. In other words, integration over any beam cross-sectional area is integration over the spatial variables y and z . Each of the variable quantities within parentheses is already the result of an integration over the cross-sectional area, and so those quantities can, at most, only be functions of the length coordinate x . Hence the quantities within parentheses are unaffected by integration over the cross-sectional coordinates y and z , and can be taken outside of their respective area integrals. Since y and z are centroidal

⁵ It can be shown that in order to include the effects of nonhomogeneity and temperature changes, the necessary modification of the end result for δW_{in}^* is the replacement of E by E_0 , A by A^* , I_{zz} by I_{zz}^* , and so on, and N by N^c , M_z by M_z^c , and so on, where the modified symbols are defined in Chapter 9. An introductory temperature change problem is discussed in Example 20.10.

coordinates, and with $d(\text{Vol.}) = dA dx$, the area integrals all reduce to either

$$\iint_A dA = A \quad \text{by definition}$$

or

$$\iint_A y dA = \iint_A z dA = 0, \quad \text{see Eq. (9.6b),}$$

or

$$\iint_A y^2 dA = I_{zz} \quad \iint_A z^2 dA = I_{yy} \quad \iint_A yz dA = 0$$

where the zero value for the latter integral, the product of inertia, is a result of the y and z axes being principal axes. The final result of the several integrations over each of n beam cross-sectional areas of the n beams of the structure is that the latter three terms are multiplied by zero, and thus the negative of the CVW, or the complementary strain energy is

$$-\delta W_{in}^* = \sum \int_0^{L_i} \left\{ \left(\frac{N \delta N}{EA} \right) + \left(\frac{M_z \delta M_z}{EI_{zz}} \right) + \left(\frac{M_y \delta M_y}{EI_{yy}} \right) \right\} dx_i$$

where the summation is over the index $i = 1, 2, \dots, n$. Therefore, the final form for beam bending and extension expressions for use in the PCVW adapted to the unit/dummy/virtual load method is, from Eq. (20.1) and the above,

$$u \delta F = \sum \int_0^{L_i} \left\{ \left(\frac{N \delta N}{EA} \right) + \left(\frac{M_z \delta M_z}{EI_{zz}} \right) + \left(\frac{M_y \delta M_y}{EI_{yy}} \right) \right\} dx_i \quad (20.5)$$

where δN , δM_z , and δM_y are a result of (i.e., functions of) δF . To fix ideas, a simple example follows.

Example 20.1. Use the dummy/virtual load method to calculate (a) the tip lateral deflection, $w(0)$; and (b) the tip bending slope, $w'(0)$, for the uniform, cantilevered beam and uniform actual loading shown in Fig. 20.2(a).

Solution. (a) Since there is only one beam, there is only one term in the summation in Eq. (20.5). Since there is only beam bending⁶ in one plane, the x, z plane, Eq. (20.5) reduces to

$$w(0) \delta F = \int_0^L \left[\frac{M_y(x) \delta M_y(x)}{EI_{yy}} \right] dx$$

(When bending is confined to one plane, which is a common occurrence in these examples, there is no need to retain coordinate subscripts for the moments and area properties because they are all the same.) The solution process requires the selection of a virtual force δF of arbitrary magnitude that does virtual complementary work in combination with the desired deflection, which in this case is the lateral tip deflection, $w(0)$. The virtual force that fulfills this requirement is shown in Fig. 20.2(b).

To explain further, from the derivation of Eq. (20.1), recall that the virtual force must be at the point and in the direction of the desired deflection in order to do the positive external

⁶ Beam shearing is discussed later.

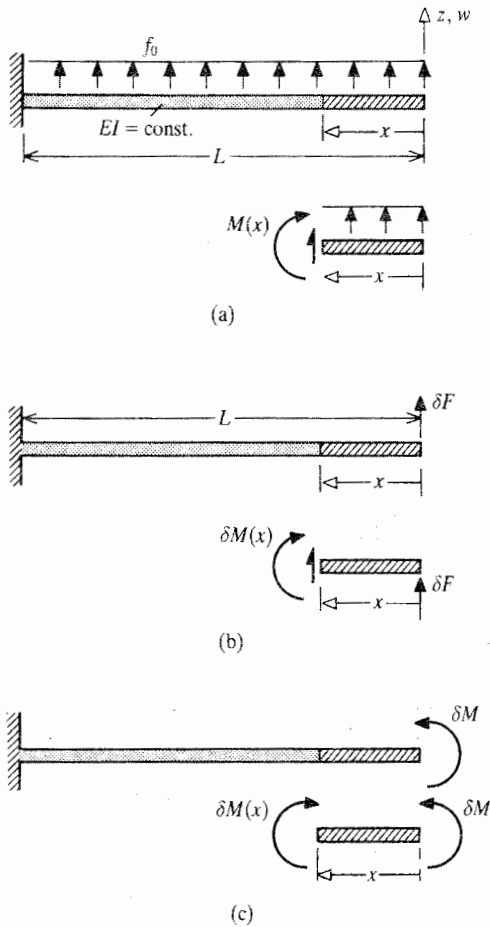


Figure 20.2. Example 20.1 (a) The applied load system (ALS) and a corresponding free body diagram of a typical portion of the beam showing the internal bending moment and the internal shearing force (unlabelled because it is of no interest) where both stress resultants are drawn, as always, according to the textbook sign convention. (b) The selected part (a) virtual load system and a corresponding FBD of a typical portion of the beam showing positive values of the internal virtual moment and internal virtual shearing force (unlabelled). (c) The selected part (b) virtual load system and FBD.

complementary virtual work shown on the left-hand side of the above equality. Sometimes, *unlike* the present problem, the loading and structural geometry are such that it is difficult to guess the correct direction of the actual deflection whose value is being sought. This is not a difficulty because if the analyst directs the virtual force in the actual direction for the deflection, then the external CVW will be positive, and the solution for the deflection will be positive. If the analyst directs the virtual force in the direction opposite to that of the actual deflection, then the solution for the deflection will have a negative value. In this way the analyst is always able to deduce from the chosen direction of the virtual force the direction of the actual deflection. Thus, for this problem, the choices of up or down for the direction of this virtual force are both equally valid choices. However, if the analyst can correctly predict the direction of the actual deflection, then choosing the virtual load in that

same direction, like checking units of measurement, is a weak check on the accuracy of the algebra and integration. Thus for this problem, the virtual force is chosen to act upward. (In a few of the other example problems, the direction of the virtual load will be purposely selected to produce a negative solution just to reinforce this point.)

As can be seen from the above discussion, there is the prescribed, actual load system (ALS), and an analyst-selected virtual load system. In the expression for the internal complementary virtual work, the actual bending moment M is determined from the ALS, while the virtual bending moment δM is determined from the virtual load system. In order to determine these two separate and independent bending moments at a typical beam cross-section, that is, at a typical value of x for insertion into the above integral solution, introduce the most convenient Cartesian coordinate system. In this case, that coordinate system is the one where the lengthwise coordinate x starts at the beam tip and proceeds to the left as shown in the two sketches. The indicated choice of FBDs makes it unnecessary to calculate the two sets of reactions at the fixed end of the beam that respectively equilibrate the actual loads and the virtual loads. Thus, from FBDs of the hatched portion of the beam shown with each load system, and from the same "happy face" moment sign convention that is used in Part III,

$$M(x) = +\frac{1}{2}f_0x^2 \quad \text{and} \quad \delta M(x) = +x \delta F$$

Since the factor EI is a constant, integration over the full length of the beam yields

$$w(0)\delta F = \frac{1}{EI} \int_0^L \left(\frac{1}{2}f_0x^2\right)(x \delta F)dx = \left(\frac{f_0L^4}{8EI}\right) \delta F$$

Canceling the nonzero quantity δF leads to the desired result that

$$w(0) = \frac{f_0L^4}{8EI}$$

Since, like all virtual forces, the selected virtual force is the fictitious creation of the analyst, it is sometimes called a "dummy" force in the "unreal" sense of that word. Also, like a dummy variable of integration, the dummy virtual load always disappears at the conclusion of the calculation.

(b) In order to determine the tip bending slope, a different form for the external complementary virtual work is necessary. Just as a force moving through a distance produces work, a moment moving through a rotation produces work. When the moment acts about the same axis about which the small structural rotation occurs, then the vector representations of the moment and small rotational angle are colinear, and the dot product of the moment and the small rotational angle reduces to the scalar product of their two magnitudes. Thus, in terms of choosing a useful form of external CVW, either

$$\delta W_{ex}^* = u \delta F \quad \text{or} \quad \delta W_{ex}^* = \theta \delta M$$

needs to be used to determine the desired deflection. In this second part of the stated problem, of course, it is the latter form that is needed. Thus a virtual moment of arbitrary magnitude is placed at the cantilevered beam tip so that the complementary virtual work done by this external virtual moment is $\delta M w'(0)$. The virtual bending moment everywhere along the length of the beam is the constant value δM . Of course the ALS and $M(x)$ are wholly

unaffected by changes in the virtual load system. Thus

$$\delta M w'(0) = \int_0^L \left(\frac{M(x) \delta M(x)}{EI} \right) dx = \frac{1}{2EI} \int_0^L (f_0 x^2) (\delta M) dx$$

or

$$\delta M w'(0) = \frac{f_0 L^3}{6EI} \delta M$$

Canceling the arbitrary virtual (dummy) moment δM from both sides of the equality yields the desired result. ■

As is suggested by the two parts of the above example, the arbitrary virtual/dummy force or virtual/dummy moment always appears as a linear factor in both the external and the internal complementary virtual work terms. Thus the virtual/dummy load always cancels when the external complementary work (the left-hand side) is equated to the negative of the internal complementary virtual work (the right-hand side). Since the virtual/dummy load always cancels, the actual canceling of the virtual/dummy load can be made into an unnecessary step by simply specifying a unit value for the arbitrary virtual load. Assigning a value of 1.0 lb or 1.0 N or 1.0 lb in or 1.0 Nm to the virtual/dummy load converts the virtual/dummy load method into the unit load method, (ULM). The following example illustrates this approach and other points with regard to organizing the calculation.

Example 20.2. Determine the midspan lateral deflection for the simply supported, uniform beam and loading shown in Fig. 20.3(a). Again, as in all of these problems, the y , z coordinates are the principal coordinates of the beam cross-section.

Solution. A unit load system (ULS) is created just as before by drawing the actual beam structure subjected to appropriate unit (virtual) loads. Since the midspan lateral deflection is the desired deflection, a unit load is placed vertically at $x = L/2$ so as to do complementary virtual work equal to $1w(x = L/2)$. As always, the ULS must be in equilibrium. In this statically determinate case, the only way that the midspan unit load can be equilibrated without having additional CVW involving other (i.e., undesired) deflection values is to react that unit load at the unmoving rigid supports with the types of reactions that are always created by those supports.⁷ Hence the ULS is as shown in Fig. 20.3(b).

In this problem, the actual loading is such that the beam is only bent, and not twisted or extended. Thus, again, only a single bending integral for a single beam is required for the solution. That is,

$$1w(x = L/2) = \int_0^L \frac{M(x) \delta M(x)}{EI} dx$$

To save time creating a complete description of the ALS, the actual support reactions are carefully checked and added to the original beam sketch.⁸ (After these first two illustrative examples, the FBDs are also drawn directly on top of the original ALS and ULS sketches for the same reason.) Now the remainder of the solution process is routine. The bending integral

⁷ Other means of reacting the chosen unit load are sometimes advantageous when symmetries are present; see Example 20.8.

⁸ Where practicable, it is recommended that the analyst twice use the usually more lengthy moment summation equations to determine the reactions, and then check the results by using the simpler summation of forces equation. By saving the simpler equation to last, it is more likely that the analyst will check the result and avoid an error at the very start of the problem.

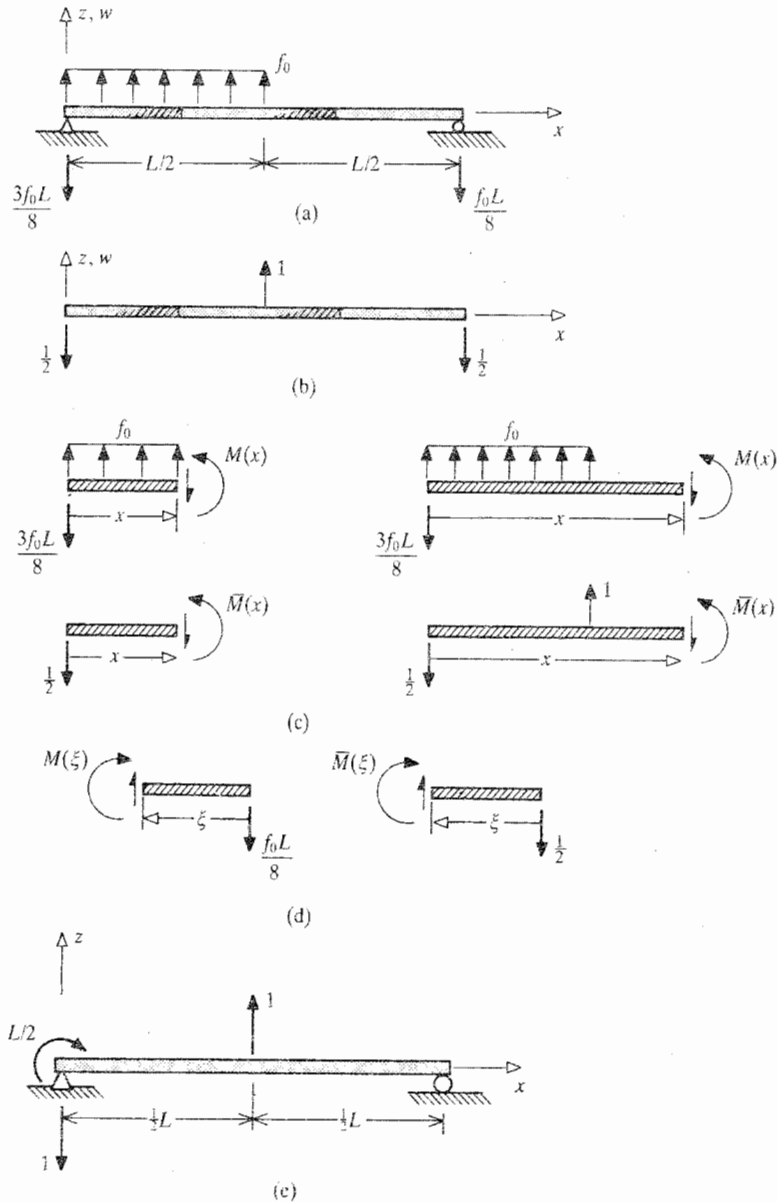


Figure 20.3. Example 20.2. (a) The actual load system with markings on the beam showing the locations of the FBDs of typical portions of the beam. (b) The selected virtual load system with the same beam markings for typical FBDs. (c) FBDs of the actual and virtual loads using only the x coordinate and left-hand portions of the beam. As always, the FBDs include all the external loads, real or virtual, on that portion of the structure plus the internal stress resultants at the partitions (cuts) that separate the free body from the remainder of the structure. (d) FBDs leading to simpler moment expressions as a result of the introduction of a second axial coordinate. (e) An example of a useless unit load system, even though the unit load system is in equilibrium.

prompts the analyst to write the bending moment expressions for the ALS and the ULS. Since there is a discontinuity in both loadings at $x = L/2$, both moment expressions have the same discontinuity. From the FBDs of Fig. 20.3(c), using the usual x coordinate, and now using an upper bar rather than the delta operator to distinguish the quantities derived from the ULS; that is, writing

$$\delta M(x) = \bar{M}(x)$$

then, for $0 \leq x \leq L/2$

$$M(x) = \frac{f_0}{8}(4x^2 - 3Lx) \quad \bar{M}(x) = -\frac{x}{2}$$

and for $L/2 \leq x \leq L$

$$M(x) = \frac{f_0 L}{8}(x - L) \quad \bar{M}(x) = \frac{1}{2}(x - L)$$

where the moment expressions have been simplified in order to reduce the work of integration to a minimum. Substituting into the integral solution,

$$w(x = L/2) = \frac{f_0}{16EI} \int_0^{L/2} (3Lx^2 - 4x^3) dx + \frac{f_0 L}{16EI} \int_{L/2}^L (x - L)^2 dx$$

or, after simplification,

$$w(x = L/2) = \frac{f_0 L^4}{256EI} + \frac{f_0 L^4}{384EI} = \frac{5f_0 L^4}{768EI}$$

Note that the above integration covered the entire beam, not just the half of the beam that bears the actual distributed load. Another point of considerable practical importance is that the tedious evaluation of the integral for the right half of the beam could be made a lot easier if a lengthwise coordinate is used for that half of the beam that simplifies both the moment expressions and the limits of integration. It is quite possible to use two or more lengthwise beam coordinates because the derivations of the PVW and the PCVW only require that the integrations of the various work quantities cover the entire volume of the structural system. There is absolutely no stipulation as to how that integration must proceed. It may proceed from right to left, or left to right, or from both ends towards the middle, and so on. Therefore, introduce a new coordinate, ξ , that starts at the right-hand end of the beam and increases to the left. The FBDs for the moments in terms of this better coordinate for the right half of the beam are shown in Fig. 20.3(d). Thus for

$$0 \leq \xi \leq L/2 \quad M(\xi) = -\frac{f_0 L}{8}\xi \quad \text{and} \quad \bar{M}(\xi) = -\frac{\xi}{2}$$

$$w(L/2) = \frac{f_0 L^4}{256EI} + \frac{f_0 L}{16EI} \int_0^{L/2} \xi^2 d\xi = \frac{5f_0 L^4}{768EI}$$

which is the same result with a lot less work and less opportunity for error. Those are two good reasons to always begin a ULM beam analysis by carefully deciding which is the best choice of lengthwise coordinates. ■

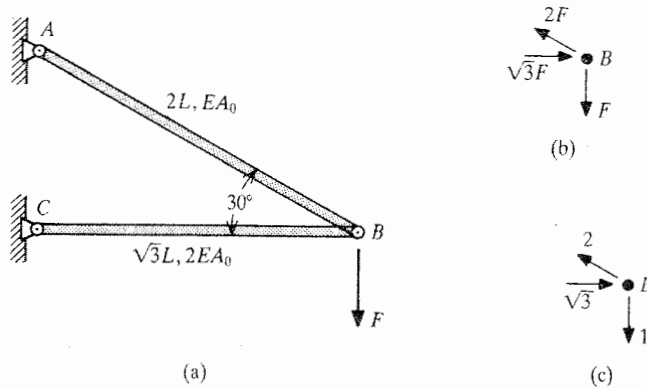


Figure 20.4. (a) A two-bar truss for which the vertical deflection at joint B is to be calculated. (b) The actual load FBD of pin B . (c) The virtual load FBD of pin B .

In review, the ULS must be in equilibrium to be valid. The ULS must also be such that it isolates the one deflection desired. On this latter point, consider the ULS shown in Fig. 20.3(e), and contrast that ULS with the one shown in Fig. 20.3(b). The ULS of Fig. 20.3(e) is also in equilibrium, but the CVW done by this new ULS is $w(L/2) - (L/2)w'(0)$. (The minus sign before the slope term is explained again in Example 20.8.) Therefore, the difficulty with the ULS of Fig. 20.3(e) is that it introduces a second unknown actual deflection, $w'(0)$, into the one equation obtainable from the one ULS. This second unknown, of course, prevents the solution of the one equation for the desired deflection. A general guide to avoiding this difficulty is to routinely use the actual supports of the statically determinate structure to react the selected unit load. (Remember this is just a guide, not an unbreakable rule that would prevent clever ULS choices later.) To elaborate, the ULS of Fig. 20.3(e) violates this guide because it involves a virtual moment at $x = 0$, while the rigid knife-edge support at $x = 0$ cannot supply such a moment. Since that virtual moment is not supplied by the rigid support, it can rotate through the actual beam bending slope at $x = 0$ and thus do the CVW indicated above. Going back to Example 20.1, note that the reactions to both unit loadings are the corresponding virtual force and virtual moment at the rigid wall. Since the rigid wall neither moves up or down, nor rotates, the CVW done by those two reactions is zero, and thus does not appear in the final ULS equation.

Example 20.3. Calculate the total deflection of joint B of the loaded planar truss of pin-jointed bars shown in Fig. 20.4(a).

Solution. Since the truss system contains only pin joints, there are no bending moments in either bar element. Furthermore, the axial forces in each bar element are constant along the bar length; that is, the actual and unit load axial forces are not functions of a lengthwise coordinate x_i for the i th bar. Therefore, from Eq. (20.5), the PCVW equation $\delta W_{ex}^* = -\delta W_{in}^*$ becomes

$$\delta W_{ex}^* = \sum \int_0^{L_i} \left(\frac{N\bar{N}}{EA} \right) dx_i = \sum \left(\frac{N\bar{N}L}{EA} \right)_i$$

To find v , the actual vertical component of the deflection at joint B , create a unit load system, which again is totally separate from the actual load system, by placing a vertical unit force

at joint B . Let the unit force act downward in anticipation of the fact that joint B moves downward under the action of the actual load. In this way a positive answer is expected. (Again, if the vertical unit force were chosen to act upward, then a negative answer of the same magnitude would result.) In this way, the complementary virtual work of the external unit (virtual) force is

$$\delta W_{ex}^* = 1v$$

The negative of the internal complementary virtual work is detailed by the above sum. Figures. 20.4(b) and (c) respectively show the ALS and ULS FBDs of the rigid pin at joint B . The actual and virtual forces on the elastic bars are equal and opposite to corresponding forces acting upon the pin joint. Thus the following table of loads and truss properties can be constructed.

Bar	(L/EA_0) coeff.	N	\bar{N}	$N\bar{N}L/EA$
AB	2	$2F$	2	$8FL/EA_0$
CB	$\sqrt{3}/2$	$-\sqrt{3}F$	$-\sqrt{3}$	$3\sqrt{3}FL/2EA_0$

Summing the last column leads to the result $v = 10.6 FL/EA_0$.

Proceeding in the same manner to determine u , the horizontal component of the deflection at joint B , place a horizontal unit force at joint B acting to the right. Since only the long horizontal bar reacts this virtual force, and since the actual load system remains the same, the table of relevant terms is

Bar	(L/EA_0) coeff.	N	\bar{N}	$N\bar{N}L/EA$
AB	2	$2F$	0	0
CB	$\sqrt{3}/2$	$-\sqrt{3}F$	+1	$-3FL/2EA_0$

Summing the last column leads to the result $u = -1.5 FL/EA_0$.

The negative sign for the complementary virtual work indicates that the actual deflection is opposite to the direction assumed for the unit force. That is, the horizontal deflection is actually to the left. This result is clearly true because of the compression in the horizontal bar. The quantities u and v are the orthogonal components of the total deflection vector. ■

The above example problem is limited to just bar extension. The first two example problems were limited to beam bending in one plane. In Eq. (20.5), the necessary integrals for dealing with bending in two orthogonal planes are presented. Since beams can do more than just bend and extend, the sequence of example problems is now interrupted to discuss other aspects of beam behavior from a work viewpoint.

20.4 Internal Complementary Virtual Work for Beam Torsion

As derived above, the derivation of the expressions for the internal complementary virtual work for beams undergoing bending and extension proceeded from the general expression for internal complementary virtual work as set forth in Eq. (16.12a), and utilized the bending and extension strain and virtual stress expressions. A similar approach can be used for the torsion of each of the four types of beam cross-sections (solid; thin open; thin closed, single cell; and thin closed, multicell) discussed in Chapters 12 and 13. That approach, which is based upon the particular stress expressions appropriate to each type of

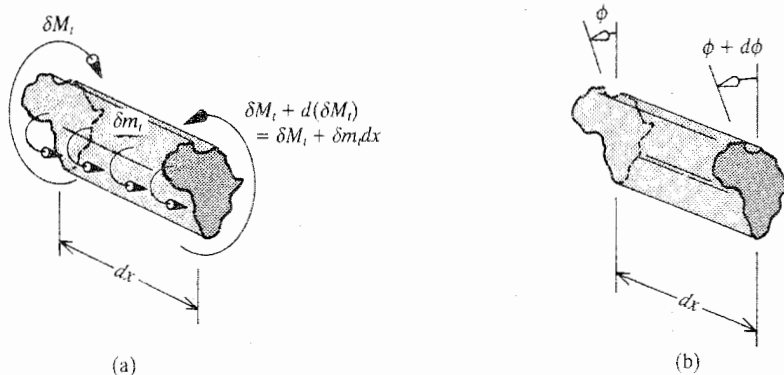


Figure 20.5. (a) A FBD showing the internal virtual twisting moments at the end cross-sections of a beam segment, and for unnecessary generality, an externally applied virtual torque per unit length. (b) The actual twisting deflections for the same beam segment. The product of a virtual torque and an associated actual twist produces complementary virtual work.

cross-section, is discussed briefly in an exercise at the end of this chapter. In each of these four cases the end result is the same as that which is developed in the following discussion. A general argument can be made for the beam torsion result by approaching the internal CVW indirectly by means of the external CVW; that is, by use of the PCVW in the form

$$-\delta W_{in}^* = +\delta W_{ex}^*$$

Figure 20.5(a) shows a FBD of a differential length of beam supporting virtual torques⁹ external to it. Figure 20.5(b) shows the actual rotations of the same differential beam segment. The differential value of the internal CVW for this differential beam length as calculated from the CVW done by the external virtual torques is

$$d(-\delta W_{in}^*) = -\delta M_t \phi + \delta m_t dx \left(\phi + \frac{d\phi}{2} \right) + [\delta M_t + d(\delta M_t)](\phi + d\phi)$$

or

$$d(-\delta W_{in}^*) = \delta M_t d\phi$$

after use of the equilibrium relation that $d(\delta M_t) = -\delta m_t dx$, and discarding higher-order differentials. From the Chapter 13 long-beam general relation between the actual twist and actual twisting moment, $GJ\phi'(x) = M_t$. Hence

$$d\phi = \frac{M_t dx}{GJ}$$

Substituting into the above, and integrating over the entire length of the beam (which alters the previous viewpoint that the δM_t are external moments on the outside cross-sectional areas of beam slices of differential length into δM_t being internal virtual moments of the

⁹ For the sake of generality, a distributed virtual torque has been included in the FBD. A distributed virtual torque is useful only for determining such seldom used quantities as the integral over the beam length of the actual twist per unit length. Also see Endnote (2).

finite length beam), yields

$$-\delta W_{in}^* = \int_L \frac{M_t \bar{M}_t}{GJ} dx$$

where $\bar{M}_t \equiv \delta M_t$ in order to make the usual change from the method of complementary virtual work to the unit load method.

Anticipating the shearing force result of the next section, a summary of all complementary virtual work results for beams in terms of the integrands of the ULM integrals over the lengths of the beams is as follows:

EXTENSION	$N(x)\bar{N}(x)/EA$	(20.6)
BENDING	$M(x)\bar{M}(x)/EI$	
SHEARING	$V(x)\bar{V}(x)/\gamma GA$	
TORSION	$M_t(x)\bar{M}_t(x)/GJ$	

where the bending term is for each of the two principal axes. If temperature changes are present, only the first three of the above integrands are modified to include the equivalent thermal stress resultants; that is, $N \rightarrow N^c$, $M \rightarrow M^c$, and $V \rightarrow V^c$.

Not all the above terms are of equal importance. The shearing force integral only has some importance if the beam experiences significant shearing deformation relative to bending deformations. That would be the situation only if the beam were short, or the beam web were very thin relative to the flanges. In all the problems that follow in this text, long beams with web thicknesses close to those of the flanges are assumed. Hence here, and in general, there is usually no need for the shear force integrals. They are derived in the only for the purpose of completing the above E versus G and A (or γA) versus I (or J) quasymmetry. The extension integral is also negligible whenever bending is also present, unless the extension is due to sizable temperature changes. Note that in the analysis of a pin-jointed truss where all actual loads are applied at the truss joints, and hence no bending is present, the extension terms are dominant. Of course, if a beam is only twisted, then the bending moments are zero and the bending integral is not used, and if a beam is only bent, then the twisting moments are zero and the torsion integral is not used.

20.5 **Internal CVW for Beam Shearing**

The internal complementary virtual work due to shear forces and shearing deformations, from the general internal CVW expression, is

$$-\delta W_{in}^* = \iiint_{Vol.} (\gamma_{xy} \delta \sigma_{xy} + \gamma_{xz} \delta \sigma_{xz}) d(Vol.)$$

For the thin beam cross-sections of vehicular structures, this same expression can be written more conveniently, since $\sigma_{xn} = 0$, as

$$-\delta W_{in}^* = \iiint_{Vol.} (\gamma_{xs} \delta \sigma_{xs}) d(Vol.)$$

where, as used in Part , the subscript s indicates the direction of the total shear stress vector, which is along the centerline of the thin cross-section. In order to make the discussion of CVW for shearing forces reasonably brief, the discussion is now limited to (i) y and z being

principal axes as has been assumed throughout this chapter; (ii) shear forces acting in the z direction only (a similar result applies for shear forces acting in the y direction); and (iii) thin, open cross-section beam cross-sections. Then, from Chapter 14, the thin, open cross-section beam shearing stress acting along the centerline of the thin cross-section at coordinate location s , where s is measured from either end of the thin, open cross-section, due to a z direction shear force only, is

$$\sigma_{xs} = \frac{V_z Q_y(s)}{I_{yy} t(s)}$$

When the shear force is that associated with the unit load system, then

$$\delta\sigma_{xs} = \frac{\bar{V}_z Q_y(s)}{I_{yy} t(s)}$$

Recall that the beam shearing strain is wholly ignored in the Bernoulli–Euler beam bending and extension theory for long beams on the basis that shearing effects are only significant in short beams. However, when the shearing strain is not approximated as having a zero value, the shearing strain is related to the shearing stress by the usual material equation, which is that the shearing strain equals the shearing stress divided by the shear modulus. That is,

$$\gamma_{xs} = \frac{V_z Q_y(s)}{GI_{yy} t(s)}$$

Substituting into the volume integral, and then iterating that integral in order to integrate first over the cross-sectional area, and then the length of the beam, yields

$$-\delta W_{in}^* = \int_0^L \frac{V_z \bar{V}_z}{\gamma AG} dx$$

where the inverse of the nondimensional factor γ that modifies the cross-sectional area is

$$\frac{1}{\gamma} = \frac{A}{I_{yy}^2} \int_{s=0}^{s=l} \frac{Q(s)^2}{t(s)} ds$$

where the line integration is over the entire length l of the centerline of the thin, open cross-section. The value of γ is usually close to 1. See the Exercises. Again, a similar expression is obtainable for shear forces in the other orthogonal plane.

20.6 Additional Illustrative Examples

The following are a series of examples that are intended to build confidence in the use of the ULM in a variety of circumstances. The first two of these examples merely illustrate what needs to be done when the stiffness of the beam varies along the length of the beam in a discontinuous manner. The next example problem illustrates the selection of different types of ULM integrals. The final two example problems illustrate different aspects of the solution process when there is symmetry of both the structure and loading.

Example 20.4. Use the ULM to calculate the counterclockwise bending slope at the free end of the nonuniform cantilevered beam loaded as shown in Fig. 20.6. That is, find $\beta = -w'(x=0)$. (The negative sign appears before the slope term $w'(0)$ because, for the chosen coordinate system, $w'(0)$ is positive as a clockwise angle while the tip rotation for the loading shown is clearly counterclockwise)

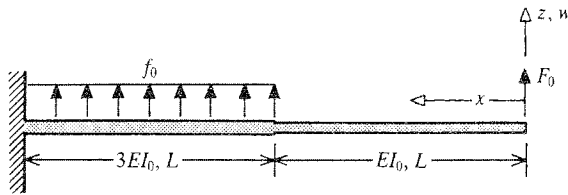


Figure 20.6. Example 20.4. A piecewise uniform, cantilevered beam.

Solution. The unit load introduced by the analyst is simply a counterclockwise unit moment at the beam tip that does the desired CVW of 1β . The equal and oppositely directed external moment at the clamped end does no external CVW because there is no actual deflection at the clamped end. A FBD shows that the ULS moment has the value $+1$ everywhere over the length of the beam. The ALS moments are as follows:

$$0 \leq x \leq L \quad M(x) = F_0x$$

$$L \leq x \leq 2L \quad M(x) = F_0x + \frac{1}{2}f_0(x - L)^2$$

Since beam bending deflections are the only type of actual deflections present in this situation, only the bending moment ULM integral is required. After multiplying both sides of the equality by the constant factor EI_0 ,

$$EI_0\beta = \int_0^L [F_0x](1)dx + \frac{1}{3} \int_L^{2L} [F_0x + \frac{1}{2}f_0(x - L)^2](1) dx$$

$$= F_0L^2 + \frac{f_0L^3}{18}$$

where the intervals of integration are determined by the discontinuity at $x = L$ in the moment expressions as well as the discontinuity at $x = L$ in the beam bending stiffness. Division by EI_0 completes the problem solution. Note again that the integration covers the entire length of the beam system. ■

Example 20.5. Use the ULM to calculate the tip torsional rotation of a nonuniform cantilevered beam loaded only by a twisting moment, M_0 , located at the beam tip, $x = L$, if the beam torsional stiffness is described by the expression $GJ_0[3 - (x/L)]$, where x originates at the fixed end of the beam.

Solution. The selected unit load is a unit torque at the beam tip in the same direction as the applied torque. Therefore, the ULS torque, $\bar{M}_t(x) = +1$ everywhere along the length of the beam. From the ALS, $M_t(x) = M_0$ everywhere along the length of the beam. Therefore, after multiplying through by the constant value GJ_0 ,

$$GJ_0\phi(x = L) = \int_0^L \frac{[M_0](1)}{3 - (x/L)} dx$$

$$GJ_0\phi(x = L) = M_0 \int_0^L \frac{dx}{3 - (x/L)} = -M_0L \int_0^L \frac{d[3 - (x/L)]}{3 - (x/L)}$$

$$= -M_0L(\ln 2 - \ln 3) = +M_0L \ln(3/2)$$

Division by the factor GJ_0 completes the solution. This particular problem, and many like it, would be no more difficult to solve using a differential equation approach. A beam bending problem with a bending stiffness that is a function of the lengthwise variable would also

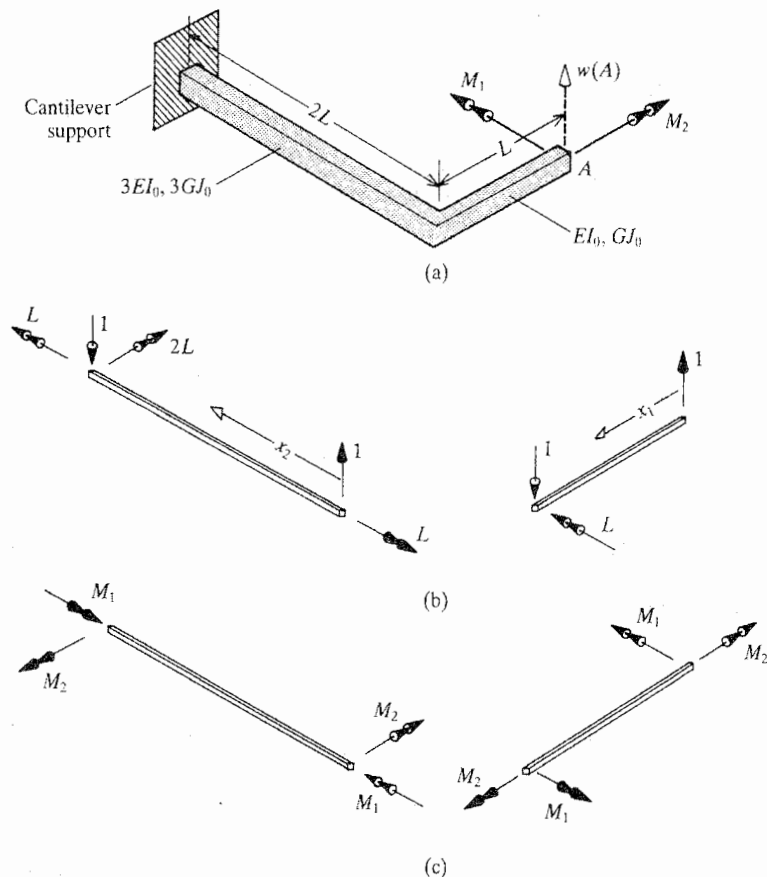


Figure 20.7. Example 20.6. (a) A cantilevered, two beam grid. (A planar combination of beams loaded so as to bend out of their plane is called a *beam grid*, while a planar combination of beams loaded to bend in their plane is called a *beam frame*.) (b) FBDs for the ULS. (c) FBDs for the ALS.

be quite manageable, although a bit messier since it would require two integrations with a nonconstant denominator. The advantage of the ULM relative to a differential equation approach becomes apparent when the torsional or bending stiffness is not easily expressible in analytical form, but rather is best expressed in tabular form or other numerical form. When the bending or torsional moments are similarly expressed, then the summation that approximates the integration is easily carried out. ■

Example 20.6. Calculate the upward lateral tip deflection, $w(A)$, of the two-beam structure shown in Fig. 20.7(a). The structure is subjected to an applied moment whose components are M_1 and M_2 .

Solution. The ULS begins with a unit force at point A and the reactions to this unit force at the clamped end. The total CVW done by the unit load and its reactions is $1w(A)$. Figure 20.7(b) shows the FBDs associated with the ULS. Note that the ULS internal reactions never do CVW because they always occur in equal and oppositely directed pairs that move through

the same actual deflections. The ALS FBDs are shown in Fig. 20.7(c). Clearly, as a result of the actual applied moment components, there is both bending and twisting of both beam elements of the overall structure.

Introduce the lengthwise coordinates x_1 and x_2 to locate positions along the axes of the two beams as shown in the FBDs of Figs. 20.7(b, c). From the FBDs the following bending and twisting moments can be determined for the intervals: For $0 \leq x_1 \leq L$ and $0 \leq x_2 \leq 2L$,

$$\begin{aligned} \bar{M}(x_1) &= +x_1 & \bar{M}(x_2) &= +x_2 & \bar{M}_t(x_1) &= 0 & \bar{M}_t(x_2) &= +L \\ M(x_1) &= -M_1 & M(x_2) &= -M_2 & M_t(x_1) &= +M_2 & M_t(x_2) &= -M_t \end{aligned}$$

Then

$$\begin{aligned} w(A) &= -\frac{M_2}{EI_0} \int_0^L x_1 dx_1 - \frac{M_2}{3EI_0} \int_0^{2L} x_2 dx_2 - \frac{M_1 L}{3GJ_0} \int_0^{2L} dx_2 \\ w(A) &= -\frac{(3M_1 + 4M_2)L^2}{6EI_0} - \frac{2M_1 L^2}{3GJ_0} \end{aligned}$$

Note that both components of the answer are negative, which means that the actual deflection is downward rather than upward as implicitly assumed with the above choice of a ULS. That both M_1 and M_2 cause the tip to move downward can be visualized when the reader rotates his or her right hand around the double headed arrows that symbolize the moments with, of course, the right thumb pointing in the direction of the arrowheads. ■

Example 20.7. Consider Fig. 20.8(a), which is a much simplified mathematical model of a high-aspect-ratio aircraft wing in level flight with its simplified net lift per span length distribution $f(x)$. The wing is represented here as a uniform beam, and the fuselage–empennage combination is represented by a centrally located weight force, $(4/3)f_0L$, that balances the total lift force. That is, the integral of the distributed load expression is equal to $(4/3)f_0L$. Thus the symmetric beam is in a state of equilibrium even though there are no beam supports. Calculate the deflection of the wing tip relative to the beam center; that is, calculate $w(0) - w(L)$. An arbitrary value could be assigned to either of these two deflections if desired.

Solution. As always, it is necessary to construct a ULS that does CVW equal to the desired deflection. In this case the ULS of Fig. 20.8(b) accomplishes this purpose because of the symmetry of the structure and actual deflections about $x = L$; that is,

$$\delta W_{ex}^* = \frac{1}{2}w(0) - 1w(L) + \frac{1}{2}(2L) = w(0) - w(L)$$

Note also that this is a valid ULS because it meets the requirement that is in equilibrium,¹⁰ and the CVW done by this ULS only involves deflections of interest.

¹⁰ Again, the fact that the ULS must be always in equilibrium is a result of requiring in the derivation of the PCVW that the virtual stresses and virtual body forces satisfy the general equilibrium equations, and that the virtual tractions be related to the virtual stresses at the boundary by Cauchy's equations. This is the only requirement that is placed upon the virtual force-type quantities in the derivation of the PCVW, which is the complete basis for the ULM.

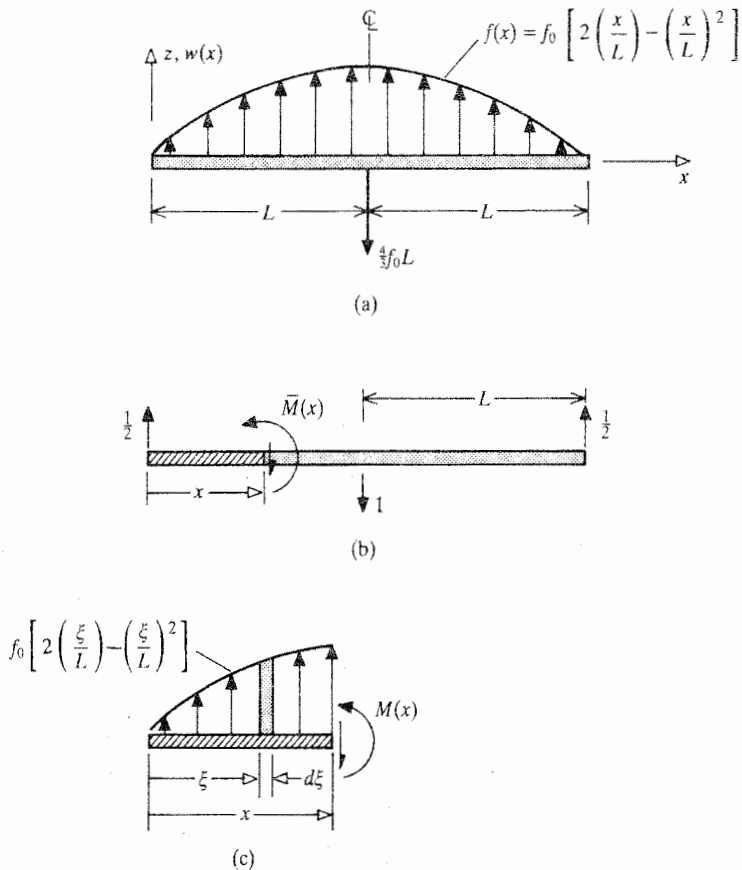


Figure 20.8. Example 20.7. (a) A much simplified wing loading mathematical model where $f(x)$ is the per unit length difference between the spanwise lift and weight distributions. (b) The selected ULS and a superimposed FBD. (c) An ALS FBD where a second spanwise coordinate is used to calculate the internal bending moment at a typical point x . The point x is, of course, the interior end of the free body.

Since beam bending is the only type of deformation occurring in this example problem, the general form of the solution can be written as

$$EI_0[w(0) - w(L)] = 2 \int_0^L M(x) \bar{M}(x) dx$$

where again advantage is taken of the symmetry about $x = L$ of both the actual and virtual loadings as well as the structure itself. Hence it is clear that the next order of business is to determine the ULS and ALS moment expressions. The ULS moment at any point x within the integration interval is simply $+x/2$. While it is possible to determine the ALS moment expression for this parabolically distributed loading using the same type of centroidal information commonly used with rectangular and triangular loading distributions, it is better to attack the problem directly by going back to basics. Consider the actual bending moment at the typical location x ; see Fig. 20.8(c). In order to calculate $M(x)$, introduce another coordinate, ξ , that starts at the left-hand wing tip and extends as far as the value x ; that is, let $0 \leq \xi \leq x$. Since the distributed force is a force per unit length, $f(\xi)d(\xi)$ is an

infinitesimal force located at the point along the beam axis that has the coordinate value ξ . The moment arm of this infinitesimal force about the point x is just $(x - \xi)$. When all such infinitesimal forces and their moment arms are added (i.e., integrated), the total bending moment at x is obtained. That is, for $0 \leq x \leq L$,

$$M(x) = \int_{\xi=0}^{\xi=x} (x - \xi) f(\xi) d\xi = x \int_0^x f(\xi) d\xi - \int_0^x \xi f(\xi) d\xi$$

In this particular case,

$$\begin{aligned} M(x) &= x f_0 L \int_0^{x/L} \left[2 \frac{\xi}{L} - \left(\frac{\xi}{L} \right)^2 \right] d \left(\frac{\xi}{L} \right) \\ &\quad - f_0 L^2 \int_0^{x/L} \frac{\xi}{L} \left[2 \frac{\xi}{L} - \left(\frac{\xi}{L} \right)^2 \right] d \left(\frac{\xi}{L} \right) \\ M(x) &= \frac{f_0 L^2}{12} \left[4 \left(\frac{x}{L} \right)^3 - \left(\frac{x}{L} \right)^4 \right] \end{aligned}$$

Now it is merely a matter of substituting the two moment expressions into the bending integral above to obtain

$$\begin{aligned} EI_0[w(0) - w(L)] &= 2 \frac{f_0 L^2}{12} \int_0^L \left[4 \left(\frac{x}{L} \right)^3 - \left(\frac{x}{L} \right)^4 \right] \left(\frac{x}{2} \right) dx \\ &= \frac{19 f_0 L^4}{360} \end{aligned}$$

If the applied load per unit length were not symmetric, then the ULM selected here would not be convenient. The use of the differential equations of Chapters 10 and 11 would be a reasonable approach to the problem. The differential equation approach also works quite well when the loading is symmetric because then the beam can be treated as clamped at the beam midspan. ■

Example 20.8. Calculate the bending slope at $x = L$ for the simply supported, symmetric, nonuniform beam of span $3L$, and symmetric loading, shown in Fig. 20.9(a). Let $f_0 L = F_0$.

Solution. First consider the ULS when no advantage is taken of the symmetry of the actual structure and loading. In that case, the most evident ULS would be as shown in Fig. 20.9(b). While this is a perfectly valid ULS, the stiffness discontinuities lead to the necessary evaluation of three definite integrals in order to determine the desired bending slope. It is true that two of those three definite integrals cancel each other. However, if that is not noticed, which is quite possible, the analyst has a lot of definite integration to carry out.

At the expense of having to think carefully, the symmetry of the structure and actual loading can be used advantageously by means of a symmetric ULS such as shown in Fig. 20.9(c). This symmetric ULS is a valid ULS because it is an equilibrated system, and because the CVW is $1w'(x=L) - 1w'(x=2L)$, which in turn is equal to $+2w'(x=L)$ because $w'(x=2L)$ is equal in magnitude to, but opposite in direction to $w'(x=L)$. To better understand the signs assigned to these bending slopes, first note that if the actual forces F_0 were not equal to $f_0 L$, and if the F_0 forces were directed downward, then the analyst might

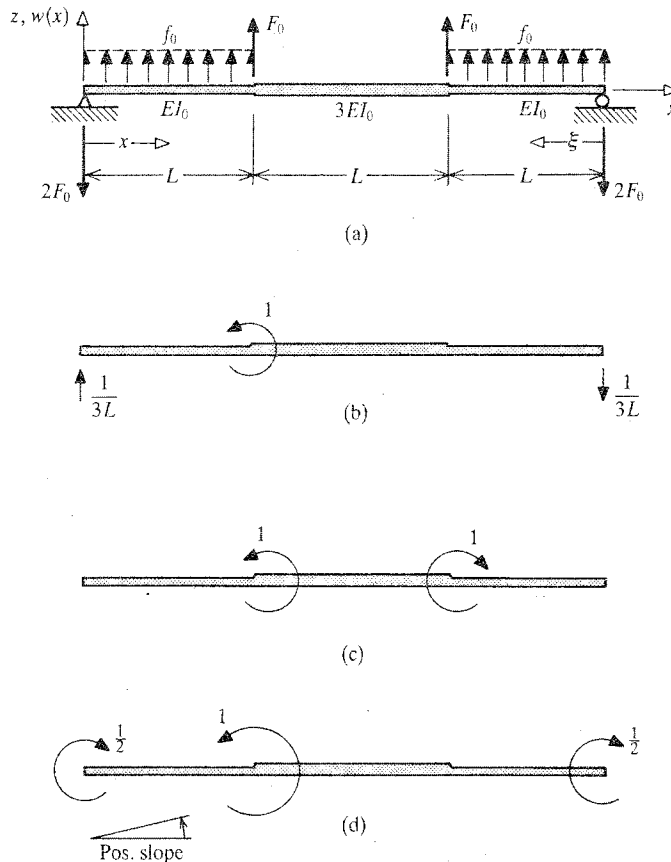
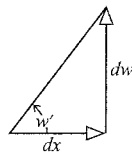


Figure 20.9. Example 20.8. (a) The ALS. (b) One possible ULS. (c) A more efficient, second possible ULS for calculating the desired bending slope. (d) Still another possible ULS.

not be sure what parts of the beam rotated upward, and what parts rotated downward. However, the analyst would know, because of the symmetry, that the bending slopes at the beam ends have opposite signs. It is useful to review the sign convention associated with derivatives of functions such as $w(x)$. In this example problem, the coordinate x is positive to the right, and the lateral deflection w is positive upward. Thus positive values of dx and dw are also to the right and upward, respectively. Put these differential quantities together in vector form as



Noting that the bending slope equals the trigonometric tangent of the rotation angle of the beam axis, dw/dx , leads to the conclusion that for the chosen coordinate axes of this example problem, the bending slope at all points along the beam axis is positive counterclockwise.

On this basis, the left-hand unit moment of Fig. 20.9(c) is in the same direction as a positive bending slope, and hence does positive CVW. The right-hand moment is directed oppositely to the positive rotation at $x = 2L$, so it does negative CVW as was stated above. Also see Endnote (1) of Chapter 11.

From the ALS and the symmetric ULS diagrams, the ULS and ALS bending moments can be obtained as follows:

$$\begin{aligned} 0 \leq x \leq L & \quad \bar{M}(x) = 0 & \quad M(x) = -2F_0x + \frac{1}{2}f_0x^2 \\ L \leq x, \xi \leq 2L & \quad \bar{M}(x) = \bar{M}(\xi) = -1 & \quad M(x) = M(\xi) = -\frac{3}{2}F_0L \\ 0 \leq \xi \leq L & \quad \bar{M}(\xi) = 0 & \quad M(\xi) = -2F_0\xi + \frac{1}{2}f_0\xi^2 \end{aligned}$$

Since two of the ULS bending moments are zero, two of the bending moment integrals are eliminated. The deflection solution reduces to the calculation

$$2w'(x = L) = \frac{1}{3EI_0} \int_{x=L}^{x=2L} \left(-\frac{3F_0L}{2} \right) (-1)dx = \frac{F_0L^2}{2EI_0}$$

or

$$w'(x = L) = \frac{F_0L^2}{4EI_0}$$

which, of course, is the same answer that would be obtained using either the first discussed ULS, or the one discussed below.

It is interesting to note that it is even possible to use the symmetry of the actual deflection pattern with a valid ULS and still not have a symmetric ULS. See Fig. 20.9(d), where the CVW is $-(1/2)w'(x = 0) + 1w'(x = L) - (1/2)w'(x = 3L) = w'(L)$ because, by symmetry, the bending slopes at the beam tips are of equal magnitude, but of opposite rotation. Since this ULS is not symmetric, it is no better the first ULS. ■

20.7 **Examples of Using the ULM for Design Purposes**

The ULM is a convenient tool for simple design problems. The following two example problems demonstrate its usefulness. The second of these two example problems also illustrates the use of the ULM when there are temperature changes.

Example 20.9. Consider the continuous, uniform beam, and uniform distributed loading shown in Figure 20.10(a). Let the span between the two supports, L_0 , be a fixed length. Determine the value of the overhang length, L , such that the right-hand tip deflection is zero.

Solution. For ease of description, let $r \equiv L/L_0$. Since L is the design variable, r too is an unknown quantity. The first step is to calculate, and then check the values of the support reactions. The results are

$$R_1 = \frac{1}{2}f_0L_0(1 - r^2) \quad \text{and} \quad R_2 = \frac{1}{2}f_0L_0(1 + r)^2$$

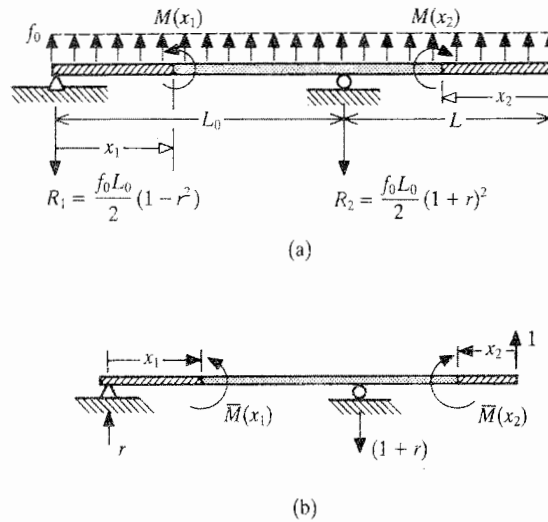


Figure 20.10. Example 20.9. (a) The ALS with support reactions and superimposed FBDs. Be sure to understand that in such compacted diagrams, quantities such as $M(x_1)$ are not part of the external loading, but are an internal stress resultant of the FBD. Externally applied bending and twisting moments are labelled as M_i , where $i = 0, 1, 2$, and so on, or some other such distinct label. (b) The selected ULS with superimposed FBDs.

Then the ALS bending moments are

$$0 \leq x_1 \leq L_0 \quad M(x_1) = \frac{1}{2} f_0 [x_1^2 - L_0 x_1 (1 - r^2)]$$

$$0 \leq x_2 \leq L \quad M(x_2) = \frac{1}{2} f_0 x_2^2$$

The unit load system must measure the lateral deflection at the tip of the overhanging beam. To this end, begin the ULS by placing an upward (or downward) unit force at that tip as shown in Fig. 20.10(b), and again calculate the support reactions. Then the ULS bending moments are

$$0 \leq x_1 \leq L_0 \quad \bar{M}(x_1) = r x_1$$

$$0 \leq x_2 \leq L \quad \bar{M}(x_2) = x_2$$

Now all is ready to calculate the bending deflection at the right-hand beam tip, and to require that deflection be zero. Write

$$EI_0 w(x_2 = 0) = 0 = \frac{f_0}{2} \int_{x_1=0}^{L_0} [x_1^2 - L_0 x_1 (1 - r^2)] [r x_1] dx_1$$

$$+ \frac{f_0}{2} \int_{x_2=0}^L [x_2^2] [x_2] dx_2$$

which after evaluation and simplification reduces to

$$0 = -L_0^3 + 4L_0 L^2 + 3L^3$$

Division by L_0^3 leads to the following cubic equation in terms of the length ratio r ,

$$0 = 3r^3 + 4r^2 - 1$$

It can be shown that this cubic equation has at most one positive root (Descartes' rule), and that root lies within the interval (0,1). (The other two roots are real and negative, and therefore have no physical meaning.) There are many ways to approximate the desired root. For example, synthetic division or Newton's method are convenient procedures. Beginning with the latter approach

$$f(r) = 3r^3 + 4r^2 - 1 \quad f'(r) = 9r^2 + 8r$$

$$f(0) = -1 \quad f(1) = +6 \quad f'(0) = 0$$

Starting Newton's method with a mediocre guess of $r = 0.5$ in the approximation equation

$$r_2 = r_1 - \frac{f(r_1)}{f'(r_1)}$$

leads to

$$r_2 = 0.5 - (0.375)/(6.25) \approx 0.44$$

$$r_3 = 0.4 + (0.168)/(4.64) \approx 0.44$$

$$r_4 = 0.44 - (0.03)/(5.2624) \approx 0.434$$

Checking (and also extending) this approximation using synthetic division,

0.4342	3.0	4.0	0.0	-1.0	
		1.3026	2.3023889	+0.9996973	
	3.0	5.3026	2.3023889	0.0003027	

Hence the approximate solution is $r = 0.434$. Thus the design length for the overhang that produces zero deflection at the tip of the overhang is $L = 0.434L_0$. Note that this solution procedure would work just as well, with a bit more work, even if the beam and loading were nonuniform. ■

Since neither the derivation of the Principle of Virtual Work nor the derivation of the Principle of Complementary Virtual Work involve the material constitutive equations, and since the effects of temperature changes appear only in the constitutive equations, those two principles are valid as they are presented in Chapter 16 for the situation where the structure undergoes temperature changes. In particular, for beams and bars where the only actual strain is ϵ_{xx} , the PCVW is

$$\delta W_{ex}^* = \iiint_{\text{Vol.}} \epsilon_{xx} \delta \sigma_{xx} d(\text{Vol.})$$

In the case of a pin-jointed truss, the total volume of the structure is the volume of the various bars. In each bar the strain due to the ALS is a constant, and the virtual stress due to the virtual or unit load system is also constant. With the volume of the i th bar being $(AL)_i$,

$$\delta W_{ex}^* = \sum (\epsilon_{xx} \delta \sigma_{xx} AL)_i = \sum (\epsilon_{xx} \bar{\sigma}_{xx} AL)_i$$

Since $\epsilon_{xx} = (\sigma_{xx}/E) + \alpha \Delta T$, $\sigma_{xx} = (N/A)$, and $\bar{\sigma}_{xx} = (\bar{N}/A)$, then the external complementary virtual work for a pin-jointed truss with homogeneous bars can be written as

follows if the temperature change is also a constant for each bar:

$$\begin{aligned}
 \delta W_{ex}^* &= \sum \left[\left[\frac{N}{EA} + \alpha \Delta T \right] \frac{\bar{N}}{A} AL \right]_i \\
 &= \sum \left[(N + EA\alpha \Delta T) \frac{\bar{N}L}{EA} \right]_i \\
 &= \sum \left[N^c \bar{N} \frac{L}{EA} \right]_i
 \end{aligned} \tag{20.7}$$

where, in keeping with previous definitions, in this special case of a uniform temperature change over the length of each bar, $N + EA\alpha \Delta T = N + N_T = N^c$. This result is used in the next example problem. See Exercise 17 for a more complete derivation of the (negative of the) internal CVW when each beam is nonhomogeneous, is loaded by bending moments as well as axial forces, and there is an arbitrary temperature change.

Example 20.10. Consider the symmetric, three-bar, nonhomogeneous, pin-jointed truss shown in Fig 20.11(a). The two diagonal bars are manufactured from material s and have the material and geometric properties E_s, A_s, L_s . The bar between the two supports is manufactured from material a and has the material and geometric properties E_a, A_a, L_a . The purpose of this three-bar truss is, by means of the different thermal expansion rates of its two materials, to maintain the unchanging vertical distance h , a focal distance of an optical system, in a spacecraft as the spacecraft undergoes gradual, uniform temperature changes in its orbit. Therefore, for a given h , and given materials with constant coefficients of thermal expansion, determine the lengths of the bar elements. (It turns out that the cross-sectional areas are not determined by this constant height requirement.)

Solution. In order for h to be a constant for an arbitrary temperature change, joint C must have a zero vertical deflection. Therefore the ULM is used to calculate the deflection of joint C , and require that it be zero. The ULS that does CVW that is just the vertical deflection of joint C is shown in Fig. 20.11(b), where

$$\bar{N}_s = -\frac{1}{2} \sec \theta \quad \text{and} \quad \bar{N}_a = +\frac{1}{2} \tan \theta.$$

Since there are no mechanical loads applied to the truss, $N_a = N_s = 0$. Thus the total actual loads are the equivalent thermal loads. Then, from the development leading to Eq. (20.7),

$$N_s^c = E_s A_s \alpha_s \Delta T \quad \text{and} \quad N_a^c = E_a A_a \alpha_a \Delta T$$

Substituting into Eq. (20.7),

$$\delta W_{ex}^* = 1 \times 0 = 0 = 2(\alpha_s \Delta T) \left(-\frac{1}{2} \sec \theta\right) L_s + (\alpha_a \Delta T) \left(\frac{1}{2} \tan \theta\right) L_a$$

Substituting $L_s = h \sec \theta$ and $L_a = 2h \tan \theta$, canceling common factors, and simplifying leads to

$$0 = -\alpha_s \sec^2 \theta + \alpha_a \tan^2 \theta$$

or

$$0 = \frac{-\alpha_s + \alpha_a \sin^2 \theta}{\cos^2 \theta}$$

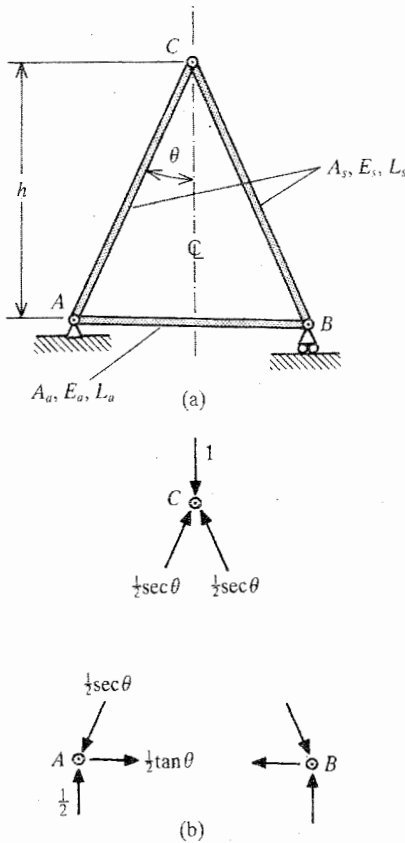


Figure 20.11. Example 20.10. (a) A planar three-bar truss to be designed to passively maintain a constant height h under the condition of a slow, uniform temperature change. (b) ULS FBDs for the purpose of calculating the deflection that causes a change in h , and then requiring that change to be zero.

Since $\cos^2 \theta$ cannot be infinite, the numerator must be zero. Hence

$$\sin \theta = \left(\frac{\alpha_s}{\alpha_a} \right)^{1/2}$$

which shows that a practical solution for $\sin \theta$ requires that α_s be less than α_a . Using this solution for θ in the above expressions for the bar lengths leads to

$$L_s = h \frac{(\alpha_a)^{1/2}}{(\alpha_a - \alpha_s)^{1/2}} \quad \text{and} \quad L_a = 2h \frac{(\alpha_s)^{1/2}}{(\alpha_a - \alpha_s)^{1/2}}$$

Now that the lengths have been determined, the next task would be to select materials that would provide a minimum-weight truss, and to consider whether or not there would be a galvanic action problem between two dissimilar metals. To accomplish the task of minimizing the weight of the truss, it is necessary to decide on the critical loads borne by the truss. For example, if the major concern is the buckling of the two diagonal bars under the action of the inertial loads produced by liftoff, and if, for example, the bars buckle when their axial stress reaches their yield stress, then without regard for cost, the best material for the diagonal bars would be the material with the highest ratio of yield stress to mass density. Among the metals, a high-strength steel or perhaps a titanium would be good

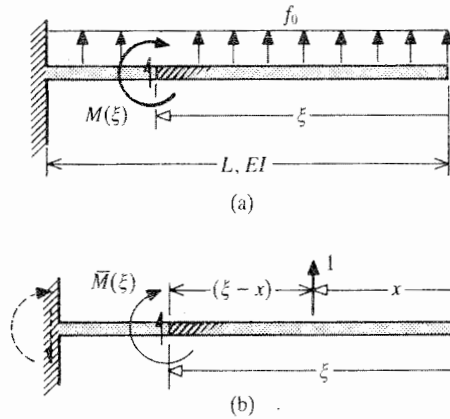


Figure 20.12. Example 20.11. (a) A cantilevered beam ALS and a superimposed FBD. (b) A ULS useful for calculating the beam lateral deflection at the arbitrary point x , and a superimposed FBD illustrating the case when the dummy variable ξ is greater than x .

candidates for selection. If AM-355 steel is chosen for the diagonal bars and 6061 aluminum is chosen for the horizontal bar, their suitable respective coefficients of thermal expansion are $\alpha_s = 6.4 \times 10^{-6}$ in/in-°F, and 12.6×10^{-6} in/in-°F. Finally, the bar cross-sectional areas, which would be inversely proportional to the yield stress, could then be calculated knowing the compressive load applied to the truss and the yield stress of each bar. ■

20.8 **General Deflection Solutions**

The ULM can be used to calculate a beam deflection pattern (i.e., the deflection at all points along a beam axis) as well as a deflection at a specific point. The following example demonstrates the procedure.

Example 20.11. Calculate the lateral deflection pattern for a uniform cantilevered beam subjected to a uniform, lateral, distributed load of magnitude f_0 . See Fig. 20.12(a).

Solution. What is desired is the lateral deflection at an arbitrary point x . To obtain that deflection, create a ULS that begins with a unit lateral force located at an arbitrary point x as is shown in Fig. 20.12(b). Since the lengthwise coordinate x is being used to locate the point where the deflection is being calculated, it is necessary to introduce another lengthwise coordinate, ξ , to integrate the ULS and ALS bending moments over the length of the beam. From the ULS and ALS diagrams of Figs. 20.12(a, b),

$$\begin{aligned} 0 \leq \xi \leq x \quad \bar{M}(\xi) &= 0 & M(\xi) &= \frac{1}{2} f_0 \xi^2 \\ x \leq \xi \leq L \quad \bar{M}(\xi) &= \xi - x & M(\xi) &= \frac{1}{2} f_0 \xi^2 \end{aligned}$$

Hence,

$$\begin{aligned} EI_0 w(x) &= 0 + \int_{\xi=x}^{\xi=L} \left(\frac{1}{2} f_0 \xi^2 \right) (\xi - x) d\xi \\ &= \frac{1}{2} f_0 \int_x^L \xi^3 d\xi - \frac{1}{2} x f_0 \int_0^L \xi^2 d\xi \end{aligned}$$

Note that because x is wholly independent of the variable of integration, it can be factored out of the integrand. The final result of the definite integration is

$$EI_0w(x) = \frac{1}{24}f_0(3L^4 - 4L^3x + x^4)$$

In this case where the beam stiffness and loading are uniform, it is a bit easier to obtain this result using the beam bending governing differential equation and the proper boundary conditions. However, if the stiffness and loading have discontinuities, it is easier to take this approach. ■

20.9 **Large Radius Curved Beams**

Curved beams whose radius of curvature is at least ten times the depth of the beam in the plane of the curvature can be analyzed with reasonable accuracy using Bernoulli–Euler straight beam theory. That is, the ULM can be applied to large radius curved beams in the same manner it is applied to straight beams, but for the need to measure distances along the beam axis by use of an arc length coordinate s rather than the Cartesian coordinate x . When the radius of curvature is less than ten times the depth of the beam, then a curved beam theory, based upon the same deflection assumptions of the Bernoulli–Euler straight beam theory, such as found in Ref. [4], can be used.

Example 20.12. Consider the cantilevered, uniform, quarter-circle curved beam shown in plan view in the ALS and ULS diagrams of Figs 20.13(a, b). The radius of curvature of the beam axis is more than 10 times the depth of the beam in the plane of the curvature. The beam is loaded at its free end by a bending moment of magnitude M_0 . Calculate the lateral deflection (downward) of the free end.

Solution. Let locations along the length of the curved beam of constant radius R be identified by use of the angular coordinate θ as shown in Figs. 20.13(a, b). Then the distance along the curved beam from the fixed end is $s = R\theta$, and a differential distance along the beam axis is $ds = R d\theta$. Integrating over the length of the curved beam is accomplished by integrating with respect to s from $s = 0$ to $s = (\pi/2)R$, or, what is exactly the same, integrating with respect to $R\theta$, or just θ , from $\theta = 0$ to $\theta = \pi/2$, where ds is replaced by $Rd\theta$.

The ULS begins with a downward unit lateral force at the beam tip. Since the applied tip bending moment, M_0 , causes both bending and torsion everywhere along the interior length of the beam as can be seen in the ALS FBD, both bending and torsional moments must be calculated for both the ALS and the ULS. Keep in mind that the double-headed vectors that represent moments are torsional moments when they are parallel to the beam axis, and are bending moments when they are perpendicular to the beam axis. Calculating the appropriate components of the applied tip moment in the case of the ALS, and calculating the appropriate moment arms in the case of the ULS, leads for $0 \leq \theta \leq \pi/2$, to

$$\begin{aligned} \overline{M}(\theta) &= -R \cos \theta & M(\theta) &= -M_0 \sin \theta \\ \overline{M}_t(\theta) &= R(1 - \sin \theta) & M_t(\theta) &= M_0 \cos \theta \end{aligned}$$

Substitution into

$$w(\theta = \pi/2) = \int_L \frac{M\overline{M}}{EI} ds + \int_L \frac{M_t\overline{M}_t}{GJ} ds$$

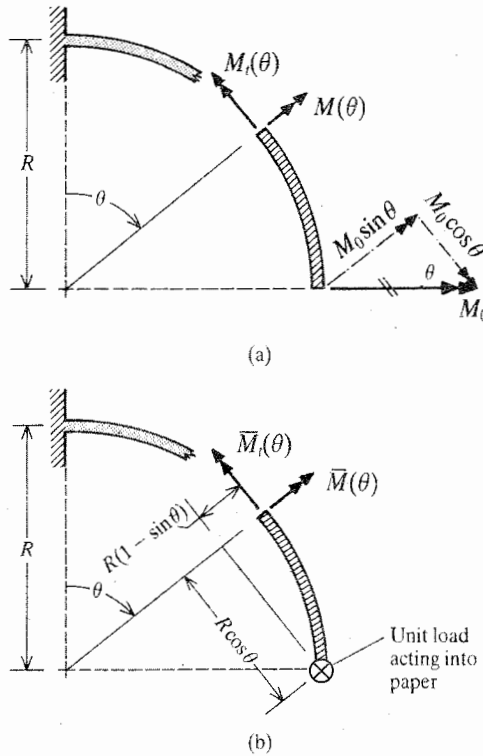


Figure 20.13. Example 20.12. (a) A plan view of a long, curved beam ALS and a superimposed FBD for the actual loads. (b) The selected ULS and a superimposed FBD for the unit (virtual) loads.

yields

$$w(\theta = \pi/2) = \frac{M_0 R^2}{EI} \int_{\theta=0}^{\theta=\pi/2} \sin \theta \cos \theta d\theta + \frac{M_0 R^2}{GJ} \int_{\theta=0}^{\theta=\pi/2} \cos \theta (1 - \sin \theta) d\theta$$

After evaluation,

$$w(\theta = \pi/2) = \frac{M_0 R^2}{2EI} + \frac{M_0 R^2}{2GJ}$$

Here is a simple illustration of a torsional stiffness influencing a lateral deflection. ■

Example 20.13. Calculate the inward travel of the right-hand support of the symmetric, uniform circular arch of Fig. 20.14(a, b) when loaded symmetrically by the actual force F_0 as shown. Again, $R > 10h$.

Solution. In this case the applied loading results in both a bending moment and an axial force at a typical beam cross-section. (Again, since the beam is a long beam, shearing deflections are negligible.) The ALS and the ULS are shown in Figs. 20.14(a, b), respectively. In terms

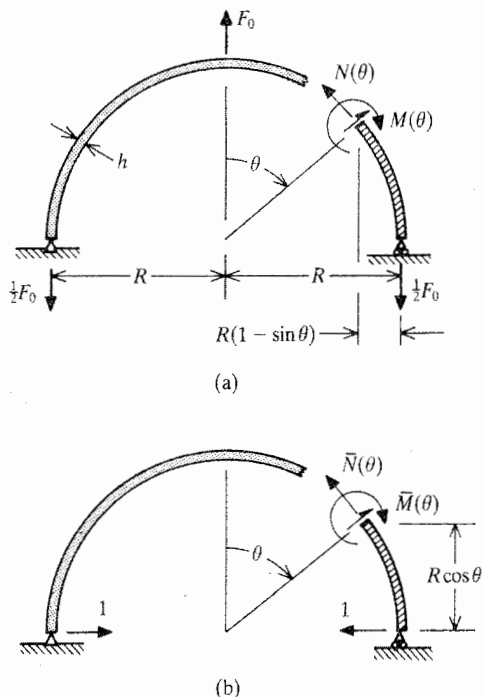


Figure 20.14. Example 20.13. (a) A long, curved beam ALS and a superimposed FBD. (b) The selected ULS and a superimposed FBD.

of the angular coordinate θ ,

$$\begin{aligned} \bar{M}(\theta) &= -R \cos \theta & M(\theta) &= -\frac{F_0 R}{2} (1 - \sin \theta) \\ \bar{N}(\theta) &= -\cos \theta & N(\theta) &= +\frac{F_0}{2} \sin \theta \end{aligned}$$

Capitalizing on the symmetry of the structure and the loading by multiplying by 2 and limiting the integration to $0 \leq \theta \leq \pi/2$, with ds replaced by $Rd\theta$, yields

$$\begin{aligned} \text{Defl.} &= 2 \frac{F_0 R^3}{2EI} \int_0^{\pi/2} \cos \theta (1 - \sin \theta) d\theta \\ &\quad - 2 \frac{F_0 R}{2EA} \int_0^{\pi/2} \sin \theta \cos \theta d\theta \end{aligned}$$

Evaluation of the two definite integrals leads to the solution

$$\text{Defl.} = \frac{F_0 R^3}{2EI} - \frac{F_0 R}{2EA}$$

Note that the ratio of the first part of the total deflection solution, the bending deflection contribution, to the second part of the solution, the axial deflection contribution, is $R^2 A / I$. Since $R^2 \gg h^2$, and since I is of the order of magnitude of Ah^2 , the numerator of this ratio is very much greater than the denominator. This illustrates the statement made at the end of Section 20.4 that, except when there are significant equivalent thermal axial forces,

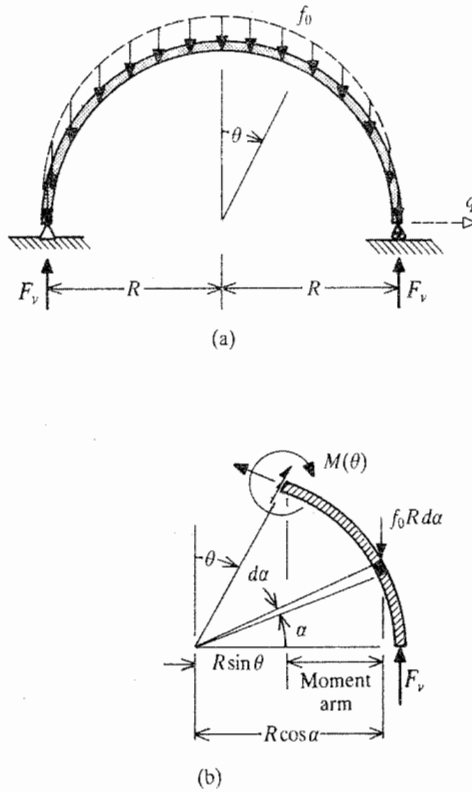


Figure 20.15. Example 20.14. (a) A long, curved beam ALS. (b) An ALS FBD illustrating the introduction of a second coordinate, α , for the purpose of calculating the actual bending moment at θ .

axial forces provide only negligible contributions to lateral deflections when actual bending moments are present. ■

Example 20.14. Repeat the above example problem, changing only the actual applied loading from a single concentrated load to a uniform load per unit of arc length of the curved beam which is everywhere directed downward; see Fig. 20.15(a). In other words, this type of loading would result from a vertical gravitational field or a vertical acceleration. As a consequence of the result for Example 20.13, axial force contributions are to be neglected in the analysis.

Solution. The ULS is the same as that of the previous example. The challenge lies with the ALS. The first step is to determine the vertical support reactions, F_v . Since the structure and loading are symmetric and the distributed force is per unit of arc length, then

$$F_v = \int_{s=0}^{s=\pi R/2} f_0 ds = \int_{\theta=0}^{\theta=\pi/2} f_0 R d\theta = \frac{\pi}{2} f_0 R$$

This result makes sense in that each support reaction is just the magnitude of the distributed load multiplied by half the length of the half circle arch. The next step is to calculate the

ALS moment at a typical location. Referring to Fig. 20.15(b),

$$M(\theta) = +F_v R(1 - \sin \theta) - \int_{\theta=0}^{\alpha=(\pi/2)-\theta} F_0 R d\alpha (R \cos \alpha - R \sin \theta)$$

So

$$M(\theta) = \frac{\pi}{2} f_0 R^2 (1 - \sin \theta) - f_0 R^2 \int_0^{(\pi/2)-\theta} \cos \alpha d\alpha - f_0 R^2 \sin \theta \int_0^{(\pi/2)-\theta} d\alpha$$

Thus

$$M(\theta) = f_0 R^2 \left(\frac{\pi}{2} - \cos \theta - \theta \sin \theta \right)$$

and

$$\bar{M}(\theta) = -R \cos \theta$$

as before, although it is evident that in this case the right-hand support moves to the right with this downward loading. Substitution of these two bending moment expressions into the bending integral, and accounting for the symmetry of the structure and loading leads to

$$\text{Defl.} = 2 \int_{\theta=0}^{\theta=\pi/2} \frac{M(\theta)\bar{M}(\theta)}{EI} R d\theta$$

$$\text{Defl.} = -\frac{2f_0 R^4}{EI} \int_0^{\pi/2} \left(\frac{\pi}{2} \cos \theta - \cos^2 \theta - \theta \sin \theta \cos \theta \right) d\theta$$

A table of integrals, or conversion to $\sin 2\theta$ and integration by parts, can be used to evaluate the last integral. The final result is

$$\text{Defl.} = -\frac{\pi f_0 R^4}{4 EI}$$

where, again, the negative sign confirms that the displacement is outward. ■

Example 20.15. Redo the same problem when the distributed loading is again of constant magnitude f_0 , but this time is directed radially inward.

Solution highlights. This time the vertical support reactions are $F_v = f_0 R$, and the bending moment $M(\theta)$ is zero. That $M(\theta)$ is zero can be understood by visualizing the half circle structure and loading extended to a full circle. Since there is no bending contribution to the support displacement, the small axial force contribution is dominant. In this case

$$\bar{P}(\theta) = \cos \theta \quad \text{and} \quad P(\theta) = f_0 R$$

so

$$\begin{aligned} \text{Defl.} &= 2 \int_0^{\pi/2} \frac{P\bar{P}}{EA} ds = 2 \frac{f_0 R^2}{EA} \int_0^{\pi/2} \cos \theta d\theta \\ &= 2 \frac{f_0 R^2}{EA} \end{aligned}$$

which is inward, and it is a much smaller displacement value than that of Example 20.14. ■

20.10 Summary

The PCVW gives rise to several very closely related methods of small deflection structural analysis that are suitable for structural systems not including plate and shell elements. The unit load method, the focus of this and the next chapter, is only a very slight variation on the virtual load method or the dummy load method in that the unit load method uses fictitious (virtual) load systems where the dummy force or moment doing the desired CVW has a magnitude of 1 lb or 1 N, or, in the case of a moment, has a magnitude of 1.0 lb/in or 1.0 N m. The reason for the choice of unit load values is merely that unit load values generally save the one step in the calculation of a desired deflection that is the canceling of the arbitrary, fictitious load (virtual or dummy) from both sides of the equation that says that the external CVW equals the negative of the internal CVW.

The PCVW is an identity that holds true for any virtual or unit load system that is in a state of equilibrium. The task of the analyst is to choose a fictitious ULS that does complementary virtual work that only involves the one or more unknown deflections that are being sought. That choice of a unit load system is usually quite routine. All that is usually necessary is to place a unit force or unit moment at the location and in the direction of the deflection that is sought. Only when the structure and the actual loading are both symmetric is more careful consideration necessary to achieve the optimum result of having a ULS that is also symmetric.

All of the example problems considered in this chapter are statically determinate. That is, merely by using summations of forces and moments, all external reactions and all internal forces and moments can be determined. Thus, in this chapter, all the integrands of the bar and beam internal complementary virtual work integrals can be specified by careful use of FBDs. Chapter 21 explains the use of the ULM with statically indeterminate structures.

It should be clear that efficient use of the ULM requires complete proficiency in writing, for example, beam bending and twisting moment expressions, and in obtaining the solutions for axial forces in the bars of trusses. If the reader does not have that proficiency, he or she cannot successfully use the ULM with statically determinate or indeterminate structures. It is essential that any remedial work necessary to obtain this proficiency be completed with this chapter. A final example problem follows that emphasizes the skill of calculating moments and selecting a satisfactory ULS.

Example 20.16. Consider the two beam structure and loading shown in Fig. 20.16(a). Calculate the bending slope at the corner where the beam of length $3L$ joins the beam of length L .

Solution. There is only one ULS that supplies the one equation that can be solved for the desired bending slope. That ULS is the particularly simple one pictured in Fig. 20.16(b). Therefore, the virtual and actual bending moments are

$$\begin{aligned} 0 \leq \xi \leq L & \quad \overline{M}(\xi) = 0 & \quad M(\xi) = \xi F_0 \\ 0 \leq x \leq 3L & \quad \overline{M}(x) = 1 & \quad M(x) = LF_0 + \frac{f_0}{18L}x^3 \end{aligned}$$

So

$$2EI_0w'(x=0) = \int_{x=0}^{3L} \left[LF_0 + \frac{f_0}{18L}x^3 \right] (1) dx$$

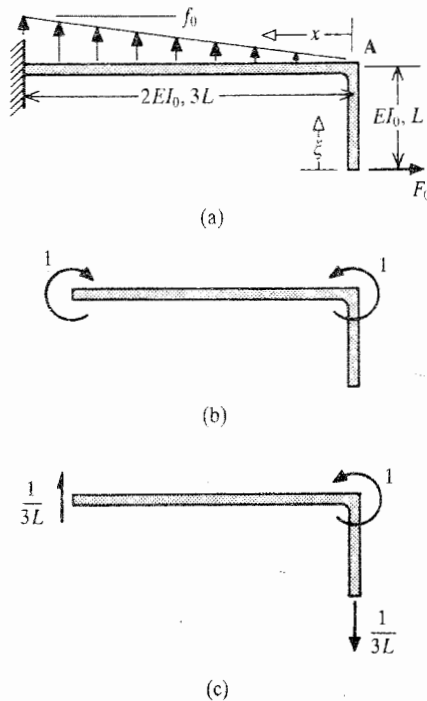


Figure 20.16. Example. 20.16. (a) A two beam frame ALS. (b) The only valid and useful ULS for this nonsymmetrical structure. (c) A remainder that not every valid ULS is useful.

Hence

$$w'(0) = \frac{9f_0L^3}{16EI_0} + \frac{3F_0L^2}{2EI_0}$$

Now consider the ULS shown in Fig. 20.16(c). The external virtual loads of that ULS are indeed in equilibrium. However, the CVW done by those virtual loads is

$$\delta W_{ex}^* = 1w'(x=0) - \frac{1}{3L}(\text{the upward deflection at } \xi = 0)$$

Since the upward deflection at $\xi = 0$ is unknown without further analysis, the ULS of Fig. 20.16(c) is unsatisfactory. ■

20.11 Maxwell's Reciprocity Theorem

Consider two distinct and wholly independent load sets separately applied to a linearly elastic structure. Call them load set one and load set two. Let there be no temperature change throughout the body. As before, let the six stresses and the six strains at each geometric point within the body that are produced by, say, the first set of loads be arranged in the 1×6 vector forms $[\sigma^{(1)}]$ and $[\gamma^{(1)}]$. Consider the integral over the entire volume of the linearly elastic structure of the first set of stresses acting through the strains separately produced by the second set of loads:

$$\iiint_{\text{Vol.}} [\sigma^{(1)}] \{ \gamma^{(2)} \} d(\text{Vol.}) \tag{20.8}$$

Recall that the product of stresses and their corresponding strains is work per unit volume. When that product is integrated over a volume, then the result is work. From Eq. (6.3), in the absence of temperature changes, $\{\sigma^{(1)}\} = [E]\{\gamma^{(1)}\}$, or transposing this matrix equation, $[\sigma^{(1)}] = [\gamma^{(1)}][E]$, where $[E]^t = [E]$. Substituting this latter form of the stress-strain equation into the above volume integral yields

$$\iiint_{\text{Vol.}} [\gamma^{(1)}][E]\{\gamma^{(2)}\} d(\text{Vol.}) = \iiint_{\text{Vol.}} [\gamma^{(1)}]\{\sigma^{(2)}\} d(\text{Vol.}) = \iiint_{\text{Vol.}} [\sigma^{(2)}]\{\gamma^{(1)}\} d(\text{Vol.})$$

That is

$$\iiint_{\text{Vol.}} [\sigma^{(1)}]\{\gamma^{(2)}\} d(\text{Vol.}) = \iiint_{\text{Vol.}} [\sigma^{(2)}]\{\gamma^{(1)}\} d(\text{Vol.})$$

The above equation is called Betti's law.

In order to give a physical interpretation to Betti's law, consider the following scenario. Let only the first load set be applied to the body, creating the first set of stresses. Then apply the second load set to the linearly elastic body. With this sequencing, the stresses from the first load set, which are fully developed before the application of the second load set, move through the full value of the strains created by the second load set. The work done by the first set of stresses moving through the second set of strains is equal to the value of the volume integral of expression (20.8).

Now reverse the above process. First let the second set of loads be applied to the body, developing the second set of stresses throughout the body. Then apply the first load set to the body creating the corresponding first set of strains. This time the stresses from the second load set move through the strains created by the first load set. Betti's law proves that the work done by the first set of stresses moving through the second set of strains is equal to the work done by the second set of stresses moving through the first set of strains. This fact is often symbolized as $W_{12} = W_{21}$.

To obtain a directly useful result from the above development that $W_{12} = W_{21}$, turn now to work done as the result of either forces moving through co-linear deflections, or moments moving through rotations. These two cases can be combined as the external generalized forces, $\{Q\}$, moving through their corresponding generalized deflections, $\{q\}$. Then $W_{12} = W_{21}$ becomes

$$[Q^{(1)}]\{q^{(2)}\} = [Q^{(2)}]\{q^{(1)}\}$$

where, for example, $\{q^{(2)}\}$ is the set of deflections caused by the second load set at the locations of the first load set. If the two force sets are now each restricted to being a single generalized force, one generalized force at point A, and the other generalized force at point B, then the above equation says that

$$Q_A^{(1)} q_A^{(2)} = Q_B^{(2)} q_B^{(1)}$$

Finally, if each of the generalized forces is required to have a unit value, then

In a linearly elastic body constrained against rigid body motions, the generalized deflection at point A, in the direction of a first generalized unit force but which is due to a second generalized unit force, is equal to the generalized deflection at point B, in the direction of the second unit force, but which is due to the first unit force.

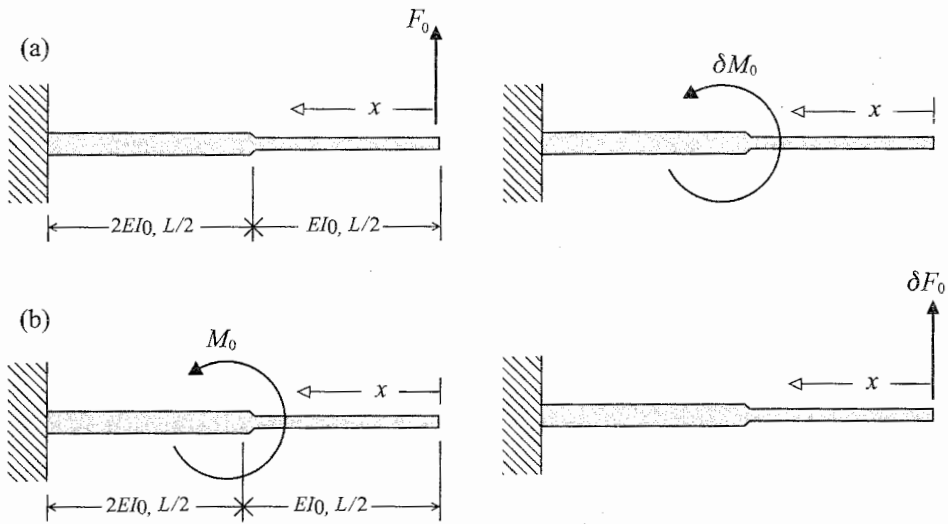


Figure 20.17. Example 20.17. (a) Actual load system and the virtual load system used to calculate the bending slope at midspan, $w'(L/2)$, positive counterclockwise. (b) (ALS and the VLS needed to calculate the lateral tip deflection, $w(0)$, for the purpose of demonstrating Maxwell's reciprocity theorem.

This is a statement of *Maxwell's reciprocity theorem*. The following example problem is an illustration of this theorem, which, hopefully, will clarify its meaning.

Example 20.17. (a) Use the virtual load method to determine the midspan bending slope of the nonuniform, cantilevered beam sketched in Fig. 20.17(a). The sole loading is the tip force F_0 .

(b) Use the virtual load method to determine the tip lateral deflection for the same beam when the sole loading is a midspan bending moment M_0 as sketched in Fig. 20.17(b).

Solution. (a) The virtual load system starts with a counterclockwise virtual moment, δM_0 , placed at center span. Then the ALS and VLS bending moments are simply $M(x) = +x F_0$ for $0 \leq x \leq L$, and $\delta M(x) = 0$ for $0 \leq x \leq L/2$ and $\delta M(x) = \delta M_0$ for $0 \leq x \leq L/2$. Therefore

$$EI_0 \delta M_0 w'(L/2) = \int_0^{L/2} [x F_0][0]dx + \frac{1}{2} \int_{L/2}^L [x F_0][\delta M_0] dx$$

So

$$EI_0 w'(L/2) = \frac{3}{16} F_0 L^2$$

(b) Here the virtual load system starts with a tip force δF_0 to measure the tip deflection $w(0)$. After multiplying through by EI_0 , the $\delta W_{ex}^* = \delta U^*$ statement becomes

$$EI_0 \delta F_0 w(0) = 0 + \frac{1}{2} \int_{L/2}^L [M_0][x \delta F_0] dx = \frac{3}{16} M_0 L^2 \delta F_0$$

$$EI_0 w(0) = \frac{3}{16} M_0 L^2$$

Note that when the applied force F_0 and the applied moment M_0 are each assigned a unit value, the magnitudes of the two deflections at, and in the direction of the other load, but due to the first load, are exactly the same as is guaranteed by Maxwell's reciprocity theorem. ■

As mentioned earlier, Maxwell's reciprocity theorem can be used to establish the symmetry of all stiffness matrices and all flexibility matrices. Again consider a linearly elastic structure constrained against rigid body motion. Again let each of the two load sets involve a single generalized force. Let the single load of the first load set act at point A , while that of the second load set acts at point B . Then, as before, $Q_A^{(1)} q_A^{(2)} = Q_B^{(2)} q_B^{(1)}$. The general flexibility matrix relationships for this two-load, two-deflection case are

$$\begin{Bmatrix} q_A \\ q_B \end{Bmatrix}^{(1)} = \begin{bmatrix} f_{AA} & f_{AB} \\ f_{BA} & f_{BB} \end{bmatrix} \begin{Bmatrix} Q_A \\ Q_B \end{Bmatrix}^{(1)} \quad \begin{Bmatrix} q_A \\ q_B \end{Bmatrix}^{(2)} = \begin{bmatrix} f_{AA} & f_{AB} \\ f_{BA} & f_{BB} \end{bmatrix} \begin{Bmatrix} Q_A \\ Q_B \end{Bmatrix}^{(2)}$$

However, in this case $Q_A^{(2)} = 0$ and $Q_B^{(1)} = 0$. Hence $q_A^{(2)} = f_{AB} Q_B^{(2)}$, and $q_B^{(1)} = f_{BA} Q_A^{(1)}$. Substituting these last two relationships into the above $Q_A^{(1)} q_A^{(2)} = Q_B^{(2)} q_B^{(1)}$ yields

$$Q_A^{(1)} f_{AB} Q_B^{(2)} = Q_B^{(2)} f_{BA} Q_A^{(1)} \quad \text{or} \quad f_{AB} = f_{BA}$$

Since the points A and B are any two points on the structure, they can be any two points of any larger set of points involved in a larger flexibility matrix. Hence that larger flexibility matrix is also a symmetric matrix.

The direct proof of the symmetry of any stiffness matrix requires a little more algebra. The general stiffness relations between these pairs of generalized forces and the generalized deflections are

$$\begin{Bmatrix} Q_A \\ Q_B \end{Bmatrix}^{(1)} = \begin{bmatrix} k_{AA} & k_{AB} \\ k_{BA} & k_{BB} \end{bmatrix} \begin{Bmatrix} q_A \\ q_B \end{Bmatrix}^{(1)} \quad \begin{Bmatrix} Q_A \\ Q_B \end{Bmatrix}^{(2)} = \begin{bmatrix} k_{AA} & k_{AB} \\ k_{BA} & k_{BB} \end{bmatrix} \begin{Bmatrix} q_A \\ q_B \end{Bmatrix}^{(2)}$$

Substituting from the above matrix equation relationships

$$Q_A^{(1)} = k_{AA} q_A^{(1)} + k_{AB} q_B^{(1)} \quad \text{and} \quad Q_B^{(2)} = k_{BA} q_A^{(2)} + k_{BB} q_B^{(2)}$$

into the Maxwell's $Q_A^{(1)} q_A^{(2)} = Q_B^{(2)} q_B^{(1)}$ yields

$$k_{AA} q_A^{(1)} q_A^{(2)} + k_{AB} q_B^{(1)} q_A^{(2)} = k_{BA} q_A^{(2)} q_B^{(1)} + k_{BB} q_B^{(1)} q_B^{(2)}$$

Again, $Q_A^{(2)} = 0$ and $Q_B^{(1)} = 0$. Thus

$$k_{AA} q_A^{(2)} = -k_{AB} q_B^{(2)} \quad \text{and} \quad k_{BB} q_B^{(1)} = -k_{BA} q_A^{(1)}$$

Substituting these stiffness relationships into the previous stiffness relationships yields

$$k_{AB} (q_B^{(1)} q_A^{(2)} - q_A^{(1)} q_B^{(2)}) = k_{BA} (q_A^{(2)} q_B^{(1)} - q_A^{(1)} q_B^{(2)})$$

or, simply

$$k_{AB} = k_{BA}$$

This statement proves the symmetry of all stiffness matrices.

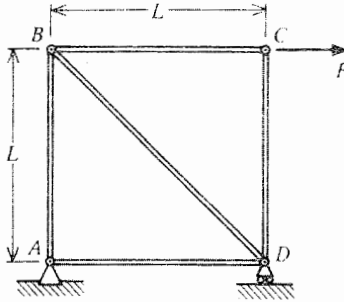


Figure 20.18. Exercise 20.2. A square, pin-jointed truss.

Chapter 20 Exercises

- 20.1.** Consider the nonuniform, simply supported beam of Fig. 20.9, without the distributed loading and concentrated forces shown in that sketch.
- Calculate the lateral deflection $w(x = L)$ resulting from an applied, counter-clockwise bending moment of unit magnitude placed at $x = 2L$.
 - Calculate the bending slope $w'(x = 2L)$ due to an upwardly directed, unit valued, lateral force placed at $x = L$.
 - Should the magnitude and sign of the answers to parts (a) and (b) be the same?
- 20.2.** For the statically determinate pin-jointed truss and loading shown in Fig. 20.18 where all bars have the same Young's modulus and cross-sectional area, calculate:
- The horizontal deflection of the right-hand (roller) support.
 - The relative motion of joints A and C along the straight line between the two joints.
 - The horizontal motion of joint C.
- 20.3.** (a) Calculate the lateral bending deflection at one-quarter of the span of a simply supported (long) beam of span length L and bending stiffness EI , which is loaded by a uniform distributed load of magnitude f_0 acting upward without using a symmetric ULS
- (b) As in part (a) but using a symmetric ULS.
- 20.4.** For the two-beam frame and loading sketched in Fig. 20.19, calculate
- the lateral deflection at, and in the direction of, the single applied load F .
 - the x direction lateral deflection at $x = L$.
 - the bending slope at $x = L$, $y = 2L$ if, in addition to the applied force F , there is also a uniformly distributed force per unit length of magnitude F/L acting in the positive x direction on both beams.
 - the bending slope at $x = 0$ when both the concentrated force F and the distributed loading of magnitude F/L are acting upon the two beam frame.
- 20.5.** (a) Find the bending slope magnitude at either support of a simply supported, beam of length L and stiffness EI that is symmetrically loaded by two upward concentrated forces of magnitude F_0 placed at the one-third and two-thirds span positions.
- Find the lateral deflection at the one-third span location.
 - Find the bending slope magnitude at either load application point.

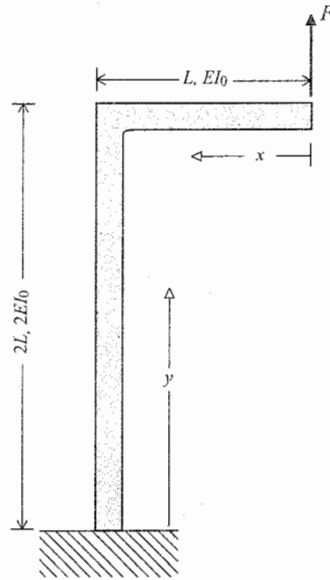


Figure 20.19. Exercise 20.4

- 20.6.** A uniform beam of overall length $4L$ is symmetrically positioned over two simple supports separated by a distance of $2L$. That is, there is an overhang of length L at each end of the beam. The entire beam is subjected to a upward distributed load per unit length of magnitude F_0 . Thus the reaction at each support is $2f_0L$ downward.
- Sketch the deflection pattern for the entire beam.
 - Calculate the vertical deflection at the right-hand beam tip.
 - Calculate the vertical deflection at the center of the beam.
 - Calculate the bending slope at either support.
 - Calculate the bending slope at either beam tip.
- 20.7.** A symmetric beam of overall length $3L$ is symmetrically positioned over two simple supports separated by a distance L . The center length of the beam has a stiffness $2EI_0$, while the two overhanging lengths have a stiffness EI_0 . The loading is an upwardly directed distributed force per unit length of magnitude f_0 acting only over the left-hand overhang length L . Note that the loading is *not* symmetric.
- Calculate the bending slope at the left-hand beam tip.
 - Calculate the lateral deflection at the left-hand beam tip.
 - Calculate the lateral deflection at the right-hand beam tip.
 - Calculate the lateral deflection at the midspan.
 - Sketch the deflection pattern.
 - Suggest a symmetric and an antisymmetric loading for this beam, which, when the two are superimposed, provide the nonsymmetric loading originally specified.
- 20.8.** (a) Calculate the tip deflection of a uniform, cantilevered beam loaded by a linearly varying distributed loading acting upward when the distributed loading has the magnitude f_0 at the clamped end, and zero magnitude at the free end.
- (b) Calculate the tip rotation (i.e., bending slope).

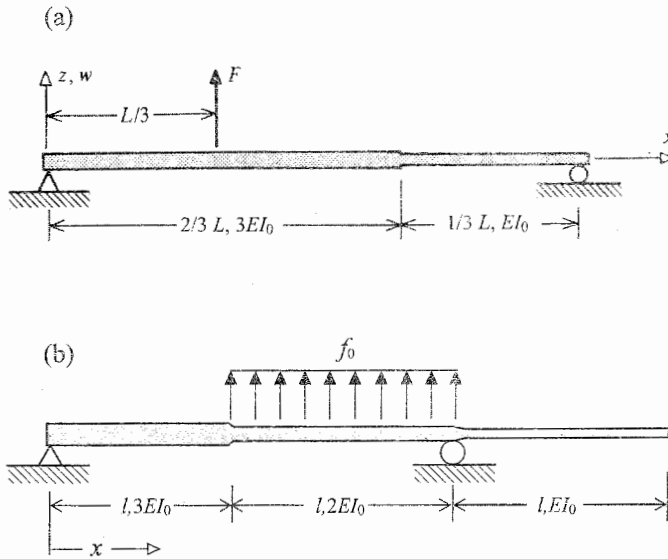


Figure 20.20. (a) Exercise 20.9 (a,b,c) A nonuniform, simply supported beam. (b) Exercise 20.9 (d). Another nonuniform, simply supported beam.

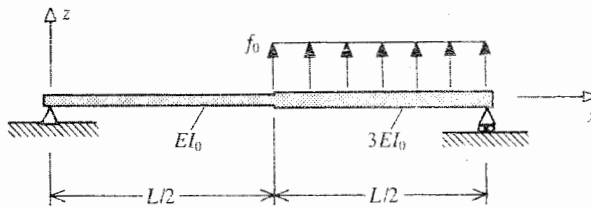


Figure 20.21. Exercise 20.10. A nonuniform, simply supported beam.

- 20.9.** (a) Calculate the bending slope at $x = L/3$ of the nonuniform, simply supported beam shown in Fig. 20.20
 (b) Calculate the lateral deflection at the same point.
 (c) Calculate the deflection at $x = 2L/3$.
 (d) Calculate the lateral deflection at $x = l$ of the beam shown in Fig. 20.20(b).
- 20.10.** (a) Calculate the bending slope at midspan of the simply supported beam shown in Fig. 20.21
 (b) Calculate the vertical deflection at midspan.
 (c) Calculate the bending slope at $x = 0$.
 (d) Calculate the bending slope at $x = L$.
- 20.11.** (a) Calculate the vertical deflection at midspan, $x = L$, of the nonuniform, simply supported beam shown in Fig. 20.22. The use of two coordinates originating at the supports is strongly advised.
 (b) Calculate the bending slope at midspan.
 (c) Calculate the bending slope at $x = 0$.
- 20.12.** (a) Calculate the vertical tip deflection, of the cantilevered, piecewise uniform, two-beam structure shown in Fig. 20.23.
 (b) Calculate the two rotations at the elbow of the structure.

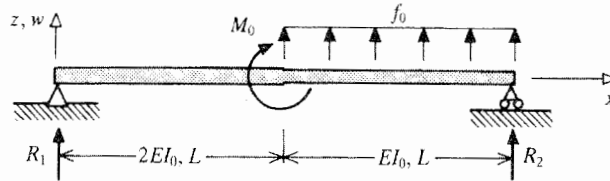


Figure 20.22. Exercise 20.11. A nonuniform, simply supported beam.

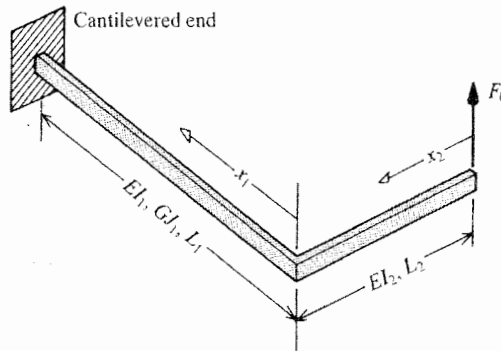


Figure 20.23. Exercise 20.12. A nonuniform, cantilevered two beam grid.

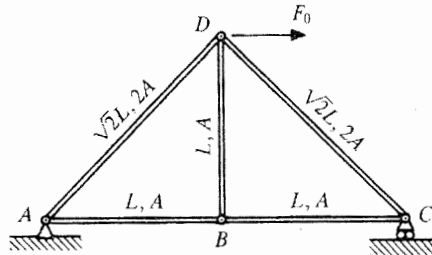


Figure 20.24. Exercise 20.13. A five-bar, pin-jointed truss.

- 20.13. (a) Calculate the horizontal deflection of joint D of the simply supported five-bar truss shown in Fig. 20.24. The modulus of elasticity is the same for all bar members.
- (b) Calculate the horizontal deflection at joint C .
- (c) Calculate the vertical deflection at joint D .
- (d) Why would the simple truss geometry shown in Fig. 20.4 be a poor design if the actual force F acted upward rather than downward? What changes in geometry would you suggest?
- 20.14. Calculate the wing tip deflection relative to the beam center deflection of the beam of Fig. 20.8(a) when the distributed lift per unit length is $f_0 \sin(\pi x/L)$.
- 20.15. Figure 20.25 shows a simply supported, nonuniform beam with an overhang. Note the applied moment at $x = 0$.
- (a) Calculate the upward deflection at $x = 0$; that is, $w(x = 0)$.
- (b) Calculate the bending slope at $x = L$; that is, $w'(x = L)$.

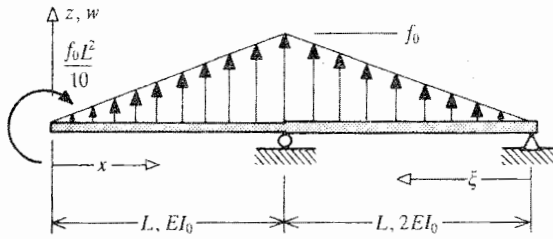


Figure 20.25. Exercise 20.15. A nonuniform, simply supported beam with an overhang.

- (c) Alter the above problem by first removing the applied moment at the left end, moving the roller support at $x = L$ to $x = 0$ (thus making a simply supported beam of length $2L$, and making the loading per unit length over the left portion of the beam uniform and of magnitude f_0 acting upward). The triangular load distribution on the right half of the beam remains the same as it was. After these changes, calculate the bending slope at $x = 0$.
- (d) As in part (c), but this time calculate the bending slope at $x = L$.
- (e) As in part (c), but this time calculate the bending slope at the right-hand end, where ξ equals zero.

FOR THE EAGER

- 20.16. Show that for a thin rectangular cross-section of depth h and width b , where $h \gg b$, and a shear force acting in the direction of the cross-section depth, the value of the nondimensional shear factor modifying the cross-sectional area in the ULM shearing deformation integral, γ , has the value $5/6$.
- 20.17. Consider a uniform, homogeneous beam which in planform is a full circle of radius R , but where the circle is broken at one cross-section by a separation between the two beam ends of negligible length. Let the beam cross-section be circular with a radius r . Let each of the two beam ends be loaded only by a force F that is normal to the plane of the circular beam, but where the two forces are oppositely directed so that the beam is in a state of static equilibrium. Assume that $R \gg r$ so that straight-beam theory is reasonably applicable, and then calculate the relative lateral deflection between the two beam ends. Use this information to obtain the stiffness (the ratio of force to deflection) of one coil of a coiled wire spring in terms of the geometric and material factors of the beam. If the stiffness of a spring with n coils is $1/n$ that of a spring of one coil, then what is the formula for the stiffness of a circular wire spring of n coils?

FOR THE ESPECIALLY EAGER

- 20.18. Rederive the beam bending and extension expressions for the internal complementary virtual work for a homogeneous beam subjected to a temperature change as well as an arbitrary mechanical loading, and thereby confirm footnote 5. Let the y and z axes be principal axes.
- 20.19. Use the uniform torsion results of Chapters 12 and 13 for the torsionally induced shearing stress $\sigma_{\tau s}$, where s is arc length coordinate within the plane of the cross-section that runs along membrane contour lines, to directly derive from the general expression for the internal CVW the ULM beam torsion integral for (a) a thin, open cross-section of length a and thickness b ; (b) a thin, closed, single-cell

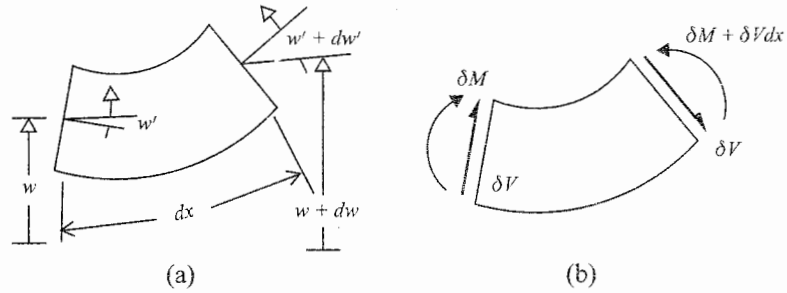


Figure 20.26. Endnote (2). (a) Geometry of bent differential beam length. (b) Virtual force system in equilibrium.

cross-section; (c) a thin, multicelled cross-section; and (d) an arbitrary, solid cross-section. *Hint:* For (a) $\sigma_{xz} = \sigma_{xy} = 2z M_t(x)/J$, so $\delta\sigma = 2z \delta M_t(x)/J$, and $\epsilon = 2z M_t(x)/GJ$ where $(-b/2) \leq z \leq (+b/2)$ and $(-a/2) \leq y \leq (+a/2)$ define the (serpentine) rectangular area, and $J = (1/3)ab^3$. For (b) use the first of Eqs. (13.11) to obtain $\epsilon_{xz} = M_t/[2G\hat{A}t(s)]$, $\delta\sigma_{xz} = \delta M_t/[2\hat{A}t(s)]$, $dA = t ds$, and the last of Eqs. (13.11) to complete the proof. For part (d) make use of the fact that for uniform torsion the virtual torque is coincident with, and thus proportional to, the actual torque, and thus all virtual load quantities, such as the virtual stress, have the same proportionality to the corresponding actual load quantities. Then see the first part of Appendix A, Section 4.

- 20.20.** Consider a beam of length L cantilevered at its left end. Calculate the internal bending moment, $M(x)$, due only to an applied lateral force per unit length of arbitrary magnitude, $f(x)$, where x is measured from the free beam end.
- 20.21.** In relation to footnote 5, derive the beam bending and extension expressions for $-\delta W_m^*$ for a beam where the y and z axes are not principal axes, the beam cross-section is not homogeneous, and there is a temperature change. To this end, use Eq. (9.8) for σ_{xx} , and

$$\epsilon_{xx} = \frac{\sigma_{xx}}{E} + \alpha \Delta T$$

and recall $\delta(\Delta T) = 0$.

Endnote (1) ULM Limitations

Even plate bending problems are unsuited to the unit/dummy/virtual load method. The plate bending complementary virtual internal work could easily be written in terms of the plate internal bending and twisting moments per unit length that are produced by both the actual and virtual load systems. However, unlike beams, plate moments per unit length and shear forces per unit length can never be rendered statically determinate by the introduction of a limited number of discrete, unknown moments and forces. That is, the calculation of those plate bending forces and moments per unit length best proceeds from the very plate displacement solutions that are sought by the use of the unit/dummy/virtual load method. Plate theory is introduced in Chapter 22.

Endnote (2) Internal Complementary Virtual Work

In Section 20.4, the complementary virtual work for beam twisting was calculated without reference to strains or virtual stresses. To test that approach for beam bending, consider the differential length of deformed beam shown in Fig. 20.26 where $I_{yz}^* = 0$.

$$\begin{aligned} d(\delta W^*) &= -\delta M w' + (\delta M + \delta V dx)(w' + dw') + \delta V w - \delta V(w + dw) \\ &= \delta M dw' + \delta V dw' dx - \delta V dw = \delta M dw' \end{aligned}$$

Since $dw' = w'' dx = \frac{M}{EI} dx$, then $\delta W^* = \int \frac{M\delta M}{EI} dx$, the same result as that previously obtained, which builds confidence in the approach taken for beam twisting and shearing.

The Unit Load Method for Indeterminate Structures

21.1 Introduction

As was previously noted, all complementary virtual work (CVW) methods of analysis, such as the unit load method (ULM), are force or flexibility types of analyses, and thus are a special case of a stress formulation. The internal CVW terms are always written in terms of force-type quantities such as actual and virtual bending moments, or actual and virtual twisting moments, or actual and virtual axial forces, and so forth. Flexibility is the inverse of stiffness, and these force-type quantities of the internal CVW expressions are always multiplied by the inverse of a corresponding structural element stiffness coefficient such as $1/(EI)$, or $1/(GJ)$, or $1/(EA)$. All force-type analyses always divide loaded structures and their supports into two categories. With respect to force-type analyses, a structure is either statically determinate or statically indeterminate, and the analysis procedure depends upon to which category the structure belongs. When a beam structure is statically determinate, all external support reactions and all internal stress resultants can be calculated by use of equations of force and moment equilibrium. Then the calculation of the internal stresses is simply a matter of algebra. See, for example, for beam extension and bending, Eq. (9.8). The only quantities not immediately derivable from the stress resultants are the deflections. Chapter 20 explains how the ULM can be used to calculate deflections when the structure is statically determinate, or when the indeterminate stress resultants have already been determined by means such as those discussed in this chapter.

When the structure to be analyzed by a force method is statically *indeterminate*, then one or more of the external support reactions and/or the internal stress resultants cannot be determined by the use of the equations of force and moment equilibrium alone. The minimum number of such force-type quantities left undetermined by the force and moment equilibrium equations is called the degree of redundancy of the structure. Those support reactions and/or internal stress resultants that need to be known in order to know all other support reactions and stress resultants, are called the “redundant” support reactions and “redundant” stress resultants. Collectively, they are called the “redundants.” Of course, the number of redundants is equal to the degree of redundancy.

The first object of force analyses is to determine the values of the redundants, and such is the case with the ULM. Hence the first step in the use of the ULM is to identify the (minimum) degree of redundancy, and to choose a valid set of redundant forces and moments. This task is not difficult for simple structures, but can get to be messy for structures with a large number of structural elements. In fact, this is an important difficulty with force methods that is not encountered with displacement methods.

21.2 Identifying Redundant Forces and Moments

The minimum number of beam structure redundants not only depends upon the structure and its supports, but that number also depends upon the loading. The one certain way of determining the minimum number of redundants for a particular structure and loading

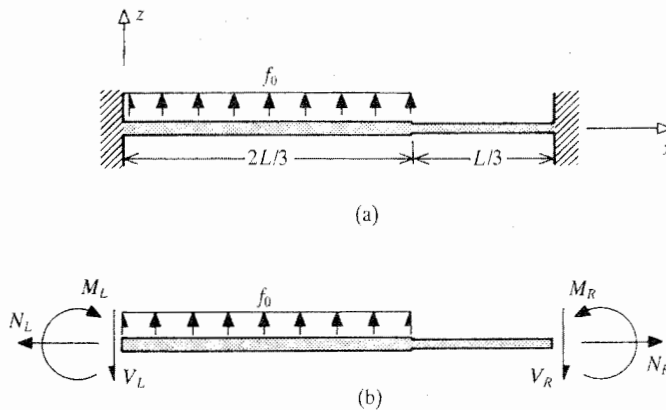


Figure 21.1. (a) A fixed–fixed, nonuniform beam. (b) A FBD of the entire beam for the purpose of investigating the support reactions.

is to systematically carry out the process of (i) identifying all the small-displacement, nonzero external reactions; (ii) actually writing the independent equations of equilibrium for the entire structure in terms of those external reactions and the applied loading; (iii) selecting the external reactions whose number exceeds the number of overall independent equations of equilibrium as the external redundants; and (iv) assuming that all external reactions are known, determining the additional number of internal reactions that need to be known in order that all internal stress resultants can then be calculated using force and moment equilibrium equations. The last step is a process of looking at FBDs of various parts of the structure – every individual beam and other simple structural element if necessary. The minimum number of redundants for that structure and load system is the minimum number of external and internal reactions that have to be known in order to determine all the other internal and external reactions in the equilibrium equations of all parts of the structure. This process is illustrated below.

In order to practice the skill of identifying redundants, consider the structure shown in Fig. 21.1(a), which is a fixed–fixed, nonuniform beam. In this case there are only two relevant independent equations of equilibrium. These two equations could be either the sum of the moments in the plane of the paper about any point on the beam axis and the sum of the forces in the vertical direction, or two moment summation equations about different points along the beam axes. Either pair of equilibrium equations would be equally valid. The sum of the forces in the horizontal direction is ignored in this case because the axial forces do not appear in the equilibrium equations that involve the bending moments and shearing forces. The beam axial forces that arise from lateral beam bending are nonlinear and depend upon the resistance to stretching provided by the beam supports. If the lateral deflections are small,¹ and the beam's supports provide little opposition to stretching, then the axial forces are sufficiently small that they can be ignored.

There is a moment and shear reaction at each fixed end of the beam in Fig. 21.1(a), for a total of four reactions. Since there are only the two previously discussed equilibrium equations to provide two relations among these four unknowns, the minimum number of redundant reactions is two. It matters little for problems of this size which two of the four

¹ Again, a small lateral beam bending deflection is one that is less than approximately one-quarter of the beam depth (Ref. [16]).

reactions are identified as the redundants.² For example, M_R and V_R are an acceptable choice as the two redundants. Again, when these two redundant reactions are calculated, the stress resultants would be known everywhere within the beam system.

As another illustration of the process for identifying redundants, consider the same beam as above, but now modified by the insertion of a hinge at $x = 2L/3$. Now the structure can be described as two coaxial, cantilevered beams joined together at their tips by a hinge. No moment can be transmitted across a hinge, only shear forces. Hence free body diagrams of each of the two cantilevered beams would have equal and opposite unknown shear forces at each beam tip at the hinge. Each cantilevered beam would be statically determinate but for that one unknown (internal) shear force. Hence the structure has one redundant reaction. Another viewpoint, useful for larger structures, is that the equilibrium equation that states that the moment at a hinge is zero augments the number of equilibrium equations for the total structure, and thereby reduces the number of redundants by the number of hinges.³ Hence, from this viewpoint as well, this modified beam structure has only one redundant reaction. As before, it matters little which one of the two moments or two shears is selected as the redundant. If, for example, V_L is chosen as the redundant, the remaining reactions can be determined in terms of V_L as follows. By summing vertical forces and then writing a moment equation at each fixed beam end for that cantilevered beam:

$$V_R = \frac{2f_0L}{3} - V_L \quad M_L = \frac{2V_L L}{3} - \frac{2f_0L^2}{9} \quad M_R = \frac{2f_0L^2}{9} - \frac{V_L L}{3}$$

Consider the four-beam grid shown in Fig. 21.2(a), which is only loaded in the negative z direction along beam BC . All four beams have the same cross-section. At supports A and B the beam grid is constrained from moving in any direction, but there is no constraint against rotations. At supports D and E the grid can move freely in the x and y directions, but not at all in the z direction, and there is no constraint against rotations. Hence there is only a vertical reaction at each of the four supports. The number of independent equations available to determine those four reactions are (1) the sum of the moments about an axis paralleling the x axis is zero; (2) the sum of the moments about an axis paralleling the y axis is zero; and (3) the sum of the vertical forces is zero. The sum of the moments about the z axis and the sum of the forces in the x and y directions are identically zero, and thus provide no information. Since there are no other equations available, the conclusion is that there is but one redundant reaction, and it does not matter which one of the four vertical reactions is chosen for that role.

Now modify the loading on the above beam grid by adding a downward loading per unit length of magnitude f_0 over the entire length of beam AC so that now both the structure and loading are symmetric about the axis that bisects the right angles ACB and DCE . This axis of symmetry means that the vertical reaction at A is equal to the vertical reaction at B , and the vertical reaction at D is equal to that at E . Thus, to begin with, there are now only two unknown vertical reactions, say F_d and F_e . There is a small price to be paid for the use

² For structures with a large number of redundants, and hence a large number of simultaneous equations to be solved, a useful guideline for selecting those redundants from among the various candidate reactions is to choose those reactions that cause larger deflections at their own location than elsewhere in the structure when the structure is modified by "releases" (explained later) at the locations of the reactions. This choice helps avoid ill-conditioning of the simultaneous equations. Moments more often than forces meet this criterion in frames.

³ More equilibrium equations than unknown reactions indicates either (i) a structure which can undergo rigid body motion; or (ii) must undergo finite (nonlinear) deflections in order to be able to resist general applied loads.

of an axis of symmetry. Now there is only one independent moment equilibrium equation. Regardless of which coordinate axis in the plane ABC is used as a moment axis, the result of that moment equation and the result of summing forces in the vertical direction is

$$4LF_a - 2LF_e = 8f_0L^2 \quad \text{and} \quad 2F_a + 2F_e = 8f_0L$$

which is clearly two equations in two unknowns. Since these equations have independent origins, they are independent equations. Thus it is concluded that both F_a and F_e can be determined, and therefore there are no redundant reactions. (The solution is $F_a = F_b = 2F_d = 2F_e = 8f_0L/3$, which could also have been determined directly by taking moments about AB and DE .) In other words, symmetry can add to the constraints imposed upon the values of the reactions, and thus may reduce the number of redundants from what it would be without symmetry.

Figure 21.2(b) provides another, related illustration of the process of identifying redundant reactions. Again, in this beam grid, there is one axis of symmetry. However, this time the external beam ends are clamped against all deflections. Since the loading on the T structure is entirely lateral, and since the lateral beam deflections are presumed to be small, there are no significant axial force reactions at any of the three supports. Deciding what reactions do exist is sometimes aided by visualizing the deflection pattern of the loaded structure. See Fig. 21.2(c). At the symmetric supports B and D , equal vertical shearing force reactions are required to hold the beam down. At the same two supports, equal but opposite bending moment reactions are necessary to achieve the zero bending slopes associated with clamped supports. Similarly, at support A , there is also a vertical shear force reaction, and a bending moment reaction. The continuity of the deflections between beams AC and BD requires that the twist in beam BD at point C be equal to the bending slope of beam AC at point C . Since beam BD twists at its center, but not at its ends, there must be twisting moment reactions at supports B and D . There is no twisting moment at support A because the symmetry of the structure and the loading prohibit any twist in beam AC . (This result of a zero twisting moment reaction at support A can be confirmed by setting the sum of the moments about axis AC equal to zero.) Therefore, in total there are eight reactions, where the three at support D are linked by symmetry to the corresponding three reactions at support B . There are only two useful equilibrium equations: (i) zero equals the sum of the vertical forces; and (ii) zero equals the sum of the moments about axis BD . The independent equilibrium equation which refers to the sum of the moments about axis AC has been replaced by the symmetric labeling of the reactions at supports B and D . Thus five different reactions less two useful equilibrium equations leaves a total of three redundant reactions. The first exercise reviews this matter.

21.3 The Coiled Spring Structural Elements

Structures in three dimensions often require much more effort than structures in two dimensions. Hence it is always desirable to model a structure in two dimensions if possible. As is explained in Section 11.2, the use of the coiled spring to model other structural elements is one means of accomplishing such a simplification in the mathematical model of a structure. As a brief review of that concept for those who skipped Part III, consider the three-beam structure shown in Fig. 21.3(a), which consists of a loaded top beam that is supported along its length by two other beams. If the top beam only rests upon the other two beams, that is, if there is no material connection between the beams, then the bottom pair of beams only supply the top beam with vertical force reactions in response to the downward deflection of the top beam. If, for example, the bottom two beams are each simply supported,

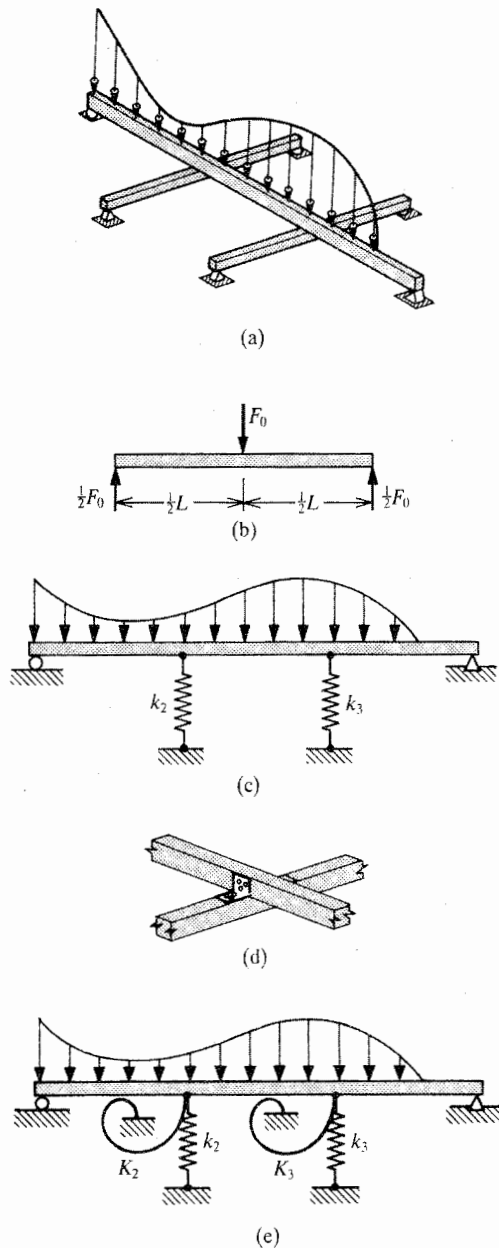


Figure 21.3. The usefulness of elastic springs as a part of structural analysis models. (a) One beam partially supported by two simply supported beams. (b) A FBD of one of the bottom, simply supported beams. (c) The top beam mathematical model when the two lower beams are replaced by equivalent rectilinear springs. (d) A detailed view of a so-called *rigid* connection, which, in this case, causes the bottom beam to resist not only the lateral deflection of the top beam by means of its midspan bending stiffness, but also to resist bending slopes in the top beam by means of its, the bottom beam's, midspan torsional stiffness. Thus the bottom beam acts as both a rectilinear and a torsional spring support for the top beam. (e) The mathematical model of the top beam modified to include the two equivalent torsional springs.

and they each support the top beam at their midspans, then a free body diagram (FBD) of either of the bottom beams would be like that shown in Fig. 21.3(b), where F_0 is the force imposed upon the bottom beam by the top beam. By Newton's third law, F_0 is also the force (elastic reaction) supplied to the top beam by that bottom beam. An analysis of that bottom beam would show that if w_m is the downward midspan lateral deflection of that bottom beam (subscript b), then the upward force acting upon the top beam is

$$F_0 = \frac{48E_b I_b}{L_b^3} w_m$$

Now, if the bottom beam were replaced by a coiled spring whose stiffness constant was $k = 48E_b I_b / L_b^3$, then the top beam would experience exactly the same support as that provided by the bottom beam. Hence the analysis of this three-beam structure could begin with the mathematical model shown in Fig. 21.3(c), where each of the bottom beams is replaced by a spring that interacts with the top beam exactly like the beam that it replaces. The analysis of the top beam would then be confined to two dimensions. One result of the analysis of the structural model shown in Fig. 21.3(c) would be the determination of the forces in the two springs, and that information would be all that would be needed to complete the analysis of the two bottom beams.

If the two bottom beams were connected in any of the usual ways to the top beam, such as being riveted or bolted or welded with the use of, for example, two small pieces of an angle beam⁴ as shown in Fig. 21.3(d), then not only would a force be transmitted from the bottom beam to the top beam as a result of the deflections of the bottom beam, but also a bending moment. That is, if the two bottom beams were constrained against rotations at their own ends, then the continuity of rotations between the top and bottom beams enforced by the connection would require that the bottom beams twist as the top beam develops a bending slope. The resisting moment provided by a bottom beam to each bending slope rotation of the top beam, θ , at the location of the bottom beam, is

$$M_{res} = \frac{4G_b J_b}{L_b} \theta$$

This linear relation between moment and rotation parallels the coiled spring relation between axial force and axial deflection. Indeed, this is the form of the relation between moment and rotation that describes a rotational spring, which is a spring that resists rotations just as the coiled spring resists axial deflections. A rotational spring is symbolized by a spiral (like the master spring of mechanical wristwatches). Thus, with both bottom beams connected to the top beam as described, the mathematical model of the top beam would be as shown in Fig. 21.3(e).

Many of the structures to be studied below include springs as well as beams because springs can be used to replace any elastic structure whose force versus deflection or moment versus rotation response is known for the points where the replaced elastic structure connects to other elastic elements. As such they are very useful in structural modeling. In order to analyze structures that include spring elements using the ULM, it is necessary to develop an expression for the internal virtual work done by virtual loads moving through actual spring

⁴ Since such a connection is very small compared to the lengths of the beams that it connects, it is relatively very stiff. For that reason it is modeled as a "rigid" connection.

deflections. The same approach used to obtain the beam torsion internal CVW expression is used here. That is,

$$-\delta W_{in}^* = +\delta W_{ex}^*$$

To determine the external complementary virtual work done by the self-equilibrating virtual forces of magnitude $\delta N = \bar{N}$ applied in tension at each end of a spring, note that the actual displacement of one end of the spring relative to the other is $+N/k$, where N is the actual tensile force acting at each end of the spring and k is the spring stiffness constant. Therefore the external virtual work, and the negative of the internal virtual work, is

$$\delta W_{ex}^* = \frac{N\bar{N}}{k}$$

For a torsional spring, the similar result in terms of applied and virtual moments is

$$\delta W_{ex}^* = \frac{M\bar{M}}{K}$$

These quantities, for each spring, are to be added to the like quantities for each beam in the structure. A nice thing about work and energy expressions is that there is no direction associated with them. That is, they simply add algebraically.

21.4 The Strategy of Releases and Reattachments

In order to understand how the ULM can be used to determine the magnitudes of redundants, a simple indeterminate structure is first analyzed by explicitly following the same steps that are implicit in the ULM. Consider the uniform, continuous, two-span beam shown in Fig. 21.4(a). This structure has one redundant reaction. Let the reaction at the center support be selected as the redundant reaction, and let all redundant reactions be symbolized as \mathcal{Y} (with subscripts if necessary later). A FBD of the continuous beam is as shown in Fig. 21.4(b) with \mathcal{Y} as an unknown force. For the moment, let \mathcal{Y} take on any value within the range of forces that produce small deflections. This would be possible if \mathcal{Y} were an externally applied force, like the distributed force f_0 , rather than a reaction to forces and moments of fixed magnitude. Therefore, to achieve that status for \mathcal{Y} of being an applied force, temporarily remove the center support from the continuous beam, leaving the beam supported only at its ends. (This is called making a release.) The beam will now either bow up or bow down at $x=L$ depending upon the magnitude of \mathcal{Y} as shown in Fig. 21.4(c). Without loss of generality, let it be assumed that the magnitude of \mathcal{Y} is such that the beam bows upward. With just two supports, the beam is now statically determinate. Hence calculating the deflection at the center of the beam due to both the distributed loading and the variable magnitude concentrated force \mathcal{Y} is now routine either by the use of the ULM or by any other method.⁵ The result, using the ULS of Fig. 21.4(d) is

$$w(x=L) = 5 \frac{f_0 L^4}{24EI_0} - 4 \frac{\mathcal{Y} L^3}{24EI_0}$$

which, of course, clearly depends upon the variable value of \mathcal{Y} . If the value of the variable applied force \mathcal{Y} is made to be that which forces the beam down into its original position in contact with the now reinstalled center roller support, that is, which causes $w(x=L)$ to be zero (reattachment), then this variable external force accomplishes exactly the same

⁵ Superposition of lateral loads is always valid whenever the lateral deflections due to the lateral loads are small.

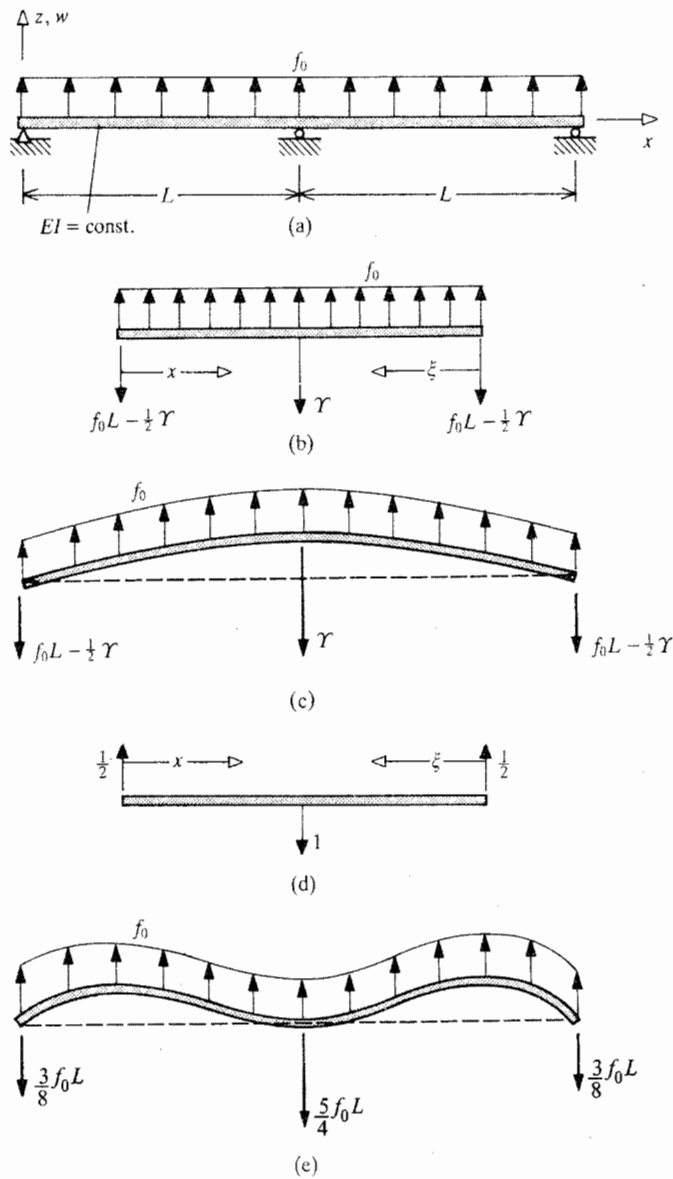


Figure 21.4. (a) A uniform, two-span beam with a uniform distributed load. (b) The ALS when the middle support reaction is chosen as the redundant reaction. (c) The exaggerated lateral deflection pattern when the beam is detached from the center support and the unknown “applied” force acting at the center of the beam has a lesser value than that of the center support reaction when the beam is attached to the center support. (d) The ULS used to calculate the beam centerspan deflection when the “applied” redundant force has an arbitrary value γ . (e) The beam loading, calculated support reactions, and exaggerated deflection pattern when the beam centerspan is required to have a zero lateral deflection. When this “reattachment” is completed, the formerly arbitrary force γ has the value of the center support reaction because it accomplishes the same task as the center support reaction.

task that the roller support reaction force at $x = L$ accomplishes in the original beam on three supports. Since the effect upon the beam is the same, this particular value of γ is, of course, the magnitude of the center reaction when the center roller is in its place. Thus the second step of this procedure is to set $w(x = L)$ equal to zero, and solve for γ ; see Fig. 21.4(e). The result is

$$\gamma = \frac{5}{4} f_0 L$$

With this knowledge, the magnitudes of the other two reactions, and those of moments everywhere along the length of the continuous beam, can be quickly determined. Then, using those moments with the ULM, lateral deflections and bending slopes can also be determined anywhere along the length of the continuous beam.

The above two-step process of (i) finding a deflection in terms of the applied loading and a variable redundant load, and then (ii) setting that deflection equal to its actual value (not necessarily zero), can be condensed into one step by use of the ULM. As in the above approach, the ULM starts with the identification of the redundants and the corresponding releases. The only difference is that the calculation of the appropriate deflections at the releases, and the subsequent reattachments, that is, the setting of those deflections equal to their prescribed values, is done simultaneously. Illustrating this latter part of the process for this problem, Fig. 21.4(d) is again the ULS for calculating the deflection at $x = L$. From Figs. 21.4(b, d), the ALS and ULS bending moments for this symmetric beam are,

$$0 \leq x \leq L \quad M(x) = \frac{1}{2} f_0 x^2 - (f_0 L - \frac{1}{2} \gamma) x \quad \bar{M}(x) = \frac{1}{2} x$$

Then

$$w(x = L) = 0 = 2 \int_0^L \frac{M\bar{M}}{EI} dx = \frac{1}{2EI} \int_0^L (f_0 x^3 - 2f_0 Lx^2 + \gamma x^2) dx$$

or

$$0 = \frac{1}{4} f_0 L^4 - \frac{2}{3} f_0 L^4 + \frac{1}{3} \gamma L^3$$

so, again,

$$\gamma = \frac{5}{4} f_0 L$$

While it should be clear that the ULM solution is exactly the same as the original superposition solution for the above problem, the question arises as to whether the ULM is always suitable for this release and reattachment strategy for solving indeterminate problems. The reason that the ULM always succeeds is that, as is demonstrated in Section 15.6, the PCVW upon which the ULM is based always enforces compatibility (continuity of the actual deflections) given a virtual force system (ULS) that is in equilibrium, and the reattachment step is always the reestablishment of the continuity of the actual deflections.

The unit load method for indeterminate beam, bar, and spring structures can be summarized in the following four steps where steps 2, 3, and 4 are essentially accomplished simultaneously.

Step 1 Identify the redundant forces and moments, internal and external.

Step 2 Make a deflection release corresponding to each redundant force and moment (i.e., allow appropriate arbitrary small axial, lateral, and rotation deflections at each redundant axial force, lateral force and moment) and thereby allow those redundants to vary. (The idea that the magnitudes of the redundants can vary permits the existence of the virtual generalized forces and thus the use of the ULM.)

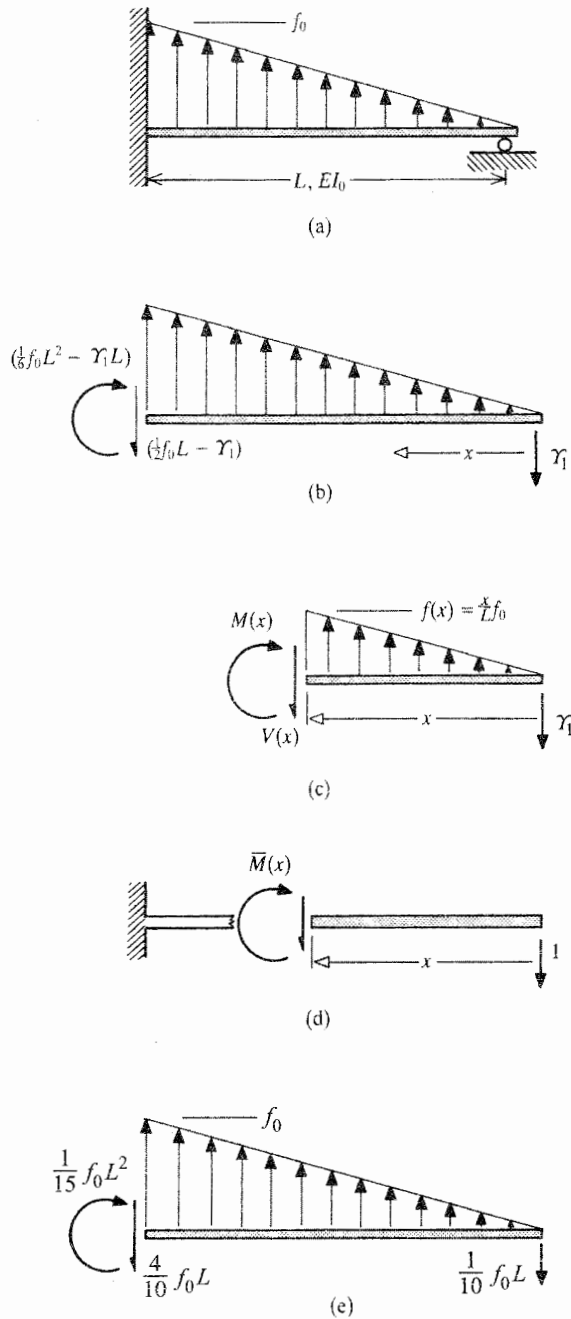


Figure 21.5. Example 21.1. (a) A uniform beam with a linearly varying distributed loading. (b) A FBD of the entire beam when the right-hand support force is chosen as redundant. It is not necessary to draw this sketch when all FBDs are chosen to be of the right-hand portion of the beam, regardless of which reaction is selected as the single redundant. (c) An ALS FBD where the intensity of the distributed loading at the point x has been determined as $(x/L)f_0$. (d) The corresponding ULS FBD. (e) The beam loading and calculated support reaction results.

- Step 3** Calculate the magnitudes (absolute or relative) of those deflections at the releases in terms of the external loads and the redundant forces and moments.
- Step 4** Require those deflections at the releases to take on their actual values (usually zero) and thus obtain the necessary number of equations required to determine the magnitudes of all redundant forces and moments.

21.5 Example Problems

This and the next section present a variety of example problems demonstrating the use of the ULM with indeterminate structures. The emphasis is upon calculating the values of the redundants. Once all the redundants have been calculated, there is no difference whatever between the calculation of stresses or deflections in determinate and indeterminate structures.

Example 21.1. The uniform, symmetric beam of Fig. 21.5(a) has one redundant reaction. Let the redundant, Υ_1 , be the roller support reaction. (A subscript is used here for the single redundant in order to distinguish this redundant from another when this problem is redone in the next illustration.) Calculate all reactions.

Solution. The solution procedure begins with a release at the roller support; that is, the roller support reaction is replaced by the redundant force of arbitrary magnitude, Υ_1 . The FBD of the entire beam is shown in Fig. 21.5(b). It should be clear that simpler moment expressions are obtained when the length coordinate starts at the right-hand end. The ALS bending moment at a typical point x is obtained from a FBD like that shown in Fig. 21.5(c). The intensity of the distributed load at point x can be determined from similar triangles; that is, $f(x) = (x/L)f_0$. Since this is a linear expression, it only needs to be checked at two points, such as $x = 0$ and $x = L$, in order to confirm that it is correct. From the ALS FBD, $0 \leq x \leq L$: $M(x) = f_0x^3/6L - \Upsilon_1x$. Now it is necessary to calculate the deflection at $x = 0$ and require that deflection be zero. The ULS of Fig. 21.5(d) shows the FBD suitable to this purpose:

$$0 \leq x \leq L \quad \overline{M}(x) = -x$$

Since beam bending is the only deformation present in this example,

$$EI_0w(0) = 0 = \int_0^L \left(\frac{f_0x^3}{6L} - \Upsilon_1x \right) (-x) dx = \frac{\Upsilon_1L^3}{3} - \frac{f_0L^4}{30}$$

The above equality is clearly one equation in the one unknown, Υ_1 . It can be solved immediately for the value of the redundant. That solution is $\Upsilon_1 = f_0L/10$. Hence a complete description of the reactions for this structure is as shown in Fig. 21.5(e). ■

Example 21.2. Redo the above problem, but this time choose the temporary release to be that of the constraint of zero slope at the left-hand end of the beam.

Solution. Call the moment at the wall Υ_2 in order to distinguish between it and the previous single redundant. Then the other reactions are as shown in Fig. 21.6(a). A FBD for the ALS at point x shows that for

$$0 \leq x \leq L \quad M(x) = \frac{f_0x^3}{6L} - \frac{f_0Lx}{6} + \frac{\Upsilon_2x}{L}$$

which, in this case, is in as simple a form for integration as can be obtained.

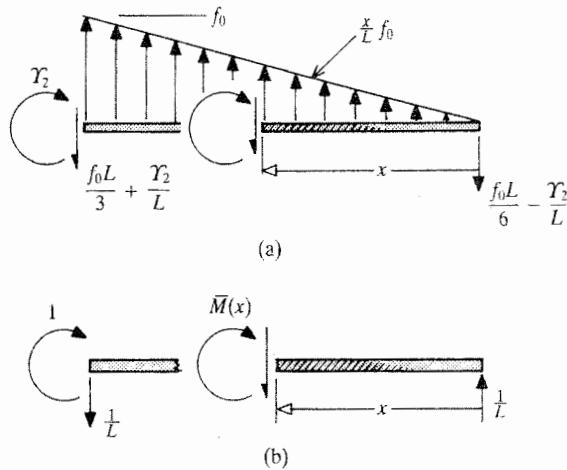


Figure 21.6. Example 21.2. The same beam and loading as the previous example, but a new ALS is needed because here a different support reaction is chosen as the redundant reaction. (b) A new ULS FBD is also required because the new ULS must calculate a different deflection (i.e., accomplish a different reattachment). Of course, the new ALS and ULS lead to the same values of the support reactions.

The ULS suitable for calculating the rotation at $x = L$ is shown in Fig. 21.6(b). Recall that there is no release for the deflections at either end of the beam. Therefore, neither of the virtual forces of magnitude $1/L$ does any virtual work. From this ULS, for

$$0 \leq x \leq L \quad \bar{M}(x) = +\frac{x}{L}$$

Substituting into the beam bending integral, and setting the rotation equal to zero produces

$$w'(x=L) = 0 = \frac{1}{EI_0} \int_0^L \left(\frac{f_0 x^3}{6L} - \frac{f_0 Lx}{6} + \frac{\gamma_2 x}{L} \right) \left(\frac{x}{L} \right) dx$$

or

$$0 = \frac{f_0 L^5}{30L^2} - \frac{f_0 L^3}{18} + \frac{\gamma_2 L}{3}$$

or

$$\gamma_2 = \frac{f_0 L^2}{15}$$

exactly as before for this moment, with of course the same results for the other two reactions. ■

Example 21.3. Determine the reactions at the supports of the beam–spring structure sketched in Fig. 21.7(a). Present your answer for the reactions in diagram form. Clearly label any coordinates that you choose to use.

Solution. It is always a good idea to include all elastic elements within the structural system. Thus, in this case, the structural system is the beam and the spring. Since there are two external reactions at the wall, and one at the bottom of the spring, but only two independent equations of equilibrium, there is one redundant reaction. Let that redundant be the force at the bottom of the spring. Then the release is also at the bottom of the spring. Therefore a ULS is necessary to calculate the deflection at the bottom of the spring so that

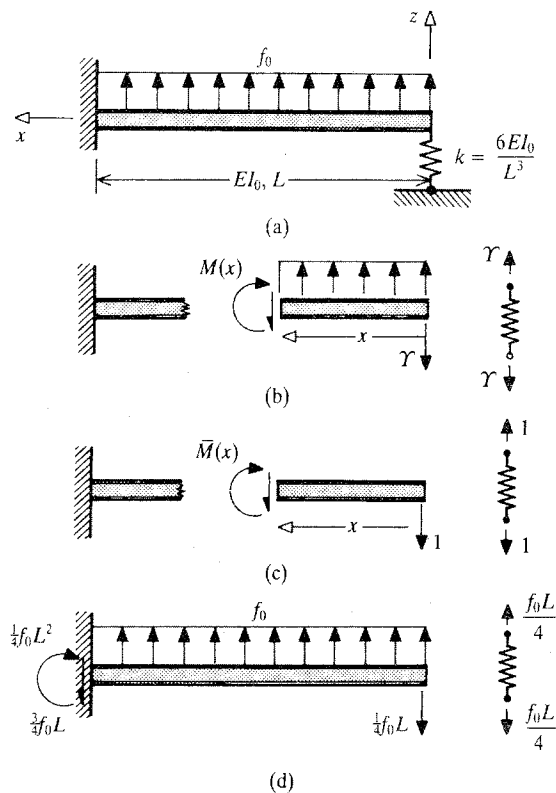


Figure 21.7. Example 21.3. (a) A spring and uniform beam structural system with one redundant reaction. (b) The ALS beam and spring FBDs. (c) The ULS beam and spring FBDs. (d) The calculated support reactions and spring force. A caution: it is not possible to solve this or any such problem by mentally detaching the spring from the beam and then *separately* analyzing the now “statically determinate” beam and thereby calculating the beam tip deflection, and thus “knowing” the deflection of the spring, calculating the force in the spring. In actuality, the beam tip deflection depends on the spring as well as the beam. After all, if the spring were rigid, then there would be no beam tip deflection.

it may be set to zero. From FBDs of the *two* structural elements for both the ALS and the ULS, as shown in Fig. 21.7(b, c), for all x

$$M(x) = \frac{1}{2} f_0 x^2 - \gamma x \quad N = +\gamma$$

$$\bar{M}(x) = -x \quad \bar{N} = +1$$

The sum of the internal CVW of the individual elements of the structure, the beam and the spring, is equal to the total internal CVW for the structure. The external CVW is equal to unity multiplied by the deflection at the bottom of the spring. This is so because the other external virtual loads, the virtual force and virtual moment at the wall have no actual deflections, and the equal and opposite forces between the spring and beam have the same deflection (deflection continuity). Hence the net CVW of all these external virtual loads is zero. Setting the external CVW to zero is setting the deflection at the bottom of the spring to zero. This leads to

$$0 = \frac{1}{EI_0} \int_0^L \left(\frac{1}{2} f_0 x^2 - \gamma x \right) (-x) dx + \frac{\gamma(1)L^3}{6EI_0}$$

or

$$0 = -\frac{1}{8}f_0L^4 + \frac{1}{3}\Upsilon L^3 + \frac{1}{6}\Upsilon L^3$$

or

$$\Upsilon = \frac{1}{4}f_0L$$

The two reactions at the wall can now be calculated by summing forces and moments for the entire beam. The final result is as shown in Fig. 21.7(d). ■

Example 21.4. Consider a fixed–fixed beam of length $2L$ loaded by a uniform, upward, distributed force per unit length of magnitude f_0 . Let the left half of the beam have stiffness $2EI_0$, while the right half has stiffness EI_0 . Calculate the reactions at the right-hand end.

Solution. There are two reactions at each fixed end, for a total of four reactions. There are only two independent equations of equilibrium. Hence there are two redundants. Since the problem statement calls for the magnitudes of the right-hand reactions, it is convenient to let Υ_1 be the counterclockwise moment at the right-hand fixed end, and let Υ_2 be the downward shear force at the right-hand fixed end. Then a FBD for the ALS shows that, for a lengthwise coordinate x originating at the right-hand end, for

$$0 \leq x \leq 2L \quad M(x) = +\Upsilon_1 - x\Upsilon_2 + \frac{1}{2}f_0x^2$$

Since there are two redundant reactions, two releases are required, and two corresponding deflections need to be calculated and set to zero using two ULSs. The ULS needed to measure the deflection at the right-hand end, $w(x = 0)$, is shown in Fig. 21.8(a). Note that this unit (virtual) load is reacted at the left-hand fixed end, and those reactions do no CVW. The reader is reminded to be sure that he or she accounts for all the CVW done by forces and moments external to the elastic system. Also note that since the deflection to be calculated will be set to zero, the direction of the unit load is wholly immaterial. The moment expression for this first ULS is

$$0 \leq x \leq 2L \quad \bar{M}(x) = +x$$

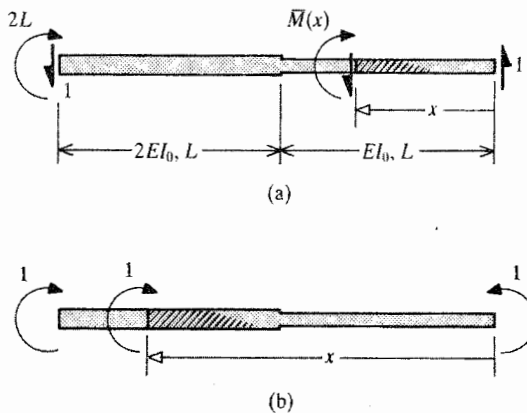


Figure 21.8. Example 21.4. A nonuniform beam with two redundant reactions. (a) A first ULS and superimposed FBD. (b) A second ULS and superimposed FBD.

The second ULS that is needed to calculate the bending slope at the right-hand end is shown in Fig. 21.8(b). The moment expression for this second ULS is

$$0 \leq x \leq 2L \quad \bar{M}(x) = +1$$

The equation that sets $w(x = 0)$ to zero, and does that much of the reattachment process, is

$$0 = \frac{1}{EI_0} \int_0^L \left(\gamma_1 - x\gamma_2 + \frac{1}{2}f_0x^2 \right) (x) dx + \frac{1}{2EI_0} \int_L^{2L} \left(\gamma_1 - x\gamma_2 + \frac{1}{2}f_0x^2 \right) (x) dx$$

The equation that sets $w'(x = 0)$ to zero, and completes the process of reattachment is

$$0 = \frac{1}{EI_0} \int_0^L \left(\gamma_1 - x\gamma_2 + \frac{1}{2}f_0x^2 \right) (1) dx + \frac{1}{2EI_0} \int_L^{2L} \left(\gamma_1 - x\gamma_2 + \frac{1}{2}f_0x^2 \right) (1) dx$$

These two simultaneous equations in the two unknowns reduce to

$$\frac{5}{4}\gamma_1 - \frac{3}{2}\gamma_2L = -\frac{17}{16}f_0L^2$$

$$\frac{3}{2}\gamma_1 - \frac{5}{4}\gamma_2L = -\frac{3}{4}f_0L^2$$

or multiples thereof. The reader is invited to confirm these results in a simpler fashion by using a second lengthwise coordinate $0 \leq \xi \leq L$ starting at the right-hand beam end. It is often worthwhile expending the effort to solve a set of two simultaneous equations in order to determine whether the solutions for the redundants are positive, that is, whether the analyst's expectation of the direction of the redundants is confirmed or not. In this case the solution is

$$\gamma_1 = +\frac{13}{44}f_0L^2 \quad \text{and} \quad \gamma_2 = +\frac{21}{22}f_0L$$

Since the moment and shear force at the left-hand end are $(17/44)f_0L^2$ and $(23/22)f_0L$ respectively, this example demonstrates again that the stiffer side of the continuous beam shoulders a bit more of the applied load total of $2f_0L$. ■

Example 21.5. Consider the fixed–fixed beam of length $3L$ shown in Fig. 21.9(a), which is subjected to a distributed torque per unit length of magnitude m_0 acting only over the left-hand length L . (a) Determine the torques at the clamped ends; and (b) determine the angle of twist at the change in the beam torsional stiffness, that is, at $x = L$.

Solution. (a) Since the loading is entirely torsional, so are the reactions. Since there is only one (nontrivial) moment equilibrium equation, one of the two reacting torques is a redundant. Let it be the torque at the right-hand end. Then the ALS and the ULS are as shown in Figs. 21.9(b, c), where for

$$0 \leq x \leq L \quad M_t(x) = m_0x - (m_0L - \gamma) \quad \bar{M}_t(x) = +1$$

$$0 \leq \xi \leq 2L \quad M_t(\xi) = +\gamma \quad \bar{M}_t(\xi) = +1$$

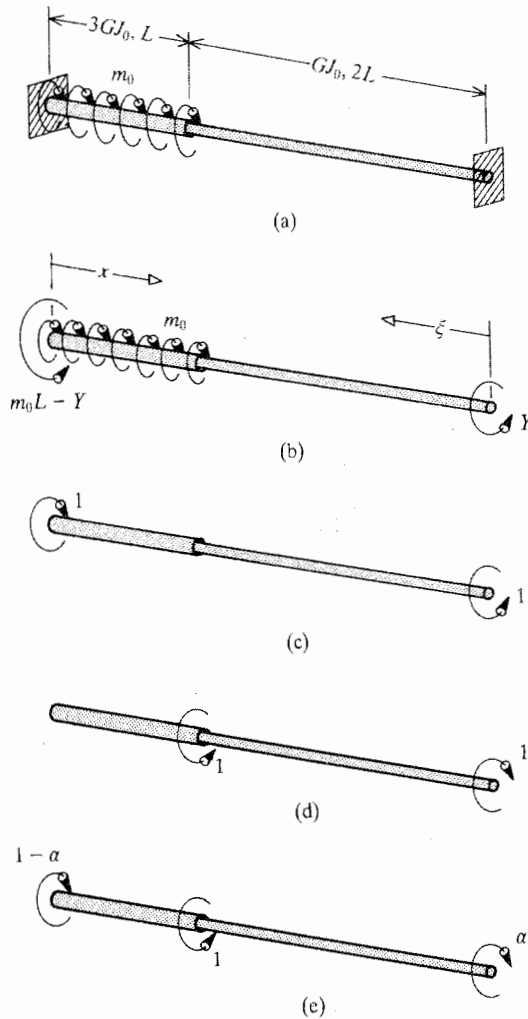


Figure 21.9. Example 21.5. (a) A nonuniform beam subjected to a partial span, twisting moment per unit length. (b) The one redundant ALS. (c) The ULS for determining the redundant reaction. (d) A ULS for determining the twist at $x = L$ ($\xi = 2L$). (e) Another possible ULS for determining the twist at $x = L$.

Requiring the twisting deflection at $\xi = 0$ to be zero produces

$$0 = \frac{1}{3} \int_0^L [m_0 x - (m_0 L - \gamma)](1) dx + \int_0^{2L} \gamma(1) d\xi$$

Integration and simplification result in the right-hand end torque solution of $\gamma = (1/14)m_0 L$. Then the left-hand torque solution is $(13/14)m_0 L$. Again, the stiffer portion of the structure shoulders most of the load.

(b) In order to find the twist at $x = L$, a unit load system that does CVW equal to that twist is needed. The simplest possibility is shown in Fig. 21.9(d). However, for this indeterminate structure, there are an infinity of other possibilities. All these other possibilities can be consolidated into the one FBD shown in Fig. 21.9(e), where α is an arbitrary parameter. Note that the CVW done by this ULS is also $1\phi(x = L)$. Note further that the unit load has

been drawn in a direction that will produce a negative solution for $\phi(L)$. The actual moment expressions are, of course, unchanged. The new virtual moment expressions are

$$0 \leq x \leq L \quad \bar{M}_i(x) = 1 - \alpha \quad \text{and} \quad 0 \leq \xi \leq 2L \quad \bar{M}_i(\xi) = -\alpha$$

Then

$$GJ_0\phi(x=L) = \frac{1}{3} \int_0^L [m_0x - (m_0L - \gamma)](1 - \alpha) dx - \int_0^{2L} [\gamma](\alpha) d\xi$$

$$GJ_0\phi(x=L) = \frac{1}{3} \left[\frac{1}{2} m_0L^2 - (m_0L - \gamma)L \right] (1 - \alpha) - 2\alpha\gamma L$$

When the above solution for γ is substituted for that quantity, then the factor multiplying α disappears, and the resulting solution is entirely independent of α . That is

$$GJ_0\phi(L) = -\frac{1}{7}m_0L^2(1 - \alpha) - \frac{1}{7}\alpha m_0L^2$$

or

$$\phi(x=L) = -\frac{m_0L^2}{7GJ_0}$$

This, of course, demonstrates that any ULS that does the desired CVW is suitable for calculating deflections. The same is true for the calculation of redundants. ■

Example 21.6. Set up, but do not bother solving, the simultaneous equations that determine the bar forces for the pin-jointed truss shown in Fig. 21.10(a). Choose a minimum number of bar redundant forces in the order of the bar numbers. Each bar has the same extensional stiffness, EA_0 .

Solution. Since two releases are necessary in order to cause the truss to be statically determinate, the degree of redundancy is 2. Thus let $N_1 = \gamma_1$, and $N_2 = \gamma_2$. The ALS for the entire structure is shown in Fig. 21.10(b). The equations of equilibrium for interior joint A are

$$\frac{\sqrt{2}}{2}\gamma_2 + N_3 + \frac{\sqrt{2}}{2}N_4 = F_1$$

$$\gamma_1 + \frac{\sqrt{2}}{2}\gamma_2 - \frac{\sqrt{2}}{2}N_4 = F_2$$

A ULS that can be used to reattach the first released bar to its pin support is shown in Fig. 21.10(c), while a ULS that can be used to reattach the second bar to its pin support is shown in Fig. 21.10(d). Using the ULM equation

$$\sum [N\bar{N}L/EA]_i = 0$$

for zero deflections at the releases, then for joint B,

$$0 = (\gamma_1)(1)L + (\gamma_2)(0)\sqrt{2}L + (N_3)(-1)L + (N_4)(\sqrt{2})\sqrt{2}L$$

or

$$\gamma_1 = N_3 - 2N_4$$

Enforcing the requirement of zero deflection at joint C yields

$$0 = (\gamma_1)(0)L + (\gamma_2)(1)\sqrt{2}L + (N_3)(-\sqrt{2})L + (N_4)(1)\sqrt{2}L$$

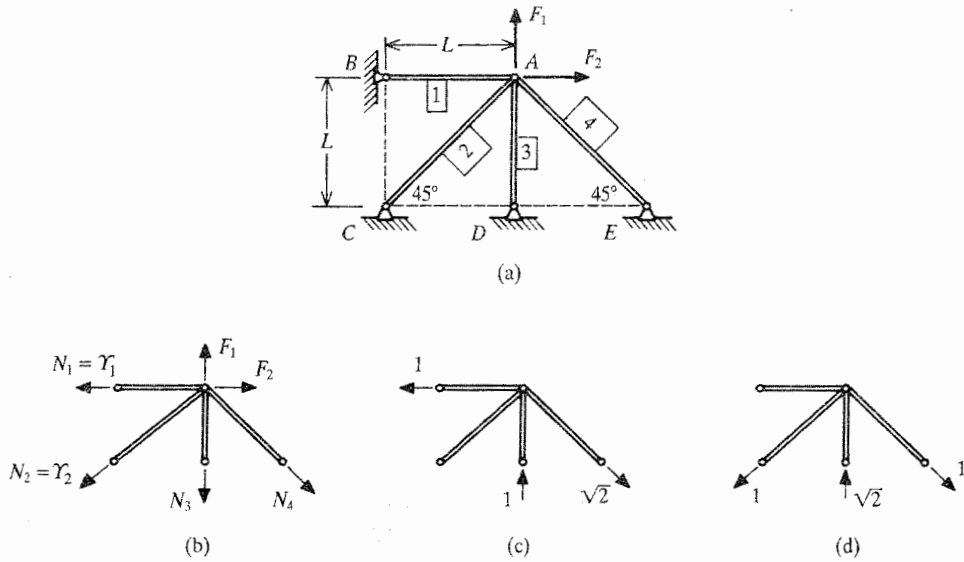


Figure 21.10. Example 21.6. (a) A pin-jointed truss where all four bars have the same modulus of elasticity and cross-sectional area. (b) The ALS after choosing two redundant bar forces. (c) A first ULS. (d) A second ULS.

or

$$\gamma_2 = N_3 - N_4$$

The two equilibrium equations for joint A obtained above plus these two compatibility equations for γ_1 and γ_2 constitute four easily solved equations in the four unknowns γ_1 , γ_2 , N_3 , and N_4 in terms of the given loading F_1 and F_2 . ■

Example 21.7. Set up, but do not bother to simplify or solve, the ULM equations necessary to determine the reactions at points A, B, C, and D for the uniform continuous beam and three-spring structure loaded as shown in Fig. 21.11(a). Each spring has the same stiffness $k = 7EI_0/L^3$. Choose the minimum number of redundants starting at the far right-hand spring with R_4 , and work up the alphabet.

Solution. There are four vertical force reactions and only two independent equations of equilibrium. Hence there are two redundant reactions. The ALS is as shown in Fig. 21.11(b). Suitable FBDs show that the moments in the beam and the forces in the springs are

$$\begin{aligned}
 0 \leq x \leq L \quad M(x) &= \left(\frac{3}{2} f_0 L - 2\gamma_1 - \gamma_2 \right) x \\
 L \leq x \leq 2L \quad M(x) &= (-f_0 L + \gamma_1 + \gamma_2) x + \left(\frac{5}{2} f_0 L^2 - 3\gamma_1 L - 2\gamma_2 L \right) \\
 0 \leq \xi \leq L \quad M(\xi) &= \frac{1}{2} f_0 \xi^2 - \gamma_1 \xi \\
 L \leq \xi \leq 2L \quad M(\xi) &= (f_0 L - \gamma_1 - \gamma_2) \xi - \left(\frac{1}{2} f_0 L^2 - \gamma_2 L \right) \\
 N_b &= \frac{5}{2} f_0 L - 3\gamma_1 - 2\gamma_2 \quad N_c = \gamma_2 \quad N_d = \gamma_1
 \end{aligned}$$

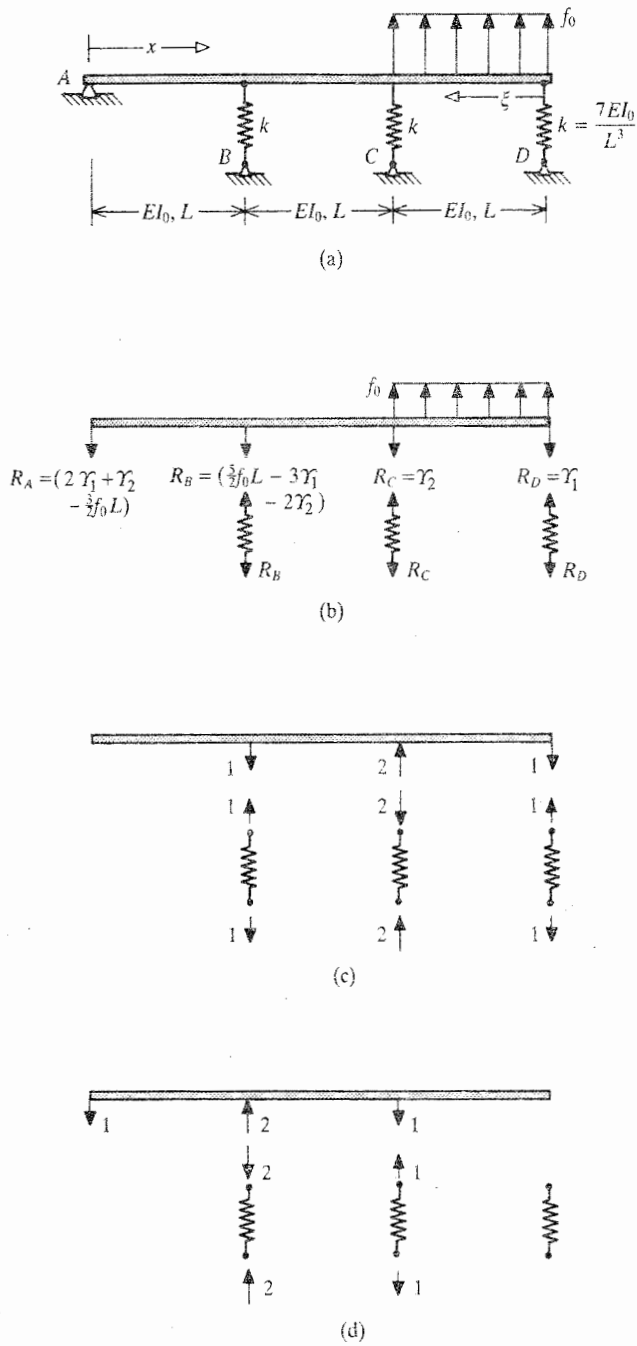


Figure 21.11. Example 21.7. (a) A continuous beam over one rigid and three elastic supports. (b) The ALS beam and spring FBDs after selection of the two redundant support reactions. (c) A first ULS suitable for reattachment at Point D. (d) A second ULS suitable for reattachment at Point C.

The second expression for the moment in the center beam span is slightly more concise, so it is used in preference to the first of these two overlapping moment expressions.

Since there are two redundants, there is a need for two independent ULSs. There are many possible ULSs. The better choices are those that result in the least computational effort. In general, a good choice of a ULS is one that causes zero virtual moments over as much of the beam structure as possible. A good choice for reattaching the far right-hand spring to its base is shown in Fig. 21.11(c). Again, the equal and opposite forces at the tops of the three springs and at the bottom of the beam do no net CVW because their actual deflections are the same. The force at the bottom of the spring connected to point *B* does no CVW because there is no deflection there. The forces at the bottom of the other two springs also do no CVW because at this point in the analysis the releases that were made there are now being simultaneously eliminated so as to again have zero deflections at points *C* and *D*. Therefore, the total CVW is zero, and nonzero moments and axial forces for this first ULS are

$$\begin{aligned} 0 \leq \xi \leq L & \quad \overline{M}(\xi) = -\xi & \quad \overline{N}_b = \overline{N}_d = +1 \\ L \leq \xi \leq 2L & \quad \overline{M}(\xi) = +\xi - 2L & \quad \overline{N}_c = -2 \end{aligned}$$

A convenient choice for a second ULS that assures reattachment at point *C* is shown in Fig. 21.11(d). Be reminded that every element of every ULS has to be in force and moment equilibrium. The nonzero moments and axial forces for this ULS are

$$\begin{aligned} 0 \leq x \leq L & \quad \overline{M}(x) = -x & \quad \overline{N}_b = -2 \\ L \leq \xi \leq 2L & \quad \overline{M}\{\xi\} = -\xi + L & \quad \overline{N}_c = +1 \end{aligned}$$

The simultaneous equations to be solved for γ_1 and γ_2 that come from the two ULSs are, after division by EI_0 , respectively,

$$\begin{aligned} 0 = & \left(\frac{5}{2}f_0L - 3\gamma_1 - 2\gamma_2 \right) (1)\frac{L^3}{7} + (\gamma_2)(-2)\frac{L^3}{7} + (\gamma_1)(1)\frac{L^3}{7} \\ & + \int_{\xi=L}^{\xi=2L} \left[(f_0L - \gamma_1 - \gamma_2)\xi - \left(\frac{1}{2}f_0L^2 - \gamma_2L \right) \right] (\xi - 2L) d\xi \\ & + \int_{\xi=0}^{\xi=L} \left(\frac{1}{2}f_0\xi^2 - \gamma_1\xi \right) (-\xi) d\xi \end{aligned}$$

and

$$\begin{aligned} 0 = & \frac{1}{7} \left(\frac{5}{2}f_0L - 3\gamma_1 - 2\gamma_2 \right) (-2)L^3 + \frac{1}{7}(\gamma_2)(1)L^3 \\ & + \int_{x=0}^{x=L} \left[\left(\frac{3}{2}f_0L - 2\gamma_1 - \gamma_2 \right) x \right] (-x) dx \\ & + \int_{\xi=L}^{\xi=2L} \left[(f_0L - \gamma_1 - \gamma_2)\xi - \left(\frac{1}{2}f_0L^2 - \gamma_2L \right) \right] (-\xi + L) d\xi \end{aligned}$$

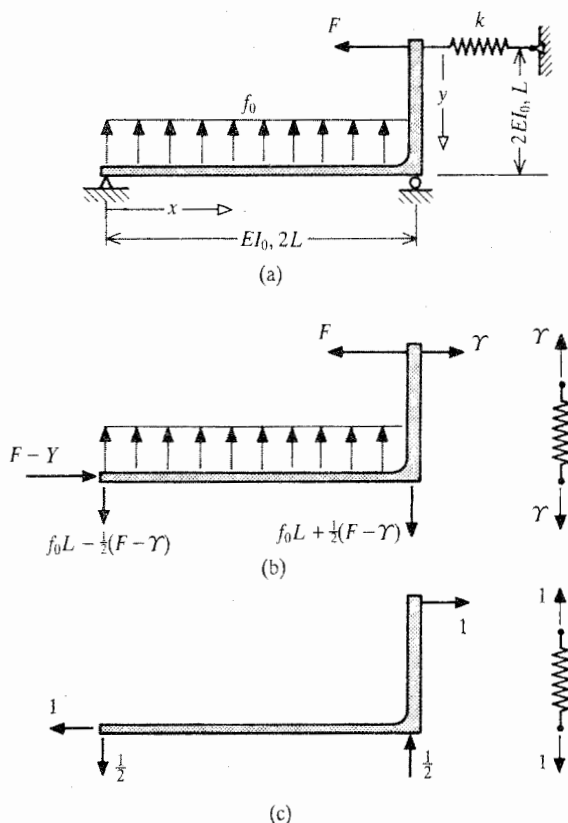


Figure 21.12. Example 21.8. (a) A two beam frame and spring structure. (b) The ALS FBDs. (c) The frame and spring ULS FBDs for reattaching the right-hand end of the spring. Note that the original detachment (“cut”) to create the redundant Y as an externally applied, variable force also can be imagined to have occurred at the point connection between the spring and the vertical beam. From this viewpoint, requiring the external CVW to be zero requires the two labeled equal and opposite internal values of Y , one at the top of the vertical beam, and the other at the left end of the spring, to move through the same real, internal deflection. These two forces move through the same real deflection when the left-hand end of the spring is reattached to the top of the vertical beam.

where the spring terms are stated first as an aid in avoiding forgetting them. At this point, evaluation of the integrals and simplifying and organizing the two simultaneous equations should be unnecessary routine effort, and as such, it is left undone. ■

Example 21.8. Determine the reactions for the two-beam, one-spring structure and loading shown in Fig. 21.12(a). If the structure is indeterminate, choose redundant reactions starting at the top, right-hand side of the structure, and then proceed down and to the left.

Solution. There are two reactions at the knife-edge support, one at the roller support, and one at the outer end of the spring, for a total of four reactions. Since there are two independent equations of force equilibrium and one equation of moment equilibrium, there is one redundant reaction. Following the directions given, choose the redundant reaction to be the force at the outer end of the spring. At this point, it goes without saying that

the corresponding release is also at the outer end of the spring. Then a FBD of the overall structure is as shown in Fig. 21.12(b), and the actual moments and axial forces are

$$\begin{aligned} 0 \leq x \leq 2L \quad M(x) &= \frac{1}{2}f_0x^2 - f_0Lx + \frac{x}{2}(F - \Upsilon) \\ 0 \leq y \leq L \quad M(y) &= -y(\Upsilon - F) \quad \text{and} \quad N = \Upsilon \end{aligned}$$

Again the effects of the axial forces and shearing forces in the beams are ignored as being negligible in comparison with the bending effects in the beams.

The ULS that measures the CVW at the release is shown in Fig. 21.12(c). The unit load moments and spring axial force are

$$\begin{aligned} 0 \leq x \leq 2L \quad \bar{M}(x) &= -\frac{x}{2} \\ 0 \leq y \leq L \quad \bar{M}(y) &= -y \quad \text{and} \quad \bar{N} = +1 \end{aligned}$$

Again, requiring a zero deflection at the release requires zero CVW. Hence,

$$\begin{aligned} 0 &= (\Upsilon)(1) \left(\frac{EI_0}{k} \right) + \frac{1}{2} \int_0^L [-y(\Upsilon - F)](-y) dy \\ &\quad + \int_0^{2L} \left(\frac{1}{2}f_0x^2 - f_0Lx + \frac{x}{2}(F - \Upsilon) \right) \left(-\frac{x}{2} \right) dx \end{aligned}$$

After integration and simplification, the solution for the redundant reaction is

$$\Upsilon = \frac{5F - 2f_0L}{5 + (6EI_0/kL^3)}$$

Be sure to realize that, even with f_0 being zero, this answer makes clear that the force in the spring is only a fraction of the applied force F . In other words, the applied force F is not only reacted by the spring, but it is also resisted by the two-beam structure. That is, together the spring and the beams share the load. A useful way of viewing this situation is to think of the applied force being split between the two load paths, and thus diffused through the structure. Note therefore, that this problem cannot be solved by applying the total external force F to the spring alone. ■

Example 21.9. Use the ULM to set up the simultaneous equations necessary to determine the reactions at the base of the “portal” frame loaded as shown in Fig. 21.13(a).

Solution. Both the structure and the loading are symmetric about the indicated centerline. This symmetry plus the equations of equilibrium permit the identification of the base reactions as shown in the ALS sketch of Fig. 21.13(b). Therefore, there are two redundant reactions, and two ULSs are needed. The first ULS reattaches the release associated with Υ_1 , and starts with a unit load in the same direction, and at the same location, as Υ_1 . That means the first ULS moments are the same as the ALS moments where Υ_1 is replaced by 1.0, and Υ_2 is replaced by zero. Similarly, the second ULS paves the way for setting the external CVW, which is 1 multiplied by the bending slope at the base of the columns, equal to zero. This ULS is the same as the ALS with Υ_2 replaced by 1.0, and Υ_1 replaced by zero. In summary,

$$\begin{aligned} 0 \leq y \leq L \quad M(y) &= \Upsilon_2 - y\Upsilon_1 & \bar{M}_1(y) &= -y & \bar{M}_2(y) &= +1 \\ 0 \leq x \leq L \quad M(x) &= \frac{1}{2}F_0x + \Upsilon_2 - \Upsilon_1L & \bar{M}_1(x) &= -L & \bar{M}_2(x) &= +1 \end{aligned}$$

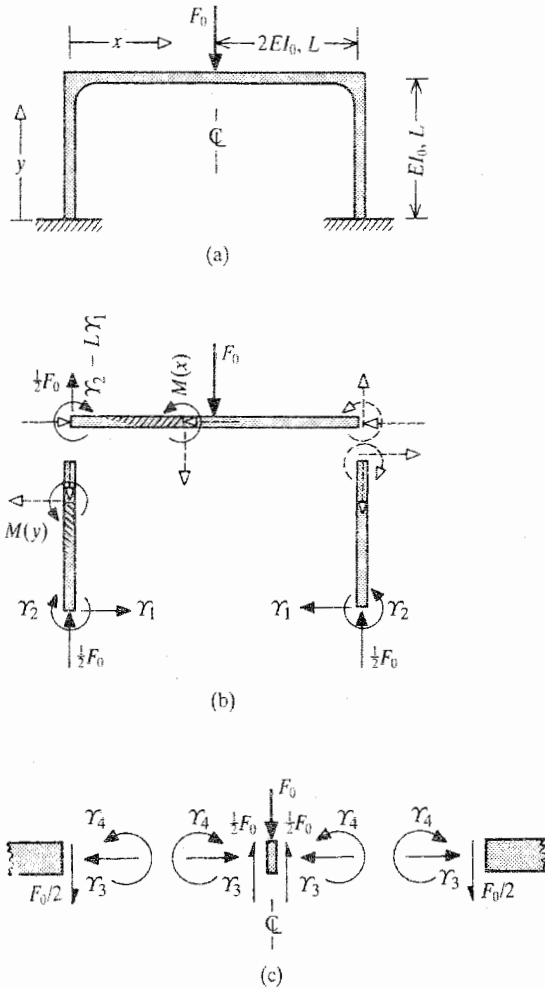


Figure 21.13. Example 21.9. (a) A symmetrically loaded, symmetric portal frame with clamped footings. (b) The selected ALS FBDs for calculating the required actual internal bending moments throughout the frame. (c) A FBD showing an alternate choice for the two redundants. In this alternate case, the two redundants are an internal force and an internal moment. Neither of these two choices is superior to the other, although the student may prefer external redundants because they are older friends. However, more complicated structures may require internal redundants.

After canceling EI_0 and the symmetry factor 2.0, the integrals for the left half of the structure are

$$0 = \int_0^L (\gamma_2 - y\gamma_1)(-y) dy + \frac{1}{2} \int_0^L \left(\frac{1}{2} F_0 x + \gamma_2 - \gamma_1 L \right) (-L) dx$$

$$0 = \int_0^L (\gamma_2 - y\gamma_1)(+1) dy + \frac{1}{2} \int_0^L \left(\frac{1}{2} F_0 x + \gamma_2 - \gamma_1 L \right) (+1) dx$$

These equations are easily simplified and solved.

It is instructive to note that releases at the base of one or both columns are not the only symmetric releases that can be used to solve this problem. For example, releases can be made at the location of the applied load as shown in Fig. 21.13(c). Again the symmetry quickly reduces the problem to that of two redundant stress resultants. Again, each of the two ULSs can be chosen to mimic the ALS by first replacing γ_3 , and then γ_4 , by a unit load, while the other redundant is replaced by zero. In this case setting the CVW of each ULS to zero means requiring that the axial deflections and bending slopes at each side of the cut are the same, thereby reattaching the cut ends. ■

21.6 **Further Example Problems**

The first two example problems (Examples 21.10 and 21.11) are simple. They are included in this section because their very simplicity is sometimes confusing to those working with the ULM for the first time. The third problem is a large-radius curved-beam problem. The fourth and fifth example problems are routine truss problems, which are included in this section only because they are more elaborate than the previously discussed problems. The sixth and last problem is an extension of the fifth problem. The sixth problem (Example 21.15) introduces a temperature change into the truss problem.

Example 21.10. Use the ULM to determine the forces in each of the two springs shown in Fig. 21.14(a). The two springs are constrained to remain horizontal.

Solution. If, for example, the force at either end of the two spring system were known, then static equilibrium equations would be able to determine the force in both springs. Therefore this two-spring system has one redundant force. Let that redundant force γ be the reaction

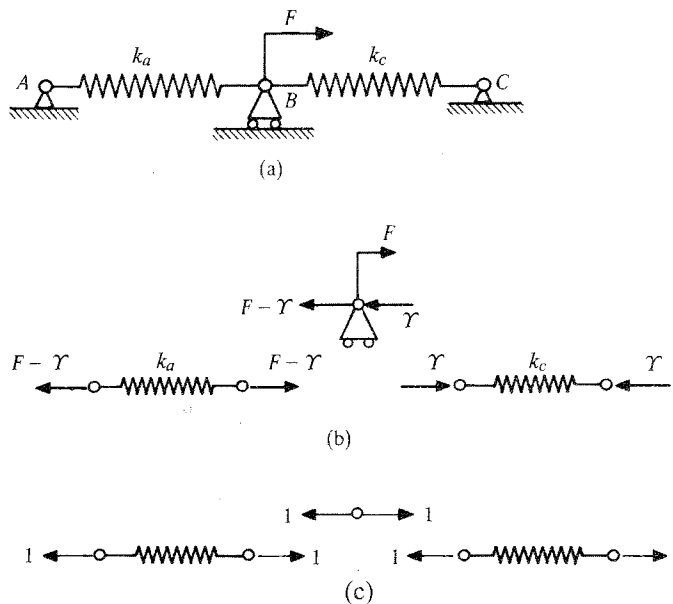


Figure 21.14. Example 21.10. (a) A two-spring structure. (b) The ALS FBDs. (c) The ULS FBDs.

at pin C , and of course, the release is at point C . The FBDs of the ALS are shown in Fig. 21.14(b). The ULS needed to calculate the deflection of the severed right-hand end of spring BC is shown in Fig. 21.14(c). Making the total CVW of the two springs zero makes that deflection zero. Hence

$$0 = \frac{(F - \gamma)(-1)}{k_a} + \frac{(-\gamma)(-1)}{k_c} \quad \text{or} \quad \gamma = \frac{k_c F}{k_a + k_c}$$

Thus the force in spring AB is $k_a F / (k_a + k_c)$, while the force in spring BC is $k_c F / (k_a + k_c)$. Thus it is clear that the applied force divides in proportion to the stiffnesses of the two linearly elastic systems (represented by springs) that jointly bear the applied load. The stiffer the element, the greater the load it bears when its deflection is the same as that of the other elastic elements. ■

Example 21.11. Calculate the shearing force and moment reactions for a fixed–fixed beam that is forced to undergo a lateral support deflection of magnitude w_0 as shown in Fig. 21.15(a). Note that neither end is rotated.

Solution. The ALS is Fig. 21.15(a). As ever, the presence of the two redundant reactions γ_1 and γ_2 indicates releases, or discontinuities in their corresponding deflections. The next step is to develop two ULSs that, when combined with the actual deflections, do CVW that involves an actual deflection equal to (i) the lateral deflection w_0 , and (ii) the zero rotation at the right-hand beam end. Such ULSs are shown in Fig. 21.15(b) and (c). The ALS and ULS moments are, for all values of x ,

$$M(x) = x\gamma_2 - \gamma_1 \quad \bar{M}_1(x) = x \quad \bar{M}_2(x) = +1$$

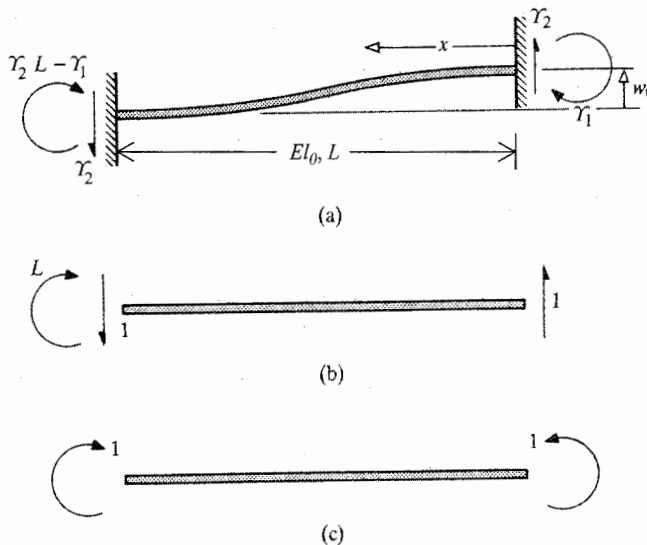


Figure 21.15. Example 21.11. (a) A clamped–clamped, uniform beam loaded only by an enforced deflection w_0 at the right-hand end. (b) The first ULS, which enforces the beam end lateral deflection, w_0 . (c) The second ULS, which enforces the zero rotation

Substitution of these moment pairs into the bending integral yields the following simultaneous equations after integration:

$$6EI_0w_0 = 2\Upsilon_2L^3 - 3\Upsilon_1L^2 \quad \text{and} \quad 0 = \Upsilon_2L^2 - 2\Upsilon_1L$$

The solution to these two equations is quickly determined to be

$$\Upsilon_1 = \frac{6EI_0}{L^2}w_0 \quad \text{and} \quad \Upsilon_2 = \frac{12EI_0}{L^3}w_0$$

from which the other two reactions are quickly calculated. The reader possibly recognizes that Υ_2 , Υ_1 , and the shearing force and bending moment at the left end of the beam constitute the third column of the beam bending element stiffness matrix, when the sign of Υ , is adjusted to the FEM sign convention. This is an alternate approach to calculating that stiffness matrix. ■

Example 21.12. Determine the bending moment in the circular ring of Fig. 21.16(a) at the location of the force F if $R > 10h$.

Solution. Note that there are two axes of symmetry for this structure and loading. The most efficient solution makes use of both of those axes of symmetry. Tentatively make bending slope, lateral deflection, and axial deflection releases (cuts) at $\theta = 0$ and 180° as shown in Fig. 21.16(b). Then the shear forces at the cut are zero as a result of the combination of (i) the

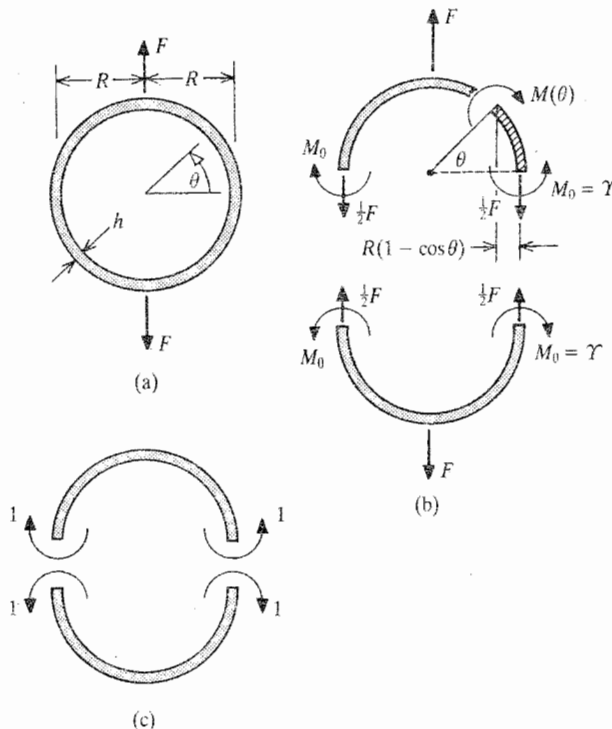


Figure 21.16. Example 21.12. (a) A circular beam frame in equilibrium where the beam radius exceeds 10 times the beam depth in the plane of bending. (b) The ALS FBDs that show that there is but one redundant stress resultant, the internal bending moment M_0 . (c) The ULS that restores the continuity of the bending slope.

axis of symmetry that is $\theta = 0$, requiring that the shear forces on the opposite faces of the cut be equal and act in the same direction, and (ii) the general requirement from Newton's third law that the shear forces on opposite sides of the cut be equal and oppositely directed. Summing vertical forces on either half-ring, while recognizing the axis of symmetry that is $\theta = 90^\circ$ means that the two axial forces must be equal, shows that the axial force at each cut has the magnitude $F/2$. Since the bending moment is not obtainable by statics, it is the only redundant. Thus $\gamma = M_0$, the moment which is located where $\theta = 0$.

It is apparent now that the only release that needs to be made is that of the bending slope at $\theta = 0$. The ULS that measures the *relative* bending slope rotations at $\theta = 0$ is shown in Fig. 21.16(c). The theta equals zero axis of symmetry requires that this bending slope be zero. From the ALS and ULS,

$$M(\theta) = M_0 - \frac{1}{2}FR(1 - \cos \theta) \quad \text{and} \quad \bar{M}(\theta) = +1$$

and so

$$0 = 4 \int_0^{\pi/2} \left(M_0 - \frac{1}{2} \right) FR(1 - \cos \theta)(+1)R \, d\theta$$

The solution to this equation is $M_0 = FR[(1/2) - (1/\pi)]$. Then the moment at $\theta = 90^\circ$ is $M(\theta = \pi/2) = -FR/\pi$, which is a moment that causes tension on the outer surface of the ring, as should be evident from the original loading. ■

Example 21.13. Consider the pin-jointed truss shown in Fig. 21.17. Use the unit load method to calculate the force in bar AC. Note that the determinate external reactions are provided.

Solution. Since the removal of one bar renders the structure statically determinate, here is only one internal redundant force (or redundant bar). Let the redundant force be the force

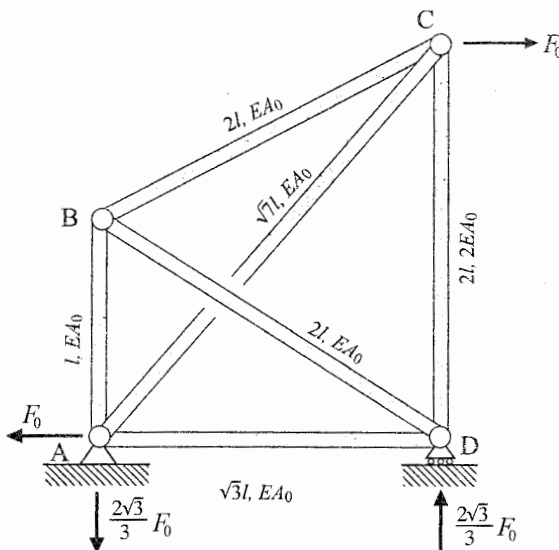


Figure 21.17. Example 21.13. Pin-jointed truss.

in bar AC, and, as usual, temporarily assume that it is a tensile force. Then, after writing a series of force equilibrium equations at the joints, the following table can be constructed:

bar	ℓ coeff	EA coeff	ALS force (N)	ULS force (\bar{N})
AB	1	1	$(2\sqrt{3}/3)F_0 - (2\sqrt{7})\Upsilon$	$-(2\sqrt{7})$
AC	$\sqrt{7}$	1	Υ	+1
AD	$\sqrt{3}$	1	$F_0 - (\sqrt{3}/\sqrt{7})\Upsilon$	$-(\sqrt{3}/\sqrt{7})$
BC	2	1	$(2\sqrt{3}/3)F_0 - (2\sqrt{7})\Upsilon$	$-(2\sqrt{7})$
BD	2	1	$-(2\sqrt{3}/3)F_0 + (2\sqrt{7})\Upsilon$	$+(2\sqrt{7})$
CD	2	2	$(\sqrt{3}/3)F_0 - (1/\sqrt{7})\Upsilon$	$+(1/\sqrt{7})$

Now it is just a matter of writing $\sum(N\bar{N}\ell/(EA)) = 0$, which is one equation in the one unknown Υ . After some simplification, the result is $\Upsilon = 0.827 F_0$. ■

Example 21.14. Write the simultaneous equations necessary to determine the redundants of the pin-jointed truss loaded as shown in Fig. 21.18. Each bar has the same stiffness coefficient, EA_0 .

Solution. The structure and its actual loading are symmetric. It is highly desirable from the viewpoint of necessary effort to have symmetric ULSs as well. Therefore make the external release at the middle support, and, for example, make the internal releases in bars CD and DG. Then, because of the symmetry of the releases, there is only one internal redundant because the forces in bars CD and DG must be the same, and with these bar forces and the external reactions as known quantities, all other bar forces can be determined by statics alone. Call that redundant bar force in bars CD and DG by the name Υ_1 . (If the symmetry of structure and loading were not recognized and the two redundant bar forces were named Υ_1 and Υ_2 , the final solution would show that $\Upsilon_1 = \Upsilon_2$.) Let the one external redundant, called Υ_3 , be the vertical reaction at the center support. The ALS forces are tabulated below. The two ULSs that reestablish deflection continuity, can as always, be modeled upon the ALS. In this case that is the simplest choice. Thus ULS1 is the ALS with

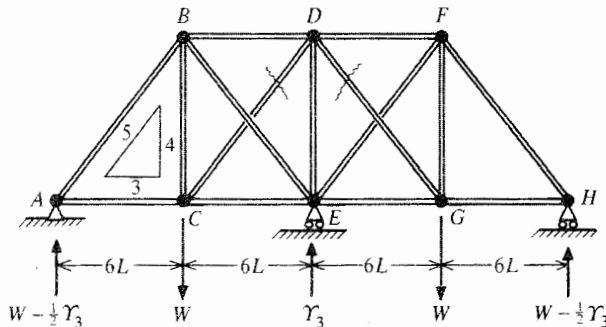


Figure 21.18. Example 21.14. An internally and externally indeterminate, pin-jointed, planar truss.

$\gamma_1 = 1.0$, $\gamma_3 = W = 0.0$, and ULS2 is the ALS with $\gamma_1 = W = 0.0$, $\gamma_3 = 1.0$. The table of results is

Bar	Length	ALS	ULS1	ULS2	
AB	10 L	$-(5/4)W$	$+(5/8)\gamma_3$	0	+5/8
AC	6 L	$(3/4)W$	$-(3/8)\gamma_3$	0	-3/8
BC	8 L	$1 W - (4/5)\gamma_1$		-4/5	0
BD	6 L	$-(3/4)W - (3/5)\gamma_1 + (3/4)\gamma_3$		-3/5	+3/4
BE	10 L	$1 \gamma_1 - (5/8)\gamma_3$		+1	-5/8
CD	10 L	$1 \gamma_1$		+1	0
CE	6 L	$-(3/4)W - (3/5)\gamma_1 + (3/8)\gamma_3$		-3/5	+3/8
DE	8 L	$-(8/5)\gamma_1$		-8/5	0

Since each bar has the same stiffness factor EA_0 , all that needs to be done now is to obtain the sum of the product of the length multiplied by the ALS force multiplied by each of the ULS forces in turn. Note that bars AB through CE need to be counted twice because of the symmetry, but bar DE has no counterpart on the other side of the truss, and so is counted only once. After simplification, the two sums, which represent the CVW of each ULS, produce the following two equations when that CVW is set to zero:

$$\begin{aligned} 79.36 \gamma_1 - 15.20 \gamma_3 &= 12.800 W \\ -15.20 \gamma_1 + 25.75 \gamma_3 &= 29.125 W \end{aligned}$$

which are easily solved for the magnitudes of the redundant forces. The solution is

$$\gamma_1 = 0.426 W \quad \text{and} \quad \gamma_3 = 1.383 W \quad \blacksquare$$

Example 21.15. What modifications would be necessary in the analysis of the above indeterminate truss with the same mechanical loading if there also was a temperature change of magnitude T_0 in bar CE?

Solution. Beyond the loss of symmetry, and thus the need for $\gamma_2 \neq \gamma_1$, the only modification to the above analysis is the inclusion in the ALS of the equivalent thermal force $EA_0\alpha T_0$ as an additional part of the total force in bar CE. Since the positions of pins C and E are fixed by bars other than bar CE, it is clear that such a temperature change does induce reactive forces in all the bars of the truss. The support reactions are also altered. \blacksquare

21.7 Summary

Indeterminate structures are commonplace in vehicular construction, especially so in flight and maritime structures. The ULM is one means for the hand calculation of the stress resultants, and hence the stresses, of simple or simplified indeterminate structures. The basis of the ULM is the Principle of Complementary Virtual work. The ULM begins with an actual load system (ALS) and one or more unit load systems (ULS) that are in equilibrium. When the complementary virtual work of each ULS is required to be zero or some other known quantity, then the releases that permitted variable values for the redundant forces and moments are eliminated, and hence continuity of all deflections is reestablished. In those two ways, force, moment, and deflection continuity are enforced for the indeterminate structure. The linear elastic material properties enter the problem in the following way. The ULM is a force method. The internal complementary virtual work is expressed in terms of force-type

quantities such as the actual and virtual (i.e., unit load) bending moments. The original internal complementary virtual work expression involves the actual strains. The material stress–strain equations are used to write the actual strains in terms of the actual stresses, which in turn are written in terms of the actual stress resultants. Displacement boundary conditions in the form of support deflections, zero or otherwise, are taken into account in the external complementary virtual work expression. Force-type boundary conditions are accounted for as the applied loads. Hence, every aspect of a general indeterminate structural analysis (force and moment equilibrium, the material constitutive equations, deflection continuity, and boundary conditions) are present in a ULM analysis.

The selection of the internal (stress resultant) and external (support reaction) redundants is the first part of a ULM indeterminate analysis that requires careful attention. In trusses, the external and internal redundants are distinct categories, but in frames and beam grids, as can be seen in Exercise 21.1(f) below, it is sometimes possible to choose the redundants so that they all fall into one or the other category, or are a mix of the two categories. The key step to choosing redundants is not stinting on drawing FBDs. Be sure to obtain all possible relations among reactions using all available equations of static equilibrium. Use symmetry, if it is present, to relate forces or moments. For the small problems that are suitable for hand calculations, it does not matter which of the forces and moments are selected as the redundant forces and moments.

Another part of the ULM indeterminate analysis that requires careful attention is the selection of the ULSs. There is, of course, one ULS for each redundant force or moment. As is illustrated in example problems 21.9 and 21.14, a foolproof way of choosing ULSs is to model them directly upon the ALS in such a manner that each redundant of the ALS is replaced in turn in that ULS by a unit load while all other loads and redundants are replaced by zero loads. This foolproof approach was not emphasized because it is sometimes possible to use more economical ULSs.⁶ However, when the analyst creates his or her own ULS, he or she must be sure that (i) the complementary virtual work done by that ULS is what is desired; (ii) the ULS is in equilibrium; and (iii) each ULS is independent of all others. On this latter point, understand that a (linearly) independent force system is just like an independent algebraic equation, or an independent vector. For example, the vectors $2\mathbf{i} + 3\mathbf{j} + 4\mathbf{k}$ (2, 3, 4) and (3, 4, 5) are independent of each other because there is no single, scalar factor that can be used to multiply one vector to obtain the other. On the other hand, the vector (4, 5, 6) is not independent of the first two vectors because it is twice the second vector less the first. All these matters are learned thoroughly with practice. The exercises below are an opportunity to obtain that practice.

A final trio of example problems, in order to review the above comments, follows. When studying these and other problems involving springs, remember that (i) springs are disguises for other structural elements, and (ii) springs only accept forces, tensile or compressive, along their line on connection.

Example 21.16. The structural system whose mathematical model is shown in Fig. 21.19(a) includes a continuous beam over three equal spans, and two springs. Set up, but do not solve, the equations necessary to determine the redundant reactions for this small structural system where the redundant reactions, if any, are to be labeled starting at point D , and then

⁶ The use of the ALS to choose ULSs is essentially what Castigliano's second theorem does every time. By coincidence, this is the approach taken in all the simple structures of the example problems except Example 21.7, where there are enough different supports to allow an advantage in doing otherwise.

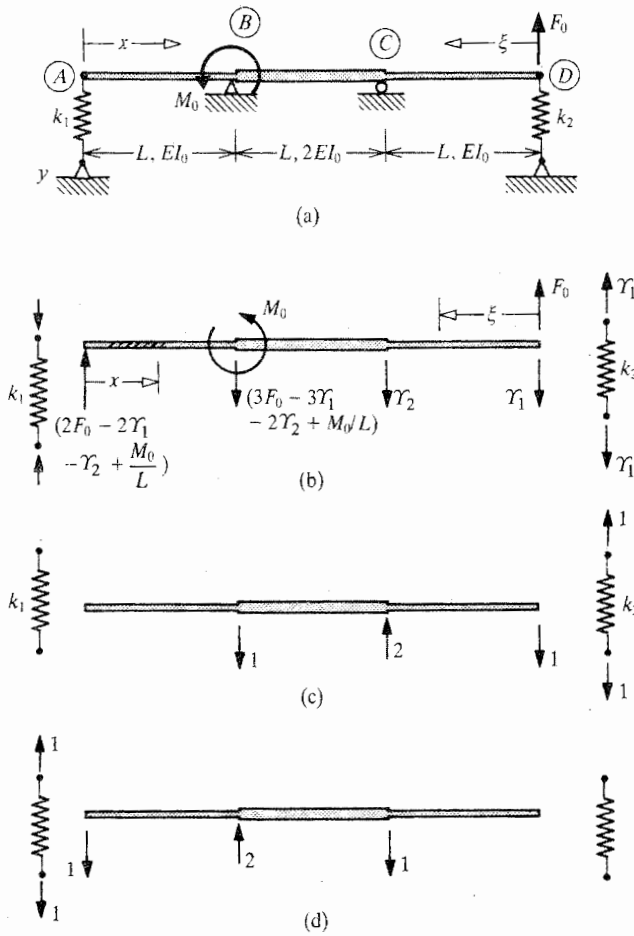


Figure 21.19. Example 21.16. (a) A beam-spring mathematical model. (b) The ALS FBDs after the selection of two redundants. (c) The first ULS FBDs. (d) The second ULS FBDs.

proceeding to the left. The required integrals do not have to be evaluated. Use only the coordinates shown.

Solution. The only beam deflections are those of beam bending. There are four vertical reactions and no horizontal reactions. Thus there are but two independent equilibrium equations, and there are two redundant reactions as labeled in Fig. 21.19(b). The actual load system spring forces and bending moments are

$$N_1 = -2F_0 + 2\gamma_1 + \gamma_2 - \frac{M_0}{L} \quad N_2 = +\gamma_1$$

$$0 \leq x \leq L \quad M(x) = \left(2F_0 - 2\gamma_1 - \gamma_2 + \frac{M_0}{L} \right) x$$

$$0 \leq \xi \leq L \quad M(\xi) = (F_0 - \gamma_1)\xi$$

$$L \leq \xi \leq 2L \quad M(\xi) = (F_0 - \gamma_1 - \gamma_2)\xi + \gamma_2 L$$

Two independent ULSs are shown in Figs. 21.19(c, d). The corresponding ULS bending moments and spring forces are, respectively,

$$\begin{aligned}
 \text{(c)} \quad & 0 \leq x \leq L & \bar{M}(x) = 0 & \bar{N}_1 = 0 \\
 & 0 \leq \xi \leq L & \bar{M}(\xi) = -\xi & \bar{N}_2 = +1 \\
 & L \leq \xi \leq 2L & \bar{M}(\xi) = -\xi + 2(\xi - L) = \xi - 2L & \\
 \\
 \text{(d)} \quad & 0 \leq x \leq L & \bar{M}(x) = -x & \bar{N}_1 = +1 \\
 & 0 \leq \xi \leq L & \bar{M}(\xi) = 0 & \bar{N}_2 = 0 \\
 & L \leq \xi \leq 2L & \bar{M}(\xi) = -(\xi - L) = L - \xi &
 \end{aligned}$$

Note that by *not* modeling the first ULS upon the ALS, a ULS is obtained which requires fewer calculations. The two equations to be solved for the two redundants, γ_1 and γ_2 , are, after multiplying through by the constant factor EI_0 ,

$$\begin{aligned}
 0 &= \gamma_1 \frac{EI_0}{k_2} - \int_{\xi=0}^L (F_0 - \gamma_1)\xi^2 d\xi + \frac{1}{2} \int_{\xi=L}^{2L} [(F_0 - \gamma_1 - \gamma_2)\xi + \gamma_2 L](\xi - 2L) d\xi \\
 0 &= \left(-2F_0 + 2\gamma_1 + \gamma_2 - \frac{M_0}{L} \right) \frac{EI_0}{k_1} - \int_{x=0}^L (2F_0 - 2\gamma_1 - \gamma_2 + M_0/L)x^2 dx \\
 &+ \frac{1}{2} \int_{\xi=L}^{2L} [(F_0 - \gamma_1 - \gamma_2)\xi + \gamma_2 L](L - \xi) d\xi \quad \blacksquare
 \end{aligned}$$

Example 21.17. All three beams that comprise the simple, planar frame shown in Fig. 21.20(a) have the same length and the same stiffness coefficient EI_0 . The two springs have the same stiffness factor $k = 3EI_0/L^3$. Set up and solve the minimum number of equations necessary to determine the redundant reactions.

Solution. Since there are five external reactions, and three equations of equilibrium in the plane, there are two external redundant reactions. The selected redundants and the other reactions are shown in Fig. 21.20(b). The consequent actual moment expressions for the three beams and the forces in the springs are

$$\begin{aligned}
 0 \leq y \leq L & \quad M(y) = (F - \gamma_1 - \gamma_2)y & \quad N_1 = \gamma_1 \\
 0 \leq x \leq L & \quad M(x) = (F - \gamma_1 - \gamma_2)L + \gamma_2 x & \quad N_2 = \gamma_2 \\
 0 \leq z \leq L & \quad M(z) = -\gamma_1 z
 \end{aligned}$$

The first ULS is illustrated in Fig. 21.20(c). The unit load moments and spring forces are

$$\begin{aligned}
 0 \leq y \leq L & \quad \bar{M}(y) = y & \quad \bar{N}_1 = 1 \\
 0 \leq x \leq L & \quad \bar{M}(x) = L & \quad \bar{N}_2 = 0 \\
 0 \leq z \leq L & \quad \bar{M}(z) = z
 \end{aligned}$$

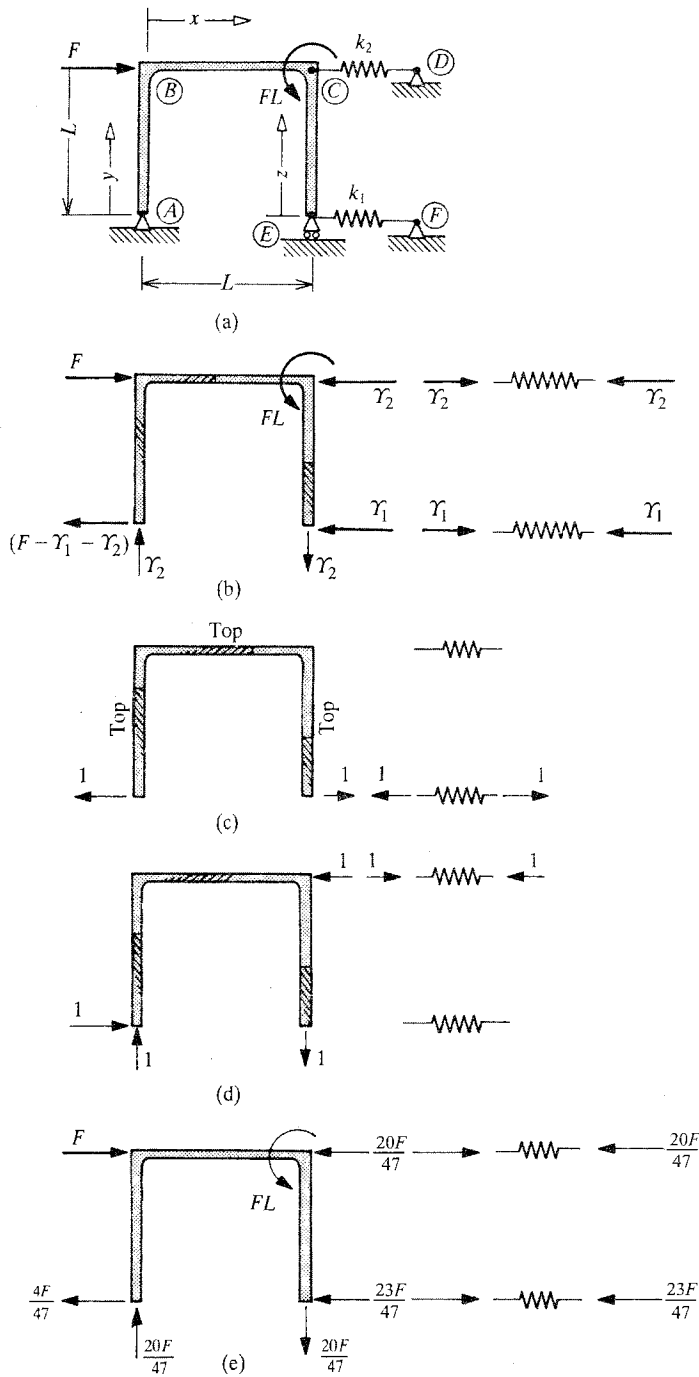


Figure 21.20. Example 21.17. (a) A portal frame, spring, mathematical model. (b) The ALS FBDs. (c) The first ULS FBDs. To assist with the moment sign convention, the “top” of each beam is labeled. (d) The second ULS FBDs. (e) The calculated support reactions.

The second ULS, which is independent of the first ULS, is shown in Fig. 21.20(d). The associated moments and spring forces are

$$\begin{aligned} 0 \leq y \leq L & \quad \overline{M}(y) = -y & \quad \overline{N}_1 = 0 \\ 0 \leq x \leq L & \quad \overline{M}(x) = -L + x & \quad \overline{N}_2 = 1 \\ 0 \leq z \leq L & \quad \overline{M}(z) = 0 \end{aligned}$$

Therefore the reattachment equation for point F , from the first ULS is, after canceling EI_0 ,

$$\begin{aligned} 0 = & \frac{(-\gamma_1)(+1)L^3}{3} + \int_{y=0}^L [(F - \gamma_1 - \gamma_2)y](y) dy \\ & + \int_{x=0}^L [(F - \gamma_1 - \gamma_2)L + \gamma_2x](L) dx + \int_{z=0}^L (-\gamma_1z)(z) dz \end{aligned}$$

The equation that requires the vertical reattachment at point E is, from the second ULS, after canceling EI_0 ,

$$\begin{aligned} 0 = & \frac{(-\gamma_2)(-1)L^3}{3} + \int_{y=0}^L [(F - \gamma_1 - \gamma_2)y](-y) dy \\ & + \int_{x=0}^L [(F - \gamma_1 - \gamma_2)L + \gamma_2x](x - L) dx \end{aligned}$$

The above equation can alternately be viewed as forcing a horizontal attachment at point C or at point D . Integration and simplification of these two simultaneous equations in terms of the redundant forces leads to

$$\begin{aligned} 12\gamma_1 + 5\gamma_2 &= 8F \\ 5\gamma_1 + 6\gamma_2 &= 5F \end{aligned}$$

whose solution is $\gamma_1 = (23/47)F$ and $\gamma_2 = (20/47)F$. The complete force system is shown in Fig. 21.20(e). ■

The final example problem illustrates the use of the ULM when the redundant forces and moments are necessarily (internal) stress resultants. There is nothing at all new when the redundants are internal forces and moments. For example, referring again to Fig. 21.20(a, b) of the previous example problem, it matters not at all whether the two redundants are the external vertical reaction at point A and the horizontal reaction at point D , or the internal horizontal forces at points C and E . However, for greater clarity, the following example illustrates the process of making releases, commonly called “cuts,” in a frame. The frame has been deliberately made nonsymmetrical in order to avoid shortcuts.

Example 21.18. Use the ULM to prepare to calculate the normal and shearing stresses in the top beam of the four-beam frame shown in Fig. 21.21(a) by preparing to calculate the axial force, bending moment, and shearing force at any point in the top beam. Use only the spatial coordinates indicated, and do not bother carrying out the integration necessary to determine the redundants. Note that the beam axial deflections and the complementary virtual work done by beam axial forces are insignificant relative to beam bending deflections and the complementary virtual work done by beam bending moments.

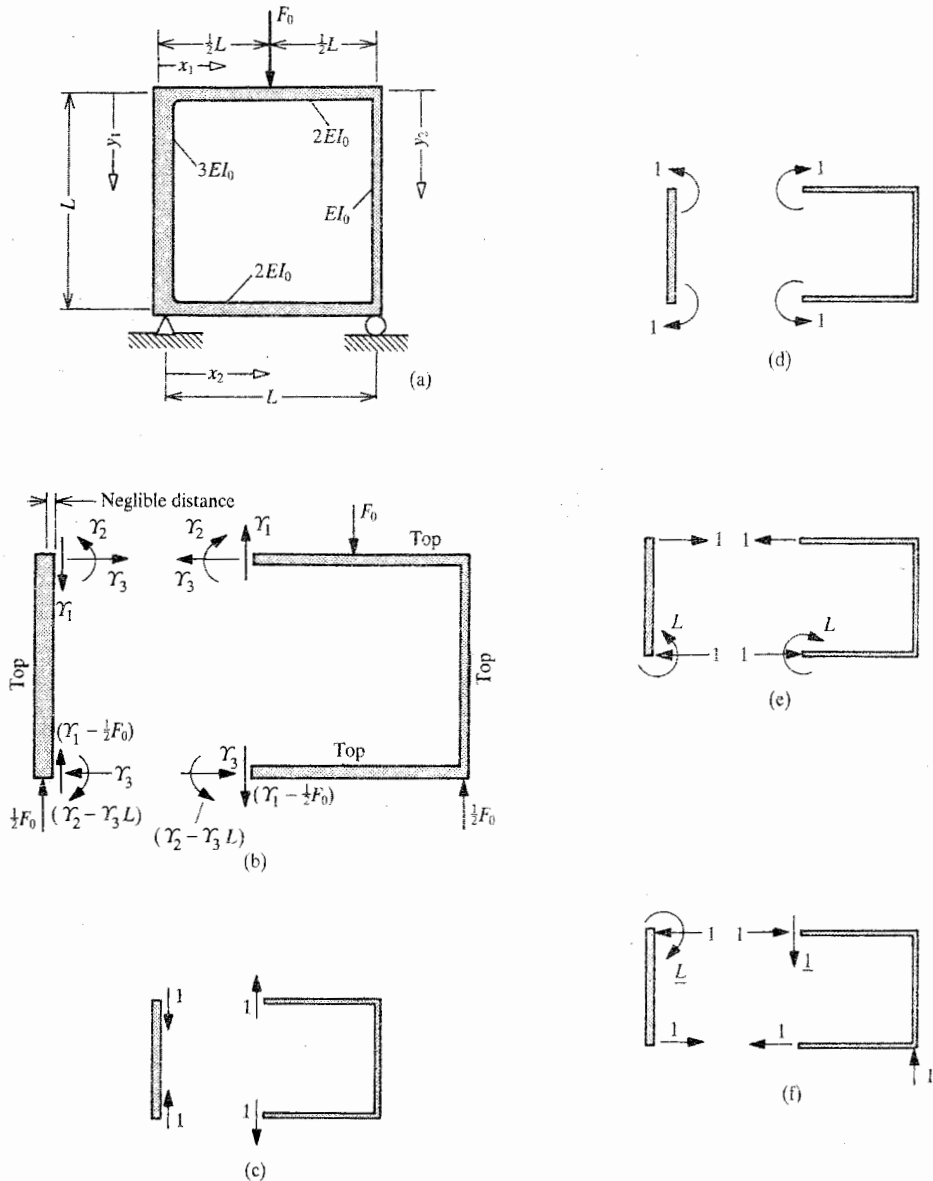


Figure 21.21. Example 21.18. An illustration of a beam frame where the redundant forces and moments are not associated with the support system. (a) A closed loop frame having statically determinate supports. (b) ALS FBDs. (c) A first ULS. (d) A second ULS. (e) A third ULS. (Locating the equilibrating moments at the top cut would also provide another ULS independent of the first two ULSs.) (f) An example of an invalid ULS. The equilibrium condition is satisfied on each of the two FBDs, but either the internal loads are not equal and oppositely directed at the two cuts, or if the underlined loads are considered to be external, they do an unknown amount of complementary virtual work.

Solution. As mentioned in the problem statement, in order to determine the bending and shearing stresses in the top beam of the four-beam frame shown in Fig. 21.21(a), it is first necessary to calculate the internal axial force and bending moment, and the internal shearing force at any point along the length of that beam. The fact that the external reactions at the base supports are easily obtained in this case does not allow the calculation of those stress resultants using only equations of equilibrium. On the contrary, the calculation of those three stress resultants requires a cut be made somewhere along the perimeter of that closed beam loop, and the labeling of the stress resultants at the cut as redundants. Since it is the top beam that is of particular interest in this case, the cut is made at a convenient point along the axis of the top beam. The left-hand end of the top beam has been chosen as the point of the cut. Figure 21.21(b) shows the labeling of the redundants. With the internal forces at the top left corner identified, the internal forces anywhere else along the perimeter of the beam loop are easily calculated. Those internal forces and moments are displayed in Fig. 21.21(b). (Note that if the structure were symmetric, as is the external loading, then it would be evident that the shearing force γ_1 could be identified immediately as having the value $F_0/2$, and then there would only be two redundants.)

In Fig. 21.21(b), for the sake of assisting with the moment sign convention, the “top” of each beam is labeled. Then the actual load system bending moments, in terms of the redundants and applied load, are

$$\begin{aligned}
 0 \leq x_1 \leq \frac{1}{2}L & \quad M(x_1) = \gamma_2 + \gamma_1 x_1 \\
 \frac{1}{2}L \leq x_1 \leq L & \quad M(x_1) = \gamma_2 + \gamma_1 x_1 - F_0 \left(x_1 - \frac{1}{2}L\right) \\
 & \quad M(x_2) = -\gamma_2 + \gamma_3 L - \left(\gamma_1 - \frac{1}{2}F_0\right) x_2 \\
 & \quad M(y_1) = \gamma_2 - \gamma_3 y_1 \\
 & \quad M(y_2) = \gamma_2 + \gamma_1 L - \frac{1}{2}F_0 L - \gamma_3 y_2
 \end{aligned}$$

In this case, as is discussed in the third paragraph of the Summary, the required three unit load systems are obtained by first setting $\gamma_1 = 1$, and the other two redundants and F_0 equal to zero, and then setting $\gamma_2 = 1$ while $F_0 = \gamma_1 = \gamma_3 = 0$, and so on. The respective unit load system diagrams are shown in Figs. 21.21(c, d, e). Of course, there are other possibilities for ULSs, but remember that all parts of the structure have to be in equilibrium for each ULS, and the value of the complementary virtual work done by each ULS has to be known (e.g., zero) in order to write a useful equation. The ULS moments are

ULS1	ULS2	ULS3
$\bar{M}(x_1) = x_1$	$\bar{M}(x_1) = 1$	$\bar{M}(x_1) = 0$
$\bar{M}(x_2) = -x_2$	$\bar{M}(x_2) = -1$	$\bar{M}(x_2) = L$
$\bar{M}(y_1) = 0$	$\bar{M}(y_1) = 1$	$\bar{M}(y_1) = -y_1$
$\bar{M}(y_2) = L$	$\bar{M}(y_2) = 1$	$\bar{M}(y_2) = -y_2$

The complementary virtual work done by the virtual forces of the first ULS moving through their respective real deflections is zero. This is because all the virtual forces and moments are internal forces and moments. For each such force and moment, equilibrium requires an equal and opposite force and moment on the opposite face of any cut. Thus the complementary virtual work done by either one of this pair of equal and opposite stress resultants is canceled by the complementary virtual work done by the other because they

both move through the same actual deflection. The same can be said for the other two ULSs. Thus the integral equations that can be used to determine the values of the three redundants are

$$\begin{aligned}
 0 &= \frac{1}{2} \int_0^{\frac{1}{2}L} (\gamma_2 + \gamma_1 x_1) x_1 dx_1 + \frac{1}{2} \int_{\frac{1}{2}L}^L \left[\gamma_2 + \gamma_1 x_1 - F_0 \left(x_1 - \frac{1}{2}L \right) \right] x_1 dx_1 \\
 &\quad + \frac{1}{2} \int_0^L \left[-\gamma_2 + \gamma_3 L - \left(\gamma_1 - \frac{1}{2}F_0 \right) x_2 \right] (-x_2) dx_2 \\
 &\quad + \int_0^L \left(\gamma_2 + \gamma_1 L - \frac{1}{2}F_0 L - \gamma_3 y_2 \right) L dy_2 \\
 0 &= \frac{1}{2} \int_0^{\frac{1}{2}L} (\gamma_2 + \gamma_1 x_1)(1) dx_1 + \frac{1}{2} \int_{\frac{1}{2}L}^L \left[\gamma_2 + \gamma_1 x_1 - F_0 \left(x_1 - \frac{1}{2}L \right) \right] (1) dx_1 \\
 &\quad + \frac{1}{2} \int_0^L \left[-\gamma_2 + \gamma_3 L - \left(\gamma_1 - \frac{1}{2}F_0 \right) x_2 \right] (-1) dx_2 + \frac{1}{3} \int_0^L (\gamma_2 - \gamma_3 y_1)(1) dy_1 \\
 &\quad + \int_0^L \left(\gamma_2 + \gamma_1 L - \frac{1}{2}F_0 L - \gamma_3 y_2 \right) (1) dy_2 \\
 0 &= \frac{1}{2} \int_0^L \left[-\gamma_2 + \gamma_3 L - \left(\gamma_1 - \frac{1}{2}F_0 \right) x_2 \right] (L) dx_2 + \frac{1}{3} \int_0^L (\gamma_2 - \gamma_3 y_1)(-y_1) dy_1 \\
 &\quad + \int_0^L \left(\gamma_2 + \gamma_1 L - \frac{1}{2}F_0 L - \gamma_3 y_2 \right) (-y_2) dy_2
 \end{aligned}$$

Finally, after the redundants at the upper left corner have been determined from the solution to the above three simultaneous equations, the values of the axial force, bending moment, and shearing force anywhere along the top beam, or anywhere else on the loop, can be quickly ascertained. Then using Eqs. (9.8) and (15.5), the normal stress and the shearing stress also can be determined provided the calculation concerns a cross-section away from the corners and away from the concentrated applied force, since those two equations are not accurate near concentrated forces or geometric irregularities. ■

Chapter 21 Exercises

- 21.1.** Determine the minimum number of redundants, external and internal, for each of the planar structural models shown in Fig. 21.22. Suggest possible choices for the redundants. Also see Exercise 21.15.
- 21.2. (a)** Recalculate the three reaction forces for the continuous beam of Fig. 21.4(a) when the stiffness of the left-hand span is nEI_0 , where n is any positive integer, and the stiffness of the right-hand span remains as EI_0 .
- (b)** Recalculate the three reaction forces when the original uniform, continuous beam is only loaded by a distributed force of magnitude f_0 over the length of the left-hand span. *Hint:* By sketching the deflection pattern of the continuous beam, the directions of the support reactions become evident.

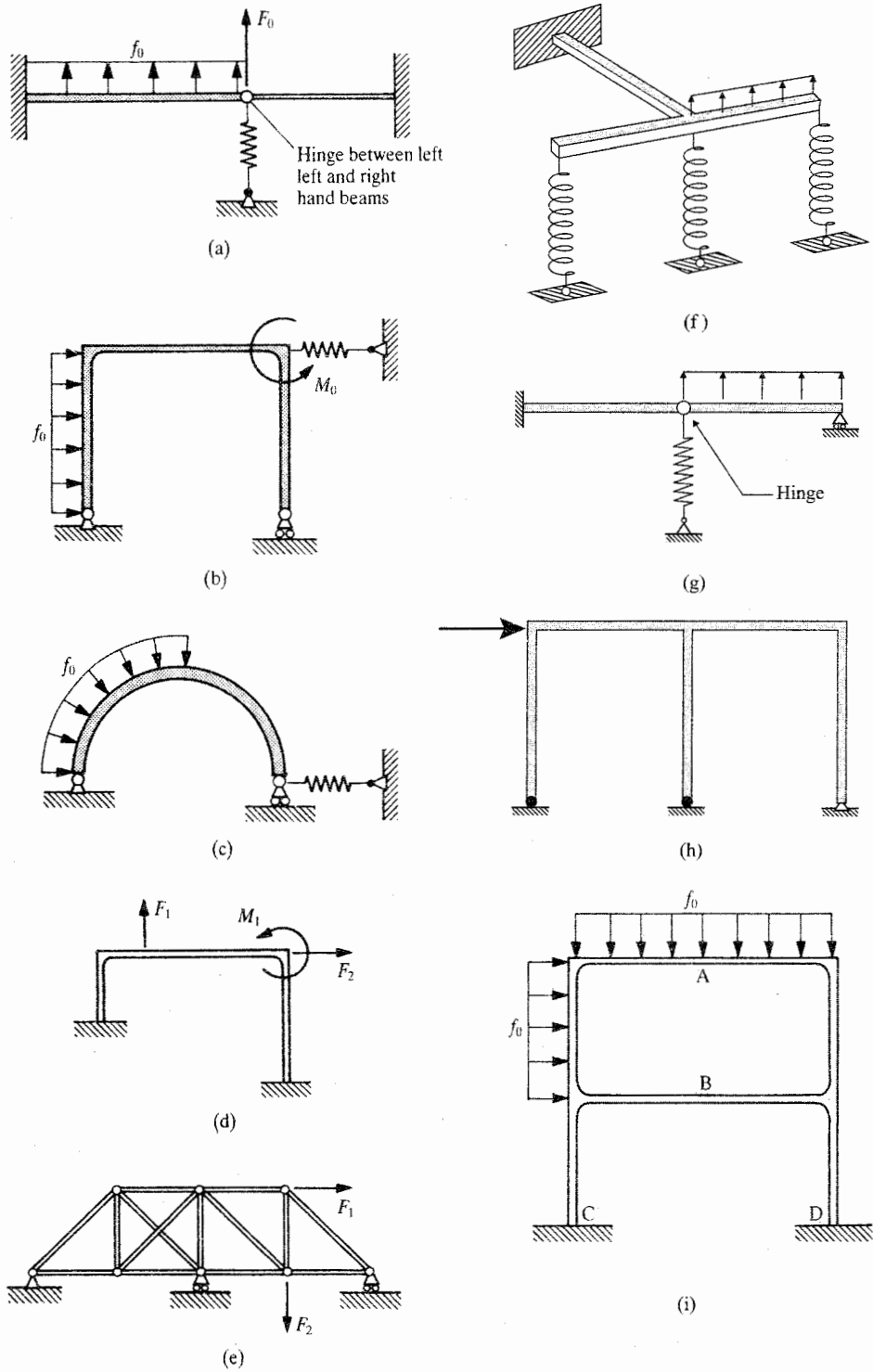


Figure 21.22. Exercise 21.1.

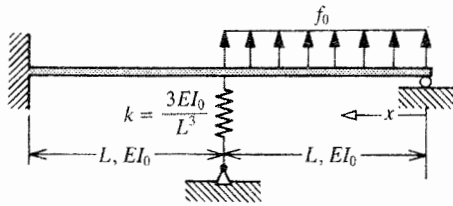


Figure 21.23. Exercise 21.4.

- (c) Calculate the deflection at the center of the left-hand span for the beam in Fig. 21.4(a). Is it greater or less than the deflection at the same point when the loading is only over the left hand span as in part (b) above?
- 21.3. (a) Before calculating the solution, decide what changes you the reader would expect to occur in the values of the reactions for the beam and spring of Fig. 21.7(a) when the spring constant is changed to $k = 10EI_0/L^3$ from $k = 6EI_0/L^3$.
- (b) Calculate the reactions for this new spring constant.
- (c) Calculate the reactions when the distributed loading extends over only the left half of the beam and the new spring value is used.
- (d) Calculate the reactions when the distributed loading extends over only the right half of the beam and the new spring value is used.
- 21.4. For the continuous beam and single spring system shown in Fig. 21.23,
- (a) State the number of redundant reactions.
- (b) Write the ULM equation(s) necessary to determine the redundant reaction(s), if any. Use only the single lengthwise coordinate shown, and label reactions as redundant starting at the right-hand end, and if necessary, proceeding to the left.
- (c) Same problem as above, but with the distributed loading acting over the left-hand span rather than the right-hand span.
- (d) Same problem as above, but with the only loading being a concentrated force of magnitude F acting upward at $x = L$.
- (e) Redo the calculation of the outer support reactions for the continuous beam of Fig. 20.11(a) when the structure is altered by replacing the right-hand spring by a roller support, lengthening the centerspan to $2L$, and lowering the spring stiffnesses to $6EI_0/L^3$. Also shift the uniform loading to the center span so that both the structure and loading are symmetric about $x = \xi = 2L$.
- 21.5. (a) Determine the three reactions for the spring–continuous beam structure and loading shown in Fig. 21.24(a).
- (b) Redo the problem of Figure 21.4(a) so as to determine the values of all three reactions. However, this time have the uniform load acting over only the right half of the two-span beam, and upgrade the stiffness coefficient of the right half of the beam to $2EI$. Remember that once one of the three reactions is determined using the ULM, the other two can be determined using two static equilibrium equations.
- (c) For the beam and loading of Figure 21.24(b) calculate the force reaction at the center support when that support is force to move upward a small distance, v_0 .

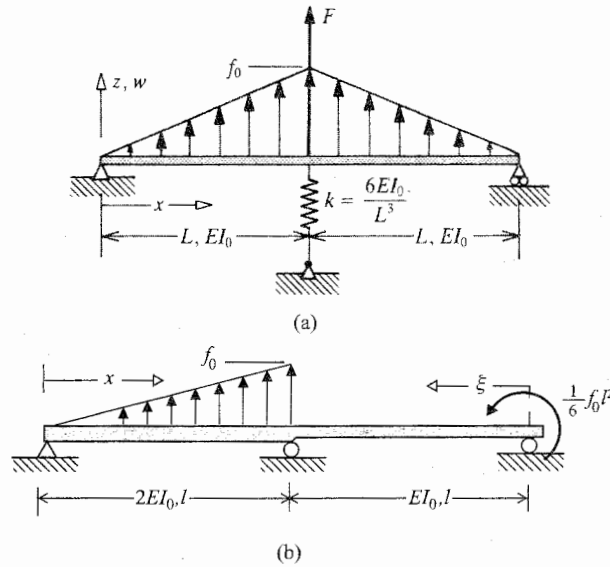


Figure 21.24. (a) Exercise 21.5(a). (b) Exercise 21.5(c).

- 21.6.** (a) Determine the values of the stresses in the aluminum bars of the three-bar truss loaded as shown in Fig. 21.25(a).
 (b) As above, but this time the force F is horizontal to the right.
 (c) Determine the axial forces in the bars AC and AD of the symmetrically loaded, symmetric truss of Fig. 21.25(b).
 (d) Calculate the axial force in the bar BC of the symmetrically loaded, symmetric truss of Fig. 21.25(c).
- 21.7.** (a) Determine the force in the vertical spring that is part of the two-spring–two-beam frame shown in Fig. 21.26(a) as a result of the applied moment M_0 . Each spring constant has the value $k = 6EI_0/L^3$.
 (b) As above, but this time let the spring stiffnesses both be $12EI_0/L^3$
 (c) As in (a), but this time let the length of the vertical beam be $2L$ rather than L .
 (d) As above with the original springs, but this time with a leftward-acting distributed force per unit length of magnitude f_0 along the entire length of the vertical beam.
 (e) The “U” shaped beam frame and spring structure shown in Fig. 21.26(b) is subjected to the applied moments shown. The redundant and other reactions are shown in Fig. 21.26(c). Draw ULSs, and provide ULS bending moment and spring force expressions.
 (f) Write the ALS bending moment and spring force expressions corresponding to Fig. 21.26(c).
- 21.8.** (a) Determine all the external reactions for the two-spring–beam frame structure and loading shown in Fig. 21.27(a). Make releases and number redundants, if any, starting at the base of the spring with stiffness k_1 , and, if necessary, proceed to the left. Use only the coordinates shown.
 (b) For the two-beam–two-spring structure of Fig. 21.27(b), number your external redundant forces starting with the reactions at points A , B , and then C , if

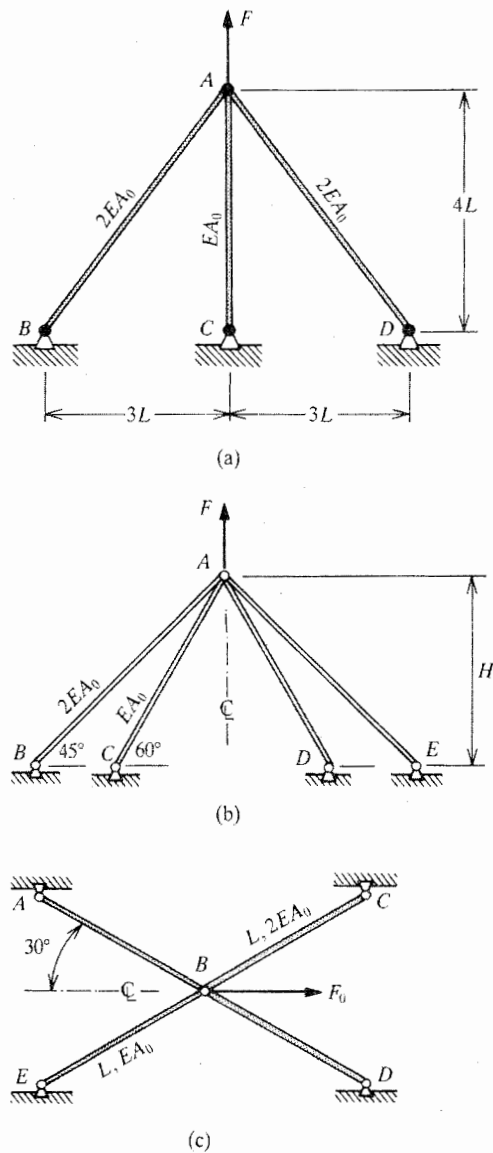


Figure 21.25. Statically indeterminate pin-jointed trusses. (a) Exercise 21.6(a). (b) Exercise 21.6(c). (c) Exercise 21.6(d).

necessary. Using only the length coordinates shown, write the expressions for the ALS moments and spring forces. Then using ULSs that replace each redundant in turn by a unit load, write the necessary ULS moment and spring force expressions.

- 21.9. (a) Calculate the reaction at the base of the bottom spring for the loading and structure shown in Fig. 21.28.
 (b) Redo the same problem with the spring stiffnesses at one-sixth of the values in part (a).

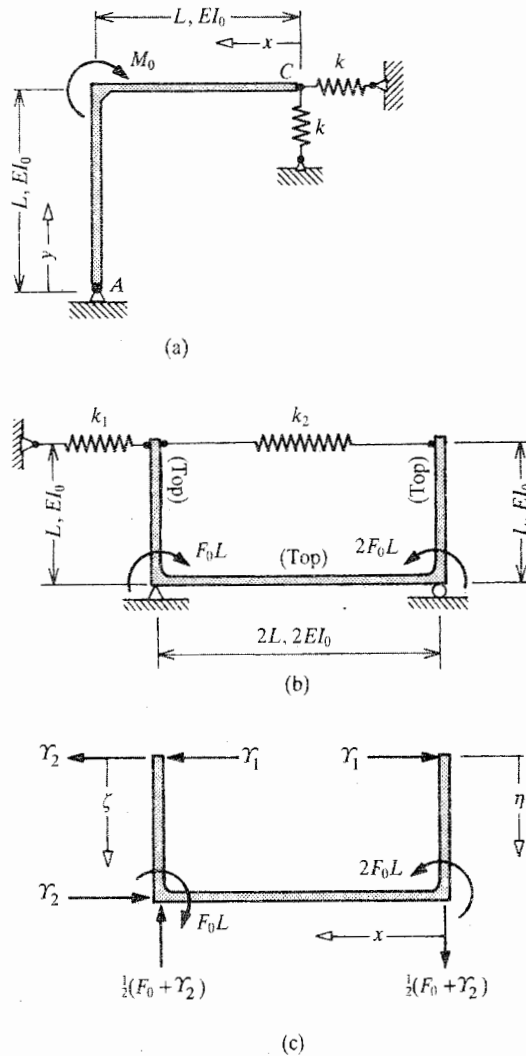


Figure 21.26. Spring-frame structures. (a) Exercise 21.7(a). (b) Exercise 21.7(e). (c) FBD for Exercise 21.7(e).

- (c) Redo the same problem with the spring stiffnesses six times their value in part (a)
- (d) For the stiffnesses of part (a), calculate the deflection at the applied load F ; that is, at the tip of the top cantilevered beam.
- (e) Redo part (a) but this time with the loading being an upward, uniform distributed load of magnitude f_0 along the entire length of the top beam.
- 21.10.** (a) Determine the forces in all the bars of the pin-jointed truss shown in Fig. 21.29 due to the loading shown if all bars have the same modulus of elasticity and cross-sectional area.
- (b) As in part (a), but this time the loading is a single horizontal force F_0 at joint D .

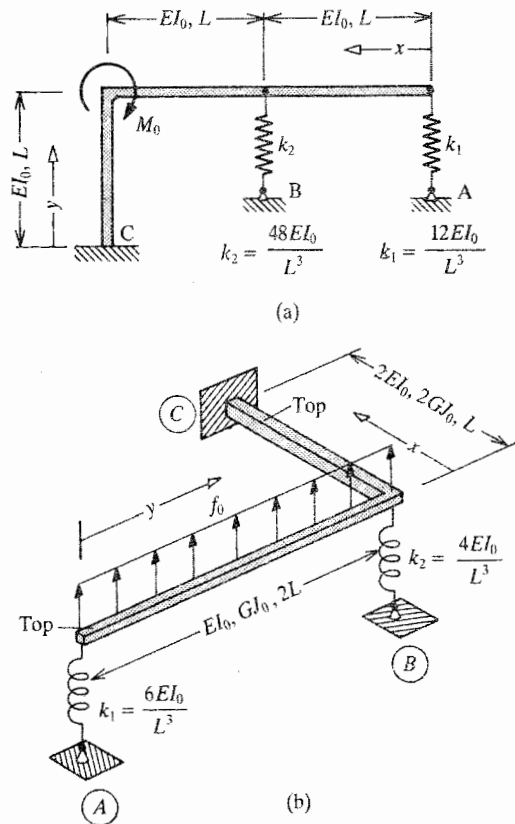


Figure 21.27. A spring-frame structure and a spring-grid structure. (a) Exercise 21.8(a). (b) Exercise 21.8(b).

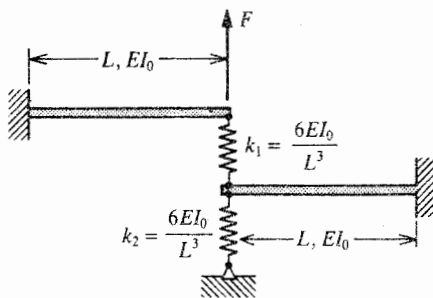


Figure 21.28. Exercise 21.9.

(c) After doing parts (a) and (b), what is the axial force in bar BD when the forces F_0 , F_1 , and F_2 of part (a) and part (b) are applied together?

21.11. Use the ULM to set up the equations needed to determine the five reactions at the rigid wall that supports the three-beam grid shown in Fig. 21.30. Do not bother to carry out the integration. Understand that the left-hand support is a fully fixed support but, while the right-hand support can resist shear forces and bending moments, the right-hand support offers no resistance to twisting moments. To

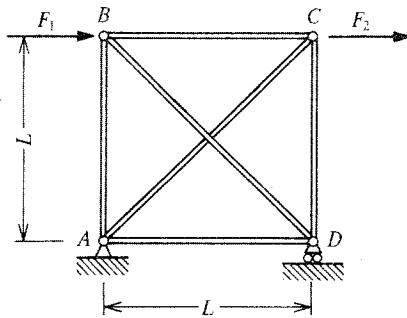


Figure 21.29. Exercise 21.10.

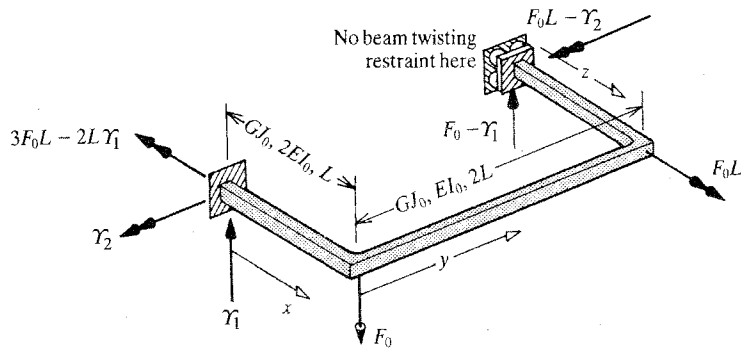


Figure 21.30. Exercise 21.11.

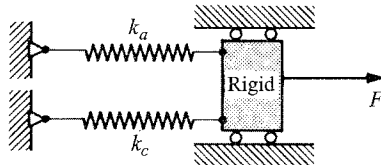


Figure 21.31. Exercise 21.12.

avoid confusion on this point, the redundants have been selected and the support reactions to the applied loads are provided. Use only the beam axis coordinates shown. See Appendix B for intended significance of this exercise with respect to engineering practice.

FOR THE EAGER

- 21.12. (a) Use the ULM to calculate the forces in each of the two springs shown in Fig. 21.31 where each spring undergoes the same deflections.
- (b) Use the ULM to calculate the forces in three springs of stiffnesses $2k_0$, $3k_0$, and $4k_0$ that are, as in the above, required to undergo the same deflection as a result of the application of a tensile or compressive force F to all three.

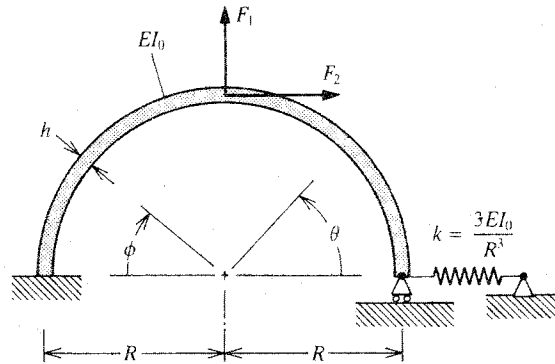


Figure 21.32. Exercise 21.13.

- 21.13. (a) Calculate the force in the spring for the loading and structure shown in Fig. 21.32.
- (b) Add a torsional spring of stiffness $4EI_0/R$ to the structure at $\theta = 0$ and then recalculate the force in the rectilinear spring. (The torsional spring resists a beam bending slope at $\theta = 0$.)
- 21.14. (a) Redo the closed ring problem of Example 21.12 where the oppositely directed applied forces F are replaced by oppositely directed applied bending moments M_1 .
- (b) Redo part (a), but this time with oppositely directed torsional moments M_2 .
- 21.15. (a) Sketch suitable, independent ULSs for the structure that is drawn in Fig. 21.22(a).
- (b) As above, for Fig. 21.22(b).
- (c) As above, for Fig. 21.22(c).
- (d) As above, for Fig. 21.22(d).
- (e) As above, for Fig. 21.22(e).
- (f) As above, for Fig. 21.22(f).
- 21.16. Redo Example 21.12 where the only deflection is
 - (a) A bending slope rotation at the right-hand beam end.
 - (b) A lateral deflection at the left-hand beam end.
 - (c) A bending slope rotation at the left-hand beam end.

FOR THE ESPECIALLY EAGER

- 21.17. A uniform bar of length L is fixed against axial deflection at its left-hand end and loaded at its right-hand end by an axial tensile force of magnitude N that is uniformly distributed over the end cross-section. If the elastic material of the bar is described by the stress–strain equations

$$(a) \sigma = \mathcal{E}\sqrt{\epsilon} \quad (b) \epsilon = \frac{\sigma}{E} + \beta \left(\frac{\sigma}{E}\right)^n$$

which are both examples of a “softening” material, what then is the deflection at the right-hand end of the bar? *Hint:* Write $-\delta W_{in}^* = \epsilon \delta \sigma AL$ where $\sigma = N/A$, and $\delta W_{ex}^* = N \delta u(L)$. Remember that the PCVW applies to all material.

- 21.18.** (a) If the truss of Fig. 19.4 is composed of a material for which $\sigma = \mathcal{E}\sqrt{\epsilon}$, what then is vertical deflection at joint B ?
- (b) As above, but here $\sigma = \mathcal{E}\epsilon^2$.
- 21.19.** Calculate the forces in the four bars of Fig. 21.10 if the only loading is a temperature change T_0 in bar (a) AB ; (b) AC ; (c) AD ; (d) AE .
- (e) If the original mechanical load pictured in Fig. 21.10 and any or all of the temperature changes mentioned above were to occur simultaneously, would it be possible to superimpose the resulting internal forces for each type of loading?

Parts IV and V Review Questions

True or False?

1. The Principles of Virtual Work and Complementary Virtual Work are valid only for elastic materials.
2. The virtual work and complementary virtual work of a entire structural system are simply the sum of the virtual work and complementary virtual work, respectively, of each part of the structural system.
3. Typical virtual work and complementary virtual work statements are $\delta W = u \delta F$, and $\delta W^* = F \delta u$, respectively.
4. The PCVW for small strains is entirely equivalent to the linear strain–displacement equations, and therefore is entirely equivalent to the linear compatibility equations.
5. One possible form of complementary virtual work is a real moment moving through a virtual rotation.
6. The PCVW requires that the virtual forces and moments form a system of forces and moments that are in equilibrium with the actual forces and moments.
7. There are only stylistic differences between the virtual load method, the unit load method, and applications of Castigliano's second theorem.
8. The unit load method is a special application of the PCVW wherein a unit load system consisting of a unit load and its equilibrating reactions are the set of virtual loads.
9. For both statically determinate *and* indeterminate structural systems, any unit load system must be distributed as if the unit load system were another actual load system where, generally, any actual load system satisfies more than just equilibrium conditions. Note that all "load systems" include support reactions.
10. There need be no connection between any unit load system and the applied load system, and each unit load system must be linearly independent of all other unit load systems used in that analysis of the indeterminate structure.
11. For any unit load system, the total external complementary virtual work does *not* include the products of (i) the reactions to the selected unit load, with (ii) their respective actual deflections.
12. Castigliano's first theorem corresponds to the PVW, and Castigliano's second theorem corresponds to the PCVW.
13. The mathematical variation of a definite integral with fixed limits is another definite integral with the same fixed limits.
14. If $u = u(x)$ is a function of unknown form, then the variation of $F(x, u'(x))$, which has a known form, is simply $(\partial F / \partial u') \delta u'$.
15. If $F(u, u'')$ is a known function of its arguments, and $u(x)$ is an unknown function of the independent variable x , then

$$\delta F = \frac{\partial F}{\partial u} \delta u + \frac{\partial F}{\partial u''} \delta u'' \quad \text{where} \quad \delta u'' = \frac{d^2(\delta u)}{dx^2}$$

16. Consider a beam of length $3L$. The x coordinate originates at the left-hand end of the beam. The beam is simply supported at $x = 0$ and at $x = 2L$. Between $x = 0$ and $x = L$, there is no loading and the beam stiffness is $3EI_0$. For $L \leq x \leq 2L$, there is a positive uniform lateral load per unit length of magnitude f_0 , and the beam stiffness is $2EI_0$. For $2L \leq x \leq 3L$, there is no loading, and the beam stiffness is just EI_0 . Then the lateral deflection at $x = L$, midway between the two simple supports, is $11 f_0 L^4 / (288 EI_0)$.
17. In statically indeterminate analyses, as opposed to statically determinate analyses, there can be only one satisfactory unit load system (ULS) for the purpose of calculating a deflection.
18. A unit load method of analysis typically has fewer, sometimes far fewer, simultaneous equations that need to be solved for an analysis solution than the deflection-based finite element method.
19. The unit load method is fully applicable to beams where the beam stiffness is an arbitrary positive function of the axial coordinate x , and the unit load method integral formulations can always be solved numerically if they cannot be solved analytically.
20. The unit load method is equally applicable to structures without rigid or elastic supports as it is to those with such supports.
21. A structure can be internally, as well as externally, statically indeterminate.
22. The number of redundant reactions that need to be determined for a given structure does not depend upon the loading.
23. There must be a redundant force associated with every spring that appears in a structural model if one end of each spring is tied to a rigid base and if there is at least one rigid support for the structure.
24. One certain way to obtain independent unit load systems for a unit load method analysis of a structure with more than one redundant reaction is to choose unit load systems based upon the actual load system where each of the redundant loads is in turn replaced by a unit load while all the other redundant loads and the actual applied loads are set equal to zero.
25. The deflection functions chosen for a Rayleigh–Ritz analysis using the PVW (i) are defined over the entire domain of the structure; (ii) must be sufficiently differentiable to continuously define the relevant strains in the structure; and (iii) must satisfy all the deflection type boundary conditions.
26. The number of DOF of a railway train consisting of two attached, rigid rail cars rolling without slipping upon rigid wheels on a fixed rail bed that goes up and down and around hills is 3 if the attachment between the two cars is a rectilinear spring.
27. The number of DOF of an elastic beam bending element undergoing only lateral deflections in one plane while subjected to one and only one type of distributed loading, such as a uniform lateral loading per unit length, is 4, the same as the beam bending element unloaded over its interior.
28. A rigid hoop rolling upright (one diameter is always vertical) without slipping upon a horizontal, flat, rigid plane has three DOF.
29. Consider a rigid bar supported by a fixed hinge at one bar end (so that the bar only rotates in a plane) and an elastic spring at the other end. The number of DOF of the rigid bar and spring is 1.
30. The commonplace finite element method is a force method, while the unit load method is a deflection method.

31. One very important advantage of a deflection method of analysis in comparison to a force method of analysis is that, in large structures, the identification of unknown generalized coordinates is much easier than the identification of redundant forces and moments.
32. In the case of beams or bars, shape functions describe the change in the finite element cross-sectional area moment of inertia or area, respectively, as a function of distance along the beam or bar axis.
33. The number of DOF of an individual beam finite element is always two less than the number of generalized coordinates used to describe the deflected position of the finite element.
34. Those columns of the assembled system stiffness matrix eliminated by imposition of zero deflection boundary conditions exactly correspond to those rows that contain unknown support reactions of one kind or another.
35. The finite element method requires the use of principal axes when dealing with beams; that is, it is a necessary preliminary step in the finite element description of a beam segment to rotate to principal axes.
36. The individual terms of the finite element method generalized force vector of a static structural analysis can include more than one concentrated force or equivalent concentrated force from more than one node if there is a rigid linkage between the nodes where those forces are applied.
37. Rigid elements are used in finite element modeling in order to avoid very large stiffness entries relative to other entries and the consequent possibility of matrix ill conditioning.
38. Regardless of the type of finite element, the shape functions always have a maximum value of 1.0 and an algebraic minimum value of zero.
39. For one-dimensional finite elements, shape functions *or* their first derivatives always take on the value +1.0 at the geometric location of the DOF with which they are associated, and the value zero at the location of all other DOF.
40. Once continuous intraelement shape functions have been chosen for a two- or three-dimensional finite element, and the matter of interelement deflection continuity has been resolved, then the element stiffness matrix is the direct result of the application of the PVW.
41. Any unit load system where all the external virtual loads are in equilibrium, and which involves the desired deflection, be it zero or otherwise, is an adequate unit load system.
42. Consider the circumstance where a clamped-clamped, uniform beam experiences an actual, enforced upward lateral deflection at its right-hand end of magnitude w_0 while the slopes at both beam ends are held to being zero. This means that the beam of length L is forced into a flattened S shape, where, because of the antisymmetry of the beam deflections, the lateral deflection at the beam midspan is $\frac{1}{2}w_0$. Let a concentrated, upward virtual force of magnitude δF be placed at the beam midspan prior to the actual deflection. Then the external complementary virtual work done by that virtual force *and* its reactions at the beam ends must be the product $(1/2)\delta Fw_0$.
43. For a linearly elastic material, the internal complementary work per unit volume equals the internal work per unit volume.
44. For a linearly elastic material, the internal complementary *virtual* work per unit volume equals the internal *virtual* work per unit volume.

45. As long as the deflections and strains are small, the PVW also applies to a structure where the stresses exceed the elastic limit and the structure has undergone elastoplastic deformations including unloading and reloading.
46. As a consequence of Newton's third law, internal beam redundants (i.e., the redundant forces and moments at the opposite sides of "cuts" in the beams of the structure) are always described as equal in magnitude and oppositely directed. When the associated virtual forces and moments of unit load systems follow this same "equal and opposite" rule the complementary virtual work of each pair of such equal and opposite virtual forces or moments is zero.
47. The presence of a hinge in a planar beam structure always means that there is one less equation of static equilibrium compared to the number of equilibrium equations that would exist in the absence of the hinge.
48. In the general three-dimensional loading case, at each of the two finite element beam segment ends, there are six beam DOF which are the two orthogonal beam end lateral deflections, the axial deflection, the two beam bending slopes, and the beam end twist.
49. Since the element stiffness matrices are always singular matrices to a degree equal to the number of rigid body motions possible to the element with its DOF, the planar beam bending finite element $(w_1, \theta_1, w_2, \theta_2)$ stiffness matrix is singular to the second degree.
50. Maxwell's reciprocity theorem guarantees that the inverse of a stiffness matrix is a flexibility matrix.

Answers

1. False. The PVW and the PCVW are valid for any material because no constitutive equations were used in the derivation of either principle.
2. True. Recall that the meaning of "energy" is stored work. From a physical point of view, both actual mechanical energy and virtual mechanical energy are associated with mass. The stored work of a larger mass is the stored work of all the component masses. From a mathematical point of view, work and energy are scalar quantities, and add as such for each part of a structure. What is true for work is also true for complementary work.
3. False. Typical virtual work and complementary virtual work statements are $\delta W = F \delta u$, and $\delta W^* = u \delta F$, respectively.
4. True. As discussed during its derivation, the Principle of Complementary Virtual Work is a necessary and sufficient condition for the linear strain-displacement equations. As discussed in Part I, the strain-displacement equations are necessary and sufficient conditions for the linear strain compatibility equations. Therefore the PCVW is entirely equivalent to the compatibility equations.
5. False. A real moment moving through a virtual rotation is virtual work, not complementary virtual work, which would be a virtual moment moving through an actual rotation.
6. False. There is no necessary relation between the actual load system and the virtual load system. Each load system must separately be in a state of static equilibrium.
7. True. All three techniques for calculating deflections are based upon the PCVW, and their procedures are essentially the same. The style of the virtual load method is to load the structure with a discrete δF or a discrete δM so as to produce external complementary virtual work in combination with the actual translation or actual

rotation that is the object of the analysis. The virtual strain energy integrals involve virtual moment, virtual torque, and/or virtual axial force expressions that involve in linear form these same selected δF or δM terms. Thus it is possible to cancel these arbitrary virtual load factors, and determine the magnitude of the selected deflection. The unit load method is exactly the same except that unit values are assigned to the selected δF or δM terms, thus saving the effort of a cancellation. Although not explained previously, in the implementation of Castigliano's second theorem, if there is not already an actual load at the point and in the direction of the deflection being sought, then a dummy load (call it Q) is so placed. Then the actual moment expression M involves the quantity Q . When the variational operator is applied to obtain δM , this quantity is expanded by the chain rule to get $(\partial M/\partial Q)\delta Q$, where the latter factor never appears because it, as before, is canceled during the setup of the procedure. If Q is a dummy load, then as a last step, it is set equal to zero.

8. True, as noted above.
9. False. The only requirement placed upon the virtual load system is that it be in a state of static equilibrium. As a matter of strategy, the CVW done by the ULS should only involve the actual deflections of interest, and be as simple as possible.
10. Both parts of the statement are True. While the actual load system for, say, an aircraft reflect the analyst's estimate of the loads resulting from steady state lift forces, weight forces, and so on, the virtual load system is based solely upon the need to create complementary virtual work in combination with the actual deflection being sought.
11. False. The reactions to the unit load are also virtual loads. Thus their products with their corresponding actual deflections do indeed contribute to the complementary virtual work, at least when the actual deflections at the locations of the reactions have nonzero values.
12. True. As explained in the answer to Question 7, Castigliano's second theorem is nearly identical to the virtual load method, and therefore utilizes the PCVW. Castigliano's first theorem is seldom used today, but it is based upon the PVW.
13. True. As proved in Endnote (1) of Chapter 16, the variational operator and a definite integral are commutative, meaning that the variational operator can pass into the integral and thus act upon the integrand, or be detached from the integrand and pass out of the integral.
14. True. Since $u'(x)$ is the only dependent function of unknown form, it is the only quantity that can be varied.
15. True. This is simply an application of the chain rule for partial derivatives.
16. False. The lateral deflection $w(x = L) = 13 f_0 L^4 / (288 E I_0)$.
17. False. Particularly where there is symmetry of the actual loading and the structure, there can be more than one satisfactory independent unit load system. See Example 21.5 for an illustration of how other ULSs can be devised.
18. True. Even for a single beam with a distributed loading, at least six beam elements would require at a minimum ten DOF, and thus ten simultaneous equations, to obtain reasonably accurate deflections. Even if the beam were clamped at both ends, there would only be two redundant loads and two simultaneous equations.
19. True. A varying EI appears in the denominator of the strain energy integrals, and thus complicates, but does not invalidate the integration.
20. True. There is an example problem demonstrating the use of the ULM with an unsupported beam. The only difference between this case and the others is that in

an unsupported structure, only relative deflections can be calculated because the structure, while in equilibrium, can undergo rigid body motions.

21. True. If there are more than three support reactions for a planar structure, or more than six for a three-dimensional structure, then the structure can be externally indeterminate. As demonstrated with two example frame problems (one a fully circular structure), if the beam structure forms a closed loop, then generally there are internal redundants.
22. False. While there is a maximum number of redundant reactions for each structure that is independent of the loading, the number of redundants that need to be determined in a given situation may depend upon the loading, with simpler loadings requiring fewer redundants. For example, if a beam structure bears no horizontal loads, it may be that there are no horizontal redundant reactions. Furthermore, the number of redundants associated with a symmetric loading upon a symmetric structure may be less than the number of redundants associated with a nonsymmetric loading action upon the same structure.
23. False. A beam with a knife edge support at one end and a rectilinear spring support at the other beam end is statically determinate, and thus disproves the statement. Furthermore, even if the introduction of a spring into a structural model were to add a redundant reaction to the model, it is not necessary that the extra redundant be the reaction at the base of the spring.
24. True. If properly chosen, each redundant is independent of the others. Thus a unit value associated with a certain redundant and a zero value there for all the other redundant guarantees an independent unit load system because no possible combination of the other unit load systems can produce a nonzero value at the location of the subject redundant. This is analogous to the fact that no additive combination of vectors of the form $\alpha \mathbf{i} + \beta \mathbf{j}$ can ever be equal to the vector $\gamma \mathbf{k}$, so this latter vector is linearly independent of all the former vectors.
25. All three parts are true. The virtual strain energy must be unambiguously integrable.
26. False. Only two DOF are required since both cars roll without slipping. One DOF is necessary to locate one of the two cars and its wheels, and another generalized coordinate (absolute or relative) is necessary to locate the other car and its wheels.
27. True. When the loading is restricted to being a single type of loading, the deflection pattern for the bending finite element cannot be altered by the use of additional loadings. Hence the two end deflections and two end bending slopes completely control the deflected shape of the element and thus qualify as the element generalized coordinates. Recall that whatever the specified distributed loading, the solution to the fourth order GDE contains exactly four constants of integration.
28. False. This is a tricky one, and a classical example of a “nonholonomic” dynamic system. (See your physics textbook.) There are four DOF. Two DOF are needed to locate the point of contact of the hoop on the plane. Another DOF is needed to specify the angular orientation of a horizontal diameter of the hoop with respect to a fixed line in the plane. Finally, a fourth DOF is needed to specify which point on the outer diameter of the hoop is in contact with the plane. The first three generalized coordinates do not determine the value of the fourth DOF because if the first three coordinates are fixed, any additional value of the fourth coordinate can be achieved by rolling the hoop in a circle of a circumference equal to that additional value, and returning to the original position of the hoop’s first three coordinates.

29. True. A single rotational angle precisely defines the position of the rigid bar. Since the bar end point is the same as that of the elastic spring, the position of the spring is also unambiguously defined by the same rotational angle for the bar.
30. False. The correct statement is the reverse of the given statement. The unknown quantities of the finite element method today are the generalized coordinates (DOF), while the unknown quantities of the unit load method are the redundant generalized forces.
31. True. Even for a three-dimensional structural model, deciding upon the number of external support reactions that cannot be evaluated by the six possible static equilibrium equations is not difficult. However, as discussed in Chapter 22, when a planar structure loops back on itself, there are necessarily internal redundants, and in three dimensions there are many possible loops of different sizes. Hence identifying internal redundants can be confusing.
32. False. For any finite element, shape functions describe the deflection pattern associated with a DOF. They have nothing to do with the undeflected cross-sectional geometry of a finite element.
33. False. The DOF and the generalized coordinates are identical, so they have the same numbers. The rank (number of rows or columns less the number of dependent rows or columns) of the planar beam bending element stiffness matrix is two less than its size because of the possibility of two element rigid body motions. For the 2×2 bar stretching and bar twisting finite elements, the order of the 2×2 stiffness matrices is 1.
34. True. In the matrix equation $\{Q\} = [K] \{q\}$, the generalized force of the j th row is located at the physical position of the j th generalized coordinate. The only locations where there are known deflections, here described as zero, are at the supports, and at the supports there are unknown reactions. Of course where there are applied (known) loads, the deflections are unknown. So, one known quantity is always coupled with one unknown quantity.
35. False. The virtual strain energy integral over the volume of the beam element, $\iiint(\dots)dA dx$, has as its integrand the product of the beam bending stress and the beam bending virtual strain. That product for bending in both the xy and the xz planes is

$$\sigma_{xx} \delta \varepsilon_{xx} = E y^2 v'' \delta v'' + E z^2 w'' \delta w'' + E y z w'' \delta v'' + E y z v'' \delta w''$$

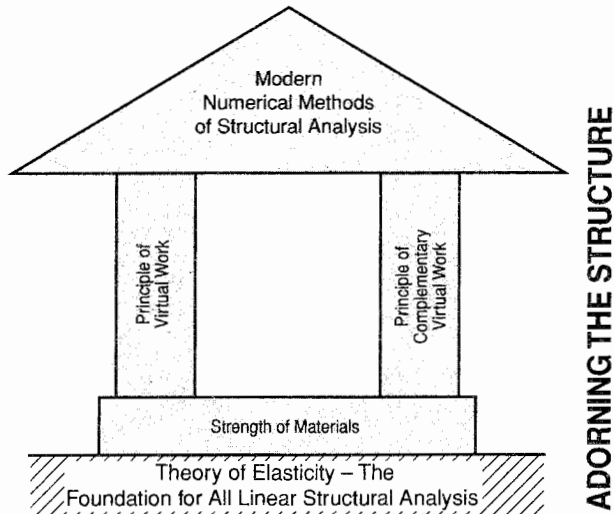
In the previous development, the integral over the cross-sectional area of the yz dA terms where $dA = dy dz$ was set equal to zero in order to limit the discussion to principal axes and thereby simplify the discussion. However, at this point that integral can be designated the nonzero quantity I_{yz} . Since both $v''(x)$ and $w''(x)$ have exactly the same polynomial expansion, the same 4×4 stiffness matrices are obtained for $E I_{yy}$, $E I_{zz}$ and $E I_{yz}$, where there are two of the latter matrices. Thus the restriction to principal axes was an unnecessary and temporary convenience.

36. True. As is illustrated by the example of an axially rigid beam where there is an axial applied force at each end of the beam, the variation of the one axial DOF causes both of these axial forces to do virtual work. Therefore the generalized force associated with that axial DOF involves both of the applied axial forces.
37. True. Large disparities in stiffness entries can lead to the mathematical loss of accuracy when the $\{Q\} = [K] \{q\}$ matrix equation is solved.

38. False. Firstly, shape functions can have negative values. The fourth beam bending shape function illustrates this fact and the fact that the maximum functional value is not always +1. While $N_4'(x = \ell) = +1$, the maximum value of $N_4(x)$ itself is zero.
39. True. This is illustrated in the answer to the previous question.
40. True. Once adequate shape functions for the relevant displacements have been established, the remainder of the derivation of the element stiffness matrix is the routine application of the strain–displacement equations to get the strains, the premultiplication of the strains by the appropriate material stiffness matrix to get the stresses, the substitution for the stress and strain vectors in the virtual strain energy integral, and then the completion of the integration.
41. False. The unit load system may be inadequate if, in addition to calculating the desired deflection in a complementary virtual work expression, it also involves unwanted, nonzero deflections that cause (additional) unknown values to enter into the complementary virtual work equation.
42. False. The external complementary virtual work done by the virtual force at the beam midspan and the virtual forces and moments at the beam supports that react and thus equilibrate the midspan virtual force depend upon what form is chosen for those virtual reactions at the beam supports. That is, since the clamped–clamped beam is statically indeterminate, there exists more than one way to react the midspan virtual force. If, for example, the midspan virtual force is equilibrated by a downward virtual force of magnitude $\frac{1}{2}\delta F$ at each support, then the complementary virtual work is $+(\delta F)(\frac{1}{2}w_0)$ at the beam midspan, and $(-\frac{1}{2}\delta F)(w_0)$ at the right-hand end, for a total of zero complementary virtual work. A total complementary virtual work of $(1/2)w_0 \delta F$ can be obtained by reacting the midspan virtual force by a downward virtual force of magnitude δF and a virtual clockwise moment of magnitude $(L/2)\delta F$ at the left support. Since there are no actual deflections at the left-hand support, these virtual reactions do no complementary virtual work. Thus the total complementary virtual work is that done by the midspan virtual force. A total complementary virtual work of $-(1/2)w_0 \delta F$ can be obtained by putting a reacting virtual force δF and a reacting counterclockwise moment $(L/2)\delta F$ at the right-hand beam end.
43. True. For a linearly elastic material, the stress–strain curve is a straight line that bisects the rectangle whose height is the stress and whose width is the strain. The equal half below the stress–strain curve is the work per unit volume, and the equal half above that straight line is the complementary work per unit volume.
44. False. While, for a linearly elastic material, the internal work per unit volume and the internal complementary work per unit volume occupy equal areas on the material stress–strain curve, the same is not necessarily true for the corresponding virtual quantities, $\sigma \delta\epsilon$ and $\epsilon \delta\sigma$. This is so because, while the actual stress and the actual strain are related, there is no necessary relation between the virtual stress and the virtual strain of these virtual work and CVW expressions. This is so because, for example, with the PVW, while there is an arbitrary value for $\delta\epsilon$, there is no $\delta\sigma$ since in the PVW stresses are regarded as independent quantities.
45. True. The PVW enforces equilibrium at the surface and within the interior of the structure. The validity of the PVW depends upon the strain–displacement equations be valid. The PVW is derived without any reference to material behavior. Therefore it applies to a material undergoing plastic deformations with unloading.

46. True. The complementary virtual work at a cut is always zero because the virtual forces and virtual moments must abide by the equal-and-opposite rule while they move through the same deflections, and thus together produce zero complementary virtual work.
47. False. The presence of the hinge means that there is always one more equilibrium equation (the moment at the hinge is zero) than there would be in the absence of the hinge.
48. True. In the order cited in the question, these six DOF here have been assigned the symbols v , w , u , θ , ψ , and ϕ .
49. True. Any matrix is singular if its determinant is zero. Any determinant is zero if it contains a row (or a column) of all zero entries. The determinant of the planar beam bending stiffness matrix can be made to have two rows of all zeros by (i) following the rules of determinants, the first row is added to the third row, which then makes the third row all zeros; and (ii) multiplying the first row by the beam element length and then subtracting the second and fourth rows, which renders the first row as being composed of all zeros.
50. False. The inverse of a stiffness matrix is always a flexibility matrix by definition of those two terms. Maxwell's reciprocity theorem guarantees that both matrices are symmetric matrices.

THIN PLATE THEORY AND STRUCTURAL STABILITY



VI.1 Introduction

While the finite element method, with occasional assistance from the unit load method or some such application of the principle of complementary virtual work, is a completely satisfactory approach to all linear structural analysis tasks, there are still many topics that need to be touched upon in this introductory textbook in order to provide a reasonably complete overview of aerospace structural analysis. The first of these topics is the mechanics of two-dimensional structural elements other than merely the equations for the out-of-plane stretching of thin membranes and the finite elements that can be used to determine the in-plane deflections and stresses of thin skins. Chapter 22 considers the strength of materials approach to thin plate bending and buckling. Again, the objective is to provide a sufficient understanding of the mechanics and the mathematics of thin plate bending so that a simple, but representative, thin plate finite element can be introduced. The next step in complexity after thin plates is thin shells. A treatment of thin shells of general geometry is complicated. Hence the analysis of thin shells is left entirely to textbooks that are specific to that topic.

Chapter 23 returns to the essential topic of elastic stability by discussing a simple finite element for beam buckling. Just as any finite element analysis is much superior to a differential equation-based analysis in its ability to address geometric and material complexities, a beam buckling finite element greatly expands the range of beam and beam frame buckling

problems that can be so analyzed. The end result of such an analysis is a matrix eigenvalue problem. Chapter 23 also provides an extension of the structural stability discussion to the challenge of aeronautical divergence and flutter. The discussion of these and other aeroelastic instabilities is necessarily brief because the aerodynamic complexities of these topics require a full textbook of their own.

Thin Plate Theory

22.1 Introduction

A thin plate is a structural element, just as a long beam is a structural element. The thin plate also is characterized by its special geometry. While a long beam has two dimensions very much shorter than the length dimension, a thin plate, as is pictured in Fig. 1.11, has one dimension that is very much less than the other two dimensions. The thin plate's least dimension is, of course, called the plate thickness. The thickness is usually a constant in most vehicular structures, but the possibility of a gradually changing thickness can be incorporated into thin plate bending theory (Ref. [16]). The difference between a thin plate and a membrane is that a thin plate can resist both stretching and bending, while a membrane can only resist lateral or inplane loads by stretching.

There are two goals for this chapter. The first and lesser goal is to develop the equations of classical thin plate bending theory. More than an introductory discussion of the extensive body of classical thin plate bending solutions is outside the purposes of this textbook. The second and more important goal is to develop the equations necessary to describe a simple plate bending finite element comparable to the previously developed beam bending finite element. The greater importance assigned to the second, rather limited, goal not only suggests the present relative importance of the two topics but also suggests that certain simplifications like constant plate thickness are appropriate for the thin plate theory to be presented here. The development of the thin plate theory in this chapter is kept *as simple as possible*, for the most part, to facilitate clarity by avoiding what otherwise can be a significant amount of algebraic detail. Thus unlike, for example, the extensive development of beam bending theory, the derivation of the plate equations is here restricted to small deflections. (Finite deflections are discussed in Ref. [16] and in the exercises for the eager.) Other limitations, such as isotropic material models for each layer of a "sandwich"-type plate construction are introduced in the next section. If desired, at the expense of much more algebra, the reader can replace the selected isotropic material model by the orthotropic material model necessary to describe the bending of plates (laminates) composed of stacks of bonded fiber composite plies.

The strength of materials basis for small-deflection, thin plate theory is essentially the same as that for small-deflection, long beam theory. This point is repeatedly emphasized by referring to the beam bending sections and equations that closely parallel the present development. That beam-plate parallelism is easily seen to be extensive because, as in the development of the long beam equations in Chapters 9 and 10, a vector equilibrium approach is used here to develop the thin plate equations. In order to elaborate on this point, recall that the alternate derivational approach to the long beam equations, the approach based upon the use of the Principle of Virtual Work or the associated Principle of the Minimum Value of the Potential Energy, is presented in Endnote (3) of Chapter 15. Thus both basic derivational approaches to the long beam equations are available as guides for the development of the thin plate equations. The vector equilibrium approach to thin plate theory is chosen because it is judged that it will seem less abstract to a person new to plate

theory. However, the application of work or energy principles has an important advantage over the vector equilibrium approach in developing the small-deflection plate equations. The use of work or energy principles yields not only the correct governing differential equations, but also the correct boundary conditions that are *not* otherwise obvious.

22.2 The Plate Midplane

As the name suggests, the plate midplane is planar. If the midsurface of the thin structural element is curved before loading, then the structural element is called a shell, or shell segment. If the plate material is homogeneous, then the location of the plate midplane is apparent. The midplane, which is the plane of symmetry for the top and bottom surfaces, must be equidistant from the possibly nonplanar plate top and bottom surfaces. Then the lateral or z direction, which is perpendicular to the midplane, is equally obvious. If the plate has a varying thickness, and the plate material is nonhomogeneous, then there is possibly material and geometric complexity. For the sake of algebraic simplicity, only constant thickness plates composed of isotropic materials are considered here. However, within the limits of those two restrictions, the possibility of layered nonhomogeneity is taken into account in the development that follows. When there are nonsymmetrically arranged layers of isotropic materials with different Young's moduli, then the midplane is no longer simply a matter of geometry. It is necessary to develop the concept of the modulus weighted midplane and the modulus weighted thickness. Before doing so, it is worth repeating that, because of the limitation to uniform layers of materials that exhibit isotropic behavior, the following development of thin plate bending theory is not applicable to laminated plates built from fiber composite plies (layers). However, the extension of the following concepts to uniform thickness plates constructed of layers of orthotropic materials with different material orientations only increases the bookkeeping associated with some steps of the derivation as opposed to altering the type of steps necessary to the plate bending theory derivation.

The thin plate modulus weighted thickness, which corresponds to A^* in beams, is measured in the geometric thickness direction as follows. Establish a convenient coordinate origin for the temporary, geometric thickness direction coordinate z_0 . The thickness coordinate z_0 corresponds to the arbitrary beam cross-sectional coordinates y_0 and z_0 . Let the top and bottom plate surfaces be located at the z_0 values t_0 and b_0 , respectively. Then, since the modulus of elasticity only varies through the plate thickness, that is, $E = E(z_0)$ only, the modulus weighted thickness is then defined as

$$h^* \equiv \int_{z_0=b_0}^{z_0=t_0} \frac{E}{E_0} dz_0 = \text{constant} \quad (22.1)$$

where, again, E_0 is the arbitrarily chosen reference modulus of elasticity. Now introduce the z coordinate. Let the yet-to-be located modulus weighted (m.w.) midplane be the origin of the z axis. The z coordinate is called the modulus weighted thickness coordinate. Since the modulus weighted midplane serves the same function for a plate as the m.w. centroid serves for a beam cross-section, it is appropriate to locate the m.w. midplane by another "first moment" balance equation. Let

$$0 = \int_{z_0=b_0}^{z_0=t_0} z \frac{E}{E_0} dz \quad (22.2)$$

As is the case with a nonhomogeneous beam cross-section, the relation between the two thickness-direction coordinates is

$$z = z_0 - z_0^* \quad (22.3)$$

where z_0^* is the yet unknown, constant distance from the arbitrary z_0 origin to the m.w. midplane. Substituting the third equation into the second quickly shows that the distance between the modulus weighted midplane and the arbitrary coordinate origin, z_0^* , is

$$z_0^* h^* = \int_{b_0}^{t_0} z_0 \frac{E}{E_0} dz_0 = \sum (\bar{z}_0)_i \left(\frac{Eh}{E_0} \right)_i \quad (22.4)$$

where $dz = dz_0$

22.3 The Plate Stress Resultants

Paralleling the beam development of Section 9.3, the next step is to define the stress resultants for thin plates in terms of the internal stresses in the plate. Following the established format for stresses, and using a Cartesian coordinate system, the stresses for a infinitesimal portion of the plate are shown in Fig. 22.1(a). In stress terms, the visible faces of the plate segment shown in the figure are one front x face and one back y face. Note that this typical plate specimen has a finite thickness h or h^* , and infinitesimal lateral dimensions. This representative infinitesimal portion could be from either the interior of the plate, or the edge of the plate if the latter happens to parallel either Cartesian coordinate axis.

Like the beam stress resultants, the plate stress resultants are moments, shear forces, and in-plane forces. However, because there are now both x face and y face cross-sections to consider, there are more plate stress resultants than beam stress resultants. For the sake of clarity, the plate force stress resultants and the moment stress resultants, which jointly act on planes perpendicular to the plate midplane, are shown in two separate figures. Figure 22.1(c) shows the shear forces Q_x and Q_y and the three in-plane force resultants N_x , N_y , and N_{xy} or N_{yx} . Figure 22.1(d) shows the three types of moments. The moments M_x and M_y are bending moments that parallel the bending moments in beams. The moments M_{xy} and M_{yx} are twisting moments that parallel the twisting moments in beams. Note that the meaning of the subscripts on the plate bending moments is different from that for beam bending moments. For plates, the single subscript indicates the plane on which the moment acts, while for beams the subscript indicates an axis about which the moment acts.

There is an important difference between the beam stress resultants and the plate stress resultants. Recall, for example, that the beam axial force N is the integral over the entire beam cross-sectional area A of the stress σ_{xx} . In plate theory it is not useful to sum stresses over an entire plate cross-section, that is, from one plate edge to another. The reason that such a summation over the entire beam cross-section is useful in engineering beam theory is that, in that theory, the normal stress σ_{xx} varies linearly with respect to both beam cross-sectional coordinates, the y and z coordinates. Even though the same linear change for the plate stresses σ_{xx} and σ_{yy} will be soon established for the z direction, there is no such simple change in the values of σ_{xx} or σ_{yy} with respect to the y and x coordinates. Thus it is necessary to allow for arbitrary variations of those stresses with the x and y coordinates. This can be accomplished by dealing with the plate forces and moments exclusively on the basis of a differential width of the plate, dx or dy , as is illustrated in Figs. 22.1(b). Thus, on this basis, each plate stress resultant is only truly a force or moment when it is multiplied by a midplane length. For example, the total in-plane, normal force at the m.w. midplane on the x face of the differential-sized specimen pictured is

$$N_x dy \equiv \int_{z=z_b}^{z=z_t} \sigma_{xx}(x, y, z) dz dy$$

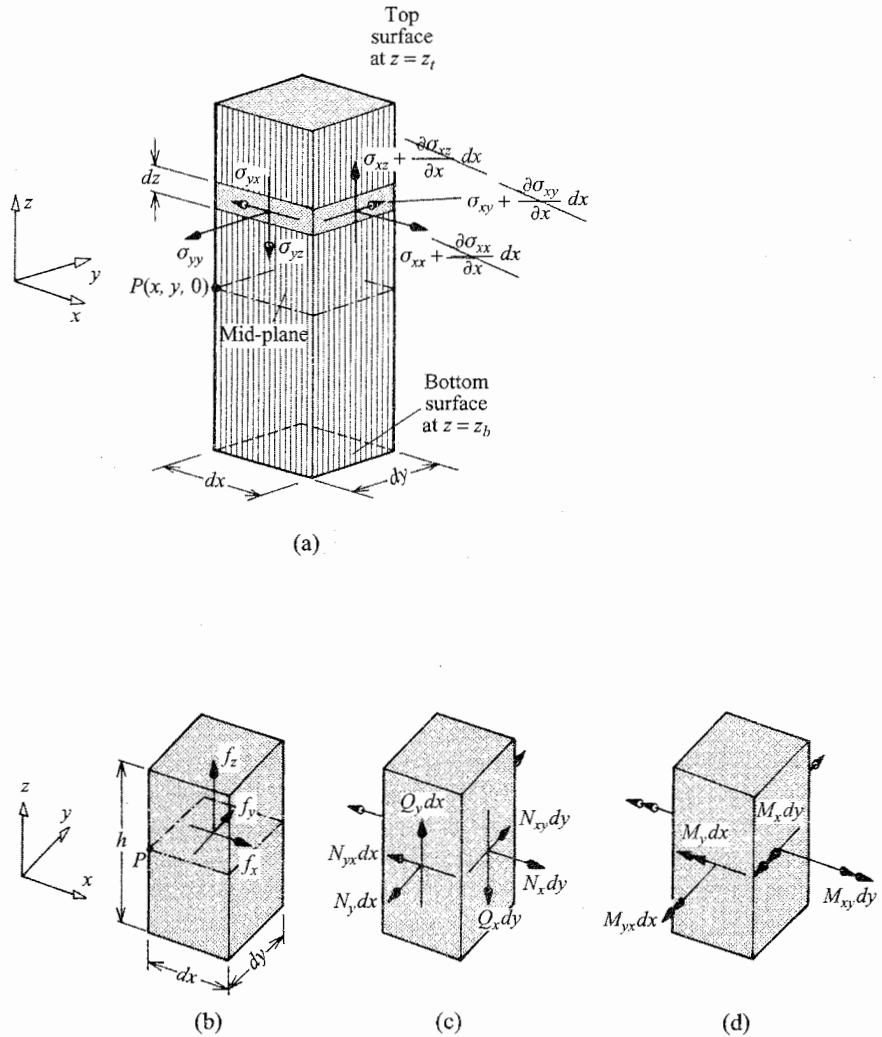


Figure 22.1. A rectangular parallelepiped piece of a plate structure located at the Point $P(x, y, 0)$. This plate segment has (the exaggerated) dimensions dx by dy in the plate inplane directions, and it extends the length of the local plate thickness in the z direction. The figures show: (a) representative back and front face stresses at a distance z above the midplane; (b) the three Cartesian components of the applied loading per unit area which are taken to act at the midplane; (c) the force per unit length stress resultants that act at the midpoint of one back y face and one front x face; and (d) the moment per unit length stress resultants at the same points on the same faces. (A similar view of all 10 stress resultants is provided in Fig. 22.2.) Be sure to note that the bending moment subscripts do *NOT* identify the coordinate axis about which the moment per unit length acts.

where z_t and z_b are the z coordinate values for the top and bottom surfaces, respectively, and where $z_t - z_b = h$, the thickness. Canceling the arbitrary dy term on both sides produces the definition of N_x at the point $P(x, y, 0)$. The quantity N_x is properly referred to as the normal force in the x direction per differential length in the y direction. The phrase “per unit length” is commonly used in place of “per differential length” without loss of usefulness.

Similarly, the other plate stress resultants per unit length are defined as

$$\begin{aligned}
 N_y &\equiv \int_h \sigma_{yy} dz & N_{xy} = N_{yx} &\equiv \int_h \sigma_{xy} dz \\
 Q_x &\equiv - \int_h \sigma_{xz} dz & Q_y &\equiv - \int_h \sigma_{yz} dz & M_x &\equiv - \int_h z \sigma_{xx} dz \\
 M_y &\equiv - \int_h z \sigma_{yy} dz & M_{xy} = -M_{yx} &\equiv - \int_h z \sigma_{xy} dz
 \end{aligned} \tag{22.5}$$

Note that in this textbook the first or only subscript indicates the face on which the force or moment acts. From this point on the qualification “per unit length” will often be omitted for the sake of brevity when referring to the plate stress resultants.

22.4 The Approximate Pattern for Plate Displacements

Analogously to Section 9.4, approximations regarding the deformations of the thin plate are accepted in order to escape from the theory of elasticity to the more efficient environment of strength of materials. These approximations are called the *Kirchhoff hypothesis*. The Kirchhoff¹ hypothesis is

1. Straight lines within the thin plate which are perpendicular to the m.w. midplane before loading remain straight and perpendicular to the m.w. midplane after loading; and
2. The perpendiculars to the m.w. midplane are unchanged in length after loading.

Analogously to Eqs. (9.2), the above approximations can be cast in mathematical terms as the displacement equations below, where θ_x is the rotation about the x axis, and θ_y is the rotation about the *negative* y axis (just as is the case in Chapter 9):

$$\begin{aligned}
 u(x, y, z) &= u(x, y, 0) - z\theta_y(x, y) \\
 v(x, y, z) &= v(x, y, 0) - z\theta_x(x, y) \\
 w(x, y, z) &= w(x, y, 0)
 \end{aligned} \tag{22.6}$$

Of course, the displacements at $z = 0$ are the m.w. midplane displacements. This strength of materials formulation of plate bending theory utilizes the midplane displacements, now called the plate deflections, in exactly the same fashion that engineering beam theory utilizes the displacements at the beam centroid. Just as is the case with beam deflections $v(x)$ and $w(x)$, the plate deflections are identified by a displacement symbol with fewer variables in the functional argument. That is,

$$u(x, y, 0) \equiv u(x, y) \quad v(x, y, 0) \equiv v(x, y)$$

and

$$w(x, y, 0) \equiv w(x, y)$$

With the above approximation to the actual displacements, the strains, stresses, and stress resultants can now be calculated using strain–displacement equations, stress–strain equations, and the stress resultant–stress equations. Again using the comma notation for

¹ Gustav Robert Kirchhoff (1824–1887), German physicist (Ref. [17]).

partial derivatives, the small deflection (i.e., linear) strains are

$$\begin{aligned}\epsilon_{xx}(x, y, z) &= \frac{\partial u(x, y, z)}{\partial x} = u_{,x} - z\theta_{y,x} \\ \epsilon_{yy}(x, y, z) &= \frac{\partial v(x, y, z)}{\partial y} = v_{,y} - z\theta_{x,y} \\ \epsilon_{zz}(x, y, z) &= \frac{\partial w(x, y, z)}{\partial z} = w_{,z} = 0 \\ \gamma_{xy}(x, y, z) &= \frac{\partial u(x, y, z)}{\partial y} + \frac{\partial v(x, y, z)}{\partial x} = u_{,y} + v_{,x} - z(\theta_{y,y} + \theta_{x,x}) \\ \gamma_{xz}(x, y, z) &= \frac{\partial u(x, y, z)}{\partial z} + \frac{\partial w(x, y, z)}{\partial x} = -\theta_y + w_{,x} \\ \gamma_{yz}(x, y, z) &= \frac{\partial v(x, y, z)}{\partial z} + \frac{\partial w(x, y, z)}{\partial y} = -\theta_x + w_{,y}\end{aligned}$$

The first Kirchhoff approximation, which requires that the right angles of the perpendiculars to the midplane remain right angles, is expressed mathematically as $\gamma_{xz} = \gamma_{yz} = 0$. The result of this approximation, just as is the case for the Bernoulli–Euler beam approximations, is that the rotations are the same as the bending slopes. The zero value of the z direction strain is consistent with the second Kirchhoff approximation. Thus the three nonzero strains can be written as

$$\begin{aligned}\epsilon_{xx}(x, y, z) &= u_{,x} - zw_{,xx} \\ \epsilon_{yy}(x, y, z) &= v_{,y} - zw_{,yy} \\ \gamma_{xy}(x, y, z) &= u_{,y} + v_{,x} - 2zw_{,xy}\end{aligned}\tag{22.7}$$

Note in passing that the strength of materials approach to thin plates leads to a plane strain problem.

As is the case with the beam, the isotropic stress–strain equations are the stage in the development of the plate equations at which the inexactness of the Kirchhoff approximations becomes visible through the appearance of apparent contradictions. For example, a lateral loading on the upper or lower plate surfaces, or a lateral shearing loading along an unsupported plate edge, certainly produces nonzero values of the σ_{xz} and σ_{yz} shearing stresses. However, the Kirchhoff approximations forbid the accompanying shearing strains in these same x, z and y, z planes. Using the same means of escape from this contradiction that is used in the beam theory development of Section 9.4, appropriate fictitious orthotropic material constants are chosen to overcome this contradiction. The lack of a strain in the z direction in the face of strains in the x and y directions requires that the coefficient of thermal expansion α_z and the Poisson's ratios ν_{xz} and ν_{yz} be zero, and that there be an infinite value for the modulus of elasticity in the z direction. These two fictitious Poisson's ratios and the zero values for all strains with z subscripts produces the following plane stress isotropic stress–strain equations:

$$\begin{aligned}\sigma_{xx} &= \frac{E}{1-\nu^2}(\epsilon_{xx} + \nu\epsilon_{yy}) - \frac{E\alpha\Delta T}{1-\nu} \\ \sigma_{yy} &= \frac{E}{1-\nu^2}(\epsilon_{yy} + \nu\epsilon_{xx}) - \frac{E\alpha\Delta T}{1-\nu} \\ \sigma_{xy} &= G\gamma_{xy} = \frac{E\gamma_{xy}}{2(1+\nu)}\end{aligned}\tag{22.8}$$

where E , ν , and α are the in-plane values of these material constants. The infinite value of E_z , and infinite values of G_{xz} and G_{yz} allow finite values for the other three stresses even though their corresponding strains are zero. Thus the zero specification for two of the six Poisson's ratios, and the infinite value specification of one of the Young's moduli and two of the shearing moduli, produces both stresses and strains that are in keeping with the Kirchhoff approximations. Substitute Eqs. (22.7) into Eqs. (22.8), to obtain

$$\begin{aligned}\sigma_{xx} &= E_0 \left[\frac{E}{E_0} \left(\frac{1}{1-\nu^2} \right) [u_{,x} + \nu v_{,y} - z(w_{,xx} + \nu w_{,yy})] - \frac{E}{E_0} \left(\frac{\alpha \Delta T}{1-\nu} \right) \right] \\ \sigma_{yy} &= E_0 \left[\frac{E}{E_0} \left(\frac{1}{1-\nu^2} \right) [v_{,y} + \nu u_{,x} - z(w_{,yy} + \nu w_{,xx})] - \frac{E}{E_0} \left(\frac{\alpha \Delta T}{1-\nu} \right) \right] \\ \sigma_{xy} &= E_0 \left[\frac{E}{E_0} \left(\frac{1}{2(1+\nu)} \right) (u_{,y} + v_{,x} - 2z w_{,xy}) \right]\end{aligned}\quad (22.9)$$

Substituting the above result into Eqs. (22.5) yields, with the use of Eqs. (22.1, 2), the stress resultant-deflection equations

$$\begin{aligned}N_x &= K^*(u_{,x} + \nu v_{,y}) - N_T & N_y &= K^*(v_{,y} + \nu u_{,x}) - N_T \\ N_{xy} &= \frac{1}{2}(1-\nu)K^*(v_{,x} + u_{,y})\end{aligned}\quad (22.10a)$$

where

$$K^* = \frac{E_0 h^*}{1-\nu^2} \quad N_T = \frac{E_0}{1-\nu} \int_h \alpha \Delta T \frac{E}{E_0} dz$$

$$\begin{aligned}M_x &= D^*(w_{,xx} + \nu w_{,yy}) - M_T & M_y &= D^*(w_{,yy} + \nu w_{,xx}) - M_T \\ M_{xy} &= (1-\nu)D^* w_{,xy}\end{aligned}\quad (22.10b)$$

where

$$\begin{aligned}D^* &= E_0 I^* & I^* &= \int_h \frac{z^2}{1-\nu^2} \frac{E}{E_0} dz \\ M_T &= -\frac{E_0}{1-\nu} \int_h z \alpha \Delta T \frac{E}{E_0} dz\end{aligned}$$

If the thin plate is homogeneous, then $K^* = K$, $D^* = D$, and

$$I = \frac{h^3}{12(1-\nu^2)}, \quad K = \frac{Eh}{1-\nu^2}, \quad \text{and} \quad D = \frac{Eh^3}{12(1-\nu^2)} \quad (22.11)$$

In the above equations, the isotropic Poisson's ratio is an average value through the plate thickness. This is acceptable if the nonconstant values of this in-plane Poisson's ratio change only slightly over the plate thickness. If there were a significant change in the Poisson's ratio over the plate thickness, as would be possible if the plate were composed of thin layers of very different materials, or had a honeycomb core that is sometimes used in sandwich constructions, then the integrations over the thickness for the stress resultants per

unit length have to account for that change. That situation can be addressed by writing, for example,

$$N_x = \sum \int_{h_i} \sigma_{xx} dz \quad \text{where of course} \quad h = \sum h_i$$

Clearly, there are several similarities between the solutions in terms of deflection derivatives for the above plate stress resultants per unit length and the beam stress resultants. Note in particular that I^* is the plate edge area moment of inertia per unit length about the x or y coordinate axes of the m.w. plate midplane. Its homogeneous value of $I = h^3/[12(1 - \nu^2)]$ is the same as that for a beam of unit width, except for the factor $[1/(1 - \nu^2)]$. The reason for the difference is that engineering beam theory completely fails to account for the Poisson effect, while engineering plate theory accounts for that effect within the plane of the plate by having a nonzero $\nu_{xy} = \nu$ while requiring all ν with z subscripts to be zero.

The stresses can be expressed in terms of the stress resultants. This is accomplished by solving Eqs. (22.10) for the deflection combinations of Eqs. (22.9) and substituting those combinations into Eqs. (22.9). With the usual type of definitions,

$$\begin{aligned} N_x^c &= N_x + N_T & N_y^c &= N_y + N_T \\ M_x^c &= M_x + M_T & M_y^c &= M_y + M_T \end{aligned} \quad (22.12)$$

the result is

$$\begin{aligned} \sigma_{xx} &= \frac{E}{E_0} \left[\frac{N_x^c}{h^*} - z \frac{M_x^c}{I^*} - \frac{E_0 \alpha \Delta T}{1 - \nu} \right] \\ \sigma_{yy} &= \frac{E}{E_0} \left[\frac{N_y^c}{h^*} - z \frac{M_y^c}{I^*} - \frac{E_0 \alpha \Delta T}{1 - \nu} \right] \\ \sigma_{xy} &= \frac{E}{E_0} \left[\frac{N_{xy}}{h^*} - z \frac{M_{xy}}{I^*} \right] \end{aligned} \quad (22.13)$$

Clearly, once the stress resultants are obtained, the stresses are known. Equations (22.10) show that the stress resultants are known once the deflections are known. The deflections can be obtained from a differential equation and boundary conditions (plus initial conditions if there is a time-varying loading) just as in the case for beams. To obtain that plate deflection equation, it is necessary to first write equilibrium equations in terms of the stress resultants. Remember that the above equations only (i) account for continuity of deflections, by means of requiring smooth deflection functions in the strain – displacement equations; (ii) approximate the actual material description via the modified orthotropic stress–strain equations; and (iii) embody the limited equilibrium relations of the stress resultant–stress equations.

22.5 The Small Deflection Thin Plate Bending Equation

Analogous to the development of long beam theory in Chapter 10, the next thin plate theory step is to draw a free body diagram of a thin plate differential element adorned with all its various stress resultant vectors and external pressures, and from that derive equilibrium equations. For the sake of understanding the most important limitation on these forthcoming equilibrium equations, recall the fundamental difference between a vector approach to a derivation of small deflection equilibrium equations and the same approach to a derivation of finite deflection equilibrium equations. A (stress resultant) vector approach to the derivation of the general thin plate, *finite* deflection equilibrium equations, as is found in Ref. [16], requires a detailed diagram of a differential-sized thin plate element, where the originally

straight line geometry of the differential element is slightly deformed by the applied loads. As a result of the twisted and bent thin plate differential element geometry, the vectors representing the plate element's internal stress resultants and the vectors representing the external pressures are slightly out of parallel. The use of the deformed geometry makes it possible to account for the interaction between the loads (as represented by the stresses) and the thin plate deflections, and thus, for example, deal with plate buckling problems. On the other hand, a (stress resultant) vector approach to the derivation of the thin plate, *small* deflection equilibrium equations, where there are no force-deflection interactions, only requires a FBD of an undeformed differential plate element. For the sake of simplicity, only the small deflection equilibrium equations are derived here. Thus the desired thin plate free body diagrams look like those of Figs. 22.1(b, c, d). (In terms of long beam theory, this choice of diagrams is analogous to using the FBD of Fig. 10.2 rather than those of Fig. 10.3 for the purpose of deriving the beam equilibrium equations.)

To begin the derivation of the plate equilibrium equations, on the front x face and the front y face of Figs. 22.1(c, d) add the appropriate differential changes in the stress resultants. For example, on the visible front x face add $\partial Q_x/\partial x dx dy$ to $Q_x dy$, and on the out-of-view front y face realize that there is a downward lateral shear force of magnitude $(Q_y + \partial Q_y/\partial y dy) dx$. Also on Fig. 22.1(c) superimpose the applied lateral pressure loading $f_z(x, y)$ that is positive in the positive z direction, and similar in-plane applied forces per unit area as shown in Fig. 22.1(b). The result of these clarifications of the details of the forces and moments acting upon the single differential element are shown in the two sketches of Fig. 22.2 where the differential lengths have been greatly exaggerated. Summing forces in the positive x , then y , then z direction for this undeformed plate differential element yields

$$\begin{aligned} \left[N_x + \frac{\partial N_x}{\partial x} dx \right] dy - N_x dy + \left[N_{yx} + \frac{\partial N_{yx}}{\partial y} dy \right] dx - N_{yx} dx &= -f_x dx dy \\ \left[N_y + \frac{\partial N_y}{\partial y} dy \right] dx - N_y dx + \left[N_{xy} + \frac{\partial N_{xy}}{\partial x} dx \right] dy - N_{xy} dy &= -f_y dx dy \\ \left[Q_x + \frac{\partial Q_x}{\partial x} dx \right] dy - Q_x dy + \left[Q_y + \frac{\partial Q_y}{\partial y} dy \right] dx - Q_y dx &= f_z dx dy \end{aligned}$$

Summing moments about axes that pass through the center of the differential element and parallel the x and then the y coordinate axes yields

$$\begin{aligned} \left[M_y + \frac{\partial M_y}{\partial y} dy \right] dx - M_y dx + \left[M_{xy} + \frac{\partial M_{xy}}{\partial x} dx \right] dy - M_{xy} dy \\ - (Q_y dx) \left(\frac{1}{2} dy \right) - \left[Q_y + \frac{\partial Q_y}{\partial y} dy \right] dx \left(\frac{1}{2} dy \right) &= 0 \\ \left[M_x + \frac{\partial M_x}{\partial x} dx \right] dy - M_x dy - \left[M_{yx} + \frac{\partial M_{yx}}{\partial y} dy \right] dx + M_{yx} dx \\ - \left[Q_x + \frac{\partial Q_x}{\partial x} dx \right] dy \left(\frac{1}{2} dx \right) - (Q_x dy) \left(\frac{1}{2} dx \right) &= 0 \end{aligned}$$

Summing moments about the z axis leads only to the already known equation that $N_{xy} = N_{yx}$. Simplifying the above five equilibrium equations produces

$$\begin{aligned} \frac{\partial N_x}{\partial x} + \frac{\partial N_{yx}}{\partial y} = -f_x \quad \frac{\partial N_y}{\partial y} + \frac{\partial N_{xy}}{\partial x} = -f_y \quad \frac{\partial Q_x}{\partial x} + \frac{\partial Q_y}{\partial y} = f_z(x, y) \quad (22.14) \\ \frac{\partial M_y}{\partial y} + \frac{\partial M_{xy}}{\partial x} - Q_y = 0 \quad \frac{\partial M_x}{\partial x} - \frac{\partial M_{yx}}{\partial y} - Q_x = 0 \end{aligned}$$

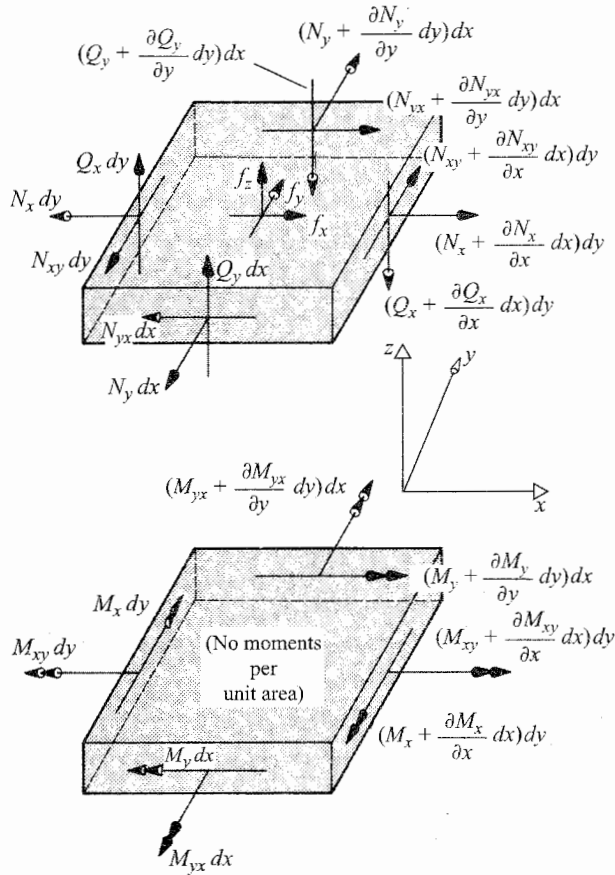


Figure 22.2. A two-part view of a single free body. Again the rectangular parallelepiped piece of plate has much exaggerated differential inplane dimensions, and the depth of the free body is the full thickness of the plate. All the forces per unit length and per unit area are shown in one sketch, while all the moments per unit length are shown in the second sketch.

Note that the first two of the above equilibrium equations are just slight variations from the plane stress equilibrium equations. Substituting Eqs. (22.10a) into these first two equilibrium equations yields, for constant m.w. thickness,

$$K^*(u_{,xx} + \nu v_{,yy}) - N_{T,x} + \frac{1}{2}(1 - \nu)K^*(v_{,xy} + u_{,yy}) = -f_x$$

$$K^*(v_{,yy} + \nu u_{,xx}) - N_{T,y} + \frac{1}{2}(1 - \nu)K^*(v_{,xx} + u_{,yy}) = -f_y$$

or

$$K^*\nabla^2 u + \frac{1}{2}(1 + \nu)K^*\frac{\partial}{\partial y}(v_{,x} - u_{,y}) - N_{T,x} = -f_x$$

$$K^*\nabla^2 v + \frac{1}{2}(1 + \nu)K^*\frac{\partial}{\partial x}(v_{,x} - u_{,y}) - N_{T,y} = -f_y$$

By adding and subtracting $u_{,xx}$ within the last parentheses of the second term, the first of the above two equations can be made to exactly parallel the first of Eqs. (7.15) when that latter equation is reduced to the plane strain case by setting w equal to a constant. Thus it is

apparent that the result of the first two plate equilibrium equations is one of the two familiar in-plane stress problems, and as such that result requires no further attention at this point.

Substituting the fourth and fifth equilibrium equations into the third equilibrium equation yields

$$\frac{\partial^2 M_x}{\partial x^2} - \frac{\partial^2 M_{yx}}{\partial x \partial y} + \frac{\partial^2 M_y}{\partial y^2} + \frac{\partial^2 M_{xy}}{\partial x \partial y} = f_z(x, y)$$

Recalling that $-M_{yx} = M_{xy}$, the above equation can be written as

$$\frac{\partial^2 M_x}{\partial x^2} + \frac{\partial^2 M_y}{\partial y^2} + 2 \frac{\partial^2 M_{xy}}{\partial x \partial y} = f_z(x, y) \quad (22.15)$$

Finally, substituting Eqs. (22.10b) into Eqs. (22.15) yields

$$\begin{aligned} \nabla^2 [D^* \nabla^2 w] - (1 - \nu) [(D^* w_{,yy})_{,xx} + (D^* w_{,xx})_{,yy} - 2(D^* w_{,xy})_{,xy}] \\ = f_z(x, y) + \nabla^2 M_T \end{aligned}$$

In this development, D^* is a constant because a constant thickness has been stipulated. Thus the second square bracketed term of the above equation goes to zero, and the remaining equation reduces to the simpler form

$$D^* \nabla^4 w(x, y) = f_z(x, y) + \nabla^2 M_T(x, y)$$

or

$$D^* [w_{,xxxx} + 2w_{,xxyy} + w_{,yyyy}] = f_z + \nabla^2 M_T \quad (22.16)$$

which is the constant-thickness, small-deflection, isotropic, thin plate bending equation. This biharmonic equation is attributed to Lagrange (Ref. [2]). Keep in mind that Eq. (22.16) is not only an equilibrium equation, but that it also incorporates the deflection continuity equations and the plate material equations.

It should be clear that this plate bending fourth order partial differential equation closely parallels, for example, the z direction beam bending fourth order ordinary differential equation without the $-Nw''$ term, which is the beam term that couples beam longitudinal to beam lateral deflections. The corresponding plate equations that incorporate the coupling between plate lateral and plate longitudinal deflections, that is, the plate finite deflection equations, are listed in Section 22.8.

Using the del-squared form of the plate bending equation makes it convenient to switch to polar coordinates if, for example, a circular plate is to be analyzed. In polar coordinates, with $w = w(r, \theta)$, Eq. (22.16) is

$$\begin{aligned} D^* \left[\frac{\partial^2}{\partial r^2} + \frac{1}{r} \frac{\partial}{\partial r} + \frac{1}{r^2} \frac{\partial^2}{\partial \theta^2} \right] \left(\frac{\partial^2 w}{\partial r^2} + \frac{1}{r} \frac{\partial w}{\partial r} + \frac{1}{r^2} \frac{\partial^2 w}{\partial \theta^2} \right) \\ = f_z(r, \theta) + \left[\frac{\partial^2}{\partial r^2} + \frac{1}{r} \frac{\partial}{\partial r} + \frac{1}{r^2} \frac{\partial^2}{\partial \theta^2} \right] M_T(r, \theta) \end{aligned}$$

Be sure to note that each term in the first set of square brackets acts upon each term within the parentheses. For example, the product

$$\left[\frac{1}{r} \frac{\partial}{\partial r} \right] \left(\frac{1}{r} \frac{\partial w}{\partial r} \right) = -\frac{1}{r^3} \frac{\partial w}{\partial r} + \frac{1}{r^2} \frac{\partial^2 w}{\partial r^2}$$

22.6 Thin Plate Boundary Conditions

The thin plate boundary conditions are much the same as those for a beam. Both the beam and plate governing differential equations are of the fourth order. Therefore in each case two boundary conditions must be stated for each boundary point. In the case of a beam the only two boundary points are the points on the beam elastic axis at the beam ends. In the case of the thin plate, there are boundary lines which are the intersection of the m.w. midplane and the edge surfaces. Each boundary line segment is, of course, a continuum of boundary points. It is possible to specify support (or lack of support) conditions (i) at individual edge points and (ii) along closed or open line intervals along a plate edge.

Just as is the case for beams, as demonstrated for beams in Endnote (3) of Chapter 15, the PVW shows that the two lateral deflection BCs for every open interval must be (i) either a bending moment statement or a statement about the plate slope normal to the plate edge, and (ii) a Kirchhoff shearing force statement (explained below) or a deflection statement. For example, for a rectangular plate with one edge defined by the equation $x = a$, "clamped" or "fixed" BCs for that entire edge would be written as

$$w(a, y) = 0 \quad \text{and} \quad w_{,x}(a, y) = 0$$

Just as for the beam, "clamped" means zero lateral deflection and zero slope normal to the edge. Of course fixed BCs at $y = b$ would be written as

$$w(x, b) = 0 \quad \text{and} \quad w_{,y}(x, b) = 0$$

If the edge at $x = a$ is "simply supported," then the lateral deflection is zero and there is no resistance to having a bending slope at that edge; that is, there is no moment about the plate edge supplied by the simple support. These circumstances at $x = a$ are written as

$$w(a, y) = 0 \quad \text{and} \quad M_x(a, y) = 0$$

The latter of these two BCs must be written in terms of the derivatives of the unknown lateral deflection function. From Eq. (22.10b),

$$M_x(a, y) = D^*[w_{,xx}(a, y) + 0] - M_T(a, y)$$

where $w_{,xy}(a, y)$ is zero because the function $w(a, y)$ is identically zero, and thus all its derivatives with respect to y are also zero. Therefore, the second BC is finally written as

$$w_{,xx}(a, y) = \frac{1}{D^*} M_T(a, y)$$

An important difference between beam and plate BCs is the difference between the BC description of a support-free beam end and a support-free plate edge. As mentioned previously, there are three plate bending stress resultants along a plate edge: (i) a bending moment; (ii) a twisting moment; and (iii) a shear force, all per unit of edge length. On the other hand, only two plate bending, twisting, and shearing BCs are possible. On the basis of the preceding work there is no way to resolve this mismatch because in this chapter the fourth order linear plate deflection equation was derived by the vector method of drawing a FBD and summing forces and moments. If, however, the small deflection (linear) plate bending equation, Eq. (22.16) had been derived on the basis of the Principle of Virtual Work or the Principle of the Minimum Value of the Total Potential Energy, then, as is demonstrated in Endnote (3) of Chapter 15, the correct boundary conditions that must be specified at each point along the edge of the plate midplane would also be part of the result of that procedure. Then it would be clear that the twisting moment and shear force stress

resultants must be combined to form one resultant shearing force per unit of edge length, called the Kirchhoff shearing force (Ref. [52]). At x face and y face edges the Kirchhoff shearing forces are symbolized as V_x and V_y , respectively. For a constant m.w. thickness, the two BCs at a free edge at $x = a$ are

$$\begin{aligned} V_x(a, y) = 0 &= D^*[w_{.xxx}(a, y) + (2 - \nu)w_{.xyy}(a, y)] - M_{T,y}(a, y) \\ M_x(a, y) = 0 &= D^*[w_{.xx}(a, y) + \nu w_{.yy}(a, y)] - M_T(a, y) \end{aligned} \quad (22.17)$$

Similarly, at a straight, unsupported edge located at $y = b$, the two BCs are

$$\begin{aligned} V_y(x, b) = 0 &= D^*[w_{.yyy}(x, b) + (2 - \nu)w_{.yxx}(x, b)] - M_{T,x}(x, b) \\ M_y(x, b) = 0 &= D^*[w_{.yy}(x, b) + \nu w_{.xx}(x, b)] - M_T(x, b) \end{aligned}$$

There is a simple explanation that can be offered for the Kirchhoff shearing force. Consider a plate edge at $x = a$. Figure 22.3(a) shows a series of twisting moments per unit length acting over a series of differential lengths along that plate edge. Recall that the twisting moment per unit length $M_{xy}(a, y)$ is the result of integrating through the plate thickness the shearing stress σ_{xy} . Figure 22.3(b) shows how partial sums of the shearing stress might change through the finite plate thickness along the same sequence of differential edge lengths so as to produce the twisting moments of Fig. 22.3(a). Figure 22.3(c) shows how those partial sums of the shearing stresses can be rearranged within each differential edge length in a statically equivalent manner. Since M_{xy} has the units of force, the partial sums that produce the twisting moments $M_{xy} dy$ can be labeled as shown in Fig. 22.3(c). Merging the two side-by-side forces in the highlighted area produces a net downward force of $M_{xy,y} dy$. When this net force is added to the shear force per unit length Q_x , which is positive downward, then the total shearing force per unit length is $V_x = Q_x + M_{xy,y}$. From Eqs. (22.14),

$$Q_x = M_{x,x} + M_{xy,y} = D^*[w_{.xxx} + \nu w_{.yyx} + (1 - \nu)w_{.xyy}] - M_{T,x}$$

and

$$M_{xy,y} = D^*(1 - \nu)[w_{.xyy}]$$

so, since $w_{.yyx} = w_{.xyy}$, as before,

$$V_x(a, y) = D^*[w_{.xxx}(a, y) + (2 - \nu)w_{.xyy}(a, y)] - M_{T,x}(a, y)$$

There is an interesting extension of the above reasoning. Figure 22.3(e) shows that there is a concentrated force of finite magnitude at the corner (0, 0) of a rectangular plate even when the twisting moment is a constant. With a constant twisting moment, along the edge $y = \text{const.}$ the vertical force arrangement shows that all the adjacent forces M_{yx} cancel out each other except at the corner where M_{yx} , acting downward, stands alone. Similarly, along the edge $x = \text{const.}$ the force M_{xy} stands alone and thus is not canceled. Since $M_{xy} = -M_{yx}$, the net downward corner force is $2M_{yx}$. The same reasoning applies at the corner when the twisting moments are not constant. The two forces $M_{yx}(0, 0)$ and $M_{xy}(0, 0)$ combine to produce the concentrated downward force $2M_{yx}$ downward, or equivalently, the upward force $2M_{xy}(0, 0)$.

The rectangular corner at (a, b) bears another downward concentrated force of the magnitude $2M_{yx}(a, b)$. The $(0, b)$ and $(a, 0)$ corners bear downward concentrated forces of magnitude $2M_{xy}(0, b)$ and $2M_{xy}(a, 0)$. These concentrated forces have no importance if they are reacted by rigid supports. However, if the plate is elastically supported by, say,

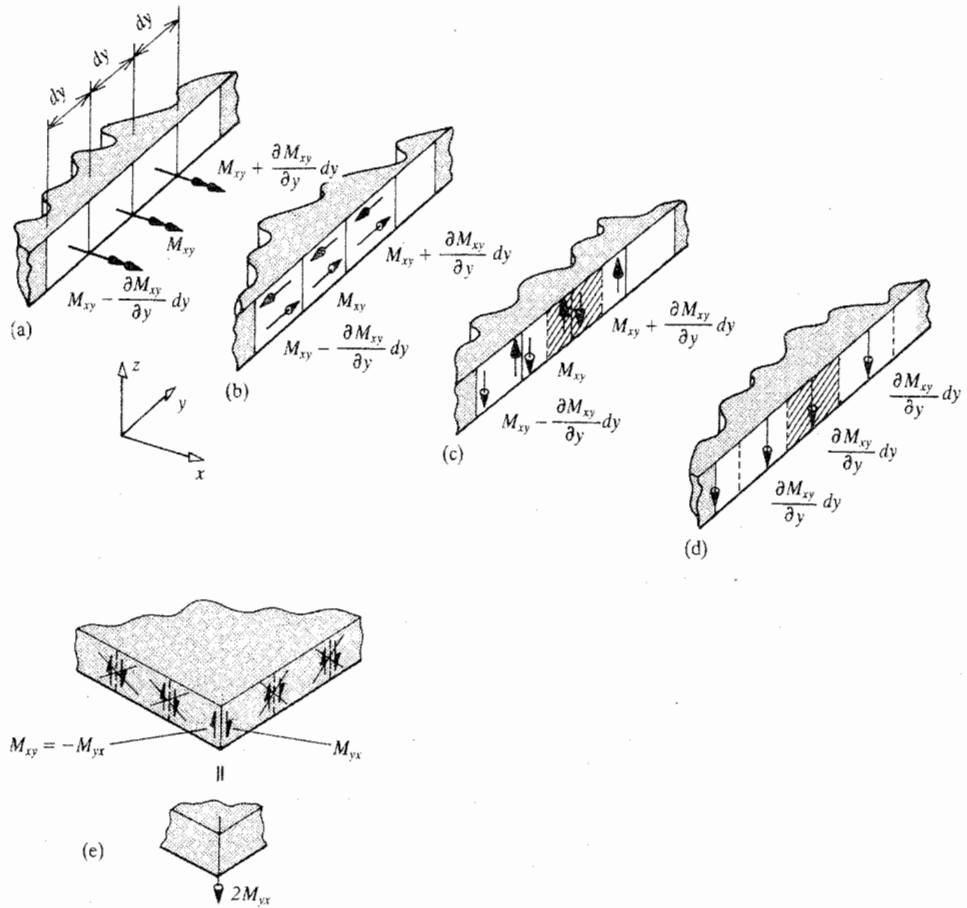


Figure 22.3. A series of differential distances along a plate edge showing: (a) how in general the twisting moment per unit length varies over three consecutive differential distances dy ; (b) how these twisting moments arose from oppositely directed shearing stresses σ_{xy} ; (c) how those equal and oppositely directed horizontal forces equivalent to the twisting moment on any one differential segment can be rearranged vertically in a statically equivalent manner; (d) the net shearing force that results from combining adjacent forces; and (e) how, even when the twisting moment per unit of length has a constant value along the plate edges, these statically equivalent vertical forces add to produce a concentrated corner force.

beams, then equal and opposite forces act upon the beam supports. In particular, in the case of beam supports at the plate straight edges, the Kirchhoff shear is transmitted as a lateral force per unit length along the length of the beam, acting upon the beam where the plate is connected to the beam, and plate edge bending moments are transmitted as twisting moments per unit length.

Boundary conditions for other than rectangular plates very closely follow the above pattern. First consider a straight edge that is not parallel to a coordinate axis such as would necessarily be found on a trapezoidal plate. For such a plate Cartesian coordinates (x, y) would still be the likely coordinate system choice. Let that skewed edge be described by the equation $y = \alpha x + \beta$. Also let there be a local Cartesian coordinate system consisting of an arc length coordinate s , and an outer normal coordinate n . Then the deflections along

that edge are simply written as $w(x, \alpha x + \beta)$ or $w((1/\alpha)(y - \beta), y)$. The normal bending slope could be written as

$$w_{,n} = w_{,x} \frac{\partial x}{\partial n} + w_{,y} \frac{\partial y}{\partial n}$$

where the values of the derivatives $\partial x/\partial n$ and $\partial y/\partial n$ are constants when the skewed edge is straight. Those constants are directly evaluated from the plate planform geometry and the usual coordinate rotation formulas. The repeated use of the chain rule allows the calculation of $w_{,nn}$ and $w_{,ns}$, and so on. For these and any other straight or curved edges, the classical BCs are

$$\text{Clamped edge : } w = 0 \quad \text{and} \quad w_{,n} = 0$$

$$\text{Simply supported edge : } w = 0 \quad \text{and} \quad w_{,nn} = \frac{M_T}{D^*}$$

$$\text{Free edge : } w_{,nn} + \nu w_{,ss} = \frac{M_T}{D^*}$$

$$\text{and} \quad w_{,nnn} + (2 - \nu)w_{,nss} = \frac{M_{T,n}}{D^*}$$

22.7 **Classical Small Deflection Plate Bending Solutions**

There are many interesting circular plate solutions. Some of those circular plate solutions can be obtained in closed form from an ordinary differential equation when the lateral loading is axisymmetric (Ref. [55]). However, few vehicular structures have non-reinforced circular plates as structural elements. Flat vehicular structures are most often rectangular beam frames or beam grids covered by an outer skin. Between the beams, the skin panel is often modeled as a rectangular plate. Closed form solutions to rectangular plate problems are unknown. Simple infinite series (open form) solutions can be obtained easily any time two opposite plate edges are simply supported. When both pairs of opposite edges are simply supported, the plate itself is called simply supported. A solution for a simply supported, thin, rectangular plate with edge lengths a and b in the x and y directions, respectively, can be obtained from the following *Navier series*:

$$w(x, y) = \sum_m \sum_n W_{mn} \sin(m\pi x/a) \sin(n\pi y/b)$$

where the series coefficients, the Fourier constants W_{mn} , are to be determined. Note that this trial function satisfies the BCs at all four plate edges: $x = 0, a$ and $y = 0, b$. When substituted into the GDE, the distributed coordinates W_{mn} can be calculated. The solution process is expedited if the applied lateral pressure $f_z(x, y)$ is also expanded into a double Fourier series. That is, also write

$$f_z(x, y) = \sum_m \sum_n f_{mn} \sin(m\pi x/a) \sin(n\pi y/b)$$

where the constant Fourier coefficients f_{mn} are calculated in the same way the Fourier coefficients c_{mn} are calculated in Example 12.3. Then, using either the orthogonality of the sine functions on the plate planform or their linear independence, the solution for the distributed coordinates is

$$W_{mn} \left[\left(\frac{m}{a} \right)^2 + \left(\frac{n}{b} \right)^2 \right]^2 = \frac{f_{mn}}{\pi^4 D}$$

Substitution of this solution in the original lateral deflection series completes the Navier series solution for the lateral deflection:

$$w(x, y) = \sum_m \sum_n \frac{f_{mn}}{\pi^4 D [(m/a)^2 + (n/b)^2]^2} \sin(m\pi x/a) \sin(n\pi y/b) \quad (22.18)$$

When two opposite plate edges are simply supported, an open form complementary solution can be obtained in the form of a *Lévy series*. For the sake of this discussion, let the simply supported sides be at $y = 0$ and at $y = b$. Then the following infinite series immediately satisfies the BCs at those two edges:

$$w_c(x, y) = \sum X_n(x) \sin(n\pi y/b)$$

Substituting into the homogeneous form of Eq. (22.16), and eliminating the sine functions as above yields the following ordinary differential equation with constant coefficients:

$$X_n''''(x) - 2 \left(\frac{n\pi}{b} \right)^2 X_n''(x) + \left(\frac{n\pi}{b} \right)^4 X_n(x) = 0$$

The solution to this equation is obtained from substituting an exponential trial function $X_n(x) = C_n \exp(r_n x)$. The algebraic equation for the parameter r_n is then

$$r_n^4 - 2 \left(\frac{n\pi}{b} \right)^2 r_n^2 + \left(\frac{n\pi}{b} \right)^4 = 0$$

The four roots of this quartic are simply obtained as

$$r_n = \frac{n\pi}{b} \quad r_n = \frac{n\pi}{b} \quad r_n = -\frac{n\pi}{b} \quad r_n = -\frac{n\pi}{b}$$

Since there are repeated roots to the characteristic equation for the homogeneous ordinary differential equation, the complementary solution must be written as

$$X_n = C_{1,n} \exp(n\pi x/b) + C_{2,n} x \exp(n\pi x/b) + C_{3,n} \exp(-n\pi x/b) + C_{4,n} x \exp(-n\pi x/b) \quad (22.19a)$$

It is usually convenient to convert the exponential functions to hyperbolic sines and cosines:

$$X_n = A_{1,n} \sinh(n\pi x/b) + A_{2,n} x \sinh(n\pi x/b) + A_{3,n} x \cosh(n\pi x/b) + A_{4,n} \cosh(n\pi x/b) \quad (22.19b)$$

In its most general form, the particular solution to Eq. (22.16) is the same double Fourier series solution that is Eq. (22.18). When Eqs. (22.18) and (22.19b) are combined as the total solution, the clamped or free or elastic BCs at $x = 0$ and $x = a$ can be used to determine the constants of integration in Eq. (22.19). Lévy series solutions often converge more quickly than Navier series solutions, especially if the applied loading is only a function of one of the spatial coordinates. In that case the particular solution can be written as a single, rather than double, Fourier series. This latter case is illustrated below.

Finally, for the case of no simply supported edges, or just one simply supported edge, or even skewed edges with any BCs, the solution of Eq. (22.16) is obtained from the superposition of up to four Lévy solutions as a complementary solution and the one Navier series as a particular solution (Ref. [45]). Many detailed plate solutions can be found in Ref. [52].

Example 22.1. A uniformly thick, homogeneous, isotropic, rectangular, simply supported plate of dimensions $a \times b$ is loaded by a uniform pressure over the left half of its area. That

is, with the midplane Cartesian coordinates x, y originating at the lower left corner of the rectangle and paralleling the plate edges, the applied loading is

$$f_z(x, y) = \begin{cases} f_0 & 0 \leq x < \frac{1}{2}a \\ 0 & \frac{1}{2}a \leq x \leq a \end{cases}$$

Write the Navier series solution for the lateral deflection for $D\nabla^4 w(x, y) = f_z(x, y)$.

Solution. The first step is to write the applied loading as a double Fourier series. As described above, let

$$f_z(x, y) = \sum \sum f_{mn} \sin(m\pi x/a) \sin(n\pi y/b) = \begin{cases} f_0 & 0 \leq x < \frac{1}{2}a \\ 0 & \frac{1}{2} \leq x \leq a \end{cases} \quad (22.20)$$

In order to utilize the orthogonality of the sine functions, multiply both sides of the above equality by sine functions with integer indices that are not the same as the summation indices; that is, multiply both sides by $(2/a) \sin(r\pi x/a)$ and $(2/b) \sin(s\pi y/b)$ where r, s are any positive integers. Then integrate that product over $0 \leq x \leq a$ and $0 \leq y \leq b$. Since the finite interval integrations and the summations are commutative, the double sum reduces to the single term

$$\begin{aligned} f_{rs} &= \frac{4f_0}{ab} \int_0^{a/2} \sin(r\pi x/a) dx \int_0^b \sin(s\pi y/b) dy \\ &= \frac{4f_0}{\pi^2 rs} [1 - \cos(r\pi/2)][1 - \cos(s\pi)] \\ &= \begin{cases} 8f_0/(\pi^2 rs) & \text{for } r, s = \text{odd, that is, } 1, 3, 5, 7, \dots \\ 16f_0/(\pi^2 rs) & \text{for } s = \text{odd, and } r = 2, 6, 10, 14, \dots \end{cases} \end{aligned}$$

Switching index r for m and index s for n , the above result can be substituted into Eq. (22.20) to complete the series representation of the applied load. Representing the lateral deflection as the double Fourier series

$$w(x, y) = \sum \sum W_{mn} \sin(m\pi x/a) \sin(n\pi y/b)$$

results in

$$D\nabla^4 w(x, y) = \sum \sum W_{mn} \left[\left(\frac{m\pi}{a} \right)^2 + \left(\frac{n\pi}{b} \right)^2 \right]^2 \sin(m\pi x/a) \sin(n\pi y/b) = f_z(x, y)$$

Equating the above series to the series representation of the applied loads, and then calling upon the linear independence of the sine functions so as to equate the coefficients of like sine functions, produces the result

$$\begin{aligned} w(x, y) &= \sum_{\text{odd}} \sum_{\text{odd}} \frac{8f_0}{\{\pi^2 mn D [(m\pi/a)^2 + (n\pi/b)^2]^2\}} \sin(m\pi x/a) \sin(n\pi y/b) \\ &\quad + \sum_{2,6,\dots} \sum_{\text{odd}} \frac{16f_0}{\{\pi^2 mn D [(m\pi/a)^2 + (n\pi/b)^2]^2\}} \sin(m\pi x/a) \sin(n\pi y/b) \end{aligned}$$

This Navier series solution is a bit slow to converge for specific values of x and y , but with modern digital computers, this particular slow convergence is not too much of a problem. ■

Example 22.2. Prepare a Lévy series solution for an isotropic, homogeneous, simply supported rectangular, thin plate of thickness h where the loading is a uniform upward pressure

of magnitude f_0 . Let the Cartesian coordinates originate at the lower left corner of the plate so that $0 \leq x \leq a$, and $0 \leq y \leq b$.

Solution. The differential equation to be solved is $D\nabla^4 w(x, y) = f_0$. Since both pairs of opposite plate edges are simply supported, the solution can be written as either

$$w(x, y) = \sum X_n(x) \sin(n\pi y/b) \quad \text{or} \quad w(x, y) = \sum Y_n(y) \sin(n\pi x/a)$$

The corresponding single series for the applied loading are, respectively,

$$f_0 = \sum f_n \sin(n\pi y/b) \quad \text{or} \quad f_0 = \sum f_n \sin(n\pi x/a)$$

For the sake of variety, the second listed matching possibilities for $w(x, y)$ and f_0 are selected for development. The first step is to obtain the Fourier coefficients for the applied loading. Multiplying both sides of the applied load series by $(2/a) \sin(m\pi x/a)$, and integrating between $x = 0$ and $x = a$, produces the following solution for f_n :

$$f_n = \begin{cases} \frac{4f_0}{n\pi} & \text{when } n = \text{odd integer} \\ 0 & \text{when } n = \text{even integer} \end{cases}$$

Thus

$$f_0 = \frac{4f_0}{\pi} \sum_{\text{odd } n} \frac{1}{n} \sin(n\pi x/a)$$

Substituting both the deflection series and the loading series into the differential equation $D\nabla^4 w(x, y) = f_0$, and using linear independence in order to isolate n th terms, the differential equation for $Y_n(y)$ reduces, for $n = \text{odd integers}$, to

$$Y_n''''(y) - 2\left(\frac{n\pi}{a}\right)^2 Y_n''(y) + \left(\frac{n\pi}{a}\right)^4 Y_n(y) = \frac{4f_0}{n\pi D}$$

and, of course, $Y_n = 0$ for all even values of the index n . The particular solution is the constant value $4f_0 b^4 / (\pi n^5 D \beta^4)$, where

$$\beta = \frac{\pi b}{a}$$

The complementary solution is merely a slight modification of Eq. (22.19b). Thus the total solution can be written as

$$Y_n = B_{1,n} \sinh(n\pi y/a) + B_{2,n} \cosh(n\pi y/a) + \bar{B}_{3,n} y \cosh(n\pi y/a) + \bar{B}_{4,n} y \cosh(n\pi y/a) + \frac{4f_0 b^4}{\pi n^5 D \beta^4}$$

where the bars over the latter two constants of integration are temporary conveniences. Letting $\xi = y/b$, the above solution can be rewritten as

$$Y_n = B_{1,n} \sinh(n\beta\xi) + B_{2,n} \cosh(n\beta\xi) + B_{3,n} \xi \cosh(n\beta\xi) + B_{4,n} \xi \cosh(n\beta\xi) + \frac{4f_0 b^4}{\pi n^5 D \beta^4} \quad (22.21)$$

If the x coordinate axis had been placed along the centerline of the thin plate, the above solution would have to be even in y . Thus it would be immediately possible to drop the first and third terms of Eq. (22.21) because they are odd functions of y . Continuing with the

original coordinate axis placement, the BCs that remain to be satisfied are those at $y = 0, b$; that is, the four conditions

$$w(x, 0) = w_{,yy}(x, 0) = w(x, b) = w_{,yy}(x, b) = 0$$

determine the four constants of integration for each value of the integer index n . Substituting the series solution $w(x, y) = \sum Y_n(y) \sin(n\pi x/a)$ into the above BCs and again using the linear independence of the sine functions yields

$$Y_n(0) = Y_n''(0) = Y_n(b) = Y_n''(b) = 0$$

The first BC quickly yields the result

$$B_{2,n} = -\frac{4f_0b^4}{\pi n^4 D\beta^3}$$

The second BC produces the result

$$B_{4,n} = +\frac{2f_0b^4}{\pi n^4 D\beta^3}$$

The latter two BCs need to be solved simultaneously. The result is

$$B_{1,n} = -\frac{2f_0b^4}{\pi n^4 D\beta^3} \operatorname{csch}(b\beta) \left(\frac{2}{n\beta} [1 - \cosh(n\beta)] - \operatorname{csch}(n\beta) + \operatorname{coth}(n\beta) \right)$$

$$B_{3,n} = +\frac{2f_0b^4}{\pi n^4 D\beta^3} [\operatorname{csch}(n\beta) - \operatorname{coth}(n\beta)]$$

Substitution of the above solutions for the constants of integration into Eq. (22.21), and the subsequent substitution of the now completely detailed expression for $Y_n(y)$ into the series $w(x, y) = \sum Y_n(y) \sin(n\pi x/a)$ completes the solution for the midplane lateral deflections. This Lévy series solution is more work than a Navier series solution, but the presence of the index n raised to the fourth power or fifth power in the denominator of each part of Y_n means that this Lévy series is very quick to converge for any point $P(x, y)$ on the plate midplane. ■

22.8 **Plate Buckling and Its Uses**

Plate buckling analyses require plate equations that account for the interaction between the plate lateral deflection, $w(x, y)$, and the plate in-plane stress resultants, N_x, N_y , and N_{xy} . The small-deflection plate bending equations studied above do not account for this interaction. Only finite deflection equations, based upon the deformed plate geometry, can describe that interaction. The added complexity of the deformed plate geometry results in a mathematical coupling between the finite deflection in-plane plate equation and the finite deflection plate bending equation. This mathematical coupling reflects, of course, the physical interaction between the lateral and in-plane plate deflections and stress resultants. Fortunately for the analyst, this coupling is similar to that for beams in one important sense. If the values of the in-plane stress resultants N_x, N_y , and N_{xy} are known, then the analyst can devote his or her entire attention to the plate bending equation, which can be written exclusively in terms of the plate lateral deflection $w(x, y)$ and the known in-plane stress resultants N_x, N_y , and N_{xy} . Thus the problem focuses on the one unknown function, $w(x, y)$.

There is a major difficulty in the case of the finite deflection, plate bending equation that is not present in the case of the finite deflection beam bending equation. Unlike the value

of the beam axial force N along the length of a beam-column when the beam-column is loaded only by axial forces at the beam ends and the beam begins to buckle, the values of the plate in-plane stress resultants N_x , N_y , and N_{xy} are not quite constant at a given plate cross-section even when the in-plane loadings at the outer plate edges have constant values along the outer plate edges while the plate begins to buckle. For example, along any interior cut through the thickness of the plate, such as at a fixed value of x , the in-plane stress resultants N_x and N_{xy} still vary with y . This circumstance means that the finite deflection plate equation has nonconstant coefficients even in the case of constant edge loadings if the buckling deflections are truly finite. However, the following reasoning can be used for the adjacent equilibrium approach to plate buckling. Consider a flat plate loaded only within its midplane. That is, let there be no lateral loading. At the critical values of the in-plane stress resultants, the plate can be either flat or very slightly buckled. When the plate is flat, the in-plane equilibrium equations $N_{x,x} + N_{xy,y} = 0$ and $N_{y,y} + N_{xy,x} = 0$ are clearly satisfied by constant values of $N_x(x, y)$, $N_y(x, y)$, and $N_{xy}(x, y)$. Furthermore, from Eqs. (22.13) and (22.8), the constant values of the in-plane forces lead to constant values for the stresses and the strains. Thus the flat plate compatibility equations are satisfied. If, also, the interior constant in-plane forces per unit length match the constant in-plane forces at the plate boundaries, then those constant values are the valid solution for the in-plane stress resultants. Now, although those in-plane forces are no longer constant when the plate undergoes finite lateral deflections, the in-plane forces can be expected to be very close to those constant values if the plate lateral deflections are very close to zero. In other words, if the plate is loaded at its outer boundaries by constant values of N_x , N_y , and N_{xy} , then it is reasonable to approximate the internal values of those in-plane forces by their constant values at the boundaries whenever the lateral deflections are very small. This is all the leeway that is needed to proceed with an adjacent equilibrium analysis using the constant boundary values of the in-plane loadings as the values of the interior, in-plane stress resultants. Here, once again, "adjacent" means very close to the flat plate equilibrium position.

Let, as before, f_x and f_y be applied forces per unit area of the midplane in the x and y directions, respectively, positive in the positive coordinate directions. Let the m.w. thickness be a constant. Then, skipping over a derivation that differs from the above derivation of the plate small deflection equations in the same way that the finite and small beam deflection equations of Sections 10.2 and 10.3 differ, the finite deflection plate bending equation is, from Ref. [16],

$$D^*\nabla^4 w = f_z + \nabla^2 M_T + (N_x w_{,xx} + 2N_{xy} w_{,xy} + N_y w_{,yy}) - (f_x w_{,x} + f_y w_{,y}) \quad (22.22a)$$

Note that the first set of terms within parentheses clearly correspond to the beam bending $-Nw''$ and $-Nv''$ terms. With the first two terms and the last two terms of the right-hand side set to zero, this is the equation that can be used to calculate the in-plane boundary forces per unit length that cause the plate to begin to buckle. For the record, the other nonlinear plate equation is stated and briefly discussed in Endnote (1).

Example 22.3. Write the GDE and BCs that determine the Euler buckling load for a simply supported rectangular plate of size a by b loaded at the edges $x = 0$ and $x = a$ by a uniform compressive load of magnitude N_0 per unit of edge length; see Fig. 22.4(a).

Comment. Plate buckling is of interest not only for itself, but it is important for understanding local buckling in the flanges and webs of open and closed section, thin-walled beams.

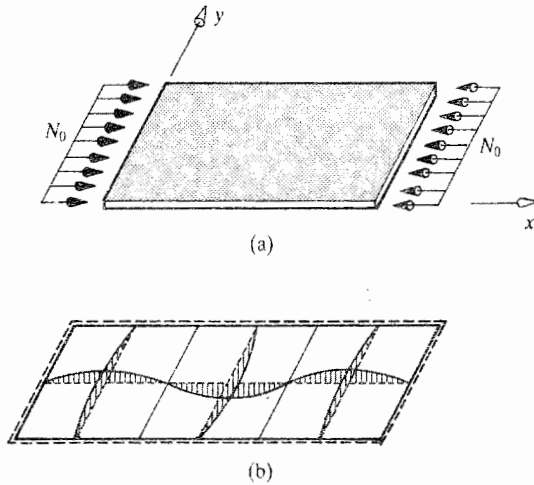


Figure 22.4. Example 22.3. (a) A simply supported plate with a uniform in-plane edge loading in the x direction, (b) The buckling pattern (mode shape) for this plate when the plate aspect ratio, a/b , has the value 3.0.

The reason is that the flanges can be modeled as long plates with simple support along one long edge, and support-free along the other long edge. Webs can be modeled as long plates with simple supports along the two near edges.

Solution. From Eqs. (22.14), the in-plane equilibrium equations for the only slightly buckled plate are

$$\frac{\partial N_x}{\partial x} + \frac{\partial N_{yx}}{\partial y} = 0 \quad \frac{\partial N_y}{\partial y} + \frac{\partial N_{xy}}{\partial x} = 0$$

Relying on the experience of Chapter 1 to guess that the equilibrium solution is $N_x = -N_0$, $N_y = N_{xy} = 0$. This solution, of course, also satisfies the in-plane BCs, and the resulting constant strains satisfy the linear strain compatibility equation. Hence $N_x = -N_0$, $N_y = N_{xy} = 0$ is an appropriate approximate solution for the in-plane stress resultants per unit length within the slightly buckled plate. With this solution, with no temperature change, and no lateral load, the lateral deflection GDE, Eq. (22.22), becomes

$$D[w_{,xxxx} + 2w_{,xxyy} + w_{,yyyy}] = -N_0 w_{,xx}$$

The BCs are that the lateral deflection and bending moment at each edge is zero. That is, $w(0, y) = w(x, b) = w(a, y) = w(x, 0) = 0$, and $w_{,xx}(0, y) = w_{,yy}(x, b) = w_{,xx}(a, y) = w_{,yy}(x, 0) = 0$. Of course this is an eigenvalue problem where N_0 , or N_0/D is the unknown eigenvalue, and $w(x, y)$ is the unknown eigenfunction. ■

Example 22.4. Solve the previous example problem for the buckling load, N_0 , and the buckling deflection mode shape.

Solution. Test as a trial buckling mode shape the function

$$w(x, y) = W_{mn} \sin(m\pi x/a) \sin(n\pi y/b)$$

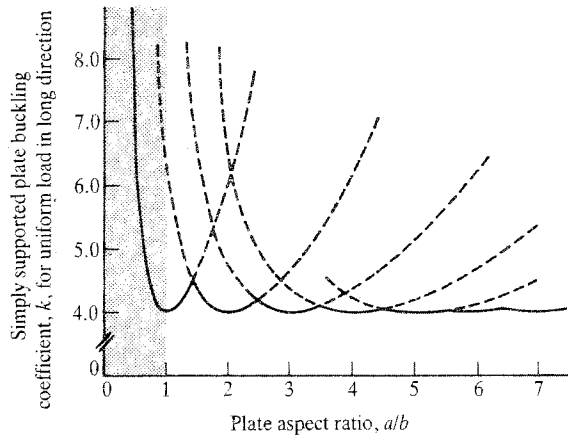


Figure 22.5. Example 22.4. A plate buckling coefficient plot.

where W_{mn} is an unknown constant value, and m and n are unknown integers. This trial function satisfies all the BCs. Substituting the trial function into the GDE yields, after canceling the sine functions and the unknown constant W_{mn} ,

$$D \left[\left(\frac{m\pi}{a} \right)^2 + \left(\frac{n\pi}{b} \right)^2 \right]^2 = + \left(\frac{m\pi}{a} \right)^2 N_0$$

Solving for the eigenvalue N_0 yields the solution for the critical value:

$$N_0 = \frac{\pi^2 D}{b^2} \left(m \frac{b}{a} + \frac{n^2 a}{m b} \right)^2 = k \frac{\pi^2 D}{b^2}$$

where the definition of the plate buckling coefficient $k = k(a/b, m, n)$ is apparent. The buckling load, $(N_0)_{cr}$, depends on the minimum value of N_0 in the above equation, which, in turn, depends upon the minimum value of k . Clearly, the minimum value of k occurs when $n = 1$. The presence of m in the denominator of the second part of k means that $m = 1$ is not necessarily the value that produces the minimum value of k . For example, if $a/b = 1$ (a square plate), then a simple tabulation shows that in this case $m = 1$ does lead to a minimum value of $k = 4$, and $(N_0)_{cr} = (2\pi/b)^2 D$. In this case the plate bulges on one side or the other with a maximum deflection at the plate center. However, if $a/b = 3$, then the minimum value for N_0 is achieved when $m = 3$. In this case, while there is still a single half sine wave in the y direction, the plate has three half sine wave undulations in the x direction. See Fig. 22.4(b). Figure 22.5 shows a plot of the minimum values of k for various plate aspect ratios. This scalloped plot is typical of other boundary conditions as well as the simply supported case discussed here (Ref. [16]). As is the case with the beam, this adjacent equilibrium analysis is insufficient to develop the actual relation between the arbitrary factor W_{mn} , which is the peak lateral deflection, and the applied load. ■

The above analysis corresponds closely to an Euler analysis for beams. In particular, if the plate is thin enough (as the beam is long enough) then the plate buckles while all stresses remain less than the yield stress. Thus, in these circumstances, when the compressive axial load is removed, the plate (or beam) snaps back to its original geometry. If the perfect plate

is sufficiently thick relative to its in-plane dimensions, the normal inplane stress reaches the yield stress value before the plate undergoes elastic buckling. In an imperfect plate, or a perfect plate with imperfect loading, that is sufficiently thick, the combination of the bending stress and the direct stress may reach the yield stress value before the plate buckles elastically. In this case the plate (or beam) buckles plastically at the load corresponding to the yield stress or a slightly lesser load. The plate (or beam) develops what is called a plastic hinge as it bends, and of course there is no complete return to the original geometry if the compressive load is removed. As discussed before, there is a smooth transition between the Euler buckling regime and the case where, prior to buckling, the applied stress reaches the yield stress over the entire plate or beam cross-section.

Postbuckling analysis of plates shows that plate behavior after buckling is much different than that for beams. As is shown in Ref. [3], very little additional load can be applied to a beam after buckling. The beam deflections become very large very quickly. The result of the large beam deflections is that the beam bending stresses quickly reach the yield stress value, and the beam collapses soon afterward. In the case of the simply supported plate, the bending deflections are restricted by the plate side supports. With the bending deflections so restricted, so too are the bending stresses. Before buckling, the perfect plate has the same stiffness at every point along the loaded edges $x = 0, a$. After buckling, because of the greater bowing out of the plate center, the plate stiffness in the loading direction along the center half of the loaded plate edges is much less than the stiffness at those portions of the loaded plate edges near the supports at $y = 0, b$. The load and the applied stress redistribute themselves accordingly, with the great majority of the stress in the direction of the load acting near the supports at $y = 0, b$. In marine structures, it has been customary to ignore the much smaller in-plane load-carrying capacity of the central portion of the plate by modeling the outer portions only of the plate as additional flange areas for the supporting beam frame/grid.

Another aspect of beam postbuckling behavior is that while the buckling load of an actual (i.e., imperfect) beam is readily determined experimentally, such is not the case for imperfect plates with side supports. The increase in the plate lateral deflections can be too gradual with increasing applied load to allow clear identification of the buckling load.

22.9 A Simple Plate Bending Finite Element

The stiffness matrices for plate finite elements with triangular and quadrilateral planforms are more complicated to derive than the stiffness matrix for a rectangular plate finite element. Thus, while recognizing the advantages of the triangular and quadrilateral shapes for representing plates with nonrectangular geometries, this introduction is limited to discussing the isotropic, rectangular plate finite element for small deflections. The rectangular plate bending finite element to be discussed here is sketched in Fig. 22.6. Somewhat similarly to the beam bending finite element, the DOF are the lateral deflections and the two orthogonal rotations at each of the four corners.

As before the plate finite element lateral deflections, $w(x, y)$, within the rectangle and at its circumference are represented by a polynomial expansion. The polynomial expression involves all polynomial terms up through a complete set of cubic terms, plus the quartic terms x^3y and xy^3 . Therefore there are 12 polynomial terms to match the same number of element DOF. The choice of those polynomial terms has several advantages. The first advantage is that there is a symmetry or balance between the x and y coordinates; that is, for each term in the finite series expansion $x^n y^m$, there is a corresponding term $x^m y^n$.

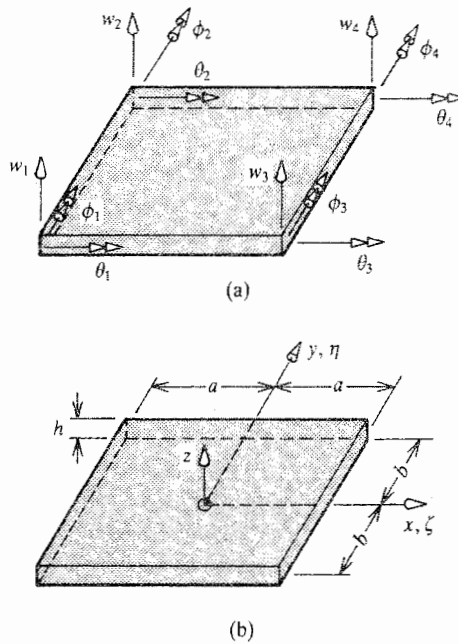


Figure 22.6. A rectangular plate bending finite element. (a) The element DOF. (b) The element coordinate systems and dimensions.

This symmetry means that the finite element behaves exactly in the same manner in the x direction as it does in the y direction. Thus an isotropic plate modeled by these elements would behave in the same manner in all directions.

The second advantage is that each polynomial term of the series expansion is a solution for Eq. (22.16). Thus, with this series expansion for $w(x, y)$, the small-deflection plate equilibrium equations, the isotropic stress-strain equations, and the strain-displacement equations are all satisfied within the element boundaries. This would not be true, for example, if the x^2y^2 polynomial term was included in the series expansion.

The third advantage of this expansion concerns interelement deflection continuity. Note that the element Cartesian coordinates system is chosen to parallel the finite element edges. Thus along any rectangular outer edge either x or y is a constant, while the other of the two Cartesian coordinates varies over the edge length. By setting either x or y equal to a constant in the 12-term polynomial expansion for the lateral deflection, it becomes evident that each lateral edge deflection is described by a cubic polynomial which has four independent polynomial coefficients. Recall from the study of the beam bending finite element that the two beam end deflection DOF and the two beam end bending slope DOF completely control the (cubic) beam deflections everywhere in the interior of the beam element. The same sort of control over the edge deflections is exercised by the corner DOF of the plate element along any element boundary edge. The argument proceeds as follows for a plate element where x has a fixed value. Since there are two shared nodes at each corner of any two adjacent rectangular elements, and since each node has a deflection and a θ DOF, then the two common nodes at the two ends of the common boundary between the two elements provide the same four controlling parameters (the four DOF) that fully specify the same cubic form of each adjacent element's lateral edge deflections at the common boundary between the two nodes. Thus this choice of polynomial terms and element DOF

ensures complete deflection continuity between these finite elements and beam elements as well.

The problem is that the lateral deflection slopes normal to a common element boundary are not the same. For example, the normal slope $\partial w/\partial x$ at the left and right element edges (fixed values of x) of the element pictured in Fig. 22.6(a), is also a cubic polynomial in terms of the variable y . However, there are only the two ϕ DOF available to specify the four parameters of this cubic polynomial. Thus the two cubic polynomials of the adjacent element edges do not necessarily coincide. Therefore this approach leads to “creases” or “folds” at the element boundaries between the nodes in this rectangular finite element representation of the deflected plate. (Of course the common nodal DOF make the normal and all other slopes the same at the common nodes.) The creases or folds between the nodes are obviously not a good mathematical description of the actual smooth plate behavior. This problem can be overcome with more complicated finite elements. However, this simple but interelement slope-discontinuous finite element is frequently used because, in addition to being simple, it has proved through repeated testing to be accurate (Ref. [50]). It seems that the increased flexibility of the finite element model caused by allowing creases between elements is largely offset by the overestimate of the bending stiffness within the finite element caused by the use of so few polynomial terms to represent the true bending deflections.

In addition to extensive analytical testing, the seriousness of this interelement slope discontinuity can be approached mathematically. In mathematical terms, this four-node rectangular element is C^0 continuous, but not C^1 continuous. Now, consider a plate modeled by a finite element grid. As is seen below, the internal virtual work (or internal potential energy) expression for a plate involves the second partial derivatives of the plate lateral deflections. These three second partial derivatives are, of course, well defined within the internal areas of each finite element. At the element boundaries where the first partial derivatives in the normal directions are discontinuous, the normal and mixed second partial derivatives are infinite. However, this singularity is not a difficulty in the evaluation of the internal virtual work area integral. This is so because the elements are C_0 continuous and thus the boundary between adjacent elements is merely a line rather than a gap or overlap. As a line, even with infinite values for the integrand along that line, the area integral is zero. Thus there is no contribution to the internal virtual work by the infinite values of two of the second partial derivatives at the boundary and hence the internal virtual work and the resulting stiffness matrix are uniquely defined.

Accepting interelement normal slope discontinuity, the above-mentioned 12 polynomial terms can be arranged in the following suitable shape functions, N_i , where $w(\zeta, \eta) = [N(\zeta, \eta)] \{q\}$. The nondimensional coordinates $\zeta = x/a$, and $\eta = y/b$ are based on the local Cartesian coordinates x, y that originate at the element center as shown in Fig. 22.6(b). Ordering the DOF as

$$\{q\} = [w_1 \quad \theta_1 \quad \phi_1 \quad w_2 \quad \cdots \quad w_4 \quad \theta_4 \quad \phi_4]$$

then

$$N_1(\zeta, \eta) = +(1/8)(1 - \zeta)(1 - \eta)(2 - \zeta - \eta - \zeta^2 - \eta^2)$$

$$N_2(\zeta, \eta) = +(b/8)(1 - \zeta)(1 - \eta)^2(1 + \eta)$$

$$N_3(\zeta, \eta) = +(a/8)(1 - \zeta)^2(1 + \zeta)(1 - \eta)$$

$$N_4(\zeta, \eta) = +(1/8)(1 - \zeta)(1 + \eta)(2 - \zeta + \eta - \zeta^2 - \eta^2)$$

$$N_5(\zeta, \eta) = -(b/8)(1 - \zeta)(1 + \eta)^2(1 - \eta)$$

$$N_6(\zeta, \eta) = +(a/8)(1 - \zeta)^2(1 + \zeta)(1 + \eta)$$

$$\begin{aligned}
 N_7(\zeta, \eta) &= +(1/8)(1 + \zeta)(1 - \eta)(2 + \zeta - \eta - \zeta^2 - \eta^2) \\
 N_8(\zeta, \eta) &= +(b/8)(1 + \zeta)(1 - \eta)^2(1 + \eta) \\
 N_9(\zeta, \eta) &= -(a/8)(1 + \zeta)^2(1 - \zeta)(1 - \eta) \\
 N_{10}(\zeta, \eta) &= +(1/8)(1 + \zeta)(1 + \eta)(2 + \zeta + \eta - \zeta^2 - \eta^2) \\
 N_{11}(\zeta, \eta) &= -(b/8)(1 + \zeta)(1 + \eta)^2(1 - \eta) \\
 N_{12}(\zeta, \eta) &= -(a/8)(1 + \zeta)^2(1 - \zeta)(1 + \eta)
 \end{aligned}$$

As an aid in checking that the above shape functions have the correct values at the four corners, note, for example,

$$\begin{aligned}
 N_{1,x} &= (1/a)N_{1,\zeta} = -(1/8a)(1 - \eta)(3 - \eta - \eta^2 - 3\zeta^2) \\
 N_{1,y} &= (1/b)N_{1,\eta} = -(1/8b)(1 - \zeta)(3 - \zeta - \zeta^2 - 3\eta^2) \\
 N_{3,x} &= (1/a)N_{3,\zeta} = -(1/8a)(1 - \eta)(1 + 2\zeta - 3\zeta^2) \\
 N_{3,y} &= (1/b)N_{3,\eta} = -(a/8b)(1 + \zeta)(1 - \zeta)^2 \\
 N_{7,x} &= (1/a)N_{4,\zeta} = +(1/8a)(1 - \eta)(3 - \eta - \eta^2 - 3\zeta^2) \\
 N_{7,y} &= (1/b)N_{4,\eta} = -(1/8b)(1 + \zeta)(3 + \zeta - \zeta^2 - 3\eta^2) \\
 N_{9,x} &= (1/a)N_{6,\zeta} = +(1/8a)(1 - \eta)(1 - 2\zeta - 3\zeta^2) \\
 N_{9,y} &= (a/8b)N_{6,\eta} = +(a/8b)(1 - \zeta)(1 + \zeta)^2
 \end{aligned}$$

Again, once the shape functions are in place, the rest of the process is routine. The three plane strains are obtained from partially differentiating $w(\zeta, \eta) = [N(\zeta, \eta)] \{q\}$ twice in each case as per Eqs. (22.7). That is, the strain vector is

$$\{\gamma\} = \begin{Bmatrix} \epsilon_{xx}(x, y, z) \\ \epsilon_{yy}(x, y, z) \\ \gamma_{xy}(x, y, z) \end{Bmatrix} = -z \begin{Bmatrix} w_{,xx} \\ w_{,yy} \\ 2w_{,xy} \end{Bmatrix} = z[B] \{q\}$$

The stress vector is obtained from Eq. (6.13). That is, $\{\sigma\} = [E] \{\gamma\} - \Delta T \{A\}$. Then, for the homogeneous, isotropic element,

$$[k] = \int_{-h/2}^{+h/2} z^2 dz \int_{-a}^a \int_{-b}^b [B]^t [E] [B] dx dy \quad (22.23)$$

The evaluation of the above integrals leads to the following symmetric 12×12 element stiffness matrix equation credited to Adini and Clough (Ref. [57]), and Melosh (Ref. [58]). From Ref. [50], which sets forth the orthotropic stiffness matrix, the isotropic matrix equation may be written as

$$\begin{Bmatrix} V_1 \\ M_{1y}/2a \\ M_{1x}/2b \\ V_2 \\ M_{2y}/2a \\ M_{2x}/2b \\ \vdots \\ M_{4x}/2b \end{Bmatrix} = \frac{D}{60ab} \begin{bmatrix} k_{1,1} & k_{1,2} & k_{1,3} & \cdots & k_{1,12} \\ k_{2,1} & k_{2,2} & k_{2,3} & \cdots & k_{2,12} \\ k_{3,1} & k_{3,2} & k_{3,3} & \cdots & k_{3,12} \\ k_{4,1} & k_{4,2} & k_{4,3} & \cdots & k_{4,12} \\ k_{5,1} & k_{5,2} & k_{5,3} & \cdots & k_{5,12} \\ k_{6,1} & k_{6,2} & k_{6,3} & \cdots & k_{6,12} \\ \vdots & \vdots & \vdots & \cdots & \vdots \\ k_{12,1} & k_{12,2} & k_{12,3} & \cdots & k_{12,12} \end{bmatrix} \begin{Bmatrix} w_1 \\ 2a\theta_1 \\ 2b\phi_1 \\ w_2 \\ 2a\theta_2 \\ 2b\phi_2 \\ \vdots \\ 2b\phi_4 \end{Bmatrix} \quad (22.24)$$

where $p = a/b$, and

$$\begin{aligned}
 k_{1,1} &= (60/p^2) + 60p^2 + 42 - 12\nu & k_{2,1} &= +30p^2 + 3 + 12\nu \\
 k_{2,2} &= +20p^2 + 4 - 4\nu & k_{3,1} &= -(30/p^2) - 3 - 12\nu \\
 k_{3,2} &= -15\nu & k_{3,3} &= (20/p^2) + 4 - 4\nu \\
 k_{4,1} &= (30/p^2) - 60p^2 - 42 + 12\nu & k_{4,2} &= -30p^2 - 3 + 3\nu \\
 k_{4,3} &= -(15/p^2) + 3 + 12\nu & k_{4,4} &= (60/p^2) + 60p^2 + 42 - 12\nu \\
 k_{5,1} &= +30p^2 + 3 - 3\nu & k_{5,2} &= +10p^2 - 1 + \nu \\
 k_{5,3} &= 0 & k_{5,4} &= -30p^2 - 3 + 12\nu \\
 k_{5,5} &= +20p^2 + 4 - 4\nu & k_{6,1} &= -(15/p^2) + 3 + 12\nu \\
 k_{6,2} &= 0 & k_{6,3} &= (10/p^2) - 4 + 4\nu \\
 k_{6,4} &= -(30/p^2) - 3 - 12\nu & k_{6,5} &= +15\nu \\
 k_{6,6} &= +(20/p^2) + 4 - 4\nu & k_{7,1} &= -(60/p^2) + 30p^2 - 42 + 12\nu \\
 k_{7,2} &= +15p^2 - 3 + 12\nu & k_{7,3} &= +(30/p^2) + 3 - 3\nu \\
 k_{7,4} &= -(30/p^2) - 30p^2 + 42 - 12\nu & k_{7,5} &= +15p^2 - 3 + 3\nu \\
 k_{7,6} &= +15p^2 - 3 + 3\nu & k_{7,7} &= (60/p^2) + 60p^2 + 42 - 12\nu \\
 k_{8,1} &= +15p^2 - 3 - 12\nu & k_{8,2} &= +10p^2 - 4 + 4\nu \\
 k_{8,3} &= 0 & k_{8,4} &= -15p^2 + 3 - 3\nu \\
 k_{8,5} &= +5p^2 + 1 - \nu & k_{8,6} &= 0 \\
 k_{8,7} &= +30p^2 + 3 + 12\nu & k_{8,8} &= 20p^2 + 4 - 4\nu \\
 k_{9,1} &= -(30/p^2) - 3 + 3\nu & k_{9,2} &= 0 \\
 k_{9,3} &= +(10/p^2) - 1 + \nu & k_{9,4} &= -(15/p^2) + 3 - 3\nu \\
 k_{9,5} &= 0 & k_{9,6} &= -(5/p^2) + 1 - \nu \\
 k_{9,7} &= +(30/p^2) + 3 + 12\nu & k_{9,8} &= 15\nu \\
 k_{9,9} &= +(20/p^2) + 4 - 4\nu & k_{10,1} &= -(30/p^2) - 30p^2 + 42 + 12\nu \\
 k_{10,2} &= -15p^2 + 3 - 3\nu & k_{10,3} &= +(15/p^2) - 3 + 3\nu \\
 k_{10,4} &= -(60/p^2) + 30p^2 - 42 + 12\nu & k_{10,5} &= -(15/p^2) + 3 + 12\nu \\
 k_{10,6} &= +(30/p^2) + 3 - 3\nu & k_{10,7} &= +(30/p^2) - 60p^2 - 42 + 12\nu \\
 k_{10,8} &= -30p^2 - 3 + 3\nu & k_{10,9} &= +(15/p^2) - 3 - 12\nu \\
 k_{10,10} &= +(60/p^2) + 60p^2 + 42 - 12\nu & k_{11,1} &= +15p^2 - 3 + 3\nu \\
 k_{11,2} &= +5p^2 + 1 - \nu & k_{11,3} &= 0 \\
 k_{11,4} &= -15p^2 + 3 + 12\nu & k_{11,5} &= +10p^2 - 4 + 4\nu \\
 k_{11,6} &= 0 & k_{11,7} &= +30p^2 + 3 - 3\nu \\
 k_{11,8} &= +10p^2 - 1 + \nu & k_{11,9} &= 0 \\
 k_{11,10} &= -30p^2 - 3 - 12\nu & k_{11,11} &= +20p^2 + 4 - 4\nu \\
 k_{12,1} &= -(15/p^2) + 3 - 3\nu & k_{12,2} &= 0 \\
 k_{12,3} &= +(5/p^2) + 1 - \nu & k_{12,4} &= -(30/p^2) - 3 + 3\nu \\
 k_{12,5} &= 0 & k_{12,6} &= +(10/p^2) - 1 + \nu \\
 k_{12,7} &= +(15/p^2) - 3 - 12\nu & k_{12,8} &= 0 \\
 k_{12,9} &= -(10/p^2) - 4 + 4\nu & k_{12,10} &= +(30/p^2) + 3 + 12\nu \\
 k_{12,11} &= -15\nu & k_{12,12} &= +(20/p^2) + 4 - 4\nu
 \end{aligned}$$

The other 66 stiffness terms are inferred from the symmetry of the stiffness matrix. Exercise 22.9 asks the reader to verify the stiffness matrix term $k_{7,7}$.

Example 22.5. Return to Example 19.2, and Fig. 19.5(d). Set up $\{Q\} = [K]\{q\}$ for the beam-plate bending problem. Make use of symmetry and use only two square plate bending finite elements. Let the relevant symmetric beam area moment of inertia be $3.0h^4$. Let the Poisson's ratio of the plate be $1/3$. Let the global DOF be identified as indicated in Fig. 22.7.

and for the half-beam

$$[k_{30}]\{q\} = \frac{Eh}{18000} \begin{bmatrix} 12 & -180h \\ -180h & 3600h^2 \end{bmatrix} \begin{Bmatrix} w_5 \\ (-\phi_5) \end{Bmatrix}$$

$$[k_{40}]\{q\} = \frac{Eh}{18000} \begin{bmatrix} 12 & 180h & -12 & 180h \\ 180h & 3600h^2 & -180h & 1800h^2 \\ -12 & -180h & 12 & -180h \\ 180h & 1800h^2 & -180h^2 & 3600h^2 \end{bmatrix} \begin{Bmatrix} w_5 \\ -\phi_5 \\ w_6 \\ -\phi_6 \end{Bmatrix}$$

or

$$[k_{30}]\{q\} = \frac{Eh}{144000} \begin{bmatrix} 96 & 1440h \\ 1440h & 28800h^2 \end{bmatrix} \begin{Bmatrix} w_5 \\ \phi_5 \end{Bmatrix}$$

$$[k_{40}]\{q\} = \frac{Eh}{144000} \begin{bmatrix} 96 & -1440h & -96 & -1440h \\ -1440h & 28800h^2 & 1440h & 14400h^2 \\ -96 & 1440h & 96 & 1440h \\ -1440h & 14400h^2 & 1440h & 28800h^2 \end{bmatrix} \begin{Bmatrix} w_5 \\ \phi_5 \\ w_6 \\ \phi_6 \end{Bmatrix}$$

where, to have the same external factor for the beam element stiffness matrices that multiplies the plate element matrices, the beam element matrix terms were multiplied by 8 while their external factor was divided by the same number. Note that this structural system is well balanced at the load point in that the beam and plate elements make approximately equal contributions to the system stiffness matrix. Assembling the four element stiffness matrices yields the system equation to be solved for the unknown nodal deflections and then all other quantities of interest. The system or global equation is

$$\begin{Bmatrix} 0 \\ 0 \\ \frac{1}{2}F \\ 0 \end{Bmatrix} = \frac{Eh}{144000} \begin{bmatrix} 508 & 0 & -164 & -2400h \\ 0 & 98400h^2 & 2400h & 22800h^2 \\ -164 & 2400h & 254 & 2550h \\ -2400h & 22800h^2 & 2550h & 49200h^2 \end{bmatrix} \begin{Bmatrix} w_5 \\ \phi_5 \\ w_6 \\ \phi_6 \end{Bmatrix}$$

Once again, while this example illustrates that hand calculations with plate bending finite elements are a bit tedious (and error-prone), the use of these and their more geometrically useful triangular and quadrilateral cousins is no problem whatsoever when a computer program handles all the bookkeeping. The solution to the above matrix equation is

$$[w_5 \quad \phi_5 \quad w_6 \quad \phi_6] = 72000 \frac{F}{Eh^2} [1.507h \times 10^{-3} \quad -1.622 \times 10^{-4} \quad 1.032h \times 10^{-2} \quad -3.862 \times 10^{-4}]$$

For a steel sheet ($E = 29 \times 10^6$ psi) of thickness 0.1 in, and a load of 100 lb, the solution for the vertical deflection at the point of application of the load (i.e., w_6) is 0.026 in. This deflection solution is over twice the thickness of the plate, and is hence beyond the applicability of the linear plate bending equations. Thus this linear analysis' deflection solution can be expected to be too high a value compared to the physical deflection. However,

it is the correct linear solution as confirmed by an independent, linear, NASTRAN² finite element analysis.³ The NASTRAN analysis used, for the same half of the structure, eight square plate elements and four beam elements to produce the same result. ■

22.10 Summary

The theory of thin plates with small lateral deflections hypothesizes that normals to the midplane remain normal and unchanged in length after loading. This hypothesis closely parallels the engineering beam theory approximation. Thus the beam and plate equations developed from those hypotheses also have parallels. The significant difference between the two theories is that beam equations involve only one spatial variable and hence total derivatives, while plate equations require two spatial coordinates and hence partial derivatives. This difference is manifested in the greater complexity of thin plate planform geometries, boundary conditions, and problem solutions. “Classical” plate bending solutions typically require the superposition of two or more series solutions.

The Bernoulli–Euler long beam approximations and the Kirchhoff thin plate hypothesis are constraints on the deflections of their respective structural elements. Like any constraints, they make a structural element less flexible. This fact about constraints may be easily illustrated by considering any beam supported against rigid body motion where, in response to the beam loading, all deflections are either above or below the undeflected beam axis. If a roller support is placed at any point along the beam axis where the beam’s original bending deflection curve is not zero, then the bending deflections everywhere in that beam are diminished. Thus the beam is stiffened by the constraint introduced by the additional roller. In the same way, the beams and plates of the strength of materials theories discussed in this text are slightly stiffer than the actual beams and plates they describe. When the beam and plate deflections are further constrained by the approximate deflection patterns represented by the shape functions of the finite element development, they are again made slightly stiffer. It appears that the simple rectangular plate bending finite element discussed above is accurate because the constraints imposed on that finite element by restricting its deflection patterns to 12 polynomial terms is closely offset by the imposed flexibility of permitting creases in the form of slope discontinuities between the element nodes.

The major difference between the above plate bending theory and actual plate behavior is the absence of shearing deflections. Just as with beams, a more sophisticated plate deflection theory has been developed that does account for shearing deflections. In this extended theory, for example, $w_{,x}$, the slope of the plate deflection curve in the x direction, is now the sum, with due attention to the sign convention, of the bending rotation θ_x and the shear angle γ_{xz} . In the plate theory presented here, of course, γ_{xz} is zero.

Chapter 22 Exercises

- 22.1. (a)** Write the BC equations for the rectangular plate edge at $x = a$ if that plate edge is supported by a series of infinitely closely packed, individual, rectilinear springs running along the entire length of that edge. The springs only oppose the lateral deflection of the plate at that edge with a spring stiffness k per unit length along the plate edge. The springs offer no resistance to

² NASTRAN is an acronym standing for *NASA Structural Analysis* program. It is one of several very large commercial finite element programs.

³ Courtesy of Dr. Suresh Chander.

rotations about the plate edge. The springs are unstretched when the plate edge is undeflected.

- (b) In terms of Cartesian coordinates, write the BCs for a triangular plate edge whose location relative to the coordinate origin is described by the equation $y = mx + b$, and when the lateral deflection along that edge and the rotation about that edge (called the slope normal to that edge) are constrained to be zero. That is, the edge is clamped. Consider that $m, b > 0$.
 - (c) As in part (b), but now the normal bending slope BC is replaced by the BC that the bending moment is zero everywhere along that edge. In other words, that entire edge is simply supported.
 - (d) Let the skewed edge of part (b) now be support-free. Now write the Kirchhoff shearing force and normal bending moment BCs.
- 22.2. (a) In terms of Cartesian coordinates, write the plate small bending deflection GDE for a vibrating plate subjected to a harmonic applied lateral pressure whose magnitude is $f_z(x, y, t) = f_0 \sin(\pi t/t_0)$, where t is time, and t_0 is a time constant such that the frequency (Hz) of the applied load is equal to $1/(2t_0)$. *Hint:* In addition to the applied force per unit area, f_z , the inertial load per unit area = $-(\text{mass density})(\text{thickness})(\text{acceleration})$ is another lateral force per unit area.
- (b) In terms of polar coordinates, write the lateral plate deflection GDE for a uniformly thick circular plate loaded by an axisymmetric loading of arbitrary magnitude $f(r)$.
 - (c) If $f(r)$ in part (b) is the constant value f_0 , determine a homogeneous and particular solution to that GDE.
 - (d) Write the small deflection GDE and BCs for a simply supported, rectangular plate with edges at $x = 0, a$ and at $y = 0, b$ when there is no applied lateral loading, but there is a temperature change that produces a constant equivalent thermal moment equal to $+M_0$.
- 22.3. (a) Write the Navier series solution for the small, lateral deflections of a homogeneous, isotropic, constant thickness, rectangular, simply supported plate of dimensions a by b subjected to a constant upward pressure of magnitude f_0 over the entire plate planform area. For your analysis use Cartesian coordinates that originate at the lower left-hand corner of the plate, with $0 \leq x \leq a$, and $0 \leq y \leq b$.
- (b) Write the Lévy (not Navier) series solution for a rectangular, homogeneous, isotropic, thin plate of constant thickness and dimensions a by b when the applied loading per unit area has the constant value f_0 for $0 \leq x \leq a/2$, and has the value zero over the other half of the plate planform area.
 - (c) Determine the deflection at the beam-supported corner of a square plate that is fully clamped along two adjacent edges, and supported by beams along the other two adjacent edges. Let the load be a single lateral force F_0 at that same corner where the two beams join. Use a single plate finite element to model the plate, and single beam elements to model each of the two beams that join at a right angle. Let the length of the beams and edge length of the square plate be $20h$, the plate thickness be h , the area moment of inertia of each beam be $I = 0.4 \text{ in}^4$. Let the beam and plate material be aluminum with $\nu = \frac{1}{3}$, and $E = 10 \times 10^6 \text{ psi}$. Note that there are only two nonzero system DOF.

FOR THE EAGER

- 22.4. Write the Lévy series solution for Exercise 22.3(a) if the boundary conditions are changed to:
- Clamped at $x = 0$, simple support elsewhere.
 - Clamped at $x = a$, simple support elsewhere.
 - Clamped at $x = 0$ and at $x = a$, simple support elsewhere.
 - Clamped at all four edges.
- 22.5. (a) Consider a thin plate extending over and supported by a grid of thin-walled I beams. Let this structure be loaded by an upward pressure. Taking into account the different buckling behavior of plates and beams, decide whether it is better to design this structure for this loading so as to place the grid of beams above the thin plate or below the thin plate. Explain your answer.
- (b) Consider developing a different shape function for the w_1 DOF of the rectangular plate bending finite element. Recall that the shape function used in Section 22.9, where $-1 \leq x/a = \zeta \leq +1$, $-1 \leq y/b = \eta \leq +1$, is $N_1(\zeta, \eta) = (1/8)(1 - \zeta)(1 - \eta)(2 - \zeta - \eta - \zeta^2 - \eta^2)$. Sampling this shape function along the lines $\eta = -1, 0$, and $+1$ shows that it has the required value of $+1$ at $\zeta = -1$ and the required value of 0 at $\zeta = +1$, and it has its maximum value of $+1$ at $\zeta = -1$. Of course, what is true for zeta is also true for eta. Thus it is a suitable shape function. The corresponding beam shape function from Eq. (17.4a), adjusted from the variable range ($0 \leq x/l \leq 1$) to ($-1 \leq \zeta \leq +1$) is the same function as above when there are fixed values of η , that is, for the beam, $N_1(\zeta) = (1/4)(\zeta^3 - 3\zeta + 2)$. Why would it be a bad idea to create a plate shape function $N_1(\zeta, \eta)$ by multiplying together the two beam shape functions $N_1(\zeta)N_1(\eta)$?
- 22.6. Write all the necessary BCs for the circular plate of Exercise 22.2(c) if the plate radius is R and the outer plate edges are clamped. Then complete the solution.

FOR THE ESPECIALLY EAGER

- 22.7. In the above derivation of the thin plate bending equations, the small-deflection longitudinal strain in the x direction is, for example, described as $\epsilon_{xx}(x, y, z) = u_{,x} - z\theta_{y,x}$ where $u = u(x, y)$, and $\theta_y = \theta_y(x, y)$. How would this strain term have to be modified to account for finite deflections in general?
- 22.8. (a) Write and solve the plate buckling problem of Examples 22.3 and 22.4 if the BCs at the unloaded edges at $y = 0$ and $y = b$ are changed from those of simply supported edges to those of clamped edges, while the loaded edges of length b remain simply supported.
- (b) As above, but this time the loaded edges of length b are clamped and the unloaded edges of length a are simply supported.
- (c) As above, let the plate be simply supported at $y = b$, free at $y = 0$, and simply supported at $x = 0$ and $x = a$.
- 22.9. (a) As a spot check on the stated isotropic, rectangular, plate bending element stiffness matrix, complete the derivation of the single matrix element at the seventh row and seventh column.
- (b) As in part (a), but for an off diagonal single stiffness matrix entry of your choosing.

22.10. Be warned that the algebra involved in this exercise is lengthy.

- (a) Consider a rectangular, uniform, isotropic, homogeneous plate of dimensions a by b . Let the Cartesian coordinate originate at the lower left corner as usual. There is no loading over the plate area. The plate is subjected to an arbitrary deflection along the edge $x = 0$ and simply supported at the other three edges. If the arbitrary deflections are described by

$$w(0, y) = \sum A_n \sin(n\pi y/b) \quad \text{and} \quad w_{,x}(0, y) = \sum B_n \sin(n\pi y/b)$$

what then is the solution for the plate deflections in terms of the Fourier coefficients A_n and B_n ? *Hint:* Use a Lévy series to obtain this solution.

- (b) Redo part (a), but this time let the edge at $x = 0$ be vibrating harmonically at the arbitrary amplitudes described above with a vibration frequency equal to f Hz; that is, let

$$w(0, y, t) = \sin(2\pi ft) \sum A_n \sin(n\pi y/b)$$

$$w_{,x}(x, y) = \sin(2\pi ft) \sum b_n \sin(n\pi y/b)$$

Endnote (1) The Second Finite Deflection Plate Equation (Ref. [16])

From Ref. [16], the nonlinear companion equation to the plate bending equation, Eq. (22.22a), which closely corresponds to the nonlinear beam extension equation introduced in Endnote (2) of Chapter 10 in both form and derivation, where again h^* is a constant, is

$$(N_x - \nu N_y)_{,yy} + (N_y - \nu N_x)_{,xx} - 2(1 + \nu)(N_{xy})_{,xy}$$

$$= -(1 - \nu)\nabla^2 N_T + E_0 h^* (w_{,xy}^2 - w_{,xx} w_{,yy})$$

This second plate deflection equation, the in-plane equation, is often written in terms of the stress resultant potential function $F(x, y)$ and a loading potential function $\bar{V}(x, y)$, where, from Eqs. (22.14), paralleling the Airy stress function

$$N_x = F_{,yy} + \bar{V} \quad N_y = F_{,xx} + \bar{V} \quad N_{xy} = -F_{,xy} \quad f_x = -\bar{V}_{,x} \quad \text{and} \quad f_y = -\bar{V}_{,y}$$

Then the second coupled, nonlinear partial differential equation is

$$\nabla^4 F = -(1 - \nu)\nabla^2(\bar{V} + N_T) + E_0 h^* [(w_{,xy})^2 - (w_{,xx})(w_{,yy})] \quad (22.25)$$

The derivation of this equation depends upon writing a compatibility equation for the in-plane strains. The familiar plane strain compatibility equation, which is Eq. (3.14a), is not adequate to this task because it was derived for small strains. However, the new compatibility equation that is specifically required for the plate finite strains and the lateral deflection can be derived by the same differentiation and in-plane deflection elimination procedure that can be used to derive Eq. (3.14a). The nonlinear strains from Eq. (3.11), combined with the Eq. (22.7) bending strains, are the basis for this new compatibility equation. Specifically, those three finite strains are

$$\epsilon_{xx} = u_{,x} + \frac{1}{2}(w_{,x})^2 - z w_{,xx} \quad \epsilon_{yy} = v_{,y} + \frac{1}{2}(w_{,y})^2 - z w_{,yy}$$

$$\gamma_{xy} = v_{,x} + u_{,y} + (w_{,x})(w_{,y}) - 2z w_{,xy}$$

See the solution to Exercise 22.7 for further comment upon these nonlinear strains. The resulting compatibility equation, an extension of the linear equation is then

$$\epsilon_{xx,yy} + \epsilon_{yy,xx} - \gamma_{xy,xy} = (w_{,xy})^2 - (w_{,xx})(w_{,yy})$$

The remainder of the derivation of the second plate equation proceeds from this compatibility equation by substituting stresses for the strains, stress resultants for the stresses, and then the above potentials for the stress resultants.

Elastic and Aeroelastic Instabilities

23.1 Introduction

The Euler beam buckling type of elastic instability, where an entire beam axis moves laterally, is discussed in Sections 11.6 and 11.7. Plate buckling and local flange and web type beam buckling are discussed in Section 22.8. These previous elastic instability discussions centered upon the solution of appropriate differential equations. In the first part of this chapter the focus is upon the use of the finite element method to calculate elastic buckling loads. The use of the finite element method makes practical the elastic buckling analysis of structures as opposed to the buckling analysis of one or two isolated structural elements. These FEM beam buckling solutions have the same limits of applicability as the Euler beam buckling solutions.

The second part of this chapter examines certain instabilities of structures that arise from fluid–structure interactions. These instabilities have much in common with the purely elastic instabilities. Whereas the object of an elastic instability analysis is to discover the critical magnitude of a particular type of load that will cause a sudden and sizable lateral deflection of the elastic structure, the object of the aeroelastic analysis is to discover the critical value of the airspeed (or Reynolds number or Mach number¹) beyond which the airloads cause an ever increasing deflection or vibration amplitude. A representative static instability (divergence) and a representative dynamic instability (wing flutter) are studied in some detail. Again the FEM is useful for describing the linear elastic properties of the structure being studied.

The last part of this chapter discusses the matrix iteration method for solving the type of matrix equations that are here developed to describe elastic and aeroelastic instabilities. Matrix iteration is one of many methods to be preferred in comparison to the previously discussed determinant method when the instability problem involves more than two or three degrees of freedom.

23.2 An Energy Formulation of the Beam Buckling Problem

The elastic (i.e., Euler) beam buckling governing differential equation (GDE) is easily solved whenever the beam has a constant bending stiffness and the axial loading is a constant. These circumstances of constant stiffness and loading are convenient for formulating a beam buckling finite element that can be used to model more complicated elastic beam buckling problems. Thus the task for this and the next section is to develop a finite element description that corresponds to the elastic buckling GDE

$$EIw''''(x) + Pw''(x) = 0 \quad (11.4)$$

where EI , and P , the compressive axial beam force, are constants.

¹ From the *Encyclopaedia Britannica*, Osborne Reynolds (1842–1912), British engineer, physicist, and educator. Ernst Mach (1838–1916), Bohemian-Austrian physicist.

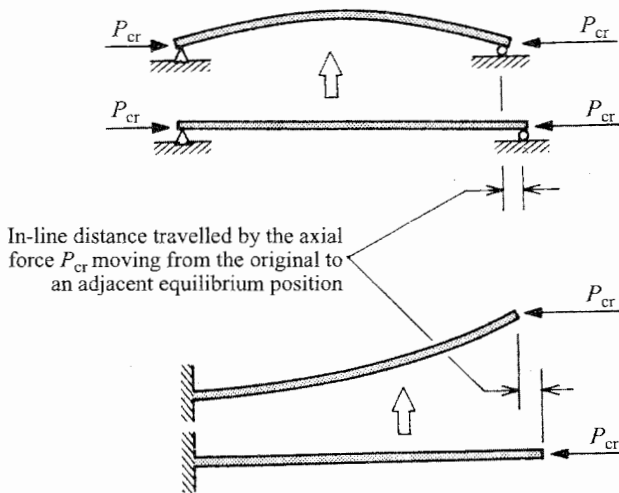


Figure 23.1. Two illustrations of the work done by the buckling force as it travels with the beam without changing its magnitude as the beam moves from the straight equilibrium position to an "adjacent," bent, equilibrium position.

In the previous finite element derivations presented in this text, the beginning point has always been the Principle of Virtual Work and suitable deflection shape functions rather than a differential equation. This approach could be used here since there is a standard technique for converting a certain type of differential equation, of which Eq. (11.4) is an example, into an equivalent virtual work statement (Ref. [3]). However, rather than proceed in that way, it is simpler at this point to validate by means of the usual variational procedure the virtual work statement corresponding to this GDE by deriving the above GDE and all possible boundary conditions (BCs) from that virtual work statement.

There is one other, rather small change to be made here, which is only stylistic. As mentioned above, the variational principle used in all previous finite element derivations has been the PVW. In elastic stability formulations it is customary to use the principle of the minimum value of the total potential energy. As explained in Chapter 15, the principle of the minimum value of the total energy is the PVW written in potential form (hence negative signs), and restricted to elastic bodies. So again, for elastic bodies, with $\delta W_{ex} = -\delta V$, and $\delta W_{in} = -\delta U$, the principle of the minimum value of the total energy becomes $\delta U + \delta V = \delta(U + V) = 0$. The principle of the minimum value of the total energy for the uniform beam bending finite element loaded by a constant axial force is

$$\delta \left(\frac{1}{2} EI \int_0^l (w'')^2 dx - \frac{1}{2} P \int_0^l (w')^2 dx \right) = 0$$

or

$$EI \int_0^l w'' \delta w'' dx - P \int_0^l w' \delta w' dx = 0 \quad (23.1)$$

The first of the above two integrals, representing δU , is familiar from Eq. (16.7b). The δV integral can be explained as follows. Consider either of the uniform beams shown in Fig 23.1. Each beam is shown in both its unbuckled, straight geometry and in a buckled shape. Two beams are sketched in order to indicate that the conclusions to be drawn from these

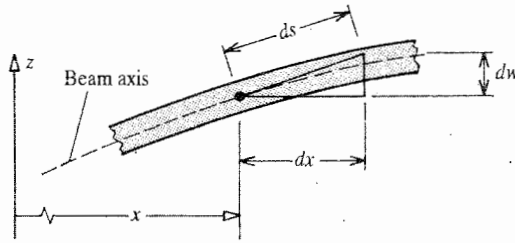


Figure 23.2. A detail of the buckled beam geometry.

figures are independent of any particular pair of boundary conditions. The external force acting upon the beam is the compressive force $P = P_{cr}$ for this beam. That is, the sketches present the situation for the perfect beam where the axial load is exactly equal to the critical load, which is a state of neutral stability as described by Eq. (11.4). In this circumstance, either the straight or buckled beam shape is associated with the critical axial force. The external work done by the critical axial force as it moves while remaining horizontal from the straight configuration to the buckled configuration is the product of the constant force magnitude, P , and the horizontal distance the force travels. Reference [3] proves that this external work value is the only external work that enters into the buckling calculation; that is, the work done by the axial force compressing the beam as the axial force increases from a zero value to the critical value is irrelevant to the buckling load calculation. Hence, from Fig. 23.2

$$W_{ex} = +P \left(\int_0^l ds - \int_0^l dx \right) = -V$$

Since $ds = [(dx)^2 + (dw)^2]^{1/2} = [1 + (dw/dx)^2]^{1/2} dx$, the integrals can be rewritten as

$$V = -P \int_0^l \{ [1 + (w')^2]^{1/2} - 1 \} dx$$

Using the binomial theorem and converting the line integral over x into an ordinary integral over x with the upper limit set at the approximate value of l , for small bending slopes

$$\begin{aligned} V &\approx -P \int_0^l \left[1 + \frac{1}{2}(w')^2 + \dots - 1 \right] dx \\ &= -\frac{P}{2} \int_0^l (w')^2 dx \end{aligned}$$

and therefore, as before,

$$\delta V = -P \int_0^l w' \delta w' dx$$

Now that the origin of the second part of Eq. (23.1) has been explained, the principle of the minimum value of the total potential energy can be integrated by parts in order to obtain the beam buckling GDE and the associated BCs as follows:

$$\begin{aligned} \delta(U + V) &= 0 \\ &= EIw'' \delta w' \Big|_0^l - \int_0^l (EIw''')' \delta w' dx - Pw' \delta w \Big|_0^l + P \int_0^l w'' \delta w dx \end{aligned}$$

or

$$0 = EIw'' \delta w' \Big|_0^l - (EIw''') \delta w \Big|_0^l + \int_0^l [(EIw''')' + Pw'''] \delta w \, dx - Pw' \delta w \Big|_0^l$$

Requiring that the first and the sum of the second and fourth terms, the terms pertaining to the BCs be individually zero, leaves the integral over the beam length equal to zero. Since the integrand of this integral contains the arbitrary function $\delta w(x)$, the only way that this integral can be zero for all choices of $\delta w(x)$ is for

$$[EIw''(x)]' + Pw''(x) = 0$$

which, for a constant EI , is identical to Eq. (11.4). Thus Eq. (23.1), the origin of this known GDE, is validated. In passing, note that with $EIw'' = M$, and $(EIw''')' = V$ in the absence of a bending moment per unit length and a temperature change, the BCs, as discussed in part in Exercise 11.12, are

$$\text{either } M = 0 \quad \text{or } w' = \text{constant}$$

and

$$\text{either } V + Pw' = 0 \quad \text{or } w = \text{constant}$$

See Exercise 23.9 for the completion of the process of demonstrating the equivalence of the above beam buckling differential equation and the virtual energy expressions.

23.3 A Beam Buckling Finite Element

Now that confidence in Eq. (23.1) has been established, developing the beam buckling finite element is a routine matter. This is so because the beam bending shape functions of Chapter 17 are just as applicable to beam bending caused by an axial force as they are to beam bending caused by lateral loadings. Thus it is simply a matter of substituting from Eq. (17.4) $w(x) = N_1w_1 + N_2\theta_1 + N_3w_2 + N_4\theta_2 = [N]\{q\}$ into

$$EI \int_0^l w'' \delta w'' \, dx - P \int_0^l w' \delta w' \, dx = 0 \quad (23.1)$$

to obtain

$$[\delta q] EI \int_0^l \{N''\} [N''] \, dx \{q\} - P [\delta q] \int_0^l \{N'\} [N'] \, dx \{q\} = 0$$

After eliminating the arbitrary row matrices $[\delta q]$, the first term is $[k]\{q\}$ exactly as developed in Chapter 17. Detailing the second matrix term is the task ahead. From Eq. (17.4a, b), and noting that $N'_i \equiv dN_i/dx = (1/l)(dN_i/d\xi)$, for $i = 1, 2, 3, 4$

$$N'_1(\xi) = +(6/l)(\xi^2 - \xi) \quad N'_2(\xi) = 3\xi^2 - 4\xi + 1$$

$$N'_3(\xi) = -(6/l)(\xi^2 - \xi) \quad N'_4(\xi) = 3\xi^2 - 2\xi$$

Thus the integrand of the second integral, the square matrix $\{N'\}[N']$, becomes

$$\{N'\}[N'] = \begin{bmatrix} g_1 & g_2 & -g_1 & g_3 \\ g_2 & g_4 & -g_2 & g_5 \\ -g_1 & -g_2 & g_1 & -g_3 \\ g_3 & g_5 & -g_3 & g_6 \end{bmatrix}$$

with the definitions

$$\begin{aligned} g_1 &= (36/l^2)(\xi^4 - 2\xi^3 + \xi^2) & g_2 &= (6/l)(3\xi^4 - 7\xi^3 + 5\xi^2 - \xi) \\ g_3 &= (6/l)(3\xi^4 - 5\xi^3 + 2\xi^2) & g_4 &= 9\xi^4 - 24\xi^3 + 22\xi^2 - 8\xi + 1 \\ g_5 &= 9\xi^4 - 18\xi^3 + 11\xi^2 - 2\xi & g_6 &= 9\xi^4 - 12\xi^3 + 4\xi^2 \end{aligned}$$

Noting that $dx = (1/l)d\xi$, and carrying out the integration over the beam element length, l , leads to

$$P[h]\{q\} = \frac{P}{30l} \begin{bmatrix} 36 & 3l & -36 & 3l \\ 3l & 4l^2 & -3l & -l^2 \\ -36 & -3l & 36 & -3l \\ 3l & -l^2 & -3l & 4l^2 \end{bmatrix} \begin{Bmatrix} w_1 \\ \theta_1 \\ w_2 \\ \theta_2 \end{Bmatrix} \quad (23.2)$$

Thus there are two element matrices, $[k]$ and $[h]$, to be used with each beam element when there is an axial buckling load. As before, the element matrices need to be assembled to produce the global matrix equation

$$[K]\{q\} = P[H]\{q\}$$

Example 23.1. Using a uniform, homogeneous, simply supported beam as a test vehicle, determine the accuracy of the above finite element formulation by using (a) first a single finite element to model the simply supported beam; and then (b) two finite elements to model the simply supported beam. Let the length of the beam be L in both cases.

Solution. (a) Applying the BCs $w_1 = w_2 = 0$ to the beam element matrices, and setting $l = L$, the result is

$$\left(\begin{bmatrix} 4L^2 & 2L^2 \\ 2L^2 & 4L^2 \end{bmatrix} - \frac{PL^2}{30EI} \begin{bmatrix} 4L^2 & -L^2 \\ -L^2 & 4L^2 \end{bmatrix} \right) \begin{Bmatrix} \theta_1 \\ \theta_2 \end{Bmatrix} = \begin{Bmatrix} 0 \\ 0 \end{Bmatrix}$$

Let $\lambda = PL^2/(30EI)$, and note as before that a nontrivial solution is only possible if the determinant of the difference of the two square matrices is zero. After canceling L^2 in each row,

$$\begin{vmatrix} 4 - 4\lambda & 2 + \lambda \\ 2 + \lambda & 4 - 4\lambda \end{vmatrix} = 0 = 15\lambda^2 - 36\lambda + 12$$

The two solutions for the eigenvalue λ are $\lambda = 0.4$ and $\lambda = 2.0$. There are only two eigenvalue, and hence buckling load, solutions because in this crude structural model there are only two DOF. This is in marked contrast to the differential equation solution where there are an infinite number of eigenvalue solutions. Nevertheless, the only eigenvalue solution of any importance is the one with the lowest value. This single-element finite element solution $\lambda = 0.4$ leads to

$$P_{cr} = \frac{12EI}{L^2}$$

This same result could have been obtained more quickly from symmetry by setting $\theta_1 = -\theta_2$ in the matrix equation, and then solving for P .

Recall that the exact (i.e., Euler) differential equation solution is $\pi^2 EI/L^2$. Therefore the above single finite element solution is slightly over twenty percent in error. That is of course an unacceptable error. The source of this error can be understood by noting that a Rayleigh-Ritz analysis of the same simply supported, uniform beam using as the single approximating

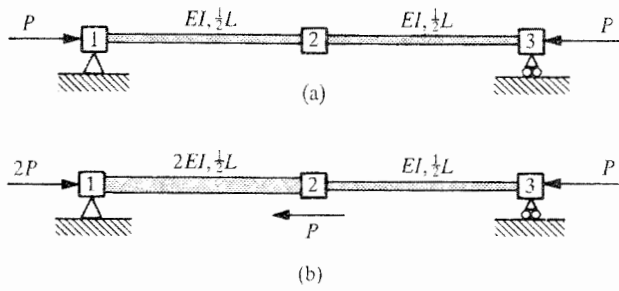


Figure 23.3. Finite element beam buckling models. (a) The uniform beam and uniform loading of Example 23.1. (b) The nonuniform beam and nonuniform loading of Example 23.2.

function the quadratic polynomial $\xi(1 - \xi)$ leads to exactly the same solution. Also note that there is no cubic polynomial (an odd function) that meets the conditions that the polynomial expression is zero at $\xi = 0$ and $\xi = 1$, and is symmetric (even) about $\xi = 1/2$. Thus the cubic terms of the shape function expansions disappear from the finite element analysis (a special case of the Rayleigh–Ritz analysis), leaving only the quadratic polynomial $\xi(1 - \xi)$. This statement can be supported by noting again that setting $\theta_1 = -\theta_2$ in the finite element analysis leads to exactly the same result. Now the quadratic expression $\xi(1 - \xi)$ is a poor choice as an approximating function for the bent beam because buckling can be viewed as being the result of bending moments developing in the beam as the beam deflects laterally. The bending moment of the Euler solution, which is proportional to $w''(x)$, actually varies sinusoidally, while $w''(x)$ of the approximating function is a constant. This is the reason for the large error.

(b) Using two finite elements requires the usual assembling of $[K]$ and $[H]$ matrices from the individual $[k]$ and $[h]$ matrices. Number the left-hand node as number 1, the middle node as number 2, and the right-hand node as number 3, as shown in Fig. 23.3(a). Then note that symmetry and the BCs require that $w_1 = \theta_2 = w_3 = 0$. Therefore, where $l \equiv \frac{1}{2}L$

$$[K]\{q\} = \frac{EI}{l^3} \begin{bmatrix} 4l^2 & -6l & 0 \\ -6l & 24 & 6l \\ 0 & 6l & 4l^2 \end{bmatrix} \begin{Bmatrix} \theta_1 \\ w_2 \\ \theta_3 \end{Bmatrix}$$

$$P[H]\{q\} = \frac{P}{30l} \begin{bmatrix} 4l^2 & -3l & 0 \\ -3l & 72 & 3l \\ 0 & 3l & 4l^2 \end{bmatrix} \begin{Bmatrix} \theta_1 \\ w_2 \\ \theta_3 \end{Bmatrix}$$

Expanding by hand a 3×3 determinant of the matrix equation $([K] - P[H])\{q\} = \{0\}$ is not difficult. However, it is simpler still to make use of the symmetry condition that $\theta_3 = -\theta_1$ by introducing the generalized coordinate transformation between the constrained and unconstrained DOF

$$\{q\} = \begin{Bmatrix} \theta_1 \\ w_2 \\ \theta_3 \end{Bmatrix} = \begin{bmatrix} 1 & 0 \\ 0 & 1 \\ -1 & 0 \end{bmatrix} \begin{Bmatrix} \theta_1 \\ w_2 \end{Bmatrix} = [T]\{q\}$$

Substituting the above DOF transformation, and premultiplying by $[T]^t$, the finite element equation becomes, after division by EI/l^3 ,

$$\left(\begin{bmatrix} 8l^2 & -12l \\ -12l & 24 \end{bmatrix} - \frac{Pl^2}{30EI} \begin{bmatrix} 8l^2 & -6l \\ -6l & 72 \end{bmatrix} \right) \begin{Bmatrix} \theta_1 \\ w_2 \end{Bmatrix} = \begin{Bmatrix} 0 \\ 0 \end{Bmatrix}$$

Writing $\lambda \equiv P l^2 / (30EI)$, the zero value of the determinant of the above matrix equation reduces, after some simplification, to the equation

$$\begin{vmatrix} 4 - 4\lambda & -6 + 3\lambda \\ -2 + \lambda & 4 - 12\lambda \end{vmatrix} = 45\lambda^2 - 52\lambda + 4 = 0$$

The lowest root of this quadratic equation is $\lambda = 0.082865 = P l^2 / (30EI) = P L^2 / (120EI)$. Thus the value of critical axial force is

$$(P_{cr})_{\text{FEM}} = 9.944 \frac{EI}{L^2} > (P_{cr})_{\text{exact}} = 9.870 \frac{EI}{L^2}$$

The error for this two-element model is the wholly acceptable value of three-quarters of 1 percent. As discussed in Chapter 16, in all Rayleigh–Ritz or finite element calculations of a buckling load, natural frequency of vibration, or anything else that is increased when the structure is further constrained beyond its existing boundary conditions, the approximate buckling load or natural frequency solution exceeds or equals the exact solution. The reason for the marked improvement in accuracy in this second analysis is that with the two-element model a cubic polynomial is used as an approximation for each half of the exact deflection pattern, which is a sine function between zero and π . Thus the exact sinusoidal bending moment is now approximated by a piecewise linear function, and that is a much better approximation than the constant function approximation of the first analysis. ■

It must be stressed that the above finite element analysis has the same practical limitation that applies to any Euler buckling analysis. That limitation is again that well-designed beam-columns do not buckle in the elastic range as is presumed in an Euler analysis. Thus an Euler analysis for the purpose of obtaining P_{cr} is only a first step towards calculating the Euler buckling stress equal to P_{cr}/A , and comparing this stress to the material yield stress and the lesser stresses of Johnson's parabola as discussed in Section 11.7.

Example 23.2. As a variation on the second part of the above example, set up the determinant equation to be solved for the critical load eigenvalue of the finite element model shown in Fig. 23.3(b). (Note that both the loading and stiffness coefficients are now different over the left half of the beam.) Expand the determinant and determine the value of the eigenvalue and the critical value of the axial force, P .

Solution. Assembling the global matrices from the element matrices in the usual fashion leads to

$$[K]\{q\} = \frac{8EI}{L^3} \begin{bmatrix} 2L^2 & -6L & L^2 & 0 \\ -6L & 36 & -3L & 3L \\ L^2 & -3L & 3L^2 & 0.5L^2 \\ 0 & 3L & 0.5L^2 & L^2 \end{bmatrix} \begin{Bmatrix} \theta_1 \\ w_2 \\ \theta_2 \\ \theta_3 \end{Bmatrix}$$

$$[H]\{q\} = \frac{P}{30L} \begin{bmatrix} 4L^2 & -6L & -L^2 & 0 \\ -6L & 216 & -3L & 3L \\ -L^2 & -3L & 6L^2 & -0.5L^2 \\ 0 & 3L & -0.5L^2 & 2L^2 \end{bmatrix} \begin{Bmatrix} \theta_1 \\ w_2 \\ \theta_2 \\ \theta_3 \end{Bmatrix}$$

where, in contrast to the previous uniform beam-column problem, it is not possible to anticipate that θ_2 is zero, nor is it likely that $\theta_1 = -\theta_3$. Hence no reductions in size are possible here. Dividing through by $P/30L$, define the eigenvalue as $\lambda = 240 EI/PL^2$. Hence the search is for the largest eigenvalue so as to obtain the smallest value of P .

Rather than attempt a solution by expanding a 4×4 determinant, the computer program *Mathematica* is now employed so as to directly deal with these matrices. In order to simplify the calculations, the matrix equation is nondimensionalized by factoring out L 's so that the θ_j unknowns are replaced by $L\theta_j$, and then dividing through those remaining rows where an L is present. Then the modified matrix equation $\lambda[K]\{q\} = [H]\{q\}$ becomes $\lambda\{q\} = [K^{-1}H]\{q\}$, where

$$[K]^{-1} = \frac{1}{24} \begin{bmatrix} 36 & 8 & 0 & -24 \\ 8 & 3 & 2 & -10 \\ 0 & 2 & 12 & -12 \\ -24 & -10 & -12 & 60 \end{bmatrix}$$

and

$$[K^{-1}H] = \frac{1}{12} \begin{bmatrix} 4 & 60 & -2 & -1 \\ 0.5 & 23.5 & 0 & -0.5 \\ -1 & 15 & 3 & -1 \\ -1 & -75 & -2 & 4 \end{bmatrix}$$

In this form the matrix equation is ready for iteration. However, since *Mathematica* has been used to this point, it might as well be also used to determine all the eigenvalues as well. The result of using that program is that the highest eigenvalue is $(26.6218/12)$. Thus the critical value for the axial load is $10.4 EI/L^2$.

The question now is how accurate is this answer. The best way to answer that question is to take the trouble to solve the differential equation eigenvalue problem. To that purpose it is necessary to write $EIw''''(x) + Pw''(x) = 0$ for both the left half (L) and the right half (R) of the beam. The critical boundary conditions are, in terms of a local axial length coordinate for each half of the beam

$$w_L(0) = w_L''(0) = w_R(L/2) = w_R''(L/2) = 0$$

along with the equations of continuity and equilibrium at the beam center, which are

$$\begin{aligned} w_L(L/2) &= w_R(0) & w_L'(L/2) &= w_R'(0) & 2w_L''(L/2) &= -w_R''(0) \\ 2w_L'''(L/2) &= -w_R'''(0) \end{aligned}$$

The first two boundary conditions produce a zero result for the first and fourth constants of integration for the left-hand beam, leaving six constants of integration to be determined by the remaining six equations. In this case, expanding the 6×6 determinant by hand by minors is not difficult. The resulting characteristic equation reduces to simply $\cos(\lambda L/2) \sin(\lambda L/2) = 0$, where $\lambda^2 = P/EI$. Hence the critical value of the axial force is $P = \pi^2 EI/L^2$. This result should not be surprising because the P/EI ratio is the same for both halves of the beam. Now the question can be answered that the FEM result of 10.4 is an acceptable 5 percent off the "exact" strength-of-materials solution of 9.87, and it is a higher value, as it should be. ■

Now consider the elastic stability of the pinned-end truss structure shown in Fig. 23.4. Let the truss be braced against buckling out of the plane of the truss so that the following discussion can be confined to two dimensions. Let the applied loads increase simultaneously and proportionally as indicated. The joints of the truss deflect and the bars rotate as the applied loads are distributed throughout the bars of the truss. Since the bars are pinned, the joint displacements and the bar rotations per se have no effect upon the stability of the bars. For the bars, those deflections are merely rigid body deflections. The quantity that

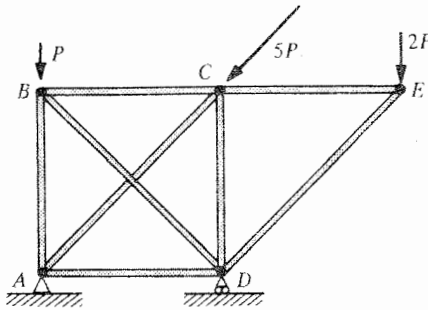


Figure 23.4. A pin-jointed truss subjected to externally applied compressive forces that increase simultaneously.

does matter is the axial force acting in each bar. Prior to the buckling of any bar member of the truss, the axial forces in the truss can be calculated by either the unit load method, the finite element method, or any comparable linear method. Then the ratio PL^2/EI can be calculated for each bar, and the first bar to approach π^2 , with the usual safety factors, is the bar that will buckle first. If the first bar to buckle were, say DE , then, recalling the shape of the stability paths for beams, the right-hand portion of the truss would soon collapse after a modest increase in the load. However, if the first bar to buckle were CD , the redundant truss is not necessarily in immediate danger of collapsing. The bar CD would not accept any appreciable further loading, but would continue to transmit its buckling load. The increased loading would be distributed among the other redundant bars. Therefore, if a flight vehicle truss structure is redundant, and if the vehicle is unmanned, then the buckling loads of a vehicle truss are not necessarily the maximum planned loads for the vehicle.

If the hinged end conditions of the bars of the truss of Fig. 23.4 were now changed from being those of discontinuous bending slopes to those of continuous bending slopes, changing the truss to a frame, then isolating individual beams is less practicable. The more straightforward elastic stability analysis approach is simply, using beam element rotation matrices for diagonal beams as discussed in Chapter 18, to assemble the finite element equations $([K] - P[H])\{q\} = \{0\}$, and solve this matrix eigenvalue problem for the lowest value of P . One method suitable for hand calculations when the number of DOF is not too large, or for machine calculation when the number of DOF is a couple hundred or so, is discussed in Section 23.8. Finally, when there are fixed loads as well as increasing loads acting simultaneously on the structure, then the analysis cannot be treated as an eigenvalue problem. Instead, the analysis is one of tracking stresses and deflections as the variable loads are increased.

23.4 Further Aspects of the Energy Formulation

The writing of the principle of the minimum value of the total potential energy, $\delta(U + V) = 0$ requires the total potential $U + V$ to be stationary. The requirement of a stationary total potential energy determines all equilibrium configurations, stable as well as unstable. If the total potential is also a minimum for an equilibrium state, then the equilibrium is stable because positive work has to be done on the structural system by additional outside forces to move it away from that equilibrium position. The total potential is a minimum in the neighborhood of the equilibrium state if the total variation of the total potential is positive for *all* small variations of the deflections about that equilibrium configuration. Recall that the total variation is the sum of the first variation plus one-half the

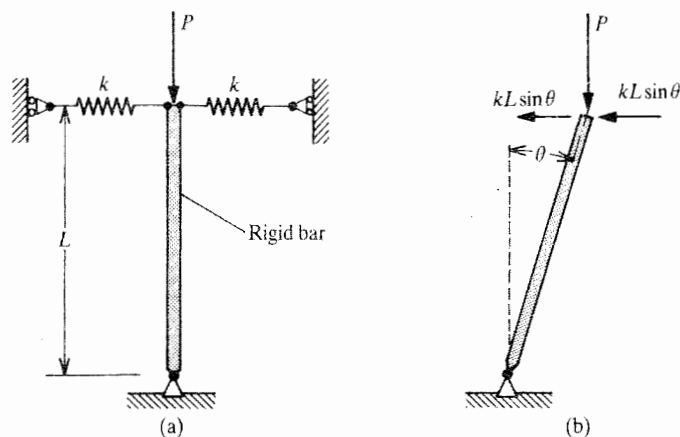


Figure 23.5. A single DOF elastic stability model. (a) The undeflected position. (b) A deflected equilibrium position. It makes no difference if the springs are preloaded as long as the rigid bar is vertical when P has a zero value.

second variation plus one-sixth the third variation, and so on. That is, as explained in the first endnote of Chapter 15, the total variation of the total potential energy, when $\Pi \equiv U + V$ is a function of a single dependent variable q , is

$$\delta^4 \Pi = \delta \Pi + \frac{1}{2!} \delta^2 \Pi + \frac{1}{3!} \delta^3 \Pi + \dots = \frac{\partial \Pi}{\partial q} \delta q + \frac{1}{2!} \frac{\partial^2 \Pi}{\partial q^2} (\delta q)^2 + \dots$$

If the total variation of the total potential energy is zero, then the equilibrium state is neutrally stable. If the total variation is negative, then the equilibrium state is unstable.

Since the variation δq must be small in order to investigate the stability of a structural system in the neighborhood of an equilibrium state, then each term in the series for the total variation of the total potential dominates all succeeding terms. Since the first term of that series is zero at an equilibrium state, the second term $\delta^2(U + V)$ is often the term that indicates the stability of the equilibrium state. The following simple example illustrates these concepts.

Example 23.3. Consider the rigid, massless bar shown in Fig. 23.5(a). Determine the stable and unstable equilibrium states of this simple structural system.

Solution. Only one generalized coordinate is required to define the deflected position of the system. Let that DOF be $q = \theta$, positive as shown in Fig. 23.5(b). In order to determine the total potential energy of this system when loaded by the static load P , consider the system in its displaced configuration as shown in Fig. 23.5(b). Then

$$U = \frac{1}{2} k (+L \sin \theta)^2 + \frac{1}{2} k (-L \sin \theta)^2$$

and

$$V = -PL(1 - \cos \theta)$$

Since the elastic coil springs remain linear through large deflections θ , it is possible to proceed with the analysis without the necessity of using a small-angle approximation. The equilibrium states of this structural system are determined by writing

$$\delta(U + V) = 0 = 2kL^2 \sin \theta \cos \theta \delta \theta - PL \sin \theta \delta \theta \quad (23.3)$$

or $(L \sin \theta)(2kL \cos \theta - P) \delta \theta = 0$

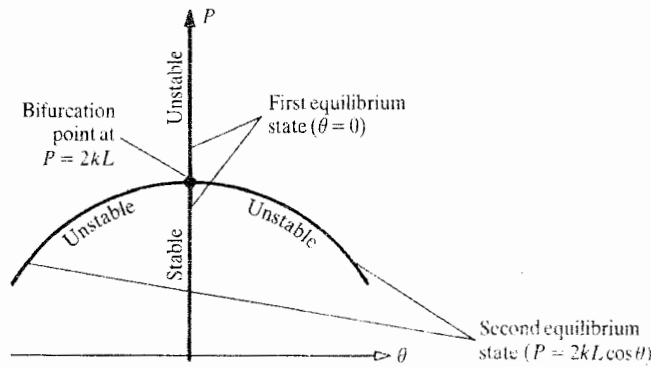


Figure 23.6. As an example of a stability diagram, the force vs. lateral deflection equilibrium paths for the perfectly constructed, perfectly vertically loaded, elastic system of Fig. 23.5.

Since $\delta\theta$ is not zero, either the first or second factor must be zero. These two factors yield the equilibrium states

- (e1) $\sin\theta = 0$ or $\theta = 0, \pi$ where $\theta = \pi$ is discarded, and
 (e2) $P = 2kL \cos\theta$

A force–displacement plot, P versus θ , of these equilibrium states is shown in Fig. 23.6. The lines of that plot are called equilibrium paths. They are so named because they illustrate all possible ways that the applied load and a representative structural deflection can change as the structure goes from one equilibrium position to another. For example, as the applied load P is increased from a zero value, the equilibrium value of θ remains at $\theta = 0$. Only when the value of the applied load reaches the magnitude $2kL$ is there a possibility of a nonzero equilibrium value for θ . The (P, θ) point on the plot equal to $(2kL, 0)$ is called a bifurcation point, (from “bifurcate,” which means to divide or fork into two or more branches). At that point it is possible for the system to be in a state of equilibrium (in the sense of balanced forces and moments) with the rigid bar deflected to the left or right or not deflected.

In order to determine which of the equilibrium paths are stable and which are not, apply the variational operator to $\delta(U + V)$ in Eq. (23.2), and note that there is no variation of $\delta\theta$ because $\delta\theta$ is not an explicit function of the dependent variable θ . (The implicit independent variable is time.) The result of $\delta[\delta(U + V)]$ is

$$\begin{aligned} \delta^2(U + V) &= (L \cos\theta)(2kL \cos\theta - P)(\delta\theta)^2 + (L \sin\theta)(2kL \sin\theta)(\delta\theta)^2 \\ &= [2kL^2(\cos^2\theta - \sin^2\theta) - PL \cos\theta](\delta\theta)^2 \end{aligned} \quad (23.4)$$

Consider the first equilibrium path where θ has the value of zero. Substituting $\theta = 0$ into the expression for the second variation of the total potential energy, Eq. (23.4), shows that, regardless of the sign of $\delta\theta$, the second variation of the total potential energy is positive whenever $P < 2kL$, and negative whenever $P > 2kL$. Thus the structural equilibrium path $\theta = 0$ is stable below the bifurcation point, and the equilibrium path $\theta = 0$ is unstable above the bifurcation point. Along the equilibrium paths where $P = 2kL \cos\theta$, the second variation of the total potential energy is equal to $-2kL \sin^2\theta$. Thus, along the equilibrium

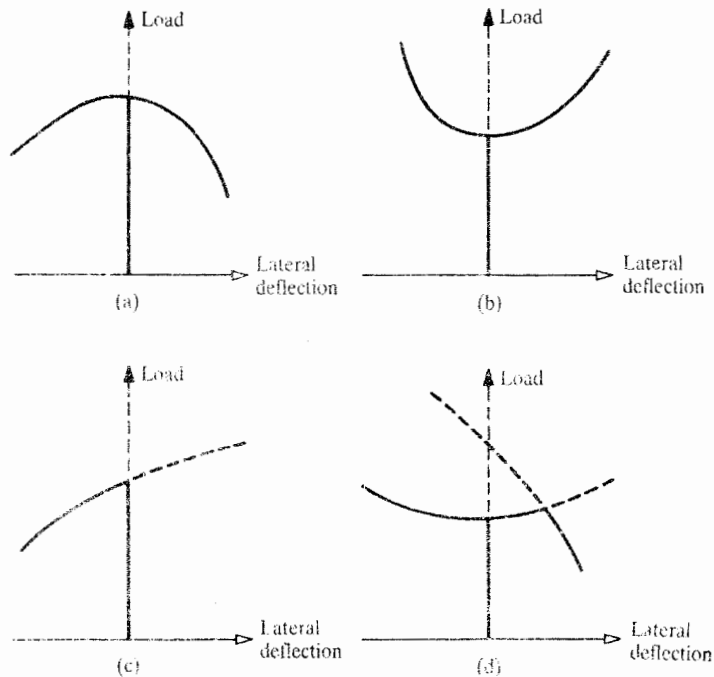


Figure 23.7. Various equilibrium load paths for perfect elastic systems. (a) Unstable equilibrium paths after the critical load. (b) Stable paths after the critical load. (c) Unstable at the critical load because even a perturbation to the right will produce a pendulum-like overshoot to the left, and any perturbation to the left will result in an accelerating, collapsing motion to the left. (d) Stable for small perturbations at the critical load, or small increases in the compressive load, but unstable for large deflections to the right. (e) Scaled plot of the equilibrium path for the structural system of Fig. 23.5 when the initial imperfection is the rather large value of 0.1 radian. (f) An equilibrium load path plot for the Fig. 23.5 system when the initial rotation imperfection is now the small value of 0.01 radian. In this case the nondimensionalized limit load has the approximate value of 0.93, showing that this system is not overly imperfection sensitive. A structural collapse at a load value even less than the imperfect limit load is possible if the structural system is given a perturbation large enough from its stable equilibrium path, say, at Point 2, to reach the unstable portion of the equilibrium path. If the extent of the perturbation is not sufficient to reach the imperfect path, as is illustrated at Point 3, then the damped system returns to its stable equilibrium position after the additional forces that caused the perturbation disappear.

paths that branch to the left and right, the second variation is everywhere negative and the system is unstable. The fact that the structural system is unstable along either of these two branch paths is evident merely from the fact that the two branch paths turn downward. That is, along either branch path, increasing deflections are associated with decreasing applied loads. Thus the deflections continue to increase with any constant-valued applied load that is in static equilibrium. Figure 23.7(a) shows, this circumstance in general, while Fig. 23.7(b) shows a stable branch path where increases in the applied load are required for increases in the lateral deflection. Plates have symmetric branch paths for large deflections of the type shown in Fig. 23.7(b). So do beams, but the upward curvature for beams is rather slight. Figures 23.7(c, d) show branch paths of the type associated with some shells where

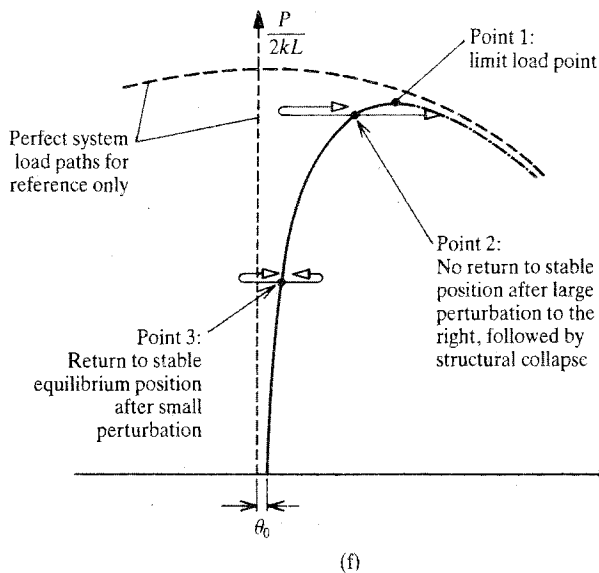
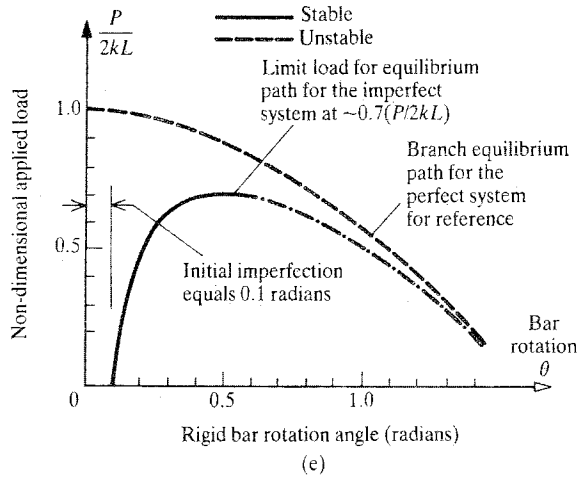


Figure 23.7 (continued).

deflections in one direction along the branch path are stable while deflections in the other direction are unstable. Since deflection perturbations will always exist in both directions, the system will always follow the downhill path.

The stability plots of Figs. 23.6 and 23.7(a, b, c, d) are drawn for perfect structural systems. A perfect structural system is one where all structural members have perfect geometries, exact dimensions, perfectly homogeneous materials, and so forth, and all loads are exactly placed on and aligned with the structure. If, for example, the system of Fig. 23.5 were perfect, then both springs would have exactly the same force-displacement properties and remain exactly horizontal, the rigid bar would be perfectly straight and perfectly vertical at zero load, and the applied force would also be exactly vertical and located at

the exact center of the top surface of the rigid bar. Obviously, any real system is an imperfect system with multiple imperfections, and some imperfections are more significant than others. If the only imperfection in the Fig. 23.5 system were that the rigid bar length was actually larger than some desired value, this particular off-design characteristic, by itself, would have no effect upon the shape of the general stability paths of Fig. 23.6 because the rigid bar length is merely a normalizing factor for the applied load. Since this change in length does not alter the shape of the stability paths, it is not an imperfection in the stability sense. However, if the applied force, or the unloaded rigid bar, is at a small angle to the vertical, either of these circumstances would affect the shape of the force–deflection plot for that system in much the same way. Consider the latter circumstance where the unloaded rigid bar has an initial rotation to the right of magnitude θ_0 , while the applied force remains vertical. With the further rotation θ measured positive to the right from the zero load position, then much like the perfect case, the equilibrium equation for this off-design circumstance is $(P/2kL) = [\sin(\theta + \theta_0) - \sin \theta_0] / \tan(\theta + \theta_0)$. A scaled plot of this equilibrium path is presented in Fig. 23.7(e) for the noticeably large imperfection $\theta_0 = 5.70^\circ$, and another in Fig. 23.7(f) for the difficult to notice imperfection $\theta_0 = 0.6^\circ$. Consider the plot for the larger imperfection. The load–deflection curve is nonlinear, and it reaches a maximum value, called the *limit load*, of approximately 0.7 of the value of the perfect system critical load. After the applied load reaches the limit load value, the system becomes unstable because after that point, greater deflections require only lesser forces. Thus, in the manner of having a maximum load below which the system is stable and beyond which it is unstable, this imperfect system is approximated by the perfect system. That approximation is even closer in the case of the smaller, more realistic, imperfection. The only cause for concern is that in the case of the gross imperfection, the load-carrying capacity of the system has been substantially reduced. However, for the case of the very small imperfection, without large perturbations, the reduction in the system load-carrying capacity is only 7 percent, which coincidentally is the usual outer limit of acceptable engineering error. Thus, the case of a small imperfection well illustrates the common circumstance that the perfect system equilibrium path solution is a boundary, and therefore a close approximation, for the actual system. This circumstance is also true for beams and plates. However, it must be pointed out that for certain shells, even with very small imperfections, the limit load can be approximately half, or less, of the magnitude of the critical load for the perfect system. Hence the usefulness and dangers of the perfect system analytical model.

One further interesting elastic stability phenomena requires mention. It is called the *snap through* phenomena. Consider the perfect, symmetric, two-bar truss of Fig. 23.8(a). Since the two bars are at a small angle to each other, even a small deflection causes a large percentage change in the original angle. Thus this is another example of an elastic stability problem because the load increase appreciably affects the geometry, which in turn further increases the bar stress beyond the increase it would have due to the change in the load without the change in geometry. The normalized force versus normalized deflection plot for this system is shown in Fig. 23.8(b). As always, once the limit load is reached, the system becomes unstable. The system accelerates downward through the horizontal plane and very quickly turns itself inside out; that is, the vee of the truss is at this loading, pointing downward. The deflections of the central joint below the unloaded position of the downward facing truss (at $w/h = 2.0$) become increasingly more linear with further increasing downward force because, now, the relative angle between the bars is increasing and the truss geometry is becoming more normal. ■

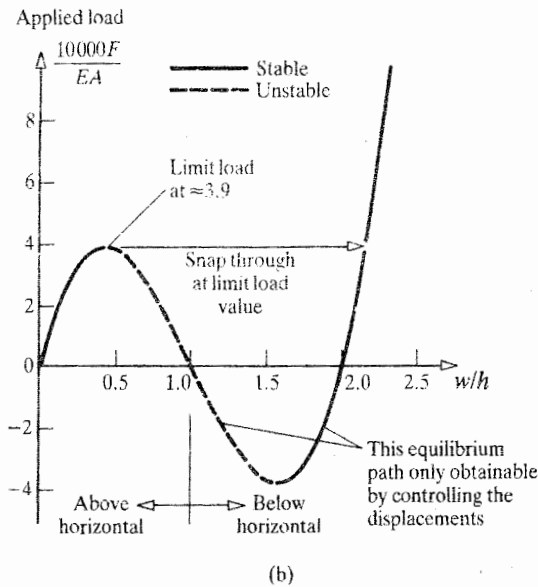
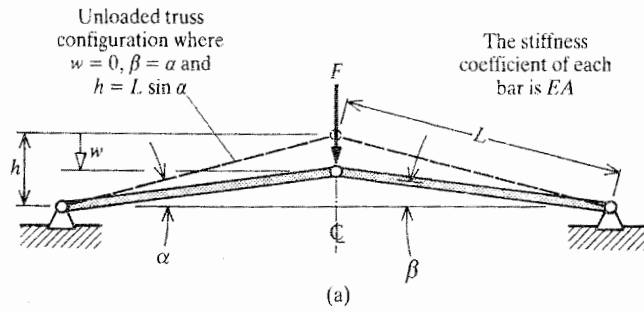


Figure 23.8. The well-known, symmetric, shallow truss problem with unmovable supports. The two bars are linearly elastic and are prevented from buckling or moving out of the plane of the paper by unshown additional constraints. (a) In terms of the rotation parameter β , after writing equilibrium, geometric compatibility, and Hooke's law, the large deflection (nonlinear) force-deflection solution is $(F/EA) = (\sin 2\beta / \cos \alpha) - 2 \sin \beta$ while $(w/h) = 1 - (\tan \beta / \tan \alpha)$, (b) A scaled plot of this normalized applied force versus the normalized center joint deflection for the special case where the initial shallow truss angle $\alpha = 0.1$ radian (5.7°). Both the applied force F and the joint deflection w are positive downward.

23.5 Types of Fluid–Structure Interaction Instabilities

The study of the various types of interactions between flight structures and the surrounding air flow is called "aeroelasticity." When the structure interacts with water, the study is called "hydroelasticity." There are a wide range of both static and dynamic, linear, and nonlinear fluid–structure interactions. An example of a linear, static, and comparatively benign instability is "aileron reversal." Figure 23.9(a) shows a wing cross-section of unit depth into the paper near the wing tip when the aileron is undeflected. In this figure, the straight line that best approximates the centerline of the wing cross-section is at a positive angle to the air stream velocity vector. This angle is called the angle of attack. If the aileron is deflected downward, as shown in Fig. 23.9(b), and if the wing is rigid, then the effective

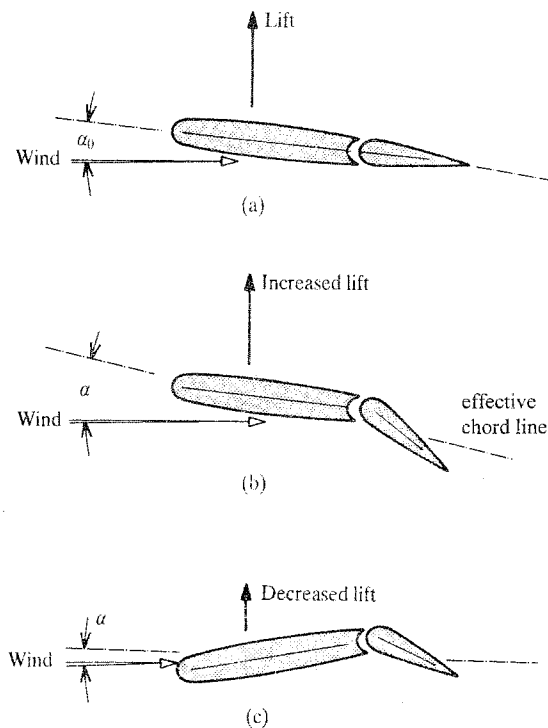


Figure 23.9. An explanation of aileron reversal. (a) The static reference case: the angle of attack is the small value α_0 , the aileron is undeflected, and the lift force is in static equilibrium with forces and moments elsewhere on the flight vehicle. (b) The aileron is deflected downward from the *rigid* wing thus increasing the effective angle of attack and increasing the lift. The increase in the lift causes this half of the wing to rise. (c) After the same downward aileron deflection, the flexible *and* torsionally weak wing rotates as shown in response to the aftward shift in the center of air pressure. The result is a marked decrease in the effective angle of attack and the lift. The decrease in the lift causes this half of the wing to sink, and the aircraft turns in the direction opposite to that intended.

angle of attack for the wing section is increased. The result is a greater lift force acting on the wing section. However, no wing is rigid along its span length. If the torsional stiffness of the wing at this outboard cross-section is sufficiently small and if the airstream dynamic pressure sufficiently large, then it is possible that with the downward deflection of the aileron, and with the consequent aftward shift of the center of pressure, the resulting aerodynamic torque on the wing section will cause the wing section to twist as shown in Fig. 23.9(c). The twist in this case is sufficient to actually decrease the angle of attack. Since the lift force increases or decreases as the small angle of attack increases or decreases, the result is that rather than the intended increase in wing section lift, there is a decrease. Hence the aircraft turns less quickly in the direction intended or may even turn in the direction opposite to that intended and opposite to that which would occur if the airstream dynamic pressure were below the critical value at which this direction reversal phenomenon begins. This phenomenon where a change in the air loads causes a change in the deflections, which, in turn, causes a further change in the air loads, and so on, is the essence of aeroelasticity. The aileron reversal phenomenon is similar to the lifting surface divergence phenomenon that is discussed in mathematical detail below.

An example of a linear dynamic instability is vibrations due to von Kármán vortices. Again consider a two-dimensional fluid flow; that is, one where all fluid velocity vectors lie in a single plane. From Ref. [59], at Reynold's numbers from 60 to 3000 for a circular cross-section, and at other low Reynold's numbers for other blunt or semiblunt bodies, vortices rotating in opposite directions are alternately shed from the body. The opposite vortex rotations produce oppositely directed reacting forces on the body at nondimensionalized frequencies (Strouhal numbers) that are dependent upon the Reynold's number of the flow. If the frequency of the loading caused by the vortices is close to or at the natural frequency of the body, then a resonance² effect is present and large amplitudes of vibration result.

Nonlinear effects are always present in a vehicular structure when the deflections or vibratory amplitudes become finite. Sometimes the nonlinear effects are beneficial. An example of a beneficial effect can be found in the case of finite amplitude "panel flutter." Panel flutter is the vibration induced in a plate or shell segment, such as a skin panel of an aircraft or a large rocket, by air flowing parallel to the panel surface. As a plate's or shell segment's lateral deflection amplitudes increase beyond the point of being equal to the plate thickness, the plate midplane must stretch appreciably in order for the plate or shell segment to further deflect laterally. Since plates and shell segments are very much stiffer for in-plane deflections than they are for bending deflections, the finite lateral deflections and peak stresses are effectively moderated by the plate or shell segment's resistance to in-plane straining.

An example of a nonbeneficial nonlinearity is found in the case of "stall flutter." When airspeed increases and the attendant increases in the aerodynamic lift cause a torsionally weak wing or other airfoil to increasingly twist to a larger angle of attack, a point can be reached where some part of the airfoil stalls. Then there is a sudden drop in the lift force, and hence a sudden drop in the airfoil rotation and the angle of attack. At the lower angle of attack the airfoil is no longer stalled. Thus the reestablished lift will cause the angle of attack to again increase until stall occurs once more and the cycle repeats itself. Thus a large rotation vibration is possible with its attendant risk of low-cycle fatigue failures.

All manner of fluid-structure interactions have plagued engineers. With such a wide variety of self-excited vibrations and instabilities, it is necessary to limit the discussion. The intention here is to provide a mathematical treatment of just two phenomena. The first topic is the divergence phenomenon, which as previously mentioned is a static instability. The second topic is the flutter problem, which, because of the mathematical complexity of the aerodynamic loads, is discussed only in broad terms. Further information can be obtained from Refs. [28, 29, 72].

23.6 Airfoil Divergence

In order to introduce the linear mathematical treatment of airfoil divergence in the simplest possible manner, the problem is first discussed as a one-dimensional problem. After that one-dimensional treatment is concluded, a more realistic two-dimensional treatment is offered. Consider the airfoil section shown in Fig. 23.10. Let the rigid airfoil's elastic properties be concentrated in and represented by the rectilinear and torsional springs shown. Let e be the distance between the aerodynamic center and the airfoil elastic axis. In subsonic

² "Resonance" is the term used to identify the situation where a significant portion of the applied load varies sinusoidally with time at an oscillatory frequency that is also one of the frequencies at which the structure vibrates "naturally"; that is, in the absence of applied loads. The significance of resonance is that when an applied load oscillates at one of the structure's lower-valued natural frequencies, the structure responds to this dynamic loading with very much larger deflection and stress amplitudes that it would if loaded by a static load of the same magnitude. After reading Section. 23.8, see Endnote (1).

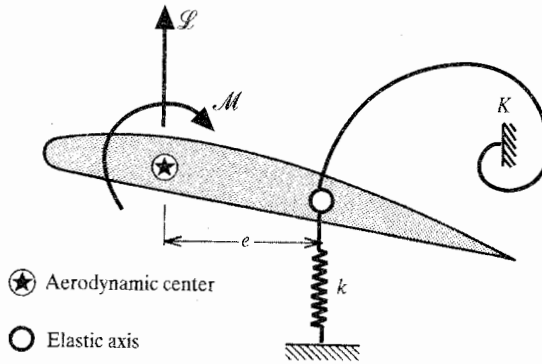


Figure 23.10. A one-dimensional analytical model for airfoil divergence.

flight, the aerodynamic center is at or very close to the airfoil section's quarterchord position. In supersonic flight, the aerodynamic center is near the centerchord position. Thus the moment arm for the destabilizing moment about the elastic axis created by the lift force is generally greater in subsonic flight than in supersonic flight. This discussion is limited to the subsonic case.

From Fig. 23.10, the moment equilibrium equation is $\mathcal{M} + e\mathcal{L} = K\alpha$ where \mathcal{M} is the aerodynamic moment, \mathcal{L} is the aerodynamic lift force, K is the torsional spring constant, and α is the equilibrium angle of rotation for the airfoil. Since $\mathcal{L} = C_l qS$, where the lift coefficient C_l is a characteristic of the airfoil shape, q is the dynamic pressure equal to the product of one-half the air mass density and the airspeed squared, and S is a characteristic area such as the airfoil planform area. The lift coefficient can be written as the product of the lift curve slope ($\partial C_l / \partial \alpha$) and the angle of attack measured from the chordline position where the torsional spring is undeflected, α , plus the rotational angle between the zero-lift line and the line where the torsional spring is unflexed, α_0 . That is, $C_l = (C_{l\alpha})(\alpha + \alpha_0)$, where $\alpha + \alpha_0$ is the total angle of attack from the zero lift line. Similarly, the aerodynamic moment can be written as $\mathcal{M} = C_m qS$. The moment coefficient, unlike the lift coefficient, does not change appreciably with the angle of attack. Thus the moment equilibrium equation can be written in terms of the airfoil angle of attack as

$$eC_{l\alpha}(\alpha + \alpha_0)qS + C_m qS = K\alpha \quad (23.5)$$

A simple way of proceeding from this point is to solve the above equation for α , and obtain

$$\alpha = \frac{[C_m + eC_{l\alpha}\alpha_0]qS}{K - eC_{l\alpha}qS} \quad (23.6)$$

Clearly, the angle of attack becomes very large as the denominator becomes very small. The denominator becomes small as the dynamic pressure q increases. Therefore, there is a critical dynamic pressure at which the angle of attack becomes so large that the airfoil structure fails. That dynamic pressure is called the airfoil divergence dynamic pressure, q_D , and the associated airspeed is the divergence airspeed. From the above equation,

$$q_D = \frac{K}{eSC_{l\alpha}} \quad (23.7)$$

The above treatment of the moment equilibrium equation is not a useful procedure for more complicated situations. Anticipating two- and three-dimensional structures, return to Eq. (23.5). This time, temporarily fix the unknown value of the dynamic pressure and take

the ordinary differential of both sides of the moment equilibrium equation, Eq. (23.5), where now the angle of attack, α is the only variable. The result is

$$[eC_{l\alpha} qS]d\alpha = K d\alpha \quad (23.8)$$

The left-hand side of this equation represents the change in the aerodynamic (upsetting) moment due to a change in the angle of attack, $d\alpha$. The right-hand side of this equation is the change in the elastic (restoring) moment due to the same change in angle of attack. When both moment increments are equal to each other, then there has been a transition from one equilibrium state at angle α to another, adjacent equilibrium state at the rotational angle $\alpha + d\alpha$, where $d\alpha$ is arbitrary. Therefore, at this particular dynamic pressure, there exists a state of neutral stability. (Neutral stability is the stability of a cylinder placed anywhere on a flat table top. No matter where the cylinder is placed upon the flat table top, the cylinder is in a state of static equilibrium.) If the dynamic pressure were to be increased, then only the magnitude of the overturning, aerodynamic moment would increase, and the overturning moment would exceed the elastic restraining moment. The result would be the loss of equilibrium and an accelerating increase in the angle of rotation. This describes an instability. Therefore the above equation represents a stability boundary between safe dynamic pressures where, after a perturbation in angle of attack, the greater increment in the elastic restoring moment safely returns the airfoil to its original equilibrium position, and unsafe dynamic pressures where the greater increment in the aerodynamic moment causes a still further departure from the original equilibrium position. The solution for the critical dynamic pressure, after canceling the arbitrary differentials, is again

$$q_D = \frac{K}{eC_{l\alpha} S}$$

The above one-dimensional analysis establishes (i) the importance of a lifting surface's torsional stiffness; and (ii) the balanced increment approach to determining the neutral stability boundary beyond which the dynamic pressure causes ever-increasing lifting surface rotations. The prediction of ever-increasing rotations must be restricted to the range of applicability of the above analysis, which is the range of angles of attack for which the aerodynamics is linear and, more restrictively, the range of elastic rotations for which the structural restoring moment is proportional to the change in airfoil twist. When small rotations are exceeded, the elastic restoring moment usually; at least initially, increases at a rate that exceeds a linear increase. However, it is certainly undesirable to put a lifting surface in such a highly stressed condition when the surface may only be flying straight and level.

Besides the lifting surface's torsional stiffness, there is one other aspect of the lifting surface structure that profoundly affects the surface's ability to avoid divergence. Referring now specifically to wings, that aspect is the sweep angle of the wing. In order to establish the importance of wing sweep angle, consider a high-aspect-ratio, cantilevered aircraft wing such as that shown in Fig. 23.11(a), which is swept forward through an angle β at the elastic axis. Modeling the wing as a cantilevered beam permits a simple discussion. As is evident from Fig. 23.11(a), a perturbation that results in an increase in the lift forces acting along the quarterchord causes the wing to not only have larger bending slope for the same wing span, but also larger twists (leading edge up, trailing edge down). This is so because of the increased bending and twisting moment arms of the outboard lift forces, particularly in increased relation to twisting at inboard points along the elastic axis. These positive increments in bending slope and twisting angle both contribute to a positive increment in the angle of attack, which, in turn, further increments the lift forces, which further increases

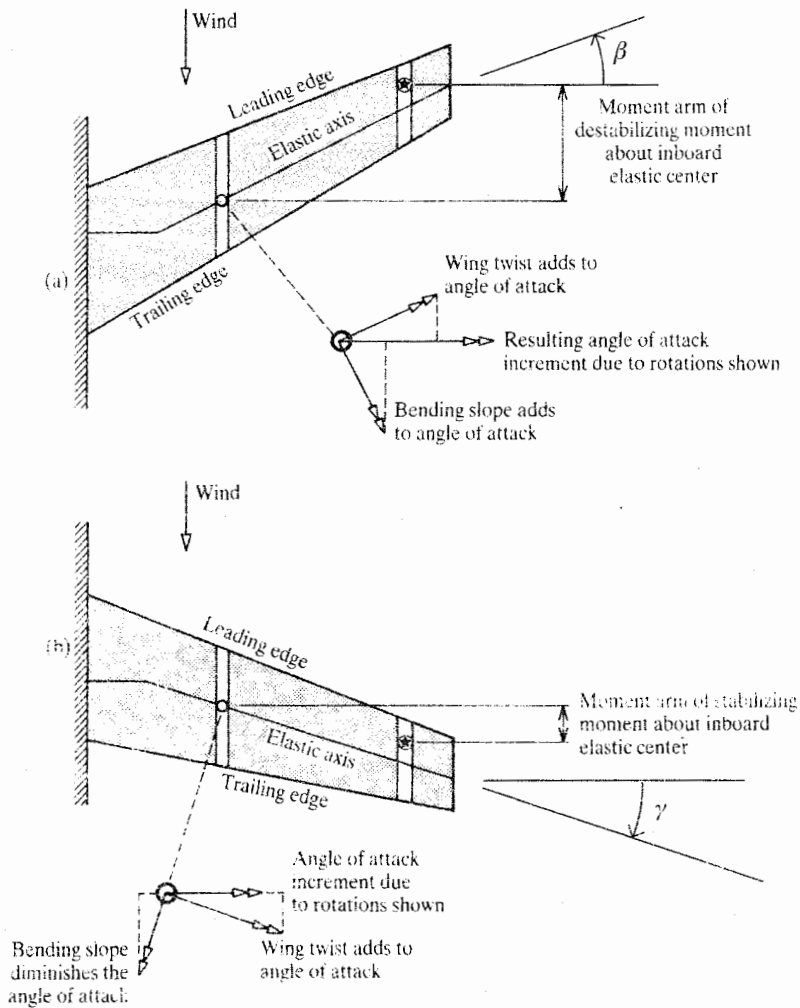


Figure 23.11. The differences with respect to wing divergence between two half wings that differ only in that one is swept forward while the other is swept backward.

the angle of attack, and so on. From the vector diagram of Fig. 23.11(a), where again ϕ is the angle of beam twist at the elastic axis, θ is the elastic axis bending slope, and α is the air stream angle of attack

$$d\alpha = d\phi \cos \beta + d\theta \sin \beta$$

As illustrated in Fig. 23.11(b), when the wing is swept back through an angle γ , an increase in the wing beam bending slope, such as would result from a transient increase in dynamic pressure, decreases the increment in the angle of attack

$$d\alpha = d\phi \cos \gamma - d\theta \sin \gamma$$

Thus, from either a change in the out-to-in twisting moment point of view, or directly from a geometric change in twisting angle and change in bending slope point of view, a swept-back wing experiences a stabilizing change in the angle of attack when the wing bends.

This stabilizing bending slope response to a destabilizing increase in lift that occurs with swept-back wings is the reason that when wings are swept, they are seldom swept forward despite certain aerodynamic and structural advantages that may exist for forward-swept wings.

A modern divergence analysis is not at all limited to modeling the wing as a beam located at the wing elastic axis. Today the wing structure is modeled as a collection of beam, plane stress, plate, and so on, finite elements. Therefore, regardless of whether the wing being modeled has a high or low aspect ratio, is tapered or not, of varying thickness, washed in or out, swept forward or aft, and so on, the wing finite element elastic equation is, as ever $\{Q\} = [K]\{q\}$. In this case, the generalized force vector, $\{Q\}$, can contain nodal forces in the plane of the wing, lateral shear forces, bending moments, and twisting moments. The generalized deflection vector $\{q\}$ contains the corresponding DOF.

Example 23.4. Consider the oversimplified, untapered, lifting surface model shown in Fig. 23.12. The cantilevered structural model is based upon dividing the lifting surface into three rigid, unconnected, spanwise airfoil shell segments as indicated by the dashed lines.

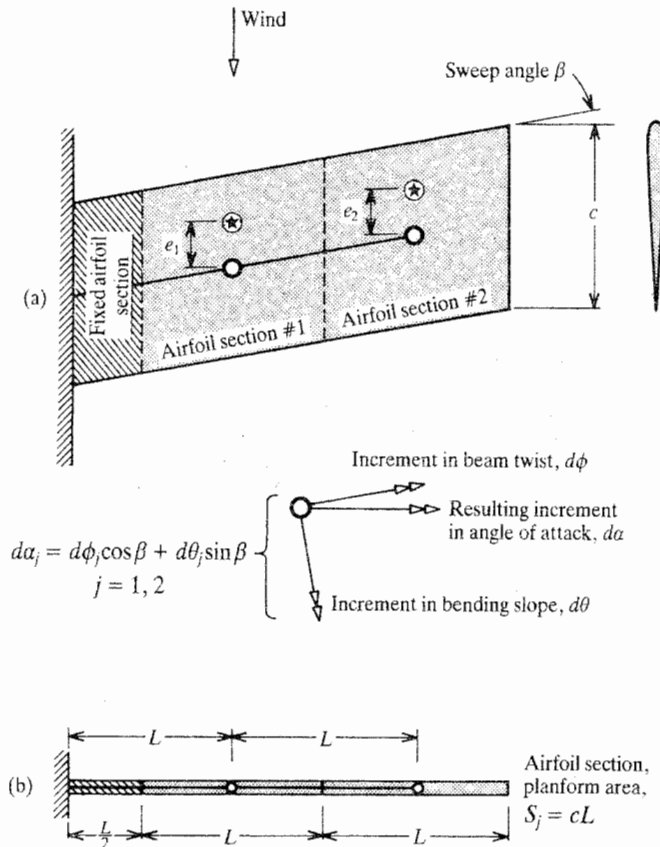


Figure 23.12. Example 23.4. An untapered airfoil of sweepforward angle β approximated, for the sake of hand calculations, by only two elastically supported, separated, rigid lifting surfaces. (a) The planview and endview. (b) The trailing edge view. The cantilevered beam represents the wing elastic axis.

The inboard rigid shell segment is attached to the cantilever support, and thus does not deflect. The two outboard shell segments are attached only at their centers to the uniform elastic beam that is swept forward at the same sweep angle as the airfoil leading and trailing edges. The single-beam model allows for simply calculated elastic reactions using the FEM. The shell segment centers of attachment are chosen as the outboard beam nodes and the inboard beam node is at the beam's cantilevered support. In this illustrative example, the subsonic aerodynamic theory is to be simplified by ignoring the low aspect ratio of this airfoil; that is, by pretending that the airflow over and under the airfoil is the same in every y, z plane (no vortices). Set up the matrix equation that defines the divergence dynamic pressure for this airfoil model.

Solution. First write the aerodynamic incremental load matrix in terms of the bending (\mathcal{H}) and twisting (\mathcal{T}) moments at the individual FEM nodes. This involves calculating the moment arms from the shell segment aerodynamic centers where the segment lift forces act, to the shell segment FEM nodes. The result is

$$\begin{Bmatrix} d\mathcal{L}_1 \\ d\mathcal{H}_1 \\ d\mathcal{T}_1 \\ d\mathcal{L}_2 \\ d\mathcal{H}_2 \\ d\mathcal{T}_2 \end{Bmatrix} = qLcC_{l\alpha} \begin{bmatrix} 1 & 0 \\ e \sin \beta & 0 \\ e \cos \beta & 0 \\ 0 & 1 \\ 0 & e \sin \beta \\ 0 & e \cos \beta \end{bmatrix} \begin{Bmatrix} d\alpha_1 \\ d\alpha_2 \end{Bmatrix}$$

After noting that for this swept-forward airfoil, $d\alpha = d\theta \sin \beta + d\phi \cos \beta$, where θ is a bending slope DOF for the cantilevered beam, and ϕ is twisting DOF

$$\begin{Bmatrix} d\mathcal{L}_1 \\ d\mathcal{H}_1 \\ d\mathcal{T}_1 \\ d\mathcal{L}_2 \\ d\mathcal{H}_2 \\ d\mathcal{T}_2 \end{Bmatrix} = qLcC_{l\alpha} \begin{bmatrix} 0 & \sin \beta & \cos \beta & 0 & 0 & 0 \\ 0 & e \sin^2 \beta & e \sin \beta \cos \beta & 0 & 0 & 0 \\ 0 & e \sin \beta \cos \beta & e \cos^2 \beta & 0 & 0 & 0 \\ 0 & 0 & 0 & 0 & \sin \beta & \cos \beta \\ 0 & 0 & 0 & 0 & e \sin^2 \beta & e \sin \beta \cos \beta \\ 0 & 0 & 0 & 0 & e \sin \beta \cos \beta & e \cos^2 \beta \end{bmatrix} \begin{Bmatrix} dw_1 \\ d\theta_1 \\ d\phi_1 \\ dw_2 \\ d\theta_2 \\ d\phi_2 \end{Bmatrix}$$

or $\{dQ\} = q[\mathcal{A}]\{dq\}$, where hopefully there is no confusion between the symbols for the generalized coordinates and the aerodynamic pressure. Note that $[\mathcal{A}]$ is not symmetric. The fact that it is singular does not present a difficulty.

The beam bending stiffness matrix is assembled as before from the two beam element bending and twisting stiffness matrices. Letting $r = GJ/EI$, the complete stiffness matrix for the elastic restoring moments acting upon the two rigid airfoil shells in the equation $\{dQ\} = [K]\{dq\}$, is

$$\begin{Bmatrix} d\mathcal{L}_1 \\ d\mathcal{H}_1 \\ d\mathcal{T}_1 \\ d\mathcal{L}_2 \\ d\mathcal{H}_2 \\ d\mathcal{T}_2 \end{Bmatrix} = [K]\{dq\} = \frac{EI}{L^3} \begin{bmatrix} 24 & 0 & 0 & -12 & 6L & 0 \\ 0 & 8L^2 & 0 & -6L & 2L^2 & 0 \\ 0 & 0 & 2rL^2 & 0 & 0 & -rL^2 \\ -12 & -6L & 0 & 12 & -6L & 0 \\ 6L & 2L^2 & 0 & -6L & 4L^2 & 0 \\ 0 & 0 & -rL^2 & 0 & 0 & rL^2 \end{bmatrix} \begin{Bmatrix} dw_1 \\ d\theta_1 \\ d\phi_1 \\ dw_2 \\ d\theta_2 \\ d\phi_2 \end{Bmatrix}$$

Equating the change in the elastic, restoring forces and moments on the rigid shells to the change in the aerodynamic, destabilizing forces and moments in order to describe the neutral stability boundary between stability and instability, leads to

$$[K]\{dq\} = q_D[\mathcal{A}]\{dq\} \quad \text{or} \quad ([K] - q_D[\mathcal{A}])\{dq\} = \{0\}$$

This is a matrix eigenvalue problem that can be solved for the divergence dynamic pressure using, for example, the iteration technique discussed in Section 23.8. ■

In a manner analogous to using a more elaborate structural model involving many types of spanwise and chordwise oriented structural elements, the description of the aerodynamic loads can be made to be much more sophisticated. For example, for a given airfoil section, the net aerodynamic force on a small portion of the planform can be described using experimental data on the change in the net pressure distribution over the chord length in response to a unit change in the airfoil angle of attack along the chord length (e.g., see Ref. [41]). Another possibility is using theoretical results that account for finite aspect ratios for the change in net pressure over the airfoil planform due to a change in angle of attack at one small area within the planform.

23.7 Airfoil Flutter

An airfoil flutter analysis is much like an airfoil divergence analysis in that they can both be treated as eigenvalue problems. However, a flutter analysis is fundamentally more complicated. Again, divergence is a static instability involving steady-state aerodynamic forces where the sole variable is the change in the angle of attack. Flutter is a dynamic instability where the airloads depend upon not only an airfoil angle of attack, but also upon the airfoil lateral and rotational velocities and accelerations. When an airfoil diverges, its rotations and lateral deflections continue to increase monotonically until the airfoil structure fails. When an airfoil flutters, the airfoil undergoes lateral and rotational vibrations. The term "flutter" usually implies that the amplitudes of the vibration continually increase or at least remain constant. When the amplitudes increase, the airfoil is dynamically unstable. When the airfoil vibration amplitudes remain constant over time, the airfoil is neutrally stable. Again, neutral stability is the boundary point between stability and instability. At neutral stability the associated dynamic pressure is called the flutter dynamic pressure, and the associated airspeed is called the flutter airspeed. Greater dynamic pressure or greater airspeeds push the airfoil into an unstable flight regime. This section approaches the flutter problem by first providing an explanation for airfoil flutter in physical terms. That discussion, which starts with the next paragraph, is followed by a mathematical treatment of the topic.

Consider the one cycle of airfoil vibration sketched in Fig. 23.13(a). In the diagram, the airfoil cross-section is simultaneously undergoing rotational and lateral vibrations. This simultaneous vibration, where both deflection components have the same vibration frequency, is called a "coupled" vibration. In the coupled vibration of Fig. 23.13(a) the angle of attack for the airfoil is not merely the twist of the airfoil. There is also the increment in the angle of attack, $\bar{\alpha}$, produced by the airfoil lateral velocity as shown in Fig. 23.13(b). In the vibration of Fig. 23.13(a), the effective angle of attack is the twist less $\bar{\alpha}$. Nevertheless, the twist predominates when the airspeed becomes large, and the oscillating lift force of the vibrating airfoil is always in the direction of the motion. Therefore, the external work done upon the airfoil by the lift force is always positive. Thus energy is being added to the airfoil by the airflow during every cycle. (It can be shown that the elastic and inertial forces and moments and the aerodynamic moment do no net work over the course of an entire cycle.) Therefore, if the energy added by the lift force is greater than the energy dissipated by the damping and drag forces, then the vibration amplitudes must increase. Continuously increasing vibration amplitudes constitute the dynamic instability called "airfoil flutter." Such a vibration would eventually, and perhaps very quickly, destroy the wing.

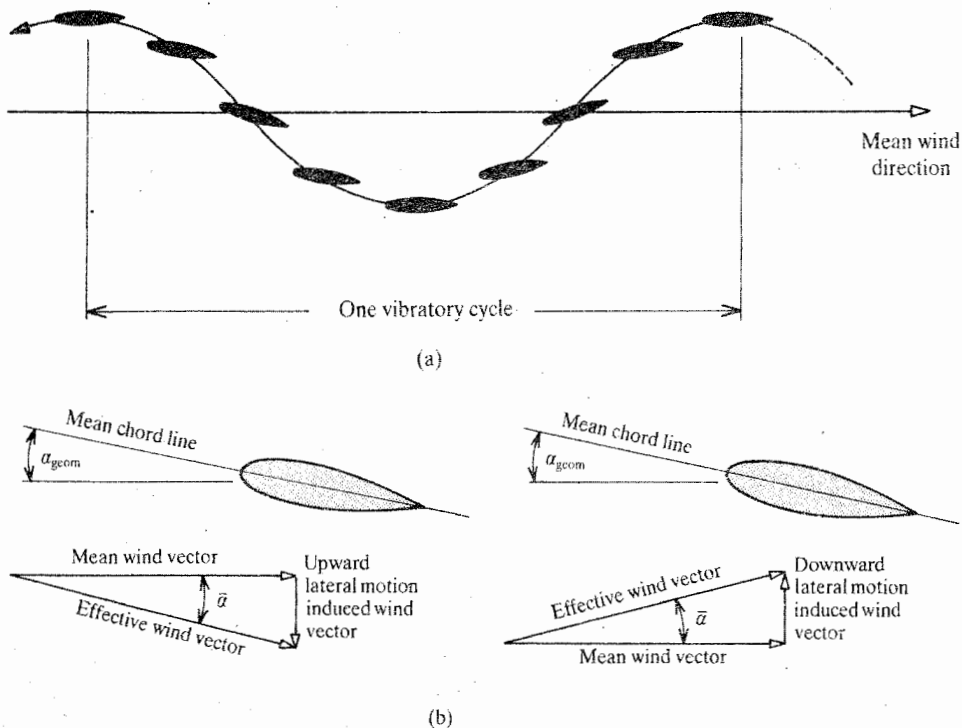


Figure 23.13. The effect on dynamic stability of different phasing between coupled twisting and bending vibrations of an airfoil in an airstream. (a) In this sketch and sketch (c), both the stationary airfoil angle of attack and the average angle of attack of the vibrating airfoil are zero. Even if the vibrating airfoil has any other geometric (static) angle of attack, it has a changing instantaneous angle of attack, and hence a time-varying lift force. The time-varying lift is a result of both the airfoil's twisting motion and the airfoil's up and down motion in the airstream. For an explanation of the latter lift force, see sketch (b). When, as pictured in sketch (a), the airfoil twists in the direction of its lateral motion, and that twisting angle exceeds the angle of attack induced by the up and down motion of the airfoil, then there will be a net lift force in the direction of the lateral motion. A net force in phase with the lateral motion increases the amplitude of the vibration because a force in the same direction as the motion does positive work on the airfoil, and thus increases its airfoil energy content. These ever increasing amplitudes (and thus ever increasing strains and stresses) are the dynamic instability called airfoil flutter. (b) Here the airfoil is undergoing only bending (i.e., up and down) vibrations. A second difference between diagrams (b) and diagrams (a) and (c) is that the (steady state) geometric angle of attack of the airfoils in diagram (b) is not zero. The constant, nonzero geometric angle of attack (within the limits of small total angles of attack) has no effect on the time-varying lift that either diminishes or increases the vibration amplitude. Now, the bending vibration induced wind vector is the vertical air velocity vector. It is equal and opposite to the airfoil lateral velocity vector. By altering the direction of the effective (total) wind vector, the induced wind vector creates an additional angle of attack, α_{vib} , that creates a vibratory lift vector in addition to the steady state lift vector. On the left where the symmetric airfoil is moving upward, the lift force is downward. On the right, where the airfoil is moving downward, the additional lift force is upward. Thus the additional lift of pure bending vibrations always opposes the vibratory motion. (c) In contrast to the vibratory cycle pictured in (a), the phasing shown here between the twisting and the bending of the airfoil results in additional lift due to twisting and the additional lift due to bending combining to directly oppose the bending vibration, and indirectly oppose the twisting vibratory motion that is tied to the bending motion. Thus the vibratory amplitudes diminish and the system is dynamically stable.

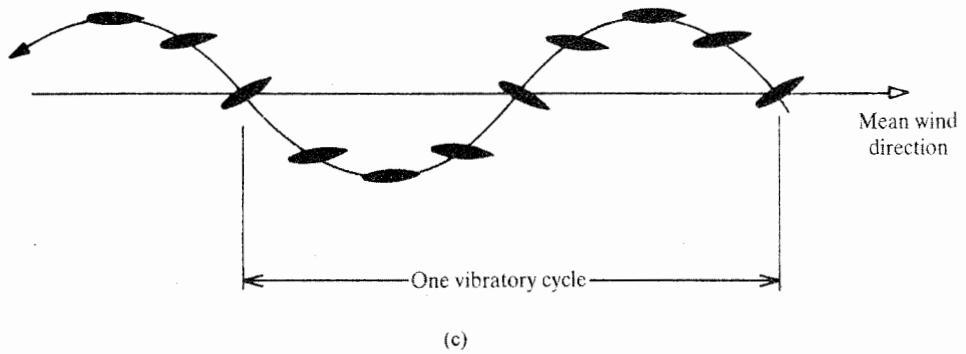


Figure 23.13 (continued).

Of course, not all airfoil vibrations are unstable. In the coupled vibration of Fig. 23.13(c), the phasing between the rotational and lateral vibration is such that the oscillatory increment in the lift force is always opposed to the motion. Thus negative work is being done on the airfoil each cycle, and thus energy is being removed from the airfoil by the airflow. The phasings between the rotational and lateral vibrations sketched in Figs. 23.13(a, c) are just two of many possible combinations. Experience has shown that for the structure of each lifting surface there is a dynamic pressure below which the vibration amplitudes will always decrease, and above which the vibration amplitudes will always increase. Thus it is concluded that for each lifting surface structure there exists a neutral stability dynamic pressure at which the vibration amplitudes remain constant. Any vibration at constant amplitude and frequency is called "harmonic motion." Mathematically, harmonic motion can be represented by a sinusoidal function of time as is done below in complex form, and in the next section using real quantities.

As noted previously, the difference between the vibration cycles of Figs. 23.13(a) and 23.13(c) is the phase relation between the lateral deflection h (positive downward) and the airfoil twist α (positive leading edge upward). The effective way to describe this all-important phasing, as is done for example with alternating electric voltages, is to use complex algebra. Complex algebra enters the flutter analysis in the description of the time-varying air loads. The time-varying, also called "unsteady," air loads for a flutter analysis are derived from the presumption that the airfoil is undergoing harmonic motion, and is therefore at its neutral stability dynamic pressure. In complex algebra terms, a harmonic deflection can be written as $d(q) = D_0 \exp(2\pi if t)$, where D_0 is the amplitude of the deflection, i is the square root of minus one, f is the frequency of the vibration in units of cycles per unit of time, and t is time. Then, with a being the nondimensional parameter that locates the elastic axis aft of the midchord position (see Fig. 23.14), the lift force and moment at the elastic axis per unit of span length due to the deflections from the static equilibrium position are, respectively (Ref. [62]),

$$\begin{aligned} \mathcal{L} &= -\pi\rho b^3 \left[\frac{\ddot{h}}{b} + 2\frac{V\dot{h}}{b^2}\mathcal{E}(k) - a\ddot{\alpha} - \frac{V\dot{\alpha}}{b}[(2a-1)\mathcal{E}(k) - 1] + 2\frac{V^2\alpha}{b^2}\mathcal{E}(k) \right] \\ \mathcal{M} &= +\pi\rho b^4 \left\{ \frac{a\ddot{h}}{b} + (1+2a)\frac{V\dot{h}}{b^2}\mathcal{E}(k) - \left(\frac{1}{8} + a^2\right)\ddot{\alpha} \right. \\ &\quad \left. + \left[a - \frac{1}{2} + \left(\frac{1}{2} - a^2\right)\mathcal{E}(k) \right] \frac{V\dot{\alpha}}{b} + (1+2a)\frac{V^2\alpha}{b^2}\mathcal{E}(k) \right\} \end{aligned} \quad (23.9)$$

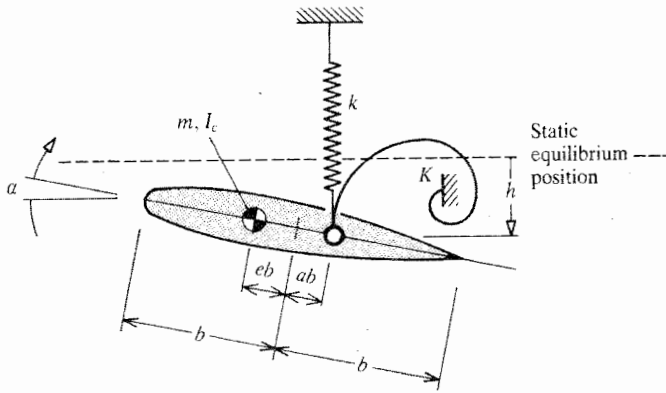


Figure 23.14. The geometry and sign convention for the elastic axis deflections h and α of the unsteady lift and moment equations, Eqs. (23.9).

where ρ = air density, b = semichord length, V = subsonic airstream velocity for neutral stability, called the flutter speed, f = the flutter vibratory frequency, and the reduced (i.e., nondimensionalized) frequency $k = 2\pi fb/V$. The Theodorsen function $\mathcal{C}(k) = \mathcal{F}(k) + i\mathcal{G}(k)$, where

$$\mathcal{F}(k) = \frac{J_1(k)[J_1(k) + Y_0(k)] + Y_1(k)[Y_1(k) - J_0(k)]}{[J_1(k) + Y_0(k)]^2 + [Y_1(k) - J_0(k)]^2}$$

and

$$\mathcal{G}(k) = -\frac{Y_1(k)Y_0(k) + J_1(k)J_0(k)}{[J_1(k) + Y_0(k)]^2 + [Y_1(k) - J_0(k)]^2}$$

The quantities J_0 and J_1 are Bessel functions of the first kind, and Y_0 and Y_1 are Bessel functions of the second kind. Since neither the Reynolds number nor the Mach number of the airflow appears in the above load descriptions, it should be clear that the above solution for the airloads involves neither viscosity nor compressibility effects.

With these two airload descriptions, the equations of motion for the two-dimensional airfoil of Fig. 23.14 are

$$\begin{bmatrix} m & meb \\ meb & (I_c + me^2b^2) \end{bmatrix} \begin{Bmatrix} \ddot{h} \\ \ddot{\alpha} \end{Bmatrix} + \begin{bmatrix} k & 0 \\ 0 & K \end{bmatrix} \begin{Bmatrix} h \\ \alpha \end{Bmatrix} = \begin{Bmatrix} s\mathcal{L}(k, \dots) \\ s\mathcal{M}(k, \dots) \end{Bmatrix} \quad (23.10)$$

where s is the depth into the paper of the two-dimensional airfoil, m is the mass of the total airfoil, and I_c is the mass moment of inertia of the airfoil about the center of mass. Note that there is no difficulty in summing the complex lift force and the complex aerodynamic moment as if they were represented in real terms because, for example, the complex algebra only indicates how the magnitude of the time-varying lift force varies in time relative to the other time-varying forces acting upon the system. That is, here, the complex algebra has nothing to do with the direction of the lift force, which, in this analysis, is always perpendicular to the mean chord line.

This simple analysis would be appropriate for a relatively rigid, thin airfoil supported elastically in a wind tunnel when the airfoil spans the distance between the wind-tunnel walls. Note that the above matrix equation makes no allowance for damping (friction) forces such as would be present in any actual situation. This omission is wholly acceptable in a well-constructed wind-tunnel model, and in an aircraft structure as well.

Since the airloads are predicated upon the harmonic motion of the airfoil, the solution process begins by writing the following phase and frequency relations for the velocities and accelerations:

$$\dot{h} = 2\pi i f h \quad \dot{\alpha} = 2\pi i f \alpha \quad \ddot{h} = -4\pi^2 f^2 h \quad \ddot{\alpha} = -4\pi^2 f^2 \alpha$$

Substituting the above relations into Eq. (23.10), replacing $2\pi f$ by kV/b , where again the nondimensional frequency k is called the "reduced frequency," and transposing the aerodynamic terms to the left-hand side, allows Eq. (23.10) to be rewritten in the form

$$\begin{bmatrix} \mathcal{L}_1(k, V) & \mathcal{L}_2(k, V) \\ \mathcal{L}_3(k, V) & \mathcal{L}_4(k, V) \end{bmatrix} \begin{Bmatrix} h \\ \alpha \end{Bmatrix} = \begin{Bmatrix} 0 \\ 0 \end{Bmatrix} \quad (23.11)$$

The coefficient matrix for the deflection amplitudes is not symmetric. As is routine for any eigenvalue problem, Eq. (23.11) can only have a nontrivial solution if the determinant of the 2×2 coefficient matrix is zero. Since the elements of that determinant are complex, setting the determinant equal to zero requires that both the real part and the imaginary part of the determinant expansion be equal to zero. This provides two real, transcendental, simultaneous equations in the two real unknowns: the flutter airspeed V , and the reduced frequency k . One way to solve those two simultaneous equations is to choose a fixed, arbitrary value for the reduced frequency, and then solve each of the two equations separately for the flutter airspeed. (Choosing a fixed value for k simplifies dealing with the Theodorsen function $\mathcal{C}(k)$.) Of course, the two solutions for the flutter airspeed will in general be different. However, if many choices of the reduced frequency are made, the many pairs of solutions for the airspeed can be separately plotted as functions of the reduced frequency. Where the two curved lines intersect, the solution for the flutter airspeed is the same for both simultaneous equations, and is thus the true solution. Thus the flutter airspeed is determined. The experimentally useful flutter frequency is determined from the value of the reduced frequency where the two curves intersect.

There are many other solution techniques for the flutter determinant. The above technique is essentially Theodorsen's method. Another, more common, technique is to introduce an artificial structural damping factor of unknown magnitude g into the equations of motion as shown below. An actual damping factor that is positive indicates damping forces that diminish the amplitudes of vibration, and an actual damping factor that is negative indicates damping forces that increase the amplitudes of vibration. On the other hand, since the damping forces associated with this artificial damping factor are part of the equilibrium of forces, a positive artificial damping factor solution indicates that the amplitudes of vibration would increase without this artificial damping. Thus positive artificial damping factor solutions are dynamically unstable, while negative ones are dynamically stable. The object of the analysis is therefore to determine the airspeed at which the damping factor, after being negative, reaches a zero value. The inclusion of this unknown artificial damping factor in the analysis increases the number of unknowns to three. The solution process is essentially to again choose an arbitrary value of k , (thus fixing the unknown vibratory frequency) and then solving the two equations simultaneously for the remaining two unknowns: V and g . A plot of the V solution versus the g solution for each chosen value of k (a V - g diagram) shows when the value of the damping factor becomes zero. The values of V and k where the artificial damping factor is zero are of course the values of the flutter airspeed and flutter frequency.

The above-described thin-airfoil, two-dimensional incompressible flow analysis corresponds to a wing of infinite aspect ratio and zero taper. In the precomputer days, this was the extent of a practical flutter speed calculation. By trial and error, it was discovered that many large-aspect-ratio, straight, tapered wings could be described by the above two degrees

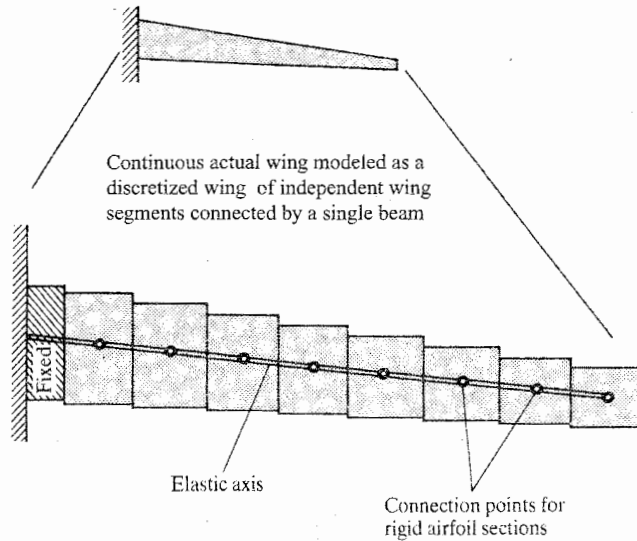


Figure 23.15. A basic strip theory analytical wing model for a high aspect ratio wing treated structurally as a beam.

of freedom analysis if the wing mass, wing stiffness, and wing geometry at 70–75 percent of the semispan were used to represent the entire wing.

With the advent of the availability of the digital computer, the above infinite-aspect-ratio unsteady aerodynamics was used fairly successfully with tapered wings of large, but finite, aspect ratios (over 8 or 10). The technique, as is used above in the divergence example, is to divide the finite wing into a series of adjacent wing panels and apply the above two-dimensional aerodynamics to each panel. To expound upon this point, consider the cantilevered, finite wing shown in Fig. 23.15. Again, in model form, such a wing might be used in a wind-tunnel test. Using the same rigid chord assumption, the wing is approximated over its semispan with a series of chordwise panels often called “strips.” Then, with a value of b , the semichord length that varies from strip to strip, the unsteady airloads of Eq. (23.9) can be used with each strip. Then the equations of motion can be written, for example, using an artificial structural damping factor g , as

$$[M]\{q\} + (1 + ig)[K]\{q\} = \{\mathcal{L}(\dot{h}_i, \ddot{h}_i, \alpha_i, \dot{\alpha}_i, \ddot{\alpha}_i, k, V)\}$$

where, as before, $\{q\} = [h_1 \ \theta_1 \ \phi_1 \ \dots \ \phi_n]$. As with the divergence analysis, a geometrical relation depending upon the sweep of the elastic axis exists between the α rotations on one hand, and the θ and ϕ rotations on the other hand. Since the matrices of the above equation are quite large considering the complexity of the solution process, a modal coordinate transformation³ is almost always used to reduce the size of the determinant equation. This type of analysis is generally called a basic strip theory flutter analysis. It can easily be 20 percent in error even when the actual airflow is almost wholly incompressible. However, the calculated solution for the flutter speed is almost always less than the wind tunnel and flight test indicated flutter speed. On those exceptional occasions when the basic strip theory-calculated flutter speed is greater than the actual flutter speed, it is so only by a couple of percent.

³ See Endnote (1) after reading Section 23.8.

When the wing is that of an aircraft in free flight, the zero eigenvalue rigid body motion of the aircraft is removed from the analysis by writing the equations that state that the change in the linear and angular momentum is zero. With DOF that are h_i , θ_i , and ϕ_i , it would be necessary to write that the linear momentum in the vertical direction is zero, the angular velocity of the total structure about the fuselage axis is zero, and the angular velocity about the pitch axis is zero.

With the tremendous increase in computing capability that has occurred in the last decade, basic strip theory is obsolete in industrial practice. It is now practicable to discard the rigid chord assumption that was inapplicable to low-aspect-ratio wings and, using finite elements, provide a truly suitable description of the structure of any airfoil. With the recent advances in aerodynamics, it is now practicable to do the resulting air pressure calculations for a compressible flow about a wing of any aspect ratio and taper. Nevertheless, it is still important to verify those calculations by flight testing. Of course, flight testing does not mean increasing the airspeed until the plane becomes unstable and the airfoil structure fails. It does mean increasing the airspeed while carefully monitoring in real time the damping and vibratory frequency of the structure after the structure has been perturbed by, for example, an aileron movement. Aerodynamic flutter is a aircraft structural problem that probably will always need to be investigated. The maximum safe airspeed of several aircraft flying today is limited by the flutter phenomenon.

23.8 Matrix Iteration for Symmetric Matrices

There are many methods and variations on methods for determining eigenvalues. The reader has already been introduced to the determinant method in Chapter 2, where the matrix equation for principal stresses in three dimensions was discussed. The determinant method is an efficient procedure when the size of the square matrices is limited to just a few rows. The determinant method becomes rapidly less efficient as the size of the matrices increases. This section introduces a matrix eigenvalue solution method that is (i) not difficult to understand, (ii) easy to use for hand calculations, and (iii) moderately efficient for moderately sized matrix machine calculations. Over the past few decades, mathematicians have developed more efficient means of solving large matrix eigenvalue problems for the many eigenvalues that usually need investigation. As of this writing, Lanczo's method is the most popular for treating the large, sparse matrices that are a commonplace means for describing the inertial and elastic characteristics of aerospace structures. Descriptions of these techniques are left to other textbooks dealing with the topic of structural dynamics.

The matrix iteration method for the solution of matrix eigenvalue problems is easily explained when the two square matrices that describe the characteristics of the structure, and possibly the applied loading as well, are both real and symmetric. Important examples of this limited circumstance are the calculation of a buckling load of a structure using finite element matrices, and the calculation of a first or fundamental natural frequency of vibration of a structural system plus higher-numbered natural frequencies. Since buckling has already been discussed in this chapter, the matrix iteration technique is explained in terms of the matrices involved in the calculation of vibratory natural frequencies. Solutions for other types of problems can be patterned exactly on the solution process for the first natural frequency.

Any natural frequency of vibration for an elastic structure is an inherent characteristic of that structure. Each natural frequency depends only upon the distribution of mass and stiffness throughout the structure. In particular, natural frequencies are not at all related to

any time-varying or time-invariant loading (other than the weight loading as it reflects the mass distribution). The characteristics of natural frequencies are revealed by the mathematics that follows. From Eq. (19.9), the $n \times n$ matrix equation that describes the motion of a force-free ($\{Q\} = \{0\}$), undamped ($[C] = [0]$) structure is

$$[M]\{\ddot{q}(t)\} + [K]\{q(t)\} = \{0\} \quad (23.12a)$$

where, again, the matrix $[M]$ describes the mass associated with each DOF. A complete solution to this matrix equation for the time-varying DOF of the structure, $\{q(t)\}$, is obtained by first describing the time variation of those deflections as⁴

$$\{q(t)\} = \{\bar{q}\} \sin(2\pi ft + \psi) \quad (23.13)$$

where $\{\bar{q}\}$ is the n -vector of constant deflection amplitudes, and f is the frequency of vibration in units of cycles per second (Hz) when time is in units of seconds. This trial solution means that when the structure vibrates at a single natural frequency, f , the amplitudes of vibration of all parts of the structure are in a fixed ratio to each other, positive or negative. Thus

$$\{\ddot{q}(t)\} = -4\pi^2 f^2 \{\bar{q}\} \sin(2\pi ft + \psi)$$

After substitution, and cancellation of $\sin(2\pi ft + \psi)$, Eq. (23.12) can be written as

$$\begin{aligned} [M]\{\bar{q}\} &= \frac{1}{4\pi^2 f^2} [K]\{\bar{q}\} \\ &= \lambda [K]\{\bar{q}\} \end{aligned} \quad (23.12b)$$

where λ is the eigenvalue containing the unknown frequency of vibration in its denominator. From a determinant method solution of Eq. (23.13), it is clear that there are n solutions for λ . Let λ_i be the i th solution, and λ_j be the j th solution. Then

$$\begin{aligned} [M]\{\bar{q}_i\} &= \lambda_i [K]\{\bar{q}_i\} \\ [M]\{\bar{q}_j\} &= \lambda_j [K]\{\bar{q}_j\} \end{aligned} \quad (23.14)$$

where $\{\bar{q}_i\}$ is the deflection amplitude solution $\{\bar{q}\}$ corresponding to λ_i , and so on. Premultiplying the first of Eqs. (23.14) by $[\bar{q}_j]$ and premultiplying the second by $[\bar{q}_i]$ leads to

$$\begin{aligned} [\bar{q}_j][M]\{\bar{q}_i\} &= \lambda_i [\bar{q}_j][K]\{\bar{q}_i\} \\ [\bar{q}_i][M]\{\bar{q}_j\} &= \lambda_j [\bar{q}_i][K]\{\bar{q}_j\} \end{aligned} \quad (23.15)$$

Transpose the second equation of the above equations. Since both the mass and stiffness matrices are symmetric, $[M]^t = [M]$ and $[K]^t = [K]$. Therefore,

$$[\bar{q}_j][M]\{\bar{q}_i\} = \lambda_j [\bar{q}_j][K]\{\bar{q}_i\}$$

Subtracting this equation from the first of Eqs. (23.15) yields

$$0 = (\lambda_i - \lambda_j) [\bar{q}_j][K]\{\bar{q}_i\}$$

It is now assumed that all the eigenvalues or natural frequencies are distinct. Only very rarely are natural frequencies repeated in an actual structure. Then the factor $(\lambda_i - \lambda_j)$ is not zero. Therefore it must be true that

$$[\bar{q}_j][K]\{\bar{q}_i\} = 0 = [\bar{q}_j][M]\{\bar{q}_i\} \quad (23.16)$$

⁴ Using coordinate transformations and matrix diagonalization techniques (see Endnote (2)), it can be proved that the time variation of the generalized coordinates must be sinusoidal.

The above equations establish the mutual orthogonality of the eigenvectors $\{\bar{q}_i\}$ and $\{\bar{q}_j\}$ when their product includes either the stiffness matrix or the mass matrix. Such an orthogonality condition is called "weighted" orthogonality.

Consider the case when i equals j in Eq. (23.15) and the following definition. A matrix $[B]$ is *positive definite* whenever $\{x\}[B]\{x\} > 0$ for any vector $\{x\}$ that is not the null vector. The above mass matrix is positive definite because the kinetic energy of the structure

$$T = \frac{1}{2}[\dot{q}(t)][M]\{\dot{q}(t)\}$$

is always greater than zero whenever there is a nonzero (i.e., positive or negative) velocity for any part of the structure. Thus it follows that the products $[\bar{q}_i][M]\{\bar{q}_i\}$ and $[\bar{q}_i][K]\{\bar{q}_i\}$ are greater than zero. It also can be argued directly that the above stiffness matrix, which already includes all boundary (and momentum) conditions, is also positive definite because the positive-valued strain energy of the structure is equal to

$$U = \frac{1}{2}[q(t)][K]\{q(t)\}$$

Note that all forms of the deflection vectors $\{q\}$, such as $\{\bar{q}_i\}$, are exclusively composed of real numbers. Therefore both $[\bar{q}_i][M]\{\bar{q}_i\} = M_i$, called the generalized mass, and $[\bar{q}_i][K]\{\bar{q}_i\} = K_i$, called the generalized stiffness, are positive real numbers. Also note from Eq. (23.15) that the eigenvalue λ_i can be written as the ratio M_i/K_i . Thus every solution for every eigenvalue must always be a positive real number.

Since the eigenvectors $\{\bar{q}_i\}$ are orthogonal, they are also linearly independent. To prove this statement, assume, by way of contradiction, that the n eigenvectors are linearly dependent. Then, by definition, there must exist a set of constants a_i not all of which are zero, such that

$$0 = a_1\{\bar{q}_1\} + a_2\{\bar{q}_2\} + a_3\{\bar{q}_3\} + \cdots + a_n\{\bar{q}_n\}$$

Multiply both sides of the above equation by $[\bar{q}_i][M]$. Because of the weighted orthogonality of the i th eigenvector with all other eigenvectors, the above equation reduces to

$$0 = a_i[\bar{q}_i][M]\{\bar{q}_i\}$$

Since $[\bar{q}_i][M]\{\bar{q}_i\}$ is greater than zero, then the coefficient a_i must be zero. When this procedure is carried out for all values of the index i , then the assumption that some of the constants a_i are not zero is contradicted. Hence the eigenvectors cannot be linearly dependent, but must be linearly independent.

Since the eigenvectors are linearly independent, an arbitrary n vector $\{\bar{q}\}$ can be expressed in terms of these eigenvectors as

$$\{\bar{q}\} = c_1\{\bar{q}_1\} + c_2\{\bar{q}_2\} + c_3\{\bar{q}_3\} + \cdots + c_n\{\bar{q}_n\} \quad (23.17)$$

where the Fourier coefficients c_i have the values $[\bar{q}_i][M]\{\bar{q}\}/M_i$. In this discussion, these coefficients are arbitrary constants because $\{\bar{q}\}$ is arbitrary. Now rewrite Eq. (23.12b) as

$$[K]^{-1}[M]\{\bar{q}\} = \lambda\{\bar{q}\} \quad \text{or} \quad [D]\{\bar{q}\} = \lambda\{\bar{q}\} \quad (23.18)$$

where $[D]$ is called the dynamic matrix. Consider the vector $\{\bar{q}\}$ of Eq. (23.17) to be the first eigenvector trial solution. Call it $\{\bar{q}\#1\}$. Substitute this series expansion of the trial solution $\{\bar{q}\#1\}$ into Eq. (23.18) so as to obtain

$$[D]\{\bar{q}\#1\} = c_1[D]\{\bar{q}_1\} + c_2[D]\{\bar{q}_2\} + c_3[D]\{\bar{q}_3\} + \cdots + c_n[D]\{\bar{q}_n\} \stackrel{?}{=} \lambda\{\bar{q}\}$$

Since $\{\bar{q}_i\}$ and λ_i are also solutions to Eq. (23.18), that is, $[D]\{\bar{q}_i\} = \lambda_i\{\bar{q}_i\}$, the right-hand side of the above equation becomes

$$[D]\{\bar{q}\#1\} = c_1\lambda_1\{\bar{q}_1\} + c_2\lambda_2\{\bar{q}_2\} + c_3\lambda_3\{\bar{q}_3\} + \cdots + c_n\lambda_n\{\bar{q}_n\}$$

Call the above sum $\{\bar{q}\#2\}$, the second trial solution. Substitute $\{\bar{q}\#2\}$ into Eq. (23.18). The result is

$$[D]\{\bar{q}\#2\} = c_1\lambda_1^2\{\bar{q}_1\} + c_2\lambda_2^2\{\bar{q}_2\} + c_3\lambda_3^2\{\bar{q}_3\} + \cdots + c_n\lambda_n^2\{\bar{q}_n\}$$

Call the right-hand side of the above equation $\{\bar{q}\#3\}$ and substitute it into the left-hand side of Eq. (23.18). After m such iterations, the result is

$$c_1\lambda_1^m\{\bar{q}_1\} + c_2\lambda_2^m\{\bar{q}_2\} + c_3\lambda_3^m\{\bar{q}_3\} + \cdots + c_n\lambda_n^m\{\bar{q}_n\} = \lambda\{\bar{q}\#m\}$$

Now let all the eigenvalues be ordered such that $\lambda_1 > \lambda_2 > \lambda_3 > \cdots > \lambda_n$. Then regardless of the relative nonzero values of the c_i (which means regardless of the original choice for $\{q\#1\}$, as long as c_1 is not zero) a value of m will be reached where the first term of the above left-hand side totally dominates all the other terms of the left-hand side. When this happens, the vector $\{\bar{q}\#m\}$ is proportional to $\{\bar{q}_1\}$, and the iteration procedure has converged to the desired answer. Since λ_1 is the largest eigenvalue, it contains the lowest natural frequency value, which is called the first or fundamental natural frequency. The following two examples illustrate the process. Note that one advantage of the iteration solution technique for hand calculations is that the worst effect of a numerical error is that it may temporarily slow the rate of convergence by moving the trial vector further from its converged state. On the other hand, judicious guessing can speed the rate of convergence.

The second, third, and higher natural frequencies can also be calculated by the matrix iteration method. To iterate for the second natural frequency, it is necessary to have an otherwise arbitrary trial vector that is completely free of all traces of the first eigenvector. That is, it is necessary to force c_1 to be zero. If the trial vector has any component "in the direction" of the first eigenvector, then that trial vector will inevitably converge to the first eigenvector for the reasons demonstrated above. To eliminate all traces of the first eigenvector, require that the trial vector for the second eigenvector, $\{q\setminus 2\}$, be constrained to be orthogonal to the now known first eigenvector; that is, write $[\bar{q}_1][M]\{q\setminus 2\}_c = 0$. The subscript c indicates that this otherwise arbitrary vector is now constrained to be free of the first eigenvector. Multiplying out this triple matrix product leads to the single equation $-Z_2q_2 - Z_3q_3 - \cdots - Z_nq_n = q_1$ where q_i is the i th element of $\{q\setminus 2\}_c$, and Z_i comes from the product $[q_1][M]$. This single equation can be used to construct the first row of the transformation matrix $[T_2]$ in the matrix equation $\{q\setminus 2\}_c = [T_2]\{q\setminus 2\}$. The remaining $n - 1$ rows of $[T_2]$ are merely the identities $q_i/2 = q_i/2$, for $i = 2, 3, \dots$. To be clearer, the first column of $[T_2]$ is all zeros, the $-Z_j$ terms make up the remainder of the first row, and the other diagonal terms are ones. Then $[D]\{q\setminus 2\}_c = [D][T_2]\{q\setminus 2\} = [D_2]\{q\setminus 2\}$, where the unconstrained form of the vector $\{q\setminus 2\}$ is wholly arbitrary. Thus the matrix $[D_2]$ carries the constraint that causes the vector $\{q\setminus 2\}$ to converge to the second eigenvector with its now dominant second eigenvalue. The third eigenvector and eigenvalue can be obtained by writing two orthogonality conditions, and so on. Other, better iteration techniques for the higher numbered vibratory eigenvectors are also possible.

The above extension of the matrix iteration method to the higher natural frequencies works quite well when a computing machine is doing the calculations and precision is maintained by carrying a large number of digits for each numerical quantity. A check on the numerical accuracy of these calculations can be made by comparing the last eigenvalue solution for $[D]$ to the first eigenvalue solution for the inverse of $[D]$, which is equal

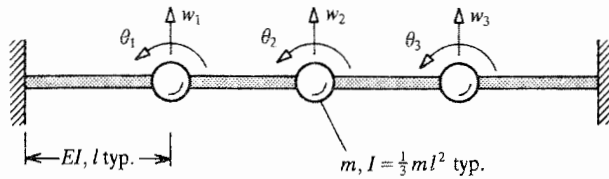


Figure 23.16. Example 23.5. A beam vibration finite element model.

to $[M]^{-1}[K]$. This check on numerical accuracy is the only use the last eigenvalue and eigenvector solution has. Again, the discretization process used to form the mass and stiffness matrices is only an approximation to the continuous, actual structure. The result of that approximation is usually that only the lower half of the calculated natural frequencies and eigenvectors are good approximations to their corresponding actual values.

Example 23.5. Consider the clamped–clamped, uniform beam shown in Fig. 23.16. The beam has been modeled using four massless, elastic beam elements and three rigid masses. Each beam element has the stiffness factor EI , and is of length l . Each discrete mass has a mass value m and a mass moment of inertia about an axis coming out of the paper of magnitude $(1/3)ml^2$. The beam has six DOF, which are labeled w_1 through θ_3 . Since the structure is symmetric about the indicated centerline, the modes of vibration are either symmetric or antisymmetric. The symmetric modes can be calculated separately from the antisymmetric modes by requiring $w_3 = w_1$, $\theta_3 = -\theta_1$, and $\theta_2 = 0$. Applying this set of constraints to the original mass and stiffness matrices in order to assure symmetric vibration amplitudes leads to the following equation of motion for free, undamped vibration:

$$\begin{bmatrix} 2 & 0 & 0 \\ 0 & 2/3 & 0 \\ 0 & 0 & 1 \end{bmatrix} \begin{Bmatrix} \ddot{w}_1 \\ l\ddot{\theta}_1 \\ \ddot{w}_2 \end{Bmatrix} + \frac{4EI}{ml^3} \begin{bmatrix} 12 & 0 & -6 \\ 0 & 4 & -3 \\ -6 & -3 & 6 \end{bmatrix} \begin{Bmatrix} w_1 \\ l\theta_1 \\ w_2 \end{Bmatrix} = \begin{Bmatrix} 0 \\ 0 \\ 0 \end{Bmatrix}$$

Iterate to find only the fundamental natural frequency and first mode shape. Check that the first natural frequency satisfies the characteristic equation provided by the determinant method.

Solution. First write $q(t) = \bar{q} \sin(2\pi ft + \psi)$ and $\ddot{q}(t) = -4\pi^2 f^2 q(t)$. Let $\lambda = EI/(\pi^2 f^2 ml^3)$, where it is important to have the frequency in the denominator of the eigenvalue because the iteration procedure always converges to the largest eigenvalue. The next step is to invert the matrix portion of $[K]$ and form the dynamic matrix $[D] = [K]^{-1}[M]$:

$$[K]^{-1} = \begin{bmatrix} 5/12 & 1/2 & 2/3 \\ 1/2 & 1 & 1 \\ 2/3 & 1 & 4/3 \end{bmatrix} \quad [D] = \frac{1}{6} \begin{bmatrix} 5 & 2 & 4 \\ 6 & 4 & 6 \\ 8 & 4 & 8 \end{bmatrix}$$

Note that the dynamic matrix is not usually symmetric.⁵ With the cancellation of the sine function, the original matrix equation now has the form $[D]\{\bar{q}\} = \lambda\{\bar{q}\}$ which is suitable

⁵ There is no advantage in matrix iteration to having a symmetric $[D]$. Certain other methods do require $[D] = [D]^t$. Symmetry can be achieved, for example, by using the coordinate transformation $\{q\} = [M]^{-1/2}\{p\}$ and premultiplying by $[M]^{-1/2}$. When the mass matrix is diagonal, its square root is particularly easy to obtain. When the mass matrix is not a diagonal matrix a Cholesky decomposition of the mass matrix is the usually chosen route to a symmetric dynamic matrix (Ref. [72]).

for iteration. To begin the iteration, guess at $\{q\#1\}$, the mode shape for the first symmetric vibratory mode. From physical experience, it can be expected that, for example, the value for w_2 is something like twice the value of w_1 , and so on. Thus a reasonable first guess could be $\{q\#1\} = [\frac{1}{2} \frac{1}{2} 1]$. However, in order to illustrate the power of this approach, a completely neutral guess of $\{q\#1\} = [1 \ 1 \ 1]$ will be used. Now substitute this latter guess into the equation $[D]\{\bar{q}\} = \lambda\{\bar{q}\}$ to test whether or not $[D]\{\bar{q}\#1\} = \lambda\{\bar{q}\#1\}$. That is, write

$$\frac{1}{6} \begin{bmatrix} 5 & 2 & 4 \\ 6 & 4 & 6 \\ 8 & 4 & 8 \end{bmatrix} \begin{Bmatrix} 1 \\ 1 \\ 1 \end{Bmatrix} = \begin{Bmatrix} 11/6 \\ 16/6 \\ 20/6 \end{Bmatrix} = 3.3 \begin{Bmatrix} 0.55 \\ 0.8 \\ 1.0 \end{Bmatrix} \neq \lambda \begin{Bmatrix} 1 \\ 1 \\ 1 \end{Bmatrix}$$

The second of the above equalities is merely the factoring of the algebraically largest of the element magnitudes ($20/6 = 3.3$) in order to make the resulting largest element of the column matrix equal to one for the sake of easy comparisons with the original vector. This factoring of the largest element is referred to as (one form of) normalizing the vector. Since the normalized vector result of the matrix multiplication does not equal the original vector, use the first result as the second guess. Note that in the early stages of the calculation only one or two significant digits are useful.

$$\frac{1}{6} \begin{bmatrix} 5 & 2 & 4 \\ 6 & 4 & 6 \\ 8 & 4 & 8 \end{bmatrix} \begin{Bmatrix} 0.5 \\ 0.8 \\ 1.0 \end{Bmatrix} = \begin{Bmatrix} 8.1/6 \\ 12.2/6 \\ 15.2/6 \end{Bmatrix} = 2.5 \begin{Bmatrix} 0.53 \\ 0.80 \\ 1.0 \end{Bmatrix} \neq \lambda \begin{Bmatrix} 0.50 \\ 0.80 \\ 1.0 \end{Bmatrix}$$

Obviously $\{q\#3\}$ is not far different from $\{q\#2\}$. Iterating again with $\{q\#3\}$,

$$\frac{1}{6} \begin{bmatrix} 5 & 2 & 4 \\ 6 & 4 & 6 \\ 8 & 4 & 8 \end{bmatrix} \begin{Bmatrix} 0.53 \\ 0.80 \\ 1.0 \end{Bmatrix} = \begin{Bmatrix} 1.375 \\ 2.063 \\ 2.573 \end{Bmatrix} = 2.573 \begin{Bmatrix} 0.5343 \\ 0.8018 \\ 1.000 \end{Bmatrix}$$

Convergence to four significant figures is achieved with one more iteration:

$$\frac{1}{6} \begin{bmatrix} 5 & 2 & 4 \\ 6 & 4 & 6 \\ 8 & 4 & 8 \end{bmatrix} \begin{Bmatrix} 0.5343 \\ 0.8018 \\ 1.000 \end{Bmatrix} = \begin{Bmatrix} 1.379 \\ 2.069 \\ 2.580 \end{Bmatrix} = 2.580 \begin{Bmatrix} 0.5345 \\ 0.8018 \\ 1.000 \end{Bmatrix}$$

Thus by comparison to $[D]\{q\} = \lambda\{q\}$, $\lambda_1 = 2.58 = EI/(\pi^2 f^2 ml^3)$, or $f_1 = 0.198(EI/ml^3)^{1/2}$, and $\{q_1\} = [0.535 \ 0.802 \ 1.00]$. This result is confirmed by the determinant method, which also reveals that the second and third symmetric natural frequencies are $f_2 = 0.780(EI/ml^3)^{1/2}$, and $f_3 = 1.08(EI/ml^3)^{1/2}$. However, these higher natural frequencies are only worth noting if the details of the simple structural model of Fig. 23.16 closely correspond to the actual structure. ■

Example 23.6. A certain beam buckling problem is described by the matrix equation $[K]\{q\} = \lambda^*[H]\{q\}$ given below. Use matrix iteration to determine the beam buckling load and the beam buckling mode shape.

$$\begin{bmatrix} 20 & -14 & 5 \\ -14 & 29 & -19 \\ 5 & -19 & 15 \end{bmatrix} \begin{Bmatrix} w_1 \\ w_2 \\ w_3 \end{Bmatrix} = \frac{PL^2}{18EI} \begin{bmatrix} 2 & -1 & 0 \\ -1 & 2 & -1 \\ 0 & -1 & 1 \end{bmatrix} \begin{Bmatrix} w_1 \\ w_2 \\ w_3 \end{Bmatrix}$$

Solution. Since it is desired to find the lowest value of P that satisfies the above matrix eigenvalue problem, it is necessary to divide both sides by the factor $\lambda^* = PL^2/(18EI)$ and

multiply both sides by $[K]^{-1}$ in order to obtain the form $\lambda\{q\} = [D]\{q\}$ where $\lambda = 1/\lambda^*$, and $[D] = [K]^{-1}[H]$. With

$$[K]^{-1} = \frac{1}{475} \begin{bmatrix} 74 & 115 & 121 \\ 115 & 275 & 310 \\ 121 & 310 & 384 \end{bmatrix} \quad [D] = \frac{1}{475} \begin{bmatrix} 33 & 35 & 6 \\ -45 & 125 & 35 \\ -68 & 115 & 74 \end{bmatrix}$$

Again starting with $\{q\} = [1 \ 1 \ 1]$, the iteration procedure is

$$\frac{1}{475} \begin{bmatrix} 33 & 35 & 6 \\ -45 & 125 & 35 \\ -68 & 115 & 74 \end{bmatrix} \begin{Bmatrix} 1 \\ 1 \\ 1 \end{Bmatrix} = \begin{Bmatrix} 74/475 \\ 115/475 \\ 121/475 \end{Bmatrix} = 0.25 \begin{Bmatrix} 0.6 \\ 0.9 \\ 1 \end{Bmatrix}$$

$$\frac{1}{475} \begin{bmatrix} 33 & 35 & 6 \\ -45 & 125 & 35 \\ -68 & 115 & 74 \end{bmatrix} \begin{Bmatrix} 0.6 \\ 0.9 \\ 1.0 \end{Bmatrix} = \begin{Bmatrix} 57.3/475 \\ 120.5/475 \\ 136.7/475 \end{Bmatrix} = 0.29 \begin{Bmatrix} 0.42 \\ 0.86 \\ 1.0 \end{Bmatrix}$$

$$\frac{1}{475} \begin{bmatrix} 33 & 35 & 6 \\ -45 & 125 & 35 \\ -68 & 115 & 74 \end{bmatrix} \begin{Bmatrix} 0.42 \\ 0.88 \\ 1.0 \end{Bmatrix} = \begin{Bmatrix} 50.66/475 \\ 126.1/475 \\ 146.6/475 \end{Bmatrix} = 0.31 \begin{Bmatrix} 0.34 \\ 0.86 \\ 1.0 \end{Bmatrix}$$

$$\frac{1}{475} \begin{bmatrix} 33 & 35 & 6 \\ -45 & 125 & 35 \\ -68 & 115 & 74 \end{bmatrix} \begin{Bmatrix} 0.34 \\ 0.86 \\ 1.0 \end{Bmatrix} = \begin{Bmatrix} 47.32/475 \\ 127.2/475 \\ 149.8/475 \end{Bmatrix} = 0.315 \begin{Bmatrix} 0.316 \\ 0.849 \\ 1.00 \end{Bmatrix}$$

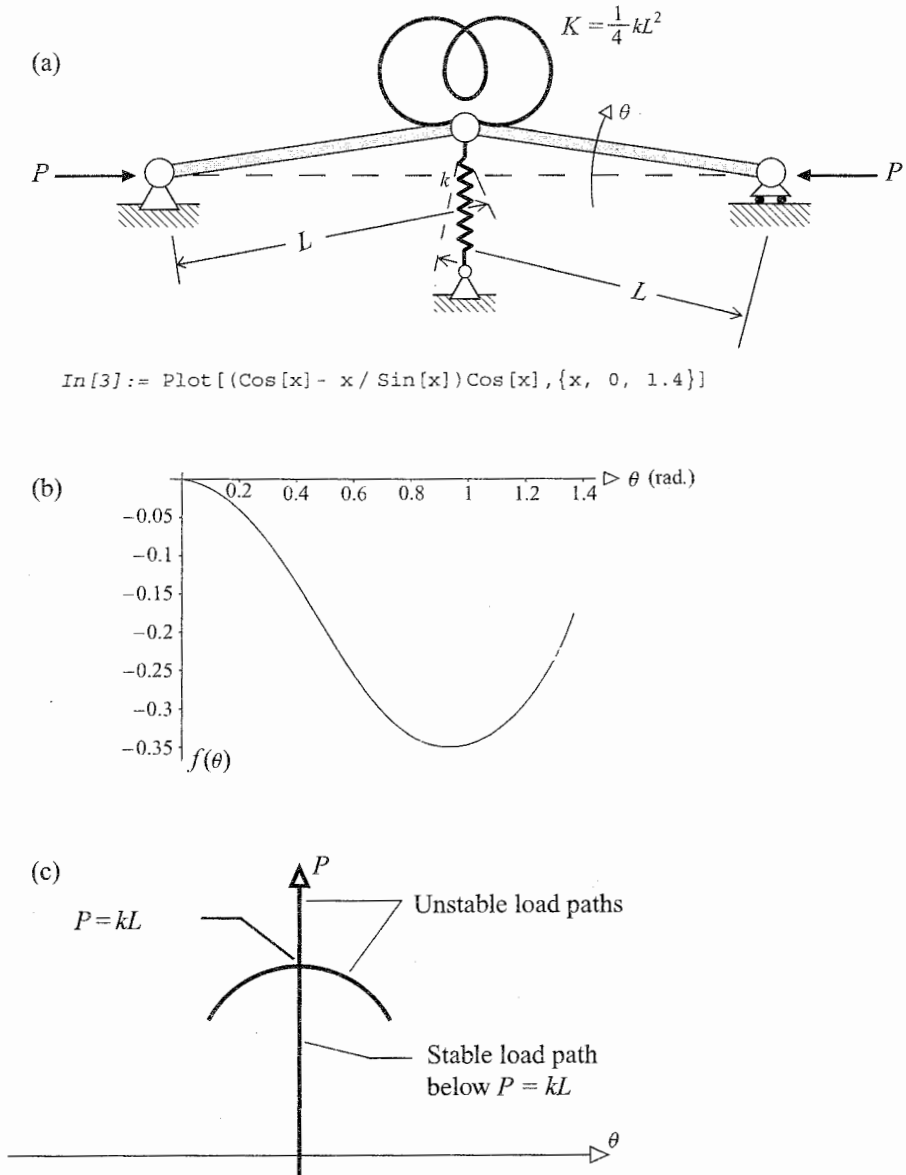
$$\frac{1}{475} \begin{bmatrix} 33 & 35 & 6 \\ -45 & 125 & 35 \\ -68 & 115 & 74 \end{bmatrix} \begin{Bmatrix} 0.316 \\ 0.849 \\ 1.00 \end{Bmatrix} = \begin{Bmatrix} 46.11/475 \\ 126.9/475 \\ 150.2/475 \end{Bmatrix} = 0.316 \begin{Bmatrix} 0.307 \\ 0.845 \\ 1.00 \end{Bmatrix}$$

After five iterations starting with a rather poor guess, convergence is close on the eigenvalue. One more time for a better accuracy:

$$\frac{1}{475} \begin{bmatrix} 33 & 35 & 6 \\ -45 & 125 & 35 \\ -68 & 115 & 74 \end{bmatrix} \begin{Bmatrix} 0.307 \\ 0.845 \\ 1.00 \end{Bmatrix} = \begin{Bmatrix} 45.70/475 \\ 126.8/475 \\ 150.3/475 \end{Bmatrix} = 0.316 \begin{Bmatrix} 0.304 \\ 0.844 \\ 1.00 \end{Bmatrix}$$

Precision for buckling eigenvectors is not as important as it is for vibratory eigenvectors because there is never any interest in the higher buckling eigenvalues. Therefore, the above answer is satisfactory because three-significant-digit convergence has been obtained for the eigenvalue $\lambda = 18EI/(PL^2) = 0.316$. Whence $P_{cr} = 57EI/L^2$. ■

Two final comments on the iteration procedure are offered. First note that with hand and machine calculations the convergence rate can be improved by noting and using the demonstrated trends of the eigenvector element values during the initial stages of the procedure. For example, instead of using $\{q\#2\} = [0.6 \ 0.9 \ 0 \ 1.0]^t$ the drop in the first element value from its initial estimate at 1 could suggest trying $[0.4 \ 0.8 \ 1.0]$. This choice would speed convergence. Second, the matrix iteration procedure works just as well when the matrices are real and nonsymmetric (Ref. [25]). The matrix iteration procedure works even when one of the square matrices is singular as well as nonsymmetric, as is illustrated in Exercise 23.7. Nonsymmetric matrices are briefly commented upon at the end of Endnote (2). See Ref. [61] for a discussion of matrix iteration for complex matrices.



```
In[3]:= Plot[(Cos[x] - x/Sin[x])Cos[x], {x, 0, 1.4}]
```

Figure 23.17. Example 23.7. (a) Two-bar system in deformed position. (b) Graph proportional to the second variation of total potential energy. (c) System stability diagram showing a single bifurcation point (neutral stability) between the initial, stable load path and the subsequent unstable load paths.

Example 23.7. Consider the two-bar system shown in Fig. 23.17 where the only loading is an axial force P . In their unloaded state the two bars are horizontal. The stiffness of the central hinge translational spring and rotational spring are sufficiently smaller than the stiffnesses of the bars that the bars are here modeled as being rigid. Draw the stability diagram for this one DOF system showing the postbuckling behavior of the structure for small values of the angle θ .

Solution. Figure 23.17(a) shows the system in its deformed configuration. Realizing that the angle of rotation experienced by the torsion spring is 2θ , the system strain energy, which resides entirely in the two springs, is

$$U = \frac{1}{2}K(2\theta)^2 + \frac{1}{2}kL^2 \sin^2 \theta = \frac{1}{2}kL^2(\theta^2 + \sin^2 \theta)$$

The system potential energy is the negative of the work done by the axial force P :

$$V = -P(2L)(1 - \cos \theta)$$

The equilibrium states of the two-bar system are determined by writing the variation of the total potential energy, $\delta\Pi = \delta(U + V) = 0$. That result is

$$[kL^2(\theta + \sin \theta \cos \theta) - 2PL \sin \theta]\delta\theta = 0$$

One solution to the above equilibrium equation is clearly θ equals zero regardless of the value of the axial force P . The second equilibrium solution is where

$$P = \frac{kL}{2} \left(\frac{\theta}{\sin \theta} + \cos \theta \right)$$

When θ approaches zero, the above value for the axial force approaches kL . To investigate the stability of these two equilibrium paths, θ equals zero and that written above, write the expression for the second variation of the total potential energy:

$$\delta^2\Pi = [kL^2(1 + \cos^2 \theta - \sin^2 \theta) - 2PL \cos \theta](\delta\theta)^2$$

or

$$\delta^2\Pi = 2L[kL \cos^2 \theta - P \cos \theta](\delta\theta)^2$$

First investigate the loading path θ equals zero. Clearly the second variation of the total potential energy is positive (and the system stable) whenever $P < kL$, and the second variation is negative (and the system unstable) whenever $P > kL$. Now investigate the case where θ is not necessarily zero. In this latter case, where P has the value stated above, after some algebra, the expression for the second variation of the total potential energy is

$$\delta^2\Pi = kL^2 \left[\cos \theta - \frac{\theta}{\sin \theta} \right] \cos \theta (\delta\theta)^2$$

Of course, there is more than one way to determine whether or not this expression is positive or negative for small values of θ . If a computer and relevant software are readily available, the graph of the above function of θ can be inspected for that purpose. Figure 23.17(b) is such a graph from *Mathematica* which shows that, for small θ , the second variation of the potential energy is negative, and hence this load path is unstable. If such software is not immediately available, then for small θ the following two approximations can be used: $\sin \theta = \theta - \theta^3/6$, and $\cos \theta = 1 - \frac{1}{2}\theta^2$, which are the first two terms of their respective Taylor's series. Substituting these approximations, and using the further approximation that $1/(1-x) \approx 1+x$, after some algebra

$$\delta^2\Pi = kL^2 \left[-\frac{1}{2}\theta^2 + \frac{1}{3}\theta^4 \right] (\delta\theta)^2$$

which is clearly negative for small θ . Hence, again this load path is unstable. The stability diagram is shown as Fig. 23.17(c). Also see Exercises 23.7(b, c). ■

Chapter 23 Exercises

- 23.1.** A “push–pull” rod of an aircraft control system has three geometries along its 76-inch length. Along the central 60 inches, the rod has a thin, annular cross-section with an outside diameter of $1\frac{1}{2}$ inches. The 2 inches of rod at each end is an adjusting screw with a solid circular cross-section of $\frac{1}{4}$ -inch diameter. Along the 6-inch length at both ends between the screws and the central portion of the rod, the rod has a tapering, near solid cross-section. If the screw area moment of inertia is approximately one-fourth of the area moment of inertia at the rod center, is it reasonable to model this rod for a buckling analysis as a uniform rod and thus use a differential equation approach?
- 23.2.** (a) Redo the elastic buckling analysis for the nonuniform beam of Fig. 23.3(b) with the left-hand support changed to that of a fixed support.
 (b) Use the FEM to verify that the buckling load of the nonuniform beam of Fig. 23.3(a) is increased fourfold if another roller support is added at the center of the beam.
- 23.3.** Set up and solve the aerodynamic divergence matrix equations for the airfoil of Fig. 23.12 when there is no sweep angle, that is, for $\beta = 0$. Let $GJ = 2EI$, and for this purpose use:
 (a) Just two twisting degrees of freedom and the determinant solution method to obtain q_D .
 (b) All six of the nonzero beam bending and twisting nodal DOF and the determinant solution method to obtain q_D . Let the ratio $e/L = 1/3$.
- 23.4.** Use the matrix iteration method to determine the first natural frequency f_1 for the structural system whose free, undamped vibration is described by the matrix equations:

$$(a) \quad m \begin{bmatrix} 2 & 0 \\ 0 & 1 \end{bmatrix} \begin{Bmatrix} \ddot{q}_1 \\ \ddot{q}_2 \end{Bmatrix} + \frac{48EI}{7L^3} \begin{bmatrix} 16 & -5 \\ -5 & 2 \end{bmatrix} \begin{Bmatrix} q_1 \\ q_2 \end{Bmatrix} = \begin{Bmatrix} 0 \\ 0 \end{Bmatrix}$$

$$(b) \quad (2\pi m/k)^2 f^2 \begin{bmatrix} 4 & 0 & 0 \\ 0 & 3 & 1 \\ 0 & 1 & 1 \end{bmatrix} \begin{Bmatrix} q_1 \\ q_2 \\ q_3 \end{Bmatrix} = \begin{bmatrix} 5 & -2 & 0 \\ -2 & 4 & 2 \\ 0 & 2 & 3 \end{bmatrix} \begin{Bmatrix} q_1 \\ q_2 \\ q_3 \end{Bmatrix}$$

where m and k are mass and stiffness parameters, respectively.

- 23.5.** Determine the beam buckling eigenvalue λ in the matrix equation $\lambda\{q\} = [D]\{q\}$ using matrix iteration when

$$(a) \quad [D] = \begin{bmatrix} 18 & 3 & 6 \\ 3 & 6 & 2 \\ 3 & 1 & 2 \end{bmatrix} \qquad (b) \quad [D] = \begin{bmatrix} 11 & 17 & 16 \\ 18 & 30 & 24 \\ 20 & 32 & 32 \end{bmatrix}$$

$$(c) \quad [D] = \begin{bmatrix} 5 & 6 & 8 \\ 6 & 12 & 12 \\ 8 & 12 & 16 \end{bmatrix} \qquad (d) \quad [D] = \begin{bmatrix} 5 & 7 & 11 \\ 6 & 12 & 18 \\ 8 & 14 & 22 \end{bmatrix}$$

- 23.6.** An uniform airfoil is elastically supported in a wind tunnel using a long, torsionally stiff “sting” mounted on an aerodynamically faired column set on the

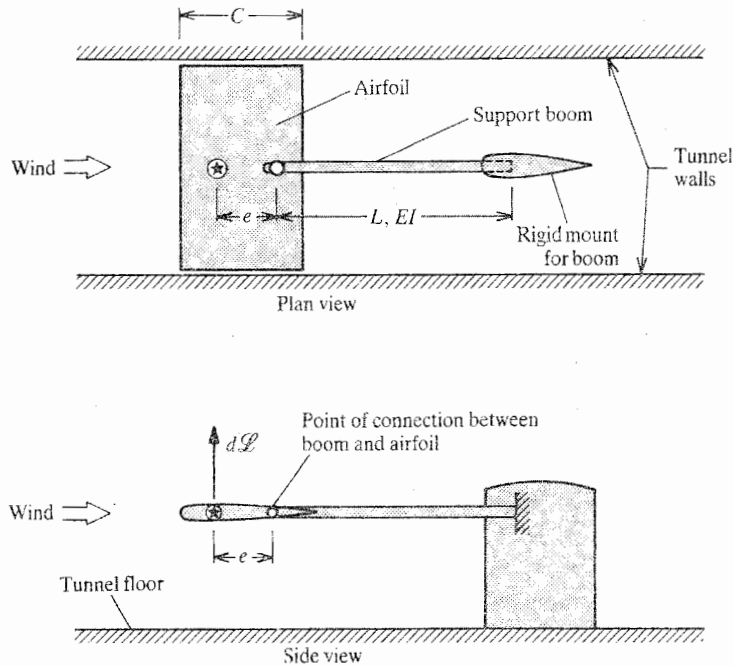


Figure 23.18. Exercise 23.6. An elastically mounted rigid airfoil in a wind tunnel.

wind-tunnel floor; see Fig. 23.18. Model the airfoil and support column as rigid, and the string as a uniform beam element having a stiffness factor EI and a length $l = L$. Write and solve the matrix equation for the divergence aerodynamic pressure, q_D when e/L equals 0.25.

FOR THE EAGER

- 23.7. (a) Determine the critical load, and draw the stability diagram, for the one DOF, rigid bar of length L sketched in Fig. 23.19. Show that its postbuckling load path is stable for small angles of rotation.
- (b) Redo Example 23.7(a), but this time let the stiffness factor for the torsional spring be four times as large; that is, let $K = kL^2$. Determine the new critical load value, and show that this increase in that stiffness factor is sufficient to make the postbuckling load path stable.
- (c) Redo part (b) above, but this time let $K = kL^2/2$.
- 23.8. In order to demonstrate the suitability of the matrix iteration method for finding the single largest eigenvalue even when one of the two square matrices is singular and nonsymmetric, redo part (b) of Exercise 23.3, but this time use matrix iteration to obtain the solution. *Hint:* The inverse of the stiffness matrix is

$$[K]^{-1} = \frac{L^3}{6EI} \begin{bmatrix} 2 & 3 & 0 & 5 & 3 & 0 \\ 3 & 6 & 0 & 9 & 6 & 0 \\ 0 & 0 & 3 & 0 & 0 & 3 \\ 5 & 9 & 0 & 16 & 12 & 0 \\ 3 & 6 & 0 & 12 & 12 & 0 \\ 0 & 0 & 3 & 0 & 0 & 6 \end{bmatrix}$$

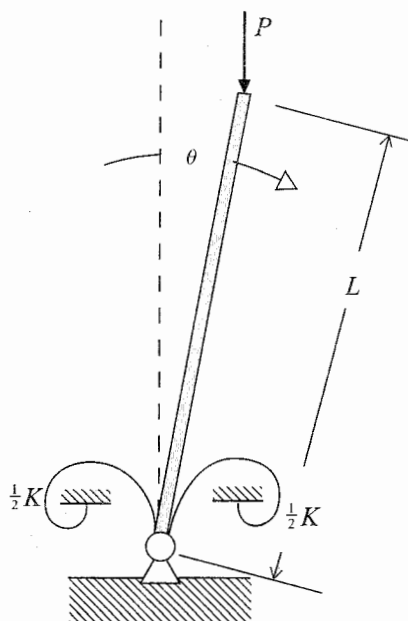


Figure 23.19. Exercise 23.7. Rigid bar supported by torsional springs.

Also note that when the aerodynamic matrix is nondimensionalized to conform with the stiffness matrix's generalized force and generalized coordinate vectors, the result, with $e/L = 1/3$, is

$$[A]q = q_D c C_{1\alpha} \begin{bmatrix} 0 & 0 & 1 & 0 & 0 & 0 \\ 0 & 0 & 0 & 0 & 0 & 0 \\ 0 & 0 & 1/3 & 0 & 0 & 0 \\ 0 & 0 & 0 & 0 & 0 & 1 \\ 0 & 0 & 0 & 0 & 0 & 0 \\ 0 & 0 & 0 & 0 & 0 & 1/3 \end{bmatrix} \begin{Bmatrix} dw_1 \\ Ld\theta_1 \\ Ld\phi_1 \\ dw_2 \\ Ld\theta_2 \\ Ld\phi_2 \end{Bmatrix}$$

- 23.9. Multiply the beam buckling equation $EIw''''(x) + Pw''(x) = 0$, where EI and P are constants, by $\delta w(x)$ and then integrate each term by parts over the beam length so as to obtain the familiar virtual strain energy expression and, more importantly, the virtual potential energy expression for beam buckling, and the appropriate boundary conditions. That is, obtain

$$\delta U = \int_0^L EIw''(x)\delta w''(x)dx \quad \text{and} \quad \delta V = - \int_0^L Pw'(x)\delta w'(x)dx$$

plus the necessary boundary conditions.

- 23.10. After reading Endnote (2), show that

$$\exp\{([A] + [B])t\} = \exp([A]t)\exp([B]t)$$

Endnote (1) Resonance

The following argument demonstrates the importance of natural frequencies by showing that large deflections, hence large strains, hence large stresses, result when an

applied sinusoidal force has an oscillatory frequency that matches, or nearly matches, the j th natural frequency of the structure, f_j . Consider the following dynamic force-deflection matrix equation for an undamped structure,

$$[M]\{\ddot{q}(t)\} + [K]\{q(t)\} = \{Q_0\} \sin(2\pi f_j t + \psi_j) \quad (23.19)$$

where $[M]$ and $[K]$ are the usual mass and stiffness matrices arising respectively from the expressions for the kinetic energy and strain energy, $\{Q_0\}$ is a constant vector of load amplitudes, t is time, and ψ is an arbitrary phase angle. Again the damping matrix $[C]$ is omitted for the sake of simplicity. To understand the solution to this nonhomogeneous equation, consider the solution to the homogeneous equation

$$[M]\{\ddot{q}(t)\} + [K]\{q(t)\} = \{0\} \quad (23.20)$$

As was discussed in Section 23.8, the solution to the above homogeneous equation is achieved by first writing

$$\{q(t)\} = \{\bar{q}\} \sin(2\pi f t + \phi) \quad (23.13)$$

where $\{\bar{q}\}$ is a set of constants. Substituting Eq. (23.13) into Eq. (23.20) yields

$$4\pi^2 f [M]\{\bar{q}\} = [K]\{\bar{q}\} \quad (23.21)$$

This \mathcal{N} -by- \mathcal{N} eigenvalue problem can be solved for the \mathcal{N} natural frequencies f_i , and the \mathcal{N} eigenvectors $\{\bar{q}_i\}$. The total complementary solution is the sum of those \mathcal{N} individual solutions. That is, with the constants of integration A_i , and ϕ_j , the general solution to the homogeneous matrix equation is

$$\{q(t)\} = \sum_{i=1}^{\mathcal{N}} A_i \{\bar{q}_i\} \sin(2\pi f t + \phi_j) \quad (23.22)$$

Each eigenvector $\{\bar{q}_i\}$ called the vibratory mode shape, reveals the relative vibratory amplitudes of the $\{q_i\}$ structure when the structure is freely vibrating at the corresponding natural frequency. A very useful way of using the normalized $\mathcal{N} \times 1$ mode shapes is to arrange all, or some lesser number, of them into a rectangular matrix where the first column is the first eigenvector, the second column is the second eigenvector, and so on. Call this rectangular matrix the *modal matrix*, $[\Phi]$. That is $[\Phi] = [\bar{q}_1 \ \bar{q}_2 \ \dots \ \bar{q}_k]$ where $k \leq \mathcal{N}$. Then introduce a new set of generalized coordinates $\{p(t)\}$, called the modal coordinates, by means of the coordinate transformation

$$\{q(t)\} = [\Phi]\{p(t)\} \quad \text{so that} \quad \{\ddot{q}(t)\} = [\Phi]\{\ddot{p}(t)\} \quad (23.23)$$

Substituting Eq. (23.23) into Eq. (23.19), and then premultiplying Eq. (23.19) by the transpose of $[\Phi]$, leads to

$$[\Phi]^t [M] [\Phi] \{\ddot{p}(t)\} + [\Phi]^t [K] [\Phi] \{p(t)\} = [\Phi]^t \{Q_0\} \sin(2\pi f t + \psi_j) \quad (23.24)$$

Since the columns of $[\Phi]$ are nothing more than the modal eigenvectors, the m, n term of the triple matrix product $[\Phi]^t [M] [\Phi]$ is $[\bar{q}_m]^t [M] \{\bar{q}_n\}$. Because of the orthogonality of these eigenvectors (see Eq. (23.16)), and the positive definiteness of the mass matrix, the product $[\bar{q}_m]^t [M] \{\bar{q}_n\}$ is (i) zero if $m \neq n$, and (ii) the positive number M_n if $m = n$. Similarly, the m, n term of the triple matrix product $[\Phi]^t [K] [\Phi]$ is $[\bar{q}_m]^t [K] \{\bar{q}_n\}$, which is (i) zero if $m \neq n$, and (ii) the positive number K_n if $m = n$. Thus $[\Phi]^t [M] [\Phi]$ and $[\Phi]^t [K] [\Phi]$ are both diagonal matrices. Call them, respectively, $[\backslash M \backslash]$ and $[\backslash K \backslash]$. Furthermore, from Eqs. (23.12b, 23.15) it can be seen that $(2\pi f_n)^2 M_n = K_n$.

With both of the matrices $[M]$ and $[K]$ being diagonal, there is no coupling between the elements of the unknown vector $\{p(t)\}$. That is, with $\{P_0\} = [\Phi]^t\{Q_0\}$, the i th row of the Eq. (23.24) is simply the uncoupled scalar equation

$$M_i \ddot{p}_i(t) + (2\pi f_i)^2 M_i p_i(t) = P_{0i} \sin(2\pi f_j t + \psi_j)$$

There are two cases to consider: (i) when $i \neq j$, and (ii) when $i = j$. In each case the mathematical solution of the above equation consists of the complementary solution and the particular solution. In each case the complementary solution is a sine function with frequency f_i . If damping were included in the differential equation, that sine function would be modified by an exponential function with a negative argument that becomes more negative as time increases. Since the exponential function makes this part of the total solution quickly disappear, the complementary solution in the damped case is called the "transient solution." The conclusion to be reached is that the complementary solution in both the undamped and the more realistic damped case is bounded in time.

In the first of the above two cases, when $f_i \neq f_j$, the particular solution for the generalized coordinate $p_i(t)$ is

$$p_i(t) = \frac{P_{0i}}{4\pi^2 M_i (f_i^2 - f_j^2)} \sin(2\pi f_j t + \psi_j)$$

Since f_i does not equal f_j , this solution, called the steady-state solution, is also bounded with respect to time. On the other hand, when $f_j = f_i$, the resonance case, the solution for the generalized coordinate $p_j(t)$,

$$p_j(t) = -\frac{P_{0j}}{4\pi M f_j} t \cos(2\pi f_j t + \psi)$$

is one that grows without bound as time increases. Hence the importance of knowing the natural frequencies. (The inclusion of an equivalent viscous damping would place an upper limit on the growth of this function.) With or without the inclusion of damping, the solution for the p_j coordinate dominates all the other solutions as it grows very large. Thus, from Eq. (23.23), the deflection vector $\{q(t)\}$ grows very large when the input generalized force vector oscillates at one of the natural frequencies of the structural system. Furthermore, even though the input vector magnitudes $\{Q_0\}$ are not necessarily proportional to $\{\bar{q}_j\}$, from Eq. (23.23), the structure's vibration amplitudes are primarily proportional to that j th modal vector. This fact is experimentally useful.

Endnote (2) Diagonalization and Functions of Matrices

Consider the $\mathcal{N} \times \mathcal{N}$ symmetric matrix $[A]$. This matrix can be written as the triple product $[A] = [\Phi][\lambda][\Phi]^t$ where $[\lambda]$ is the diagonal matrix of the eigenvalues (i.e., the (i, i) element of $[\lambda]$ is λ_i), and $[\Phi]$ is the eigenvector matrix whose i th column is the i th eigenvector. The proof of this statement proceeds directly from the solutions

$$[A]\{q_i\} = \lambda_i\{q_i\} \quad \text{and} \quad [A]\{q_j\} = \lambda_j\{q_j\} \quad (23.25)$$

where $1 \leq i, j \leq \mathcal{N}$. When the above two solutions are combined into one matrix equation, the result, from the rules of matrix multiplication, can be written as

$$[A][q_i \ q_j] = [q_i \ q_j] \begin{bmatrix} \lambda_i & 0 \\ 0 & \lambda_j \end{bmatrix}$$

When the same thing is done for all \mathcal{N} eigenvalues and eigenvectors, the result is $[A][\Phi] = [\Phi][\lambda]$. Following a similar argument to that presented in the section on matrix iteration, let the first of Eqs. (23.25) be premultiplied by $[q_j]$ and the second be premultiplied by $[q_i]$. Then

$$[q_j][A]\{q_i\} = \lambda_i [q_j]\{q_i\} \quad \text{and} \quad [q_i][A]\{q_j\} = \lambda_j [q_i]\{q_j\}$$

Transpose the second of the above equations, and note that $[A]^t = [A]$. Then subtract the second equation from the first to obtain

$$(\lambda_i - \lambda_j)[q_j]\{q_i\} = 0$$

With distinct eigenvalues, by far the usual case, the above difference between eigenvalues is not zero. Thus the two orthogonality conditions for $i \neq j$ are

$$[q_j]\{q_i\} = 0 \quad \text{and} \quad [q_j][A]\{q_i\} = 0$$

Now let the eigenvectors be normalized so that, for all i ,

$$[q_i]\{q_i\} = 1 \quad \text{whence} \quad [q_i][A]\{q_i\} = \lambda_i \quad (23.26)$$

This form of normalization is easily achieved. If the original value of the product $[q_i]\{q_i\} = c$, then division of the vector $\{q_i\}$ by \sqrt{c} accomplishes the desired result. These normalized eigenvectors are termed "orthonormal." For the sake of distinction, let these orthonormal eigenvectors now be denoted as $\{\hat{q}_i\}$. Then, using this symbolism, Eq. (23.26) is rewritten as

$$[\hat{q}_i]\{\hat{q}_i\} = 1 \quad \text{and} \quad [\hat{q}_i][A]\{\hat{q}_i\} = \lambda_i \quad (23.26)$$

When the orthonormal eigenvectors are assembled into $[\hat{\Phi}]$, then

$$[\hat{\Phi}]^t[\hat{\Phi}] = [I] \quad \text{and} \quad [\hat{\Phi}]^t[A][\hat{\Phi}] = [\lambda]$$

or

$$[A] = [\hat{\Phi}][\lambda][\hat{\Phi}]^t \quad (23.27)$$

In the latter form of Eq. (23.27), the symmetric matrix $[A]$ is said to be diagonalized. This diagonal form has many uses. For example, if the square root of the matrix $[A]$ is desired, it can be written immediately as

$$[A]^{1/2} = [\hat{\Phi}][\lambda^{1/2}][\hat{\Phi}]^t$$

where the i, i element of $[\lambda^{1/2}]$ is simply $(\lambda_i)^{1/2}$. This solution for the square root is quickly verified by multiplying it by itself, and noting the first of Eqs. (23.27). Similarly, the inverse of $[A]$ is

$$[A]^{-1} = [\hat{\Phi}][\lambda^{-1}][\hat{\Phi}]^t$$

Consider the following homogeneous matrix equation where the symmetric matrices $[M]$ and $[K]$ are real and constant:

$$[M]\{\ddot{q}\} + [K]\{q\} = \{0\} \quad (23.28)$$

Write the coordinate transformation $\{q\} = [M]^{-1/2}\{p\}$ and substitute it into the above equation. Premultiplying Eq. (23.28) by the symmetric matrix $[M]^{-1/2}$ then yields

$$\{\ddot{p}\} + [M]^{-1/2}[K][M]^{-1/2}\{p\} = \{0\} \quad (23.29)$$

or $\{\ddot{p}\} + [A]\{p\} = \{0\}$

An alternative to decoupling this equation is to write the solution for $\{p(t)\}$ as

$$\{p\} = \sin([A]^{1/2}t)\{C_1\} + \cos([A]^{1/2}t)\{C_2\}$$

Where $\{C_1\}$ and $\{C_2\}$ are vectors of constants of integration that can be determined from initial conditions. In order to demonstrate that this is indeed a solution to Eq. (23.29), assume for the moment, as is proved below, that these sine and cosine functions have the same derivatives and integral forms that are possessed by ordinary sine and cosine functions. Then substitute

$$\{\dot{p}\} = -[A] \sin([A]^{1/2}t)\{C_1\} - [A] \cos([A]^{1/2}t)\{C_2\}$$

as well as the alleged solution for $\{p\}$ into Eq. (23.29). The result is the zero vector, which shows that the alleged solution is indeed a solution. The solution for the original vector $\{q\} = [M]^{-1/2}\{p\}$ follows immediately.

The only questions remaining concern the calculation and differentiation of, for example, $\sin([B]x)$, where $[B]$ is a matrix of constants. To calculate the matrix $\sin[B]$, first write $[B] = [\hat{\phi}][\lambda][\hat{\phi}]^t$. Note that the n th power of $[B]$ can be written as $[B]^n = [\hat{\phi}][\lambda^n][\hat{\phi}]^t$. Recall that the series expansion for the sine function is

$$\sin \theta = \theta - \frac{\theta^3}{3!} + \frac{\theta^5}{5!} - \frac{\theta^7}{7!} + \dots$$

Consider the matrix $[\hat{\phi}][\sin \lambda][\hat{\phi}]^t$, where $[\sin \lambda]$ is just the diagonal matrix of the sines of the eigenvalues. That is, the i th element along the diagonals is $\sin(\lambda_i)$. Since the sine function is applicable to any real number,

$$\begin{aligned} [\hat{\phi}][\sin \lambda][\hat{\phi}]^t &= [\hat{\phi}] \left([\lambda] - \frac{1}{3!}[\lambda^3] + \frac{1}{5!}[\lambda^5] - \dots \right) [\hat{\phi}]^t \\ &= [\hat{\phi}][\lambda][\hat{\phi}]^t - \frac{1}{3!}[\hat{\phi}][\lambda^3][\hat{\phi}]^t \\ &\quad + \frac{1}{5!}[\hat{\phi}][\lambda^5][\hat{\phi}]^t - \dots \end{aligned}$$

In the above series expansion for $[\hat{\phi}][\sin \lambda][\hat{\phi}]^t$, insert the identity matrix $[I] = [\hat{\phi}]^t[\hat{\phi}]$ in each right-hand-side term of the series expansion in such a way that, for example, the matrix $[\lambda^3] = [\lambda][\lambda][\lambda]$ becomes $[\lambda][\hat{\phi}]^t[\hat{\phi}][\lambda][\hat{\phi}]^t[\hat{\phi}][\lambda]$. Since $[B] = [\hat{\phi}][\lambda][\hat{\phi}]^t$, it should be clear that, after grouping each succeeding product of three matrices in each right-hand-side term of the series expansion, the result is

$$[\hat{\phi}][\sin \lambda][\hat{\phi}]^t = [B] - \frac{1}{3!}[B]^3 + \frac{1}{5!}[B]^5 - \dots$$

The parallel between the $\sin \theta$ series and the $[\hat{\phi}][\sin \lambda][\hat{\phi}]^t$ series permits calling the triple product $[\hat{\phi}][\sin \lambda][\hat{\phi}]^t$ by the name $\sin[B]$. Thus there is now a meaning for the symbol $\sin[B]$. Of course the means for calculating $\sin[B]$ is not the infinitely long series expansion, rather the calculation is accomplished by means of using the functional values of the individual eigenvalues for $[B]$; that is,

$$\sin[B] = [\hat{\phi}][\sin \lambda][\hat{\phi}]^t$$

Similarly, $\cos[B] = [\hat{\phi}][\cos \lambda][\hat{\phi}]^t$, and $\exp[B] = [\hat{\phi}][\exp \lambda][\hat{\phi}]^t$, and so on. As for differentiation of functions of matrices, note that, where again $[B]$ is a matrix of constants,

$$\begin{aligned}\sin([B]x) &= [B]x - \frac{1}{3!}[B]^3x^3 + \frac{1}{5!}[B]^5x^5 - \dots \\ \frac{d}{dx} \sin([B]x) &= [B] - 3\frac{1}{3!}[B]^3x^2 + 5\frac{1}{5!}[B]^5x^4 - \dots \\ \frac{d}{dx} \sin([B]x) &= [B] \left([I] - \frac{1}{2!}[B]^2x^2 + \frac{1}{4!}[B]^4x^4 - \dots \right) \\ &= [B] \cos([B]x)\end{aligned}$$

or

$$\begin{aligned}\frac{d}{dx} \sin([B]x) &= \left([I] - \frac{1}{2!}[B]^2x^2 + \frac{1}{4!}[B]^4x^4 - \dots \right) [B] \\ &= \cos([B]x)[B]\end{aligned}$$

Similar expressions can be written for nonsymmetric matrices. However, with nonsymmetric matrices, everything is a bit more complicated. First of all, with a nonsymmetric matrix $[N]$ it is necessary to obtain the eigenvalues and eigenvectors of $[N]^t$ as well as those of $[N]$. The determinant method for calculating eigenvalues shows that the two sets of eigenvalues are identical because a determinant is not altered by interchanging the rows and columns. Let the orthonormal eigenvectors of $[N]^t$ be $\{\hat{p}_i\}$ and those of $[N]$ be $\{\hat{q}_i\}$. Then following the by now familiar process of premultiplying

$$[N]\{\hat{q}_i\} = \lambda_i\{\hat{q}_i\} \quad \text{and} \quad [N]^t\{\hat{p}_j\} = \lambda_j\{\hat{p}_j\}$$

by $[\hat{p}_j]$ and $[\hat{q}_i]$ respectively, transposing the second equation, and subtracting one from the other, yields $(\lambda_i - \lambda_j)[\hat{p}_j][\hat{q}_i] = 0$. With unequal eigenvalues, the orthogonality conditions are

$$[\hat{p}_j][\hat{q}_i] = 0 = [\hat{p}_j][N]\{\hat{q}_i\}$$

These two sets of orthonormal vectors can be used to diagonalize $[N]$ much the same way as is done with symmetric matrices. The following brief example illustrates the process.

Example 23.8. Diagonalize the matrix

$$[N] = \begin{bmatrix} 2 & 1 \\ 4 & 5 \end{bmatrix}$$

Solution. Matrix iteration followed by the normalization process quickly shows that the eigenvalues and eigenvectors are

$$\begin{aligned}\lambda_1 &= 6 & [\hat{q}_1] &= [1/4 \quad 1] & [\hat{p}_1] &= [4/5 \quad 4/5] \\ \lambda_2 &= 1 & [\hat{q}_2] &= [-1 \quad +1] & [\hat{p}_2] &= [-4/5 \quad 1/5]\end{aligned}$$

A quick check verifies that the above eigenvectors are indeed orthonormal. That is,

$$\begin{bmatrix} 4/5 & 4/5 \\ -4/5 & 1/5 \end{bmatrix} \begin{bmatrix} 1/4 & -1 \\ 1 & 1 \end{bmatrix} = \begin{bmatrix} 1 & 0 \\ 0 & 1 \end{bmatrix} = \begin{bmatrix} 1/4 & -1 \\ 1 & 1 \end{bmatrix} \begin{bmatrix} 4/5 & 4/5 \\ -4/5 & 1/5 \end{bmatrix}$$

Carrying out the triple matrix multiplication $[\Phi_p]^t[N][\Phi_q]$ verifies that

$$\frac{1}{5} \begin{bmatrix} 4 & 4 \\ -4 & 1 \end{bmatrix} \begin{bmatrix} 2 & 1 \\ 4 & 5 \end{bmatrix} \begin{bmatrix} 1/4 & -1 \\ 1 & 1 \end{bmatrix} = \begin{bmatrix} 6 & 0 \\ 0 & 1 \end{bmatrix}$$

Thus the diagonalization of $[N]$ is

$$\begin{bmatrix} 2 & 1 \\ 4 & 5 \end{bmatrix} = \begin{bmatrix} 1/4 & -1 \\ 1 & 1 \end{bmatrix} \begin{bmatrix} 6 & 0 \\ 0 & 1 \end{bmatrix} \begin{bmatrix} 4/5 & 4/5 \\ -4/5 & 1/5 \end{bmatrix}$$

In more general terms, if $[Q]$ and $[P]$ are the matrices whose columns are the eigenvectors $\{\hat{q}\}$ and $\{\hat{p}\}$, then $[N][Q] = [Q][\lambda]$ and $[N]^t[P] = [P][\lambda]$ or $[P]^t[N] = [\lambda][P]^t$. With $[P]^t[Q] = [I] = [Q]^t[P]$, then $[P]^t[N][Q] = [\lambda]$. Since the $\{\hat{p}\}$ are linearly independent (proof as before), the inverse of $[P]$ exists. Define $[R] = [N][P]^{-t}$ or $[N] = [R][P]^t$. Substitute this latter expression into $[N][Q] = [Q][\lambda]$ to obtain $[R][P]^t[Q] = [R] = [Q][\lambda]$. Then postmultiply the latter equality by $[P]^t$ to finally obtain $[N] = [Q][\lambda][P]^t$. Then $[N]^{1/2} = [Q][\lambda^{1/2}][P]^t$, and so on. ■

Additional Topics

A.1 Integration of the Strains to Obtain Displacements

There are two aspects to the following discussion of strains and displacements. The first aspect is an outline of the process that is the general integration of the six strains to obtain the three displacements. The second aspect is the redirection of the series of equations developed during the process of obtaining the displacements towards the second goal, which is the partial differential equations that relate the strains to each other. The equations that relate the strains are called the compatibility equations. In this textbook, the compatibility equations are of more immediate concern than the process of integrating the strains to obtain the displacements. As is proved in Endnote (1) of Chapter 3 there are six second order compatibility equations that occur in two sets or three equations of similar form. The second of the two sets of three compatibility equations is rederived here because the form of those compatibility equations is less obvious than that of the first set.

Throughout the process begun below for obtaining the displacements from the strains, it is of course presumed that the strains are known functions of the cartesian coordinates, and if necessary, time as well. The process begins with the first order partial differential equations that are the linear form of the strain–displacement equations. Consider determining $u(x, y, z)$ from the strain $\epsilon_{xx}(x, y, z) = \partial u / \partial x$. Indefinite integration with respect to x leads to

$$u(x, y, z) = \int_x \frac{\partial u}{\partial x} dx = \int_x \epsilon_{xx} dx + f(y, z) \quad (\text{A.1})$$

The above integration of the partial derivative produces a function of integration that is here labeled $f(y, z)$. This function of integration is similar to the constant of integration that always accompanies the indefinite integration of a total derivative. The function of integration is always a function of the variables that are not involved in the integration. Thus partially differentiating Eq. (A.1) with respect to the variable of integration, which in this case is x , leads to the original first order derivative. Such a differentiation, of course, verifies Eq. (A.1).

The key point of this derivation is that the left-hand integral can be identified as $u(x, y, z)$ because integration is the reverse of partial differentiation. That is,

$$u(x, y, z) = \int_x \epsilon_{xx} dx + f(y, z) = \bar{u}(x, y, z) + f(y, z) \quad (\text{A.2})$$

where the known function $\bar{u}(x, y, z)$, which is one part of the solution for $u(x, y, z)$, represents the immediate result of the integration of the function ϵ_{xx} with respect to x . Similar intermediate solutions for the displacements $v(x, y, z)$ and $w(x, y, z)$ can be obtained, with their associated functions of integration $g(x, z)$ and $h(x, y)$. They are, respectively,

$$\begin{aligned} v(x, y, z) &= \int_y \epsilon_{yy} dy + g(x, z) = \bar{v}(x, y, z) + g(x, z) \\ w(x, y, z) &= \int_z \epsilon_{zz} dz + h(x, y) = \bar{w}(x, y, z) + h(x, y) \end{aligned} \quad (\text{A.3})$$

Since there are three unknown functions, three additional pieces of information are required. This additional information is available in part in the form of the three known shearing strains. Substitution of the above solutions for the displacements into the shearing strain expressions yields

$$\begin{aligned}\gamma_{xy}(x, y, z) &= \frac{\partial \tilde{u}}{\partial y} + \frac{\partial f}{\partial y} + \frac{\partial \tilde{v}}{\partial x} + \frac{\partial g}{\partial x} \\ \gamma_{xz}(x, y, z) &= \frac{\partial \tilde{u}}{\partial z} + \frac{\partial f}{\partial z} + \frac{\partial \tilde{w}}{\partial x} + \frac{\partial h}{\partial x} \\ \gamma_{yz}(x, y, z) &= \frac{\partial \tilde{v}}{\partial z} + \frac{\partial g}{\partial z} + \frac{\partial \tilde{w}}{\partial y} + \frac{\partial h}{\partial y}\end{aligned}\tag{A.4}$$

Equations (A.4) constitute three simultaneous, first order, partial differential equations for the three unknown functions of integration f , g , and h . The progress that has been made so far is that these unknown functions of integration have one fewer variable than the unknown displacements. To work further towards the goal of determining the displacements, differentiate the first of Eqs. (A.4) with respect to z , the second equation with respect to y , and the third with respect to x . The result is

$$\begin{aligned}\frac{\partial^2 f}{\partial y \partial z} + \frac{\partial^2 g}{\partial x \partial z} &= \frac{\partial \gamma_{xy}}{\partial z} - \frac{\partial^2 \tilde{u}}{\partial y \partial z} - \frac{\partial^2 \tilde{v}}{\partial x \partial z} \\ \frac{\partial^2 f}{\partial y \partial z} + \frac{\partial^2 h}{\partial x \partial y} &= \frac{\partial \gamma_{xz}}{\partial y} - \frac{\partial^2 \tilde{u}}{\partial y \partial z} - \frac{\partial^2 \tilde{w}}{\partial x \partial y} \\ \frac{\partial^2 g}{\partial x \partial z} + \frac{\partial^2 h}{\partial x \partial y} &= \frac{\partial \gamma_{yz}}{\partial x} - \frac{\partial^2 \tilde{v}}{\partial x \partial z} - \frac{\partial^2 \tilde{w}}{\partial x \partial y}\end{aligned}\tag{A.5}$$

The symmetry of Eqs. (A.5) is evident. Hence it is possible, for example, to isolate the function of integration $f(y, z)$ by adding the first of the above two equations and subtracting the third. That result and similar results for the other two functions of integration are

$$\begin{aligned}2 \frac{\partial^2 f}{\partial y \partial z} &= \frac{\partial \gamma_{xy}}{\partial z} + \frac{\partial \gamma_{xz}}{\partial y} - \frac{\partial \gamma_{yz}}{\partial x} - 2 \frac{\partial^2 \tilde{u}}{\partial y \partial z} \\ 2 \frac{\partial^2 g}{\partial x \partial z} &= \frac{\partial \gamma_{xy}}{\partial z} + \frac{\partial \gamma_{yz}}{\partial x} - \frac{\partial \gamma_{xz}}{\partial y} - 2 \frac{\partial^2 \tilde{v}}{\partial x \partial z} \\ 2 \frac{\partial^2 h}{\partial x \partial y} &= \frac{\partial \gamma_{xz}}{\partial y} + \frac{\partial \gamma_{yz}}{\partial x} - \frac{\partial \gamma_{xy}}{\partial z} - 2 \frac{\partial^2 \tilde{w}}{\partial x \partial y}\end{aligned}\tag{A.6}$$

Now it is a matter of directly integrating each of the above three equations twice in order to obtain the unknown functions f , g , and h . For example, integrating the first of the above three equations first with respect to y and then with respect to z would first produce a new function of integration $\hat{f}(z)$ and then just a constant of integration. Clearly this procedure has greatly simplified the unknown functions. Now it is a matter of using whatever displacement boundary conditions are available for a particular problem. When these simpler integration functions have been determined from the BCs, the results can be substituted into Eqs. (A.2) and (A.3) to complete the solution for the displacements.

Turning now to the purpose of discovering the necessary relations between the strains, let the purpose of further manipulation of Equations (A.6) be the elimination of the functions

of integration. To this end, differentiate the first of the above three equations with respect to x , and note

$$\frac{\partial}{\partial x} \left(\frac{\partial^2 f}{\partial y \partial z} \right) = \frac{\partial^2}{\partial y \partial z} \left(\frac{\partial f(y, z)}{\partial x} \right) = 0$$

and

$$\frac{\partial}{\partial x} \left(\frac{\partial^2 \tilde{u}}{\partial y \partial z} \right) = \frac{\partial^2}{\partial y \partial z} \left(\frac{\partial}{\partial x} \int_x \epsilon_{xx} dx \right) = \frac{\partial^2 \epsilon_{xx}}{\partial y \partial z}$$

Therefore,

$$0 = \frac{\partial}{\partial x} \left(\frac{\partial \gamma_{xy}}{\partial z} + \frac{\partial \gamma_{xz}}{\partial y} - \frac{\partial \gamma_{yz}}{\partial x} \right) - 2 \frac{\partial^2 \epsilon_{xx}}{\partial y \partial z}$$

and similarly

$$0 = \frac{\partial}{\partial y} \left(\frac{\partial \gamma_{xy}}{\partial z} + \frac{\partial \gamma_{yz}}{\partial x} - \frac{\partial \gamma_{xz}}{\partial y} \right) - 2 \frac{\partial^2 \epsilon_{yy}}{\partial x \partial z}$$

$$0 = \frac{\partial}{\partial z} \left(\frac{\partial \gamma_{xz}}{\partial y} + \frac{\partial \gamma_{yz}}{\partial x} - \frac{\partial \gamma_{xy}}{\partial z} \right) - 2 \frac{\partial^2 \epsilon_{zz}}{\partial x \partial y}$$

The above are the second of the two sets of three compatibility equations. This completes the proof that these equations are necessary conditions for the six strain–displacement equations.

A.2 Proof of the Symmetry of the Compliance Matrix

Section 20.11 offered a proof of Betti's law, sometimes called Betti's reciprocal theorem, that depended upon the observed symmetry of the material stiffness matrix, $[E]$, for orthotropic and isotropic materials. Since $[E]$ is symmetric, its inverse, the material compliance matrix $[S]$, must also be symmetric. The proof of this assertion is as follows. Since $[E] = [E]^t$, premultiplying by $[E]^{-1}$ yields $[I] = [E]^{-1}[E]^t$. Transposing both sides of this latter matrix equation leads to $[I] = [E][E]^{-t}$. Then premultiplying by $[E]^{-1}$ provides the final statement that $[E]^{-1} = [E]^{-t}$, or $[S] = [S]^t$. Hence using the previously developed Betti's law to prove the symmetry of the compliance matrix would be using circular reasoning. Therefore this section takes another approach to Betti's law that doesn't depend upon the observed symmetry of the material stiffness matrix. However, this is not a superior approach because, as will be seen, it simply makes another observation as a key step in the proof.

To begin this alternate proof of Betti's reciprocal theorem, consider a differential-sized rectangular parallelepiped that has no temperature change and is in the process of being loaded by a *single* normal stress, say σ_{xx} . That is, let the stress σ_{xx} increase from zero to some end value σ_{xx}^e while the parallelepiped deforms accordingly. In the discussion that follows, the focus is upon a typical intermediate value of the single normal stress, which is simply designated as σ_{xx} and the corresponding strain ϵ_{xx} .

To start simply, let the material of the differential rectangular parallelepiped be orthotropic, and let the boundary planes of the rectangular parallelepiped coincide with the material planes of symmetry. Then the differential element has three normal strains and no shearing strains. The first task is to calculate the work done by the single stress σ_{xx} . Recall that the differential of work is defined as the dot product of the applied force vector and the vector form of the differential of distance through which the force moves; that is,

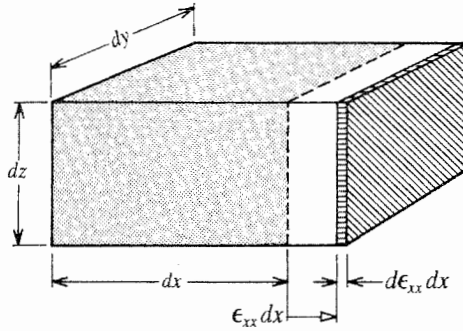


Figure A.1. An infinitesimal rectangular parallelepiped deformed in the x direction only.

$dW = \mathbf{F} \cdot d\mathbf{D}$. As can be seen from Fig. A.1, the applied force during the loading process is $\sigma_{xx} dy dz$, where, as before, the change in area due to the loading is neglected. The differential distance through which this force moves can be determined by first noting that the distance the force has moved to reach this intermediate deformation is the intermediate change in length of the original length of the parallelepiped. Since the strain corresponding to the intermediate deformation, ϵ_{xx} , is defined as the change in length of the original length divided by the original length, dx , then the intermediate distance moved by the force is $\epsilon_{xx} dx$, as is shown in an exaggerated fashion in the figure. In order to form the work integral, it is necessary to take the differential of this intermediate distance $\epsilon_{xx} dx$. Since the original length dx is a fixed quantity, and since the strain varies from an initial value of zero corresponding to zero stress to a end value ϵ_{xx}^e , the differential of this distance is the product $d\epsilon_{xx} dx$. Furthermore, the force and displacement vectors are collinear. Hence the dot product is an ordinary product. Substituting the above force and differential distance expressions into the definition for the differential of work done on the differential element yields

$$dW = (\sigma_{xx} dy dz)(d\epsilon_{xx} dx) = \sigma_{xx} d\epsilon_{xx} d(\text{Vol.})$$

Note that while the left-hand side of the above equality has the appearance of a single differential, the right-hand side clearly has four differential factors. The number of differential factors must be the same on both sides of any equality. Hence, just as $d(\text{Vol.})$ incorporates three differentials, here the work differential incorporates four differentials. In order to avoid the appearance of differential mismatches, and to save continually writing the differential volume term, it is convenient to introduce the work per unit volume, W_0 , in the definition

$$dW = dW_0 d(\text{Vol.})$$

Thus, the expression for the work per unit volume for a single normal stress is

$$dW_0 = \sigma_{xx} d\epsilon_{xx}$$

It is a simple matter to integrate the above expression to obtain the work per unit volume in the case of a linearly elastic material, because at every point in the progress of the stress and strain, they are linearly proportional to each other. That is, because there are no other stresses, and no temperature change, $\epsilon_{xx} = \sigma_{xx}/E_x$. Using this latter equation to solve for the stress, and substituting for the stress in the work expression, and integrating over the range of strains from zero strain to the end strain, produces

$$W_0 = \int_0^{\epsilon_{xx}^e} E_x \epsilon_{xx} d\epsilon_{xx} = \frac{1}{2} E_x (\epsilon_{xx}^e)^2 = \frac{1}{2} \sigma_{xx}^e \epsilon_{xx}^e$$

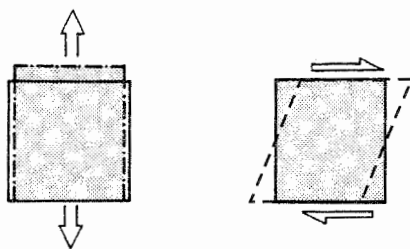


Figure A.2. The lack of interaction between normal stresses and shearing strains, and vice versa, when the stresses parallel the orthotropic axes of symmetry, or the material is isotropic.

Now consider the same rectangular parallelepiped subjected to all six stresses, and thus experiencing all six strains. Figure A.2 shows a side view of a pair of normal and shear stresses acting on one pair of the six faces of the rectangular parallelepiped, and the exaggerated deformation associated with each pair of stresses. From this diagram it should be clear that the normal force acts perpendicularly to the displacement caused by the shear stress, and the shear force acts perpendicularly to the displacement caused by the normal force. Since the definition of work involves a dot product, it should be clear that the work done by the normal and shear forces moving through the shearing and longitudinal displacements, respectively, is zero. Hence the conclusion, patterned after the previous result, that

$$dW_0 = \sigma_{xx} d\epsilon_{xx} + \sigma_{yy} d\epsilon_{yy} + \cdots + \sigma_{yz} d\gamma_{yz}$$

where, for example, the shear term $\sigma_{zx} d\gamma_{zx}$ comes from the shear force ($\sigma_{zx} dx dy$) moving through the distance ($\gamma_{zx} dz$), where the sine of the shearing strain is equal to the shearing strain. The integration of this expression for the work done on the body per unit volume is not straightforward because each normal stress depends on the three longitudinal strains, and vice versa. This difficulty can be side-stepped. In general, the integral of the differential of work is a line integral, and as such it is path-dependent. That is, in general, an integration over different paths produces different results for the same integrand (i.e., same force). However, in this case of a linearly elastic, orthotropic material without a temperature change, from the first law of thermodynamics as discussed in Section 6.1, the path-dependent differential of work is equal to the differential of the internal (i.e., strain) energy, which is a point function. (The differentials of point functions are called “exact differentials.”) The integrals of the differentials of all point functions are path-independent. Thus the integral of the work differential for the linearly¹ elastic material is path-independent. Since any path leads to the same result for the value of the integral, it is useful to choose a convenient path. The path chosen here is the one where all the stresses increase at exactly the same rate from their zero values to their final values. That is, let $\tilde{\alpha}(t)$ be the time-varying proportionality factor for each stress such that $0 \leq \tilde{\alpha}(t) \leq 1.0$, and

$$\begin{aligned} \sigma_{xx} &= \tilde{\alpha} \sigma_{xx}^e & \sigma_{yy} &= \tilde{\alpha} \sigma_{yy}^e & \sigma_{zz} &= \tilde{\alpha} \sigma_{zz}^e \\ \sigma_{xy} &= \tilde{\alpha} \sigma_{xy}^e & \sigma_{xz} &= \tilde{\alpha} \sigma_{xz}^e & \sigma_{yz} &= \tilde{\alpha} \sigma_{yz}^e \end{aligned}$$

¹ The linearity of the elastic material is actually immaterial to this argument.

In the absence of a temperature change, substitution of the above expressions for the stresses into the strain–stress equations for any linearly elastic material shows that the strains can be represented in exactly the same way. That is,

$$\{\gamma\} = [S]\{\sigma\} = [S]\{\tilde{\alpha}\sigma^e\} = \tilde{\alpha}[S]\{\sigma^e\} = \tilde{\alpha}\{\gamma^e\}$$

Since the end values of stress and strain are constants, substituting these forms into the general stress state expression for the work differential per unit volume yields

$$\begin{aligned} W_0 &= \sigma_{xx}^e \epsilon_{xx}^e \int_0^1 \tilde{\alpha} d\tilde{\alpha} + \sigma_{yy}^e \epsilon_{yy}^e \int_0^1 \tilde{\alpha} d\tilde{\alpha} + \cdots + \sigma_{yz}^e \epsilon_{yz}^e \int_0^1 \tilde{\alpha} d\tilde{\alpha} \\ W_0 &= \frac{1}{2}(\sigma_{xx}\epsilon_{xx} + \sigma_{yy}\epsilon_{yy} + \cdots + \sigma_{yz}\gamma_{yz}) = \frac{1}{2}[\sigma]\{\gamma\} \end{aligned} \quad (\text{A.7})$$

where in the last two equalities, in a change in symbols, the superscript e is dropped, and now the usual, unmodified symbols indicate the end values of stress and strain. (It is a simple matter to show, as a major step in proving that the above argument works equally well for any analytical function of $\tilde{\alpha}(t)$, that exactly the same result is obtained if $\tilde{\alpha}(t)$ is replaced by $\tilde{\alpha}(t)$ raised to the n th power.)

Now consider the situation where the same differential rectangular parallelepiped is loaded sequentially by two different sets of stresses. Let the first set be designated as $\{\sigma^{(1)}\}$ and the second set as $\{\sigma^{(2)}\}$, and let the corresponding strains be similarly denoted. The work done on the parallelepiped per unit volume by the first set of stresses when that set is the only set of stresses applied to the parallelepiped is

$$W_0 = \frac{1}{2}[\sigma^{(1)}]\{\gamma^{(1)}\}$$

If the second set of stresses is then applied to the parallelepiped with the first set still acting upon the parallelepiped, the work per unit volume increases to

$$W_0 = \frac{1}{2}[\sigma^{(2)}]\{\gamma^{(2)}\} + [\sigma^{(1)}]\{\gamma^{(2)}\} + \frac{1}{2}[\sigma^{(1)}]\{\gamma^{(1)}\}$$

The second term does *not* have a factor of one-half because the first set of stresses are fully developed, that is, they have their constant end values before and during the displacements associated with the second set of strains. A constant force integrated over a displacement is simply the force multiplied by the total displacement. (Thus the factor one-half is an indication that the force grows proportionally with the displacement.) If now the stresses are removed and reapplied in reverse order, then the work done by both sets of forces is

$$W_0 = \frac{1}{2}[\sigma^{(1)}]\{\gamma^{(1)}\} + [\sigma^{(2)}]\{\gamma^{(1)}\} + \frac{1}{2}[\sigma^{(2)}]\{\gamma^{(2)}\}$$

For an elastic material, the sequencing of the loads (i.e., the loading path) has no effect on the total work done. This is illustrated in Fig. A.3 for the case of two increments of a single stress. Equating the two expressions for the work per unit volume leads to the conclusion that

$$[\sigma^{(1)}]\{\gamma^{(2)}\} = [\sigma^{(2)}]\{\gamma^{(1)}\} \quad (\text{A.8})$$

Equation (A.8) is *Betti's law* or *Betti's reciprocal theorem*. This theorem can be reshaped to prove the slightly more general statement that the work done by one set of forces moving through the displacements produced by a second set of forces is equal to the work done by the second set of forces moving through the displacements produced by the first set of forces. The proof of this statement is thoroughly outlined in the exercises of Ref. [3], Chapter 1. When this statement is rendered in terms of single forces, it is *Maxwell's reciprocal theorem* or *Maxwell's reciprocity theorem*.

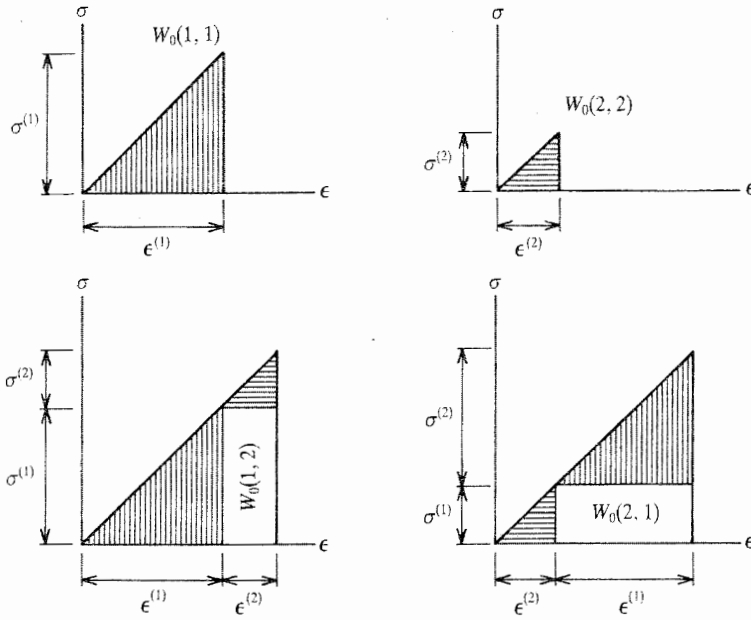


Figure A.3. The work per unit volume done by two stresses of the same type when the two stresses are applied sequentially to a (linearly) elastic body. The conclusion is that the work per unit volume done by the first stress moving through the strain of the second stress, $W_0(1, 2)$, is equal to the work per unit volume done by the second stress moving through the strain of the first stress, $W_0(2, 1)$.

Equation (A.7), and as a result everything afterwards, was derived for an orthotropic material where the coordinate axes are aligned with the material axes. The rotation equations in Section 6.5 can be used to show the Betti's reciprocal theorem applies to an orthotropic material for any set of orthogonal axes. Thus these equations also apply to an isotropic material for any set of orthogonal axes.

The proof of the symmetry of the compliance matrix is a short step from Betti's theorem. It begins with writing the strain-stress equations for each load set; that is,

$$\{\gamma^{(1)}\} = [S]\{\sigma^{(1)}\} \quad \text{and} \quad \{\gamma^{(2)}\} = [S]\{\sigma^{(2)}\}$$

Then Betti's theorem becomes

$$[\sigma^{(1)}][S]\{\sigma^{(2)}\} = [\sigma^{(2)}][S]\{\sigma^{(1)}\}$$

or

$$[\sigma^{(1)}][S]\{\sigma^{(2)}\} = [\sigma^{(1)}][S]^t\{\sigma^{(2)}\}$$

where the last step is just a matrix product transposition of the scalar quantity on the right hand side of the equal sign. Since both sets of stresses are unrelated to each other, and wholly arbitrary, the conclusion from the last equation is that the compliance matrix is equal to its transpose, and thus is symmetric. This conclusion can be justified in the following way. Rewrite the above equations as

$$([\sigma^{(1)}][S] - [\sigma^{(1)}][S]^t)\{\sigma^{(2)}\} = 0$$

The above left-hand side is the product of two unrelated quantities. The first of these two quantities is a row vector. The second is a column vector that can take on any set of nonzero real values. The matrix product of the row and column vector is simply the finite sum of products of the corresponding elements of the two matrices. Since that matrix product is zero regardless of the nonzero values of the elements of the column vector, then it must be concluded that each element of the row vector, and thus the row vector itself, is necessarily zero. This row vector equation can be rewritten after factoring and transposition as

$$([S] - [S]^t)\{\sigma^{(1)}\} = \{0\}$$

Now the above argument is repeated with one small change. Consider the product of each row of the square matrix and the arbitrary column vector separately as above to arrive at the conclusion that each row of the square matrix within the parentheses is necessarily null. Thus the final result is that the compliance matrix is symmetric; that is,

$$[S] = [S]^t \quad (\text{A.9})$$

A cautionary note: the above argument concerning the square matrix depends on the triple matrix product being of the form $[x][m]\{y\}$ where $[x]$ and $\{y\}$ are both arbitrary and unrelated. The triple product $[x][m]\{x\}$ being always equal to zero for an arbitrary $\{x\}$ is not sufficient information in itself to conclude that $[m]$ is null. In this latter case, all that can be said is that $[m]$ is a skew-symmetric matrix; that is, a matrix where the (i, j) th element is equal to the negative of the (j, i) th element.

A.3 Uniform Torsion Stress Resultants for Multiply Connected Cross-Sections

In this section it is proved that the two shearing force components

$$V_y = + \oint_{\partial A} \psi dy \quad \text{and} \quad V_z = + \oint_{\partial A} \psi dz$$

are zero for the multiply connected cross-section as well as the singly connected cross-section, and the more general expression for the torque is derived.

Consider the multiply connected cross-section of Fig. A.4 where the outer boundary is linked to the two inner boundaries by arbitrary paths that are traversed in both directions as any line integral proceeds along the outer and inner boundaries in one continuous loop. Since the contribution of that portion of any line integral that is derived from the oppositely traversed paths to the total value of the line integral cancels, the indicated single loop can be substituted for the separate outer and inner boundary loops. Thus consider the line integral for the y component of the total shearing force to have this single loop as its integration path. Then

$$V_y = + \oint_{\partial A_{net}} \psi dy = \oint_{\partial C_0} \psi dy + \oint_{\partial C_1} \psi dy + \oint_{\partial C_2} \psi dy + \dots$$

The value of the Prandtl stress function is a constant on each of the boundary curves. Thus each such constant can be factored out of each integral leaving a line integral about a closed loop of the exact differential dy . Since dy is an exact differential, its integral is simply the value of y at the beginning of the loop less the value of y at the end of the loop. Since these two values are the same, each integral has the value zero. Thus the y direction shearing force component is zero and, by a similar argument, so too is the z component of the total shearing force.

The evaluation of the integral that is the torsional moment proceeds initially in much the same way for the multiply connected cross-section as it does for the singly connected

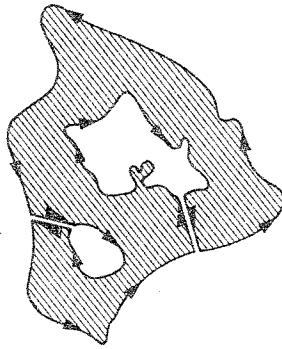


Figure A.4. A multiply connected cross-section showing a single boundary integration path that encompasses all inner boundaries and the outer boundary.

cross-section. The only difference between the present and previous moment integrals is, of course, that here the area integral is limited to that part of the cross-sectional area where stresses are possible. That is, the present form of the moment integral does not include the inner voids of the multiply connected cross-section. Thus

$$M_t = - \iint_{A_{net}} \left(y \frac{\partial \Psi}{\partial y} + z \frac{\partial \Psi}{\partial z} \right) dA$$

The use of an obvious identity and then the Green–Gauss theorem produces

$$M_t = - \iint_{A_{net}} \left[\frac{\partial(y\Psi)}{\partial y} + \frac{\partial(z\Psi)}{\partial z} \right] dA + 2 \iint_{A_{net}} \Psi dA$$

$$M_t = - \int_{\partial A_{net}} [y\Psi dz - z\Psi dy] + 2 \iint_{A_{net}} \Psi dA$$

Recall that the ∂ attached to the line integral is to be read as “the boundary of.” The last of the above three equalities requires that the multiply connected cross-sectional area of Fig. A.4 be divided into y and z direction single interval sub-areas as per the derivation of the Green–Gauss theorem. This is always possible for cross-sections of engineering interest. (The division into sub-areas is not shown in Fig. A.4., but is illustrated in Fig. IV.2.) Again, with that division, the above line integral around the boundaries of the net cross-sectional area is the sum of (i) the counterclockwise line integral around the outer boundary of the cross-section; (ii) all the line integrals that run both ways over the analyst-selected internal boundaries between the single-interval sub-areas required by the Green–Gauss theorem; and (iii) the clockwise line integrals around the boundaries of the internal voids. All these line integrals, of course, have the form of the line integral that is part of the above third equality. Since Ψ is zero on the outer boundary, and since the line integrals over the internal boundaries always occur in pairs that traverse the internal boundary in opposite directions, the line integrals in categories (i) and (ii) each sum to zero. Around each inner boundary the Prandtl stress function has a (unknown) nonzero constant value Ψ_i . Hence with clockwise line integration around the boundaries of the inner voids

$$M_t = - \sum \Psi_i \oint_{\partial C_i} [y dz - z dy] + 2 \iint_{A_{net}} \Psi dA$$

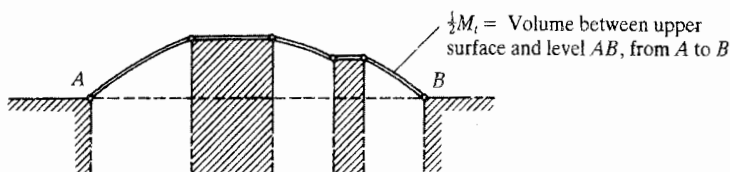


Figure A.5. A sectional view of a membrane (Prandtl stress function) attached to constant height interior plateaus (the inner boundaries of a multiply connected cross-section).

or, after reversing the direction of the line integration to counterclockwise

$$M_t = + \sum \Psi_i \oint_{\partial C_i} [y dz - z dy] + 2 \iint_{A_{net}} \Psi dA$$

The easiest way of evaluating the remaining line integrals around the internal voids is to use the Green–Gauss theorem. That is, for any general area A_i

$$\oint [y dz - z dy] = \iint_{A_i} \left[\frac{\partial y}{\partial y} + \frac{\partial z}{\partial z} \right] dA = 2A_i \quad (\text{A.10})$$

Thus

$$M_t = +2 \iint_{A_{net}} \Psi dA + 2 \sum \Psi_i A_i \quad (\text{A.11})$$

where, of course, A_i is the area of the i th void. This final expression for the torque has an important parallel to the expression for the torque acting upon a singly connected cross-section. In the latter case, in geometric terms, the torque is twice the volume between the Prandtl stress function and the y, z plane as the Prandtl stress function spans the entire cross-sectional area. In the multiply connected case, the torque is twice the volume under the Prandtl stress function as it spans the net cross-sectional area, plus twice the product of the constant values of the Prandtl stress function at the edges of the voids multiplied by the areas of the voids. This latter result may be interpreted as twice the volume of a Prandtl stress function that is flattened over the voids inside the outer boundary. This interpretation is illustrated in Fig. A.5.

A.4 The Uniform Torsion GDE for Multiply Connected Cross-Sections

In this section the unit load method is used to calculate the twist per unit length for the uniform torsion problem. The actual load system consists of a uniform beam of length L with a multiply connected cross-section and equal and opposite torques of magnitude M_t acting at the beam ends. The unit load system consists of the same beam with the same arrangement of torques, but in this case the torques are of unit magnitude. Hence the actual stresses are, as always,

$$\sigma_{xy} \equiv \frac{\partial \Psi(y, z)}{\partial z} \quad \text{and} \quad \gamma_{xz} \equiv -\frac{\partial \Psi(y, z)}{\partial y}$$

The actual strains, using the isotropic strain–stress equations, are

$$\gamma_{xy} = \frac{1}{G} \frac{\partial \Psi(y, z)}{\partial z} \quad \text{and} \quad \gamma_{xz} = -\frac{1}{G} \frac{\partial \Psi(y, z)}{\partial y}$$

The unit load stresses in this linear system can be calculated by setting up the proportionality that the actual stresses are to the actual torque as the unit load stresses are to the unit torque. The result is

$$\bar{\sigma}_{xy} = \frac{1}{M_t} \frac{\partial \Psi(y, z)}{\partial z} \quad \text{and} \quad \bar{\sigma}_{xz} = -\frac{1}{M_t} \frac{\partial \Psi(y, z)}{\partial y}$$

The twist per unit length, θ , multiplied by the beam length L is the total twist of one beam end relative to the other beam end. The total twist multiplied by the unit moment is the external complementary virtual work of the unit load system, which in turn is equal to the negative of the internal complementary virtual work of the unit load system. The latter quantity is the integral over the entire volume of the beam material of the product of the nonzero unit load stresses and the actual strains. This result may be written as

$$\theta = \frac{1}{L} \iiint_{V_{net}} [\bar{\sigma}_{xy} \gamma_{xy} + \bar{\sigma}_{xz} \gamma_{xz}] dA_{net} dx$$

or

$$\theta = \frac{1}{LGM_t} \int_L \iint_{A_{net}} \left[\left(\frac{\partial \Psi}{\partial z} \right)^2 + \left(\frac{\partial \Psi}{\partial y} \right)^2 \right] dA dx$$

Since $\Psi(y, z)$ and its derivatives are not functions of x , the integration over the interval $0 \leq x \leq L$ can be carried out separately to produce a factor L , which cancels the same quantity in the denominator of the ratio before the integrals. The Green–Gauss theorem can be used to carry out the integration with respect to y and z . Recall that the Green–Gauss theorem states

$$\iint_A \left[\frac{\partial F}{\partial z} + \frac{\partial G}{\partial y} \right] dA = - \oint [F dy - G dz]$$

For present purposes, let $F = \Psi(\partial \Psi / \partial z)$, and let $G = \Psi(\partial \Psi / \partial y)$. Then these substitutions transform the Green–Gauss theorem into the following form, one of the many variations on the Green–Gauss theorem

$$\iint_{A_{net}} \left[\left(\frac{\partial \Psi}{\partial z} \right)^2 + \left(\frac{\partial \Psi}{\partial y} \right)^2 \right] dA = - \iint_{A_{net}} \Psi \nabla^2 \Psi dA + \oint \Psi \left[\frac{\partial \Psi}{\partial y} dz - \frac{\partial \Psi}{\partial z} dy \right]$$

where, as usual, for this multiply connected region the counterclockwise path around the entire boundary of the net area includes the outer boundary, the two-way paths between the outer boundary, and the various inner boundaries in such a manner that the paths subdivide the original area into sub-areas for which the Green–Gauss theorem is valid, and the various boundaries of the internal voids. As before, the general counterclockwise movement over the total boundary path means a clockwise movement around the internal boundaries. Now it is a matter of evaluating the two integrals of the right-hand side of the above equality.

Since $\nabla^2 \Psi = C$ is a constant, it can be factored out of the second area integral regardless of the nature of the boundary of the cross-section. The remaining net area integral of the Prandtl stress function can be determined from Eq. (A.11) above as

$$\iint_{A_{net}} \Psi dA = \frac{M_t}{2} - \sum \Psi_i A_i$$

The final task is to evaluate the right-hand side line integral, which for the sake of convenience is termed Λ_0 . That is,

$$\Lambda_0 = + \oint \Psi \left[\frac{\partial \Psi}{\partial y} dz - \frac{\partial \Psi}{\partial z} dy \right]$$

Since $\Psi(s)$ is zero on the outer boundary, and it is the unknown constant Ψ_i on the i th inner boundary, the Λ_0 clockwise line integral becomes the sum of the product of those constants and their respective line integrals around each of the inner boundaries. That is,

$$\Lambda_0 = \sum \Psi_i \oint_{\partial C_i} \left[\frac{\partial \Psi}{\partial y} dz - \frac{\partial \Psi}{\partial z} dy \right]$$

Now the task is to evaluate each of the above line integrals about the inner voids. Let a typical such line integral be identified as Λ_i so that $\Lambda_0 = \sum \Psi_i \Lambda_i$, where, by use of the Green–Gauss theorem

$$\begin{aligned} \Lambda_i &= \oint_{\partial C_i} \left[\frac{\partial \Psi}{\partial y} dz - \frac{\partial \Psi}{\partial z} dy \right] = \iint_{A_i} \left[\frac{\partial}{\partial y} \left(\frac{\partial \Psi}{\partial y} \right) + \frac{\partial}{\partial z} \left(\frac{\partial \Psi}{\partial z} \right) \right] dA \\ &= \iint_{A_i} \nabla^2 \Psi dA = C A_i \end{aligned}$$

So

$$\Lambda_0 = C \sum \Psi_i A_i$$

Therefore, from

$$\theta = \frac{1}{GM_t} \iint_{A_{net}} \left[\left(\frac{\partial \Psi}{\partial z} \right)^2 + \left(\frac{\partial \Psi}{\partial y} \right)^2 \right] dA$$

the result is

$$GM_t \theta = -C \left(\frac{1}{2} M_t - \sum \Psi_i A_i \right) + C \sum \Psi_i A_i$$

from which

$$C = -2G\theta$$

and thus

$$\nabla^2 \Psi(y, z) = -2G\theta$$

is the uniform torsion GDE for a multiply connected cross-section.

A.5 Calculation of the Twist Per Unit Length of a Single Cell of an N -Cell Cross-Section

This uniform torsion twist per unit length calculation in terms of the quantities particular to an N -cell, thin cross-section is conveniently accomplished using the unit load method. Let the equilibrium unit load system consist of two oppositely directed unit torques acting at the ends of a multicell beam of length L . Let each unit torque have the form of a shear flow loop around the i th cell, as sketched in Fig. A.6. The external work done by this unit load system is the unit load multiplied by the twist of the i th cell front-face cross-section

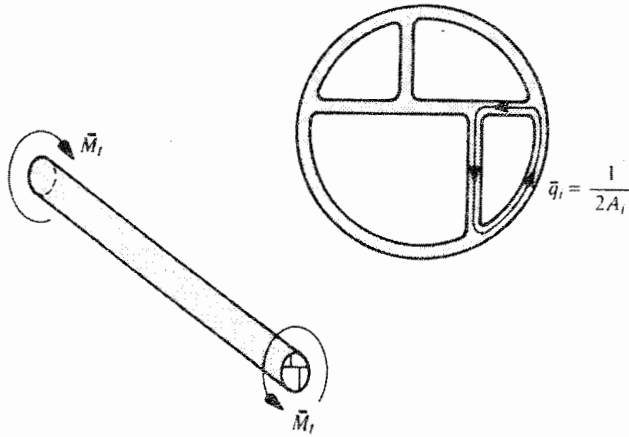


Figure A.6. A uniform torsion FBD for calculating the twist in a single cell of a multicell cross-section.

relative to its back face. Thus, with no warping constraint, and with all the actual stresses other than σ_{xy} and σ_{xz} being zero, the unit load solution for the twist of the i th cell is

$$1\phi_i = \int_L \iint_A [\bar{\sigma}_{xy}\epsilon_{xy} + \bar{\sigma}_{xz}\epsilon_{xz}]dA dx$$

Since the integrand is independent of the x coordinate, the integration over the length can be accomplished immediately to obtain the length as a right-hand side factor. Dividing both sides of the equality by L produces on the left-hand side the twist per unit length of the i th cell, θ_i .

Cartesian coordinates are obviously not convenient to the present situation. Referring to the coordinate axes of Fig. 12.3 and the inverse forms of Eqs. (12.12), with σ_{xn} equaling zero, leads to

$$\sigma_{xy} = -\sigma_{xs} \sin \beta \quad \text{and} \quad \sigma_{xz} = +\sigma_{xs} \cos \beta$$

so

$$\begin{aligned} \bar{\sigma}_{xy} &= -\bar{\sigma}_{xs} \sin \beta & \text{and} & & \bar{\sigma}_{xz} &= +\bar{\sigma}_{xs} \cos \beta \\ \epsilon_{xy} &= -\epsilon_{xs} \sin \beta & \text{and} & & \epsilon_{xz} &= +\epsilon_{xs} \cos \beta \end{aligned}$$

Substitution of the last two pairs of relations into the above integrand yields

$$\theta_i = \iint_{A_i} \bar{\sigma}_{xs}\epsilon_{xs}dA = \oint_{\partial C_i} \bar{\sigma}_{xs}\epsilon_{xs}t ds$$

where $dA = tds$ and $t = t(s)$ is the local thickness. Recall that $\bar{\sigma}_{xs}$ is equal to the unit load shear flow divided by the local thickness. With the unit load moment having the magnitude 1, and with the unit load shear flow being that of a single loop, the unit load shear flow divided by the local thickness equals $(1/2\hat{A}_i t)$. The actual shearing strain is the actual shearing stress divided by the local shear modulus, that is, q/Gt . Then, making these substitutions, introducing a reference shear modulus G_0 in order to account for nonhomogeneous cross-sections, and defining $t^* \equiv (G/G_0)t$, leads to

$$\theta_i = \frac{1}{2G_0\hat{A}_i} \oint_{\partial C_i} \frac{q}{t^*} ds \tag{A.12}$$

Note that q is the total actual shear flow at any point s on the centerline going around the i th cell. Thus it is one of the numerically subscripted shear flows, or the difference of two of those shear flows. In any event, the shear flow q is piecewise constant. With wall thicknesses also generally being piecewise constant, the evaluation of these line integrals usually reduces to the simple matter of dividing thin-wall cross-section lengths by their thicknesses for each cell wall segment.

Selected Answers to Exercises

- 1.1.** Let L equal Lexa's present age, S equal Sara's present age, and T equal the elapsed time between "now" and "before." Now $L = 12$, and before, Lexa's age was $12 - T$. Before, Sara's age was $S - T$. Then from the problem statement, $12 = 2(S - T)$, and $12 - T = S$. Thus $S = 9$, and $T = 3$.
- 1.2.** The first step is to locate the point P on the infinitesimal body, which is the corner point with the lowest coordinate values. Then the orthogonal planes passing through the point P are the back faces where all the stress vectors are positive in the directions that are opposite to the positive directions of the coordinates. The other three faces are front faces where the stress vectors are positive in the direction of increasing coordinate values. For example, in the third figure where the point P is already labeled, the normal stress $\sigma_{\phi\phi}$ on the top surface points upward; and the normal stress $\sigma_{\rho\rho}$ on the front face points outward in the direction of increasing ρ .
- 1.3.** (a) The edges of the rectangle are defined mathematically by $x = 0$, $x = a$, $y = 0$, and $y = b$. These coordinate values are inserted into the traction arguments. For example, $T_x(0, y) = -2p_0$ and $T_y(0, y) = 0$; $T_x(a, y) = +2p_0$, and $T_y(a, y) = 0$. Similarly, $T_x(x, 0) = 0$, and $T_y(x, 0) = +p_0$. It is left to the reader to write the tractions for the upper edge.
- (b) Yes, these constant values for the stresses are a solution for the equilibrium and Cauchy equations. It can be learned later that these stress values also satisfy the equations for small deformations, and the equations for linearly elastic materials. Thus these stress values are a solution for the elastically deformed piece of metal.
- (c) $T_x = T_z = 0$, and $T_y = \frac{1}{2}\sigma_0$.
- 1.4.** For $x = -a$: $\cos(n, x) = -1.0$; $\cos(n, y) = \cos(n, z) = 0$. For $z = +c$: $\cos(n, x) = \cos(n, y) = 0$; $\cos(n, z) = +1.0$. The direction cosines c_{yx} , c_{yy} , and c_{yz} are left to the reader.
- 1.5.** (a) $C = +6$.
- (b) $T_x(a, y) = T_x(-a, y) = 0$, $T_y(a, y) = -T_y(-a, y) = -3\sigma_0$. On any surface, all z subscripted tractions are zero because this is a plane stress problem.
- (d) All tractions upon the surfaces $z = +c$ and $z = -c$ are zero.
- 1.6.** (a) Interior equilibrium equations only require that $B \equiv D$, while both A and C can have any value.
- (b) At $x = 0$: $\cos(n, x) = -1.0$; $\cos(n, y) = \cos(n, z) = 0$. Thus the matrix $[v] = [-1 \ 0 \ 0]$. From the relation $\{T\} = [\sigma][v]$, $[T] = [0 \ (-1 + Ay - By^2) \ 0]$, where all tractions are positive in the positive coordinate directions irrespective of the orientation of the surface on which they act.
- 1.7.** (a) The external forces $ta\sigma_0$, $\frac{1}{2}ta\sigma_0$ and $(\sqrt{3}ta/2)\sigma_0$ do form a closed force triangle, and therefore the triangular sheet of material is in a state of external equilibrium.

- (b) The given plane stress solution satisfies the interior and boundary (i.e., Cauchy) equilibrium equations. On the hypotenuse edge, where $\cos(n, x) = 0.866$, $\cos(n, y) = 0.5$, the normal traction $-\sigma_0$ is the vector sum of the two Cartesian components, $T_x = -(\sqrt{3}/2)\sigma_0$, and $T_y = -\frac{1}{2}\sigma_0$.
- 1.8. The positive directions of the tractions acting upon the outer boundary are, of course, in the positive coordinate directions. The other two edge planes are, of course, back faces. Summing forces in the x direction yields $T_x ds dz = \sigma_{xx} dy dz + \sigma_{yx} dx dz - \frac{1}{2}\rho B_x dx dy dz$. The body force term is insignificant relative to the other three terms, and thus must be discarded. Dividing through by the nonzero quantities ds and dz , and noting that $\cos\theta = dy/ds$, and so forth, yields $T_x = \sigma_{xx} \cos\theta + \sigma_{xy} \sin\theta$. The y direction traction equation is $T_y = \sigma_{xy} \cos\theta + \sigma_{yy} \sin\theta$. These two solutions exactly match Eqs. (1.11).
- 1.9. (b, c, d) Setting moments about the element center equal to zero shows that the order of cylindrical coordinate subscripts for stresses is immaterial.
- 1.10. (c) For example, extending the r direction interior equilibrium equation to three dimensions only requires the addition of the term $+r \partial\sigma_r/\partial z$ to the plane stress equation.
- 1.11. Yes, as is necessary, each term has the same units as every other term in the same equation.
- 1.12. (a) $\sigma_{xx} = +N/A$ satisfies the interior equilibrium equations since both N and A are constants. The boundary equilibrium equations are also satisfied on the cylindrical surface particularly because $\cos(n, x) = 0$, and they are satisfied at $x = 0$ since $\cos(n, x) = -1.0$.
- (b) The oblique area is now $\sqrt{2}A_0$ because A_0 is the projected area, which is equal to the oblique area multiplied by the cosine of the angle between the normals to the two areas. Thus, at $x = L$, the new $T_x = N/\sqrt{2}A$, and the same stress solution is valid in this case. In particular, the Cauchy matrix equation is satisfied where σ_{xx} is again N/A and all other stresses are zero. The extension to a multifaceted surface of a general body can be achieved by breaking up that surface into smaller and smaller planes at different inclinations where, as above, there is no effect on the stress state solution.
- 1.13. Two vectors along the edges of the triangular area are $(-a\mathbf{i} + 2a\mathbf{j})$ and $(-a\mathbf{i} + 3a\mathbf{k})$. Their cross product gives both the magnitude of twice the area of the triangle and a normal vector. The normal vector can be converted into a unit normal vector by dividing it by its own magnitude. The result is a unit outward normal vector $\mathbf{n} = (6/7)\mathbf{i} + (3/7)\mathbf{j} + (2/7)\mathbf{k}$, and the area of the triangular face is determined to be $(7/2)a^2$. Then for case (a) the normal stress, $(4N/49a^2)$, is then the dot product of $(N/A) \equiv (N/A)\mathbf{k}$ and \mathbf{n} . The total shear stress can be obtained using the Pythagorean theorem with the triangle formed by the total stress vector N/A , the normal stress vector and the shearing stress vector. The result is $(6\sqrt{5}/49)(N/a^2)$. The stress in the z direction is simply $N/A = 2N/(7a^2)$, while those in the other two coordinate directions are zero.
- 1.14. An intermediate step could be to obtain $d\bar{A} = \frac{1}{2}[-dx\mathbf{i} + dy\mathbf{j}] \times [-dx\mathbf{i} + dz\mathbf{k}] = \frac{1}{2}[dy dz \mathbf{i} + dx dz \mathbf{j} + dx dy \mathbf{k}] = dA_x \mathbf{i} + dA_y \mathbf{j} + dA_z \mathbf{k}$. Dividing this vector by its magnitude, dA , provides the unit normal to the oblique face. Dot products with the unit vectors \mathbf{i} , \mathbf{j} , and \mathbf{k} provide the desired result.
- 1.15. Distances in the θ direction are measured by the product $r\theta$. The factor r in this product has the fixed value of the radius of the circular arc along which $r\theta$ measures distance; that is, this particular value of r is a constant. In order to distinguish this constant radius from the coordinate r , which can take on any value, let it

be temporarily labeled with a zero subscript as r_0 . Then, for example, using the chain rule for partial differentiation, where F is any function of the cylindrical coordinates: $\partial F/\partial(r_0\theta) = (\partial F/\partial r)(\partial r/\partial(r_0\theta)) + (\partial F/\partial\theta)(\partial\theta/\partial r_0\theta) + (\partial F/\partial z)(\partial z/\partial r_0\theta)$. The second factors in the first and third products are zero because the coordinates r and z do not vary with $r_0\theta$. The partial derivative of θ with respect to $r_0\theta$ equals $(1/r_0)$. Thus the final result, after changing r_0 back to r , which is still a constant in this discussion, is $\partial F/\partial(r\theta) = (1/r)(\partial F/\partial\theta)$.

- 1.17. (a) After deleting terms of magnitudes that are infinitesimal compared to those retained, and canceling $r dr d\theta d\phi$, the r direction equilibrium equation becomes

$$r \frac{\partial \sigma_{rr}}{\partial r} + 2\sigma_{rr} + \frac{\partial \sigma_{\phi r}}{\partial \phi} + \sigma_{\phi r} \cot \phi - (\sigma_{\phi\phi} + \sigma_{\theta\theta}) + \frac{\partial \sigma_{\theta r}}{\partial \theta} \csc \phi + \rho r B_r = 0$$

- 1.18. (a) $B_r = r\Omega^2 \sin^2 \phi - \frac{r}{R}g_0$, $B_\theta = 0$, and $B_\phi = r\Omega^2 \sin \phi \cos \phi$.
 (b) $\sigma_{\theta r} = \sigma_{\theta\phi} = 0$.
 (c) All derivatives with respect to θ are zero.

- 2.1. (a, b) This is simply a matter of carrying out the matrix multiplication to the extent of calculating the (1, 1) and (1, 2) entries of the matrix of rotated stresses.

- 2.2. Your plane stress result can be checked by specializing the three-dimensional rotation equations, Eqs. (2.1) and (2.2), to the present circumstances. Here

$$\begin{aligned} c_{xx} &= \cos \theta & c_{xy} &= \sin \theta & c_{xz} &= 0 \\ c_{yx} &= -\sin \theta & c_{yy} &= \cos \theta & c_{yz} &= 0 \end{aligned}$$

- 2.3. (a) The point of this exercise is that with the use of Cartesian coordinates the concept of back faces and front faces only applies to rectangular parallelepipeds. The given sketch can be justified by drawing the rectangular parallelepiped at point P that lies above the wedge of the given sketch and noting that Newton's third law requires the stresses on the oblique face of the wedge to be equal and oppositely directed from those on the adjacent face of the rectangular parallelepiped.

- 2.4. (b) The z^* and x axes coincide; the y^* and y axes coincide; and the x^* and z axes are oppositely directed.

- 2.5. Let $|\sigma_{sz}|$ be the absolute magnitude of the maximum shearing stress in the z plane, and $|\sigma_{sm}|$ be the absolute magnitude of the maximum shearing stress in any plane. Let α be the counterclockwise rotation in units of degrees of the original differential element from its original orientation to the orientation on which the principal stresses act. Let β be the counterclockwise rotation in units of degrees of the original differential element to the orientation on which the maximum shearing stresses (and mean normal stresses) act. Recall that in all cases the difference between these counterclockwise rotation angles, α and β , is 45° . Then selected solutions are

Case	Units	σ_{11}	σ_{22}	σ_{33}	$ \sigma_{sz} $	$ \sigma_{sm} $	α	β
(1)	MPa	121	0	-161	141	141	22.5	-22.5
(2)	ksi	9	0	-21	15	15	-18.4	26.6
(3)	ksi	25	10	-1	13	13	-11.3	33.7
(4)	ksi	15	-5	-8	10	11.5	-30	15
(5)	MPa	300	-90	-100	200	200	30	-15
(6)	MPa	70	70	70	0	0	any	any
(7)	MPa	18	-12	-34	26	26	-11	34

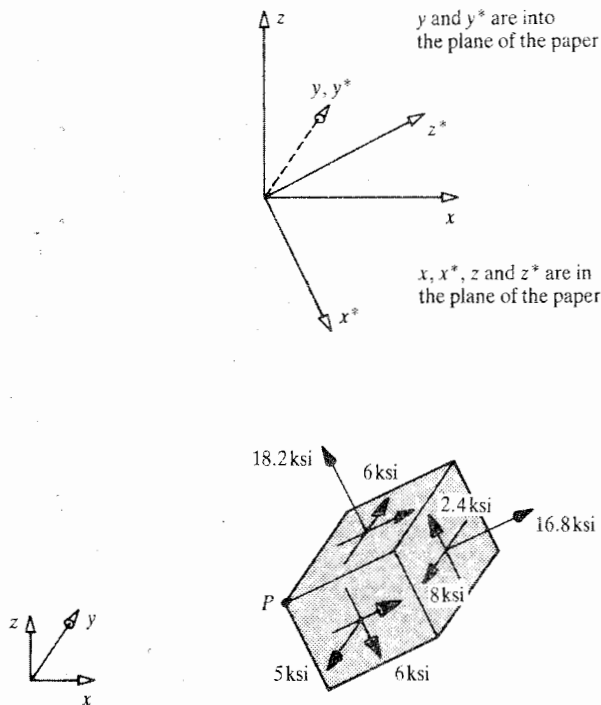


Figure B.1. Ans. 2.6

- 2.6. (a) Eq. (2.3) provides the stresses in the rotated coordinate system in matrix form, which are

$$\frac{1}{5} \begin{bmatrix} 91 & -30 & -12 \\ -30 & 25 & -40 \\ -12 & -40 & -84 \end{bmatrix} \text{ ksi} = \begin{bmatrix} 18.2 & -6 & -2.4 \\ -6 & 5 & -8 \\ -2.4 & -8 & -16.8 \end{bmatrix} \text{ ksi}$$

- (b) Inspection of the second row of the matrix of direction cosines shows that the y and y^* axes coincide. With this knowledge, the problem reduces to one in the two dimensions of the plane formed by the x and z axes. The signs of the nonzero direction cosines show, with very little trial and error, that the z^* axis lies between the z and x axes, closer to the x axis than the z axis, and the angle between the x^* axis and the z axis is obtuse. This result, and the rectangular parallelepiped, are sketched in Fig. B.1.
- 2.7. This exercise, as in the case of Exercise 1.4, requires the determination of the unit normal to the given plane. The components of the unit normal are the three direction cosines for the angles between the unit normal vector and the Cartesian coordinate axes. Once those quantities are obtained, it is just a matter of applying the Cauchy matrix equation. As for the details, a normal vector is again determined by taking the cross product of two vectors in the plane for which a normal vector is sought. Two such suitable vectors are $(-2\mathbf{i} + 3\mathbf{j})$ and $(-2\mathbf{i} + 4\mathbf{k})$. The unit normal vector is obtained from a normal vector by dividing by the magnitude of the normal vector, which in this case is $\sqrt{61}$. The results are that the unit normal, that is, the vector of direction cosines, $[\nu] = [6/\sqrt{61} \ 4/\sqrt{61} \ 3/\sqrt{61}]$, and $[T] = [6.4 \ -5.1 \ 7.7]$ ksi, where the final number of significant figures is reduced to

two so as to match the number of significant figures of the input. The magnitude of the total traction vector is a little over 11 ksi.

- 2.8. (a)** The middle root is approximately 3.1864. Thus $\sigma_{22} \approx 3.2$ MPa. The other two roots are a little bit less than +4 MPa and -10 MPa.
- (b)** The middle root is approximately 13.873 ksi ≈ 13.9 ksi.
- (c)** The quadratic is $\sigma^2 + (5.7178)\sigma - 38.8712 = 0$, which has one root at $\sigma = 4.0000$ ksi.
- 2.9. (a)** The coefficients of the cubic polynomial that is the characteristic equation are: +1, +20, +43, -160. The roots of the derivative of that cubic are the points where the cubic has a zero slope. These points bracket the middle root of the cubic and aid in sketching the cubic. Those two points are -12.15 and -1.18 ksi. Checking to see whether there are any integer roots in the vicinity of half-way between those two points shows that -5 is an integer root. With this information the cubic can be reduced to a quadratic in the remaining two unknown roots that is easily solved. The principal stresses in order of magnitude are: 1.89 ksi, -5.00 ksi (an exact solution), and -16.9 ksi.
- (b)** The coefficients for the cubic polynomial equation for the principal stresses are: +1, -180, +8000, -100 000 MPa. The roots, in order of magnitude are 120.5 MPa, 37.2 MPa, and 22.3 MPa, which sum to the negative of the second coefficient, and their product is 99 962, which is a close approximation to the negative of the last coefficient. These roots should, after all the calculations are completed, be rounded off to comply with the (presumably) two significant figures of the input stress matrix.
- (d)** The cubic coefficients are, for descending powers of the unknown eigenvalue: 1, -12, -214, and +2454. Application of Descartes' rule shows that there are two positive roots. The three roots turn out to be +15.658 MPa, +10.823 MPa, and -14.481 MPa, which need to be rounded off as 15.7, 10.9, and 14.5 MPa respectively.
- (e)** The cubic coefficients are, for descending powers of the eigenvalue: 1, -22, -5, and +1498. The ordered values of the principal stresses are: 17.264 ksi ≈ 17.3 ksi; 11.979 ksi ≈ 12.0 ksi; and -7.243 ksi ≈ -7.3 ksi. Note that the sum of the roots adds to the negative of the second coefficient, and the product of the roots is very close to the negative of the last coefficient.
- (f)** The cubic coefficients are, for descending powers of the eigenvalue: 1, -5, -375, and +875.
- (g)** The cubic coefficients are, for descending powers of the eigenvalue: 1, +8, -612, and -3568. Descartes' rule shows that there are one positive root and two negative roots.
- 3.1. (a)** $\epsilon_{xx} = C; \epsilon_{yy} = -C; \epsilon_{zz} = -C; \gamma_{xy} = \gamma_{xz} = \gamma_{yz} = 0$.
- 3.2.** Even though the displacement function $u(x, y, z) = C|x|$ is a single-valued, continuous function, these two mathematical conditions are insufficient for the physical reality of a continuous body when the origin of the coordinate system (*where u is nondifferentiable*), is located within the body under study. This, is because $\epsilon_{xx} = +C$ for all $x > 0$, and $\epsilon_{xx} = -C$ for all $x < 0$. These strain expressions mean that the body would have to be uniformly stretched to the right of the origin of the coordinate axes, and uniformly compressed to the left of the origin, without any transition region in between. This state of strain is physically impossible because equilibrium is not possible where $x = 0$. In other words, the displacement functions must be everywhere differentiable, not just continuous.

- 3.3. (a) Since $d\hat{y} = dy + [v + (\partial v/\partial y) dy] - v = [dy + (\partial v/\partial y) dy]$, then $(d\hat{y} - dy)/dy = \partial v/\partial y$.
- (b) Referring to Fig. 3.3, the longitudinal strain ϵ_{yy} is equal to the limit of the ratio of $(P'R' - PR)/PR$ as PR is diminished to zero. An intermediate step is

$$\overrightarrow{P'R'} = \frac{\partial u}{\partial y} dy \mathbf{i} + \left(1 + \frac{\partial v}{\partial y}\right) dy \mathbf{j} + \frac{\partial w}{\partial y} dy \mathbf{k}$$

The remainder of the deduction can now proceed as is detailed for ϵ_{xx} with the single exception that the squares as well as the higher powers of the partial derivatives are now discarded. The discarding of the squared terms is equivalent to ignoring the deflections in the x and z directions of the original differential segment, dy . In order to establish this geometric interpretation of the algebraic step of discarding second order terms, note that the change in length over length definition of ϵ_{yy} , is

$$\epsilon_{yy} = \frac{d\hat{y} - dy}{dy} = \frac{dy + [v + (\partial v/\partial y) dy] - v}{dy}$$

or

$$\epsilon_{yy} = \frac{\partial v}{\partial y}$$

- 3.4. (a) $C = 4A$

(c) $A = C = -B$

- 3.6. $A = C = +1; B = -1$.

- 3.7. (a) Recall that any compatibility equation for linear strain expressions only involves strains, and derivatives of strains. In particular, such a compatibility equation never involves displacement functions. Thus the task is to devise a means of linking together the nonzero strains by eliminating displacements. In this case, with $v = w = 0$, and $u(x, y)$ only being a function of x and y , the only nonzero strains are $\epsilon_{xx} = \partial u/\partial x$ and, for this case, $\gamma_{xy} = \partial u/\partial y$. Since the strains are differentiable functions, $(\partial/\partial y)(\partial u/\partial x) = (\partial/\partial x)(\partial u/\partial y)$. Thus $\partial\epsilon_{xx}/\partial y = \partial\gamma_{xy}/\partial x$, which is the desired compatibility equation.

- (b) Partially differentiate $\gamma_{r\theta}$ with respect to θ and interchange the order of differentiation in the first term to achieve

$$\frac{\partial\gamma_{r\theta}}{\partial\theta} = \frac{\partial}{\partial r} \left(\frac{\partial v}{\partial\theta} \right) - \frac{1}{r} \left(\frac{\partial v}{\partial\theta} \right) = \frac{\partial}{\partial r} (r\epsilon_{\theta\theta}) - \epsilon_{\theta\theta}$$

Carrying out the above partial differentiation, $(\partial/\partial r)(r\epsilon_{\theta\theta})$, leads to $\partial\gamma_{r\theta}/\partial\theta = r(\partial\epsilon_{\theta\theta}/\partial r)$, which is the desired compatibility equation.

- (c) First of all, since this is a case of plane strain, the only nonzero strains are ϵ_{xx} , ϵ_{yy} , and γ_{xy} . The goal here is to find a partial differential equation that relates these three strain functions, but which does not involve either of the two displacement functions. The simplest approach is to replace $u(x, y)$ by $f(x)v(x, y)$ so as to have all three plane strains in terms of the single displacement function v and, of course, the function f , and their derivatives. That is, the intermediate step is

$$\epsilon_{xx} = f'v + f\frac{\partial v}{\partial x} \quad \epsilon_{yy} = \frac{\partial v}{\partial y} \quad \gamma_{xy} = f\frac{\partial v}{\partial y} + \frac{\partial v}{\partial x}$$

One way of proceeding is to solve the shearing strain expression for $\partial v/\partial x$ in terms of γ_{xy} , and the normal strain $\epsilon_{yy} = \partial v/\partial y$. Then substitute that expression for $\partial v/\partial x$ into the x direction strain expression. To eliminate v , differentiate both sides of the combined expression with respect to y and again replace $\partial v/\partial x$ by the y direction strain. The final result is the following first order partial differential equation. Since it only involves the strains, it is a compatibility equation:

$$\frac{\partial \epsilon_{xx}}{\partial y} = f' \epsilon_{yy} + f \frac{\partial \gamma_{xy}}{\partial y} - f^2 \frac{\partial \epsilon_{yy}}{\partial y}$$

A closely related approach, after writing the strains in terms of v and f and their derivatives, is to first partially differentiate to obtain

$$\frac{\partial \epsilon_{xx}}{\partial y} = f' \epsilon_{yy} + f \frac{\partial \epsilon_{yy}}{\partial x}$$

and

$$\frac{\partial \gamma_{xy}}{\partial y} = f \frac{\partial \epsilon_{yy}}{\partial y} + \frac{\partial \epsilon_{yy}}{\partial x}$$

These two equations can be combined to obtain the result above by algebraically eliminating $\partial \epsilon_{yy}/\partial x$.

- 3.9.** The units of the second term (inverse of length) do not match the units of all the other terms (radians) in the equation.
- 3.10.** (a), (b), and (d) are true. (c) can be made to be true by changing the plus sign on the right-hand side to a minus sign.
- 4.2.** (b) $[\epsilon] = [c]^t[\epsilon^*][c]$ and $[\sigma] = [c]^t[\sigma^*][c]$.
- 4.3.** The direction cosines of the matrix are in accord with the six equations of constraint developed from the six different dot products that are incorporated into the matrix equation $[c][c]^t = [I]$. That is, the product of the given matrix with its own transpose is indeed the identity matrix, and thus the matrix is a valid matrix of direction cosines.
- 4.4.** (a) $\epsilon_{xx} = (1/3)(-\epsilon_a + 2\epsilon_b + 2\epsilon_c)$
 $\gamma_{xy} = (2/\sqrt{3})(\epsilon_b - \epsilon_c)$
 $\epsilon_{yy} = \epsilon_a$
- (c) $\epsilon_{xx} = \epsilon_b$
 $\gamma_{xy} = (2/\sqrt{3})(\epsilon_c - \epsilon_a)$
 $\epsilon_{yy} = (1/3)(2\epsilon_a - \epsilon_b + 2\epsilon_c)$
- (e) $\epsilon_{xx} = \epsilon_b$
 $\gamma_{xy} = \epsilon_c - \epsilon_a$
 $\epsilon_{yy} = \epsilon_a - \epsilon_b + \epsilon_c$
- 5.1.** For example, the strain $\epsilon_{zz} = (b - b_0)/b_0 = -\nu\epsilon_{xx}$, and of course, $A/A_0 = ab/a_0b_0$. Hence $\frac{A(\sigma)}{A} = 1 - 2\nu\epsilon_{xx} + \nu^2\epsilon_{xx}^2$.
- 5.2.** From Military Handbook 5D (a) $E \approx 29.4 \times 10^3$ ksi = 29.4×10^6 psi. (b) $E \approx 10.6 \times 10^3$ ksi = 10.6×10^6 psi.
- 5.3.** (a) The room-temperature values for the tensile and compressive yield stresses are, respectively, 65 and 64 ksi. There is a 50 percent reduction in the tensile yield stress at 400 °F after $\frac{1}{2}$ hour of exposure; therefore, the tensile yield stress

is then 32 ksi. The compressive yield stress is 49 percent of room-temperature (RT) value, or 31 ksi.

- (d) The compressive yield stress is 73 ksi, and the temperature reduction factor is 0.68. Therefore the A basis compressive yield stress after a one-half hour at 350 °F is 49 ksi.

5.4. (a) Steel; (b, c) Aluminum.

5.5. (a) From Fig. 5.11, the number of allowable stress cycles for the 20 ksi, 20 ksi loading is approximately 5×10^6 cycles. To arrive at that approximation, realize that the interpolation is not linear, but logarithmic or even more than logarithmic. For logarithmic interpolation, half the distance between 1 and 10 is not 5.5 but 3, because $\log 3 = 0.4771$, and seven-tenths of the distance has the value 5, since $\log 5 = 0.6990$. If the reader looks at a slide rule, then the logarithmic proportionalities will be evident. Similarly, the number of allowable cycles for the 25 ksi, 10 ksi loading is approximately 1×10^6 . With the number of allowable cycles estimated, the next step is to form the ratios, for corresponding stress states, of the actual number of cycles to the allowable number of cycles, and then convert those ratios to a percentage. The sum of the estimated percentages is the estimate of the total damage; that is, Total damage = $[5 \times 10^6 / 5 \times 10^6] + (5 \times 10^5 / 10 \times 10^5)$ 100 percent = 150 percent. Since the total damage estimate exceeds 100 percent, it is estimated that failure will occur. Remember that this is a crude estimate, and failure is by no means guaranteed even for damage estimates as high as 300 percent in some instances.

- (b) Using Fig. 5.10, the mean allowable number of cycles to failure in each case is approximately 3×10^6 cycles, 3.5×10^5 (or maybe 3.6×10^5) cycles, and 5×10^5 cycles, respectively. Therefore the percentage damage is approximately $(100) [(1/3) + (2/7) + (1/5)]$. Since this is only 81 percent, the probability of failure is less than 1/2. The fact that the thin sheet under investigation is slightly thicker than the test specimens means that the thinner, test specimen data is on the safe side with respect to the thicker sheet under investigation.
- (c) Here it is necessary to obtain test data that is not presented in the textbook. Appropriate data can be found on page 3–345 of Military Handbook 5E, where $K_t = 1.5$. In order to match the given loadings to the given data, note that the two minimum stresses are –30 ksi and 0 ksi, respectively, and the two mean stresses are 0 ksi and 20 ksi, respectively. Then from the $S-N$ diagram, the corresponding numbers of cycles to failure are approximately 52 000 and 75 000 cycles. Then the percentage damage calculation and conclusion is

$$\%D = (100) \left(\frac{30\,000}{52\,000} + \frac{50\,000}{75\,000} \right) = 125 \text{ percent}$$

thus more likely to fail than not.

- 5.6. The area under the uniaxial loading curve is the product of the normal stress and the corresponding longitudinal strain. Stress is force over area, where the area is perpendicular to the stress vector. Strain is change (i.e., increment) in length over original length, where both the increment and original length are in the same direction as the stress vector. Thus their product is force multiplied by increment in length (i.e., work) over area multiplied by perpendicular length (i.e., volume).

5.7. Volume = $bhL = (b - \Delta b)(h - \Delta h)(L + \Delta L)$; thus

$$1 = [1 - (\Delta b/b)][1 - (\Delta h/h)][1 + (\Delta L/L)]$$

$$1 = 1 - (\Delta b/b) - (\Delta h/h) + (\Delta L/L) + (\text{higher order terms})$$

Hence

$$\Delta L/L = \Delta h/h + \Delta b/b \rightarrow \epsilon_{xx} = -\epsilon_{yy} - \epsilon_{zz} = -2\epsilon_{zz}$$

where, in this uniaxial loading case, the strain in all directions normal to the x axis must be equal. Thus the relation between any lateral strain and the longitudinal strain is $\epsilon_{zz} = -\frac{1}{2}\epsilon_{xx}$. Hence in this case Poisson's ratio is very close to $\frac{1}{2}$.

- 5.8. (a) On the stress state plot, the portion of the hexagon in the first quadrant is a pair of perpendicular lines that are normal to the stress axes and extend into the first quadrant from the tensile yield stress points on the two axes. The portion of the hexagon in the third quadrant is similar in that the two perpendicular lines extend into the third quadrant from the compressive yield stress points for each direction of loading. The single sides of the hexagon in the second and fourth quadrants are lines at 45° (if all four yield stresses have the same magnitude) to the stress axes, and they close the hexagon. All points on this hexagonal boundary have the same associated maximum shearing stress.
- (b) Now the plot has three stress axes, one for each orthogonal direction of loading. When the stress in the third direction is zero, then the plot from part (a) is the three-dimensional solution. That is, the part (a) hexagonal boundary curve solution is the cross-section of the boundary surface at a zero value of the stress in the third direction. Note that if the three principal stresses increase with the same magnitude from zero to some other value, tensile or compressive, then the corresponding three Mohr's circles are three coincident points. Thus these three stresses can increase without bound without creating any shearing stresses or plastic deformations. Similarly, consider the corner of the hexagonal boundary of part (a) that lies in the first quadrant where $\sigma_1 = \sigma_2 =$ (the tensile yield stress). If σ_3 is twice the tensile yield stress, then the three Mohr's circles form a single point at the tensile yield stress and two coincident circles between the tensile yield stress and twice that value. The coincident circles have a radius (associated shearing stress) equal to the critical shearing stress. Hence this stress point lies upon the boundary surface for the triaxial loading case. Now note that these three stress values and their associated Mohr's circles can be translated in lock step to any extent and in either direction along the horizontal axis of the Mohr's circle diagram without increasing the associated shearing stress. This shows that the boundary surface has constant inclinations to the three stress axes. Obviously this unbounded bounding surface is unrealistic, particularly in tension.
- 6.1. The material compliance matrix was developed on the basis of the strain that results from the stresses in the same and orthogonal directions. It matters not how those orthogonal directions are labeled. That is, the orthogonal directions can be referenced using any orthogonal coordinate system. Thus a material compliance matrix of the same form as that developed for a Cartesian coordinate system relates strains and stresses in a cylindrical or spherical coordinate system as well. It is only a matter of changing from one set of orthogonal coordinate subscripts to another.

- 6.2. (a) After writing $[I] = [E]'[S]' = [E]'[S]$, postmultiply by $[E]$ to obtain $[E] = [E]'$, which establishes the symmetry of the material stiffness matrix.
- (b) In all circumstances; because, regardless of the directions of the principal axes of strain, a shear stress is equal to the product of the shear modulus and the corresponding shearing strain. Thus, if the corresponding shearing strain is zero, then so too is the shearing stress, and that plane is also a plane of principal stress.
- (c) When the material is orthotropic, the same simple relation between a shearing stress and the corresponding shearing strain cited above only occurs when the axes of principal stress or the axes of principal strain are the same as the material axes of symmetry. That is, in general, the axes of principal strain and the axes of principal stress are not the same for an orthotropic material because when those axes are rotated away from the material axes of symmetry, any one shearing stress depends upon not just that one corresponding shearing strain, but all strains.
- 6.3. $\epsilon_{zz} = -[\nu/(1-\nu)](\epsilon_{xx} + \epsilon_{yy}) + [(1+\nu)/(1-\nu)]\alpha \Delta T$.
- 6.4. This solution depends upon recalling that $G = E/[2(1+\nu)]$, and, of course, that $\sigma_{xy} = G\gamma_{xy}$. Then, to the proper number of significant figures, $\sigma_{xy} = 3.9$ ksi.
- 6.5. FBDs for each of the bars show that the stresses are constant from one cross-section to another within the same bar. A FBD of an end cap provides the equation

$$2A_1\sigma_1 + A_2\sigma_2 = 0$$

The rigid caps require that the bars move the same distances, and since the lengths of the bars are the same, the strains in the bar are the same. Thus the strain compatibility equation is $\epsilon_1 = \epsilon_2$. The strain–stress equations are $\epsilon_1 = (\sigma_1/E_1) + \alpha_1 T_0$, and the same form for bar 2. Substituting the strain–stress equations into the strain compatibility equation, and solving simultaneously with the equilibrium equation, leads to, for example,

$$\sigma_1 = \frac{E_1 E_2 (\alpha_2 - \alpha_1) T_0}{E_2 + E_1 (2A_1/A_2)}$$

If $\alpha_1 = \alpha_2$, then the stress is zero, as might be expected.

- 6.6. $|r| = (\cos^2 \theta + \sin^2 \theta)^3 = 1.0$.
- 6.8. As in the solution to Exercise 6.5, the longitudinal stresses within any bar are constant, and the FBD of the rigid cap provides exactly the same equation as in that exercise. The strain–stress equations are both of the form $\epsilon = \sigma/E$. The tricky part is the strain–displacement equation. The outer bars have to stretch a distance ($L\epsilon_1$), while the middle bar has to be compressed a distance ($-L\epsilon_2$), and these two distances add to δ . Substituting the strain–stress equations into the strain–displacement equation, and simultaneously with the equilibrium equation yields, for example,

$$\sigma_1 = \frac{E_1 E_2 A_2 (\delta/L)}{2E_1 A_1 + E_2 A_2}$$

- 6.9. On the basis of the theory that all directions have the same material constants, and on the basis of actual computation, $[E^*] = [E]$.
- 6.10. These equations are the correct plane strain equations.
- 6.11. The strain compatibility equations are $\{\epsilon^*\} = \{\epsilon^{(1)*}\} = \dots = \{\epsilon^{(2N)*}\}$. The stress–strain equations for each ply in the laminate axes are $\{\sigma^{(P)*}\} = [E^{(P)*}]\{\epsilon^*\}$ where

the above compatibility equations were used to replace the strains in the individual plies in the laminate coordinate system. Substitution of these last equations into the given equilibrium equation permits the solution for the strains $\{\epsilon^*\}$. The use of the rotation and stress-strain equations in either order leads to the solution for the stresses in each ply.

- 7.1. (b) Since the total moment acting upon the disk is $M = bT_{\theta t}(2\pi b)$, then $\sigma_{r\theta} = M/(2\pi tr^2)$:
- (c) Yes, equilibrium requires that the moment at the inner edge be equal to the moment at the outer edge. Since the moment arm for the traction at the inner edge, a , is smaller than the moment arm at the outer edge, b , the traction at the inner edge must be larger than that at the outer edge by the factor $(b/a)^2$.
- (e) The displacement solutions would be the same except now there would be additional terms that represent rigid body motion.
- 7.2. (a) For the same reasons as in Example 7.4, that is, because (i) all partial derivatives with respect to θ and ϕ are zero due to the symmetry of the structure and loading; (ii) the partial derivatives with respect to r are then total derivatives; (iii) the stress $\sigma_{\theta\theta} = \sigma_{\phi\phi}$ due to the same symmetry; and (iv) the body force per unit volume is negligible in comparison to the internal pressure; the equilibrium equation for the r direction is again: $r\sigma'_{rr} + 2(\sigma_{rr} - \sigma_{\theta\theta}) = 0$
- (b) B, C.
- (c) A, D.
- (d) $\sigma_{rr}(b) = 0$ and $\sigma_{rr}(a) = -p_0$.
- (e) The above stress BCs can be rewritten in terms of the displacement function $u(r)$ and its derivatives by substituting for the stresses by use of the spherical stress-strain equations, and then substituting for the strains by use of the spherical strain-displacement equations.
- (f) Since the spherical coordinate system is an orthogonal coordinate system, the isotropic strain-stress equations are

$$E\epsilon_{rr} = \sigma_{rr} - \nu\sigma_{\theta\theta} - \nu\sigma_{\phi\phi} + E\alpha \Delta T \quad G\gamma_{r\theta} = \sigma_{r\theta} \quad \text{etc.}$$

- 7.3. (a, b) The radial and hoop stresses are both zero.
- (c) There would be no difference between the two solutions because the differential equations of this problem are all linear differential equations. Thus the problem is "linear" and superposition of solutions is possible. Superimposing a zero solution on a second solution does not alter the second solution.
- 7.4. (a) $\sigma_{rr} = p_i[a^2/(b^2 - a^2)][1 - (b/r)^2]$.
 $\sigma_{\theta\theta} = p_i[a^2/(b^2 - a^2)][1 + (b/r)^2]$.
- (b) Yes.
- (c) Both the hoop and radial stress take on their maximum values at the inner radius, that is, at $r = a$.
- (d) $\sigma_{rr} = -[p_0b^2/(b^2 - a^2)][1 - (a/r)^2]$.
- (e) Yes. An intermediate check point is the following solution for the constants of integration:

$$A = \frac{(p_0 - p_i)a^2b^2}{b^2 - a^2} \quad \text{and} \quad B = -\frac{p_0b^2 - p_ia^2}{b^2 - a^2}$$

Note that p_i and p_0 are magnitudes of (traction) vectors, and therefore are positive quantities. With these constants of integration, the radial stresses at both circular boundaries are compressive.

- 7.5. (a) $u(r) = \alpha T_0 r$.
 (b) The inner radius increases when the constant temperature change is an increase in temperature.
- 7.6. (a) If Σ_{rr} and $U(r)$ represent the radial stress and displacement in the outer tube, respectively, while the usual lower-case notation applies for the inner tube, then the necessary four boundary conditions are

$$\begin{aligned} (1) \sigma_{rr}(r = 5'') &= 0 & (2) \Sigma_{rr}(r = 7'') &= 0 \\ (3) \sigma_{rr}(r = 6'') &= \Sigma_{rr}(r = 6'') & (4) u(r = 6'') &= U(r = 6'') \end{aligned}$$

The third and fourth BC above would be far more accurate descriptions of the conditions at the interface between the two cylinders when well-manufactured than would the measured displacement. Therefore, the information on the shrinkage of the outer radius of the inner tube is unnecessary information.

- (e) The differential equation for the radial displacement of either tube is Eq. (7.14) but with the temperature change and the angular velocity set to zero.
- 7.8. (b)

$$C_1 = \frac{1-\nu}{R^2} \left[\int_{r=R} r \alpha \Delta T(r) dr \right] + (3+\nu)(1-\nu) \frac{\rho \Omega^2 R^2}{8E}$$

- (e) Yes, the same result is obtained by this more general approach.
- 8.2. (a) Differentiating the displacements to obtain the strains leads to $\epsilon_{xx} = (u_0/a)$, $\epsilon_{yy} = (v_0/b)$, and $\gamma_{xy} = 0$. Using the plane stress stress-strain equations leads to $\sigma_{xy} = 0$, and

$$\begin{aligned} \sigma_{xx}(x, y) &= \frac{E}{1-\nu^2} \left(\frac{u_0}{a} + \nu \frac{v_0}{b} \right) - \frac{E\alpha T_0}{1-\nu} \\ \sigma_{yy}(x, y) &= \frac{E}{1-\nu^2} \left(\frac{v_0}{a} + \nu \frac{u_0}{a} \right) - \frac{E\alpha T_0}{1-\nu} \end{aligned}$$

which are also constant values throughout the sheet. Use of the Cauchy equations shows that the edge tractions that have stretched the sheet have the constant values $T_x(a, y) = \sigma_{xx}$, and $T_y(x, b) = \sigma_{yy}$. It is also true, of course, that $T_y(a, y) = T_x(x, b) = 0$.

- (b) No. To make the tractions zero means making the above stress expressions equal to zero simultaneously. The only way that there can be a single solution for αT_0 is for $u_0/a = v_0/b$. When there is such an equality, then $\alpha T_0 = u_0/a$.
- 8.3. The equilibrium equations and Eq. (8.2) are satisfied identically. Therefore, all interior requirements are met. The traction boundary conditions at the top and bottom surface are also identically satisfied. At the end $x = a$, the x direction tractions must be and are zero, and the y direction tractions must sum to $+F$. The latter condition produces the result $c = +3$.
- 8.4. (a) The equilibrium equations, Eqs. (1.6), and the compatibility equation in terms of stresses, Eq. (8.2), are satisfied identically. Thus the candidate plane stress solution is a theory of elasticity solution within any interior.
- (b) $T_x = T_y = (\sigma_0/a)(2\sqrt{2}y - a) = (\sigma_0/a)(a - 2\sqrt{2}x)$.
- (d) $T_z = 0$, $T_n = \sqrt{2}T_x = (\sigma_0/a)(4y - \sqrt{2}a) = (\sigma_0/a)(\sqrt{2}a - 4x)$.
- (f) Since, for example, $s = \sqrt{2}y$, $T_n = \sqrt{2}(\sigma_0/a)(2s - a)$.
- (g) Setting the given expression for the stresses equal to zero shows that the line of zero stress is the line $y = x$.

- 8.5. (a)** The direction cosines for the outer normal at the boundary surface $y = +b$ are $c_{nx} = 0$, and $c_{ny} = +1$. The Cauchy equations lead to $\sigma_{xy}(x, b) = 0$, and $\sigma_{yy}(x, b) = 0$, and $\sigma_{yy}(x, b) = -p_0$. The use of the strain–stress equations yields $\gamma_{xy}(x, b) = 0$, and $-(1 - \nu^2)(p_0/E) = \epsilon_{yy} + \nu\epsilon_{xx}$. The use of the strain–displacement equations produces the displacement BCs

$$\frac{\partial u(x, b)}{\partial y} + \frac{\partial v(x, b)}{\partial x} = 0$$

and

$$\frac{\partial v(x, b)}{\partial y} + \nu \frac{\partial u(x, b)}{\partial x} = -(1 - \nu^2) \frac{p_0}{E}$$

Note that it is essential that all the stresses, strains and displacements in the above switch from a pair of stress-type BCs to a pair of displacement-type BCs be identified as being at the boundary $y = +b$. The above equations would not be correct otherwise.

- (b)** The stress BCs are $\sigma_{xx}(-a, 0) = -p_0$, $\sigma_{xy}(-a, 0) = 0$. Use of two corresponding plane stress–strain equations and the strain–displacement equations leads immediately to

$$u_{,x}(-a, y) + v_{,y}(-a, y) = -(1 - \nu^2) \frac{p_0}{E}$$

and

$$u_{,y}(-a, y) + v_{,x}(-a, y) = 0$$

- 8.6. (a, b)** The given stresses satisfy the equilibrium, constitutive, and primary compatibility equations. The equilibrium equations reduce to

$$\sigma_{r\theta,\theta} + \sigma_{rr} - \sigma_{\theta\theta} = 0 \quad \text{and} \quad \sigma_{\theta\theta,\theta} + 2\sigma_{r\theta} = 0$$

The compatibility equation in terms of stresses referenced to polar coordinates is determined by recalling (i) that, at any point, the sum of the normal stresses in one orthogonal coordinate system is equal to the sum of the normal stresses in a rotated coordinate system; that is, $\sigma_{xx} + \sigma_{yy} = \sigma_{rr} + \sigma_{\theta\theta}$, and (ii) that ∇^2 in polar coordinates, with the two derivatives with respect to r being zero, reduces to merely the second partial derivative with respect to θ .

- (c)** At $\theta = 0$, $-T_\theta(0) \equiv T_n(0) = +\sigma_{\theta\theta}(0) = 2\sigma_0[\alpha - \tan \alpha]$ = a negative constant since $\tan \alpha > \alpha$, and

$$-T_r(0) \equiv T_s(0) = +\sigma_{r\theta}(0) = 0$$

- (d)** At $\theta = \alpha$,

$$T_\theta(\alpha) \equiv T_n(\alpha) = +\sigma_{\theta\theta}(\alpha) = 0$$

$$T_r(\alpha) \equiv T_s(\alpha) = +\sigma_{r\theta}(\alpha) = 0$$

- (e)** Therefore, the only traction acting upon the wedge is a constant upward normal traction along the bottom surface of the wedge.

- 8.7. (a)** The given stresses do satisfy the equilibrium equations, and do require tractions on the three outer boundaries that are similar to those of Fig. 1.12(b).
(b) The given stresses do satisfy the primary compatibility equation in terms of stresses, and thus they are a solution.
(c) An additional constant compressive σ_{yy} stress of suitable magnitude would provide a rationale for the “frictional” tractions on the top and bottom surfaces;

the length of the body in the x direction could be made finite while the very slight T_x at the far end could be offset, on average, by a constant σ_{xx} ; and so on.

- 8.9. (a) Normal tensile tractions on edges $x = \pm a$ of magnitude $2C$ only. This is a case of uniform tension, or from a beam viewpoint, a constant axial force.
 (b) Linearly varying tractions on edges $x = \pm a$ that are tensile above the x axis and compressive below. The equal maximum traction magnitudes are $6C$.
 (c) $\sigma_{xx} = 2C$, and all other stresses are zero. Thus $T_x = \sigma_{xx} \cos(n, x)$. Thus if the usual counterclockwise polar coordinate θ , which is zero along the x axis, is used, $T_x = 2C \cos \theta$. Thus the circular disk is loaded by tensile tractions in the x directions that are maximum at the disk equator and are zero at the poles.
 (d) The only tractions are shearing tractions on all four edges of magnitude C .
- 8.11. (a) $v(a, 0) = (F/2Et)(a/b)^3 + (3/4)(F/Gt)(a/b)$
 (b) Effective area equals $(4/3)bt$, and therefore $k = 2/3$.
 (c) Ratio = $(4/3)[1/(1 + \nu)](a/2b)^2$.
- 9.1. (a) $y_0^* = 1.375a$, $z_0^* = 0.958a + 1.208t$.
 (b) $y_0^* = -0.223t$, $z_0^* = 9.64t$.
- 9.2. (a) $y_0^* = 0$, $z_0^* = 1.825a$; $I_{y_0z_0}^* = a^3t = a^4/10$, $I_{yz}^* = a^4/10$.
 (b) $y_0^* = 1.89t$, $z_0^* = 4.21t$, $I_{y_0y_0}^* = 1423t^4$, $I_{y_0z_0}^* = 0$, $I_{yy}^* = 884t^4$ and $I_{yz}^* = -242t^4$.
 (c) $y_0^* = 2.92t$, $I_{y_0y_0}^* = 1903t^4$, $I_{yy}^* = 275t^4$, $I_{y_0z_0}^* = 665.6t^4$, and $I_{yz}^* = 128t^4$.
- 9.3. (a) $y_0^* = 3b/8$, $z_0^* = -(1/2)(b + t)$; $I_{y_0y_0}^* = (2/3)bt(8b^2 + 6bt + 5t^2)$,
 $I_{yy}^* = (2/3)bt(5b^2 + 2t^2)$; $I_{y_0z_0}^* = -bt^2(b + t)$, $I_{yz}^* = (bt/2)(3b^2 + bt - 2t^2)$.
 (b) $I_{zz}^* = 376t^4$, $I_{yz}^* = -45t^4$.
 (c) $A^* = 25.2t$, $y_0^* = 5.71t$, $z_0^* = 5.62t$, $I_{zz}^* = 178t^4$, and $I_{yz}^* = 16.9t^4$.
- 9.4. (a) With the y_0 axis originating at the center of the corner, $y_0^* = z_0^* = 1.0$ in; ($I_{y_0y_0} = 4.27$ in⁴), $I_{yy} = I_{zz} = 2.67$ in⁴; $I_{yz} = -1.60$ in⁴.
 (b) The centroid is located $7t/3$ down from the inner (horizontal) edge, and $t/3$ to the left of inner (vertical) edge. (The rest is up to you.)
 (c) The centroid is 1.111 in from bottom; $I_{y_0y_0} = 0.27573$ in⁴ about horizontal axis at bottom; $I_{yy} = 0.0389 \rightarrow 0.039$ in⁴. $I_{yz} = 0$ by symmetry. Thus the y , z axes are principal axes.
 (d) $I_{YY} = 4.27$ in⁴, $I_{ZZ} = 1.07$ in⁴.
- 9.5. $y_0^* = 0.519a$, and $z_0^* = 1.074a$.
- 9.6. (a) From double integration: $I_{y_0y_0} = ab^3/12$, $I_{y_0z_0} = a^2b^2/8$; $I_{yy} = ab^3/36$,
 $I_{yz} = a^2b^2/72$.
 (b) $I_{yy} = 19.26$ cm⁴, $I_{zz} = 3.24$ cm⁴.
- 9.7. I_{yz}^* = zero due to symmetry, and $I_{zz}^* = 2965t^4 \rightarrow 2900t^4$, where the answer is rounded down to be on the safe side.
- 9.8. (a) $I_{y_0y_0}^* = 88\,800$ mm⁴, $I_{y_0z_0}^* = 51\,100$ mm⁴, $I_{yy}^* = 4550$ mm⁴, $I_{yz}^* = (51\,100$ mm⁴) - (12.8 mm)(22.95 mm)(160 mm²) = 4070 mm⁴. A direct calculation of the area product of inertia, where the units have been omitted from the parentheses, is

$$I_{yz}^* = (2.1/0.7)[(2.05)(3.2)(40)] + (1.0)[(1.05)(-4.8)(16)] \\ + (1.0)[(-12.8)(-10.95)(24)] = 4070 \text{ mm}^4 = 0.407 \text{ cm}^4$$

- (b) $y_0^* = 51t/24$; $z_0^* = 213t/24$; $I_{y_0y_0}^* = 3068t^4$, $I_{yy}^* = 1178t^4$ before rounding off; $I_{y_0z_0}^* = 702t^4$, $I_{yz}^* = 249t^4$ before rounding off. I_{zz}^* is left to the reader.

- (c) $M_{yT} = 86t^3 E_\alpha T_0$
 (d) $N_T = 5E_0\alpha T_0 at$,
 $M_{yT} = 1.59E_0\alpha T_0 a^2 t$,
 $M_{zT} = 0.873E_0\alpha T_0 a^2 t$.
 (e) $N_T = 26.4E_0\alpha T_0 t^2$,
 $M_{zT} = 48.3E_0\alpha T_0 t^3$.
 (f) $N_T = 26.4E_0\alpha T_0 t^2$,
 $M_{zT} = 48.3E_0\alpha T_0 t^3$.

9.9. (a) $M_{yT} = 35.6 \text{ N m}$.

(b) $M_{yT} = -76E_0\alpha_0 T_0 t^3$.

9.10. Since $z = z_0 - z_0^*$, then

$$\begin{aligned} M_{yT} &= - \iint_A z E \alpha \Delta T dA = - \iint_A z_0 E \alpha \Delta T dA + z_0^* \iint_A E \alpha \Delta T dA \\ &= M_{y_0T} + Z_0^* N_T \end{aligned}$$

9.11. $M_{yT} = -96E\alpha T_0 t^3$.

9.12. (a) $z_0^* = (3a + t)/4$; $N_T = 3at E_\alpha T_0$, $M_{yT} = -\frac{1}{4} E\alpha T_0 (a^2 t + at^2)$, and $M_{zT} = 0$ by symmetry.

(b) $M_{yT} = -158E_0\alpha T_0 t^3$.

9.14. (d) The equation for the neutral axis is $z = -1.387y$. Hence point T is the point of maximum tensile stress with a stress magnitude of $(0.0279 \text{ in}^{-3})M_0$.

9.15. At the bottom of the web ($z = -6.25t$), $\sigma_{xx} = +0.35E\alpha T_0$.

9.17. $N_T = AE\alpha T_1$, $M_{yT} = -EI_{yy}\alpha T_3$, and $M_{zT} = -EI_{zz}\alpha T_2$. (The same result applies to an arbitrary nonsymmetric, homogeneous cross-section; and the same result applies to a symmetric, nonhomogeneous cross-section).

9.18. Draw a FBD of a slice of beam of length dx . The first time through, let the geometry of the beam cross-section be the same at both ends of the beam slice. At one end, say the front end, draw the stress vectors acting at point P as in Fig. 9.1(a), but this time point P on the front face is really just a projection of the actual point P on the back face, which is at the coordinate value x . On this front face the differential increments in the values of the stresses can be attached to the stress values, but these differential increments will always remain with the finite stress values, and thus in the end they can be dropped as infinitesimals. Place the *stress resultants* on the beam slice back face as shown in Fig. 9.1(a). Now sum forces and sum moments about each of the coordinate axes to obtain Eqs. (9.1) as before.

10.2. (a) $N(x) = EA(x)u'(x) - N_T(x)$. The GDE and BCs are $(d/dx)[EA(x)u'(x)] = -f_0 + N_T'(x)$ and $u(0) = N(L) = 0$. Integrating the GDE: $EA(x)u'(x) = -f_0x + N_T(x) + C_1$. Applying the second BC: $N_T(L) = -f_0L + N_T(L) + C_1$. Hence $C_1 = f_0L$. Therefore $N(x) = f_0(L - X) = f_0(L - x)$, as it should be.

(b) Since the solution for part (a) did not depend upon the particular form of either $A(x)$ or $N_T(x)$, the solution here is the same as there.

(c) The GDE is $Eu''(x) = -x\rho\Omega^2$. The BCs are $u(0) = u'(L) = 0$. Integrating the GDE $u'(x) = C_1 - x^2\rho\Omega^2/(2E)$, where $C_1 = \rho\Omega^2L^2/(2E)$. Integrating again $u(x) = \rho\Omega^2L^2x/(2E) - \rho\Omega^2x^3/(6E) + C_2$ where $C_2 = 0$. Therefore $u(L) = \rho\Omega^2L^3/(3E)$.

- 10.3. (a)** Firstly $u(x) = v(x) = 0$. In this case the BC at the free end are $w''(L) = w'''(L) = 0$. Hence,

$$w(x) = \frac{f_0[(L-x)^5 + 5L^4x - L^5]}{120EI_{yy}L}$$

- (b)** Since the bending moment in this problem can be calculated easily in terms of the given loading, this problem is better solved using the second order differential equation, Eq. (9.7b). However, there is very little extra effort involved in using the fourth order differential equation instead. That equation reduces to $EI_{yy}w''''(x) = 0$ with BC $w(0) = w'(0) = 0$, $EI_{yy}w'''(L) = -F_0$, and finally $EI_{yy}w''(L) = +M_0$. The solution for the deflection function is

$$EI_{yy}w(x) = \frac{1}{2}(M_0 + F_0L)x^2 - \frac{1}{6}F_0x^3$$

Note that, since the first expression involving F_0 is larger than the second, both M_0 and F_0 make a positive contribution to the deflection. It should be clear from your sketch that this effect on the deflections is as it should be.

- 10.4. (a), (b)** $N'_T(x) = -f_0$. Therefore the GDE is $E Au''(x) = -f_0 - f_0 = -2f_0$. The BCs are $u(0) = 0$; and $N(L) = -\frac{1}{2}f_0L = EAu'(L) - N_T(L)$. Thus the second BC is $u'(L) = f_0L/(2EA)$.

(c) $E Au(x) = x f_0 (\frac{5}{2}L - x)$.

- 10.5.** Since there is no temperature change, the GDE is $E Au''(x) = +\rho g A$. The first BC is $u(0) = 0$. The second BC is $E Au'(L) = -Mg$. After integrating and applying the BC, $E Au(x) = \frac{1}{2}\rho g Ax^2 - (Mg + \rho g AL)x$. The axial stress is $\sigma_{xx} = EAu'(x) = N/A = -\rho g(L-x) - Mg/A$.

- 10.6.** This is mostly a matter of substituting the given data and writing expressions for the distributed loads as shown on the diagram. From the diagram

$$f_y(x) = -3f_0 \left[1 - \frac{x}{L}\right] \quad f_z(x) = -2f_0 \frac{x}{L}$$

where the initial negative signs are due to the distributed loading acting in the negative coordinate directions. The equivalent thermal distributed loading is obtained from twice differentiating the thermal moments according to the given formulas.

$$f_{yT} = M''_{zT} = -\frac{f_0}{15} \quad f_{zT} = M''_{yT} = -\frac{f_0}{10}$$

Therefore the two governing differential equations for the bending of this beam are

$$3EI_0v''''(x) - EI_0w''''(x) = -3f_0 \left(1 - \frac{x}{L}\right) - \frac{f_0}{15} = -3f_0 \left(\frac{46}{45} - \frac{x}{L}\right)$$

$$-EI_0v''''(x) - 2EI_0w''''(x) = -2f_0 \frac{x}{L} - \frac{f_0}{10}$$

Note that it is always best to combine terms as is done in the first of the two above equations on the right-hand side. In this case there would be one less step for each of the four integrations necessary to solve these equations.

- 10.7.** The GDEs are $ER_{zz}w'''' = -ER_{yz}v'''' = f_0[1 - (x/L)^2]$. The second of these equations is obtained after cancelling I_{yy} , and dividing by I_{yz} . The BCs are $w(0) = w'(0) = v(0) = v'(0) = 0$, $w(L) = +d_0$, and $v(L) = v''(L) = w''(L) = 0$. Since the two GDEs and BCs are wholly decoupled and similar, it is only necessary for the sake of confirmation to integrate the w -deflection equation. The first and

second constants of integration, as numbered in the usual order, are

$$C_1 = -\frac{61f_0L}{120} - \frac{3ER_{zz}d_0}{L^3}$$

$$C_2 = +\frac{11f_0L^2}{120} + \frac{3ER_{zz}d_0}{L^2}$$

with the result

$$w'(L) = \frac{3d_0}{2L} - \frac{f_0L^3}{80ER_{zz}}$$

Note that the enforced upward deflection at the right-hand support should produce a positive bending slope, while the distributed loading should produce a negative bending slope, and the signs in the above answer reflect these two facts.

- 10.8.** $N(x) = u(x) = 0$, and $v(x) = -(I_{yz}/I_{zz})w(x)$. Define $\xi = x/L$. Then

$$120w(\xi) = \frac{f_0L^4}{ER_{zz}}(\xi^5 - 5\xi^4 + 8\xi^3 - 4\xi^2) - \frac{30M_0L^2}{ER_{zz}}(\xi^3 - \xi^2)$$

- 10.9.** The GDE is $EI_{zz}v''''(x) = pt$, where $I_{zz} = 2b^3t/3$. The BCs are $v(-a) = v(+a) = v''(-a) = v''(+a) = 0$. After integrating, and using the BCs to determine the constants of integration, the deflection solution, where $\xi = x/a$, is

$$v(x) = (pt a^4)[\xi^4 - 6\xi^2 + 5]/(24 EI_{zz})$$

which is, as it should be, an even function in the beam length coordinate. At the beam center, where $x = \xi = 0$, this strength of materials solution is $v(0) = (5 pa^4)/(16Eb^3)$. The corresponding theory of elasticity solution is Eq. (8.5). The above strength of materials solution has only one part, which is identical to the first portion of the theory of elasticity solution. This first part represents the beam deflection due to bending deformation. The second portion of the theory of elasticity solution, which includes a Poisson's ratio and the factor (b/a) squared, is due to the beam undergoing shearing deformation. Shearing deformations are prohibited in the Bernoulli–Euler postulates. In short beams, this second term can have significance. In long beams, $a > 10b$, this shearing deflection portion is only a few percent of the total solution. This is why Bernoulli–Euler beam theory is limited to long beams.

If the problem is pursued to the point of obtaining the strength of materials axial stress solution, the result is

$$\sigma_{xx} = -(M_z/I_{zz})y = -yEv''(x) = (3/4)p(a/b)^2 [1 - (x/a)^2] (y/b)$$

The corresponding theory of elasticity stress solution is shown in Eq. (8.1). The same conclusions can be drawn with regard to the strength of materials stress solution and the theory of elasticity stress solution.

- 10.10.** $N_T = E\alpha T_1 Ax$, and $M_{yT} = 10M_{zT} = -E\alpha T_2 I$. Other intermediate steps are $w''''(x) = v''''(x) = 0$, $w'''(L) = v'''(L) = 0$, $v''(L) = 0$ and $w''(L) = -\alpha T_2$. Then $u(L) = \alpha T_1 L^2/2$, $v(L) = 0$, and $w(L) = -\alpha T_2 L^2/2$.
- 10.11. (a)** $21.6EIw(x) = -21.6EIV(x) = f_0x^2(L-x)^2$. $M_z(x) = 0$, and $12M_y(x) = f_0L^2[6(x/L)^2 - 6(x/L) + 1]$, in which it is only necessary to substitute $x = L/2$ and $x = 0$ or L to obtain the desired results.
- 10.14.** The result of including the bending–twisting interaction terms is to add to the left-hand sides of Eqs. (10.5a) and (10.5b), respectively, the quantities $[(M_z\phi)' - (M_yv'')]$ and $[(M_yw'') - (M_z\phi)']$.

10.15. Define the nondimensional factors $\beta^4 = kL^4/4EI_{yy}$ and $\xi = x/L$. Then define the temporary functional symbols $F(x) = \cos(x) \sinh(x)$, $G(x) = \sin(x) \cosh(x)$, and $H(x) = \cos(x) \cosh(x)$. Then from $w(x) = C_1 \sinh \beta x \cos \beta x + C_2 \cosh \beta x \cos \beta x + C_3 \cosh \beta x \sin \beta x + C_4 \sinh \beta x \sin \beta x - f_0/k$,

$$\text{get: } w(\xi) = \frac{f_0}{k} \{ [1 - H(\beta\xi)] + (\cosh \beta - \cos \beta) \Omega(\xi) \}$$

where

$$\Omega(\xi) = \frac{\sinh(\beta) F(\beta\xi) - \sin(\beta) G(\beta\xi)}{F^2(\beta) + G^2(\beta)}$$

10.17. To determine the deflections $u(x)$, that is to carry out the integration, it would be necessary to isolate $u'(x)$ by dividing through by the $EA(x)$ term as follows:

$$EA_0 u'(x) = f_0 L \left(\frac{1 - \frac{x}{L}}{4 - 3\frac{x}{L}} \right) - N_0 \left(\frac{2 - \frac{x^2}{L^2}}{4 - 3\frac{x}{L}} \right)$$

Switching to the nondimensional variable $\xi = x/L$, then $du/dx = (1/L)(du/d\xi)$, then

$$\frac{EA_0}{L} \frac{du(\xi)}{d\xi} = f_0 L \left(\frac{1 - \xi}{4 - 3\xi} \right) - N_0 \left(\frac{2 - \xi^2}{4 - 3\xi} \right)$$

In order to integrate the above equation to obtain $u(\xi)$, it is necessary to evaluate the integrals

$$I_1 = \int \frac{1 d\xi}{4 - 3\xi} \quad I_2 = \int \frac{\xi d\xi}{4 - 3\xi} \quad I_3 = \int \frac{\xi^2 d\xi}{4 - 3\xi}$$

The first integral can be done without using a computer or table of integrals

$$I_1 = \int \frac{1 d\xi}{4 - 3\xi} = -\frac{1}{3} \int \frac{d(4 - 3\xi)}{4 - 3\xi} = -\frac{1}{3} \ln(4 - 3\xi)$$

The second integral requires a wee bit of cleverness

$$\int \frac{4 - 3\xi}{4 - 3\xi} d\xi = \int d\xi = \xi = + \int \frac{4 d\xi}{4 - 3\xi} - \int \frac{3\xi d\xi}{4 - 3\xi} \rightarrow \xi = 4I_1 - 3I_2$$

from which the value of I_2 can be determined. Proceeding in a similar manner,

$$\int \frac{(4 - 3\xi)^2}{4 - 3\xi} d\xi = \int (4 - 3\xi) d\xi = 4\xi - \frac{3}{2}\xi^2 = 16I_1 - 24I_2 + 9I_3$$

from which the value of the third integral can be obtained. The rest is simple algebra. The result is that for the tapered beam, the axial deflections are described not only by polynomials, but involve logarithmic terms as well. Note that the arguments of the natural logarithms are always positive, so it is not necessary to include the absolute value symbol.

- 11.1.** (a) This integral becomes $\int_0^x d[\delta(x - a)] = \delta(x - a) - \delta(0 - a) = \delta(x - a)$.
 (b) One approach is to add and subtract the quantity $b\delta(x - b)$ so as to be able to write this term as $(x - b) \delta(x - b) + b\delta(x - b)$. The first of these two terms is the product of two quantities, the first of which is very small in the very near vicinity of $x = b$, while the second is very large in that vicinity. Their product and definite integral should be treated as a zero because of the reasoning to follow. The second of these terms when integrated is simply $b \text{stp}(x - b)$.

A better way to approach this integral is to integrate by parts between the limits of zero and x . Let “ u ” equal x , and “ dv ” equal $\delta(x - b) dx$. Then $\int_0^x x \delta(x - b) dx = x \operatorname{stp}(x - b)|_0^x - \int_0^x \operatorname{stp}(x - b) dx$. Applying the limits yields $x \operatorname{stp}(x - b) - (x - b) \operatorname{stp}(x - b) = +b \operatorname{stp}(x - b)$. As an aside, the more general definition of the Dirac delta function would have provided this answer immediately.

- (c) Rewrite as $[x - b + b - a] \operatorname{stp}(x - b) = (x - b) \operatorname{stp}(x - b) + (b - a) \operatorname{stp}(x - b)$. Then, since $(b - a)$ is a constant, the integration is straight forward. The answer is, of course, $1/2(x - b)^2 \operatorname{stp}(x - b) + (b - a)(x - b) \operatorname{stp}(x - b)$.
- (d) Rewrite as $[x - b + b - b]^2 \operatorname{stp}(x - b) = [(x - b)^2 + 2(b - a)(x - b) + (b - a)^2] \operatorname{stp}(x - b)$. From this point, the integration is again straight forward.
- (e) The integration proceeds almost effortlessly if the term to be integrated is in a form where the step $(x - x_0)$ polynomial factor involving the coordinate x has the form $(x - x_0)^n$. Thus rewrite the right-hand side as $(2f_0/L)(\frac{1}{2}L - x) \operatorname{stp}(x - \frac{1}{2}L) = -(2f_0/L)(x - \frac{1}{2}L) \operatorname{stp}(x - \frac{1}{2}L)$. Then the first integral between the limits zero and x of the right-hand side is simply

$$C_1 - \frac{f_0}{L} \left(x - \frac{1}{2}L\right)^2 \operatorname{stp}\left(x - \frac{1}{2}L\right)$$

- (g) The first integral of the right-hand side is

$$C_1 + M_0 \delta(x - a) + m_0 \operatorname{stp}(x - b) + f_0(x - c) \operatorname{stp}(x - c)$$

- 11.2.** (a) $f_y(x) - f_0 \sin(2\pi x/L)$ is continuous over the entire span; and $f_z(x) = f_0[1 - \operatorname{stp}(x - L/2)] - f_0 \operatorname{stp}(x - L/2) = f_0 - 2f_0 \operatorname{stp}(x - \frac{1}{2}L)$.
- (b) $m_z(x) = -M_0 \delta(x - L/3)$, $f_z(x) = (x/L)f_0 + f_0 \delta(x - 2L/3)$.
- (c) $m_z(x) = -m_0[1 - \operatorname{stp}(x - L/2)]$, $f_z(x) = 2(x/L)f_0 \operatorname{stp}(x - L/2)$. Note that in the GDE, $m'_z(x) = +m_0 \delta(x - L/2)$.

- 11.3.** (a)

$$E_0 I_{zz}^* v''''(x) = \frac{2f_0}{l} \left(x - \frac{l}{2}\right) \left[1 - \operatorname{stp}\left(x - \frac{l}{2}\right)\right] + F_0 \delta\left(x - \frac{l}{2}\right) - \frac{2f_0}{l} \left(x - \frac{l}{2}\right) \operatorname{stp}\left(x - \frac{l}{2}\right)$$

$$E_0 I_{yy}^* w''''(x) = +M_0 \delta'\left(x - \frac{l}{3}\right) - M_0 \delta'\left(x - \frac{2l}{3}\right)$$

- (b)

$$f_y(x) = -F_0 \delta\left(x - \frac{L}{2}\right), \quad f_z(x) = \frac{2f_0}{L} \left(x - \frac{L}{2}\right) \left[1 - \operatorname{stp}\left(x - \frac{L}{2}\right)\right] - \frac{2f_0}{L} \left(x - \frac{L}{2}\right) \operatorname{stp}\left(x - \frac{L}{2}\right)$$

The latter expression can be obtained as follows. First write the equations for the two straight lines associated with the loadings, and apply a negative sign to account for the fact that both loadings are opposite to the positive coordinate directions. From the standard straight line formula $y = mx + b$, these expressions are.

$$f_{z1} = -\left(-\frac{2f_0}{L}x + f_0\right) \quad f_{z2} = -\left(\frac{2f_0}{L}x - f_0\right)$$

Be sure to check the validity of these straight line formulas at two separate points. The rest is simply a matter of simplifying the expressions *at least* to the point of

$$f_{z1}(x) = f_0 \left(\frac{2x}{L} - 1 \right) \quad f_{z2} = f_0 \left(1 - \frac{2x}{L} \right)$$

and the combining these two expressions with the Heaviside step function filters to get the full expression as started.

As for the moments per unit length, the concentrated moment about the z axis is negative because the z axis is positive out of the paper.

$$(c) \quad m_y(x) = 0 \quad m_z(x) = -M_0 \delta \left(x - \frac{L}{2} \right)$$

$$f_y(x) = -2f_0 \left(1 - \frac{2x}{l} \right) \left[1 - \text{stp} \left(x - \frac{l}{2} \right) \right]$$

$$f_z(x) = -f_0 \left[\text{stp} \left(x - \frac{l}{4} \right) - \text{stp} \left(x - \frac{3l}{4} \right) \right] - \frac{f_0 l}{4} \delta \left(x - \frac{l}{4} \right)$$

$$(d) \quad m_y = +\frac{f_0 l^2}{8} \delta \left(x - \frac{3l}{4} \right) \quad m_z = -\frac{f_0 l^2}{12} \delta \left(x - \frac{l}{2} \right)$$

$$f_y(x) = -f_0 \left[\text{stp} \left(x - \frac{l}{3} \right) - \text{stp} \left(x - \frac{2l}{3} \right) \right] - \frac{1}{2} f_0 l^2 \delta \left(x - \frac{2l}{3} \right)$$

$$f_z(x) = -f_0 \left[1 - \text{stp} \left(x - \frac{2l}{3} \right) \right]$$

$$m_z(x) = -\frac{1}{7} f_0 l^2 \delta \left(x - \frac{l}{3} \right)$$

$$m_y(x) = +\frac{1}{8} f_0 l^2 \delta \left(x - \frac{l}{3} \right) - \frac{1}{9} f_0 l^2 \delta \left(x - \frac{2l}{3} \right)$$

(e) Since the y axis is into the paper, the moment per unit length is negative. Hence

$$f_z(x) + m'_y(x) = -f_0 \left[1 - \text{stp} \left(x - \frac{l}{3} \right) \right] - \left[-\frac{3f_0 x}{2l} + \frac{3f_0}{2} \right] \text{stp} \left(x - \frac{l}{3} \right) - M_0 \delta' \left(x - \frac{l}{3} \right)$$

In order to integrate easily, it is convenient to simplify the above in order to obtain

$$f_z(x) + m'_y(x) = -f_0 + f_0 \text{stp} \left(x - \frac{l}{3} \right)$$

$$+ \frac{3f_0}{2l} \left(x - l - \frac{l}{3} + \frac{l}{3} \right) \text{stp} \left(x - \frac{l}{3} \right) - M_0 \delta' \left(x - \frac{l}{3} \right)$$

or

$$f_z(x) + m'_y(x) = -f_0 + \frac{3f_0}{2l} \left(x - \frac{l}{3} \right) \text{stp} \left(x - \frac{l}{3} \right) - M_0 \delta' \left(x - \frac{l}{3} \right)$$

Integration can now proceed easily as follows

$$\text{1st integ.} = C_1 - F_0x + \frac{3f_0}{4l} \left(x - \frac{l}{3}\right)^2 \text{stp} \left(x - \frac{l}{3}\right) - M_0 \delta \left(x - \frac{l}{3}\right)$$

$$\begin{aligned} \text{2nd integ.} = C_1x + C_2 - \frac{F_0x^2}{2} + \frac{f_0}{4l} \left(x - \frac{l}{3}\right)^3 \text{stp} \left(x - \frac{l}{3}\right) \\ - M_0 \text{stp} \left(x - \frac{l}{3}\right) \end{aligned}$$

11.4. (a) $M_z(L) + K_1v'(L) = -M_1$, and $M_y(L) + K_2w'(L) = +M_2$ are the two preliminary force-type BCs that accompany $v(L) = w(L) = 0$.

(d) $V_y(0) = k_1v(0) = +F_1$, $M_z(0) = 0$, $V_z(0) + k_2w(0) = 0$, and $M_y(0) = +M_2$ are the preliminary equations.

11.5. (a) The preliminary BCs are

$$M_y(0) = 0 \quad V_z(0) + \frac{5EI_0}{L^3} w(0) = F_0$$

$$M_z(0) + \frac{EI_0}{L} v'(0) = -\frac{1}{8} F_0L \quad V_y(0) + \frac{3EI_0}{L^3} v(0) = 0$$

Since the product of inertia and the temperature change are zero, it is a simple matter substituting for the stress resultants. The results are

$$3EI_0w''(0) = 0 \quad 3EI_0w'''(0) + \frac{5EI_0}{L^3} w(0) = F_0$$

$$2EI_0v''(0) + \frac{EI_0}{L} v'(0) = -\frac{1}{8} F_0L \quad 2EI_0v'''(0) + \frac{3EI_0}{L^3} v(0) = 0$$

(b) Summing forces and moments from FBDs leads to the preliminary equations

$$V_y(L) - \frac{3EI_0}{L^3} v(L) = 0 \quad M_z(L) = -\frac{f_0L^2}{20}$$

$$V_z(L) = -\frac{f_0L}{10} \quad M_y(L) + \frac{EI_0}{L} w'(L) = 0$$

Substituting the supplied shear and moment equations into the above equations leads to (eventually) the following corresponding V_y , V_z , M_y , and M_z equations in that order

$$2EI_0v'''(L) - \frac{EI_0}{L} v''(L) - \frac{3EI_0}{L^3} v(L) + 2EI_0w'''(L) - \frac{EI_0}{L} w''(L) = -\frac{f_0L}{50}$$

$$2EI_0v'''(L) - \frac{EI_0}{L^3} v''(L) + 4EI_0w'''(L) - \frac{2EI_0}{L} w''(L) = -\frac{f_0L}{25} - \frac{f_0L}{10}$$

$$2EI_0v''(L) + 4EI_0w''(L) + \frac{EI_0}{L} w'(L) = \frac{f_0L^2}{25}$$

$$2EI_0v''(L) + 2EI_0w''(L) = \frac{f_0L^2}{50} - \frac{f_0L^2}{20}$$

(c) From free body diagrams translated, in the one case, and rotated in both cases, according to the adopted sign convention, the kinematic and equilibrium equations at the beam end are

$$v(L) = 0 \quad M_z(L) = \frac{1}{2} F_0L \quad M_y(L) + K w'(L) = 0$$

$$V_z(L) - k w(L) = F_0$$

The second, third, and fourth BC equations become, where $V_z = F_0$ (and $V_{yT} = -F_0$)

$$\begin{aligned} 3EI_0v''(L) - EI_0w''(L) &= \frac{1}{2}F_0L \\ -EI_0v''(L) + 2EI_0w''(L) + \frac{EI_0}{L}w'(L) &= 2F_0L \\ -EI_0v'''(L) + 2EI_0w'''(L) - \frac{5EI_0}{L^3}w(L) &= 2F_0 \end{aligned}$$

The above equations should be simplified as

$$\begin{aligned} 3v''(L) - w''(L) &= \frac{1}{2} \frac{F_0L}{EI_0} \\ -v''(L) + 2w''(L) + \frac{w'(L)}{L} &= 2 \frac{F_0L}{EI_0} \\ -v'''(L) + 2w'''(L) - \frac{5}{L^3}w(L) &= 2 \frac{F_0}{EI_0} \end{aligned}$$

These equations cannot be decoupled, which makes the solution for the constants of integration more lengthy than it would be otherwise.

- 11.6.** With the x axis originating at the left-hand end, $f_z(x) = -f_0 \text{stp}(x - L/2)$, and $f_y(x) = -F_0 \delta(x - L/2)$. Since the product of inertia is zero, the eight BCs reduce to $v(0) = v(L) = w(0) = w(L) = v''(0) = v''(L) = w''(0) = w''(L) = 0$.
- 11.9.** $6EI_{yy}w(x) = -F_0[(bx/L)(L^2 - b^2 - x^2) + (x - a)^3 \text{stp}(x - a)]$, and $v(x) = u(x) = 0$.
- 11.10.** $w(L) = -F_0L^3/(3ER_{zz})$, and $v(L) = +F_0L^3/(3ER_{yz})$.
- 11.11.** $R_{zz} = (5/3)I_0$, etc. $f_z(x) = F_1\delta(x - L) - f_0[1 - (x/L)] \text{stp}(x - L)$, $f_y(x) = m_y(x) = 0$, and $m_z(x) = -M_2 \delta(x - L)$. Therefore,
- (a) $5EI_0v''''(x) = 2M_2\delta'(x - L) - F_1\delta(x - L) - \frac{f_0}{L}(x - L) \text{stp}(x - L)$
 $5EI_0w''''(x) = -M_2\delta'(x - L) + 3F_1\delta(x - L) + \frac{3f_0}{L}(x - L) \text{stp}(x - L)$
- (b) BCs: $w(0) = d_0$, $w(2L) = w'(2L) = v(2L) = 0$, $w''(0) = \gamma/L$, $v''(0) = (\beta - 2\gamma)/L$, $\alpha v'(2L) + 3Lv''(2L) + Lw''(2L) = \beta$, and $4\alpha v(0) + 3L^3v'''(0) + L^3w'''(0) + \beta L = 0$.
- (c) $5EI_0v(x) = C_4 + C_3x + \frac{C_2x^2}{2} + \frac{C_1x^3}{6} + M_2(x - L)^2 \text{stp}(x - L)$
 $-\frac{F_1}{6}(x - L)^3 \text{stp}(x - L) - \frac{f_0}{120L}(x - L)^5 \text{stp}(x - L)$
- 11.12.** (b) $v(0) = v(L) = w(0) = w(L) = 0$, $w'(L) = -r_0$. The three force-type BCs $m_z(0) = M_y(0) = M_z(L) + kv'(L) = 0$ reduce to

$$w''(0) = \frac{10}{7} \frac{\beta}{L} \quad v''(0) = \frac{19}{7} \frac{\beta}{L}$$

and

$$2Lv''(L) - Lw''(L) + \alpha v'(L) = \beta$$

- 11.13.** (a) Since the axial force is not zero, it is necessary to use the coupled form of the beam bending GDE's. With the second derivatives of the thermal moments

about the y and z axes are zero and $2f_0$, respectively, and $m_z(x) = 0$, the GDE's, before simplification, are

$$\begin{aligned} 3EI_0v''''(x) + EI_0w''''(x) - f_0Lv''(x) &= -2f_0 \operatorname{stp}\left(x - \frac{1}{2}L\right) + 2f_0 \\ &\quad - f_0L\delta\left(x - \frac{1}{4}L\right) \\ 2EI_0w''''(x) + EI_0v''''(x) - f_0Lw''(x) \\ &= -3f_0\left(1 - \frac{2x}{L}\right)\left[1 - \operatorname{stp}\left(x - \frac{1}{2}L\right)\right] - f_0L^2\delta'\left(x - \frac{1}{2}L\right) \end{aligned}$$

(b) The eight BCs are

$$\begin{aligned} w(L) &= v(L) = 0 \\ 3L^3v''''(0) + L^3w''''(0) + 3v(0) &= -\frac{4f_0L^4}{EI_0} \\ 3L^2v''(0) + L^2w''(0) - 2Lv'(0) &= +\frac{4f_0L^4}{EI_0} \\ L^3v''''(0) + 2L^3w''''(0) + 6w(0) &= +\frac{f_0L^4}{EI_0} \\ L^2v''(0) + 2L^2w''(0) &= +\frac{f_0L^4}{EI_0} \end{aligned}$$

where the thermal moments were evaluated at $x = 0$, and the thermal shearing forces at the left-hand end are $V_{yT}(0) = -4f_0L$, and $V_{zT}(0) = f_0L$. The above two moment equations can be written in a better form using the second BC table. However, that is not so for the two shearing force equations. The two force-type BCs at the right-hand end are

$$L^2w''(L) = +\frac{8f_0L^4}{5EI_0} \quad L^2v''(L) = -\frac{1f_0L^4}{5EI_0}$$

where

$$M_{yT}(L) = 2f_0L^2 \quad \text{and} \quad M_{zT}(L) = f_0L^2$$

11.14. (a) The critical buckling force for the clamped-clamped beam-column is four times that for the simply supported beam-column. The critical buckling shape is $A[1 - \cos(2\pi x/L)]$. The details of the analysis are as follows. Start with the beam GDE solution which, as always, is $w(x) = A + B(x) + C \sin(\lambda x) + D \cos(\lambda x)$, where $\lambda^2 = P/EI$. The BCs are $w(0) = w'(0) = w(L) = w'(L) = 0$. Substituting the GDE solution into the BCs yields the four equations: (i) $A + D = 0$; (ii) $B + \lambda C = 0$; (iii) $A + BL + C \sin(\lambda L) + D \cos(\lambda L) = 0$; and (iv) $B + \lambda C \cos(\lambda L) - \lambda D \sin(\lambda L) = 0$. An easy way to solve these equations is to write them in the matrix form $[c]\{A\} = \{0\}$, where $\{A\}$ is the 4×1 vector of the unknown coefficients A, B, C , and D . Since the equations are homogeneous (i.e., their right-hand side vector is zero), in order to have other than a trivial solution the determinant of the coefficient matrix must be zero. Expanding the determinant of the coefficient matrix yields the eigenvalue equation

$$2[1 - \cos(\lambda L)] = \lambda L \sin(\lambda L)$$

The solution process for this eigenvalue equation in terms of the unknown value of λL is simplified if the following substitution, suggested by the form of the left-hand side of the above equation, is used. Let $\theta = \lambda L/2$. Then this equation becomes $2[1 - \cos(2\theta)] = 2\theta \sin(2\theta)$, or in equivalent terms,

$$4 \sin^4 \theta = 2\theta \sin \theta \cos \theta \quad \text{or} \quad \sin \theta [\sin \theta - \theta \cos \theta] = 0$$

The solution to the last of the above equations is either the solution to (i) $\sin \theta = 0$, or (ii) $\sin \theta = \theta \cos \theta$, whichever yields the smaller, nontrivial solution for θ . The first non-zero solution of (i) is $\theta = \pi$, while that for (ii) is $\theta \approx 4.5$ (See Example 11.11.) Therefore, the critical value of $\theta = \frac{1}{2}\lambda L = \pi$, which leads immediately, to $P_{cr} = 4\pi^2 EI/L^2$. This is four times the critical load value for the simply supported beam.

The buckling mode shape can be determined by eliminating all but one of the constants of integration. In this case, start with $D = -A$, and $B = -\lambda C$. Hence, after substituting $\lambda L = 2\pi$, the third BC equation becomes $A - C(2\pi) + C \sin 2(2\pi) - A \cos(2\pi) = 0$. Simplifying this equation shows that $C = 0$. The fourth BC equation only yields the useless identity $0 = 0$. Then with $B = 0$, and again $D = -A$, and again $\lambda = 2\pi/L$, the GDE solution reduces to

$$w(x) = A[1 - \cos(2\pi x/L)]$$

The unknown value of A is seen to be the (unknowable by this method) value $\frac{1}{2}w(L/2)$. This buckling mode shape is a bit more complicated than the sine mode shape of the simply supported beam case. This mode shape involves two reversals of curvature. It will be seen in Chapter 15 that structural systems seek the loaded deflection shape that stores the least energy. Hopefully, it is evident to the reader that this "one minus cosine" shape requires more energy, and hence a larger applied load for a given midspan deflection, than the sine mode shape.

- (b) From Example 10.4, or a similar analysis, the axial force N in the beam-column has the value $-E\alpha T_0 A$. Then, from the result of part (a), $P_{cr} = EA(\alpha T_0)_{cr}$, or $(\alpha T_0)_{cr} = 4\pi^2 I/AL^2$. Thus thermal buckling problems for beams are solved by knowing the mechanical buckling load and the equivalent thermal axial force.
- (c) As always, the Euler buckling load solution is

$$v(x) = B_1 + B_2 x + B_3 \sin \lambda x + B_4 \cos \lambda x \quad \text{where} \quad \lambda^2 = \frac{P}{EI}$$

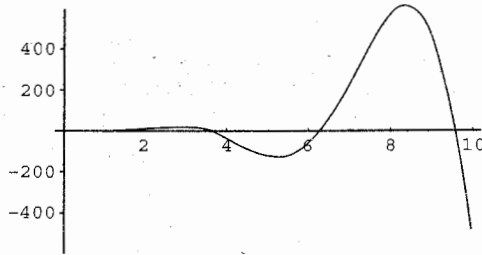
The first task is to write the BCs. The kinematic BCs are $v(0) = v'(0) = v'(L) = 0$. From a FBD at $x = L$, obtain

$$V_y(L) - \frac{2EI}{L^3}v(L) = 0 \quad \text{or} \quad L^3 v'''(L) - 2v(L) = 0$$

Hence the determinant equation to be solved for the eigenvalue is

$$\begin{vmatrix} 1 & 0 & 0 & 1 \\ 0 & 1 & \lambda & 0 \\ 0 & 1 & \lambda \cos \lambda L & -\lambda \sin \lambda L \\ 2 & 2L & (2 \sin \lambda L + \lambda^3 L^3 \cos \lambda L) & (2 \cos \lambda L - \lambda^3 L^3 \sin \lambda L) \end{vmatrix} = 0$$

```
In[14]:= Plot[4(1 - Cos[x]) + (x^3 - 2x) Sin[x], {x, 0.1, 10.0}]
```



```
Out[14]= -Graphics-
```

```
In [16]:= FindRoot[4(1 - Cos[x]) + (x^3 - 2x) Sin[x], {x, 3.5}]
```

```
Out[16]= {x -> 3.38915}
```

Figure B.2. Ans. 11.14(a)

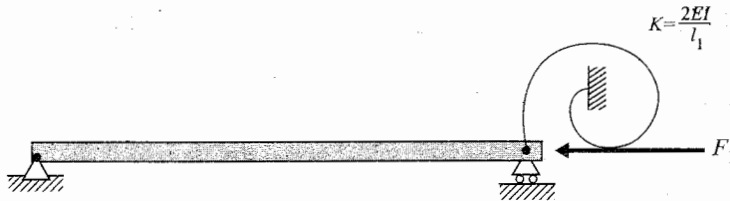


Figure B.3. Ans. 11.14(d)

After expanding the determinant by hand and by using *Mathematica* 4.2, the eigenvalue equation becomes

$$4 \cos \lambda L - [(\lambda L)^3 - 2\lambda L] \sin \lambda L = 4$$

A *Mathematica* plot of this function is shown in Fig. B.2. The lowest, nonzero, root has the approximate value 3.38915, which is equivalent to a critical compressive load of $P_{cr} = 11.5 EI/L^2$.

- (d) With just F_1 acting upon the frame, the single beam that represents the frame is that of length L . The beam of length l_2 (the beam with the unsupported end) is unloaded and therefore makes no contribution to the frame stiffness. The beam of length l_1 must also bend when the simply supported beam of length L bends. Thus it contributes rotational stiffness at the point of application of the axial load. A beam bending analysis shows that this rotational stiffness is $K = 2EI/l_1$. Hence the single beam model for a beam buckling analysis (an eigenvalue problem) is shown in Fig. B.3.
- (e) With just F_2 acting upon the frame, the single beam that represents the frame is again that of length L . The beam of length l_2 provides a moment arm for F_2 . Again the beam of length l_1 provides a rotational spring of stiffness $K = 2EI/l_1$. Hence the single beam model is that of the boundary value problem shown in Fig. B.4.

11.15. (a) The solution to the Euler beam bending differential equation is, as always

$$w(x) = A_1 + A_2x + A_3 \sin \lambda x + A_4 \cos \lambda x \quad \text{where} \quad \lambda = \sqrt{\frac{P}{EI}}$$

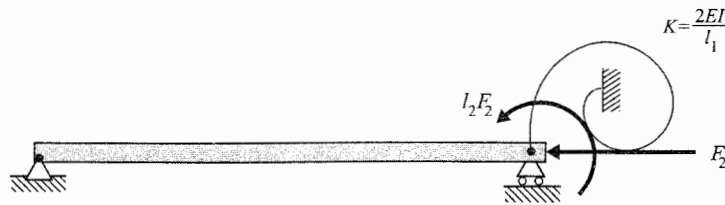


Figure B.4. Ans. 11.14(e)

The two kinematic BCs are $w(0) = w'(0) = 0$. From a free body diagram of the beam tip, where the beam tip is given a positive deflection $w(x)$ ((up)), and a positive bending slope $w'(x)$ ((up and rotated counterclockwise)), the remaining two BCs are

$$w''(L) = 0 \quad w'''(L) + \lambda^2 w'(L) - \frac{4}{L^3} w(L) = 0$$

Write the above four BC equations in the homogeneous matrix form: $[C]\{A\} = \{0\}$, where $\{A\}$ is the vector of the unknown constants of integration. Then set the determinant of the singular coefficient matrix $[C]$ equal to zero; that is, write

$$\begin{vmatrix} 1 & 0 & 0 & 1 \\ 0 & 1 & \lambda & 0 \\ 0 & 0 & -\lambda^2 \sin \lambda L & -\lambda^2 \cos \lambda L \\ -\frac{4}{L^3} & \left(\lambda^2 - \frac{4}{L^2}\right) & -\frac{4}{L^3} \sin \lambda L & -\frac{4}{L^3} \cos \lambda L \end{vmatrix} = 0$$

Expanding the determinant, and simplifying, including dividing by $\lambda^2 \cos \lambda L$, yields

$$\tan \lambda L = \lambda L - \frac{(\lambda L)^3}{4}$$

to be solved for λL . A rough sketch shows that the smallest root of this transcendental equation is near 2.3. Applying the Newton–Raphson procedure yields a solution of 2.373. Thus

$$P_{critical} = 5.63 \frac{EI}{L^2}$$

- (b) The deflection BCs are simply $w(0) = w(L) = 0$. For the moment BCs, it is necessary that the beam tips be rotated according to the deflection sign convention, which here means that the beam tips need to be rotated counterclockwise. The results of the FBDs are

$$EI w''(0) - \frac{2EI}{L} w'(0) = 0 \quad EI w''(L) + \frac{3EI}{L} w'(L) = 0$$

where the EI factors can be canceled. Substituting the standard Euler beam-column deflection solution $w(x) = A_1 + A_2 x + A_3 \sin \lambda x + A_4 \cos \lambda x$ into these four BCs results in the following determinant to be solved for the eigenvalue λ

$$\begin{vmatrix} 1 & 0 & 0 & 1 \\ 0 & 2L & 2\lambda L & (\lambda L)^2 \\ 1 & L & \sin \lambda L & \cos \lambda L \\ 0 & 3L & (3\lambda L \cos \lambda L - \lambda^2 L^2 \sin \lambda L) & -(3\lambda L \sin \lambda L + \lambda^2 L^2 \cos \lambda L) \end{vmatrix} = 0$$

- (c) The beam will buckle about the z axis. Therefore the GDE and its solution are

$$EI_0 v''''(x) + P v''(x) = 0$$

and

$$v(x) = C_1 + C_2 x + C_3 \sin \lambda x + C_4 \cos \lambda x$$

where λ^2 equals P/EI_0 . Now it is a matter of writing the BCs, using FBDs where necessary. From the sketch, after dividing by EI_0 and other tidying, the BCs are

$$v(0) = 0, \quad Lv''(0) - v'(0) = 0, \quad v''(L) = 0,$$

$$L^3 v'''(L) - 3v(L) + L^3 \lambda^2 v'(L) = 0$$

Now it is a matter of substituting the above solution for $v(x)$ into these BCs, arranging the result in the matrix form [coeff.] $\{C\} = \{0\}$, and requiring |coeff. | = 0. Hence

$$\begin{vmatrix} 1 & 0 & 0 & 1 \\ 0 & L & \lambda L & (\lambda L)^2 \\ 0 & 0 & \sin \lambda L & \cos \lambda L \\ 3 & L(3 - \lambda^2 L^2) & 3 \sin \lambda L & 3 \cos \lambda L \end{vmatrix} = 0$$

The expansion of this determinant leads to the characteristic equation for $\lambda L = x$, which is

$$x(3 - x^2) \cos x - x^2(3 - x^2) \sin x - 3 \sin x = 0$$

$$\text{or } \tan x = \frac{3x - x^3}{3 + 3x^2 - x^4}$$

- (d) The axial force acting upon the beam is the first thing to investigate because it is basic to the GDE and the eigenvalue. From the FBDs, the axial force $-N \equiv P = F \cos[\theta + w'(L)]$, $F = P_0 \sec \theta$. From the geometry of the deflections, the quantity $\sec \theta$ is equal to the square root of one minus the square of the ratio $[w(L)/\ell]$. The beam tip deflection $w(L)$, while finite, is still a small fraction of the length of the rigid link, ℓ , and the square of that ratio is much smaller still. Hence the good approximation that $\sec \theta \approx 1.0$. Now, $\cos[\theta + w'(L)] = \cos \theta \cos[w'(L)] - \sin \theta \sin[w'(L)]$, and $\sin \theta = w(L)/\ell$. Since both theta and beam tip bending slope are also small quantities, their sines can be approximated as their arguments, and their cosines can be approximated as one. Thus, because the product of small quantities is smaller still

$$P = P_0[1 - w(L)w'(L)/\ell] = P_0$$

and the GDE does not require any modification. The first boundary condition is that the beam tip moment is zero, or $w''(L) = 0$. The beam tip shearing force $V_z = EI w'''(L) = -F \sin[\theta + w'(L)] = -P_0[w'(L) + w(L)/\ell]$. After

division of this latter BC by EI , and recognizing the ratio P_0/EI as the square of the eigenvalue, the writing of the two force-type BCs is complete.

- 12.1.** Note that all forces per unit length are equal to their corresponding stress multiplied by the constant thickness. Then both results are immediate with the use of Mohr's circle, which in this case is just a point. Alternately, Eqs. (2.6) provide the same result.
- 12.2. (a)** In terms of the temporary coordinates y_0, z_0 specified in the problem statement, the double sine series would have the form

$$\Psi(y_0, z_0) = \sum_m \sum_n C_{mn} \sin(m\pi y_0/a) \sin(n\pi z_0/b)$$

where each double sine term in the series satisfies all the BCs. There is one more condition that can be satisfied at this point. Both m and n can be restricted to being odd integers so that each sine term is an even function about the center of the rectangle; that is, the symmetry of the Prandtl stress function about the axes of symmetry of the rectangle, as dictated by the membrane analogy, is established immediately. If this condition of restricting the indices to being odd is not met at the beginning of the analysis, it will simply be a necessary conclusion to be drawn after the application of the orthogonality conditions associated with the sine functions, which are the same as those associated with the cosine functions, as in Eq. (12.15).

- (b)** The two series solutions have the same algebra and result.
- 12.3.** At points B and D the stress magnitude is zero. From Fig. 12.12, where for $a/b = 1$, $\alpha = 0.21$. Then for points A and C , the stress magnitude is $4.8M_t/a^3$, and the applied stress direction is the same as that of the torque while paralleling the edge.
- 12.5.** Recall that (i) the outer and inner boundaries of any cross-section are always contour lines; and (ii) the shearing stresses are greatest wherever the contour lines are closest together.
- 12.6. (a)** One way of answering this question is to picture the membrane over the thin beam cross-section as roughly a long cylinder with, say, an arch being the cross-sectional shape of the membrane. Let the arch have an easily imaged finite slope (corresponding to a finite stress) at the edge of the thin beam cross-section. Then picture that cylinder cut cross-wise into four equal parts and placed on top of the thick beam cross-section, completely covering its area. A single arch spanning the thickness of the thick cross-section and having the same edge slope stress would enclose a much greater volume torque. Therefore, for the same maximum stress, the thicker cross-section can bear a much greater torque.
- (b)** By a slight adjustment to the above argument, it can be seen that for the same torque volume, the stress slope on thick beam cross-section is much less than that for the thin beam cross-section.
- 12.7. (a)** The trial function does satisfy the BC of being zero at each point on the four segments of the cross-sectional boundary. That is, at all points $y = -a$, at $y = +a$, and along the arcs of the circle $y^2 + z^2 = R^2$, the trial function takes on the value zero. However, the trial function is not a valid stress function because its units are incorrect (Ψ has units of force over length), and when subjected to the harmonic operator there is a result other than $-2G\theta$. Since the result is not a constant it cannot be adjusted to achieve the desired result, $-2G\theta$.

- (b) Again the BCs $\Psi = 0$ are satisfied at every point along the outer boundary lines $r = R$, $\alpha = 0$, and $\alpha = \pi/2$. However, again, the GDE is not satisfied because the result of applying the ∇^2 operator to the candidate Prandtl stress function is zero rather than the required value $-2G\theta$. Since zero cannot be made into the required finite value $-2G\theta$, this is not an acceptable Prandtl stress function.
- (c) The equations for the three boundaries of the isosceles triangle are $y = -a/2$, $z = -a/2$, and $y + z = \frac{1}{2}a$. Substitution of these values for y and z into the given candidate Prandtl stress function expression leads to zero values. Thus the BCs are satisfied.
- (d) Substitution of the candidate Prandtl stress function into the GDE produces a right-hand side of $-2G\theta(y + z)$ rather than the required value of $-2G\theta$. Hence the GDE is not satisfied, and the candidate function fails.
- 12.8.** (a) The trial function does satisfy the GDE. It also satisfies the BC of $\Psi(s) = 0$ for every point on the boundary. This fact is established by first writing the equations for all points upon the boundary, which are: $y = -a/3$; $z = [(y/\sqrt{3}) - (2a/3\sqrt{3})]$; and $z = -[(y/\sqrt{3}) - (2a/3\sqrt{3})]$; and then substituting these equalities into the trial function. The zero result shows that the trial function is zero on the three sides of the equilateral triangle. Since the GDE and BC are both satisfied, the trial function is valid.
- (b) The maximum shearing stress is at the center of each of the three sides. Since all three sides are the same, choose to work with the side $y = -a/3$, where the normal direction, $n = -y$. Then $\sigma_{max} = -\partial\Psi/\partial(-y) = \partial\Psi/\partial y = -G\theta[y - 3(y^2 + z^2)/2a]$, which when evaluated at $y = -a/3$, $z = 0$ yields $\sigma_{max} = G\theta a/2$.
- (c) $M_t = G\theta a^4/15\sqrt{3}$ from which $J = a^4/15\sqrt{3}$. Then $G\theta$ can be replaced by M_t/J in the maximum stress equation.
- 12.9.** A computer-generated plot of the function $\Psi(y, z)$ is shown in Fig. B.5. Clearly there is no closed curve, and hence no possible bar cross-section.
- 12.10.** The general third order polynomial term in two variables has the form

$$P_3(y, z) = Ay^3 + By^2z + Cyz^2 + Dz^3$$

Substitution of this expression into the equation

$$\left[\frac{\partial^2}{\partial y^2} + \frac{\partial^2}{\partial z^2} \right] P_3(y, z) = 0$$

reveals the relations that must exist between the constant coefficients A , B , C , and D for the resulting identity to hold true. That is, the coefficient of each linearly independent (see comment immediately below) polynomial term of the resulting identity must be zero. Substitution of the relations between the constants back into the original expression, and renaming the constants, yields the general form of the third order, harmonic polynomial term as

$$H_3(y, z) = C_7(y^3 - 3yz^2) + C_8(z^3 - 3y^2z)$$

Recall that polynomial terms or functions, such as $f_1(x)$, $f_2(x)$, ... are linearly independent if and only if $B_1f_1(x) + B_2f_2(x) + \dots = 0$ implies $B_1 = B_2 = \dots = 0$. For example, with y , z being independent variables, and α , β and γ being a set of constants, then $\alpha y^2 + \beta yz + \gamma z^2 = 0$ can only be true for all values of y , z if $\alpha = \beta = \gamma = 0$. Thus it is concluded that the terms y^2 , yz , and z^2 are (mutually)

```
In[1]:= Needs["Graphics`ImplicitPlot`"]
In[3]:= ImplicitPlot[x^4 - 6x^2 y^2 + y^4 - x^2/2 - y^2/2 = 0, {x, -10, +10}]
```

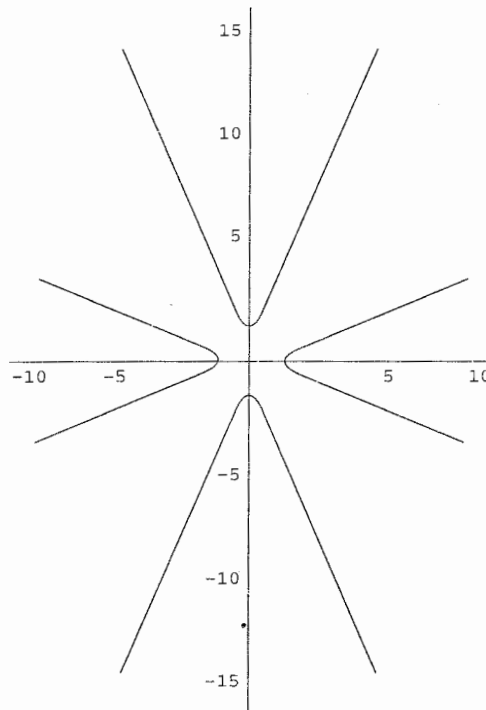


Figure B.5. Ans. 12.9. Source: *Mathematica 4.1*, Wolfram Research

linearly independent terms. A definitive test for linear independence is to evaluate a determinant called the Wronskian determinant. See Section III.3.

- 12.11.** Consider the geometry of the laterally loaded taut (i.e., preloaded) cable. Since it spans the same straight-line distance as the unloaded taut cable, it has to stretch beyond its initial strains when the cable is no longer straight. Consider differential length, ds , of the deflected cable. The projection of ds upon the original cable position is dx . The length dx is also the length of the taut cable segment of length ds before the cable was deflected laterally. Let the change in the deflection over the differential length ds , (i.e., from one end of ds to the other), be dw . Then, by use of the Pythagorean theorem, $ds = [(dx)^2 + (dw)^2]^{1/2} = [1 + (w')^2]^{1/2} dx$. The change in the strain in the taut cable as it is laterally deflected is $\Delta\epsilon = (ds - dx)/dx = (ds/dx) - 1$. Using the binomial expansion for $ds/dx = [1 + (w')^2]^{1/2} = 1 + \frac{1}{2}(w')^2 + \dots$, and substituting for ds/dx into $\Delta\epsilon$, yields $\Delta\epsilon \approx \frac{1}{2}(w')^2$. The change in the stress and hence the change in the cable force can now be calculated from the change in the strain. Specifically, $\Delta N = \frac{1}{2}EA(w')^2$.

In order to more clearly establish the point that the change in the axial preloading due to finite deflections can be neglected, consider a steel wire where $E = 29\,000\,000$ psi, the yield stress is 40 000 psi, and the cross-sectional area is 0.01 in^2 . Hence the diameter of the circular wire is 0.113 in. Let the pre-load, N_0 , be half the force that would bring the wire to the verge of undergoing plastic behavior. That is let $N_0 = 1/2\sigma_{\text{yield}}A = 200$ lbs. Then, if the 40-inch wire is plucked at its

center, say, one-fifth of an inch, which is almost twice its diameter, and thus is easily discernable, then the slope of the deflected wire is everywhere one-fifth of an inch divided by 20 inches, or 0.01. Then the change in the axial force is $1/2 EA(w')^2 = 14.5$ lbs. By saying the change in the axial force is zero, the error is 7 percent, which is just within engineering tolerance.

- 13.1. (a) $J = (1/3)(2h + d)t^3$, then $\theta = M_t/GJ$, and the maximum stress is $M_t t/J$.
 (b) same as in (a).
 (c) $J = 16at^3/3$.
- 13.2. (a) The cross-section is doubly symmetric, so it is only necessary to integrate from $\zeta = 0$ to $\zeta = c/2$, and multiply by 2. However, if the integration is carried out over the entire length of the centerline, the thickness expressions are

$$b(\zeta) = \frac{3t\zeta}{c} \quad 0 \leq \zeta \leq \frac{c}{3}$$

$$b(\zeta) = t \quad \text{for } \frac{c}{3} \leq \zeta \leq \frac{2c}{3}$$

$$b(\zeta) = \frac{3t}{c}(c - \zeta) \quad \frac{2c}{3} \leq \zeta \leq c$$

Then

$$J = \frac{1}{3} \left(\frac{ct^3}{12} + \frac{ct^3}{3} + \frac{ct^3}{12} \right) = \frac{ct^3}{6}$$

and the maximum stress is equal to $(M_t b_{max}/J) = 6M_t/(ct^2)$.

- (b) From any table of integrals, the integral of $(\sin^3 ax)$ is equal to

$$-\frac{1}{a} \cos ax + \frac{1}{3a} \cos^3 ax$$

Here $a = \pi/20$. Now it is a matter of applying the limits of zero and 10.

- 13.3. (a) The value of $\hat{A} = 150t^2$; and thus the shear flow $q = M_t/(300t^2)$. The stress is the value of the shear flow divided by the thickness, that is, q/t . The line integral of the inverse of the thickness is $(1/t)(50t)$. Hence $J = 1800t^4$.
 (b) $q = 1590$ lb/in; the maximum stress equals the shear flow divided by the minimum thickness, that is, 12 700 psi; and for $G_0 = 2.5 \times 10^4$ psi, the line integral of the inverse of the m.w. thickness equals 8π radians, so $J = \pi/2 \text{in}^4$.
 (c) To calculate the torsion constant, use is again made of the third of Eqs. (13.11), where $\hat{A} = 2c^2$, and the line integral has the value $2(c)/[2(2t)] + (4c)/1(t) = 4.5c/t$. In these calculations, on the basis of the membrane analogy, the contribution to the torsion constant of that part of the top plate and the hat cross-section beyond the central void of dimensions $2c$ by c is ignored. Thus $J^* = 3.5c^3t$.

- 13.4. In the case of the open cross-section, $J = 3bt^3$. In the case of the closed cross-section, it is necessary to calculate J from the relation $M_t = GJ\theta$, which first requires the determination of the shear flows and then the calculation of θ . So, for q_1 being the shear flow around the smaller of the two cells, the equilibrium is $M_t = 2q_1b^2 + 4q_2b^2$, and $\theta_1 = \theta_2$ yields $9q_1 = 8q_2$. Hence

$$q_1 = \frac{2M_t}{13b^2} \quad \text{and} \quad J = \frac{104b^3t}{23}$$

- 13.5. (a) The equilibrium equation is $M_t = 64\pi t^2 q_1 + 64(\pi + 8)t^2 q_2$. The solution of the twist continuity equation $\theta_1 = \theta_2$ is $q_1 = 0.8023q_2 = M_t/(1090t^2)$. Therefore, $J = 10\,300t^4$.
- (b) The equilibrium equation is $M_t = 5.712R^2 q_1 + 0.571R^2 q_2$. The twist equilibrium equation yields $7.100q_1 = 10.954q_2$.
- (c) $M_t = 19.635q_1 + 60q_2$; $q_1 = 1.0226q_2$.
- 13.6. (a) $\phi(L) = m_0 L^2/2GJ$.
- (b) $\phi(L) = M_0 L/GJ$.
- (c) $GJ\phi''(x) = m_0 L \delta(x - \frac{1}{2}L) - m_0 \text{stp}(x - \frac{1}{2}L)$ or the negative thereof, The BCs are $\phi(0) = \phi'(L) = 0$. Thus the first constant of integration equals $-m_0 L/2$, and the second is zero. Thus $\phi(L) = m_0 L^2/8GJ$ in the direction of the concentrated torque, which was here chosen to be negative.
- 13.7. $\phi(L) - \phi(0) = m_0 L^2/(2\pi GJ)$.
- 13.8. In a form that is ready to be integrated easily, the GDE is

$$GJ\phi''(x) = -M_5\delta(x - \frac{1}{2}L) - (m_0/L)(x - \frac{1}{2}L)\text{stp}(x - \frac{1}{2}L) - (3m_0/2)\text{stp}(x - \frac{1}{2}L)$$

The two BCs are

- i. $3L\phi'(0) - \phi(0) = 0$
- ii. $\phi'(L) = M_4/GJ$

- 13.9. The correctness of any suggested solution, of course, can be confirmed or denied by integrating the GDE and applying the BC. However, the easiest approach is usually to substitute the suggested solution into the GDE and BC equations and see whether these equations are satisfied. This exercise is therefore a review of differentiating expressions involving step functions. Differentiating the given solution once yields

$$GJ\phi'(x) = \left[M_4 + M_5 + \frac{7}{4}m_0L \right] - M_5 \text{stp}(x - L) - m_0L \left[\frac{1}{4} \left(\frac{x}{L} \right)^2 + \frac{x}{L} - \frac{5}{4} \right] \text{stp}(x - L)$$

A second differentiation yields the original GDE, so that part of the problem is satisfied. It is important to note that in this exercise, the process of taking the derivative of products involving the step function, the coefficient of the resulting Dirac delta function is always zero where the delta function is nonzero. Thus those product terms drop out. The next equations to check are the BC equations:

$$GJ\phi'(2L) = \left[M_4 + M_5 + \frac{7}{4}m_0L \right] - M_5 - m_0L \left[1 + 2 - \frac{5}{4} \right] = M_4$$

so this BC is satisfied.

$$GJ\phi'(0) = \left[M_4 + M_5 + \frac{7}{4}m_0L \right] = K\phi(0)$$

so this BC is also satisfied. Hence the suggested solution is the (unique) correct solution to the problem posed by Example 13.10.

- 13.10. (a) There is a one J_3 for the horizontal rectangle for which the appropriate β is $\beta(14) \approx 0.32$; and another J_3 for the vertical rectangle for which $\beta \approx 0.33$;

and an αD^4 term is also needed. Hence $J = (0.33)(10t^4) + (0.32)(7t^4) + (0.185)(2t)^4 = (3.30 + 2.24 + 2.96)t^4 = 8.5t^4$.

(b) The web requires J_3 with a $\beta(6) = 0.229$; the flange takes a J_2 with a $\beta(8) = 0.308$; and $\alpha = 0.20$ for the bulge.

13.11. The manufacturing difficulty presented by having the channels face inward (i.e., []) might be overcome to some extent by having lightening holes cut in the web of the channels. Sufficient holes might provide access to the interior of the box beam so that riveting or bolting would be possible.

13.12. After applying the BC $\phi(0) = 0$, the solution reduces to

$$GJ\phi(x) = (m_0L^2 - C_1L)\ln\left(1 - \frac{x}{L}\right) + m_0Lx$$

What can be said about the twist at the end $x = L$ of this cantilevered beam is that the twist is finite. However, setting $x = L$ in the above solution causes the first term to become infinite. Since that is not physically possible, the constant coefficient of the natural logarithm term must be zero. Thus $GJ\phi(x) = m_0Lx$.

14.1. (a) The partial area moments in simplified form are

$$\text{Top flange: } Q_y(y) = at(a - 2y) \quad Q_z(y) = t\left(\frac{1}{4}a^2 - y^2\right).$$

$$\text{Web: } Q_y(z) = 2a^2t + \frac{1}{2}(a^2 - z^2) \quad Q_z(z) = -\frac{1}{2}at(a - z).$$

$$\text{Bottom flange: } Q_y(y) = \frac{3}{2}a^2t - yat \quad Q_z(y) = -a^2t + \frac{1}{2}t\left(y^2 - \frac{1}{4}a^2\right)$$

(b) With $I_{yy} = (29/6)a^3t$, $I_{zz} = (13/6)a^3t$, and $I_{yy} = -a^3t$, calculation of the shear stress due to a shearing force with both horizontal and vertical components is now only a matter of substituting into Eq. (14.5) with $q_0 = 0$.

(e) Starting at $(y, z) = (+8.1t, +4.9t)$ so as to easily have positive values for the centerline coordinate z

$$\text{upper flange: } Q_y = (4.9t)(8.1t - y)t = 39.69t^3 - 4.9yt^2$$

$$Q_z = \frac{1}{2}(8.1t + y)(8.1t - y) = \frac{t}{2}(65.6t^2 - y^2)$$

$$\text{web: } Q_y = 49t^3 + \frac{t}{2}(4.9t + z)(4.9t - z) = 61t^3 - \frac{1}{2}z^2t$$

$$Q_z = 31t^3 + t(-1.9t)(4.9t - z) = 21.7t^3 + 1.9zt^2$$

where the $49t^3$ and $31t^3$ terms at the start of the web calculation are the first moments of the top flange in its entirety. The small error at the end of the centerline, where $z = -11.1t$, is due to round-off.

14.2. (c) The shear center is at the juncture of the web and the flange.

(d) The vertical force F at the left tip of the T can be replaced by the statically equivalent combination of a force F acting along the T centerline and a counterclockwise moment of magnitude $(0.9 \text{ in})F$. The force F now passes through the shear center and creates shearing stresses described by Eq. (14.5) with q_0 equal to zero. These shearing stresses are essentially uniform across the thickness of each segment of the T , and their maximum value is determined from the result of part (a). On the other hand, the torsional moment creates shearing stresses that vary linearly across the thickness, and their maximum value

$$\frac{M_t b}{J} = \frac{3(0.9'')F}{(3.2'')(0.06'')^2}$$

is the same everywhere on the outer boundary of the cross-section, except perhaps at the fillets. Thus this torsional moment maximum shearing stress coincides with the shear force maximum shearing stress at the point where the shear force-induced maximum shearing stress occurs, and those two values are then added to obtain the overall maximum shearing stress.

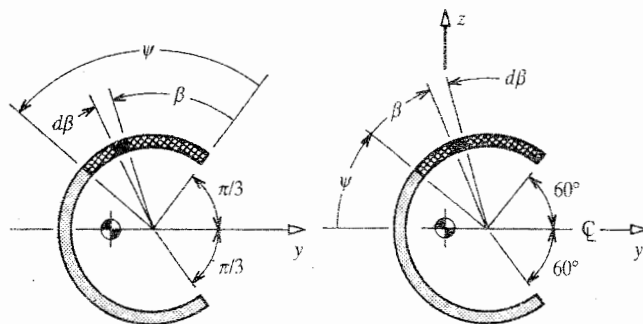
- 14.4.** As explained, $q_0 = \text{zero}$ at $\alpha = s = 0$ because of the symmetry of the cross-section and loading. In other words, the shear flow cannot go in opposite directions at the same point. Therefore $Q_y(\alpha)$ equals the integral from zero to α of the product of the differential area $Rt d\beta$ at β and its moment arm about the y axis, $R \cos \beta$. Therefore, with $I_{yy} = \pi R^3 t$, $q(\alpha) = F \sin \alpha / (\pi R)$.
- 14.5.** (a) The first moment of the partial area is exactly the same as that of the previous exercise; that is, $Q_y(\alpha) = R^2 t \sin \alpha$.
- (b) The shear center lies on the cross-section axis of symmetry, the y axis, which passes through the circle center and the slit. To find the horizontal location of the shear center, a vertical force of arbitrary magnitude F is applied at the unknown location of the shear center. The shear flow solution is $q(\alpha) = (F/R)(1 - \cos \alpha)$. Then, taking moments about the center of the circle yields $F e_y =$ (the integral from zero to π of) $R q(\alpha) R d\alpha$. Thus $e_y = 2R$ to the left of the circle center.
- (c) Again the shear center lies upon the axis of symmetry. Two solution approaches are presented that differ only in the choice of coordinates used to locate positions along the centerline of the beam cross-section material. See Fig. B.6. In the first solution approach, the angle ψ , whose origin is at one end of the material centerline, locates the limit of the partial area under consideration. See the two left-hand diagrams of the figure. The angle β has the same origin, but it locates positions within the partial area. In other words, the limiting upper value for β is the value $\beta = \Psi$. In order to locate the shear center, it is first necessary to calculate the shear flow due to a (say, positive, i.e., downward) shearing force F that is perpendicular to the cross-section axis of symmetry. To this end,

$$Q_y = \iint_{A(s)} z dA = \oint z (tR d\beta) \quad \text{where} \quad ds = R d\beta$$

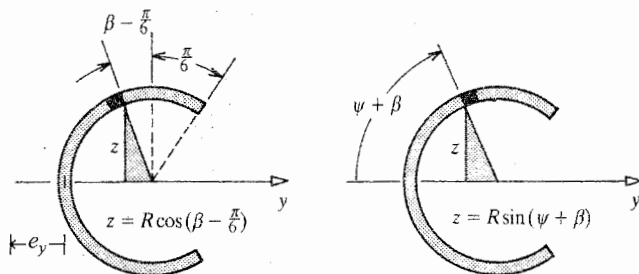
Since $z = R \cos[\beta - (\pi/6)]$,

$$\begin{aligned} Q_y(\Psi) &= - \int_{\beta=0}^{\beta=\Psi} R \cos\left(\beta - \frac{\pi}{6}\right) R t d\beta \\ &= R^2 t \left[\frac{\sqrt{3}}{3} \sin \Psi + \frac{1}{2} (1 - \cos \Psi) \right] \end{aligned}$$

where the integration can be completed either by writing $d\beta = d[\beta - (\pi/6)]$, or by expanding the cosine function in the integrand and noting that $\sin(\pi/6) = 1/2$ and $\cos(\pi/6) = \sqrt{3}/2$. Since $q(\Psi) = F Q_y(\Psi) / I_{yy}$, it is now possible to write the twisting moment equilibrium equation that locates the shear center. Letting e_y be positive to the left of the intersection of the cross-section axis of symmetry and the thin cross-section material centerline, then the twisting moment equilibrium equation, where all moments are taken about the center



Two possible coordinate choices



Corresponding typical moment arm expressions

Figure B.6. Ans. 14.5.

of the circle, is

$$\begin{aligned}
 F(e_y + R) &= -\oint Rq(\Psi)ds = +\oint R^2q(\Psi)d\Psi \\
 &= \frac{F}{I_{yy}} \int_{\Psi=0}^{\Psi=4\pi/3} R^2t \left[\frac{\sqrt{3}}{2} \sin \Psi + \frac{1}{2}(1 - \cos \Psi) \right] R^2d\Psi
 \end{aligned}$$

or

$$F(e_y + R) = R^4t[(2\pi/3) + \sqrt{3}](F/I_{yy})$$

Hence

$$e_y = R \left(\frac{(2\pi/3) + \sqrt{3}}{(2\pi/3) - (\sqrt{3}/4)} \right) - R$$

If the angles Ψ and β are defined as shown in the two right-hand diagrams of Fig. B.6, then

$$\begin{aligned}
 Q_y(\Psi) &= \int_{s=0}^s zt ds = -t \int_{\beta=(2\pi/3)-\Psi}^{\beta=0} R \sin(\Psi + \beta)R d\beta \\
 &= -R^2t[\cos(2\pi/3) - \cos \Psi] = +R^2t \left(\frac{1}{2} + \cos \Psi \right)
 \end{aligned}$$

Then

$$F(e_y + R) = \frac{F}{I_{yy}} R \int_{\psi=-2\pi/3}^{\psi=2\pi/3} R^2 t \left(\frac{1}{2} + \cos \Psi \right) R d\Psi$$

which, of course, yields exactly the same result for e_y as the previous calculation using different definitions of Ψ and β .

- (d) Briefly; (i) $y_0^* = \frac{2\sqrt{2}}{3\pi} R$ to the closed side of the cross-section from the geometric center; (ii) $I_{yy} = \frac{1}{4}(3\pi + 2)R^3 t$; (iii) with the y axis as the axis of symmetry, and measuring the angle ψ from where the cross-section begins at an angle 45° above the horizontal, so that $\frac{\pi}{4} \leq \Psi \leq \frac{7\pi}{4}$, the shear flow $q(\Psi) = \frac{4}{(3\pi+2)} \frac{F}{R} \left(\frac{\sqrt{2}}{2} - \cos \Psi \right)$; and (iv) from the geometric center to the left

$$e_y = \frac{\sqrt{2}R}{3\pi + 2} (3\pi + 4)$$

- 14.6. (a) Starting the calculation of the first moments of partial area at the upper right, for the right segment

$$Q_y(z) = (t/2)(144t^2 - z^2) \quad \text{and} \quad Q_z(z) = 120t^3 - 10zt^2$$

for the middle segment

$$Q_y(y) = 72t^3 \quad \text{and} \quad Q_z(y) = 170t^3 - 1/2 ty^2$$

for the left segment

$$Q_y(z) = 72t^3 - \frac{1}{2}tz^2 \quad \text{and} \quad Q_z(z) = 120t^3 + 10zt^2$$

- (b) Since $R_{zz} = 478t^4$ and $R_{yz} = 1019t^4$, then the expression for the shear flow is $q(s) = (V_z Q_y / R_{zz}) - (V_z Q_z / R_{yz})$, where $V_z = F$. Now it is simply a matter of substitution. The sketch of the reacting shear flow is as shown in Fig. B.7.
- (c) The shear flow distribution clearly shows that the shear center has to lie along the z axis. To be certain that the shear center also lies along the y axis, the above process would have to be repeated with an applied shear force in the y direction. That calculation would confirm that result.

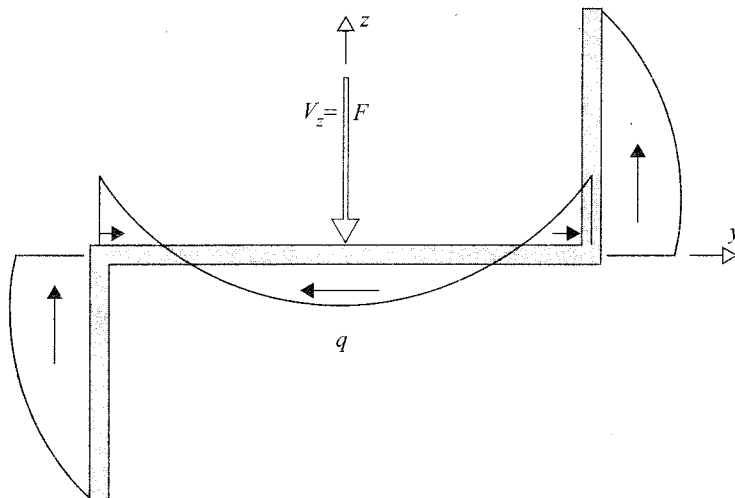


Figure B.7. Ans. 14.6.

- 14.10.** Starting the calculation of the first moments of partial area at the upper left, for the top flange

$$Q_y(y) = (10t)[(7.5t) + y]t = 75t^3 + 10yt^2$$

and

$$Q_z(z) = -\frac{1}{2}(7.5t - y)(7.5t + y)t = -\frac{1}{2}(56.25t^3 - ty^2)$$

for the web

$$Q_y(z) = 100t^3 + \frac{1}{2}(10t + z)(10t - z)t = 100t^3 + (t/2)(100t^2 - z^2)$$

and

$$Q_z(z) = (-2.5t)(10t^2) + (2.5t)(10t - z)t = -25t^3 + \frac{1}{2}t^2(50t - 5z)$$

for the bottom flange

$$Q_y(y) = 100t^3 - (-10t)(2.5t - y)t = 75t^3 + 10yt^2$$

and

$$Q_z(y) = 25t^3 + t(2.5t - y)(\frac{1}{2})(2.5t + y) = 25t^3 + 1/2t^3(6.25t^2 - y^2)$$

Note that $Q_y(-7.5t) = Q_z(-7.5t) = 0$, which, as always, is a good check on the calculation.

- 14.11.** The shear flow due to the twisting moment, aF_0 , is simply the constant counter-clockwise quantity $q = aF_0/(2 * 2a^2) = \frac{1}{4}(F_0/a)$. The calculation of the shear flow due to the shear force at the shear center begins with the recognition that the symmetry of the cross-section and this latter loading means that this shear flow is zero where the z axis crosses the flanges. Let the center point of the top flange be the origin of the s coordinate, and in order to have positive values of y , let s go clockwise around the right-hand portion of the cross-section. The equation for this shear flow is $q(s) = F_0Q_y/I_{yy}$. This moment of inertia has the approximate value $7a^3t/6$. Hence the next step is to calculate the first moments of partial area about the y axis (only) for the right-hand side of the cross-section. These values are

$$0 \leq y \leq a \text{ (top and bot. flange)} \quad Q_y(y) = \frac{1}{2}aty$$

$$-\frac{a}{2} \leq z \leq \frac{a}{2} \text{ (web)} \quad Q_y(z) = \frac{a^2t}{2} + \frac{t}{2} \left(\frac{a^2}{4} - z^2 \right)$$

Hence the *resisting* shear flows due to the moment and the shear force are as shown in Fig. B.8.

- 15.1.** (b) For F_1 , the work done along any path is $+(ab/L)F_0$. The work done by F_2 for the three paths is, respectively, $+(ab/L)F_0$, 0, and $-(ab/L)F_0$.
- 15.2.** (a) $2(u + xy)v \delta u + (u + xy)^2 \delta v$
 (b) $\delta u + y \delta u_{,x} = \delta u + y \partial/\partial x(\delta u)$
 (c) $\partial G/\partial u_{,x} \delta v_{,x} + \partial G/\partial v_{,x} \delta v_{,x}$
 (d) $\sin(u_{,x}) \delta u + u \cos(u_{,x}) \delta u_{,x}$
- 15.3.** (a) $\delta W_{ex} = F_1 \delta v(L/3) - F_2 \delta v(2L/3)$. There are no virtual deflections at the rigid support reactions because the fixed values of the deflections at the rigid supports are constraints upon the beam. In other words, even though the deflections at the supports are dependent quantities from the virtual work viewpoint,

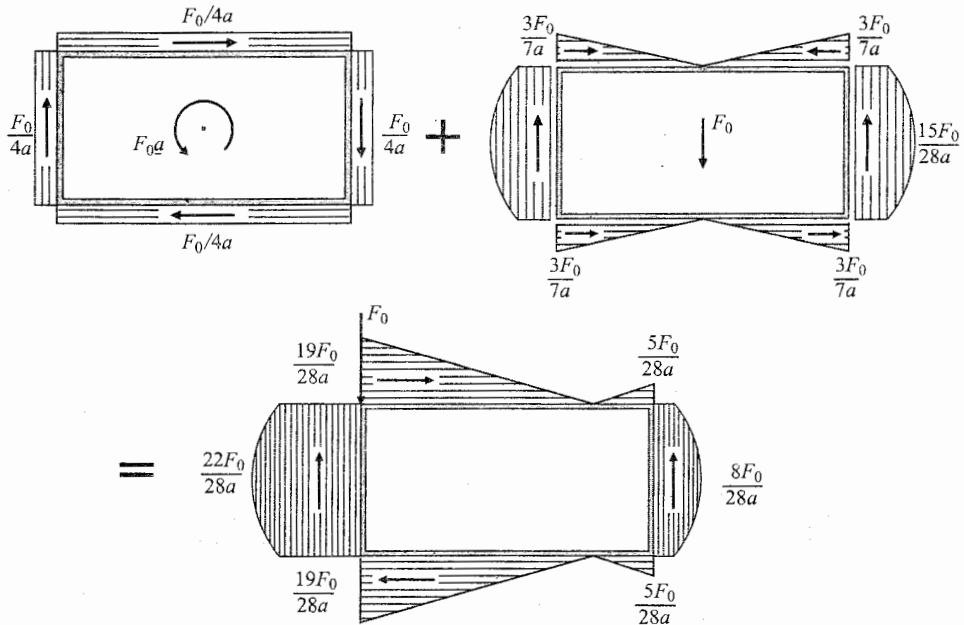


Figure B.8. Ans. 14.11.

when the deflections are known, constant values, they do not admit a variation. On the other hand, the deflections within the interior of the beam are unknown, dependent quantities. Hence they can have variations.

- (b) $\delta W_{ex}^* = d_0 \delta R_3$. Once again, from the CVW viewpoint, the three reactions are unknown, dependent quantities. From the CVW viewpoint, they can vary, and thus have variations. The actual deflections at the first two reactions are zero, so they do zero CVW. On the other hand, the forces F_1 and F_2 have no variations, since these two forces have known, fixed values. With either CVW or virtual work, fixed quantities have no variations.
- (c) $\delta W_{ex} = T_r(2\pi Rh)\delta u(R)$, where δu , in keeping with the symmetry of the problem, is constrained to not being a function of the coordinate θ , and thus is in this case a constant value around the circumference.
- (d) The component of the gravitational force in the tangential direction of the pendulum bob is $mg \sin \theta$. Giving the bob a virtual displacement $+\delta\theta$, where $\delta\theta$ has of course the same sign convention as θ , leads to $\delta W_{ex} = -(mg \sin \theta)(L\delta\theta) = -mgL \sin \theta \delta\theta$. The negative sign is necessary because the force is directed opposite to the positive direction of the angle θ . In another view, if the virtual deflection is in the direction of the force, then the virtual angle $\delta\theta$ is opposite to the positive direction for the angle θ , and must be written as $-\delta\theta$.
- (e) Since, at the outer boundary, the actual tractions are known and the displacements are unknown, there can only be variations on the displacements leading to external virtual work, but no variations upon the tractions leading to complementary virtual work. That is, $\delta W_{ex}^* = 0$ because δT_r is zero.
- 15.5. (a) $\delta W_{ex} = F_r \delta u + F_0 \delta v + F_z \delta w$ where, as before, the displacement components $u, v, w(r, \theta, z)$ parallel the cylindrical coordinates axes at any point.

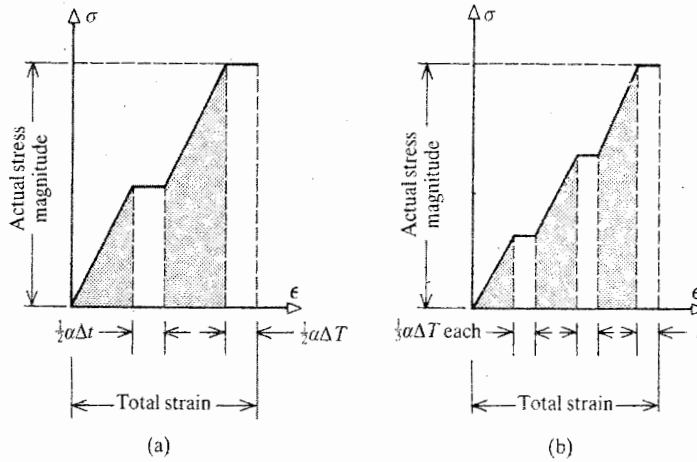


Figure B.9. Ans. 15.6

This result may be proved by simply letting \hat{i} and \hat{j} be the unit vectors in the r and θ directions respectively, and (i) noting that $\delta r = \delta u \hat{i} + \delta v \hat{j} + \delta w \hat{k}$; (ii) decomposing \mathbf{F} into its cylindrical components; and (iii) then taking the dot product.

(b) $\delta W_{ex}^* = u \delta F_r + v \delta F_\theta + w \delta F_z.$

15.6. Consider U_0 first. Approach the simultaneous application of the temperature and mechanical loading in discrete steps. That is, let half the mechanical load be followed by half the thermal load followed by the last half of the mechanical load followed by the last half of the thermal load as shown in Fig. B.9. In this case it should be clear that the shaded area representing $U_o = \frac{1}{2} \sigma (\epsilon - \alpha \Delta T)$ is the same as that shown in Figs. 15.7(a, b). Figure B.9 shows the same result when pairs of one third of each loading are taken sequentially. By varying the order and size of the discrete loading segments, any loading path involving the simultaneous application of the thermal and mechanical loads can be approximated while maintaining the constant area under the mechanical loading portion of the total curve that is represented by $U_o = \frac{1}{2} \sigma (\epsilon - \alpha \Delta T)$. In the limit as the size of the segments becomes infinitesimal, an exact representation of any loading curve is obtained. Furthermore, since $U_o^* = \sigma \epsilon - U_0$, it too is the same regardless of the load path.

15.7. With $\delta u = \text{const.}$, then $\delta \epsilon_{xx} = (\partial/\partial x) \delta u$ and all other virtual strains are zero. Then, after canceling the constant value of δu , the virtual work statement reduces to the surface integral of T_x and the volume integral of ρB_x equaling zero. Substitution of the Cauchy equation for T_x and the use of the Green–Gauss theorem completes the derivation.

15.9. Since $T = T(q_i, \dot{q}_i, t)$, then $\delta T = \Sigma[(\partial T/\partial \dot{q}_i) \delta \dot{q}_i + (\partial T/\partial q_i) \delta q_i]$, where the sum is over $i = 1, 2, \dots, N$, where N is the number of generalized coordinates. Integrate the first of these two terms by parts. Since for all values of i , $\delta q_i(t_2) = \delta q_i(t_1) = 0$, the uv part of the result of integration by parts is zero. Thus the terms that remain in the time integrand for δT are

$$-\frac{d}{dt} \left(\frac{\partial T}{\partial \dot{q}_i} \right) + \frac{\partial T}{\partial q_i}$$

The virtual work can be separated into two parts. The first part of the total virtual work is that part that pertains to conservative forces that the analyst wishes to describe in terms of one or more potential energies that are collectively symbolized as Π . Since potentials have signs opposite to their corresponding work terms, for this part

$$\delta W = - \sum \frac{\partial \Pi}{\partial q_i} \delta q_i$$

The second part of the total virtual work is the product of all the other generalized forces, conservative or nonconservative, moving through their virtual displacements. Therefore, the total virtual work is

$$\delta W = - \sum \frac{\partial \Pi}{\partial q_i} \delta q_i + \sum Q_i \delta q_i$$

Following the usual argument that calls for all of the arbitrary δq_i to be zero but one, and noting the arbitrariness of the time interval of integration, the end result, which is applicable to both conservative and nonconservative forces, is immediate.

- 15.10.** Since $\delta W_{ex} = F_r \delta u + F_\theta \delta v + F_z \delta w$, then $Q_r = F_r$, $Q_\theta = F_\theta$, and $Q_z = F_z$. In this case the generalized forces are none other than the ordinary force components. However, in the case of Exercise 15.3(b), the generalized force Q_θ is the moment $-mgR \sin \theta$.

- 16.2.** (a) The strength of materials solution for the beam cantilevered at $x = 0$ is $w(x) = F_0 x^2 (3L - x) / (6EI)$. Thus the choice of $f_1(x) = x^2$, and $f_2(x) = x^3$ will lead to the above exact solution. Of course, these two functions both have the anticipated deflection shape, both satisfy the lateral deflection and slope BCs at $x = 0$, and the resulting polynomial products are very easy to integrate. As is generally the case in a RRM analysis, here simultaneous equations in number equal to the number of selected functions (two) must be solved for the unknown coefficients, q_i . In this case, where the approximating functions are all the functions that are part of the exact solution, if the analyst adds an additional function (such as x^4), then the coefficient of that additional function turns out to have a zero value.

- (b) A trigonometric function that approximates the anticipated deflection pattern is $f_1(x) = 1 - \cos(\pi x / 2L)$. A second such function that serves as a correction to the first function is $f_2(x) = 1 - \cos(\pi x / L)$.

- 16.3.** (a) With $w(x, t) = q(t)(x/L)^2$, then $T = (1/2)[M + (1/5)\rho AL]\dot{q}^2$, and $U = (2EI/L^3)q^2$. Thus $f^2 = EI/\{\pi^2[ML^3 + (1/5)\rho AL^4]\}$

- (b) Note the correspondence between the single function used in Example 16.2 and this choice of functions.

16.4. (a) $f^2 = \frac{\pi^2}{4} \left(\frac{EI}{2ML^3 + \rho AL^4} \right)$

- 16.5.** (a) Since, for the sake of a quick calculation, a single approximating function is to be used, and since the beam is simply supported, and since the stiffness nonuniformity is merely piecewise constant, then the probable best choice is $\sin(\pi x / L)$, which satisfies the deflection boundary conditions (and the moment boundary conditions). Also, $\delta W(w')$ and $\delta U(w'')$ are easily calculated.

- (b) Probably the best choice for a single approximating function is, where x is measured from the clamped end, is $[1 - \cos(\pi x / 2L)]$. Of course the way to

judge the better of two choices is to calculate which choice provides the lower estimate for the buckling load.

- (c) This exercise differs from the above two only in that it is the δW integral that requires division into that for two intervals along the beam length. Since the beam is simply supported, $\sin(\pi x/L)$ would be a good choice for the single approximating function.
- (e) This exercise is redone using a finite element formulation in a later chapter.
- 16.6. (a)** This is a matter of first writing $w(x, y) = q_1 \sin(\pi x/a) \sin(\pi y/b)$. Then evaluating the δW_{ex} integral is just a matter of applying the variational operator to the lateral deflection approximating function to get $\delta w(x, y) = \delta q_1 \sin(\pi x/a) \sin(\pi y/b)$, and substituting. In order to evaluate δU , it is first necessary to apply the variational operator to U , and use the product rule from the ordinary calculus for the quadratic functions of the deflection derivatives. Substitution of $w(x, y)$ and $\delta w(x, y)$ then carrying out the integration provides a result involving both q_1 and δq_1 . The δq_1 of the work and strain energy integrals cancels leaving one equation to be solved for the unknown q_1 . In other words, doing a RRM analysis for a plate differs from that of a beam only in that the strain energy expression is a bit more complicated.
- (c) Such a series of sine functions is called a Navier series. This series of sine functions in the two spatial variables is used to find an exact plate bending series solution, via the plate differential equation, in Chapter 22.
- 16.7.** Since the plate geometry, material distribution, and the loading are axial symmetric, the approximating functions should not involve the polar angular coordinate, but only the radial coordinate, r . One possible choice of approximating functions for the lateral deflection $w(r)$ would be $\cos(\pi r/2R)$, $\cos(3\pi r/2R)$, $\cos(5\pi r/2R)$ etc. All these terms meet the deflection boundary condition requirement at $r = R$. This is a case where writing an expression for the applied concentrated force using a Dirac delta function is confusing. It is better just to write that $\delta W_{ex} = F \delta w(r = 0) = F \sum q_j$.
- 16.8.** Because the slab/plate is symmetric, but the loading is antisymmetric, σ_{xx} can be expected to be odd in y , but even in x . If the pattern of the other two stresses is not as clear, consider the fact that differentiation of an even function yields an odd function, and vice versa. Then use the first of the two general equilibrium equations as $\partial \sigma_{xx} / \partial x = -\partial \sigma_{xy} / \partial y$. This suggests that σ_{xy} is odd in x , and even in y . The second equilibrium equation can be used in a similar manner to judge σ_{yy} . A place to start with polynomial series for the three stresses is

$$\sigma_{xx} = \sigma_0(y/b) + (a^2 - x^2)(p_0 + p_1 y + p_2 x^2 + p_3 y^3)$$

$$\sigma_{xy} = (a^2 - x^2)(b^2 - y^2)(p_4 + p_5 x + p_6 y^2 + p_7 x^3)$$

$$\sigma_{yy} = (b^2 - y^2)(p_8 + p_9 y + p_{10} x^2 + p_{11} x^4)$$

If these finite series cannot be used to satisfy the equilibrium equations, then make adjustments until three nontrivial finite series are found that do satisfy those equations.

- 16.9. (a)** The series terms selected for the two plane stress displacements do not have to meet any deflection boundary conditions. The applied loading enters the problem through the external virtual work integral

$$\delta W_{ex} = h \oint T_x(y) \delta u(x, y) ds = h \oint \sigma_0(y/b) \delta u(x, y) ds$$

Since the applied traction is antisymmetric about the x axis, the selected x direction displacement terms should also be odd in y , as well as in x . On the basis that this particular applied traction mimics the stress distribution in a beam, the y direction deflection should be even in x , and possibly even in y also. Therefore start with the estimate

$$u(x, y) = q_1x + q_2y + q_3xy + q_4xy^3 + q_5x^3y + q_6x^3y^3$$

$$v(x, y) = q_7 + q_8y^2 + q_9x^2 + q_{10}x^2y^2 + q_{11}x^2y^4 + q_{12}x^4y^2$$

Proceeding on the basis that the above series is adequate, now the above virtual work integral can be evaluated. First integrate where $x = a$ (on the right side of the rectangle), from $y = -b$ to $y = +b$, where $ds = +dy$. Understand that along this right side $\delta u = \delta u(a, y)$. Along the top edge there are no tractions, so the next integration is down the left side, from $+b$ to $-b$, where $\delta u = \delta u(-a, y)$, $ds = -dy$, and from the sign convention for tractions $T_x(y) = -\sigma_0(y/b)$. So the line integral becomes just two ordinary integrals as described. The next step is to convert the plane stress form for the strain energy into a statement entirely in terms of strains (using the isotropic material equations), and then, using the strain-displacement equations, convert from the strains into derivatives of the displacements. After applying the variational operator to U , equate δU to δW_{ex} , and equate the coefficients of the arbitrary δq 's to solve for the unknown weighting factors that determine the displacements.

- 17.1. (a)** One set of generalized coordinates could be two rectilinear measures that locate the scissor hinge plus one angle that locates the orientation of each scissor blade relative to a fixed table top edge, for a total of four generalized coordinates. A second set of four generalized coordinates could be the straight-line distance from a fixed point on the table top to the scissor hinge, the angle between the table top edge and the aforementioned straight line, and the relative angle of each blade makes with the same straight line.
- (b)** Eight generalized coordinates are required.
- (c)** Four generalized coordinates are required, one to locate the outer end of the first link along the straight line, and, say, three angles relative to the horizontal, positive counterclockwise, to locate the links relative to each other. Two angles are insufficient because of the possibility of ambiguity. Two coordinates locating the ends of the three links along the straight line, plus one angle can also lead to an ambiguity.
- (d)** Two generalized coordinates are required. One could be the arc length distance along the rigid wire, and the second generalized coordinate could be the rotation of the bead about the wire relative to the plane of curvature of the wire where the wire is not straight, and the rotation relative to an appropriately fixed plane where the wire is straight. An alternate second generalized coordinate could be the rotation relative to a series of appropriately fixed planes.
- (e)** The rigid watch base requires six generalized coordinates like any rigid body in space. One additional generalized coordinate is required to locate the hour hand relative to the watch. Thus a total of seven generalized coordinates are required.
- 17.2.(a)** Figure 17.13 shows both the two degrees of freedom and the two generalized forces for the bar element. Since the equations for the stress in a bar of a general cross-sectional shape depend upon the classification of the cross-section, it is

easier to directly fill in the 2×2 element stiffness matrix. Begin with a positive ϕ_2 and a zero value of ϕ_1 . The zero value of ϕ_1 means that the left end of the bar is fixed. The torque M_{12} necessary to achieve the rotation ϕ_2 is of course $+(GJ/l)\phi_2$. The torque M_{21} that equilibrates M_{12} is then $-(GJ/l)\phi_2$. This pair of results fills in the second column of the 2×2 bar element torsional stiffness matrix. It is up to the reader to reason out the first column.

- (b) The linearly varying lateral force per unit length can be replaced by a lateral force of magnitude $(1/3)f_0l$ at the left end of the beam element, and a lateral force of magnitude $(1/6)f_0l$ at the right end. Such a replacement is statically equivalent to the original distributed force. It is also possible to obtain a more consistent answer from Eqs. (17.6) and (17.4b). Then $\{Q\} = f_0l[7/20 \quad 1/20 \quad 3/20 \quad -1/30]$. See Exercise 17.7.
- 17.3.(a) The presence of the concentrated force at the midspan of the cantilevered beam makes it necessary to use two beam elements to form the finite element model. See Fig. B.10.
- (b) The approach to the beam bending finite element employed here requires that the beam finite element have a constant stiffness coefficient. If a single beam finite element with the average stiffness coefficient $3EI_0$ were used, then that model would not well represent the changes in curvature, and hence stress, that actually occur in this tapered beam. Therefore, at a minimum, two beam elements should be used. When two beam elements are used, the average stiffness coefficient over the inboard half-span is $4EI_0$. The average stiffness coefficient over the outboard half-span is $2EI_0$. Thus a minimum finite element model for such a structure would be that shown in Fig. B.10.
- (c) The matrix equation $\{\tilde{Q}\} = [\tilde{K}]\{\tilde{q}\}$, without recognizing the symmetry of this particular structure and loading, is

$$\begin{Bmatrix} F_0 \\ 0 \end{Bmatrix} = \frac{EI_0}{L^3} \begin{bmatrix} 24 & 0 \\ 0 & 8L^2 \end{bmatrix} \begin{Bmatrix} \hat{w}_2 \\ \hat{\theta}_2 \end{Bmatrix}$$

Obviously the solution for $\hat{\theta}_2$ is zero, as it must be because of the above-noted symmetry. The solution for the midspan deflection is $\hat{w}_2 = F_0L^3/(24EI_0)$. With practice in using the finite element method, this finite element solution is easier to obtain than the unit load method solution discussed in later chapters, which because of the symmetry, has a single redundant.

- (d) Let $\hat{\alpha}$ be the bending slope to the left of the hinge at midspan, that is, $\hat{\alpha} = \theta_2$ for the left-hand beam element. Let $\hat{\beta}$ be θ_1 for the right-hand beam element, that is, the bending slope to the right of the hinge. Then $\{\tilde{Q}\} = [\tilde{K}]\{\tilde{q}\}$ in this case is

$$\begin{Bmatrix} F_0 \\ 0 \\ 0 \end{Bmatrix} = \frac{EI_0}{L^3} \begin{bmatrix} 24 & -6L & 6L \\ -6L & 4L^2 & 0 \\ 6L & 0 & 4L^2 \end{bmatrix} \begin{Bmatrix} \hat{w}_2 \\ \hat{\alpha} \\ \hat{\beta} \end{Bmatrix}$$

Now all three global DOF are algebraically coupled, and, for the form shown, a simultaneous solution is necessary for these three unknowns. However, it may be recognized from the symmetry of the problem that $\hat{\beta} = -\hat{\alpha}$. Then the above matrix equation reduces to

$$\begin{Bmatrix} F_0 \\ 0 \end{Bmatrix} = \frac{EI_0}{L^3} \begin{bmatrix} 24 & -12L \\ -12L & 8L^2 \end{bmatrix} \begin{Bmatrix} \hat{w}_2 \\ \hat{\alpha} \end{Bmatrix}$$

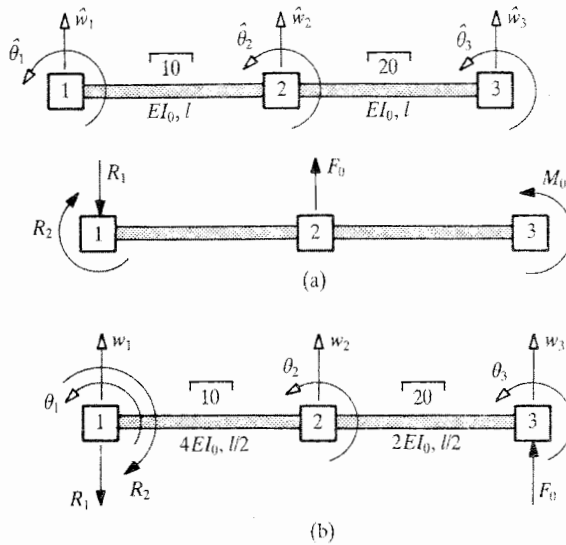


Figure B.10. Ans. 17.3 (a) Sketches of the global degrees of freedom and the loading. For very small structures, it is useful to guess the directions of the reactions. However, for larger structures, it is better to have all reactions positive in the same direction as their corresponding DOF. (b) In order to accurately represent the deflections and curvatures (stresses) of this simple structure, it is necessary to model the change in stiffness coefficient. Two is the minimum number of uniform finite elements that reflect the change in stiffness coefficient. The use of more elements would produce greater accuracy. Each of the two uniform elements uses the average stiffness coefficient for the element span. For good accuracy, eight beam elements would be adequate.

This reduction of global DOF from three to two allows the contrasting of this solution to the case where there is no hinge at the midspan. The solution is easily obtained by hand as, $\hat{w}_2 = F_0 L^3 / (6EI_0)$, and $\hat{\alpha} = F_0 L^2 / (4EI_0)$. Note that with respect to a lateral deflection at midspan, the hinged structure is four times more flexible, or one-fourth as stiff, as the clamped-clamped beam without the hinge. Lastly, note that if the reader has memorized the tip deflection of a cantilevered beam due to a tip lateral force F_0 , which is $F_0 L^3 / (3EI_0)$, then replacing the two beams by two springs with stiffness $3EI_3 / L^3$ leads immediately to the solution for the midspan deflection for the hinged beam.

- 17.4.(a) As a result of the BCs $\hat{w}_1 = \hat{\theta}_1 = \hat{w}_3 = \hat{w}_4 = \hat{w}_5 = 0$, the reduced system matrix equation is

$$\begin{Bmatrix} +F_0 \\ 0 \\ -M_0 \end{Bmatrix} = \frac{EI_0}{l^3} \begin{bmatrix} 48 & 6l & 12l \\ 6l & 12l^2 & 4l^2 \\ 12l & 4l^2 & 8l^2 \end{bmatrix} \begin{Bmatrix} \hat{w}_2 \\ \hat{\theta}_2 \\ \hat{\theta}_3 \end{Bmatrix}$$

The (1, 1) entry of $[\tilde{K}]$, for example, is the sum $12 + 24 + 5 + 7 = 48$.

- (b) With u_2 being the horizontal deflection of the left-hand cart, u_3 being the DOF of the middle cart, and u_4 being the DOF of the right-hand cart, with all three

DOF being positive to the right, then the system FEM matrix equation is

$$\begin{Bmatrix} 0 \\ 0 \\ F_1 \end{Bmatrix} = \begin{bmatrix} k_1 + k_2 + k_3 & -k_2 & -k_3 \\ -k_2 & k_2 + k_4 & -k_4 \\ -k_3 & -k_4 & k_3 + k_4 + k_5 \end{bmatrix} \begin{Bmatrix} u_2 \\ u_3 \\ u_4 \end{Bmatrix}$$

- (c) The nonuniform beam of Fig. 17.17 has one clamped support, one rigid simple support, one rectilinear spring support, and one support-free end. Since all beam segments are collinear, there is only beam bending with which to be concerned, and hence only beam bending DOF. The beam bending element stiffness matrixes, in terms of the global DOF, are

$$[K_{10}]\{\hat{q}\} = \frac{EI_0}{l^3} \begin{bmatrix} 24 & 12l & -24 & 12l \\ 12l & 8l^2 & -12l & 4l^2 \\ -24 & -12l & 24 & -12l^2 \\ 12l & 4l^2 & -12l & 8l^2 \end{bmatrix} \begin{Bmatrix} \hat{w}_1 \\ \hat{\theta}_1 \\ \hat{w}_2 \\ \hat{\theta}_2 \end{Bmatrix}$$

$$[K_{20}]\{\hat{q}\} = \frac{EI_0}{l^3} \begin{bmatrix} 12 & 6l & -12 & 6l \\ 6l & 4l^2 & -6l & 2l^2 \\ -12 & -6l & 12 & -6l^2 \\ 6l & 2l^2 & -6l & 4l^2 \end{bmatrix} \begin{Bmatrix} \hat{w}_2 \\ \hat{\theta}_2 \\ \hat{w}_4 \\ \hat{\theta}_4 \end{Bmatrix}$$

$$[K_{30}]\{\hat{q}\} = \frac{EI_0}{l^3} \begin{bmatrix} 24 & 12l & -24 & 12l \\ 12l & 8l^2 & -12l & 4l^2 \\ -24 & -12l & 24 & -12l^2 \\ 12l & 4l^2 & -12l & 8l^2 \end{bmatrix} \begin{Bmatrix} \hat{w}_4 \\ \hat{\theta}_4 \\ \hat{w}_5 \\ \hat{\theta}_5 \end{Bmatrix}$$

$$[K_{40}]\{\hat{q}\} = \frac{EI_0}{l^3} \begin{bmatrix} +4 & -4 \\ -4 & +4 \end{bmatrix} \begin{Bmatrix} \hat{w}_2 \\ \hat{w}_3 \end{Bmatrix}$$

Assembling the global structural matrix and (i) applying the BCs that $\hat{w}_3 = \hat{w}_4 = \hat{w}_5 = 0$ and (ii) writing the external virtual work expression to define the load vector, produces the following $\{\tilde{Q}\} = [\tilde{K}]\{\tilde{q}\}$ equation:

$$\begin{Bmatrix} F_1 \\ 0 \\ F_2 \\ 0 \\ 0 \end{Bmatrix} = \frac{EI_0}{l^3} \begin{bmatrix} 24 & 12l & -24 & 12l & 0 \\ 12l & 8l^2 & -12l & 4l^2 & 0 \\ -24 & -12l & 40 & -6l & 6l \\ 12l & 4l^2 & -6l & 12l^2 & 2l^2 \\ 0 & 0 & 6l & 2l^2 & 12l^2 \end{bmatrix} \begin{Bmatrix} \hat{w}_1 \\ \hat{\theta}_1 \\ \hat{w}_2 \\ \hat{\theta}_2 \\ \hat{\theta}_4 \end{Bmatrix}$$

The above simultaneous equations in matrix equation form can now be solved for the unknown structural DOF, $\{\tilde{q}\}$. Then these structural DOF can be used in the set-aside rows (rows 5, 6, 8, and 9) to determine the support reactions at nodes 3, 4, and 5. The solution for the structural DOF can also be used in the above element stiffness matrix equations in order to determine the beam element stress resultants.

- (d) The element stiffness matrix equations in terms of the global DOF shown in Fig. 17.18(b) are as follows:

$$\{Q_{10}\} = \frac{EI_0}{l^3} \begin{bmatrix} 12 & 6l & 0 & -12 & 6l & 0 \\ 6l & 4l^2 & 0 & -6l & 2l^2 & 0 \\ 0 & 0 & \beta l^2 & 0 & 0 & -\beta l^2 \\ -12 & -6l & 0 & 12 & -6l & 0 \\ 6l & 2l^2 & 0 & -6l & 4l^2 & 0 \\ 0 & 0 & -\beta l^2 & 0 & 0 & \beta l^2 \end{bmatrix} \begin{Bmatrix} \hat{w}_1 \\ \hat{\theta}_1 \\ \hat{\phi}_1 \\ \hat{w}_2 \\ \hat{\theta}_2 \\ \hat{\phi}_2 \end{Bmatrix}$$

$$\{Q_{20}\} = \frac{EI_0}{l^3} \begin{bmatrix} 24 & 12l & 0 & -24 & 12l & 0 \\ 12l & 8l^2 & 0 & -12l & 4l^2 & 0 \\ 0 & 0 & \beta l^2 & 0 & 0 & -\beta l^2 \\ -24 & -12l & 0 & 24 & -12l & 0 \\ 12l & 4l^2 & 0 & -12l & 8l^2 & 0 \\ 0 & 0 & -\beta l^2 & 0 & 0 & \beta l^2 \end{bmatrix} \begin{Bmatrix} \hat{w}_2 \\ -\hat{\phi}_2 \\ \hat{\theta}_2 \\ \hat{w}_3 \\ -\hat{\phi}_3 \\ \hat{\theta}_3 \end{Bmatrix}$$

$$[K_{30}]\{\hat{q}\} = \frac{EI_0}{l^3} \begin{bmatrix} +\gamma & -\gamma \\ -\gamma & +\gamma \end{bmatrix} \begin{Bmatrix} \hat{w}_2 \\ \hat{w}_4 \end{Bmatrix}$$

The assembly of the global stiffness matrix is facilitated by rewriting the element stiffness matrix of beam element number 20 so that all deflection quantities have positive signs, and the global DOF are in the same order as that of the global deflection vector. These two steps require that the second and fifth rows and columns be multiplied through by -1 , and then the second and third, and the fifth and sixth rows and columns be interchanged. The result is

$$\{Q_{20}\} = \frac{EI_0}{l^3} \begin{bmatrix} 24 & 0 & -12l & -24 & 0 & -12l \\ 0 & \beta l^2 & 0 & 0 & -\beta l^2 & 0 \\ -12l & 0 & 8l^2 & 12l & 0 & 4l^2 \\ -24 & 0 & 12l & 24 & 0 & 12l \\ 0 & -\beta l^2 & 0 & 0 & \beta l^2 & 0 \\ -12l & 0 & 4l^2 & 12l & 0 & 8l^2 \end{bmatrix} \begin{Bmatrix} \hat{w}_2 \\ \hat{\theta}_2 \\ \hat{\phi}_2 \\ \hat{w}_3 \\ \hat{\theta}_3 \\ \hat{\phi}_3 \end{Bmatrix}$$

Now the assembly of the global stiffness matrix can proceed without any difficulty. After writing the external virtual work expressions to obtain the global generalized forces, and after applying the BCs $\hat{w}_1 = \hat{\phi}_1 = \hat{w}_3 = \hat{\theta}_3 = \hat{w}_4 = 0$, the result is

$$\begin{Bmatrix} 0 \\ +F_0 \\ 0 \\ 0 \\ +F_0l \end{Bmatrix} = \frac{EI_0}{l^3} \begin{bmatrix} 4l^2 & -6l & 2l^2 & 0 & 0 \\ -6l & (36 + \gamma) & -6l & -12l & -12l \\ 2l^2 & -6l & (4 + \beta)l^2 & 0 & 0 \\ 0 & -12l & 0 & (8 + \beta)l^2 & 4l^2 \\ 0 & -12l & 0 & 4l^2 & 8l^2 \end{bmatrix} \begin{Bmatrix} \hat{\theta}_1 \\ \hat{w}_2 \\ \hat{\theta}_2 \\ \hat{\phi}_2 \\ \hat{\phi}_3 \end{Bmatrix}$$

(e) The final matrix equation is

$$\begin{Bmatrix} 0 \\ -M_0 \\ 0 \\ F_0 \\ 0 \\ 0 \end{Bmatrix} = \frac{EI_0}{L^3} \begin{bmatrix} 36 & -6L & -12L & -24 & 0 & -12L \\ -6L & 5L^2 & 0 & 0 & -L^2 & 0 \\ -12L & 0 & 8.5L^2 & 12L & 0 & 4L^2 \\ -24 & 0 & 12L & 36 & 6L & 12L \\ 0 & -L^2 & 0 & 6L & 5L^2 & 0 \\ -12L & 0 & 4L^2 & 12L & 0 & 8.5L^2 \end{bmatrix} \begin{Bmatrix} \hat{w}_2 \\ \hat{\theta}_2 \\ \hat{\phi}_2 \\ \hat{w}_3 \\ \hat{\theta}_3 \\ \hat{\phi}_3 \end{Bmatrix}$$

- (l) In Fig. 21.22(a), the distributed load per unit length along the left-hand beam axis, f_0 , is divided into two, equal, concentrated loads which have the magnitude $\frac{1}{2}f_0l$. One of these two loads is absorbed by the left-hand rigid support (and thus does not enter into the FEM analysis), while the second is placed at the hinge, making the total upward, vertical force at the hinge have a magnitude of $(\frac{1}{2}f_0l + F_0)$. Remember that the hinge between the two beam ends means that the θ_2 bending rotation for the left-hand beam element and the θ_1 bending rotation for the right-hand beam element require different global DOF.
- (m) In terms of the global DOF, the bending-twisting element stiffness matrix for beam element number 10 is exactly the same as that given above in part

(d), except that all the bending terms need to be multiplied by 2 in order to account for the given bending stiffness factor being $2EI_0$ rather than just EI_0 . The stiffness matrices for the other two beams require either changes in sign or interchanges of rows and columns. In addition, the element stiffness matrix for beam 20 needs to have l changed to $2l$ both in the multiplicative factor outside the matrix and in all terms containing l within the matrix. The result in the most complicated case, that of beam 20 is

$$\{Q_{20}\} = \frac{EI_0}{l^3} \begin{bmatrix} \frac{3}{2} & 0 & 3l/2 & -\frac{3}{2} & 0 & 3l/2 \\ 0 & \frac{1}{2}\beta l^2 & 0 & 0 & -\frac{1}{2}\beta l^2 & 0 \\ 3l/2 & 0 & 2l^2 & -3l/2 & 0 & l^2 \\ -\frac{3}{2} & 0 & -3l/2 & \frac{3}{2} & 0 & -3l/2 \\ 0 & -\frac{1}{2}\beta l^2 & 0 & 0 & \frac{1}{2}\beta l^2 & 0 \\ 3l/2 & 0 & l^2 & -3l/2 & 0 & 2l^2 \end{bmatrix} \begin{Bmatrix} \hat{w}_2 \\ \hat{\theta}_2 \\ \hat{\phi}_2 \\ \hat{w}_3 \\ \hat{\theta}_3 \\ \hat{\phi}_3 \end{Bmatrix}$$

The BCs in this problem are $\hat{w}_1 = \hat{\theta}_1 = \hat{\phi}_1 = \hat{w}_4 = \hat{\theta}_4 = 0$, and the nonzero external virtual work equals $\delta W_{ex} = -F_0 \delta \hat{w}_2 + F_0 l \delta \hat{\phi}_3$. The final matrix equation is

$$\begin{Bmatrix} -F_0 \\ 0 \\ 0 \\ 0 \\ 0 \\ F_0 l \\ 0 \end{Bmatrix} = \frac{EI_0}{l^3} \begin{bmatrix} 25.2 & 12l & 1.5l & -1.5 & 0 & 1.5l & 0 \\ -12l & (8 + \frac{1}{2}\beta)l^2 & 0 & 0 & -\frac{1}{2}\beta l^2 & 0 & 0 \\ 1.5l & 0 & (2 + \beta)l^2 & -1.5l & 0 & l^2 & 0 \\ -1.5l & 0 & -1.5l & 25.5 & -12l & -1.5l & 0 \\ 0 & -\frac{1}{2}\beta l^2 & 0 & -12l & (8 + \frac{1}{2}\beta)l^2 & 0 & 0 \\ 1.5l & 0 & l^2 & -1.5l & 0 & (2 + \beta)l^2 & -\beta l^2 \\ 0 & 0 & 0 & 0 & 0 & -\beta l^2 & \beta l^2 \end{bmatrix} \begin{Bmatrix} \hat{w}_2 \\ \hat{\theta}_2 \\ \hat{\phi}_2 \\ \hat{w}_3 \\ \hat{\theta}_3 \\ \hat{\phi}_3 \\ \hat{\phi}_4 \end{Bmatrix}$$

- (p) Only the DOF at the grid corner are nonzero. The assembled stiffness matrix equation after imposition of the BCs is

$$\begin{Bmatrix} +F_0 \\ 0 \\ +M_0 \end{Bmatrix} = \frac{EI_0}{L^3} \begin{bmatrix} 15 & -3L & 6L \\ -3L & 4.5L^2 & 0 \\ 6L & 0 & 4.5L^2 \end{bmatrix} \begin{Bmatrix} \hat{w}_2 \\ \hat{\theta}_2 \\ \hat{\phi}_2 \end{Bmatrix}$$

- 17.5. (a) All vertical DOF are zero. All horizontal DOF at the ground level are zero. All horizontal DOF at the first-floor level are u_1 , and at the second level are u_2 . All rotational DOF are distinct unless the load and structure are both symmetric.

(c)

$$[\tilde{K}] = \frac{EI_0}{l^3} \begin{bmatrix} 24 & -6l & 6l \\ -6l & 8l^2 & 2l^2 \\ 6l & 2l^2 & 8l^2 \end{bmatrix}$$

- 17.6. (a) When there is a constant temperature change, T_0 , the $\delta \epsilon_{xx} \sigma_{xx}$ term in the PVW is replaced by $\delta \epsilon_{xx} E(\epsilon_{xx} - \alpha T_0)$. When the equality $\epsilon_{xx} = u'(x) = [N'(x)]\{q\}$ is substituted into the above expression, the first of the two terms, after integration over the volume of the bar, becomes the previously derived stiffness matrix multiplied by $\{q\}$. The second term, which involves the temperature change, becomes $(EA\alpha T_0/l)$ multiplied by the integral of $\{N'(x)\}$ over the bar length. The second result is $[Q_T] = E\alpha T_0 A [-1 \quad +1] = N_T [-1 \quad +1]$. See Section 18.3 for further details.

- 17.7. (a) The virtual work done by the uniform distributed load per unit length f_0 acting upon a differential length of beam is equal to $(f_0 dx)(\delta w(x))$. Thus, using

the beam bending shape functions, the total external virtual work done by the distributed lateral load is

$$\delta W_{ex} = \int_0^l f_0 \delta w \, dx = f_0 [\delta q] \int_0^l \{N(x)\} \, dx$$

Since in all cases, $\delta W_{ex} = [\delta q] \{Q\}$, then

$$\{Q\} = f_0 \int_0^l \{N(x)\} \, dx$$

where the integration is left to the reader. Clearly, any specified form of a distributed load can be dealt with in exactly the same way.

- (b) Following the same procedure outlined above, the integration for the generalized force vector leads to

$$\{Q\} = f_0 l \begin{bmatrix} +3/20 & -1/30 & 7/20 & +1/20 \end{bmatrix}^t$$

- 18.2. (b) From the third column of the beam 40 element stiffness matrix, and the θ_2 and θ_3 rows, the equivalent system load vector is

$$+ \frac{6EI_0}{L^2} \begin{Bmatrix} 0 \\ 0 \\ 1 \\ 1 \end{Bmatrix}$$

- (c) Yes.

- 18.3. (a) There are only two nonzero DOF in the case of this truss. Therefore, the two simultaneous equations can be solved for the horizontal deflection at pin D . Use of that deflection in the bar AD element stiffness matrix produces the result that the bar force has the tensile magnitude $3F/4$.

- (b) The matrix equation for this truss and loading is

$$\begin{Bmatrix} 0 \\ 0 \\ 0 \\ -F_0 \end{Bmatrix} + EA_0 \alpha T_0 \begin{Bmatrix} +\frac{1}{2} & +0 \\ +\frac{\sqrt{3}}{2} & +0 \\ 0 & +4 \\ 0 & +0 \end{Bmatrix} + \frac{EA_0 D_0}{2l} \begin{Bmatrix} \frac{\sqrt{3}}{4} \\ \frac{3}{4} \\ 0 \\ 0 \end{Bmatrix} \\ = \frac{EA_0}{l} \begin{bmatrix} 1.25 & 0 & -0.125 & 0.217 \\ 0 & 0.75 & 0.217 & -0.375 \\ -0.125 & 0.217 & 1.341 & -0.404 \\ 0.217 & -0.375 & -0.404 & 0.537 \end{bmatrix} \begin{Bmatrix} \hat{u}_3 \\ \hat{v}_3 \\ \hat{u}_4 \\ \hat{v}_4 \end{Bmatrix}$$

- 18.6. The formula to be used in the evaluation of T_{av} is, from section 18.3, $T_{av} = \frac{1}{L} \int_0^L T(x) \, dx$. In this exercise it has the value $\frac{1}{2}T$.

- 18.7. (a) The small vertical deflection at joint B is a wholly lateral deflection for bar BA , and hence does not strain, or stress, or load bar BA or any other bar of the truss.

- 18.8. The three-beam element stiffness matrices reduce to

$$[k_{10}]\{q\} = \frac{EI_0}{L^3} \begin{bmatrix} 4L^2 & 2L^2 \\ 2L^2 & 4L^2 \end{bmatrix} \begin{Bmatrix} \hat{\theta}_1 \\ \hat{\theta}_2 \end{Bmatrix}$$

$$[k_{20}]\{q\} = \frac{EI_0}{L^3} \begin{bmatrix} 4L^2 & -6L & 2L^2 \\ 2L^2 & -6L & 4L^2 \end{bmatrix} \begin{Bmatrix} \hat{\theta}_2 \\ -w_0 \\ \hat{\theta}_3 \end{Bmatrix}$$

$$[k_{30}]\{q\} = \frac{EI_0}{L^3} \begin{bmatrix} 6L & 4L^2 & 2L^2 \\ 6L & 2L^2 & 4L^2 \end{bmatrix} \begin{Bmatrix} -w_0 \\ \hat{\theta}_3 \\ \hat{\theta}_4 \end{Bmatrix}$$

Thus, after assembly, transposition, and factoring, the system matrix equation is

$$\frac{w_0}{L} \begin{Bmatrix} 0 \\ -6 \\ 0 \\ 6 \end{Bmatrix} = \begin{bmatrix} 4 & 2 & 0 & 0 \\ 2 & 8 & 2 & 0 \\ 0 & 2 & 8 & 2 \\ 0 & 0 & 2 & 0 \end{bmatrix} \begin{Bmatrix} \hat{\theta}_1 \\ \hat{\theta}_2 \\ \hat{\theta}_3 \\ \hat{\theta}_4 \end{Bmatrix}$$

which, interestingly, does not involve the bending stiffness coefficient, EI_0 . It is just a matter of geometry.

- 18.9.** The solutions for each part of this exercise are the same as when ϵ_0 is replaced by αT_0 .
- 18.10. (a)** Let the superscript f refer to the axial deflection u , the lateral deflection v , and the rotational deflection θ that are the “body fixed” DOF. That is, these DOF rotate with the beam through the counterclockwise angle β . Let generalized coordinates with an “o” superscript refer to the original horizontal and vertical orientation of the u and v DOF. Then at one end of the beam rotated in the plane

$$\begin{Bmatrix} u \\ v \\ \theta \end{Bmatrix}^f = \begin{bmatrix} \cos \beta & \sin \beta & 0 \\ -\sin \beta & \cos \beta & 0 \\ 0 & 0 & 1 \end{bmatrix} \begin{Bmatrix} u \\ v \\ \theta \end{Bmatrix}^o$$

If the above square matrix is symbolized as $[c]$, then the relationship between the two six by one DOF vectors is

$$\{q\}^f = \begin{bmatrix} c & 0 \\ 0 & c \end{bmatrix} \{q\}^o$$

Since the beam is being modeled as axially rigid, the two u coordinates of the right hand six by one vector have the same value. Hence the necessity of altering this vector to reflect the axial rigidity of the beam.

$$\begin{Bmatrix} u_1 \\ v_1 \\ \theta_1 \\ u_2 \\ v_2 \\ \theta_2 \end{Bmatrix}^{UC} = \begin{bmatrix} 1 & 0 & 0 & 0 & 0 \\ 0 & 1 & 0 & 0 & 0 \\ 0 & 0 & 1 & 0 & 0 \\ 1 & 0 & 0 & 0 & 0 \\ 0 & 0 & 0 & 1 & 0 \\ 0 & 0 & 0 & 0 & 1 \end{bmatrix} \begin{Bmatrix} u_1 \\ v_1 \\ \theta_1 \\ v_2 \\ \theta_2 \end{Bmatrix}^C \quad \text{or} \quad \{q\}^{UC} = [T_r]\{q\}^C$$

Hence the force-deflection relationship for the rotated beam in terms of the five by one (horizontal and vertical) original DOF is

$$[T_r]^t \begin{bmatrix} c & 0 \\ 0 & c \end{bmatrix}^t \{Q\}^{UC} = [T_r]^t \begin{bmatrix} c & 0 \\ 0 & c \end{bmatrix}^t [k_0] \begin{bmatrix} c & 0 \\ 0 & c \end{bmatrix} [T_r]\{q\}^C$$

or $\{Q\} = [k]\{q\}$ for the rotated beam element.

- (b)** As before, let $[c]$ be the matrix of direction cosines. Then, with $\{q^*\}$ being the rotated generalized coordinates at one bar end, $\{q^*\} = [c]\{q^0\}$. Also let the upper left quarter of the expanded bar element stiffness matrix be identified as

$$[n] = \begin{bmatrix} 1 & 0 & 0 \\ 0 & 0 & 0 \\ 0 & 0 & 0 \end{bmatrix}$$

Then

$$[k^*] = \frac{E_0 A^*}{l} \begin{bmatrix} c & 0 \\ 0 & c \end{bmatrix} \begin{bmatrix} n & -n \\ -n & n \end{bmatrix} \begin{bmatrix} c & 0 \\ 0 & c \end{bmatrix}^t$$

- (c) Basically, yes. However, the two-headed vector that represents the bending slope rotation about the y axis is positive in the negative y direction, while the torsional rotation vector and the bending slope about the z axis vector are positive in the positive x and z directions.
- 18.11.** Start the analysis with each bar modulus being E_1 . Apply the full value of the loads and calculate the nodal deflections. Use the nodal deflections to calculate the element strains. If none of the bar strains exceeds ϵ_1 , then the analysis is essentially concluded. If one or more bars have strains that exceed ϵ_1 , then linearly scale down the external loads so that the strain in no bar exceed ϵ_1 . The linear scaling of the loads in the bars is possible because the deflections are small and up to this point the material behavior is linear. Those bars where the strain has reached ϵ_1 now have their modulus entry changed to E_2 . Now a new analysis is completed where the remainder of the external loads are applied to the truss, which now consists of two different linear materials. The results of this second analysis are superimposed upon the first analysis, strain values are checked, loads are linearly scaled down, moduli are changed, and the procedure is repeated.
- 19.1.** (a) The BCs for this exercise are $u_1 = v_1 = v_2 = u_3 = v_3 = v_4 = 0$, leaving only the horizontal deflections at nodes 2 and 4 as the global DOF. The bar between nodes 1 and 3 is constrained not to deflect by the system BCs. Similarly, the bar between nodes 2 and 4 does not stretch or shrink because its ends are fixed against axial motion. Therefore, neither bar can be stressed or be subjected to a virtual strain. Thus neither bar stores internal virtual work. Thus neither bar contributes an element stiffness matrix to this analysis. The element stiffness matrix and global DOF product for the bar between nodes 3 and 4, for example, reduces to the scalar product $(EA/l)(+1)u_4 = 0.6Ehu_4$. The rest is left to the reader.
- 19.2.** (a) The virtual work expression is $\delta W = (Lf_z(t)/6)\delta w_1 + (Lf_z(t)/6)\delta w_2 + (Lf_z(t)/12)\delta w_3$. Therefore, using the order of the generalized coordinates that is used in Example 19.3, the load vector is $[Q] = (Lf_z(t)/12)[2 \ 2 \ 1 \ 0 \ 0 \ 0]$
- (b) The inertial loads are $-m_1\ddot{u}_2$ and $-m_2\ddot{u}_4$. The kinetic energy is $T = \frac{1}{2}m_1\dot{u}_2^2 + \frac{1}{2}m_2\dot{u}_4^2$. From either approach the mass matrix is a 2×2 diagonal matrix with the diagonal elements m_1 and m_2 . The the linear equation of motion are

$$\begin{bmatrix} m_1 & 0 \\ 0 & m_2 \end{bmatrix} \begin{Bmatrix} \ddot{u}_2 \\ \ddot{u}_4 \end{Bmatrix} + \begin{bmatrix} (k_1 + k_2 + k_3) & -k_3 \\ -k_3 & (k_3 + k_4) \end{bmatrix} \begin{Bmatrix} u_2 \\ u_4 \end{Bmatrix} = \begin{Bmatrix} 0 \\ 0 \end{Bmatrix}$$

The static force F does not appear in the above matrix equation because this matrix equation only involves the time-varying deflections measured from the static equilibrium position. The static force only contributes to establishing that static equilibrium position. Since there are no time-varying applied loads, this matrix equation describes what is called a (force-) free vibration. (The simple solution to this matrix equation shows that the motion of the masses is sinusoidal in time with an amplitude and phase dependent upon the initial deflections and initial velocities.)

- (c) Having u_i being the single generalized coordinate that describes the horizontal motion of the i th mass, the mass matrix is a diagonal matrix whose three

elements are respectively m_1 , m_2 , and m_3 . The generalized force vector is $[0 \ 0 \ F]$. The rest is up to the reader.

- (d) For a generalized coordinate vector of $[w_2 \ \theta_2 \ w_4 \ \theta_4]$, the lumped mass matrix is again diagonal with diagonal terms $\frac{1}{2}M$, 0 , M , and 0 , respectively. The generalized force vector is $[F_0 \ -M_0 \ 0 \ 0]$. The rest is up to the reader.
- (e) For a $[q] = [w_2 \ \theta_2 \ \theta_3]$, the three diagonal terms of the diagonal mass matrix are $3M/2$, 0 , and 0 respectively. The generalized force vector is $[Q] = [F_0 \ 0 \ -M_0]$.
- (f) The three diagonal terms of the diagonal mass matrix would now be $3M/2$, 0 , and ML^2 . The mass value $9M$ does not enter into the analysis because there is no rectilinear motion of this nonstructural mass when the structural system is confined to small deflections.

19.4. The x direction deflection expansion includes a constant term to account for rigid body motion without straining. The expansion includes linear terms to provide for the possibility of constant strain. The expansion is a single-valued, continuous function, and thus intraelement continuity is assured. As for interelement continuity, first consider the left-hand edge of the element where $y = bx/c$. Along this edge,

$$u\left(x, \frac{bx}{c}\right) = \alpha_0 + \left(\alpha_1 + \frac{\alpha_2 b}{c}\right)x$$

Along the right-hand edge where $y = (b/c)(x - a)$,

$$u(x, \cdot) = \left(\alpha_0 - \alpha_2 \frac{ab}{c} + \alpha_3 \frac{a^2 b}{c}\right) + x \left(\alpha_1 + \alpha_2 \frac{b}{c} + \alpha_3 \frac{ab}{c}\right)$$

It is easy to see that along the top and bottom edges where $y = b$ and $y = 0$, respectively, $u(x, \cdot)$ is also a linear function of x . Since these four linear deflection functions are fully controlled by their respective corner deflections, the straight-line deformed edges of this finite element are continuous with other finite elements like themselves as well as the four-node rectangular and three-node triangular finite elements discussed in this chapter.

- (b) If the exact same series expansion, but with β 's replacing α 's, is chosen for $v(x, y)$, then the exact same conclusions can be drawn with respect to that deflection.
- (c) No. The first of Eqs. (1.6) is not satisfied within the interior of this plane stress finite element.

19.5. A serendipity-type shape function for degrees of freedom at say, $X = Y = 0$ for the nine-node rectangle could be

$$N(X, Y) = 4(1 - X) \left(\frac{1}{2} - X\right) \left(\frac{1}{2} - Y\right) (1 - Y)$$

which, of course, is easily obtained by multiplying together the expressions that when set equal to zero are the equations for the straight lines that pass through all the element nodes other than the one for which the function is being written. The shape function contains only the polynomial term $X^2 Y^2$ beyond those used for the eight-node rectangle. Therefore here, too, all edge in-plane deflections are parabolic, and since there are three nodes on each side, this shape function would be consistent with interelement compatibility. Of course other straight and curved lines can be considered in this nine-node case for this corner node. For example,

$$N(X, Y) = \frac{1}{3}(1 - 2X - 2Y)(1 - X - Y) \left(\frac{3}{2} - X - Y\right) (2 - X - Y)$$

is a possibility, but a very poor one because it is immediately evident that this candidate shape function would contribute x^4 and y^4 polynomial terms to the deflection series expansion, and by itself it would result in discontinuities between the edge deflections of adjacent rectangular elements.

There is another systematic way of crafting shape functions for finite elements that have nodes in rows and columns in the interior just as they do at the edges. (The nine-node rectangular finite element discussed in this exercise is an example of an element that has three rows and three columns of three nodes. After the explanation below, it will be an easy matter to consider a 16-node element with four rows and columns of four nodes.) Shape functions for any such finite element are simply a matter of multiplying together (i) a polynomial in X that has the value 1.0 at the appropriate element node, and zero values at all other nodes and (ii) another such polynomial where Y is the variable. These polynomials for n nodes in a row or column are of order $n - 1$. In terms of X , the polynomial that has the value 1.0 at the m th node, where $X = X_m$, is obtained from the form

$$L_{n,m}(X) = \frac{(X - X_1)(X - X_2) \cdots (X - X_{m-1})(X - X_{m+1}) \cdots (X - X_n)}{(X_m - X_1)(X_m - X_2) \cdots (X_m - X_{m-1})(X_m - X_{m+1}) \cdots (X_m - X_n)}$$

The above polynomial is known as a Lagrange polynomial. Its application to this nine-node element at the node where $X_m = Y_m = 0$ is

$$N(X, Y) = \frac{(X - \frac{1}{2})(X - 1)(Y - \frac{1}{2})(Y - 1)}{(0 - \frac{1}{2})(0 - 1)(0 - \frac{1}{2})(0 - 1)} = 4(1 - X)(1 - Y)(\frac{1}{2} - X)(\frac{1}{2} - Y)$$

just as before.

- 19.6. (a)** Since the slab is unconstrained, it is able to undergo rigid body displacements within its own plane. Thus it is necessary to have some reference for all deflections. A convenient reference (datum) for all deflections is the slab center. That is, let the horizontal and vertical deflections at the center of the slab be arbitrarily assigned the values zero. This choice in effect introduces one constraint on the nodal deflections. Furthermore, the symmetry of the structure and loading allows the analysis to be restricted to the upper right quarter of the slab. (The advantage that the right side has with respect to the left side is that in the right side most of the deflections have positive values.) That same symmetry requires that along the vertical centerline there cannot be any horizontal deflections and along the horizontal centerline there cannot be any vertical deflections. The assembly of the global stiffness matrix from the element stiffness matrices and the imposition of the symmetry and datum BCs to reduce the vector of generalized coordinates is routine. The original (i.e., unreduced) vector of generalized forces is composed entirely of equivalent thermal load terms that are assembled in exactly the same fashion as is the global stiffness matrix. See Section 18.3 and Example 18.3 for further elaboration on this point.
- (b)** The stresses in any element are determined from the plane stress stress-strain equations and the strain-nodal deflection equations for that element, which are, again

$$\{\sigma\} = [E]\{\gamma\} - \bar{T}A \quad \text{and} \quad \{\gamma\} = [B]\{q\}$$

where, of course, $\{q\}$ is the vector of only those global DOF obtained from the deflection solution that are identical to the element DOF.

- 19.7. (a) The partial differential equation whose solution is the continuous deflection function $w(x, t)$ is, where primes are partial derivatives with respect to x , and dots are partial derivatives with respect to t ,

$$EIw''''(x, t) + \rho A\ddot{w}(x, t) = f_z(t)$$

- (b) The BCs are $w(0, t) = w(L, t) = w''(0, t) = w''(L, t) = 0$
 (c) Let $\rho A/EI = c^4$. Then substituting $w = WT$ leads to

$$W''''(x)T(t) + c^4 W(x)\ddot{T}(t) = 0 \quad \text{or} \quad \frac{W''''}{c^4 W} = -\frac{\ddot{T}}{T}$$

The standard argument is now that the left-hand side of the second equation depends entirely upon x while the right-hand side of the second equation depends entirely upon t . Therefore, the only way these two ratios can be equal is for each of them to be equal to the same constant, p^2 . (A positive constant is chosen because otherwise the solution for $T(t)$ would grow exponentially with time, that is, be unstable.) In this way, the following two ordinary differential equations are obtained:

$$W''''(x) - c^4 p^2 W(x) = 0 \quad \ddot{T}(t) + p^2 T(t) = 0$$

These two ordinary differential equations are connected through the presence of the parameter p^2 in both equations. The solutions to these two differential equations are

$$W(x) = C_1 \sinh(cx\sqrt{p}) + C_2 \cosh(cx\sqrt{p}) + C_3 \sin(cx\sqrt{p}) + C_4 \cos(cx\sqrt{p}),$$

and

$$T(t) = \sin(pt + \beta)$$

where β is a phase angle determined by the initial conditions. No constant of integration has been used as a multiplier for $\sin(pt + \beta)$ because it would just be absorbed into the constants of integration attached to the solution for $W(x)$ when $W(x)$ and $T(t)$ are multiplied together in order to write the homogeneous solution for $w(x, t)$. Nevertheless, there are six unknown quantities: the four C_j , p , and β .

- (d) After substituting $w(x, t) = W(x)T(t)$ into the BCs, the result is: $W(0) = W(L) = W''(0) = W''(L) = 0$.
 (e) C_3 cannot be zero because, if it were, then so too would C_1 equal zero. In that case $W(x)$ would equal zero, which would be the trivial solution to the homogeneous GDE. Since C_3 is not zero, then $\sin(cL\sqrt{p}) = 0$, or $cL\sqrt{p} = \pm n\pi$. Thus there are multiple solutions for the parameter p . Call them p_n , where $p_n = (n\pi/cL)^2$. Substituting back into the solution for $w(x, t) = W(x)T(t)$, and dropping the subscript 3 from the constant of integration,

$$w(x, t) = \sum_n C_n \sin(n\pi x/L) \sin(p_n t + \beta_n)$$

This solution, in addition to being the free vibration solution for the beam where the sets of constants C_n and β_n are determined by the initial conditions of the free vibration (but only at this point when there is no applied force), is also the basis of a modal series solution for the nonhomogeneous equation. The mode shapes (modal functions, or eigenfunctions) of the beam are the

functions $\sin(n\pi x/L)$, and the eigenvalues are the natural frequencies of vibration, $p_n = (n\pi/cL)^2$.

- (f) The procedure to be followed after the substitution of the trial function is much like that already discussed in the uniform torsion solution for the rectangular beam cross-section that is found in Chapter 12. This same procedure is also discussed later in Chapter 22 when Lévy series are discussed. Note that once the homogeneous and particular solutions are combined, not before then, the initial conditions can be used to determine the constants of integration C_n and β_n .

$$20.1. \quad (a) \quad EI_0 w(x=L) = \int_0^L \left[\frac{x}{3L} \right] \left[-\frac{2x}{3} \right] dx + \frac{1}{3} \int_L^{2L} \left[\frac{x}{3L} \right] \left[\frac{x-3L}{3} \right] dx + \int_0^L \left[-\frac{\xi}{3L} \right] \left[-\frac{\xi}{3} \right] d\xi = -\frac{19L^2}{162}$$

$$(b) \quad EI_0 w'(x=2L) = \int_0^L \left[-\frac{2x}{3} \right] \left[\frac{x}{3L} \right] dx + \frac{1}{3} \int_L^{2L} \left[\frac{x-3L}{3} \right] \left[\frac{x}{3L} \right] dx + \int_0^L \left[-\frac{\xi}{3} \right] \left[-\frac{\xi}{3L} \right] d\xi = -\frac{19L^2}{162}$$

(c) yes

- 20.2. (a) The unit load system is a unit force at joint D , say, acting to the right. This unit force is reacted at support joint A by an equal and opposite force. Only bar AD transmits this force. Thus, with the actual force in bar AD being $+F$, the horizontal deflection at D is FL/EA .
- (b) The unit load system is a unit force at joint C directed towards joint A plus a unit force at joint A directed towards joint C . This way the complementary virtual work is the distance that joints A and C move towards each other. The table of relevant factors is

Bar	L/EA coeff.	N	\bar{N}	$N\bar{N}L/EA$
AB	1	F	$-\sqrt{2}/2$	$-\sqrt{2}/2 FL/EA$
BC	1	F	$-\sqrt{2}/2$	$-\sqrt{2}/2 FL/EA$
CD	1	0	$-\sqrt{2}/2$	0
DA	1	F	$-\sqrt{2}/2$	$-\sqrt{2}/2 FL/EA$
DB	$\sqrt{2}$	$-\sqrt{2}F$	1	$-2 FL/EA$

Hence the relative motion of joints A and C along the line between them is a distance of $4.12 FL/EA$ away from each other.

(c) $5.83 FL/EA$.

- 20.3. (a) Only beam bending is of concern here. Hence the only integral that must be selected is the integral over the entire beam length of the product of the ALS and ULS bending moments divided by EI . Each end reaction force is $f_0L/2$. Starting the beam length coordinate at either support, the ALS $M(x) = \frac{1}{2}f_0x^2 - \frac{1}{2}f_0Lx$. The ULS consists of an upward unit lateral force at the quarter point, and the downward reactions of magnitude $3/4$ at the nearer support, and $1/4$ at the farther support. Of course, neither of these reactions does any CVW, and thus the total external CVW is just $1w(L/4)$. The ULS moments are $-(3x/4)$ and $(x/4) - (L/4)$ for $0 \leq x \leq L/4$ and $L/4 \leq x \leq L$, respectively. However, the problem is simplified if a second coordinate, ξ , is introduced that starts at $x=L$ and proceeds in the opposite direction. Then for $0 \leq \xi \leq 3L/4$, the ALS moment is $\frac{1}{2}f_0\xi^2 - \frac{1}{2}f_0L\xi$, while the ULS moment is just $-\xi/4$. Substituting and carrying out the integration over the intervals $0 \leq x \leq L/4$ and $0 \leq \xi \leq 3L/4$, which cover the entire beam, leads to $w(L/4) = 19f_0L^4/(2048EI)$.

- (b) Here there is no great advantage to setting up a symmetric ULS to accompany the symmetric ALS, but it can be done by placing one unit load at $x = L/4$ and another at $x = 3L/4$, with unit reactions that do no CVW at the end supports. In this case, due to the equality of the lateral deflections at $x = L/4$ and at $x = 3L/4$, the external CVW is $2w(L/4)$. Integrating over the intervals $0 \leq x \leq L/4$ and $L/4 \leq x \leq L/2$, and then multiplying by 2 to account for the other half of the beam, leads to the same result.

20.4. (a) $EI_0v(0) = \frac{4}{3}FL^3$

- 20.5. (a) The ULS might consist of a unit bending moment that is placed at either beam end and that is equilibrated by vertical forces of magnitude $1/L$ at the supports, or it might consist of counterclockwise-directed unit bending moment applied to the left beam end, and a clockwise-directed unit bending moment applied to the right-hand end. The latter case is a possibility because the CVW done by the two bending moments is the same and its total is twice the desired deflection. In either case, the magnitude of the bending slope at the beam ends is $F_0L^2/(9EI)$. If the first mentioned ULS is used, the sign accompanying the solution depends upon the beam end chosen and the direction of the selected unit moment.

- 20.6. (a) A calculation is necessary to determine whether the beam ends and beam center are deflected upward or downward.

- (b) Tip displacement $= 7f_0L^4/(24EI_0)$ upward. This answer is obtainable in the following fashion. With an x coordinate originating at either beam tip, the ALS moments are

$$0 \leq x \leq L \quad M(x) = \frac{1}{2}f_0x^2$$

$$L \leq x \leq 2L \quad M(x) = \frac{1}{2}f_0x^2 - 2f_0Lx + 2f_0L^2$$

There is a choice of unit load systems. For example, one ULS choice is to put (i) a unit load, say upward, at the right-hand beam tip, (ii) a downward force of magnitude $\frac{3}{2}$ at the right-hand support, and (iii) an upward force of magnitude $\frac{1}{2}$ at the left-hand support, farthest from the unit load. This ULS is in equilibrium, and only the unit load does external CVW for a total external CVW equal to the value of the beam tip deflection. Thus it is a suitable ULS. However, because the beam and actual loading are symmetrical, a better ULS choice would be a ULS that is also symmetrical. One symmetrical ULS is one where there are upward unit loads at both beam tips, and downward unit loads at both beam supports. Then because of the symmetrical pattern for the actual deflections, the nonzero CVW is twice the value of either beam tip deflection, that is, $\delta W_{ex} = 2w(0)$. The integration of the CVW integrals can now be limited to one-half of the total length of the beam provided that the two-part integration from $x = 0$ to $x = 2L$ is multiplied by 2 in order to account for both halves of the beam of length $4L$. When this symmetrical ULS is chosen, the unit load moments are particularly simple. They are

$$0 \leq x \leq L \quad \overline{M}(x) = +x$$

and

$$L \leq x \leq 2L \quad \overline{M}(x) = +L$$

- (c) Center displacement = $f_0 L^4 / (24EI_0)$ downward.
- 20.7. (a) Left-hand end rotation = $f_0 L^3 / (4EI_0)$.
- 20.8. (a) For ease of calculation, choose a coordinate x that starts at the free end of the beam. Then for all x , the ALS moment is $f_0 x^3 / 6L$, while the ULS moment is $+x$. A simple integration yields $w(0) = f_0 L^4 / (30EI)$.
- (b) The tip bending slope is $f_0 L^3 / (24EI)$.
- 20.9. (a) Only the beam bending integral is of importance here. The ULS consists of a counterclockwise unit-valued bending moment at $x = L/3$ that does CVW equal to $1w'(x = L/3)$, and the reactions at the supports that do no CVW. There is a small advantage to introducing a new coordinate ξ that originates at the right-hand support. In either case the bending moments are

$$0 \leq x \leq L/3 \quad \bar{M}(x) = \frac{x}{L} \quad M(x) = -\frac{2}{3}Fx$$

$$L/3 \leq x \leq L \quad \bar{M}(x) = \frac{x}{L} - 1 \quad M(x) = \frac{F}{3}(x - L)$$

or

$$0 \leq \xi \leq 2L/3 \quad \bar{M}(\xi) = -(\xi/L) \quad M(\xi) = -\frac{1}{3}F\xi$$

The important thing to note here is that, because of the discontinuity in the bending stiffness at $x = 2L/3$ or $\xi = L/3$, there are three integrals in the solution for the rotation $w'(x = L/3)$. The best choice of integration intervals to cover the entire length of the beam is $0 \leq x \leq L/3$, $0 \leq \xi \leq L/3$, and $L/3 \leq \xi \leq 2L/3$. The solution is

$$w'(x = L/3) = \frac{8FL^2}{729EI_0}$$

(d) $w(x = l) = \frac{13}{288} \frac{f_0 l^4}{EI_0}$

- 20.10. (a) The ULS consists of a unit moment at midspan, say clockwise, an upward reaction of magnitude $1/L$ at the right-hand end, and a downward reaction of the same magnitude at the left-hand end. It is better to use one Cartesian coordinate, x , that originates at the left-hand end, and another coordinate ξ that is positive to the left and originates at the right-hand end. Then

$$0 \leq x \leq \frac{1}{2}L \quad \bar{M}(x) = -\frac{x}{L} \quad M(x) = -\frac{f_0 Lx}{8}$$

$$0 \leq \xi \leq \frac{1}{2}L \quad \bar{M}(\xi) = +\frac{\xi}{L} \quad M(\xi) = -\frac{3f_0 L\xi}{8} + \frac{f_0 \xi^2}{2}$$

Integrating over both halves of the beam, and accounting for the change in beam stiffness, leads to the solution

$$w'(x = \frac{1}{2}L) = +\frac{f_0 L^3}{384EI_0}$$

where the positive sign means that the slope is in the same direction as the chosen unit moment.

- 20.11. (a) $w(L) = f_0 L^4 / (12EI_0) - M_0 L^2 / (2EI_0)$, which is, of course, positive upward. Note that the distributed loading and the concentrated moment are counter-vailing, and this is reflected in the opposite signs of their two contributions to the total solution.

20.12. (a) Tip vertical displacement = $F_0 L_1^3 / (3EI_1) + F_0 L_2^3 / (3EI_2) + F_0 L_2^2 L_1 / (GJ_1)$.

20.13. (a) Note that the ULS is exactly the same as the ALS if F_0 is set equal to a value of 1.0. The table of results is

Bar	L/EA coeff.	N	\bar{N}	$N\bar{N}L/EA$ coeff.
AB	1	$F_0/2$	$1/2$	$1/4$
AD	$\sqrt{2}/2$	$\sqrt{2}F_0/2$	$\sqrt{2}/2$	$\sqrt{2}/4$
BC	1	$F_0/2$	$1/2$	$1/4$
BD	1	0	0	0
CD	$\sqrt{2}/2$	$-\sqrt{2}F_0/2$	$-\sqrt{2}/2$	$\sqrt{2}/4$

Thus the horizontal deflection at joint D is $1.21 F_0 L / EA$.

(d) It would be a poor design because the longest member, which also has the least cross-sectional area, would now be the member in compression, and thus would be more likely to buckle.

20.15. (a) $w(0) = 7f_0 L^4 / (60EI_0)$.

(b) $w'(x=L) = -f_0 L^3 / (30EI_0)$, where the negative sign indicates that the bending slope is clockwise. In both cases $M(x) = (1/10)f_0 L^2 + (f_0/6L)x^3$, while $M(\xi) = (1/10)f_0 L\xi + (f_0/6L)\xi^3$. The first ULS could simply be an upward unit load at $x = 0$ and at $\xi = 0$ with a downward reaction of 2 at $x = \xi = L$. The second ULS could be a counterclockwise unit moment at $x = \xi = L$, reacted by forces of magnitude $1/L$ at the two supports.

(c) With the change in supports and loading, the left-hand reacting force has a downward magnitude of $11f_0 L / 12$, while the downward force at the right-hand support has the magnitude $7f_0 L / 12$. With a counterclockwise unit moment at the left-hand end, the ULS moments for $0 \leq x \leq L$, and $0 \leq \xi \leq L$, respectively, are

$$\bar{M}(x) = \frac{x}{2L} - 1 \quad \text{and} \quad \bar{M}(\xi) = -\frac{\xi}{2L}$$

The ALS moments are $M(x) = f_0 x^2 / 2 - 11f_0 Lx / 12$, and $M(\xi) = f_0 \xi^3 / 6L - 7f_0 L\xi / 12$. Carrying out the laborious integration, remembering that the stiffness along the right half of the beam of length $2L$ is $2EI_0$, yields the result that $w'(x=0) = +29f_0 L^3 / (120EI_0)$, where the positive sign means that the bending slope at the left-hand support is indeed counterclockwise

20.18. The key equations are as follows:

$$\sigma = \frac{E}{E_0} \left(\frac{N^c}{A^*} - z \frac{M_y^c}{I_{yy}^*} - E_0 \alpha \Delta T \right)$$

$$\delta \sigma = \frac{E}{E_0} \left(\frac{\delta N}{A^*} - z \frac{\delta M_y}{I_{yy}^*} \right) \quad \text{and} \quad \epsilon = \frac{\sigma}{E} + \alpha \Delta T$$

Integrating the product of the actual strain and the virtual stress over the cross-sectional area and then the beam length produces the result

$$\delta W_{in}^* = \int_0^L \left(\frac{N^c \delta N}{E_0 A^*} + \frac{M_y^c \delta M_y}{E_0 I_{yy}^*} \right) dx$$

20.20. The moment is

$$M(x) = + \int_{\xi=0}^{\xi=x} (x - \xi) f(\xi) d\xi$$

- 21.1. (a) This is the second of the previously discussed problems of Section 21.2 altered by the addition of a spring. The reaction at the base of the spring adds one redundant. Hence the minimum number of redundants is two.
- (b) There are four reactions: horizontal and vertical forces at the left support, a vertical force at the right footing, and a horizontal force at the far end of the spring. There are but three independent equations of equilibrium. Since there is no symmetry or other special circumstances associated with this structure, there is one redundant reaction. This is confirmed by choosing the force in the spring as that redundant, and demonstrating that all the other three reactions can be written in terms of that unknown force and the given loading, f_0 and M_0 .
- (c) Four reactions less three independent equilibrium equations equals one redundant, say the force in the spring.
- (d) Six reactions minus three independent equilibrium equations equals three redundant reactions. They could be all three reactions (moment, shear force, and axial force) at either support.
- (e) There are three external vertical reactions and one external horizontal reaction. There are three applicable equations of equilibrium for the structure as a whole. Thus there is one external redundant, say the vertical reaction at the right hand support. There is also one internal redundant bar force because each joint in the second of the four bays joins four bars. If, for example, the force in one of the diagonals of that second bay were known (as well as all external reactions), then all the bar forces in that truss could be determined using static equilibrium equations for the pin joints. Hence the total number of redundant forces is 2.
- (j) The easiest approach to this frame is to cut the "floor" beams at points A and B . At each cut there are three internal reactions: a shear force, an axial force, and a bending moment. If these six quantities are known, then all the stress resultants everywhere throughout the left-hand and right-hand portions of the structure would be known, including the support reactions at both base supports, by the use of static equilibrium equations. If fewer than these six pieces of information are available, then, for example, all the base support reactions could not be determined. Therefore, this frame has a total of six redundant reactions. They could be chosen to be the six quantities discussed above, or the six base reactions, or they could be, for example, the three support reactions at point C plus the three internal stress resultants at point B . As an aside, a ULM analysis of this structure and loading would require the solution of six simultaneous equations, which is beyond the pale of reasonable handwork today. However, the new hand-held calculators with their algebraic equation solution capabilities do make this problem a candidate for a ULM solution in the absence of computer facilities.
- 21.2 (a) The reactions have the same value of $(3/8)f_0L$ at the end supports and $(5/4)f_0L$ at the center support. The reason that the increased stiffness of the left-hand span does not affect the magnitudes of the reactions is that, in this very unusual case, the change in stiffness does not change the deflection pattern. It only changes the magnitudes of the deflections. Hence there is no

change in the relative distribution of the forces, and of course there is no change in the sum of all the forces.

- (b) The left-hand support reaction is a force of magnitude $7f_0L/16$ acting downward; $10f_0L/16$ downward at the center support; and $f_0L/16$ upward at the right-hand support.

21.3. (a) A stiffer spring shoulders more of the loading. Therefore, the force in the spring can be expected to increase, while the force at the wall decreases. The moment at the wall should also decrease because of the increase in the magnitude of the force in the spring.

- (b) The force in the spring is now $(15/52)f_0L$, up from a value of $(13/52)f_0L$.

21.4. (a) There are four reactions, and two independent equations of equilibrium. Thus there are two redundant reactions.

- (b) Following instructions, the redundant reactions are the downward force at the roller, γ_1 , and the downward force at the base of the spring, γ_2 . Since a coordinate is being used that starts at the right-hand end, there is no need to calculate the two reactions at the wall. That is, the ALS moments can be obtained without involving that moment and shear force. Two likely choices among the possible ULSs are (i) a ULS with a downward unit load at the right end of the beam reacted at the wall with an upward unit force and a counterclockwise moment of magnitude $2L$ (and no force in the spring); and (ii) a unit tensile force in the spring that leads to a unit downward force on the beam at midspan that is reacted at the wall with an upward unit force and a counterclockwise moment of magnitude L . Another possible choice of ULS is one like the second of the above, but with upward force reactions of magnitude $\frac{1}{2}$ at each end of the beam. The ALS and ULS moments and spring forces are

$$0 \leq x \leq L \quad M(x) = \frac{1}{2}f_0x^2 - x\gamma_1 \quad N = +\gamma_2$$

$$L \leq x \leq 2L \quad M(x) = f_0Lx - \frac{f_0L^2}{2} - x\gamma_1 - \gamma_2(x-L)$$

$$(i) \quad 0 \leq x \leq L \quad \bar{M}(x) = -x \quad \bar{N} = 0$$

$$L \leq x \leq 2L \quad \bar{M}(x) = -x$$

$$(ii) \quad 0 \leq x \leq L \quad \bar{M}(x) = 0 \quad \bar{N} = +1$$

$$L \leq x \leq 2L \quad \bar{M}(x) = -x + L$$

All that is necessary to do now is to substitute the above ALS quantities and, successively, the ULS quantities into the spring CVW term and the beam bending CVW integrals and set each sum equal to zero.

- 21.5. (a) With or without using symmetry, there is one more reaction than there are independent equations of equilibrium. Let that one redundant be the downward reaction at the base of the spring. Then the two equal downward outboard reactions at the beam ends have the magnitudes $R = \frac{1}{2}[f_0L + F - \gamma]$. Since the structure and loading are symmetric about midspan, it is only necessary to study the left-hand side of the beam where, for $0 \leq x \leq L$,

$$M(x) = \frac{1}{6} \frac{f_0x^3}{L} - \frac{1}{2}x[f_0L + F - \gamma] \quad \text{and} \quad N = +\gamma$$

A symmetric ULS is desired. The only choice is a unit tensile force in the spring causing a downward unit force on the beam at midspan, which is reacted by

upward forces of magnitude $\frac{1}{2}$ at each beam end. Then setting the sum of (i) the spring CVW term, and (ii) twice the CVW bending integral over the left-hand side of the beam, equal to zero yields

$$\Upsilon = \frac{1}{2}F + \frac{2}{5}f_0L \quad \text{and} \quad R = \frac{1}{4}F + \frac{3}{10}f_0L$$

- (b) If the right-hand reaction is declared redundant, then the center reaction is $\frac{3}{2}f_0L - 2\Upsilon$, and so on. The ULS consists of, say, two unit forces acting downward at the beam ends while an upward force of magnitude 2 is at the center. Note that the ULS is in both force and moment equilibrium.

$$M(x) = \left(\frac{1}{2}f_0L - \Upsilon\right)x \quad \bar{M}(x) = -x, \quad M(\xi) = \frac{1}{2}f_0\xi^2 - \Upsilon\xi \quad \bar{M}(\xi) = -\xi$$

After integration, $\Upsilon = 11f_0L/24$, downward. If, on the other hand, the left-hand reaction is chosen to be redundant, the ALS reactions and moments change, but the ULS turns out to be the same as (or the negative of) that above. The solution for that redundant is $\Upsilon = f_0L/24$, upward. If the center reaction is chosen to be the redundant, again the ULS is proportional to the others. The solution for the center support turns out to be $14f_0L/24$, downward.

- (c) If the center reaction is Υ upward, the end reactions are $(\frac{1}{4}f_0l + \frac{1}{2}\Upsilon)$ downward. Then $\Upsilon = 8\frac{EI_0}{l^3}v_0 - \frac{f_0l}{10}$.

- 21.6. (a) There is one redundant bar force/reaction. Let it be the reaction at point C. Then the ULS begins with, say, a downward unit force at the bottom end of bar AC. Then

Member	(L/EA) coeff.	N	\bar{N}	$N\bar{N}L/(EA_0)$
AB 1	5/2	(5/8)(F - Υ)	-5/8	-(125/128)(F - Υ)L/EA ₀
AC 2	4	Υ	1	4 Υ L/EA ₀
AD 3	5/2	(5/8)(F - Υ)	-5/8	-(125/128)(F - Υ)L/EA ₀

The sum of the terms in the last column is the total CVW, and setting it to zero nullifies the release at support C, and creates a single equation for Υ . Its solution, and the solutions for the stresses are

$$\Upsilon = \frac{125}{381}F \quad \sigma_1 = \sigma_3 = \frac{80}{381}\frac{F}{A_0}, \quad \sigma_2 = \frac{125}{381}\frac{F}{A_0}$$

- (c) Since the structure and loading are symmetric, there is only a single redundant bar force. Select, for example, as the tensile force in bar AC, and thus for bar AD as well, the redundant Υ . Then summing vertical force components at joint A leads to the conclusion that the tensile forces in bars AB and AE are of magnitude $F/\sqrt{2} - (\sqrt{3}/\sqrt{2})\Upsilon$. The single ULS can be unit tensile forces in bars AC and AD, and compressive forces of magnitude $\sqrt{3}/\sqrt{2}$ in bars AB and AE. This ULS is, of course, in equilibrium, and it does zero CVW when the deflections at supports C and D are required to be zero. Now it is simply a matter of setting the sum of the $N\bar{N}(L/EA)$ terms for the four bars equal to zero. Then $\Upsilon = 0.28F$.
- (d) Let the compressive force in bar BC (and bar BD) be the single redundant Υ . Then the tensile forces in bars AB and BE are $(F/\sqrt{3}) - \Upsilon$. Several simple ULSs are evident. Compressive unit forces in all four bars is one possibility.

Another possibility is tensile or compressive unit forces in collinear bars such as AB and AD . Regardless of the choice of ULS, setting the sum of $N\bar{N}(L/EA)$ terms to zero yields the solution $\Upsilon = (2\sqrt{3}/9)F = 0.385F$. In this case where the geometry of the deflection of all four bars is the same, it is again clear that the stiffer pair of bars, BC and BD , take most (77 percent) of the applied load.

- 21.7. (a) There is one redundant reaction. Let it be the compressive force in the vertical spring. Ignoring the beam axial force CVW in preference to beam bending CVW, for the ALS: $M(x) = x\Upsilon$, $M(y) = -y[(M_0/L) - \Upsilon]$, $N_v = -\Upsilon$, and $N_h = -(M_0/L) + \Upsilon$. The ULS starts with a unit force at the base of the vertical spring. The final solution is $\Upsilon = M_0/(2L)$.
- (b) Again, $\Upsilon = M_0/(2L)$. The answer could have been anticipated without any resort to a ULM analysis by rotating the two-beam frame about point A while viewing the radial line AC . The equal leg geometry of the frame causes the movement of point C to compress the two springs equally. With the knowledge that the forces in the two springs are equal, the problem becomes statically determinate.
- (c) One choice for the two ULSs is the pair obtained from Fig. 21.26(c) by first setting $\Upsilon_1 = 1$, F_0 and Υ_2 equal to zero, and then $\Upsilon_2 = 1$, F_0 and Υ_1 equal to zero. In case 1,

$$\bar{M}(\zeta) = -\zeta \quad \bar{M}(\eta) = -\eta \quad \bar{M}(x) = -L \quad \bar{N}_1 = 0 \quad \bar{N}_2 = -1$$

In the case of the second ULS described above,

$$\bar{M}(\zeta) = -\zeta \quad \bar{M}(\eta) = 0 \quad \bar{M}(x) = -\frac{1}{2}x \quad \bar{N}_1 = 1 \quad \bar{N}_2 = 0$$

- 21.8. (a) The horizontal reaction at point C is zero. Therefore, there are four nonzero reactions, and but two equilibrium equations. Choose the tensile force in the spring at point A to be Υ_1 , and the tensile force in the spring at point B to be Υ_2 . (Negative solutions are to be expected.) Then the vertical reaction at point C is $(\Upsilon_1 + \Upsilon_2)$ upward, and the counterclockwise moment at point C is $(M_0 + 2\Upsilon_1L + \Upsilon_2L)$. A sure way to obtain independent ULSs is to start each ULS with a unit tensile force in one spring with no ULS force in the other spring. Another ULS that is independent of either, but not both, of the first two suggested ULSs is one where there is a unit force in inner spring that is balanced by forces of magnitude $\frac{1}{2}$ acting in the opposite direction at the outer spring base and at point C . This ULS has the advantage of there not being a ULS moment in the vertical beam. There are still other possibilities.
- (b) There are two redundant reactions: Υ_1 at point A , and Υ_2 at point B . Let these two reactions be directed so that the two springs are in tension. Then the moment expressions and spring forces are

ALS	ULS1	ULS2
$M(y) = \frac{1}{2}f_0y^2 - \Upsilon_1y$	$\bar{M}(y) = -y$	$\bar{M}(y) = 0$
$M_t(y) = 0$	$\bar{M}_t(y) = 0$	$\bar{M}_t(y) = 0$
$M(x) = (2f_0L - \Upsilon_1 - \Upsilon_2)x$	$\bar{M}(x) = -x$	$\bar{M}(x) = -x$
$M_t(x) = -2L(f_0L - \Upsilon_1)$	$\bar{M}_t(x) = 2L$	$\bar{M}_t(x) = 0$
$N_1 = \Upsilon_1, N_2 = \Upsilon_2$	$\bar{N}_1 = 1, \bar{N}_2 = 0$	$\bar{N}_1 = 0, \bar{N}_2 = 1$

The second of the two simultaneous equations reduces to $2f_0L = \Upsilon_1 + 2\Upsilon_2$.

- 21.9. This is an interesting problem because of the various load paths that diffuse the applied load F , which also permit a wide variety of choice for ULSs. The best way to decide upon the number of redundants here is sketch FBDs of each of the four elastic elements. Again, there are no horizontal reactions. On the top cantilevered beam, the spring reaction is one redundant, which carries through to the bottom cantilevered beam. The reaction of the bottom spring on the bottom cantilevered beam is the second redundant. Thus choose the forces in the springs as the two redundants. When they are calculated, the stress resultants in the beams will also be known. This is a problem where not requiring the ULS's unit loads to follow the pattern of the redundant loads of the ALS saves computational effort.
- (a) The reaction at the base of the bottom spring is $12F/33$.
 - (d) The tip deflection is $5FL^3/(33EI_0)$. (As a result of the special circumstances of the one applied loading having the simple form and location that it has, this problem as it stands is most easily done by the "equivalent spring" stiffness method rather than the ULM force/flexibility approach. However, a small change in the loading, such as in part (e), would greatly complicate the "equivalent spring" approach. The "equivalent spring" approach is explained in most mechanical vibration textbooks.)
- 21.10. (a) While the external reactions of the truss are statically determinate, there is one internal redundancy. A suitable choice for the redundant bar force is any one of the bar forces. If the bar force in member AC is chosen, call it γ . Then all the other bar forces of the ALS can be calculated in terms of γ and the two applied forces. The release associated with this redundant can be visualized as a cut entirely through the bar anywhere along its length with a pipe acting as a sleeve around the cut so as to maintain the geometry of the truss as a whole. In less graphic terms, the release is a nullification of the continuity of the deflections of the bar while maintaining the continuity of the force in the bar. The ULS that is needed to reestablish that deflection continuity would start with oppositely directed unit forces on the two faces of the cut. Setting the CVW done by these two unit forces to zero means that the two unit forces are required to have the same deflection, and that reestablishes the deflection continuity and provides an equation by which the redundant force may be calculated.
- (c) Superposition of the external loads results in superposition of the internal reactions whenever the deflections are small.
- 21.11. Not only do engineers have to analyze structural designs with various load combinations, but in addition to analyzing structures as they are intended to be, engineers may also have to analyze various modifications to the ideal structure. Modifications on the ideal structure may result from poor workmanship, improper maintenance, mismanagement by vehicular operators (such as following banned fuel burn sequences in a large aircraft, resulting in unfavorable weight distributions), and limited structural failures. There also may be significant loadings imposed upon the structure during the course of its construction. This exercise is meant to reflect those various circumstances. In this exercise, the otherwise fully symmetric structure's right-hand support is without (has lost?) the capability of resisting torques.

The ALS contains both bending moments and twisting moments, and so too do the two ULSs. The ALS is pictured in Fig. 21.30, but it might be beneficial to redraw it for clarity. The first ULS can be obtained from the ALS by deleting the

applied force F_0 and moment F_0L , and setting $\gamma_1 = 0$, and $\gamma_2 = 0$. The second ULS can be determined by again removing the applied loads and setting $\gamma_1 = 0$, and $\gamma_2 = 1$. The moment expressions for each of the three beams are, for $0 \leq x \leq L$, $0 \leq y \leq 2L$, and $0 \leq z \leq L$ respectively,

ALS	ULS1	ULS2
$M(x) = \gamma_1 x - \gamma_2$	$\overline{M}(x) = +x$	$\overline{M}(x) = -1$
$M_t(x) = 3F_0L - 2\gamma_1L$	$\overline{M}_t(x) = -2L$	$\overline{M}_t(x) = 0$
$M(y) = 3F_0L - 2L\gamma_1 + (\gamma_1 - F_0)y$	$\overline{M}(y) = -2L + y$	$\overline{M}(y) = 0$
$M_t(y) = \gamma_2 - \gamma_1L$	$\overline{M}_t(y) = -L$	$\overline{M}_t(y) = +1$
$M(z) = (F_0 - \gamma_1)z - F_0L + \gamma_2$	$\overline{M}(z) = -z$	$\overline{M}(z) = +1$
$M_t(z) = 0$	$M_t(z) = 0$	$M_t(z) = 0$

Now it is necessary to substitute these bending and twisting moments into their integral expressions, taking care to insert the correct bending and twisting stiffness factors in each integral, and using the limits of integration stated above.

- 21.12.** (a) The answer is the same as in Example 21.10.
 (b) The respective forces are $2F/9$, $3F/9$, and $4F/9$.
- 21.13.** (a) Neither the loading nor the half-ring structure, because of the different supports, is symmetric. There are three reactions at the fixed support at $\phi = 0$, and one vertical force reaction at $\theta = 0$, and a horizontal force reaction at the far end of the spring. There are only three independent equations of equilibrium. Let the two redundant reactions be the tensile force in the spring, γ_1 , and the vertical reaction, γ_2 , positive downward, at $\theta = 0$. At $\phi = 0$, the upward axial force is $(\gamma_2 - F_1)$; the leftward shear force is $(\gamma_1 + F_2)$; and the bending moment reaction is $R(F_1 - F_2 - 2\gamma_2)$. The first ULS starts with a unit tensile force applied to the spring. It is finally reacted by a unit shear force at $\phi = 0$. The second ULS starts with a positive unit axial force at $\theta = 0$, no force in the spring, and it is finally reacted at $\phi = 0$ by a compressive unit axial force and a counterclockwise moment of magnitude $2R$. The moments for $0 \leq \theta, \phi \leq \pi/2$ are

$$\begin{aligned}
 \text{ALS: } M(\theta) &= R[\gamma_1 \sin \theta - \gamma_2(1 - \cos \theta)] & N &= +\gamma_1 \\
 M(\phi) &= R[F_1 \cos \phi - F_2(1 - \sin \phi) + \gamma_1 \sin \phi - \gamma_2(1 - \cos \phi)] \\
 \text{ULS1: } \overline{M}(\theta) &= R \sin \theta & \text{ULS2: } \overline{M}(\theta) &= -R(1 - \cos \theta) \\
 \overline{M}(\phi) &= R \sin \phi & \overline{M}(\phi) &= -R(1 + \cos \phi) \\
 \overline{N} &= +1 & \overline{N} &= 0
 \end{aligned}$$

The problem is completed when, for each ULS, the above moments and spring forces are substituted appropriately into a bending moment integral between zero and $\pi/2$ for θ , another such for ϕ , and the spring CVW term.

- 21.17.** (b) The key equations are $N(x) = N$, $\sigma = N/A$, $\delta\sigma = \delta N/A$, $\epsilon = \text{constant} = (N/EA) + \beta(N/EA)^n$. Then substitution into the PCVW yields $u(L) = (NL/EA) + \beta L(N/EA)^n$.
- 21.19.** (e) Yes, superposition is valid because both the mechanical and thermal force resultants are determined from linear analyses just as they were when the beam differential equations were derived.
- 22.1.** (a) Since there is no resistance to a bending slope $w_{,x}$, the reacting bending moment $M_x(a, y)$ must be zero. Hence, in the absence of a temperature change,

$w_{,xx}(a, y) + \nu w_{,yy}(a, y) = 0$. The second term is present in this case because neither $w(a, y)$ nor $w_{,y}(a, y)$ are zero as they would be at a simply supported edge. The second boundary condition is arrived at by drawing a FBD of “one” of the spring edge supports at a differential length of the plate edge. The force acting at the point the spring is attached to the plate is $V_x(a, y)dy$. The force acting at the outer end of the spring is $(k dy)w(a, y)$. These two oppositely directed forces are in equilibrium, and are therefore equal to each other. Thus the second BC is

$$w_{,xxx}(a, y) + (2 - \nu)w_{,xyy}(a, y) = \frac{k}{D}w(a, y)$$

- (b) The deflection BC is simply $w(x, mx + b) = 0$. Note that along this skewed edge, as along any line, only one parameter is needed to locate a position. In this case x has been chosen as that parameter. As for the slope BC, let the local coordinates (s, n) be such that the counterclockwise arc length coordinate s runs down to the left, while the outer normal coordinate n runs upward to the left. Then using the chain rule: $w_{,n} = (w_{,x})(x_{,n}) + (w_{,y})(y_{,n})$. The second factor in each term is a constant because the edge is straight. With θ being the angle between the positive x axis and the negative s axis, the coordinate relations $x = -s \cos \theta - n \sin \theta$ and $y = -s \sin \theta + n \cos \theta$ show that $x_{,n} = -\sin \theta$ while $y_{,n} = +\cos \theta$. Since $m = \tan \theta$, setting up a triangle with a base length of 1, a height of m , and a hypotenuse of $[1 + m^2]^{1/2}$ shows that $\sin \theta = m/[1 + m^2]^{1/2}$, while $\cos \theta = 1/[1 + m^2]^{1/2}$. Therefore, the slope BC can be written as

$$0 = -mw_{,x}(x, mx + b) + w_{,y}(x, mx + b)$$

- (c) The bending moment equation reduces to $w_{,nn}(x, mx + b) = 0$. To put this entirely in Cartesian coordinate terms, the chain rule is used twice. That is, from the above answer for $w_{,n}$ where $x_{,n}$ and $y_{,n}$ are constants, write

$$\begin{aligned} w_{,nn} &\equiv \frac{\partial(w_{,n})}{\partial n} = \frac{\partial w_{,n}}{\partial x}x_{,n} + \frac{\partial w_{,n}}{\partial y}y_{,n} \\ &= w_{,xx}(x_{,n})^2 + 2w_{,xy}y_{,n}x_{,n} + w_{,yy}(y_{,n})^2 \end{aligned}$$

The reader can finish by inserting the proper argument for the deflection function and the values for $x_{,n}$ and $y_{,n}$ found above.

- 22.2. (a)** The GDE for the harmonically vibrating thin plate is

$$D[w_{,xxxx} + 2w_{,xxyy} + w_{,yyyy}] + \rho h w_{,tt} = f_0 \sin(\pi t/t_0)$$

It can be shown that there exists what is called a “variables separable” solution for the above equation that must have the form $w(x, y; t) = W(x, y) \sin(\pi t/t_0)$. Thus the time variable in the above partial differential equation can be quickly removed so as to arrive at the simpler equation

$$D[W_{,xxxx} + 2W_{,xxyy} + W_{,yyyy}] - \left(\frac{\pi}{t_0}\right)^2 \rho h W = f_0$$

- (b) The second partial derivative with respect to θ can be dropped from the ∇^2 operator in polar coordinates because the lateral deflection is only a function of the radial coordinate when the loading is axisymmetric. The remaining

partial derivatives with respect to r become total derivatives. The ∇^2 operator acting upon the ∇^2 produces the following GDE:

$$D \left[w''''(r) + \frac{2}{r} w'''(r) - \frac{1}{r^2} w''(r) + \frac{1}{r^3} w'(r) \right] = f(r)$$

However, this form is *not* the best way to approach this problem. It is better to leave the GDE as

$$\left[\frac{d^2}{dr^2} + \frac{1}{r} \frac{d}{dr} \right] \left[\frac{d^2 w}{dr^2} + \frac{1}{r} \frac{dw}{dr} \right] = \frac{f_0}{D}$$

In fact the above GDE can be expressed entirely as a product of four derivative operators, (Ref. [55]) but that is not really necessary.

- (c) The complementary solution is obtained as follows. Let $[(d^2 w/dr^2) + (1/r)(dw/dr)] \equiv F(r)$. Then $[(d^2 F/dr^2) + (1/r)(dF/dr)] = 0$. Let $F' \equiv G$. Then $G' + (1/r)G = 0$. The solution to this first order equation is simply $G = C_1/r$. Then integrate $G(r)$ once to obtain $F = C_1 \ln r + C_2$. Let $w' \equiv H$. Then $H' + (1/r)H = C_1 \ln r + C_2 = C_1 (\ln r - 1) + (C_1 + C_2)$. The complementary solution is again $H = C_3/r$. The particular solution is $C_1[\frac{1}{2}r \ln r - \frac{3}{4}r] + \frac{1}{2}(C_1 + C_2)r = \frac{1}{2}C_1 r \ln r - \frac{1}{4}C_1 r + \frac{1}{2}C_2 r$. Integrating the total solution for $H = w'$, and simplifying the constants of integration yields the complementary solution

$$w_c(r) = A_1 + A_2 r^2 + A_3 \ln r + A_4 r^2 \ln r$$

The particular solution for a constant pressure can be found from the trial function $w = cr^4$. Substitution in either form of the GDE quickly leads to $w_p(r) = f_0 r^4 / (64D)$. Of course, the total solution is $w = w_c + w_p$.

- (d) The GDE is simply $\nabla^4 w(x, y)$ equals zero. The constant thermal moment enters into the BCs, which are

$$w(0, y) = w(a, y) = w(x, 0) = w(x, b) = 0$$

$$w_{,xx}(0, y) = w_{,xx}(a, y) = w_{,yy}(x, 0) = w_{,yy}(x, b) = \frac{M_0}{D}$$

- 22.3. (a) As developed in Eq. (22.18), the small, lateral deflection solution for a simply supported rectangular plate can be written as

$$w(x, y) = \sum \sum \frac{f_{mn}}{D[(m\pi/a)^2 + (n\pi/b)^2]^2} \sin(m\pi x/a) \sin(n\pi y/b)$$

In the uniform load case, each of the above summations is limited to odd values only, and $f_{mn} = 16f_0/(\pi^2 mn)$.

- 22.5. It is better to place the grid of beams above the plate so that the plate is in compression and the beams are mostly in tension. When the plate buckles, it can continue to support even greater pressure loadings until there is general material yielding in the plate. The reverse design would have the beams buckling, locally or over their entire length, and not being able to support significant increases in the pressure loading.
- 22.6. At the outer edges, $w(R) = w'(R) = 0$. It is equally clear that $w'(0) = 0$. This last statement includes the statement that the deflection is a maximum at $r = 0$. Applying this last BC to the general solution for $w(r)$ leads to the immediate conclusion that A_3 must equal zero in order for the slope to be zero at $r = 0$.

Another reason A_3 has to be zero is that the deflection needs to be finite at $r = 0$. One more BC needs to be found at $r = 0$. To this end, note that $w''(r) = 9f_0r^2/(64D) + 2A_2 + A_4(2\ln r + 3)$. In order for this curvature to be finite, A_4 must be zero. Then using the first two BCs to solve for A_1 and A_2 leads to the final solution.

$$w(r) = \frac{f_0}{64D}(R^2 - r^2)^2$$

This is a good example of a case where it might be a lot less work to guess a polynomial answer to begin with.

- 22.7. In the strain equation, $\epsilon_{xx}(x, y, z) = u_{,x} - z\theta_{y,x}$, the first linear term is the strain of the midplane (where $z = 0$), while the second linear term provides the change in that strain away from the midplane according to the Kirchhoff hypothesis. While accounting for finite deflections, the Kirchhoff hypothesis, and hence the second of the two strain terms, remains the same. However, the first term must now include the dominant nonlinear part of Eq. (3.12). That is, since $u', v' \ll w'$ in any direction, the single nonlinear term to be added to the above strain expression is $+\frac{1}{2}(w_{,x})^2$. Just as is the case for beams, this nonlinear term is not necessary if the midplane does not have to stretch so that the thin plate can bend to amplitudes greater than its thickness. An example of a situation where the midplane would not have to stretch is the case where the thin plate bent into a "deveopable" surface, such as a cylindrical surface. A *deveopable* surface is one that can be achieved by bending a flat plane (like a piece of paper) without stretching or cutting it. The surface of a cone, for example, is a developable surface, but a spherical surface is not. Developable midplane surfaces for plates are unusual in engineering. In almost all engineering applications, the plate boundary conditions are such that the midsurface must stretch in order for the plate to have small or finite deflections.
- 22.8. (a) For large values of a/b , the factor k approaches 7 rapidly; that is, after $a/b = 3.0$, k is everywhere very close to 7.0.
 (b) For large values of a/b , the factor k approaches 4 slowly.
 (c) For values of a/b greater than 3.0, $k \approx 0.4$ from Ref. [63].
- 22.9. The equation for the isotropic, rectangular plate bending element stiffness matrix is Eq. (22.23). The first of the three integrals produces the result $h^3/12$. The second part of this equation involves a double integral of a triple matrix product that results in a 12×12 matrix. Since the goal is just the (7, 7) element of the 12×12 matrix, it is only necessary to calculate the seventh row of $[B]^t$ and the seventh column of $[E][B]$. The matrix $[B]$ is specified immediately above Eq. (22.23). That is, since $w(\zeta, \eta) = [N(\zeta, \eta)]\{q\}$, the seventh column of the 3×7 matrix $[B]$ is $[N_{7,xx} \ N_{7,yy} \ 2N_{7,xy}]^t$. Now, from Eq. (6.18), the matrix

$$[E] = \frac{E}{1 - \nu^2} \begin{bmatrix} 1 & \nu & 0 \\ \nu & 1 & 0 \\ 0 & 0 & \frac{1}{2}(1 - \nu) \end{bmatrix}$$

Thus the seventh column of $[EB]$ has the elements $(N_{7,xx} + \nu N_{7,yy})$, $(\nu N_{7,xx} + N_{7,yy})$, $(1 - \nu)N_{7,xy}$, all with the factor $E/(1 - \nu^2)$. Therefore, the (7, 7) element of $[B]^t EB]$ is the four-term sum

$$\frac{E}{1 - \nu^2} [(N_{7,xx})^2 + (N_{7,yy})^2 + 2\nu N_{7,xx}N_{7,yy} + 2(1 - \nu)(N_{7,xy})^2]$$

Thus now it is merely a matter of fighting one's way through the algebra. First of all, with $\zeta = x/a$, and $\eta = y/b$,

$$N_7(\zeta, \eta) = +\frac{1}{8}(1 + \zeta)(1 - \eta)(2 + \zeta - \eta - \zeta^2 - \eta^2)$$

so

$$N_{7,xx} = -\frac{3}{4a^2} \frac{x}{a} \left(1 - \frac{y}{b}\right)$$

$$N_{7,yy} = +\frac{3}{4b^2} \frac{y}{b} \left(1 + \frac{x}{a}\right)$$

$$N_{7,xy} = -\frac{1}{8ab} \left[4 - 3\left(\frac{x}{a}\right)^2 - 3\left(\frac{y}{b}\right)^2\right]$$

and

$$(N_{7,xx})^2 = \frac{9}{16a^4} \left(\frac{x}{a}\right)^2 \left[1 - 2\frac{y}{b} + \left(\frac{y}{b}\right)^2\right]$$

$$(N_{7,yy})^2 = \frac{9}{16a^4} \left(\frac{y}{b}\right)^2 \left[1 + 2\frac{x}{a} + \left(\frac{x}{a}\right)^2\right]$$

$$(N_{7,xy})^2 = \frac{1}{64a^2b^2} \left[16 - 24\left(\frac{x}{a}\right)^2 - 24\left(\frac{y}{b}\right)^2 + 18\left(\frac{x}{a}\right)^2 \left(\frac{y}{b}\right)^2 + 9\left(\frac{x}{a}\right)^4 + 9\left(\frac{y}{b}\right)^4\right]$$

$$(N_{7,xx})(N_{7,yy}) = -\frac{9}{16a^2b^2} \left[\frac{xy}{ab} + \left(\frac{x}{a}\right)^2 \frac{y}{b} - \frac{x}{a} \left(\frac{y}{b}\right)^2 - \left(\frac{x}{a}\right)^2 \left(\frac{y}{b}\right)^2\right]$$

Now it is a matter of integrating. The easiest thing to do is to modify the iterated double integral by multiplying and dividing by (ab) so that the variables are ζ and η and the limits of integration are now $(-1, +1)$ for both the x or ζ , and the y or η integrals. The integrals of

$$\frac{E}{1 - \nu^2} [(N_{7,xx})^2 + (N_{7,yy})^2 + 2\nu N_{7,xx}N_{7,yy} + 2(1 - \nu)(N_{7,xy})^2]$$

are

$$\frac{E}{1 - \nu^2} \left(\frac{9}{16a^4} (2/3)(8/3) + \frac{9}{16b^4} (8/3)(2/3) - 2\nu \frac{9}{16a^2b^2} [0 + 0 - 0 - (4/9)] + 2(1 - \nu) \frac{1}{64a^2b^2} [64 - 32 - 32 + 8 + (36/5) + (36/5)] \right)$$

Therefore,

$$\begin{aligned} k_{7,7} &= ab \frac{Eh^3}{12(1 - \nu^2)} \left(\frac{1}{a^4} + \frac{1}{b^4} + \frac{\nu}{2a^2b^2} + (1 - \nu) \frac{7}{10a^2b^2} \right) \\ &= \frac{Dab}{60a^2b^2} \left(\frac{60}{p^2} + 60p^2 + 42 - 12\nu \right) \end{aligned}$$

Q.E.D

22.10. (b) Let the time-varying deflection solution have the form

$$w(x, y, t) = \sin(ft/2\pi) \sum X_n(x) \sin(n\pi y/b)$$

Then substituting this solution form into the GDE (see the solution to Exercise 22.2) produces the following differential equation to be solved for each $X_n(x)$:

$$X_n''''(x) - 2 \left(\frac{n\pi}{b} \right)^2 X_n''(x) + \left[\left(\frac{n\pi}{b} \right)^4 - \frac{\rho f^2 h}{4\pi^2 D} \right] X_n(x) = 0$$

The characteristic equation for an exponential solution is

$$r^4 - 2 \left(\frac{n\pi}{b} \right)^2 r^2 + \left[\left(\frac{n\pi}{b} \right)^4 - \frac{\rho f^2 h}{4\pi^2 D} \right] = 0$$

The four roots to this quartic are r_n , $-r_n$, s_n , and $-s_n$, where

$$r_n = \left[\left(\frac{n\pi}{b} \right)^2 + \frac{f}{2\pi} \left(\frac{\rho h}{D} \right)^{1/2} \right]^{1/2}$$

$$s_n = \left[\frac{f}{2\pi} \left(\frac{\rho h}{D} \right)^{1/2} - \left(\frac{n\pi}{b} \right)^2 \right]^{1/2} \quad \text{if } n < \bar{n}$$

$$s_n = \left[\left(\frac{n\pi}{b} \right)^2 - \frac{f}{2\pi} \left(\frac{\rho h}{D} \right)^{1/2} \right]^{1/2} \quad \text{if } n \geq \bar{n}$$

where

$$\bar{n} = \frac{b}{\pi} \left(\frac{f}{2\pi} \right)^{1/2} \left(\frac{\rho h}{D} \right)^{1/4}$$

Then, converting the exponential solutions to circular and hyperbolic functions, the total solution can be written as

$$X_n(x) = C_{1,n} \sinh(r_n x) + C_{2,n} \cosh(r_n x) \\ + C_{3,n} \sin(\text{h})(s_n x) + C_{4,n} \cos(\text{h})(s_n x)$$

where, for example,

$$\sin(\text{h})(s_n x) = \begin{cases} \sin s_n x & \text{if } n < \bar{n} \\ \sinh s_n x & \text{if } n \geq \bar{n} \end{cases}$$

It now remains for the above constants of integration to be determined by use of the BCs. The BCs at $y = 0, b$ are identically satisfied, and require no further attention. The BCs at $x = 0$ lead to $X_n(0) = C_{2,n} + C_{4,n} = A_n$, and $X_n'(0) = r_n C_{1,n} + s_n C_{3,n} = B_n$. The BCs at $x = a$ lead to $X_n(a) = X_n''(a) = 0$. Completing the algebra yields the solution necessary to determine the four constants of integration with the result

$$w(x, y; t) = W(x, y) \sin(ft/2\pi)$$

where

$$W(x, y) = \sum J_n \{ A_n [s_n \cos(\text{h}) s_n a \sinh r_n (a - x) \\ - r_n \cosh r_n a \sin(\text{h}) s_n (a - x)] \sin(n\pi y/b) \\ + \sum J_n \{ B_n [\sin(\text{h}) s_n a \sinh r_n (a - x) \\ - \sinh r_n a \sin(\text{h}) s_n (a - x)] \sin(n\pi y/b) \}$$

where

$$1/J_n = s_n \sinh r_n a \cos(h) s_n a - r_n \cosh r_n a \sin(h) s_n a$$

The quantity $1/J_n$ is often the small difference of two large numbers. A loss of three significant figures would not be unusual. Therefore, this value should be calculated by using as many significant figures as possible.

- 23.1.** Yes. The reason that the uniform modeling is acceptable is that the beam bending moments that cause the bar to buckle are greatest at the center of the rod where the rod is truly uniform. However, a better solution can be obtained using several finite elements that can account for the changes in geometry at the bar ends.
- 23.2. (a)** The global BCs are now that $w_1 = \theta_1 = w_3 = 0$, that is, in particular, θ_2 is not zero. The axial loading matrices for the left and right-hand halves of the beam, respectively, with $l = L/2$, are

$$P[h]\{q\} = \frac{P}{30l} \begin{bmatrix} 72 & -6l \\ -6l & 8l^2 \end{bmatrix} \begin{Bmatrix} w_2 \\ \theta_2 \end{Bmatrix}$$

$$P[h]\{q\} = \frac{P}{30l} \begin{bmatrix} 36 & 3l & 3l \\ 3l & 4l^2 & -l^2 \\ 3l & -l^2 & 4l^2 \end{bmatrix} \begin{Bmatrix} w_2 \\ \theta_2 \\ \theta_3 \end{Bmatrix}$$

The stiffness matrices for the two beam halves are written as usual. Then the matrix eigenvalue problem is composed and solved for the lowest value of P .

- 23.3. (a)** Since the beam-wing can twist without bending, and vice versa, the matrix eigenvalue problem becomes

$$\frac{GJ}{L} \begin{bmatrix} 2 & -1 \\ -1 & 1 \end{bmatrix} \begin{Bmatrix} d\phi_1 \\ d\phi_2 \end{Bmatrix} = q_D L c e C_{l\alpha} \begin{bmatrix} 1 & 0 \\ 0 & 1 \end{bmatrix} \begin{Bmatrix} d\phi_1 \\ d\phi_2 \end{Bmatrix}$$

Letting $\lambda = q_D L^2 c e C_{l\alpha} / GJ$, the determinant of the single coefficient matrix of the twists is

$$\begin{vmatrix} 2 - \lambda & -1 \\ -1 & 1 - \lambda \end{vmatrix} = 0$$

Thus the characteristic polynomial is $\lambda^2 - 3\lambda + 1 = 0$. The smallest root is $(3/2) - (\sqrt{5}/2) = 0.3820$. Thus $q_D = 0.38GJ/(L^2 c e C_{l\alpha})$.

(b)

$$[A]\{dq\} = q_D L c C_{l\alpha} \begin{bmatrix} 0 & 0 & 1 & 0 & 0 & 0 \\ 0 & 0 & 0 & 0 & 0 & 0 \\ 0 & 0 & e & 0 & 0 & 0 \\ 0 & 0 & 0 & 0 & 0 & 1 \\ 0 & 0 & 0 & 0 & 0 & 0 \\ 0 & 0 & 0 & 0 & 0 & e \end{bmatrix} \begin{Bmatrix} dw_1 \\ d\theta_1 \\ d\phi_1 \\ dw_2 \\ d\theta_2 \\ d\phi_2 \end{Bmatrix}$$

Using a force vector $[Q] = [V_1 \ M_1/L \ T_1/L \ V_2 \ M_2/L \ T_2/L]$, where V is a shear force, T is a torque, and M is a bending moment, then the elastic forces can be written in terms of the following stiffness matrix:

$$\{dQ\} = [K]\{dq\} = \frac{EI}{L^3} \begin{bmatrix} 24 & 0 & 0 & -12 & 6 & 0 \\ 0 & 8 & 0 & -6 & 2 & 0 \\ 0 & 0 & 4 & 0 & 0 & -2 \\ -12 & -6 & 0 & 12 & -6 & 0 \\ 6 & 2 & 0 & -6 & 4 & 0 \\ 0 & 0 & -2 & 0 & 0 & -2 \end{bmatrix} \begin{Bmatrix} dw_1 \\ L d\theta_1 \\ L d\phi_1 \\ dw_2 \\ L d\theta_2 \\ L d\phi_2 \end{Bmatrix}$$

The resulting 6×6 determinant of the matrix eigenvalue equation can be efficiently expanded by minors starting with the fourth row. The first of those two 5×5 determinants reduces to -576 . The second reduces to $576(2 - 3\lambda + \lambda^2)$. Since these two terms sum to zero, they combine to produce exactly the same characteristic equation found in part (a). Note that there are still only two eigenvalues because the $6 \times 6 [A]$ has four dependent rows or four dependent columns.

- 23.4. (a) Because undamped free vibration motion is always such that $\{\ddot{q}\} = -4\pi^2 f^2 \{q\}$, the matrix equation can be rewritten as

$$-4\pi^2 f^2 m \begin{bmatrix} 2 & 0 \\ 0 & 1 \end{bmatrix} \begin{Bmatrix} q_1 \\ q_2 \end{Bmatrix} + \frac{48EI}{7L^3} \begin{bmatrix} 16 & -5 \\ -5 & 2 \end{bmatrix} \begin{Bmatrix} q_1 \\ q_2 \end{Bmatrix} = \begin{Bmatrix} 0 \\ 0 \end{Bmatrix}$$

To put this equation in the form required for matrix iteration for the first natural frequency, divide by the scalar factor containing the frequency and multiply through by the inverse of the second matrix. The result is

$$\frac{12EI}{7\pi^2 m L^3 f^2} \begin{Bmatrix} q_1 \\ q_2 \end{Bmatrix} = \frac{1}{7} \begin{bmatrix} 4 & 5 \\ 10 & 16 \end{bmatrix} \begin{Bmatrix} q_1 \\ q_2 \end{Bmatrix}$$

Cancel the sevens in the two denominators, define $\lambda = 12EI/(\pi^2 m L^3 f^2)$, and iterate to obtain $\lambda = 19.33$ and $\{q_1\} = [0.327 \ 1.00]$. Therefore, $f_1^2 = 0.0629(EI/mL^3)$

- 23.5. (a) $\lambda = 19.82$, and $\{q_1\} = [1.000 \ 0.2434 \ 0.1820]$.

- 23.6. The two nodal DOF for the structural system are the lateral translation w and the bending slope θ at the end of the beam where it connects to the airfoil. Then, equating increments in the aerodynamic loads to increments in the restoring elastic loads

$$\begin{aligned} \begin{Bmatrix} d\mathcal{L} \\ d\mathcal{M} \end{Bmatrix} &= \begin{Bmatrix} 1 \\ -e \end{Bmatrix} d\mathcal{L} = q L c C_{l\alpha} \begin{Bmatrix} 1 \\ -e \end{Bmatrix} (-d\theta) \\ &= q L c C_{l\alpha} \begin{bmatrix} 0 & -1 \\ 0 & -e \end{bmatrix} \begin{Bmatrix} dw \\ d\theta \end{Bmatrix} = \frac{EI}{L^2} \begin{bmatrix} 12 & 6L \\ 6L & L^2 \end{bmatrix} \begin{Bmatrix} dw \\ d\theta \end{Bmatrix} \end{aligned}$$

With $e/L = 1/4$

$$\begin{bmatrix} 12 & 6 \\ 6 & 4 \end{bmatrix} \begin{Bmatrix} dw \\ Ld\theta \end{Bmatrix} = \frac{q L^3 c C_{l\alpha}}{EI} \begin{bmatrix} 0 & -1 \\ 0 & 1/4 \end{bmatrix} \begin{Bmatrix} dw \\ Ld\theta \end{Bmatrix}$$

Thus, using the determinant method to determine the eigenvalue, $q_D = 4EI/(3L^3 c C_{l\alpha})$.

- 23.7. (a) The equilibrium equation is $\delta\Pi = \delta(U + V) = (K\theta - PL \sin\theta)\delta\theta$, which has two solution paths. The first path is θ equals zero regardless of the value of the applied load, and the second path is $P = (K/L)(\theta/\sin\theta)$ from which it is determined that the critical load is $P = (K/L)$. The second variation of the total potential energy, $\delta^2\Pi = (K - PL \cos\theta)(\delta\theta)^2$ shows that, as per usual, the load path θ equals zero is stable below the critical load value and unstable above the critical load value. The approximate formula for the bifurcated path is $K = (\theta^2/3)(\delta\theta)^2$, which is everywhere positive, and hence stable.
- (b) With $K = kL^2$, the equilibrium equation is

$$[kL^2(4\theta + \sin\theta \cos\theta) - 2PL \sin\theta]\delta\theta = 0$$

which has the two solutions: (i) theta equals zero regardless of the value of P ; and (ii) $P = (kL/2)[(4\theta/\sin\theta) + \cos\theta]$. This shows that the value of the critical load is $P = (5/2)kL$. The second variation of the total potential energy shows, as per usual, that the load path θ equals zero is stable below the critical load value and unstable above it. The approximate value of the second variation of the total potential for small values of θ along the bifurcated path is $+(kL^2/3)\theta^2$, which is everywhere positive, and hence stable.

- (c) With $K = kL^2/2$, critical load value is $P = (3/2)kL$, and the approximate value of second variation of the total potential energy for small values of theta is $-(kL^2/3)\theta^2$.

23.8. To obtain the matrix eigenvalue form $\lambda\{q\} = [D]\{q\}$ for matrix iteration, it is necessary to premultiply the first of the 6×6 matrices in the problem statement by the second in order to obtain $[D]$. In order to obtain the smallest solution for φ_D , define $\lambda = 6EI/(\varphi_D c C_{1\alpha} L^3)$. The $[D]$ matrix is

$$[D] = \begin{bmatrix} 0 & 0 & 2 & 0 & 0 & 5 \\ 0 & 0 & 3 & 0 & 0 & 9 \\ 0 & 0 & 1 & 0 & 0 & 1 \\ 0 & 0 & 5 & 0 & 0 & 16 \\ 0 & 0 & 3 & 0 & 0 & 12 \\ 0 & 0 & 1 & 0 & 0 & 2 \end{bmatrix}$$

After iteration, which initially can be confined to the third and sixth elements of $\{q\}$, the converged result is $\lambda = 2.6178$ and $[q] = [0.3267 \ 0.5686 \ 0.08475 \ 1.000 \ 0.7257 \ 0.1371]$. Thus $\varphi_D = 2.292EI/(cC_{1\alpha}L^3)$ and the ratio of the two torsional rotations is 0.618. When EI is replaced by $GJ/2$, the numerator and denominator are multiplied by e , and e/L is set equal to $1/3$, then the result of Exercise 23.3, $\varphi_D = 0.382 GJ/(L^2 c e C_{1\alpha})$, is obtained again.

References

1. Taylor, A. E., *Advanced Calculus*, Ginn & Co., Boston, 1955.
2. Volterra, E., and E. C. Zachmanoglou, *Dynamics of Vibrations*, Charles E. Merrill Books, Inc., Columbus, Ohio, 1965.
3. Shames, I. H., and C. L. Dym, *Energy and Finite Element Methods in Structural Mechanics*, Taylor and Francis, New York, 1991.
4. Boresi, A. P., and O. M. Sidebottom, *Advanced Mechanics of Materials*, Wiley, New York, 1985.
5. Weiss, M., *Higher Algebra for the Undergraduate*, Wiley, New York, 1949.
6. Allen, D. H., and W. E. Haisler, *Introduction to Aerospace Structural Analysis*, Wiley, New York, 1985.
7. Flugge W. (Ed.), *Handbook of Engineering Mechanics*, McGraw-Hill, New York, 1962.
8. Malvern, L. E., *Introduction to the Mechanics of a Continuous Medium*, Prentice-Hall, Englewood Cliffs, New Jersey, 1969.
9. Love, A. E. H., *A Treatise on the Mathematical Theory of Elasticity*, Fourth edition. Dover Publications, New York, 1944.
10. *ASM Metals Reference Book*, American Society for Metals, Metals Park, Ohio.
11. *Metals Handbook* (many volumes), American Society for Metals, Metals Park, Ohio.
12. *Manual of Steel Construction*, Eighth edition, American Institute of Steel Construction, Chicago, Illinois, 1980.
13. *Alloy Digest*, Engineering Alloy Digest, Inc., Upper Montclair, New Jersey.
14. Military Standardization Handbook (MIL-HDBK-5D) *Metallic Materials and Elements for Aerospace Vehicle Structures* (two volumes) FSC 1560, 1983.
15. *Aluminum Developments Digest*, Winter 85–86, The Aluminum Association, Washington, D.C.
16. Rivello, R. M., *Theory and Analysis of Flight Structures*, McGraw-Hill, New York, 1969.
17. Fuchs, H. O., and R. I. Stephens, *Metal Fatigue in Engineering*, Wiley, New York 1980.
18. Peterson, R. E., *Stress Concentration Factors*, Wiley, New York, 1974.
19. Jones, R. M., *Mechanics of Composite Materials*, Scripta Book Co., Washington, D.C., and McGraw-Hill, New York, 1975.
20. Wilf, H. S., *Mathematics for the Physical Sciences*, Wiley, New York, 1962.
21. Timoshenko, S., and J. N. Goodier, *Theory of Elasticity*, McGraw-Hill, Inc., New York, 1951.
22. Engineering Data for Aluminum Structures, *Aluminum Construction Manual*, Section 3, The Aluminum Association, Washington, D.C.
23. Brush, D. O., and B. O. Almroth, *Buckling of Bars, Plates, and Shells*, McGraw-Hill, New York, 1975.
24. Zeigler, H., *Principles of Structural Stability*, Blaisdell, Waltham, Massachusetts, 1968.
25. Meirovitch, L., *Analytical Methods in Vibrations*, Macmillan, New York, 1967.
26. Miner, M. A., "Cumulative damage in fatigue," *Trans. ASME*, Vol. 67, A-159, 1945.
27. Schwartz, M. M., *Composite Materials Handbook*, McGraw-Hill, New York, 1984.
28. Bisplinghoff, R. L., H. Ashley, and R. L. Halfman, *Aeroelasticity*. Addison-Wesley, Reading, Massachusetts, 1955.
29. Bisplinghoff, R. L., and H. Ashley, *Principles of Aeroelasticity*, Wiley, New York, 1962.
30. Oden, J. T., *Mechanics of Elastic Structures*, McGraw-Hill, New York, 1967.
31. Roark, R. J., *Formulas for Stress and Strain*, McGraw-Hill, New York, 1965.
32. Trayer, G. W., and H. W. March, "The Torsion of Members Having Sections Common in Aircraft Construction," NACA Report 334, 1929.

33. Timoshenko, S. P., and J. M. Gere, *Theory of Elastic Stability*, McGraw-Hill, New York, 1961.
34. Bodner, S. R., "On the conservativeness of various distributed force systems," *Journal of the Aeronautical Sciences*, Vol. 25, pp. 132-133, Feb. 1958.
35. Venkatraman, B., and S. A. Patel, *Structural Mechanics with Introductions to Elasticity and Plasticity*, McGraw-Hill, New York, 1970.
36. Weeton, J. W., D. M. Peters, and K. L. Thomas, *Engineer's Guide to Composite Materials*, American Society for Metals, Metals Park, Ohio, 1987.
37. Sokolnikoff, I. S., *Mathematical Theory of Elasticity*, Second edition, McGraw-Hill, New York, 1956.
38. Meirovitch, L., *Computational Methods in Structural Dynamics*, Sijthoff and Noordhoff, Rockville, Maryland, 1980.
39. Kaplan, W., *Advanced Calculus*, Addison-Wesley, Reading, Massachusetts, 1952.
40. *Journal of the Structural Division, Proceedings of the American Society of Civil Engineers (ASCE)*, Vol. 108, No. ST1, Jan. 1982.
41. Abbot, I. H., and A. E. von Doenhoff, *Theory of Wing Sections*, McGraw-Hill, New York, 1949 (also Dover, New York, 1959).
42. Timoshenko, S. P., *Collected Papers*, McGraw-Hill, New York, 1953.
43. Lin, Y. K., and B. K. Donaldson, "A brief survey of transfer matrix techniques with special reference to the analysis of aircraft panels," U.S. Airforce Materials Lab. TR-67-285, Wright-Patterson AFB, Ohio, 1967.
44. Gleick, J., *Chaos, Making a New Science*, Viking, New York, 1987.
45. Donaldson, B. K., S. Chander, and H. Negm, "Improved extended field method numerical results," *Journal of Sound and Vibration*, Vol. 66, No. 1, 1979.
46. Richtmyer, R. D., and R. W. Morton, *Difference Methods for Initial Value Problems*, Second edition, Interscience, New York, 1967.
47. Temple, G., and W. G. Bickley, *Rayleigh's Principle and its Application to Engineering*, Dover, New York, 1956.
48. *Structural Design with Aluminum*, (Buildings and Bridges), The Aluminum Association, No. 38, May 1987.
49. Turner, M. J., R. W. Clough, H. C. Martin, and L. J. Topp, "Stiffness and deflection analysis of complex structures," *Journal of Aeronautical Sciences*, Vol. 23, No. 9, Sept. 1956.
50. Zienkiewicz, O. C., *The Finite Element Method*, Third edition, McGraw-Hill, London, 1977.
51. Strang, G., "A chaotic search for i ," *The College Math. J.*, Vol. 22, No. 1, Jan. 1991.
52. Timoshenko, S. P., and S. Woinowsky-Krieger, *Theory of Plates and Shells*, Second edition, McGraw-Hill, New York, 1959.
53. Lin, Y. K., *Probabilistic Theory of Structural Dynamics*, McGraw-Hill, New York, 1967.
54. Martin, H. C., and G. F. Carey, *Introduction to Finite Element Analysis, Theory and Application*, McGraw-Hill, New York, 1973.
55. Vinson, J. R., *Structural Mechanics: The Behavior of Plates and Shells*, Wiley, New York, 1974.
56. Reddy, J. N., *An Introduction to the Finite Element Method*, McGraw-Hill, New York, 1984.
57. Clough, R. W., and J. L. Tocher, "Finite element stiffness matrices for analysis of plate bending," Proceedings of (first) Conference on Matrix Methods in Structural Mechanics, AFFDL-TR-66-80, Wright-Patterson AFB, 1965.
58. Melosh, R. J., "Basis for derivation of matrices for the direct stiffness method," *AIAA Journal*, Vol. 1, 1631, 1963.
59. Schlichting, H., *Boundary Layer theory*, Fourth edition, McGraw-Hill, New York, 1960.
60. Parris, R., "The root finding route to chaos," *The College Math. J.*, Vol. 22, No. 1, Jan. 1991.
61. Hurty, W. C., and M. F. Rubinstein, *Dynamics of Structures*, Prentice-Hall, Englewood Cliffs, New Jersey, 1964.
62. Scanlan, R. H., and R. Rosenbaum, *Aircraft Vibration and Flutter*, Macmillan, New York, 1960.
63. Gerard, G., *Handbook of Structural Stability, Part V: Compressive Strength of Flat Stiffened Panels*, NACA Technical Note 3785, 1957.

64. Chajes, A., *Principles of Structural Stability Theory*, Prentice-Hall, Englewood Cliffs, New Jersey, 1974.
65. Megson, T. H. G., *Aircraft Structures for Engineering Students*, Crane, Russak & Co., New York, 1972.
66. Higdon, A., E. H. Ohlsen, W. B. Stiles, J. A. Wesse, and W. F. Riley, *Mechanics of Materials*, Third edition, Wiley, New York, 1976.
67. Rizzo, F., "An integral equation approach to boundary value problems of classical elastostatics," *Quarterly of Applied Mathematics*, Vol. 25, No. 1, April 1967.
68. Mendelson, A., "Boundary-integral methods in elasticity and plasticity," NASA TN D-7418, Nov. 1973.
69. Paz, M., *Structural Dynamics, Theory and Computation*, Second edition, Van Nostrand Reinhold, New York, 1985.
70. Gurtin, M. E., Mechanics of Solids II, *Encyclopedia of Physics*, Vol. VIa/2, Springer-Verlag, Berlin, 1972.
71. Wylie, C. R., and L. C. Barrett, *Advanced Engineering Mathematics*, Fifth edition, McGraw-Hill, New York, 1982.
72. Donaldson, B. K., *Introduction to Structural Dynamics*, Cambridge University Press, New York, 2006.



Index

- "A" and "B" bases for material properties, 125
aeroelasticity, 806
aileron reversal, 807
Airy Stress function, 202, 791
anisotropic materials, 156
applied elasticity. *See* strength of materials
applied loads per unit of beam length, 272
- bar, 6
basic strip theory, 819
Bauschinger effect, 124
beam bending slopes, 233
beam boundary condition equations, 282
beam buckling, 792
beam cross-sectional properties. *See also* St. Venant's
 constant uniform torsion
 bending and extension, 241
 modified area for shearing, 670
 torsion of thin beam cross-sections, 405, 415, 416
beam cross-sections, thin open or thin closed,
 403
beam deflection differential equations, 282
beams, short beam solution, 195, 198
Beltrami–Michell equations, 188
Bernoulli–Euler beam theory, 231
Betti's law, 690
Bianchi's identities, 93
biaxial and triaxial loadings, 136
binomial series, 3
boundary conditions
 derived for beam bending and extension, 518
 derived for uniform beam torsion, 519
 general stress formulation, 188
 stated for plates, 770, 773
boundary element/integral method, 540
boundary value problems, 282
Bredt's equations, 417
brick finite element, 637
buckling. *See* beam buckling; plate buckling
bulkheads. *See* frames
- calculus of variations, 512
Castigliano's first theorem, 747
Castigliano's method/second theorem. *See* unit load
 method
Cauchy equations, 21, 514
center of twist, 473
chain rule for partial differentiation, 4
characteristic equation of an o.d.e., 328
characteristic value problem, 56. *See also* eigenvalue
 problem
compact beam cross-sections, 238
compatibility equations
 Cartesian coordinates, 84, 371
 cylindrical coordinates, 94
complementary strain energy, 504, 538
complementary strain energy/CVW
 beam bending and extension, 660
 beam shearing, 669
 beam torsion, 667
complementary virtual work, 498, 538
compliance matrix, 152
composite materials, 157
concentrated forces, 316
conservative forces, 483
constitutive equations, 153
coordinate axis rotations, 39
crack propagation, 133, 145
creep, 114, 127
curved beams, large radius, 683
"cuts," 734. *See also* releases (of constraints)
- damping, 123
deflection interactions, 306, 310, 327, 365
deflection type analyses. *See* stiffness type analyses
deflections, 69, 232, 763
deformations, 69
degrees of freedom. *See* generalized coordinates
determinate structures. *See* indeterminacy
Dirac delta function, limited definition and use, 317
direction cosines, 20, 41
displacement formulations, 173. *See also* Navier
 equations
displacements, 68
distributed generalized coordinates, 598
divergence, 220, 336, 356, 808
ductility, 119, 124
dummy load method. *See* unit load method
dynamic equilibrium, 17, 645
- effective beam length for buckling, 334
eigenvalue problem
 differential equation, 332
 matrix, 56, 814
eigenvector weighted orthogonality, 822
elastic axis, 444, 457
elastic foundation, 304
elastic limit, 122

- elastic stability. *See* beam buckling; plate buckling
 elastic supports and their BCs, 312
 elasticity, 123, 146
 energy, 122
 energy of distortion, maximum, 62. *See also* von Mises shearing stresses
 enforced deflection boundary conditions, in the finite element method, 611
 engineering accuracy, 227
 engineering theory of beams. *See* Bernoulli–Euler beam theory
 equation(s) of motion, 647, 817
 equilibrium equations
 for beam stress resultants, 272, 279
 boundary. *See* Cauchy equations
 general, 19, 370
 for plate stress resultants, 670
 Euler–Lagrange equation, 513
 exact solutions, 192
 external virtual work, beam buckling, 531
- faces of differential-sized volumes
 back, 14
 front, 14
 factor of safety, 125. *See also* limit load factor; ultimate load factor
 false strains, finite element, 653
 fatigue in metals, 129, 144
 fillets
 maximum shearing stress, 409
 need for, 382, 409
 finite difference method, 524
 finite element analysis accuracy, 600
 finite element method, 545
 deflection boundary conditions, 565
 refined elements, 637
 finite element structural model, 558
 flexibility influence coefficient matrix,
 flexibility type analyses, 700. *See also* stress formulations
- flutter
 airfoil, 814
 general, 220, 336, 646
 force type analyses. *See* flexibility type analyses
 forces, body, 17
 frames, 220
 free vibrations. *See* natural vibrations
 functions of integration, 839
 functions of matrices, 833
- Galerkin method, 525
 Gauss's theorem. *See* Green–Gauss theorem
 generalized coordinates, 546. *See also* distributed generalized coordinates
 generalized forces, 510, 553
 Greek alphabet, ix
 Green–Gauss theorem, 475
 Green's theorem. *See* Green–Gauss theorem
 Guyan reduction, 622
- Hamilton's principle, 480, 508
 Heaviside step function, 318
 Hellinger–Reissner principle, 504
 homogeneity, 115
 Hooke's law, 122, 146
 hysteresis loop, 125
- imperfections, structural, 126, 805
 indeterminacy, 22, 271, 700
 inertia force, 17, 645
 inertia matrix. *See* mass matrix
 infinite series, use of, 387
 initial strains/stresses, 610
 intergration of strains, 195, 209
 inverse method, 193, 203, 370
 isotropic materials, 153. *See also* transversely isotropic materials
- kinetic energy, 510
 Kirchoff hypothesis, 763
- Lagrange equations of motion, 459, 480
 Lamé (material) constants, 154
 Lévy series, 401, 774
 limit load factor, 126
 linear independence or dependence, 223, 730
 longitudinal (structural component). *See* stringer
- margin of safety, 126
 mass, in Newton's second theorem, 12. *See also* weight
 mass matrix, 821
 material flexibility matrix. *See* compliance matrix
 material stiffness matrix, 153
 matrix ill-conditioning, 579
 matrix iteration, 820
 Maxwell–Mohr method. *See* unit load method
 Maxwell's reciprocity theorem, 689
 mean value theorem, 224, 608
 membrane analogy, 378
 modulus of elasticity, 120, 124
 secant, 122, 333
 tangent, 120, 333
 modulus of rigidity, 125. *See also* shear modulus
 modulus weighted properties
 beam bending and extension, 235
 plate bending and extension, 760
 Mohr's circle, 47
 moment of inertia, 236
 polar, 393
 principal, 252, 271
 monocoque, 219
 Mueller–Breslau method. *See* unit load method
 multiconnectivity, 240, 371
- natural vibrations
 beam, 533
 system modeling, 582
 Navier equations, 187

- Navier series, 401
- neutral axis, beam bending, 253
- Newton's method for finding roots, 2
- nodes, finite element, 552
- numerical solutions, 225

- octahedral shearing stresses. *See* von Mises shearing stresses
- orthogonality, in functions, 388, 400
- orthotropic materials, 148

- parallel axes theorems, 245
- percent elongation, 120
- permanent set, 123
- plane strain, 85, 162
- plane stress finite element. *See* stiffness matrix
- plasticity, 123, 138
- plate buckling, 777
- plate theory, 759
- Poisson's ratio, 118, 142
- potential energy, 502
- Prandtl stress function, 371, 518
- principal axes, beam cross-section, 252
- principle of complementary virtual work, 499–500, 518, 655
- principle of the total complementary potential energy, 504
- principle of the total potential energy, 503
- principle of virtual work, 493–497, 626
- products of inertia, 236
- proportional limit, regular or offset, 120

- Ramberg–Osgood curve fit, 139
- Rayleigh–Ritz method, 525
- redundant forces/moments or reactions, 700
- reference coefficient of thermal expansion, α_0 , 608
- reference modulus of elasticity, E_0 , 234, 554
- refined finite elements. *See* finite element method
- Reissner principle, 504–508
- releases, 707, 734
- residual stresses, 140–143. *See also* initial strain/stresses,
- resonance, 831
- rib, 220
- rigid body motions of structures, 556, 607
- rigidity in finite elements, 569–579, 587
- rings. *See* frames
- Ritz method. *See* Rayleigh–Ritz method

- safety factor. *See* factor of safety
- semimonocoque, 219
- separation of variables, 401
- series
 - binomial, 3
 - Taylor's, 2
- series representations, truncated infinite, finite element displacements, 626
- shape functions, finite element, 628, 639
- shear center, 444, 457, 462
- shear flow due to shear forces, 447
 - in closed cross-sections, 459, 480
 - in open cross-sections, 448
- shear flow due to twisting moments, 411
- shear lag, 239
- shear modulus, 125, 150, 156
- skin, 219–220, 623
- slenderness ratio, for beams, 333
- snap through instability, 805
- software, 523
- spar, 220
- springs used for structural modeling, 311, 704
- St. Venant's constant for uniform torsion, 375
- St. Venant's principle, 199
- stability, neutral, 810
- stability diagrams, 802, 820, 828
- stability energy criteria, 801
- static condensation. *See* Guyan reduction
- stiffener (structural component). *See* stringer
- stiffness matrix
 - additional, beam shearing, 597
 - element beam bending, 555, 726
 - element beam extension, 557
 - global/system assembly, 560
 - plane stress rectangular element, 625
 - rectangular plate element bending, 784
 - rotated bar element, 604
 - spring element, 558
 - when product of inertia not zero, 589
- stiffness type analyses, 545. *See also* displacement formulations
- strain energy, 147
- strain energy, actual and virtual, 503
- strain gauge, 99
- strain gauge rosette, 99
- strain hardening, 123, 138
- strain rate, 127
- strain–displacement equations, linear and nonlinear, 80
- strains
 - Green, 79
 - longitudinal or normal, 75
 - in rotated coordinate systems, 95
 - shear or shearing, 77
 - thermal, 150
 - true, 80
- strain–stress equations
 - isotropic materials, 154
 - orthotropic materials, 152
- strength of materials, 368
- stress
 - generalized plane, 53
 - offset yield, 120
 - plane, 23, 157, 189, 202
 - ultimate, 119
 - yield, 119, 124
- stress concentration factors, 129, 130, 133, 238, 387
- stress formulations, 168. *See also* Beltrami–Michell equations

- stress resultants
 in beams, 227
 in plates, 761
- stress, axial normal, in beams, 237, 567
- stresses
 based on original cross-sectional area, 119
 double subscript notation, 10
 initial, 126. *See also* residual stresses
 maximum values, 46
 octahedral/von Mises shearing, 59
 in rotated coordinate systems, 42
- stress-strain equations, 153
- stringer, 220, 631
- substructuring,
- symmetry of a structure and loading, as a constraint
 on number of unknowns, 170, 180, 388, 702,
 722, 726
- Taylor's series, 2
- temperature change effects, 127, 504
- tensors, 63, 79, 89
- tests, tensile, 119
- tetrahedron finite element, 636
- Theodorsen function, 817
- theory of elasticity, overview and solutions
 approaches, 167. *See also* displacement
 formulations; stress formulations
- thermal forces and moments, equivalent, 235, 249
- thin plate bending and extension. *See* plate theory
- time-varying loads, 642
- Timoshenko beam theory, 231
- torsion box, 220
- torsion constant. *See* St. Venant's constant for uniform
 torsion
- total potential energy, 503, 801
- tractions, 19
- transversely isotropic materials, 157
- trial solutions for differential equations, an example,
 327
- triangular plane stress finite element, 635
- trivial solution, 55, 331
- ultimate load factor, 126
- undetermined coefficients, method of, 221
- uniform torsion, 369, 518, 846
- unit load method, 655
 for simple design purposes, 677
- unit step function, 318. *See also* Heaviside step
 function
- unitary matrices, 106
- variation
 first or second, 511
 total, 511, 800
- variational operator, 487-510
- varied paths, 489
- vibrations. *See* time-varying loads
- virtual displacement, 484
- virtual forces, virtual stresses, 499
- virtual load method. *See* unit load method
- virtual potential energy, 484
- virtual work, 484
 used to define equivalent nodal loads, 597
- virtual work method. *See* unit load method
- viscoelasticity, 128
- Von Mises shearing stresses, 59
- warping constant, for beam torsion, 421, 442
- warping deflections, 368
- weight, vehicular, 1
- well-formulated problems, 104
- Winkler foundation. *See* elastic foundation
- work, 122, 482
 lost, 122
 per unit volume, 122
- Young's modulus. *See* modulus of elasticity,
 120





As with the first edition, this textbook provides a clear introduction to the fundamental theory of structural analysis as applied to aircraft, spacecraft, automobiles, and ships. The emphasis is on the application of fundamental concepts of structural analysis that are employed in everyday engineering practice. All

approximations are accompanied by a full explanation of their validity. Repetition is an important learning tool; therefore, some redundancy is used to dispel misunderstanding. In this new edition, more topics, figures, examples, and exercises have been added. There is also a greater emphasis on the finite element method of analysis. Clarity remains the hallmark of this text.

Bruce K. Donaldson was first exposed to aircraft inertia loads when he was a carrier-based U.S. Navy antisubmarine pilot. He subsequently worked in the structural dynamics area at the Boeing Company and at the Beech Aircraft Corporation in Wichita, Kansas, before returning to school and embarking on an academic career in the area of structural analysis. He became a professor of aerospace engineering and then a professor of civil and environmental engineering at the University of Maryland. Professor Donaldson is the recipient of numerous teaching awards and has maintained industry contacts, working various summers at government agencies and for commercial enterprises, the last being Lockheed Martin in Fort Worth, Texas. He is the author of *Introduction to Structural Dynamics* also published by Cambridge University Press.

STERLING BOOK HOUSE, MUMBAI
Ph # (+91 22) 22612*21
ANALYSIS OF AIRCRAFT STRUCTURES

B.K. DONALDSON

MRP Rs 695



S-109404

9781107038167

L-0

This edition is for sale in South Asia only, not for export elsewhere.



9 781107 638167